Fundamental constants

Quantity	Symbol	Value	SI unit	Auxiliary value
Speed of light in vacuum	c	$2.997\,925 \times 10^{8}$	$m\,s^{-1}$	
Elementary charge	e	$1.602\,189 \times 10^{-19}$	C	
Planck constant	h	$6.626\,18 \times 10^{-34}$	Js	$= 4.135\,70 \times 10^{-15}$ eV s; $\hbar = h/2\pi$
Avogadro constant	N_A	$6.022\,04 \times 10^{23}$	mol^{-1}	
Atomic mass unit	1 u	$1.660\,566 \times 10^{-27}$	kg	= 931.501 6 MeV: mass of $^{12}C = 12$ u
Electron rest mass	m_e	$0.910\,953 \times 10^{-30}$	kg	$M_e = N_A \cdot m_e = 0.000\,548\,580$ u = 0.511 003 4 MeV
Proton rest mass	m_P	$1.672\,649 \times 10^{-27}$	kg	$M_P = N_A \cdot m_P = 1.007\,276\,5$ u = 938.279 6 MeV
Neutron rest mass	m_n	$1.674\,954 \times 10^{-27}$	kg	$M_n = N_A \cdot m_n = 1.008\,665\,0$ u = 939.573 1 MeV
Faraday constant	F	$9.648\,46 \times 10^{4}$	$C\,mol^{-1}$	$= N_A \cdot e$
Rydberg constant	R_∞	$1.097\,373 \times 10^{7}$	m^{-1}	$R_\infty h \cdot c = 13.605\,8$ eV
Bohr radius	a_0	$0.529\,177 \times 10^{-10}$	m	$= \alpha/4\pi R_\infty$
Electron magnetic moment	μ_e	$9.284\,83 \times 10^{-24}$	$J\,T^{-1}$	
Proton magnetic moment	μ_P	$1.410\,617 \times 10^{-26}$	$J\,T^{-1}$	
Bohr magneton	μ_B	$9.274\,08 \times 10^{-24}$	$J\,T^{-1}$	$= e \cdot /2 \cdot m_e$ ($1\,J\,T^{-1} = 10^3$ erg gauss^{-1})
Nuclear magneton	μ_N	$5.050\,82 \times 10^{-27}$	$J\,T^{-1}$	$= e \cdot /2 \cdot m_P$
Molar gas constant	R	8.314 41	$J\,mol^{-1}\,K^{-1}$	= 0.082 057 lit atm $mol^{-1}\,K^{-1}$ = 1.987 2 cal $mol^{-1}\,K^{-1}$
Molar volume of ideal gas (s.t.p.)	V_m	0.022 413 8	$m^3\,mol^{-1}$	$= R \cdot T_0/p_0$, $T_0 = 273.15$ K, $p_0 = 1$ atm
Boltzmann constant	k	$1.380\,662 \times 10^{-23}$	$J\,K^{-1}$	$= R/N_A$; $= 8.617\,35 \times 10^{-5}$ eV K^{-1}; $1/k = 11\,604.5$ K eV^{-1}

Pressure	Pa	bar	kp/m^2
1 Pa (Pascal) = $1\,N/m^2$	1	10^{-5}	1.019716×10^{-1}
1 bar = $10^6\,dyn/cm^2$	10^5	1	10.19716×10^3
$1\,kp/m^2$ = 1 mm H_2O	9.80665	0.980665×10^{-4}	1
1 at = $1\,kp/cm^2$	0.980665×10^5	0.980665	10^4
1 atm = 760 Torr	1.01325×10^5	1.01325	1.033227×10^4
1 Torr = 1 mm Hg	133.3224	1.333224×10^{-3}	13.59510
$1\,lb/in^2$ = 1 psi	6.89476×10^3	68.9476×10^{-3}	703.069

Useful conversion factors

Work, energy, heat	J	kWh	kcal	Btu	MeV
1 J (Joule) = 1 Ws = 1 Nm = 10^7 erg	1	2.778×10^{-7}	2.39006×10^{-4}	9.4781×10^{-4}	6.242×10^{12}
1 kWh	3.6×10^6	1	860.4	3412.14	2.247×10^{19}
1 kcal	4184.0	1.1622×10^{-3}	1	3.96566	2.6117×10^{16}
1 Btu (British thermal unit)	1055.06	2.93071×10^{-4}	0.25164	1	6.5858×10^{15}
1 MeV	1.602×10^{-13}	4.450×10^{-20}	3.8289×10^{-17}	1.51840×10^{-16}	1

Molecular energy	J/mol	cm^{-1}/molecule	K*/molecule	eV/molecule
1 J/mol	1	0.0835935	0.12027	0.0103643
1 cm^{-1}/molecule	11.96266	1	1.43879	1.2398×10^{-4}
1 K/molecule	8.31444	0.69503	1	8.6173×10^{-5}
1 eV/molecule	96484.6	8065.5	11604.5	1

* Kelvin (temperature unit)

Power	kW	PS	kp m/s	kcal/s
1 kW = 10^{10} erg/s	1	1.35962	101.972	0.239006
1 PS	0.73550	1	75	0.17579
1 kp m/s	9.80665×10^{-3}	0.01333	1	2.34384×10^{-3}
1 kcal/s	4.1840	5.6886	426.650	1

at	atm	Torr	lb/in^2
1.019716×10^{-5}	0.986923×10^{-5}	0.750062×10^{-2}	145.0378×10^{-6}
1.019716	0.986923	750.062	14.50378
10^{-4}	0.967841×10^{-4}	0.735559×10^{-1}	1.422335×10^{-3}
1	0.967841	735.559	14.22335
1.033227	1	760	14.69595
1.359510×10^{-3}	1.315789×10^{-3}	1	19.33678×10^{-3}
70.3069×10^{-3}	68.0460×10^{-3}	51.7149	1

THE CHEMISTRY OF THE ACTINIDE ELEMENTS

This work is dedicated to
Professor Burris B. Cunningham
University of California, Berkeley
1912–1971
Pioneer in the chemistry of
the transuranium elements

THE CHEMISTRY OF THE ACTINIDE ELEMENTS

SECOND EDITION

Volume 2

EDITED BY

Joseph J. Katz
Chemistry Division
Argonne National Laboratory, USA

Glenn T. Seaborg
Chemistry Division
Lawrence Berkeley Laboratory, USA

Lester R. Morss
Chemistry Division
Argonne National Laboratory, USA

LONDON NEW YORK
Chapman and Hall

First published in 1957 by Methuen Ltd
Published in 1986 in two volumes by
Chapman and Hall Ltd
11 New Fetter Lane, London EC4P 4EE
Published in the USA by
Chapman and Hall
29 West 35th Street, New York NY 10001

ISBN-13:978-94-010-7918-1

British Library Cataloguing in Publication Data

Katz, Joseph J.
The chemistry of the actinide elements—
2nd ed.
1. Actinide elements
I. Title II. Seaborg, Glenn T. III. Morss,
Lester R.
546'.4 QD172.A3

ISBN-13:978-94-010-7918-1 e-ISBN-13:978-94-009-3155-8
DOI: 10.1007/978-94-009-3155-8

Library of Congress Cataloging-in-Publication Data

The chemistry of the actinide elements.
Bibliography: p.
Includes indexes.
1. Actinide elements. I. Katz, Joseph J.
(Joseph Jacob), 1912– . II. Seaborg, Glenn
Theodore, 1912– . III. Morss, Lester R.
QD172.A3C46 1986 546'.7 86–8284
ISBN-13:978-94-010-7918-1

CONTENTS

Volume 1

Volume 2

CONTRIBUTORS

Irshad Ahmad
Chemistry and Physics Divisions, Argonne National Laboratory, USA

Sten Ahrland
Inorganic Chemistry 1, Chemical Center, University of Lund, Sweden

Jean Blaise
Laboratoire Aimé Cotton, Centre National de la Recherche Scientifique, Université de Paris-Sud, France

Merwyn B. Brodsky
Materials Science and Technology Division, Argonne National Laboratory, USA

John H. Burns
Chemistry Division, Oak Ridge National Laboratory, USA

William T. Carnall
Chemistry Division, Argonne National Laboratory, USA

John G. Conway
Materials and Molecular Research Division, Lawrence Berkeley Laboratory, USA

Henry M. Crosswhite
Chemistry Division, Argonne National Laboratory, USA

Norman M. Edelstein
Materials and Molecular Research Division, Lawrence Berkeley Laboratory, USA

P. Gary Eller
Isotope and Nuclear Chemistry Division, Los Alamos National Laboratory, USA

James A. Fahey
Bronx Community College of the City University of New York, New York, USA

Paul R. Fields
Chemistry Division, Argonne National Laboratory, USA

Mark S. Fred
Chemistry Division, Argonne National Laboratory, USA

Jean Goffart
Laboratory of Analytical Chemistry and Radiochemistry, Université de Liège, Belgium

Richard G. Haire
Chemistry Division, Oak Ridge National Laboratory, USA

David E. Hobart
Isotope and Nuclear Chemistry Division, Los Alamos National Laboratory, USA

E. Kenneth Hulet
Nuclear Chemistry Division, Lawrence Livermore National Laboratory, USA

Joseph J. Katz
Chemistry Division, Argonne National Laboratory, USA

Leonard I. Katzin
Chemistry Division, Argonne National Laboratory, USA

O. Lewin Keller, Jr
Chemistry Division, Oak Ridge National Laboratory, USA

H. W. Kirby
Mound Laboratory, Monsanto Research Corporation, Miamisburg, USA

Tobin J. Marks
Department of Chemistry, Northwestern University, Evanston, USA

Lester R. Morss
Chemistry Division, Argonne National Laboratory, USA

Michael V. Nevitt
Materials Science and Technology Division, Argonne National Laboratory, USA

Robert A. Penneman
Isotope and Nuclear Chemistry Division, Los Alamos National Laboratory, USA

Joseph R. Peterson
Department of Chemistry, University of Tennessee and Chemistry Division, Oak Ridge National Laboratory, USA

Wallace W. Schulz
Rockwell Hanford Operations, Energy Systems Group, Richland, USA

Glenn T. Seaborg
Department of Chemistry, University of California, Berkeley and Nuclear Science Division, Lawrence Berkeley Laboratory, USA

Robert J. Silva
Nuclear Chemistry Division, Lawrence Livermore National Laboratory, USA

Gary L. Silver
Mound Laboratory, Monsanto Research Corporation, Miamisburg, USA

David C. Sonnenberger
Chemistry Division, Argonne National Laboratory, USA

Andrew Streitwieser, Jr
Department of Chemistry, University of California, Berkeley and Materials and Molecular Research Division, Lawrence Berkeley Laboratory, USA

Fritz Weigel
Radiochemistry Laboratory, Institute of Inorganic Chemistry, University of Munich, Federal Republic of Germany

PREFACE

The first edition of this work appeared almost thirty years ago, when, as we can see in retrospect, the study of the actinide elements was in its first bloom. Although the broad features of the chemistry of the actinide elements were by then quite well delineated, the treatment of the subject in the first edition was of necessity largely descriptive in nature. A detailed understanding of the chemical consequences of the characteristic presence of 5f electrons in most of the members of the actinide series was still for the future, and many of the systematic features of the actinide elements were only dimly apprehended. In the past thirty years all this has changed. The application of new spectroscopic techniques, which came into general use during this period, and new theoretical insights, which came from a better understanding of chemical bonding, inorganic chemistry, and solid state phenomena, were among the important factors that led to a great expansion and maturation in actinide element research and a large number of new and important findings.

The first edition consisted of a serial description of the individual actinide elements, with a single chapter devoted to the six heaviest elements (lawrencium, the heaviest actinide, was yet to be discovered). Less than 15% of the text was devoted to a consideration of the systematics of the actinide elements. In this edition nearly half of the work consists of survey chapters in which such subjects as the metallic state, thermochemistry, solid state chemistry, solution chemistry, atomic and electronic spectroscopy, magnetic properties, organometallic chemistry, and the biological and environmental properties of the actinide elements are treated in comparative fashion. Because of the expansion of the discipline and of the scope of the second edition, many colleagues were asked to contribute chapters that reflected their expert knowledge.

The editors of this edition are deeply indebted to the contributors of individual chapters for their cooperation in the preparation of the book. We are also grateful to colleagues who helped us in many ways. We acknowledge the planning and organization of this edition undertaken by the late Burris B. Cunningham and by Robert A. Penneman. We wish to thank Gary L. Silver for contributing to and editing of the plutonium chapter; Thomas W. Newton and James C. Sullivan for timely assistance on the redox reactions and kinetics of the actinide elements; Henry R. Hoekstra and Jack L. Ryan for their contributions to the chapter on uranium in the early stages of its preparation; to Irshad Ahmad for tables of isotopes of each element; to Sue Morss for bibliographies and SI unit conversion; to Sherman M. Fried for the first draft of the neptunium chapter; and to Beth A. Mustari for her expert secretarial assistance. We take especial pleasure in thanking Richard T. Stileman of Chapman and Hall Ltd without whose encouragement and guidance this volume could not have been completed.

All of us who have been involved in the writing, editing, and publishing the new edition of *The Chemistry of the Actinide Elements* express our sincere hope that this new work will make a substantive contribution to research in this important field, and that it will serve as a convenient source of factual information on the actinide elements for researchers, teachers, students, and those who will have responsibility for far-reaching decisions involving the actinide elements in nuclear energy production and in the control of nuclear weapons.

JJK
GTS
LRM

CHAPTER EIGHT

AMERICIUM

Wallace W. Schulz and Robert A. Penneman

8.1 HISTORICAL

Americium, element 95, was discovered in 1944–45 by Seaborg *et al.* [1] at the Metallurgical Laboratory of the University of Chicago. The reaction used was:

$$^{239}\mathrm{Pu(n,\gamma)}^{240}\mathrm{Pu(n,\gamma)}^{241}\mathrm{Pu} \xrightarrow[14\ \mathrm{yr}]{\beta^-} {}^{241}\mathrm{Am}$$

Americium-241 is an alpha emitter with a half-life of 433 years. This reaction is still the best source of the pure ^{241}Am available today.

In post-war work at Chicago, Cunningham isolated $Am(OH)_3$ and measured the absorption spectrum of the Am^{3+} aquo ion [2]. By the 1950s, the major center for americium chemistry research in the world was at Los Alamos. In the 1970s, the bulk of publications on americium came from the USSR and West Germany.

The longest-lived americium isotope is ^{243}Am ($t_{1/2}$ = 7380 years). While americium isotopes with mass numbers from 234 to 247 are known, ^{241}Am and ^{243}Am are the most important and the most useful for chemical research. Extensive reviews can be found in refs 3–16 and 367.

8.2 NUCLEAR PROPERTIES

Data in Table 8.1 are taken primarily from the comprehensive compilations of Hyde in *Gmelin* [4] and others [16–23].

Table 8.1 *Nuclear properties of americium isotopes.*

Mass number	*Half-life*	*Mode of decay*	*Main radiations* (MeV)	*Method of production*
234	2.6 min	EC		^{230}Th(^{10}B, 6n) ^{10}B, ^{11}B on ^{233}U
237	1.22 h	EC >99% α 0.025%	α 6.042 γ 0.280 (47%)	^{237}Np(α, 4n) ^{237}Np(^{3}He, 3n)
238	1.63 h	EC >99% α 1.0×10^{-4}%	α 5.94 γ 0.963 (29%)	^{237}Np(α, 3n)
239	11.9 h	EC >99% α 0.010%	α 5.776 (84%) 5.734 (13.8%) γ 0.278 (15%)	^{237}Np(α, 2n) ^{239}Pu(d, 2n)
240	50.8 h	EC >99% α 1.9×10^{-4}%	α 5.378 (87%) 5.337 (12.0%) γ 0.988 (73%)	^{237}Np(α, n) ^{239}Pu(d, n)
241	432.7 yr 1.15×10^{14} yr	α SF	α 5.486 (84.0%) 5.443 (13.1%) γ 0.059 (35.7%)	^{241}Pu daughter multiple n capture
242	16.01 h	β^- 82.7% EC 17.3%	β^- 0.667 γ 0.042 weak	^{241}Am(n, γ)
242 m	141 yr 9.5×10^{11} yr	IT 99.55% SF α 0.45%	α 5.207 (89%) 5.141 (6.0%) γ 0.0493 (41%)	^{241}Am(n, γ) ^{241}Am(n, γ)
243	7.38×10^{3} yr 2.0×10^{14} yr	α SF	α 5.277 (88%) 5.234 (10.6%) γ 0.075 (68%)	multiple n capture
244	10.1 h	β^-	β^- 0.387 γ 0.746 (67%)	^{243}Am(n, γ)
244 m	26 min	β^- >99% EC 0.041%	β^- 1.50	^{243}Am(n, γ)
245	2.05 h	β^-	β^- 0.895 γ 0.253 (6.1%)	^{245}Pu daughter
246[a]	25.0 min	β^-	β^- 2.38 γ 0.799 (25%)	^{246}Pu daughter
246[a]	39 min	β^-	γ 0.679 (52%)	^{244}Pu(α, d) ^{244}Pu(^{3}He, p)
247	24 min	β^-	γ 0.285 (23%)	^{244}Pu(α, p)

[a] Not known whether ground-state nuclide or isomer.

8.3 PREPARATION AND PURIFICATION

8.3.1 Production

The important isotopes of americium, ^{243}Am ($t_{1/2}$ = 7380 years) and ^{241}Am ($t_{1/2}$ = 433 years), have been made in kilogram amounts as nearly pure isotopes. A third, ^{242}Am ($t_{1/2}$ = 141 years), can be produced to the extent of only a few percent in ^{241}Am by neutron capture.

(a) Production of ^{241}Am by irradiation of ^{239}Pu

Neutron irradiation of ^{239}Pu that normally occurs during its production yields ^{241}Pu, which decays by beta emission with a half-life of 14.4 ± 0.3 years to ^{241}Am. In 1977 more than 1.5 kg of ^{241}Am were isolated from rework of aged plutonium at the Rocky Flats site (USA). In 1980 a similar amount was isolated at Los Alamos.

(b) Production of ^{243}Am by irradiation of ^{242}Pu

Nearly isotopically pure ^{243}Am results from irradiation of ^{242}Pu with thermal neutrons:

$$^{242}\mathrm{Pu}(\mathrm{n},\gamma)^{243}\mathrm{Pu} \xrightarrow[5\,\mathrm{h}]{\beta^-} {}^{243}\mathrm{Am}$$

(c) Availability of ^{241}Am and ^{243}Am from power reactors

Power reactors will produce kilogram quantities of ^{241}Am and ^{243}Am with an isotopic composition dependent on reactor exposure. About 1 kg of ^{241}Am and ^{243}Am were recovered at Hanford during reprocessing of the Shippingport blanket fuel [24]. No industrial fuel reprocessor in the USA has undertaken the systematic recovery of americium. However, a potentially large source of americium is the high-level Purex-process liquid waste from plutonium processing; indeed, future waste storage may require the separation of americium.

8.3.2 Applications of ^{241}Am

(a) Uses based on characteristic radiations

As a source of nearly monoenergetic alpha (5.44 and 5.49 MeV) and gamma (59.6 keV) radiation, ^{241}Am is widely used in thickness gaging, and density and radiographic measurements. Seaborg [25] states that the list of applications of ^{241}Am may well be the longest of any actinide nuclide. Crandall [26] points out that in terms of cost, convenience, spectral purity, and lifetime, ^{241}Am is superior to all competing radioisotopes as a low-energy gamma source. In the USA, an expanding use is in smoke-detector alarms. Many neutron sources use ^{241}Am to furnish alpha particles for the (α, n) reaction on beryllium and this is the major use for ^{241}Am. Many specific uses of ^{241}Am have been recapitulated by LeVert and Helminski [27].

(b) Use in production of ^{242}Cm and ^{238}Pu

The ^{238}Pu produced by the decay of ^{242}Cm contains little (< 0.02 ppm) of the undesirable ^{236}Pu contaminant, compared to about 10 ppm in the ^{238}Pu produced by ^{237}Np neutron irradiation in a light-water reactor; a low ^{238}Pu

content is a distinct advantage for cardiac pacemaker use [16]. Because of its high power output (122 W g^{-1}) and minor shielding requirements, ^{242}Cm has been used in the preparation of heat sources. The thermal-neutron capture sequence involved in producing ^{242}Cm from ^{241}Am is:

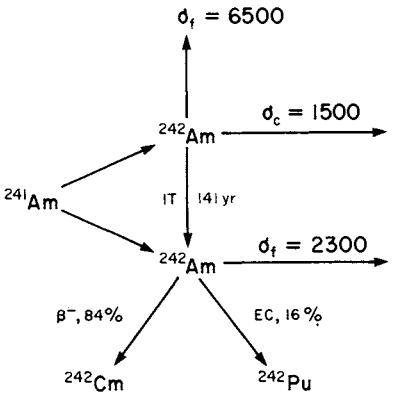

Hennelly notes an optimum yield of about 0.65 g of ^{242}Cm per gram of ^{241}Am consumed [28].

(c) Applications of ^{243}Am

Its lower specific activity compared to ^{241}Am makes ^{243}Am particularly useful in chemical studies. Of importance also is the use of ^{243}Am as a target material for the production of ^{244}Cm, $^{249}Bk/Cf$, ^{252}Cf, and other transcurium elements in high neutron-flux reactors. The Savannah River reactors in the USA produced about 9 kg of a ^{243}Am–^{244}Cm mixture [14].

8.3.3 Separation processes

Traditionally, the recovery and purification of americium has utilized primarily aqueous ion-exchange, solvent extraction, and precipitation processes. Departures are represented by the pyrochemical process and distillation of americium metal in high vacuum used at the Rocky Flats plant (Colorado) [333].

(a) Pyrochemical processes

A two-stage, countercurrent molten-salt extraction process is used to extract ^{241}Am from many kilograms of aged plutonium metal in which ^{241}Am has grown-in by beta decay of ^{241}Pu. The purification scheme, based partly on molten-halide/molten-metal studies at the Los Alamos Scientific Laboratory and Argonne National Laboratory, removes about 90% of the americium from plutonium metal, typically containing 200–2000 ppm ^{241}Am [16].

Mullins and Leary [29] patented a method of separating americium from plutonium which involves bubbling a mixture of oxygen and argon gas into a molten salt containing both elements. Plutonium precipitates as PuO_2, whereas americium stays in solution.

Ferris and his co-workers [30] determined the equilibrium distribution of americium (and other transuranium elements) between liquid bismuth and molten LiCl, LiBr, and several $LiF–BeF_2–ThF_4$ solutions at temperatures of 600–750°C. Some of the americium appeared to be in the divalent state in the $Am/PuCl_3$ system [29]. The distribution coefficient, D = (g Am/g metal phase)/(g Am/g salt phase), of americium between molten aluminum metal and molten $AlCl_3$–KCl is 1.96 [31].

Foos and Guillaumont [32] measured the partition of americium at 150–160°C between molten $LiNO_3$–KNO_3 phases and tri-n-butyl phosphate (TBP) and other extractants.

(b) Precipitation processes

Ion-exchange and solvent extraction technologies have largely supplanted precipitation processes for recovering americium. However, some precipitation processes still find applications, using the insolubility and other special properties of AmF_3, $K_8Am_2(SO_4)_7$, $Am_2(C_2O_4)_3$, or $K_3AmO_2(CO_3)_2$. The latter two compounds are in use because oxalate prevents certain impurities from accompanying americium in the precipitate and is a convenient source of AmO_2. The insoluble Am(v) carbonate complex has been particularly useful for the large-scale separation from curium [33, 34].

Following a suggestion by Penneman, Hermann demonstrated that a substantial separation of americium from lanthanum could be obtained by fractional precipitation of americium and lanthanum oxalates. The precipitation is effected in homogeneous solution; the precipitant is generated by the slow hydrolysis of dimethyl oxalate. The oxalate precipitate is greatly enriched in americium (50% of the lanthanum can be rejected at each stage, with about 4% of the americium) [35].

Stephanou and Penneman [36] found that Cm(III) could be separated from americium by oxidizing the latter to Am(VI) with potassium persulfate and precipitating CmF_3; Am(VI) fluoride is soluble under these conditions.

Proctor *et al.* [37] at the Rocky Flats plant used precipitation of cerium peroxide to purify gram quantities of americium from cerium. Based on an earlier finding by Penneman and Asprey that Am(VI) is soluble in aqueous hydrofluoric acid, Proctor [38] separated Am(VI) from large quantities of rare earths by precipitation of their trifluorides.

(c) Solvent extraction processes

Solvent extraction processes and systems using amine and organophosphorus extractants are extensively used for the initial recovery and separation of gram

amounts of americium. Weaver has published an excellent review of the solvent extraction chemistry of trivalent americium [15], and Myasoedov [5] has discussed solvent extraction systems for the analysis of americium. (See also Shoun and McDowell [39].)

(*i*) *Organophosphorus extractants* [40]

Tri-n-butyl phosphate (TBP) is the extractant in widest use for nuclear fuel processing. Extraction of Am^{3+} from nitrate media by TBP conforms to the reaction [15]:

$$Am^{3+}(aq) + 3NO_3^-(aq) + 3TBP(org) \rightarrow Am(NO_3)_3 \cdot 3TBP(org)$$

The equilibrium constant, $K_{ex} = [Am(NO_3)_3 \cdot 3TBP]/[Am^{3+}]\,[NO_3^-]^3[TBP]^3$, has the value of 0·4 at zero ionic strength [41]. While TBP, even undiluted, extracts americium only weakly from strong nitric acid solutions, americium is extracted by TBP quite strongly from neutral (or low-acid), highly salted nitrate solutions.

Formation constants of complexes formed by Am(III) with aminopolycarboxylic acids are larger than for the comparable complexes of the light lanthanides ($Z = 57$–61). Thus, addition of an aminopolycarboxylic acid to a lithium or aluminum nitrate solution containing Am(III) and rare earths enhances TBP extraction of the lanthanides relative to americium [42].

Penneman and Keenan [334] report that Am(III) can be separated from rare earths by TBP extraction from 1 M ammonium thiocyanate solutions. The mechanism of extraction of Am(III) and Eu(III) from 1 M ammonium thiocyanate media by TBP both in the presence or absence of a quaternary ammonium thiocyanate was recently investigated by Indian scientists [43].

Dibutyl butylphosphonate

Dibutyl butylphosphonate (DBBP), $(C_4H_9O)_2(C_4H_9)PO$, extracts Am(III) from nitrate media more strongly than TBP and was used in a production process at Hanford [16].

Neutral bifunctional organophosphorus compounds

Since TBP leaves Am(III) behind in an acidic raffinate, an effective extractant is needed to remove Am(III) from such media. Siddall found that bidentate extractants have this desirable property [44]. Schulz [45] and McIsaac [46] at the Hanford and Idaho Falls sites, respectively, have recently revived interest in plant-scale application of neutral bidentate organophosphorus extractants, particularly dihexyl-*N*,*N*-diethylcarbamoyl methylenephosphonate (DHDECMP) and dibutyl-*N*,*N*-diethylcarbamoyl methylenephosphonate (DBDECMP). The binding of actinide ions to DHDECMP has not been elucidated fully. Horwitz [335] states that in perchloric acid the extractant is

indeed bidentate, but when nitrate is present, it competes for the second coordination site.

There has as yet been no crystal structure of a trivalent actinide complex with DHDECMP but R. T. Paine, University of New Mexico, has prepared $Sm(NO_3)_3 \cdot 2CMP$ and $Th(NO_3)_4 \cdot 2CMP$ and finds oxygen binding to these metals from CMP [47].

Bis(2-ethylhexyl)phosphoric acid

An excellent extractant for Am^{3+} is bis(2-ethylhexyl) phosphoric acid (HDEHP). This extractant is commercially available in large quantities, can be readily purified, and has been widely used for both analytical and plant-scale recovery and purification of americium [48, 49]. Extraction of Am(III) is very sensitive to the nature of the diluent [49]. Kinetics of extraction were studied by Choppin and Nash [336].

A countercurrent HDEHP extraction process was used at Hanford in the late 1960s as part of the processing sequence for recovering and purifying 1 kg of Am and 50 g of Cm from irradiated Shippingport reactor fuel [50].

An HDEHP batch extraction–strip process (Cleanex process) is routinely used in the Transuranium Processing Plant at the Oak Ridge National Laboratory to reclaim americium, curium, and other transplutonium elements from rework solutions and/or to convert from nitrate to chloride media [337]. The Talspeak HDEHP processes are based on the results of Weaver and Kappelman [51], who were the first to show that HDEHP extracts lanthanides much more strongly than actinides from aqueous carboxylic acid solutions containing an aminopolycarboxylic acid chelating agent. Lactic acid is used to avoid precipitation where the concentration of lanthanides is high. The extraction of Am(VI) from Cm(III) in HDEHP has been studied [338] but Am(VI) reduces rather rapidly.

Other organophosphorus acid extractants

Only HDEHP has found large-scale use for the recovery and separation of americium; however, other organophosphorus acids have been evaluated. Bis(2-ethylhexyl)phenylphosphonic acid (HEHØP) was used to separate americium and curium from transcurium elements contained in 1 M HCl [52].

(*ii*) *Amine extractants*

Nitrogen-based extractants, especially tertiary amines and quaternary ammonium compounds, are particularly effective in separating and recovering americium and other actinide elements from aqueous media.

Tertiary amine salts

Tertiary amine salts extract Am^{3+} poorly from concentrated nitric or hydrochloric acids but extract it very strongly from concentrated nitrate or chloride solutions of low acidity [5]. Marcus, Givon, and Choppin [53] and Horwitz *et al.*

[54] find that Am^{3+} is extracted from nitrate media as the complex $(R_3NH)_2Am(NO_3)_5$.

Distribution coefficients of Am^{3+} and other trivalent transplutonium elements from concentrated LiCl solutions are from 150-fold to more than 1000-fold higher than those of trivalent lanthanides [55]. This phenomenon was used by Moore [56] in various analytical applications; it was also exploited at ORNL in the development of the Tramex process for plant-scale separation of americium, curium, and other transplutonium elements from fission product lanthanides [7, 57].

Quaternary ammonium salts

Quaternary alkylammonium nitrate salts were shown by Horwitz *et al.* [54] to extract Am^{3+} considerably more efficiently from low-acid, highly salted aqueous nitrate solutions than do tertiary alkylamines. The extraction sequence for trivalent actinides into either Aliquat 336 (a mixture of trioctylmethylammonium and tridecylmethylammonium salts made by General Mills, Inc.) nitrate or trilaurylmethylammonium nitrate is Cm < Cf < Am < Es.

(d) Ion-exchange processes

The combination of chromatographic elution techniques with cation-exchange resins provides a powerful and sophisticated tool for purifying americium from lanthanides and other trivalent actinides. Elution chromatography involves the use of organic chelating agents to produce the largest possible difference in the distribution coefficients of the metal ions to be separated.

Both elution-development and displacement-development (also known as barrier-ion or retaining-ion) chromatography have been used in cation-exchange separation and purification of americium. Ryan [55] points out that displacement-development chromatography is capable of separating *macro*quantities only, whereas, unless very large columns are used, elution-development chromatography is applicable only to the separation of tracer amounts. Jenkins and Wain [58] have listed publications covering the use of ion exchange for recovering and purifying ^{241}Am and ^{243}Am.

(*i*) *Anion-exchange resin systems*

For routine, large-scale purification of americium, application of anion-exchange resins is limited to sorption from thiocyanate, chloride, and, to a smaller extent, nitrate solutions [55].

Thiocyanate solutions

Americium(III) forms relatively strong complexes ($AmSCN^{2+}$, $Am(SCN)_2^+$, and $Am(SCN)_3$) in concentrated aqueous thiocyanate solutions, and its thiocyanate

species are sorbed on anion-exchange resins considerably more strongly than are the corresponding lanthanide thiocyanate complexes [59, 60]

Thiocyanate anion-exchange systems have been used to purify americium from rare earths; until recently supplanted, a plant-scale thiocyanate ion-exchange process was in long use at the Rocky Flats plant (1960–75) for routine purification of ^{241}Am recovered from aged plutonium metal [16]. This purification scheme was developed at the Los Alamos Scientific Laboratory by Coleman *et al.* [59].

Chloride solutions

Am(III) is sorbed much more strongly onto anion-exchange resins from concentrated lithium chloride solutions than are the lanthanides [61]. Americium distribution ratios increase with increased lithium chloride concentration (Fig. 8.1), whereas increased temperature enhances the separation of americium from rare earths. A lithium-chloride-based anion-exchange process for separating multigram amounts of americium and curium from lanthanide fission products and to isolate an Am–Cm fraction free of heavier actinides is routinely operated at the Oak Ridge facility [14].

(*ii*) *Cation-exchange resin systems*

Cation-exchange resins sorb Am^{3+} very strongly from dilute acid solutions. An important application is to concentrate Am^{3+} and other trivalent and tetravalent

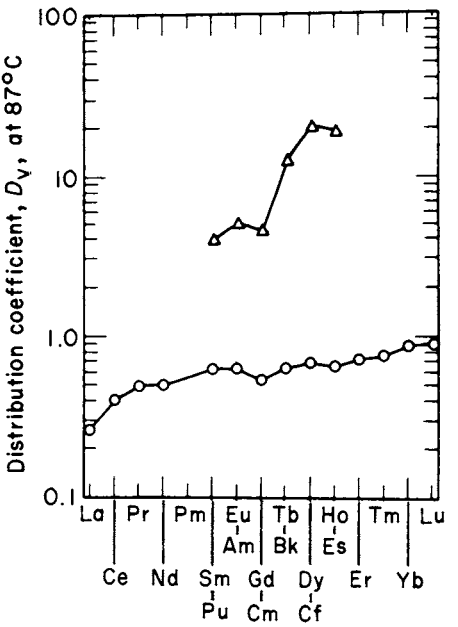

Fig. 8.1 *Distribution coefficients of actinides* (△) *and lanthanides* (○) *into Dowex* 1 × 8 *resin from* 10 M *LiCl* [61].

ions from dilute acid solutions to separate them, at least partially, from many impurities [55, 62].

A cation–anion exchange process has recently replaced the hydroxide precipitation and thiocyanate ion-exchange systems formerly used at the Rocky Flats plant for recovering ^{241}Am from solutions of spent $NaCl–KCl–MgCl_2$ salt residues [63].

Distribution coefficients: separation factors

Data for the distribution of Am^{3+} between cation-exchange resins and many aqueous solutions have been analyzed in a comprehensive review by Ryan [55].

Solutions of α-hydroxycarboxylic and aminopolycarboxylic acids are commonly used to elute americium from cation-exchange resins. When these reagents are used in a displacement elution system, they provide excellent separation of americium from trivalent lanthanides and other trivalent actinides. Separation factors, α_{Cm}^{Am}, for americium from curium range from 1.2 to 1.4 for α-hydroxycarboxylic acids and from 1.2 to 2 for the separation of americium from curium with aminocarboxylic acids [16].

Chromatographic elution schemes

Although citric acid has found use, both lactic and α-hydroxyisobutyric acids provide better separation of americium from curium. Using chromatographic elution from Dowex 50-X12 resin with α-hydroxyisobutyric acid, Campbell [64] demonstrated the effective use of high-pressure ion-exchange methods for the rapid separation of americium from curium. Highly efficient displacement chromatographic separation schemes that use nitrilotriacetic acid (NTA) and/or diethylenetriaminepentaacetic acid as eluents have been applied at Hanford and at Savannah River to purify kilogram amounts of americium from curium and lanthanides [65]. Wheelwright [24] successfully used a two-cycle cation-exchange process to separate and purify 1 kg of ^{241}Am and ^{243}Am, about 60 g of ^{244}Cm, and 140 g of ^{147}Pm extracted from 13.5 tons of blanket fuel elements of the Shippingport reactor. Highly purified americium and curium fractions were obtained by americium–curium displacement elution at 60°C through a series of four Zn^{2+}-form Dowex 50 resin beds with a 0.105 M NTA solution buffered to pH 6.5 with NH_4OH. Harbour *et al.* [65] at the Savannah River plant adapted the displacement elution scheme to pressurized columns.

Inorganic exchangers

Most studies have been concerned with the sorption of Am^{3+} by zirconium phosphate. The order of the distribution coefficients of trivalent actinides and lanthanides on zirconium phosphate is the reverse of the order observed with a typical strong-base resin exchanger [66]. Both American [67] and Russian [68]

scientists have recently utilized the fact that the singly charged AmO_2^+ ion is not sorbed by zirconium phosphate from dilute acid media to separate americium from curium and other metal ions. Inorganic exchangers formed by hydrolysis of the alkoxides of titanium, niobium or zirconium have been developed for actinide/lanthanide separation [69] and possible disposal.

Extraction chromatographic processes

Extraction chromatography (formerly called reversed-phase partition chromatography) combines the best features of solvent extraction and chromatographic separation techniques. Extraction chromatographic systems consist of a mobile liquid phase and a stationary liquid phase on an inert support. Separations are achieved by taking advantage of the difference in the distribution of ions between the two liquid phases.

Many systems using either HDEHP or Aliquat 336 as the stationary phase have been studied for extraction chromatographic separation of americium tracer. An Aliquat 336 (nitrate-form)–kieselguhr system has been used recently both in the USA and in Europe to separate milligram to gram amounts of americium from curium [70, 71].

8.4 ATOMIC PROPERTIES

8.4.1 Electron configuration

Electron configurations of gaseous americium species as determined from spectroscopic and atomic-beam experiments show a $5f^7 7s^2$ ground state and $(5f^7)^{2+}$ state [72 and Tables 14.3 and 15.6]. Americium is the sixth member of the actinide series, with electron configurations in its ground and ionized states analogous to those of its lanthanide homolog, europium. Note, however, that the solution chemistries of these two elements show substantial differences, the major ones being the absence of Am(II, aq) and the absence of Eu(IV), (V) and (VI).

8.4.2 Atomic and ionic radii

Metallic, covalent, and ionic radii of americium in various oxidation states were first calculated by Zachariasen [73] (see Section 20.7 and Table 20.8). The radius of americium metal (coordination number (CN) 12) is 1.73 Å [74]. On the basis of a refined crystal structure for $AmCl_3$, Burns and Peterson [75] calculated the ionic radius (CN 6) of Am^{3+} in $AmCl_3$ to be 0.984 ± 0.003 Å. It is beneficial to introduce the summary bond length–bond strength formulas of Zachariasen [76] at this point. They provide, as a function of americium valence and coordination number, a condensation of the many americium–oxygen and americium–halogen

distances derived from the best-known structures. (See also Shannon's compilation [339].)

Zachariasen's bond length–bond strength relations [76]

(1) A bond strength $s_{ij} = s_{ji}$ is assigned to a bond between the ith and jth atoms of a structure so that

$$\sum_j s_{ij} = v_i \qquad \sum_i s_{ij} = v_j$$

where v_i and v_j are the valences of the two atoms.

(2) The length of a bond D_{AB} between two atoms of species A and B is a function only of the strength of the bond. A universal function $D_{AB}(s)$, valid for all structures containing A–B bonds, is postulated: $D = D_1 - B \ln s$, where D_1 is normalized to unit bond strength ($s = 1$).

Unit Am–X bond lengths (D_1 values, Å) (for calculation of actual bond distances).

	Am(III)	*Am(IV)*	*Am(V)*	*Am(VI)*		*B*(Å)
Am–O	2.131	2.083	2.07	2.05	$s \leqslant 1$	0.35
					$s \geqslant 1$	$0.35 + 0.12(s-1)$
Am–F	1.978	1.955	1.949	1.946		0.40
Am–Cl	2.448					0.40
Am–Br	2.59					0.40

Example

In $BaAmO_3$, Am(IV) is surrounded by six equidistant oxygens. The bond strength $s = 4/6$ and the Am–O distance should be 2.22 Å. However, $BaAmO_3$ is said to be cubic and, if classic perovskite, the Am–O distance will be half the cell edge of 5.357 Å, or 2.18 Å. This is clearly too short, and Penneman and Eller [340] suggest that the AmO_6 octahedra are tilted to allow lengthening of the AmO bonds, requiring that the symmetry be lower than cubic.

Example

In AmO_2, there are eight oxygens equidistant from each americium; the bond strength is then $s = 4/8 = 1/2$. Thus, $D_{Am-O} = 2.083 - 0.35 \ln(\frac{1}{2}) = 2.33$ Å compared with the observed Am–O distance in AmO_2 of 2.327 Å.

8.4.3 Ionization potentials

Carlson, Nestor, Wasserman, and McDowell [77] calculated these ionization potentials (eV): 5.66, Am^0; 12.15, Am^{1+}; 18.8, Am^{2+}. Penneman and Mann's values [78], based on *jj* coupling, underestimate the first ionization potential, but

are in close agreement for higher ionizations. (For a tabulation of values for the actinide series, see Sugar [341] and Table 17.4 of this volume.)

8.4.4 Emission spectra

Studies of the arc and spark spectra of americium have been summarized by Carnall in *Gmelin* [4]. Corresponding to the absolute term value (48 767 cm^{-1}) of the ground state, the ionization potential of Am I is 6.0 eV [77].

8.4.5 X-ray spectra

Atomic energy levels (binding energies) of americium have been calculated from experimental measurements of x-ray emission wavelengths; for example, the value for $K–M_{III}$ is 120.319 keV [4].

8.4.6 Mössbauer spectra

Beta decay of ^{243}Pu ($t_{1/2}$ = 4.98 h) to the 83.9 keV level of ^{243}Am produces an excited nuclear state ($t_{1/2}$ = 2.34 ns) of ^{243}Am, suitable for Mössbauer spectroscopy [79]. Data obtained with a $^{243}PuO_2$ source at 4.2 K showed the shift of the $^{243}AmF_3$ resonance line relative to $^{243}AmO_2$ to have the unusually large value of 55 mm s^{-1} [79].

8.4.7 Critical mass

The calculated minimum critical mass of aqueous ^{242}Am is 23 g at a concentration of 5 $g\,l^{-1}$ [80]. Note that mass separation of ^{242}Am from ^{241}Am is required to obtain pure ^{242}Am.

8.5 THE METALLIC STATE

8.5.1 Metal preparation

Americium metal has been prepared by the following methods: (1) reduction of AmF_3 with barium (or lithium) metal; (2) reduction of AmO_2 with lanthanum metal; (3) bomb reduction of AmF_4 with calcium metal; (4) thermal decomposition of Pt_5Am. Lanthanum reduction of AmO_2 in tantalum equipment and subsequent distillation of the americium metal from the reaction mixture yields americium of very high (> 99.9%) purity. There is about 10^4-fold difference in americium–lanthanum volatility. Extensive application of this technique by the Euratom group has led to important new measurements of the physical properties and thermodynamic properties of americium metal [81, 342]. Rocky Flats workers have reported similar success with vacuum distillation [333].

Preparation of americium metal by thermal decomposition of the intermetallic compound Pt_5Am is a recent development. Müller, Reul, and Spirlet [343] produced high-purity americium metal by thermal decomposition of 4 g of Pt_5Am at 1550°C and 10^{-6} torr, followed by further distillation.

8.5.2 Properties

Americium metal is silvery, ductile, non-magnetic, and very malleable. Selected physical properties are listed in Table 8.2. There are two well-established forms of americium metal, a double hexagonal close-packed (dhcp) α phase, stable at room temperature, and a face-centered cubic (fcc) β phase [74, 81, 342]. The expected body-centered cubic (bcc) phase has not been found, although there is a phase transition to an unknown structure at 1050–1074°C [83, 84, 345]. Sari *et al.* [83], in studies with high-purity americium metal, concluded that there is no phase transition between 600 and 700°C. Americium metal has recently been found to be superconducting at temperatures as high as 0.79 K for the room-temperature dhcp phase [346]. Under high pressure, americium metal is converted to fcc and other structures (Table 8.2), one of which is the orthorhombic α-uranium structure of Roof *et al.* [82], but, from dilatometry and differential thermal analysis (DTA) experiments on americium metal, evidence was recently presented [84] for at least three phases existing between room temperature and the melting point (1170°C): an α phase existing up to 658°C, a β phase existing between 793 and 1004°C, and a γ phase which forms at 1050°C (see also Chapter 19 and Table 19.2).

Heated americium metal reacts with halogens, H_2, O_2, N_2, carbon, boron, antimony, etc., forms dihalides with $HgBr_2$ and HgI_2, and forms alloys with a number of metals (e.g. beryllium and platinum) (see Table 8.3). Americium dissolves readily in aqueous hydrochloric acid but is insoluble in liquid ammonia.

8.5.3 Alloys and intermetallic compounds

Runnals [85] patented a method for making americium–aluminum alloys in which a mixture of aluminum metal and an americium halide is heated in a vacuum of 10^{-3} torr at 700–1200°C until the americium is reduced and alloyed. Homogeneous americium–aluminum alloys suitable for irradiation of americium can be prepared by reaction of aluminum, AmO_2, and Na_3AlF_6 (cryolite) at 1100–1200°C [86]. δ-Plutonium and β-americium form a continuous series of fcc solid solutions that are stable at room temperature in the composition range from about 6 to 80 at% americium [294]. Other alloys and intermetallic compounds are listed in Table 8.3.

8.6 SIMPLE AND COMPLEX COMPOUNDS

The crystal structures (where known) and references to the preparation of about 150 compounds and alloys of americium are collected in Table 8.3. The table is

Table 8.2 *Selected properties of americium metal (adopted from refs* 16 *and* 342*; see also Chapter* 19).

Property	*Value(s)*[a]
Crystallographic data	
symmetry	< 658°C, dhcp (α) 793–1004°C, fcc (β) ~ 1050–1173°C, bcc (?)
space group	$P6_3/mmc$
lattice parameters	dhcp: $a = 3.4681$ Å, $c = 11.241$ Å fcc: $a = 4.894$ Å
density	13.671 g cm^{-3} (calc.) 13.671 g cm^{-3} (obs.)[b]
high-pressure structures[c]	0–5 GPa, dhcp 5–10 GPa, fcc 10–15 GPa, double body-centered monoclinic > 15 GPa, orthorhombic α-uranium or monoclinic (α″-uranium alloys)
metallic radius (CN 12)	1.73 Å
melting point	1176, 1173 or 1170°C
boiling point	2067°C (calc.)
coefficient of thermal expansion	$\alpha_a = 7.5 \pm 0.2 \times 10^{-6}$ K^{-1} $\alpha_c = 6.2 \pm 0.2 \times 10^{-6}$ K^{-1}
compressibility at 1 atm	0.002 77 kbar^{-1} at 23°C
vapor pressure[d]	$\log(p/\text{atm}) = (6.578 \pm 0.046) - (14\,315 \pm 55)/T$ at 990–1358 K
magnetic susceptibility	$\chi_{20°C} = (881 \pm 46) \times 10^{-6}$ cm^3 mol^{-1}
magnetic moment	~ 0
microhardness (Vickers) at 25°C	800 MN m^{-2}
electrical resistivity	68 μΩ cm (300 K), 71 μΩ cm (298 K)
crystal entropy, S°_{298}	55 J K^{-1} mol^{-1}
heat of vaporization at boiling point	230.2 kJ mol^{-1} (calc.)
entropy of vaporization at boiling point	100.8 J K^{-1} mol^{-1} (calc.)
heat of transformation	5.9 kJ mol^{-1}
heat of fusion	14.4 kJ mol^{-1}
heat of solution in aqueous HCl	
1 M HCl	−616.3 kJ mol^{-1}
1.5 M HCl	−615.5 kJ mol^{-1}
6 M HCl	−618.0 kJ mol^{-1}

[a] For the dhcp form unless otherwise indicated.
[b] By immersion in monobromobenzene.
[c] From ref. 82.
[d] Ward *et al.* [344] give the following equation for americium above its melting point: $\log(p/\text{atm}) = 5.185 - 13\,191/T$.

arranged with the anionic constituent (or metallic partner, if an alloy) listed alphabetically. A group of compounds in which americium could be considered as part of the anionic constituent appears under the heading 'Oxides, ternary'. Inorganic compounds containing either oxygen or the halides far outnumber those containing other elements. Many of these resulted from research aimed at stabilizing valence states other than III.

Table 8.3 *Compounds of americium.*

Class	*Formula*	*Symmetry*	*Space group or structure type*	*Lattice constants*				*Comments*	*Refs*
				a (Å)	*b* (Å)	*c* (Å)	*Angle* (deg)		
aluminate	$AmAlO_3$	hexagonal	$R\bar{3}m$, $LaAlO_3$	5.336		12.91		$Am(OH)_3/Al(OH)_3/H_2$/heat	87, 88
aluminide	$AmAl_2$		$MgCu_2$	7.861				arc melt	196
antimonides	AmSb	fcc	*Fm3m*	6.239				Am/Sb/heat	89, 90
	$AmSb_2$		$LaSb_2$						168
	Am_4Sb_3	bcc	anti-Th_3P_4	9.239				AmH_3/Sb/heat	91
arsenate	$AmAsO_4$	monoclinic	$P2_1/n$	6.89	7.06	6.62	$\beta = 105.5$		87, 92
arsenide	AmAs	fcc	*Fm3m*	5.880				Am/As	89
				5.875				AmH_3/As	93
beryllide	$AmBe_{13}$	fcc	*Fm3c*	10.283				AmF_3/Be/vac./heat	85, 94, 95
								AmO_2/Be/vac./heat	96
bismuthide	AmBi	fcc	*Fm3c*	6.338				Am(or AmH_3)/Bi vapor	89
	Am_2O_2Bi			3.950		13.434			97
borate	$AmBO_3$	orthorhombic	*Pnam*	5.053	8.092	5.738		AmO_2/B_2O_3/heat	87, 88
borides	AmB_4	tetragonal	*P4/mbm*	7.105		4.006		vac. heat Am/B 1:2	98
	AmB_6	simple cubic	*Pm3m*	4.115				arc melt Am/B	98
bromides	$AmBr_2$	tetragonal	*P4/n*, $EuBr_2$	11.59		7.121		$Am/HgBr_2$/vac./heat	99, 100
	$AmBr_3$	orthorhombic	*Cmcm*, $PuBr_3$	4.064	12.66	9.144			101–106
	$AmBr_3 \cdot 6H_2O$	monoclinic	*P2/n*	9.955	6.783	8.166	$\beta = 91.75$	$AmBr_3$, H_2O vapor	104
	$[(C_6H_5)_3PH]_3AmBr_6$							ethanol pptn	107
	AmOBr	tetragonal	*P4/nmm*	3.982		7.644			347
carbide	Am_2C_3	bcc	$I\bar{4}3d$	8.276				Am/C arc melt	108
cobaltide	$AmCo_2$		$MgCu_2$					arc melt	196
carbonates	$Am_2(CO_3)_3 \cdot 2H_2O$							Am(III)/trichloroacetate	109
	$Am_2(CO_3)_3 \cdot 4H_2O$							Am(III)/$NaHCO_3$, CO_2	110
	$NH_4AmO_2CO_3$	hexagonal	*C6/mmc*					Am(III)/$(NH_4)_2CO_3 + O_3$	111
	$CsAmO_2CO_3$	hexagonal	*C6/mmc*	5.123		11.538		Am(III)/$CsHCO_3 + O_3$	112
	$KAmO_2CO_3(nH_2O)$	hexagonal	*C6/mmc*	5.112		9.740		*c* is variable with H_2O	113, 114, 348
	$K_3AmO_2(CO_3)_2 \cdot nH_2O$	rhombic (a, b)		5.32	9.21	8.76		(a) 4.7 M, (b) 2.3 M K_2CO_3	348
				5.29	9.11	8.83		Am(III)/3.5 M $K_2CO_3 + O_3$	115
	$K_5AmO_2(CO_3)_3$	orthorhombic						Am(III)/>5 M $K_2CO_3 + O_3$	111, 116
	$(NH_4)_5AmO_2(CO_3)_3$							Am(VI)/NH_4^+	320

	$RbAmO_2CO_3$	hexagonal	C6/*mmc*	5.12		10.46		Am(III)/10 M $Rb_2CO_3 + O_3$	111, 117
	$Na_{2x+1}AmO_2(CO_3)_{1+x}$							Am(VI)/Na_2CO_3/heat	111, 114
chlorides	$AmCl_2$	orthorhombic	P*bnm*	8.963	7.573	4.532		Am/$HgCl_2$/heat	99, 100
	$AmCl_3$	hexagonal	$P6_3/m$	7.382		4.214		AmO_2/HCl	75, 101–105
	$AmCl_3 \cdot 6H_2O$	monoclinic	P2/*n*	9.702	6.567	8.009	$\beta = 93.62$		75, 119, 120
	AmOCl	tetragonal	P4/*nmm*	4.00		6.78			121
chloride complexes	$CsAmCl_4$							Am(III)/HCl + CsCl	122
	$CsAmCl_4 \cdot 4H_2O$							Am(III)/HCl + CsCl	122, 123
	Cs_3AmCl_6							Am(III)/HCl/CsCl/NaCl	124
	$Cs_2NaAmCl_6$	fcc	F*m3m*	10.86				Am(v)/HCl/CsCl/NaCl	122, 123
	$[(C_6H_5)_3PH]_3AmCl_6$		$Cs_3NpO_2Cl_4$					ethanol pptn	107, 125
	$Rb_2AmO_2Cl_4$	monoclinic	C2/*c*	11.53	7.48	5.65	$\beta = 99.19$	Am(v)/HCl/RbCl	320, 321
	$Cs_2AmO_2Cl_4$	monoclinic	C2/*c*	11.92	7.61	11.67	$\beta = 99.56$	Am(v)/HCl/CsCl	320, 321
fluorides	AmF_3	hexagonal	$P\bar{3}c1$, LaF_3	7.044		7.225		m.p. 1400°C/v.p.	129–131
	AmF_4	monoclinic	C2/*c*, UF_4	12.538	10.516	8.204	$\beta = 126.8$	AmF_3/F_2/v.p.	132–136
	AmO_2F_2	hexagonal (rhomb.)	$R\bar{3}m$	4.136		15.85			137
	AmF_6							KrF_2/HF (li); dark brn	312
fluoride complexes	$NaAmF_4$	hexagonal	P6	6.109	3.731			AmO_2/HF–H_2/NaF	138, 139
	$KAmF_4$	orthorhombic	P*nma*	6.13	3.71	15.2			349
	K_3AmF_6	hexagonal	K_3LaF_6	22.75		7.56		AmO_2/HF-H_2/KF/650°C	349
	K_2AmF_5		K_2PrF_5						349
	KAm_2F_7	cubic	KEu_2F_7	5.857					139, 349
	$(NH_4)_4AmF_8$	monoclinic	C2/*c*, $(NH_4)_4UF_8$					$Am(OH)_4/NH_4F$	140
	$LiAmF_5$	tetragonal	$I4_1/a$	14.63		6.449			141
	$K_7Am_6F_{31}$	hexagonal (rhomb.)	$R\bar{3}$	14.938		10.293		Am(III)/KF	142, 143
	$Na_7Am_6F_{31}$	hexagonal (rhomb.)	$R\bar{3}$	14.48		9.665			143
	$RbAmF_4$	orthorhombic	P*nma*	6.43	3.76	16.0			349
	Rb_2AmF_6	orthorhombic	C*mcm*	6.962	12.001	7.579			144, 145
	$KAmO_2F_2$	rhombohedral	$R\bar{3}m$, $CaUO_4$	6.78			$\alpha = 36.25$	AmO_2^+/KF	146
	$RbAmO_2F_2$	rhombohedral	$R\bar{3}m$	6.789			$\alpha = 36.25$	AmO_2^+/RbF	147

Table 8.3 (*Contd.*)

Class	Formula	Symmetry	Space group or structure type	Lattice constants a_0 (Å)	b_0 (Å)	c_0 (Å)	Angle (deg)	Comments	Refs
germanate	$AmGeO_4$	tetragonal	$I4_1/a$	5.04		11.03			148
hydrides	AmH_2	fcc	$Fm3m$	5.348				AmH_{2+x}, $x = 0$–0.7	149, 150
	AmH_3	triagonal	$P\bar{3}c1$	6.68		6.75			150
hydroperoxide									152
hydroxide	$Am(OH)_3$	hexagonal	$Nd(OH)_3$	6.426		3.745		$K_{sp} \sim 3 \times 10^{-18}$	153, 155
hydrousoxide	$Am(OH)_4$ (?)							$Am(OH)_3 + NaOCl$	156, 157
iodides	AmI_2	monoclinic		7.677	8.311	7.925	$\beta = 98.46$	$Am/H_2/I_2$/vac.	329
	α-AmI_3	orthorhombic	$Ccmm$	4.31	14.03	9.92		AmO_2/AlI_3	103, 158
	β-AmI_3	hexagonal	$R\bar{3}$	7.42		20.55			103, 158
	AmOI	tetragonal		4.011		9.204			103, 158
iridium	Ir_2Am	cubic	$Fd3m$, Cu_2Mg	7.55				$AmO_2/H_2/Ir/1550°C$	159–161
iron	Fe_2Am	cubic	Cu_2Mg	7.30				arc melt, ferromagnetic	196
molybdates	α-$Am_2(MoO_4)_3$	tetragonal	$I4_1/a$	5.24		11.52		$AmO_2/MoO_3/\sim 825°C$	162, 163
	β-$Am_2(MoO_4)_3$	orthorhombic		9.095	10.527	10.820		$AmO_2/MoO_3/> 850°C$	162, 163
	$LiAm(MoO_4)_2$	tetragonal	$I4_1/a$, $LiGd(MoO_4)_2$	5.20		11.39		$Am_2(MoO_4)_3/Li_2MoO_4$	163
	$NaAm(MoO_4)_2$	tetragonal	scheelite	5.25		11.55			163
	$Na_5Am(MoO_4)_4$		$Na_5La(WO_4)_4$	11.515		11.429		solid-state reaction	163
	$K_2Am_2(MoO_4)_4$							solid-state reaction	163
	$K_{10}Am_2(MoO_4)_8$							solid-state reaction	163
nickel	Ni_2Am	cubic	$Fd3m$, Cu_2Mg	6.99				Am/Ni arc melt	164
nitride	AmN	fcc	$Fm3m$, NaCl	5.000				$Am(AmH_3)/N_2$	165–168
osmium	Os_2Am	hexagonal	$P6_3/mmc$	5.320		8.849		Am/Os arc melt	164
oxides, binary	AmO (?)	fcc	$Fm3m$	5.045				Am/Ag_2O	165–167, 169
	A-Am_2O_3	hexagonal	$P\bar{3}m1$	3.817		5.971		$AmO_2/H_2/800°C$	170, 176
	B-Am_2O_3	monoclinic	$C2/m$	14.38	3.52	8.92	$\beta = 100.4$		171–174
	C-Am_2O_3	cubic	$Ia3$	11.03				600°C	170, 175, 176
	AmO_2	fcc	$Fm3m$	5.374				$^{241}AmO_2$, $^{243}AmO_2$	176, 350
	AmO_{2-x}							phase studies	171, 172, 217

oxides, ternary								(Am valence)	
lithium	$LiAmO_2$							Am(III)	87, 177 178
	Li_2AmO_3							Am(IV)	87, 177, 178
	Li_8AmO_6	hexagonal	Li_8PbO_6	5.62		15.96			87, 177, 178
	Li_3AmO_4	tetragonal	Li_3UO_4	4.459		8.355		Am(v)	87, 177, 178
	Li_7AmO_6	hexagonal	$R\bar{3}$	5.54		15.65		Am((v)	87, 177, 178
	Li_4AmO_5	tetragonal	$I4/m$	6.666		4.415		Am(VI)	87, 177, 178
	Li_6AmO_6	hexagonal	Li_6ReO_6	5.174		14.59		Am(VI)	87, 177, 178
potassium (Rb, Cs)	K_2AmO_4	tetragonal	I_4/mmm	4.286		13.05		Am(VI)	178
sodium	Na_2AmO_3	monoclinic	$C2/c$	5.92	10.26	11.23	$\beta = 100.12$	Am(IV)	87, 177, 178
	Na_3AmO_4	fcc	$Fm3m$	4.757				Am(v)	87, 177, 178
	Na_4AmO_5	fcc	$Fm3m$	4.70				Am(VI)	87, 177, 178
	Na_6AmO_6	hexagonal	Li_6ReO_6	4.76		16.10		Am(VI)	87, 177, 178
barium and strontium	$BaAm_2O_4$							Am(III)	87, 179
	$BaAmO_3$	cubic	perovskite	4.356				Am(IV)	87, 179
	Ba_3AmO_6	cubic	$F\bar{4}3m$	8.81				Am(VI)	87, 179
	$SrAm_2O_4$							Am(III)	87, 179
	$SrAmO_3$	cubic	perovskite	4.23				Am(VI)	87, 179
	Sr_3AmO_6	cubic	Ba_3WO_6					Am(VI)	87, 179
curium	$(Am_{0.30}, Cm_{0.70})O_{2.00}$	fcc		5.368				350°C in O_2	180
	$(Am_{0.30}, Cm_{0.70})O_{1.83}$	fcc		5.433				550°C in O_2	180
	$(Am_{0.30}, Cm_{0.70})O_{1.685}$	rhombohedral		6.687			$\alpha = 99.47$	760°C in He	180
	$(Am_{0.30}, Cm_{0.7})O_x$	bcc		10.935				900°C in He	180
	$(Am_{0.64}, Cm_{0.36})O_{1.5}$	monoclinic		14.321	3.665	8.926	$\beta = 100.17$	1100°C in H_2/He	180
	$(Am_{0.64}, Cm_{0.36})O_{1.5}$	hexagonal		3.812		5.980		1500°C in H_2/He	180

Table 8.3 (*Contd.*)

Class	Formula	Symmetry	Space group or structure type	Lattice constants a (Å)	b (Å)	c (Å)	Angle (deg)	Comments	Refs
zirconium hafnium	AmO_2–ZrO_2 AmO_2HfO_2	cubic	fluorite					18–100% AmO_2/ZrO_2, SS SS, extent unknown	87, 181 87, 181
thorium	AmO_2–ThO_2	cubic	fluorite					ThO_2/AmO_2, complete SS	87
niobium, tantalum and protactinium	α-$AmNbO_4$	monoclinic	I2	5.444	11.25	5.141	$\beta = 94.95$	AmO_2/Nb_2O_5	87, 92
	β-$AmNbO_4$	tetragonal	$I4_1/a$	5.30		11.34		$\alpha \rightarrow \beta \sim 600°C$	87, 92
	$Am_{0.33}NbO_3$	pseudo-tetragonal	P4/*mm*, $La_{0.33}TaO_3$	3.819		7.835			87, 88
	Ba_2AmNbO_6	cubic	$F\bar{4}3m$	8.520				$AmNbO_4/BaO$	87, 88
	$AmNbTiO_6$	orthorhombic	P*nam*	5.34	11.00	7.53		$AmNbO_4/TiO_2$	87, 88
	$AmTaO_4$	monoclinic	I2	5.489	11.21	5.115	$\beta = 95.37$	AmO_2/Ta_2O_5	87, 88, 92
	$Am_{0.33}TaO_3$	tetragonal	$I4_1/a$	3.889		7.820		AmO_2/Ta_2O_5	87, 88, 92
	Ba_2AmTaO_6	cubic	$F\bar{4}3m$	8.518					87, 92
	$AmTaTiO_6$	orthorhombic	P*nam*	5.33	10.95	7.49			92
	$AmPaO_4$	fcc	F*m*3*m*	5.458				AmO_2/Pa_2O_5	87, 92
	Ba_2AmPaO_6	cubic	$F\bar{4}3m$	8.793				$(Am_{0.5}Pa_{0.5})O_2/BaO$	87, 92, 182
palladium phosphates	Pd_3Am	simple cubic	P*m*3*m*	4.158				$Am_2O_3/H_2/Pd$	159
	$AmPO_4$	monoclinic	$P2_1/n$	6.73	6.93	6.41	$\beta = 103.5$	stable to 1000°C	92
	$AmPO_4 \cdot 0.5H_2O$	hexagonal		6.99		6.39		pptn, dried 200°C	92
phosphates, complex	$(NH_4)AmO_2PO_4 \cdot$	tetragonal	?	6.99		9.06			
	$KAmO_2PO_4 \cdot$	tetragonal	?	6.91		9.00			
	$RbAmO_2PO_4 \cdot$	tetragonal	?	6.94		9.02			
	$CsAmO_2PO_4 \cdot$	tetragonal	?	6.94		8.82			
	$(NH_4)AmO_2AsO_4 \cdot$	tetragonal	?	7.11		8.95			320, 321
	$KAmO_2AsO_4 \cdot$	tetragonal	?	7.10		9.09			
	$RbAmO_2AsO_4 \cdot$	tetragonal	?	7.15		17.73			
	$CsAmO_2AsO_4 \cdot$ $\cdot xH_2O$, $x \sim 2$–3	tetragonal	?	7.09		17.72			

phosphide	AmP	cubic	NaCl	5.711				$AmH_3/P/580°C$	91, 168
platinum	Pt_2Am	cubic	F*d*3*m*	7.615				$AmO_2/H_2/Pt$	159, 160
	Pt_5Am		$CaCu_5$	5.312		4.411		$Am_2O_3/H_2/Pt$	159, 160
rhodium	Rh_2Am	cubic	R*d*3*m*, Cu_2Mg	7.548					
	Rh_3Am	cubic	P*m*3*m*, Cu_3Au	4.098				$Am_2O_3/H_2/Rh$	160
ruthenium	Ru_2Am	hexagonal	$MgZn_2$	5.26		8.73			196
scandate	$AmScO_3$	orthorhombic	P6*mm*, $GdFeO_3$	5.540	5.785	8.005		$AmO_2/H_2/Sc_2O_3$	183
								oxidation yields fluorite	174
selenides	AmSe	cubic	NaCl	5.821				AmH_3/Se	168
	$AmSe_{2-x}$	tetragonal		4.096		8.347			184
	Am_3Se_4	bcc	$I\bar{4}3d$, Th_3P_4	8.799					89, 90, 91, 168
silicate	$AmSiO_4$	tetragonal	zircon	6.87		6.20		hydrothermal	148
silicide	Am_5Si_3			11.419		5.538		$AmF_3/Si/1050°C$	351
	AmSi	orthorhombic		8.39	4.09	6.01		$AmF_3/Si/1050°C$	195
	$Am_3Si_5 \ldots Am_2Si_3$	hexagonal	Pu_3Si_5	3.871		4.120		$AmF_3/Si/1050°C$	351
	$AmSi_x (x < 2)$	tetragonal	α-$ThSi_2$	4.02		13.7			195
sulfates	$Am_2(SO_4)_3 \cdot 8H_2O$	monoclinic	C2/*c*	13.619	6.837	18.405	$\beta = 102.7$		185
	$Am_2O_2SO_4$	orthorhombic	I222	4.225	4.103	13.328			154
	$Am_2(SO_4)_3 \cdot 5H_2O$							anh. at 500°C	186, 118
	$KAm(SO_4)_2$								187
	$NaAm(SO_4)_2 \cdot H_2O$								135
	$KAm(SO_4)_2 \cdot 2H_2O$								135
	$RbAm(SO_4)_2 \cdot 4H_2O$								135
	$CsAm(SO_4)_2 \cdot 4H_2O$								135
	$TlAm(SO_4)_2 \cdot 4H_2O$								135
	$K_3Am(SO_4)_3 \cdot H_2O$								135
	$K_8Am_2(SO_4)_7$								135
	$Cs_8Am_2(SO_4)_7$								135
	$Tl_8Am_2(SO_4)_7$								135
	$\{[Co(NH_3)_6]HSO_4)_2 \cdot [AmO_2(SO_4)_3] \cdot nH_2O$	cubic							135, 188

Table 8.3 (*Contd.*)

Class	*Formula*	*Symmetry*	*Space group or structure type*	*Lattice constants*				*Comments*	*Refs*
				a (Å)	*b* (Å)	*c* (Å)	*Angle* (deg)		
sulfides	AmS	fcc	$Fm3m$	5.592					189
	Am_2O_2S	trigonal	$P3m$	3.91		6.772			154
	$AmS_{1.9}$	tetragonal		3.938		7.981			154
	α-Am_2S_3	orthorhombic	$Pnma$	3.98	7.39	15.36		$\alpha \rightarrow \gamma$ 1300°C	189, 190
	β-Am_2S_3								191
	γ-Am_2S_3	bcc	$I\bar{4}3d$	8.434					191
	$Am_{10}S_{14}O_3$								191
tellurides	AmTe								
	$AmTe_2$	tetragonal		4.366		8.969		AmH_3/Te/heat	168, 192
	$AmTe_3$	orthorhombic	$Bmmb$	4.399	4.339	25.57			192
	Am_2Te_3	orthorhombic	$Pbnm$	11.93	12.12	4.33			193
	Am_3Te_4	bcc	$I\bar{4}3d$	9.394					90, 193
tungstate	$Am_2(WO_4)_3$	tetragonal	$I4_1/a$						162
vanadates	$AmVO_3$	orthorhombic	$Pbnm$, $GdFeO_3$	5.45	5.58	7.76		AmO_2/V_2O_5	87, 88, 92
	$AmVO_4$	tetragonal	zircon	7.31		6.42			87, 88, 92
xenate	$Am_4(XeO_6)_3 \cdot 40H_2O$								194

8.6.1 Oxides

The binary (simple) americium oxides are limited to AmO, Am_2O_3, and non-stoichiometric phases between Am_2O_3 and AmO_2. Although AmO has been reported twice [165, 169], the lattice parameter of the earlier preparation (4.95 Å) is not consistent with that of the more recent one (5.045 Å). An accidental exposure of an AmH_{2+x} sample to air at 300°C also led to an fcc phase [352], in agreement with Akimoto's AmO [165]. The difficulty of achieving Am(II) in solution and in other compounds makes it likely that the monoxide could only be synthesized under high pressure from Am and Am_2O_3, which is parallel with the lanthanide monoxide SmO [327]. Recent evidence that 'PuO' and surface-layer lanthanide 'monoxides' are really oxycarbides or nitrides [328] reinforces the uncertainty whether any claim for 'AmO' is valid.

The dioxide was the first reported compound of americium [169]. It can be prepared by heating a variety of americium compounds (hydroxide, carbonate, oxalate, nitrate) in air or oxygen at temperatures of 600–800°C [175, 176, 217, 219, 313]. This black oxide is believed to be stoichiometric $AmO_{2.00}$ [172, 217] and even at 1000°C in oxygen is better than $AmO_{1.99}$ [217]. It undergoes an expansion of its face-centered cubic lattice constant due to radiation damage [176], and the lattice parameter quoted in Table 8.3 represents an extrapolation to zero time for both $^{241}AmO_2$ and $^{243}AmO_2$ [176, 350].

Phase relationships and thermodynamic data in the $AmO_{1.5}$–AmO_2 system are well-established. The red-brown ('persimmon') sesquioxide is easily prepared in H_2 at temperatures as low as 600°C; it oxidizes very readily in air, even at room temperature. Baybarz [332] has summarized the transition temperatures of the low-temperature (body-centered cubic, C-phase) to medium-temperature (monoclinic, B-phase) and to high-temperature (hexagonal, A-phase) sesquioxides. The C → B transition temperature appears to lie between 460 and 650°C and the B → A transition is at 800–900°C [172, 176]. The hexagonal sesquioxide undergoes slight swelling with time but self-irradiation causes cubic Am_2O_3 to transform to hexagonal at room temperature over about 3 years [176]. It is possible that monoclinic Am_2O_3 is stabilized by small amounts of rare-earth impurities [173, 174] and that pure Am_2O_3 passes directly from C- to A-phase; it is also possible that the C → B transition occurs well below 650°C and is therefore sluggish. The hexagonal sesquioxide is stoichiometric but the cubic form may have a lower oxygen limit of $AmO_{1.513}$ [172].

Recent studies on americium oxides include measurement of the melting point of Am_2O_3, 2205 ± 15°C [171], and the enthalpy of formation of AmO_2 (see also Chapter 17) [313].

There is no evidence for any binary oxide of Am higher than AmO_2 [170, 353]. However, ternary oxides are known for Am(III) through Am(VI) [174, 177–183]. Stabilization of high oxidation states in complex oxides is frequently observed [87, 179, 326]; excellent examples are the thermally stable Cs_2AmO_4 and Ba_3AmO_6. Most complex oxides of americium have been prepared by Keller and Hoekstra and their co-workers.

8.6.2 Hydrides

Olson and Mulford [150] characterized the americium–hydrogen system with ^{241}Am and found parallels to the lanthanides. There is an AmH_{2+x} (fcc) phase, isostructural with NpH_{2+x}, PuH_{2+x}, and most of the rare-earth dihydrides [151]. There is also a phase that approximates AmH_3, which is hexagonal. Although the hexagonal lattice parameters were reported [150] to be $a_0 = 3.77$ Å and $c_0 = 6.75$ Å, Keller [3] has pointed out that recent data on HoD_3 makes the most probable space group $P\bar{3}c1$ with lattice parameters in Table 8.3. A more recent study with ^{243}Am [352] essentially confirms the earlier report.

8.6.3 Halides

Known halides are described in Table 8.3 and have been reviewed extensively [3, 4, 10–12]. The only remarkable halides are those of extreme oxidation states. Dihalides of americium cannot be prepared by hydrogen reduction of trihalides, although hydrogen reduction is successful for the lanthanides Sm, Eu (the 4f analog of americium), and Yb. Instead, americium metal must be reacted with a halide such as HgI_2 [329] or $HgCl_2$ [100]. It is likely that the reaction

$$Am(s) + 2AmX_3(s) \rightarrow 3AmX_2(s)$$

would also succeed, in analogy with the least stable lanthanide dihalides. It may also be found that ternary americium(II) halides can be prepared with americium metal or lithium metal as reductant [330].

At the other extreme of oxidation states, AmF_6 has recently been claimed as the result of oxidation of AmF_3 by KrF_2 in anhydrous HF at 40–60°C [312]. The evidence for AmF_6 was three-fold: presence of ^{241}Am in the vapor above the HF–KrF_2, identified from its gamma spectrum; upon evaporation of solvent, a dark-brown solid residue vaporized to give a symmetric infrared absorption at $604 \pm 3\ cm^{-1}$; and a hydrolysis of this solid yielded AmO_2^+. Chloro complex compounds of Am(VI) have also been reported (Table 8.3), and appear to be sufficiently stable to permit x-ray crystallographic studies.

8.6.4 Compounds of americium with organic ligands

Relatively few solid compounds of americium with organic ligands have yet been prepared; these are listed in Table 8.4. For reviews see Kanellakopulos [204] and Chapters 22 and 23.

8.7 SOLUTION CHEMISTRY

8.7.1 Oxidation states

Americium in aqueous solutions has well-established III, IV, V, and VI oxidation states. Simple aquo ions of Am^{3+} and AmO_2^{2+} are stable in dilute acid, and AmO_2^+

Table 8.4 *Compounds of americium with organic ligands.*

Organic reagent ligand	*Formula of compound*	*Comments*	*Ref.*
acetate	$NaAmO_2(OOCCH_3)_3$	lemon yellow	197–199
acetylacetone	$Am(C_5H_7O_2)_3 \cdot H_2O$	pale rose	200
benzoyltrifluoroacetone	$Am(C_{10}H_6F_3O_2)_3 \cdot 3H_2O$	pale rose	200
cyclooctatetraene	$KAm(C_8H_8)_2 \cdot 2THF$[a]	yellow	201, 316
cyclopentadiene	$Am(C_5H_5)_3$	flesh	202–209, 292
dipivaloylmethane	$Am(C_{11}H_{19}O_2)_3$		205, 210, 211
formate	$Am(HCOO)_3 \cdot 0.2H_2O$	pink	223
hexafluoroacetylacetone	$CsAm(C_5HF_6O_2)_4 \cdot H_2O$	yellow	210–213
hexafluoroacetylacetone/ TBP	$Am(C_5HF_6O_2)_3 \cdot 2(C_4H_9O)_3PO$	volatile, 175°C	224
8-hydroxyquinoline	$Am(C_9H_6NO)_3$	yellow-green	214
5-chloro-8-hydroxyquinoline	$Am(C_9H_5ClNO)_3$	dark green	214
5,7-dichloro-8-hydroxyquinoline	$Am(C_9H_4Cl_2NO)_3$	green	214
oxalate	$Am_2(C_2O_4)_3 \cdot 10H_2O$	pink	109, 135, 175, 215–222
phthalocyanine	$Am(C_{32}H_{16}N_2)_2$	dark violet	225, 354
pyridine-2-carboxylic acid	$AmO_2(C_5H_4NCOO)_2$	red-brown	226, 227
pyridine-2-carboxylic acid	$HAmO_2(C_5H_4NCOO)_3$	red-brown	226, 227
pyridine-*N*-oxide carboxylic acid	$AmO_2[C_5H_4N(O)COO]_2$		227
salicylate	$Am(C_7H_5O_3)_3 \cdot H_2O$		232
thenoyltrifluoroacetone	$Am(C_5H_4F_3O_2S)_3 \cdot 3H_2O$	pale rose	200

[a] THF = tetrahydrofuran.

disproportionates so slowly that in ^{241}Am(v) solutions radiation-induced reduction dominates. The tetravalent state in the form of aqueous Am(IV) is unknown in the absence of complexing agents. Russian workers [228] have announced evidence for the production of Am(VII) in alkaline solutions, and compared it with Np(VII) and Pu(VII) [355].

(a) Am(II)

Americium, unlike europium, does not have a divalent state in aqueous solution; this was long greeted with some surprise. However, Am(II) has been prepared in the solid compounds $AmCl_2$, $AmBr_2$, and AmI_2 and demonstrated as a dilute solution in CaF_2 [99–102, 105]. Reduction conditions used to prepare Eu^{2+} and Sm^{2+} do not reduce Am^{3+} (aq) to Am^{2+} (aq) [229]. Myasoedov *et al.* claim electrochemical evidence for unstable Am(II) in acetonitrile, instantly oxidized by water in the solvent [230]. Sullivan *et al.* [356] formed transient Am(II) by pulse radiolysis, with an absorption maximum at 313 nm, and $t_{1/2} \sim 5 \times 10^{-6}$ s for disappearance.

(b) Am(III)

The trivalent state of americium is the stable aqueous oxidation state. Although americium is the homolog of europium, the Am^{3+} radius (0.975 Å) is closer to that of Nd^{3+} (radius 0.983 Å) [76]. It is a convenient 'rule of thumb' that the radii of the light lanthanide ions are nearly identical to the radii of the corresponding actinides shifted three elements to the right in the periodic table, e.g. $r(La^{3+}) \simeq r(U^{3+})$. In some early purification schemes, fission-product promethium accompanied americium. Am(III) is precipitated by hydroxide, fluoride, phosphate, and oxalate ions from aqueous solution.

Désiré *et al.* [231] calculate for the first hydrolysis constant, $K_1 = [MOH^{2+}][H^+]/[M^{3+}] = 1.2 \times 10^{-6}$, and Shalinets and Stepanov [233] report $K_2 = [MOH^{2+}][H^+]/[M^{3+}]K_w = 5 \times 10^{10}$.

Contrary to such simple representations, Korotkin and others [234, 235] state that Am^{3+} hydrolysis is complicated, starting at pH values as low as 0.5–1.0 and dependent on the nature of other cations (e.g. Li^+, Na^+, and H^+) that may be present.

From diffusion measurements, Fourest *et al.* [361] have determined the hydration number of Am^{3+} to be 13 and the hydrated Am^{3+} radius to be 4.52 Å. They found that the hydrated Am^{3+} parallels its lanthanide homolog Eu^{3+}. (Hydrated radii increase as a function of atomic number in both the lanthanide and actinide series because increased covalency increases the number of water ligands.)

(c) Am(IV)

Tetravalent americium is unstable in non-complexing mineral acid solutions. Aqueous solutions of tetravalent americium were first prepared by Asprey and Penneman [140] by dissolution of $Am(OH)_4$ in concentrated solutions of ammonium fluoride. In 13 M NH_4F at 25°C the solubility of Am(IV) is 0.02 M, giving a rose-colored solution. Ozone oxidizes Am(IV) in 13 M NH_4F to Am(VI), whereas iodide reduces it to Am(III). Reduction of Am(IV) to Am(III) occurs spontaneously because of alpha-radiation effects. Yanir *et al.* [261] have demonstrated that Am(IV) is stable in phosphoric acid and pyrophosphate media. Myasoedov *et al.* [236] report that pure Am(IV) is obtained in 8–15 M phosphoric acid by anodic oxidation. In lower phosphoric acid concentrations some Am(VI) is formed. Similar results were obtained with an oxidizing mixture of Ag_3PO_4 and $(NH_4)_2S_2O_8$; with 94% ^{243}Am, the half-life for reduction is 20 h. Saprykin *et al.* [357] and Kosyakov and co-workers [317, 358] have stabilized Am(IV) by heteropolyanions and find that the reduction to Am(III) is caused solely by radiolytic effects. An approximate value of 10^9 for the formation constant β of $Am(P_2W_{17}O_{61})_2$ has been reported [230]. Produced by pulse radiolysis, the occurrence of transient Am(IV) has been observed [356]. Hobart *et al.* [362] report the stabilization of Am(IV) in alkali-metal carbonate media. Electrolytic

oxidation of Am(III) in 2–5.5 M carbonate solutions results in a dark red-brown Am(IV) carbonate complex which is stable to disproportionation.

(d) Am(V)

Oxidation of Am(III) yields only Am(VI) in acid solution but both Am(V) and Am(VI) in alkaline solution. Solutions of Am(V) are conventionally prepared by oxidation of Am(III) (which is soluble in alkali carbonate media) with ozone [112], peroxydisulfate [111], or hypochlorite ion [116], or by electrolysis [362]. Various insoluble carbonates containing Am(V) are precipitated [348]; these yield solutions of AmO_2^+ (usually containing several percent Am^{3+}) upon dissolution in dilute acid. Americium(V) solutions free of Am(III) can be prepared by intermediate preparation of Am(VI) in 2 M Na_2CO_3 solution [114]. After 5% ozone is bubbled through the solution for 1 h at room temperature to oxidize Am(III) to Am(VI), $NaAmO_2CO_3$ is precipitated by heating the solution for 30–60 min at 60°C and the precipitate is then dissolved in dilute acid.

Hara [237] prepared perchlorate, sulfate, and acetate solutions containing AmO_2^+ free of Am^{3+} by first extracting AmO_2^+ from buffered 1 M acetate (pH $\sim$ 3) solutions of Am(III) and Am(V) into 0.1 M thenoyltrifluoroacetone in isobutanol and back-extracting the Am(V) into an aqueous phase. More exotic methods for obtaining the AmO_2^+ ion in aqueous solution include dissolution of solid Li_3AmO_4 in dilute perchloric acid or the electrolytic oxidation of Am(III) in 2 M $LiIO_3$/0.7 M HIO_3 (pH 1.47) solution [3].

(e) Am(VI)

In dilute, non-reducing acid solutions, powerful chemical oxidants such as peroxydisulfate and Ag(II) oxidize both Am(III) and Am(V) to Am(VI); these oxidants were used in the discovery of Am(VI) [198]. Peroxydisulfate, however, will not oxidize Am(III) to Am(VI) completely at acidities above about 0.5 M, since acid hydrolysis of $S_2O_8^{2-}$ interferes [9]. In perchloric acid solution, Ce(IV) oxidizes Am(V) to Am(VI) but only partly oxidizes Am(III) to Am(VI) [9]. Similarly, ozone readily oxidizes Am(V) to Am(VI) in heated nitric or perchloric acid solution but will not oxidize Am(III) to Am(VI) in acid media. Electrolytic oxidation of Am(III) in 2 M H_3PO_4, in 6 M $HClO_4$ [236], or in 2 M Na_2CO_3 [362, 363] produces the AmO_2^{2+} ion [236], as does peroxydisulfate in dilute phosphotungstate solutions [317].

Ozone or peroxydisulfate oxidation of either Am(III) or Am(V) in aqueous sodium carbonate or bicarbonate yields an intensely colored red-brown solution thought to contain a carbonate complex of Am(VI) [114]. This same complex is also obtained by dissolution of solid sodium americyl acetate in sodium carbonate solutions. Nugent [238] speculates that an Am(VII)–carbonate complex may actually be present in such solutions. Americium(VI) in 0.1–0.5 M $NaHCO_3$

solution is stable at 90°C to reduction by H_2O, Cl^-, and Br^- but is readily reduced by I^-, N_2H_4, H_2O_2, NO_2^-, and NH_2OH. Reduction by water occurs at 90°C in 2 M Na_2CO_3.

Ozone oxidation of Am(III) in 2 M Na_2CO_3 yields AmO_2^{2+} only if the temperature is maintained at 25°C or below; at 90°C oxidation does not proceed past Am(V). Surprisingly, Am(VI) is not produced by ozone oxidation of either $Am(OH)_3$ or $KAmO_2CO_3$ in 0.03–0.1 M $KHCO_3$ solution [114]. Similarly $K_2S_2O_8$ will not oxidize either $Am(OH)_3$ or $NaAmO_2CO_3$ in 0.1 M $NaHCO_3$ to Am(VI), although such an oxidation is accomplished readily with $Na_2S_2O_8$. This difference is attributed to the lower solubility of $KAmO_2CO_3$ as compared to that of $NaAmO_2CO_3$.

Alkali hydroxide solutions of Am(VI) are yellow in color and, according to Cohen [239], can be prepared by ozone oxidation of a slurry of $Am(OH)_3$ in any alkali hydroxide. Reduction of Am(VI) is observed on going from acid to alkaline pH and back again. A light-tan solid gradually precipitates from alkali hydroxide solutions of Am(VI). Dissolution of this substance in dilute mineral acids yields a solution of Am(V). It is claimed that Am(VI) disproportionates into Am(VII) and Am(V) in > 10 M NaOH [235].

There is recent evidence for production of AmF_6 by the reaction of KrF_2 and AmF_4 in anhydrous HF, yielding a dark-brown solid of vapor pressure about that of UF_6, and IR absorption at 604 ± 3 cm^{-1}, the position expected for the ν_3 mode of AmF_6 [312].

(f) Am(VII)

The first report on the preparation of Am(VII) in alkaline solution was found to be in error because of contamination by Fe(VI) [240]. Attempts to prepare a solid compound containing Am(VII) by heating Li_2O–AmO_2 mixtures in oxygen at 300–400°C were not successful. However, Krot *et al.* [228] reported that aqueous solutions containing Am(VII) can be prepared by oxidation at 0–7°C of Am(VI) in alkaline solutions. Passage of air/ozone for 30–60 min through a cold, light-yellow 3–4 M sodium hydroxide solution containing 0.001–0.002 M Am(VI) yields a green-colored solution containing some Am(VII). A similar green-colored solution results on gamma irradiation by ^{60}Co at 0°C of a 3 M NaOH solution containing 0.001–0.002 M Am(VI) and previously saturated with nitrous oxide. (N_2O scavenges hydrated electrons by the reaction $N_2O + e^-(aq) \rightarrow N_2 + O^-$; $S_2O_8^{2-}$ may be substituted for N_2O.)

The Russian scientists made spectrophotometric studies in 1–2 M NaOH solutions of the reactions: Pu(VI) + Am(VII) → Pu(VII) + Am(VI), and 2Np(VI) + Am(VII) → 2Np(VII) + Am(V). Appearance of the characteristic spectrum of Pu(VII) provides strong evidence that the green solutions of americium prepared as described above do indeed contain a powerful oxidant such as Am(VII) is expected to be.

8.7.2 Thermodynamic values

The heats of solution of americium metal in aqueous hydrochloric acid solutions at 298.15 ± 0.05 K were redetermined in 1972 by Fuger, Spirlet, and Müller [241] with pure americium metal prepared by distillation. Combined with earlier results, the standard enthalpy of formation of Am^{3+} (aq) at 198 K of $-616.7 \pm 1.3\,kJ\,mol^{-1}$ was calculated [242]. For hydration enthalpy and entropy, see Choppin [359].

Fuger and Oetting [242] have critically evaluated available existing enthalpy and e.m.f. data, and their thermodynamic values for americium ions are listed in Table 8.5.

A correlation function $P(M)$ that connects the trivalent gaseous lanthanide atoms with their aqueous ions changes systematically as a function of atomic number [322]. The same property is moderately well-behaved for trivalent actinides [322–324, or 368]. Each experimental datum needed to calculate $P(Am)$ is well-established but $P(Am)$ is about 20 kJ greater than expected from neighboring actinides (see 17.5.2 and Fig. 17.6). This anomaly has been attributed to the large positive change in entropy of vaporization of Am [325].

8.7.3 Electrode potentials

Table 8.6 lists electrode potentials [3, 9, 16, 236, 243] (1969 IUPAC sign convention) for americium in various aqueous media. The potential diagram for americium in 1 M $HClO_4$ reflects the latest values of Martinot and Fuger for the Am(III)/(0), Am(III)/(II), and Am(IV)/(III) couples [243]. (See also Nugent's papers on the chemical oxidation states of lanthanides and actinides [238, 254]).

(a) Potentials in 1 M $HClO_4$

(*i*) *Am(VI)/(V)*

The potential, 1.60 ± 0.01 V, of the Am(VI)/Am(V) couple in 1 M $HClO_4$ was measured directly [244]. Potentials of all the other couples are calculated from indirect measurements. Since the potentials of both the Am(VI)/(III) and Am(VI)/(V) couples are based on results of older measurements with ^{241}Am, repetition with long-lived ^{243}Am would be valuable. In 1 M K_2CO_3, E°(Am(VI)/Am(V)) is 0.9 V [348].

(*ii*) *Am(III)/(0)*

Using their carefully determined value of $-616.7 \pm 1.3\,kJ\,mol^{-1}$ for the heat of formation of Am^{3+}(aq), Fuger, Spirlet, and Müller [241] estimate the potential of the Am(III)/Am(0) couple in 1 M $HClO_4$ to be -2.06 ± 0.01 V. Martinot and Fuger give -2.07 V [243]. (An earlier estimate was -2.36 ± 0.04 V.)

Table 8.5 *Americium ions in aqueous solution.*

Oxidation state	*Ion*	*Color*	*Preparation*	ΔH_f°(298 K) (kJ mol^{-1})	ΔG_f°(298 K) (kJ mol^{-1})	S° (298 K) (J K^{-1} mol^{-1})
III	Am^{3+}	pink-orange	AmO_2 + hot HCl or red. agent; Am(> III) + I^-, SO_2	-616.7 ± 1.3	-599 ± 4	-201 ± 13
IV	Am^{4+}	rose, > 1 mM	$Am(OH)_3$ + OCl^-, O_3 or $S_2O_8^{2-}$; $Am(OH)_4$ + sat. F^-, H_3PO_4, $P_2W_{17}O_{64}$ complex; electrochem. in $NaHCO_3/Na_2CO_3$	-406 ± 6	-347 ± 9	(-408)
V	AmO_2^+	yellow-tan	$Am(OH)_3$ in $K_2CO_3 + O_3$, OCl^-	-805 ± 5	-741 ± 5	(-21 ± 8)
VI	AmO_2^{2+}	light yellow; brown in SO_4^{2-}; magenta in CO_3^{2-}	$Am^{3+} + S_2O_8^{2-}$, hot dil. H^+; electrochemistry; O_3 + Am(III) in $NaHCO_3$	-652 ± 2	-587 ± 3	(-88 ± 8)
VII		green	Am(VI) + O_3 or γ irradiation in N_2O sat. cold NaOH			

Table 8.6 *Electrode potentials (V) of americium (IUPAC sign convention)* [16, 362, 363].

(a) 1 M $HClO_4$

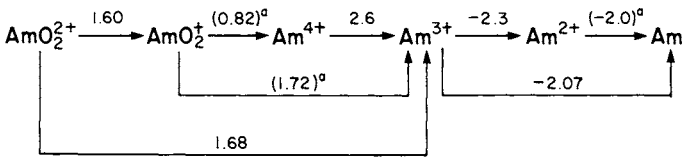

(b) 1 M OH^-

$$AmO_2(OH)_2 \xrightarrow{0.9} AmO_2OH \xrightarrow{(0.7)^a} Am(OH)_4 \xrightarrow{0.5} Am(OH)_3 \xrightarrow{-2.53} Am$$

(c) Phosphoric acid

$$Am(IV) \xrightarrow[10.0\text{–}14.5\,M\ H_3PO_4]{1.75\text{–}1.78} Am(III)$$

$$Am(VI) \xrightarrow[0.54\,M\ H_3PO_4]{1.43} Am(V)$$

$$Am(VI) \xrightarrow[4.34\,M\ H_3PO_4]{1.32} Am(V)$$

(d) Carbonate media

$$Am(IV) \xrightarrow[2\,M\ Na_2CO_3]{0.92} Am(III)$$

$$Am(VI) \xrightarrow[2\,M\ Na_2CO_3]{0.975} Am(V)$$

[a] Values determined by difference.

(*iii*) *Am(III)/(II)*

Nugent *et al.* [245, 246] estimate that the best value for the Am(III)/Am(II) couple is -2.3 V (earlier listed as $\leqslant -1.5$ V [3, 9, 247–249]) and note that this calculated value is in agreement with chemical evidence.

(*iv*) *Am(IV)/(III)*

The standard potential of the Am(IV)/Am(III) couple in 1 M $HClO_4$ was originally estimated at 2.44 V [250]. This value was suggested to be too small by at least 0.2 V from work on oxidation of $Am(OH)_3$ to $Am(OH)_4$ [157]. From their measured value of 1.78 V for the Am(IV)/(III) couple in 10 M H_3PO_4, Nugent, Baybarz, *et al.* [251] calculate a value of 2.34 V for the couple in 1 M $HClO_4$. A value of 2.6 ± 0.09 V has been reported from enthalpy measurements [313], and has been confirmed by electrochemical measurements in carbonate [318]; this

value for the Am(IV)/(III) couple is shown in Table 8.6. The stabilizing of Am(IV) by phosphotungstate drops this potential to 1.52 V [358]. The potential is quite low in carbonate media, at a value of 0.92 V [362, 363].

(v) *Am(VI)/(III) and Am(II)/(0)*

Gunn [252], from measurements of the heat of reduction of Am(VI) to Am(III) by Fe^{2+} ion, estimated the potential of the Am(VI)/Am(III) couple at 1.70 V. A value of 1.67 V for this couple was estimated by Nigon (cited in ref. 9) on the basis of the oxidation of Am(III) to Am(VI) by Ce(IV) ion.

Potentials shown in Table 8.6 for the Am(II)/Am(0), Am(V)/Am(III), and Am(V)/Am(IV) couples are estimated. The new values assigned to the Am(III)/(0) and Am(III)/(II) couples lead to a value of -1.96 V for the Am(II)/(0) couple, which is substantially changed from the potential of below -2.7 V customarily shown [3, 9]. Nugent [254] assigns a value of -2.0 V. to the Am(II)/(0) couple.

(b) Potentials in H_3PO_4

The formal potentials of the Am(IV)/Am(III) and Am(VI)/Am(V) couples in phosphoric acid solutions (Table 8.6) were determined by potentiometry [236, 251, 255].

(c) Potentials in CO_3^{2-} media

The formal potentials of the Am(IV)/Am(III) [362] and Am(VI)/Am(V) [363] couples (Table 8.6) were determined by cyclic voltammetry and potentiometric titration, respectively.

(d) Potentials in 1 M OH^-

Standard potentials of americium in 1 M OH^- solution were based on Latimer's old estimates of the solubility products of $Am(OH)_3$ and $Am(OH)_4$. New values of $K_{sp}(Am(OH)_3) = 10^{23.3}$ and $K_{sp}(Am(OH)_4) = 10^{64}$ are given in Table 17.3 and lead to the values of the standard potentials in 1 M OH^- solution shown in Table 8.6. Earlier, Penneman, Coleman, and Keenan [157] suggested that the standard potential of the $Am(OH)_4/Am(OH)_3$ couple should be revised from -0.4 V to at least $+0.5$ V. From recent studies of the reaction of Am(VI) and Np(VI) with Pu(VI) in NaOH, Nikolaevskii, Shilov, and Krot [257] estimate that the potential of the Am(VI)/Am(V) couple in 1 M NaOH is about 0.65 V rather than 1.1 V (Table 8.6).

Peretrukhin, Nikolaevskii, and Shilov [258] have investigated the polarographic behavior of Am(V) and Am(VI) in 1–10 M NaOH. From their data these authors give the following potential scheme:

1 M *NaOH*

$$\mathrm{Am(VI)} \xrightarrow{0.68} \mathrm{Am(V)} \xrightarrow{0.25 < E_0 < 0.50} \mathrm{Am(IV)} \xrightarrow{E_0 < 0.25} \mathrm{Am(III)}$$

10 M *NaOH*

$$\mathrm{Am(VI)} \xrightarrow{0.63} \mathrm{Am(V)} \xrightarrow{0.17 < E_0 < 0.50} \mathrm{Am(IV)} \xrightarrow{E_0 < 0.18} \mathrm{Am(III)}$$

Shilov reports a value of about 1.05 V for the Am(VII)/Am(VI) couple in 1 M OH^- [256], and Peretrukhin and Spitsyn report 0.78 V for this couple in 10 M OH^- [331].

8.7.4 Autoreduction effects

Species (e.g. hydrogen peroxide and HO_2 radicals) produced by radiolysis of water by alpha particles reduce the higher oxidation states of americium to Am(III). Because of its lower specific acitivity, the rates of autoreduction of ^{243}Am species are much less than those of ^{241}Am species. Zaitsev *et al.* [259] account for the kinetics of autoreduction of aqueous AmO_2^{2+} and AmO_2^+ ions by assuming that H_2O_2 is consumed only in reducing Am(VI), Am(V) is reduced only by HO_2 radicals, but Am(V) may be oxidized to Am(VI) by OH radicals.

All investigators concur that autoreduction of Am(VI) is kinetically zero order with respect to the AmO_2^{2+} ion and first order with respect to total americium concentration:

$$-\mathrm{d[Am(VI)]}/\mathrm{d}t = \mathrm{d[Am(V)]}/\mathrm{d}t = k_1[\mathrm{Am_{total}}]$$

In both perchloric and sulfuric acid media, the value of the rate constant k_1 decreases with increasing acid concentration (0.04 h^{-1} in dilute acid to zero in 12 M $HClO_4$) [259]. The autoreduction rate of $^{241}Am(VI)$ approaches 10% per hour in 9 M HNO_3 [259]; a slower rate was found in a later study [253]. The rate of autoreduction of $^{243}Am(VI)$ in 2 M $HClO_4$ solution at 76°C is about six times that at room temperature [259].

The autoreduction of Am(V) to Am(III) is usually stated to depend only on the total americium concentration and to be independent of Am(V) concentration. Zaitsev *et al.* [259, 260] find that under some conditions the rate of autoreduction of Am(V) to Am(III) does depend on Am(V) concentration. The autoreduction of $^{241}AmO_2^+$ proceeds more slowly in 0.5 M HCl than in 0.2 M $HClO_4$. The maximum reduction rate of AmO_2^+ is about 1% per hour in 0.5 M HNO_3 and 0.8% per hour in 3.0 M HNO_3 [259].

In 13 M NH_4F, $^{241}Am(IV)$ autoreduces at a rate of about 4% per hour [140], increasing to 10% per hour in 3 M fluoride solution [261]. Self-reduction of Am(IV) to Am(III) in phosphoric acid solution follows first-order reaction kinetics [261–263].

(a) Self-reduction of Am(VI) and Am(V) in acid peroxydisulfate solution

No Am(III) is observed until all the Am(VI) is reduced to Am(V). In the presence of $S_2O_2^{2-}$ ions, radiolytic reduction of Am(V) proceeds more slowly than that of Am(VI) [264].

8.7.5 Disproportionation

(a) Am(IV)

In nitric and perchloric acid solutions, Am(IV) rapidly disproportionates according to the reaction [157]:

$$2\text{Am(IV)} \rightarrow \text{Am(III)} + \text{Am(V)}$$

Assuming a reaction that is second order in Am(IV), Penneman, Coleman, and Keenan [157] estimated k_1 in the equation:

$$-\text{d[Am(IV)]}/\text{d}t = k_1[\text{Am(IV)}]^2$$

to be greater than 3.7×10^{-4} l mol^{-1} h^{-1} in 0.05 M HNO_3 at 0°C.

Conversely, dissolution of $Am(OH)_4$ in 0.05–2 M H_2SO_4 solutions at either 0 or 25°C or of solid AmO_2 in 1 M H_2SO_4 yields solutions containing Am^{3+} and AmO_2^{2+} [157, 135]. These results are explained on the basis of the following mechanism.

Stage 1, *simple disproportionation*

$$2\text{Am(IV)} \rightarrow \text{Am(III)} + \text{Am(V)}$$

Stage 2, *redox reaction*

$$\text{Am}^{4+} + \text{AmO}_2^{+} \rightarrow \text{AmO}_2^{2+} + \text{Am}^{3+}$$

The proportion of AmO_2^{2+} increases with increasing SO_4^{2-} and HSO_4^- concentrations at constant H^+ concentration, possibly a result of SO_4^{2-} (or HSO_4^-) stabilization of an Am(IV) complex. Am(IV) is stable only in concentrated H_3PO_4, $K_4P_2O_7$, phosphotungstate and fluoride (NH_4F, KF, etc.) solutions.

Significantly, the average oxidation number of americium remains IV when $Am(OH)_4$ is dissolved in either perchloric, nitric or sulfuric acids [157], indicating no significant reduction by water, in contrast to the reduction of Cm(IV) [358].

(b) Am(V)

The most definitive study of the kinetics of the disproportionation of Am(V) was made by Coleman [266] who used ^{243}Am to minimize the radiolytic complications associated with ^{241}Am. Coleman investigated disproportionation of Am(V) in 3–8 M $HClO_4$ at 25°C, in 1–2 M $HClO_4$ at 75.7°C, and in about 2 M HCl,

H_2SO_4, and HNO_3 solutions at 75.7°C. His data for disproportionation in 6 M $HClO_4$ at 25°C are shown in Fig. 8.2. Coleman [266] finds that the stoichiometry of the disproportionation reaction in all media except hydrochloric acid corresponds to:

$$3\,AmO_2^+ + 4H^+ \rightarrow 2AmO_2^{2+} + Am^{3+} + 2H_2O$$

Coleman's rate law for the disproportionation of Am(v) is

$$-d[Am(v)]/dt = k_2[AmO_2^+]^2[H^+]^2 + k_3[AmO_2^+]^2[H^+]^3$$

with $k_2 = (6.94 \pm 1.01) \times 10^{-4} l^3\,mol^{-3}\,s^{-1}$ and
$k_3 = (4.63 \pm 0.71) \times 10^{-4} l^4\,mol^{-4}\,s^{-1}$.

Coleman also notes that at 75.7°C the disproportionation rates in 2 M HNO_3, HCl, and H_2SO_4 are, respectively, 4.0, 4.6, and 24 times as great as that in 1 M $HClO_4$, whereas at 25°C the reaction rate increased 450 times in going from 3 to 8 M $HClO_4$.

Using, in part, temperature-dependence data obtained by Coleman, Newton [267] estimated thermodynamic quantities of activation for the disproportionation of Am(v). Results of his calculations are given in Table 8.7.

8.7.6 Kinetics of oxidation–reduction reactions

Data for a few oxidation–reduction reactions that have been studied in detail can now be summarized and this supplements information presented by Hindman [268], Newton and Baker [269], and Gourisse [270]. An important recent reference to this subject is the critical review by Newton [267].

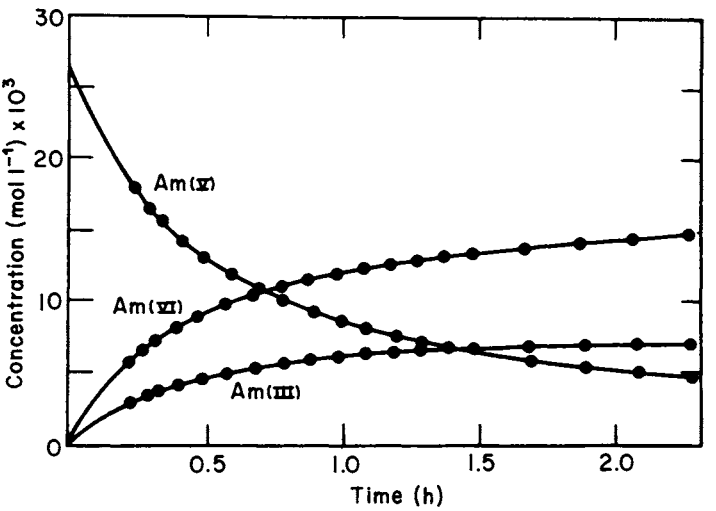

Fig. 8.2 *Disproportionation of Am(V) in 6 M $HClO_4$* [266].

Table 8.7 *Net activation processes and thermodynamic quantities for the disproportionation of Am(v)*[a].

Net activation process	ΔG^* (kJ mol^{-1})	ΔH^* (kJ mol^{-1})	ΔS^* (J K^{-1} mol^{-1})
$2AmO_2^+ + 2H^+ \rightarrow [*]^{4+}$	109.5	64.4 ± 1.3	-130 ± 4
$2AmO_2^+ + 3H^+ \rightarrow [*]^{5+}$	112.2	39.3	-209 ± 5

[a] Adapted from Newton [267].

(a) Peroxydisulfate oxidation of Am(III) in acid media

Early exploratory work by Asprey, Stephanou and Penneman [197], the discoverers of the reaction between $S_2O_8^{2-}$ and Am(III) that produces Am(VI), established that the reaction proceeded in the concentration range from 10^{-8} to 10^{-1} M Am(III), implying a low-order dependence of the rate on Am(III) concentration. They further found that acidities greater than a few tenths molar were deleterious, presumably due to the acid-catalyzed decomposition path of $S_2O_8^{2-}$ [9].

The general pattern of the oxidation (Fig. 8.3) involves an induction period and

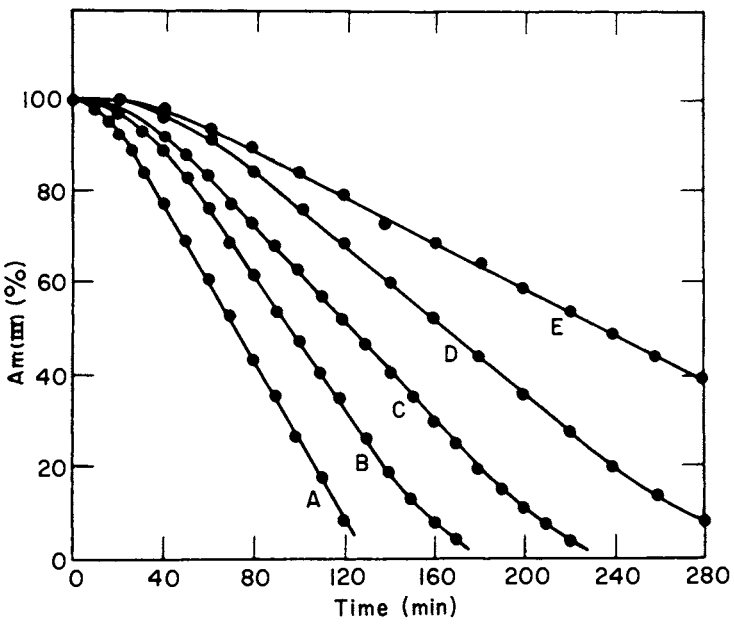

Fig. 8.3 *Kinetics of oxidation of Am(III) by peroxydisulfate* (50.6°C, $[S_2O_8^{2-}]_0$ = 0.40 M) [272]. *HNO_3 concentration: A*, 0.09 M; *B*, 0.14 M; *C*, 0.19 M; *D*, 0.24 M; *E*, 0.28 M.

a linear region of constant rate followed by a region of gradually decreasing rate at high nitric acid concentrations. Reaction rates are dependent on temperature and on the concentration of HNO_3, $S_2O_8^{2-}$, and, when present, Ag^+. Newton [267] states that the stoichiometry of the oxidation reaction is

$$\tfrac{3}{2}S_2O_8^{2-} + Am^{3+} + 2H_2O \rightarrow 3SO_4^{2-} + AmO_2^{2+} + 4H^+$$

All workers concur that the oxidizing agent is not the $S_2O_8^{2-}$ ion itself but its thermal decomposition products (e.g. SO_4^-, OH, and $HS_2O_8^-$).

In contrast to conclusions of Japanese workers who used *micro*molar Am(III), Ermakov *et al.* [272], on the basis of studies with *milli*molar amounts of ^{243}Am(III), claim that (in the absence of Ag^+) the rate of oxidation of Am(III) in the linear portion of kinetic curves does *not* depend on the Am(III) concentration and that the rate is given by

$$-\mathrm{d}[\mathrm{Am(III)}]/\mathrm{d}t = (a - b[H^+])\,[S_2O_8^{2-}]\,[\mathrm{Am(III)}]^0$$

$$= \tfrac{2}{3}k_1 - \frac{k_4[H^+]}{1+x}[S_2O_8^{2-}]_0 = k_{III}$$

At 50.6°C, $a = 4.9 \times 10^{-5}\,\mathrm{min}^{-1}$ and $b = 0.9 \times 10^{-4}\,\mathrm{l\,mol}^{-1}\,\mathrm{min}^{-1}$. In this equation $[S_2O_8^{2-}]_0$ is the initial concentration of the peroxydisulfate ion, $x = k_5/k_6[H_2O]$, and k_1, k_4–k_6 are rate constants for the following reactions:

$$S_2O_8^{2-} \xrightarrow{k_1} 2SO_4^{\cdot -}$$

$$S_2O_8^{2-} + H^+ \xrightarrow{k_4} HSO_4^- + SO_4^{\cdot}$$

$$SO_4^{\cdot} \xrightarrow{k_5} SO_3 + O$$

$$SO_4^{\cdot} + H_2O \xrightarrow{k_6} H_2O_2 + SO_3$$

(b) Peroxydisulfate oxidation of Am(V) in HNO_3

Ermakov *et al.* [272] have also investigated the kinetics of the oxidation of Am(V) by $S_2O_8^{2-}$ ion in 0.09–0.6 M HNO_3 media at 45.6–60°C. According to Newton [267] the stoichiometry of this reaction is

$$\tfrac{1}{2}S_2O_8^{2-} + AmO_2^+ \rightarrow SO_4^{2-} + AmO_2^{2+}$$

Ermakov gives the rate law:

$$-\mathrm{d}[\mathrm{Am(V)}]/\mathrm{d}t = (a' - b'[H^+])\,[S_2O_8^{2-}]\,[\mathrm{Am(V)}]^0$$

At 50.6°C, $a' = 15 \times 10^{-5}\,\mathrm{min}^{-1}$ and $b' = 2.7 \times 10^{-4}\,\mathrm{l\,mol}^{-1}\,\mathrm{min}^{-1}$. It follows from this and the discussion in the preceding section that

$$-\mathrm{d}[\mathrm{Am(III)}]/\mathrm{d}t = -\tfrac{1}{3}\mathrm{d}[\mathrm{Am(V)}]/\mathrm{d}t$$

The results of Rykov *et al.* [264] indicate that the mechanism of reduction of

Am(VI) in the presence of $S_2O_8^{2-}$ ions is identical with that proposed for the oxidation of Am(V).

(c) Peroxydisulfate oxidation of Am(III) in carbonate media

Peroxydisulfate oxidation of Am(III) in carbonate solutions proceeds through the intermediate formation of Am(V). Ermakov *et al.* [272] found that the rate of oxidation of Am(III) to Am(V) is independent of the total Am and potassium carbonate concentrations and is equal to the rate of decomposition of $S_2O_8^{2-}$ ions. However, the rate of oxidation of Am(V) to Am(VI) is directly proportional to both the total americium concentration and the $S_2O_8^{2-}$ concentration, and is inversely proportional to the K_2CO_3 concentration. The effective activation energy of the $S_2O_8^{2-}$ oxidation of Am(III) to Am(V) in potassium carbonate solutions is close to the activation energy (140 kJ mol^{-1}) of the thermal decomposition of $S_2O_8^{2-}$ ions. Recall that $Na_2S_2O_8$ will oxidize either Am(III) or Am(V) to Am(VI) in Na_2CO_3 or $NaHCO_3$.

(d) Reduction of Am(VI) by hydrogen peroxide

Using ^{243}Am in $LiClO_4$–$HClO_4$ media, Woods, Cain, and Sullivan [273] studied the kinetics of the reaction and found the reduction of Am(VI) to be first order in both Am(VI) and H_2O_2:

$$2AmO_2^{2+} + H_2O_2 \rightarrow 2AmO_2^{+} + 2H^{+} + O_2$$

(e) Reduction of Am(VI) by other reductants

Woods and Sullivan [271] studied the reaction between AmO_2^{2+} and NpO_2^{+} in 1 M (H,Li)ClO_4. The rate law is

$$-d[Am(VI)]/dt = k[Am(VI)][Np(V)]$$

At 25°C, k is $(2.45 \pm 0.4) \times 10^4$ $l\,mol^{-1}\,s^{-1}$; for this reaction, $\Delta H^* = 27.87 \pm 0.33$ kJ mol^{-1} and $\Delta S^* = -67.8 \pm 1.3$ J K^{-1} mol^{-1}. Oxalic acid reduces Am(VI) rapidly to approximately equal mixtures of Am(III) and Am(V), whereas reagents such as H_2O_2, HCl, HCOOH, HCHO, etc., reduce Am(VI) initially only to Am(V). The reduction of Am(VI) by nitrous acid is first order in each [360].

(f) Reduction of Am(V) by hydrogen peroxide

From studies of the reduction of AmO_2^{+} to Am^{3+} by hydrogen peroxide in 0.1 M $HClO_4$, Zaitsev *et al.* [274] deduced the rate law:

$$-d[AmO_2^{+}]/dt = k[AmO_2^{+}][H_2O_2]$$

where $k = 14.8 \pm 1.5$, 21.6 ± 2.2, and 30.3 ± 3.01 $mol^{-1}\,h^{-1}$ at 25, 30 and 35°C, respectively. The activation energy deduced for the reduction reaction is 55.23 kJ

mol^{-1}. The only other reported studies of the Am(III)–Am(V)–H_2O_2–$HClO_4$ system have been made by Damien and Pages [275, 276]. They report that the rate at which AmO_2^+ is reduced is inversely proportional to the perchloric acid concentration and is also strongly dependent on the initial $[Am^{3+}]_0/[AmO_2^+]_0$ and $[H_2O_2]_0/[AmO_2^+]_0$ concentration ratios.

(g) Reduction of Am(V) by Np(IV) in perchloric acid media

Blokhin, Ermakov, and Rykov [277] used spectrophotometry to study the kinetics of the Np(IV)–Am(V) reaction in 0.23–1.97 M $HClO_4$ at temperatures in the range 35.0–54.6°C. Depending on the initial concentrations of Np(IV) and Am(V), the reaction products are either Np(V) and Am(III) or Np(VI) and Am(III). The reaction rate falls rapidly with increasing acidity. Under the assumption of constant Am(IV) concentration, the kinetic data follow the rate law:

$$d[Am^{3+}]/dt = k_1'[Np^{4+}][AmO_2^+] + k_2'[NpO_2^+][AmO_2^+]$$

The authors report the following values: $\Delta H^* = 126 \pm 4$ kJ mol^{-1}, $\Delta G^* = 87 \pm 4$ kJ mol^{-1}, and $\Delta S^* = 130 \pm 13$ J K^{-1} mol^{-1}.

(h) Reduction of Am(V) by Np(V) in perchloric acid

Rykov, Timofeev, and Chistyakov [278] have determined spectrophotometrically the rate of the reaction:

$$2NpO_2^+ + AmO_2^+ + 4H^+ \rightarrow 2NpO_2^{2+} + Am^{3+} + 2H_2O$$

Kinetic data were collected in perchlorate media ($\mu = 2.0$ M) at temperatures in the range 24.7–44.1°C. These workers claim that reduction of Am(V) by Np(V) is an irreversible, second-order reaction.

(i) Reduction of Am(V) by Np(V) in sodium carbonate

Kinetics of the reduction of Am(V) by Np(V) in Na_2CO_3 solutions have been investigated spectrophotometrically [279]. The stoichiometry of the reduction is

$$4H^+ + AmO_2^+ + 2NpO_2^+ \rightarrow Am^{3+} + 2NpO_2^{2+} + 2H_2O$$

The kinetics of the Am(V) reactions in Na_2CO_3 media follow the same rate law as in $HClO_4$ media.

(j) Reduction of Am(V) by U(IV) in perchloric acid

At 11.2–3.60°C in 0.51–2.60 M $HClO_4$, the reaction between Am(V) and U(IV) proceeds according to the equation:

$$AmO_2^+ + U^{4+} \rightarrow Am^{3+} + UO_2^{2+}$$

Blokhin, Ermakov, and Rykov [280] derive the following rate law:

$$d[Am^{3+}]/dt = k[AmO_2^{2+}][U^{4+}]$$

In 2.0 M $HClO_4$ at 9.5°C, $k = 725 \pm 30\,l\,mol^{-1}\,min^{-1}$. Standard thermodynamic activation parameters are $\Delta H^* = 75 \pm 4\,kJ\,mol^{-1}$, $\Delta G^* = 63.6 \pm 0.8\,kJ\,mol^{-1}$, and $\Delta S^* = 37.7 \pm 12.5\,J\,K^{-1}\,mol^{-1}$.

(k) Oxidation of Am(II) by water

In an elegant experiment carried out at the Argonne Laboratory, the absorption spectra of both divalent americium and tetravalent americium were obtained [356]. The technique involved irradiation of americium(III) solutions with single electron pulses and recording the spectra with a streak camera at post-irradiation times of 50 μs for Am(II) and 100 μs for Am(IV). Am(II) disappeared by reaction with water while the Am(IV) species disproportionated, that is, reacted with each other to yield Am(III) and Am(V).

8.7.7 Solution (electronic transition) absorption spectra

(a) Am(III)

The absorption spectra of the Am^{3+} ion have been measured in various solutions and Schulz lists molar absorptivity maxima for Am(III) in various media [16]. Data for the narrowest peaks of Am(III), (V), and (VI) should be used with some caution, paying attention to the effect of spectral slit widths. In perchlorate media [229], the major peaks in the absorption spectrum of Am^{3+} occur at 503 and 811 nm, with $\varepsilon \approx 378$ and 64, respectively. Shifts in the position of these peaks and/or changes in molar absorptivity that occur in other media (HNO_3 (Fig. 8.4) or HCl) are evidence for complex formation [124, 126, 127]. Theoretical calculations of the electronic energy bands in the Am^{3+} ion have been performed by several investigators [281–284]. Such calculations predicted an unexpected $^7F_0 \leftrightarrow {}^5D_1$ transition at about 17 600 cm^{-1}, which was subsequently observed in a concentrated americium solution. See also Chapter 16.

(b) Am(IV)

The solution spectrum [285, 140] of Am(IV), characterized by broad absorption features, has been measured in 13 M NH_4F [140, 285] (Fig. 8.5), in 12 M KF [291], in 12 M H_3PO_4 [236], and in 2 M Na_2CO_3 [362, 363]. The spectrum in 13 M NH_4F and 12 M KF also resembles very closely that of solid AmF_4.

(c) Am(V)

The solution spectrum of Am(V) has been measured in 0.1 M H_2SO_4 [286], in 0.5–5.0 M HCl [287], in dilute $HClO_4$ [9, 198, 288] (Fig. 8.6), and in 2 M Na_2CO_3

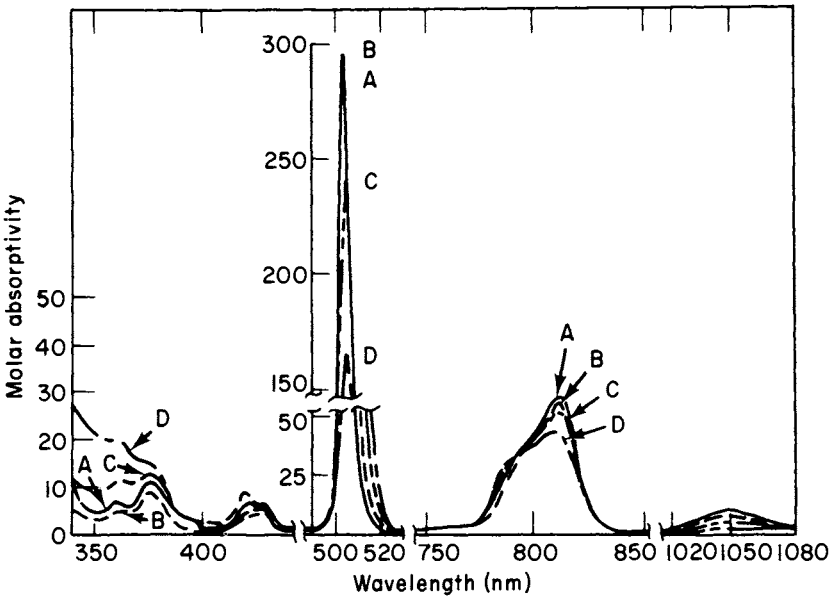

Fig. 8.4 *Absorption spectrum of Am(III) in HNO_3* [135]. *HNO_3 concentration: A,* 0.20 *M; B,* 1.00 *M; C,* 5.02 *M; D,* 10.04 *M.*

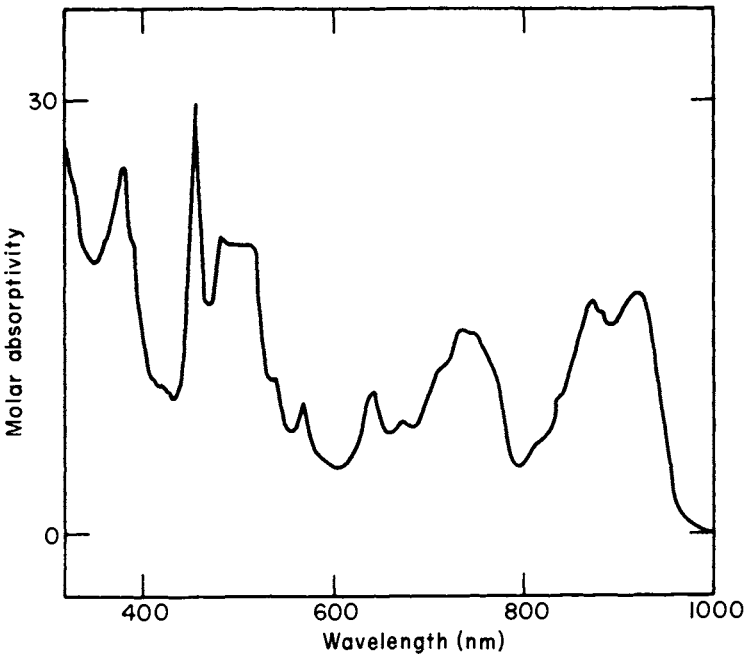

Fig. 8.5 *Absorption spectrum of Am(IV) in* 13 *M NH_4F* [140].

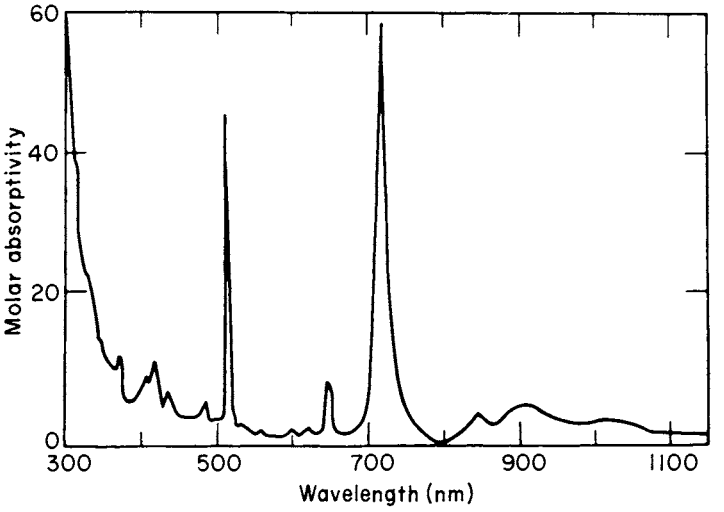

Fig. 8.6 *Absorption spectrum of Am(V) in* 1 M $HClO_4$ [9].

[362, 363]. Molar absorptivities at maximum absorption peaks are 715–720 nm, $\varepsilon \sim 60$, and 513–515 nm, $\varepsilon \approx 45$.

(d) Am(VI)

The spectrum of Am(VI) in acid media is characterized by a sharp absorption feature at about 996 nm with $\varepsilon \sim 100$ in $HClO_4$ and $\varepsilon \sim 200$ in H_3PO_4 (Fig. 8.7). There are some shifts in band energies and/or intensities in different acids (HNO_3 for example) [135, 262, 289]. However, the spectra of Am(VI) in hydroxide solutions (Fig. 8.8) and in acid solutions differ markedly.

Bell [290] has compared band positions of the transuranium actinyl spectra, including those of AmO_2^+ and AmO_2^{2+}, with the spacings between positions of the UO_2^{2+} bands. His results indicate that a single molecular-orbital model can represent any of the actinyl ions when the uranyl ion is assumed to have the bonding orbitals exactly filled, and the transuranium actinyl ions are represented with the uranyl core and a progressive increase of electrons in the first two orbitals lying above the bonding orbitals. Jorgensen has also recently considered the electronic structure of uranyl ion [265].

Jones and Penneman [293] studied the infrared absorption involving the O–M–O asymmetric stretch of actinyl(V) and (VI) ions, concluding that these ions were linear or very nearly so.

(e) Am(VII)

Green-colored solutions believed to contain Am(VII) are prepared by oxidation of Am(VI) in 3–5 M NaOH at 0–7°C with either O_3 or the O^- ion radical. The

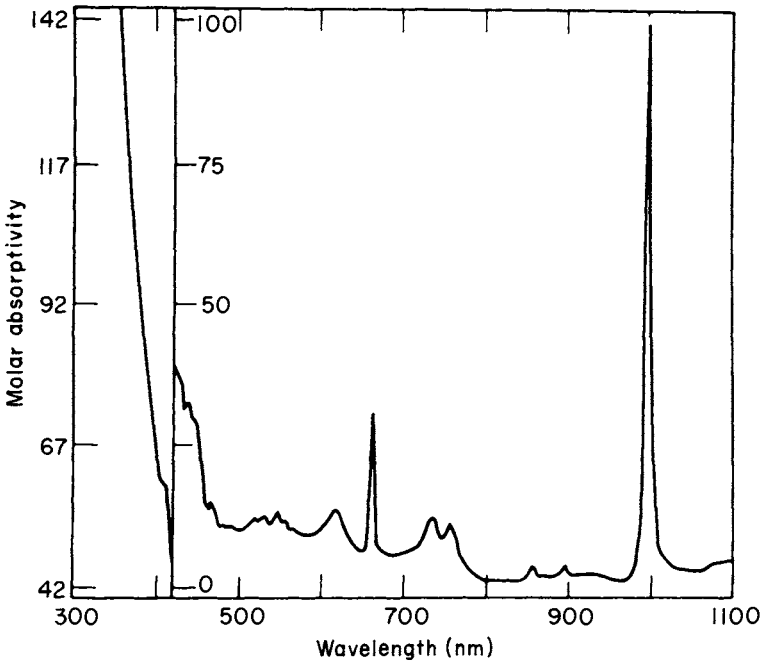

Fig. 8.7 *Absorption spectrum of Am(VI) in 1 M $HClO_4$* [9].

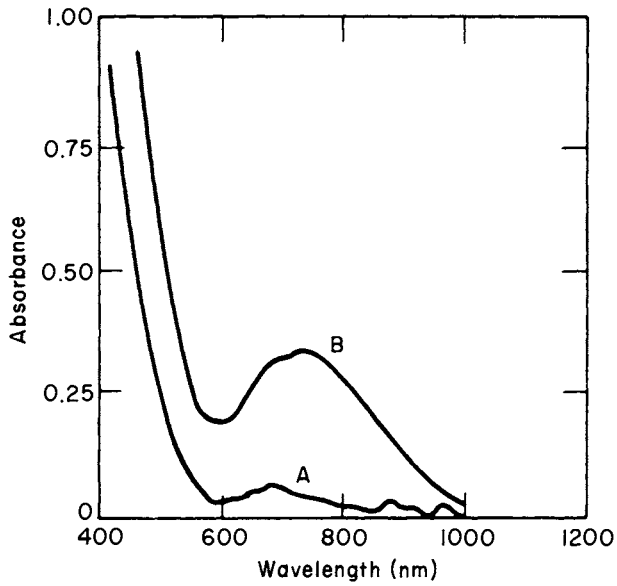

Fig. 8.8 *Absorption spectra of Am(VI) and Am(VII) in 3.5 M NaOH: A, 0.0194 M Am(VI); B, 0.00194 M Am + 50% Am(VII) and 50% Am(VI)* [228].

absorption spectra of Am(VI) and Am(VII) in 3.5 M NaOH as measured by Krot *et al.* [228] are shown in Fig. 8.8. See also Nikolaevskii *et al.* for charge-transfer spectra of heptavalent Np, Pu, and Am [355].

8.7.8 Raman (vibrational) spectra

The results of Raman scattering experiments on Am(V) and Am(VI) ions in perchloric acid solutions have been reported [364]. The values for the polarized symmetric stretching frequencies (ν_1) of the oxycations were found to be 730 cm^{-1} for Am(V) and 796 cm^{-1} for Am(VI) [364]. The Raman scattering of Am ions in carbonate solution showed a shift of ν_1 to 760 cm^{-1} for Am(VI) [365] and to 747 cm^{-1} for Am(V) [366]. A study of the correlation of the Raman spectra of actinyl(V) and actinyl(VI) ions in non-complexing perchlorate and complexing carbonate solutions, as well as the spectra of solid actinide(V) double-carbonate compounds, was published by Madic *et al.* [366].

8.7.9 Complex-ion formation constants

Formation constants and pertinent experimental conditions under which they were determined are collected in Tables 8.8 and 8.9 for complexes of Am^{3+} with inorganic and organic ligands, respectively. Earlier compilations of formation constants of americium complexes are those of Jones and Choppin [8], Martell and Sillen [295], Marcus, Givon, and Shiloh [296], Keller [3], Gel'man *et al.* [297], and Rogozina *et al.* [298].

In Tables 8.8 and 8.9, the following abbreviations are used: Spec, spectrophotometry; Sol, solubility; SX, solvent extraction; IX, ion exchange; Relax, relaxation; EM, electromigration; PT, potentiometric titration; and PEP, paper electrophoresis. The constants k_i and β_i are defined for the reaction of a cation M with a ligand L as follows:

$$K_1 = \beta_1 = \frac{[ML]}{[M][L]} \qquad K_2 = \frac{[ML_2]}{[ML][L]} \qquad K_3 = \frac{[ML_3]}{[ML_2][L]} \qquad \text{etc.}$$

$$\beta_2 = \frac{[ML_2]}{[M][L]^2} \qquad \beta_3 = \frac{[ML_3]}{[M][L]^3} \qquad \text{etc.}$$

and

$$\beta_2 = K_1K_2 \qquad \beta_3 = K_1K_2K_3 \qquad \text{etc.}$$

(a) Complexes with inorganic ligands

Nearly all of the formation constants listed in Table 8.8 are for complexes formed by Am(III), as little work has been done on complexes of americium with oxidation states higher than III. Color changes indicate existence of Am(VI) nitrate, sulfate, and fluoride complexes. There is also spectrophotometric evidence [299] for the existence in 1 M NaOH solution of a peroxide complex of

Table 8.8 *Complexes of americium(III) with inorganic ligands*[a].

Ligand	*Ref.*[a]	*Method*	*Temp.* (°C)	*Ionic strength,* μ(mol l^{-1})	*Medium*	*Log of formation constants* β_1	β_2	*Other*
bromide (Br^-)								
	126	Spec	25		8.74–11.4 M LiBr	-3.3 ± 0.1 ($AmBr^{2+}$)		
carbonate (CO_3^{2-})								
	126	Sol	25		0.1–0.6 M K_2CO_3			$[Am(OH)(CO_3)_3]^{4-}$
	319	SX	25	1.0	1 M $NaClO_4$	5.81 ± 0.04	9.72 ± 0.10	
chloride (Cl^-)								
	124	Spec	25(?)		13.7 M LiCl	-2.21 ± 0.08 ($AmCl^{2+}$)	-4.70 ± 0.08 ($AmCl_2^+$)	
	43	SX	30 ± 0.1	1.0	$LiClO_4$–LiCl	0.25 ± 0.015		
					$HClO_4$–HCl	0.14 ± 0.024	-0.53 ± 0.044	
					$NaClO_4$–NaCl	0.027 ± 0.01	-0.55 ± 0.13	
					NH_4ClO_4–NH_4Cl	0.117 ± 0.017	0.033 ± 0.020	
		IX	26 ± 1	1.0	$HClO_4$–HCl	-0.057 ± 0.098	-0.82	
					$NaClO_4$–NaCl, pH 3.0	0.15 ± 0.03		
	48	SX	22 ± 1	1.0	$HClO_4$–HCl	-0.046 ± 0.010		
		SX	25	4.0	4 M $NaClO_4$	-0.15 ± 0.07	-0.69 ± 0.10	
		IX		0.5	0.5 M $HClO_4$	-0.24		
		Relax				0.03	-1.0	
		IX	20	4.0	$HClO_4$–HCl	-0.16 ± 0.02	-0.75 ± 0.14	
	125	Spec	25(?)		[b]			$K_6 = 150 \pm 20$[c]
	303	Relax	?	?	[d]	1.8 ± 0.5	0.5 ± 0.03	$K_6 = 60 \pm 20$[c]
fluoride (F^-)								
		SX	25	0.5	$NaClO_4$–NaF	3.39 ± 0.01 (AmF^{2+})	6.11 ± 0.03 (AmF_2^+)	$\beta_3 = 9.0$ (AmF_3)
	310	SX	25	1.0	$NaClO_4$	2.49 ± 0.02		
	304	EM	25	0.1	$NaClO_4$	3.32		
	391	IX	25	0.1	$NaClO_4$	2.59 ± 0.01	4.75 ± 0.04	$\Delta H_1 = 22.9$ kJ mol^{-1}
hydroxide (OH^-)								
	233	EM	25	0.005	$HClO_4$–NH_4ClO_4	10.7 ± 0.1 ($AmOH^{2+}$)	20.9 ($Am(OH)_2^+$)[e]	
	307	SX	10–40	0.1	$HClO_4$–$LiClO_4$			$\Delta G° = 30.5$ kJ mol^{-1} ($AmOH^{2+}$)
		PEP	15 ± 1	0.005	HCl–KCl	11.32 ± 0.02		
	231	SX	23 ± 1	0.1	$HClO_4$–$LiClO_4$	8.3		
	370	SX	22 ± 2	0		$\leqslant 5.8$	10.9	$NoAmCOH_4^-$

Table 8.8 (*Contd.*)

Ligand	*Ref.*[a]	*Method*	*Temp.* (°C)	*Ionic strength,* μ(mol l^{-1})	*Medium*	*Log of formation constants* β_1	β_2	*Other*
nitrate (NO_3^-)								
	126	Spec	25		8.0 M $LiNO_3$	-1.3 ± 0.1 ($AmNO_3^{2+}$)		
	223	IX	20–25	1.0	1.0 M NH_4ClO_4, pH 1.5	0.60		
	310	SX	25 ± 0.02	1.0	$HClO_4$–HNO_3	0.25 ± 0.02		
	43	SX	30 ± 0.1	1.0	NH_4ClO_4–HNO_3	0.23	0.13 ($Am(NO_3)_2^+$)	
		IX	26 ± 1		$NaClO_4$–$NaNO_3$, pH 3.0	0.20 ± 0.03		
					$HClO_4$–HNO_3, pH 1.0	0.15 ± 0.03	-0.40	
	48	SX	22 ± 1	1.0	$HClO_4$–HNO_3	0.25 ± 0.07		
		SX	20 ± 1	8.0	8.0 M $HClO_4$	-0.33	-0.77	$\beta_3=-1.4$ ($Am(NO_3)_3$)
		SX		1.0	1.0 M $NaClO_4$, pH 3.0	-0.26		
		SX	25	2.01	NH_4NO_3–HNO_3	0.20 ± 0.03		$[AmO_2(NO_3)_2(H_2O)_2]$
	309	Spec			0–10 M HNO_3			$[AmO_2(H_2O)_6]^{2+}$
nitrite (NO_2^-)								
	315	SX	25	1.0	$NaClO_4$	0.96 ± 0.03		
perchlorate (ClO_4^-)								
		SX	25	2.0	HBF_4–$HClO_4$	-0.07 ± 0.03 ($AmClO_4^{2+}$)		
phosphate ($H_2PO_4^-$)								
	300	IX	20 ± 1	1.0	1.0 M NH_4Cl	1.48 ($Am(H_2PO_4)^{2+}$)	2.10 ($Am(H_2PO_4)_2^+$)	$\beta_3=2.85$ ($Am(H_2PO_4)_3$)
								$\beta_4=3.4$ ($Am(H_2PO_4)_4^-$)
	314	Spec			0.001–12 M H_3PO_4		4.61$[AmO_2(H_2O)_{x-2}(H_2PO_4)_2]^0$	

sulfate (SO_4^{2-})								
		IX	26±1	1–1.3	$NaClO_4$, pH 3.0	1.49 ($AmSO_4^+$)	2.47 ($Am(SO_4)_2^-$)	
		SX		1–1.3	$NaClO_4$, pH 3.0	1.47	2.59	
	223	IX	20–25	0.75	0.75 M $NaClO_4$, pH 3.5	1.78		
		IX		1.5	1.5 M NH_4ClO_4, pH 3.5	1.76	2.11	
		SX	25	1.0	1.0 M $NaClO_4$	1.57±0.09	2.66±0.08	
	302	SX	25±0.1	2.0	2.0 M $NaClO_4$	1.43±0.06	1.83±0.12	
		IX	27	1.0	$HClO_4$–H_2SO_4	1.22±0.01		$\beta' = 0.54 \pm 0.03$ ($Am(HSO_4)_2^+$)
					$NaClO_4$–Na_2SO_4, pH 3.0	1.48±0.01	2.35±0.01	
		SX	24–25	0.5	0.5 M $NaClO_4$	1.85±0.01	2.79±0.01	
		IX	27	0.5	0.5 M $NaClO_4$	1.86±0.01	2.73±0.01	
thiocyanate (SCN^-)								
	43	SX	30±0.1	1.0	$LiClO_4$ + LiSCN	0.06±0.04 ($AmSCN^{2+}$)	0.24±0.03 ($Am(SCN)_2^+$)	
					$NaClO_4$–NaSCN	0.17±0.05	0.51±0.03	
					NH_4ClO_4–NH_4SCN	0.12±0.06	0.56±0.02	
		SX	25	5.0	5.0 M $NaClO_4$	0.85±0.05		$\beta_3 = 0.55 \pm 0.15$ ($Am(SCN)_3$) $\beta_4 = 0.0 \pm 0.15$($Am(SCN)_4^-$)
		SX	25	2.0	NH_4NO_3–NH_4SCN	−0.55±0.15	0.74±0.03	$\beta_3 = 0.87 \pm 0.03$
	223	IX		0.5	0.5 M NH_4ClO_4	0.66±0.03 ($\mu = 0$)		
				5.0	5.0 M NH_4ClO_4	0.24		$\beta_3 = -0.04$
	310	IX	25	1.0	$NaClO_4$–NaSCN	0.50±0.01	0.84±0.07	
		SX		5.0	5.0 M $NaClO_4$	0.60±0.06		
		SX	25±0.1	1.0	$NaClO_4$ + NaSCN, pH 2.0	0.36±0.03	−0.01±0.20	$\beta_3 = 0.22 \pm 0.26$
		Spec	22±1	1.0	1.0 M $NaClO_4$	0.76±0.03	0.83±0.07	
		SX	25	5.0	$NaClO_4$ + NaSCN	0.59±0.05		
trimetaphosphate ($P_3O_9^{3-}$)								
		IX	25±0.1	0.2	NH_4ClO_4, pH 2–4	2.48±0.04 (AmP_3O_9)		$\beta'_1 = 2.21 \pm 0.21$ ($AmHP_3O_9^+$)

[a] Unless otherwise noted, see the compilation by Schulz [16] and references therein.
[b] 85 vol% succinonitrile–15 vol% acetonitrile.
[c] Equilibrium constant for reaction $AmCl_5^{2-} + Cl^- \rightarrow AmCl_6^{3-}$.
[d] Propylene carbonate.

Table 8.9 *Complexes of americium(III) with organic ligands*[a].

Ligand	*Ref.*[a]	*Method*	*Temp.* (°C)	*Ionic strength,* μ (mol l^{-1})	*Medium*	*Log of formation constants* β_1	β_2	*Other*
acetic acid (HAc)								
	300	IX	20	0.5	9.0 M HAc	2.28 ($AmAc^{2+}$)	3.84 ($AmAc_2^+$)	$\beta_3 = 4.78$ ($AmAc_3$) $\beta_4 = 5.7$ ($AmAc_4^-$) $\beta_5 = 6.66$ ($AmAc_5^{2-}$) $\beta_6 = 7.62$ ($AmAc_6^{3-}$)
	300	PT	20	1.0	1.0 M NH_4ClO_4	1.81	3.20	$\beta_3 = 4.57$; $\beta_4 = 5.7$ $\beta_5 = 6.73$; $\beta_6 = 7.73$
	310	SX	25 ± 0.1	2.0	2.0 M NH_4ClO_4	1.95 ± 0.11		
	40	IX	20	0.5	0.5 M $NaClO_4$	1.99 ± 0.01	3.27 ± 0.07	$\beta_3 = 3.9$
		IX	25(?)	0.2	?	2.15	3.83	
			25(?)	0.5	?	2.30	3.81	
			25(?)	1.0	?	2.08	3.62	
	234	SX	~25		0.1–1.0 M Ac	1.40 (AmO_2Ac)	2.51 ($AmO_2Ac_2^-$)	
α-alanine (Ala)								
		SX	25	2.0	2.0 M $NaClO_4$	0.79 ($AmAla^{2+}$)		
	298	Spec	18 ± 2	1.0	KCl	3.9 ± 0.2		
anthranil-*N*,*N*-diacetic acid (H_3ADA)								
		IX	25	0.1	0.1 M NH_4ClO_4	8.92 (AmADA)	14.5 ($Am(ADA)_2^{3-}$)	
arginine	298					3.8 ± 0.3		
arsenazo(III) (AZ)								
		Spec			HAc; HNO_3	AmAZ	$AmAZ_2$	$AmAZ_3$
		Spec			pH 3–6	AmO_2AZ		
aspartic acid	298	Spec	18 ± 2	1.0	KCl	5.1 ± 0.02		
N-benzoylphenylhydroxylamine (NBPHA)								
		SX						$\beta = ?$ ($Am(NBPHA)_3$)
benzoyltrifluoroacetone (HBTA)								
	200	SX	25	0.1	NH_4ClO_4			$\beta_3 = 14.84$ ($Am(BTA)_3$)

citric acid (H_3Cit)								
		Spec	25	1.0	1.0 M $NaClO_4$	6.96 (AmCit)	10.3 ($Am(Cit)_2^{3-}$)	$\beta'_1 = 4.53$ ($AmHCit^+$)
	307	SX	25	0.1	$(H,Li)ClO_4$		12.15	$\Delta G° = 44.98$ kJ mol^{-1} ($AmHCit^{2-}$)
		IX	25	0.1	0.1 M $NaClO_4$	9.16 ± 0.03		$\beta'_1 = 7.00$
				0.5	0.5 M $NaClO_4$	8.73 ± 0.066		$\beta'_1 = 6.29$
				1.0	1.0 M $NaClO_4$	6.72 ± 0.05		$\beta'_1 = 4.24$
		IX	25	0.1	0.1 M NaH_2Cit	6.74	11.55	$\beta'_1 = 5.31$
								$\beta'_2 = 8.23$ ($Am(HCit)_2^-$)
	297	IX			1.0 M NH_4Cl	7.11	14.0	$\beta''_3 = 8.29$ ($Am(H_2Cit)_3$)
	298	PEP			0.04 M		9.66	
cysteine	298	Spec	18 ± 2	1.0	KCl	4.3 ± 0.3		
decanohydroxamic acid (HDHA)								
		SX	20	0.1	0.1 M $NaClO_4$			$\beta(?) = [Am(DHA)_3 \cdot 2H_2(DHA)_2]$
1,2-diaminocyclohexanetetraacetic acid (H_4DCTA)								
		EM	20 ± 0.5	0.1	KCl + HCl	18.34 ($AmDCTA^-$)		$\beta'_1 = 2.87$ ($AmHDCTA^-$)
		IX	25 ± 1	0.1	0.1 M NH_4ClO_4	18.79		
		IX	80		0.001 M H_4DCTA + 0.02 M ammonium α-hydroxyisobutyrate	18.79[e]		
	308	SX	20	0.1	0.1 M NH_4Cl	18.21		$\beta''_1 = 2.85 \pm 0.04$
		Spec	25	0.1				$(AmO_2 \cdot H_2DTPA)^{2-}$
1,2-diaminopropanetetraacetic acid (H_4DTPrA^-)								
		IX	25	0.1	0.1 M $NaClO_4$	17.69 ($AmDTPrA^-$)		$\beta'_1 = 9.79$ ($AmHDTPrA$)
dibutyl-P,P'-ethane-1,2-diphosphonic acid (H_2B_2EDP)								
		SX	25	1.0	1.0 M $NaClO_4$			$\beta'_1 = 14.52$ ($Am(HB_2EDP)_3$)
5,7-dichloro-8-hydroxyquinoline (HDCO)								
	214	SX	25 ± 0.5	0.1	0.1 M $(NH_4,H)ClO_4$			$\beta_3 = 21.93$ ($Am(DCO)_3$)
diethylenetriaminepentaacetic acid (H_5DTPA)								
		IX	25	0.1	0.1 M NH_4ClO_4	23.07 ($AmDTPA^{2-}$)		$\beta'_1 = 14.06$ ($AmHDTPA^-$)
		IX	25	0.1	0.1 M NH_4ClO_4	22.92		
		EM	25 ± 0.2	0.1	0.1 M KNO_3	22.74		$\beta'_1 = 14.3$
		SX		0.1		23.2		
		Spec	25	0.1		23.2		
		Spec	25	0.1	0.1 M NH_4ClO_4	24.03		
		Spec	20 ± 0.1	0.5	$HClO_4$; HNO_3	22.09		
		IX	25	0.1	0.1 M NH_4ClO_4	23.32		
	300	IX	25	1.0	1.0 M NH_4ClO_4	21.3		$\beta'_1 = 15.46$

Table 8.9 (*Contd.*)

Ligand	*Ref.*[a]	*Method*	*Temp.* (°C)	*Ionic strength,* μ (mol l^{-1})	*Medium*	*Log of formation constants* β_1	β_2	*Other*
diethylphosphinylpropionic acid (HDEPP)								
		IX	25	0.5	NH_4ClO_4; $HClO_4$	1.76 ($AmDEPP^{2+}$)	3.16 ($Am(DEPP)_2^+$)	
diglycolic acid (H_2DGA)								
	311	Spec	25.2	0.1	0.1 M NH_4ClO_4	6.47 ($AmDGA^+$)	10.96 ($Am(DGA)_2^-$)	$\beta_3 = 13.83$ ($Am(DGA)_3^{3-}$)
dioctyl-P,P′-ethane-1,2-diphosphonic acid (H_2O_2 EDP)								
		SX	25	1.0	1.0 M $NaClO_4$			$\beta'_1 = 19.53$ ($Am(HO_2EDP)_3$)
diphosphine dioxides[b]								
		SX	25	2.0	2.0 M $NaNO_3$	1.43 ($Am(NO_3)_3 \cdot$(1,1-DiPO))		
						6.56 ($Am(NO_3)_3 \cdot 2$ (1,4-DiPO))		
						5.92 ($Am(NO_3)_3 \cdot 2$ (1,5-DiPO))		
ethylenediaminebis(isopropyl)phosphonic acid (H_4EDIP)								
		EM	25	0.1	0.1 M KNO_3	18.00 ($AmEDIP^-$)		$\beta'_1 = 6.26$ (AmH_3EDIP^{2+})
								$\beta''_1 = 8.94$ (AmH_2EDIP^+)
								$\beta'''_1 = 13.95$ (AmHEDIP)
ethylenediaminebis(methyl)phosphonic acid (H_4EDMP)								
	233	EM	25	0.1	0.1 M KNO_3	16.52 ($AmEDMP^-$)		$\beta'_1 = 6.3$ (AmH_3EDMP^{2+})
								$\beta''_1 = 8.48$ (AmH_2EDMP^+)
								$\beta'''_1 = 12.3$ (AmHEDMP)
		IX	25	0.5	0.5 M NH_4ClO_4			$\beta'_1 = 6.12$ (AmH_2EDMP^+)
ethylenediaminetetraacetic acid (H_4EDTA)								
		IX	25	0.1	0.1 M $NaClO_4$	18.15 ($AmEDTA^-$)		
				0.5	0.5 M $NaClO_4$	16.36		$\beta'_1 = 9.68$ (AmHEDTA)
				1.0	1.0 M $NaClO_4$	15.72		
		Spec	25 ± 0.2	1.0	$NaClO_4$; $HClO_4$	15.33	22.10 ($Am(EDTA)_2^{5-}$)	$\beta'_1 = 8.94$ (AmHEDTA)
		SX	20	0.1	0.1 M NH_4Cl	16.91 ± 0.04		
		Spec	25	0.1	0.1 M NH_4ClO_4	18.06		
		IX	25 ± 0.02	0.1	0.1 M NH_4ClO_4	18.16 ± 0.10		
		IX		1.0	1.0 M NH_4ClO_4	18.03 ± 0.13		$\beta'_1 = 10.29$ (AmHEDTA)
		EM	25 ± 0.5	0.1	HCl + KCl	17.0		$\beta'_1 = 9.21$ (AmHEDTA)
		IX	80	0.1	0.001 M H_4EDTA + 0.2 M α-hydroxyisobutyrate	17.14		
		EM	25 ± 0.1	0.1	0.1 M KNO_3	17.00 ± 0.09		$\beta'_1 = 9.21$ (AmHEDTA)
	308	Spec	25	0.1				$\beta = 19.98$ (AmO_2HEDTA^{2-})
								$\beta''' = 4.88 \pm 0.05$ (AmO_2HEDTA^{2-})

ethylenediaminetetramethylphosphonic acid (H_8EDTMP)								
		EM	25 ± 0.1	0.1	0.1 M KNO_3	22.47 ± 0.08 ($AmEDTMP^{5-}$)		$\beta'_1 = 4.8 \pm 0.6$ (AmH_5EDTMP) $\beta''_1 = 7.33 \pm 0.09$ (AmH_4EDTMP) $\beta'''_1 = 11.17 \pm 0.07$ (AmH_3EDTMP) $\beta''''_1 = 14.90 \pm 0.06$ (AmH_2EDTMP) $\beta'''''_1 = 18.45 \pm 0.08$ (AmHEDTMP)
ethylenediaminetetrapropionic acid (H_4EDTP)								
		Spec	25 ± 0.2	1.0	$NaClO_4$; $HClO_4$	18.84 ± 0.02 ($AmEDTP^-$)		$\beta'_1 = 12.31$ (AmHEDTP)
ethyleneglycol*bis*(2-aminoethyl)tetraacetic acid (H_4EGTA)								
		IX	25	0.1	0.1 M NH_4ClO_4	18.22 (AmEGTA)		
fulvic acid	305							
glutamic acid	298	Spec	18 ± 2	1.0	KCl	5.6 ± 0.1		
glycine (HGlyn)								
		SX	25	2.0	2.0 M $NaClO_4$	0.69 ± 0.02 ($AmGlyn^{2+}$)		
	298	Spec	18 ± 2	1.0	KCl	4.1 ± 0.02		
glycolic acid (HGlyc)								
		IX	20	0.5	0.5 M $NaClO_4$	2.82 ($AmGlyc^{2+}$)	4.85 ($Am(Glyc)_2^+$)	$\beta_3 = 6.30$ ($Am(Glyc)_3$)
	310	SX	25	2.0	2.0 M $NaClO_4$	2.59		
		Spec	25 ± 0.2	1.0	$NaClO_4$; $HClO_4$	2.44 ± 0.02	4.29 ± 0.2	$\beta_3 = 5.20$
		IX	25	0.5	0.5 M $NaClO_4$	2.57 ± 0.02	4.01 ± 0.1	
histadine	298	Spec	18 ± 2	1.0	KCl	4.8 ± 0.2		
humic acid	305							
hydrazine-*N*,*N*-diacetic acid (H_2HyDA)								
		IX	25	0.1	0.1 M $NaClO_4$	10.74 ($AmHyDA^+$)	20.20 ($Am(HyDA)_2^-$)	
	233	EM	25	0.1		11.01	19.78	
hydrazineiminodiacetic acid (H_2HyIDA)								
		EM	25	0.1	0.1 M KNO_3	10.98 ($AmHyIDA^+$)	19.97 ($Am(HyIDA)_2^-$)	$\beta'_1 = 4.13$ ($AmHHyIDA^{2+}$)
2-hydroxycyclohexylethylenediaminetriacetic acid (H_3HCEDTA)								
		IX	25	0.1	0.1 M $NaClO_4$	16.09 (AmHCEDTA)		$\beta'_1 = 7.44$ ($AmHHCEDTA^+$)
N (2-hydroxyethyl)ethylene-*N*,*N*,*N*′-triacetic acid (H_3NHEDTA)								
		IX	25	0.1	$HClO_4$; NH_4ClO_4	15.72 (AmNHEDTA)	22.47 ($Am(NHEDTA)_2^{3-}$)	
		Spec	25 ± 0.2	1.0	$HClO_4$; NH_4ClO_4	14.84	22.18	
		Spec	25	0.1	0.1 M NH_4ClO_4	16.18		
		IX	22	0.15	HCl; KCl	15.34		

Table 8.9 (*Contd.*)

Ligand	*Ref.*[a]	*Method*	*Temp.* (°C)	*Ionic strength,* μ (mol l^{-1})	*Medium*	*Log of formation constants* β_1	β_2	*Other*
hydroxyethylidenediphosphonic acid (HEDPA)								
		SX	25	0.1	HNO_3–$NaNO_3$			$\beta_3 = ?\,(Am(H_3EDPA)_3^{3-})$
N'(2-hydroxyethyl)iminodiacetic acid (H_2NHIDA)								
		IX	25	0.1	0.1 M NH_4ClO_4	9.14 ($AmNHIDA^+$)	17.04 ($Am(NHIDA)_2^-$)	
		Spec	25	0.1	0.1 M NH_4ClO_4	9.80	17.01	
		SX		0.1		9.3 ± 0.1		
		EM	25	0.1	0.1 M KNO_3	9.3 ± 0.13	16.5 ± 0.2	
α-hydroxyisobutyric acid (HIBA)								
		Spec	25 ± 0.2	1.0	$HClO_4$; $NaClO_4$	2.68 ($AmIBA^{2+}$)	4.38 ($Am(IBA)_2^+$)	
		IX	25 ± 0.2	0.5	0.5 M NH_4ClO_4	2.88 ± 0.01	4.03 ± 0.02	
		IX		0.5	$NH_4ClO_4 + NH_4IBA$	2.38	4.67	$\beta_3 = 5.12$ ($Am(IBA)_3$)
		IX				2.72	4.69	$\beta_3 = 5.64$
		SX		0.5				$\beta_3 = 6.1$
bis(hydroxymethyl)phosphinic acid (HMPA)								
		IX	25	0.2		1.76 ± 0.06 ($AmMPA^{2+}$)	2.48 ± 0.02 ($Am(MPA)_2^+$)	
hydroxymethylphosphonic acid (HMP'A)								
		IX	25	0.2	0.2 M NH_4ClO_4	1.55 ($AmMP'A^{2+}$)	3.18 ($Am(MP'A)_2^+$)	
o-hydroxyphenyliminodiacetic acid (H_2HPIDA)								
		SX	25 ± 0.1	0.1	0.1 M NH_4ClO_4	6.80 ($Am(HPIDA)^{2+}$)	11.9 ($Am(HPIDA_2^+$)	
2-hydroxypropane-1,3-diaminetetraacetic acid (H_4PDTA)								
		Spec	25	0.1	0.1 M NH_4ClO_4	$AmPDTA^-$		Am_2PDTA^{2+}
8-hydroxyquinoline (HOX)								
		SX						$Am(OX)_3$
	214	SX	25 ± 0.5	0.1 M (NH_4, H)ClO_4				$Am(OH)(OX)_2$
8-hydroxyquinoline-5-sulfonic acid (H_2OXSA)								
		IX	25 ± 0.2	0.1	0.1 M NH_4ClO_4	8.64 ± 0.09 ($AmOXSA^+$)		

iminodiacetic acid (H_2IDA)							
	IX	25	0.1	0.1 M NH_4ClO_4	7.37 ($AmIDA^+$)	12.39 ($Am(IDA)_2$)	
	Spec	25 ± 0.2	1.0	$HClO_4$; $NaClO_4$	6.14		$\beta_1 = 3.34$ ($Am(IDA)_5^{7-}$)
	Spec	25	0.1	0.1 M NH_4ClO_4	6.94		$Am(IDA)_3^3$
	Spec	25		0.005 M H_2IDA			
7-iodo-8-hydroxyquinoline-5-sulfonic acid (H_2IOXSA)							
	IX	25 ± 0.2	0.1	0.1 M NH_4ClO_4	6.92 ($AmIOXSA^+$)		
β-isopropyltropolone (HIPT)							
200	SX	25	0.1	NH_4ClO_4			$\beta_3 = 22.22 \pm 0.15$ ($Am(IPT)_3$)
306	SX	25	0.1	NH_4ClO_4			$\beta_3 = 21.37$
lactic acid (HLact)							
	SX	25	2.0	2.0 M NH_4ClO_4	2.52 ($AmLact^{2+}$)	4.77 ($Am(Lact)_2^+$)	$\beta_3 = 5.98$ ($Am(Lact)_3$)
	IX		0.5	0.5 M NH_4ClO_4	2.77	4.64	
	SX	20	0.5	0.5 M NH_4ClO_4			$\beta_3 = 5.71 \pm 0.03$
	IX	20	0.5	0.5 M NH_4ClO_4			$\beta_3 = 5.73$
	PEP	10	1.5	KCl + HLact	2.57	4.21	
methionine							
298	Spec	18 ± 2	1.0	KCl	4.8 ± 0.2		
N-methyliminodiacetic acid (H_2MIDA)							
	IX	25	0.1	0.1 M NH_4ClO_4	7.01 ($AmMIDA^+$)	12.51 ($Am(MIDA)_2^-$)	
6-methyl-2-picoline acid (HMAPS)							
	IX	25 ± 0.2	0.1	0.1 M NH_4ClO_4	4.26 ($AmMAPS^{2+}$)		
6-methyl-2-picolyliminodiacetic acid (H_2MPIDA)							
	IX	25	0.1	0.1 M NH_4ClO_4	8.38 ($AmMPIDA^+$)		
methylolethylphosphoric acid (HMEPA)							
	IX	25	0.2	0.2 M NH_4ClO_4	1.79 ± 0.12 ($AmMEPA^{2+}$)		
(methylphenylphosphinyl)methylphenylphosphinic acid (HMPPA)							
	SX	25	0.2	0.2 M NH_4ClO_4	3.35 ($AmMPPA^{2+}$)		
methylphosphinic acid (HMPA)							
	IX	25 ± 0.2	0.5	NH_4ClO_4	2.79 ($AmMPA^{2+}$)[c]		
naphthoyltrifluoroacetone (HNTA)							
200	SX	25	0.1	NH_4ClO_4			$\beta_3 = 18.31$ ($Am(NTA)_3$)
nitrilodiacetomonobutyric acid (H_3NDMBA)							
	IX	25	0.1	NH_4ClO_4			$\beta'_1 = 3.53$ (AmHNDMBA)
nitrilodiacetomonopropionic acid (H_3NDAPA)							
	IX	25	0.1	NH_4ClO_4	10.54 (AmNDAPA)	17.83 ($Am(NDAPA)_2^{3-}$)	$\beta'_1 = 4.02$ (AmHNDAPA)

Table 8.9 (*Contd.*)

Ligand	*Ref.*[a]	*Method*	*Temp.* (°C)	*Ionic strength,* μ (mol l^{-1})	*Medium*	*Log of formation constants* β_1	β_2	*Other*
nitrilodiacetomonovaleric acid (H_3NDAVA)								
		IX	25	0.1	NH_4ClO_4			$\beta'_1 = 3.47$ (AmHNDAVA)
nitrilotriacetic acid (H_3NTA)								
		IX	25 ± 0.2	0.1	0.1 M $NaClO_4$	11.72 ± 0.02 (AmNTA)		
				0.5	0.5 M $NaClO_4$	10.84 ± 0.06		
		SX	20	0.1	0.1 M NH_4ClO_4	10.70	19.71 ($Am(NTA)_2^{3-}$)	
	300	IX	20	1.0	1.0 M NH_4ClO_4	10.87		
	311	IX	25.6	0.1	0.1 M NH_4ClO_4	11.91	20.18	
		IX	25	0.1	NH_4ClO_4–$HClO_4$	11.52	20.24	
		IX	25	0.1	0.1 M (NH_4, $HClO_4$)	11.68	20.47	
		Spec	24.6	0.1	0.1 M NH_4ClO_4	11.99	21.1	
			20	0.1		11.65	19.52	$\beta_3 = 13.56$ (AmNTA(HNTA)$^{2-}$)
nitrosophenylhydroxylamine (cupferron)								
		SX					$Am(Cupf)_2$	
oxalic acid (H_2Ox)								
		SX	20	0.1	0.1 M NH_4Cl		8.3 ($Am(Ox)_2^-$)	$\beta_3 = 11.8$ ($Am(Ox)_3^{3-}$)
		IX		1.0	1.0 M NH_4Cl		9.95	$\beta'_4 = 11.0$ ($Am(HOx)_4^-$)
	215	Sol	25		$HClO_4$–H_2Ox	7.10 ($AmOx^+$)	11.2	$\beta_3 = 12.3$
		IX	20–25	0.2	0.2 M NH_4ClO_4	5.99	10.1	
		EM	25	0.1	NH_4Cl–HCl	6.45	10.5	
		SX	25	1.0	1.0 M $NaClO_4$	4.63	8.35	$\beta_3 = 11.2$
		IX	25	0.5	0.5 M $NaClO_4$	3.8 ± 0.02	8.61 ± 0.01	
		Spec	$25 + 0.1$	0.25	oxalate, pH 1–5	3.27 (AmO_2Ox^+)	2.09 ($AmO_2(Ox)_2^{3-}$)	
phenylalanine								
	298	Spec	18 ± 2	1.0	KCl	5.1 ± 0.3		
1-phenyl-3-methyl-4-acetylpyrazolone-5 (HPMAP)								
		SX	25	0.1	0.1 M NH_4ClO_4			$\beta_3 = 12.23$ ($Am(PMAP)_3$)
1-phenyl-3-methyl-4-benzoylpyrazolone-5 (HPMBP)								
		SX	25	0.1	0.1 M NH_4ClO_4			$\beta_3 = 16.49$ ($Am(PMBP)_3$)
1-phenyl-3-methyl-4-trichloroacetylpyrazolone-5 (HPMTCP)								
		SX	25	0.1	0.1 M NH_4ClO_4			$\beta_3 = 7.47$ ($Am(PMTCP)_3$)
1-phenyl-3-methyl-4-trifluoroacetylpyrazolone-5 (HPMTFP)								
		SX	25	0.1	0.1 M NH_4ClO_4			$\beta_3 = 9.70$ ($Am(PMTFP)_3$)

phosphonoacetic acid (H_3PAA)							
	IX	25	0.2	NH_4ClO_4			$\beta_1'' = 2.75$ ($Am(H_2PAA)^{2+}$) $\beta_1'' = 5.15$ ($AmHPAA^{+}$) $\beta_2'' = 8.5$ ($Am(HPAA)_2^{-}$)
pyridine-2-carbonic acid (HAPS)							
	IX	25 ± 0.2	0.1	0.1 M NH_4ClO_4	4.28 ± 0.05 ($AmAPS^{2+}$)	7.99 ± 0.03 ($Am(APS)_2^{+}$)	$\beta_3 = 10.51 \pm 0.05$ ($Am(APS)_3$)
α-picolinic acid-*N*-oxide (HAPSNO)							
	IX	25 ± 0.2	0.1	0.1 M NH_4ClO_4	3.09 ± 0.07 ($AmAPSNO^{2+}$)	5.49 ± 0.07 ($Am(APSNO)_2^{+}$)	
2-picolyliminodiacetic acid (H_2PIDA)							
	IX	25	0.1	0.1 M NH_4ClO_4	8.96 ($Am(PIDA^{+})$)	17.71 ($Am(PIDA)_2^{-}$)	
propanetricarboxylic acid (H_3PTA)							
	Spec	25	1.0	1.0 M $NaClO_4$	5.61 ± 0.07 (AmPTA)		$\beta_1' = 4.96 \pm 0.02$ ($AmHPTA^{+}$)
α-pyridylacetic acid (HAPAA)							
	IX	25 ± 0.2	0.1	0.1 M NH_4ClO_4	3.63 ± 0.07 ($AmAPPA^{2+}$)		
pyridine-3-carboxylic acid (Nicotinic acid) (HNIC)							
	IX	25 ± 0.2	0.1	0.1 M NH_4ClO_4	3.18 ± 0.07 ($AmNIC^{2+}$)		
pyridine-2,6-dicarboxylic acid (H_2PDA)							
	IX	25 ± 0.2	0.1	0.1 M NH_4ClO_4	9.33 ± 0.09 ($AmPDA^{+}$)	16.51 ± 0.09 ($Am(PDA)_2^{-}$)	
pyruvic acid (HPruv)							
	SX	25	2.0	2.0 M $NaClO_4$	2.03 ($AmPruv^{2+}$)	3.34 ($Am(Pruv)_2^{+}$)	$\beta_3 = 3.87$ ($Am(Pruv)_3$)
bis(3-methoxysalicylidenaldehyde)ethylenediimine (B3MoxSEDI)							
	SX	25(?)	0.3	0.3 M KNO_3			$\beta_2' = 0.59$ ($AmH(B3MoxSEDI)_2$)
bis(salicylidenaldehyde)ethylenediimine (BSEDI)							
	SX	25(?)	0.3	0.3 M KNO_3			$\beta_2' = 4.94$ ($AmH(BSEDI)_2$)
serine 298	Spec	18 ± 2	1.0	KCl	4.3 ± 0.1		
squaric acid (H_2Sq)[d]							
	IX	25	1.0	$HClO_4$–NH_4ClO_4	2.17 ($AmSq^{+}$)	3.10 ($Am(Sq)_2$)	
tartaric acid (H_2Tart)							
297	IX			1.0 M NH_4Cl		10.7 ($Am(Tart)_2^{-}$)	
	SX	20	0.1	0.1 M NH_4Cl	3.9 ($AmTart^{+}$)	6.8	
	PEP	(?)	(?)	(?)		7.88	

Table 8.9 (*Contd.*)

Ligand	*Ref.*[a]	*Method*	*Temp.* (°C)	*Ionic strength,* μ (mol l^{-1})	*Medium*	*Log of formation constants* β_1	β_2	*Other*
taurine-*N*,*N*-diacetic acid (H_3TDA)								
		IX	25	0.1	0.1 M NH_4ClO_4	8.08 ($AmTDA$)		$\beta'_1 = 2.29$ ($AmHTDA^+$)
tetraethylenepentaamineheptaacetic acid (H_7TPHA)								
		Spec	20 ± 0.1	0.1	0.1 M NH_4ClO_4	(?) ($AmTHPA^{4-}$)	(?) $(AmTHPA)_2^{11-}$)	
thenoyltrifluoroacetone (HTTA)								
	200	SX	25	0.1	NH_4ClO_4	3.4 ($AmTTA^{2+}$)	8.5 $(Am(TTA)_2^+)$	$\beta_3 = 13.3$ ($Am(TTA)_3$)
	307	SX	10.40	0.1	$HClO_4$–ClO_4			$\Delta G° = 43.9$ kJ mol^{-1} ($Am(TTA)_3$)
thiodiglycolic acid (H_2TDGA)								
	311	Spec	25.6	0.1	0.1 M NH_4ClO_4	3.52 ± 0.08 ($AmTDGA^+$)	5.66 ± 0.07 $(Am(TDGA)_2^-)$	$\beta'_1 = 2.06 \pm 0.08$ ($AmHTDGA^{2+}$)
thioglycolic acid (HTGlyc)								
		IX	20	0.5	0.5 M NH_4ClO_4	1.55 ($AmGlyc^{2+}$)	2.60 $(Am(TGlyc)_2^+)$	(?) $(Am(TGlyc)_3)$
p-toluenesulfonic acid (pTSAH)								
		SX	25	2.0	$HClO_4$–pTSAH	-0.028 ± 0.028 ($AmpTSA^{2+}$)		
		SX	25	2.0	HBF_4–pTSAH	0.075 ± 0.018		
triethylenetetraaminehexaacetic acid (H_6TTHA)								
		IX	25	0.1	0.1 M NH_4ClO_4			$\beta'_1 = 18.13$ ($AmHTTHA^{2+}$)
								$\beta''_1 = 11.85$ (AmH_2TTHA^-)
	300	Spec	25	0.1	0.1 M NH_4ClO_4	27.61 ($AmTTHA^{3-}$)		$\beta = 30.97$ (Am_2TTHA)
								$\beta = 9.15$ $(Am_2H_2(TTHA)_3^{10-})$
tropolene	306	SX	25	0.1	0.1 N $HyClO_4$			$\beta_3 = 16.17 \pm 0.08$
tryptophan								
	298	Spec	18 ± 2	1.0	KCl	4.7 ± 0.2		

[a] Unless otherwise noted, see the compilation by Schulz [16] and references therein.
[b] 1,1-DiPO = $(C_6H_{13})_2P(O)CH_2(O)P(C_6H_{13})_2$; 1,4-DiPO = $(C_6H_{11})_2P(O)(CH_2)_4(O)P(C_6H_{11})_2$; 1,5-DiPO = $(C_6H_{11})_2P(O)(CH_2)_5(O)P(C_6H_{11})_2$.
[c] At $\mu = 0$.
[d] Diketocyclobutenediol.
[e] Calculated value at 25°C and $\mu = 0.1$ mol l^{-1}.

Am(v). Jones and Choppin [8] point out that correlations of formation constant data for actinide complexes are rendered more difficult by the wide range of experimental conditions used. However, at an ionic strength of 1.0–2.0 M, the stability sequence for complexes of Am(III) with monovalent inorganic ligands appears to be

$$F^- > H_2PO_4^- > SCN^- > NO_3^- > Cl > ClO_4^-$$

As a Chatt–Ahrland type 'A' or Pearson 'hard' cation, association of Am^{3+} with inorganic ligands proceeds initially through electrostatic interactions to form outer-sphere complexes. However, in some cases (e.g. F^-, SO_4^{2-}), there is evidence that the ligand displaces the water of hydration, at least to some extent, to form inner-sphere complexes. Spectrophotometric results of Marcus and Shiloh [124] also provide evidence for inner-sphere complexation of chloride and nitrate ions to Am^{3+} in concentrated LiCl and $LiNO_3$ solutions, respectively. Preparation of the solid compound $[(C_6H_5)_3PH]_3AmCl_6$, containing the octahedral hexahalide complex $AmCl_6^{3-}$, has been described by Ryan [107].

The stability of Am^{3+} complexes in many cases is similar to that of complexes of lanthanides of equal ionic radius. In some cases (where bonding may presumably involve f electrons) the stability of the Am^{3+} complex is slightly greater than that of the corresponding lanthanide complex [300]. As discussed earlier, this difference in stability can be used to effect a separation of Am^{3+} from lanthanide elements. The properties of Am^{3+} chloride and thiocyanato complexes are particularly useful for this latter purpose. Ion-exchange studies [61, 296, 301] with both anion resins and long-chain amine hydrohalides show that Am^{3+} in concentrated LiCl and HCl solutions forms anionic chloride complexes.

(b) Complexes with organic ligands

With few exceptions, the data in Table 8.9 are for complexes of Am(III). The higher oxidation states of americium are generally reduced by organic complexing agents.

Examination of Table 8.9 reveals that aminopolycarboxylic acids complex Am(III) more strongly than do either hydroxycarboxylic or aminoalkylpolyphosphoric acids (e.g. ethylenediamine*bis*(methylene)phosphonic acid). Keller [3] observes that in the series of α-hydroxycarboxylic acids (e.g. glycolic and lactic) the stability of the americium complex decreases with increasing number of carbon atoms. The logarithm of the stability constant of the complexes of Am^{3+} with aminopolycarboxylic acids increases linearly (Fig. 8.9) with the number of bound donor atoms of the ligand.

Methods are being sought to estimate and correlate the strengths of complexes of Am^{3+} and other trivalent actinides and lanthanides with various organic ligands. Shalinets [233] suggests a 'rule of additivity of the strength of rings' according to which, under similar steric conditions, the logarithm of the thermodynamic formation constant of the complex is proportional to the sum of

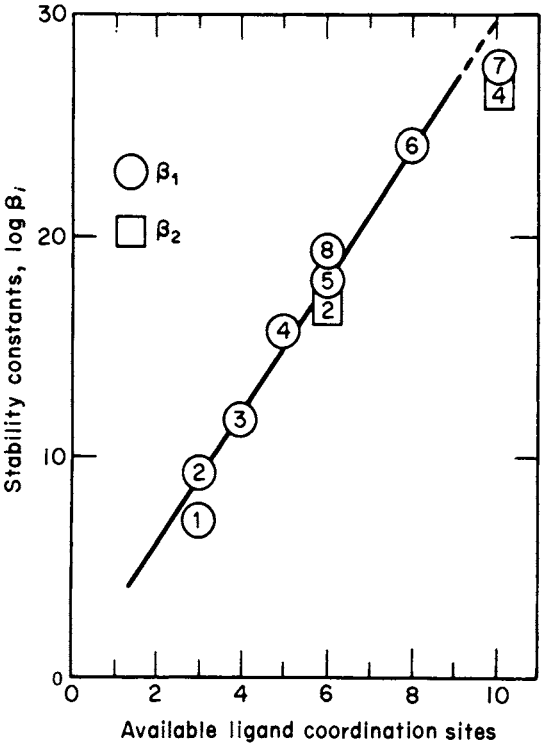

Fig. 8.9 *Correlation of stability constants with number of available coordination sites:* 1, *iminodiacetic acid;* 2, *N-hydroxyethyliminodiacetic acid;* 3, *nitrilotriacetic acid;* 4, *N-hydroxyethylethylenediaminetriacetic acid;* 5, *ethylenediaminetetracetic acid;* 6, *diethylenetriaminepentaacetic acid;* 7, *triethylenetetraaminehexaacetic acid;* 8, *diaminocyclohexanetetraacetic acid* [3].

the strengths of the individual rings. In a few test cases, formation constants of americium chelates calculated by Shalinets are in good agreement with experimental data.

(c) Thermodynamics and kinetics

Thermodynamic functions have been determined for only a few complexes of Am^{3+}. These data, which are collected in Table 8.10, provide evidence for the structures of these complexes in aqueous solution. The thermodynamic changes on complexation of Am^{3+} are the result of two contributions: exothermic enthalpy and negative entropy changes due to the association of the cation with the ligand, and endothermic enthalpy and positive entropy changes arising from the dehydration of the cation and anion. A high positive net change of the entropy indicates inner-sphere complexing. Thus, from the magnitude of the ΔH and ΔS terms for $AmSO_4^+$, Carvalho and Choppin [302] conclude that the degree of

Table 8.10 *Thermodynamic functions for complexes of Am(III)*[a].

Complex	*Method*[b]	*Conditions*	*Reaction*	ΔG (kJ mol^{-1})	ΔH (kJ mol^{-1})	ΔS (J K^{-1} mol^{-1})	*Ref.*
acetic acid (HAc)							
	Tdm(SX)	2.0 M NH_4ClO_4	$Am^{3+} + Ac^- \rightarrow AmAc^{2+}$	-11.21 ± 0.13	18.0 ± 1.3	97.9 ± 4	
diglycolic acid (H_2DGA)							
	Tdm(Spec)	0.1 M NH_4ClO_4	$Am^{3+} + DGA^{2-} \rightarrow AmDGA^+$	-36.61 ± 0.13	2.51 ± 2.97	130 ± 8	311
			$AmDGA^+ + DGA^{2-} \rightarrow Am(DGA)_2^-$	-25.94 ± 0.29	6.7 ± 3.3	109 ± 13	311
			$Am(DGA)_2^- + DGA^{2-} \rightarrow Am(DGA)_3^{3-}$	-16.44 ± 0.33	3.3 ± 0.8	70 ± 4	311
ethylenediaminetetraacetic acid (H_4EDTA)							
	Cal	0.1 M KCl; 25°C	$Am^{3+} + EDTA^{4-} \rightarrow AmEDTA^-$	-103.68	-19.54 ± 1.05	282.4 ± 8	
fluoride (F^-)							
	Tdm(SX)	1.0 M $NaClO_4$	$Am^{3+} + F^- \rightarrow AmF^{2+}$	-17.15 ± 3.35	31.97	164.4	
	Tdm(Sol)	0.1 M $HClO_4$	$Am^{3+} + F^- \rightarrow AmF^{2+}$	-23.35	21.88	133.1	
glycine (HGlyn)							
	Tdm(SX)	2.0 M $NaClO_4$	$Am^{3+} + Glyn^- \rightarrow AmGlyn^{2+}$	-3.89 ± 0.08	12.1 ± 1.7	54 ± 8	
iminodiacetic acid (H_2IDA)							
	Tdm(Spec)	0.1 M NH_4ClO_4	$Am^{3+} + HIDA^- \rightarrow AmHIDA^{2+}$	-7.49 ± 0.63	-62.72 ± 6.36	-185.4 ± 23.8	311
			$Am^{3+} + IDA^{2-} \rightarrow AmIDA^+$	-40.33 ± 0.04	-4.98 ± 1.34	118.8 ± 4.6	311
			$AmIDA^+ + IDA^{2-} \rightarrow Am(IDA)_2^-$	-31.76 ± 0.17	-13.14 ± 7.03	62.3 ± 23.4	311
			$Am(IDA)_2^-$ (aq) $\rightarrow Am(IDA)_2(OH)^{2-}$	44.77 ± 0.37	45.2 ± 5.0		311
	Tdm(Spec)	0.005 M H_2IDA; 15–90°C	$Am + IDA^{2-} \rightarrow AmIDA^+$	-12.5 to -8.4	28.9 ± 5.0	54.8 ± 15.5	
nitrilotriacetic acid (H_3NTA)							
	Tdm(Spec)	0.1 M NH_4ClO_4	$Am^{3+} + NTA^{3-} \rightarrow AmNTA$	-68.24 ± 0.17	2.80 ± 1.92	234.7 ± 1.9	311
			$AmNTA + NTA^{3-} \rightarrow Am(NTA)_2^{3-}$	-51.55 ± 0.37	-23.8 ± 3.3	93.3 ± 11.7	311

Table 8.10 (*Contd.*)

Complex	*Method*[b]	*Conditions*	*Reaction*	ΔG (kJ mol^{-1})	ΔH (kJ mol^{-1})	ΔS (J K^{-1} mol^{-1})	*Ref.*
sulfate (SO_4^{2-})	Tdm(SX)	2.0 M $NaClO_4$	$Am^{3+} + SO_4^{2-} \rightarrow AmSO_4^+$	−8.4	18.4	87.9	302
thiocyanate (SCN^-)							
	Tdm(SX)	1.0 M $NaClO_4$	$Am^{3+} + SCN^- \rightarrow AmSCN^{2+}$	−2.89 ± 0.08	−18.24 ± 1.26	−51.5 ± 4.2	310
			$Am^{3+} + SCN^- \rightarrow AmSCN^{2+}$	−3.39 ± 0.29	10.59 ± 1.21	46.9	
	Tdm(SX)	1.0 M $NaClO_4$	$Am^{3+} + SCN^- \rightarrow AmSCN^{2+}$	−1.97 ± 0.08	6.7 ± 2.9	29.3 ± 8.4	
			$Am^{3+} + 3SCN^- \rightarrow Am(SCN)_3$	−0.79 ± 0.63	−26.8	−83.7 ± 62.8	
			$AmSCN^{2+} + 2SCN^- \rightarrow Am(SCN)_3$	1.17 ± 0.67	−35.6	−113.0 ± 66.9	
	Tdm(SX)	5.0 M (ClO_4 + SCN); 10–55°C	$Am^{3+} + 3SCN^- \rightarrow Am(SCN)^{2+}$	−3.40 ± 0.31	11.76 ± 2.05	50.2 ± 6.7	
thiodiglycolic acid (H_2TDGA)							
	Tdm(Spec)	0.1 M NH_4ClO_4	$Am^{3+} + HTDGA^- \rightarrow AmHTDGA^{2+}$	−11.51 ± 0.79	−29.62 ± 4.10	−60.7 ± 16.3	311
			$Am^{3+} + TDGA^{2-} \rightarrow AmTDGA^{2+}$	−20.42 ± 0.38	28.28 ± 4.69	163.6 ± 17.6	311
			$AmTDGA^+ + TDGA^{2-} \rightarrow Am(TDGA)_2^-$	−11.92 ± 0.50	37.15 ± 2.76	164.8 ± 10.0	311

[a] Unless otherwise noted, see the compilation by Schulz [16] and references therein.
[b] Tdm, temperature-dependence measurements.

inner-sphere complexation present is at least comparable to, and probably exceeds, that of the outer-sphere complexation. By the same criteria, monodentate complexes of Am^{3+} with fluoride, glycine, and ethylenediaminetetraacetic, nitrilotriacetic, and diglycolic acids are also inner-sphere complexes. Jones and Choppin [8] emphasize the thermodynamic importance of the disruption of the hydration sphere of Am^{3+} and other actinide ions on complexing. Their estimates of the entropy and enthalpy of hydration of Am^{3+} and Am^{4+} are listed in Table 8.10.

On the basis of the limited data available, Moskvin [300] has presented some generalizations of the thermodynamics of the formation of actinide ions in aqueous solutions. His analysis includes discussion of the heat capacities of triply charged actinide ions and the changes in their heat capacities on hydration and when transferred from a crystal lattice to solution. Moskvin concludes that further accumulation of thermochemical data for actinide ions, including those of americium, is one of the most urgent contemporary problems in actinide chemistry.

Complexation and stability of americium ions in various media, including solids used for waste storage, are of increasing importance because of americium occurrence in nuclear process waste. Solutions to the problems of long-term, safe storage of americium must be found. To answer such questions, an increase in the study of americium chemistry is to be anticipated.

ACKNOWLEDGMENTS

This work was performed under the auspices of the US Department of Energy.

REFERENCES

1. Seaborg, G. T., James, R. A., Ghiorso, A., and Morgan, L. O. (1949) *The Transuranium Elements* (eds G. T. Seaborg, J. J. Katz, and W. M. Manning) McGraw-Hill, New York, pp. 1525–53; (1950) *Phys. Rev.*, **78**, 472.
2. Cunningham, B. B. (1948) *Isolation and Chemistry of Americium*, USAEC Report ANL-JJK-124, Argonne National Laboratory.
3. Keller, C. (1971) *Chemistry of the Transuranium Elements*, Verlag Chemie, Weinheim.
4. *Gmelin Handbook of Inorganic Chemistry*, Suppl. Work, 8th edn, *Transuranium*, Verlag Chemie, Weinheim, vol. 4, part C, Compounds (1972), vol. 7a, part A1, The Elements (1973), vol. 8, part A2, The Elements (1973).
5. Myasoedov, B. F., Guseva, L. I., Lebedev, I. A., Milyukova, M. S., and Chmutova, M. S. (1974) *Analytical Chemistry of the Transplutonium Elements* (English translation), John Wiley, New York.
6. Bagnall, K. W. (1972) *The Actinide Elements*, Elsevier, New York.
7. Leuze, R. E. and Lloyd, M. H. (1970) in *Progress in Nuclear Energy*, ser. III, vol. 4,

Process Chemistry (eds C. E. Stevenson, E. A. Mason, and A. T. Gresky). Pergamon Press, New York, p. 549.
8. Jones, A. D. and Choppin, G. R. (1969) *Actinides Rev.*, **1**, 311.
9. Penneman, R. A. and Asprey, L. B. (1956) *Proc. First Int. Conf. on the Peaceful Uses of Atomic Energy*, Geneva, 1955, vol. 7, United Nations, New York, p. 355.
10. Penneman, R. A., Ryan, R. R., and Rosenzweig, A. (1973) *Struct. Bonding (Berlin)*, **13**, 1–52.
11. Brown, D. (1968) *Halides of the Lanthanides and Actinides*, John Wiley, New York.
12. Trotman-Dickenson, A. F. (ed.) (1973) *Comprehensive Inorganic Chemistry – Actinides, Master Index*, vol. 5, Pergamon Press, Oxford.
13. Freeman, A. J. and Darby, J. B. Jr (eds) (1974) *The Actinides: Electronic Structure and Related Properties*, vols I and II, Academic Press, New York.
14. Baybarz, R. D. (1970) *At. Energy Rev.*, **8**, 327–60.
15. Weaver, B. (1974) in *Ion Exchange and Solvent Extraction, A Series of Advances*, vol. 6 (eds J. A. Marinsky and Y. Marcus), Marcel Dekker, New York.
16. Schulz, W. W. (1976) *The Chemistry of Americium*, ERDA Critical Review Series, Report No. TID-26971.
17. Ellis, Y. A. and Wapstra, A. H. (1969) *Nucl. Data Sheets*, **3** (2), 1 (A = 243–261); Ellis, Y. A. (1970) *Nucl. Data Sheets*, **4**, 635–60, (A = 238); Schmorak, M. R. (1970) *Nucl. Data Sheets*, **4**, 661–82, (A = 240); Ellis, Y. A. (1970) *Nucl. Data Sheets*, **4**, 683–97, (A = 242); Ellis, Y. A. (1971) *Nucl. Data Sheets*, **6**, 539–76 (A = 237).
18. Lederer, C. M. and Shirkey (eds) (1978) *Table of Isotopes*, 6th edn, John Wiley, New York.
19. Dzhelepov, B. S. and Peker, L. K. (1961) *Decay Schemes of Radioactive Nuclei* (Engl. transl.) (ed. D. L. Allen), Pergamon Press, New York.
20. Mughabghab, S. F. and Garber, D. I. (1973) *Neutron Cross Sections*, vol. I, *Resonance Parameters*, USAEC Report BNL-325, vol. 1, 3rd edn, Brookhaven National Laboratory.
21. Howerton, R. J. (1959) *Tabulated Neutron Cross Sections*, part I, 0.001–14.5 *MeV*, USAEC Report UCRL-5226, University of California Lawrence Radiation Laboratory.
22. Wapstra, A. H. and Gove, N. B. (1971) *Nucl. Data Tables*, **9**, 265–468.
23. Hyde, E. K., Perlman, I., and Seaborg, G. T. (1971) *The Nuclear Properties of the Heavy Elements*, vol. II, Prentice-Hall, Englewood Cliffs, NJ.
24. Wheelwright, E. J., Roberts, F. P., and Bray, L. A. (1968) *Simultaneous Recovery and Purification of Pm, Am, and Cm by the Use of Alternating DTPA and NTA Cation-Exchange Flowsheets*, USAEC Report BNWL-SA-1492, Battelle Memorial Institute, Pacific Northwest Laboratories.
25. Seaborg, G. T. (1970) *Nucl. Appl. Technol.*, **9**, 830–50.
26. Crandall, J. L. (1971) *Applications of Transplutonium Elements*, USAEC Report DP-MS-71-52, Savannah River Laboratory.
27. LeVert, F. E. and Helminski, E. L. (1973) *Literature Review and Commercial Source Evaluation of Americium*-241, USAEC Report ORO-4333-1, Tuskegee Institute.
28. Hennelly, E. J. (1972) in *Radioisotope Engineering* (ed. G. G. Eichholz), Marcel Dekker, New York, pp. 47–134.
29. Mullins, L. J. and Leary, J. A. (1969) US Patent no. 3420639.
30. Ferris, L. M., Smith, F. J., Mailen, J. C., and Bell, M. J. (1972) *J. Inorg. Nucl. Chem.*, **34**, 2921–33.

31. Moore, R. H. and Lyon, W. L. (1959) *Distribution of the Actinide Elements in Molten System KCl–$AlCl_3$–Al*, USAEC Report HW-59147, General Electric Company, Hanford Atomic Products Operation.
32. Foos, J. and Guillaumont, R. (1971) *Bull. Soc. Chim. Fr.*, **9**, 3129–35.
33. King, L. J., Bigelow, J. E., and Collins, E. D. (1973) *Transuranium Processing Plant Semiannual Report of Production, Status, and Plans for Period Ending June* 30, 1972, USAEC Report ORNL-4833, Oak Ridge National Laboratory.
34. Buijs, K., Müller, W., Reul, J., and Toussaint, J. C. (1973) *Separation and Purification of Americium on the Multigramme Scale*, Euratom Report EUR-5040.
35. Hermann, J. A. (1956) *Coprecipitation of Am(III) with Lanthanum Oxalate*, USAEC Report LA-2013, Los Alamos Scientific Laboratory.
36. Stephanou, S. E. and Penneman, R. A. (1952) *J. Am. Chem. Soc.*, **74**, 3701–2.
37. Proctor, S. G. and Connor, W. V. (1970) *J. Inorg. Nucl. Chem.*, **32**, 3699–701.
38. Proctor, S. G. (1976) *J. Less Common Metals*, **44**, 195–9; (1973) US Patent no. 3723 594.
39. Shoun, R. R. and McDowell, W. J. (1980) in *Actinide Separations* (ACS Symp. Ser. 117), American Chemical Society, Washington DC, ch. 6.
40. Gureev, E. S., Dedov, V. B., Karpacheva, S. M., Shvetsov, I. K., Ryzhov, M. N., Trukchlayev, P. S., Yakovlev, G. N., and Lebedev, I. A. (1970) in *Progress in Nuclear Energy*, Ser. III, vol. 4, *Process Chemistry* (eds C. E. Stevenson, E. A. Mason, and A. T. Gresky), Pergamon Press, New York, p. 631.
41. Zemlyanukhin, V. I., Savoskina, G. P., and Pushlenkov, M. F. (1962) *Radiokhimiya*, **4**, 570–5 (*Sov. Radiochem.*, **4**, 501–5).
42. Koehly, G. and Hoffert, F. (1967) in *Semiannual Report of the Chemistry Department, Center for Nuclear Studies at Fontenay-Aux-Roses, December* 1966–*May* 1967, French Report CEA-N-856; also USAEC Report ANL-Trans-628, Argonne National Laboratory.
43. Khopkar, P. K. and Narayankutty, P. (1971) *J. Inorg. Nucl. Chem.*, **33**, 495–502.
44. Siddall, T. H., III (1963) *J. Inorg. Nucl. Chem.*, **25**, 883–92.
45. Schulz, W. W. (1974) *Bidentate Organophosphorus Extraction of Americium and Plutonium from Hanford Plutonium Reclamation Facility Waste*, USAEC Report ARH-SA-203, Atlantic Richfield Hanford Company; (1975) *Trans. Am. Nucl. Soc.*, **21**, 262–3.
46. Schulz, W. W. and McIsaac, L. D. (1975) *Removal of Actinides from Nuclear Fuel Reprocessing Waste Solutions with Bidentate Organophosphorus Extractants*, ERDA Report ARH-SA-217 (CONF-750913-13), Atlantic Richfield Hanford Company.
47. Bowen, S., Paine, R. T., and Eller, P. G. (1980) *Actinide Workshop–IV*, Los Alamos, NM, May; Paine, R. T., *et al.* (1982) *Inorg. Chem.*, **21**, 261; (1982) *Inorg. Chim. Acta*, **61**, 155.
48. Peppard, D. F., Mason, G. W., Driscoll, W. J., and Sironen, R. J. (1958) *J. Inorg. Nucl. Chem.*, 7, 276–85; (1962) *J. Inorg. Nucl. Chem.*, **24**, 881–8.
49. Gureev, E. S., Kosyakov, V. N., and Yakovlev, G. N. (1964) *Radiokhimiya*, **6**, 655–65; *Sov. Radiochem.*, **6**, 639–47.
50. Boldt, A. L. and Ritter, G. L. (1969) *Recovery of Am, Cm, and Pm from Shippingport Reactor Fuel Reprocessing Wastes by Successive TBP and D2EHPA Extractions*, USAEC Report ARH-1354. Atlantic Richfield Hanford Company.
51. Weaver, B. and Kappelmann, F. A. (1964) *Talspeak: A New Method of Separating Americium and Curium from the Lanthanides by Extraction from an Aqueous Solution*

of an Aminopolyacetic Acid Complex with a Monoacidic Organophosphate or Phosphonate, USAEC Report ORNL-3559, Oak Ridge National Laboratory.
52. Lueze, R. E., Baybarz, R. D., and Weaver, B. (1963) *Nucl. Sci. Eng.*, **17**, 252–8.
53. Marcus, Y., Givon, M., and Choppin, G. R. (1963) *J. Inorg. Nucl. Chem.*, **25**, 1457–63; also (1962) Israeli Report IA-783.
54. Horwitz, E. P., Bloomquist, C. A. A., Sauro, L. J., and Henderson, D. J. (1966) *J. Inorg. Nucl. Chem.*, **28**, 2313–24.
55. Ryan, J. L. (1974) in ref. 4, vol. 21, part D2 (1974).
56. Moore, F. L. (1965) *Anal. Chem.*, **37**, 419–20.
57. Baybarz, R. D., Weaver, B. S., and Kinser, H. B. (1963) *Nucl. Sci. Eng.*, **17**, 457–62.
58. Jenkins, I. L. and Wain, A. G. (1972) *Rep. Prog. Appl. Chem.* **57**, 308–19.
59. Coleman, J. S., Armstrong, D. E., Asprey, L. B., Keenan, T. K., LaMar, L. E., and Penneman, R. A. (1955) *Purification of Gram Amounts of Americium*, USAEC Report LA-1975, Los Alamos Scientific Laboratory; (1957) *J. Inorg. Nucl. Chem.*, **3**, 327–8.
60. Surls, J. P. Jr and Choppin, G. R. (1957) *J. Inorg. Nucl. Chem.*, **4**, 62–73.
61. Hulet, E. K., Gutmacher, R. G., and Coops, M. S. (1961) *J. Inorg. Nucl. Chem.*, **17**, 350–60.
62. Hale, W. H. and Lowe, J. T. (1969) *Inorg. Nucl. Chem. Lett.*, **5**, 363–9.
63. Proctor, S. G. (1975) *Cation Exchange Process for Molten Salt Extraction Residues*, USERDA Report RFP-2347, Rocky Flats Plant, Dow Chemical Company.
64. Campbell, D. O. (1970) *Ind. Eng. Chem. Process Des. Dev.* **9**, 95–9.
65. Harbour, R. M., Hale, W. H., Burney, G. A., and Lowe, J. T. (1972) *At. Energy Rev.*, **10**, 379–99.
66. Horwitz, E. P. (1966) *J. Inorg. Nucl. Chem.* **28**, 1469–78.
67. Moore, F. L. (1973) US Patent no. 3687641.
68. Shafiev, A. I., Efremov, Yu. V., Nikolaev, V. M., and Yakovlev, G. N. (1971) *Radiokhimiya*, **13**, 129–31; (1971) *Sov. Radiochem.*, **13**, 123–5.
69. Lynch, R. W., Dosch, R. G., Kenna, B. T., Johnstone, J. K., and Nowak, E. J. (1975) *The Sandia Solidification Process – A Broad Range Aqueous Waste Solidification Method*, Report No. IAEA-SM-207/75.
70. Horwitz, E. P., Bloomquist, C. A. A., Orlandini, K. A., and Henderson, D. J. (1967) *Radiochim. Acta*, **8**, 127–32.
71. Müller, W. (1971) *Angew. Chem.*, **83**, 625; (1971) *Angew. Chem. Int. Edn*, **10**, 580–1.
72. Tomkins, F. S. and Fred, M. (1949) *J. Opt. Soc. Am.*, **39**, 357–63; (1948) USAEC Report AECD-2478.
73. Zachariasen, W. H. (1954) in *The Actinide Elements* (eds G. T. Seaborg and J. J. Katz), Natl Nucl. En. Ser., Div. IV, 14A, McGraw-Hill, New York, ch. 18, pp. 769–95.
74. McWhan, D. B., Wallmann, J. C., Cunningham, B. B., Asprey, L. B., Ellinger, F. H., and Zachariasen, W. H. (1960) *J. Inorg. Nucl. Chem.*, **15**, 185–7.
75. Burns, J. H. and Peterson, J. R. (1970) *Acta Crystallogr. B*, **26**, 1885–7; (1971) *Inorg. Chem.*, **10**, 147–51.
76. Zachariasen, W. H. (1978) *J. Less Common Metals*, **62**, 1–7.
77. Carlson, T. A., Nestor, C. W. Jr, Wasserman, N., and McDowell, J. D. (1970) *Comprehensive Calculations of Ionization Potentials and Binding Energies for Multiply-Charged Ions*, USAEC Report ORNL-4562, Oak Ridge National Laboratory.
78. Penneman, R. A. and Mann, J. B. (1976) *J. Inorg. Nucl. Chem.*, Suppl., 257–63.
79. Kalvius, G. M., Ruby, S. L., Dunlap, B. D., Shenoy, G. K., Cohen, D., and Brodsky,

M. B. (1969) *Phys. Lett. B*, **29**, 489–90; Bode, D. D., Wild, J. F., and Hulet, E. K. (1976) *J. Inorg. Nucl. Chem.*, **38**, 1291–7.
80. Bierman, S. R. and Clayton, E. D. (1969) *Trans. Am. Nucl. Soc.*, **12**, 887–8.
81. Baybarz, R. D. *et al.* (1976) in *Transplutonium* 1975, *Proc. 4th Int. Symp.*, Baden-Baden, Sept. 13–17, 1975 (eds W. Müller and R. Lindner), North-Holland, Amsterdam, pp. 61–8.
82. Roof, R. B., Haire, R. G., Schiferl, D., Schwalbe, L., Kmetko, E. A., and Smith, J. L. (1980) *Science*, **207**, 1353–5; Smith, G. S., Akella, J., Reichlin, R., Johnson, Q., Schock, R. N., and Schwab, M. (1981) *Actinides–1981*, Report LBL-1244; Roof, R. B. (1982) *Z. Krist.*, **158**, 307–12.
83. Sari, C., Müller, W., and Benedict, U. (1972/73) *J. Nucl. Mater.*, **45**, 73–5.
84. Rose, R. L., Kelley, R. G., and Lesuer, D. R. (1979) *J. Nucl. Mater.*, **48**, 114–16.
85. Runnals, O. J. C. (1975) US Patent no. 2809 887; (1956) Br. Patent no. 741 441.
86. Wede, U. (1971) *Radiochim. Acta*, **15**, 102–3.
87. Keller, C. (1967) in *Lanthanide/Actinide Chemistry* (ed. R. F. Gould) (ACS Adv. Chem. Ser.), American Chemical Society, Washington DC, pp. 228–47.
88. Keller, C. and Walter, K. H. (1965) *J. Inorg. Nucl. Chem.*, **27**, 1247–51.
89. Roddy, J. W. (1974) *J. Inorg. Nucl. Chem.*, **36**, 2531–3.
90. Mitchell, A. W. and Lam, D. J. (1970) *J. Nucl. Mater.*, **37**, 349–52.
91. Charvillat, J. P., Benedict, U., Damien, D., and Müller, W. (1975) *Radiochem. Radioanal. Lett.*, **20**, 371–81.
92. Keller, C. and Walter, K. H. (1965) *J. Inorg. Nucl. Chem.*, **27**, 1253–60.
93. Charvillat, J. P. and Damien, D. (1973) *Inorg. Nucl. Chem. Lett.*, **9**, 559–63.
94. Benedict, U., Buijs, K., Dufuor, S., and Toussaint, J. Cl. (1975) *J. Less Common Metals*, **42**, 345–54.
95. Runnals, O. J. C. and Boucher, R. R. (1955) *Nature*, **176**, 1019–20; (1956) *Can. J. Phys.*, **34**, 949–58.
96. Brachet, G. and Vasseur, C. (1969) *Reduction of Americium Oxide by Beryllium for Neutron-Source Productuon*, French Report CEA-R-3875.
97. Charvillat, J. P. and Zachariasen, W. H. (1977) *Inorg. Nucl. Chem. Lett.*, **13**, 161–3.
98. Eick, H. A. and Mulford, R. N. R. (1969) *J. Inorg. Nucl. Chem.*, **31**, 371–5.
99. Peterson, J. R. (1973) in *Proc. Tenth Rare Earth Research Conf.*, Carefree, Ariz., April 30–May 3, 1973 (eds C. J. Kevane and T. Moeller), USAEC Report CONF-730402, pt 1.
100. Baybarz, R. D. (1973) *J. Inorg. Nucl. Chem.*, **35**, 483–7.
101. Fried, S. (1951) *J. Am. Chem. Soc.*, **73**, 416–18.
102. Pappalardo, R. G., Carnall, W. T., and Fields, P. R. (1969) *J. Chem. Phys.*, **51**, 1182–200.
103. Asprey, L. B., Keenan, T. K., and Kruse, F. H. (1965) *Inorg. Chem.*, **4**, 985–6.
104. Brown, D., Fletcher, S., and Holah, D. G. (1968) *J. Chem. Soc.* **A**, 1889–94.
105. Zachariasen, W. H. (1948) *Acta Crystallogr.*, **1**, 265–9.
106. Brown, D., Holah, D. G., and Rickard, C. E. F. (1968) *Chem. Commun.*, **11**, 651–2.
107. Ryan, J. L. (1967) in *Lanthanide/Actinide Chemistry* (ed. R. F. Gould) (ACS Adv. Chem. Ser.), American Chemical Society, Washington DC, pp. 331–4.
108. Mitchell, A. W. and Lam, D. J. (1970) *J. Nucl. Mater.*, **36**, 110–12.
109. Weigel, F. and ter Meer, N. (1967) *Inorg. Nucl. Chem. Lett.*, **3**, 403–8.
110. Fang, D. (1967) Dissertation, Karlsruhe, cited in Fang, D. and Keller, C. (1969) *Radiochim. Acta*, **11**, 123–7.

111. Nigon, J. P., Penneman, R. A., Staritzky, E., Keenan, T. K., and Asprey, L. B. (1954) *J. Phys. Chem.*, **58**, 403–4.
112. Keenan, T. K. (1965) *Inorg. Chem.*, **4**, 1500–1.
113. Keenan, T. K. and Kruse, F. H. (1964) *Inorg. Chem.*, **3**, 1231–2.
114. Coleman, J. S., Keenan, T. K., Jones, L. H., Carnall, W. T., and Penneman, R. A. (1963) *Inorg. Chem.*, **2**, 58–61.
115. Burney, G. A. (1968) *Nucl. Appl.*, **4**, 217–21.
116. Yakovlev, G. N. and Gorbenko–Germanov, D. S. (1956) in *Proc. Int. Conf. on the Peaceful Uses of Atomic Energy*, Geneva, 1955, vol. 7, United Nations, New York, pp. 306–8.
117. Ellinger, F. H. and Zachariasen, W. H. (1954) *J. Phys. Chem.*, **58**, 405–8.
118. Hall, G. R. and Markin, T. L. (1957) *J. Inorg. Nucl. Chem.*, **4**, 137–42.
119. Fuger, J. and Cunningham, B. B. (1963) *J. Inorg. Nucl. Chem.*, **25**, 1423–9.
120. Lohr, H. R. and Cunningham, B. B. (1951) *J. Am. Chem. Soc.*, **73**, 2025–8; (1950) USAEC Report AECD-2902, University of California Radiation Laboratory.
121. Weigel, F., Wishnevsky, V., and Hauske, H. (1976) in *Transplutonium* 1975, *Proc. 4th Int. Symp.*, Baden-Baden, Sept. 13–17, 1975, (eds W. Müller and R. Lindner), North-Holland, Amsterdam, pp. 217–26.
122. Bagnall, K. W., Laidler, J. B., and Stewart, M. A. A. (1968) *J. Chem. Soc.* A, 133–6.
123. Bagnall, K. W., Laidler, J. B., and Stewart, M. A. A. (1967) *Chem. Commun.*, **1**, 24–5.
124. Marcus, Y. and Shiloh, M. (1969) *Israel J. Chem.*, **7**, 31–43.
125. Marcus, Y. and Bomse, M. (1970) *Israel J. Chem.*, **8**, 901–11.
126. Shiloh, M., Givon, M., and Marcus, Y. (1969) *J. Inorg. Nucl. Chem.*, **31**, 1807–14.
127. Barbanel, Yu. A., Gorskii, A. G., and Kotlin, V. P. (1971) *Radiokhimiya*, **13**, 305–7; (1971) *Sov. Radiochem.*, **13**, 314–16; (1976) *J. Inorg. Nucl. Chem.*, Suppl., 79–84.
128. Vodavatov, V. A., Kolokoltsov, V. G., Kovaleva, T. V., Mashirov, L. G., Suglobov, D. N., and Sles, V. G. (1976) in *Transplutonium 1975, Proc. Int. Symp.*, Baden-Baden, Sept. 13–17, 1975 (eds W. Müller and R. Lindner), North-Holland, Amsterdam, pp. 247–56.
129. Burnett, J. L. (1966) *J. Inorg. Nucl. Chem.*, **28**, 2454–6; (1965) *Trans. Am. Nucl. Soc.*, **8**, 335.
130. Jones, M. E. (1951) *The Vapor Pressure of Americium Trifluoride* (Thesis), USAEC Report UCRL-1438, University of California Radiation Laboratory.
131. Carniglia, S. C. and Cunningham, B. B. (1955) *J. Am. Chem. Soc.*, **77**, 1451–3.
132. Asprey, L. B. (1954) *J. Am. Chem. Soc.*, **76**, 2019–20.
133. Asprey, L. B. and Keenan, T. K. (1958) *J. Inorg. Nucl. Chem.*, **7**, 27–31.
134. Conner, W. V. (1971) *J. Less Common Metals*, **25**, 379–84; (1968) USAEC Report RFP-1188, Dow Chemical Co., Rocky Flats.
135. Yakovlev, G. N. and Kosyakov, V. N. (1958) *Proc. Second Int. Conf. on the Peaceful Uses of Atomic Energy*, Geneva, 1958, United Nations, New York, vol. 7, pp. 363–8, vol. 28, pp. 373–84.
136. Chudinov, E. G. and Choporov, D. Ya. (1970) *At. Energ. (USSR)*, **28**, 62–4; (1970) *Sov. At. Energy*, **28**, 71–3.
137. Keenan, T. K. (1968) *Inorg. Nucl. Chem. Lett.*, **4**, 381–4.
138. Keller, C. and Schmutz, H. (1964) *Z. Naturf. B*, **19**, 1080.
139. Schmutz, H. (1966) *Untersuchungen in den Systemem Alkalifluorid-Lanthaniden/Actinidenfluorid (Li, Na, K, Rb-La, S. E., Y/Np, Pu, Am)*, West German Report KFK-431.
140. Asprey, L. B. and Penneman, R. A. (1962) *Inorg. Chem.*, **1**, 134–6.

141. Keenan, T. K. (1966) *Inorg. Nucl. Chem. Lett.*, **2**, 153–6.
142. Keenan, T. K. (1967) *Inorg. Nucl. Chem. Lett.*, **3**, 391–6.
143. Keenan, T. K. (1966) *Inorg. Nucl. Chem. Lett.*, **2**, 211–14.
144. Keenan, T. K. (1967) *Inorg. Nucl. Chem. Lett.*, **3**, 463–7.
145. Kruse, F. H. and Asprey, L. B. (1962) *Inorg. Chem.*, **1**, 137–9.
146. Asprey, L. B., Ellinger, F. H., and Zachariasen, W. H. (1954) *J. Am. Chem. Soc.*, **76**, 5235–7.
147. Keenan, T. K. (1965) *Inorg. Chem.*, **4**, 1500–1.
148. Keller, C. (1963) *Nukleonik*, **5**, 41–8.
149. Katz, J. J. and Seaborg, G. T. (1957) *The Chemistry of the Actinide Elements*, Methuen, London, p. 349.
150. Olson, W. M. and Mulford, R. N. R. (1966) *J. Phys. Chem.*, **70**, 2934–7.
151. Roddy, J. W. (1973) *J. Inorg. Nucl. Chem.*, **35**, 4141–8.
152. Buijs, K. and Louwrier, K. P. (1966) *J. Inorg. Nucl. Chem.*, **28**, 2463–4.
153. Haire, R. G., Lloyd, M. H., Milligan, W. O., and Beasley, M. C. (1977) *J. Inorg. Nucl. Chem.*, **39**, 843–7.
154. Haire, R. G. and Fahey, J. A. (1977) *J. Inorg. Nucl. Chem.*, **39**, 837–41.
155. Weaver, B. and Shoun, R. R. (1971) in *Proc. 9th Rare Earth Research Conf.*, Oct. 10–14, 1971, Blacksburg, Va., USAEC Report CONF-711001, vol. 1, p. 322.
156. Cunningham, B. B. (1949) in *The Transuranium Elements* (eds G. T. Seaborg and J. J. Katz), Natl. Nucl En. Ser., Div. IV, 14B, McGraw-Hill, New York, pp. 1363–70.
157. Penneman, R. A., Coleman, J. S., and Keenan, T. H. (1961) *J. Inorg. Nucl. Chem.*, **17**, 138–45.
158. Asprey, L. B., Keenan, T. K., and Kruse, F. H. (1964) *Inorg. Chem.*, **3**, 1137–40.
159. Erdmann, B. (1971) *Darstellung von Actiniden/Lanthaniden-Edelmetall (Pt, Pd, Ir, Rh) – Legierungsphases durch Gekoppelte Reduktion*, West German Report KFK-1444; Rebizant, J. and Benedict, U. (1978) *J. Less Common Metals*, **58**, 31–3.
160. Erdmann, B. and Keller, C. (1971) *Inorg. Nucl. Chem. Lett.*, **7**, 675–83.
161. Erdmann, B. and Keller, C. (1973) *J. Solid State Chem.*, **7**, 40–8.
162. Tabuteau, A. and Pages, M. (1978) *J Solid State Chem.*, **26**(2), 153–8.
163. Tabuteau, A., Pages, M., and Freundich, W. (1972) *Radiochem. Radioanal. Lett.*, **12**, 139–44.
164. Lam, D. J. and Mitchell, A. W. (1972) *J. Nucl. Mater.*, **44**, 279–84.
165. Akimoto, Y. (1967) *J. Inorg. Nucl. Chem.*, **29**, 2650–2.
166. *Chemistry Division Semiannual Report for December* 1958 *Through May* 1959, USAEC Report UCRL-8867, University of California Radiation Laboratory.
167. *Chemistry Division Semiannual Report for June Through December* 1959, USAEC Report UCRL-9093, University of California Radiation Laboratory.
168. Charvillat, J. P., Benedict, U., Damien, D., de Novion, Ch., Wojakowski, A., and Müller, W. (1976) in *Transplutonium 1975, Proc. 4th Int. Symp.*, Baden-Baden, Sept. 13–17, 1975 (eds W. Müller and R. Lindner), North-Holland, Amsterdam, pp. 79–93; (1977) *Rev. Chim. Minér.*, **14**, 178–88.
169. Zachariasen, W. H. (1949) *Acta Crystallogr.*, **2**, 288–91; *Phys. Rev.*, **73**, 1104.
170. Templeton, D. H. and Dauben, C. H. (1953) *J. Am. Chem. Soc.*, **75**, 4560–2; (1953) USAEC Report UCRL-2101, University of California Radiation Laboratory.
171. Chikalla, T. D., McNeilly, C. E., Bates, J. L., and Rasmussen, J. J. (1973) in *Proc. Int. Colloq. on High Temperature Phase Transformations*, CNRS Publ. no. 205, pp. 351–60.
172. Chikalla, T. D. and Eyring, L. (1968) *J. Inorg. Nucl. Chem.*, **30**, 133–45.

173. Berndt, U., Tanamas, R., Maier, D., and Keller, C. (1974) *Inorg. Nucl. Chem. Lett.*, **10**, 315–21.
174. Keller, C. and Berndt, U. (1976) in *Transplutonium 1975, Proc. 4th Int. Symp.*, Baden-Baden, Sept. 13–17, 1975 (eds W. Müller and R. Lindner), North-Holland, Amsterdam, pp. 85–93.
175. Eyring, L., Lohr, H. R., and Cunningham, B. B. (1952) *J. Am. Chem. Soc.*, **74**, 1186–90; (1949) USAEC Report UCRL-327, University of California Radiation Laboratory.
176. Hurtgen, C. and Fuger, J. (1977) *Inorg. Nucl. Chem. Lett.*, **13**, 179–88.
177. Keller, C., Koch, L., and Walter, K. H. (1965) *J. Inorg. Nucl. Chem.*, **27**, 1205–23, 1225–32.
178. Hoekstra, H. R. and Gebert, E. (1978) *Inorg. Nucl. Chem. Lett.*, **14**, 189–91.
179. Keller, C. (1964) *Uber die Festkörperchimie der Actinides-Oxide*, West German Report KFK-225.
180. Mosley, W. C. (1970) in *Plutonium 1970 and Other Actinides, Proc. 4th Int. Conf. on Plutonium and Other Actinides*, Santa Fe, N. Mex., Oct. 5–9, 1970, (ed. W. N. Miner), Nuclear Materials, vol. 17; (1970) USAEC Report CONF-701001, pts I and II.
181. Radzewitz, H. (1966) *Festkörperchemische Untersuchungen über die Systeme* $SeO_{1.5}$–ZrO_2 (HfO_2), $AmO_{1.5}$–ZrO_2 (HfO_2, ThO_2)–O_2, *und* TiO_2–NpO_2 (PuO_2), West German Report KFK-433.
182. Keller, C. (1965) *J. Inorg. Nucl. Chem.*, **27**, 321–7.
183. Keller, C., Berndt, U., Debbabi, M., and Engerer, H. (1972) *J. Nucl. Mater.*, **42**, 23–31.
184. Damien, D. and Jove, J. (1971) *Inorg. Nucl. Chem. Lett.*, **7**, 685–8.
185. Burns, J. H. and Baybarz, R. D. (1972) *Inorg. Chem.*, **11**, 2233–7.
186. Yakovlev, G. N., Gorbenko-Germanov, D. S., Zenkova, R. A., Razbitnoi, V. L., and Kazanskii, K. S. (1958) *J. Gen. Chem. USSR*, **28**, 2653.
187. Staritzky, E. and Walker, D. I. (1952) *Optical Properties of Some Compounds of Uranium, Plutonium, and Related Elements*, USAEC Report LA-1439, Los Alamos Scientific Laboratory.
188. Ueno, K. and Hoshi, M. (1971) *J. Inorg. Nucl. Chem.*, **33**, 2631–3.
189. Damien, D. (1971) *Inorg. Nucl. Chem. Lett.*, **7**, 291–7.
190. Zachariasen, W. H. (1949) *Acta Crystallogr.*, **2**, 57–60.
191. Damien, D., Marcon, J. P., and Jove, J. (1972) *Inorg. Nucl. Chem. Lett.*, **8**, 317–20; (1976) *Bull. Int. Sci. Tech. Iommes. Energ. At. (Fr.)*, **217**, 67; (1975) *Radiochem. Radioanal. Lett.*, **23**, 145–54.
192. Burns, J. H., Damien, D., and Haire, R. G. (1979) *Acta Crystallogr. B*, **35**, 143–4.
193. Damien, D. and Charvillat, J. P. (1972) *Inorg. Nucl. Chem. Lett.*, **8**, 705–8.
194. Marcus, Y. and Cohen, D. (1966) *Inorg. Chem.*, **5**, 1740–3.
195. Weigel, F., Wittmann, F. D., and Marquart, R. (1977) *J. Less Common Metals*, **56**, 47–53.
196. Aldred, A. T., Dunlap, B. D., Lam, D. J., and Shenoy, G. K. (1976) in *Transplutonium 1975, Proc. 4th Int. Symp.*, Baden-Baden, Sept. 13–17, 1975 (eds W. Müller and R. Lindner), North-Holland, Amsterdam, pp. 191–5.
197. Asprey, L. B., Stephanou, S. E., and Penneman, R. A. (1950) *J. Am. Chem. Soc.*, **72**, 1425–6; (1954) US Patent no. 2681 923.
198. Asprey, L. B., Stephanou, S. E., and Penneman, R. A. (1951) *J. Am. Chem. Soc.*, **73**, 5715–17.
199. Asprey, L. B., Stephanou, S. E., and Penneman, R. A. (1954) US Patent no. 2681 923.
200. Keller, C. and Schrock, H. (1969) *J. Inorg. Nucl. Chem.*, **31**, 1121–32.

201. Karraker, D. G. (1976) in *Transplutonium 1975, Proc. 4th Int. Symp.*, Baden-Baden, Sept. 13–17, 1975 (eds W. Müller and R. Lindner), North-Holland, Amsterdam, pp. 131–5.
202. Baumgärtner, F., Fisher, E. O., Kanellakopulos, B., and Laubereau, P. (1966) *Angew. Chem.*, **78**, 112–13; (1966) *Angew. Chem. Int. Edn*, **5**, 134–5; (1977) *J. Inorg. Nucl. Chem.*, **39**, 87–9.
203. Seaborg, G. T. (1972) *Pure Appl. Chem.*, **30**, 539–49.
204. Kanellakopulos, B. (1979) in *Organometallics of the f-Elements* (eds T. J. Marks and R. D. Fischer), Reidel, Dordrecht, pp. 1–35.
205. Moore, G. E. (ed.) (1970) *Chemistry Division Annual Progress Report for Period Ending May* 20, 1970, USAEC Report ORNL-4581, Oak Ridge National Laboratory.
206. Kanellakopulos, B., Fisher, E. O., Dornberger, E., and Baumgärtner, F. (1970) *J. Organometal. Chem. (Amsterdam)*, **24**, 507–14.
207. Pappalardo, R., Carnall, W. T., and Fields, P. R. (1969) *J. Chem. Phys.*, **51**, 842–3.
208. Nugent, L. J., Laubereau, P. G., Werner, G. K., and Vander Sluis, K. L. (1971) *J. Organometal. Chem. (Amsterdam)*, **27**, 365–72.
209. Fischer, R. D., Laubereau, P., and Kanellakopulos, B. (1971) in *Third Int. Transplutonium Element Symp.*, Argonne, Ill., Oct. 20–22, 1971; Report CONF-711078 (Abstracts).
210. Danford, M. D., Burns, J. H., Higgins, C. E., Stokeley, J. R., Jr, and Baldwin, W. H. (1970) *Inorg. Chem.*, **9**, 1953–5.
211. Sakanoue, M. and Amano, R. (1976) in *Transplutonium 1975, Proc. 4th Int. Symp.*, Baden-Baden, Sept. 13–17, 1975 (eds W. Müller and R. Lindner), North-Holland, Amsterdam, pp. 123–9.
212. Burns, J. H. and Danford, M. D. (1969) *Inorg. Chem.*, **8**, 1780–4.
213. Bagnall, K. W. (1972) in ref. 4, vol. 4, part C, p. 264.
214. Keller, C., Eberle, S. H., and Mosdzelewski, K. (1965) *Radiochim. Acta*, **4**, 141–5; (1966) *Radiochim. Acta*, **5**, 185–8.
215. Lebedev, I. A., Pirozhkov, S. V., Razbitnoi, V. M., and Yakovlev, G. N. (1960) *Radiokhimiya*, **2**, 351–6; (1960) *Sov. Radiochem.*, **2**, 89–94.
216. Burney, G. A. and Porter, J. A. (1967) *Inorg. Nucl. Chem. Lett.*, **3**, 79–85.
217. Chikalla, T. D. and Eyring, L. (1967) *J. Inorg. Nucl. Chem.*, **29**, 2281–93.
218. Staritzky, E. and Truitt, A. L. (1954) in *The Actinide Elements* (eds G. T. Seaborg and J. J. Katz), Natl Nucl. En. Ser., Div. IV, 14A, McGraw-Hill, New York, ch. 19.
219. Baybarz, R. D. (1960) *Preparation of Americium Dioxide by Thermal Decomposition of Americium Oxalate in Air*, USAEC Report ORNL-3003, Oak Ridge National Laboratory.
220. Markin, T. L. (1958) *J. Inorg. Nucl. Chem.*, **7**, 290–2.
221. Weigel, F., Ollendorff, W., Scherer, V., and Hagenbruch, R. (1966) *Z. Anorg. Allg. Chem.*, **345**, 119–28.
222. Weigel, F. and ter Meer, N. (1971) *Z. Naturf. B*, **26**, 504–12.
223. Lebedev, I. A., Pirozhkov, S. V., and Yakovlev, G. N. (1960) *Radiokhimiya*, **2**, 549–58; (1962) *Radiokhimiya*, **4**, 304–8; (1960) *Sov. Radiochem.*, **2**, 39–47; (1962) *Sov. Radiochem.*, **4**, 273–5.
224. Davydov, A. V., Myasoedov, B. F., and Travnikov, S. S. (1975) *Dokl. Akad. Nauk SSSR*, **225**, 1075–8; (1975) *Dokl. Acad. Sci. USSR*, **224–225**, 672–4.

225. Lux, F. (1973) in *Proc. Tenth Rare Earth Research Conf.*, Carefree, Ariz., April 30–May 3, 1973 (eds C. J. Kevane and T. Moeller), pp. 871–80; USAEC Report CONF-730402, pt 2.
226. Eberle, S. H. and Robel, W. (1970) *Inorg. Nucl. Chem. Lett.*, **6**, 359–65.
227. Robel, W. (1970) *Complex Compounds of Hexavalent Actinides with Pyridine Carboxylic Acids*, West German Report KFK-1070.
228. Krot, N. N., Shilov, V. P., Nikolaevskii, V. B., Nikaev, A. K., Gel'man, A. D., and Spitsyn, V. I. (1974) *Dokl. Akad. Nauk SSSR*, **217**(3), 589–92; (1974) USAEC Report ORNL-tr-2828; (1974) *Dokl. Acad. Sci. USSR*, **217**, 525–7.
229. Keenan, T. H. (1959) *J. Chem. Educ.*, **36**, 27–31.
230. Milyukova, M. S., Litvina, M. N., and Myasoedov, B. F. (1980) *Radiochem. Radioanal. Lett.*, **44**(4), 259–68.
231. Désiré, B., Hussonois, M., and Guillaumont, R. (1969) *C. R. Acad. Sci. Paris C*, **269**, 448–51.
232. Burns, J. H. and Baldwin, W. H. (1977) *Inorg. Chem.*, **16**, 289–94.
233. Shalinets, A. B. and Stepanov, A. V. (1971, 1972) *Radiokhimiya*, **13**, 566–70; **14**, 280–3; *Sov. Radiochem.*, **13**, 583–6; **14**, 290–3.
234. Korotkin, Yu. S. (1973) *Radiokhimiya*, **15**, 766–72; (1973) *Sov. Radiochem.*, **15**, 682–5, 677–81, 776–81.
235. Nikolaevskii, V. B., Shilov, V. P., Krot, N. N., and Peretrukhin, V. F. (1975) *Radiokhimiya*, **17**, 431–3; (1975) *Sov. Radiochem.*, **17**, 420–2.
236. Myasoedov, B. F., Lebedev, I. A., and Milyukova, M. S. (1977) *Rev. Chem. Minér.*, **14**, 160–71.
237. Hara, M. (1970) *Bull. Chem. Soc. Jap.*, **43**, 89–94.
238. Nugent, L. J., Baybarz, R. D., Burnett, J. L., and Ryan, J. L. (1976) *J. Inorg. Nucl. Chem.*, Suppl., 37–9.
239. Cohen, D. (1972) *Inorg. Nucl. Chem. Lett.*, **8**, 533–5.
240. Zaitseva, V. P. (1971) *Radiokhimiya*, **13**, 658–9; (1971) *Sov. Radiochem.*, **13**, 679.
241. Fuger, J., Spirlet, J. C., and Müller, W. (1972) *Inorg. Nucl. Chem. Lett.*, **8**, 709–23.
242. Fuger, J. and Oetting, F. L. (1976) *The Chemical Thermodynamics of Actinide Elements and Compounds*, part 2, *The Actinide Aqueous Ions*, IAEA, Vienna.
243. Martinot, L. and Fuger, J. (1985) *Oxidation–Reduction Potentials of Aqueous Solutions: A Selective and Critical Source Book* (eds A. Bard, R. Parsons, and J. Jordan).
244. Penneman, R. A. and Asprey, L. B. (1950) *The Formal Potential of the Am(V)–Am(VI) Couple*, USAEC Report AECU-936, Los Alamos Scientific Laboratory.
245. Nugent, L. J., Baybarz, R. D., and Burnett, J. L. (1969) *J. Phys. Chem.* **73**, 1177–8.
246. Nugent, L. J., Baybarz, R. D., Burnett, J. L., and Ryan, J. L. (1973) *J. Phys. Chem.*, **77**, 1528–39.
247. Jove, J. and Pages, M. (1972) *Radiochem. Radioanal. Lett.*, **11**, 7–17.
248. David, F. (1970) *C. R. Acad. Sci. Paris*, **271**, 440–2.
249. Jorgensen, C. K. (1968) *Chem. Phys. Lett.*, **2**, 549–50.
250. Gunn, S. R. and Cunningham, B. B. (1957) *J. Am. Chem. Soc.*, **79**, 1563–5.
251. Nugent, L. J., Baybarz, R. D., Burnett, J. L., and Ryan, J. L. (1971) *J. Inorg. Nucl. Chem.*, **33**, 2503–30.
252. Gunn, S. R. (1954) *Thermodynamics of the Aqueous Ions of Americium* (Thesis),

USAEC Report UCRL-2541, University of California, Lawrence Radiation Laboratory.
253. Myasoedov, B. F., Lebedev, I. A., Frankel, V. Ya., and Vyatkina, I. I. (1974) *Radiokhimiya*, **16**, 822–7; (1974) *Sov. Radiochem.*, **16**, 803–7.
254. Nugent, L. J. (1975) *J. Inorg. Nucl. Chem.*, **37**, 1767–70.
255. Yanir, E., Givon, M., and Marcus, Y. (1959) *Inorg. Nucl. Chem. Lett.*, **6**, 415–19.
256. Shilov, V. P. (1976) *Radiokhimiya*, **18**, 659–60; (1976) *Sov. Radiochem.*, **18**, 567–8.
257. Nikolaevskii, V. B., Shilov, V. P., and Krot, N. N. (1974) *Radiokhimiya*, **16**, 122–3; (1974) *Sov. Radiochem.*, **16**, 120–1.
258. Peretrukhin, V. F., Nikolaevskii, V. B., and Shilov, V. P. (1974) *Radiokhimiya*, **16**, 833–6; (1974) *Sov. Radiochem.*, **16**, 813–15.
259. Zaitsev, A. A., Kosyakov, V. N., Rykov, A. G., Sobolov, Yu. P., and Yakovlev, G. N. (1960) *Sov. At. Energy*, **7**, 562–9.
260. Yakovlev, G. N., Zaitsev, A. A., Kosyakov, V. N., Rykov, A. G., and Sobolev, Yu. B. *Izdaniya AN SSSR*, **195**, 326, cited in ref. 259.
261. Yanir, E., Givon, M., and Marcus, Y. (1969) *Inorg. Nucl. Chem. Lett.*, **5**, 369–72.
262. Myasoedov, B. F., Mikhailov, V. M., Lebedev, I. A., Koiro, O. E., and Frenkel, V. Ya. (1973) *Radiochem. Radioanal. Lett.*, **14**, 17–24.
263. Myasoedov, B. F., Milyukova, M. S., Lebedev, I. A., Litvina, M. N., and Frenkel, V. Ya. (1975) *J. Inorg. Nucl. Chem.*, **37**, 1475–8.
264. Rykov, A. G., Ermakov, V. A., Timofeev, G. A., Chistyakov, V. M., and Yakovlev, G. N. (1970) *Radiokhimiya*, **13**, 832–6; (1970) *Sov. Radiochem.*, **13**, 858–61.
265. Jorgensen, C. K. (1977) *Rev. Chim. Minér.*, **14**, 127–38.
266. Coleman, J. S. (1963) *Inorg. Chem.*, **2**, 53–7.
267. Newton, T. W. (1975) *The Kinetics of the Oxidation–Reduction Reactions of Uranium, Neptunium, Plutonium, and Americium Ions in Aqueous Solutions*, ERDA Critical Review Series, TID-26506.
268. Hindman, J. C. (1958) in *Proc. Second Int. Conf. on the Peaceful Uses of Atomic Energy*, Geneva, 1958, vol. 28, United Nations, New York, pp. 349–60.
269. Newton, T. W. and Baker, F. (1967) in *Lanthanide/Actinide Chemistry* (ed. R. F. Gould), ACS Adv. Chem. Ser., American Chemical Society, Washington DC, pp. 268–95.
270. Gourisse, D. (1966) *Cinetique des Reactions D'Oxydo-Reduction des Elements Transuraniens en Solution*, French Report CEA-R-3079.
271. Woods, M. and Sullivan, J. C. (1974) *Inorg. Chem.*, **13**, 2774–5.
272. Ermakov, V. A., Rykov, A. G., Timofeev, G. A., and Yakovlev, G. N. (1971, 1973, 1974) *Radiokhimiya*, **13**, 826–32; **15**, 380–5; **16**, 810–17; *Sov. Radiochem.*, **13**, 851–7; **15**, 381–5; **16**, 793–8.
273. Woods, M., Cain, A., and Sullivan, J. C. (1974) *J. Inorg. Nucl. Chem.*, **36**, 2605–7.
274. Zaitsev, A. A., Kosyakov, V. N., Rykov, A. G., Sobolev, Yu. P., and Yakovlev, G. N. (1960) *Radiokhimiya*, **2**(3), 348–50; (1960) *Sov. Radiochem.*, **2**, 86–8.
275. Damien, N. and Pages, M. (1969) in *Rapport Semestriel du Department de Chimie No. 6, Juin* 1968–*Novembre* 1968, French Report CEA-N-1148, p. 407.
276. Damien, N. and Pages, M. (1970) in *Rapport Semestriel du Department de Chimie No. 8, Juin* 1969–*Novembre* 1969, French Report CEA-N-1341, p. 472.
277. Blokhin, N. B., Ermakov, V. A., and Rykov, A. G. (1973) *Radiokhimiya*, **16**, 189–92; (1973) *Sov. Radiochem.*, **16**, 191–3.

278. Rykov, A. G., Timofeev, G. A., and Chistyakov, V. M. (1973) *Radiokhimiya*, **15**, 872–4; (1973) *Sov. Radiochem.*, **15**, 883–5.
279. Chistyakov, V. M., Ermakov, V. A., and Rykov, A. G. (1974) *Radiokhimiya*, **16**, 553–5; (1974) *Sov. Radiochem.*, **16**, 545–7.
280. Blokhin, N. B., Ermakov, V. A., and Rykov, A. G. (1974) *Radiokhimiya*, **16**, 551–3; (1974) *Sov. Radiochem.*, **16**, 543–4.
281. Carnall, W. T. and Fields, P. R. (1967) in *Lanthanide/Actinide Chemistry* (ed. R. F. Gould) (ACS Adv. Chem. Ser.), American Chemical Society, Washington DC, pp. 86–101.
282. Conway, J. G. (1964) *J. Chem. Phys.*, **40**, 2504–7; (1963) USAEC Report UCRL-11099, University of California, Lawrence Laboratory.
283. Carnall, W. T. and Wybourne, B. G. (1964) *J. Chem. Phys.*, **40**, 3428–33.
284. Carnall, W. T., Fields, P. R., and Wybourne, B. G. (1964) *J. Chem. Phys.*, **41**, 2195–6.
285. Asprey, L. B. and Penneman, R. A. (1961) *J. Am. Chem. Soc.*, **83**, 2200.
286. Werner, L. B. and Perlman, I. (1950) *J. Am. Chem. Soc.*, **73**, 495–6; (1950) USAEC Report AECD-2898.
287. Hall, G. R. and Herniman, P. D. (1954) *J. Chem. Soc.*, 2214.
288. Stephanou, S. E., Nigon, J. P., and Penneman, R. A. (1953) *J. Chem. Phys.*, **21**, 42–45; (1952) USAEC Report LADC-1147, Los Alamos Scientific Laboratory.
289. Hall, G. R. and Markin, T. L. (1957) *J. Inorg. Nucl. Chem.*, **4**, 296–303.
290. Bell, J. T. (1969) *J. Inorg. Nucl. Chem.*, **31**, 703–10.
291. Varga, L. P., Baybarz, R. D., Reisfeld, M. J., and Asprey, L. B. (1973) *J. Inorg. Nucl. Chem.*, **35**, 2775–85.
292. Kanellakopulos, B., Aderhold, C., Dornberger, E., Müller, W., and Baybarz, R. D. (1978) *Radiochim. Acta*, **25**, 89–92.
293. Jones, L. H. and Penneman, R. A. (1953) *J. Chem. Phys.*, **21**, 542–4.
294. Ellinger, F. H., Johnson, K. A., and Struebing, V. O. (1966) *J. Nucl. Mater.*, **20**, 83–6.
295. Martell, A. E. and Sillen, L. G. (1964) *Stability Constants of Metal–Ion Complexes*, Special Publication no. 17, 2nd edn, The Chemical Society, London.
296. Marcus, Y., Givon, M., and Shiloh, M. (1965) *Proc. Third Int. Conf. on the Peaceful Uses of Atomic Energy*, Geneva, 1964, vol. 10, United Nations, New York, pp. 588–98.
297. Gel'man, A. D., Moskvin, A. I., Zaitsev, L. M., and Medfod'eva, M. P. (1967) *Complex Compounds of Transuranides* (Engl. transl.), Israel Program for Scientific Translations, Jerusalem.
298. Rogozina, E. M., Konkina, L. F., and Popov, D. K. (1974) *Radiokhimiya*, **16**, 383–6; (1974) *Sov. Radiochem.*, **16**, 382–5.
299. Musikas, C. (1973) *Radiochem. Radioanal. Lett.*, **13**, 255–8.
300. Moskvin, A. I. (1967, 1971, 1973) *Radiokhimiya*, **9**, 718–20; **13**, 221–3, 224–30, 575–81, 668–74; **15**, 504–13; *Sov. Radiochem.*, **9**, 677–9; **13**, 220–3, 224–9, 592–7, 688–93; **15**, 511–18.
301. Moore, F. L. (1961) *Anal. Chem.*, **33**, 748–51.
302. De Carvalho, R. G. and Choppin, G. R. (1967) *J. Inorg. Nucl. Chem.*, **29**, 737–43.
303. Vdovenko, V. M., Kolokol'tsov, V. B., and Stebunov, O. B. (1966) *Radiokhimiya*, **8**, 286–90; (1966) *Sov. Radiochem.*, **8**, 266–9.
304. Makarova, T., Stepanov, A. V., and Shestakov, B. I. (1973) *Zh. Neorg. Khim.*, **18**, 1485–8; (1973) *Russ. J. Inorg. Chem.*, **18**, 783–5.
305. Bertha, E. L. and Choppin, G. R. (1978) *J. Inorg. Nucl. Chem.*, **40**, 655–8.
306. Cilindro, L. G. and Keller, C. (1974) *Radiochim. Acta*, **21**, 29–32.

307. Hubert, S., Hussonois, M., Brillard, L., and Guillaumont, R. (1976) *Transplutonium 1975, Proc. 4th Int. Symp.*, Baden-Baden, Sept. 13–17, 1975 (eds W. Müller and R. Lindner), North-Holland/American Elsevier, New York, pp. 109–18.
308. Shilov, V. P., Nikalagevsky, V. B., and Krot, N. N. (1976) *Chemistry of Transuranium Elements* (eds V. I. Spitsyn and J. J. Katz), Pergamon Press, New York, pp. 225–8.
309. Rozen, A. M., Nikolotova, Z. I., Kartasheva, N. A., and Yudina, K. S. (1976) *Americium and Curium Complexing with Organic Dioxides*, Report INIS-mf-3283; see *INIS Atomindex*, **8**, 295483.
310. Choppin, G. R. *et al.* (1976) in *Transplutonium 1975, Proc. 4th Int. Symp.*, Baden-Baden, Sept. 13–17, 1975 (eds W. Müller and R. Lindner), North-Holland, Amsterdam; (1965) *Inorg. Chem.*, **4**, 1250–4; (1965) *J. Inorg. Nucl. Chem.*, **27**, 1335–9; (1970) *J. Inorg. Nucl. Chem.*, **32**, 3283–8; (1972) *J. Inorg. Nucl. Chem.*, **34**, 3473–7.
311. Grigorescu-Sabau, C. S. (1972) *Uber die Temperaturabhangigkeit von Komplexgleichgewichten der Transplutone*, German Report KFK-1620.
312. Drobyshevskii, Iu. V., Prusakov, V. N., Serik, V. F., and Sokolov, V. B. (1980) *Radiokhimiya*, **22**(4), 591–4.
313. Morss, L. R. and Fuger, J. (1981) *J. Inorg. Nucl. Chem.*, **43**, 2059–64.
314. Lebedev, I. A., Frenkel, V. Ya., Kulyako, Yu. M., and Myasoedov, B. F. (1980) UDC 541.49:546.799.5, Plenum, New York; Koltunov, V. S. (1974) *Kinetics of Actinide Reactions*, Moscow, Atomizdat, p. 216.
315. Vasudeva Rao, P. R., Kusumakumari, M., and Patil, S. K. (1978) *Radiochem. Radioanal. Lett.* **33** (5–6), 305–14.
316. Karraker, D. G. (1977) *J. Inorg. Nucl. Chem.*, **39**, 87–9.
317. Erin, E. A., Kopytov, V. V., Rykov, A. G., and Kosyakov, V. N. (1979) *Radiokhimiya (Radkau)*, **21**, 63–7.
318. Hobart, D. E., Samhoun, K., and Peterson, J. R. (1982) *Radiochim. Acta*, **31**, 133–45.
319. Lundqvist, R. (1982) *Acta Chem. Scand. A*, **36**, 741–50.
320. Lawaldt, D. (1981) MS Thesis, Univ. of Munich; Weigel, F. (1981) private communication.
321. Werner, G. D. (1981) Doctoral Thesis, Univ. of Munich; Weigel, F. (1981) private communication.
322. Nugent, L. J., Burnett, J. L., and Morss, L. R. (1973) *J. Chem. Thermodyn.*, **5**, 665–75.
323. David, F., Samhoun, K., Guillaumont, R., and Edelstein, N. (1978) *J. Inorg. Nucl. Chem.*, **40**, 69–74.
324. Morss, L. R. (1983) *J. Less Common Metals*, **93**, 301–21.
325. Ward, J. W. and Hill, H. H. (1976) *Heavy Element Properties* (eds W. Müller and H. Blank), North-Holland, Amsterdam, pp. 65–79.
326. Morss, L. R. (1982) *Actinides in Perspective* (ed. N. Edelstein), Pergamon Press, Oxford, pp. 381–407.
327. Leger, J. M., Yacoubi, N., and Loriers, J. (1981) *J. Solid State Chem.*, **36**, 261–70.
328. Larson, D. T. and Haschke, J. M. (1981) *Inorg. Chem.*, **20**, 1945–50.
329. Baybarz, R. D., Asprey, L. B., Strouse, C. E., and Fukushima E. (1972) *J. Inorg. Nucl. Chem.*, **34**, 3427–31.
330. Meyer, G. (1983) *J. Less Common Metals*, **93**, 371–80.
331. Peretrukhin, V. F. and Spitsyn, V. I. (1982) *Izv. Akad. Nauk SSSR, Ser. Khim.*, **31**, 826–31.
332. Baybarz, R. D. (1973) *J. Inorg. Nucl. Chem.*, **35**, 4149–58.

333. Berry, J. W., Knighton, J. B., and Nannie, C. A. (1982) *Vacuum Distillation of Americium Metal*, USDOE Report RFP-3211.
334. Penneman, R. A. and Keenan, T. K. (1960) *The Radiochemistry of Americium and Curium*, National Academy of Sciences – National Research Council Report NAS-NS-3006.
335. Horwitz, E. P. (1980) private communication; see also Horwitz, E. P. *et al.* (1981) *Sep. Sci. Tech.*, **16**, 417–37.
336. Choppin, G. R. and Nash, K. L. (1977) *Rev. Chim. Minér.*, **14**, 230–6.
337. Bigelow, J. E., Collins, E. D., and King, L. J. (1979) in *Actinide Separations* (ACS Symp. Ser. 117), American Chemical Society, Washington DC, pp. 147–55.
338. Musikas, C., Germain, M., and Bathellier, A. (1980) in *Actinide Separations* (ACS Symp. Ser. 117), American Chemical Society, Washington DC, pp. 157–73.
339. Shannon, R. D. (1976) *Acta Crystallogr. A*, **32**, 751.
340. Penneman, R. A. and Eller, P. G. (1983) *Radiochim. Acta*, **32**, 81–7.
341. Sugar, J. (1974) *J. Chem. Phys.*, **60**, 4103.
342. Oetting, F. L., Rand, M. H., and Ackermann, R. J. (1976) in *The Chemical Thermodynamics of Actinide Elements and Compounds*, part 1, *The Actinide Elements*, IAEA, Vienna.
343. Müller, W., Reul, J., and Spirlet, J. C. (1972) *Atomwirtschaft*, **17**, 415.
344. Ward, J. W., Müller, W., and Kramer, G. F. (1976) in *Transplutonium 1975, Proc. 4th Int. Symp.*, Baden-Baden, Sept. 13–17, 1975 (eds W. Müller and R. Lindner), North-Holland, Amsterdam, pp. 161–71.
345. Stephens, D. R., Stromberg, H. D., and Lilley, E. M. (1968) *J. Phys. Chem. Solids*, **29**, 815–21.
346. Smith, J. L. and Haire, R. G. (1978) *Science*, **200**, 535–7.
347. Weigel, F., Wishnevsky, V., and Wolf, M. (1979) *J. Less Common Metals*, **63**, 81–6.
348. Volkov, T. F., Kapshukov, I. I., Visyashcheva, G. I., and Yakovlev, G. N. (1974) *Radiokhimiya*, **16**, 859–63, 863–7, 868–73; *Sov. Radiochem.*, **16**, 838–50.
349. Jove, J. and Pages, M. (1977) *Inorg. Nucl. Chem. Lett.*, **13**, 329–34.
350. Fahey, J. A., Turcotte, R. P., and Chikalla, T. D. (1974) *Inorg. Nucl. Chem. Lett.*, **10**, 459–65.
351. Wittmann, F. D. (1980) Doctoral Thesis, University of Munich; Weigel, F. (1981) private communication.
352. Roddy, J. W. (1973) *J. Inorg. Nucl. Chem.*, **35**, 4141–8.
353. Katz, J. J. and Gruen, D. M. (1949) *J. Am. Chem. Soc.*, **71**, 2106–12.
354. Kirin, I. S., Moskalev, P. N., and Mishin, V. Ya. (1967) *Zh. Obshch. Khim.*, **37**, 1065–8.
355. Nikolaevskii, V. B., Shilov, V. P., Krot, N. N., and Peretrukhin, V. F. (1975) *Radiokhimiya*, **17**, 426–30.
356. Sullivan, J. C., Gordon, S., Mulac, W. A., Schmidt, K. M., Cohen, D., and Sjoblom, R. (1976) *Inorg. Nucl. Chem. Lett.*, **12**, 599–601; (1978) *Inorg. Chem.*, **17**, 294–6.
357. Saprykin, A. S., Spitsyn, V. I., and Krot, N. N. (1976) *Dokl. Akad. Nauk SSSR*, **228**, 649–51.
358. Kosyakov, V. N., Timofeev, G. A., Erin, E. A., Andreev, V. I., Kopytov, V. V., and Simakin, G. A. (1977) *Radiokhimiya*, **19**, 511–17.
359. Ensor, D. D. and Choppin, G. R. (1980) *J. Inorg. Nucl. Chem.*, **42**, 1477–80.
360. Woods, M., Montag, T. A., and Sullivan, J. C. (1976) *J. Inorg. Nucl. Chem.*, **38**, 2059–61.
361. Fourest, B., Duplessis, J., and David, F. (1982) *C. R. Acad. Sci. Paris*, **294**, 1179–81.

362. Hobart, D. E., Samhoun, K., and Peterson, J. R. (1983) *Radiochim. Acta*, **31**, 139–45.
363. Bourges, J. Y., Guillaume, B., Koehly, G., Hobart, D. E., and Peterson, J. R. (1983) *Inorg. Chem.*, **22**, 1179–84.
364. Basile, L. J., Sullivan, J. C., Ferraro, J. R., and LaBonville, P. (1974) *Appl. Spectrosc.*, **28**, 142–5.
365. Basile, L. J., Ferraro, J. R., Mitchell, M. L., and Sullivan, J. C. (1978) *Appl. Spectrosc.*, **32**, 535–7.
366. Madic, C., Hobart, D. E., and Begun, G. M. (1983) *Inorg. Chem.*, **22**, 1494–503.
367. Endlestein, N. M., Navratil, J. D., and Schulz, W. W., eds (1985) *Americium and Curium Chemistry and Technology*. D. Reidel, Dordrecht, Holland.
368. Morss, L. R. and Sonnenberger, D. C. (1985) *J. Nucl. Mater.*, **130**, 266–72.
369. Nash, K. L. and Cleveland, J. M. (1984) *Radiochim. Acta*, **37**, 19–24.
370. Rai, D., Strickert, R. G., Moore, D. A., and Ryan, J. L. (1983) *Radiochim. Acta*, **33**, 201–6.

CHAPTER NINE

CURIUM

P. Gary Eller and Robert A. Penneman

9.1 INTRODUCTION

Curium, like americium, is a transplutonium element in which there is renewed interest. These elements are produced in plutonium power reactors and cause many of the long-term radiological and thermal problems associated with reactor waste storage and disposal. It is evident that such problems will become more acute, and a sounder understanding of the basic chemistry of these elements is mandated.

Several excellent reviews describe some chemical aspects of curium [1–6]. This chapter is an overview of curium chemistry with emphasis on recent advances.

Curium, element 96, is the element of highest atomic number that is available on the multigram scale. Even so, microchemical handling techniques are usually used [7, 8]. The element, unknown in nature, is named after Pierre and Marie Curie, by analogy with its lanthanide congener, gadolinium (named after the Finnish chemist, J. Gadolin). The discovery of curium preceded that of americium (element 95).

The first curium isotope, ^{242}Cm, was prepared by Seaborg, James, and Ghiorso in mid-1944 by cyclotron α bombardment of ^{239}Pu, and was identified by its characteristic α radiation [9]. Werner and Perlman separated the first weighable quantity of curium (40 μg of impure ^{242}Cm oxide), which was prepared by prolonged neutron irradiation of ^{241}Am [10].

Owing to the limited availability of long-lived isotopes (especially ^{248}Cm), the high radioactivity of its most common isotopes (^{242}Cm and ^{244}Cm), and its general occurrence in aqueous systems as a 3 + ion, considerably less physical and chemical information about curium is available than for americium.

9.2 NUCLEAR PROPERTIES

Properties of the known curium isotopes, which range in mass from 238 to 251, are summarized in Table 9.1. Electron binding energies, x-ray spectra, and L-shell fluorescence data for curium are available, as well as both α and spontaneous fission data [11–13]. Three isotopes (^{242}Cm, ^{244}Cm, and ^{248}Cm) are available in quantities sufficient for chemical study. Macroscopic studies with ^{242}Cm and ^{244}Cm are complicated by the high α activities of these isotopes (half-lives of 163 days and 18.11 years, respectively). The isotope ^{248}Cm is desirable for chemical studies (half-life 3.40×10^5 years). Approximately 100 mg of ^{248}Cm are

Table 9.1 *Nuclear properties of curium isotopes*[a]

Mass number	*Half-life*	*Mode of decay*	*Main radiations* (MeV)	*Method of production*
238	2.3 h	EC <90% α >10%	α 6.52	^{239}Pu(α, 5n)
239	2.9 h	EC	γ 0.188	^{239}Pu(α, 4n)
240	27 d	α	α 6.291 (71%)	^{239}Pu(α, 3n)
	1.9×10^6 yr	SF	6.248 (29%)	
241	32.8 d	EC 99.0% α 1.0%	α 5.939 (69%) 5.929 (18%) γ 0.472 (71%)	^{239}Pu(α, 2n)
242	162.9 d	α	α 6.113 (74.0%)	^{239}Pu(α, n)
	6.1×10^6 yr	SF	6.070 (26.0%)	^{242}Am daughter
243	28.5 yr	α 99.76% EC 0.24%	α 5.785 (73.5%) 5.742 (10.6%) γ 0.278 (14.0%)	^{242}Cm(n, γ)
244	18.11 yr	α	α 5.805 (76.4%)	multiple n capture
	1.35×10^7 yr	SF	5.764 (23.6%)	^{244}Am daughter
245	8.5×10^3 yr	α	α 5.362 (93.2%) 5.304 (5.0%) γ 0.175	multiple n capture
246	4.73×10^3 yr	α	α 5.386 (79%)	multiple n capture
	1.80×10^7 yr	SF β stable	5.343 (21%)	
247	1.56×10^7 yr	α	α 5.266 (14%) 4.869 (71%) γ 0.402 (72%)	multiple n capture
248	3.40×10^5 yr	α 91.74% SF 8.26%	α 5.078 (82%) 5.035 (18%)	multiple n capture
249	64.2 min	β^-	β^- 0.90 γ 0.634 (1.5%)	^{248}Cm(n, γ)
250	$< 1.13 \times 10^4$ yr	SF		multiple n capture
251	16.8 min	β^-	β^- 1.42 γ 0.543 (12%)	^{250}Cm(n, γ)

[a] See also refs 5, 12, 13, 151, and 152; *Nuclear Data Sheets*, Academic Press, New York, vol. 4 (1970) and vols 17–19 (1976); and Report ORNL-5146 (1976).

produced yearly after purification from parent ^{252}Cf. The practical limit for chemical operations with ^{248}Cm in glove boxes is 10–20 mg because of the significant neutron dose due to the 8% spontaneous fission of this isotope.

Both ^{242}Cm and ^{244}Cm have been used in radionuclide batteries as power sources (thermal and electrical) for space and medical applications [14]. The isotope ^{242}Cm has a specific heat output (122 $W\,g^{-1}$) about 43 times higher than that of ^{244}Cm (2.8 $W\,g^{-1}$) and a cake of $^{242}Cm_2O_3$ weighing a few grams can be photographed using its own incandescence for illumination. These isotopes provide convenient choices of energy sources for short-period/high-output and long-period/moderate-output applications. As a radioactive heat source, ^{242}Cm is a useful alternative to ^{210}Po. However, ^{238}Pu is now made on the kilogram scale from ^{237}Np and has supplanted both ^{242}Cm and ^{244}Cm for many such uses. The isotope ^{248}Cm has been a favored nuclide for accelerator studies attempting to form superheavy elements [150].

Most curium isotopes heavier than ^{244}Cm have longer half-lives but cannot be prepared isotopically pure by neutron capture, and, except for ^{248}Cm, isotope enrichment is accomplished in a mass separator. Approximately 1 kg of high-mass curium has received substantial neutron exposure at the Savannah River plant. The major isotopes formed are ^{246}Cm (54%), ^{244}Cm (34%), and ^{248}Cm (10%), with lesser amounts of the odd-mass isotopes, ^{245}Cm ($< 0.5\%$) and ^{247}Cm ($\sim 1.5\%$).

9.3 PREPARATION AND PURIFICATION

By far the greatest quantity of curium exists as the isotope ^{244}Cm, which has been produced on the several kilogram scale at the Savannah River plant [1, 14, 15]. This isotope is produced by successive neutron capture starting with ^{239}Pu (or better, with the higher-mass isotopes ^{242}Pu and ^{243}Am):

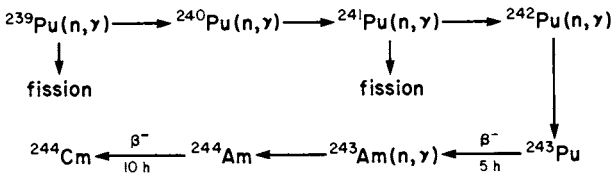

At Savannah River this reaction sequence is carried out in stages, the first involving progressive irradiation of Pu/Al alloys to build up ^{242}Pu and ^{243}Am and to reduce the ^{241}Pu content to about 1%. During this period, the heat from fission of ^{239}Pu and ^{241}Pu must be dissipated. After separation of the americium and plutonium, $AmO_2(PuO_2)/Al$ ceramic metals (cermets) are fabricated and irradiated further to produce the ^{244}Cm product. The ^{244}Cm yield is about 8% of the ^{239}Pu starting material.

To isolate ^{244}Cm, the irradiated material is dissolved in nitric acid and the tetravalent plutonium is removed by solvent extraction [14, 15]. The trivalent

species (americium, curium, and the lanthanides) remaining in the aqueous phase are then extracted with 50% tributyl phosphate (TBP) in kerosene and back-extracted into dilute acid. For purification from lanthanides, Am/Cm chlorides are extracted with tertiary amines from slightly acidic 11 M LiCl (Tramex process) [15], and back-extracted into aqueous 7 M HCl. Separation of curium from americium is achieved by adjusting the solution to a concentration of 10 g Am(Cm) per litre and 3.5 M K_2CO_3, oxidizing the Am(III) to Am(V) with potassium hypochlorite, peroxydisulfate, or ozone, and precipitating the double carbonate $K_5AmO_2(CO_3)_3$ at 85°C. A second precipitation is sometimes used to remove residual Am from the Cm solution.

The isotope ^{242}Cm is best obtained by neutron irradiation of ^{241}Am at an intermediate flux level:

$$^{241}\text{Am}(n,\gamma) \longrightarrow {}^{242}\text{Am} \xrightarrow[16\,\text{h}]{\beta^-\,(84\%)} {}^{242}\text{Cm}$$

High neutron fluxes diminish the yield of ^{242}Cm because of the increased fission of ^{242}Am. Following irradiation, the sample (in the form of an AmO_2/Al cermet) can be treated with hot sodium hydroxide to dissolve the aluminum. Dissolution in hydrochloric acid can also be used, in which case Al^{3+} must be removed prior to further processing. For small-scale separations the Am/Cm/lanthanide fraction is dissolved in hydrochloric acid; the solution is then made 11 M in LiCl, and passed through an anion-exchange column. Under these conditions, trivalent actinides (but not rare-earth elements) are retained on the column. Alternatively, a tertiary amine extractant can be substituted for the anion-exchange resin and this provides a group separation between actinides (extracted) and lanthanides [15]. A subsequent americium/curium separation step is then required.

The relatively stable isotope ^{248}Cm is obtained in multi-milligram quantities by milking aged, prepurified ^{252}Cf samples, which decay by α emission:

$$^{252}\text{Cf} \xrightarrow[2.6\,\text{yr}]{\alpha} {}^{248}\text{Cm}$$

This method routinely yields milligram amounts of ^{248}Cm with an isotopic purity of 97%. A sample containing 99.9% ^{248}Cm has been obtained [16]. Even in the 97% enriched samples, more than 99% of the alpha activity arises from ^{244}Cm and ^{246}Cm impurities. Small (microgram) amounts of ^{245}Cm have been separated from α decay products of ^{249}Cf, itself a daughter of ^{249}Bk.

Numerous other techniques, including high-pressure ion exchange, extraction chromatography, and di(2-ethylhexyl)phosphoric acid (HDEHP) extraction have also been used to effect Cm separation and purification [1, 15, 17–19, 156–158]. Pressurized displacement ion-exchange chromatography has been applied to large-scale ^{244}Cm/^{243}Am separation using Dowex 50 in Zn^{2+} form and DTPA (diethylenetriaminepentaacetic acid) as eluant [17]. Where sufficient quantities of Cm are present to give a substantial band, a pure curium cut can be obtained, since it leads the americium band. A combination of anion and cation exchange

was used successfully to separate about 1 g of ^{242}Cm from neutron-irradiated ^{241}Am [156].

9.4 ATOMIC PROPERTIES

9.4.1 General

The f^8s^2–f^7ds^2 energy difference for curium has been determined to be about 9700 cm^{-1} greater than that for the corresponding electronic states in gadolinium [20]. This is a reversal of the actinide–lanthanide relationship observed in the lighter actinides and corresponds to a change in sign for the f–d parameter coefficients. This situation is consistent with the increasing tendency of heavier actinides to resemble lanthanides in chemical behavior [20].

The great stability of the nf^7 configuration of Cm(III) and of Gd(III) is shown by their large M(III)–(IV) oxidation potentials (see Section 9.7.1 and Chapter 17). In contrast, it is noteworthy that the tendency of americium to attain the nf^7 configuration by assuming a divalent state is much weaker than that displayed by europium.

9.4.2 Absorption spectra

The spectra of the Cm^{3+} aquo ion and of a metastable Cm(IV) aqueous fluoride complex ion are shown in Figs 9.1 and 9.2. As is the case for Gd(III) [23], aqueous

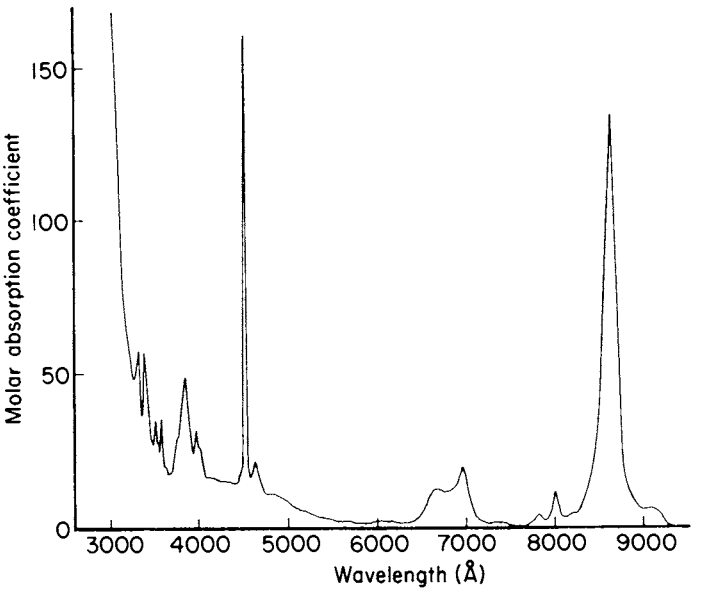

Fig. 9.1 *The absorption spectrum of Cm(IV) in 15 M CsF (aq).*

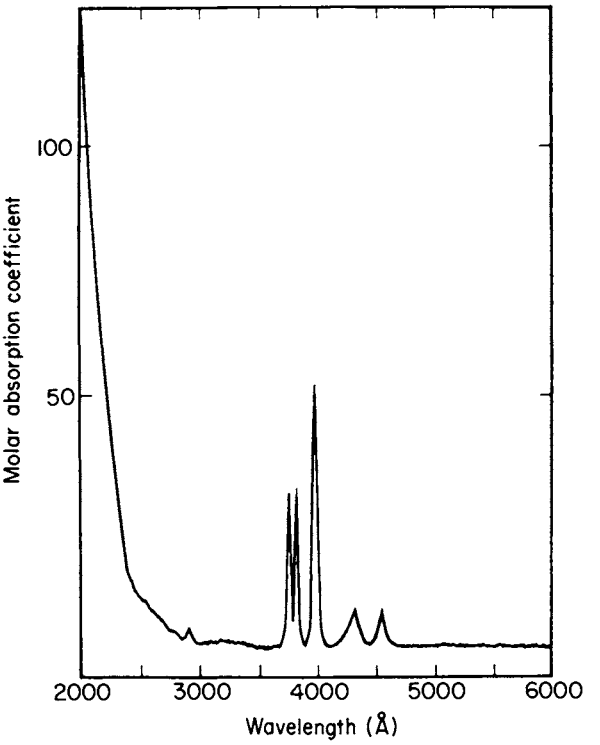

Fig. 9.2 *The absorption spectrum of aqueous Cm(III).*

solutions of Cm(III) have no absorption bands in the visible region, although intense absorptions are present in the ultraviolet [21, 22, 159]. Both aqueous Cm(III) and solid CmF_3 show well-defined spectra with a strong resemblance to that of GdF_3 [21].

Electronic transitions for Cm(III) are shifted 20–30 Å to longer wavelengths in solution compared to the solid state. Typically, addition of complexing ions produces a diminution of intensities, and small changes in band positions. The transition energies for CmF_3 are lower than for GdF_3, an effect attributed to weaker binding of f electrons in the actinide series. The spectra in both cases may be interpreted in terms of an nf^7 ground-state configuration. Recently the spectrum of $Cs_2NaCmCl_6$, which contains octahedrally coordinated Cm(III), was reported for both the solid and molten phases [22]. The most notable spectral effect is a sharp diminution in intensity due to the highly symmetric curium coordination compared to that of aqueous Cm(III).

Spectroscopic measurements have been performed on Cm doped into crystalline CaF_2 [24]. The trivalent curium occupies the cubic site and two different trigonal sites of the CaF_2 lattice. For each of the three sites, the crystal field splitting for Cm(III) is large and the g-value is within experimental error of

that for divalent Am in CaF_2. Cm(IV), formed by alpha irradiation, was also identified spectroscopically. Self-luminescence of Cm doped into SrF_2, BaF_2, and $SrCl_2$ has also been reported [160].

Varga and co-workers [25, 26] have reported calculations and estimates of free-ion spectroscopic parameters for Cm^{3+} and Cm^{4+}, allowing construction of intermediate spin–orbit coupling diagrams for f^7 and f^6 configurations. The treatment was based in part on a fitting of parameters for the Bk^{4+} ion [25, 26]. Values of the spectroscopic parameters obtained for Cm^{3+} were $F_2 = 251\ cm^{-1}$ and $\zeta = 2839\ cm^{-1}$, respectively. Analysis of nine ultraviolet bands for Cm^{4+} gave the derived values of $F_2 = 276\ cm^{-1}$ and of the spin–orbit coupling parameter $\zeta = 3103\ cm^{-1}$. For thorough discussions of absorption and luminescence spectra, see the sections on this subject by Carnall and Crosswhite in ref. 1 and Chapter 16.

9.5 THE METALLIC STATE

9.5.1 Physical properties

Curium is a lustrous, malleable, silvery metal with many properties quite comparable to those of the lighter actinide elements. The melting point of Cm (dhcp form) is $1345 \pm 50°C$ [71], much higher than for the immediately preceding actinide elements, Np–Am (639–1173°C), but very similar to that of gadolinium (1312°C), its lanthanide analog [27, 162].

Curium metal exists in two modifications, a double hexagonal close-packed (dhcp) structure (α-lanthanum type) and a high-temperature cubic close-packed (fcc) structure. Using ^{244}Cm, the dhcp form was found to have lattice constants $a = 3.496(3)$ and $c = 11.331(5)$ Å, giving a calculated density of $13.5\ g\ cm^{-3}$ and a metallic radius of 1.74 Å [27, 97]. In a recent pressure study, slightly less accurate lattice constants were obtained (yielding a calculated density of $13.8\ g\ cm^{-3}$) but did establish that the dhcp phase was stable at least to 6.5 GPa [162].

These data cast further doubt on the report of an fcc phase with $a = 4.382$ Å, attributed to metallic curium of valence 4+ [28]. Since no transformations to other phases were observed, this result must be regarded with suspicion [28]. Baybarz and Adair [29] reported a high-temperature fcc phase with $a = 5.039(2)$ Å, prepared by metal volatilization at 1650°C [29, 30]. Using ^{248}Cm, Stevenson and Peterson have obtained this phase with $a = 5.065$ Å [97].

Conversion to the dhcp form was observed on cooling as well as by cold-working samples, indicating that metallic curium was indeed present. This apparently rules out possible stabilization of the fcc phase by trace amounts of CmN, which has a very similar lattice constant, $a = 5.041(2)$ Å, although there is an unusually large difference in the two reported values for the fcc metal. A phase attributed to CmO, fcc, $a = 5.09$ Å, was seen in early preparations of curium metal [27]. Zachariasen used a metallic radius of 1.743 Å for curium [32].

Other preparations of Cm metal using ^{248}Cm have been reported. They exhibit the dhcp structure with $a = 3.500 \pm 0.003$ Å and $c = 11.34 \pm 0.01$ Å [97], and $a = 3.490 \pm 0.006$ Å and $c = 11.308 \pm 0.018$ Å [162].

Curium metal has an entropy of vaporization remarkably similar to that of gadolinium, although its vapor pressure is about double that of gadolinium over the measured range [33]. The metal vapor pressure of triply distilled ^{244}Cm metal has been measured between 1300 and 2000 K and obeys the following relations [33]:

$$\log_{10}(p/\text{atm}) = (6.082 \pm 0.129) - (19\,618 \pm 193)/T \quad \text{(solid, 1327–1639 K)}$$

$$\log_{10}(p/\text{atm}) = (5.586 \pm 0.157) - (18\,894 \pm 275)/T \quad \text{(liquid, 1640–1972 K)}$$

From the latter equation the calculated boiling point of Cm is 3110°C. The derived heat of fusion, entropy of fusion, and average second-law entropy are 13.85 kJ mol^{-1}, 9.16 J K^{-1} mol^{-1}, and 106.7 ± 3.0 J K^{-1} mol^{-1}, respectively. Low-temperature condensed-phase thermodynamic parameters await the availability of long-lived isotopes. For excellent discussions of thermodynamic, electronic, and magnetic effects in curium and other actinide and lanthanide metals, the reader is referred to recent articles by Ward and Hill [34].

Metallic curium obeys a Curie–Weiss magnetic susceptibility relationship between 100 and 550 K with a magnetic moment of 8.07 μ_B [35], comparable to earlier values of 7.85–8.15 μ_B [36], although a lower value of 6.0 μ_B was reported recently [37]. However, the form of the metal was not identified by x-ray diffraction in the latter case. Schenkel performed electrical resistance measurements on ^{244}Cm metal, and confirmed that curium is the first magnetically ordering actinide metal, with a Néel temperature of 52.5 K [38]. A neutron diffraction study of the dhcp (α-La) form indicated no structure change down to 5 K and also showed antiferromagnetic ordering below 52 K [39]. A recent careful susceptibility study with ^{248}Cm metal has confirmed an antiferromagnetic transition at about 65 K, but the fcc phase reveals a ferrimagnetic transition near 200 K [153].

9.5.2 Preparation of curium metal

Curium metal can be prepared from CmF_3 by reduction with barium or lithium metal [27, 37, 40, 97, 162]. Dry, oxygen-free CmF_3 is required and temperatures (> 1600 K) are used which are well above the melting points of the metals and slag. On a small scale, tungsten coils and tantalum crucibles are used (tantalum is reported to dissolve slightly in Cm) [27, 97, 162]. Larger quantities of the metal have been prepared in 75–90 % yield by reduction with a magnesium–zinc alloy of CmO_2 suspended in a $MgF_2/MgCl_2$ melt [41]. When CmO_2 or Cm_2O_3 and pure hydrogen are heated to temperatures between 1200 and 1500°C in the presence of Pt, Ir, or Rh, alloy phases result with compositions Pt_5Cm, Pt_2Cm, Ir_2Cm, Pd_3Cm, and Rh_3Cm [42]. Pure curium metal has been prepared by

decomposition of these intermetallic compounds [43]. The dhcp form of curium has also been prepared by reducing the dioxide or sesquioxide with thorium metal, followed by volatilization and condensation of the curium metal vapor on a tantalum condenser [29, 30, 47].

9.5.3 Chemical properties of the metallic state

Metallic curium appears to be even more susceptible to corrosion than the earlier actinide elements, a property due at least in part to radioactive self-heating. The metal dissolves rapidly in dilute acid solutions and its enthalpy of solution has been measured in HCl (aq) [44, 164]. The metal reacts with hydrogen at 200–250°C to give fcc CmH_{2+x} ($a = 5.344$ Å) [45]. Recently hexagonal $CmH_{3-\delta}$ also has been reported [173]. The metal surface rapidly oxidizes in air to form a film, which may begin as CmO [27, 161, 162], progresses to Cm_2O_3 at room temperature, and further to CmO_2 at elevated temperatures. The metal is pyrophoric when finely divided.

The direct reactions of curium metal with non-metals such as P, As, Sb, S, and Se have been reported, and binary compounds with N, P, As, and Sb have been prepared by reactions using curium hydride (see next section) [31, 46, 47].

9.6 SIMPLE AND COMPLEX COMPOUNDS

9.6.1 General

Curium is the actinide element of highest atomic number (96) for which multigram quantities are available for chemical study. Even so, special microchemical techniques are necessarily applied to most studies with the 18 year α emitter ^{244}Cm and the 163 day α emitter ^{242}Cm. The 3.4×10^5 year isotope ^{248}Cm, only recently available in milligram quantities, greatly facilitates chemical progress with this element.

The most important chemical characteristic that distinguishes curium from the lighter actinides is the great stability of the 3+ state with respect to oxidation or reduction. The stability of Cm(III) has been attributed to the relative stability of a half-filled ($5f^7$) configuration, an observation which, in turn, has been used as a key argument in favor of the actinide hypothesis. The predominance of the 3+ state causes a chemical resemblance to lanthanides.

In contrast to americium, the oxidation of Cm(III) to Cm(IV) is achieved only with the strongest oxidizing agents and only one report [48] claims evidence for an oxidation state greater than IV. Transient divalent and tetravalent states have been observed in aqueous perchlorate media using pulse radiolysis techniques [49]. Attempts have been made to induce Cm(III)–Cm(IV) oxidation chemically (using ozone [50] and perxenate [51]) or electrochemically [52]. These early attempts have failed, an effect clearly not attributable solely to radiolytic reduction.

Recently, however, formation of a red Cm(IV) complex in phosphotungstate solution was achieved by the use of peroxydisulfate as the oxidant [53]. Kosyakov *et al.* [54] demonstrated that in such solutions the Cm(IV) is reduced much faster than can be accounted for by radiolytic effects, while Am(IV) in such solutions is much more stable, being reduced at a rate attributable to radiolytic effects alone. No value for the $E^\circ(Cm^{4+}/Cm^{3+})$ is known but from existing data it is substantially more positive than E° (Am^{4+}/Am^{3+}) and probably about as positive as $E^\circ(Pr^{4+}/Pr^{3+})$. The recent success of generating soluble carbonate solutions of Pr(IV) suggests that similar soluble Cm(IV) species may be prepared [55]. All known Cm(IV) compounds are either fluorides or oxides, but a broader chemistry has been developed for Cm(III).

With the more common isotopes ^{242}Cm and ^{244}Cm, intense α self-irradiation and heating effects cause aqueous-solution instability (peroxide is always present) and solid-state instability (lattice changes and compound alteration). In some cases these effects are sufficiently large that certain compounds may be identified in bulk only with the more stable isotope, e.g. $^{244}CmF_4$ and $^{248}Cm(\pi\text{-}C_5H_5)_3$ [21, 57].

9.6.2 Halides

To date, the halides represent by far the most extensively characterized class of curium compounds (refer to Table 9.2). The complete CmX_3 series (X = F, Cl, Br, I), as well as CmF_4 and several complex Cm(IV) fluorides, have been prepared and studied. Several reviews deal specifically with actinide halides and for further information (especially for cross-comparisons of Cm with other actinide halides) the reader is referred to these articles [2, 3, 58, 59].

Curium trifluoride is a white, sparingly soluble ($\sim$ 10 mg l^{-1}) compound [60] with the LaF_3 structure, which precipitates when fluoride ion is added to weakly acidic Cm(III) solutions (or HF to $Cm(OH)_3$). The anhydrous trifluoride is obtained by desiccation over P_2O_5 or by treatment with hot HF(g). Lattice constants of $a = 7.019$, $c = 7.198$ Å and $a = 7.014$, $c = 7.194$ Å for trigonal CmF_3 have been reported using ^{244}Cm and ^{248}Cm, respectively [61]. The trifluoride metals at 1406 ± 20°C and has an estimated standard entropy of 121 J K^{-1} mol^{-1} at 298 K [60, 63]. Curium has an irregular tricapped trigonal prismatic coordination in CmF_3 [2].

Magnetic susceptibilities of Cm(III) compounds have been reported by several authors. A recent determination gave an effective magnetic moment of 7.65 ± 0.1 μ_B for Cm^{3+} in CmF_3, CmOCl, and 5.6 mol% Cm^{3+} in LaF_3 [36, 64]. This value indicates a significant departure from Russell–Saunders coupling. Electron paramagnetic resonance experiments on several Cm^{3+} samples (doped into CaF_2 [65], ThO_2 and CeO_2 [66], and $LaCl_3$ and lanthanum ethylsulfate [67]) revealed a single-line spectrum and not a seven-line spectrum as earlier reported, which was apparently due to a Gd^{3+} impurity. Crystal field splittings for the nominally $^8S_{7/2}$ Cm^{3+} ion are about 250 times larger than for Gd^{3+}, a

Table 9.2 *Crystallographic data for curium metal, alloys, and compounds.*

				Lattice constants			
	Ref.	*Lattice type*	*Crystal system–space group*	a_0 (Å)	b_0 (Å)	c_0 (Å)	*Angle* (deg)
metal							
α-Cm	27, 40	α-La	hexagonal–$P6_3/mmc$	3.496(3)		11.331(5)	
β-Cm	29, 30		fcc	5.039(2)			
alloys							
Pd_3Cm	42	Cu_3Au	cubic–$Pm3m$	4.147			
Rh_3Cm	42	Cu_3Au	cubic–$Pm3m$	4.106			
Ir_2Cm	42	Cu_2Mg	cubic–$Fd3m$	7.561			
Pt_5Cm	42	Pt_5Sm	orthorhombic	5.329	9.108	26.38	
Pt_2Cm	42	Cu_2Mg	cubic–$Fd3m$	7.625			
oxides and chalcogenides							
A-Cm_2O_3	163	A-La_2O_3	hexagonal–$P\bar{3}m1$	3.792(9)		5.985(12)	
B-Cm_2O_3	87, 163	B-La_2O_3	monoclinic–$C2/m$	14.282(9)	3.641(3)	8.883(8)	$\beta = 100.29(7)$
C-Cm_2O_3	163	C-Mn_2O_3	cubic–$Ia3$	11.002(1)			
CmO_2	83, 86	fluorite	cubic–$Pm3m$	5.3584			
CmO(?)	27		cubic–$Fm3m$	5.09			
CmS	94		fcc	5.5754(6)			
CmSe	94		fcc	5.791(1)			
CmTe	94		fcc	6.150(4)			
Cm_2S_3	47	Th_3P_4	bcc	8.452(5)			
$CmS_{1.98}$	47	Fe_2As	tetragonal	3.926(5)		8.01(5)	
Cm_2Se_3	47	Th_3P_4	bcc	8.788			
$CmSe_{1.98}$	47	Fe_2As	tetragonal	4.096(3)		8.396(6)	
$CmTe_3$	96	$NdTe_3$	orthorhombic (pseudotetragonal)	4.34(2)		25.7(1)	
$CmTe_2$	96	Fe_2As	tetragonal	4.328(7)		8.93(1)	
Cm_2Te_3	96	η-U_2S_3	orthorhombic	11.94(2)	12.13(3)	4.330(6)	
Cm_2O_2S	92	Pu_2O_2S	hexagonal	3.889(2)		6.736(3)	
Cm_2O_2Te	96	La_2O_2Te	tetragonal	3.98(3)		12.58(7)	
$Cm_2O_2SO_4$	92	$Nd_2O_2SO_4$	orthorhombic	4.209(2)	4.087(2)	13.270(6)	
$BaCmO_3$	103	perovskite					
$CmAlO_3$	102	perovskite					
pnictides							
CmN	31	NaCl	fcc	5.041(2)			
CmP	94	NaCl	fcc	5.743(3)			
CmAs	94	NaCl	fcc	5.887			
CmSb	94	NaCl	fcc	6.242			
Cm_2O_2Sb	95	La_2O_2Te	tetragonal–$I4/mmm$	3.920(3)		13.41(2)	
Cm_2O_2Bi	95	La_2O_2Te	tetragonal–$I4/mmm$	3.957(1)		13.359(5)	
halides							
CmF_3	61, 62	LaF_3	trigonal–$P\bar{3}C1$	7.019(18)		7.198(20)	
$CmCl_3$	62, 69	UCl_3	hexagonal–$P6_3/m$	7.3743(11)		4.1850(7)	
$CmBr_3$	62, 72	$PuBr_3$	orthorhombic–$Cmcm$	4.041(2)	12.70(2)	9.135(2)	
CmI_3	62	BiI_3	hexagonal-$R\bar{3}$	7.44(9)		20.4(1)	
CmF_4	74	UF_4	monoclinic–$C2/c$	12.500(9)	10.488(10)	8.183(6)	$\beta = 126.10(5)$
$LiCmF_5$	78	$LiUF_5$	tetragonal–$I4_1/a$	14.57(2)		6.437(5)	
$Na_7Cm_6F_{31}$	75	$Na_7Zr_6F_{31}$	hexagonal-$R\bar{3}$	14.41(2)		9.661(3)	
$K_7Cm_6F_{31}$	76	$Na_7Zr_6F_{31}$	hexagonal-$R\bar{3}$	14.89(1)		10.254(9)	
Rb_2CmF_6	77	Rb_2UF_6	orthorhombic–$Cmcm$	6.931(14)	11.996(25)	7.567(16)	
CmOCl	79	PbClF	hexagonal	3.985(3)		6.752(8)	
hydrides							
CmH_{2+x}	173	fluorite	fcc	6.322			
$CmH_{3-\delta}$	173	PuH_3	trigonal–$P\bar{3}C1$	6.528		6.732	

result attributed to intermediate-coupling effects induced by the relatively large spin–orbit coupling energies of the actinide ions [65, see also 172].

Curium trichloride is a white compound that can be obtained by treating curium oxides or CmOCl with anhydrous hydrogen chloride at 400–600°C [68]. The hydrate has been reported to be light green. A single-crystal study showed that $CmCl_3$ has the hexagonal UCl_3-type structure common among the actinide trichlorides with $a = 7.3743$ and $c = 4.1850$ Å, giving a radius of 0.971 Å for Cm(III) [69]. Curium has nine chloride neighbors in the form of a tricapped trigonal prism, with Cm–Cl lengths of 2.859 and 2.914 Å. A melting point of 695°C [69] and an enthalpy of formation (298 K) of -974 ± 4 kJ mol^{-1} [44, 71, Table 17.14] have been reported.

Curium tribromide has been prepared by heating the trichloride with NH_4Br at 400–450°C in a hydrogen atmosphere [62] and also by hydrogen bromide treatment of the calcined oxide at 600°C [72]. The compound melts at 625°C and has the $PuBr_3$ (orthorhombic) structure [72]. The metal ion is surrounded by eight bromide ions, two at 2.865 Å, four at 2.983 Å, and two at 3.137 Å. An analogous procedure ($CmCl_3 + NH_4I$) has been used to prepare CmI_3, a colorless material having the BiI_3 structure [62]. Preparation from elemental curium and iodine has also been reported [1].

The halides of tetravalent curium include the simple fluoride CmF_4 [73, 74], and a series of complex fluorides of the type $M_7Cm_6F_{31}$ [75, 76], M_2CmF_6 [77], and $MCmF_5$ [78], where M is an alkali metal. As with terbium, the only reported method for preparing the tetrafluoride is by fluorine oxidation of the trifluoride. CmF_4 is a brownish-tan solid with a monoclinic ZrF_4-type structure ($C2/c$), in which curium has an antiprismatic eight coordination [2, 74]. Magnetic susceptibility measurements suggest a fluoride-deficient structure, CmF_{4-x} [70, 172].

A prominent series of isostructural complex actinide(IV) fluorides, $M_7An_6F_{31}$, with the $Na_7Zr_6F_{31}$ structure have been prepared [75,76]. With curium, the Na and K salts are known. The compounds were prepared by direct fluorination of evaporated salt mixtures of MX and CmX_3 at about 300°C. This 7:6 type of compound predominates with the larger alkali cations. The basic coordination polyhedron is a square antiprism [2]. In tetragonal $LiCmF_5$ the curium coordination is tricapped trigonal prismatic [2]. The compound Rb_2CmF_6 is orthorhombic with the Rb_2UF_6 structure, which consists of chains of fluoride dodecahedra [2].

The oxychloride CmOCl has been synthesized by treatment of $CmCl_3$ (or Cm_2O_3) at 500–600°C, with the vapor in equilibrium with a 10 M HCl solution [79]:

$$CmCl_3 + H_2O \rightleftharpoons CmOCl + 2HCl$$

From the equilibrium and known heats of formation, ΔH°_{f298} for CmOCl was calculated [80], see Table 17.4. Marei and Cunningham found that the magnetic susceptibility of CmOCl follows the Curie–Weiss law over the temperature range 77–298 K, with $\mu_{eff} \sim 7.58\,\mu_B$ and a Curie constant of approximately 22 K [36].

The structure of CmOCl is of the PbClF type (hexagonal), with each metal surrounded by four oxygens and five chlorides [79].

9.6.3 Oxides

The white to faint tan sesquioxide Cm_2O_3 (m.p. 2260 ± 25°C [81]) was prepared by thermal decomposition of $^{244}CmO_2$ at 600°C and 10^{-4} torr pressure [82]. This material has the Mn_2O_3-type cubic-C lattice, which gradually changes at room temperature to a hexagonal A-form because of self-irradiation effects [83, 163]. Haug prepared monoclinic B-type Cm_2O_3 by reduction of $^{244}CmO_2$ with hydrogen [84]. This study showed the cubic form described by Asprey *et al.* [82] to predominate at reaction temperatures below 800°C, changing to the monoclinic B-form at higher temperatures [84]. These three crystal modifications correspond to the three types observed for lanthanide sesquioxides. Structural data enthalpy of formation, and magnetic susceptibility have been obtained by Morss *et al.* [87] with B-form $^{248}Cm_2O_3$.

Preparation of the black curium dioxide by ignition in air was first claimed by Asprey and co-workers [82]. The product had a cubic (fcc) structure with $a = 5.372(3)$ Å. The compound is also formed by thermal decomposition of ^{244}Cm(III)-loaded resin [85] and by heating $^{244}Cm_2O_3$ to 650°C in 1 atm of oxygen, followed by cooling in oxygen [86]. Others have shown that the dioxide is the stable oxide form in an oxygen atmosphere at temperatures below 400°C [88]. A study with $^{248}CmO_2$ determined the lattice constant to be 5.359(2) Å [86]. This parameter yields a computed radius of 0.880 Å for the Cm^{4+} ion, a value which minimizes but does not entirely eliminate the cusp at Cm when tetravalent actinide radii are plotted against atomic number. These results have been interpreted to suggest that the 'dioxide', originally prepared [82] using ^{244}Cm, is a substoichiometric compound with approximate formula $CmO_{1.98}$. The black color is consistent with this hypothesis and recent magnetic susceptibility data imply even greater substoichiometry [154, 172]. Studies of the electronic structure of actinide dioxides (including CmO_2) by ESCA and theoretical calculations have appeared recently [89]. An x-ray diffraction study of the stability of ^{244}Cm oxides has also appeared [148].

Metal–oxygen phase diagram studies show a great similarity to analogous Pu, Pr, and Tb systems, and indicate the possible existence of two additional Cm_2O_3 phases which have not yet been isolated [8, 170]. Two intermediate oxides, $CmO_{1.72}$ and $CmO_{1.82}$, and two other non-stoichiometric phases close to the composition of CmO_2 and $CmO_{1.5}$ have also been detected [88]. A cubic (fcc) phase, CmO, was reported in an early preparation of the metal [27].

Curium oxalate, $Cm_2(C_2O_4)_3$, is routinely used for calcination to CmO_2. Oxalate precipitation has also been used to process kilograms of ^{244}Cm, with subsequent metathesis with 0.5 M hydroxide to $Cm(OH)_3$ [90, 91].

Hale and Mosley [85] have reported the preparation of curium oxysulfate, $^{244}Cm_2O_2SO_4$, by heating Cm^{3+}-loaded resin (sulfonate form) in a stream of

oxygen at 900°C. Heating to 1175°C under otherwise similar conditions yielded Cm_2O_3, which on cooling formed CmO_2. Haire and Fahey have prepared $Cm_2O_2SO_4$ by calcination of the hydrated sulfate in air at about 750°C [92]. The brown $Cm_2O_2SO_4$ has a body-centered orthorhombic structure with lattice parameters $a = 4.209(2)$, $b = 4.087(2)$, and $c = 13.270(6)$ Å [92], similar to $Nd_2O_2SO_4$ and $Cf_2O_2SO_4$ [93]. The computed Cm^{3+} radius in $Cm_2O_2SO_4$, namely 0.980 Å, agrees with the value 0.979 Å derived from Cm_2O_3. The oxysulfide Cm_2O_2S is formed when the sulfate is heated to about 800°C in H_2/Ar [92].

9.6.4 Chalcogenides

Damien *et al.* [47] prepared $^{244}CmS_2$ and $^{244}CmSe_2$ by slow reaction of excess sulfur or selenium vapor with curium hydride in vacuum. The resulting solids gave powder patterns indicating the tetragonal Fe_2As-type cell (isostructural with AmS_2 and $AmSe_2$) with lattice parameters (Table 9.2) indicating the materials to be non-stoichiometric.

The sesquisulfide Cm_2S_3 forms a defect body-centered cubic phase of the Th_3P_4 type with lattice parameter 8.452(5) Å [47]. The sesquiselenide was obtained by thermal dissociation of $CmSe_2$ at 620°C, again yielding a Th_3P_4-type phase, with cell parameter $a = 8.788$ Å [47]. Unlike gadolinium or plutonium, no other sesquiselenide forms were observed, even after thermal treatment at various temperatures.

The monochalcogenides were prepared by heating stoichiometric mixtures of chalcogen and curium metal at 700–750°C for 15 h followed by heating at 1250–1500°C under high vacuum [94]. The monochalcogenides have fcc structures. In these preparations accessory phases, possibly γ-Cm_2S_3, Cm_2O_2S, γ-Cm_2Se_3, and Cm_2O_2Te, were detected. Cell constants for Cm_2O_2Sb and Cm_2O_2Bi have been reported [95].

The oxysulfide Cm_2O_2S was prepared by partial oxidation of CmS_2 at 700°C [47, 92]. The resulting hexagonal phase has lattice parameters $a = 3.889(2)$ and $c = 6.736(3)$ Å, and is isostructural with the Np, Pu, and Cf analogs [92].

Damien *et al.* [96] have recently reported the preparation of $CmTe_3$ by the reaction of the hydride with tellurium at 400°C. At temperatures above 400°C the tritelluride decomposes to form the successive lower tellurides $CmTe_2$ and Cm_2Te_3. At 1100°C in a quartz tube, the oxytelluride Cm_2O_2Te is formed.

9.6.5 Pnictides

Charvillat *et al.* [31, 35, 46] and Peterson *et al.* [94, 97] have reported the syntheses of the pnictide compounds CmX, where X = N, P, As, and Sb. The compounds were obtained by heating curium hydride or metal with the respective pnictide element is a sealed tube to temperatures of 350–950°C. The N, P, As, and Sb compounds all have the NaCl structure, cell parameters for CmN and CmAs

being $a = 5.041$ and 5.887 Å, respectively [31, 35, 46, 94]. Recently Damien *et al.* [94] prepared the monopnictides (N, P, As, Sb) by directly heating stoichiometric mixtures of the elements. Lattice parameters for these preparations are given in Table 9.2. CmN and CmAs are ferromagnetic with T_c of 109 and 88 K, respectively [35]. The calculated effective magnetic moments are 7.02 and 6.58 μ_B, lower than expected for a pure $5f^7$ configuration, probably due to strong spin–orbit coupling and crystal field effects [35]. The silicides CmSi, $CmSi_2$, and Cm_2Si_3 have recently been reported [171].

9.6.6 Miscellaneous compounds

The trihydroxide, $Cm(OH)_3$, has been prepared from aqueous solution and crystallized by aging in water [98]. The compound has the lanthanide trihydroxide (hexagonal) structure.

The oxalate $Cm_2(C_2O_4)_3 \cdot 10H_2O$ forms when aqueous Cm(III) and oxalic acid are mixed. The compound dehydrates in a stepwise fashion when heated *in vacuo*, yielding the anhydrous oxalate at 280°C, which then converts to a carbonate above 360°C [91]. Further heating leads to oxides. The hydrated oxalate dissolves readily in aqueous alkali-metal carbonate solutions [90, 99]. The compound has a lower solubility than that of americium ($\sim$ 0.8 mg Cm per litre at 23°C) in 0.1 M $H_2C_2O_4$/0.2 M HNO_3; the solubility increases rapidly with temperature.

Complex sulfates of the type $MAn(SO_4)_2 \cdot xH_2O$, where M = alkali metal, have been precipitated from solutions of M_2SO_4 and the appropriate trivalent actinide ion in dilute HCl or H_2SO_4 [158]. Structural characterization is lacking for these compounds.

A series of actinide phosphates having the formulation $AnPO_4 \cdot 0.5H_2O$ have been prepared (An = Pu, Am, Cm) [100]. These compounds form when aqueous Cm(III) solutions are mixed with Na_2HPO_4 or $(NH_4)_2HPO_4$. Their structures are unknown. The hydrated phosphate of Cm(III) dehydrates at 300°C to $CmPO_4$, which has the monazite structure [100].

The compounds $CmNbO_4$ and $CmTaO_4$ are isotypic with the corresponding lanthanide compounds and are obtained by heating the precipitated, mixed hydroxide/hydrous oxides at 1200°C [101].

Heating mixtures of curium oxide and alumina affords $CmAlO_3$, which gives either a rhombohedral or cubic product depending upon the quenching conditions [102]. The rhombohedral phase transforms to the cubic phase at room temperature. $BaCmO_3$ has also been reported [103, 172].

The addition of K_2CO_3 to Cm^{3+} solution causes $Cm_2(CO_3)_3$ to precipitate [158]. The compound is soluble in 40% K_2CO_3. Utilizing the insolubility of $Cm(OH)_3$ in $NaHCO_3$ and the solubility of the Am(VI) carbonate complex (which is intensely colored), it is possible to reduce the americium content in curium to low levels. Sodium, rather than potassium, ion is necessary here to avoid precipitation of $KAmO_2CO_3$ [104].

9.6.7 Organometallics

Despite substantial recent advances in the organometallic chemistry of other actinide elements, progress with curium has been slow. This lack of progress apparently is due to the nuclear properties of the element rather than to an inherent chemical instability of the organometallic compounds. For more detailed discussion of this topic, especially comparison with organometallics containing other actinide metals, the reader is directed to Chapters 22 and 23 of this volume.

The synthesis and spectroscopic characterization of milligram quantities of white, crystalline tris(η^5-cyclopentadienyl)curium, $Cm(C_5H_5)_3$, has been reported from the reaction of $^{248}CmCl_3$ with $Be(C_5H_5)_2$ [57, 105]. The compound can be sublimed in vacuum at 180°C and is isostructural with the Pr, Pm, Sm, Gd, Tb, Bk, and Cf analogs [57, 106]. Mass-spectrometric evidence for volatile $Cm(C_5H_5)_3$ using microgram amounts of ^{244}Cm was obtained [105], but large-scale preparations are not stable due to radiolytic decomposition.

In terms of structural properties, volatility, thermal stability, and solubility, $Cm(C_5H_5)_3$ closely resembles other actinide and lanthanide tris(cyclopentadienide) compounds and hence the bonding must be similar. Nugent *et al.* [107] studied the optical spectrum of $^{248}Cm(C_5H_5)_3$ and found weak bands, typical for Cm^{3+}. These workers derived a value for the nephelauxetic parameter $d\beta$ of 0.050 ± 0.004, corresponding to very weak covalency in the organometallic bond. Thus, like the lanthanide analogs, the bonding in $Cm(C_5H_5)_3$ appears to have rather little covalent character. The ^{248}Cm compound fluoresces bright red under 360 nm irradiation [107].

Certain properties of the salt $CsCm(HFAA)_4 \cdot H_2O$ where HFAA = hexafluoroacetylacetone, have been studied in detail [108]. This compound, as well as the Eu, Gd, Tb, Nd, Am, Bk, Cf, and Es analogs, forms readily when the ligand is added to ethanol solutions of Cm(III) in the presence of cesium ion. Of the actinides studied for possible laser properties, only Cm displayed UV-excited sharp-line sensitized luminescence [108]. Cm(III) was found to be a highly efficient emitter (resembling Eu(III)) in the crystalline state, in ethanol solution, and doped into the $CsGd(HFAA)_4$ crystal matrix; hence laser emission should be demonstrable. Strong luminescence has been observed from ^{244}Cm(III) on an anion-exchange resin and in solution [109].

A number of adducts of the type $CmL_3 \cdot nQ$ have been prepared, where L is a fluorinated β-diketonate and Q is tributyl phosphate or trioctylphosphine oxide [110]. The volatility, thermal and radiation stabilities were studied with consideration of such compounds for gas chromatographic separation of Am and Cm.

9.7 SOLUTION CHEMISTRY

9.7.1 Inorganic

The aqueous-solution chemistry of curium is almost exclusively that of Cm(III). Little non-aqueous-solution chemistry has been reported with curium other than that related to solvent extraction [149]. Dilute Cm(III) solutions are normally colorless, but Cm(III) in concentrated HCl appears greenish. With ^{242}Cm, solutions with concentrations of about 1 $g\,l^{-1}$ will boil unless cooled.

Cm(III) is a 'class A' or 'hard' metal ion and thus complexes far more strongly to oxygen and fluoride donors than to more polarizable donors such as chloride or sulfur. Solution reactions of Cm^{3+} resemble those of the trivalent lanthanides and actinides. The fluoride, oxalate, phosphate, iodate, and hydroxide are essentially water-insoluble and the chloride, iodide, perchlorate, nitrate, and sulfate are water-soluble. The first hydrolysis constant for Cm^{3+}, i.e. for the reaction:

$$M^{n+} + H_2O \rightarrow MOH^{(n-1)+} + H^+$$

is 1.2×10^{-6} ($\mu = 0.1$; 23°C), which is within experimental error of the value for Am^{3+} but 10 times greater than for Pu^{3+} [111, 112].

There is no evidence for an oxidation state in solution less than II. A fluoride complex of tetravalent curium was obtained in aqueous solution when separately prepared CmF_4 was dissolved in concentrated (15 M) MF solution (M = alkali-metal ion) [21, 159]. Even under these conditions, and using ^{244}Cm, the self-reduction rate due to α decay is about 1% per minute. When CmF_4 is added to aqueous NH_4F, an immediate oxidation–reduction reaction occurs, with deposition of CmF_3. This is a sharp contrast to the stability of Am(IV) in NH_4F solution [113]. Other than the CmF_4/MF system, the only claims for chemically generated Cm(IV) in solution are the reports [53, 54] that red solutions result when aqueous Cm(III) solutions are mixed with potassium peroxydisulfate and heteropolyanions such as $[P_2W_{17}O_{61}]^{10-}$. Electrochemical generation of Cm(IV) in phosphate solutions was unsuccessful, owing to the large Cm(IV)/Cm(III) potential, estimated to be greater than 2 V in these systems [52]. Evidence was presented that the observed Cm(IV) reduction rate ($\sim 45\%$ per hour) was due both to radiolysis and to direct reduction by water. Other attempts to prepare Cm(IV) by oxidation of Cm(III) in solution have failed. These attempts include electrochemical methods [52, 114] and the use of sodium perxenate [51] and ozone [50], agents which readily oxidize Am(III) to Am(V) or Am(VI). $Cm(OH)_3$ in $NaHCO_3$ is not oxidized by ozone or $Na_2S_2O_8$, oxidants which produce Am(VI) as a carbonate complex [104]. An earlier report [169] that ozone oxidises Cm^{3+} apparently is in error, the oxidized material actually being the ozonized anion-exchange resin [50].

For dissolution of dhcp Cm metal in 1 M hydrochloric acid, the value of ΔH is $-615 \pm 4\,kJ\,mol^{-1}$ at 298.2 K, which with an estimated $s^\circ = -194\,J\,mol^{-1}\,h^{-1}$ for

the Cm^{3+} (aquo) ion yields an estimated -2.06 ± 0.03 V for the Cm(III)/Cm(0) couple [44] (Chapter 17). Raschella *et al.* found -606.5 ± 11.7 kJ mol^{-1} using ^{248}Cm [164]. From electron-transfer spectra, the Cm(III)/Cm(II) couple was estimated at -4.4 V [56], but the results of the pulse radiolysis study and the potential of the hydrated electron place a lower value on this couple [49]. From studies in a melt, Mikheev obtained -2.8 V for E° (Cm^{3+}/Cm^{2+}) [165]. On the basis of UV spectra the Cm(IV)/Cm(III) couple had been estimated as about $+3.3$ V [115], while a recent compilation gives E° (Cm^{4+}/Cm^{3+}) as $+3.1$ V [166].

Despite the numerous unsuccessful attempts to oxidize Cm(III) and Cm(IV) compounds to higher oxidation states, some theoretical work suggests the possibility that Cm(VI) may be even more stable than Am(VI), and the lack of success in preparing Cm(VI) may be due to low stability of Cm(V) and the high Cm(IV)/Cm(III) potential [114, 116]. A recent Russian report [48], in fact, claims the synthesis of Cm(VI) by the transmutation reaction of $^{242}AmO_2^+$:

$$^{242}AmO_2^+ \xrightarrow[16.07\ h]{\beta^-} CmO_2^{2+}$$

The $K_3AmO_2(CO_3)_2$ starting material was aged 18–40 h and then dissolved in 0.1 M $NaHCO_3$ in the presence of ozone, followed by addition of $Na_4UO_2(CO_3)_3/K_2CO_3$ solution to precipitate MO_2^{2+} species as $K_4MO_2(CO_3)_3$. From the enhancement of Cm in the precipitate over that expected for Cm(III), it was concluded that a 30–60% conversion to Cm(VI) had occurred.

Other than as a transient aqueous species and species co-precipitated from melts, and possibly in CmO, Cm(II) is unknown. Pulse radiolysis, producing OH radicals as oxidant and the aquo electron as reductant, produced changes in aqueous americium and curium perchlorate solutions. The new absorbances were attributed to transient formation of Cm(II), λ_{max} 240 nm, and Cm(IV), λ_{max} 260 nm [49]. A recent study has shown that the two polarographic waves earlier found for acetonitrile solutions of hydrated Am^{3+} and Cm^{3+} perchlorates are not, as claimed, evidence for Am(II) and Cm(II), but in fact correspond to reduction of hydration water and to the An(III) → An(0) reduction [117].

Stability constants for Cm(III) complexes have been determined for only a few halides, pseudohalides, and oxyanions: (F^-) [118, 119], (Cl^-) [120], (NO_2^-) [121], (NO_3^-) [122], ($C_2O_4^{2-}$) [167], (SO_4^{2-}) [122, 125], and (SCN^-) [122, 124]. However, vastly different constants have been reported from experiments conducted under seemingly similar conditions. For example, β_2 values for the Cm(III)–SCN systems vary by an order of magnitude, and evidence for a third complexation step is found by some workers and not others [122–124]. Therefore, caution is advisable in quantitative comparisons of stability constants given in Table 9.3. Also see Chapter 21 and Baes and Mesmer [155].

The curium absorption spectrum changes very little with increasing acid concentration (HCl, HNO_3, H_2SO_4); a decrease in intensity may be observed but

Table 9.3 *Stability constants for selected Cm(III) complexes.*

Ligand	*Conditions*	*Stability constants*	*Ref.*
F^-	extraction with di(2-ethylhexyl)phosphoric acid, pH = 3.6, $\mu = 0.50$	$\beta_1 = 2.21 \times 10^3$ $\beta_2 = 1.50 \times 10^6$ $\beta_3 = 1.2 \times 10^9$	118
	extraction, $\mu = 1.0$	$\beta_1 = 4 \times 10^2$	119
SCN^-	extraction with dinonylnaphthalene sulfonic acid, pH = 2.8, $\mu = 1.0$	$\beta_1 = 1.53$ $\beta_2 = 4.08$	124
NO_3^-	ion exchange, $\mu = 1$, $T = 30°C$	$\beta_1 = 2.2$ $\beta_2 = 1.3$	122
SO_4^{2-}	extraction, pH = 3.0, $\mu = 2.0$, $T = 25°C$	$\beta_1 = 22$ $\beta_2 = 73$	139
	ion exchange	$\beta_1 = 32$ $\beta_2 = 241$	122
$C_2O_4^{2-}$	solubility, ion exchange, $\mu = 0.2$	$\beta_1 = 9.1 \times 10^5$ $\beta_2 = 1.40 \times 10^{10}$	167
$P_3O_9^{3-}$	ion exchange	$\beta_1 = 4.4 \times 10^3$	140
Cl^-	ion exchange	$\beta_1 = 1.6$ $\beta_2 = 0.9$	120, 122
NO_2^-	extraction with dinonylnaphthalene sulfonic acid	$\beta_1 = 6.6$	121
acetate	ion exchange, $\mu = 0.5$, $T = 20°C$	$\beta_1 = 114$ $\beta_2 = 1240$	141
lactic acid/di(2-ethylhexyl)phosphoric acid	extraction, $\mu = 0.5$	$\beta_1 = 5.5 \times 10^2$ $\beta_2 = 3.0 \times 10^4$ $\beta_3 = 1.3 \times 10^6$	142
citrate	extraction, $\mu = 0.1$	$\log \beta_1 = 10.69$ $\log \beta_2 = 11.93$	143
glycinate	extraction, $\mu = 2.0$, $T = 25°C$	$\beta_1 = 6.4$	133
ethylenediaminetetraacetic acid	cation exchange, $\mu = 0.1$	$\log \beta_1 = 17.4$	144
α-hydroxyisobutyric acid	cation exchange, $\mu = 0.5$	$\log \beta_1 = 3.43$ $\log \beta_2 = 4.71$ $\log \beta_3 = 5.23$	145
thenoyltrifluoroacetone	extraction ($CHCl_3$), $\mu = 0.1$, $T = 25°C$	$\log \beta_3 = 13.4$	134

Table 9.3 (*Contd.*)

Ligand	*Conditions*	*Stability constants*	*Ref.*
nitrilotriacetic acid	ion exchange, $\mu = 0.1$, $T = 25°C$	$\log \beta_1 = 11.8$ $\log \beta_2 = 20.6$	146
ethylenediamine-bis(methyl)phosphonic acid	ion exchange, $\mu = 0.5$, $T = 25°C$	$\log \beta_1 = 6.40$	147

little shifting of band positions. Generally inorganic ligands and organic chelating agents complex americium and curium about equally well, but the binding to Cm^{3+} appears to be stronger than to the light lanthanides. However, in comparing binding constants of Cm^{3+} with trivalent lanthanides, it should be remembered that the appropriate comparison is with the earlier lanthanides (e.g. Nd or Pm) for which the ionic radii are more nearly the same, rather than with the nf^7 counterpart Gd(III), which is smaller than Cm(III) by 0.05 Å [2]. For extensive radii comparison, see Shannon [168].

9.7.2 Organic

Very few curium compounds containing organic ligands have actually been isolated (see earlier section on organometallic compounds), although it seems likely that efforts to isolate such compounds would prove to be fruitful. Because of interest in extraction schemes for treating radioactive wastes, a substantial number of studies have determined stability constants and distribution coefficients for solutions containing curium and various organic ligating agents. However, these experiments have often involved tracer amounts of curium and have employed a variety of experimental conditions (ionic strength, temperature, concentrations, etc.), and therefore quantitative comparisons of the determined values are rendered difficult. As with the inorganic anions, values, and in some cases even trends, can vary markedly under seemingly similar conditions. Most studies do not involve isolation or definitive formulation of the actual species in solution and it is possible that complicated structures occur, e.g. $CmF_3 \cdot (HDEHP)_x$ [118].

Furthermore, recent crystal structure determinations for a number of lanthanide and actinide extractant complexes illustrate that surprises may be expected when more definitive structural information becomes available [126, 127]. Owing to these complications we will not try to analyze the voluminous extraction data that are available, but will include in Table 9.3 data for only a few of the more important extractants. The reader is referred to a recent, more extensive compilation for additional data of this type [128].

Special attention has been given to extraction studies involving amine and organophosphorus derivatives. In general, it is found that methyl-containing trialkylamines are more effective in extracting Am than Cf and Cm, whereas long-chain, symmetric alkylamines extract Cf more efficiently [129]. The basicities as well as the polydentate nature of organophosphorus esters, amides, amine oxides, and amine salts appear to be factors in extraction of the actinides [130–132]. The nature of the coordination in these systems is unknown.

Tanner and Choppin [133] have determined by solvent extraction techniques the first stability constants and thermodynamic parameters for glycine–M^{3+} complexation at pH 3.64 and ionic strength 2.0 M ($NaClO_4$). The results indicate that the amino acid is coordinated predominantly in the zwitterionic ($NH_3^+CH_2CO_2^-$) form, in contrast to previous reports claiming the glycine ligand to be in the cationic form.

Keller and Schreck [134] have shown that Cm(III), as well as Ac(III), Am(III), and Cf(III), are extracted with β-diketone ligands as 1:3 chelates only, with stability constants ($\log \beta_3$) decreasing in the series Cf > Cm ~ Am > Ac. Keller *et al.* [135] have also shown that Am(III) and Cm(III) are extracted from aqueous solutions into chloroform solutions of 8-hydroxyquinoline ligands as AnL_2Y, where L is the 8-hydroxyquinolate anion and Y is probably OH^-, in contrast to the lanthanides which are extracted as LnL_3 chelates.

Distribution ratios (chloroform–water) have also been reported for curium complexes with 8-hydroxyquinoline (oxine), cupferron, and *N*-benzoyl-phenylhydroxylamine (NBPHA) [136]. Only 1:3 complexes with Cm(III) and Am(III) were reported, and extraction into the organic phase appears to be very high at pH values above 5. Solution interaction of Cm(III) with bis(salicylidene)ethylenediimine (SALEN) and derivatives has also been studied [137]. With the reagent arsenazo(III), both Cm(III) and Am(III) form 1:1 and 1:2 complexes [138].

ACKNOWLEDGMENT

Work performed under the auspices of the US Department of Energy.

REFERENCES

1. *Gmelin Handbook of Inorganic Chemistry*, Suppl. Work, 8th edn, *Transuranium*, Verlag Chemie, Weinheim, part A1, II (1973), part A1, II (1974), part A2 (1973), part C (1972). See also *Notes added in proof* (p. 988).
2. Penneman, R. A., Ryan, R. R., and Rosenzweig, A. (1973) *Struct. Bonding*, **13**, 1–52.
3. Brown, D. (1968) *Halides of the Lanthanides and Actinides*, Wiley-Interscience, New York.
4. Katz, J. J. and Seaborg, G. T. (1957) *The Chemistry of the Actinide Elements*, Methuen, London.

5. Keller, C. (1971) *The Chemistry of the Transuranium Elements*, Verlag Chemie, Weinheim.
6. Bagnall, K. W. (1972) *The Actinide Elements*, Elsevier, New York.
7. Seaborg, G. T. (1972) *Pure Appl. Chem.*, **30**, 539–49.
8. Stevenson, J. N. and Peterson, J. R. (1975) *Microchem. J.*, **20**, 213–20.
9. Seaborg, G. T., James, R. A., and Ghiorso, A. (1949) in *The Transuranium Elements* (eds G. T. Seaborg, J. J. Katz, and W. W. Manning), Natl Nucl. En. Ser., Div. IV, 14B, McGraw-Hill, New York, pp. 1554–71.
10. Werner, L. B. and Perlman, I. (1951) *J. Am. Chem. Soc.*, **73**, 5215–17.
11. Chu, Y. Y. (1972) *Phys. Rev. A*, **5**(1), 67–72.
12. Lederer, C. M. and Shirley, V. S. (eds) (1978) *Table of Isotopes*, 7th edn, Wiley, New York, supplemented.
13. Kerrigan, W. J. and Banick, C. J. (1975) *J. Inorg. Nucl. Chem.*, **37**, 641; Lougheed, R. W., Wild, J. F., Hulet, E. K., Hoff, R. W., and Landrum, J. H. (1978) *J. Inorg. Nucl. Chem.*, **40**, 1865–9.
14. Groh, H. J., Huntoon, R. T., Schlea, C. S., Smith, J. A., and Springer, F. H. (1965) *Nucl. Appl.*, **1**, 327–36.
15. Baybarz, R. D. (1970) *At. Energy Rev.*, **8**, 327–60.
16. Bigelow, J. (1976) personal communication.
17. Haug, H. O. (1974) *J. Radioanal. Chem.*, **21**, 187–98.
18. Lebedev, I. A., Myasoedov, B. F., and Guseva, L. I. (1974) *J. Radioanal. Chem.*, **21**, 259–66.
19. Buijs, K., Müller, W., Reul, J., and Toussaint, J. C. (1973) Euratom Rep. 5040; *Nucl. Sci. Abstr.*, **29**, 02573, 38 p.
20. Brewer, L. (1971) *J. Opt. Soc. Am.*, **61**, 1101–11; Nugent, L. J. and Vander Sluis, K. L. (1971) *J. Opt. Soc. Am.*, **61**, 1112–15.
21. Asprey, L. B. and Keenan, T. K. (1958) *J. Inorg. Nucl. Chem.*, **7**, 27–31.
22. Barbanel, Yu. A., Kotlin, V. P., and Kolin, V. V. (1977) *Radiokhimiya*, **19**, 497–501; *Sov. Radiochem.*, **19**, 406–9.
23. Moeller, T. and Moss, F. A. J. (1951) *J. Am. Chem. Soc.*, **73**, 3149–51.
24. Edelstein, N., Easley, W., and McLaughlin, R. (1967) *Lanthanide/Actinide Chemistry* (ACS Adv. Chem. Ser. 71), American Chemical Society, Washington DC, ch. 15, pp. 203–10.
25. Varga, L. P., Baybarz, R. D., and Reisfeld, M. J. (1973) *J. Inorg. Nucl. Chem.*, **35**, 4313–17.
26. Varga, L. P., Baybarz, R. D., Reisfeld, M. J., and Volz, W. B. (1973) *J. Inorg. Nucl. Chem.*, **35**, 2787–94.
27. Cunningham, B. B. and Wallmann, J. C. (1964) *J. Inorg. Nucl. Chem.*, **26**, 271–5.
28. Smith, P. K., Hale, W. M., and Thompson, M. C. (1969) *J. Chem. Phys.*, **50**, 5066–76.
29. Baybarz, R. D. and Adair, M. L. (1972) *J. Inorg. Nucl. Chem.*, **34**, 3127–30.
30. Baybarz, R. D., Bohet, J., Buijs, K., Colsen, L., Müller, W., Reul, J., Spirlet, J. C., and Toussaint, J. C. (1976) *Transplutonium* 1975 (eds W. Müller and R. Lindner), North-Holland, Amsterdam, pp. 61–8.
31. Charvillat, J. P., Benedict, U., Damien, D., de Novion, C. H., Wojakowski, A., and Müller, W. (1976) *Transplutonium* 1975 (eds W. Müller and R. Lindner), North-Holland, Amsterdam, pp. 79–84.
32. Zachariasen, W. H. (1973) *J. Inorg. Nucl. Chem.*, **35**, 3487–97.

33. Ward, J., Ohse, R. W., and Reul, R. (1975) *J. Chem. Phys.*, **62**, 2366–72.
34. Ward, J. W. and Hill, H. H. (1975) *Heavy Element Properties* (eds W. Müller and M. Blank), North-Holland, Amsterdam, vol. I, pp. 65–79; Ward, J. W., Kleinschmidt, P. D., Haire, R. G., and Brown, D. (1980) in *Lanthanide and Actinide Chemistry and Spectroscopy* (ACS Symp. Ser. 131), American Chemical Society, Washington DC, pp. 199–220.
35. Kanellakopulos, B., Charvillat, J. P., Maino, F., and Müller, W. (1976) *Transplutonium* 1975 (eds W. Müller and R. Lindner), North-Holland, Amsterdam, pp. 181–90. See also ref. 175.
36. Marei, S. A. and Cunningham, B. B. (1972) *J. Inorg. Nucl. Chem.*, **34**, 1203–6.
37. Fujita, D. K., Parsons, T. C., Edelstein, N., Noe, M., and Peterson, J. R. (1976) *Transplutonium* 1975 (eds W. Müller and R. Lindner), North-Holland, Amsterdam, pp. 173–8.
38. Schenkel, R. (1977) *Solid State Commun.*, **23**, 389–92.
39. Fournier, J. M., Blaise, A., Müller, W., and Spirlet, J. C. (1977) *Physica*, **87-88B**, 30–1.
40. Müller, W., Reul, J., and Spirlet, J. C. (1977) *Rev. Chim. Minér.*, **14**, 212–24.
41. Eubanks, I. D. and Thompson, M. C. (1969) *Inorg. Nucl. Chem. Lett.*, **5**, 187–91.
42. Erdmann, B. and Keller, C. (1973) *J. Solid State Chem.*, **7**, 40–8; (1971) *Inorg. Nucl. Chem. Lett.*, 7, 675–83. See also ref. 174.
43. Müller, W., Reul, J., and Spirlet, J. C. (1972) *Atomwirt. Atomtech.*, **17**, 415–16.
44. Fuger, J., Reul, J., and Müller, W. (1975) *Inorg. Nucl. Chem. Lett.*, **11**, 265–75.
45. Bansal, B. M. and Damien, D. (1970) *Inorg. Nucl. Chem. Lett.*, **6**, 603–6.
46. Charvillat, J. P., Benedict, U., Damien, D., and Müller, W. (1975) *Radiochem. Radioanal. Lett.*, **20**, 371–81.
47. Damien, D., Charvillat, J. P., and Müller, W. (1975) *Inorg. Nucl. Chem. Lett.*, **11**, 451–7.
48. Peretrukhin, V. F., Erin, E. A., Dzyubenko, V. I., Kopytov, V. V., Polyukhov, V. G., Vasil'ev, V. Ya., Timofeev, G. A., Rykov, A. G., Krot, N. N., and Spitsyn, V. I. (1978) *Dokl. Akad. Nauk SSSR*, **242**, 1359–62; *Dokl. Acad. Sci. USSR*, **242**, 503–6.
49. Sullivan, J. C., Gordon, S., Mulac, W. A., Schmidt, K. M., Cohen, D., and Sjoblom, R. (1976) *Inorg. Nucl. Chem. Lett.*, **12**, 599–601.
50. Pages, M. and Demichelis, R. (1966) *C. R. Acad. Sci. Paris C*, **263**, 938–40.
51. Holcomb, H. P. (1967) *J. Inorg. Nucl. Chem.*, **29**, 2885–8.
52. Myasoedov, B. F., Lebedev, I. A., Mikhailov, V. M., and Frenkel, V. Ya. (1973) *Radiochem. Radioanal. Lett.*, **14**, 131–4; (1974) *Radiochem. Radioanal. Lett.*, **17**, 359–65.
53. Saprykin, A. S., Shilov, V. P., Spitsyn, V. I., and Krot, N. N. (1976) *Dokl. Akad. Nauk SSSR*, **226**, 853–6; *Dokl. Acad. Sci. USSR*, **226**, 114–16.
54. Kosyakov, V. N., Timofeev, G. A., Erin, E. A., Andreev, V. I., Kopytov, V. V., and Simakin, G. A. (1977) *Radiokhimiya*, **19**, 511–17; *Sov. Radiochem.*, **19**, 418–23.
55. Hobart, D. E., Samhoun, K., Young, J. P., Norvell, V. E., Mamantov, G., and Peterson, J. R. (1980) *Inorg. Nucl. Chem. Lett.*, **16**, 321–8. See also ref. 177.
56. Nugent, L. J., Baybarz, R. D., Burnett, J. L., and Ryan, J. L. (1973) *J. Phys. Chem.*, **77**, 1528–39.
57. Laubereau, P. G. and Burns, J. H. (1970) *Inorg. Nucl. Chem. Lett.*, **6**, 59–63.
58. Bagnall, K. W. (1967) *Coord. Chem. Rev.*, **2**, 145–62.
59. Katz, J. J. and Sheft, I. (1960) *Adv. Inorg. Chem. Radiochem.*, **2**, 195–236.
60. Cunningham, B. B. (1966) *Prep. Inorg. Reactions*, **3**, 79–121.

61. Stevenson, J. N. (1973) Oak Ridge National Laboratory Report TID-26453, **28**, 30534; (1974) *Chem. Abstr.*, **80**, 90432w.
62. Asprey, L. B., Keenan, T. K., and Kruse, F. H. (1965) *Inorg. Chem.*, **4**, 985–6.
63. Burnett, J. (1966) *J. Inorg. Nucl. Chem.*, **28**, 2454–6.
64. Marei, S. A. (1965) USAEC Report UCRL-11984; *Chem. Abstr.*, **63**, 9213c.
65. Edelstein, N. and Easley, W. (1968) *J. Chem. Phys.*, **48**, 2110–15.
66. Abraham, M., Finch, C. B., and Clarke, G. W. (1968) *Phys. Rev.*, **168**, 933–5.
67. Abraham, M., Judd, B. R., and Wickman, H. H. (1963) *Phys. Rev.*, **130**, 611–12.
68. Wallmann, J. C., Fuger, J., Peterson, J. R., and Green, J. L. (1967) *J. Inorg. Nucl. Chem.*, **29**, 2745–51.
69. Peterson, J. R. and Burns, J. H. (1973) *J. Inorg. Nucl. Chem.*, **35**, 1525–30.
70. Haire, R. G., Nave, S. E., and Huray, P. G. (1982) *12th Journée des Actinides*, Orsay.
71. Oetting, F. L., Rand, M. H., and Ackermann, R. J. (1976) *The Chemical Thermodynamics of Actinide Elements and Compounds*, part 1, *The Actinide Elements*, IAEA, Vienna, p. 34; Fuger, J. and Oetting, F. L. (1976) *The Chemical Thermodynamics of Actinide Elements and Compounds*, part 2, *The Actinide Aqueous Ions*, IAEA, Vienna, p. 48.
72. Burns, J. H., Peterson, J. R., and Stevenson, J. N. (1975) *J. Inorg. Nucl. Chem.*, **37**, 743–9.
73. Keenan, T. K. and Asprey, L. B. (1969) *Inorg. Chem.*, **8**, 235–8.
74. Asprey, L. B. and Haire, R. G. (1973) *Inorg. Nucl. Chem. Lett.*, **9**, 1121–8; Haug, H. O. and Baybarz, R. D. (1975) *Inorg. Nucl. Chem. Lett.*, **11**, 847–55.
75. Keenan, T. K. (1966) *Inorg. Nucl. Chem. Lett.*, **2**, 211–14.
76. Keenan, T. K. (1967) *Inorg. Nucl. Chem. Lett.*, **3**, 391–6.
77. Keenan, T. K. (1967) *Inorg. Nucl. Chem. Lett.*, **3**, 463–7.
78. Keenan, T. K. (1966) *Inorg. Nucl. Chem. Lett.*, **2**, 153–6.
79. Peterson, J. R. (1972) *J. Inorg. Nucl. Chem.*, **34**, 1603–7.
80. Weigel, F., Wishnevsky, V., and Hauske, H. (1977) *J. Less Common Metals*, **56**, 113–23.
81. Baybarz, R. D. (1973) *J. Inorg. Nucl. Chem.*, **35**, 4149–58.
82. Asprey, L. B., Ellinger, F. H., Fried, S., and Zachariasen, W. H. (1955) *J. Am. Chem. Soc.*, **77**, 1707–8.
83. Wallmann, J. C. (1964) *J. Inorg. Nucl. Chem.*, **26**, 2053–7.
84. Haug, H. O. (1967) *J. Inorg. Nucl. Chem.*, **29**, 2753–8.
85. Hale, W. H. Jr and Mosley, W. C. (1973) *J. Inorg. Nucl. Chem.*, **35**, 165–71.
86. Peterson, J. R. and Fuger, J. (1971) *J. Inorg. Nucl. Chem.*, **33**, 4111–17; Noé, M. and Fuger, J. (1971) *Inorg. Nucl. Chem. Lett.*, **7**, 421–30.
87. Morss, L. R., Fuger, J., Goffart, J., and Haire, R. G. (1983) *Inorg. Chem.*, **22**, 1993.
88. Chikalla, T. D. and Eyring, L. (1969) *J. Inorg. Nucl. Chem.*, **31**, 85–93.
89. Gubanov, V. A., Rosen, A., and Ellis, D. E. (1979) *J. Phys. Chem. Solids*, **40**, 17–28; Gubanov, V. A. and Chirkov, A. K. (1978) *Inorg. Nucl. Chem. Lett.*, **14**, 139–42.
90. Bibler, N. E. (1972) *Inorg. Nucl. Chem. Lett.*, **8**, 153–6.
91. Scherer, V. and Fochler, M. (1968) *J. Inorg. Nucl. Chem.*, **30**, 1433–7.
92. Haire, R. G. and Fahey, J. A. (1977) *J. Inorg. Nucl. Chem.*, **39**, 837–41.
93. Baybarz, R. D., Fahey, J. A., and Haire, R. G. (1974) *J. Inorg. Nucl. Chem.*, **36**, 2023–7.
94. Damien, D. A., Haire, R. G., and Peterson, J. R. (1979) *J. Less Common Metals*, **68**, 159–65; (1979) *J. Phys. Colloq.*, 95–100.
95. Charvillat, J. P. and Zachariasen, W. H. (1977) *Inorg. Nucl. Chem. Lett.*, **13**, 161–3.

96. Damien, D., Wojakowski, W., and Müller, W. (1976) *Inorg. Nucl. Chem. Lett.*, **12**, 441–9.
97. Stevenson, J. N. and Peterson, J. R. (1979) *J. Less Common Metals*, **66**, 201–10.
98. Haire, R. G., Lloyd, M. H., Milligan, W. O., and Beasley, M. L. (1977) *J. Inorg. Nucl. Chem.*, **39**, 843–7.
99. Burney, G. A. and Porter, J. A. (1967) *Inorg. Nucl. Chem. Lett.*, **3**, 79–85.
100. Weigel, F. and Haug, H. (1965) *Radiochim. Acta*, **4**, 227–228. See also ref. 176.
101. Keller, C. and Walter, K. H. (1965) *J. Inorg. Nucl. Chem.*, **27**, 1253–60.
102. Mosley, W. C. (1971) *J. Am. Ceram. Soc.*, **54**, 475–9.
103. Haire, R. G. (1980) *Proc. 10th Journée des Actinides*, Stockholm, p. 19.
104. Coleman, J. S., Keenan, T. K., Jones, L. H., Carnall, W. T., and Penneman, R. A. (1963) *Inorg. Chem.*, **2**, 58–61.
105. Baumgärtner, F., Fischer, E. O., Billich, H., Dornberger, E., Kanellakopulos, B., Roth, W., and Stieglitz, L. (1970) *J. Organomet. Chem.*, **22**, C17–18.
106. Laubereau, P. G. and Burns, J. H. (1970) *Inorg. Chem.*, **9**, 1091–5.
107. Nugent, L. J., Laubereau, P. G., Werner, G. K., and Vander Sluis, K. L. (1971) *J. Organomet. Chem.*, **27**, 365–72.
108. Nugent, L. J., Burnett, J. L., Baybarz, R. D., Werner, G. K., Tanner, J. P., Tarrant, J. R., and Keller, O. L. (1969) *J. Phys. Chem.*, **73**, 1540–9.
109. Gutmacher, R. G., Hulet, E. K., and Conway, J. G. (1964) *J. Opt. Soc. Am.*, **54**, 1403–4; Beitz, J. V. and Hessler, J. P. (1980). *Nucl. Tech.*, **51**, 169–77.
110. Davydov, A. V., Myasoedov, B. F., Travnikov, S. S., and Fedoseev, E. V. (1978) *Radiokhimiya*, **20**, 257–64; *Sov. Radiochem.*, **20**, 217–24.
111. Désiré, B., Hussonnois, M., and Guillaumont, R. (1969) *C. R. Acad. Sci. Paris C*, **269**, 448–51.
112. Korotkin, Yu. S. (1974) *Radiokhimiya*, **16**, 221–5; *Sov. Radiochem.*, **16**, 223–6.
113. Asprey, L. B. and Penneman, R. A. (1962) *Inorg. Chem.*, **1**, 134–6.
114. Ionova, G. V. and Spitsyn, V. I. (1978) *Dokl. Akad. Nauk SSSR*, **241**, 590–1; *Dokl. Acad. Sci. USSR*, **241**, 348–9.
115. Miles, J. H. (1965) *J. Inorg. Nucl. Chem.*, **27**, 1595–600.
116. Spitsyn, V. I. and Ionova, G. V. (1978) *Radiokhimiya*, **20**, 328–32; *Sov. Radiochem.*, **20**, 279–83.
117. Friedman, H. A. and Stokely, J. R. (1976) *Inorg. Nucl. Chem. Lett.*, **12**, 505–13.
118. Aziz, A. and Lyle, S. J. (1969) *J. Inorg. Nucl. Chem.*, **31**, 3471–80.
119. Choppin, G. R. and Unrein, P. J. (1976) *Transplutonium* 1975 (eds W. Müller and R. Lindner), North-Holland, Amsterdam, pp. 97–105.
120. Ward, M. and Welch, G. A. (1956) *J. Inorg. Nucl. Chem.*, **2**, 395–402.
121. Vasudeva Rao, P. R., Kusumakumari, M., and Patil, S. K. (1978) *Radiochem. Radioanal. Lett.*, **33**, 305–14.
122. Khopkar, P. K. and Mathur, J. N. (1980) *J. Inorg. Nucl. Chem.*, **42**, 109–13.
123. Harmon, H. D., Peterson, J. R., McDowell, W. J., and Coleman, C. F. (1972) *J. Inorg. Nucl. Chem.*, **34**, 1381–97.
124. Khopkar, P. K. and Mathur, J. N. (1974) *J. Inorg. Nucl. Chem.*, **36**, 3819–25; (1980) *Thermochim. Acta*, **37**, 71–8.
125. Stepanov, A. V. (1973) *Zh. Neorg. Khim.*, **18**, 371–4; *Sov. J. Inorg. Chem.*, **18**, 194–6.
126. Burns, J. H. (1982) *Oak Ridge Nat. Lab. Rept.* ORNL/TM-8221.
127. For example, see Bowen, S. M., Dresler, E. N., and Paine, R. T. (1984) *Inorg. Chim. Acta*, **84**, 221, and earlier articles by these authors.

128. Jones, A. D. and Choppin, G. R. (1969) *Actinide Rev.*, **1**, 311–36.
129. See, for example, Chudinov, E. G., Pirozhkov, S. V., Bebikh, G. F., and Kuznetsova, L. K. (1973) *Vestn. Mosk. Univ. Khim.*, **28**, 77–82 (Engl. transl. **28**, 51–4); (1973) *Chem. Abstr.*, **78**, 164890b; Chmertova, M. K., Kochetkova, N. E., and Myasoedov, B. F. (1980) *J. Inorg. Nucl. Chem.*, **42**, 897–903.
130. See, for example, Shmidt, V. S. and Shesterikov, V. N. (1971) *Radiokhimiya*, **13**, 815–21; *Sov. Radiochem.*, **13**, 840–5.
131. Shalinets, A. B. (1971) *Radiokhimiya*, **13**, 566–70; *Sov. Radiochem.*, **13**, 583–6.
132. Zeitsev, A. A., Nazarova, I. I., Fetukhova, I. V., Filimonov, V. T., and Yakovlev, G. N. (1973) *Radiokhimiya*, **16**, 176–9; *Sov. Radiochem.*, **16**, 177–80.
133. Tanner, S. P. and Choppin, G. R. (1968) *Inorg. Chem.*, **7**, 2046–8.
134. Keller, C. and Schreck, H. (1969) *J. Inorg. Nucl. Chem.*, **31**, 1121–32.
135. Keller, C., Eberle, S. H., and Mosdzelewski, K. (1966) *Radiochim. Acta*, **5**, 185–8.
136. Akatsu, E., Hoshi, M., Ono, R., and Ueno, K. (1968) *J. Nucl. Sci. Tech.*, **5**, 252–5.
137. Stroński, I. and Rekas, M. (1973) *Radiochem. Radioanal. Lett.*, **14**, 297–304.
138. Myasoedov, B. F., Milyukova, M. S., and Ryzhova, L. V. (1970) *Radiochem. Radioanal. Lett.*, **5**, 19–23.
139. de Carvalho, R. G. and Choppin, G. R. (1967) *J. Inorg. Nucl. Chem.*, **29**, 725–35.
140. Elesin, A. A., Lebedev, I. A., Piskunov, E. M., and Yakovlev, G. N. (1967) *Radiokhimiya*, **9**, 161–6; *Sov. Radiochem.*, **9**, 159–63.
141. Grenthe, I. (1963) *Acta. Chem. Scand.*, **17**, 1814–15.
142. Nikolaev, V. M. and Lebedev, V. M. (1975) *Zh. Neorg. Khim.*, **20**, 1359–61; *Sov. J. Inorg. Chem.*, **20**, 765–7.
143. Hubert, S., Hussonnois, M., Brillard, L., Goby, G., and Guillaumont, R. (1974) *J. Inorg. Nucl. Chem.*, **36**, 2361–6.
144. Elesin, A. A. and Zaitsev, A. A. (1971) *Radiokhimiya*, **13**, 775–8; *Sov. Radiochem.*, **13**, 798–801.
145. Dedov, V. B., Lebedev, I. A., Ryzhov, M. N., Trukhlyaev, P. S., and Yakovlev, G. N. (1961) *Radiokhimiya*, **3**, 701–5; *Sov. Radiochem.*, **3**, 197–201.
146. Eberle, S. H. and Ali, S. A. (1968) *Z. Anorg. Allg. Chem.*, **361**, 1–14.
147. Elesin, A. A., Zaitsev, A. A., Sergeev, G. M., and Nazarova, I. I. (1973) *Radiokhimiya*, **15**, 64–8; *Sov. Radiochem.*, **15**, 62–6.
148. Sudakov, L. V., Kapshukov, I. I., Baranov, A.-Yu., Shimbarev, E. V., and Lyalyushkin, N. V. (1976) *Radiokhimiya*, **19**, 490–6; *Sov. Radiochem.*, **19**, 400–5.
149. For a review of curium chemistry in the nuclear fuel cycle, see Keller, O. L. (1978) *Radiochim. Acta*, **25**, 211–23.
150. See, for example, Illige, J. D., Hulet, E. K., Nitschke, J. M., Dougan, R. J., Lougheed, R. W., Ghiorso, A., and Landrum, J. H. (1978) *Phys. Lett. B*, **78**, 209–12.
151. Diamond, H., Bentley, W. C., Jaffey, A. H., and Flynn, K. F. (1977) *Phys. Rev. C*, **15**, 1034–42.
152. Polyukhov, V. G., Timofeev, G. A., Privalova, P. A., Gabeskiriya, V. Ya., and Chetverikov, A. P. (1977) *Radiokhimiya*, **19**, 507–10; *Sov. Radiochem.*, **19**, 414–17.
153. Huray, P. G., Nave, S. E., Peterson, J. R., and Haire, R. G. (1980) *Physica B/C*, **102**, 217–20.
154. Kannelakopulos, B. (1978) AED-Conf-78-074-002; *INIS Atomindex*, **10**, 425–659; Morss, L. R., *et al.* (1981) *Actinides*–1981, Lawrence Berkeley Laboratory Report LBL-12441, p. 263; Haire, R. G., Nave, S. E., and Huray, P. G. (1982) *12th Journee des Actinides*, Orsay. See also ref. 172.

155. Baes, C. F. and Mesmer, R. E. (1976) *Hydrolysis of Cations*, Wiley, New York.
156. Thompson, G. H. (1972) *Ion Exch. Membranes*, **1**, 87–9.
157. Bigelow, J. E., Collins, E. D., and King, L. J. (1980) in *Actinide Separations* (ACS Symp. Ser. 117), American Chemical Society, Washington DC, pp. 147–55; Bond, W. D. and Leuze, R. E. (1980) *ibid.*, pp. 441–53.
158. Dedov, V. B., *et al.* (1965) *Radiokhimiya*, **7**, 453–61; *Sov. Radiochem.*, **7**, 452–8.
159. Keenan, T. K. (1961) *J. Am. Chem. Soc.*, **83**, 3719–20.
160. Finch, C. B., Fellows, R. L., and Young, J. P. (1978) *J. Luminesc.*, **16**, 109–15.
161. Burney, G. A. (1980) *Sep. Sci. and Technol.*, **15**, 163–82.
162. Reichlin, R. L., Akella, J., Smith, G. S., and Schwab, M. (1981) in *Actinides*–1981, Lawrence Berkeley Laboratory Report LBL-12441.
163. Noé, M., Fuger, J., and Duyckaerts, G. (1970) *Inorg. Nucl. Chem. Lett.*, **6**, 111–19.
164. Raschella, D. L., Fellows, R. L., and Peterson, J. R. (1981) *J. Chem. Thermodyn.*, **13**, 303–12.
165. Mikheev, N. B. (1983) *Radiochim. Acta*, **32**, 69.
166. Martinot, L. and Fuger, J. (1900) in *Oxidation–Reduction Potentials* (eds A. J. Bard, R. Parsens, and J. Jordan), IUPAC, in press.
167. Lebedev, I. A., Pirozhkov, S. V., and Yakovlev, G. N. (1960, 1962) *Radiokhimiya*, **2**, 549–58; **4**, 304–8; *Sov. Radiochem.*, **2**(5), 39–47; **4**, 273–6.
168. Shannon, R. D. (1976) *Acta Crystallogr. A*, **32**, 751–67.
169. Akatsu, J. (1965) *Radiochim. Acta*, **4**, 58–60.
170. Eyring, L. (1967) *Adv. Chem. Ser.*, **71**, American Chemical Society, Washington, D.C., pp. 67–85.
171. Weigel, F. and Marquardt, R. (1983) *J. Less-Common Metals*, **90**, 283–90.
172. Nave, S. E., Haire, R. G., and Huray, P. G. (1983) *Phys. Rev. B*, **28**, 2317–27.
173. Gibson, J. K. and Haire, R. G. (1985) *J. Solid State Chem.*, **59**, 317–23.
174. Radchenko, V. M., Seleznev, A. G., Shushakov, V. D., Ryabinin, M. A., Lebedeva, L. S., Karelin, E. A., and Visel'ev, V. Ya (1985) *Radiokhimiya*, **27**, 33–37; *ibid.*, 38–42.
175. Nave, S. E., Huray, P. G., Peterson, J. R., Damien, D. A., and Haire, R. G. (1981) *Physica*, **107B**, 253–4.
176. Kazantsev, G. N., Skiba, O. V., Burnaevà, A. A., Kolesnikov, V. P., Volkov, Yu. F., Kryukova, A. I., and Korshunov, I. A. (1982) *Radiokhimiya*, **24**, 88–91.
177. Hobart, D. E., Varlashkin, P. G., Samhoun, K., Haire, R. G., and Peterson, J. R. (1983) *Rev. Chim. Minerale*, **20**, 817–26.

Notes added in proof. X-ray diffraction studies of ^{248}Cm metal have yielded an orthorhombic form as well as delocalization and compressibility data: Benedict, U., Haire, R. G., Peterson, J. R., and Itié, J. P. (1985) *J. Phys.* F, **15**, L29–35; Haire, R. G., Benedict, U., Peterson, J. R., Dufour, C., and Itié, J. P. (1985) *J. Less-Common Metals*, **109**, 71–8. An EPR study of Cm-doped $LuPO_4$ single crystals has appeared: Boatner, L. A. and Abraham, M. M. (1982) *Phys. Rev. B*, **26**, 1434–7. A calorimetric study of Cm complexation by EDTA and acetate has been published: Choppin, G. R., Liu, Q., and Sullivan, J. C. (1985) *Inorg. Chem.*, **24**, 3968–9. Many papers on basic and applied curium chemistry from the 1984 International Chemical Congress of Pacific Basin Societies have been published: Edelstein, N. M., Navratil, J. D., Schulz, W. W. (1985) *Americium and Curium Chemistry and Technology*, D. Reidel, Dordrecht, Holland.

CHAPTER TEN

BERKELIUM

David E. Hobart and Joseph R. Peterson

10.1 INTRODUCTION

As was the case for the previously discovered transuranium elements, element 97 was first produced via a nuclear bombardment reaction. In December 1949 ion-exchange separation of the products formed by the bombardment of ^{241}Am with accelerated alpha particles provided a new electron-capture activity eluting just ahead of curium [1, 2]. This activity was assigned to an isotope (mass number 243) of element 97. The new element was named berkelium after Berkeley, California, the city of its discovery, in a parallel manner to the naming of its lanthanide analog, terbium, after Ytterby, Sweden. The initial investigations of the chemical properties of berkelium were limited to tracer experiments (ion exchange and co-precipitation), but these were sufficient to establish the stability of Bk(III) and the accessibility of Bk(IV) in aqueous solution and to estimate the electrochemical potential of the Bk(IV)/Bk(III) couple [2, 3].

Since a complete study of the chemistry of an element is not possible by tracer methods alone, a program for long-term neutron irradiation of about 8 g of ^{239}Pu was initiated in 1952 in the Materials Testing Reactor (Arco, Idaho) to provide macroquantities of berkelium [4]. In 1958 about 0.6 μg of ^{249}Bk was separated, purified, and used in experiments to determine the absorption spectrum of Bk(III) in aqueous solution and to measure the magnetic susceptibility of Bk(III) [4]. No Bk(III) absorption was observed over the wavelength range 450–750 nm, but an upper limit of about 20 was set for the molar absorptivity of any absorption by Bk(III) in this wavelength region. The magnetic susceptibility, measured from 77 to 298 K with the Bk(III) ions sorbed in a single

bead of cation-exchange resin, was found to conform to the Curie–Weiss law with an effective moment of 8.7 μ_B, suggesting a $5f^8$ electronic configuration for the Bk(III) ion.

The first structure determination of a compound of berkelium, the dioxide, was carried out in 1962 [5]. Four x-ray diffraction lines were obtained from 4 ng of BkO_2 and indexed on the basis of a face-centered cubic structure with $a_0 = 0.533 \pm 0.001$ nm. In the intervening 24 years, considerable information about the physicochemical properties of berkelium has been obtained in spite of the rather limited availability and short half-life of ^{249}Bk, the only isotope available in bulk quantities.

The authors have focused this review of the chemistry of berkelium on open-literature references in English or English translation, except where it was deemed necessary to cite a research institution report or technical memorandum. Thus also minimized are references to theses, dissertations, and patents. The biologic and metabolic effects on man and animals of exposure to and/or ingestion of berkelium have not been reviewed here. Also excluded are references dealing with the determination and/or use of the nuclear properties of the various isotopes of berkelium. The references cited are not necessarily inclusive or the original ones, yet they should be adequate to permit the interested reader to access easily the broader areas beyond.

Earlier reviews of the physicochemical properties of berkelium are available in several new supplement series volumes of the *Gmelin Handbuch der Anorganishen Chemie* (Springer-Verlag, New York, 1972 onward), in Keller's *The Chemistry of the Transuranium Elements* (Verlag Chemie, Weinheim, 1971), and in volume 28 of *Advances in Inorganic Chemistry and Radiochemistry* (Academic Press, New York, 1984).

10.2 NUCLEAR PROPERTIES, AVAILABILITY, AND APPLICATIONS

Selected nuclear properties of the principal isotopes of berkelium are listed in Table 10.1 [6]. In addition to these isotopes, ranging from mass numbers 240 to 251, there are spontaneously fissioning isomers known for berkelium mass numbers 242, 243, 244, and 245, all with half-lives less than 1 μs. Only ^{249}Bk is available in bulk quantities for chemical studies, as a result of prolonged neutron irradiation of Pu, Am, or Cm [7]. About 0.73 g of this isotope has been isolated from target rods irradiated with neutrons in the High Flux Isotope Reactor (Oak Ridge, Tennessee) over the period 1967 through 1985 [8–10]. The relative atomic mass of berkelium-249 was given as 249.075 by the International Union of Pure and Applied Chemistry (IUPAC) [11]; the most recent determination of its half-life yielded a value of 329 ± 4 days [12].

Besides the research use of ^{249}Bk for the characterization of the chemical and physical properties of element 97, its relatively rapid decay to ^{249}Cf (0.2% per

Table 10.1 *Nuclear properties of berkelium isotopes.*

Mass number	*Half-life*	*Mode of decay*	*Main radiations (MeV)*		*Method of production*
240	5 min	EC			^{232}Th(^{14}N,6n)
242	7 min	EC			^{235}U(^{11}B,4n)
					^{232}Th(^{15}N,5n)
243	4.5 h	EC 99.85%	α	6.758 (15%)	^{243}Am(α,4n)
		α 0.15%		6.574 (26%)	
			γ	0.755	
244	4.35 h	EC > 99%	α	6.667 (~ 50%)	^{243}Am(α,3n)
		α 6×10^{-3}%		6.625 (~ 50%)	
			γ	0.218	
245	4.90 d	EC 99.88%	α	6.349 (15.5%)	^{243}Am(α,2n)
		α 0.12%		6.145 (18.3%)	
			γ	0.253 (31%)	
246	1.80 d	EC	γ	0.799 (61%)	^{243}Am(α,n)
247	1.38×10^3 yr	α	α	5.712 (17%)	^{247}Cf daughter
				5.532 (45%)	^{244}Cm(α,p)
			γ	0.084 (40%)	
248[a]	23.7 h	β^- 70%	β^-	0.86	^{248}Cm(d,2n)
		EC 30%	γ	0.551	
248[a]	> 9 yr	decay not observed			^{246}Cm(α,pn)
249	320 d	β^- > 99%	α	5.417 (74.8%)	multiple n capture
		α 1.45×10^{-3}%		5.390 (16.0%)	
			β^-	0.125	
			γ	0.327 weak	
250	3.217 h	β^-	β^-	1.781	^{254}Es daughter
			γ	0.989 (45%)	^{249}Bk(n,γ)
251	56 min	β^-	β^-	~ 1.1	^{255}Es daughter
			γ	0.178	

[a] Not known whether ground-state nuclide or isomer.

day) makes it a valuable source of this important isotope of californium for chemical study. Recently this genetic relationship has been exploited in studies of the chemical consequences of beta (β^-) decay in the bulk-phase solid state [13, 14].

There have been no reports of practical applications for any of the isotopes of berkelium.

10.3 SEPARATION AND PURIFICATION

Berkelium may be purified by many methods that are also applicable to other actinide elements. Therefore, only those methods that apply specifically to berkelium separation and purification will be treated here.

Since berkelium can be readily oxidized to Bk(IV), it can be separated from other, non-oxidizable transplutonium elements by combining oxidation–

reduction (redox) methods with other separation techniques. The first application of this approach was performed by oxidizing Bk(III) with BrO_3^- in nitric acid solution [15]. The resultant Bk(IV) was then extracted with hydrogen di(2-ethylhexyl)orthophosphoric acid (HDEHP) in heptane followed by back-extraction with nitric acid containing H_2O_2 reducing agent. In addition to other reports of the use of BrO_3^- as an oxidizing agent in berkelium purification procedures [16–20], the use of CrO_4^{2-} [17, 21], $Cr_2O_7^{2-}$ [21–23], $Ag(I)/S_2O_8^{2-}$ [21, 24], PbO_2 [22, 25, 26], BiO_3^- [22], O_3 [25], and photochemical oxidation [25] has also been reported. Separation of the oxidized berkelium has been accomplished by the use of: (a) liquid–liquid extraction with HDEHP [15, 17, 20, 27, 28], trioctylphosphine oxide [29], alkylpyrocatechol [30], 2-thenoyltrifluoroacetone [23, 31], primary, tertiary or quaternary amines [21, 24, 31–33], or tributyl phosphate [34, 35]; (b) extraction chromatography with HDEHP [19, 36–38] or zirconium phosphate adsorbant [22, 25, 26, 39]; (c) precipitation of the iodate [16, 18]; or (d) ion exchange [19, 39, 40]; the techniques can be applied separately or in combination with one another.

The purification procedures outlined above provide separation of berkelium from all trivalent lanthanides and actinides with the notable exception of cerium. Since berkelium and cerium exhibit nearly identical redox behavior, most redox separation procedures include a Bk–Ce separation step [22, 39–43]. Separation of Bk(III) from Ce(III) and other trivalent lanthanide and actinide elements can also be accomplished without the use of redox procedures [39, 41–52].

Personnel in the Transuranium Processing Plant (TRU) at the Oak Ridge National Laboratory have isolated and purified 0.73 g of ^{249}Bk during the period 1967 through 1985 [9, 10] using the procedure outlined in Fig. 10.1 [53]. The transcurium elements, partitioned by LiCl-based anion exchange, are precipitated as hydroxides, filtered, and dissolved in nitric acid. Initial isolation is accomplished by high-pressure elution from cation-exchange resins with α-hydroxyisobutyrate (BUT) solution. The berkelium fraction is oxidized and extracted into HDEHP/dodecane from HNO_3–$NaBrO_3$ solution. The organic fraction containing Bk(IV) is treated with 2,5-di(t-butyl)hydroquinone (DBHQ) to reduce the Bk(IV) to Bk(III) before back-extracting (stripping) it into HNO_3–H_2O_2 solution. Then another oxidation/extraction, reduction/back-extraction cycle is carried out. The solution at this point is radiochemically pure except for fission-product cerium. After solvent clean-up and evaporation to dryness, the berkelium is dissolved in 0.1 M HCl for final ion-exchange purification steps including alcoholic–HCl elution from cation-exchange resin and cation clean-up columns [53].

A procedure for the rapid separation of berkelium from other actinides, lanthanides, and fission products was developed in order to measure the decay properties of short-lived isotopes [54]. Bk and Ce were separated from other elements using solvent extraction with HDEHP followed by cation-exchange high-pressure liquid chromatography (HPLC) using α-hydroxyisobutyrate as the eluant. The elution curve, showing a clean separation of Bk from Ce, is shown in

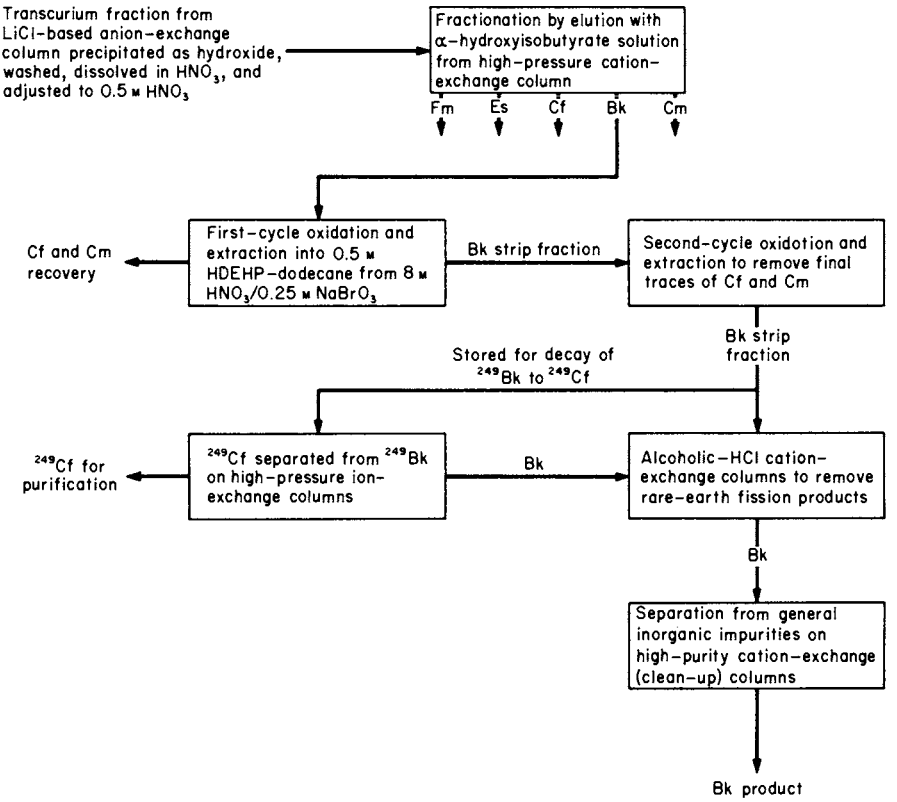

Fig. 10.1 *Schematic diagram of procedures used in the final isolation and purification of berkelium in the Transuranium Processing Plant (TRU) at the Oak Ridge National Laboratory (ORNL). (Adapted from ref.* 53.)

Fig. 10.2. The total separation time was reported to be 8 min. The fast separation of berkelium from beryllium foil targets and gold catcher foils has been published [55].

For additional discussion of berkelium separation procedures, the reader is referred to several reviews and comprehensive texts on the subject [56–62].

10.4 ATOMIC PROPERTIES

10.4.1 Electronic energies

The ionization potential of neutral berkelium ($5f^9 7s^2$) has been derived from spectroscopic data to be 6.229 ± 0.025 eV [63]. The changes in entropy associated with the stepwise ionization of gaseous berkelium atoms have also been

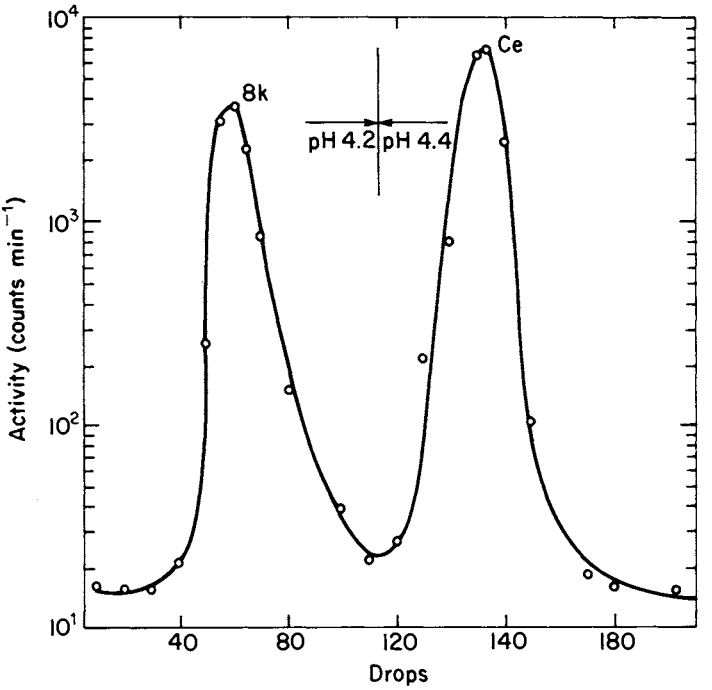

Fig. 10.2 *HPLC elution curve of Bk and Ce using* 0.5 M *ammonium α-hydroxyisobutyrate on a cation-exchange column* [54]. (*Reproduced with permission of the authors and Pergamon Press.*)

calculated [64]. The energy interval between the ground level ($^7H_8$) and first excited level ($^5H_7$) of singly ionized berkelium was determined from measurements on plates taken with a high-resolution emission spectrograph and found to be $1.487\,52 \times 10^5\ m^{-1}$ [65]. Several authors have calculated the energies of and energy intervals between the lowest-lying levels of the various electronic configurations of neutral berkelium [66–69] and of singly, doubly, and triply ionized berkelium [69, 70].

From measurements of the energies of a number of internal conversion lines in berkelium-249 (produced by the alpha decay of einsteinium-253), the atomic electron binding energies in berkelium were calculated for the K through O shells [71]. The K-series x-ray energies and intensities of berkelium were later measured, and the K-shell electron binding energy calculated [72]. The measured energies and relative transition probabilities agreed well with theoretical predictions [73, 74].

Also available are the results of relativistic relaxed-orbital *ab initio* calculations of L-shell Coster–Kronig transition energies for all possible transitions in berkelium atoms [75], relativistic relaxed-orbital Hartree–Fock–Slater calculations of the neutral-atom electron binding energies in berkelium [76], and

calculations of the K- through O-shell binding energies and K and L x-ray energies for berkelium [77]. Relativistic Hartree–Slater values of the x-ray emission rates for the filling of K- and L-shell vacancies in berkelium have been tabulated [78]. X-ray emission rates for the filling of all possible single inner-shell vacancies in berkelium by electric dipole transitions have been calculated using non-relativistic Hartree–Slater wavefunctions [79].

10.4.2 Emission spectra

Twenty emission lines, produced from 0.2 μg of berkelium in a high-voltage spark, were reported in 1965 [80]. In 1967 between 3000 and 5000 lines were recorded in the wavelength region 250–900 nm from 38 μg of ^{249}Bk in an electrodeless discharge lamp [81]. Many of the emission lines exhibited well-resolved eight-component hyperfine structure, which established the nuclear spin of ^{249}Bk to be 7/2 [81]. This value is in agreement with that derived from nuclear decay systematics.

The ground-state electronic configurations (levels) of neutral and singly ionized berkelium were identified as $5f^9\,7s^2$ ($^6H_{15/2}$) and $5f^9 7s^1$ ($^7H_8$), respectively [82]. A nuclear magnetic dipole moment of 1.5 μ_N [65] and a quadrupole moment of 4.7 barn [83] were determined for ^{249}Bk, based on analysis of the hyperfine structure in the berkelium emission spectrum.

The wavenumbers, wavelengths, and relative intensities of 1930 of the stronger emission lines from ^{249}Bk in the 254–980 nm wavelength region are available [84]. The infrared emission spectrum of ^{249}Bk from 830 to 2700 nm has been recorded [85].

A preliminary report on the self-luminescence of ^{249}Bk(III) in a $LaCl_3$ host lattice was published in 1963 [86], and the self-luminescence spectra of ^{249}Bk-doped BaF_2 and $SrCl_2$ were reported in 1978 [87]. The absence of ultraviolet-excited sharp-line sensitized luminescence of ^{249}Bk-doped gadolinium hexafluoroacetyl acetonate has been noted [88, 89]. Such luminescence was absent also in cesium berkelium hexafluoroacetyl acetonate chelate in anhydrous ethanol [88]. A study of Bk^{3+} fluorescence in H_2O and D_2O solutions has been reported, and a basis for assessing the use of fluorescence detection for transuranic ions has been established [90].

10.4.3 Solution absorption spectra

The first attempts to measure the absorption spectrum of Bk(III) involved the use of a single ion-exchange resin bead [4]. Later the spectrum of a 3.6×10^{-3} M Bk(III) solution was recorded in a microcell [91]. Sixteen absorption bands of Bk(III) were identified in the solution spectrum recorded in a 'suspended-drop' microcell over the wavelength range 320–680 nm [92]. The results of additional observations identified a total of 23 absorption bands in the 280–1500 nm wavelength region [93].

The first attempts to record the Bk(IV) solution absorption spectrum were hindered by the presence of cerium impurities [91]. The positions of the Bk(IV) absorption bands, superimposed on the strong Ce(IV) bands, suggested the assignment of $5f^7$ for the electronic configuration of Bk(IV), in agreement with the actinide hypothesis.

The absorption spectra of Bk(III) and Bk(IV) have been recorded in various media [94]. New absorption bands were reported as the result of using larger quantities of ^{249}Bk of higher purity. Observations of the spectrum of Bk(III) were extended further into the ultraviolet wavelength region (to 200 nm), and nine new absorption bands were reported [95]. An interpretation of the low-energy bands in the solution absorption spectra of Bk(III) and Bk(IV) was published [96]. Recent experimental work using larger quantities of Bk than had been available previously, coupled with a new technique for rapidly separating small quantities of daughter ^{249}Cf, has resulted in a Bk(III) solution absorption spectrum with minimal interference from radiolysis products and significantly higher resolution than those of previously published spectra [97]. A parametric fit of the data was performed in order to obtain the energy level structure of the Bk^{3+} aquo ion. The band intensities were analyzed using the Judd–Ofelt theory and fluorescent branching ratios were computed from theoretical parameters [97].

Solution absorption spectra of Bk(III) and Bk(IV) are shown in Fig. 10.3. The spectrum of Bk(III) is characterized by sharp absorption bands of low molar absorptivity attributed to 'Laporte-forbidden' f–f transitions and by intense absorption bands in the ultraviolet region attributed to f–d transitions [95]. The spectrum of Bk(IV) is dominated by a strong absorption band at 250–290 nm, the peak position of which is strongly dependent on the degree of complexation of Bk(IV) by the solvent medium. This band is attributed to a charge-transfer mechanism [95].

Electronic spectra of Bk(III) [97, 98] and Bk(IV) [99] and a prediction of the electronic spectrum of Bk(II) [100] have been published. Spin–orbit coupling diagrams for these berkelium ions, based on a free-ion interpretation of the f–f spectra, were proposed.

10.4.4 Solid-state absorption spectra

The absorption spectrum of Bk(III) in a lanthanum chloride host matrix at 77 K was first obtained in 1964 [101]. A prediction of the energy level structure of Bk(III) was made by others the same year [102]. Extensive, low-temperature spectroscopic studies of $BkCl_3$ showed the absence of transitions to excited $J = 0$ and $J = 1$ states [103, 104]. This provided good evidence for a $\mu = 0$ ground level for Bk(III), consistent with that of Tb(III):$LaCl_3$ [105]. Experimental and theoretical studies of the crystal field parameters of Bk(III) in a $LaCl_3$ host lattice have also been reported [106].

Microscale spectrophotometric techniques, using 0.5–10 μg berkelium samples, have been applied for identification and characterization of berkelium

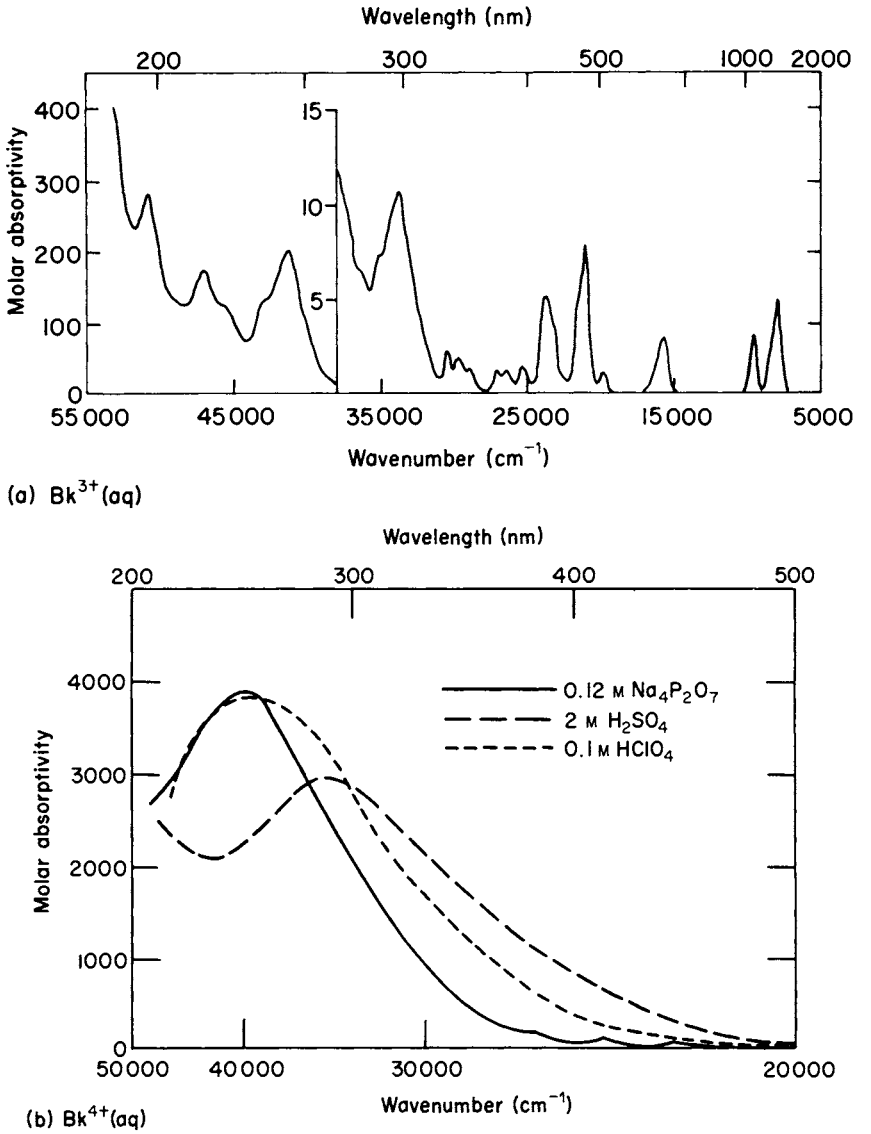

Fig. 10.3 *Solution absorption spectra of (a) Bk(III) in 0.2 M $HClO_4$ (DCl solutions were used for portions of the infrared spectrum) [97] and (b) Bk(IV) in various media [95]. (Reproduced with permission of the authors, and the American Institute of Physics and Pergamon Press, respectively.)*

halides and oxyhalides [107]. The spectra of orthorhombic and hexagonal $BkCl_3$ have been recorded and are shown in Fig. 10.4 [108]. Spectra of orthorhombic and monoclinic $BkBr_3$ [109], trigonal and orthorhombic BkF_3 [14], and monoclinic BkF_4 [14] have been reported. This technique has also been applied to the study of the chemical consequences of radioactive decay in bulk-phase

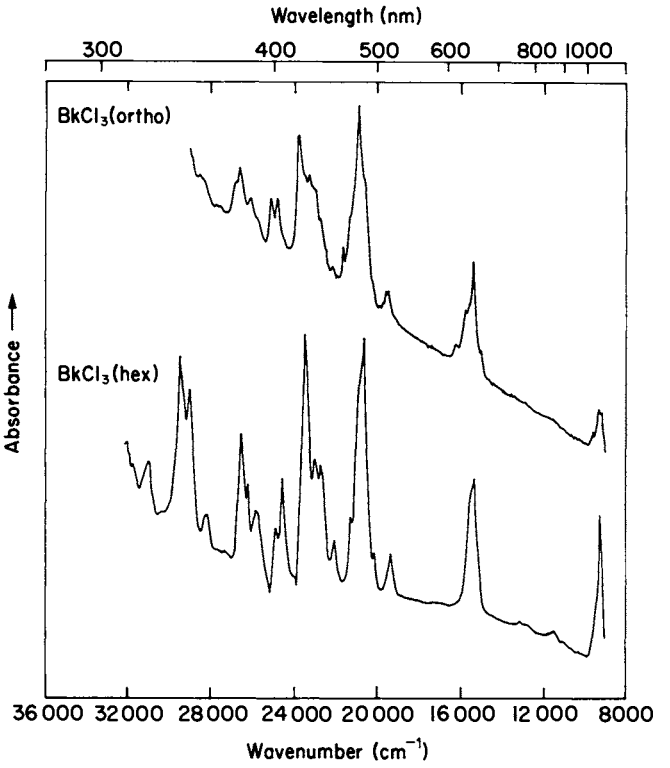

Fig. 10.4 *Solid-state absorption spectra of orthorhombic and hexagonal* $BkCl_3$ [108].

solid-state samples [13, 110]. It was found that the ^{249}Cf daughter growing into crystalline $^{249}BkBr_3$ exhibited the same oxidation state and crystal structure as its berkelium parent [13].

The absorption spectra of Bk(III) and Bk(IV) hydroxides as suspensions in 1 M NaOH have been reported [111]. The solid-state absorption spectrum [112] and Raman spectrum [113] of berkelium(III) orthophosphate have been obtained. Line lists of the absorption bands of two organoberkelium compounds, $Bk(C_5H_5)_3$ [114] and $[Bk(C_5H_5)_2Cl]_2$ [115], have been published.

For additional information [116] and discussion of the development of the theoretical treatment of berkelium spectra, the reader is referred to other sources [83, 97, 105] and to Chapter 16.

10.5 METALLIC STATE

10.5.1 Preparation

The first bulk (> 1 μg) samples of berkelium metal were prepared in early 1969 by the reduction at about 1300 K of BkF_3 with lithium metal vapor [117]. The

BkF_3 samples were suspended in a tungsten wire spiral above a charge of Li metal in a tantalum crucible. More recently berkelium metal samples up to 0.5 mg each have been prepared via the same chemical procedure [118]. Elemental berkelium can also be prepared by reduction of BkF_4 with lithium metal and by reduction of BkO_2 with either thorium or lanthanum metal. The latter reduction process is better suited to the preparation of thin metal foils unless multi-milligram quantities of berkelium are available.

10.5.2 Physical properties

Berkelium metal exhibits two crystallographic modifications, double hexagonal close-packed (dhcp) and face-centered cubic (fcc). Thus it is isostructural with the two preceding elements, both of which exhibit the fcc structure at high temperature. The room-temperature lattice constants of the dhcp (α) form are $a_0 = 0.3416 \pm 0.0003$ and $c_0 = 1.1069 \pm 0.0007$ nm, yielding a calculated density of 14.78 g cm^{-3} and a metallic radius (CN 12) of 0.170 nm [117]. The room-temperature metastable fcc (β) lattice parameter is $a_0 = 0.4997 \pm 0.0004$ nm, from which the x-ray density and metallic radius (CN 12) are calculated to be 13.25 g cm^{-3} and 0.177 nm, respectively [117]. The metallic radius of berkelium, assuming a metallic valence of 3 and 12-fold coordination, has been calculated to be 0.1739 nm [119]. On the other hand the radii (CN 12) of berkelium were predicted to be 0.184 nm for trivalent metal and 0.1704 nm for tetravalent metal, so that the observed dhcp form corresponds to tetravalent metal while the fcc form represents a metallic valence of 3.5 [120].

Although berkelium metal is dimorphic, the transformation temperature is not known with certainty. A change in the appearance of Bk metal samples at 1203 ± 30 K during the course of two melting-point determinations might correspond to the dhcp → fcc phase transformation, which should be accompanied by a 12% change in the volume of the sample [121]. The melting point of berkelium metal has been determined to be 1259 ± 25 K from measurements on two samples [121]. The melting and boiling points of elemental berkelium have been estimated to be 1323 ± 50 K and 2900 ± 50 K, respectively [122].

The first studies of berkelium metal under pressure were performed with a diamond anvil pressure cell using energy-dispersive x-ray powder diffraction analysis [123]. Three different metallic phases were observed as the pressure was increased to 57 GPa. The normal-pressure dhcp form changed to an fcc form at about 8 GPa. At about 22 GPa, the fcc form was transformed to the α-uranium-type orthorhombic structure [123]. A 12% shrinkage in volume accompanied the latter transition. This collapse was associated with delocalization of the 5f electrons [124]. Below 22 GPa, a bulk modulus (compressibility) of 30 ± 10 GPa was estimated for berkelium metal. Berkelium metal under pressure behaves similarly to americium, curium, and some light lanthanide metals and does not appear to undergo an isostructural phase transition corresponding to a change in metallic valence before delocalization of the 5f electrons [125].

In the first experiments to measure the vapor pressure of metallic berkelium using Knudsen effusion target-collection techniques, the preliminary data were fitted with a least-squares line to give a provisional vaporization equation for the temperature range 1326–1582 K and $\Delta H^\circ_{298} = 382 \pm 18$ kJ mol^{-1} [126]. More recent measurements of the vapor pressure of Bk metal over the temperature range 1100–1500 K, using combined Knudsen effusion mass-spectrometric and target-collection techniques, have been completed [122]. The vaporization equations obtained were

$$\log(P/\text{atm}) = (5.78 \pm 0.21) - (15\,718 \pm 253)/T$$

for solid Bk between 1107 and 1319 K, and

$$\log(P/\text{atm}) = (5.14 \pm 0.17) - (14\,902 \pm 244)/T$$

for liquid Bk between 1345 and 1528 K. The enthalpy of fusion was calculated to be 7.92 kJ mol^{-1}, and the enthalpy associated with the dhcp → fcc transition was calculated to be 3.66 kJ mol^{-1} [122]. The crystal entropy, S°_{298}, of berkelium was estimated to be 76.2 ± 1.3 J K^{-1} mol^{-1} [127] and more recently to be 78.2 ± 1.3 J K^{-1} mol^{-1}, and the average of data according to the second and third laws yielded 310 ± 6 kJ mol^{-1} for its enthalpy of vaporization, ΔH°_{298} [122]. Correlation systematics have suggested that the standard enthalpy of sublimation of berkelium metal, ΔH°_f (Bk (g)), is 280 kJ mol^{-1} and that the standard enthalpy of formation of aqueous Bk(III), ΔH°_f (Bk^{3+} (aq)), is −615 kJ mol^{-1} [128, 129]. A later modification of the systematics [128] led to values of 320 ± 8 kJ mol^{-1} and -590 ± 21 kJ mol^{-1} for ΔH°_f(Bk(g)) and ΔH°_f(Bk^{3+} (aq)), respectively [130].

The enthalpy of solution of Bk metal (dhcp) to Bk^{3+}(aq) in 1 M HCl at 298 K was determined from five measurements to be -576 ± 25 kJ mol^{-1} [118]. The error limits reported did not reflect the precision of the calorimetric measurements but rather the uncertainties in the purity of the berkelium metal. A new determination of the enthalpy of solution of Bk metal (dhcp) in 1 M HCl at 298.15 ± 0.05 K has yielded a value of -600.2 ± 5.1 kJ mol^{-1} [131]. From this value ΔH°_f (Bk^{3+}(aq)) was derived to be -601 ± 5 kJ mol^{-1} and, using reasonable entropy estimates, the standard potential of the Bk(III)/Bk(0) couple was calculated to be -2.01 ± 0.03 V.

Studies of the magnetic susceptibility of berkelium metal have been hampered by the difficulty in obtaining well-characterized, single-phase, bulk samples containing minimal amounts of daughter californium. Recent results obtained from a 21 μg sample of dhcp Bk metal (~ 12 at% Cf) indicated a transition to antiferromagnetic behavior at about 34 K and paramagnetic behavior between 70 and 250 K [132]. Applying the Curie–Weiss susceptibility relationship to the berkelium data obtained at fields greater than 0.08 T (where the field dependency was saturated) yielded $\mu_{eff} = 9.69\,\mu_B$ and $\Theta = 101.6$ K. The agreement of this value with the theoretical free-ion effective moment ($9.72\,\mu_B$) calculated for trivalent berkelium with LS coupling suggests that dhcp Bk metal exhibits high-

temperature magnetic behavior like its lanthanide homolog terbium. The results of earlier magnetic measurements on smaller samples of berkelium metal exhibiting mixed phases were reported by others [93, 133].

10.5.3 Chemical properties

During the handling of microgram-sized samples of berkelium metal, it was observed that the rate of oxidation in air at room temperature is not extremely rapid, possibly due to the formation of a 'protective' oxide film on the metal surface [133]. Berkelium is a chemically reactive metal, and berkelium hydride [121], some chalcogenides [121, 134, 135], and pnictides [136, 137] have been prepared directly from the reaction of Bk metal with the appropriate non-metallic element.

Berkelium metal dissolves rapidly in aqueous mineral acids liberating hydrogen gas and forming Bk(III) in solution.

10.5.4 Theoretical treatment

In 1972 a hybridized non-degenerate 6d and 5f virtual-bound-states model was used to describe the properties of the actinide metals, including berkelium [138]. It accounted for the occurrence of localized magnetism in Bk metal. In 1974 a review of the understanding of the electronic properties of berkelium metal as derived from electronic band theory was published [139]. Included was the relativistic energy band structure of face-centered cubic Bk metal ($5f^8 6d^1 7s^2$), and the conclusion was that berkelium is a rare-earth-like metal with localized (ionic) 5f electrons resulting from less hybridization with the 6d and 7s itinerant bands than occurs in the lighter actinides.

A phenomenological model based on crystal structure, metallic radius, melting point, and enthalpy of sublimation has been used to arrive at the electronic configuration of berkelium metal [140]. An energy difference of 0.92 eV was calculated between the $5f^9 7s^2$ ground state and the $5f^8 6d^1 7s^2$ first excited state. The enthalpy of sublimation of trivalent Bk metal was calculated to be 2.99 eV (288 kJ mol^{-1}), reflecting the fact that berkelium metal is more volatile than curium metal. It was also concluded that the metallic valence of the face-centered cubic form of berkelium metal is less than that of the double hexagonal close-packed modification [140].

A relativistic Hartree–Fock–Wigner–Seitz band calculation has been performed for Bk metal in order to estimate the Coulomb term U (the energy required for a 5f electron to hop from one atomic site to an adjacent one) and the 5f-electron excitation energies [141]. The results for berkelium in comparison to those for the lighter actinides show increasing localization of the 5f states, i.e. the magnitude of the Coulomb term U increases through the first half of the actinide series with a concomitant decrease in the width of the 5f level.

10.6 COMPOUNDS

10.6.1 General summary

The trivalent oxidation state of berkelium prevails in the known berkelium compounds, although the tetravalent state is exhibited in BkO_2, BkF_4, and Cs_2BkCl_6. Selected crystallographic data for Bk metal and a number of berkelium compounds are collected in Table 10.2. In cases where there have been multiple reports of lattice parameters for a particular compound, the later values or the ones considered more reliable by the present authors are given in Table 10.2. The interested reader is encouraged to refer to the citations given in the table and text for complete details. An inherent difficulty, not addressed here, in the determination of lattice constants of 'pure' berkelium-249 compounds concerns the ingrowth of daughter californium-249 at the rate of about 0.22% per day. Two experimental methods to address this problem are: (1) the determination of the lattice parameters of berkelium compounds as a function of californium content and then extrapolation to zero californium content; and (2) the utilization of Vegard's law to correct measured berkelium lattice parameters for the presence of a known amount of californium (this assumes, of course, that the lattice parameters of the isostructural 'pure' californium compound are known).

A summary and discussion of the structural aspects of solid-state actinide chemistry are presented in Chapter 20 of this book, so no attempt is made to do so here for the compounds of berkelium.

An empirical set of 'effective' ionic radii in oxides and fluorides, taking into account the electronic spin state and coordination of both the cation and anion, have been calculated [156]. For six-coordinate Bk(III), the radii values are 0.096 nm, based on a six-coordinate oxide ion radius of 0.140 nm, and 0.110 nm, based on a six-coordinate fluoride ion radius of 0.119 nm. For eight-coordinate Bk(IV), the corresponding values are 0.093 and 0.107 nm, based on the same anion radii [156]. Other self-consistent sets of trivalent and tetravalent lanthanide and actinide ionic radii, based on isomorphous series of oxides [143, 157] and fluorides [146, 157], have been published. Based on a crystal radius for Cf(III), the ionic radius of isoelectronic Bk(II) was calculated to be 0.114 nm [158]. It is important to note, however, that meaningful comparisons of ionic radii can only be made if the values compared are calculated in like fashion from the same type of compound, with respect to both composition and crystal structure [157].

The thermal decomposition of $Bk(NO_3)_3 \cdot 4H_2O$, $BkCl_3 \cdot 6H_2O$, $Bk_2(SO_4)_3 \cdot 12H_2O$, and $Bk_2(C_2O_4)_3 \cdot 4H_2O$ has been studied in air, argon, and H_2–Ar atmospheres and compared to that of the corresponding hydrates of cerium, gadolinium, and terbium [159]. In air or Ar the final berkelium product was BkO_2; in H_2–Ar it was Bk_2O_3.

10.6.2 Oxides

The first compound of berkelium identified on the basis of its characteristic x-ray powder diffraction pattern was BkO_2 [5]. Other workers have since

Table 10.2 *Selected crystallographic data for berkelium metal and compounds.*

Substance	*Structure type*	*Crystal system*	*Lattice parameters*[a] a_0 (nm)	b_0 (nm)	c_0 (nm)	β (deg)	*Other*[b]	*Ref.*
metal								
Bk	α-La	hexagonal (dhcp)	0.3416		1.1069		$\rho = 14.78$ $V = 27.96$	117
Bk	Cu(A1)	fcc	0.4997				$\rho = 13.25$ $V = 31.19$	117
oxides								
BkO_2	CaF_2	fcc	0.53315					142
Bk_2O_3	$(Fe, Mn)_2O_3$	bcc	1.0887					143
Bk_2O_3	Sm_2O_3	monoclinic	1.4197	0.3606	0.8846	100.23		144
Bk_2O_3	La_2O_3	hexagonal	0.3754		0.5958		$V = 72.7$	144
halides								
BkF_4	UF_4	monoclinic	1.2396	1.0466	0.8118	126.33	$V = 70.7$	145
BkF_3	LaF_3	trigonal	0.697		0.714		$\rho = 10.15$	146
BkF_3	YF_3	orthorhombic	0.670	0.709	0.441		$\rho = 9.70$	146
$BkCl_3$	UCl_3	hexagonal	0.7382		0.4127			147
Cs_2BkCl_6	Rb_2MnF_6	hexagonal	0.7451		1.2097		$\rho = 4.155$	148
$Cs_2NaBkCl_6$	$(NH_4)_3AlF_6$	fcc	1.0805				$\rho = 3.952$	148
$BkCl_3 \cdot 6H_2O$	$GdCl_3 \cdot 6H_2O$	monoclinic	0.966	0.654	0.797	93.77	$\rho = 3.06$	149
$BkBr_3$	$PuBr_3$	orthorhombic	0.403	1.271	0.912		$V = 116.8$	150
$BkBr_3$	$AlCl_3$	monoclinic	0.723	1.253	0.683	110.6	$V = 144.8$	150
γ-$BkBr_3$	$FeCl_3$	rhombohedral	0.766				$\alpha = 56.6$	150
BkI_3	BiI_3	hexagonal	0.7584		2.087			151
oxyhalides								
BkOCl	PbFCl	tetragonal	0.3966		0.6710		$\rho = 9.45$	152
BkOBr	PbFCl	tetragonal	0.395		0.81			153
BkOI	PbFCl	tetragonal	0.3986		0.9149			151
pnictides								
BkN	NaCl	fcc	0.4951					136
BkP	NaCl	fcc	0.5669					136
BkAs	NaCl	fcc	0.5829					136
BkSb	NaCl	fcc	0.6191					136
chalcogenides								
BkS_{2-x}	anti-Fe_2As	tetragonal	0.3902		0.792			135
Bk_2S_3	deficit Th_3P_4	bcc	0.8358					135
$BkSe_{2-x}$	anti-Fe_2As	tetragonal	0.404		0.828			135
Bk_2Se_3	deficit Th_3P_4	bcc	0.8712					135
$BkTe_3$	$NdTe_3$	orthorhombic	0.4318	0.4319	2.5467			134, 135
$BkTe_{2-x}$	anti-Fe_2As	tetragonal	0.4314		0.8945			134
Bk_2Te_3	Sc_2S_3	orthorhombic	1.226	0.8685	2.605			134
miscellaneous								
BkH_{2+x}	CaF_2	fcc	0.523					121
BkH_{2+x}	CaF_2	fcc	0.5248					154
BkH_{3-x}	LaF_3	trigonal	0.6454		0.6663			154
$Bk_2O_2SO_4$	$La_2O_2SO_4$	orthorhombic	0.4195	0.4083	1.3110			155
Bk_2O_2S	Pu_2O_2S	trigonal	0.3861		0.6686			155
$Bk(C_5H_5)_3$	$Pr(C_5H_5)_3$	orthorhombic	1.411	1.755	0.963		$\rho = 2.47$ $V = 298$	114

[a] See original source for precision claimed on these room-temperature values and for information regarding sample purity.

[b] ρ = density in 10^3 kg m^{-3} (g cm^{-3}); V = formula volume in 10^6 pm^3 (Å^3).

confirmed its CaF_2-type face-centered cubic structure with $a_0 = 0.533$ nm [142–144, 160, 161]. The thermal expansion of BkO_2 in 1 atm oxygen was determined and shown to be reversible with temperature [142]. The data were fitted by the expression

$$a_0(T) = 5.3304 + (4.32 \times 10^{-5})T + (15.00 \times 10^{-9})T^2$$

where $a_0(T)$ is the unit cell edge (in Å) at temperature T(in °C). In addition the instantaneous expansion coefficients at 25°C (298 K) and 900°C (1173 K) were calculated to be 8.25×10^{-6} K^{-1} and 13.2×10^{-6} K^{-1}, respectively [142].

The results of a preliminary study of a sample of berkelium oxide (BkO_2, Bk_2O_3, or a mixture of the two) via x-ray photoelectron spectroscopy (XPS) included measured core- and valence-electron binding energies [162]. The valence-band XPS spectrum, which was limited in resolution by phonon broadening, was dominated by 5f-electron emission.

A capacitance manometer system was used to measure the equilibrium oxygen decomposition pressures over non-stoichiometric BkO_x ($1.5 < x < 2.0$) [163]. Three broad non-stoichiometric phases were defined: $BkO_{1.5-1.77}$, $BkO_{1.81-1.91}$, and BkO_{2-x} ($x \leqslant 0.07$). More recently an x-ray diffraction investigation of this BkO_x system under equilibrium conditions was undertaken to correlate the above data with structural behavior [164]. A phase diagram was suggested, showing above 673 K two widely non-stoichiometric phases: body-centered cubic for $1.5 < O/Bk \lesssim 1.70$ and face-centered cubic for $1.78 \lesssim O/Bk < 2.00$. Interestingly, no evidence was found for the formation of Bk_7O_{12}, expected to exhibit a rhombohedral structure based on its common presence in other MO_x ($1.5 < x < 2.0$) systems.

The stable room-temperature form of berkelium sesquioxide exhibits the bixbyite-type body-centered cubic structure with $a_0 = 1.0887$ nm [143]. This has been corroborated by an independent worker [144, 160]. The cubic sesquioxide has also been analyzed by electron diffraction [165]. The high-temperature behavior of Bk_2O_3 has been studied, with the finding that the cubic-to-monoclinic transition at 1473 ± 50 K is irreversible, while the monoclinic-to-hexagonal transition at about 2025 K is reversible [144]. In addition, the melting point of Bk_2O_3 was determined to be 2193 ± 25 K. Thus berkelium continues the trend of actinide sesquioxides exhibiting trimorphisim: with increasing temperature, the structure of Bk_2O_3 changes from body-centered cubic (C-form) to monoclinic (B-form) to hexagonal (A-form).

The possibility of the existence of BkO has been raised [121]. The true identity of the brittle, gray material exhibiting a face-centered cubic structure with $a_0 = 0.4964$ nm is still in doubt. Not to be excluded from consideration is that this phase represents a nitride or an oxide nitride.

10.6.3 Halides and oxyhalides

The only reported binary Bk(IV) halide is BkF_4 [145, 166, 167], prepared by fluorination of BkO_2 or BkF_3. Although these workers agree that it exhibits the

UF_4-type monoclinic structure, there is some variance in the reported lattice parameters. This stems from the complexity of the x-ray powder diffraction pattern of BkF_4. A molecular volume of 7.07×10^7 pm^3 is calculated from the lattice constants given in Table 10.2, in contrast to those of 7.148×10^7 pm^3 [166] and 7.28×10^7 pm^3 [167] derived from the other reported lattice parameters. Recently the solid-state absorption spectrum of BkF_4 was obtained [14]. Mixed alkali-metal(M)–Bk(IV) fluoride compounds of the types $MBkF_5$, M_2BkF_6, M_3BkF_7, and $M_7Bk_6F_{31}$, although at present unreported, should be readily prepared. The structural systematics of such actinide fluoride complexes have been discussed elsewhere [168, 169].

One other Bk(IV) halide compound, Cs_2BkCl_6, has been characterized by its crystallographic properties [148]. This orange compound precipitated upon dissolution of Bk(IV) hydroxide in chilled, concentrated HCl solution containing CsCl, and was found to crystallize in the Rb_2MnF_6-type hexagonal structure with $a_0 = 0.7451$ and $c_0 = 1.2097$ nm. Using a separated halogen-atom model, the lattice energy of this compound has been calculated to be 1295 kJ mol^{-1} and the average radius of the $BkCl_6^{2-}$ ion to be 0.270 nm [170].

The trihalides of berkelium can be prepared by hydrohalogenation of BkO_2, Bk_2O_3, or a lighter berkelium halide. BkF_3 [14, 146], $BkCl_3$ [107, 147, 171], and $BkBr_3$ [150, 172] have been shown by x-ray powder diffraction and absorption spectrophotometric studies to be dimorphic. Berkelium is the first actinide whose trifluoride exhibits the YF_3-type orthorhombic structure as the room-temperature alpha phase and the LaF_3-type trigonal structure as the high-temperature phase [146].

In the case of dimorphic $BkCl_3$, the UCl_3-type hexagonal structure [147] represents the low-temperature form, while the $PuBr_3$-type orthorhombic structure is exhibited by the high-temperature modification [171]. The phase transition temperature appears to be close [171] to the $BkCl_3$ melting point, 876 K [173]. The volatilization behavior of many of the binary actinide chlorides including $BkCl_3$ has been studied and correlated with the oxidation state and atomic number ($Z < 92$ or $Z \geqslant 92$) of the actinide [174]. White $Cs_2NaBkCl_6$ was crystallized from aqueous CsCl–HCl solution by increasing the HCl concentration and cooling, and was found to exhibit a face-centered cubic structure in which the Bk(III) ions (O_h site symmetry) are octahedrally coordinated by chloride ions [148]. The unique properties of such compounds stimulated the synthesis and study of an isostructural set of Cs_2NaMCl_6 compounds containing trivalent cations (M) whose ionic radii ranged from 0.065 to 0.106 nm [175].

X-ray diffraction by a powder sample of $BkCl_3 \cdot 6H_2O$ showed that it is isostructural with $AmCl_3 \cdot 6H_2O$, whose structure was refined by single-crystal diffraction methods [149]. By analogy the basic units of the berkelium structure are $BkCl_2(OH_2)_6^+$ cations and Cl^- anions, the latter being octahedrally coordinated by water molecules.

From x-ray powder diffraction patterns of $BkBr_3$ obtained as a function of the sample's thermal treatment, it was concluded that the $PuBr_3$-type orthorhombic

structure is the low-temperature form of $BkBr_3$ and the $AlCl_3$-type monoclinic structure is the high-temperature form [150]. Since these two crystallographic modifications differ by 2 in the Bk(III) coordination number, absorption spectrophotometric analysis easily distinguishes between them [172]. The possibility of a third polymorph of $BkBr_3$ has been suggested on the basis of eight lines of low intensity in one powder pattern [150]. If it does exist, it would be the form intermediate between the $PuBr_3$- and $AlCl_3$-type structures and exhibit the $FeCl_3$-type rhombohedral structure with $a_0 = 0.766$ nm and $\alpha = 56.6°$ [150]. There is one additional report [153] with lattice parameters for the orthorhombic form of $BkBr_3$ and for BiI_3-type hexagonal BkI_3.

BkOCl [155], BkOBr [153], and BkOI [151, 153] have been synthesized and found to exhibit the PbFCl-type tetragonal structure. Although presently unreported, BkOF certainly can be prepared and probably exhibits polymorphism.

10.6.4 Pnictides, chalcogenides, and other compounds

The berkelium monopnictides have been prepared on the multi-microgram scale by direct combination of the elements [136]. In all cases the lattice constants of the NaCl-type cubic structures were smaller than those of the corresponding curium monopnictides but comparable to those of the corresponding terbium compounds. This supports the semimetallic classification for these compounds. One additional report of BkN has appeared [137]. The lattice parameter derived from the sample exhibiting a single phase was 0.5010 ± 0.0004 nm, whereas that extracted from the mixed-phase sample of BkN resulting from incomplete conversion of a hydride was 0.4948 ± 0.0003 nm. Clearly additional samples of BkN should be prepared to establish more firmly its lattice constant.

The only other crystallographic result reported for a berkelium chalcogenide besides those summarized in Table 10.2 is a cubic lattice parameter of 0.844 nm for Bk_2S_3 [153]. The microscale synthesis of the brownish-black sesquisulfide was carried out by treatment of berkelium oxide at 1400 K with a mixture of H_2S and CS_2 vapors. In the more recent work [134, 135], the higher chalcogenides were prepared on the 20–30 μg scale in quartz capillaries by direct combination of the elements. These were then thermally decomposed *in situ* to yield the lower chalcogenides. The stoichiometries of these compounds have not been determined directly.

The preparation of berkelium hydride has been accomplished by treatment of berkelium metal at 500 K with H_2 gas derived from thermal decomposition of UH_3 [121]. The product exhibited a face-centered cubic (fcc) structure with lattice parameter $a_0 = 0.523 \pm 0.001$ nm determined from nine observed x-ray diffraction lines. By analogy with the behavior of the lanthanide hydrides [176], the superdihydride stoichiometry, BkH_{2+x} ($0 < x < 1$), was assigned. Later studies of the berkelium–hydrogen system resulted in products with either fcc symmetry, identified as the dihydride, or hexagonal symmetry, which was taken to be

berkelium trihydride, BkH_{3-x} ($0 < x < 1$) [154]. Additional work is required to characterize fully the berkelium–hydrogen system.

Both the oxysulfate (body-centered orthorhombic) and oxysulfide (trigonal) of Bk(III) have been studied by x-ray powder diffraction [155]. $Bk_2O_2SO_4$ resulted from the decomposition of $Bk_2(SO_4)_3 \cdot nH_2O$ in an argon atmosphere (to prevent oxidation to BkO_2) at about 875 K, whereas Bk_2O_2S formed upon thermal decomposition of the sulfate hydrate in a 4% H_2/96% Ar atmosphere. No decomposition of the oxysulfide was observed up to 1300 K in the H_2/Ar gas mixture [155]. Both $Bk_2O_2SO_4$ and Bk_2O_2S are isostructural with the corresponding lanthanide and actinide compounds.

Berkelium(III) orthophosphate has been prepared and characterized by x-ray powder diffraction and solid-state absorption and Raman spectroscopy [112, 113]. Analysis of the x-ray data has shown this compound to be isostructural with samarium and europium orthophosphates and to exhibit similar lattice parameters [112]. The structure type was confirmed by the direct correlation of the Raman spectrum of $BkPO_4$ with those of the isostructural lanthanide orthophosphates [113].

Two cyclopentadienylberkelium(III) compounds have been reported, but only one of them, $Bk(C_5H_5)_3$, has been characterized crystallographically [114]. In addition to the data given in Table 10.2, the formula volume of this compound is 2.98×10^8 pm^3. The amber-colored tris(cyclopentadienyl)berkelium(III) was isolated from a reaction mixture of $BkCl_3$ and molten $Be(C_5H_5)_2$ by sublimation in vacuum at 475–495 K. It decomposes to an orange melt at 610 K. By vacuum sublimation at temperatures above 500 K (up to 600 K), a second berkelium fraction was obtained [115]. Its identity was established to be bis(cyclopentadienyl)berkelium(III) chloride dimer, $[Bk(C_5H_5)_2Cl]_2$, based on the similarities of its x-ray powder diffraction pattern and sublimation behavior to those of known $[Sm(C_5H_5)_2Cl]_2$. The solid-state absorption spectrum of $[Bk(C_5H_5)_2Cl]_2$ was obtained and noted to be very similar to that of $Bk(C_5H_5)_3$ [115].

A β-diketonate compound of Bk(III) has been prepared and reported to be stable when volatilized. The possibility of using this volatile compound in transport and subsequent separation of berkelium from other actinides has been proposed [177].

10.6.5 Magnetic behavior of berkelium ions

In order to improve upon the precision ($\pm 10\%$) of the initial measurements of the magnetic susceptibility of Bk(III) ions [4] and to extend the range of measurements to lower temperatures, single beads of cation-exchange resin were saturated with Bk(III) and subjected to susceptibility measurements over the temperature range 9–298 K [93]. The magnetic behavior of Bk(III) over the entire temperature range was described well by the Curie–Weiss relationship with $\mu_{eff} = 9.40 \pm 0.06\,\mu_B$ and $\Theta = 11.0 \pm 1.9$ K. The magnetic susceptibility of Bk(III)

in an octahedral environment of host matrix $Cs_2NaLuCl_6$ was measured and temperature-independent paramagnetism observed over the temperature range 10–40 K, the lowest level of Bk(III) determined to be Γ_1, and a Γ_1–Γ_4 separation of 8.5×10^3 m^{-1} derived [178].

Results of electron paramagnetic resonance [179] and magnetic susceptibility [180] studies of Bk(IV) in ThO_2 have been reported. The eight-line hyperfine pattern confirmed that the nuclear spin of ^{249}Bk is 7/2; the estimated nuclear moment was $2.2 \pm 0.4\,\mu_N$ [179]. Two regions of temperature-dependent paramagnetism of BkO_2 in ThO_2 were observed over the temperature range 10–220 K; the possibility of an antiferromagnetic transition at 3 K was noted [180].

The first measurements of the magnetic susceptibilities of bulk-phase samples of some berkelium compounds (BkO_2, BkF_3, BkF_4, and BkN) were made in 1981. The effective moments were found to agree with the calculated free-ion values assuming Bk(IV) or Bk(III) cores and *LS* coupling [181]. The paramagnetic effective moments for BkF_4 and BkO_2 were determined from a Curie–Weiss fit to

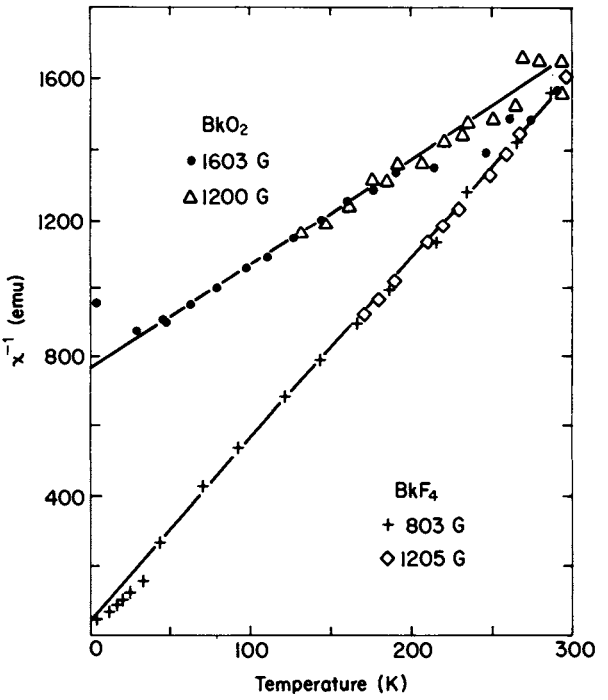

Fig. 10.5 *Inverse magnetic susceptibility of BkF_4 at 803 and 1205 G and BkO_2 at 1200 and 1603 G as a function of temperature. The solid lines are least-squares fits of the data to the Curie–Weiss law* [182]. *(Reproduced with permission of the authors and the American Physical Society.)*

the inverse magnetic susceptibility versus temperature data displayed in Fig. 10.5. The experimentally determined μ_{eff} values for BkF_4 and BkO_2 of $7.93 \pm 0.03\,\mu_B$ and $7.92 \pm 0.1\,\mu_B$, respectively, are in good agreement with a localized $5f^7$ ionic model where μ_{eff} (theory) $= 7.94\,\mu_B$ [182].

10.7 SOLUTION CHEMISTRY

10.7.1 Ionic species

Berkelium exhibits both the III and IV oxidation states, as would be expected from the oxidation states displayed by its lanthanide counterpart, terbium. Bk(III) is the most stable oxidation state in non-complexing aqueous solution. Bk(IV) is reasonably stable in solution, undoubtedly because of the stabilizing influence of the half-filled $5f^7$ electronic configuration. Bk(III) and Bk(IV) exist in aqueous solution as the simple hydrated ions $Bk^{3+}(aq)$ and $Bk^{4+}(aq)$, respectively, unless complexed by ligands. Bk(III) is green in most mineral acid solutions. Bk(IV) is yellow in HCl solution and is orange-yellow in H_2SO_4 solution. A discussion of the absorption spectra of berkelium ions in solution can be found in Section 10.4.3.

The possible existence of divalent berkelium was studied by polarography in acetonitrile solution. Because of high background currents (caused by radiolysis products) obscuring the polarographic wave, evidence for Bk(II) was not obtained [183]. Divalent berkelium has been reported to exist in mixed lanthanide chloride–strontium chloride melts. The claim is based on the results of the distribution of trace amounts of berkelium between the melt and a solid crystalline phase (co-crystallization technique) [184, 185].

10.7.2 Thermodynamic properties

Values of thermodynamic properties for the formation of berkelium ions in solution, according to the reactions:

$$Bk(c, dhcp) + 3H^+(aq) \rightarrow Bk^{3+}(aq) + \tfrac{3}{2}H_2(g)$$

and

$$Bk(c, dhcp) + 4H^+(aq) \rightarrow Bk^{4+}(aq) + 2H_2(g)$$

are summarized in Table 10.3.

Table 10.3 *Thermodynamic quantities for aqueous berkelium ions at 298 K.*

	ΔH_f° (kJ mol^{-1})	ΔG_f° (kJ mol^{-1})	S° (J K^{-1} mol^{-1})	*Ref.*
$Bk^{3+}(aq)$	-601 ± 5	-581 ± 7	-188 ± 17	131, 186
$Bk^{4+}(aq)$	-483 ± 5	-417 ± 13	-406 ± 42	186, 187

An electrostatic hydration model has been applied to the trivalent lanthanide and actinide ions in order to predict the standard free energy (ΔG_t°) and enthalpy (ΔH_t°) of hydration for these series. Assuming crystallographic and gas-phase radii for Bk(III) to be 0.096 and 0.1534 nm, respectively, and using 6.1 as the primary hydration number, ΔG_{298}° was calculated to be $-3357\ \text{kJ mol}^{-1}$ and ΔH_{298}° was calculated to be $-3503\ \text{kJ mol}^{-1}$ [188].

Activity coefficients for Bk(III) in aqueous $NaNO_3$ solutions have been calculated from distribution data for the ion between the aqueous phase and a tertiary alkylamine organic phase [189]. The activity coefficient values were reported as a function of the $NaNO_3$ concentration.

10.7.3 Stability constants and other properties

Although Bk(IV) is well-known in solution, only stability constants of complexes with Bk(III) have been reported, most of which were determined during investigations of separation procedures. A compilation of the stability constants of Bk(III) complexes with various anions is given in Table 10.4. In most cases the lack of replicate results precludes an assessment here of the accuracy of the reported values. The reader should consult the original sources for any information regarding the precision of the stability constant values. Although the number of directly measured stability constants for complexes of Bk(III) is rather small, a number of additional, reasonably accurate values for other complexes of Bk(III) can be obtained by interpolation of the stability constant data for the corresponding complexes of Am(III), Cm(III), and Cf(III).

Attempts to obtain thermodynamic data for solvent extraction of Bk(III) by thenoyltrifluoroacetone in benzene and for complexation of Bk(III) by hydroxide and citrate ions were unsuccessful [203]. The high extractibility and complexibility of the easily accessible tetravalent state of berkelium probably accounts for the difficulty encountered in this work.

Aside from the fact that no quantitative information was reported for a Bk(IV) complex with nitrate ions, a recent report is worthy of note [204]. The hexanitro complexes of Bk(IV) were studied in nitric acid solution by electromigration. An ionic mobility corresponding to a negatively charged Bk(IV) ion was evident only at HNO_3 concentrations higher than 10 M. The data indicated that at concentrations between 3 and 6 M HNO_3, Bk(IV) exists mainly as $[Bk(H_2O)_x(NO_3)_3]^+$. This study provides an explanation for the differences observed in the ion-exchange and solvent extraction behavior of Bk(IV) as compared to that of Ce(IV), Th(IV), and Np(IV) [204].

The extraction of Bk(III) by organophosphorus acids has been studied, and activity coefficients for Bk(III) in nitric acid solution were estimated [205]. In addition a mechanism for the extraction of Bk(IV) by hydrogen di(2-ethylhexyl)orthophosphoric acid (HDEHP) from nitric acid solution was proposed.

The kinetics of exchange of Bk(III) with $EuEDTA^-$ in aqueous acetate solutions of 0.1 M ionic strength has been studied [206]. The exchange was found

Table 10.4 *Stability constants of Bk(III) complexes with various anions.*

Ligand	*Conditions*[b]	*Stability constants*[a]	*Ref.*
fluoride ion, F^-	solv. extr., 298 K, $\mu = 1.0$, pH = 2.72	$\beta_1 = 7.8 \times 10^2$	190
chloride ion, Cl^-	solv. extr., 298 K, $\mu = 1.0$, pH = 2	$\beta_1 = 0.96$	191
hydroxide ion, OH^-	$\mu = 0.1$	$\beta_1 = 7.9 \times 10^8$	192
sulfate ion, SO_4^{2-}	solv. extr., 298 K, calc. values for $\mu = 0$ (meas. $\mu \leqslant 0.5$)	$\beta_1 = 5.1 \times 10^3$ $\beta_2 = 3.9 \times 10^5$ $\beta_3 = 1.1 \times 10^5$	193
thiocyanate ion, SCN^-	solv. extr., 298 K, $\mu = 5.0$	$\beta_1 = 7.21$	194
	$\mu = 1.0$, pH = 2	$\beta_1 = 3.11$, $\beta_2 = 0.31$ $\beta_3 = 2.34$	195
oxalate ion, $C_2O_4^{2-}$	electromigr. rates, 298 K, $\mu = 0.1$, pH $\simeq$ 1.8	$\beta_1 = 2.8 \times 10^5$ $\beta_2 = 1.4 \times 10^9$	196
acetate ion, CH_3COO^-	solv. extr., 298 K, 2.0 M $NaClO_4$	$\beta_1 = 1.11 \times 10^2$	197
glycolate ion, $CH_2(OH)COO^-$	solv. extr., 298 K, 2.0 M $NaClO_4$	$\beta_1 = 4.4 \times 10^2$ $\beta_2 = 5.0 \times 10^4$	198
lactate ion, $CH_3CH(OH)COO^-$	ion exch., $\mu = 0.5$	$\beta_3 = 7.9 \times 10^5$ (est.)	199
2-methyllactate ion, $(CH_3)_2C(OH)COO^-$	solv. extr., 10^{-2}–1 M	$\beta_1 = 6.39 \times 10^3$	49
α-hydroxyisobutyrate ion, $(CH_3)_2C(OH)COO^-$	ion exch., $\mu = 0.5$	$\beta_3 = 4.0 \times 10^6$ (est.)	199
malate ion, $CH(OH)(COO)CH_2COO^{2-}$	solv. extr., 10^{-2}–1 M	$\beta_1 = 1.07 \times 10^7$	49
tartrate ion, $[CH(OH)COO]_2^{2-}$	solv. extr., 10^{-2}–1 M	$\beta_1 = 6.80 \times 10^5$	49
citrate ion, $C(OH)(COO)(CH_2COO)_2^{3-}$	electromigr. rates, 298 K, $\mu = 0.1$	$\beta_1 = 7.8 \times 10^7$ $\beta_2 = 1.5 \times 10^{11}$	196
	solv. extr., 10^{-2}–1 M	$\beta_1 = 3.00 \times 10^{11}$	49
ethylenediamine-tetraacetate ion (EDTA), $C_2H_4N_2(CH_2COO)_4^{4-}$	ion exch., 298 K, $\mu = 0.1$	$\beta_1 = 7.59 \times 10^{18}$	200
1,2-diaminecyclohexane-tetraacetate ion (DACTA), $C_6H_{10}N_2(CH_2COO)_4^{4-}$	ion exch., 298 K, $\mu = 0.1$	$\beta_1 = 1.44 \times 10^{19}$	201
diethylenetriamine-pentaacetate ion (DTPA), $C_4H_8N_3(CH_2COO)_5^{5-}$	ion exch., 298 K, $\mu = 0.1$	$\beta_1 = 6.2 \times 10^{22}$	202

[a] Overall stability constants,

$$\beta_1 = \frac{[BkL^{(3-n)+}]}{[Bk^{3+}][L^{n-}]}, \quad \beta_2 = \frac{[BkL_2^{(3-2n)+}]}{[Bk^{3+}][L^{n-}]^2} \quad \text{and} \quad \beta_3 = \frac{[BkL_3^{(3-3n)+}]}{[Bk^{3+}][L^{n-}]^3}$$

[b] See footnote to Table 10.5.

to be first order with both acid-dependent and acid-independent rate terms. Rate values were calculated and compared to other actinide reaction rates [206].

The solubilities of Bk(III) oxalate and Bk(IV) iodate have been reported to be 1.5 $mg\,l^{-1}$ and 10 $mg\,l^{-1}$, respectively [207].

10.7.4 Oxidation–reduction behavior and potentials

Berkelium(III) in solution can be oxidized by strong oxidizing agents such as BrO_3^- [16–20, 208], AgO [209], Ag(I)/$S_2O_8^{2-}$ [21, 24, 210], perxenate [211], and ozone [25, 212, 213].

Oxidation of green Bk(III) hydroxide as a suspension in 1 M NaOH to yellow Bk(IV) hydroxide was performed by bubbling ozone through the slurry [111]. In basic solution Bk(III) is unstable toward oxidation by radiolytically produced peroxide. This 'self-oxidation' had been previously observed in carbonate solution [94]. Bk(III) can be stabilized, however, by the presence of a reducing agent such as hydrazine hydrate [111].

$BkCl_3$ is reported to be soluble in acetonitrile saturated with tetraethylammonium chloride [214]. A colorless, 7.6×10^{-4} M $BkCl_6^{3-}$ solution was formed that could be completely oxidized to red-orange $BkCl_6^{2-}$ by treatment with chlorine gas. The color of this Bk(IV) solution was quite similar to that observed for crystalline Cs_2BkCl_6 [148].

Investigation of the amalgamation behavior of trivalent actinides in acetate and citrate solutions by treatment with sodium amalgam showed that Bk(III) does not readily form the amalgam. This behavior is in contrast to that of the heavier actinides californium, einsteinium, and fermium, which readily amalgamate [215, 216].

Bk(IV) is a strong oxidizing agent, comparable to Ce(IV) [217]. It can be coprecipitated with cerium iodate [18] or zirconium phosphate [4]. The stability of Bk(IV) solutions is a function of the degree of complexation of Bk(IV) by the solvent medium [94]. Bk(IV) is reduced by radiolytically generated peroxide in acidic and neutral solutions. The rate of reduction of Bk(IV) can be accelerated by the introduction of a reducing agent such as hydrogen peroxide [15, 218], hydroxylamine hydrochloride [218], or ascorbic acid [218].

The first estimate of the Bk(IV)/Bk(III) potential was made in 1950, only a short time after the discovery of the element. A value of 1.6 V was reported, based on tracer experiments [3]. Later, in 1959, a refined value of 1.62 ± 0.01 V was reported for the couple, based on the results of experiments with microgram quantities of berkelium [4]. The potential of the Bk(IV)/Bk(III) couple has subsequently been determined by several workers using direct potentiometry [219–223] or indirect methods [217, 224, 225]. All of the above-mentioned determinations were performed in media of relatively low complexing capability. The formal potential of the Bk(IV)/Bk(III) couple is significantly shifted to less positive values in media containing anions which strongly complex Bk(IV), such as PO_4^{3-} and CO_3^{2-} ions [226]. This behavior closely parallels that of the

Ce(IV)/Ce(III) couple. In fact the Bk(IV)/Bk(III) couple markedly resembles the Ce(IV)/Ce(III) couple in its oxidation–reduction chemistry.

The potential of the Bk(III)/Bk(0) couple has been investigated using radiopolarography [227, 228] and theoretical calculations [229], as well as by correlation with data concerning enthalpy of formation [130, 131]. Estimates of the potentials of berkelium redox couples have also been made from correlation plots of electron-transfer and f–d absorption band energies versus redox potential and by theoretical calculations [214, 219, 230, 231].

Potentials of berkelium redox couples are summarized in Table 10.5. Replicate values for the Bk(IV)/Bk(III) couple are in reasonable agreement with one another. The effect of anions that strongly complex Bk(IV) is clearly reflected in the values

Table 10.5 *Potentials of berkelium redox couples.*

Redox couple	*Potential* (volts vs NHE)	*Conditions*[a]	*Ref.*
Bk(IV)/Bk(III)	1.6 ± 0.2	calc.	219, 230
	1.664	calc.	232
	1.54 ± 0.1	1 M $HClO_4$, dir. pot.	226
	1.597 ± 0.005	1 M $HClO_4$, dir. pot.	222
	1.735 ± 0.005	9 M $HClO_4$, dir. pot.	222
	1.54 ± 0.1	1 M HNO_3, dir. pot.	226
	1.562 ± 0.005	1 M HNO_3, dir. pot.	222
	1.56	6 M HNO_3, solv. extr.	225
	1.6	3–8 M HNO_3, co-precip.	3
	1.543 ± 0.005	8 M HNO_3, dir. pot.	222
	1.43	0.1 M H_2SO_4, dir. pot.	220
	1.44	0.25 M H_2SO_4, solv. extr.	225
	1.38	0.5 M H_2SO_4, dir. pot.	221
	1.42	0.5 M H_2SO_4, solv. extr.	225
	1.37	1 M H_2SO_4, dir. pot.	221, 223
	1.36	2 M H_2SO_4, dir. pot.	221, 223
	1.12 ± 0.1	7.5 M H_3PO_4, dir. pot.	226
	0.85	0.006 M $K_{10}P_2W_{17}O_{61}$, pH = 0, dir. pot.	233
	0.65	0.006 M $K_{10}P_2W_{17}O_{61}$, pH > 4, dir. pot.	233
	0.26 ± 0.1	2 M K_2CO_3, dir. pot.	226
Bk(III)/Bk(II)	-2.8 ± 0.2	calc.	230
	−2.75	calc.	234
Bk(III)/Bk(0)	-2.03 ± 0.05	calc.	231
	−2.4	calc.	229
	-1.99 ± 0.09	calc.	130
	-2.18 ± 0.09	0.1 M LiCl, radiopol.	227, 228
	-2.01 ± 0.03	calc.	131

[a] calc. = calculated value; dir. pot. = direct potentiometry; solv. extr. = solvent extraction; co-precip. = co-precipitation; and radiopol. = radiopolarography.

of the formal potential for the Bk(IV)/Bk(III) couple. Values of 1.36 V [221, 223] and 1.12 V [226] have been reported for the couple in sulfuric and phosphoric acid solutions, respectively. Carbonate ions, apparently forming the strongest complex with Bk(IV) of the anions listed in Table 10.5, provide conditions for the least positive potential, 0.26 V [226], as compared to the potential of 1.6 V for the couple in non-complexing perchlorate solutions [222, 226]. The overall thermodynamic and electrochemical data support a value of 1.67 ± 0.07 V for the standard potential ($E°$) for the Bk(IV)/Bk(III) couple, which is 0.07 V less positive than the accepted value of 1.74 V for the corresponding cerium couple [186]. The scatter in the potential values for the Bk(III)/Bk(II) and Bk(III)/Bk(0) couples reflects the necessary requirement of making estimates of thermodynamic quantities which have not been directly determined.

Theoretical estimates of the potentials for the Bk(V)/Bk(0) and Bk(V)/Bk(IV) couples have been reported as 0.2 and 3.5 V, respectively [130]. These estimates suggest that Bk(V) is very unstable in aqueous solution.

Additional information on the oxidation–reduction behavior of berkelium can be found in a recent review [235].

10.8 CONCLUDING REMARKS

Although the berkelium oxidation states, 0 III, and IV are known in bulk phase, further work is required to characterize more completely the solid-state and solution chemistries of this element. The synthesis of divalent berkelium in bulk should be possible via the metallothermic reduction of its trihalides, e.g.

$$Bk + 2BkBr_3 \rightarrow 3BkBr_2$$

It is quite possible that nature can accomplish this synthesis through alpha decay of the dihalides of einsteinium-253. A direct synthesis would allow both absorption spectrophotometric and x-ray powder diffraction analyses, the results of which would aid in the identification of Bk(II) species in aged einsteinium dihalide samples which also contain Cf(II) [110, 236].

Intermetallic compounds, various alloys, and additional semimetallic compounds of berkelium should be prepared and characterized to extend the knowledge of the physicochemical behavior of berkelium in these kinds of solids. Studies of such materials under pressure would be of interest in determining the effects of the non-berkelium component on physical properties such as bulk modulus (compressibility), pressure for the onset of 5f-electron delocalization, and possible volume collapse associated with a change in the metallic valence of Bk from 3 to 4.

In solution, the range of oxidation states accessible to berkelium should be further examined by using strong complexing agents in an effort to stabilize Bk(II), Bk(IV), and possibly Bk(V), produced chemically or electrochemically in non-aqueous or molten-salt media. New organometallic complexes of Bk(III)

should be studied to improve solvent extraction separation procedures. Also lacking to date, but experimentally obtainable, are stability constants of any complexes of Bk(IV).

Berkelium is the first member of the second half of the actinide series of elements. Extended knowledge of the stability and accessibility of the various oxidation states of berkelium is important to the understanding and predictability of its physicochemical behavior. In addition, such information would enable more accurate extrapolations to the physicochemical behavior of the transberkelium elements for which experimental studies are severely limited by lack of material and/or by intense radioactivity.

ACKNOWLEDGMENTS

The authors gratefully acknowledge the early assistance of J. N. Stevenson and D. L. Raschella in gathering the references included here. The more recent cooperation of numerous colleagues in supplying and/or verifying information, identifying oversights, and in commenting on the assembled manuscript was greatly appreciated. One of us (JRP) remembers with gratitude Professor B. B. Cunningham, whose guidance, inspiration, and personal interest during the first systematic study of the physicochemical properties of berkelium are still fondly remembered.

The preparation of this chapter was sponsored by the Division of Chemical Sciences, US Department of Energy, under contracts DE-AS05-76ER04447 with the University of Tennessee, Knoxville, and W-7405-eng-26 with Union Carbide Corporation.

REFERENCES

1. Thompson, S. G., Ghiorso, A., and Seaborg, G. T. (1950) *Phys. Rev.*, **77**, 838–9.
2. Thompson, S. G., Ghiorso, A., and Seaborg, G. T. (1950) *Phys. Rev.*, **80**, 781–9.
3. Thompson, S. G., Cunningham, B. B., and Seaborg, G. T. (1950) *J. Am. Chem. Soc.*, **72**, 2798–801.
4. Cunningham, B. B. (1959) *J. Chem. Ed.*, **36**, 32–7.
5. Cunningham, B. B. (1963) *Proc. Robert A. Welch Foundation Conf. on Chemical Research*, vol. VI, *Topics in Modern Inorganic Chemistry*, Houston, Texas, November 1962, (ed. W. O. Milligan) The Robert A. Welch Foundation, Houston, pp. 237–59.
6. Browne, E., Dairiki, J. M., and Doebler, R. E. (1978) *Table of Isotopes*, 7th edn (eds C. M. Lederer and V. S. Shirley), Wiley, New York, pp. 1479–508.
7. Bigelow, J. E., Corbett, B. L., King, L. J., McGuire, S. C., and Sims, T. M. (1981) in *Transplutonium Elements – Production and Recovery* (eds J. D. Navratil and W. W. Schulz), (ACS Symp. Ser. 161), American Chemical Society, Washington DC, pp. 3–18.
8. Ferguson, D. E. and Bigelow, J. E. (1969) *Actinides Rev.*, **1**, 213–21.

9. King, L. J., Bigelow, J. E., and Collins, E. D. (1981) in *Transplutonium Elements–Production and Recovery* (eds J. D. Navratil and W. W. Schulz), (ACS Symp. Ser. 161), American Chemical Society, Washington DC, pp. 133–45.
10. Bigelow, J. E. (1985) personal communication.
11. IUPAC Inorganic Chemistry Division Commission on Atomic Weights (1976) *Pure Appl. Chem.*, **47**, 75–95.
12. Polyukov, V. G., Timofeev, G. A., and Levakov, B. I. (1981) *Sov. Radiochem.*, **23**, 712–15.
13. Young, J. P., Haire, R. G., Peterson, J. R., Ensor, D. D., and Fellows, R. L. (1980) *Inorg. Chem.*, **19**, 2209–12.
14. Ensor, D. D., Peterson, J. R., Haire, R. G., and Young, J. P. (1981) *J. Inorg. Nucl. Chem.*, **43**, 1001–3.
15. Peppard, D. F., Moline, S. W., and Mason, G. W. (1957) *J. Inorg. Nucl. Chem.*, **4**, 344–8.
16. Fardy, J. J. and Weaver, B. (1969) *Anal. Chem.*, **41**, 1299–302.
17. Knauer, J. B. and Weaver, B. (1968) *Separation of Berkelium from Trivalent Actinides by Chromate Oxidation and HDEHP Extraction*, US Atomic Energy Commission Document ORNL-TM-2428, Oak Ridge National Laboratory.
18. Weaver, B. (1968) *Anal. Chem.*, **40**, 1894–6.
19. Overman, R. F. (1971) *Anal. Chem.*, **43**, 600–1.
20. Erin, E. A., Vityutnev, V. M., Kopytov, V. V., and Vasil'ev, V. Ya. (1979) *Sov. Radiochem.*, **21**, 487–9.
21. Milyukova, M. S., Malikov, D. A., and Myasoedov, B. F. (1980) *Sov. Radiochem.*, **22**, 267–72.
22. Shafiev, A. I., Efremov, Yu. V., and Yakovlev, G. N. (1974) *Sov. Radiochem.*, **16**, 31–4.
23. Moore, F. L. (1966) *Anal. Chem.*, **38**, 1872–6.
24. Milyukova, M. S., Malikov, D. A., and Myasoedov, B. F. (1978) *Sov. Radiochem.*, **20**, 762–8.
25. Myasoedov, B. F. (1974) *Sov. Radiochem.*, **16**, 716–21.
26. Myasoedov, B. F., Barsukova, K. V., and Radionova, G. N. (1971) *Radiochem. Radioanal. Lett.*, **7**, 269–74.
27. Yakovlev, N. G. and Kosyakov, V. N. (1983) *Sov. Radiochem.*, **25**, 687–92.
28. Kosyakov, V. N., Yakovlev, N. G., Kazakova, G. M., Erin, E. A., and Kopytov, V. V. (1977) *Sov. Radiochem.*, **19**, 397–400.
29. Kosyakov, V. N. and Yakovlev, N. G. (1983) *Sov. Radiochem.*, **25**, 172–5.
30. Karalova, Z. K., Myasoedov, B. F., Rodionova, L. M., and Kuznetsov, V. S. (1983) *Sov. Radiochem.*, **25**, 175–9.
31. Moore, F. L. (1969) *Anal. Chem.*, **41**, 1658–61.
32. Milyukova, M. S. and Myasoedov, B. F. (1978) *Sov. Radiochem.*, **20**, 324–30.
33. Malikov, D. A., Milyukova, M. S., Kuzovkina, E. V., and Myasoedov, B. F. (1983) *Sov. Radiochem.*, **25**, 293–6.
34. Milyukova, M. S., Malikov, D. A., Kuzovkina, E. V., and Myasoedov, B. F. (1981) *Radiochem. Radioanal. Lett.*, **48**, 355–61.
35. Yakovlev, N. G., Kosyakov, V. N., and Kazakova, G. M. (1982) *J. Radioanal. Chem.*, **75**, 113–20.
36. Kooi, J., Boden, R., and Wijkstra, J. (1964) *J. Inorg. Nucl. Chem.*, **26**, 2300–2.
37. Kooi, J. and Boden, R. (1964) *Radiochim. Acta*, **3**, 226.

38. Erin, E. A., Vityutnev, V. M., Kopytov, V. V., and Vasil'ev, V. Yu. (1979) *Sov. Radiochem.*, **21**, 85–8.
39. Shafiev, A. I. and Efremov, Yu, V. (1972) *Sov. Radiochem.*, **14**, 754–6.
40. Moore, F. L. (1967) *Anal. Chem.* **39**, 1874–6.
41. Chudinov, E. G. and Pirozhkov, S. V. (1972) *J. Radioanal. Chem.*, **10**, 41–6.
42. Guseva, L. I., Gregor'eva, S. I., and Tikhomirova, G. S. (1971) *Sov. Radiochem.*, **13**, 802–4.
43. Horwitz, E. P., Bloomquist, C. A. A., Henderson, D. J., and Nelson, D. E. (1969) *J. Inorg. Nucl. Chem.*, **31**, 3255–71.
44. Harbour, R. M. (1972) *J. Inorg. Nucl. Chem.*, **34**, 2680–1.
45. Farrar, L. G., Cooper, J. H., and Moore, F. L. (1968) *Anal. Chem.*, **40**, 1602–4.
46. Moore, F. L. and Jurriaanse, A. (1967) *Anal. Chem.*, **39**, 733–6.
47. Horwitz, E. P. and Bloomquist, C. A. A. (1973) *J. Inorg. Nucl. Chem.*, **35**, 271–84.
48. Korpusov, G. V., Patrusheva, E. N., and Dolidze, M. S. (1975) *Sov. Radiochem.*, **17**, 230–6.
49. Aly, H. F. and Latimer, R. M. (1970) *Radiochim. Acta*, **14**, 27–31.
50. Khopkar, P. K. and Mathur, J. N. (1980) *J. Radioanal. Chem.*, **60**, 131–40.
51. Mathur, J. N. and Khopkar, P. K. (1982) *Sep. Sci. Technol.*, **17**, 985–1002.
52. Ensor, D. D. and Shah, A. H. (1984) *Solvent Extr. Ion Exch.*, **2**, 591–605.
53. Baybarz, R. D., Knauer, J. B., and Orr, P. B. (1973) *Final Isolation and Purification of the Transplutonium Elements from the Twelve Campaigns Conducted at TRU During the Period August 1967–December 1971*, US Atomic Energy Commission Document ORNL-4672, Oak Ridge National Laboratory.
54. Liu, Y.-F., Luo, C., von Gunten, H. R., and Seaborg, G. T. (1981) *Inorg. Nucl. Chem. Lett.*, **17**, 257–9.
55. Liu, Y.-F., Lou, C., Moody, K. J., Lee, D., Seaborg, G. T., and von Gunten, H. R. (1983) *J. Radioanal. Chem.*, **76**, 119–24.
56. Korkisch, J. (1966) *Oesterr. Chem. Ztg.*, **67**, 273–9.
57. Ulstrup, J. (1966) *At. Energy Rev.*, **4** (4), 3–82.
58. Myasoedov, B. F., Guseva, L. I., Lebedev, I. A., Milyukova, M. S., and Chmutova, M. K. (1974) in *Analytical Chemistry of Transplutonium Elements*, (ed. D. Slutzkin), Wiley, New York, pp. 122–32.
59. Bigelow, J. E. (1974) in *Gmelin Handbuch der Anorganischen Chemie*, System No. 71, *Transurane*, Suppl. vol. 7b, part A1, II, *The Elements*, Springer-Verlag, New York, pp. 326–36.
60. Müller, W. (1967) *Actinides Rev.*, **1**, 71–119.
61. Collins, E. D., Benker, D. E., Chattin, F. R., Orr, P. B., and Ross, R. G. (1981) in *Transplutonium Elements – Production and Recovery* (eds J. D. Navratil and W. W. Schulz), (ACS Symp. Ser. 161), American Chemical Society, Washington DC, pp. 147–60.
62. Campbell, D. O. (1981) in *Transplutonium Elements – Production and Recovery* (eds J. D. Navratil and W. W. Schulz), (ACS Symp. Ser. 161), American Chemical Society, Washington DC, pp. 189–201.
63. Sugar, J. (1974) *J. Chem. Phys.*, **60**, 4103.
64. Krestov, G. A. (1966) *Sov. Radiochem.*, **8**, 200–3.
65. Worden, E. F., Gutmacher, R. G., Conway, J. G., and Mehlhorn, R. J. (1969) *J. Opt. Soc. Am.*, **59**, 1526.

66. Brewer, L. (1971) *J. Opt. Soc. Am.*, **61**, 1101–11.
67. Nugent, L. J. and Vander Sluis, K. L. (1971) *J. Opt. Soc. Am.*, **61**, 1112–15.
68. Vander Sluis, K. L. and Nugent, L. J. (1972) *Phys. Rev. A*, **6**, 86–94.
69. Vander Sluis, K. L. and Nugent, L. J. (1974) *J. Opt. Soc. Am.*, **64**, 687–95.
70. Brewer, L. (1971) *J. Opt. Soc. Am.*, **61**, 1666–82.
71. Hollander, J. M., Holtz, M. D., Novakov, T., and Graham, R. L. (1965) *Ark. Fys.*, **28**, 375–9.
72. Dittner, P. F. and Bemis, C. E. Jr (1972) *Phys. Rev. A*, **5**, 481–4.
73. Carlson, T. A., Nestor, C. W. Jr, Malik, F. B., and Tucker, T. C. (1969) *Nucl. Phys. A*, **135**, 57–64.
74. Lu, C. C., Malik, F. B., and Carlson, T. A. (1971) *Nucl. Phys. A*, **175**, 289–99.
75. Chen, M. H., Crasemann, B., Huang, K., Aoyagi, M., and Mark, H. (1977) *At. Data Nucl. Data Tables*, **19**, 97–151.
76. Huang, K., Aoyagi, M., Chen, M. H., Crasemann, B., and Mark, H. (1976) *At. Data Nucl. Data Tables*, **18**, 243–91.
77. Carlson, T. A. and Nestor, C. W. Jr (1977) *At. Data Nucl. Data Tables*, **19**, 153–73.
78. Scofield, J. H. (1974) *At. Data Nucl. Data Tables*, **14**, 121–37.
79. Manson, S. T. and Kennedy, D. J. (1974) *At. Data Nucl. Data Tables*, **14**, 111–20.
80. Gutmacher, R. G., Hulet, E. K., and Lougheed, R. (1965) *J. Opt. Soc. Am.*, **55**, 1029–30.
81. Worden, E. F., Hulet, E. K., Lougheed, R., and Conway, J. G. (1967) *J. Opt. Soc. Am.*, **57**, 550.
82. Worden, E. F., Gutmacher, R. G., Lougheed, R. W., and Conway, J. G. (1970) *J. Opt. Soc. Am.*, **60**, 1555.
83. Conway, J. G. (1976) *Proc. Symp. Commemorating the 25th Anniversary of Elements 97 and 98*, January 20, 1975, US Energy Research and Development Administration Document LBL-4366, University of California, Lawrence Berkeley Laboratory, pp. 70–5.
84. Worden, E. F. and Conway, J. G. (1978) *At. Data Nucl. Data Tables*, **22**, 329–66.
85. Conway, J. G., Worden, E. F., Blaise, J., Camus, P., and Vergès, J. (1977) *Spectrochim. Acta*, **32B**, 101–6.
86. Gutmacher, R. G., Hulet, E. K., Worden, E. F., and Conway, J. G. (1963) *J. Opt. Soc. Am.*, **53**, 506.
87. Finch, C. B., Fellows, R. L., and Young, J. P. (1978) *J. Luminesc.* **16**, 109–15.
88. Nugent, L. J., Burnett, J. L., Baybarz, R. D., Werner, G. K., Tanner, S. P., Tarrant, J. R., and Keller, O. L. Jr (1969) *J. Phys. Chem.*, **73**, 1540–9.
89. Nugent, L. J., Baybarz, R. D., Werner, G. K., and Friedman, H. A. (1970) *Chem. Phys. Lett.*, **7**, 179–82.
90. Beitz, J. V., Carnall, W. T., Wester, D. W., and Williams, C. W. (1981) *Actinides–1981*, Pacific Grove, California, September 1981, Abstracts Volume (ed. N. M. Edelstein), US Department of Energy Document LBL-12441, University of California, Lawrence Berkeley Laboratory, pp. 108–9.
91. Gutmacher, R. G., Hulet, E. K., Lougheed, R., Conway, J. G., Carnall, W. T., Cohen, D., Keenan, T. K., and Baybarz, R. D. (1967) *J. Inorg. Nucl. Chem.*, **29**, 2341–5.
92. Peterson, J. R. (1980) in *Lanthanide and Actinide Chemistry and Spectroscopy* (ed. N. M. Edelstein), (ACS Symp. Ser. 131), American Chemical Society, Washington DC, pp. 221–38; Peterson, J. R. (1967) *The Solution Absorption Spectrum of* Bk^{3+} *and*

the Crystallography of Berkelium Dioxide, Sesquioxide, Trichloride, Oxychloride, and Trifluoride, PhD Thesis, US Atomic Energy Commission Document UCRL-17875, University of California, Lawrence Berkeley Radiation Laboratory.

93. Fujita, D. K. (1969) *Some Magnetic, Spectroscopic, and Crystallographic Properties of Berkelium, Californium and Einsteinium* (PhD Thesis), US Atomic Energy Commission Document UCRL-19507, University of California, Lawrence Berkeley Radiation Laboratory.
94. Baybarz, R. D., Stokely, J. R., and Peterson, J. R. (1972) *J. Inorg. Nucl. Chem.*, **34**, 739–46.
95. Gutmacher, R. G., Bodé, D. D., Lougheed, R. W., and Hulet, E. K. (1973) *J. Inorg. Nucl. Chem.*, **35**, 979–94.
96. Carnall, W. T., Sjoblom, R. K., Barnes, R. F., and Fields, P. R. (1971) *Inorg. Nucl. Chem. Lett.*, **7**, 651–7.
97. Carnall, W. T., Beitz, J. V., and Crosswhite, H. (1984) *J. Chem. Phys.*, **80**, 2301–8.
98. Varga, L. P., Baybarz, R. D., Reisfeld, M. J., and Volz, W. B. (1973) *J. Inorg. Nucl. Chem.*, **35**, 2787–94.
99. Varga, L. P., Baybarz, R. D., and Reisfeld, M. J. (1973) *J. Inorg. Nucl. Chem.*, **35**, 4313–17.
100. Varga, L. P., Baybarz, R. D., Reisfeld, M. J., and Asprey, L. B. (1973) *J. Inorg. Nucl. Chem.*, **35**, 2775–85.
101. Gutmacher, R. G. (1964) *Atomic Spectroscopy of Berkelium* (Abstract), US Atomic Energy Commission Document UCRL-12275-T, University of California Lawrence Livermore Radiation Laboratory.
102. Fields, P. R., Wybourne, B. G., and Carnall, W. T. (1964) *The Electronic Energy Levels of the Heavy Actinides* Bk^{3+} ($5f^8$), Cf^{3+} ($5f^9$), Es^{3+} ($5f^{10}$), *and* Fm^{3+} ($5f^{11}$), US Atomic Energy Commission Document ANL-6911, Argonne National Laboratory.
103. Carnall, W. T., Fried, S., and Wagner, F. Jr (1973) *J. Chem. Phys.*, **58**, 3614–24.
104. Carnall, W. T., Fried, S., Wagner, F. Jr, Barnes, R. F., Sjoblom, R. K., and Fields, P. R. (1972) *Inorg. Nucl. Chem. Lett.*, **8**, 773–4.
105. Carnall, W. T. and Fried, S. (1976) *Proc. Symp. Commemorating the 25th Anniversary of Elements 97 and 98*, January 20, 1975, US Energy Research and Development Administration Document LBL-4366, University of California Lawrence Berkeley Laboratory, pp. 61–9.
106. Carnall, W. T., Crosswhite, H. M., Crosswhite, H., Hessler, J. P., Aderhold, C., Caird, J. A., Paszek, A., and Wagner, F. W. (1977) *Proc. 2nd Int. Conf. on the Electronic Structure of the Actinides*, Wrocław, Poland, September 1976 (eds J. Mulak, W. Suski, and R. Troć), Ossolineum, Wrocław, pp. 105–10.
107. Young, J. P., Haire, R. G., Fellows, R. L., and Peterson, J. R. (1978) *J. Radioanal. Chem.*, **43**, 479–88.
108. Peterson, J. R., Young, J. P., Ensor, D. D., and Haire, R. G., submitted to *Inorg. Chem.*
109. Peterson, J. R., Fellows, R. L., Young, J. P., and Haire, R. G. (1977) *Proc. 2nd Int. Conf. on the Electronic Structure of the Actinides*, Wrocław, Poland, September 1976 (eds J. Mulak, W. Suski, and R. Troć), Ossolineum, Wrocław, pp. 111–16; (1977) *Rev. Chim. Minér.*, **14**, 172–7.
110. Young, J. P., Haire, R. G., Peterson, J. R., Ensor, D. D., and Fellows, R. L. (1981) *Inorg. Chem.*, **20**, 3979–83.
111. Cohen, D. (1976) *J. Inorg. Nucl. Chem.* Suppl., 41–9.

112. Haire, R. G., Hellwege, H. E., Hobart, D. E., and Young, J. P. (1983) *J. Less Common Metals*, **93**, 358–9.
113. Hobart, D. E., Begun, G. M., Haire, R. G., and Hellwege, H. E. (1983) *J. Raman Spectrosc.*, **14**, 59–62.
114. Laubereau, P. G. and Burns, J. H. (1970) *Inorg. Chem.*, **9**, 1091–95.
115. Laubereau, P. G. (1970) *Inorg. Nucl. Chem. Lett.*, **6**, 611–16.
116. Carnall, W. T. (1973) in *Gmelin Handbuch der Anorganischen Chemie*, System No. 71, *Transurane*, New Suppl. Ser., vol. 8, part A2, *The Elements*, Springer-Verlag, New York, pp. 35–80.
117. Peterson, J. R., Fahey, J. A., and Baybarz, R. D. (1971) *J. Inorg. Nucl. Chem.*, **33**, 3345–51.
118. Fuger, J., Peterson, J. R., Stevenson, J. N., Noé, M., and Haire, R. G. (1975) *J. Inorg. Nucl. Chem.*, **37**, 1725–8.
119. Sarkisov, E. S. (1966) *Dokl. Akad. Nauk SSSR*, **166**, 627–30.
120. Zachariasen, W. H. (1973) *J. Inorg. Nucl. Chem.*, **35**, 3487–97.
121. Fahey, J. A., Peterson, J. R., and Baybarz, R. D. (1972) *Inorg. Nucl. Chem. Lett.*, **8**, 101–7.
122. Ward, J. W., Kleinschmidt, P. D., and Haire, R. G. (1982) *J. Chem. Phys.*, **77**, 1464–8.
123. Haire, R. G., Peterson, J. R., Benedict, U., and Dufour, C. (1984) *J. Less Common Metals*, **102**, 119–26.
124. Benedict, U., Peterson, J. R., Haire, R. G., and Dufour, C. (1984) *J. Phys. F: Metal Phys.*, **14**, L43–7.
125. Johansson, B., Skriver, H. L., and Andersen, O. K. (1981) *Physics of Solids Under High Pressure* (eds J. S. Schilling and R. N. Shelton), North-Holland, Amsterdam, pp. 245–62.
126. Ward, J. W., Kleinschmidt, P. D., Haire, R. G., and Brown, D. (1980) in *Lanthanide and Actinide Chemistry and Spectroscopy* (ed. N. M. Edelstein), (ACS Symp. Ser. 131), American Chemical Society, Washington DC, pp. 199–220.
127. Ward, J. W. and Hill, H. H. (1976) in *Heavy Element Properties* (eds W. Müller and H. Blank), *Proc. Joint Session, 4th Int. Transplutonium Element Symp. & 5th Int. Conf. on Plutonium and Other Actinides*, Baden-Baden, September 1975, North-Holland, Amsterdam, pp. 65–79.
128. Nugent, L. J., Burnett, J. L., and Morss, L. R. (1973) *J. Chem. Thermodyn.*, **5**, 665–78.
129. Johansson, B. and Rosengren, A. (1975) *Phys. Rev. B*, **11**, 1367–73.
130. David, F., Samhoun, K., Guillaumont, R., and Nugent, L. J. (1976) in *Heavy Element Properties* (eds W. Müller and H. Blank), *Proc. Joint Session, 4th Int. Transplutonium Element Symp. & 5th Int. Conf. on Plutonium and Other Actinides*, Baden-Baden, September 1975, North-Holland, Amsterdam, pp. 97–104.
131. Fuger, J., Haire, R. G., and Peterson, J. R. (1981) *J. Inorg. Nucl. Chem.*, **43**, 3209–12.
132. Nave, S. E., Huray, P. G., and Haire, R. G. (1980) in *Crystalline Electric Field and Structural Effects in f-Electron Systems* (eds J. E. Crow, R. P. Guertin, and T. W. Mihalisin), Plenum, New York, pp. 269–74.
133. Peterson, J. R., Fahey, J. A., and Baybarz, R. D. (1970) *Nucl. Metallurgy*, **17**, 20–34.
134. Damien, D. A., Haire, R. G., and Peterson, J. R. (1979) *J. Physique*, **40**(C4), 95–100.
135. Damien, D., Haire, R. G., and Peterson, J. R. (1981) preliminary values of results to be published.
136. Damien, D., Haire, R. G., and Peterson, J. R. (1980) *J. Inorg. Nucl. Chem.*, **42**, 995–8.
137. Stevenson, J. N. and Peterson, J. R. (1979) *J. Less Common Metals*, **66**, 201–10.

138. Jullien, R., Galleani d'Agliano, E., and Coqblin, B. (1972) *Phys. Rev. B*, **6**, 2139–55.
139. Freeman, A. J. and Koelling, D. D. (1974) in *The Actinides: Electronic Structure and Related Properties*, vol. 1 (eds A. J. Freeman and J. B. Darby Jr), Academic Press, New York, pp. 51–108.
140. Fournier, J. M. (1976) *J. Phys. Chem. Solids*, **37**, 235–44.
141. Herbst, J. F., Watson, R. E., and Lindgren, I. (1976) *Phys. Rev. B*, **14**, 3265–72.
142. Fahey, J. A., Turcotte, R. P., and Chikalla, T. D. (1974) *Inorg. Nucl. Chem. Lett.*, **10**, 459–65.
143. Peterson, J. R. and Cunningham, B. B. (1967) *Inorg. Nucl. Chem. Lett.*, **3**, 327–36.
144. Baybarz, R. D. (1973) *J. Inorg. Nucl. Chem.*, **35**, 4149–58.
145. Haug, H. O. and Baybarz, R. D. (1975) *Inorg. Nucl. Chem. Lett.*, **11**, 847–55.
146. Peterson, J. R. and Cunningham, B. B. (1968) *J. Inorg. Nucl. Chem.*, **30**, 1775–84.
147. Peterson, J. R. and Cunningham, B. B. (1968) *J. Inorg. Nucl. Chem.*, **30**, 823–8.
148. Morss, L. R. and Fuger, J. (1969) *Inorg. Chem.*, **8**, 1433–9.
149. Burns, J. H. and Peterson, J. R. (1971) *Inorg. Chem.*, **10**, 147–51.
150. Burns, J. H., Peterson, J. R., and Stevenson, J. N. (1975) *J. Inorg. Nucl. Chem.*, **37**, 743–9.
151. Fellows, R. L., Young, J. P., and Haire, R. G. (1977) *Physical–Chemical Studies of Transuranium Elements* (Progress Report April 1976–March 1977) (ed. J. R. Peterson), US Energy Research and Development Administration Document ORO-4447-048, University of Tennessee, Knoxville, pp. 5–15.
152. Peterson, J. R. and Cunningham, B. B. (1967) *Inorg. Nucl. Chem. Lett.*, **3**, 579–83.
153. Cohen, D., Fried, S., Siegel, S., and Tani, B. (1968) *Inorg. Nucl. Chem. Lett.*, **4**, 257–60.
154. Gibson, J. K. and Haire, R. G. (1985) *J. Less Common Metals*, **109**, 251–59.
155. Haire, R. G. and Fahey, J. A. (1977) *J. Inorg. Nucl. Chem.*, **39**, 837–41.
156. Shannon, R. D. and Prewitt, C. T. (1969) *Acta Crystallogr. B*, **25**, 925–46.
157. Shannon, R. D. (1976) *Acta Crystallogr. A*, **32**, 751–67.
158. Ionova, G. V., Spitsyn, V. I., and Mikheev, N. B. (1977) *Proc. 2nd Int. Conf. on the Electronic Structure of the Actinides*, Wrocław, Poland, September 1976 (eds J. Mulak, W. Suski, and R. Troć), Ossolineum, Wrocław, pp. 39–47.
159. Haire, R. G. (1973) *Proc. 10th Rare Earth Research Conf.*, Carefree, Arizona, April–May 1973, vol. II (eds C. J. Kevane and T. Moeller), National Technical Information Service, US Department of Commerce, Springfield VA, pp. 882–91.
160. Baybarz, R. D. (1968) *J. Inorg. Nucl. Chem.*, **30**, 1769–73.
161. Sudakov, L. V., Erin, E. A., Kopytov, V. V., Baranov, A. Yu., Shimbarev, E. V., Vasil'ev, V. Ya., and Kapshukov, I. I. (1977) *Sov. Radiochem.*, **19**, 394–6.
162. Veal, B. W., Lam, D. J., Diamond, H., and Hoekstra, H. R. (1977) *Phys. Rev. B*, **15**, 2929–42.
163. Turcotte, R. P., Chikalla, T. D., and Eyring, L. (1971) *J. Inorg. Nucl. Chem.*, **33**, 3749–63.
164. Turcotte, R. P., Chikalla, T. D., Haire, R. G., and Fahey, J. A. (1980) *J. Inorg. Nucl. Chem.*, **42**, 1729–33.
165. Haire, R. G. and Baybarz, R. D. (1973) *J. Inorg. Nucl. Chem.*, **35**, 489–96.
166. Asprey, L. B. and Haire, R. G. (1973) *Inorg. Nucl. Chem. Lett.*, **9**, 1121–8.
167. Asprey, L. B. and Keenan, T. K. (1968) *Inorg. Nucl. Chem. Lett.*, **4**, 537–41; Keenan, T. K. and Asprey, L. B. (1969) *Inorg. Chem.*, **8**, 235–8.
168. Penneman, R. A., Ryan, R. R., and Rosenzweig, A. (1973) *Struct. Bonding*, **13**, 1–52.
169. Thoma, R. E. (1962) *Inorg. Chem.*, **1**, 220–6.

170. Jenkins, H. D. B. and Pratt, K. F. (1979) *Prog. Solid State Chem.*, **12**, 125–76.
171. Peterson, J. R., Young, J. P., Ensor, D. D., and Haire, R. G. (1981) *Actinides–1981*, Pacific Grove, California, September 1981, Abstracts Volume (ed. N. M. Edelstein), US Department of Energy Document LBL-12441, University of California, Lawrence Berkeley Laboratory, pp. 118–20.
172. Peterson, J. R., Fellows, R. L., Young, J. P., and Haire, R. G. (1977) *Rev. Chim. Minér.*, **14**, 172–7.
173. Peterson, J. R. and Burns, J. H. (1973) *J. Inorg. Nucl. Chem.*, **35**, 1525–30.
174. Merinis, J., Legoux, Y., and Bouissières, G. (1970) *Radiochem. Radioanal. Lett.*, **3**, 255–61.
175. Morss, L. R., Siegal, M., Stenger, L., and Edelstein, N. (1970) *Inorg. Chem.*, **9**, 1771–5.
176. Holley, C. E. Jr, Mulford, R. N. R., Ellinger, F. H., Koehler, W. C., and Zachariasen, W. H. (1955) *J. Phys. Chem.*, **59**, 1226–8.
177. Fedoseev, E. V., Ivanova, L. A., Travnikov, S. S., Davidov, A. V., and Myasoedov, B. F. (1983) *Sov. Radiochem.*, **25**, 343–7.
178. Hendricks, M. E., Jones, E. R. Jr, Stone, J. A., and Karraker, D. G. (1974) *J. Chem. Phys.*, **60**, 2095–103.
179. Boatner, L. A., Reynolds, R. W., Finch, C. B., and Abraham, M. M. (1972) *Phys. Lett. A*, **42**, 93–4.
180. Karraker, D. G. (1975) *J. Chem. Phys.*, **62**, 1444–6.
181. Nave, S. E., Haire, R. G., and Huray, P. G. (1981) *Actinides–1981*, Pacific Grove, California, September 1981, Abstracts Volume (ed. N. M. Edelstein), US Department of Energy Document LBL-12441, University of California, Lawrence Berkeley Laboratory, pp. 144–6.
182. Nave, S. E., Haire, R. G., and Huray, P. G. (1983) *Phys. Rev. B*, **28**, 2317–27.
183. Friedman, H. A. and Stokely, J. R. (1976) *Inorg. Nucl. Chem. Lett.*, **12**, 505–13.
184. Mikheev, N. B., D'yachkova, R. A., and Spitsyn, V. I. (1979) *Dokl. Chem. (Chem. Sec.)*, **244**, 18–20.
185. D'yachkova, R. A., Auérman, L. N., Mikheev, N. B., and Spitsyn, V. I. (1980) *Sov. Radiochem.*, **22**, 234–8.
186. Fuger, J. and Oetting, F. L. (1976) in *The Chemical Thermodynamics of Actinide Elements and Compounds*, part 2, *The Actinide Aqueous Ions* (eds V. Medvedev, M. H. Rand, E. F. Westrum, Jr, and F. L. Oetting), IAEA, Vienna, pp. 50–3.
187. Fuger, J. (1982) *Actinides in Perspective, Proc. Actinides–1981*, Pacific Grove, California, September 1981 (ed. N. M. Edelstein), Pergamon Press, New York, pp. 409–31.
188. Goldman, S. and Morss, L. R. (1975) *Can. J. Chem.*, **53**, 2695–700.
189. Chudinov, E. G. and Pirozhkov, S. V. (1973) *Sov. Radiochem.*, **15**, 195–9.
190. Choppin, G. R. and Unrein, P. J. (1976) *Transplutonium Elements 1975* (eds W. Müller and R. Lindner), *Proc. 4th Int. Transplutonium Element Symp.*, Baden-Baden, September 1975, North-Holland, Amsterdam, pp. 97–107.
191. Harmon, H. D., Peterson, J. R., and McDowell, W. J. (1972) *Inorg. Nucl. Chem. Lett.*, **8**, 57–63.
192. Hussonnois, M., Hubert, S., Brillard, L., and Guillaumont, R. (1973) *Radiochem. Radioanal. Lett.*, **15**, 47–56; Désiré, B., Hussonnois, M., and Guillaumont, R. (1969) *C. R. Acad. Sci. Paris C*, **269**, 448–51.
193. McDowell, W. J. and Coleman, C. F. (1972) *J. Inorg. Nucl. Chem.*, **34**, 2837–50.
194. Kinard, W. F. and Choppin, G. R. (1974) *J. Inorg. Nucl. Chem.*, **36**, 1131–4.

195. Harmon, H. D., Peterson, J. R., McDowell, W. J., and Coleman, C. F. (1972) *J. Inorg. Nucl. Chem.*, **34**, 1381–97.
196. Stepanov, A. V. (1971) *Russ. J. Inorg. Chem.*, **16**, 1583–6.
197. Choppin, G. R. and Schneider, J. K. (1970) *J. Inorg. Nucl. Chem.*, **32**, 3283–8.
198. Choppin, G. R. and Degischer, G. (1972) *J. Inorg. Nucl. Chem.*, **34**, 3473–7.
199. Stary, J. (1966) *Talanta*, **13**, 421–37.
200. Fuger, J. (1961) *J. Inorg. Nucl. Chem.*, **18**, 263–9.
201. Baybarz, R. D. (1966) *J. Inorg. Nucl. Chem.*, **28**, 1055–61.
202. Baybarz, R. D. (1965) *J. Inorg. Nucl. Chem.*, **27**, 1831–9.
203. Hubert, S., Hussonnois, M., Brillard, L., and Guillaumont, R. (1976) *Transplutonium 1975* (eds W. Müller and R. Lindner), *Proc. 4th Int. Transplutonium Element Symp.*, Baden-Baden, September 1975, North-Holland, Amsterdam, pp. 109–18.
204. Makarova, T. P., Fridkin, A. M., Kosyakov, V. N., and Yerin, E. A. (1979) *J. Radioanal. Chem.*, **53**, 17–24.
205. Chudinov, E. G., Kosyakov, V. N., Shvetsov, I. K., and Vereshchaguin, Yu. I. (1976) *Transplutonium 1975* (eds W. Müller and R. Lindner), *Proc. 4th Int. Transplutonium Element Symp.*, Baden-Baden, September 1975, North-Holland, Amsterdam, pp. 49–56.
206. Williams, K. R. and Choppin, G. R. (1974) *J. Inorg. Nucl. Chem.*, **36**, 1849–53.
207. Erin, E. A., Kopytov, V. V., Vasil'ev, V. Ya., and Vityutnev, V. M. (1977) *Sov. Radiochem.*, **19**, 380–2.
208. Malikov, D. A., Almasova, E. V., Milyukova, M. S., and Myasoedov, B. F. (1980) *Radiochem. Radioanal. Lett.*, **44**, 297–306.
209. Erin, E. A., Kopytov, V. V., and Vityutnev, V. M. (1976) *Sov. Radiochem.*, **18**, 446–8.
210. Milyukova, M. S., Malikov, D. A., and Myasoedov, B. F. (1977) *Radiochem. Radioanal. Lett.*, **29**, 93–102.
211. Lebedev, I. A., Chepovoy, V. I., and Myasoedov, B. F. (1975) *Radiochem. Radioanal. Lett.*, **22**, 239–42.
212. Myasoedov, B. F., Chepovoy, V. I., and Lebedev, I. A. (1973) *Radiochem. Radioanal. Lett.*, **15**, 39–45.
213. Myasoedov, B. F., Chepovoy, V. I., and Lebedev, I. A. (1975) *Radiochem. Radioanal. Lett.*, **22**, 233–8.
214. Nugent, L. J., Baybarz, R. D., Burnett, J. L., and Ryan, J. L. (1971) *J. Inorg. Nucl. Chem.*, **33**, 2503–30.
215. Malý, J. (1967) *Inorg. Nucl. Chem. Lett.*, **3**, 373–81.
216. Malý, J. (1968) *J. Inorg. Nucl. Chem.*, **31**, 1007–17.
217. Weaver, B. and Stevenson, J. N. (1971) *J. Inorg. Nucl. Chem.*, **33**, 1877–81.
218. Kazakova, G. M., Kosyakov, V. N., and Erin, E. A. (1975) *Sov. Radiochem.*, **17**, 315–18.
219. Nugent, L. J., Baybarz, R. D., Burnett, J. L., and Ryan, J. L. (1973) *J. Phys. Chem.*, **77**, 1528–39.
220. Propst, R. C. and Hyder, M. L. (1970) *J. Inorg. Nucl. Chem.*, **32**, 2205–16.
221. Stokely, J. R., Baybarz, R. D., and Shults, W. D. (1969) *Inorg. Nucl. Chem. Lett.*, **5**, 877–84.
222. Simakin, G. A., Kosyakov, V. N., Baranov, A. A., Erin, E. A., Kopytov, V. V., and Timofeev, G. A. (1977) *Sov. Radiochem.*, **19**, 302–7.
223. Kulyako, Yu. M., Frenkel, V. Ya., Lebedev, I. A., Trofimov, T. I., Myasoedov, B. F., and Mogilevskii, A. N. (1981) *Radiochim. Acta*, **28**, 119–22.

224. Weaver, B. and Fardy, J. J. (1969) *Inorg. Nucl. Chem. Lett.*, **5**, 145–6.
225. Musikas, C. and Berger, R. (1967) in *Lanthanide/Actinide Chemistry* (eds P. R. Fields and T. Moeller) (ACS Adv. Chem. Ser. 71), American Chemical Society, Washington DC, pp. 296–307.
226. Stokely, J. R., Baybarz, R. D., and Peterson, J. R. (1972) *J. Inorg. Nucl. Chem.*, **34**, 392–93.
227. Samhoun, K. and David, F. (1976) in *Transplutonium Elements 1975* (eds W. Müller and R. Lindner), *Proc. 4th Int. Transplutonium Element Symp.*, Baden-Baden, September 1975, North-Holland, Amsterdam, pp. 297–304.
228. Samhoun, K. and David, F. (1979) *J. Inorg. Nucl. Chem.*, **41**, 357–63.
229. Krestov, G. A. (1965) *Sov. Radiochem.*, **7**, 69–77.
230. Nugent, L. J., Baybarz, R. D., Burnett, J. L., and Ryan, J. L. (1976) *J. Inorg. Nucl. Chem.* Suppl. 37–9.
231. Nugent, L. J. (1975) *J. Inorg. Nucl. Chem.*, **37**, 1767–70.
232. Simakin, G. A., Baranov, A. A., Kosyakov, V. N., Timofeev, G. A., Erin, E. A., and Lebedev, I. A. (1977) *Sov. Radiochem.*, **19**, 307–9.
233. Baranov, A. A., Simakin, G. A., Kosyakov, V. N., Erin, E. A., Kopytov, V. V., Timofeev, G. A., and Rykov, A. G. (1981) *Sov. Radiochem.*, **23**, 104–6.
234. Lebedev, I. A. (1978) *Sov. Radiochem.*, **20**, 556–62.
235. Martinot, L. (1978) in *Encyclopedia of Electrochemistry of the Elements*, (ed. A. J. Bard), Marcel Dekker, New York, ch. VIII-2, pp. 196–8.
236. Peterson, J. R., Ensor, D. D., Fellows, R. L., Haire, R. G., and Young, J. P. (1979) *J. Physique*, **40** (C4), 111–13.

CHAPTER ELEVEN

CALIFORNIUM

Richard G. Haire

11.1 INTRODUCTION

The discovery of the element californium, like many of the other actinide elements, hinged on the development of new experimental techniques together with predictions of the nuclear systematics of the new materials. Element 98, named californium after the University and State of California where many of the transuranium elements were first identified, was discovered by Thompson, Street, Ghiorso, and Seaborg [1] in February, 1950. The discovery of californium came only two months after the preparation of the first isotope of berkelium, element 97. The first preparative method for californium [1] was to bombard microgram targets of ^{242}Cm with 35 MeV helium ions in a 60 inch cyclotron. This produced $^{244}_{98}$Cf by an (α,2n) reaction, which decays primarily by alpha emission ($t_{1/2} = 19 \pm 3$ min) but also has a small degree of decay by electron capture [2]. Since element 98 ('eka-dysprosium') was expected to have a tripositive oxidation state in aqueous solution, its elution behavior in chromatographic separation schemes was estimated to decide which fractions should be examined for the new element. In addition to requiring a high degree of decontamination from other radionuclides, it was also necessary that the chemical separations be completed within approximately 1 h, because of the short half-life of this californium isotope.

When the existence of the element californium was established, efforts naturally progressed to preparing other isotopes, studying their nuclear properties, and investigating the chemistry of the element. These initial studies were

performed using only small numbers of atoms but it is to the credit of the early investigators that a considerable amount of chemical and nuclear data were accumulated from that work. The tracer experiments were sufficient to establish the stability of Cf(III) in solution, and some of the element's basic chemistry. Additional information on the chemistry of californium was generated as microgram quantities became available and permitted the preparation and study of solid compounds. The need for even larger quantities of the transplutonium elements was satisfied by the development of a reactor irradiation program by the USAEC, two decades ago, which is currently producing subgram amounts of ^{252}Cf per year. Smaller quantities of californium are also produced in various reactors in other countries. Reactor-produced californium consists of several different isotopes, with the major one being ^{252}Cf.

This chapter focuses on the chemistry and physical properties of californium as available in the open literature. An effort was made to minimize references to theses, technical reports, and unpublished information except for cases when a citation was warranted. The references cited are not necessarily inclusive, or to the original reference, but are given as sources for the material being presented.

The applications and studies on ^{252}Cf where the main interest was as a neutron source are only briefly covered. There are numerous references to work done with ^{252}Cf, covering biological studies, radiotherapy, neutron radiography, neutron activation analyses, dosimetry, etc.; see Sections 11.3 and 14.11.

11.2 PREPARATION AND NUCLEAR PROPERTIES

There is no evidence, and it is very unlikely, that primordial californium is present in nature in modern times. Isotopes of californium with mass numbers between 239 and 256 have been prepared as man-made isotopes. A summary of methods for the preparation of and nuclear data for these isotopes is given in Table 11.1. The lighter masses (neutron deficient) can be produced by helium bombardment of curium isotopes but they can also be prepared by heavy-ion bombardment of elements other than curium. Examples of the latter are bombarding thorium with oxygen ions, and uranium with carbon or nitrogen ions (see Table 11.1). These preparations involve high-energy accelerators and produce limited numbers of atoms of the product nucleus, and therefore are not useful when weighable quantities (> 1 μg) of californium are needed. An excellent discussion on the preparation and nuclear properties of californium isotopes is given by Hyde *et al.* [2].

Californium isotopes with a higher neutron content are usually prepared by irradiation in nuclear reactors having a high neutron flux ($\geqslant 10^{15}$ n cm^{-2} s^{-1}). These isotopes are also generated in nuclear explosions, where for short periods of time the neutron flux is much higher ($> 10^{30}$ n cm^{-2} s^{-1}). In the latter case it would be expected that higher-Z elements and heavier isotopes would be favored,

Table 11.1 *Nuclear properties of californium isotopes.*

Mass number	*Half-life*	*Mode of decay*	*Main radiations (MeV)*	*Method of production*
239	39 s	α	α 7.63	^{243}Fm daughter
240	1.1 min	α	α 7.59	^{233}U(^{12}C,5n)
241	3.8 min	α	α 7.335	^{233}U(^{12}C,4n)
242	3.5 min	α	α 7.385 (~ 80%)	^{233}U(^{12}C,3n)
			7.351 (~ 20%)	^{235}U(^{12}C,5n)
243	10.7 min	EC ~ 86%	α 7.06	^{235}U(^{12}C,4n)
		α ~ 14%		
244	19.4 min	α	α 7.210 (75%)	^{244}Cm(α,4n)
			7.168 (25%)	^{236}U(^{12}C,4n)
245	43.6 min	EC ~ 70%	α 7.137	^{244}Cm(α,3n)
		α ~ 30%		^{238}U(^{12}C,5n)
246	35.7 h	α	α 6.758 (78%)	^{244}Cm(α,2n)
		SF		
	2.0×10^3 yr	β stable	6.719 (22%)	^{246}Cm(α,4n)
247	3.11 h	EC 99.96%	α 6.296 (95%)	^{246}Cm(α,3n)
		α 0.035%	γ 0.294 (1.0%)	^{244}Cm(α,n)
248	334 d	α	α 6.258 (80.0%)	^{246}Cm(α,2n)
		SF		
	3.2×10^4 yr	β stable	6.217 (19.6%)	
249	351 yr	α	α 6.194 (2.2%)	^{249}Bk daughter
	6.9×10^{10} yr	SF	5.812 (84.4%)	
			γ 0.388 (66%)	
250	13.08 yr	α	α 6.031 (83%)	multiple n capture
	1.7×10^4 yr	SF	5.989 (17%)	
251	898 yr	α	α 5.851 (27%)	multiple n capture
			5.677 (35%)	
			γ 0.177 (17%)	
252	2.645 yr	α 96.91%	α 6.118 (84%)	multiple n capture
		SF 3.09%	6.076 (15.8%)	
253	17.81 d	β⁻ 99.69%	α 5.979 (95%)	multiple n capture
		α 0.31%	5.921 (5%)	
254	60.5 d	SF 99.69%	α 5.834 (83%)	multiple n capture
		α 0.31%	5.792 (17%)	
255	1.4 h	β⁻		^{254}Cf(n,γ)
256	12.3 min	SF		^{254}Cf(t,p)

due to the high density of neutrons in timespans that are short relative to the various decay half-lives of the materials formed. In principle the object would be to favor the capture process over the decay process, and to build rapidly beyond a short-lived isotope before it decays appreciably. Although some transplutonium elements have been produced in underground nuclear explosions, the processing of large amounts of 'ore material' (rock debris) in reasonable time periods makes the procedure impracticable for most of these materials. Thus, weighable quantities of californium are normally obtained as direct or indirect products from nuclear reactors.

Irradiating $^{239}_{94}$Pu or other actinides such as $^{241}_{95}$Am, $^{243}_{95}$Am, $^{244}_{96}$Cm, etc., with neutrons in a reactor produces a mixture of californium isotopes (mass numbers 249 through 254) with ^{252}Cf being one of the major constituents. The High-Flux Isotope Reactor (HFIR) located at Oak Ridge National Laboratory currently produces about 0.5 g of ^{252}Cf (together with other californium isotopes) per year. By using larger reactors, this quantity could be increased to produce several grams of ^{252}Cf per year. The ^{252}Cf isotope has a 2.6 year alpha decay half-life, and a 66 year spontaneous fission half-life. The latter makes this isotope an excellent source of neutrons, and this material has been used in several applications where a neutron source was desired. However, the neutron field and the gamma radiation accompanying fission of ^{252}Cf (3×10^6 n s^{-1} μg^{-1}, 7 MeV gamma) normally preclude the use of this isotope for basic chemical/physical studies, since considerable shielding is required to protect personnel and equipment from even microgram amounts of it. As a result, the mixture of californium isotopes obtained directly from a reactor is not generally considered when microgram or larger amounts are used outside of shielded cells. Although in principle the isotopes ^{251}Cf or ^{249}Cf could be isolated from reactor products by a mass separator, the cost and low yield ($\sim 10\%$) would make this process unattractive. The ^{251}Cf isotope ($t_{1/2} = 800$ years) is probably the most desirable isotope for non-nuclear studies, but is only formed at low concentrations as a result of its high neutron-capture and fission cross-sections. One isotope, ^{253}Cf, is important as a parent for isotopically pure ^{253}Es. If the Cf reactor product is sufficiently purified and the ^{253}Cf allowed to decay, then a subsequent chemical separation allows recovery of the isotopically pure ^{253}Es daughter.

For basic studies on weighable quantities of californium, the ^{249}Cf isotope is used. Its alpha half-life of 351 ± 4 years [2, 3] makes it suitable for chemical/physical experiments, where weighable quantities of californium are required. The ^{249}Cf isotope is available as an isotopically pure material from the decay of ^{249}Bk (beta emitter, half-life of 320 days), the latter being the major berkelium isotope obtained from reactors (^{250}Bk is also formed, but it has a 3.5 h half-life). To obtain ^{249}Cf free of other californium isotopes, it is first necessary to separate berkelium chemically from the californium produced in a reactor, and then permit the ^{249}Bk to decay to ^{249}Cf, which can subsequently be chemically separated from the berkelium. Currently, up to 60 mg per year of ^{249}Bk are produced in the HFIR at ORNL, which is sufficient to provide multi-milligram amounts of ^{249}Cf [4]. The only other known production of ^{249}Bk, and hence isotopically pure ^{249}Cf (excluding the use of a mass separator), is in the USSR. The quantity of these materials available in the USSR is believed to be less than that produced by the HFIR.

11.3 APPLICATIONS

As mentioned in the last section, the californium produced in nuclear reactors comprises several isotopes, with ^{252}Cf being the major one. Although

chemical/physical studies could be done on this isotope mixture, only a few micrograms of ^{252}Cf can be tolerated outside of hot-cell facilities. Thus, the main use for ^{252}Cf is: (1) where its neutron emission is desired; (2) where it serves as a target material for producing transcalifornium elements; (3) for Cf tracer work; and/or (4) when it serves as a parent for ^{248}Cm. This long-lived isotope of curium is very useful for basic studies of curium. In practice, a mixture of ^{248}Cm and small amounts of other curium isotopes are obtained from californium reactor products (97% ^{248}Cm, 3% ^{246}Cm from the decay of californium isotopes plus any residual curium isotopes that may be present from the reactor). Although it is beyond the scope of this work to review such applications fully, the potential usefulness of ^{252}Cf warrants some brief coverage. The reader is referred to the ^{252}Cf Information Center [5] for more extensive information.

When ^{252}Cf is used as a neutron source, the data listed in Table 11.2 are useful. Practical applications of ^{252}Cf make use of the spontaneous-fission neutrons generated by this isotope. Neutrons from ^{252}Cf sources have been useful in such areas as neutron activation analysis, neutron radiography (complements x-ray radiography), and medical therapy. These neutron sources are most useful where access to nuclear reactors is not possible, not convenient, and/or where a lower neutron flux is adequate. For example, portable neutron activation analysis systems have been designed for use in deep-sea exploration for minerals. Various sizes and forms of ^{252}Cf sources have been designed for medical applications, both for external irradiation and internal implantation. How extensive the practical application of ^{252}Cf may become will be determined by the success of experiments using this nuclide.

11.4 SEPARATION AND PURIFICATION

The choice of a separation and purification scheme depends on the nature of the californium source, the particular isotopes of californium involved, the amount of material, the impurities present, as well as several other factors. In short, the procedure should be customized to the particular needs at hand. Usually ion exchange is involved either as the main separative technique or in some secondary

Table 11.2 *Data for ^{252}Cf neutron sources.*

alpha radiation	partial half-life	2.730 yr
	average energy	6.11 MeV
	specific activity	520 Ci g^{-1}
neutron emission	partial half-life	85.5 yr
	specific activity	
	Al (α,n)	1.3×10^{7} n s^{-1} g^{-1}
	SF	2.3×10^{12} n s^{-1} g^{-1}
specific heat		38 W g^{-1}

capacity. Since californium in aqueous solutions is normally stable only in the tripositive state, oxidation–reduction cycles of it are not useful for separation. Because of the very similar chemical behavior of the tripositive transplutonium elements, as well as lanthanide ions of comparable ionic radii (Sm–Tb), the separation chemistry must often rely on small differences in chemical behavior.

The separation procedure most suitable for californium isotopes generated in accelerators may not be the same as that used for californium produced in reactor targets. In some accelerator experiments the desired californium isotopes may be physically separated via recoil mechanisms, which simplifies the rapid separations required for short-lived isotopes. The need for nuclear or radioactive purity, as opposed to chemical purity, will also affect the particular separative processes to be used. A considerable amount of information on californium chemistry was determined using tracer levels of californium. The major purification schemes for californium at the tracer level involved ion-exchange techniques to separate californium from other transcurium elements.

For purposes of separation, the transplutonium elements can be placed into two groups: (1) americium and curium, and (2) the next several transplutonium elements, which includes californium. The separation of californium from its neighbors, especially einsteinium, is therefore more difficult than separating it from americium/curium or from the lighter actinides. Separation from berkelium is simplified by the ability to oxidize berkelium in aqueous medium, which permits solvent extraction of Bk(IV) from Cf(III). A number of procedures have been used for the separation/purification of californium. One of the early ion-exchange methods involved the use of cation-exchange resin (Dowex 50) and ammonium citrate or ammonium lactate as eluants [6, 7]. A superior eluant, ammonium α-hydroxyisobutyrate, was first used 30 years ago [8] and is still in use today. A thiocyanate system with both anion and cation resins has also been used [9] for the separation of californium from other actinides. A very useful group separation between the lanthanides and actinides can be accomplished using concentrated hydrochloric acid as an eluant for the transcurium elements sorbed on cation resin [10]; the separation is improved by using an alcoholic hydrochloric acid eluant. The greater complexing ability of the transplutonium elements is evident as they desorb ahead of the lanthanide elements when using this eluant. The separation of californium from its actinide neighbors, using cation- or anion-exchange resins, and elution with either hydrochloric or alcoholic hydrochloric acid, is not practicable. Anion-exchange separation procedures using slightly acidic $LiNO_3$ or $Al(NO_3)_3$ solutions [11–13] or ethylenediaminetetraacetic acid (EDTA) as an eluant [14] have also been reported. Several extraction procedures have been used, such as the extraction of trivalent actinides from concentrated LiCl or $LiNO_3$ (slightly acidic) solutions using trilaurylamine or other trialkylamines [15], or quaternary ammonium salts [16–18]. Extraction chromatography using quaternary ammonium salts or di(2-ethylhexyl)phosphoric acid (HDEHP) as a stationary phase has also been employed [19–22]. Inorganic ion exchangers, such as zirconium phosphate

materials, have limited applications for californium separations due to their lower selectivity as compared to organic-type extractants. Several summaries of transplutonium element separation schemes involving californium have been published [23–31].

Most extraction procedures are useful for separating californium from americium/curium or from lighter actinides, but are limited for separating it from other transcurium elements. For example, HDEHP dissolved in an aromatic diluent has been used to separate Cf and Cm (separation factor 50). Efforts continue to find new and better extractants with the aim of improving separation factors and selectivity. It is unlikely that a specific extractant for californium will be developed but new materials may provide improved separation factors. Recent reviews that discuss californium extraction chemistry are available [32–34].

One application of HDEHP on an inert support material, such as porous glass (Bioglass), is worth noting. An excellent separation of curium and californium, which is important in recovering ^{248}Cm from its ^{252}Cf parent, can be achieved. In this procedure, the curium is eluted before the californium from the column using 0.1 M HNO_3 as the eluant.

It is also useful to note that berkelium and californium can be readily separated by extracting Bk(IV) away from Cf(III). This separation is important since isotopically pure ^{249}Cf is obtained from the beta decay of ^{249}Bk. The Bk(IV) can be generated by oxidizing Bk(III) with a strong oxidant ($NaBrO_3$) in nitric acid solution.

Since the majority of californium is produced in nuclear reactors, or obtained as a by-product from reactor-produced ^{249}Bk, it is appropriate to discuss briefly the separation techniques employed for reactor targets. If uranium or plutonium is contained as the main target material, then these elements must be separated from the californium in addition to fission products (lanthanide elements, transition metals, etc.) and other products (aluminum from target assemblies, etc.). If americium or some higher transplutonium element is the main target material, then only small amounts of the lighter actinides may be present. The general separation scheme for separating and purifying californium from the High-Flux Isotope Reactor targets (originally plutonium or higher actinides) at Oak Ridge National Laboratory is shown in Fig. 11.1. Reports on the purification processes are available [28, 35]. The procedure begins with alkali dissolution of the aluminum target holders. This leaves the insoluble actinide oxides, which are dissolved in hydrochloric or nitric acid. Solvent extraction (HDEHP in aromatic diluent) removes plutonium and zirconium. The transplutonium elements are then extracted with HDEHP in an aliphatic solvent, and a subsequent amine extraction of these actinides removes them from most of the fission products. At this point the product contains the transplutonium elements and the lanthanides. A LiCl anion-exchange process partitions the actinides from the lanthanides. The transcurium elements (Bk, Cf, Es, and some Fm) are separated on high-pressure cation-exchange columns, using α-hydroxyisobutyric acid as the eluant. Californium is obtained as a separate fraction from the high-pressure ion-

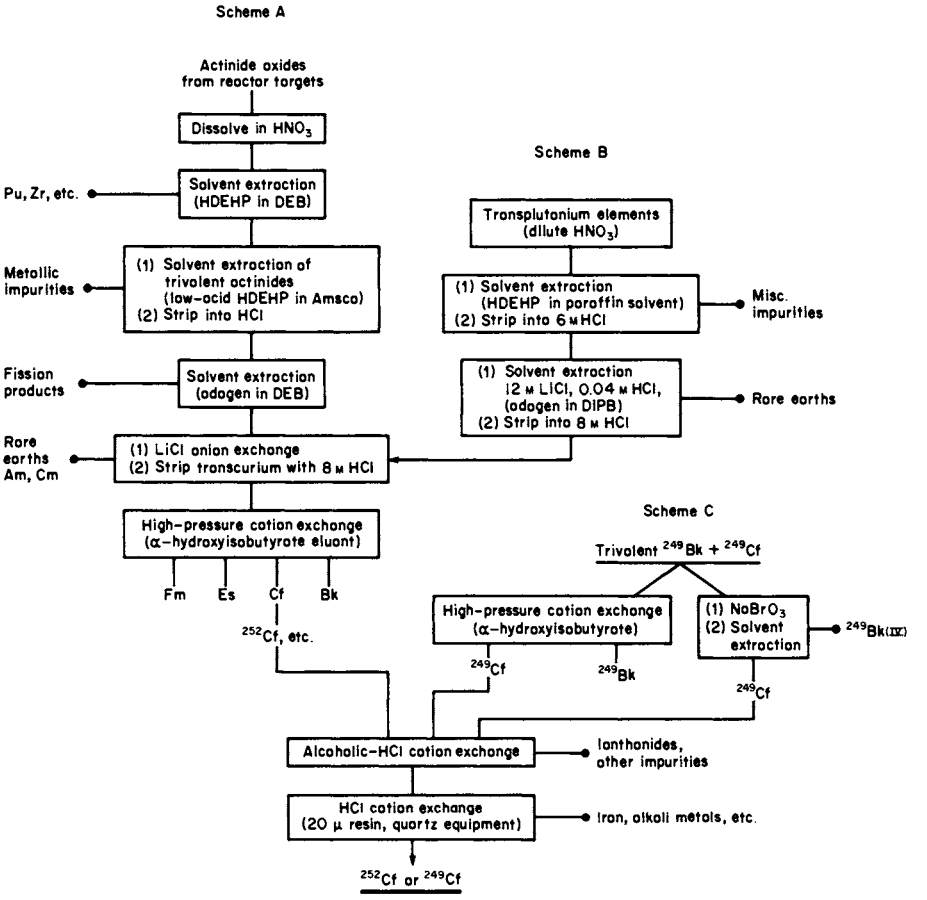

Fig. 11.1 *Purification scheme for californium produced in reactors.*

exchange process (very small resin particles, elevated temperature). The subsequent treatment of this fraction depends on several factors, which include the final use of the material. Since most basic research studies make use of ^{249}Cf obtained from decay of ^{249}Bk, the purification requirements for the californium isotopes produced directly in the reactor are based on whether ^{253}Es or ^{248}Cm daughters will be recovered, or on the medical or industrial uses of the californium isotopes.

For basic studies, researchers desire very high chemical purity. The ^{249}Bk precursor for ^{249}Cf normally is available as a reactor product (see Chapter 10) in a highly pure state, so that the eventual separation of ^{249}Cf is often made from a relatively pure parent material. However, often the ^{249}Bk has itself been used for various studies, and the ^{249}Cf must be separated from a large assortment of materials involved in these studies. Generally, ion-exchange procedures are used

to separate and purify the ^{249}Cf, although the Cf–Bk separation could be accomplished by oxidizing the Bk, and then extracting the Bk(IV) from the Cf(III). The final or so-called ultra-purification of ^{249}Cf normally involves several pressurized cation-exchange columns: (1) with ethanolic hydrochloric acid as an eluant (the latter serves to remove any lanthanide elements); (2) with 0.25 M α-hydroxyisobutyric acid as an eluant (variable pH of 3.8–4.2 at 80°C, separates californium from other transplutonium elements and provides general purification); and (3) with hydrochloric acid eluants (general purification, alkaline earths, alkali metals, iron, nickel, etc.). The latter often consists of two columns, with the final column and product receiver being constructed of acid-leached quartz. Special alpha detectors are used to determine the fractions that contain the ^{249}Cf. Using this process, a very pure californium chloride product is obtained, which can be used for preparing compounds or the metal of californium.

A fused salt–molten metal process has also been examined for separating californium [36, 37]. In principle, it may also be possible to reduce actinide oxides with thorium metal and distill away the more volatile californium metal (see Section 11.6.1). The separation of californium oxide from curium oxide using a vacuum sublimation procedure has also been reported [38].

11.5 ELECTRONIC PROPERTIES AND STRUCTURE

A considerable amount of spectroscopic data have been obtained for californium, and a number of theoretical calculations have been made concerning the energy levels in californium atoms. The neutral californium atom's ground state is assigned as $5f^{10}7s^2$ ($^5I_8$) and the Cf^{3+} ground state as $5f^9$ ($^6H^\circ_{15/2}$) [39, 40]. The ionization energy for the neutral californium atom has been calculated from spectroscopic data to be 6.298 ± 25 eV [41]. For the singly charged ion, the ground-level configuration is $5f^{10}7s$ ($5f^{10}$ ($^5I_8$) 7s $(8, 1/2)_{17/2}$) [39, 40]; the second level is at 1180.54 cm^{-1} [40]. From limited absorption and self-luminescence spectra for Cf(III), a partial energy level scheme was published for the $5f^9$ configuration [42]. Predictions of the energy level structure for Cf(III) appeared as early as 1964 [43]. Additional work on the triply ionized form of californium has also been published [44, 45]. Absorption spectra of Cf(III) are mainly characteristic of f–f transitions (Laporte forbidden) within the $5f^n$ configuration. Spectra of Cf(III) in $DClO_4$–D_2O have been used to make term assignments and energy levels for californium [45]. The electronic spectrum of Cf(IV) has also been predicted from spin–orbit coupling diagrams [46]. Estimated energies of the electronic configurations for californium had appeared earlier [47], where values were given for singly, doubly, and triply charged californium ions. A detailed theoretical interpretation of solid-state absorption spectra of $CfCl_3$ has also been published, and energy level assignments made for the several californium absorption bands [44]. The observed and calculated free-ion energy

levels for Cf(III) have also been compared to the lower energy levels in californium's analog, Dy(III) [44]. An attempt to correlate the electronic excitation energies for 4f and 5f elements has suggested that the values for the $f^n s^2 \rightarrow f^{n-1} ds^2$ excitation for californium compare best with the lighter lanthanide elements [48]. A valence-band approach for high-coordination bonding in californium compounds has also been suggested [49]; this approach implies d- and f-orbital splitting into bonding hybrids. From quantum chemistry considerations, the monopositive ion of californium should be more stable than a monopositive lanthanide or lighter actinide ion, based on its lower calculated excitation energy [50]. Calculations have also shown that, from berkelium to nobelium, the excitation energy for $f^n s^2 \rightarrow f^{n-1} ds^2$, which is taken as a measure of the stability of the divalent state, increases with the atomic number [51]. Thus, Cf(II) should be more stable than Bk(II) but less stable than Es(II). Predictions for excitation energies for $7s^2 \rightarrow 7s7p$ and $7s^2 \rightarrow 7s6d$ have also been given [52]. Experimental data have been obtained and crystal field calculations have been made for Cf(III) in crystal hosts [52]. Relativistic Hartree–Fock–Slater calculations have yielded neutral-atom electron binding energies for californium [53]. Relativistic relaxed-orbital calculations of L-shell Coster–Kronig transition energies have also been reported for californium [54]. An interpolation scheme for cohesive energies provides binding energies for electrons, which can correlate the divalent nature of transplutonium elements; this approach has predicted a divalent metallic state for einsteinium rather than for californium [55].

11.5.1 Emission spectra

The first emission spectrum for californium was reported in 1962 [56] and was obtained via the copper-spark method. The majority of subsequent work on californium has been carried out using electrodeless lamps, where multimicrogram amounts of material are sealed in quartz envelopes and the californium is excited by external radiation. Emission spectra of californium have been observed from 2400 to 2.5 μm, with approximately 25 000 lines having been recorded and accurately measured [57]. Fourier transform analyses of data obtained from californium lamps have been carried out with the goal of resolving the hyperfine structure [58]. The $5f^{10}7s^2$ ground state, the $5f^{10}7s8s$ and $5f^9 6d7s^2$ configurations, and a nuclear spin of 9/2 have been established from californium spectra [57, 59]. For further details see Chapter 15.

11.5.2 X-ray emission spectroscopy

The characteristic x-rays resulting from atomic readjustment to inner-shell vacancies provide a very useful means for identification of an element. Present theory permits the calculation of several x-ray emissions for heavy elements, and their bonding energies, and a tabulated list of such data has been reported for californium [60].

Similar calculations using non-relativistic Hartree–Slater wavefunctions [61] and relativistic Hartree–Slater theory [62] have also provided data for californium. The atomic form factors, the incoherent scattering functions [63], and a total Compton profile have been tabulated for californium [64].

Systematic x-ray photoelectron spectroscopy (XPS) studies have also been carried out on transplutonium oxides through californium, providing experimental binding energies for their electrons, which can be compared to the calculated energies [65]. An interpolation scheme has also been reported for determining the binding energies of some lanthanides and actinides, including californium [55]. The nature of the 5f electrons in the actinide series including californium has also been discussed [66].

11.6 METALLIC STATE

11.6.1 Preparation

The first attempt to prepare californium metal was reported in 1969 [67]. Subsequently, several additional attempts have been made to prepare and study this metal [68–72]. The relatively high volatility of californium metal has made its preparation and study on the microscale more difficult than the first three transplutonium metals. The possibility that the metal may exist in two different metallic valence states has made it an interesting candidate for study, but it has also complicated the full understanding of californium's metallic state.

Two preparative approaches have been utilized for preparing Cf metal. The first approach utilizes the reduction of the trifluoride with lithium metal at elevated temperatures; the excess reductant and lithium fluoride are removed by vacuum distillation. The second preparative method employs thorium or lanthanum metal to reduce a Cf oxide, permitting the distillation and subsequent condensation of the metal. Each technique has both advantages and disadvantages. With the halide reduction, the high volatility of Cf metal, which is greater than that of lithium fluoride, makes it difficult to remove the lithium fluoride completely from the product without simultaneous volatilization of significantly large amounts of Cf metal. In the oxide reduction procedure, the distillation of microgram quantities of metal yields thin films that are difficult to remove from collection devices. Also, a very good vacuum (free of residual materials such as hydrogen, oxygen, water or oil vapor, etc.) is required to avoid the formation of undesired compounds during the distillation of the reactive metal. With multi-milligram or larger quantities, the distillation procedure is probably the best preparative route. The limited availability of the ^{249}Cf isotope and the radiation fields encountered with this isotope in unshielded glove-box facilities tend to limit the amount of ^{249}Cf metal that can be prepared to less than 20 mg. The preparations of ^{249}Cf metal made to date have been in the 2–10 mg range [73, 74]. A more detailed account of the metal preparations can be found in Chapter 19 or in ref. 74.

These limited quantities of californium metal place restrictions on the amount of analytical data that can be obtained for the products; normally, analyses for hydrogen, nitrogen, and oxygen contents are not performed. The quality of the metal products has been determined by spark-source mass spectrometry, x-ray diffraction analysis, physical properties, appearance, and behavior in an experiment (such as the rate and extent of dissolution for heat-of-solution measurements).

Ideally, a larger quantity of metal would be prepared, characterized, and then used for a number of scientific measurements or experiments. But with californium (and some of the other transplutonium metals), the preparation of the metal often becomes an integral part of a subsequent study, and either the major portion or the entire preparation is needed and often consumed (i.e. dissolution in acid) in an experiment.

11.6.2 Physical properties

A summary of the reported crystallographic data for californium metal is given in Table 11.3. Based on an extrapolation of data for trivalent americium, curium, and berkelium metals, californium metal would be expected to have a double hexagonal close-packed (dhcp) low-temperature phase, with parameters of approximately $a_0 = 0.34$ and $c_0 = 1.10$ nm, and a face-centered cubic (fcc) high-temperature phase with an $a_0 \simeq 0.49$ nm. Based on other extrapolations [75], a divalent form of californium metal would be expected to be cubic and have a larger lattice parameter than a trivalent cubic form. From the values in Table 11.3, the dhcp form with parameters $a_0 = 0.3384$ and $c_0 = 1.1040$ nm [71, 72] is accepted to be the low-temperature form of trivalent californium metal. The fcc material, with $a_0 = 0.494$ nm [72], is very likely a high-temperature form of the trivalent metal, comparable to the fcc forms of americium, curium, and berkelium metals. The second fcc structure listed in Table 11.3, with $a_0 = 0.574$ nm [70, 72], has been observed by other workers using different preparative techniques.

Table 11.3 *Crystallographic data reported for californium metal.*

Crystal system	*Lattice parameters* a_0 (nm)	c_0 (nm)	*Atomic volume* (Å^3)	*Crystal density* (g cm^{-3})	*Metallic radius* (Å)	*Ref.*
fcc	0.540	–	39.4	10.5	1.91	68
fcc	0.5743	–	47.4	8.72	2.03	70
hcp	0.3988	6.887	47.4	8.72	2.07	70
dhcp	0.4002	1.2804	44.4	9.31	1.99	71
dhcp	0.3384	1.1040	27.4	15.1	1.69	71
fcc	0.494	–	30.1	13.7	1.75	72
fcc	0.575	–	47.4	8.72	2.03	72
dhcp	0.339	1.101	27.4	15.1	1.69	72

Additional support for this latter structure being a form of metallic californium is that samples exhibiting this structure have been converted by thermal treatment to the fcc structure having the parameter $a_0 = 0.494$ nm, and vice versa [72]. The second dhcp structure [71] listed in Table 11.3 and the other hexagonal structure [70] may represent the same material. If they are metallic californium, they would represent a hexagonal structure for the divalent form of the metal. They are at present not well-established structures for the metal. The fcc structure with the parameter $a_0 = 0.540$ nm [68, 69] has been observed in earlier work, where very small quantities of californium were prepared. In a later study [70], this structure ($a_0 = 0.540$ nm) was also observed in thin films of californium metal that had been heated to 200–300°C in air. It should be noted that poorly crystallized samples of californium sesquioxide (Cf_2O_{3+x}, body-centered cubic, $a_0 = 1.080$–1.083 nm; see Section 11.7.2) can be indexed as an fcc structure with $a_0 = 0.540$–0.542 nm. If the fcc structure with $a_0 = 0.540$ nm was indeed a metallic phase of californium, the lattice parameter would imply that the metal had an intermediate valence between 2 and 3.

If it is assumed that californium metal does exhibit two metallic valences, then two phases for each valence form can be selected from the crystallographic data in Table 11.3. For the trivalent form, metallic radii of 1.69 and 1.75 Å would be obtained, which is in accord with the radii obtained for the first three transplutonium metals, when allowing for a small systematic decrease in radius in going across the series. The divalent form would yield a radius of 2.0 Å, which is similar to the radii of divalent europium or ytterbium metals. The trivalent form of californium metal is well-established; if a divalent form does exist, it is favored in small quantities (thin films) obtained from higher temperatures (quenched from the vapor or molten states). Only a limited effort has been made to establish transition temperatures for californium metal [72].

Although bulk samarium metal is trivalent, divalent surface states have been demonstrated for this metal [76]. The next lanthanide metal, europium, is a divalent metal. It may be possible that californium metal is similar to samarium metal, and that the divalent state for californium metal may only be stable in thin films, very small samples, or in surface layers of atoms, as found for samarium.

There has been only one reported value for the melting point of californium metal, which was estimated to be 900 ± 30°C from the 'puddling' of metal particles in a thin film of the metal [70]. This melting point is lower than those reported for americium, curium or berkelium metals, but it is in accord with the higher volatility of californium metal, and the increasing trend toward divalency across the actinide series.

The first attempts to examine californium metal by high-pressure x-ray diffraction, on samples assumed to represent both the trivalent and divalent metal forms, did not provide additional insight into the valence state of the metal; the compressibility data obtained from this study were not conclusive [77]. A subsequent study on the dhcp (trivalent) form of californium metal found that this structure transformed into an fcc structure under pressures of 10–16 GPa

[78]. A bulk modulus of 50 ± 5 GPa was derived for the dhcp form of californium metal, which compares favorably with the bulk moduli for many of the lanthanide metals but is significantly lower than the moduli of thorium to plutonium metals. In recent studies of californium metal under pressures up to 48 GPa, it was found that the metal transforms into an α-uranium orthorhombic-type structure which corresponds to the onset of 5f-electron participation in the metallic bonding [79].

The vapor pressure and the heat of sublimation of californium metal have been measured using the Knudsen effusion technique [80]. The vaporization of californium metal (originally dhcp, trivalent form) over the temperature range 733–973 K is described by the equation:

$$\log(P/\text{atm}) = 5.675 \pm 0.039 - (9895 \pm 34)/T$$

The ΔH°_{298} was calculated to be 196.23 ± 1.26 kJ mol^{-1}, and ΔS°_{298} was derived to be 80.54 J K^{-1} mol^{-1}. The estimated boiling point for the metal is 1745 K. Nugent *et al.* [81] had estimated the heat of sublimation to be 163 kJ mol^{-1} and David *et al.* [82] had predicted a value of 197 kJ mol^{-1}. The vapor pressure of californium metal is intermediate between that of samarium metal (trivalent) and of europium metal (divalent) [80]. The data show that the californium metal was clearly trivalent up to 1026 K, and that it is one of the most volatile actinide metals. Its high volatility precludes bulk vaporization studies above 1073 K by the Knudsen technique. No evidence by mass spectrometry was obtained in this latter work for the presence of CfO.

The first data for the enthalpy of solution of californium metal (dhcp, higher-valence form) in 1.0 N HCl at 298 K yielded a value of -617 ± 11 kJ mol^{-1} [83]. A more recent measurement using larger samples of well-characterized metal has yielded a value of -576.1 ± 3.1 kJ mol^{-1} [84]. This latter value indicates a trend of less negative heat of solution with increasing atomic number for the elements americium to californium, which supports the expected trend of increasing divalent character in progressing across the series of elements. The heat of formation, $\Delta H^\circ_f(Cf^{3+}(aq))$ was derived as being -577 ± 5 kJ mol^{-1}. Using these values and estimates for entropies, $S^\circ(Cf(s, \alpha)) = 80.54 \pm 0.80$ and $S^\circ(Cf^{3+}(aq)) = -188 \pm 17$ J K^{-1} mol^{-1}, a standard potential for the Cf(III)/Cf(0) couple was calculated to be -1.92 ± 0.03 V [84]. Earlier estimates for this potential ranged from -1.95 to -2.03 V [85–88].

Efforts have been made to determine the magnetic susceptibility of californium metal. Although it would seem that susceptibility data would be very valuable in ascertaining the metallic valence of californium metal, it turns out that this information does not differentiate between the divalent form (presumably $5f^{10}$ state, $\mu_{eff} = 10.22\ \mu_B$) and the trivalent state (for $5f^9$ state, $\mu_{eff} = 10.18\ \mu_B$ [89]). The first magnetic susceptibility measurements [89] were made over the temperature range 22–298 K on two samples reported to be the divalent, fcc form of the metal. Both samples followed the Curie–Weiss relationship, and an average moment of 9.75 μ_B was derived from the data. Subsequent magnetic measurements have been made on the dhcp, trivalent form of californium for the

temperature range 4.2–350 K and in applied fields of up to 50 kG [90]. Data from these measurements indicate that californium metal exhibits at least two regions of differing magnetic behavior as a function of temperature. Below 51 K, the metal was either ferro- or ferrimagnetic; a distinction between the transition type could not be made owing to the inability to obtain a saturation moment greater than 6.1 μ_B in the highest applied field of 50 kG. There was evidence in some samples for antiferromagnetic behavior in the temperature range 48–66 K. Additional studies on pure californium oxides and nitrides must be made to determine if such impurities may have been responsible for this latter behavior. Above 160 K, the californium metal exhibited paramagnetic behavior. An average effective moment of $10.6 \pm 0.2\ \mu_B$ was obtained for three samples of the metal, whereas a fourth sample produced a value of $9.7 \pm 0.2\ \mu_B$. Results from this study [90] indicate that the magnetic behavior of californium metal is similar in some ways to that of its lanthanide electronic homolog, dysprosium metal.

11.6.3 Chemical properties

Californium metal is a fairly reactive metal, comparable to the lighter lanthanide metals but not as reactive as europium metal. One of the problems of preparing small quantities of transplutonium metals is that they are sufficiently reactive to form compounds with small amounts of impurities that may be present. At room temperature, small samples of californium metal are slowly oxidized in air, the rate increasing as the moisture content of the air increases. The metal is oxidized when warmed in air [70], and reacts when heated with nitrogen, hydrogen, or a chalcogen, or a pnictogen (see Section 11.7). Metal foils exposed to dry nitrogen at ambient temperature will slowly change from a bright silver appearance to a golden color; the change tends to be mainly at the surface. When metal samples are heated in evacuated quartz containers up to 300°C, their quality deteriorates; this change becomes more severe when the temperature is above 300°C. The products from the above treatment may be silicates or oxides. Appreciable sublimation can occur when the metal is heated to only 200–300°C in evacuated containers.

The metal reacts very rapidly with dry hydrogen halides and with aqueous mineral acids. In the latter case, hydrogen gas is evolved and a solution of Cf(III) is obtained, except with fluoride ion, where the insoluble trifluoride is formed.

Californium metal forms alloys with the lanthanide metals but definite compounds have not been reported. When heated, the metal 'wets' and appears to form an alloy with tantalum, which usually prohibits the use of tantalum containers for high-temperature work. Tungsten metal is the preferred container material.

11.6.4 Theoretical treatment

The chemistry of the actinide series is complex, and attempts to develop a self-consistent model for these elements have had limited success. Efforts have been

made to describe their properties and to correlate them with other members in the periodic table [81, 82, 85–88, 91–93]. The important questions are: what role do the 5f electrons have in the series, and what is their position with regard to the Fermi level? In progressing across the series, band narrowing is appreciable at americium [85], where the 5f electrons are more localized and behave more like the 4f electrons in the lanthanides. At californium's position in the series, the 5f electrons are fully localized.

Several properties of californium were considered in making correlations of the 5f-electron status across the series [81, 82, 85–88, 91–93]; one prediction was that californium metal would be close to the divalent–trivalent metallic boundary [85]. Californium is the first element in the actinide series to show strong divalent tendencies, owing to the progressive stabilization of the divalent ground state [92] that is probably complete at fermium.

A correlation [93] relating crystal entropy to metallic radius, atomic weight, magnetic properties, and electronic structure has permitted the accurate calculation of unknown entropies for these elements. This approach does require a defined electronic structure in order to predict accurate entropy values. Thermodynamics for the transplutonium metals have been summarized [94, 95].

The pattern of superconductivity in f-band metals has received considerable attention. It is unlikely that californium metal would show superconductivity, as a result of its magnetic moment and localized 5f electrons, but prospects for superconducting behavior in other actinides have been discussed [96, 97].

11.7 COMPOUNDS

11.7.1 General

Californium is presently known to exist in compounds where it has oxidation states of II, III, and IV, with the trivalent state being the most prevalent. The tetravalent state is exhibited in CfO_2, $BaCfO_3$, and CfF_4, and the divalent state has been observed in $CfCl_2$, $CfBr_2$, and CfI_2. There are also several compounds of californium where the oxidation state is less well-defined, such as in compounds with pnictigens, chalcogens, hydrides, etc. Ionic radii for each oxidation state can be established from crystallographic data on these compounds, and some values of radii are given in Table 11.4. It is important that the comparison of radii be made using calculated values obtained from a specific set of conventions. In many instances, lanthanides and actinides with similar ionic radii will form the same type of solid compound and will have comparable lattice parameters. Thus, the behavior of the transplutonium elements in forming these compounds and the resulting lattice parameters of such compounds are more predictable than in the metallic state, or for other compounds where bonding may be more complex. Where changes in crystal structure or other properties depend mainly on the ionic size of the metal ion, they occur earlier in the lanthanide series than in the comparable actinide series. As a consequence,

Table 11.4 *Comparison of selected radii of californium and some lanthanides.*

Ion	*Compound*	*Radius* (Å)	*Ref.*
Cf^{2+} Eu^{2+}	$CfBr_2$ $EuBr_2$	$Eu^{2+} \sim 0.01 > Cf^{2+}$	98
Cf^{3+}	$CfCl_3$	0.932[a]	99
Gd^{3+}	$GdCl_3$	0.938[a]	99
Cf^{3+}	Cf_2O_3	0.942[b]	100
Cf^{3+}	Cf_2O_3	0.95	101
Gd^{3+}	Gd_2O_3	0.938[b]	102[e]
Eu^{3+}	Eu_2O_3	0.950[b]	102[e]
Cf^{4+}	CfO_2	0.859[c]	100
Cf^{4+}	–	0.821[d]	101
Ce^{4+}	CeO_2	0.898[c]	–[f]
Pr^{4+}	PrO_2	0.890[c]	–[f]
Tb^{4+}	TbO_2	0.817[c]	–[f]

[a] Derived from apical distances of hexagonal trichloride cells; six-coordinated metal atom.
[b] Derived from sesquioxide lattice parameters, using an oxygen radius of 1.46 Å and adding 0.08 Å for covalent M–O bond character; six-coordinate metal ion.
[c] Derived from dioxide lattice parameters, using an oxygen radius of 1.46 Å, correcting for covalent character of M–O bond (+0.10 Å) and for coordination number of 8 to 6 (−0.08 Å).
[d] Radius from plot of r^3 vs volume.
[e] Source of lattice parameters: refs 103 and 104.
[f] Source of lattice parameters: ref. 105.

trivalent californium compounds are often comparable to gadolinium compounds rather than to those of dysprosium, which is the electronic homolog of californium. Crystallographic data for a number of californium compounds are given in Table 11.5. The reader is also referred to Chapter 20 on structural aspects of solid-state actinide chemistry.

11.7.2 Oxides

The oxides of new elements are often among the first compounds to be investigated, due to the basic importance of the oxides, their ease of formation, and the fact that the oxide often serves as an intermediate in preparing other materials. Californium oxides can be obtained by calcination in air of several compounds such as oxalates, hydroxides, nitrates, etc. The stoichiometry (O/M ratio), as well as the crystalline form of the californium oxide obtained, depends on the particular experimental parameters employed in the calcination. Both the

Table 11.5 *Crystallographic data for californium compounds.*

Substance	*Structure type*	*Crystal system*	*Lattice parameters* a_0 (nm)	b_0 (nm)	c_0 (nm)	*Angle* (deg)	*Ref.*
oxides							
Cf_2O_3	Mn_2O_3	bcc	1.0839				106, 238
	Sm_2O_3	monoclinic	1.412	0.3591	0.8809	$\beta = 100.3$	107
	La_2O_3	hexagonal	0.372		0.596		108, 109
Cf_7O_{12}	Tb_7O_{12}	rhombohedral	0.6596			$\alpha = 99.40$	110
CfO_2	CaF_2	fcc	0.5310				100, 111
halides							
CfF_3	LaF_3	trigonal	0.6945		0.7101		112
CfF_3	YF_3	orthorhombic	0.6653	0.7039	0.4393		112
CfF_4	UF_4	monoclinic	1.242	1.047	0.8126	$\beta = 126.0$	113
	UF_4	monoclinic	1.233	1.040	0.8113	$\beta = 126.44$	114
$CfCl_3$	UCl_3	hexagonal	0.7379		0.4090		107
$CfCl_3$	$PuBr_3$	orthorhombic	0.3859	1.1748	0.8561		99
$CfBr_2$	$SrBr_2$	tetragonal	1.150		0.7109		98
$CfBr_3$	$AlCl_3$	monoclinic	0.7215	1.2423	0.6825	$\beta = 110.7$	115
$CfBr_3$	$FeCl_3$	rhombohedral	0.758			$\alpha = 56.2$	116
CfI_2	$CdCl_2$	rhombohedral	0.7434			$\alpha = 35.83$	117
	CdI_2	hexagonal	0.4557		0.6992		
CfI_3	BiI_3	hexagonal indexing	0.7587		2.0814		117
		rhombohedral indexing	0.8205			$\alpha = 55.08$	117

oxyhalides						
$CfOF$	CaF_2	cubic	0.5561			118
$CfOCl$	PbFCl	tetragonal	0.3956		0.6662	106
$CfOBr$	PbFCl	tetragonal	0.390		0.812	115
$CfOI$	PbFCl	tetragonal	0.397		0.914	115
pnictides						
CfN	NaCl	fcc	(0.498)[a]			119
$CfAs$	NaCl	fcc	0.5809			120
$CfSb$	NaCl	fcc	0.6165			120
hydride						
CfH_{2+x}	NaCl	cubic	0.5285			235
oxysulfide and oxysulfate						
CfO_2S	La_2O_2S	trigonal	0.3844		0.6656	121
$Cf_2O_2SO_4$	$La_2O_2SO_4$	orthorhombic	0.4187	0.4072	1.3008	121
cyclopentadienyl						
$Cf(C_5H_5)_3$		orthorhombic	1.410	1.750	0.969	122

[a] Preliminary lattice parameters.

sesquioxide and dioxide are known, and oxides of intermediate composition have also been established. Three crystalline forms of the sesquioxide are known. There has been no evidence for a monoxide of californium, although other compounds containing divalent californium have been prepared. The preparation of lanthanide monoxides by reacting the metal and oxide under high pressure and temperature [123] may be applicable to californium. Californium monoxide would be expected to have an fcc type of structure and to exhibit a lattice parameter similar to that for the mononitride ($a_0 = 0.48$–0.50 nm).

Crystallographic data for the oxides are listed in Table 11.5. The monoclinic form (Sm_2O_3 type) of the sesquioxide was established in 1967 [107] and the bcc (α-Mn_2O_3 type) form was observed later [106], where it was also noted that slight oxidation of the bcc form could occur when it was heated in air. The fcc dioxide has been prepared by heating lower oxides of californium with high-pressure molecular oxygen or with atomic oxygen [100, 111]. The hexagonal form (La_2O_3 type) of Cf_2O_3 [108, 109] is difficult to prepare, as it exists in a narrow phase region between the liquid state and the monoclinic form. This form of Cf_2O_3 has also been observed in old samples of hexagonal Bk_2O_3 after five half-lives of ^{249}Bk decay [108]. The melting point of Cf_2O_3 is reported to be 1750°C, which continues the trend of decreasing melting points of the actinide sesquioxide beyond Cm_2O_3 [108, 109]. This behavior is in contrast to that observed in the lanthanide sesquioxides where the trend is for a general increase in melting points across the series. The phase diagram for the transplutonium sesquioxides through californium [108, 109] is similar to that known for the lanthanide sesquioxides.

The transition temperature for the bcc form to the monoclinic form of Cf_2O_3 has been reported as both 1100°C [107] and 1400°C [100]; the transition for the monoclinic form to the hexagonal form of Cf_2O_3 is 1700°C [108, 109]. The cubic to monoclinic transition appears to be irreversible, while the hexagonal to monoclinic transition is believed to be readily reversible.

A capacitance manometer system, capable of analyzing oxygen overpressures for as little as 1.4 mg of californium, together with x-ray powder diffraction analyses, established the californium–oxygen system for $1.50 < O/Cf < 1.72$ [110]. That work showed that Cf_7O_{12} (rhombohedral) was the stable oxide obtained by heating californium in air or oxygen up to 750°C. At higher temperatures, Cf_7O_{12} loses oxygen to form Cf_2O_3. The existence of oxide stoichiometries between Cf_2O_3 and CfO_2 had been noted earlier by other workers [100]. The sesquioxide of californium ($O/Cf = 1.50$, bcc form) can be prepared by heating an air-calcined oxide in hydrogen or carbon monoxide (850–1000°C), or by quenching such an oxide from 900–1000°C, preferably in a vacuum. The dioxide is known to be thermally unstable, with some decomposition in air occurring at temperatures as low as 200°C; by 400°C, the Cf_7O_{12} compound is formed [111].

Although the preparation of CfO_2 normally requires strong oxidizing conditions, under certain conditions lower californium oxides stored in air or oxygen can be oxidized, presumably due to active oxygen species generated by the

alpha radiation [93]. With small samples of CfO_2 [100], this self-irradiation may, instead, bring about the loss of oxygen. The exact composition of aged samples is difficult to ascertain since the lattice parameters derived from these samples reflect radiation damage to the lattice, as well as the O/Cf ratios of the samples. An earlier review on radiation effects in actinide oxides is recommended [124].

At the present time, the californium–oxygen system is believed to involve three crystal forms (trimorphic) of the sesquioxide, a rhombohedral Cf_7O_{12} compound that only exists over narrow O/Cf ratios, and an fcc CfO_2. It appears that the bcc form of Cf_2O_3 can accept additional oxygen up to an O/Cf $\leqslant$ 1.7, with an appropriate decrease in the Cf_2O_3 lattice parameter. Between O/Cf ratios of 1.8 and 2.0, an fcc-type structure is encountered with the lattice parameter decreasing with greater O/Cf ratios. The californium–oxygen system exhibits some similarity to the terbium–oxygen system.

One recent study examined the oxidation behavior of (Bk, Cf) oxides as a function of the californium content [125]. The conclusion reached was that, when the californium content was up to 25 mol%, the californium was readily oxidized in air to O/M = 2, behaving like pure berkelium oxide; when the californium content reached 64 mol%, the californium controlled the berkelium oxidation and limited the mixed cation product to a stoichiometry of M_7O_{12}.

A systematic treatment of data from the lanthanide and actinide oxides has generated estimated thermochemical values for the oxides of californium [126].

11.7.3 Halides and oxyhalides

In view of the estimated IV–III reduction potentials [87, 127] for californium, it is reasonable that the only stable, bulk binary Cf(IV) halide would be CfF_4, which can be prepared by fluorinating (F_2 or ClF_3) CfF_3, Cf_2O_3 (see Table 11.6), or possibly other materials [113, 114, 128, 129] at 300–400°C. The tetrafluoride has limited thermal stability, decomposing to form CfF_3 [113]. There has been some

Table 11.6 *Preparative reactions for californium halides.*

tetrafluoride
CfF_3 or Cf oxide + $F_2 \rightarrow CfF_4$
trihalides
Cf oxide + $HX \rightarrow CfX_3$ (X = F, Cl, Br)
$Cf^0 + HX \rightarrow CfX_3$
$Cf^0 + X_2 \rightarrow CfX_3$
$CfX_3 + 3HI \rightarrow CfI_3 + 3HX$
oxyhalides
Cf oxide or $CfX_3 + HX/H_2O \rightarrow CfOX$
dihalides (X = Cl_3, Br, I)
$CfX_3 + Cf^0 \rightarrow CfX_2$
$CfX_3 + H_2 \rightarrow CfX_2$

variance in the UF_4-type, monoclinic lattice parameters reported for CfF_4 [113, 114] (see Table 11.5); the reason for this variance is due to indexing the complicated powder patterns. Additional work has been done on CfF_4; the solid-state absorption spectrum has been obtained, the thermal stability examined, and new x-ray powder data evaluated [130]. Mixed alkali-metal fluoride complexes of the types $MCfF_5$, M_2CfF_6, M_3CfF_7, and $M_7Cf_6F_{31}$ are expected to exist, and may provide additional stability for Cf(IV). The existence of CfF_4 in the vapor state has also been claimed in high-temperature chromatographic studies using tracer quantities of californium [131, 132].

All the trihalides and oxyhalides of Cf(III) are known (see Table 11.5), and were among the first compounds of californium to be reported. They can be prepared by hydrohalogenation of Cf_2O_3, hydrohalogenation of a californium trihalide containing a halogen with a lower atomic number, or via treatment of an oxide at elevated temperature with interhalogens. The reaction of Cf_2O_3 with hydrogen iodide does not give satisfactory results.

The trifluoride is dimorphic (orthorhombic, YF_3 type; trigonal, LaF_3 type) with the transition temperature to the trigonal form occurring above 600°C [112, 133, 134]. Treatment of the trifluoride with water vapor above 700°C produces CfOF [118].

Californium trichloride is also dimorphic, exhibiting the UCl_3-type hexagonal structure (low temperature) and the $PuBr_3$-type orthorhombic structure [99, 107]. The melting point was reported to be 545°C [99]. Treatment of Cf_2O_3 with moist hydrogen chloride, or $CfCl_3$ with water vapor, at elevated temperatures produces tetragonal CfOCl [106].

Californium tribromide is trimorphic, but only two of the three forms have been prepared in a direct fashion. The high-temperature form (> 500°C) is an $AlCl_3$-type monoclinic structure [115, 116, 135]; a less well-characterized, $FeCl_3$-type rhombohedral structure has also been reported [116]. A third form, a $PuBr_3$-type orthorhombic structure, has been obtained from an aged (several half-lives) orthorhombic $^{249}BkBr_3$ parent [136]. Synthesis of the tribromides from (Bk, Cf) oxides has shown that orthorhombic $BkBr_3$ could not be prepared by thermal treatment once the californium content of the mixed oxide reached 45 mol% [136]. Heating orthorhombic $CfBr_3$ (produced from the decay of $BkBr_3$) above 330°C immediately transforms it to the monoclinic form [136]. The oxybromide of californium [115] is isostructural with CfOCl [106] and can be prepared by the methods (see Table 11.6) used for making CfOCl and by applying a pressure of 3 GPa to monoclinic $CfBr_3$ [236].

Californium tri-iodide is monophasic, exhibiting the BiI_3-type hexagonal structure [115, 117]. It has been prepared by treating 'californium hydroxide' with hydrogen iodide at 800°C [115], but a preferred procedure would be to heat $CfCl_3$ or $CfBr_3$ with hydrogen iodide [117]. The oxyiodide [115] is isostructural with CfOCl and CfOBr, and it is obtained by the same preparative procedure used for the latter compounds.

The dichloride, dibromide, and di-iodide of californium have been prepared but the difluoride has not been reported. The first compound of Cf(II) was $CfBr_2$ prepared by hydrogen reduction of $CfBr_3$ [98, 137]. Subsequently, it was observed, and shown by absorption spectra, that lime-green $CfBr_3$ could be thermally reduced (760°C) to produce amber-colored $CfBr_2$ [138]. The structure of $CfBr_2$ is tetragonal ($SrBr_2$ type) [98]. It is expected that the free-energy change between the di- and trivalent compounds would be the least for the iodides, and hence the di-iodide would be the most stable. The first preparations of CfI_2 produced the high-temperature CdI_2-type hexagonal form [139]; subsequently, a second structural form ($CdCl_2$-type rhombohedral structure) was reported [117]. The di-iodide is obtained via hydrogen reduction of the tri-iodide (see Table 11.6). Of the three dihalides, $CfCl_2$ proved to be the most difficult to prepare; early attempts to prepare it were unsuccessful [136, 140]. It was eventually prepared by hydrogen reduction of the trichloride at 700°C [141]. The x-ray structure of $CfCl_2$ has not been resolved; it is expected that $CfCl_2$ would exhibit either the $PbCl_2$-type orthorhombic or the $SrBr_2$-type tetragonal structure [137].

There is evidence that californium halides may form so-called mixed-valence compounds (M_5X_{11}, $M_{11}X_{24}$, or M_6X_{13}, where M = metal ion and X = halide ion) like those reported for some of the lanthanide elements [142–144]. To avoid the necessity of carefully controlling reduction of californium to the proper stoichiometry, mixtures of gadolinium and californium (comparable radii, see Table 11.4) were used such that total reduction of the californium to Cf(II) would produce the desired structures, Cf_4GdCl_{11} and Cf_4GdBr_{11} [145].

Except for the trifluoride, anhydrous californium trihalides are hygroscopic and must be protected from moisture. The dihalides are very sensitive to both moisture and oxygen. Normally, their syntheses are carried out in glass (except for fluorides) so that products can be flame-sealed *in situ*, avoiding subsequent transfers of the products. Some preparative and experimental techniques for studying californium halides have been reviewed [74, 146].

11.7.4 Other compounds of californium

In addition to the oxides and halides, several other compounds of californium have been prepared and their crystallographic data reported (see Table 11.5). Some of these data represent preliminary values or results from single experiments. In some cases (pnictides, chalcogenides, etc.), the limited supply of californium metal has precluded the preparation of specific compounds, especially where close control of the stoichiometries is required (for example, CfS). The general preparative techniques for pnictides and chalcogenides of the transuranium elements has been reviewed [147].

Stoichiometries other than 1:1 are not expected for californium pnictides. These materials can be prepared by direct combinations of the elements at elevated temperatures; the products exhibit the NaCl-type, cubic structure. From

a single preparation of CfN, a lattice constant of 0.498 nm [119] has been derived. This parameter is slightly larger than that reported for one form of fcc californium metal [72]. The monophosphide of californium has not been reported. The monoarsenide and monoantimonide of californium have also been prepared [120] (see Table 11.5).

In contrast to the pnictides, californium chalcogenides of different stoichiometries can be prepared [147]. Preparation of monochalcogenides requires close control of the reactant stoichiometries to avoid the formation of higher chalcogenides, and attempts to prepare californium monochalcogenides as single-phase products have not been successful to date. The tritelluride, ditelluride, diselenide, disulfide, sesquiselenide, and sesquisulfide of californium have been prepared [147]. These higher chalcogenides are prepared by direct combination of the elements, and lower stoichiometries can be obtained by thermal decomposition of the higher compositions. Lattice parameters for these californium compounds have been determined but have not yet been published [148]. The tritelluride of californium is an orthorhombic structure that is isomorphous with the $NdFe_3$ structure. The dichalcogenide compounds all crystallize in the anti-Fe_2As type of tetragonal structure (as do the corresponding plutonium, americium, curium, and berkelium compounds). Four transuranium sesquichalcogenide structure types are known; the sesquisulfide and sesquiselenide of californium have been obtained as the α form (body-centered cubic; anti-Th_3P_4 type of structure) [147].

There has been one report on the preparation of californium hydrides [235]. The hydrides were prepared by reaction of californium metal with hydrogen at elevated temperatures. It was believed that the stoichiometries were close to that for the dihydride (CfH_{2+x}). The products exhibited fcc structures with an average lattice parameter of $a_0 = 0.5285$ nm, which is slightly larger than expected for the compound based on extrapolations of parameters for preceding actinide dihydrides. This larger parameter and the inability to prepare a trihydride of californium were believed to reflect a tendency for californium to be divalent. In the lanthanide-hydrogen system, the hydrides of divalent europium and ytterbium metals deviate from the behavior of the other lanthanide hydrides [149].

The oxysulfate (orthorhombic) and the oxysulfide (trigonal) of californium have been reported (see Table 11.5) [121]. These compounds can be prepared by thermally decomposing either Dowex ion-exchange resin beads containing Cf(III) or hydrated $Cf_2(SO_4)_3$; the oxysulfide is obtained in vacuum or reducing (hydrogen-containing) atmospheres. The oxysulfate does not decompose to the sesquioxide when heated in air until the temperature exceeds 860°C.

An organocalifornium compound, $Cf(C_5H_5)_3$, has been prepared and characterized crystallographically [122, 150] (see Table 11.5). Both powder and single-crystal x-ray data were obtained for this orthorhombic, cyclopentadienyl compound, which was prepared from $CfCl_3$ and molten $Be(C_5H_5)_2$, and isolated by vacuum sublimation (135–200°C). A solid-state absorption spectrum of $Cf(C_5H_5)_3$ was obtained from the crystals; a broad absorption from 600 nm to lower wavelengths was accredited to an electron-transfer process [122].

Some work has also been reported on a californium dipivaloylmethanato complex, where the volatility of the complex was compared to complexes of other lanthanides and actinides [151]. These tracer studies suggested that the californium complex deposited at lower temperatures than the americium or plutonium complexes.

11.7.5 Magnetic behavior of californium in compounds

Only a limited amount of magnetic work has been reported for californium, some of which was discussed in the earlier section on the metal (Section 11.6). The transplutonium metals with localized 5f electrons behave as though they consist of ions embedded in a sea of conduction electrons. These 5f electrons are mainly responsible for the susceptibility. With this simple model, the effective moment for californium metal can be considered to be the same as that for a californium ion that had the same number of electrons involved in bonding in a compound. In Table 11.7 are listed some metal ions and their calculated magnetic moments based on *LS* coupling and Hund's rule. On this basis, the moments of Cf(IV) and Tb(III) or Bk(III) would be the same, the moments of Cf(III) and Dy(III) or Es(IV) would be identical, and the moments of Cf(II) and Es(III) or Ho(III) would be equal. As was pointed out earlier (Section 11.6), it is unfortunate that the measured moment cannot differentiate between Cf(II) and Cf(III), and that the calculated difference between Cf(III) and Cf(IV) is only 0.9 μ_B. However, the magnetic behavior as a function of temperature and/or magnetic field still provides very useful information, which by itself may even be sufficient to differentiate between these states.

The first magnetic data reported for californium compounds were obtained from 56 ng of californium [152]; this small quantity required a microscope to measure the deflections of a Faraday apparatus. The object of the experiment was to confirm that Cf^{3+}, deposited on an ion-exchange resin bead, had a radon core plus $5f^9$ electrons. The results showed that the sample followed the Curie–Weiss law and produced a moment of 9.2 μ_B for the Cf(III). A later experiment with larger samples (0.3–1.2 μg) of californium on resin beads gave effective moments of 9.1–9.2 μ_B [153]. More recently, magnetic studies on oxides (Cf_2O_3, Cf_7O_{12}, CfO_2, and $BaCfO_3$ [237, 238]) have been reported. The

Table 11.7 *Electronic states (3+) and effective magnetic moments given by LS coupling and Hund's rule: expected moments of californium.*

Lanthanide	*Actinide*	*3+ ion configuration*	*Basic level*	*L*	*S*	*J*	g_J	$g_J[J(J+1)]^{1/2}$	μ_{eff}[a]
Gd	Cm	f^7	$^8S_{7/2}$	0	7/2	7/2	2	7.94	7.66
Tb	Bk	f^8	$^9F_6$	3	3	6	3/2	9.72	9.40
Dy	Cf	f^9	$^6H_{15/2}$	5	5/2	15/2	4/3	10.63	10.22
Ho	Es	f^{10}	$^5I_8$	6	2	8	5/4	10.60	10.18

Therefore, based on these assumptions, Cf(II) $\simeq$ 10.60 μ_B, Cf(III) $\simeq$ 10.63 μ_B, and Cf(IV) $\simeq$ 9.72 μ_B

[a] Ref. 154; based on intermediate coupling as opposed to pure *LS* coupling.

magnetic moments obtained in these studies were in agreement with the charge states assigned to californium based on the stoichiometries in the materials. Magnetic studies have also been carried out on three pnictides (CfN, CfAs, and CfSb) [239] and on two structures of $CfCl_3$ [240]. Magnetic data for the metallic state are described in Section 11.6.

An electron paramagnetic resonance study on Cf(III) in a $Cs_2NaLuCl_6$ host (< 1% Cf by weight) [154] produced a 10-line spectrum to confirm the nuclear spin to be 9/2. The crystal field ground state was also identified in this work and the nuclear dipole moment of ^{249}Cf determined to be 0.28 μ_N.

11.7.6 Solid-state absorption spectra

The anhydrous transplutonium halides have been extensively studied by absorption spectrophotometry. The f–f and f–d transitions in californium spectra can be utilized to ascertain the oxidation state and coordination number of californium in the compounds. Some of the experimental techniques employed for studying microgram quantities of californium halides have been reported [146, 153, 155, 156]. One of the first absorption spectra for californium was obtained from a single crystal of anhydrous $CfCl_3$ [155]. Subsequently, other spectra have also been obtained for this compound [141, 155–158] and for $CfCl_2$ [141]. Absorption spectra have also been obtained for anhydrous $CfBr_3$ [135, 136, 138], $CfBr_2$ [138], CfI_3 and CfI_2 [117], and CfF_4 and CfF_3 [130]. Solid-state absorption spectra for $CfCl_2$ and the hexagonal crystal form of $CfCl_3$ are shown in Fig. 11.2. Laser-induced fluorescence of Cf^{3+} in an $LaCl_3$ host has also been reported [159, 160]. A limited amount of spectral information was reported for dicyclopentadienylcalifornium [122]. The infrared spectrum of californium has also been obtained [161]. Crystal field calculations and parameters for the 3+ actinides in crystal hosts have been published [161–164]. The spectroscopic properties of californium compounds pertinent to laser applications have been discussed, and the transition from the $J = 11/2$ state at 6500 cm^{-1} to the $^6H_{15/2}$ ground state appears to be a candidate [165]. Free-ion energy levels and the optical properties for californium have also been published [166]. In addition, absorption spectra of californium halides have been obtained and examined as daughter or granddaughter products in studies of the chemical and structural consequences of radioactive decay processes [136, 167, 168].

11.8 SOLUTION CHEMISTRY

11.8.1 General

Although californium exhibits oxidation states of II, III, and IV in the solid state, its solution chemistry is basically that of a trivalent ion. There have been no substantiated reports of an oxidation state above IV in solution or in a solid compound, even though Cf(v) presumably would have the stabilizing influence of a half-filled $5f^7$ state. The tetravalent state requires a high degree of complexation

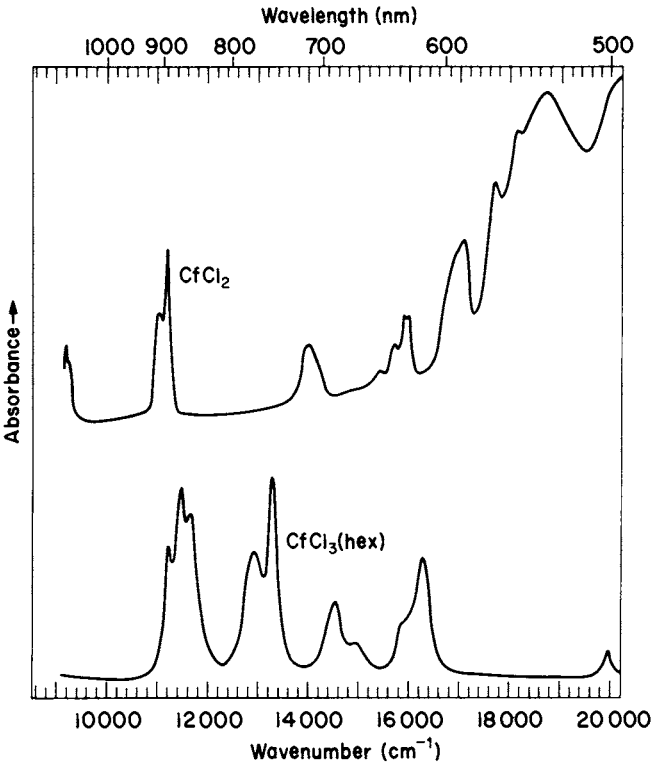

Fig. 11.2 *Solid-state absorption spectra of $CfCl_2$ and $CfCl_3$ (hexagonal crystal form)* [141].

to be stable in aqueous media. It has been reported [169] that Cf(IV) has been stabilized in phosphotungstate solutions, where M(IV)/M(III) couples can be shifted 1.0 V [170]. It is expected that it would be easier to stabilize Cf(II) than Cf(IV) in aqueous solutions, and non-aqueous solvents offer even greater promise for obtaining these oxidation states.

Although californium is the electronic homolog of dysprosium, its divalent–trivalent behavior in solution may be more similar to that of samarium, and its trivalent–tetravalent behavior may be comparable to that of terbium.

Trivalent californium in solution behaves similarly to the trivalent lanthanide ions, but it has a greater tendency to form complexes. The higher degree of complexation of the transplutonium(III) ions in alcoholic solution, as compared to the lanthanide(III) ions, has been used as a method for group separation (see Section 11.4). Fluoride and oxalate ions will precipitate trivalent californium from dilute acid solutions. Addition of hydroxide to a californium(III) solution produces a gelatinous precipitate, which is presumably the trihydroxide. In non-complexing solutions (i.e. dilute acid solutions, 0.1 M HCl), Cf(III) exists as a hydrated cation; at higher acid concentrations (i.e. 6 M HCl), complexation is sufficient so that the californium will not be held by cation-exchange resin.

11.8.2 Oxidation–reduction reactions

Several reduction potentials for californium have been derived both from experimental data and from systematic calculations, and these values are given in Table 11.8. The calculated Cf(IV)/(III) couple of 3.2 V [127] is in accord with the inability to obtain Cf(IV) in most aqueous media. This value for californium can be compared to the Tb(IV)/Tb(III) couple of 3.1–3.3 V, the Am(IV)/Am(III) couple of 2.2–2.5 V, and the Cm(IV)/Cm(III) couple of 3.1–3.5 V [127, 171]. Thus, the ease of forming Cf(IV) should be comparable to forming Tb(IV) or Cm(IV) but more difficult than forming Am(IV) in solution. The solution behavior can be compared to that in the solid state, where the formation of californium dioxide is comparable to preparing terbium dioxide, with both being more difficult to prepare than americium or curium dioxide (see Section 11.7.2).

The ability to oxidize Cf(III) to Cf(IV) in a phosphotungstate solution has been summarized in a paper on the solution behavior of the transplutonium elements [172]. Tb(IV) [173] and Am(IV) [174] can be stabilized in strong carbonate; thus, it would appear possible to prepare Cf(IV) in a strong carbonate medium, utilizing an expected shift of 1.7 V in the Cf(IV)/Cf(III) couple due to carbonate complexation of the Cf(IV). Two conflicting reports exist on the oxidation of Cf(III) in carbonate. One group [175] was unable to find evidence for Cf(IV) after chemical or electrical treatment, while a second group [241] reported that 20% of the Cf(III) present in a K_2CO_3 solution could be oxidized electrochemically.

A number of studies have supported the existence of Cf(II); in one study [182] the tendency for californium to form amalgams rapidly is compared to the behavior of divalent lanthanides [85, 182–186]. In early work, the inability to reduce Cf(III) in 0.1 M NH_4Cl suggested a limit of -1.4 V for the Cf(III)/Cf(II)

Table 11.8 *Reduction potentials for californium.*

Couple	*Potential* (V vs NHE)	*Method*	*Ref.*
Cf(IV)/Cf(III)	3.3; 3.2	calculated	127, 176
Cf(III)/Cf(II)	−2.0; −1.9	calculated; spectra	177
	−1.4	calculated	178
	−1.6	calculated; spectra	176
	−1.47	polarographic/voltammetric	179
	−1.6	polarography (acetonitrile)	180
Cf(III)/Cf(0)	−2.32	calculated	178
	−2.01	radiopolarography	87, 181
	−2.06	calculated	83
Cf(III)/Cf(Hg)	−1.61	calculated	179
Cf(III)/Cf(Hg)	−1.503	radiopolarography	181
Cf(II)/Cf(Hg)	−1.68	polarographic/voltammetric	179

couple [186]. David [178, 187, 188] proposed a value of -1.4 V from radiopolarographic and amalgamation behavior using tracers.

Studies on the co-precipitation behavior of californium [189–191] also have supported the existence of Cf(II) in solution. The difference in formal potentials of Sm(III)/Sm(II) and Cf(III)/Cf(II) couples has been estimated to be 0.045 V (californium more negative) by studies on co-precipitation of chloride salts in aqueous ethanol solution [192]. Another comparison between the reduction behavior of californium and samarium was made in anhydrous acetonitrile [180], where the Cf(III)/Cf(II) and Sm(III)/Sm(II) couples were found to be nearly identical; a value of -1.58 V was proposed for the Cf(III)/Cf(II) couple. Essentially the same value (-1.60 V) for this couple was reported from co-crystallization studies [192]. Nugent *et al.* [176, 177] have given a potential for the Cf(III)/Cf(II) couple as -1.6 V, based on their systematic analysis of electron-transfer bands. Radiopolarographic experiments on californium have resulted in two reports. The first report [178] suggested two couples: -2.32 V for Cf(III)/Cf(0), and -1.4 V for Cf(III)/Cf(II). Subsequent work [181] concluded that the first radiopolarographic results were incorrect, and that Cf(III) is reduced directly to Cf(Hg) in one step ($E_{1/2} = -1.503$ V; correcting for the amalgamation process yields Cf(III)/Cf(0) $= -2.01$ V). Subsequently, a polarographic and voltammetric study [179] on larger amounts of californium concluded that californium is reduced via a two-step process like samarium: (1) Cf(III) → Cf(II), and (2) Cf(II) → Cf(Hg). Potentials for these processes were given as -1.47 and -1.68 V, respectively. These data yield a calculated value of -1.61 V for Cf(III)/Cf(0). An evaluation of earlier amalgamation experiments has also led to a proposed value of -2.2 V for the Cf(II)/Cf(0) couple [85].

These reported differences for californium have not been resolved and additional work needs to be done to resolve the system. Since Cf(II) can be prepared and maintained in the solid state, there still remains a strong possibility that Cf(II) can be stabilized in aqueous and/or non-aqueous solvents.

Evidence for Cf(II) in molten-salt systems has been reported [193]. The distribution coefficient of californium between molten lithium chloride and lithium–bismuth metals at 640°C indicated that divalent californium was present in the salt phase. However, evidence for the existence of Cf(II) was not found in lithium fluoride–beryllium fluoride melts [193, 194].

It is generally accepted that the stability of the divalent state increases for the second half of the actinide series of elements. Starting with californium, the potentials of the M(III)/M(II) couples increase regularly in the order No > Md > Fm > Es > Cf, with values ranging from 1.45 V for nobelium to -1.60 V for californium [172].

In discussing the oxidation states of californium, the possibility of attaining Cf(V) must be addressed. In principle, this oxidation state would be stabilized by the attainment of a $5f^7$ electronic state. Some early coulometric data obtained with a few micrograms of californium suggested that Cf(V) may have been attained in a 1 M H_2SO_4 solution [195], but these results have not been confirmed

and are likely to be incorrect. More recently, a claim for the generation of Cf(v) in carbonate media was made as a result of co-precipitation experiments [196]. In this work, small amounts ($< 10\%$) of the californium, generated from the decay of Bk(IV) in solution, were found in $Na_4UO_2(CO_3)_3$ solids that were precipitated from the solutions. The presence of californium in the precipitates was interpreted as arising from the co-precipitation of a CfO_2^+ ion with the uranium precipitate. Thermodynamic [87] and quantum-chemical [197] calculations have been made which indicate that it may be possible to form Cf(v) in an aqueous medium. It may also be possible to obtain this oxidation state in the solid state.

11.8.3 Complexation chemistry/stability constants

A considerable portion of the published data dealing with californium concerns the complexation and solvent extraction chemistry of Cf(III). This is in part a consequence of the fact that a large amount of this information could be obtained using tracer quantities of the more abundant ^{252}Cf isotope. In addition, there was an impetus to perform this type of study during the investigation/development of californium's separation chemistry. A compilation of stability constants for californium complexes and chelates is given in Table 11.9.

Table 11.9 *Stability constants of Cf(III) complexes and chelates.*

Ligand	*Experimental method*	*Log of stability constants*[a] *at 25°C*	*Ref.*
fluoride ion	solv. extract.	$\beta_1 = 3.03$ $\mu = 1.0$	205
hydroxide ion	solv. extract.	$\beta_1 = 5.62$	203
		$\beta_1 = 5.05$ $\mu = 2.00$	204
sulfate ion	solv. extract.	$\beta_1 = 1.36$ $\beta_2 = 2.07$ $\mu = 2.0$	199
	solv. extract.	$K_{01} = -3.73$ $K_{02} = -5.58$ $K_{03} = -5.09$ $\mu = 0$	200
thiocyanate ion	solv. extract.	$\beta_1 = 3.06$	201
	solv. extract.	$\beta_1 = 3.71$ $\beta_2 = 0.28$ $\beta_3 = 2.65$	202
acetate ion	solv. extract.	$\beta_1 = 2.11$ $\mu = 1.0$	206
oxalate ion	–	$\beta_3 = 12.5$ $\mu = 0.1$	207
	electromigr.	$\beta_1 = 5.50$ $\beta_2 = 3.87$ $\mu = 0.1$	208

Table 11.9 (*Contd.*)

Ligand	*Experimental method*	*Log of stability constants*[a] *at 25°C*	*Ref.*
lactic acid	–	$\beta_3 = 6.08$ $\mu = 0.15$	207
	solv. extract.	$\beta_3 = 6.09$ $\mu = 0.5$	209
	ion exchange	$\beta_3 = 6.08$ $\mu = 0.5$	209
α-hydroxyisobutyric acid	ion exchange	$\beta_3 = 6.9$ $\mu = 0.5$	203
tartaric acid	–	$\beta_2 = 6.8$ $\mu = 0.1$	203
	solv. extract.	$\beta_2 = 5.86$	210
ethylenediaminetetraacetic acid	ion exchange	$\beta_1 = 19.09$	211
1,2-diaminocyclohexane-tetraacetic acid	ion exchange	$\beta_1 = 19.42$	212
diethylenetriaminepenta-acetic acid	–	$\beta_1 = 22.6$ $\mu = 0.1$	207
	ion exchange	$\beta_1 = 22.57$	213
	ion exchange	$\beta_1 = 25.19$	214
glycolate ion	solv. extract.	$\beta_1 = 2.63$ $\beta_2 = 1.97$ $\mu = 2.0$ (53°C)	215
2-methyllactic acid	solv. extract.	$\beta_1 = 4.10$ $\mu = 0.1$	210
malic acid	solv. extract.	$\beta_1 = 7.02$ $\mu = 0.1$	210
citric acid	solv. extract.	$\beta_1 = 11.61$ $\mu = 0.1$	210
	electromigr.	$\beta_1 = 7.93$ $\beta_2 = 3.3$ $\mu = 0.1$	208
	solv. extract.	$\beta(C_2^{2-}) = 10.90$ $\beta(C_2^{3-}) = 12.26$ $\mu = 0.1$	216
	solv. extract.	$\beta(M(HCit^-)_2) = 5.8$ $\beta(M(HCit)(Cit^{2-})) = 9.9$ $\mu = 0.1$	217
thenoyltrifluoroacetone	solv. extract.	$\beta_3 = 14.94$ $\mu = 0.1$	218
benzoyltrifluoroacetone	solv. extract.	$\beta = 16.06$ $\mu = 0.1$	218
naphthoyltrifluoroacetone	solv. extract.	$\beta = 18.83$ $\mu = 0.1$	218
nitrilodiaceto-monopropionic acid	ion exchange	$\beta_1 = 10.94$ $\beta_2 = 18.45$	219
nitrilotriacetic acid	ion exchange	$\beta_1 = 11.92$	219
	–	$\beta_1 = 11.3$ $\beta_2 = 21.0$ $\mu = 0.1$	207

Table 11.9 (*Contd.*)

Ligand	*Experimental method*	*Log of stability constants*[a] *at 25°C*	*Ref.*
N-2-hydroxyethylethylene-diaminetriacetic acid	ion exchange	$\beta_1 = 16.27$ $\beta_2 = 28.5$ $\mu = 0.1$	220
2-hydroxy-1,3-diaminopropane tetraacetic acid	ion exchange	$\beta_1 = 13.18$ $\mu = 0.1$	221
5,7-dichloro-8-hydroxyquinoline	solv. extract.	$\beta_3 = 22.59$	222
4-benzolyl-3-methyl-1-phenyl-2-pyrozolin-5-one	solv. extract.	$\beta_3 = 17.78$ $\mu = 0.1$	23
4-acetyl-3-methyl-1-phenyl-2-pyrozolin-5-one	solv. extract.	$\beta_3 = 13.48$ $\mu = 0.1$	23
2-hydroxyethyliminodiacetic acid	solv. extract.	$\beta_1 = 9.61$ $\mu = 0.1$	223
O-hydroxyphenyliminodi-acetic acid	solv. extract.	$\beta_1 = 7.38$ $\beta_2 = 12.28$ $\mu = 0.1$	224
2-ethylhexylphenylphosphoric acid	solv. extract.	$\beta_1 = 6.03$ $\beta_2 = 2.00$ $\mu = 0.1$	225
thenoyltrifluoroacetone	solv. extract.	$\beta_1 = 6.90$ $\mu = 0.1$	226

[a] Overall formation constants

$$\beta_1 = \frac{[CfA^{(3-n)+}]}{[Cf^{3+}][A^{n-}]} \qquad \beta_2 = \frac{[CfA_2^{(3-2n)+}]}{[Cf^{3+}][A^{n-}]^2} \qquad \text{etc.}$$

and stepwise constants

$$K_2 = \frac{[CfA^{(3-2n)+}]}{[CfA^{(3-n)+}][A^{n-}]} \qquad \text{etc.}$$

Some of the first data on californium complexes involved materials such as the halides, citrate, lactate, α-hydroxyisobutyrate, etc., as these materials played a role in early separation/purification schemes [7, 23] (also see Section 11.4). In general, it is expected that only small differences in stability would exist between Cf(III) and its trivalent neighbors Bk(III) and Es(III), with larger differences being found between Cf(III) and Am(III). A general discussion of actinide complexes (including californium) in aqueous solution is available [198].

The initial studies on Cf(III) and sulfate ions [199] concluded that 1:1 and 1:2 complexes ($Cf(SO_4)^+$ and $Cf(SO_4)_2^-$) were formed, but subsequent work in the sulfate system suggested that mono-, di-, and trisulfate species were formed [200]. A similar situation exists for thiocyanate complexes of Cf(III). Initially a 1:1 complex ($Cf(SCN)_2^+$) was reported [201], but later work indicated that three complexes could form ($CfSCN^{2+}$, $Cf(SCN)_2^+$, and $Cf(SCN)_3$), where the 1:3 complex was of the inner-sphere type [202].

The hydrolysis behavior of Cf(III) is expected to be similar to that of the trivalent lanthanides, and more specifically to that of Eu(III) or Gd(III), which have similar ionic radii. The first hydrolysis reaction ($Cf^{3+} + H_2O \rightarrow CfOH^{2+} + H^+$) has also been determined for Cf(III); log K_1 values have been reported as -5.62 [203] and -5.05 [204].

Several quite stable complexes can be formed with Cf(III) (see Table 11.9). Complexes of diketones and aminopolycarboxylic acids are considerably more stable than those of tartrate, lactate, oxalate, etc. In some cases, adduct chelates can be formed with Cf(III), as with californium thenoyltrifluoroacetone chelate and methyl isobutyl ketone ($Cf(TTA)_3 + MIBK \rightarrow Cf(TTA) \cdot MIBK$ or $Cf(TTA)_3 \cdot 2MIBK$) [23]. With the monodentate ligand tributyl phosphate, the extractable californium adduct from nitric acid solution has been assigned as the 1:3 species $Cf(NO_3)_3 \cdot 3TBP$ [227]. Quaternary ammonium bases and alkylpyrocatechols (i.e. 4-(α,α'-dioctylethyl)pyrocatechol) can form complexes in alkaline solutions [228]. One recent extraction study has examined the influence of the extractant's structure on the extraction behavior of californium [229]. A large number of materials have been investigated for forming extractable complexes of californium and the reader is referred to reviews on the subject [27, 32, 33].

The kinetics of exchange of californium(III) with europium ethylenediaminetetraacetate ($EuEDTA^-$) in aqueous solution ($\mu = 0.1$) has been reported [230]. The exchange was found to be a first-order reaction with both acid-dependent and acid-independent terms.

From a study of the relationship of distribution coefficients of californium with sodium nitrate in extractions with organic ammonium nitrates, the apparent mean molar activity coefficient of Cf(III) was calculated in terms of a polynomial ($\log \gamma_{\pm} = a + bm + cm^2 + dm^3$, where $a = 0.00397$, $b = -0.154$, $c = 0.0252$, and $d = -0.00119$) [231].

11.8.4 Thermodynamic data

Thermodynamic data for the formation of Cf(III) in solution, according to the following reaction:

$$Cf(s, \alpha) + 3H^+(aq) = Cf(III)(aq) + \tfrac{3}{2}H_2(g)$$

are given in Table 11.10 (also see Section 11.6.2 for heat of solution of californium metal). The best value for the heat of formation, $\Delta H_f(Cf^{3+}(aq))$, appears to be

Table 11.10 *Thermodynamic data for aqueous Cf(III) ion at* 298 K.

$\Delta H_f^\circ(Cf^{3+}(aq))$ (kJ mol^{-1})	$\Delta G_f^\circ(Cf^{3+}(aq))$ (kJ mol^{-1})	$S^\circ(Cf^{3+}(aq))$ (J K^{-1} mol^{-1})	*Ref.*
-617 ± 11	-596 ± 15	-184	77
-577 ± 5	-555 ± 7	-188 ± 17	84

-577 ± 5 kJ mol^{-1} [84]. The entropy, $S°$ (Cf^{3+}(aq)), has been estimated to be -188 ± 17 J K^{-1} mol^{-1} [84]. Several estimates for ΔH_f(Cf^{3+}(aq)) have appeared in the literature. Nugent *et al.* [81] proposed a value of -623 kJ mol^{-1}, David *et al.* [86] suggested -586 ± 21 kJ mol^{-1}, and Nugent [85] subsequently arrived at -602 ± 21 kJ mol^{-1}. A value of -603 kJ mol^{-1} was estimated in a recent comparison of thermochemical properties among the lanthanide and actinide elements [126]. This latter work also presents other thermochemical values for californium. Predictions of the standard free energy ($\Delta G_f°$) and the enthalpy ($\Delta H_f°$) of hydration for the trivalent californium ion have been made based on an electrostatic hydration model [232]. Assuming a crystallographic radius of 0.094 nm and a gas-phase radius of 0.1516 nm for Cf(III), and using a primary hydration number of 6.1, $\Delta G°_{298}$ and $\Delta H°_{298}$ were calculated to be -3385 and -3582 kJ mol^{-1}, respectively. Recently, $\Delta H_f°$ (Cf_2O_3, bcc, 298 K) was determined to be -1653 ± 10 kJ mol^{-1} by solution calorimetry [238]. Other thermodynamic data have also been reported for californium [87, Chapter 17].

Thermodynamic data for the 1:1 complex, $Cf(SO_4)^+$, have been calculated from the temperature dependence of the stability constant [233]. Values for this complex are: $\Delta G_{298} = -7.9$ kJ mol^{-1}, $\Delta H_{298} = 19$ kJ mol^{-1}, and $\Delta S_{298} = 88$ J K^{-1} mol^{-1}. Similarly, data for the 1:1 complex, CfF^{2+}, have been calculated [176]. Data for this californium complex are: $\Delta G_{298} = -17.3$ kJ mol^{-1}, $\Delta H_{298} = 27.2$ kJ mol^{-1}, and $\Delta S_{298} = 149$ J K^{-1} mol^{-1}.

11.8.5 Solution absorption spectra of californium

The first absorption spectrum of pure Cf(III) was obtained from the solid state (see Section 11.7.6) [155]. The first solution absorption spectrum was obtained shortly thereafter [164, 234], using 592 μg of mainly the ^{252}Cf isotope, which introduced problems of shielding and radiolytic gassing to the experiment. Nineteen absorption bands were recorded between 280 and 1600 nm from a 1 M $DClO_4$ solution (see Table 11.11). The absorption spectrum from this work [234]

Table 11.11 *Absorption data for Cf(III) in 1 M $DClO_4$* [234].

Wavelength (nm)	*Wavenumber* (cm^{-1})	*Absorption coefficient, μ* (l mol^{-1} cm^{-1})	*Wavelength* (nm)	*Wavenumber* (cm^{-1})	*Absorption coefficient, μ* (l mol^{-1} cm^{-1})
1560	6410	5.3	469.9	21 280	8.9
1211	8260	1.6	442.1	22 620	10.3
840.3	11 900	2.5	434.8	23 000	9.8
769.8	12 990	6.3	401.9	24 880	0.9
745.2	13 420	6.4	353.4	28 300	1.0
673.8	14 840	2.5	334.0	29 940	1.5
640.2	15 620	1.7	325.0	30 770	3.8
602.0	16 610	4.9	304.9	32 800	1.1
490.0	20 410	1.9	295.0	33 900	2.4
			284.0	35 210	1.9

was later confirmed using milligram amounts of the ^{249}Cf isotope [164]. Fig. 11.3 shows the Cf(III) absorption spectrum obtained from a 0.1 M $HClO_4$–$DClO_4$ solution. The absorption spectrum of Cf(III) in 2 M Na_2CO_3 [175] is shown in Fig. 11.4, and the intensities of the absorption are summarized in Table 11.12. The spectrum of Cf(III) in Na_2CO_3 solution is similar to that in 1 M $DClO_4$, but shifts in wavelength and enhancement of intensity can be observed for some of the peaks. See Chapter 16 for a comprehensive overview.

The absorption spectrum of Cf(IV) and Cf(III) in a potassium phosphotungstate medium has been reported [169, 172]. The phosphotungstate stabilizes

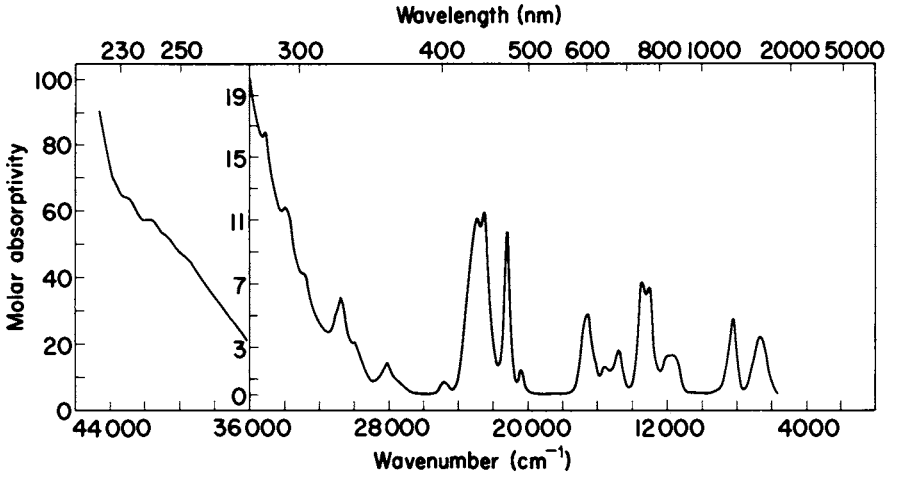

Fig. 11.3 *Solution absorption spectrum of Cf(III) in* 0.1 M $HClO_4$–$DClO_4$ [166].

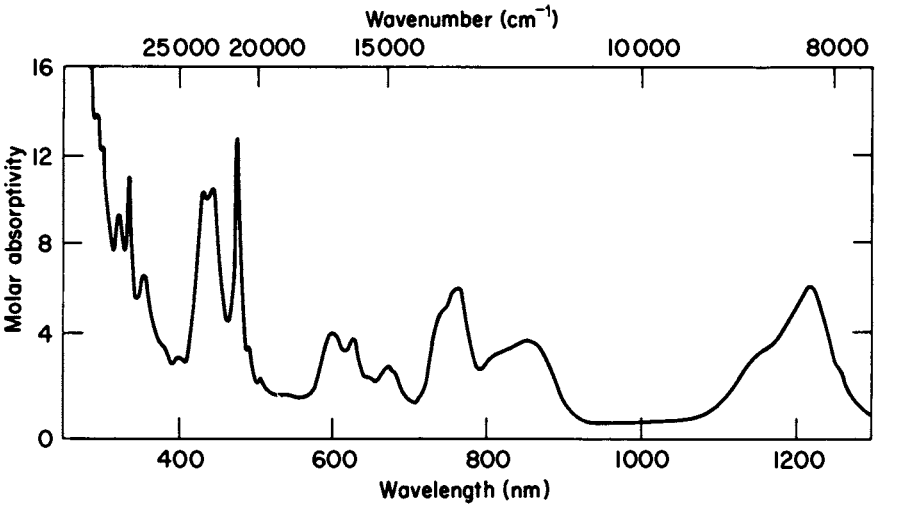

Fig. 11.4 *Solution absorption spectrum of Cf(III) in* 0.12 M Na_2CO_3 *at pH* 12 [175].

Table 11.12 *Absorption data for Cf(III) in 2 M Na_2CO_3 at pH 12 [175].*

Wavelength (nm)	*Wavenumber* (cm^{-1})	*Absorption coefficient, μ* ($l\,mol^{-1}\,cm^{-1}$)	*Wavelength* (nm)	*Wavenumber* (cm^{-1})	*Absorption coefficient, μ* ($l\,mol^{-1}\,cm^{-1}$)
293	34 100	14	491	20 400	3.3
303	33 000	12	506	19 800	2.0
322	31 000	9.3	600	16 700	4.0
336	29 800	11	625	16 000	3.8
355	28 200	6.5	674	14 800	2.4
402	24 900	2.9	740	13 500	4.9
430	23 200	10	757	13 200	6.0
443	22 600	11	850	11 800	3.7
474	21 100	13	1140	8770	2.8
			1214	8240	6.1

the Cf(IV) oxidation state sufficiently to permit spectra to be obtained (half-life approximately 70 min at room temperature). The oxidation was achieved using potassium persulfate at elevated temperatures; attempts to oxidize Cf(III) electrochemically in this medium were not successful. The absorption spectrum of ^{249}Cf(IV) is characterized by a broad absorption band beginning at 1030 nm and increasing in intensity to 390 nm. The maximum absorption appears at about 450 nm, which is similar to the absorption maximum for Cm(IV) and Tb(IV) in this medium [172]. The absorption of a comparable Cf(III) phosphotungstate solution did not show a significant absorbance over this spectral region.

11.9 CONCLUDING REMARKS

Much chemical and physical data have been acquired for californium. In many instances this information was obtained using only tracer or microgram quantities of the element. With the availability of multi-milligram amounts of the ^{249}Cf isotope, it was possible to expand the studies of californium; acquiring the heats of solution [83, 84] and sublimation of the metal [80] are two such examples. Because of the limited supply of ^{249}Cf, and other experimental limitations, such as its radioactive decay process and the accompanying heat, it may not be possible to perform all the experiments or to carry them out to the degree of perfection that scientists may desire. However, californium is the element with the highest atomic number that is expected to be available in weighable amounts (micrograms or more), with a reasonable half-life. The next element, einsteinium, is available in multi-microgram amounts, but its very high specific radioactivity severely limits the experiments that can be performed with it. Therefore, data on californium can provide insight into the chemical/physical properties of the higher members of the actinide series, in addition to the importance of its data in providing a better understanding of the periodic table.

The oxidation states of 0, II, III, and IV have been established for californium, with the III state being most prevalent and the only state presently known to have reasonable stability in aqueous solution. The existence of Cf(v) needs confirmation. Future investigations may place more emphasis on stabilizing oxidation states other than Cf(III), and may probe the possibility of attaining states which are presently unreported.

Although a considerable amount of information has been acquired for californium metal, there are still unanswered questions about it, particularly concerning the divalent form of the metal. There is also a considerable amount of work to be done on compounds, such as the mononitride, monosulfate, hydrides, etc. Investigations of the metal and/or compounds by high-pressure x-ray diffraction have provided valuable data on the bonding present in these materials, where very high pressures perturb the 5f electrons sufficiently to alter the bonding. Indeed, recent work on californium metal [79] shows that, at pressures greater than 40 GPa, the metal forms an α-uranium structure, which supports the notion that 5f electrons are involved in the metal's bonding (see Section 11.6.2).

In short, there is a considerable amount of scientific work that needs to be done on californium, the scope of which will be limited mainly by the imagination and skills of the investigators.

ACKNOWLEDGMENTS

The author gratefully acknowledges the assistance of several personnel at the Oak Ridge National Laboratory, as well as other institutions, for helpful discussions, references, and typing and commenting upon the manuscript.

The research reported herein was sponsored by the Division of Chemical Sciences, US Department of Energy, under contract W-7405-Eng-26 with Union Carbide Corporation.

REFERENCES

1. Thompson, S. G., Street, K. Jr, Ghiorso, A., and Seaborg, G. T. (1950) *Phys. Rev.*, **78**(3), 298–9; *Phys. Rev.*, **80**, 790–6.
2. Hyde, E. K., Perlman, I., and Seaborg, G. T. (1971) *The Nuclear Properties of the Heavy Elements*, vol. II, Dover, New York, pp. 926–43.
3. *Table of Isotopes*, Lederer, C. M. and Shirley, V. S. (eds) (1978) 7th edn, Wiley, New York, pp. 1472–515.
4. Bigelow, J. E., Corbett, B. L., King, L. J., McGuire, S. C., and Sims, T. M. (1981) in *Transplutonium Elements – Production and Recovery* (eds J. D. Navratil and W. W. Schulz), (ACS Symp. Ser. 161), American Chemical Society, Washington DC, pp. 3–18.

5. Californium 252 Progress Reports and Bibliography are available from: Californium Information Center, Savannah River Laboratory, Aiken, SC 29801, USA.
6. Thompson, S. G., Harvey, B. H., Choppin, G. R., and Seaborg, G. T. (1954) *J. Am. Chem. Soc.*, **76**, 6229–36.
7. Katz, J. J. and Seaborg, G. T. (1957) *The Chemistry of the Actinide Elements*, Methuen, New York, pp. 386–99.
8. Choppin, G. R., Harvey, B. G., and Thompson, S. G. (1956) *J. Inorg. Nucl. Chem.*, **2**, 66–8.
9. Surls, J. P. Jr (1956) Thesis, University of California Radiation Laboratory Report UCRL-3209.
10. Street, K. Jr and Seaborg, G. T. (1950) *J. Am. Chem. Soc.*, **72**, 2790–2.
11. Surls, J. P. Jr and Choppin, G. R. (1957) *J. Inorg. Nucl. Chem.*, **4**, 62–73.
12. Marcus, Y., Givon, H., and Choppin, G. R. (1963) *J. Inorg. Nucl. Chem.*, **25**, 1457–63.
13. Adar, S., Sjoblom, R. K., Barnes, R. F., Fields, P. R., Hulet, E. K., and Wilson, H. D. (1963) *J. Inorg. Nucl. Chem.*, **25**, 447–52.
14. Baybarz, R. D. (1966) *J. Inorg. Nucl. Chem.*, **28**, 1723–31.
15. Baybarz, R. D., Weaver, B. S., and Kinser, H. B. (1963) *Nucl. Sci. Eng.*, **17**, 457–62.
16. Moore, F. L. (1966) *Anal. Chem.*, **38**, 510–14.
17. Moore, F. L. (1964) *Anal. Chem.*, **36**, 2158–62.
18. Horwitz, E. P., Bloomquist, C. A. A., Sauro, L. J., and Henderson, D. J. (1966) *J. Inorg. Nucl. Chem.*, **28**, 2313–24.
19. Horwitz, E. P., Sauro, L. J., and Bloomquist, C. A. A. (1967) *J. Inorg. Nucl. Chem.*, **29**, 2033–40.
20. Gavrilov, K. A., Gvuzdz, E., Stary, J. and Seng, W. T. (1966) *Talanta*, **13**, 471–6.
21. Horwitz, E. P., Bloomquist, C. A. A., and Henderson, D. J. (1969) *J. Inorg. Nucl. Chem.*, **31**, 1149–66.
22. Horwitz, E. P., Bloomquist, C. A. A., Henderson, D. J., and Nelson, D. E. (1969) *J. Inorg. Nucl. Chem.*, **31**, 3255–71.
23. Keller, C. (1971) *The Chemistry of the Transuranium Elements*, Verlag Chemie, Weinheim, pp. 217–49 and 565–80.
24. Myasoedov, B. F., Guseva, L. I., Lebedev, I. A., Milyukova, M. S., and Chmutova, M. K. (1974) *Analytical Chemistry of Transplutonium Elements* (ed. D. Slutzkin), Wiley, New York, pp. 122–32.
25. Bigelow, J. E. (1974) in *Gmelin Handbuch der Anorganischen Chemie*, Suppl. Ser., *Transuranium*, Springer-Verlag, New York, vol. 7b, part A1, II, The Elements (1974), pp. 326–36.
26. Müller, W. (1967) *Actinides Rev.*, **1**, 71–119.
27. Ishimori, T. (1980) in *Actinide Separations* (eds J. D. Navratil and W. W. Schulz), (ACS Symp. Ser. 117), American Chemical Society, Washington DC, pp. 333–50.
28. King, L. J., Bigelow, J. E., and Collins, E. D. (1981) in *Transplutonium Elements – Production and Recovery* (eds. J. D. Navratil and W. W. Schulz) (ACS Symp. Ser. 161), American Chemical Society, Washington DC, pp. 133–46.
29. Collins, E. D., Benker, D. E., Chattin, F. R., Orr, P. B., and Ross, R. G. (1981) in *Transplutonium Elements – Production and Recovery* (eds J. D. Navratil and W. W. Schulz) (ACS Symp. Ser. 161), American Chemical Society, Washington DC, pp. 147–60.
30. Benker, D. E., Chattin, F. R., Collins, E. D., Knauer, J. B., Orr, P. B., Ross, R. G., and Wiggins, J. T. (1981) in *Transplutonium Elements – Production and Recovery* (eds J. D.

Navratil and W. W. Schulz), (ACS Symp. Ser. 161), American Chemical Society, Washington DC, pp. 161–72.
31. Campbell, D. O. (1981) in *Transplutonium Elements – Production and Recovery* (eds J. D. Navratil and W. W. Schulz), (ACS Symp. Ser. 161), American Chemical Society, Washington DC, pp. 189–202.
32. Shoun, R. R. and McDowell, W. J. (1980) in *Actinide Separations* (eds J. D. Navratil and W. W. Schulz), (ACS Symp. Ser. 117), American Chemical Society, Washington DC, pp. 71–87.
33. Myasoedov, B. F., Chmutova, M. K., and Karalova, Z. K. (1980) in *Actinide Separations* (eds J. D. Navratil and W. W. Schulz), (ACS Symp. Ser. 117), American Chemical Society, Washington DC, pp. 101–15.
34. Bigelow, J. E., Collins, E. D., and King, L. J. (1980) in *Actinide Separations* (eds J. D. Navratil and W. W. Schulz), (ACS Symp. Ser. 117), American Chemical Society, Washington DC, pp. 147–55.
35. Baybarz, R. D., Knauer, J. B., and Orr, P. B. (1973) USAEC Report ORNL-4672, Oak Ridge National Laboratory.
36. Knighton, J. B. and Steunenberg, R. K. (1966) US Patent 3276861.
37. Mailen, J. C. and Ferris, L. M. (1971) *Inorg. Nucl. Chem. Lett.*, **7**, 431–8.
38. Aleksandrov, B. M., Malysheva, L. P., Savoskina, G. P., Smirnova, E. A., and Krivokhat-skii, A. S. (1972) *Radiokhimiya*, **19**, 472–7.
39. Martin, W. C., Hagan, L., Reader, J., and Sugar, J. (1974) *J. Phys. Chem. Ref. Data*, **3**(3), 771–5.
40. Worden, E. F. and Conway, J. G. (1970) *J. Opt. Soc. Am.*, **60**, 1144–5.
41. Sugar, J. (1973) *J. Chem. Phys.*, **59**, 788; (1974) *J. Chem. Phys.*, **60**, 4103.
42. Conway, J. G., Bruger, J. B., Hulet, E. K., Morrow, R. J., and Gutmacher, R. G. (1962) *J. Chem. Phys.*, **36**, 189–90.
43. Fields, P. R., Wybourne, B. G., and Carnall, W. T. (1964) Argonne National Laboratory Report ANL-6911.
44. Carnall, W. T., Fried, S., and Wagner, F. Jr (1973) *J. Chem. Phys.*, **58**, 1938–49.
45. Varga, L. P., Baybarz, R. D., Reisfeld, M. J., and Asprey, L. B. (1973) *J. Inorg. Nucl. Chem.*, **35**, 2775–86.
46. Varga, L. P., Baybarz, R. D., Reisfeld, M. J., and Volz, W. B. (1973) *J. Inorg. Nucl. Chem.*, **35**, 2787–94.
47. Brewer, L. (1971) *J. Opt. Soc. Am.*, **61**, 1666–82.
48. Mikheev, N. B., Spitsyn, V. I., Dyachkova, R. A., and Auerman, L. N. (1979) *J. Physique*, Suppl. **C-4**, 230–2.
49. Carter, F. L. (1979) *J. Physique*, Suppl. **C-4**, 228–9.
50. Ionova, G. V., Spitsyn, V. I., and Mikheev, N. B. (1977) in *Proc. 2nd Int. Conf. on Electronic Structure of the Actinides* (eds J. Mulak, W. Suski, and R. Troc), Wrocław, Poland, pp. 39–47.
51. Spitsyn, V. I. (1977) in *Proc. 2nd Int. Conf. on Electronic Structure of the Actinides* (eds J. Mulak, W. Suski, and R. Troc), Wrocław, Poland, pp. 25–38.
52. Carnall, W. T., Crosswhite, H. M., Crosswhite, H., Hessler, J. P., Aderhold, C., Caird, J. A., Paszek, A., and Wagner, F. W. (1977) in *Proc. 2nd Int. Conf. on Electronic Structure of the Actinides* (eds J. Mulak, W. Suski, and R. Troc), Wrocław, Poland, pp. 105–10.
53. Haung, K., Aoyagi, M., Chen, M. H., Crasemann, B., and Mark, H. (1976) *At. Data Nucl. Data Tables*, **18**, 243–91.

54. Chen, M. H., Crasemann, B., Huang, K.-N., Aoyagi, M., and Mark, H. (1977) *At. Data Nucl. Data Tables*, **19** (2), 97–151.
55. Johansson, B. and Rosengren, A. (1975) *Phy. Rev. B*, **11**, 1367–73.
56. Conway, J. G., Hulet, E. K., and Morrow, R. J. (1962) *J. Opt. Soc. Am.*, **52**, 222.
57. Conway, J. (1976) *Proc. Symp. Commemorating the 25th Anniversary of the Elements 97 and 98*, Lawrence Berkeley Report LBL 4366, pp. 70–5.
58. Blaise, J., Verges, J., Wyart, J. F., Conway, J. C., and Worden, E. F., unpublished data.
59. Warden, J., Gutmacher, R. G., and Lougheed, R. W. (1970) *J. Opt. Soc. Am.*, **60**, 1555.
60. Carlson, T. A. and Nestor, C. W. Jr (1977) *At. Data Nucl. Data Tables*, **19** (2), 153–73.
61. Mauson, S. T. and Kennedy, D. J. (1974) *At. Data Nucl. Data Tables*, **14** (2), 111–20.
62. Scofield, J. H. (1974) *At. Data Nucl. Data Tables*, **14** (2), 121–37.
63. Hubbell, J. H., Veigele, W. J., Briggs, E. A., Brown, R. T., Cromer, D. T., and Howerton, R. J. (1975) *J. Phys. Chem. Ref. Data*, **4** (3), 471–538.
64. Biggs, F., Mendelsohn, L. B., and Mann, J. B. (1975) *At. Data Nucl. Data Tables*, **16**, 201–309.
65. Veal, B. W., Lam, D. J., Diamond, H., and Hoekstra, H. R. (1977) *Phys. Rev. B*, **15** (6), 2929–42.
66. Johansson, B. and Rosengren, A. (1975) *Phys. Rev. B*, **11** (4), 2740–3.
67. Fujita, D. K. and Cunningham, B. B. (1969) USAEC Report UCRL-19507.
68. Cunningham, B. B. and Parsons, T. C. (1970) USAEC Report UCRL-205426, pp. 239–40.
69. Asprey, L. B. (1971) Reported at the *Third Int. Transplutonium Element Symp.*, Argonne, Illinois, October 20–22; also cited in ref. 64.
70. Haire, R. G. and Baybarz, R. D. (1973) *J. Inorg. Nucl. Chem.*, **36**, 1295–302.
71. Haire, R. G. and Asprey, L. B. (1976) *Inorg. Nucl. Chem. Lett.*, **12**, 73–84.
72. Noe, M. and Peterson, J. R. (1976) in *Transplutonium 1975* (eds W. Muller and R. Lindner), North-Holland, Amsterdam, pp. 69–77.
73. Haire, R. G. (1978) USDOE Report ORNL-5485, p. 52; (1980) USDOE Report ORNL-5665, p. 71; (1981) USDOE Report-5817.
74. Haire, R. G. (1982) in *Actinides in Perspective* (ed. N. Edelstein), Pergamon Press, New York, pp. 309–42.
75. Zachariasen, W. H. (1973) *J. Inorg. Nucl. Chem.*, **35**, 3487–97.
76. Allen, J. W., Johanson, L. I., Bauer, R. S., and Lindau, I. (1978) *Phys. Rev. Lett.*, **41**, 1499–502.
77. Burns, J. H. and Peterson, J. R. (1978) in *Rare Earths and Actinides 1977* (eds W. D. Corner and B. K. Tanner), (Inst. Phys. Conf. Ser. 37), Institute of Physics, Bristol and London, pp. 52–5.
78. Peterson, J. R., Benedict, U., Dufour, C., Birkel, I., and Haire, R. G. (1983) *J. Less Common Metals*, **93**, 353–6.
79. Benedict, U., Peterson, J. R., Haire, R. G., and Dufour, C. (1984) *J. Phys. F: Metal Phys.*, **14**, L 43–7.
80. Ward, J. W., Kleinschmidt, P. D., and Haire, R. G. (1979) *J. Physique*, Suppl. **C-4**, 233–5.
81. Nugent, L. J., Burnett, J. L., and Morss, L. R. (1973) *J. Chem. Thermodyn.*, **5**, 665–78.

82. David, F., Samhoun, K., and Guillaumont, R. (1976) in *Transplutonium 1975* (eds W. Müller and R. Lindner), North-Holland, Amsterdam, pp. 297–304.
83. Raschella, D. L., Haire, R. G., and Peterson, J. R. (1982) *Radiochim. Acta*, **30**, 41–3.
84. Fuger, J., Haire, R. G., and Peterson, J. R. (1984) *J. Less Common Metals*, **98**, 315–21.
85. Nugent, L. J. (1975) *J. Inorg. Nucl. Chem.*, **37**, 1767–75.
86. David, F., Samhoun, K., Guillaumont, R., and Nugent, L. J. (1976) *Heavy Element Properties* (eds W. Müller and H. Blank), North-Holland, Amsterdam, pp. 97–104.
87. David, F., Samhoun, K., Guillaumont, R., and Edelstein, N. (1978) *J. Inorg. Nucl. Chem.*, **40**, 69–74.
88. Samhoun, K. and David, F. (1979) *J. Inorg. Nucl. Chem.*, **41**, 357–63.
89. Fujita, D. K., Parsons, T. C., Edelstein, N., Noe, M., and Peterson, J. R. (1976) *Transplutonium Elements 1975* (eds W. Müller and R. Lindner), North-Holland, Amsterdam, pp. 173–9.
90. Nave, S. E., Haire, R. G., and Huray, P. G. (1983) USDOE Report ORNL-5954, pp. 63–5; (1984) *Proc. Conf. on Electronic Structure and Properties of Rare Earth and Actinide Intermetallics*, St Polten, Austria, Sept. 3–6; (1985) *Physica B*, **130B**, 225–7.
91. Brewer, L. (1971) *J. Opt. Soc. Am.*, **61**, 1101–11.
92. Johnansson, B. (1975) *Phys. Rev. B*, **11**, 2740–4; Johansson, B. and Rosengren, A. (1975) *Phys. Rev. B*, **11**, 1367–73.
93. Ward, J. W. and Hill, H. H. (1976) in *Heavy Element Properties* (eds W. Müller and H. Blank), North-Holland, Amsterdam, pp. 65–79.
94. Ward, J. W., Kleinschmidt, P. D., Haire, R. G., and Brown, D. (1980) in *Lanthanide and Actinide Chemistry and Spectroscopy* (ed. N. M. Edelstein), (ACS Symp. Ser. 131), American Chemical Society, Washington DC, pp. 199–220.
95. Ward, J. W. (1983) *J. Less Common Metals*, **93**, 279–92.
96. Smith, J. L. (1979) USDOE Report LA-UR-79-1666, pp. 1–13.
97. Smith, J. L. (1980) USDOE Report LA-UR-80-762, pp. 1–5.
98. Peterson, J. R. and Baybarz, R. D. (1972) *Inorg. Nucl. Chem. Lett.*, **8**, 423–31.
99. Burns, J. H., Peterson, J. R., and Baybarz, R. D. (1973) *J. Inorg. Nucl. Chem.*, **35**, 1171–7.
100. Baybarz, R. D., Haire, R. G., and Fahey, J. A. (1972) *J. Inorg. Nucl. Chem.*, **34**, 557–65.
101. Shannon, R. D. (1976) *Acta. Crystallogr. A*, **32**, 751–64.
102. Haire, R. G. and Baybarz, R. D. (1973) *J. Inorg. Nucl. Chem.*, **35**, 489–96.
103. International Centre for Diffraction Data, JCPDS Data Card 12-797.
104. International Centre for Diffraction Data, JCPDS Data Card 12-393.
105. Gruen, D. M., Koehler, W. C., and Katz, J. J. (1951) *J. Am. Chem. Soc.*, **73**, 1475–9.
106. Copeland, J. C. and Cunningham, B. B. (1969) *J. Inorg. Nucl. Chem.*, **31**, 733–40.
107. Green, J. L. and Cunningham, B. B. (1967) *Inorg. Nucl. Chem. Lett.*, **3**, 343–9.
108. Baybarz, R. D. (1973) *J. Inorg. Nucl. Chem.*, **35**, 4149–58.
109. Baybarz, R. D. and Haire, R. G. (1976) *J. Inorg. Nucl. Chem.*, Suppl. 7–12.
110. Turcotte, R. P. and Haire, R. G. (1976) in *Transplutonium Elements 1975* (eds W. Müller and R. Lindner), North-Holland, Amsterdam, pp. 267–77.
111. Haire, R. G. (1976) in *Proc. 12th Rare Earth Research Conf.*, vol. II (ed. C. E. Lundin), Vail, Colo., July 1976, Denver Research Institute, pp. 584–93.
112. Stevenson, J. N. and Peterson, J. R. (1973) *J. Inorg. Nucl. Chem.*, **35**, 3481–6.

113. Haire, R. G. and Asprey, L. B. (1973) *Inorg. Nucl. Chem. Lett.*, **9**, 869–74.
114. Haug, H. W. and Baybarz, R. D. (1975) *Inorg. Nucl. Chem. Lett.*, **11**, 847–55.
115. Fried, S., Cohen, D., Siegal, S., and Taire, B. (1968) *Inorg. Nucl. Chem. Lett.*, **4**, 494–8.
116. Burns, J. H., Peterson, J. R., and Stevenson, S. N. (1975) *J. Inorg. Nucl. Chem.*, **37**, 743–9.
117. Wild, J. F., Hulet, E. K., Lougheed, R. W., Hayes, W. N., Peterson, J. R., Fellows, R. L., and Young, J. P. (1978) *J. Inorg. Nucl. Chem.*, **40**, 811–17.
118. Peterson, J. R. and Burns, J. H. (1968) *J. Inorg. Nucl. Chem.*, **30**, 2955–8.
119. Haire, R. G. (1974) USAEC Report 4966, p. 19.
120. Damien, D., Haire, R. G., and Peterson, J. R. (1980) *Inorg. Nucl. Chem. Lett.*, **16**, 537–41.
121. Baybarz, R. D., Fahey, J. A., and Haire, R. G. (1974) *J. Inorg. Nucl. Chem.*, **36**, 2023–7.
122. Laubereau, P. G. and Burns, J. H. (1970) *Inorg. Chem.*, **9**, 1091–5.
123. Leger, J. M., Yacoubi, N., and Loriers, J. (1980) in *The Rare Earths in Modern Science and Technology*, vol. II, (eds G. J. McCarthy, J. J. Rhyne, and H. B. Silber), Plenum Press, New York, pp. 203–8.
124. Fuger, J. (1975) in *MTP International Review of Science*, Inorganic Chemistry, ser. II, vol. 7 (eds H. J. Emeleus and K. W. Bagnall), Butterworths, London, pp. 151–94.
125. Turcotte, R. P. (1980) *J. Inorg. Nucl. Chem.*, **42**, 1735–7.
126. Morss, L. R. (1983) *J. Less Common Metals*, **93**, 301–21.
127. Nugent, L. J., Baybarz, R. D., Burnett, J. L., and Ryan, J. L. (1971) *J. Inorg. Nucl. Chem.*, **33**, 2503–30.
128. Asprey, L. B. (1970) unpublished results, cited in ref. 100.
129. Asprey, L. B. and Haire, R. G. (1973) *Inorg. Nucl. Chem. Lett.*, **9**, 1121–8.
130. Haire, R. G., Young, J. P., Peterson, J. R., Ensor, D. D., and Asprey, L. B. (1980) unpublished data, presented at SE/SW Regional ACS Meeting, December 1980, New Orleans.
131. Jouniaux, B. (1979) Thesis, University of Paris, pp. 34–86.
132. Bouissieres, G., Jouniaux, B., Legoux, Y., Merinis, J., David, F., and Samhoun, K. (1980) *Radiochem. Radioanal. Lett.*, **45** (2), 121–8.
133. Cunningham, B. B. and Ehrlich, P. (1970) USAEC Report UCRL-20426, p. 239.
134. Peterson, J. R. and Cunningham, B. B. (1968) *J. Inorg. Nucl. Chem.*, **30**, 1775–84.
135. Young, J. P., Haire, R. G., Fellows, R. L., Noe, M., and Peterson, J. R. (1976) in *Transplutonium 1975* (eds W. Müller and R. Lindner), North-Holland, Amsterdam, pp. 227–34.
136. Young, J. P., Haire, R. G., Peterson, J. R., Ensor, D. D., and Fellows, R. L. (1980) *Inorg. Chem.*, **19**, 2209–12.
137. Fried, S. M., Wagner, F. Jr, and Carnall, W. T. (1973) Argonne National Laboratory Report ANL-7996, p. 5.
138. Young, J. P., Vander Sluis, K. L., Werner, G. K., Peterson, J. R., and Noe, M. (1975) *J. Inorg. Nucl. Chem.*, **37**, 2497–501.
139. Hulet, E. K., Wild, J. F., Lougheed, R. W., and Hayes, W. N. (1975) *Radiokhimiya*, **17**, 632.
140. Fujita, D. D. (1969) UCRL Report 19507, p. 136.
141. Peterson, J. R., Fellows, R. L., Young, J. P., and Haire, R. G. (1977) *Radiochem. Radional. Lett.*, **31**, (4–5), 277–82.

142. Haschke, J. M. (1976) *Inorg. Chem.*, **15**, 298–303.
143. Barringhausen, H. (1976) in *Proc. 12th Rare Earth Research Conf.* (ed. C. E. Lundin), Vail, Colo., July 1976, pp. 404–13.
144. Luke, H. and Eick, H. A. (1976) *Proc. 12th Rare Earth Research Conf.* (ed. C. E. Lundin), Vail, Colo., July 1976, Denver Research Institute, pp. 424–32.
145. Haire, R. G., Young, J. P., Peterson, J. R., and Fellows, R. L. (1978) in *The Rare Earths in Modern Science and Technology* (eds G. J. McCarthy and J. J. Rhyne), Plenum, New York, pp. 501–6.
146. Young, J. P., Haire, R. G., Fellows, R. L., and Peterson, J. R. (1978) *J. Radioanal. Chem.*, **43**, 479–88.
147. Damien, D. A., Haire, R. G., and Peterson, J. R. (1979) *J. Physique*, Suppl. **C-4**, 95–100.
148. Damien, D., Haire, R. G., and Peterson, J. R., unpublished data.
149. Topp, N. E. (1965) *Chemistry of the Rare Earth Elements*, Elsevier, New York, pp. 71–3.
150. Laubereau, P. G. and Burns, J. H. (1970) in *Proc. 8th Rare Earth Research Conf.*, vol. I (eds T. Henrie and R. Lindstrom), Reno, Nev., pp. 258–65.
151. Sakangue, M. and Amano, R. (1976) in *Transplutonium 1975* (eds W. Muller and R. Lindner), North-Holland, Amsterdam, pp. 123–9.
152. Cunningham, B. B. (1959) *J. Chem. Educ.*, **36**, 32–7.
153. Fujita, D. K. (1969) Thesis, UCRL-19507.
154. Edelstein, N. and Karraker, D. (1976) *Proc. Symp. Commemorating the 25th Anniversary of Elements 97 and 98*, Lawrence Berkeley Laboratory Report LBL-4366, pp. 75–84; (1975) *J. Chem. Phys.*, **62**, 3–8.
155. Green, J. L. (1965) PhD Thesis, UCRL Report 16516, pp. 41–9.
156. Green, J. L. and Cunningham, B. B. (1966) *Inorg. Nucl. Chem. Lett.*, **2**, 365–71.
157. Carnall, W. T., Fried, S. M., Wagner, F. Jr, Barnes, R. F., Sjoblom, R. K., and Fields, P. R. (1972) *Inorg. Nucl. Chem. Lett.*, **8**, 773-4.
158. Carnall, W. T., Fried, S., and Wagner, F. Jr (1973) *J. Chem. Phys.*, **58**, 1938–49.
159. Caird, J. A., Hessler, J. P., Paszek, A. P., Carnall, W. T., Crosswhite, H. M., Crosswhite, H., Diamond, H., and Williams, C. W. (1976) *Bull. Am. Phys. Soc.*, **21**, 1284.
160. Hessler, J. P., Caird, J. A., Carnall, W. T., Crosswhite, H. M., Sjoblom, R. K., and Wagner, F. Jr (1978) in *The Rare Earths in Modern Science and Technology* (eds G. J. McCarthy and J. J. Rhyne), Plenum, New York, pp. 507–12.
161. Conway, J. G., Worden, E. F., Blaise, J. and Verges, J. (1977) *Spectrochim. Acta B*, **32**, 97–9.
162. Carnall, W. T., Crosswhite, H. M., Crosswhite, H., Hessler, J. P., Aderhold, C., Carid, J. A., Paszek, A., and Wagner, F. W. (1976) in *Proc. 2nd Int. Conf. on Electronic Structure of the Actinides* (eds J. Mulak, W. Suski, and R. Troc), Ossolineum Press, Warsaw, pp. 105–10.
163. Crosswhite, H. M. (1977) *Coll. Int. CNRS*, Spectroscopie des Elements de Transition et des Elements Lourds dan les Solides, Editions du CNRS, Paris, pp. 65–9.
164. Carnall, W. T. and Fried, S. (1976) *Proc. Symp. Commemorating the 25th Anniversary of the Elements 97 and 98*. Lawrence Berkeley Laboratory LBL-Report 4366, pp. 61–9.
165. Weber, M. J. (1980) in *Lanthanide and Actinide Chemistry and Spectroscopy* (ed.

N. M. Edelstein), (ACS Symp. Ser. 131), American Chemical Society, Washington DC, pp. 275–311.
166. Hessler, J. P. and Carnall, W. T. (1980) in *Lanthanide and Actinide Chemistry and Spectroscopy* (ed. N. M. Edelstein), (ACS Symp. Ser. 131), American Chemical Society, Washington DC, pp. 349–68.
167. Young, J. P., Haire, R. G., Peterson, J. R., Ensor, D. D., and Fellows, R. L. (1981) *Inorg. Chem.*, **20**, 3979–83.
168. Young, J. P., Haire, R. G., Peterson, J. R., and Ensor, D. D. (1984) in *Geochemical Behavior of Disposed Radioactive Waste* (eds G. S. Barney, J. D. Navratil, and W. W. Schulz), (ACS Symp. Ser. 246), American Chemical Society, Washington DC, pp. 335–46.
169. Kosyakov, V. N., Timofeev, G. A., Erin, E. A., Kopytov, V. V., and Andreev, V. J. (1977) *Radiokhimiya*, **19** (1), 82–4; (1977) *Sov. Radiochem.* **19**, 66–7.
170. Barnanov, A. A., Simakin, G. A., Kosyakov, V. N., Rin, E. A., Kopytov, V. V., Timofeev, G. A., and Rykov, A. G. (1981) *Radiokhimiya*, **23** (1), 127–9; *Sov. Radiochem.*, **23**, 104–6.
171. Nugent, L. J., Baybarz, R. D., Burnett, J. L., and Ryan, J. L. (1973) *J. Phys. Chem.*, **77** (12), 1528–39.
172. Myasoedov, B. F. (1982) in *Actinides in Perspective* (ed. N. M. Edelstein), Pergamon Press, New York, pp. 509–40.
173. Hobart, D. E., Samhoun, K., Young, J. P., Norvell, V. E., Mamantov, G., and Peterson, J. R. (1981) *Inorg. Nucl. Chem. Lett.*, **16**, 321–8.
174. Hobart, D. E., Samhoun, K., and Peterson, J. R. (1982) *Radiochim. Acta*, **31**, 139–45.
175. Hobart, D. E., Varlashkin, P. G., Samhoun, K., Haire, R. G., and Peterson, J. R. (1983) *Rev. Chim. Minér.*, **20**, 817–27.
176. Nugent, L. J., Baybarz, R. D., Burnett, J. L., and Ryan, J. L. (1973) *J. Phys. Chem.*, **77**, (12), 1528–39.
177. Nugent, L. J., Baybarz, R. D., and Burnett, J. L. (1969) *J. Phys. Chem.*, **73**, 1177–8.
178. David, F. (1970) *Radiochem. Radioanal. Lett.*, **5**, 279–85.
179. Musikas, C., Haire, R. G., and Peterson, J. R. (1981) *J. Inorg. Nucl. Chem.*, **43**, 2935–41.
180. Friedman, H. A., Stokely, J. R., and Baybarz, R. D. (1972) *Inorg. Nucl. Chem. Lett.*, **8**, 433–41.
181. Samhoun, K. and David, F. (1976) in *Transplutonium 1975* (eds W. Muller and R. Lindner), North-Holland, Amsterdam, pp. 297–304.
182. Malý, J. (1967) *Inorg. Nucl. Chem. Lett.*, **3**, 373–81.
183. Malý, J. and Cunningham, B. B. (1967) *Inorg. Nucl. Chem. Lett.*, **3**, 445–51.
184. David, F. and Bouissieres, G. (1968) *Inorg. Nucl. Chem. Lett.*, **4**, 153–9.
185. Malý, J. (1969) *J. Inorg. Nucl. Chem.*, **31**, 1007–18.
186. Cunningham, B. B., Morss, L. R., and Parsons, T. C. (1970) USAEC Report UCRL-19530, p. 276.
187. David, F. (1970) *Rev. Chem. Minér.*, **7**, 1–10.
188. David, F. (1970) *C.R. Acad. Sci. Paris C*, **270**, 2112–15; **271**, 440–2.
189. Cohen, L. H., Aten, A. H. Jr, and Kooi, J. (1968) *Inorg. Nucl. Chem. Lett.*, **4**, 249–52.
190. Fried, S. and Cohen, A. (1968) *Inorg. Nucl. Chem. Lett.*, **4**, 611–15.
191. Mikheev, N. B., Spitsyn, V. I., Kamenskaya, A. N., Rozenkevich, N. A., Rumer,

I. A., and Auerman, L. N. (1971) *Radiokhimiya.*, **14**, 486–7; (1972) *Sov. Radiochem.*, **14**, 494–5.
192. Mikheev, N. B., Kamenskaia, A. N., Rumer, I. A., Spitsyn, V. I., Diatokova, R. A., and Rosenkevitch, N. A. (1972) *Radiochem. Radioanal. Lett.*, **9**, 247–54.
193. Ferris, L. M. and Mailen, J. C. (1971) *J. Inorg. Nucl. Chem.*, **33**, 1325–35.
194. Ferris, L. M. and Mailen, J. C. (1970) *J. Inorg. Nucl. Chem.*, **32**, 2019–35.
195. Propst, R. L. and Hyder, M. L. (1969) *Nature*, **221**, 1141–2.
196. Kosyakov, V. N., Erin, E. A., Vityutnev, V. M., Kopytov, V. V., and Rykov, A. G. (1982) *Radiokhimiya*, **24**, 551–3.
197. Ionova, G. V., Spitsyn, V. I., and Pershina, V. G. (1980) in *Proc. 10ème Journées des Actinides* (eds B. Johansson and A. Rosengren), Stockholm, Sweden, May 27–28, 1980, pp. 126–59.
198. Jones, A. D. and Choppin, G. R. (1969) *Actinides Rev.*, **1**, 311–36.
199. De Carvalho, R. H. and Choppin, G. R. (1967) *J. Inorg. Nucl. Chem.*, **29**, 725–36.
200. McDowell, W. J. and Coleman, C. F. (1972) *J. Inorg. Nucl. Chem.*, **34**, 2837–50.
201. Choppin, G. R. and Ketels, J. (1965) *J. Inorg. Nucl. Chem.*, **27**, 1335–9.
202. Coleman, C. F. (1972) *J. Inorg. Nucl. Chem.*, **34**, 1381–97.
203. Désiré, B., Hussonnois, M., and Guillaumont, R. (1969) *C.R. Acad. Sci. Paris C*, **269**, 448–51.
204. Hussonnois, M., Hubert, S., Brillard, L., and Guillaumont, R. (1973) *Radiochem. Radioanal. Lett.*, **15**, 47–56.
205. Choppin, G. R. and Unrein, P. J. (1976) in *Transplutonium 1975* (eds W. Muller and R. Lindner), North-Holland, Amsterdam, pp. 97–107.
206. Choppin, G. R. and Schneider, J. K. (1970) *J. Inorg. Nucl. Chem.*, **32**, 3283–8.
207. Stary, J. (1966) *Talanta*, **13**, 421–37.
208. Stepanov, A. V. (1971) *Russ. J. Inorg. Chem.*, **16**, 1583–6.
209. Ermakov, V. A. and Stary, J. (1967) *Sov. Radiochem.*, **9**, 195–8.
210. Aly, H. F. and Latimer, R. M. (1970) *Radiochim. Acta*, **14**, 27–31.
211. Fuger, J. (1958) *J. Inorg. Nucl. Chem.*, **5**, 332–8.
212. Baybarz, R. D. (1966) *J. Inorg. Nucl. Chem.*, **28**, 1055–61.
213. Baybarz, R. D. (1965) *J. Inorg. Nucl. Chem.*, **27**, 1831–9.
214. Brandau, E. (1971) *Inorg. Nucl. Chem. Lett.*, **7**, 1177–81.
215. Choppin, G. R. and Segischer, G. (1972) *J. Inorg. Nucl. Chem.*, **34**, 3473–7.
216. Hubert, S., Hussonnois, M., Brillard, L., Goby, G., and Guillaumont, R. (1974) *J. Inorg. Nucl. Chem.*, **36**, 2361–6.
217. Guillaumont, R. and Bourderie, L. (1971) *Bull. Soc. Chim. Fr.*, **8**, 2806–9.
218. Keller, C. and Schreck, H. (1969) *J. Inorg. Nucl. Chem.*, **31**, 1121–32.
219. Eberle, S. H. and Ali, S. A. (1968) *Z. Anorg. Allg. Chem.*, **361**, 1–14.
220. Eberle, S. H. and Bayat, I. (1967) *Radiochim. Acta*, **7**, 214–17.
221. Baybarz, R. D. (1967) USAEC Report ORNL-4145, p. 225.
222. Feinauser, D. and Keller, C. (1969) *Inorg. Nucl. Chem. Lett.*, **5**, 625–30.
223. Ermakov, V. A., Vorob'eva, V. V., Zaitsev, A. A., and Yakovlev, G. N. (1971) *Sov. Radiochem.*, **13**, 866–8.
224. Ermakov, V. A., Vorob'eva, V. V., Zaitsev, A. A., and Yakovlev, G. N. (1971) *Sov. Radiochem.*, **13**, 710–13.
225. Barketov, E. S., Zaitsev, A. A., and Felermonov, V. T. (1975) *Sov. Radiochem.*, **17**, 383–7.
226. Khopkar, P. K. and Mathur, J. N. (1977) *J. Inorg. Nucl. Chem.*, **39**, 2063–7.

227. Healy, T. V. and McKay, H. A. C. (1956) *Rec. Trav. Chem. Pay-Bas*, **75**, 730–6.
228. Derevyanko, E. P., Pirozkhov, S. V., and Chudinov, E. G. (1975) *Radiokhimiya*, **17** (2), 291–6.
229. Derevyanko, E. P., Pirozkhov, S. V., and Chudinov, E. G. (1976) *Sov. Radiochem.*, **17**, 295–9.
230. Williams, K. R. and Choppin, G. R. (1974) *J. Inorg. Nucl. Chem.*, **36**, 1849–53.
231. Chudinov, E. G. and Pirozhkov, S. V. (1973) *Sov. Radiochem.*, **15**, 195–9.
232. Goldman, S. and Morss, L. R. (1975) *Can. J. Chem.*, **53**, 2685–700.
233. De Carvalho, R. G. and Choppin, G. R. (1967) *J. Inorg. Nucl. Chem.*, **29**, 737–43.
234. Conway, J. G., Fried, S., Latimer, R. M., McLaughlin, R., Gutmacher, R. G., Carnall, W. T., and Fields, P. (1966) AEC Report UCRL-16971, pp. 1–8; (1966) *J. Inorg. Nucl. Chem.*, **28**, 3064–6.
235. Gibson, J. K. and Haire, R. G. (1985) *Radiochimica Acta*, **38**, 193–96.
236. Peterson, J. R., Young, J. P., Haire, R. G., Begun, G., and Benedict, U. (1985) *Inorg. Chem.*, **24**, 2466–68.
237. Moore, J. R., Nave, S. E., Haire, R. G., and Huray, P. G. (1986) in *Proc. Actinides 85*, Aix-en-Provence, France, Sept. 1985, *J. Less Common Metals* (to be published).
238. Morss, L. R., Fuger, J., Goffart, J., Edelstein, N., and Shalimoff, G. V. in *Proc. 17th Rare Earth Research Conference*, Hamilton, Ontario, Canada, June 1986, *J. Less Common Metals* (to be published).
239. Nave, S. E., Moore, J. R., Haire, R. G., Peterson, J. R., and Damien, D. A. in *Proc. Actinides 85*, Aix-en-Provence, France, Sept. 1985, *J. Less Common Metals* (to be published).
240. Nave, S. E., Moore, J. R., Peterson, J. R., and Haire, R. G. in *Proc. 17th Rare Earth Research Conference*, Hamilton, Ontario, Canada, June 1986, *J. Less Common Metals* (to be published).
241. Myasoedov, B. F., Lebedev, I. A., Khizhnyak, P. L., Timofeev, G. A., and Frenkel, V. Ya. in *Proc. Actinides 85*, Aix-en-Provence, France, Sept., 1985, *J. Less Common Metals* (to be published).

CHAPTER TWELVE

EINSTEINIUM

E.K. Hulet

12.1 INTRODUCTION

Einsteinium (chemical symbol Es) was discovered unexpectedly together with fermium in a test of the first thermonuclear bomb at Eniwetok Atoll in 1952. Very large numbers of neutrons created from fusion reactions in the fuel were captured by large quantities of ^{238}U surrounding the Mike device. In an exceedingly brief instant, as many as 17 neutrons were captured successively by a fraction of the ^{238}U nuclei to yield very neutron-rich uranium isotopes. The rapid beta decay of these massive uranium nuclides produced intermediate isotopes of Np, Pu, Am, Bk, Cf, and Es which continued to beta decay until β-stable masses of all these elements and Fm were reached. From debris collected by aircraft sampling of the mushroom cloud, nuclear chemists at the Los Alamos National Laboratory, the Lawrence Berkeley Laboratory, and the Argonne National Laboratory identified the new elements Es and Fm as well as many new isotopes of Pu, Am, Cm, and Cf [1]. This first discovery was largely based on the identification of 20 day ^{253}Es, which is also the major einsteinium isotope now produced in nuclear reactors. Naming of the element after Albert Einstein was considered an appropriate tribute to this great physicist.

12.2 NUCLEAR PROPERTIES

The primary nuclear properties of the known isotopes of einsteinium are listed in Table 12.1 (see also refs 2 and 3). From detailed studies of their nuclear decay, the nuclear levels of their daughters have been obtained and the precise atomic mass

Table 12.1 *Nuclear properties of einsteinium isotopes.*

Mass number	*Half-life*	*Mode of decay*	*Main radiations* (MeV)	*Method of production*
243	21 s	α	α 7.89	^{233}U (^{15}N, 5n)
244	37 s	EC 96%	α 7.57	^{233}U (^{15}N, 4n)
		α ~ 4%		^{237}Np (^{12}C, 5n)
245	1.3 min	EC 60%	α 7.73	^{237}Np (^{12}C, 4n)
		α 40%		
246	7.7 min	EC 90%	α 7.35	^{241}Am (^{12}C, α3n)
		α 10%		
247	4.7 min	EC ~93%	α 7.32	^{241}Am (^{12}C, α2n)
		α ~ 7%		^{238}U (^{14}N, 5n)
248	27 min	EC 99.7%	α 6.87	^{249}Cf (d,3n)
		α ~ 0.3%	γ 0.551	
249	1.70 h	EC 99.4%	α 6.770	^{249}Cf (d,2n)
		α 0.57%	γ 0.380	
250[a]	8.6 h	EC	γ 0.829	^{249}Cf (d,n)
250[a]	2.22 h	EC	γ 0.989	^{249}Cf (d,n)
251	33 h	EC 99.5%	α 6.492 (81%)	^{249}Bk (α,2n)
		α 0.49%	6.463 (9%)	
252	472 d	α 78%	α 6.632 (80%)	^{249}Bk (α,n)
		EC 22%	6.562 (13.6%)	
			γ 0.785	
253	20.47 d	α	α 6.633 (89.8%)	multiple
	6.3×10^5 yr SF	β stable	6.592 (7.3%)	n capture
			γ 0.389	
254 g	275.7 d	α	α 6.429 (93.2%)	multiple
	$>2.5 \times 10^7$ yr	SF	6.359 (2.4%)	n capture
			γ 0.062	
254 m	39.3 h	β^- 99.6%	α 6.382 (75%)	^{253}Es (n,γ)
	$>1 \times 10^5$ yr SF	α 0.33%	6.357 (8%)	
		EC 0.08%	γ 0.649	
255	39.8 d	β^- 92.0%	α 6.300 (88%)	multiple
		α 8.0%	6.260 (10%)	n capture
		SF 4×10^{-3}%		
256[a]	25.0 min	β^-		^{255}Es (n,γ)
256[a]	~ 7.6 h	β^-		^{254}Es (t,p)

[a] Not known whether ground-state nuclide or isomer.

of each isotope deduced by relating the total decay energy to the mass of the daughter nuclide.

For the synthetic transuranium elements, nuclear properties and methods of production have an overwhelming impact upon the development of knowledge concerning their chemical properties. In the case of einsteinium, only the isotopes ^{253}Es and ^{254g}Es can be produced in quantities sufficient for chemical investigations and even the more abundant of the two isotopes, ^{253}Es, is limited to amounts of 2 mg or less. In addition, the 20 day alpha decay half-life of ^{253}Es

imposes a severe experimental obstacle and a serious restriction on the kinds of chemical and physical information that can be obtained. As an example, the radiation damage occurring in solid compounds obliterates the crystal structures within an hour, which makes it extremely difficult to obtain structural data.

Starting with neutron capture by ^{238}U, the production of ^{253}Es proceeds through a long chain of further captures and beta decays by intermediate nuclides during prolonged neutron irradiations. The yearly production of ^{253}Es from 1962 onward in the USA is shown in Fig. 12.1. Prior to 1969, einsteinium and other transplutonium elements were produced by the individual National Laboratories but an overall US production program, centered at the Oak Ridge National Laboratory, later superseded these individual efforts. The production of ^{253}Es has now leveled off at a rate of about 2 mg per year while ^{254}Es and ^{255}Es are about 0.3 and 0.06% of the ^{253}Es quantities, respectively [4].

Outside of the USA, only the USSR maintains a program for the production of transplutonium elements [5]. A large-volume reactor (MIR loop reactor) is used to produce the feed supply of ^{242}Pu, ^{243}Am, and ^{244}Cm target isotopes for the high-flux (3.9×10^{15} thermal neutron flux) SM-2 reactor. The power level and the volume of the flux trap in the SM-2 are approximately equal to the HFIR reactor at Oak Ridge; therefore, their potential production capabilities for producing transplutonium elements should be about the same.

12.3 PREPARATION AND PURIFICATION

The chemical recovery of einsteinium (and Bk, Cf, and Fm) after irradiation is performed remotely in large shielded cells. Details of the chemical separation

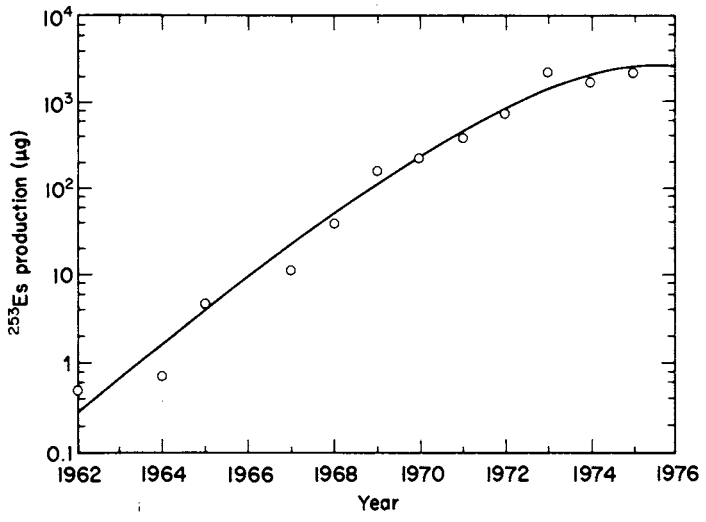

Fig. 12.1 *Yearly production of ^{253}Es in the USA.*

processes used in the USA and in the USSR at the Kurchatov Institute of Atomic Energy have been reviewed by Hulet and Bodé [6] and by Kosyakov and coworkers [7], respectively. Nearly all of the separation steps used in these large-scale processes were developed earlier for applications in laboratory separations, but extensive modifications were required to adapt them to the special and nearly always adverse conditions encountered in remote operations with very high levels of radioactivity present. These separation processes are unlikely to be scaled up further as, for instance, for the recovery of transplutonium elements during the reprocessing of fuel from power reactors. This is largely because they were born in the laboratory where corrosive chemicals could be easily contained in glass apparatus and where the chemist could oversee the difficult chromatographic separations.

Purification of einsteinium requires two difficult separations: (1) from lanthanide fission products and (2) from adjacent actinides. The main difficulty arises from the great similarity in the chemical properties of their trivalent ions. Forunately, the contraction in size of the aqueous ions with increasing atomic number can be exploited with complexing ligands to offer slight variations in complex strengths between members of either series of f elements. Chromatographic methods then exploit these small chemical differences many times over to give useful separation factors for the tripositive elements.

Separation of einsteinium from the lanthanides is usually accomplished by elution with either 13 M HCl or 20 vol % ethanol saturated with HCl from an ion-exchange column containing a strongly acidic cation-exchange resin [8]. Einsteinium and the other actinides are rapidly eluted in a band while the trivalent lanthanides are retained and eluted somewhat later. The purification of einsteinium from many milligrams of lanthanides necessitates an anion-exchange procedure using 10 M LiCl as an eluant [9]. With this elution method, Cf, Es, and Fm are separated from all lanthanides, Pu, Am, and Cm with separation factors ranging from 4 to 23.

The intragroup separation of einsteinium from adjacent actinides can be performed by either of two chromatographic methods. In the ion-exchange method, the trivalent actinides are eluted with a complexing agent such as 2-hydroxy-2-methylpropanoic acid (α-hydroxyisobutyric acid, α HIB) from a heated column of cation-exchange resin containing a strongly acidic, highly crosslinked resin [10]. Such columns are often run at pressures up to 17.2 MPa to force the eluant through the very fine particles of ion-exchange resin [11]. The second method employs extraction chromatography in which the extractants, either bis(2-ethylhexyl)phosphoric acid (HDEHP) or 2-ethylhexylphenylphosphonic acid (HEM ϕ P), are adsorbed on an inert support material [6]. An eluant of approximately 0.3–0.4 M HCl or HNO_3 provides distribution coefficients appropriate for Es–Fm separations. Table 12.2 summarizes the separation factors (ratio of distribution coefficients) obtainable by each of these methods. Clearly, the purification of Cf from Es is the poorest; hence, the cation-exchange method is preferred because of the larger separation factor. The major difference

Table 12.2 *Separation factors, $S = K_{d(Z)}/K_{d(Z+1)}$, for Es/Fm and Cf/Es obtained with acidic extractants and by cation exchange. Average values from ref. 6 (p. 11) and ref. 12 are listed.*

Elements	αHIB (87°C)	HDEHP (60°C)		HEHϕP (25°C)
		HCl	HNO_3	HCl
Cf	1.5	0.99	1.02	1.3
Es	1.7	2.04	2.20	2.5
Fm				

between the two methods of chromatographic separation lies in a reversal of the elution sequence with atomic number.

12.4 ATOMIC PROPERTIES

The electronic configurations of einsteinium in neutral and singly ionized gaseous atoms have been determined from emission spectra taken with electrodeless discharge lamps containing EsI_3. Although the first emission spectrum of einsteinium revealed only nine lines [13], the most recent exposures using the 10 m spectrograph at the Argonne National Laboratory are expected to show some 20 000 lines [14]. Unfortunately, the measurements on these photographic plates are incomplete and the electronic configurations given in Table 12.3 are based on term assignments to a portion of the 290 lines observed earlier by Worden *et al.* [15]. It should be noted that not all of the lowest-energy electronic configurations have been observed yet. Brewer has tabulated his estimated energies of the lowest level of the lowest spectroscopic term for each electron configuration [16, 17]. For the singly ionized free atom, it is apparent from his estimates that the $f^{10}s^2$, f^{12}, and $f^{11}d$ should be lower in energy than the first excited level $f^{11}p$ observed by Worden *et al.* [15]. Other atomic properties from atomic-beam and x-ray measurements are listed in Table 12.3.

12.5 METALLIC STATE

The high specific radioactivity of einsteinium has greatly limited the investigations of the metal. Of the two attempts to prepare the metal and determine its structure, the successful method employed electron diffraction rather than x-ray diffraction. The latter was largely inconclusive because of degradation of the metal's crystallinity caused by self-irradiation. The electron diffraction lines from 11 samples were indexed on the basis of a face-centered cubic structure with $a_0 = 0.575 \pm 0.001$ nm [22]. This fcc form of einsteinium metal is believed to be

Table 12.3 *Atomic properties of einsteinium* (^{253}Es).

	Ground level	*Other levels*	*Energy* (mm^{-1})
neutral, I	$5f^{11}7s^2, {}^4I^o_{15/2}$	$5f^{11}7s7p, {}^6I_{15/2}$	1780.289
		$5f^{10}6d7s^2, {}^6I_{17/2}$	1936.793
		$5f^{11}7s8s, {}^4I_{15/2}, {}^3S_1$	3382.935
singly ionized, II	$5f^{11}7s, {}^5I^o_8$	$5f^{11}7p, {}^5I_7$	2775.112
		$5f^{10}6d7s$	3289.777[a]

Property	*Value*	*Ref.*
first ionization potential	6.42 ± 0.03 eV (calc.)	18, 19
nuclear spin	7/2	15
nuclear dipole moment, μ_I	$4.10 \pm 0.07\ \mu_N$	20
nuclear quadrupole moment, Q_s	6.7 ± 0.8 barn	20
K x-ray energies	$K\alpha_2$ 112.501 ± 0.01 keV	21
	$K\alpha_1$ 118.018 ± 0.01	
	$K\beta_3$ 131.848 ± 0.02	
	$K\beta_1$ 133.188 ± 0.02	

[a] May not be the lowest level of this configuration.

divalent because it has the same lattice parameter as that reported for the divalent form of californium metal. The calculated atomic radius (CN 12) is 0.203 nm.

A melting point for the metal was also noted while heating the samples in the electron microscope used for the diffraction measurements. Micropuddles of the metal formed during the heating and, after calibrating with metals of known melting points, a temperature of 860 ± 50°C was established as the melting point of einsteinium metal.

Further evidence for divalency in Es metal has come from studies comparing the condensation temperatures of elemental lanthanides and actinides in thermochromatographic columns [23]. The trivalent metals Sc, La, and Bk were not volatilized at the initial temperature of 1425 K, whereas the metals of Yb, Es, Fm, and Md were vaporized and later condensed at the same temperature (~ 700 K). The behavior of divalent Eu, Sm, and Ca metals was intermediate between those extremes. Since volatilities are correlated with promotional energies and the number and energy of the valence bonds, the more volatile actinides are associated with the divalent metals. The estimates of Nugent *et al.* [24] for the enthalpy of sublimation of lanthanide and actinide metals agree closely with the relative volatilities found in the thermochromatographic study reported above. Furthermore, Ward and colleagues [52] have recently completed detailed analyses of the cohesive energy of the actinide metals (entropies and heats of

sublimation), in which they also indicate that einsteinium is a divalent metal. A recent measurement of the heat of vaporization by this group gave a value of 133 kJ mol^{-1}, the lowest value for any divalent metal [65].

The thermal conductivity of einsteinium has been estimated to be 10 W m^{-1} K^{-1} at 300 K [25].

12.6 COMPOUNDS

Only a few simple compounds of einsteinium have been prepared and structurally identified. Aside from self-destruction of the crystal structures, there is a rapid ingrowth of the α daughter ^{249}Bk, and the L, M, and N x-rays, following α decay, blacken the x-ray film used in Debye–Scherrer cameras within 10–20 min with microgram samples of ^{253}Es or ^{254g}Es. A synchrotron radiation source may be the only way of overwhelming this sample background source of radiation with sufficient intensity of monochromatic radiation to permit diffraction measurements.

The known compounds of einsteinium are listed in Table 12.4 together with the rather sparse information detailing their properties. Divalent compounds were not identified by their crystal structure, but by absorption spectra of their halides, taken with crystallites, or of samples first melted and then quenched. These spectra show a sharp difference in the f–f absorption bands when compared to the corresponding spectra of the trivalent halides (Fig. 12.2). We emphasize that the apparent stability of the divalent oxidation state in einsteinium was not realized until a decade ago and that this feature in the heavier actinides clearly sets this series of elements apart from the later elements in the 4f series. The stability of the divalent state is due to a marked lowering of the 5f energy levels with respect to the Fermi level, with the consequence that the 5f electrons in the latter part of the actinide series are more tightly bound to the atom than are the analogous 4f electrons. Quantitative information about the stability of divalent einsteinium can be found in a later section of this chapter.

Electron paramagnetic resonance spectra of divalent einsteinium have been recorded in single-crystal hosts of CaF_2 [33], BaF_2, and SrF_2 [34]. Reduction of Es^{3+} to Es^{2+} was spontaneous from electron displacement caused by the α radiation. A $5f^{11}$ configuration with a ground state close to the $^4I_{15/2}$ level, but with a small admixture of the $^2K_{15/2}$, was found, which indicated that the cubic crystal field only slightly perturbs the inner 5f orbitals.

A possible tetravalent compound EsF_4 may also exist, as judged by comparing the volatility of an einsteinium fluoride with PuF_4, AmF_4, CmF_4, BkF_4, and CfF_4 [35]. The f–f electronic spectrum of the Es^{4+} free ion has been calculated by Varga and co-workers [36]. Nugent *et al.* [37] and Lebedev [54] estimated the $E°(Es^{4+}/Es^{3+})$ reduction potential as +4.6 V, which Nugent thought might allow the synthesis of the compound Cs_3EsF_7.

Table 12.4 *Simple compounds of di- and trivalent einsteinium characterized by either structural or spectroscopic analysis.*

Compound	*Structural type*	*Lattice parameters* a_0 (nm)	b_0 (nm)	c_0 (nm)	β (deg)	*Major absorption bands* (cm^{-1})	*Ref.*
Es_2O_3	Mn_2O_3–bcc	1.0766 ± 0.0006				–	26
Es_2O_3	monoclinic	1.41	0.359	0.880	100	–	67
Es_2O_3	La_2O_3–hexagonal	0.37		0.60		–	67
$EsCl_3$	UCl_3–hexagonal	0.740 ± 0.002		0.407 ± 0.002		(see ref. 66)	31, 29, 66
$EsCl_2$	–					11100, 18500, 24500	27, 32
EsOCl	PbFCl–tetragonal	0.3948 ± 0.0004		0.6702 ± 0.0019		–	31, 29
$EsBr_3$	$AlCl_3$–monoclinic	0.727 ± 0.002	1.259 ± 0.003	0.681 ± 0.002	110.8 ± 0.2	12600, 19800	28, 66
$EsBr_2$	–					11200, 18300	27
EsOBr	–					(no published data)	29
EsI_3	BiI_3–hexagonal	0.753		2.084		(see ref. 29)	29, 30, 66
EsI_2	–					11200, 18500	27
EsOI	–					(no published data)	29
EsF_3	–					13200, 20300, 27000	62

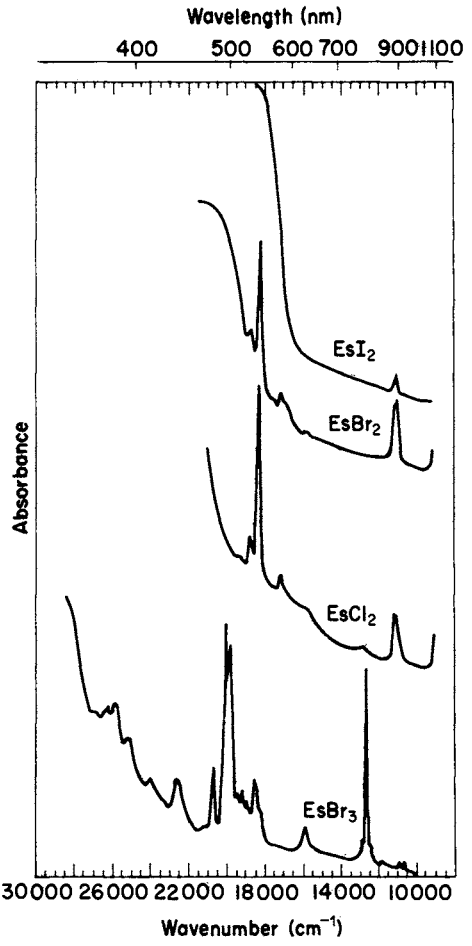

Fig. 12.2 *Absorption spectra of divalent einsteinium halides and comparison with* $EsBr_3$ [27]. *Reproduced with permission of J. R. Peterson and J. Phys. Colloq.*

12.7 SOLUTION CHEMISTRY

12.7.1 Trivalent ions

Across the actinide series from Pu to Lr, the solution properties of the tripositive actinide ions vary only slowly and in a regular manner. Thus, much of the behavior described in prior chapters for trivalent actinide ions can be safely extrapolated to estimate that of Es^{3+}. Bonding with ligands is almost entirely attributed to electrostatic forces, but with some second-order contribution from covalent sharing of electrons due to the relatively large radial extension of the 5f orbitals. The ionic radius of Es^{3+} has been calculated from the six-coordinated

sesquioxide to give a value of 0.0925 nm [26], or about 1 pm smaller than the radius of Cf^{3+}. Einsteinium is stable only as the trivalent ion in aqueous solution.

A number of measurements of the absorption spectrum of $^{253}Es^{3+}$ have been made over the energy range 943–3400 mm^{-1} [38–41]. The band structure (12 peaks) observed could be reasonably well-fitted in both energy and intensity by assuming that Es^{3+} behaved as a free ion and that the f–f transitions arose from eigenstates that were strongly mixed because of coupling intermediate between *LS* and *jj* [39–42]. These assumptions closely follow those used in fitting calculated levels to identified absorption bands in preceding members of the actinide (and lanthanide) series.

Studies of the complex-ion chemistry of Es^{3+} have been made in conjunction with measurements of the stability constants of other trivalent actinides. A summary of the known stability constants for einsteinium complexes is shown in Table 12.5. With the possible exception of the two lower thiocyanate complexes, chloride is the only outer-sphere complex in which water of hydration lies between the ligand and einsteinium ion. The remaining complexes are believed to be inner-sphere as inferred from the increase of a given stability constant with increase in atomic number and from the enthalpy and entropy of formation of the complex.

Hydrated radii and hydration numbers for the tripositive actinide ions have recently been derived from Stokes' law using migration rates in an electric field or

Table 12.5 *The stability constants of Es^{3+} complexes.*

	Log stability constants			
Complex[a]	β_1	β_2	β_3	*Ref.*
$EsCl^{2+}$	−0.18			43
$EsOH^{2+}$	8.86			44
$Es(SO_4)_n^{3-2n}$	−2.19	−4.3	−4.93	45
$Es(SCN)_n^{3-n}$	0.559	−1.4	0.468	46
$EsHCit^{2-}$	10.6			47
$Es(Cit)_2^{3-}$	12.1			47
$Es(\alpha HIB)^{2+}$	4.29			48
$Es(tartrate)^{+}$	5.86			48
$Es(malate)^{+}$	7.06			48
$EsDETPA^{2-}$	22.62			49
$EsDACTA^{-}$	19.43			49
$EsEDTA^{-}$	19.11			49

[a] Cit = citrate ion.
αHIB = 2-hydroxy-2-methylpropanoate ion.
DETPA = diethylenetriaminepentaacetate ion.
DACTA = 1,2-diaminecyclohexanetetraacetate ion.
EDTA = ethylenediaminetetraacetate ion.

diffusion coefficients of the tracer ions in a supporting electrolyte [50, 63, 64]. The hydrated ions of einsteinium and fermium are the largest in the series Am^{3+} to Md^{3+}; the hydrated radius of einsteinium is 0.492 nm, which allows 16.6 molecules of water in the total hydration sphere. Several parameters of thermodynamic interest have been measured or estimated, e.g. the molar activity coefficient of Es^{3+} in $NaNO_3$ solution [51] and the free energy, enthalpy, and entropy of formation of Es^{3+} in aqueous solution [53, 54, 56]. The values $\Delta H_f^\circ = -603\ kJ\ mol^{-1}$, $\Delta S_f^\circ = -100\ J\ K^{-1}\ mol^{-1}$, and $\Delta G_f^\circ = -573\ kJ\ mol^{-1}$ given by David and colleagues [53] were obtained from an entropy prescription and the standard reduction potential, III → 0, described in the following paragraph.

For the purpose of measuring the electropotential, reduction of the trivalent einsteinium ion to the metal (Hg amalgam) has been performed by polarographic methods. A single half-wave representing the III → 0 reduction potential was observed [55]. The potential found for the combined reactions of reduction and amalgamation was -1.460 ± 0.005 V. After correcting for the amalgamation energy by an empirical method suggested by Nugent [56], the standard potential derived was -1.98 V relative to the standard hydrogen potential. Because the amalgamation energy represents a large correction, caution should be exercised in using this standard potential in thermodynamic calculations.

12.7.2 Divalent ions

The divalent state is of major importance and has attracted the interest of many experimenters since 1967 when the appreciable stability of this state was first recognized in the actinides. The III → II reduction potential of einsteinium was first estimated to be -1.6 V from the lowest-energy electron-transfer band [57]. A later estimate of -1.21 V was given for chloroaluminate melts [58], as well as another estimate of the standard potential of -1.18 V [54]. Mikheev and co-workers identified Es(II) from the co-crystallization of einsteinium tracer with $SmCl_2$ in an ethanol solution [59]. Einsteinium was only partially reduced to the II state by $SmCl_2$, which allowed them to conclude that the standard reduction potential of Es^{3+} was close to that of Sm^{3+}, or -1.55 ± 0.06 V [60]. An ionic radius of 0.105 nm was estimated from the radius of maximum electron density obtained in Hartree–Fock calculations, which was then corrected to obtain the crystalline radius by an empirical proportionality constant [61].

ACKNOWLEDGMENT

The preparation of this chapter was performed under the auspices of the US Department of Energy by the Lawrence Livermore Laboratory under contract number W-7405-Eng-48.

REFERENCES

1. Ghiorso, A., Thompson, S. G., Higgins, G. H., Seaborg, G. T., Studier, M. H., Fields, P. R., Fried, S. M., Diamond, H., Mech, J. F., Pyle, G. L., Huizenga, J. R., Hirsch, A., Manning, W. M., Browne, C. I., Smith, H. L., and Spence, R. W. (1955) *Phys. Rev.*, **99**, 1048–9.
2. Schmorak, M. R. (1981) *Nucl. Data Sheets*, **32**, 87–193.
3. Lederer, C. M. and Shirley, V. S. (eds) (1978) *Table of Isotopes*, 7th edn, Wiley, New York.
4. Ferguson, D. E. (1978) in ref. 29, p. 35.
5. Davidenko, V. A. and 21 co-authors (1972) *Sov. At. Energy*, **33**, 936.
6. Hulet, E. K. and Bodé, D. D. (1972) in *MTP International Review of Science, Inorganic Chemistry*, ser. I, vol. 7, *Lanthanides and Actinides* (ed. K. W. Bagnall), Butterworths, London, pp. 1–46.
7. Kosyakov, V. N., Chudinov, É. G., and Shvetsov, I. K. (1974) *Sov. Radiochem.*, **16**, 722–8.
8. Street, K. Jr and Seaborg, G. T. (1950) *J. Am. Chem. Soc.*, **72**, 2790–2.
9. Hulet, E. K., Gutmacher, R. G., and Coops, M. S. (1961) *J. Inorg. Nucl. Chem.*, **17**, 350–60.
10. Choppin, G. R. and Silva, R. J. (1956) *J. Inorg. Nucl. Chem.*, **3**, 153–4.
11. Campbell, D. O. (1970) *Ind. Eng. Chem. Process Des. Dev.*, **9**, 95.
12. Harbour, R. M. (1972) *J. Inorg. Nucl. Chem.*, **34**, 2680–1.
13. Gutmacher, R. G., Evans, J. E., and Hulet, E. K. (1967) *J. Opt. Soc. Am.*, **57**, 1389–90.
14. Conway, J. G. (1978) in ref. 29, p. 69.
15. Worden, E. F., Lougheed, R. W., Gutmacher, R. G., and Conway, J. G. (1974) *J. Opt. Soc. Am.*, **64**, 77–85.
16. Brewer, L. (1971) *J. Opt. Soc. Am.*, **61**, 1101–11.
17. Brewer, L. (1971) *J. Opt. Soc. Am.*, **61**, 1666–82.
18. Sugar, J. (1974) *J. Chem. Phys.*, **60**, 4103.
19. Rajnak, K. and Shore, B. W. (1978) *J. Opt. Soc. Am.*, **68**, 360–7.
20. Goodman, L. S., Diamond, H., and Stanton, H. E. (1975) *Phys. Rev. A*, **11**, 499–504.
21. Dittner, P. F. and Bemis, C. E. Jr (1972) *Phys. Rev. A*, **5**, 481–4.
22. Haire, R. G. and Baybarz, R. D. (1979) *J. Phys. Colloq.*, **49** (C4), 101–2.
23. Hübener, S. (1980) *Radiochem. Radioanal. Lett.*, **44**, 79–86.
24. Nugent, L. J., Burnett, J. L., and Morss, L. R. (1973) *J. Chem. Thermodyn.*, **5**, 665–78.
25. Ho, C. Y., Powell, R. W., and Lilly, P. E. (1972) *J. Phys. Chem. Ref. Data*, **1**, 418.
26. Haire, R. G. and Baybarz, R. D. (1973) *J. Inorg. Nucl. Chem.*, **35**, 489–96.
27. Peterson, J. R., Ensor, D. D., Fellows, R. L., Haire, R. G., and Young, J. P. (1979) *J. Phys. Colloq.*, **49** (C4), 111–13.
28. Fellows, R. L., Peterson, J. R., Noe, M., Young, J. P., and Haire, R. G. (1975) *Inorg. Nucl. Chem. Lett.*, **11**, 737–42.
29. Peterson, J. R. (1979) in *Proc. Symp. Commemorating the 25th Anniversary of Elements 99 and 100* (ed. G. T. Seaborg), Report LBL-7701, National Technical Information Service, Springfield, Va, p. 55.
30. Fellows, R. L., Young, J. P., Haire, R. G., and Peterson, J. R. (1978) in ref. 29, and private communication.
31. Fujita, D. K., Cunningham, B. B., and Parsons, T. C. (1969) *Inorg. Nucl. Chem. Lett.*, **5**, 307–13.

32. Fellows, R. L., Peterson, J. R., Young, J. P., and Haire, R. G. (1977) in *The Rare Earths in Modern Science and Technology* (eds G. J. McCarthy and J. J. Ryne), Plenum Press, New York, pp. 493–9.
33. Edelstein, N. (1971) *J. Chem. Phys.*, **54**, 2488–91.
34. Boatner, L. A., Reynolds, R. W., Finch, C. B., and Abraham, M. M. (1975) *Phys. Rev. B*, **13**, 953–8.
35. Bouissières, G., Jouniaux, B., Legoux, Y., Merinis, J., David, F., and Samhoun, K. (1980) *Radiochem. Radioanal. Lett.*, **45**, 121–8.
36. Varga, L. P., Baybarz, R. D., Reisfeld, M. J., and Asprey, L. B. (1973) *J. Inorg. Nucl. Chem.*, **35**, 2775–85.
37. Nugent, L. J., Baybarz, R. D., Burnett, J. L., and Ryan, J. L. (1971) *J. Inorg. Nucl. Chem.*, **33**, 2503–30.
38. Fujita, D. K., Cunningham, B. B., Parsons, T. C., and Peterson, J. R. (1969) *Inorg. Nucl. Chem. Lett.*, **5**, 245–50.
39. Nugent, L. J., Baybarz, R. D., Werner, G. K., and Friedman, H. A. (1970) *Chem. Phys. Lett.*, **7**, 179–82.
40. Varga, L. P., Baybarz, R. D., Reisfeld, M. J., and Mann, J. B. (1973) *J. Inorg. Nucl. Chem.*, **35**, 2303–10.
41. Carnall, W. T., Cohen, D., Fields, P. R., Sjoblom, R. K., and Barnes, R. F. (1973) *J. Chem. Phys.*, **59**, 1785–9.
42. Nugent, L. J., Burnett, J. L., Baybarz, R. D., Werner, G. K., Tanner, S. R., Tarrant, J. B., and Keller, O. L. Jr (1969) *J. Phys. Chem.*, **73**, 1540–9.
43. Harmon, H. D. and Peterson, J. R. (1972) *Inorg. Nucl. Chem. Lett.*, **8**, 57–63.
44. Hussonnois, M., Hubert, S., Brillard, L., and Guillaumont, R. (1973) *Radiochem. Radioanal. Lett.*, **15**, 47–56.
45. McDowell, W. J. and Coleman, C. F. (1972) *J. Inorg. Nucl. Chem.*, **34**, 2837–50.
46. Harmon, H. D. and Peterson, J. R. (1972) *J. Inorg. Nucl. Chem.*, **34**, 1381–97.
47. Hubert, S., Hussonnois, M., Brillard, L., Goby, G., and Guillaumont, R. (1974) *J. Inorg. Nucl. Chem.*, **36**, 2361–6.
48. Aly, H. F. and Latimer, R. M. (1970) *Radiochim. Acta*, **14**, 27–31.
49. Myasoedov, B. F., Guseva, L. I., Milyukova, M. S., and Chmutova, M. K. (1974) *Analytical Chemistry of the Transplutonium Elements*, Kester, Jerusalem, p. 358.
50. Lundqvist, R. D., Hulet, E. K., and Baisden, P. A. (1981) *Acta Chem. Scand. A*, **35**, 653–61.
51. Chudinov, E. G. and Pirozhkov, S. V. (1973) *Sov. Radiochem.*, **15**, 195–9.
52. Ward, J. W., Kleinschmidt, P. D., Haire, R. G., and Brown, D. (1980) in *Lanthanide and Actinide Chemistry and Spectroscopy* (ed. N. Edelstein), (ACS Symp. Ser. 131), American Chemical Society, Washington DC, p. 199.
53. David, F., Samhoun, K., Guillaumont, R., and Edelstein, N. (1978) *J. Inorg. Nucl. Chem.*, **40**, 69–74.
54. Lebedev, I. A. (1978) *Sov. Radiochem.*, **20**, 556–62.
55. Samhoun, K. and David, F. (1979) *J. Inorg. Nucl. Chem.*, **41**, 357–63.
56. Nugent, L. J. (1975) *J. Inorg. Nucl. Chem.*, **37**, 1767–70.
57. Nugent, L. J., Baybarz, R. D., and Burnett, J. L. (1969) *J. Phys. Chem.*, **73**, 1177–8.
58. Duyckaerts, G. and Gilbert, B. (1977) *Inorg. Nucl. Chem. Lett.*, **13**, 537–42.
59. Mikheev, N. B., Spitsyn, V. I., Kamenskaya, A. N., Rozenkevich, N. A., Rumer, I. A., and Auerman, L. N. (1972) *Sov. Radiochem.*, **14**, 494–5.
60. Mikheev, N. B. and Rumer, I. A. (1972) *Sov. Radiochem.*, **14**, 502–3.

61. Ionova, G. V., Mikheev, N. B., and Spitsyn, V. I. (1978) *Sov. Radiochem.*, **20**, 89–92.
62. Ensor, D. D., Peterson, J. R., Haire, R. G., and Young, J. P. (1981) *J. Inorg. Nucl. Chem.*, **43**, 2425–7.
63. Fourest, B., Duplessis, J., and David, F. (1983) *J. Less Common Metals*, **92**, 17–27.
64. Latrous, H., Oliver, J., and Chemla, M. (1982) *Radiochem. Radioanal. Lett.*, **53**, 81–8.
65. Kleinschmidt, P. D., Ward, J. W., Matlack, G. M., and Haire, R. G. (1984) *J. Chem. Phys.*, **81**, 473–7.
66. Young, J. P., Haire, R. G., Peterson, J. R., Ensor, D. D., and Fellows, R. L. (1981) *Inorg. Chem.*, **20**, 3979–83.
67. Haire, R. G. (1985) Abstract NUCL-24, *American Chemical Society*, 189th National Meeting, Miami Beach; to be published.

CHAPTER THIRTEEN

TRANSEINSTEINIUM ELEMENTS

R.J. Silva

13.1 GENERAL

As of this writing, the number of known elements has been increased from the naturally occurring 92 to perhaps as many as 109. In fact, over 50 isotopes of elements with atomic numbers 100 through 109 have been reported, ranging in half-lives from as long as 100 days for ^{257}Fm to as short as a few milliseconds for ^{266}109. The end of the actinide or 5f series of elements has been reached with the production of lawrencium, atomic number 103, and elements 104–109 begin the next series, the 6d series of elements.

There have been a number of recent predictions of chemical properties of the heavy actinide and transactinide elements based on both atomic calculations and extrapolations of the periodic table, e.g. ground-state electronic configurations, electron binding energies, oxidation states, etc. Thus, we are presently in the exciting position of testing the predictions of the periodic system and the underlying quantum-mechanical calculations on which it is based.

Owing to the short half-lives and low production yields of the heaviest elements, all available chemical information has been obtained from experiments with tracer quantities. In fact, in many cases, chemical experiments were performed with only a few atoms or even one atom at a time. These experiments have of necessity been rather simple in principle, aimed primarily at making comparative studies with elements of known chemical behavior. Nevertheless, they have succeeded in establishing the chemical relationships of elements 100–105 to one another and their positions in the periodic table.

Though the 3+ oxidation state remains a dominant feature of the heavier actinides, a tendency toward the formation of lower oxidation states has emerged. Divalency has been observed in solution for californium through nobelium. The 2+ oxidation state is much more stable in the heavy actinides than in the corresponding lanthanides as the end of the series is approached and, in fact, the increased 5f-electron binding makes the 2+ oxidation state the most stable in aqueous solution for nobelium. However, lawrencium, the last member of the actinide series, returns to the 3+ state as the most stable in solution, as expected.

Though ion exchange is still a very important separation technique for the heaviest elements, fast solvent extraction and gas-phase separation schemes have been developed and are particularly useful for the transactinide elements.

The purpose of this chapter is to investigate in more detail the chemistry of the elements of atomic numbers 100 to 109.

13.2 FERMIUM

13.2.1 Introduction

The first isotope of element 100 was found in heavy-element samples obtained from the 'Mike' thermonuclear explosion of 1952, during the same set of experiments that resulted in the discovery of element 99. A combined effort by researchers from the Lawrence Berkeley Laboratory, the Argonne National Laboratory, and the Los Alamos National Laboratory resulted in the isolation and identification of the 20 h half-life ^{255}Fm [1]. The production path involved rapid, multiple neutron capture by uranium in the device to form isotopes of very heavy mass, followed by beta decay to elements of higher atomic number. The ^{255}Fm in the samples, produced from the beta decay of the longer-lived ^{255}Es, was purified and chemically identified by cation-exchange chromatography and detected by alpha-particle energy analysis. The name, fermium, in honor of the leader in nuclear energy, Enrico Fermi, was proposed in 1955 and subsequently accepted by the International Union of Pure and Applied Chemistry (IUPAC).

13.2.2 Isotopes of fermium

There are now 18 known isotopes of element 100, from atomic masses 242 through 259 (Table 13.1). Several isotopes, masses 254 through 257, have been identified in samples of plutonium or elements of higher atomic number following neutron irradiation in reactors. All of the other isotopes can only be made by charged-particle bombardments of elements of lower atomic number at charged-particle accelerators.

The isotope that can be produced in the largest quantities is ^{257}Fm. It is also the nuclide of highest atomic and mass numbers ever isolated from either reactor- or thermonuclear-produced materials. The neutron-production chain essentially terminates at mass 257 owing to the very short half-lives of the heavier isotopes.

Table 13.1 *Nuclear properties of fermium isotopes.*

Mass number	*Half-life*	*Mode of decay*	*Main radiations* (MeV)	*Method of production*
242	0.8 ms	SF		$^{204}Pb(^{40}Ar, 2n)$
243	0.18 s	α	α 9.55	$^{206}Pb(^{40}Ar, 3n)$
244	3.3 ms	SF		$^{206}Pb(^{40}Ar, 2n)$
				$^{233}U(^{16}O, 5n)$
245	4.2 s	α	α 8.15	$^{233}U(^{16}O, 4n)$
246	1.1 s	α 92%	α 8.24	$^{235}U(^{16}O, 5n)$
		SF 8%		$^{239}Pu(^{12}C, 5n)$
247[a]	35 s	α ⩾ 50%	α 7.93 (~ 30%)	$^{239}Pu(^{12}C, 4n)$
		EC ⩽ 50%	7.87 (~ 70%)	
247[a]	9 s	α	α 8.18	$^{239}Pu(^{12}C, 4n)$
248	36 s	α 99.9%	α 7.87 (80%)	$^{240}Pu(^{12}C, 4n)$
		SF 0.1%	7.83 (20%)	
249	2.6 min	α	α 7.53	$^{238}U(^{16}O, 5n)$
				$^{249}Cf(\alpha, 4n)$
250	30 min	α	α 7.43	$^{249}Cf(\alpha, 3n)$
		SF 5.7×10^{-4}%		$^{238}U(^{16}O, 4n)$
250 m	1.8 s	IT		$^{249}Cf(\alpha, 3n)$
251	5.30 h	EC 98.2%	α 6.834 (87%)	$^{249}Cf(\alpha, 2n)$
		α 1.8%	6.783 (4.8%)	
252	25.39 h	α	α 7.039 (84.0%)	$^{249}Cf(\alpha, n)$
		SF 2.3×10^{-3}%	6.998 (15.0%)	
253	3.0 d	EC 88%	α 6.943 (43%)	$^{252}Cf(\alpha, 3n)$
		α 12%	6.674 (23%)	
			γ 0.272	
254	3.240 h	α > 99%	α 7.192 (85.0%)	^{254m}Es daughter
		SF 0.0592%	7.150 (14.2%)	
255	20.07 h	α	α 7.022 (93.4%)	^{255}Es daughter
		SF 2.4×10^{-5}%	6.963 (5.0%)	
256	2.63 h	SF 91.9%	α 6.915	^{256}Md daughter
		α 8.1%		^{256}Es duaghter
257	100.5 d	α 99.79%	α 6.695 (3.5%)	multiple n capture
		SF 0.210%	6.520 (93.6%)	
			γ 0.241	
258	0.38 ms	SF		$^{257}Fm(d, p)$
259	1.5 s	SF		$^{257}Fm(t, p)$

[a] Not known whether ground-state nuclide, isomer, or identification error.

The current annual reactor production rate is about 10^9 atoms [2]. However, in the thermonuclear explosion of 1969 called 'Hutch', about 10^8 higher production was achieved [3], but only one ten-millionth of the total number of atoms of ^{257}Fm imbedded in tons of debris was recovered, i.e. a 10 kg sample of debris yielded about 10^{10} atoms.

Though ^{257}Fm is produced in larger quantities, ^{255}Fm is more available on a regular basis from the beta decay of reactor-produced ^{255}Es and is more frequently used for chemical studies on the tracer level.

13.2.3 Preparation and purification

The isotope ^{255}Es is available only in mixed isotope samples along with ^{253}Es and ^{254m}Es. Tenths of micrograms of ^{255}Es are produced per year along with milligrams of ^{253}Es and micrograms of ^{254m}Es from reactor irradiations of ^{242}Pu or ^{243}Am–^{244}Cm targets in the High-Flux Isotope Reactor at Oak Ridge [2, 3]. Radioactivity levels in excess of 10^6 alpha disintegrations per minute of ^{255}Fm can be obtained from periodic 'milkings' of purified Es samples containing only a few nanograms of ^{255}Es.

Because of their great chemical similarity, the only satisfactory methods of separation of the trivalent actinides is by cation-exchange or solvent extraction chromatography. The procedure nearly always selected is separation by elution from a cation-exchange resin column, e.g. Dowex 50 × 8 or × 12 resin, using the chelating agent α-hydroxyisobutyric acid as eluant. This combination, developed in 1956 [4] for the isolation and identification of new actinide elements, still remains the main process method for separation of the heavy trivalent actinides [5]. The elements exhibit slightly increasing complexation strength with the organic ligand with increasing atomic number (usually attributed to the decreasing ionic radii) and are eluted from the column in a regular sequence with the higher-atomic-number elements eluting first. Fig. 13.1 shows a typical separation of trace amounts of a number of 3 + actinides. The predicted elution position of Lr^{3+} is also shown.

When this column procedure is used to 'milk' the Fm from rather large amounts of Es, one or two further successive column separations are usually made on the Fm fraction from the first column in order to obtain satisfactory purification. The final step in the Fm purification usually involves adsorbing the Fm onto a small Dowex 50 × 4 resin column, e.g. 2 mm diameter by 6 cm high, from the α-hydroxyisobutyric acid solution from the last column (which has been acidified to 0.25 M in HCl), washing the α-hydroxyisobutyric acid off the column with 0.5 M HCl, and then 'stripping' the Fm from the column with 6 M HCl [6].

13.2.4 Atomic properties

Goodman, Diamond, Stanton, and Fred have used the atomic-beam magnetic resonance technique, adapted to the measurement of radioactive samples, to determine the magnetic moment of the atomic ground state of neutral atoms of the 3.24 h half-life ^{254}Fm [7]. A comparison of the experimentally measured value with those obtained from intermediate-coupling calculations for several likely configurations was made. The measured value of g_j was found to be in close agreement only with that calculated for the $^3H_6$ level of the $5f^{12}\ 7s^2$ electron configuration. This agreement was taken as conclusive evidence for the assignment of this configuration to the ground state of fermium.

The inner-shell binding energies and x-ray energies for the heavy elements have

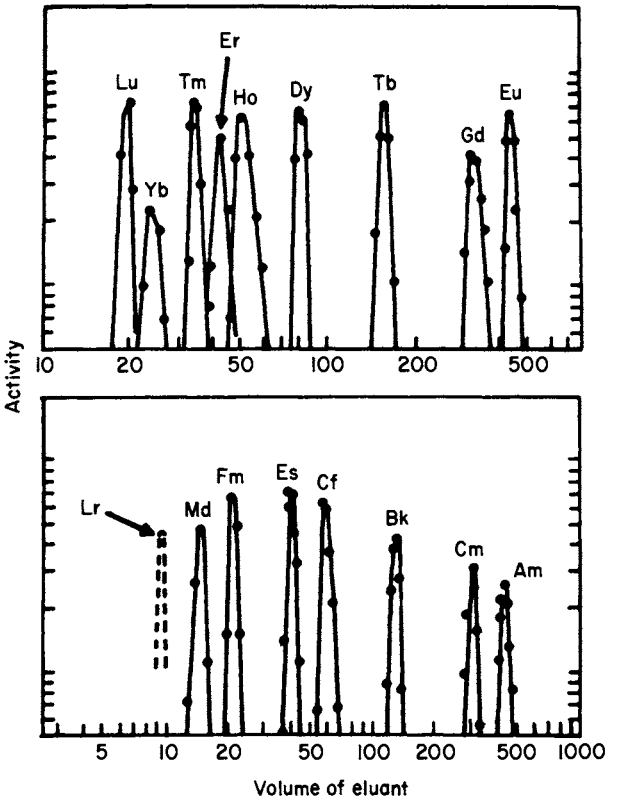

Fig. 13.1 *Elution of homologous trivalent actinides and lanthanides from a Dowex 50 resin column at 87°C with α-hydroxyisobutyrate as eluant. The broken curve for element 103 (Lr) is a prediction.*

been estimated from total energies obtained from a Dirac–Fock computer code of Desclaux by Carlson and Nestor [8]. In these calculations, small empirical corrections were added as a result of comparing calculations with experimentally determined binding energies for elements of $Z < 95$. Where comparisons have been made for higher-Z elements, the results of the calculations have agreed remarkably well with the experimentally measured values. For example, Porter and Freedman have determined the atomic binding energies of the K, L, M, N, O, and P shells for fermium via spectroscopic measurements of internal conversion electrons emitted following the beta decay of ^{254m}Es [9]. Also Dittner *et al.* have measured the K-series x-rays of ^{251}Fm emitted following the alpha decay of ^{255}No [10]. The energies derived from these works are compared with the values calculated by Carlson and Nestor in Table 13.2. These types of calculations should be quite useful for predictive purposes.

Table 13.2 *Comparison of calculated and measured electron binding and x-ray energies for Fm.*

	Binding energy (eV)			*X-ray energy* (keV)	
Shell	*Calc.* [8]	*Meas.* [9]	*Transition*	*Calc.* [8]	*Meas.* [10]
1s	141 943	141 963			
2s	27 584	27 573			
$2p_{1/2}$	26 643	26 644	$K\alpha_2(2p_{1/2} \rightarrow 1s)$	115.300	115.280
$2p_{3/2}$	20 872	20 868	$K\alpha_1(2p_{3/2} \rightarrow 1s)$	121.071	121.070
3s	7 206	7 200			
$3p_{1/2}$	6 783	6 779	$K\beta_3(3p_{1/2} \rightarrow 1s)$	135.160	135.2
$3p_{3/2}$	5 414	5 408	$K\beta_1(3p_{3/2} \rightarrow 1s)$	136.529	136.6
$3d_{3/2}$	4 757	4 746			
$3d_{5/2}$	4 497	4 484			
4s	1 954	1 940			
$4p_{1/2}$	1 753	1 743	$K\beta_2(4p_{1/2} \rightarrow 1s)$	140.190	140.1
$4p_{3/2}$	1 383	1 371	$(4p_{3/2} \rightarrow 1s)$	140.560	
$4d_{3/2}$	1 071	1 059			
$4d_{5/2}$	1 005	989			

13.2.5 The metallic state

Fermium metal has not yet been prepared; however, some predictions about it have been made. Johannson and Rosengren have correlated the measured and predicted cohesive energies of the lanthanide and actinide elements in both the divalent and trivalent metallic states [11]. They conclude that the gain in energy of binding of the $5f^n\ 6d^1\ 7s^2$ (trivalent) configuration over the $5f^{n+1}\ 7s^2$ (divalent) configuration is less than the energy necessary to promote one 5f electron to the 6d state in the final members of the actinide series. Therefore, Es, Fm, Md, and No prefer a divalent metallic state similar to Eu and Yb rather than the trivalent one. However, the energy difference is very small for Es and Fm and, at modest compression, the divalent metallic state may turn into the trivalent one. From estimates of the cohesive energy, lawrencium should prefer the trivalent metallic state. David *et al.* have estimated a divalent metallic radius of 1.94 Å for Fm [12].

Since the heaviest actinides are available only in trace amounts, unusual experimental approaches must be used in order to characterize their elemental state properties. Recently, Zvara and co-workers compared the evaporation rates of trace amounts of Es, Fm, and Md from molten La with those of Ce, Eu, Yb, Am, and Cf in order to obtain information on their metallic states [13], while Huebener compared the thermochromatographic behavior of Es, Fm, and Md evaporated from molten La in titanium columns with those of Na, Sc, Sm, Eu, Yb, Bk, and Cf [14]. From their results, both authors concluded that Es, Fm, and Md prefer the divalent metallic state.

13.2.6 Solution chemistry

The chemical behavior of fermium has been studied only with tracer quantities. The chemical properties have been discussed by Thompson, Harvey, Choppin, and Seaborg [15]. Under normal conditions, fermium behaves in aqueous solution as expected for a trivalent actinide ion. It is co-precipitated on rare-earth fluorides and hydroxides. The elution of fermium just prior to einsteinium from cation-exchange resin columns with hydrogen ion, citric acid, lactic acid, and α-hydroxyisobutyric acid is consistent with the existence of a trivalent ion [16]. In concentrated hydrochloric acid, nitric acid, and ammonium thiocyanate solutions, fermium forms anion complexes with the ligands which can be adsorbed on and subsequently eluted from anion-exchange resin columns [13]. In this case, fermium just follows einsteinium in the elution sequence. Both types of column results indicate that Fm forms a slightly stronger complex than Es, which is consistent with the slightly smaller ionic radius expected for Fm from the actinide contraction [17]. Fermium also exhibits a more acid behavior than the preceding actinides in aqueous solution, having a first hydrolysis constant of 1.6×10^{-4} [18].

David and co-workers have reported estimates of the thermodynamic properties of the 5f elements obtained from theoretical considerations and empirical correlations drawn from trends in the 4f series [12]. They suggest an ionic radius of 0.922 Å for Fm^{3+}. Lundqvist *et al.* have studied the migration rates of Fm in an electrical potential gradient using paper electrophoresis and report a hydrated radius of 4.95 Å and a hydration number of 16.9 in aqueous perchlorate solutions [19].

Fermium readily forms complexes with a variety of organic ligands, e.g. β-diketones [18], hydroxycarboxylic acids [4, 15, 20–22], organophosphorus esters [23–25], and alkylamines [26]. Lactic and α-hydroxyisobutyric acids have long been used as eluants for inner-series separation of trivalent actinides by cation-exchange chromatography. However, more recently, di-2-ethylhexyl-orthophosphoric acid [27] and Alamine 336 (a mixed n-octyl and n-decyl tertiary amine) [28] have been used for similar separations of Fm by solvent extraction chromatography.

The tendency of Fm to form a divalent ion under strong reducing conditions was first suggested by the work of Maly [29]. Using radiopolarographic techniques, David measured the half-wave potential for the $Fm^{2+} \rightarrow Fm(Hg)$ electrode process as -1.47 ± 0.01 V. By applying an estimated amalgamation potential correction, a value for $E^{\circ}(Fm^{2+} \rightarrow Fm)$ of -2.37 ± 0.1 V was reported [30]. An estimate of $E^{\circ}(Fm^{3+} \rightarrow Fm^{2+})$ of -0.8 V has been made by David [31] from his electrochemical experiments, and a value -1.15 V obtained from reduction/co-crystallization experiments with Yb by Mikheev *et al.* [32]. The former value is in reasonable agreement with the value of -1.1 ± 0.2 V calculated using refined electron-spin-pairing theory by Nugent [68]. Using this latter value of Nugent, and David's value for $E^{\circ}(Fm^{2+} \rightarrow Fm)$, a value of -1.95 ± 0.13 V

was calculated for $E°(Fm^{3+} \rightarrow Fm)$ [12, 30]. Nugent has also estimated $E°(Fm^{4+} \rightarrow Fm^{3+})$ to be +4.9 V [68]. All electrode potentials in this chapter are with reference to the normal hydrogen electrode (NHE) and the 1969 IUPAC convention, i.e. the more positive the potential the more stable the reduced form [33].

13.3 MENDELEVIUM

13.3.1 Introduction

The first isotope of element 101 was produced in 1955 by Ghiorso, Harvey, Choppin, Thompson, and Seaborg [34]. It was synthesized in the bombardment of approximately 10^9 atoms of ^{253}Es with 41 MeV alpha particles and produced at the rate of only about two atoms per 3 h bombardment. A chemical identification was made on the basis of its elution position just prior to Fm from a cation-exchange resin column using α-hydroxyisobutyric acid as eluant. It was not detected directly but by the observation of spontaneous fission events arising from its electron-capture daughter ^{256}Fm. Subsequent analysis of the data, coupled with further experimentation, showed the isotope to have mass 256 and to decay by electron capture with a half-life of 1.5 h. The name mendelevium was proposed in honor of Dimitri Mendeleev, in recognition of his contributions to the development of the periodic system, and has been accepted by IUPAC.

13.3.2 Isotopes of mendelevium

All the isotopes of mendelevium from mass 247 through mass 259 are known, with the exception of ^{253}Md; they can only be produced through charged-particle irradiations at accelerators (Table 13.3). Although ^{258}Md, with a half-life of 56 days, is the longest-lived isotope, ^{256}Md remains the isotope most often used in chemical experiments since it can be produced in relatively larger quantities. With the microgram amounts of ^{253}Es presently available, it is now possible to produce about 10^6 atoms per hour of ^{256}Md by alpha-particle bombardment [35].

13.3.3 Preparation and purification

The isotope ^{256}Md can best be produced for chemical study by the ^{253}Es(α,n) or ^{254}Es(α,2n) reactions at cyclotrons or linear accelerators. The peak cross-sections are approximately 1 mbarn at an alpha-particle bombarding energy of 38 MeV for the first reaction [36] and about 2 mbarn at a bombarding energy of 34 MeV for the second [37]. ^{254}Es would be the target material of choice if available. It has a half-life of 276 days compared to only 20.5 days for ^{253}Es and thus it would have a longer usable target lifetime.

The discovery experiments on mendelevium were the first in which the recoil momentum imparted to a product atom during its formation by the bombarding

Table 13.3 *Nuclear properties of mendelevium isotopes.*

Mass number	*Half-life*	*Mode of decay*	*Main radiations* (MeV)	*Method of production*
247	2.9 s	α	α 8.43	^{209}Bi (^{40}Ar, 2n)
248	7 s	EC ~ 80%	α 8.36 (~25%)	^{241}Am (^{12}C, 5n)
		α ~ 20%	8.32 (~75%)	^{239}Pu (^{14}N, 5n)
249	24 s	EC ⩽80%	α 8.03	^{241}Am (^{12}C, 4n)
		α ⩾20%		
250	52 s	EC 94%	α 7.82 (~30%)	^{243}Am (^{12}C, 5n)
		α 6%	7.75 (~70%)	^{240}Pu (^{15}N, 5n)
251	4.0 min	EC ⩾94%	α 7.55	^{243}Am (^{12}C, 4n)
		α ⩽6%		^{240}Pu (^{15}N, 4n)
252	2.3 min	EC		^{243}Am (^{13}C, 4n)
				^{238}U (^{19}F, 5n)
254[a]	10 min	EC		^{253}Es (α, 3n)
254[a]	28 min	EC		^{253}Es (α, 3n)
255	27 min	EC 92%	α 7.333	^{253}Es (α, 2n)
		α 8%	γ 0.453	^{254}Es (α, 3n)
256	1.27 h	EC 90.7%	α 7.205 (63%)	^{253}Es (α, n)
		α 9.3%	7.139 (16%)	
257	5.4 h	EC 90%	α 7.069	^{254}Es (α, n)
		α 10%		
258[a]	55 d	α	α 6.790 (28%)	^{255}Es (α, n)
			6.716 (72%)	
258[a]	43 min	EC ?		^{255}Es (α, n)
259	1.6 h	SF		^{259}No daughter

[a] Not known whether ground-state nuclide or isomer.

ion was used to carry out an instantaneous physical separation of the atom from the target material [38]. The recoil atoms were collected on a foil placed behind the target in the evacuated reaction chamber. This greatly shortened the separation time and made it possible to use the same valuable target in repeated bombardments. In later developments, it was found that the recoil atoms could be slowed down and stopped in a gaseous atmosphere, frequently helium. The gas could be pumped out of the reaction chamber through a small orifice to form a 'gas jet'. If this jet was impinged onto the surface of a foil, some fraction (frequently 70–80%) of the non-volatile product atoms carried along with the gas were deposited permanently on the surface [39, 40]. The foil could be removed periodically for processing and a new foil installed. By the 'gas jet' method, it is possible to transport and collect individual product atoms in a fraction of a second. Therefore, this method is quite generally used in the production and isolation of transeinsteinium elements.

After removal of the ^{256}Md atoms from the collector foil by acid etching or dissolution of the foil, they can be separated from other product activities and isolated by several different techniques.

The Md can be separated from the dissolved 'catcher' foil material, e.g. Be, Al, Pt or Au, and most fission-product activities by co-precipitation with lanthanum fluoride. Subsequent separation of trivalent actinides from lanthanide fission products and carrier can be accomplished with a cation-exchange resin column using a 90% water/10% ethanol solution saturated with HCl as eluant [15]. Final isolation of Md^{3+} from other trivalent actinides can be accomplished by selective elution from a cation-exchange resin column using α-hydroxyisobutyric acid [4]. Recently, inner-group separation of the 3+ actinides has been achieved by solvent extraction chromatography using di-2-ethylhexylorthophosphoric acid (HDEHP) as the stationary organic phase and HNO_3 as the mobile aqueous phase. Here, the actinide elution sequence is reversed from that of the cation-exchange resin columns and Md elutes just after Fm [41]. The method gives a somewhat better final separation of Md from Fm, but it has the disadvantage that Md elutes after Fm late in the sequence.

A separation scheme based on the reduction of Md to the 2+ state followed by isolation using solvent extraction chromatography has also been reported [19, 37]. After the initial steps of dissolution from the 'catcher' foil and co-precipitation with terbium fluoride, the mendelevium and 50 mg of Cr (added as a holding reductant) in 0.1 M HCl are co-reduced with Zn(Hg). The solution is passed through a solvent extraction column containing HDEHP adsorbed on an inert support as the stationary organic phase. The trivalent actinides and lanthanides are extracted by the HDEHP and held on the column while the divalent Md is not appreciably extracted and appears in the 0.1 M HCl washes of the column. After reoxidation of the Md and Cr to the trivalent states with H_2O_2, the residual impurities, including the Cr, are separated from Md by selective elution with 2 M (to remove impurities) and 6 M HCl (to remove Md) from a small column of Dowex 50 × 12 colloidal resin.

13.3.4 Atomic properties

The electronic structure of the ground state of gaseous mendelevium atoms has been predicted to be the $^2F^\circ_{7/2}$ level of the $5f^{13}7s^2$ configuration [42]. Experimental confirmation has not yet been attempted. No experimental measurements of inner-shell binding energies or x-ray energies have been reported.

13.3.5 Solution chemistry

Before its discovery, the trivalent state was predicted to be the most stable in aqueous solution and, therefore, Md was expected to exhibit a chemical behavior similar to the other 3+ actinides and lanthanides [43]. The elution of Md just prior to Fm in the elution sequence of trivalent actinides from a cation-exchange column observed in the discovery experiments appeared to confirm this prediction. Mendelevium forms insoluble hydroxides and fluorides that are

quantitatively co-precipitated with trivalent lanthanides [35]. Both the cation-exchange resin and HDEHP solvent extraction elution data are consistent with a trivalent state and an ionic radius slightly smaller than Fm.

David and co-workers have estimated an ionic radius of 0.912 Å for Md^{3+} and a divalent metallic radius of 1.94 Å [12]. Lundqvist *et al.* have studied the migration of Md^{3+} using electrophoresis techniques and reported a hydrated radius of 4.88 Å and hydration number of 16.2 [19].

Hulet and co-workers first noticed an anomalous chemical behavior for Md in certain chemical systems involving reducing conditions. With 10^5–10^6 atoms per experiment, co-precipitation with $BaSO_4$ and solvent extraction chromatography experiments with HDEHP were carried out in the presence of various reducing agents. These experiments showed that Md^{3+} could be readily reduced to a fairly stable Md^{2+} in aqueous solution [35]. Further, an estimate was obtained for the potential of the half-reaction $E^\circ(Md^{3+} \rightarrow Md^{2+}) \simeq -0.2$ V. Maly and Cunningham also produced the divalent state of Md and, from experiments similar to Hulet, estimated $E^\circ(Md^{3+} \rightarrow Md^{2+})$ at -0.1 V [44]. David and co-workers have reported the potentials for the couples $Md^{3+} \rightarrow Md$ and $Md^{2+} \rightarrow Md$ as -1.7 and -2.4 V, respectively [12]. Nugent predicted a value of $+5.4$ V for $E^\circ(Md^{4+} \rightarrow Md^{3+})$ [68].

In 1973, Mikheev *et al.* reported that a stable, monovalent Md ion could be produced in ethanol solutions and that it co-crystallized with CsCl [45]. However, Samhoun and co-workers studied the overall reduction of Md^{3+} to the amalgam using controlled potential electrolysis; they concluded that Md could not be considered a cesium-like element and no evidence was obtained consistent with a monovalent state [46, 47]. Hulet *et al.* have recently repeated some of the co-crystallization experiments of Mikheev and performed a series of new experiments in an attempt to prepare Md^{+} by reduction with Sm^{2+} in ethanol solutions and also in fused KCl media [37]. In these experiments, the behavior of Md was compared to tracer amounts of 3+, 2+, and 1+ions and Md consistently followed the 2+ ions. They concluded that Md cannot be reduced to a monovalent state with Sm^{2+} as claimed by Mikheev. However, on the basis of the results of thermodynamic studies of the co-crystallization process of mendelevium with chlorides of alkali metals, the Russian investigators maintain that Md can be reduced to the monovalent state in water–ethanol solutions and that the co-crystallization of Md^{+} with salts of divalent ions can be explained as being due to the formation of mixed crystals [102, 103]. An ionic radius of 1.17 Å was calculated for Md^{+} from the results of the co-crystallization studies [104].

Unsuccessful attempts have been made to oxidize Md^{3+} to Md^{4+} using the strong oxidant sodium bismuthate [35]. Thus, Md^{3+} is not readily oxidized, in agreement with Nugent's predicted value of 5.4 V for the couple.

13.4 NOBELIUM

13.4.1 Introduction

The discovery of element 102 was first reported in 1957 by an international research team working at the Nobel Institute in Stockholm [48]. During the bombardment of a ^{244}Cm target with ^{13}C ions, an 8.5 MeV alpha activity was observed which decayed with a half-life of approximately 10 min. The alpha activity eluted just prior to Es and Fm from a cation-exchange resin column using α-hydroxyisobutyric acid as eluant and appeared in the trivalent actinide fraction with Cf and Fm, also produced in the irradiations, from a cation-exchange resin column using 6 N HCl as eluant. This behavior was taken as chemical evidence for the production of an isotope of element 102, and a mass number of 251 or 253 was suggested. The name, nobelium, was proposed in honor of Alfred Nobel, in recognition of his support of the natural sciences, and in honor of the Nobel Institute where the experiments took place.

In the following 10 years, researchers at both the Lawrence Berkeley Laboratory and the Dubna Research Center attempted to repeat the Nobel Institute experiments, but were unsuccessful. However, the Berkeley group did succeed in identifying an isotope of element 102 for the first time in 1958 [49]. Isotopes of element 102 from mass 251 through 259 are now known, and, where the same isotopes have been studied, the Dubna and Berkeley groups are substantially in agreement [50]. The results of both efforts exclude the likelihood of any isotope of element 102 having a half-life of 10 min with the emission of 8.5 MeV alpha particles. Furthermore, chemical studies [51] showed that, because of its divalency, element 102 could not have exhibited the cation-exchange behavior attributed to the 10 min activity. A discussion of the history of the discovery of element 102 was published by Ghiorso and Sikkeland in 1967 [50] and, because of the wide use of the name over many years, the suggestion was made that nobelium be retained as the name of element 102.

Because No is normally a divalent ion in aqueous solution and is difficult to oxidize and hold in the trivalent state, it has not been possible to make a chemical identification of the atomic number in the same manner as the preceding 3+ actinides, i.e. identification by their unique positions in the elution sequence from cation-exchange resin columns. However, in 1971, the atomic number of ^{255}No was unequivocally determined through the observation of characteristic K-series x-rays of the daughter isotope ^{251}Fm in coincidence with the alpha particles from the decay of the parent, ^{255}No [10].

13.4.2 Isotopes of nobelium

The isotopes of nobelium, masses 251 through 259, have been produced (Table 13.4). The isotope ^{259}No is the longest-lived, with a half-life of 58 min. However, the peak production rate via the ^{248}Cm(^{18}O,α3n) reaction is only about 100

Table 13.4 *Nuclear properties of nobelium isotopes.*

Mass number	*Half-life*	*Mode of decay*	*Main radiations* (MeV)	*Method of production*
250[a]	0.25 ms	SF		$^{233}U(^{22}Ne, 5n)$
251	0.8 s	α	α 8.68 (20%) 8.60 (80%)	$^{244}Cm(^{12}C, 5n)$
252	2.3 s	α 73% SF 27%	α 8.415 (~ 75%) 8.372 (~ 25%)	$^{244}Cm(^{12}C, 4n)$ $^{239}Pu(^{18}O, 5n)$
253	1.7 min	α	α 8.01	$^{246}Cm(^{12}C, 5n)$ $^{242}Pu(^{16}O, 5n)$
254	68 s	α	α 8.086	$^{246}Cm(^{12}C, 4n)$ $^{242}Pu(^{16}O, 4n)$
254 m	0.28 s	IT		$^{246}Cm(^{12}C, 4n)$ $^{249}Cf(^{12}C, \alpha 3n)$
255	3.1 min	α 61.4% EC 38.6%	α 8.121 (46%) 8.077 (12%)	$^{248}Cm(^{12}C, 5n)$ $^{249}Cf(^{12}C, \alpha 2n)$
256	3.3 s	α ~99.7% SF ~0.3%	α 8.43	$^{248}Cm(^{12}C, 4n)$
257	25 s	α	α 8.27 (26%) 8.22 (55%)	$^{248}Cm(^{12}C, 3n)$
258	1.2 ms	SF		$^{248}Cm(^{13}C, 3n)$
259	1.00 h	α ~78% EC ~22%	α 7.533 (23%) 7.500 (38%)	$^{248}Cm(^{18}O, \alpha 3n)$

[a] The identity of this nuclide is not well-established.

atoms per hour [52]. The next longest-lived isotope is ^{255}No, with a half-life of 3 min. A considerably higher production rate, several hundred atoms per minute, can be achieved for ^{255}No using the $^{249}Cf(^{12}C,\alpha 2n)$ reaction. Thus, this isotope has most often been used for chemical studies.

13.4.3 Preparation and purification

The isotope ^{255}No can be produced for chemical study via the $^{249}Cf(^{12}C,\alpha 2n)$ reaction; about 1200 atoms were produced in a 10 min irradiation of a 350 $\mu g\ cm^{-2}$ target of ^{249}Cf with 3×10^{12} particles per second of 73 MeV ^{12}C ions [10].

As with Md, the physical separation of the nobelium atoms from the target material can be made using the recoil-atom catcher technique. It is preferable to combine this with the 'gas jet' technique since the atoms are deposited on the 'catcher' foil in nearly a monolayer and can be easily rinsed off the surface with dilute acid without complete dissolution of the foil. Isolation of the No from other actinides produced in the bombardment and from any target material transferred to the foil can be readily made using schemes based on the separation of divalent ions from trivalent ones, e.g. selective elution by solvent extraction chromatography using HDEHP as the stationary organic phase and 0.05 N HCl

as the mobile aqueous phase [53]. Under these conditions, No passes through the column in the first few column volumes while the trivalent actinides are strongly adsorbed. Selective elution from a cation-exchange resin column, e.g. Dowex 50 × 4, can also be made using 3 N HCl as eluant. Here, No again elutes in a few column volumes and the trivalent actinides remain on the column [52].

13.4.4 Atomic properties

The electronic ground state of gaseous nobelium atoms has been predicted to be the $^1S_0$ level of the $5f^{14}7s^2$ configuration [42]. No experimental information is available.

The characteristic K-series x-rays of ^{253}No emitted following the alpha decay of ^{257}104 have been measured in alpha/x-ray coincidence experiments [54]. Values for $K\alpha_2$ and $K\alpha_1$ were given as 120.9 ± 0.3 and 127.2 ± 0.3 keV, respectively. Carlson and Nestor have predicted values of 120.967 and 127.368 keV for these x-rays [8].

13.4.5 Solution chemistry

Before its discovery, nobelium was expected to be a trivalent ion in aqueous solution and to exhibit a chemical behavior similar to the elements preceding it in the actinide series. However, in 1949, Seaborg predicted that a relatively stable 2+ state might exist for element 102 due to the special stability of the filled $5f^{14}$ electronic configuration [55]. Twenty years later, this prediction was confirmed.

In over 600 experiments, Maly *et al.* subjected about 50 000 atoms of ^{255}No to cation-exchange and co-precipitation studies [51]. These tracer experiments showed that nobelium exhibits a chemical behavior substantially different from the trivalent actinides but similar to the divalent alkaline-earth elements, Sr, Ba, and Ra. Thus, the divalent ion of nobelium is the most stable species in aqueous solution. Additional experiments, which used the technique of solvent extraction chromatography, were performed under a variety of oxidizing conditions and allowed an estimate of $+1.45$ V for $E^\circ(No^{3+} \rightarrow No^{2+})$ [53].

Chuburkov and co-workers have compared the behavior of nobelium with those of Tb, Cf, and Fm during chlorination and adsorption experiments [56]. They concluded that the chloride of element 102 undergoes strong adsorption on solid surfaces and therefore is not very volatile; its volatility is close to the chlorides of Tb, Cf, and Fm. The chloride of either divalent or trivalent nobelium would be expected to exhibit a low volatility.

Silva, McDowell, Keller, and Tarrant have made further solvent extraction and cation-exchange studies of nobelium [57]. Its complexing ability with chloride ions was compared with that of divalent mercury, cadmium, copper, cobalt, and barium, and it was found to be most similar to the relatively weakly complexed alkaline earth. The elution behavior of nobelium was compared with the alkaline earths in a cation-exchange resin/HCl system and found to be most like Ca^{2+};

comparison with these elements in a di-2-ethylhexylorthophosphoric acid (HDEHP) liquid–liquid extraction system showed nobelium to have an extraction behavior between that of Ca^{2+} and Sr^{2+}. The determination of the distribution coefficients of nobelium in an $HDEHP/HNO_3$ system as a function of pH allowed a direct determination of the valence as 2+. The ionic radius of No^{2+} was estimated from a linear correlation of ionic radius with distribution coefficient for several divalent ions. A value of 1.0 Å was obtained from ion-exchange data and 1.1 Å from liquid–liquid extraction data, with theoretical calculations giving a value of 1.1 Å. The single-ion heat of hydration, obtained from a Born-type calculation, was -1486 kJ mol^{-1}. David *et al.* have estimated a divalent metallic radius of 1.94 Å for No and an ionic radius of 0.900 Å for No^{3+} [12].

The tendency of divalent No to form complexes with citrate, oxalate, and acetate ions in aqueous solution has been studied by McDowell *et al.* using solvent extraction techniques [58]. In general, the complexing tendency of nobelium is between that of Ca and Sr, being more like Sr. Formation constants for the 1:1 complexes of 151.9 ± 18.5, 48 ± 5.6, and -5 ± 5 l mol^{-1} for citrate, oxalate, and acetate were reported.

Meyer *et al.*, using a modified radiopolarographic technique, have measured the half-wave potential for the reduction of nobelium at a mercury electrode and report a value for $E^{\circ}(No^{2+} \rightarrow No(Hg))$ of -1.6 V [59]. After applying an estimated amalgamation potential correction, a value of -2.6 V was calculated for the standard potential of the $No^{2+} \rightarrow No$ couple. This couple, combined with the measured III/II couple, results in an estimated value for $E^{\circ}(No^{3+} \rightarrow No)$ of -1.25 V. Nugent has calculated a value of $+6.5$ V for $E^{\circ}(No^{4+} \rightarrow No^{3+})$ [68].

13.5 LAWRENCIUM

13.5.1 Introduction

In 1961, Ghiorso, Sikkeland, Larsh, and Latimer of the Lawrence Berkeley Laboratory reported the discovery of element 103 [60]. An 8.6 MeV alpha activity with a half-life of 8 s was produced in bombardments of a Cf target with both ^{10}B and ^{11}B ions. Owing to the short half-life, a chemical identification was not possible but the alpha activity was attributed to an isotope of element 103 on the basis of convincing nuclear evidence, i.e. the results of cross-bombardments with other targets and projectiles. However, because the target consisted of a mixture of californium isotopes, $^{249-252}Cf$, an unambiguous mass assignment was not possible. Though isotopes with masses 255–259 could have been produced, the highest yield was expected for mass 257. The discoverers suggested the name lawrencium, symbol Lw, for the new element in honor of E. O. Lawrence, inventor of the cyclotron and founder of the Lawrence Berkeley Laboratory. The name was accepted by IUPAC but the symbol was changed to Lr.

The results of subsequent studies on the production and identification of ^{255}Lr, ^{256}Lr, and ^{257}Lr by researchers at the Joint Institute for Nuclear Research (JINR) at Dubna, USSR, seemed to conflict with the Berkeley mass assignment since none of these isotopes appeared to have the decay properties of the original Berkeley alpha activity [61]. However in 1971, six alpha-emitting isotopes of lawrencium, masses 255–260, were produced at Berkeley in bombardments of nearly isotopically pure targets of ^{248}Cm with ^{14}N and ^{15}N ions and ^{249}Cf with ^{10}B and ^{11}B ions, and the apparent discrepancy was resolved [62]. From the Berkeley experiments, ^{257}Lr was found to emit alpha particles of 8.8 MeV with a half-life of only 0.6 s but ^{258}Lr was found to have a half-life of 4.2 s with the emission of 8.62 MeV alpha particles. Thus, Ghiorso and associates considered that the mass assignment made in 1961 should have been 258. The difference in this new half-life value compared to the 1961 value was attributed to relatively poor counting statistics resulting from the small number of alpha-particle events observed in the earlier work.

13.5.2 Isotopes of lawrencium

Seven isotopes of lawrencium are now known with masses 254–260 (Table 13.5). The longest-lived isotope is ^{260}Lr, with a half-life of approximately 3 min. However, this isotope can be produced only by rather low-yield reactions, e.g. ^{248}Cm(^{15}N,3n) and ^{249}Bk(^{18}O,α3n), at rates of about one atom per 10 min bombardment [62]. Though shorter-lived, ^{256}Lr, with a half-life of 31 s, can be produced at an appreciably higher rate and has been the only isotope used in chemical studies.

Table 13.5 *Nuclear properties of lawrencium isotopes.*

Mass number	*Half-life*	*Mode of decay*	*Main radiations* (MeV)	*Method of production*
253	1.3 s	α	α 8.800 (56%)	^{257}105 daughter
254	13 s	α	α 8.460 (54%)	^{258}105 daughter
255	22 s	α	α 8.43 (40%)	^{243}Am (^{16}O, 4n)
			8.37 (60%)	^{249}Cf (^{11}B, 5n)
256	28 s	α	α 8.52 (19%)	^{243}Am (^{18}O, 5n)
			8.43 (37%)	^{249}Cf (^{11}B, 4n)
257	0.65 s	α	α 8.86 (85%)	^{249}Cf (^{11}B, 3n)
			8.80 (15%)	^{249}Cf (^{14}N, α2n)
258	4.3 s	α	α 8.621 (25%)	^{248}Cm (^{15}N, 5n)
			8.595 (46%)	^{249}Cf (^{15}N, α2n)
259	5.4 s	α	α 8.45	^{248}Cm (^{15}N, 4n)
260	3.0 min	α	α 8.03	^{248}Cm (^{15}N, 3n)

13.5.3 Preparation and purification

The isotope ^{256}Lr can be produced in the highest yields by the ^{249}Cf(^{11}B,4n) reaction; an average of about 10 atoms per irradiation were produced in 3 min bombardments of a 250 μg cm^{-2} target of ^{249}Cf with about 5×10^{12} particles per second of 70 MeV ^{11}B ions [63].

As with Md and No, the physical separation of the Lr atoms from the target material and subsequent rapid collection is best accomplished using a recoil-atom gas-jet system of some type. Because of the short half-life of ^{256}Lr, further chemical purification is not feasible before study. It is distinguished from other possible alpha-emitting nuclides in the sample by its unique alpha-particle energy of 8.24 MeV.

13.5.4 Atomic properties

The electronic structure of the ground state of neutral atoms of Lr has been predicted to be the $^2D_{3/2}$ level of the $5f^{14}6d^17s^2$ configuration [64]. However, recent relativistic Dirac–Hartree–Fock calculations have been made for the low-lying electronic states of Lr, and the ground state of Lr could be either the $5f^{14}6d^17s^2$ or the $5f^{14}7p^17s^2$ configuration [65]. The separation in the calculated energy difference between these two levels is less than the uncertainty in their calculated energies. No experimental information is available.

The characteristic L-series x-rays of ^{256}Lr have been observed in coincidence with alpha particles of the parent ^{260}105 by Bemis *et al.* [66]. Their results are compared with the calculations of Carlson and Nestor in Table 13.6.

13.5.5 Solution chemistry

In 1949, element 103 was predicted by Seaborg to be the last member of the

Table 13.6 *Comparison of calculated and measured L-series x-rays for Lr.*

	X-ray energy (keV)	
Transition	*Calc.* [8]	*Meas.* [66][a]
$L\beta_4$ ($3p_{1/2} \rightarrow 2s$)	22.616	22.61 (18)
$L\beta_1$ ($3d_{3/2} \rightarrow 2p_{1/2}$)	23.926	24.03 (14)
$L\gamma_1$ ($4d_{3/2} \rightarrow 2p_{1/2}$)	27.910	27.97 (15)
Ll ($3s \rightarrow 2p_{3/2}$)	14.439	14.43 (20)
$L\alpha_1$ ($3d_{5/2} \rightarrow 2p_{3/2}$)	17.482	17.57 (12)
$L\beta_2$ ($4d_{5/2} \rightarrow 2p_{3/2}$)	21.248	21.35 (20)

[a] Error in last two digits is given in parentheses.

proposed actinide or 5f series of elements and to be similar to lutetium with respect to the stability of the 3+ oxidation state in aqueous solution [55]. It required nearly 20 years finally to synthesize this element and to conduct chemical experiments to confirm this prediction.

Silva and co-workers employed a fast solvent extraction procedure using methyl isobutyl ketone containing the chelating agent thenoyltrifluoroacetone (TTA) as the organic phase and buffered acetate solutions as the aqueous phase to distinguish between the 2+, 3+, and 4+ oxidation states [63]. In over 200 separate experiments, approximately 1500 atoms of ^{256}Lr were produced for study and the extraction behavior of Lr was compared with that of a number of tetravalent (Th, Pu) and trivalent (Fm, Cf, Cm, Am, Ac) actinides as well as several divalent ions (No, Ba, Ra). In these experiments, lawrencium was found to extract into the organic phase at the lower end of the pH range for the 3+ ions along with Fm and Cf. It was therefore concluded that 3+ is the most stable oxidation state for Lr in aqueous solution.

From comparative studies of the retention times of chlorinated atoms of several different actinides and transactinides as they passed through a heated glass column, Chuburkov *et al.* concluded that the chloride of element 103 has an adsorbability on solid surfaces, and hence volatility, similar to the chlorides of Cm, Fm, and No and to be much less volatile than the chlorides of element 104 or Hf [67]. This result was said to be consistent with element 103 being eka-lutetium.

Since Lr is a trivalent ion in aqueous solution, it should exhibit a chemical behavior similar to the other 3+ actinides and lanthanides, e.g. insoluble fluoride and hydroxide. One would expect Lr^{3+} to have a slightly smaller ionic radius than Md^{3+} and to elute before Md from a Dowex 50 cation-exchange resin column using α-hydroxyisobutyric acid as eluant (see Fig. 13.1). David *et al.* have estimated an ionic radius of 0.893 Å for Lr^{3+} and a metallic radius of 1.71 Å for trivalent Lr [12]. Nugent has calculated values of -2.0 V for $E^\circ(Lr^{3+} \rightarrow Lr)$ and $+7.9$ V for $E^\circ(Lr^{4+} \rightarrow Lr^{3+})$ [68].

Nugent has made correlations of the III/II oxidation potentials for the actinides and lanthanides using Jorgensen's refined spin-pairing electronic energy theory [68]. In Fig. 13.2, the known III/II oxidation potentials of the actinides are compared with the lanthanides and with calculated values. The excellent correlation of the measured potentials with the potentials calculated on the basis of the actinide theory supports the notion that the end of the 5f series has been reached with Lr. Thus, all the available experimental and theoretical evidence supports the original prediction [43] that element 103 is the last member of the actinide series of elements and that element 104 would be expected to fall into the next chemical group, i.e. the IV B group, of the periodic table.

A summary of some of the chemical properties of elements 100–103 is given in Table 13.7.

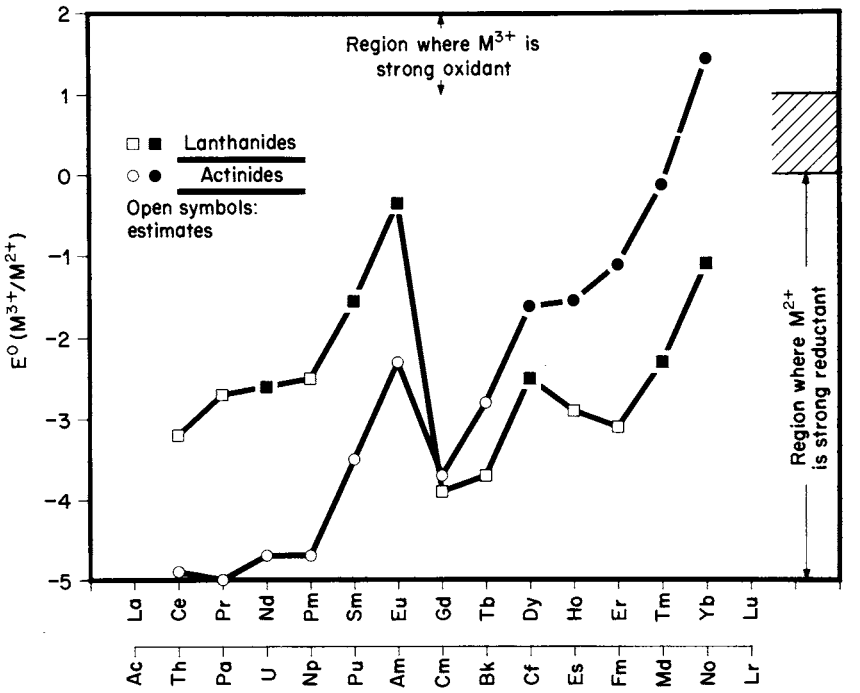

Fig. 13.2 *Correlations of the III–II reduction potentials for the actinides and lanthanides. The points are experimental values for the actinides.*

Table 13.7 *Summary of chemical peoperties of elements* 100–103.

	100	101	102	103
electron configuration[a]	$5f^{12}7s^2$	$5f^{13}7s^2$	$5f^{14}7s^2$	$5f^{14}6d^17s^2$
stable oxidation states[b]	3	3, 2	3, 2	3
ionic radius of indicated ion (Å)	0.922(3+)	0.912(3+)	1.05(2+)	0.893(3+)
standard electrode potential (V)	−2.07(3+ → 0)	−1.74(3+ → 0)	−2.6(2+ → 0)	−2.06(3+ → 0)
first ionization potential (V)[c]	6.50	6.58	6.65	

[a] Electronic ground-state configuration of free neutral atom + Rn core.
[b] Most stable state in aqueous solution underlined.
[c] From ref. 42.

13.6 ELEMENT 104

13.6.1 Introduction

In 1964, Flerov and co-workers at Dubna reported the production of an isotope of element 104 [69]. Bombardments of ^{242}Pu with ^{22}Ne ions were carried out inside the cyclotron and a spontaneous-fission activity with a half-life of about

0.3 s was detected using mica track detectors. A mass of 260 was assigned on the basis of the measured excitation functions. The name kurchatovium, Ku, was suggested for the new element.

In 1969, after bombardments of ^{246}Cm and ^{248}Cm with ^{18}O and ^{16}O ions to produce the same compound nucleus as in the Dubna experiments at expected higher production rates, Ghiorso and associates reported that they were unable to confirm the Dubna results [71]. Also, in 1969, the Berkeley group published the results of their bombardments of ^{249}Cf with ^{12}C and ^{13}C ions [72]. Two new alpha-emitting isotopes of element 104 were produced (Table 13.8). Though the measured excitation functions agreed with those calculated for ^{257}104 and ^{259}104, the final proof of atomic number and mass assignments came from the establishment of genetic linkages to the known daughter isotopes ^{253}No and ^{255}No, respectively. On the basis of their own results and the failure to confirm the Dubna results, Ghiorso and co-workers claimed the discovery of element 104 and suggested the name rutherfordium, Rf. Since that time, the atomic number of ^{257}104 has been confirmed by Bemis *et al.* in experiments where the characteristic K-series x-rays emitted by the daughter isotope ^{253}No were observed in coincidence with the alpha particles emitted in the decay of the parent ^{257}104 [54].

Shortly after publication of the Berkeley results, the Dubna research team repeated their original experiments using an external beam of Ne ions rather than an internal beam. They detected a spontaneous-fission activity with a half-life three times shorter than originally reported in 1964 or about 0.1 s [70]. The Dubna researchers attributed this discrepancy to a high background in their track

Table 13.8 *Nuclear properties of element* 104 *isotopes.*

Mass number	*Half-life*	*Mode of decay*	*Main radiations* (MeV)	*Method of production*
253[a]	~ 1.8 s	SF ~50%		^{206}Pb(^{50}Ti, 3n)
254[a]	0.5 ms	SF		^{206}Pb(^{50}Ti, 2n)
255	1.4 s	α ~55% SF ~45%	α 8.73	^{207}Pu(^{50}Ti, 2n)
256	7.4 ms	SF, α	α 8.812	^{208}Pb(^{50}Ti, 2n)
257	4.3 s	α ~ 70% SF ~14% (?) EC ~ 16%	α 9.012 (18%) 8.977 (29%)	^{208}Pb(^{50}Ti, n)
258[a]	13 ms	SF		^{249}Cf(^{12}C, 3n) ^{246}Cm(^{16}O, 4n)
259	3.4 s	α 91% SF 9%	α 8.87 (~ 40%) 8.77 (~ 60%)	^{249}Cf(^{13}C, 3n) ^{248}Cm(^{16}O, 5n)
260[a]	21 ms	SF		^{248}Cm(^{16}O, 4n)
261	1.1 min	α	α 8.28	^{248}Cm(^{18}O, 5n)
262[a]	47 ms	SF		^{248}Cm (^{18}O, 4n)

[a] The identity of this nuclide is not well-established.

detectors produced by the intense neutron field inside the cyclotron accelerating chamber. A re-evaluation of the original excitation function data led to a relaxation in the mass assignment to 260 ± 1. The shorter half-life value implied that detection of this activity might have been missed by the Berkeley scientists since the Berkeley experiments were designed to look for half-lives in the vicinity of 0.3 s. However, numerous attempts have been made by the Berkeley group to produce this activity in the intervening years, using a variety of targets and projectiles, but a 0.1 s spontaneous-fission activity has never been detected [73].

The disagreement between the Berkeley and Dubna groups has not been resolved and neither of the names suggested for element 104 have been officially accepted by IUPAC. In this connection, it should be mentioned that a group of nuclear scientists, composed of members from France, West Germany, and the USA, have attempted to provide guidelines for establishing the discovery of chemical elements and published a set of criteria in 1976 [74]. Briefly, they suggested that the basic criteria must be proof that the atomic number of a new nuclide is different from all previously known elements, i.e. the experiments, chemical or nuclear, should be of such a nature as to establish a direct and unambiguous connection to atomic number.

13.6.2 Predicted chemical properties

Since element 103, Lr, is the last member of the actinide or 5f series of elements, element 104 was expected to be the first member of the next group of the periodic table, i.e. the group IV B elements. Indeed, from the results of relativistic Dirac–Fock calculations, the electronic ground-state configuration for a neutral free atom of element 104 was predicted to be $5f^{14}6d^{2}7s^{2}$ [75]. It is expected to have a valence and ionic radius similar to Zr and Hf and to exhibit similar chemical properties [76, 77]. Using equations developed by Jorgensen, Penneman and Mann have predicted that element 104 should be predominantly tetravalent in aqueous solution and solid compounds; however, the chemistry of element 104 may involve 2+ and 3+ as well [78]. Further, the hydrolytic properties and the solubility of compounds of element 104 are expected to be similar to Hf [75]. Some of the chemical properties predicted for element 104 are given later in Table 13.10.

13.6.3 Measured chemical properties

In a collaborative experiment, Berkeley and Oak Ridge experimenters working at the Lawrence Berkeley Laboratory employed the technique of ion-exchange chromatography for their chemical studies of element 104 [79]. The atoms of $^{261}104$ produced in the $^{248}Cm(^{18}O,5n)$ reaction were passed through a small Dowex 50 cation-exchange resin column using α-hydroxyisobutyric acid as eluant. The elution behavior of $^{261}104$ was compared with those of a number of other elements, including trivalent actinides, No^{2+}, Hf^{4+}, and Zr^{4+}. In several

hundred repetitive experiments, approximately 100 atoms of element 104 were produced for study. From these comparative measurements, the column elution behavior of element 104 was found to be entirely different from the trivalent actinides and nobelium but similar to Hf and Zr.

In further ion-exchange experiments using solvent extraction chromatography, Hulet and co-workers investigated the chloride complexation of element 104 and compared it to that of the actinides and Hf [80]. The anionic chloride complexes of $^{261}104$ were compared to those of Hf, Cm, and Fm by testing their relative adsorbabilities onto a column containing a quaternary amine. The results showed that in 12 M HCl solutions the chloride complexation of element 104 was clearly stronger than those of the trivalent actinides and quite similar to that of Hf.

Researchers at JINR, Dubna, concentrated their efforts to separate element 104 from the actinides on a rapid gas-phase technique [81]. Atoms of a spontaneously fissioning activity, produced in the bombardment of ^{242}Pu with ^{22}Ne ions (the compound nucleus would be element 104), were collected in a gas stream and mixed with the chlorinating agents and carrier gases thionyl chloride, niobium pentachloride, and zirconium tetrachloride. After passing through a 2 m long heated glass column, the gases flowed between mica track detectors for recording fission events. The retention times in the column, i.e. the adsorbabilities, were measured for a number of elements and correlated with known heats of vaporization. From comparative measurements, the Dubna group reported that the chloride volatility of the spontaneous-fission activity was similar to Hf and Zr but quite different from those of the actinides [82]. At the time of these chemistry experiments at Dubna, it was assumed that the spontaneous-fission activity being studied was the 0.3 s activity reported in 1964. After the half-life of the spontaneous-fission activity ascribed to element 104 was reduced to 0.1 s, it became clear to the Dubna researchers that such a short-lived activity could not have survived passage through the column, owing to the relatively long column retention time of about 0.4 s, and that the half-life of the activity studied must have been 1 s or more [83]. Later, the Dubna chemists argued that the nuclide they had been studying was $^{259}104$, the alpha-emitting isotope discovered by the Berkeley group, and that it must have a small spontaneous-fission decay branch [84].

Thus, all the available experimental information is consistent with the contention that element 104 is eka-hafnium.

13.7 ELEMENT 105

13.7.1 Introduction

In 1968, Flerov and co-workers reported the synthesis of two short-lived alpha emitters of energies 9.4 and 9.7 MeV produced in the bombardment of ^{243}Am with ^{22}Ne ions and, on the basis of delayed coincidence correlations with their suspected daughter alpha activities, tentatively assigned them to $^{261}105$ and

^{260}105, respectively [85]. There were, however, interfering alpha activities produced by the interaction of the Ne ions with small amounts of Pb in the Am target. Thus, an unambiguous interpretation was not possible and it is not certain whether either of these alpha activities was associated with element 105. Attention was then shifted to spontaneous-fission studies.

In early 1970, Ghiorso and colleagues published data from experiments to produce isotopes of element 105 via the ^{249}Cf(^{15}N,*x*n) reactions [86]. They were unable to confirm the earlier Dubna assignments of 9.4 and 9.7 MeV alpha emitters to element 105 but reported the discovery of an alpha emitter of 9.06, 9.10, and 9.14 MeV particles with a half-life of 1.6 s. The alpha activity was assigned to ^{260}105 from the establishment of a genetic linkage to the known daughter isotope ^{256}Lr by coincidence correlations in the time sequence between the decay of the two nuclides. Shortly thereafter, the Berkeley group synthesized two additional isotopes, ^{261}105 and ^{262}105 [87] (Table 13.9). On the basis of their discovery of ^{260}105, the Berkeley group proposed that element 105 be named hahnium, Ha.

In 1977, Bemis *et al.* confirmed the atomic number assigned to the 1.6 s alpha emitter through the observation of the characteristic L-series x-rays emitted by the element 103 daughter following and in coincidence with the alpha particles [66]. The mass number was confirmed as well by establishment of a genetic linkage between the alpha decay of the 1.6 s activity and the alpha decay of the known isotope ^{256}Lr.

Also in early 1970, the Dubna group published several reports on the production of a spontaneously fissioning nuclide with a half-life of 2 s in the irradiations of ^{243}Am with ^{22}Ne ions [88, 89]. The measured excitation function followed that expected for the ^{243}Am(^{22}Ne,4n) reaction and the activity was assigned to ^{261}105; however, the assignment to ^{260}105, produced by the 5n reaction, was not excluded. A few months later, Zvara and associates performed chemical experiments on an approximately 2 s fission activity using gas-phase techniques and reported that its chloride was less volatile than niobium chloride but more volatile than hafnium chloride, a property predicted for eka-tantalum [90]. In mid-1970, after the Berkeley report on the discovery of ^{260}105, the Dubna group reported the results of further attempts to produce and identify alpha-particle-emitting isotopes of element 105 using a new ^{243}Am target containing 100 times less Pb impurity than the target used in their earlier experiments. A time correlation was reported between observed alpha particles of 8.9 and 9.1 MeV ($\sim$ 2 s half-life) and 8.25–8.6 MeV alpha particles of the 35 s daughter, ^{256}Lr or ^{257}Lr. Thus, the alpha activity was assigned to ^{260}105 or ^{261}105 [91]. It was later shown, however, that ^{257}Lr emits alpha particles of 8.87 MeV with a half-life of 0.6 s [62] and thus the isotope ^{261}105 could not have been identified by this correlation.

An exchange of letters on the priority of discovery of element 105 has appeared in *Science* [92]. As yet no official name has been accepted by IUPAC for element 105.

13.7.2 Predicted chemical properties

From the results of relativistic Dirac–Fock calculations, the electronic ground-state configuration of the free neutral atom of element 105 was predicted to be $5f^{14}6d^{3}7s^{2}$ [75]. It is expected to belong to the group V B elements of the periodic table and to exhibit chemical properties resembling Nb and Ta [75]. The pentavalent state is predicted to be the most important for element 105; however, it could exhibit several oxidation states, i.e. 3+ and 4+, as well [78]. Like Ta, element 105 should form an extensive range of complex ions. Some of the predicted chemical properties of element 105 are given later in Table 13.10.

13.7.3 Measured chemical properties

Experiments have been performed on the chemical separation of radioactive products formed in the bombardment of ^{243}Am with ^{22}Ne ions (the compound nucleus is element 105) [90, 93, 94]. Gaseous chlorides of the products were allowed to flow through a glass chromatographic column over which a temperature gradient from 300 to 50°C was established. The products were adsorbed from the flowing carrier gas onto the walls and formed zones in different temperature regions. Contained in the tube were mica detectors for recording spontaneous-fission events. From the position of the zone of an unknown nuclide relative to the zones of known elements, it is possible to estimate the volatility of its chloride. On the basis of 18 events, the spontaneous-fission activity was reported to form a chloride less volatile than niobium pentachloride but more volatile than hafnium tetrachloride, a property predicted for element 105, eka-tantalum, on the basis of the periodic system. There is no information on the solution chemistry of element 105.

13.8 ELEMENT 106

13.8.1 Introduction

In 1974, Ghiorso and associates at the Lawrence Berkeley Laboratory reported evidence for the discovery of element 106 [95]. An alpha emitter with a half-life of 0.9 s and principal alpha energy of 9.06 MeV was produced in the bombardments of ^{249}Cf with ^{18}O ions. This alpha activity was assigned to ^{263}106 (Table 13.9) from the establishment of a genetic relationship with the known daughter ^{259}104 and granddaughter ^{255}No using correlated decay-sequence data.

Also in 1974, Oganesyan and co-workers of JINR, Dubna, reported the production of spontaneously fissioning nuclei with a half-life of several milliseconds in bombardments of ^{207}Pb and ^{208}Pb with ^{54}Cr ions [96]. On the basis of their new understanding of spontaneous-fission systematics derived from studies on elements 100–104 and from the results of cross-bombardments of targets of different Pb and Bi isotopes with ^{51}V, ^{52}Cr, and ^{54}Cr ions, the Dubna

researchers considered that it was reasonable to assume that the new spontaneous-fission activity was associated with the element 106, probably $^{259}106$ (Table 13.9). However, a direct connection to atomic number was not established and other interpretations are equally possible.

In view of the simultaneity of the experiments at Berkeley and Dubna, and their very different nature, the suggestion of a name for element 106 has been postponed until the situation has been clarified. See also Armbruster [106].

13.8.2 Predicted chemical properties

The results of relativistic Dirac–Fock calculations suggest the electronic ground-state configuration of the free neutral atom of element 106 to be $5f^{14}6d^{4}7s^{2}$ and

Table 13.9 *Nuclear properties of elements 105–109 isotopes.*

Mass number	*Half-life*	*Mode of decay*	*Main radiations (MeV)*	*Method of production*
Element 105				
255[a]	1.5 s	SF ~20%		$^{207}Pb(^{51}V, 3n)$ $^{206}Pb(^{51}V, 2n)$
257	1.4 s	α, SF	α 9.160 (30%) 8.970 (40%)	$^{209}Bi(^{50}Ti, 2n)$
258	4.4 s	α	α 9.172 (59%) 9.08 (28%)	$^{209}Bi(^{50}Ti, n)$
260	1.5 s	α ≥90% SF ≤9.6% EC ≤2.5%	α 9.08 (28%) 9.05 (53%)	$^{249}Cf(^{15}N, 4n)$ $^{243}Am(^{22}Ne, 5n)$
261	1.8 s	α ~75% SF ~25%	α 8.93	$^{243}Am(^{22}Ne, 4n)$ $^{249}Bk(^{16}O, 4n)$
262	34 s	SF ~78% α ~22% EC <5%	α 8.530 (16%) 8.45 (80%)	$^{249}Bk(^{18}O, 5n)$
Element 106				
259	0.48 s	α	α 9.63	$^{207}Pb(^{54}Cr, 2n)$
260	3.6 ms	α, SF	α 9.76	$^{208}Pb(^{54}Cr, 2n)$
261	0.26 s	α	α 9.56	$^{208}Pb(^{54}Cr, n)$
263	0.9 s	α	α 9.25	$^{249}Cf(^{18}O, 4n)$
Element 107				
261[a]	1.5 ms	SF		$^{209}Bi(^{54}Cr, 2n)$ $^{208}Pb(^{55}Mn, 2n)$
262	4.7 ms	α	α 10.38	$^{209}Bi(^{54}Cr, n)$
Element 108				
265	1.8 ms	α	α 10.36	$^{208}Pb(^{58}Fe, n)$
Element 109				
266	3.5 ms	α	α 11.10	$^{209}Bi(^{58}Fe, n)$

[a] The identity of this nuclide is not well-established.

therefore it is expected to belong to the group VI B elements [75]. The chemical properties are predicted to be similar to those of W and Mo and perhaps to offer an even greater variety of complex ions. The hexafluoride is expected to be quite volatile and the hexachloride, pentachloride, and oxychloride moderately volatile [75]. Penneman and Mann predict a 4+ oxidation state in aqueous solution [78]; however, this estimate was for the hydrated cation and does not account for stabilizing effects of complex-ion formation. Since the 6+ oxidation state of tungsten is stabilized in the tungstate ion, a similar behavior might be expected for element 106 [97]. Cunningham predicted a 6+ valence for element 106 in the oxide [77]. Some of the predicted chemical properties of element 106 are given in Table 13.10.

There have been no measured chemical properties reported.

13.9 ELEMENT 107

13.9.1 Introduction

In 1976, Oganesyan *et al.* reported the observation of two spontaneously fissioning activities with half-lives of about 5 s and 2 ms produced during irradiations of ^{209}Bi with ^{54}Cr ions [98]. The researchers suggested that the results of cross-bombardments with other targets and projectiles gave grounds for assuming that the approximately 5 s activity was due to the spontaneous fission of ^{257}105, which is formed as a result of the alpha decay of ^{261}107, and the approximately 2 ms activity was due to an approximately 20% fission branch in the decay of ^{261}107 (Table 13.9). Other interpretations are, however, possible.

In 1981, Munzenberg *et al.* reported the results of a series of elegant experiments on the production of element 107 by the bombardment of ^{209}Bi targets with ^{54}Cr ions in the Unilac accelerator located at Darmstadt, Germany [100]. After passing through a velocity filter and time-of-flight apparatus, the recoiling product atoms produced in the reaction were implanted into an array of seven position-sensitive Si surface barrier detectors. Since these detectors and the related equipment were capable of measuring the energy and time correlations of any subsequent alpha decay events associated with the implanted product atoms, alpha decay chains could be detected and parent–daughter relationships established. The point of this identification scheme is that all decays belonging to a given chain must occur at the implantation position of the original product atoms. A position group of six alpha decay events was observed: five alpha decays, in the energy range 10.35–10.40 MeV, occurred 1–13 ms after implantation and one, of 9.70 MeV, at 165 ms after implantation. These events were position-correlated with subsequent alpha events with energies and decay times that could be associated with the decay-chain daughters ^{258}105 and ^{254}Lr, and ended in known transitions of ^{250}Fm and ^{250}Md. Thus, the results indicated the discovery of the alpha decay of ^{262}107 (Table 13.9). See also Armbruster [106].

Table 13.10 *Predicted chemical properties of elements* 104–109.

	104	105	106	107	108	109
chemical group	IV B	V B	VI B	VII B	VIII	VIII
electron configuration[a]	$6d^2 7s^2$	$6d^3 7s^2$	$6d^4 7s^2$	$6d^5 7s^2$	$6d^6 7s^2$	$6d^7 7s^2$
stable oxidation states[b,d]	4, 3	5, 4	6, 4	7–3	8–2	6–1
ionic radius of indicated ion (Å)[c]	0.71 (4+)	0.68 (5+)	0.86 (4+)	0.83 (5+)	0.80 (4+)	0.83 (3+)
standard electrode potential of aqueous ion to metal (V)[b]	−1.8 (4+ → 0)	−0.8 (5+ → 0)	−0.6 (4+ → 0)	+0.1 (5+ → 0)	+0.4 (4+ → 0)	+0.8 (3+ → 0)
first ionization energy (eV)[c]	5.6	6.6	7.6	6.9	7.8	8.7

[a] Electronic ground-state configuration of free neutral atom + $5f^{14}$ + Rn core.
[b] From ref. 97.
[c] From ref. 75.
[d] Predicted most stable state in solution underlined.

13.9.2 Predicted chemical properties

The electronic ground-state configuration of the free neutral atom was predicted to be $5f^{14}6d^{5}7s^{2}$ and thus it should belong to the group VII B elements [75]. It is expected to be eka-rhenium and to exhibit similar chemical properties, e.g. a volatile hexafluoride [75]. Several oxidation states have been predicted as the most stable in aqueous solution; for example, Cunningham [77] suggests 7+, Fricke and Waber [99] give 5+, and Penneman and Mann [78] predict 3+. This wide range in the predictions suggests that all the oxidation states may be possible, with the higher oxidation states being stabilized by the formation of oxyanions as is the case with Re [97]. Some of the predicted chemical properties of element 107 are given in Table 13.10.

There have been no measured chemical properties reported.

13.10 ELEMENT 108

13.10.1 Introduction

In 1984 Munzenberg *et al.* reported the results of experiments to produce element 108 by bombardment of ^{208}Pb targets with ^{58}Fe ions in the Unilac [105]. Three atoms of ^{265}108 (Table 13.9) were identified through their correlated alpha decay chains using the same experimental set-up and identification schemes as in previous experiments to produce element 107, described in Section 13.9.

13.10.2 Predicted chemical properties

The electronic ground-state configuration of the free neutral atom of element 108 has been predicted to be $5f^{14}6d^{6}7s^{2}$ [75]. It is expected to belong to the group VIII elements and to exhibit chemical properties similar to osmium, e.g. a volatile tetraoxide [75]. As with element 107, a variety of oxidation states have been predicted to be stable, including the 8+ [77], the 4+ [99], and the 2+ [78]. The higher oxidation states would be expected to be stabilized by the formation of oxyanions [97]. Some of the predicted chemical properties of element 108 are given in Table 13.10.

13.11 ELEMENT 109

13.11.1 Introduction

In 1982, Munzenberg and co-workers reported the observation of one correlated alpha decay event during the irradiation of ^{209}Bi targets with ^{58}Fe ions in the Unilac, which was interpreted as resulting from the production and decay of ^{266}109 [101] (Table 13.9). The experimental set-up and isotope identification scheme were similar to those used in their experiments to produce element 107 described in Section 13.9. One high-energy alpha decay, 11.10 MeV, occurred at

the point of implantation of the nuclear reaction product nucleus and was followed in sequence by a second alpha decay and a fission decay. This series of events was interpreted as resulting from the decay chain $^{266}109$ (alpha decay), $^{262}107$ (alpha decay), $^{258}105$ (electron-capture decay), and $^{258}104$ (fission decay). However, this interpretation should be considered tentative until confirmed by further experimentation. See also Armbruster [106].

13.11.2 Predicted chemical properties

The electronic ground-state configuration of the free neutral atom of element 109 has been predicted to be $5f^{14}6d^{7}7s^{2}$ and thus it should belong to the group VIII elements of the periodic table [75]. Element 109 is expected to have a chemical behavior similar to iridium but may exhibit an even more noble character [75]. The oxidation states 6+ [77], 3+ [99], and 1+ [78] have been predicted to be stable, and a wide variety of valence states are anticipated in aqueous solution for element 109 [75]. Like Ir, element 109 should form numerous solution complexes [75]. Some of the predicted chemical properties of element 109 are given in Table 13.10.

There have been no reported attempts to measure any chemical properties.

REFERENCES

1. Ghiorso, A., Thompson, S. G., Higgens, G. H., Seaborg, G. T., Studier, M. H., Fields, P. R., Fried, S. M., Diamond, H., Mech, J. F., Pyle, G. L., Huizenga, J. R., Hirsch, A., Manning, W. M., Browne, C. I., Smith, H. L., and Spence, R. W. (1955) *Phys. Rev.*, **99**, 1048–9.
2. King, L. J., Bigelow, J. E., and Collins, E. D. (1978) Oak Ridge Natl Lab. Rep. ORNL 5358, Oak Ridge, Tenn.
3. Hoff, R. W. and Hulet, E. K. (1970) *Proc. Am. Nucl. Soc. Symp. on Engineering with Nuclear Explosives*, vol. 2, pp. 1283–94.
4. Choppin, G. R., Harvey, B. G., and Thompson, S. G. (1956) *J. Inorg. Nucl. Chem.*, **2**, 66–8.
5. Hulet, E. K. and Bode, D. D. (1972) *MTP International Review of Science, Inorganic Chemistry*, ser. 1, vol. 7, (ed. K. W. Bagnall), Butterworths, London, pp. 1–46.
6. Diamond, R. M., Street, K. Jr, and Seaborg, G. T. (1954) *J. Am. Chem. Soc.*, **76**, 1461–9.
7. Goodman, L. S., Diamond, H., Stanton, H. E., and Fred, M. S. (1971) *Phys. Rev. A*, **4**, 473–5.
8. Carlson, T. A. and Nestor, C. W. Jr (1977) *At. Data Nucl. Data Tables*, **19**, 153–73.
9. Porter, F. T. and Freedman, M. S. (1971) *Phys. Rev. Lett.*, **27**, 293–7.
10. Dittner, P. F., Bemis, C. E. Jr, Hensley, D. C., Silva, R. J., and Goodman, C. D. (1971) *Phys. Rev. Lett.*, **26**, 1037–40.
11. Johansson, B. and Rosengren, A. (1975) *Phys. Rev. B*, **11**, 1367–73.
12. David, F., Samhoun, K., Guillaumont, R., and Edelstein, N. (1978) *J. Inorg. Nucl. Chem.*, **40**, 69–74.
13. Zvara, I., Belov, V. Z., Domanov, V. P., Zhuikov, B. L., Reetz, T., Huebener, S., and

Shalaevskii, M. R. (1976) Joint Inst. Nucl. Res. Rep. JINR P6-10334, Dubna.
14. Huebener, S. (1980) Joint Inst. Nucl. Res. Rep. JINR E6-80-291, Dubna.
15. Thompson, S. G., Harvey, B. G., Choppin, G. R., and Seaborg, G. T. (1954) *J. Am. Chem. Soc.*, **76**, 6229–36.
16. Katz, J. J. and Seaborg, G. T. (1957) *Chemistry of the Actinide Elements*, Methuen, London, p. 404.
17. *Ibid.*, p. 428.
18. Hussonnois, H., Hubert, S., Aubin, L., Guillaumont, R., and Boussieres, G. (1972) *Radiochem. Radioanal. Lett.*, **10**, 231–8.
19. Lundqvist, R., Hulet, E. K., and Baisden, T. A. (1981) *Acta. Chem. Scand.*, **A35**, 653–61.
20. Ermakov, V. A. and Stary, I. (1967) *Radiokhimiya*, **9**, 197–201.
21. Baybarz, R. D. (1965) *J. Inorg. Nucl. Chem.*, **27**, 1831–9.
22. Baybarz, R. D. (1966) *J. Inorg. Nucl. Chem.*, **28**, 1055–61.
23. Baybarz, R. D. (1963) *Nucl. Sci. Eng.*, **17**, 463–7.
24. Stary, I. (1966) *Talanta*, **13**, 421–37.
25. Horwitz, E. P., Bloomquist, C. A. A., and Henderson, D. J. (1969) *J. Inorg. Nucl. Chem.*, **31**, 1149–66.
26. Müller, W. (1967) *Actinides Rev.*, **1**, 71–119.
27. Horwitz, E. P. and Bloomquist, C. A. A. (1973) *J. Inorg. Nucl. Chem.*, **35**, 271–84.
28. Leuze, R. E., Baybarz, R. D., and Weaver, B. (1963) *Nucl. Sci. Eng.*, **17**, 252–8.
29. Maly, J. (1967) *Inorg. Nucl. Chem. Lett.*, **3**, 373–81.
30. Samhoun, K. and David, F. (1976) *Transplutonium 1975, Proc. 4th Int. Symp.*, Baden-Baden, (eds W. Müller and R. Lindner), North-Holland, Amsterdam, pp. 297–304.
31. David, F. and Hussonnois, M. (1972) *Radiochem. Radioanal. Lett.*, **11**, 1–5.
32. Mikheev, N. B., Spitsyn, V. I., Kamenskaya, A. N., Konovalova, N. A., Rumer, I. A., Auerman, L. N., and Podorozhnyi, A. M. (1977) *Inorg. Nucl. Chem. Lett.*, **13**, 651–6.
33. McGlashan, M. L. (1970) *J. Pure Appl. Chem.*, **21**, 1–44.
34. Ghiorso, A., Harvey, B. G., Choppin, G. R., Thompson, S. G., and Seaborg, G. T. (1955) *Phys. Rev.*, **5**, 1518–19.
35. Hulet, E. K., Lougheed, R. W., Brady, J. D., Stone, R. E., and Coops, M. S. (1967) *Science*, **158**, 486–8.
36. Hoff, R. W., Hulet, E. K., Dupzyk, R. J., Lougheed, R. W., and Evans, J. E. (1971) *Nucl. Phys. A*, **169**, 641–50.
37. Hulet, E. K., Lougheed, R. W., Baisden, P. A., Landrum, J. H., Wild, J. F., and Lundqvist, R. F. D. (1979) *J. Inorg. Nucl. Chem.*, **41**, 1743–7.
38. Seaborg, G. T. (1963) *Man-Made Transuranium Elements*, Prentice-Hall, Englewood Cliffs, NJ, pp. 26–30.
39. Macfarlane, R. D. and Griffioen, R. D. (1963) *Nucl. Inst. Meth.*, **24**, 461–4.
40. Ghiorso, A. (1959) Lawrence Berkeley Lab. Report UCRL-8714, Berkeley.
41. Horwitz, E. P. and Bloomquist, C. A. A. (1969) *Chem. Lett.*, **5**, 753–9.
42. Martin, W. C., Hagan, L., Reader, J., and Sugar, J. (1974) *J. Phys. Chem. Ref. Data*, **3**, 771–80.
43. Seaborg, G. T. and Katz, J. J. (1954) in *The Transuranium Elements*, Natl Nucl. En. Ser., Div. IV, 14A, McGraw-Hill, New York, pp. 733–68.
44. Maly, J. and Cunningham, B. B. (1967) *Inorg. Nucl. Chem. Lett.*, **2**, 445–51.
45. Mikheev, N. B., Spitsyn, V. I., Kamenskaya, A. M., Rumer, I. A., Gvozdev, B. A., Rozenkevich, N. A., and Auerman, L. N. (1973) *Dokl. Akad. Nauk SSSR*, **208**, 1146–9.

46. Samhoun, K., David, F., Hahn, R. L., O'Kelley, G. D., Tarrant, J. R., and Hobart, D. E. (1979) *J. Inorg. Nucl. Chem.*, **41**, 1749–54.
47. David, F., Samhoun, K., Hulet, E. K., Baisden, P. A., Dougan, R., Landrum, J. H., Lougheed, R. W., Wild, J. F., and O'Kelley, G. D. (1981) *J. Inorg. Nucl. Chem.*, **43**, 2941–5.
48. Fields, P. R., Friedman, A. M., Milstead, J., Atterling, H., Forsling, W., Holm, L. W., and Aström, B. (1957) *Phys. Rev.*, **107**, 1460–2.
49. Ghiorso, A., Sikkeland, T., Walton, J. R., and Seaborg, G. T. (1958) *Phys. Rev. Lett.*, **1**, 18–20.
50. Ghiorso, A. and Sikkeland, T. (1967) *Phys. Today*, **20** (9), 25–32.
51. Maly, J., Sikkeland, T., Silva, R. J., and Ghiorso, A. (1968) *Science*, **160**, 1114–15.
52. Silva, R. J., Dittner, P. F., Mallory, M. L., Keller, O. L. Jr, Eskola, K., Eskola, P., Nurmia, M., and Ghiorso, A. (1973) *Nucl. Phys. A*, **216**, 97–108.
53. Silva, R. J., Sikkeland, T., Nurmia, M., and Ghiorso, A. (1969) *J. Inorg. Nucl. Chem.*, **31**, 3405–9.
54. Bemis, C. E. Jr, Silva, R. J., Hensley, D. C., Keller, O. L. Jr, Tarrant, J. R., Hunt, L. D., Dittner, P. F., Hahn, R. L., and Goodman, C. D. (1973) *Phys. Rev. Lett.*, **31**, 647–50.
55. Seaborg, G. T., Katz, J. J. and Manning, W. M. (1949) in *The Transuranium Elements*, Natl Nucl. En. Ser., Div. IV, 14B, McGraw-Hill, New York, pp. 1492–524.
56. Chuburkov, Y. T., Caletka, R., Shalaevskii, M. R., and Zvara, I. (1967) *Radiokhimiya*, **9**, 637–42.
57. Silva, R. J., McDowell, W. J., Keller, O. L. Jr, and Tarrant, J. R. (1974) *J. Inorg. Chem.*, **13**, 2233–7.
58. McDowell, W. J., Keller, O. L. Jr, Dittner, P. F., Tarrant, J. R., and Case, G. N. (1976) *J. Inorg. Nucl. Chem.*, **38**, 1207–10.
59. Meyer, R. E., McDowell, J. W., Dittner, P. F., Silva, R. J., and Tarrant, J. R. (1976) *J. Inorg. Nucl. Chem.*, **38**, 1171–3.
60. Ghiorso, A., Sikkeland, T., Larsh, A. E., and Latimer, R. M. (1961) *Phys. Rev. Lett.*, **6**, 473–5.
61. Druin, V. A. (1971) *Sov. J. Nucl. Phys.*, **12**, 146–7.
62. Eskola, K., Eskola, P., Nurmia, M., and Ghiorso, A. (1971) *Phys. Rev. C*, **4**, 632–42.
63. Silva, R. J., Sikkeland, T., Nurmia, M., and Ghiorso, A. (1970) *Inorg. Nucl. Chem. Lett.*, **6**, 733–9.
64. Moeller, T. (1970) *J. Chem. Educ.*, **47**, 417–23.
65. Nugent, L. J., VanderSluis, K. L., Fricke, B., and Mann, J. B. (1974) *Phys. Rev. A*, **9**, 2270–2.
66. Bemis, C. E. Jr, Dittner, P. F., Silva, R. J., Hahn, R. L., Tarrant, J. R., Hunt, L. D., and Hensley, D. C. (1977) *Phys. Rev. C*, **16**, 1146–58.
67. Chuburkov, Y. T., Belov, V. Z., Caletka, R., Shalaevskii, M. R., and Zvara, I. (1968) *Radiokhimiya*, **11**, 394–9.
68. Nugent, L. J. (1975) in *MTP International Review of Science, Inorganic Chemistry*, ser. 2, vol. 7 (ed. K. W. Bagnall), Butterworths, London, pp. 195–219.
69. Flerov, G. N., Oganesyan, Y. T., Lobanov, Y. V., Kuznetsov, V. I., Druin, V. A., Perelygin, V. P., Gavrilov, K. A., Tretiakova, S. P., and Plotko, V. M. (1964) *Phys. Lett.*, **13**, 73–5.
70. Oganesyan, Y. T., Lobanov, Y. V., Tretyokova, S. P., Lasarev, Y. A., Kolesov, I. V., Gavrilov, K. A., Plotko, V. M., and Poluboyarinov, Y. V. (1969) Joint Inst. Nucl. Res. Rep. JINR P7-4797, Dubna.

71. Ghiorso, A. (1969) *Proc. Robert A. Welch Found. Conf. Chem. Res.*, **13**, *The Transuranium Elements* (ed. W. O. Milligan), Houston, pp. 107–50.
72. Ghiorso, A., Nurmia, M., Harris, J., Eskola, K., and Eskola, P. (1969) *Phys. Rev. Lett.*, **22**, 1317–20.
73. Nitschke, J. M., Fowler, M., Ghiorso, A., Leber, R. E., Nurmia, M. J., Somerville, L. P., Williams, K. E., Hulet, E. K., Landrum, J. H., Lougheed, R. W., Wild, J. F., Bemis, C. E. Jr, Silva, R. J., and Eskola, P. *Nucl. Phys. A*, **352**, 138–45.
74. Harvey, B. G., Herrman, G., Hoff, R. W., Hoffman, D. C., Hyde, E. K., Katz, J. J., Keller, O. L. Jr, Lefort, M., and Seaborg, G. T. (1976) *Science*, **193**, 1271–2.
75. Fricke, B. (1975) *Struct. Bonding*, **21**, 89–104.
76. Seaborg, G. T. (1958) *The Transuranium Elements*, Yale University Press, New Haven, pp. 279–82.
77. Cunningham, B. B. (1969) *Proc. Robert A. Welch Found. Conf. Chem. Res.*, 13, *The Transuranium Elements* (ed. W. O. Milligan), Houston, pp. 307–22.
78. Penneman, R. A. and Mann, J. B. (1976) *J. Inorg. Nucl. Chem.*, Suppl., *Proc. Moscow Symp. Chem. Transuranium Elements* (eds V. I. Spitsyn and J. J. Katz), Pergamon Press, Oxford, pp. 257–63.
79. Silva, R., Harris, J., Nurmia, M., Eskola, K., and Eskola, P. (1970) *Inorg. Nucl. Chem. Lett.*, **6**, 871–7.
80. Hulet, E. K., Lougheed, R. W., Wild, J. F., Landrum, J. H., Nitschke, J. M., and Ghiorso, A. (1979) *J. Inorg. Nucl. Chem.*, **42**, 79–82.
81. Zvara, I., Chuburkov, Y. T., Caletka, R., Zvarova, T. S., Shalaevskii, M. R., and Shilov, B. V. (1966) *Atomn. Energiya*, **21**, 83–4.
82. Zvara, I., Chuburkov, Y. T., Belov, V. Z., Buklanov, G. V., Zakhvataev, B. B., Zvarova, T. S., Maslov, O. D., Caletka, R., and Shalaevskii, M. R. (1970) *J. Inorg. Nucl. Chem.*, **32**, 1885–94.
83. Zvara, I. (1969) *Proc. Robert A. Welch Found. Conf. Chem. Res.*, **13**, *The Transuranium Elements* (ed. W. O. Milligan), Houston, pp. 153–85.
84. Zvara, I., Belov, V. Z., Chelnokov, L. P., Domanov, V. P., Hussonois, M., Korotkin, Y. S., Schegolev, V. A., and Shalayevsky, M. R. (1971) *Inorg. Nucl. Chem. Lett.*, **7**, 1109–16.
85. Flerov, G. N., Durin, V. A., Demin, A. G., Lobanov, Y. V., Skobelev, N. K., Akapiev, G. N., Fefilov, B. V., Kolesov, I. V., Davrilov, K. A., Kharitonov, Y. P., and Chelnokov, L. P. (1968) Joint Inst. Nucl. Res. Rep. JINR P7-3808, Dubna.
86. Ghiorso, A., Nurmia, M., Eskola, K., Harris, J., and Eskola, P. (1970) Lawrence Berkeley Lab. Rep. UCRL-19577, Berkeley.
87. Ghiorso, A., Nurmia, M., Eskola, K., and Eskola, P. (1971) *Phys. Rev. C*, **4**, 1850–5.
88. Flerov, G. N., Oganesyan, Y. T., Lobanov, Y. V., Lazarev, Y. A., and Tretiakova, S. P. (1970) Joint Inst. Nucl. Res. Rep. JINR P7-4932, Dubna.
89. Flerov, G. N., Oganesyan, Y. T., Lobanov, Y. V., Lazarev, Y. A., and Tretiakova, S. P. (1970) Joint Inst. Nucl. Res. Rep. JINR P7-5108, Dubna.
90. Zvara, I., Belov, V. Z., Korotin, Y. S., Shalaevsky, M. R., Shchegolev, V. A., Hussonnois, M., and Zager, B. A. (1970) Joint Inst. Nucl. Res. Rep. JINR P12-5120, Dubna.
91. Druin, V. A., Demi, A. G., Kharitonov, Y. P., Akapiev, G. N., Rud, V. I., Sun-Tzin-Yan, G. Y., Chelnokov, L. P., and Gavrilov, K. A. (1970) Joint Inst. Nucl. Res. Rep. JINR P7-5161, Dubna.
92. Flerov, G. N. (1970) *Science*, **170**, 15; Ghiorso, A. (1971) *Science*, **171**, 127.

93. Zvara, I., Belov, V. Z., Domanov, V. P., and Shalaevsky, M. R. (1975) Joint Inst. Nucl. Res. Rep. JINR P6-8740, Dubna.
94. Zvara, I. (1973) *Proc. 24th Int. IUPAC Congr.*, Hamburg, vol. 6, pp. 73–90.
95. Ghiorso, A., Nitschke, J. M., Alonso, J. R., Alonso, C. T., Nurmia, M., Seaborg, G. T., Hulet, E. K., and Lougheed, R. W. (1974) *Phys. Rev. Lett.*, **33**, 1490–3.
96. Oganesyan, Y. T., Tretyakov, Y. P., Ll'inov, A. S., Demin, A. G., Pleve, A. A., Tretyakova, S. P., Plotko, V. M., Ivanov, M. P., Danilov, N. A., Korotkin, Y. S., and Flerov, G. N. (1974) Joint Inst. Nucl. Res. Rep. JINR D7-8099, Dubna.
97. Keller, O. L. Jr and Seaborg, G. T. (1977) *Annu. Rev. Nucl. Sci.*, **27**, 139–66.
98. Oganesyan, Y. T., Demin, A. G., Danilov, N. A., Ivanov, M. P., Ll'inov, A. S., Kolesnikov, N. N., Markov, B. N., Plotko, V. M., Tretyakova, S. P., and Flerov, G. N. (1976) *JETP Lett.*, **23**, 277–9.
99. Fricke, B. and Waber, J. T. (1972) *J. Chem. Phys.*, **56**, 3246–8.
100. Munzenberg, G., Hofmann, S., Hessberger, F. P., Reisdorf, W., Schmidt, K. H., Schneider, J. R. H., Armbruster, P., Sahm, C. C., and Thuma, B. (1981) *Z. Phys. A*, **300**, 107–8.
101. Munzenberg, G., Armbruster, P., Hessberger, F. P., Hofmann, S., Poppensieker, K., Reisdorf, W., Schneider, J. H. R., Schneider, W. F. W., Schmidt, K.-H., Sahm, C. C., and Vermeulen, D. (1982) *Z. Phys. A*, **309**, 89–90.
102. Mikheev, N. B., Kamenskaya, A. N., Spitsyn, V. I., Mikul'skii, Ya., Petryna, T., and Konovalova, N. A. (1981) *Radiokhimiya*, **23**, 736–43.
103. Spitsyn, V. I., Mikheev, N. B., Kamenskaya, A. N., Berdonosov, S. S., and Mikul'skii, Ya. (1982) *Radiokhimiya*, **24**, 615–17.
104. Mikheev, N. B., Kamenskaya, A. N., Berdonosov, S. S., and Kilimov, S. I. (1981) *Radiokhimiya*, **23**, 793–5.
105. Munzenberg, G., Armbruster, P., Folger, H., Hessburger, F. P., Hofmann, S., Keller, J., Poppensieker, K., Reisdorf, W., Schmidt, K-H., Schött, H-J., Leino, M. E., and Hingmann, R. (1984) *Z. Phys. A*, **317**, 235–6.
106. Armbruster, P. (1985) *Ann. Rev. Nucl. Part. Sci.*, **35**, 135–94.

PART TWO

CHAPTER FOURTEEN

SUMMARY AND COMPARATIVE ASPECTS OF THE ACTINIDE ELEMENTS

Joseph J. Katz, Lester R. Morss and Glenn T. Seaborg

14.1 INTRODUCTION

14.1.1 Scope

This chapter is intended to provide a unified view of selected aspects of the physical, chemical, and biological properties of the actinide elements. The f-block elements have many unique features, and a comparison of the lanthanide and actinide transition series provides valuable insights into the properties of both. Comparative data are presented on the electronic configurations, oxidation states, redox potentials, thermochemical data, crystal structures, and ionic radii of the actinide elements, together with a miscellany of topics related to their environmental and health aspects. Much of this material is assembled in tabular and graphical form to facilitate rapid access. Many of the topics covered in this chapter, and some that are not discussed here, are the subjects of subsequent chapters of this work, and these may be consulted for more comprehensive treatments. This chapter provides a welcome opportunity to discuss the biological and environmental aspects of the actinide elements, subjects that were barely mentioned in the first edition of this work but have assumed great importance in recent times.

14.1.2 The actinide concept

The actinide concept has by now achieved well-nigh universal acceptance as a way of integrating the transuranium elements into the periodic table. A succinct summary of this important principle will therefore be sufficient here. The actinide concept considers the elements with atomic numbers 90–103 to be members of a transition series, the first member of which is actinium (atomic number 89). The elements with atomic numbers 89–103 are thus analogs of the lanthanide transition series that starts with lanthanum (atomic number 57) and includes the rare-earth elements cerium through lutetium (atomic number 71). It is important, in comparing the lanthanide and actinide transition series, to keep in mind that the electronic configuration of any given element may be significantly different in the gaseous atoms, in ions in solution, or in the metallic state. In the lanthanide series, fourteen 4f electrons are added in sequence beginning with cerium (atomic number 58). In the actinide series, fourteen 5f electrons are added successively beginning formally with thorium (atomic number 90) and ending with lawrencium (atomic number 103). Note the qualification 'formally'. No compelling evidence exists to show that thorium metal or any of its well-defined compounds contain 5f electrons. There is, however, convincing evidence that protactinium metal and certain of its compounds contain the two 5f electrons expected for the third member of an actinide series. The subsequent trivalent ions of the actinide series appear to contain their appropriate complements of 5f electrons. Although there are important differences between the actinide and lanthanide elements, there are also striking similarities. The elements with half-filled f-electron shells, for example, are of special interest because of the enhanced stability of this particular electron configuration. The elements gadolinium (atomic number 64), with seven 4f electrons, and curium (atomic number 96), with seven 5f electrons, have remarkably similar magnetic, optical and chemical properties, as would be expected from the actinide concept. The principal differences between the two transition series arise largely from the lower binding energies and less effective shielding by outer electrons of 5f as compared to 4f electrons. Both the similarities and the differences between the actinide and lanthanide series have had great heuristic value in actinide element research. Further discussion of the electronic structure of the actinide elements is to be found in Section 14.4. Much more detailed expositions of the actinide elements as a 5f transition series are given in Chapters 15, 16, 18 and 19.

14.2 SOURCES

14.2.1 Natural sources

The elements actinium through plutonium occur in nature. Neptunium (^{237}Np and ^{239}Np) and plutonium (^{239}Pu) are present in minute amounts in nature as a result of neutron reactions in uranium ores. The longer-lived ^{244}Pu has been

found in the rare-earth mineral bastnasite to the extent of 1 part in 10^{18}, and may possibly be a primordial endowment (cf. Section 14.8.1). Only the elements thorium, protactinium, and uranium are present in amounts sufficient to warrant extraction from natural sources. Uranium and thorium are widely disseminated in the Earth's crust, and, in the case of uranium, in significant concentrations in the oceans. More importantly, thorium and uranium are found highly enriched in certain mineral formations, and are obtained by normal mining operations. The richest deposits of uranium are found in northern Saskatchewan, Canada. The leading producers of uranium ore (for which statistics are available) and their estimated 1984 production in metric tons of uranium oxide are Canada (10 790), USA (5990), South Africa (5700), Australia (3850), and Namibia (3650) [1]. Extraction of thorium and uranium from their ores had been practiced for many years prior to the discovery of the transuranium elements, and an extensive technology exists for the extraction of thorium and uranium from many different types of ores.

14.2.2 Neutron irradiation

Actinium and protactinium are decay products of the naturally occurring uranium isotope ^{235}U and are present in uranium minerals in such low concentration that recovery from natural sources is a very difficult and unrewarding task. By comparison, it is relatively straightforward to obtain actinium, protactinium, and most of the remaining transuranium elements by neutron irradiation of elements of lower atomic number in nuclear reactors [2–4]. Thus, actinium has been produced in multigram quantities by the transmutation of radium with neutrons produced in a high-flux nuclear reactor:

$$^{226}Ra + n \rightarrow {}^{227}Ra + \gamma$$

$$^{227}Ra \rightarrow {}^{227}Ac + \beta^-$$

The product actinium can be separated from the precursor radium by solvent extraction or ion exchange, and gram amounts of actinium have been obtained by this procedure. This is not at all an easy task, considering the highly radioactive substances involved, but is preferable by far to extraction from natural sources.

Protactinium can be produced by the nuclear reactions:

$$^{230}Th + n \rightarrow {}^{231}Th + \gamma$$

$$^{231}Th \rightarrow {}^{231}Pa + \beta^-$$

The amount of ^{231}Pa produced in this way, however, is much less than the amounts (more than 100 g) of protactinium that have been obtained from residues accumulated from the very large-scale extraction of uranium from ores. Because of the extreme tendency of protactinium(v) to form colloidal polymers that are easily lost by adsorption on solid surfaces, and cannot be removed from aqueous

media by solvent extraction, the recovery of protactinium from uranium ore processing residues can only be described as a heroic enterprise.

Neptunium-237 is a long-lived isotope of element 93 that is produced in kilogram amounts. It is formed as a by-product in nuclear reactors when neutrons produced in the fission of uranium-235 react with uranium-238:

$$^{238}\mathrm{U} + \mathrm{n} \rightarrow {}^{237}\mathrm{U} + 2\mathrm{n}$$

$$^{237}\mathrm{U} \rightarrow {}^{237}\mathrm{Np} + \beta^-$$

Neptunium-237 is also formed by neutron capture in uranium-235:

$$^{235}\mathrm{U} + \mathrm{n} \rightarrow {}^{236}\mathrm{U} + \gamma$$

$$^{236}\mathrm{U} + \mathrm{n} \rightarrow {}^{237}\mathrm{U} + \gamma$$

$$^{237}\mathrm{U} \rightarrow {}^{237}\mathrm{Np} + \beta^-$$

The waste solutions from the processing of irradiated uranium fuel usually contain the neptunium, which can be isolated and purified by a combination of solvent extraction, ion exchange, and precipitation techniques.

The important isotope ^{239}Pu is produced by the ton in nuclear reactors. Excess neutrons from the fission of uranium-235 are captured by uranium-238 to yield plutonium-239:

$$^{235}\mathrm{U} + \mathrm{n} \rightarrow \text{fission products} + 2.5\mathrm{n} + 200\ \text{MeV}$$

$$^{238}\mathrm{U} + \mathrm{n} \rightarrow {}^{239}\mathrm{U} \rightarrow {}^{239}\mathrm{Np} \rightarrow {}^{239}\mathrm{Pu}$$

Plutonium produced in nuclear reactors in which the fuel is irradiated for long periods of time contains plutonium isotopes with mass numbers up to 244, formed from ^{239}Pu by successive neutron capture. A variety of industrial-scale processes for the separation and purification of plutonium are described in detail in Chapter 7.

The isotope ^{238}Pu is an important heat source for terrestrial and extra-terrestrial applications. It is available in kilogram quantities from the neutron irradiation of neptunium-237:

$$^{237}\mathrm{Np} + \mathrm{n} \rightarrow {}^{238}\mathrm{Np} \rightarrow {}^{238}\mathrm{Pu}$$

High-level waste from the isolation of plutonium-239 contains massive amounts of plutonium-238 formed by various nuclear reactions in reactor fuel elements. A rough estimate indicates that as of 1985 there may be as much as 2 tons of plutonium-238 mixed with heavier plutonium isotopes in stored spent fuel elements and process residues accumulated in the USA and by the European Economic Community [5].

The elements americium through fermium are obtained as by-products of the large-scale production of plutonium-239, or by irradiation of plutonium-239 or isotopes of transplutonium elements in special high-neutron-flux reactors. Kilogram quantities of americium-241 can be obtained from ^{241}Pu, which is

formed in nuclear reactors from ^{239}Pu. The americium-241 that accumulates from the beta decay of plutonium-241 can be separated by a combination of precipitation, ion exchange, and solvent extraction.

Isotopes of curium are also found in waste streams from plutonium-239 production, but in amounts smaller than those of americium. Curium is produced by the beta decay of ^{242}Am and ^{244}Am formed by neutron capture in ^{241}Am and ^{243}Am. The amount of curium-244 accumulated in process wastes and in unprocessed irradiated fuel elements as of 1985 is estimated at more than 100 kg [5]. Separation and purification of curium and americium is best carried out by the ion-exchange procedures described below (see Section 14.3.5).

The sequence of neutron captures and beta decays that forms transuranium elements by slow neutron capture starting with plutonium-239 is shown in Fig. 14.1 [6]. A high neutron flux is essential to expedite the production of transplutonium elements. Fig. 14.2 shows that, even with a neutron flux in excess of 10^{14} cm^{-2} s^{-1}, years of irradiation may be required to attain useful conversions. Starting with 1 kg of ^{239}Pu, about 1 mg of ^{252}Cf would be present after 5–10 years of continuous irradiation at a neutron flux of 3×10^{14} cm^{-2} s^{-1}. To increase the production rate, large quantities of ^{239}Pu can first be irradiated in production reactors, followed by continued irradiation in higher-neutron-flux reactors. The High Flux Isotope Reactor (HFIR) at Oak Ridge National Laboratory in Tennessee, and reactors at the Savannah River Plant in South Carolina, can provide neutron fluxes of about 10^{15} cm^{-2} s^{-1} and thus have made major contributions to the production of transcurium elements. A special facility called the Transuranium Processing Plant (TRU) at Oak Ridge was established to fabricate plutonium targets, and to extract transplutonium elements from the highly irradiated targets. Neutron irradiation cannot be used to prepare the elements beyond fermium (^{257}Fm) because some of the intermediate nuclides

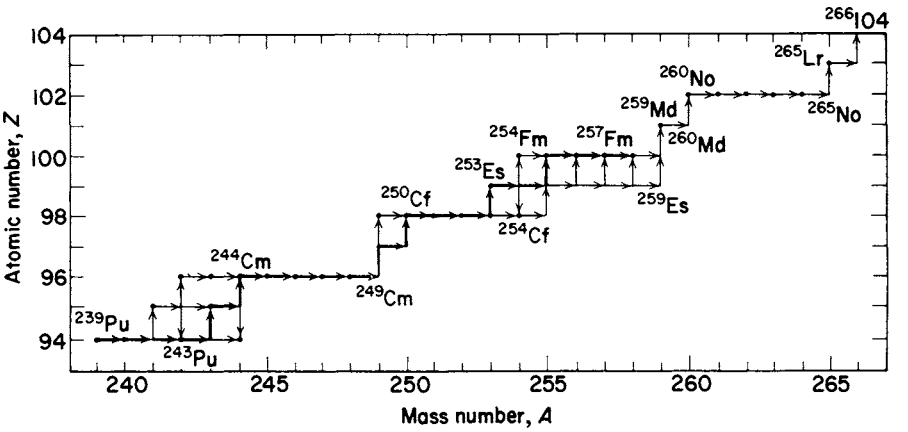

Fig. 14.1 *Nuclear reaction sequence for production of transplutonium elements by intensive slow-neutron irradiation. The principal path is shown by heavy arrows (horizontal, neutron capture; vertical, beta decay). The sequence above ^{258}Fm is a prediction.*

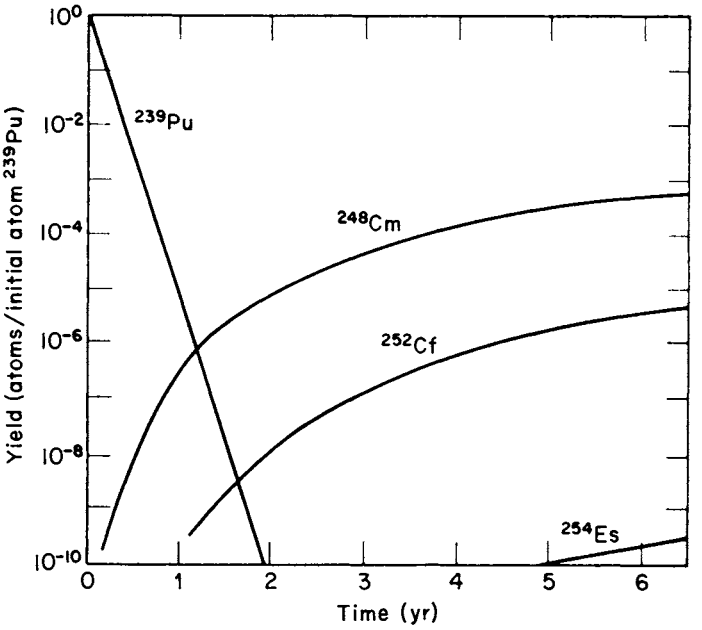

Fig. 14.2 *Production of some transplutonium nuclides by irradiation of* ^{239}Pu *at a neutron flux of* $3 \times 10^{14}\ cm^{-2}\ s^{-1}$.

have such short half-lives that the low equilibrium concentrations present effectively prevent the formation of significant amounts of the desired isotopes. Thus, only milligram amounts of einsteinium and picogram amounts of fermium can be obtained by protracted neutron irradiation even under the most favorable circumstances. Table 14.1 lists the routine production rate of isotopes of elements from curium-248 to fermium-257 in the Oak Ridge HFIR/TRU operation [6, 7]. Isotopes that are sufficiently long-lived for work in weighable amounts are obtainable at least in principle for all of the actinide elements through fermium. The elements above fermium, however, appear likely to remain amenable to chemical study only by tracer techniques because only isotopes with short half-

Table 14.1 *Production of transcurium isotopes.*

Isotope	*Half-life*	*Amount/year*
^{248}Cm	3.5×10^5 yr	150 mg
^{249}Bk	320 d	50 mg
^{252}Cf	2.64 yr	500 mg
^{253}Es	20.3 d	2 mg
^{254}Es	277 d	3 μg
^{257}Fm	100 d	1 pg

lives are known. Nor is it likely that isotopes of the elements beyond fermium sufficiently long-lived to be useful can be formed in neutron irradiation.

Very heavy elements have been detected under circumstances where very intense neutron fluxes were produced. Such is the case for a few microseconds after a thermonuclear explosion. Isotopes of einsteinium and fermium were first discovered in the debris of the first thermonuclear explosion detonated at Eniwetok Atoll in November 1952 [2, 5]. It is possible that elements of atomic number greater than 100 might have been detected had the debris been examined immediately after the explosion. The route whereby elements of high atomic number are formed in the detonation of a thermonuclear device is again multiple neutron capture in ^{238}U, which is a component of the device. Thus, the synthesis of ^{255}Fm in the explosion occurred by way of ^{255}U (formed by the capture of 17 neutrons in ^{238}U) followed by a long sequence of short-lived beta decays that take place after the neutron capture reactions are complete:

$$^{238}U + 17n \rightarrow {}^{255}U \rightarrow {}^{255}Np \rightarrow {}^{255}Pu \rightarrow \ldots \rightarrow {}^{255}Fm$$

14.2.3 Heavy-ion bombardment

In lieu of the extraordinarily intense neutron fluxes associated with a thermonuclear explosion, synthesis of the transfermium elements in amounts sufficient to study their chemical properties has depended on nuclear reactions of charged particles (i.e. ^{4}He, ^{10}B, ^{12}C, and ^{16}O accelerated to appropriate energies in heavy-ion accelerators) with targets of an actinide element of a lower atomic number. Such syntheses are made very difficult by the limited availability of target materials of high atomic number, by the low reaction yields, and by the difficulties inherent in the isolation and characterization of very short-lived radioactive substances. A distinctive feature of these procedures is that the product nuclide is produced and collected one atom at a time, necessitating isolation and identification procedures that are anything but conventional. However, the obstacles have been successfully surmounted, and numerous isotopes of the heaviest actinide elements mendelevium, nobelium, and lawrencium have been produced, their nuclear properties measured, and salient features of their chemical properties established ([8] and Chapter 13, this volume).

14.2.4 Atomic weights

The question of atomic weights deserves a brief comment. Many of the radionuclides listed in Table 14.2 can be obtained in high isotopic purity. Compounds of curium, for example, will have different formula weights depending on the particular curium isotope present in the compound. Atomic and molecular weights must be calculated from the relative abundancies of isotopes present in a given sample.

14.3 EXPERIMENTAL TECHNIQUES

14.3.1 Hazards

All of the actinide elements, with the exception of uranium and thorium, are radioactive to such a degree that handling requires special equipment and shielded facilities [9, 10]. The special containment and manipulation techniques for work with the actinide elements are necessitated by the potential health hazards to the investigator and other occupants of the laboratory. Containment in the form of glove boxes is now standard, and these are available through normal commercial channels. Shielded facilities are more specialized, and, for the most part, are found in laboratories devoted to the study or processing of the actinide elements.

The toxicity of the actinide elements which requires an absolute barrier between the experiment and the experimenter is dictated to only a small extent by external radiation hazards. Plutonium-239 is intensely radioactive, emitting 1.4×10^8 α particles per milligram per minute. However, the alpha radiation from plutonium-239 can easily be shielded by even a thin sheet of paper. It is the consequences of ingestion that make plutonium-239 and the other actinide elements such toxic substances. Plutonium-239, inhaled into the lungs as fine particulate matter, is translocated to the bone, and, over a period of time, may give rise to bone neoplasms (cf. Section 14.10). The biological properties of the actinide elements are discussed in more detail in Sections 14.9 and 14.10.

14.3.2 Long-lived actinide nuclides

Isotopes sufficiently long-lived for work with weighable amounts are in principle available for all the actinide elements through einsteinium (element 99). Long-lived actinide isotopes particularly suitable for physical and chemical investigations by more or less ordinary laboratory procedures are listed in Table 14.2. Not all of these are available in high isotopic purity. The elements above fermium, it appears, will always require tracer techniques for their investigation. This is not as restrictive a prospect as it may seem, for an astonishing amount of chemical information has been acquired from the few atoms of the heaviest actinide and transactinide elements that have already been prepared.

Most of the chemical studies with plutonium have been carried out with ^{239}Pu, but the isotopes ^{242}Pu and ^{244}Pu are more suitable because of their longer half-lives and therefore lower specific activities. The solution chemistry of shorter-lived actinide ions in concentrated aqueous solution is complicated by hydrogen peroxide rapidly formed by the high-energy alpha particles produced by radioactive decay. In solid compounds, the high-energy heavy recoil particles can seriously damage or even destroy the crystal lattice. Americium chemistry, often studied with ^{241}Am, which emits about 7×10^9 alpha particles per milligram per minute, has fewer ambiguities when the studies are performed with ^{243}Am, which

Table 14.2 *Long-lived actinide nuclides suitable for physical and chemical investigation.*

Element	*Isotope*	*Half-life*
actinium	^{227}Ac	21.8 yr
thorium	^{232}Th	1.41×10^{10} yr
protactinium	^{231}Pa	3.28×10^{4} yr
uranium	^{238}U[a]	4.47×10^{9} yr
neptunium	^{236}Np[b]	1.55×10^{5} yr
	^{237}Np	2.14×10^{6} yr
plutonium	^{239}Pu	24 150 yr
	^{240}Pu	6570 yr
	^{242}Pu	3.76×10^{5} yr
	^{244}Pu	8.1×10^{7} yr
americium	^{241}Am	433 yr
	^{243}Am	7380 yr
curium	^{244}Cm	18.1 yr
	^{245}Cm	8540 yr
	^{246}Cm	4700 yr
	^{247}Cm	1.6×10^{7} yr
	^{248}Cm	3.4×10^{5} yr
	^{250}Cm[b]	1.1×10^{4} yr
berkelium	^{247}Bk[c]	1380 yr
	^{249}Bk	320 d
californium	^{249}Cf	350 yr
	^{252}Cf	2.6 yr
einsteinium	^{253}Es	20.5 d
	^{254}Es	277 d
	^{255}Es	39.8 d
fermium	^{257}Fm	100 d

[a] Natural mixture (99.3% ^{238}U, 0.72% ^{235}U and 0.006% ^{234}U). Half-life given is for the major constituent ^{238}U.
[b] Available only in very small amounts from neutron irradiations in thermonuclear explosions.
[c] Available so far only in tracer quantities from charged particle irradiations.

has a specific alpha activity about 20 times less than ^{241}Am. Much of the early research with curium used the isotopes ^{242}Cm and ^{244}Cm. The heavier curium isotopes, especially ^{248}Cm, obtained in relatively high isotopic purity as the alpha-particle decay daughter of ^{252}Cf, make life much simpler for the investigator, although ^{248}Cm decays in part by spontaneous fission, which creates a significant neutron hazard. The same can be said for ^{237}Np as compared to ^{239}Np. The isotope ^{249}Bk and californium as a mixture of the isotopes ^{249}Cf, ^{250}Cf, ^{251}Cf, and ^{252}Cf are available from the intense neutron irradiation of lighter elements. The most useful isotope for the study of californium is ^{249}Cf, which can be isolated in pure form from the beta decay of its parent ^{249}Bk. The isotope ^{253}Es (half-life 20 days), another product of intense neutron irradiation, is

used to study the chemical properties of einsteinium, but the longer-lived ^{254}Es (half-life 276 days) would be more useful for work with macroscopic quantities. However, it is not produced initially free of einsteinium-253. There are severe problems in working with weighable amounts of berkelium, californium, and einsteinium because of their intense radioactivity. Spontaneous fission is an important mode of decay for ^{252}Cf (half-life 2.6 years): 1 microgram of this isotope emits approximately 2×10^8 neutrons per minute. The principal mode of decay of ^{254}Cf (half-life 56 days) is spontaneous fission, which emits approximately 8×10^{10} neutrons per minute per microgram. Californium produced in the highest-flux reactors contains sufficient ^{252}Cf to make for very severe handling and shielding problems. Remote control manipulation is essential when more than a few micrograms of ^{252}Cf are used. While spontaneous fission makes for problems in chemical studies, ^{252}Cf provides very convenient neutron and fission fragment sources, which have important scientific, medical, and industrial uses (cf. Section 14.11.4).

14.3.3 Tracer techniques

Investigations may be carried out on the tracer level, where solutions are handled in ordinary-sized laboratory equipment, but where the substance studied is present in extremely low concentrations. Concentrations of the radioactive species of the order of 10^{-12} M or much less are not unusual in tracer work with radioactive nuclides. A much larger amount of a suitably chosen non-radioactive host or carrier is subjected to chemical manipulation, and the behavior of the radioactive species (as monitored by its radioactivity) is determined relative to the carrier. Thus the solubility of an actinide compound can be judged by whether the radioactive ion is carried by a precipitate formed by the non-radioactive carrier. Interpretation of such studies is made difficult by the formation of radiocolloids, and by adsorption on glass surfaces or precipitates. Tracer studies provide information on the oxidation states of ions and complex-ion formation, and are used in the development of liquid–liquid solvent extraction and chromatographic separation procedures. Tracer techniques are not applicable to solid-state and spectroscopic studies. Despite the difficulties inherent in tracer experiments, these methods continue to be used with the heaviest actinide and transactinide elements, where only a few to a few score atoms may be available [11].

14.3.4 Ultramicrochemical manipulations

Chemistry under the microscope provides an alternative to tracer techniques. It is possible to work with microgram or even smaller amounts of material in very small volumes of solution not visible to the naked eye at ordinary concentrations, say 10^{-1} M to 10^{-3} M. Ultramicrochemical investigations yield results of normal validity, but skill, experience, a good microscope, and much patience are

necessary to carry out such experiments. X-ray diffraction methods can be applied to very small samples of solid compounds. Many actinide element compounds have been identified and their molecular formulas established on samples of a few micrograms synthesized directly in the capillary used to record the x-ray diffraction pattern. With milligram amounts, operations can be readily carried out in a conventional manner. Most of the chemical results described in this book were obtained on about the milligram scale by semi-microprocedures. With highly radioactive substances (e.g. ^{253}Es), the microgram scale may still be preferred even when larger amounts of material are available. In the past, usable x-ray diffraction patterns were difficult to obtain from highly radioactive crystals because of radiation damage. Such problems are considerably ameliorated when smaller samples and modern methods of recording x-ray diffraction patterns are used.

14.3.5 Ion-exchange chromatography

Ion exchange plays two very important roles in actinide element research: first, as a powerful separations technique, and secondly, as a rapid and positive method for the identification of the transcurium elements. In this chromatographic technique, ions, either as cations or anions, partition themselves between an aqueous phase and a solid phase that has binding sites for either cations or anions. The ion exchanger may be an inorganic substance that contains binding sites for cations (e.g. zirconium phosphate) or, more commonly, it will be an organic resin or polymer (e.g. polystyrene) containing sulfonic acid or carboxylic acid groups. Alternatively, the polymer may contain quaternary ammonium groups that can exchange anions. Actinide ions of the III, IV, V and VI oxidation states can be taken up by cation-exchange resins, and can be desorbed by elution with aqueous solutions of chloride, nitrate, citrate, lactate, ethylenediaminetetraacetate, α-hydroxyisobutyrate, and other anions [12, 13] (see Chapter 13). Metal ions can also be separated by solid phases that can exchange anions. In anion exchange, lanthanide or actinide ions must be present as negatively charged complex ions. The anion-exchange resins Dowex 1 (a copolymer of styrene and divinylbenzene containing quaternary ammonium groups) and Amberlite IRA-400 (a quaternary ammonium polystyrene) have been used successfully for actinide separations. The order of elution of the anionic actinide species is often the inverse of the order in which actinide cations are eluted from a cation-exchange column.

Ion exchange is rapid and selective, and because the elution order and approximate peak positions can be predicted with considerable confidence, ion exchange has been the key to the discovery of the transcurium elements. The power of the method can be judged from Fig. 14.3, which compares the order of elution of the lanthanide and actinide ions from the ion-exchange resin Dowex 50 (a copolymer of styrene and divinylbenzene containing sulfonic acid groups). The eluting agent was an aqueous solution of ammonium hydroxyisobutyrate. In this system elution occurs in the inverse order of atomic number for both lanthanide

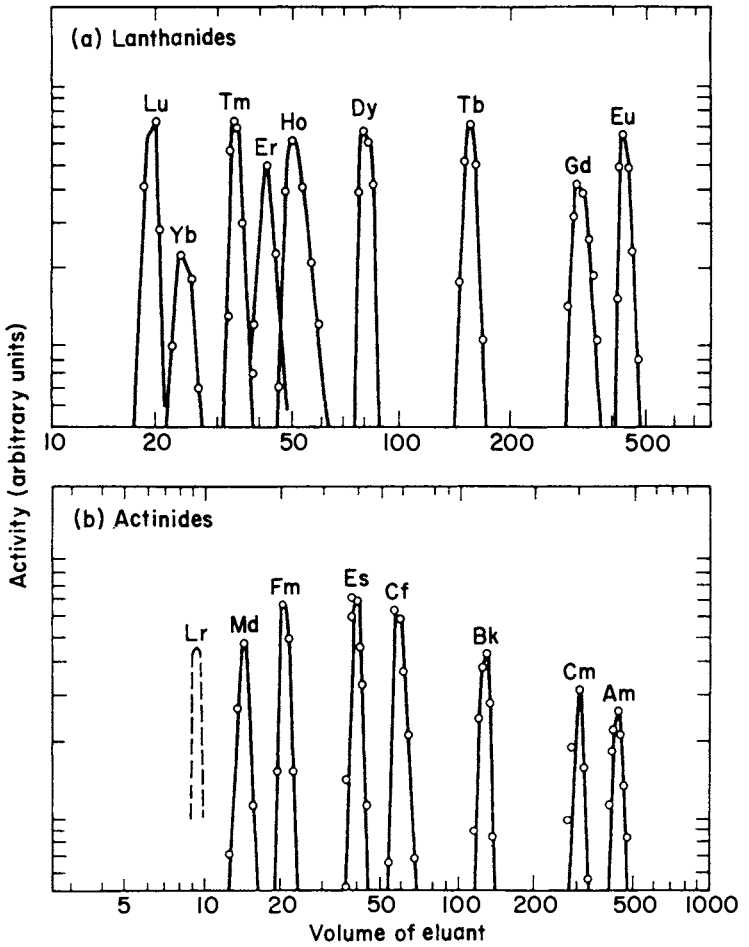

Fig. 14.3 *Elution of tripositive lanthanide and actinide ions on Dowex 50 cation-exchange resin and ammonium α-hydroxyisobutyrate eluant. Lr^{3+} band (dashed line) is predicted.*

and actinide elements. There are many similarities between the 4f and 5f transition element series, but few parallels, if any, are more striking than those observed in ion exchange. The elution sequence reflects the balance between the strength of binding to the ion-exchange resin and the tendency to form a complex ion with the eluting agent. The differences between these two interactions may be correlated with the variation of ionic radius with atomic number.

14.3.6 Liquid–liquid extraction

Liquid–liquid (or solvent) extraction is a separation technique that depends on the partition of ions between two immiscible liquid phases, one of which is usually

an aqueous solution. The organic phase often contains an extracting agent that is capable of interacting with a metal cation to form a soluble non-ionic (neutral) complex. Useful cation extractants include tri-n-butyl phosphate, bis(2-ethylhexyl)phosphoric acid, and mono(2-ethylhexyl)phosphonic acid. Reagents that complex anionic species strongly are tertiary amines (e.g. tricaprylamine or trilaurylamine) or quaternary amines (e.g. tricaprylammonium chloride). All of the extractants have only very limited solubility in the aqueous phase and high miscibility in the organic phase. These systems have an obvious resemblance to those used in organic phase transfer catalysis. Separations are achieved because the partition coefficients for a mixture of actinide ions are significantly different, and excellent separations can be realized in a countercurrent multistage process. Solvent extraction is widely used for actinide element separations both in laboratory investigations and on a large industrial scale.

14.3.7 Column partition chromatography

A technique closely related to liquid–liquid extraction is column partition chromatography, sometimes referred to as extraction chromatography. In its essential features, partition chromatography is a solvent extraction system in which one of the liquid phases is made stationary by adsorption on a solid support. The other liquid phase is mobile. Either the aqueous or the organic phase can be immobilized. The aqueous phase can be made stationary by adsorption on silica gel, diatomaceous earth, or microspheres of 5–10 μm silica. The same extracting agents that are used in ordinary solvent extraction can be used in partition chromatography. The organic phase can be adsorbed on beads (50–200 μm in diameter) of poly(vinyl chloride), poly(tetrafluoroethylene), or poly(monochlorotrifluoroethylene). When the stationary phase is organic, the technique is referred to as reversed-phase LPC. The stationary phase is used in a column just as in ion exchange. High-pressure pumps are necessary to force the liquid phase through these columns, just as in conventional high-performance liquid chromatography. Reversed-phase LPC has been used to separate Cm(III) and Am(III), and to effect other difficult separations.

14.4 ELECTRONIC CONFIGURATION

14.4.1 General considerations

Establishing the electronic configuration of the elements has historically been a primary objective in physical and chemical research. This stems from the conviction that it ought to be possible to deduce *a priori* many of the properties of an element and its compounds from a detailed knowledge of its electronic configuration, a goal that is still a long way from full realization. There are other reasons why such information is of particular interest in actinide chemistry. The f-block elements have unusual electronic configurations, and the comparative

aspects of lanthanide and actinide electronic structures, as manifested in the chemical and physical properties of homologous elements, is a matter of keen interest. The striking similarities and differences between corresponding elements of the two series provide important insights into the contributions that the valence-electron quantum number makes to the physical and chemical properties of the f-block elements.

Information relevant to the electronic configuration can be obtained from atomic emission spectroscopy, x-ray photoelectron spectroscopy, paramagnetic susceptibility measurements, electron paramagnetic resonance, electronic transition spectroscopy, crystal structure data, and atomic-beam experiments. Discussions of the theoretical and experimental aspects of atomic spectroscopy, magnetic properties, crystal structures of solids, and electronic absorption spectroscopy are to be found in the later chapters of this work.

14.4.2 Spectroscopic studies

In atomic emission spectroscopy the frequency of light emitted from excited atoms is used to derive the energy of the electronic transitions. The data are obtained from free atoms in the gas phase. Most of these have all of their valence electrons, i.e. the atoms are electrically neutral, but among them are small numbers of ionized species that have lost one, two, or three of their valence electrons. Since the spectra result from changes in the quantum numbers of the valence electrons present in the atom, it is possible in principle to make deductions about the electronic energy levels of the emitting species. In practice, however, there are very severe problems in the interpretation of the emission spectra of the actinide elements. In the free atoms in the gas phase, the valence electrons interact strongly with the 5f electrons and also with each other. Each 5f level is split by these interactions to give many energy levels that are more widely split than the 5f levels themselves. The result is an enormous number of lines in the actinide emission spectra. In the uranium spectrum, 100 000 lines have been measured, and between 5000 and 20 000 lines have been measured for each of the elements from plutonium to berkelium. The number of assigned lines varies considerably, from about 2500 for uranium to about 100 for curium. The electronic configurations of actinium, thorium, uranium, americium, berkelium, californium, and einsteinium were determined by atomic spectroscopy. The electronic structures of protactinium, neptunium, plutonium, curium, and fermium were deduced from atomic-beam experiments [10].

The dominant features of the electronic transition spectra of actinide ions in solution or in solid crystals, as in those obtained from gas-phase ions, arise for the most part from transitions within the 5f shell. However, in the gas phase the predominant population consists of neutral atoms, which possess all of their valence electrons and therefore experience more interactions between the 5f electrons and the d- and s-shell valence electrons. The 5f electrons in actinide ions, either in crystals or in solution, are perturbed to a lesser extent because valence

electrons in the 6d and 7s shells are missing, and the 5f electrons are shielded from the electric fields of other ions by the remaining 6s and 6p electrons. The electronic transition spectra of actinide ions in solution therefore provide more information about the structure of the 5f levels, but the free-atom spectra provide more information about the interactions between the 5f and the valence electrons.

14.4.3 Electronic structure

Table 14.3 shows the best assignments at the time of writing of the configuration (beyond the radon structure) of the ground-state gas-phase neutral atom of each of the elements from actinium to lawrencium, as well as the configurations of the singly charged, doubly charged, and triply charged gaseous atoms. Included for comparison are the ground-state neutral-atom electronic configurations (beyond the xenon structure) of the 4f lanthanide elements. The similarities between the lanthanide and actinide elements were recognized from very early work on the actinides [14, 15]. It can be seen from Table 14.3 that the incorporation of the fourteen 5f electrons into the elements of the actinide series is not as regular as in the 4f series, especially in the actinide elements preceding curium.

The atomic spectra indicate quite clearly that the 6d levels of thorium in the gas-phase neutral atom are lower in energy than the 5f levels. As in other

Table 14.3 *Electronic configurations of f-block atoms and ions.*[a]

Lanthanide series			*Actinide series*					
Element	*Gaseous atom*	$M^{3+}(g)$	*Element*	*Gaseous atom*	$M^{+}(g)$	$M^{2+}(g)$	$M^{3+}(g)$	$M^{4+}(g)$
La	$5d6s^2$		Ac	$6d7s^2$	$7s^2$	7s		
Ce	$4f5d6s^2$	4f	Th	$6d^27s^2$	$6d7s^2$	5f6d	5f	
Pr	$4f^36s^2$	$4f^2$	Pa	$5f^26d7s^2$	$5f^27s^2$	$5f^26d$	$5f^2$	5f
Nd	$4f^46s^2$	$4f^3$	U	$5f^36d7s^2$	$5f^37s^2$	$5f^36d?$	$5f^3$	$5f^2$
Pm	$4f^56s^2$	$4f^4$	Np	$5f^46d7s^2$	$5f^57s?$	$5f^5?$	$5f^4$	$5f^3$
Sm	$4f^66s^2$	$4f^5$	Pu	$5f^67s^2$	$5f^67s$	$5f^6$	$5f^5$	$5f^4$
Eu	$4f^76s^2$	$4f^6$	Am	$5f^77s^2$	$5f^77s$	$5f^7$	$5f^6$	$5f^5$
Gd	$4f^75d6s^2$	$4f^7$	Cm	$5f^76d7s^2$	$5f^77s^2$	$5f^8$	$5f^7$	$5f^6$
Tb	$4f^96s^2$	$4f^8$	Bk	$5f^97s^2$	$5f^97s$	$5f^9$	$5f^8$	$5f^7$
Dy	$4f^{10}6s^2$	$4f^9$	Cf	$5f^{10}7s^2$	$5f^{10}7s$	$5f^{10}$	$5f^9$	$5f^8$
Ho	$4f^{11}6s^2$	$4f^{10}$	Es	$5f^{11}7s^2$	$5f^{11}7s$	$5f^{11}$	$5f^{10}$	$(5f^9)$
Er	$4f^{12}6s^2$	$4f^{11}$	Fm	$5f^{12}7s^2$	$(5f^{12}7s)$	$(5f^{12})$	$(5f^{11})$	$(5f^{10})$
Tm	$4f^{13}6s^2$	$4f^{12}$	Md	$(5f^{13}7s^2)$	$(5f^{13}7s)$	$(5f^{13})$	$(5f^{12})$	$(5f^{11})$
Yb	$4f^{14}6s^2$	$4f^{13}$	No	$(5f^{14}7s^2)$	$(5f^{14}7s)$	$(5f^{14})$	$(5f^{13})$	$(5f^{12})$
Lu	$4f^{14}5d6s^2$	$4f^{14}$	Lr	$(5f^{14}6d7s^2$ or $5f^{14}7s^27p)$	$(5f^{14}7s^2)$	$(5f^{14}7s)$	$(5f^{14})$	$(5f^{13})$
			Rf	$(5f^{14}6d^27s^2)$				$(5f^{14})$

[a] Predicted configurations in parentheses.

transition series, the relative energy levels of the electron shell being filled become lower as successive electrons are added, and, in the elements following thorium, the 5f shell appears clearly to be of lower energy than the 6d shell. Doubly ionized Th^{2+} appears to have one 5f electron in the gas phase, but this is not an oxidation state that is found in thorium compounds. For the elements beyond neptunium, the electronic configurations of the 4f and 5f elements strongly resemble each other. That the relative energy levels of the outer d- and s-shell electrons relative to the 5f electrons are not identical to those observed in the 4f-block elements is not unexpected. Fig. 14.4 represents the relative energies of electron configurations that interchange 5f and 6d electrons for most of the actinide elements; as the curves intersect, inversion of behavior is inevitable. There are reasons to suppose that spatial characteristics of the f-shell orbitals may change abruptly at certain atomic numbers; that is, the f-shell electrons may be shielded much more strongly in some elements than in others where the f orbitals extend close to the surface of the electron cloud, and where the 5f electrons are in closer contact with d- and s-shell electrons. As the 5f electrons are shielded to a greater extent from the nucleus of the atom than in the 4f elements, the energy differences between 5f, 6d, and 7s electrons will be smaller than in the lanthanide series. There can be little doubt that 5f electrons are present in all of the actinide elements after protactinium, and that they participate in bonding interactions [16].

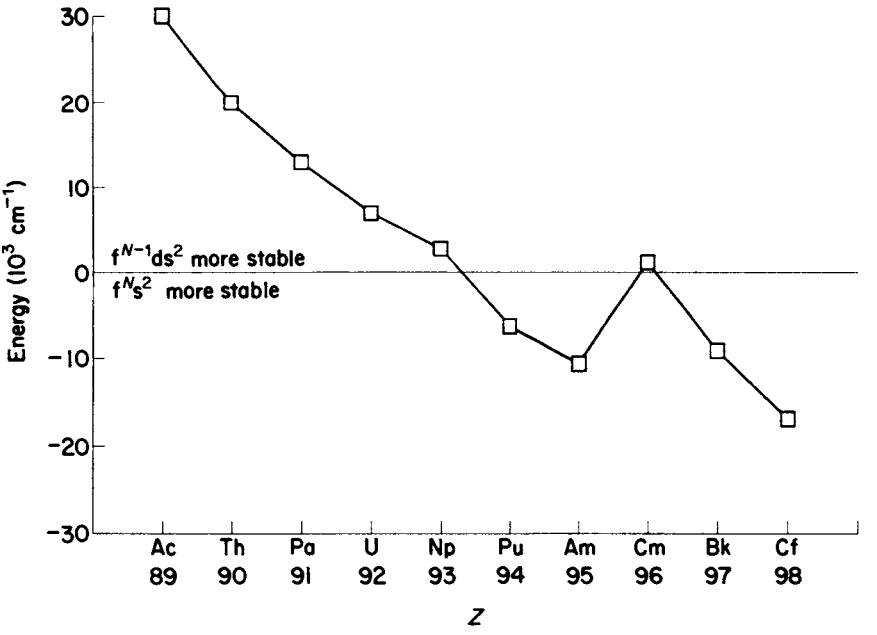

Fig. 14.4 *Relative energies of the* f^Ns^2 *and* $f^{N-1}ds^2$ *electron configurations in gaseous actinide atoms.* $N = Z - 88$. *Based on Fig.* 15.3(*a*).

14.4.4 Position in the periodic table

Prior to 1944, the elements thorium, protactinium, and uranium were assigned positions in the periodic table immediately below the elements hafnium, tantalum, and tungsten. It became evident that to accommodate the transuranium elements in the periodic table would require a radically new arrangement. The arguments for positioning them as a new 'actinide' transition series, similar to the rare earths, became strong by 1944 but experimental data to support this view were still scanty. With the passage of time the evidence in favor of a new transition series has become very convincing. Fig. 14.5 shows a modern periodic table, which not only includes the actinide elements as a transition series, but also indicates the predicted location of the transactinides and a new superactinide transition series that may never be discovered.

14.5 OXIDATION STATES

14.5.1 Ions in aqueous solution

Tables 14.4 and 14.5 list the oxidation states of the actinide elements and the color of the actinide ions, respectively. It is clear that the actinide oxidation states are far more variable than the lanthanides. The close proximity of the energy levels of the 7s, 6d, and 5f electrons almost guarantees multiple oxidation states for the actinide ions, at least in the first half of the actinide series. The multiplicity of oxidation states, coupled with the hydrolytic behavior of the ions, make the chemical behavior of the elements from protactinium to americium among the most complex of the elements in the periodic table.

In Table 14.4, the most stable states are shown in bold type and the most unstable states are indicated by parentheses. (Oxidation states that have been claimed to exist, but not independently substantiated, are indicated with question marks.) The most unstable oxidation states have only been observed in solid compounds, or produced as transient species in solution by pulse radiolysis [17–20]. In this very interesting technique, a beam of electrons is injected into an aqueous solution of the ion under investigation. These have been mainly the 3+ actinide ions. When N_2O is present in the reaction mixture, the hydrated electrons formed by the injection of the electrons into water are converted into OH radicals, which are strong oxidants. If t-butanol is present in place of nitrous oxide, the OH radicals are scavenged, and only the hydrated electron, e^-(aq), a powerful reducing agent, is formed. The reactions of these reagents with actinide ions is followed spectrophotometrically. Reaction of the III ions in 0.1 M perchloric acid with e^-(aq) forms Am(II), Cm(II), and Cf(II). When OH radicals react, Am(IV) and Cm(IV), but no Cf(IV), are produced. All of the 2+ and 4+ species are transient. The II species disappear with rate constants of about $10^5\ s^{-1}$ by what appears to be a first-order process. Am(II), Cm(II), and Cf(II) have half-lives of the order of 5–20 μs; Am(IV) appears to be appreciably more stable and

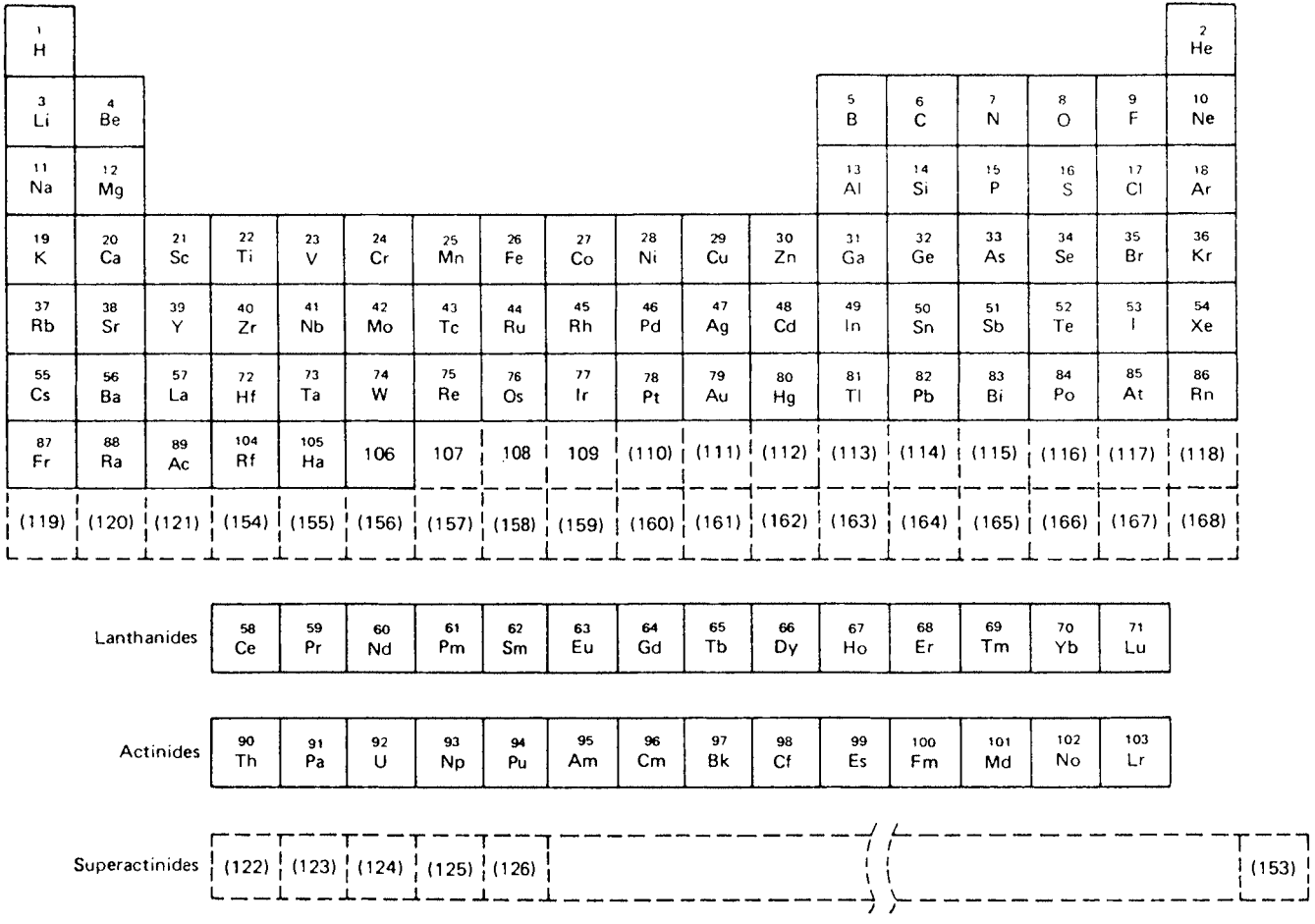

Fig. 14.5 *Modern periodic table showing predicted locations of many undiscovered transuranium elements (atomic numbers in parentheses).*

Table 14.4 *The oxidation states of the actinide elements.*

Atomic number	89	90	91	92	93	94	95	96	97	98	99	100	101	102	103
Element	*Ac*	*Th*	*Pa*	*U*	*Np*	*Pu*	*Am*	*Cm*	*Bk*	*Cf*	*Es*	*Fm*	*Md*	*No*	*Lr*
Oxidation states													1?		
							(2)			(2)	(2)	2	2	**2**	
	3	(3)	(3)	3	3	3	**3**	**3**	**3**	**3**	**3**	**3**	**3**	3	**3**
		4	4	4	4	**4**	4	4	4	(4)	4?				
			5	5	**5**	5	5	5?		5?					
				6	6	6	6	6?							
					7	(7)	7?								

Bold type = most stable; ( ) = unstable; ? = claimed but not substantiated.

has a half-life of about 1 ms. Pulse radiolysis has been shown to be a widely applicable method for producing ionic species in oxidation states that are difficult or impossible to access by conventional chemical procedures.

With the exception of thorium and protactinium, all of the actinide elements show a III state in aqueous solution, although the III state does not become the preferred or stable oxidation state under ordinary conditions until americium is reached. A stable IV state is observed in the elements thorium through plutonium and in berkelium. The V oxidation state is well-established for the elements protactinium through americium, and the VI state in the elements uranium through americium. The IV state in curium is confined to a few solid compounds, particularly CmO_2 and CmF_4, and appears to be present in a stable complex ion that exists in concentrated cesium fluoride solution. The californium(IV) state is limited to the solid compounds CfO_2, CmF_4, and a complex oxide $BaCfO_3$. The II state first appears at californium in the second half of the series and becomes increasingly more stable in proceeding to nobelium. Mendelevium(II) and nobelium(II) have been observed in aqueous solution and this appears to be the most stable oxidation state for nobelium. Americium(II) has been encountered only in solid compounds and in pulse radiolysis experiments in acetonitrile solution. The formation of berkelium(IV) probably is associated with enhanced stability of the half-filled 5f configuration ($5f^7$), and the nobelium(II) state may be taken to reflect the stability of the full 5f shell ($5f^{14}$). The increase in the stability of the lower oxidation states of the heavier actinide elements relative to the lanthanides may be the result of stronger binding of the 5f (and 6d) electrons in the elements near the heavy end of the actinide series. Claims have been advanced that all the elements from plutonium to nobelium can be prepared in the II state, and that this is a stable oxidation state for the elements fermium to nobelium [21]. There has been no confirmation of these claims. The findings from pulse radiolysis show that even the II state of the actinides preceding einsteinium are transient species, and have very short lifetimes [19, 20]. Mendelevium has been

reported to possess a stable I oxidation state [21], but we believe that the evidence for monovalent ions of the actinide elements is doubtful.

14.5.2 Ion types

Actinide ions in the same oxidation state have essentially the same structures. In aqueous solutions at a pH < 3, four structural types of actinide cations exist. Formulas and colors of these ions are listed in Table 14.5. Only simple ions are listed. The ions of the type M^{3+} or M^{4+}, as is the case for cations with a high charge, show a strong inclination to solvation, hydrolysis, and polymerization (see Section 14.5.3 below). For the actinide elements in higher oxidation states, the effective charge on the simple ion is decreased by the formation of oxygenated species of the general type MO_2^+ and MO_2^{2+}. The actinyl ions MO_2^+ and MO_2^{2+} are remarkably stable entities, and travel as a unit through a great variety of chemical transformations. Infrared spectroscopy shows conclusively that the ion MO_2^{2+} exists as a symmetrical, linear or very nearly linear, group. The corresponding V state actinyl ions of neptunium and americium likewise have the structures NpO_2^+ and AmO_2^+. There is a regular decrease in the strength of the metal–oxygen bond with increasing atomic number in the actinyl ions from uranium to americium. The VII oxidation state found in some compounds of neptunium and plutonium in alkaline aqueous solution probably contains ions of the type MO_5^{3-}. In acid solution, actinide ions in the VII oxidation state oxidize water rapidly.

Reduction potentials for the actinide elements are shown in Fig. 14.6. These show formal potentials, defined as the measured potentials relative to the hydrogen ion/hydrogen couple taken as zero volts. The redox potentials are corrected to unit concentration of the reactants, but are not corrected for activity. The measured potentials were determined by electrochemical cells, equilibria, and enthalpy of reaction measurements. The potentials for acid solution were

Table 14.5 *Ion types and colors for actinide ions.*

Element	M^{3+}	M^{4+}	MO_2^+	MO_2^{2+}	MO_5^{3-}
actinium	colorless				
thorium		colorless			
protactinium		colorless	colorless		
uranium	red	green	color unknown	yellow	
neptunium	blue to purple	yellow-green	green	pink to red	dark green
plutonium	blue to violet	tan to orange-brown	reddish-purple	yellow to pink-orange	dark green
americium	pink or yellow	color unknown	yellow	rum-colored	
curium	pale green	color unknown			
berkelium	green	yellow			
californium	green				

generally measured in 1 M perchloric acid, and those for alkaline solution in 1 M sodium hydroxide. Estimated values are indicated in parentheses.

The M^{4+}/M^{3+} and the MO_2^{2+}/MO_2^{+} couples are reversible, and, as expected, rapid reactions occur with one-electron oxidizing and reducing agents when no bond breaking or making takes place. The MO_2^{+}/M^{3+}, MO_2^{+}/M^{4+}, and MO_2^{2+}/M^{4+} couples are not reversible, presumably because of the barrier introduced by formation and rupture of bonds and the subsequent reorganization of the solvent shell.

A summary of qualitative information about the oxidation–reduction characteristics of the actinide ions is presented in Table 14.6. The disproportionation and redox reactions of UO_2^{+}, Pu^{4+}, PuO_2^{+}, and AmO_2^{+} are especially complex, and, despite extensive study, many aspects of these reactions still remain to be explored. In the case of plutonium, the situation is especially complicated, for ions in all four oxidation states III, IV, V, and VI can exist simultaneously in aqueous solution in equilibrium with each other in comparable concentrations. The kinetics of the redox reactions of the actinide elements have been ably summarized by Newton [22].

14.5.3 Hydrolysis and polymerization

All metal cations in aqueous solution interact extensively with the solvent water, and to a lesser or greater extent exist as aquo cations [23, 24]. The more highly charged the naked cation, the greater the extent of interaction with the solvent. Aquo cations, especially those of 4+, 3+, and small 2+ ions, tend to act as acids in solution:

$$M(OH_2)_x^{n+} = M(OH_2)_{x-1}(OH)^{(n-1)+} + H^+$$

This reaction illustrates the increase in acidity of protic ligands coordinated to metal cations. Since the acidity of water coordinated to 3+ and 4+ species is the more strongly enhanced the higher the charge on the metal cation, it is no surprise that actinide elements in their most frequently encountered oxidation states undergo extensive hydrolytic reactions. Th^{4+}(aq) exists as unhydrolyzed $Th(OH)^{3+}$(aq) at a pH below about 0.5 in 0.5 M Th(IV) solutions. At higher pH, hydrolyzed thorium(IV) species begin to predominate. The mononuclear protactinium (V) species PaO^{2+} (aq) or $Pa(OH)_2^{2+}$ (aq) have been claimed to exist at low concentrations; however, polymers are already evident at protactinium concentrations well below micromolar in tracer experiments. Uranium(IV) begins to undergo hydrolysis in aqueous solution above pH > 2.9, and, at somewhat higher pH, is largely present as hydrolyzed species. $U(OH)^{3+}$ has been identified as the predominant U(IV) species in solution at low uranium concentrations and high acidities. Plutonium(IV) requires strongly acid conditions to exist as a simple Pu^{4+}(aq) ion. In moderately acid solutions, Pu(IV) hydrolyzes extensively, and may form polymers of high molecular weight. The actinyl ions typical of the V and VI states presumably are formed with great speed whenever oxidation to the V and

Actinium

Acid

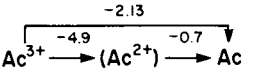

Base

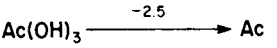

Thorium

Acid

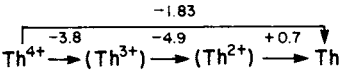

Base

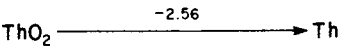

Protactinium

Acid

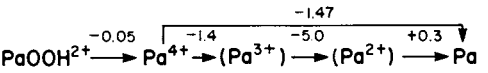

Uranium

Acid

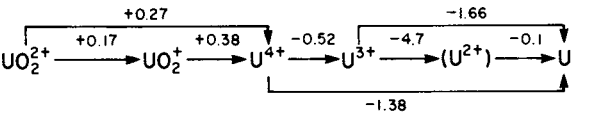

Base

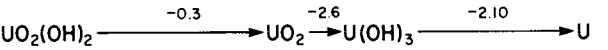

Neptunium

Acid

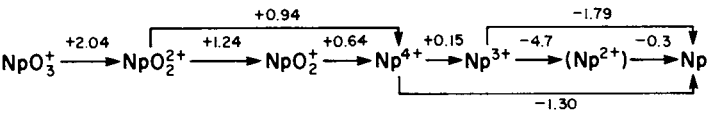

Base

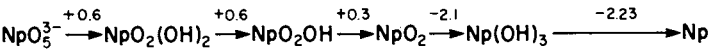

Plutonium

Acid

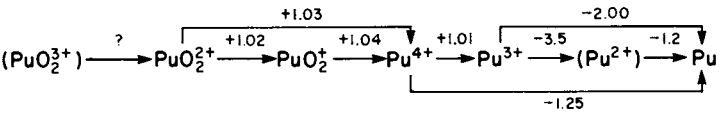

Base

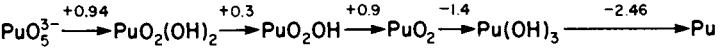

Americium

Acid

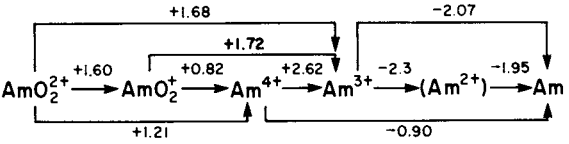

Base

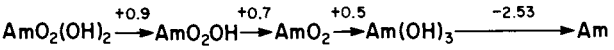

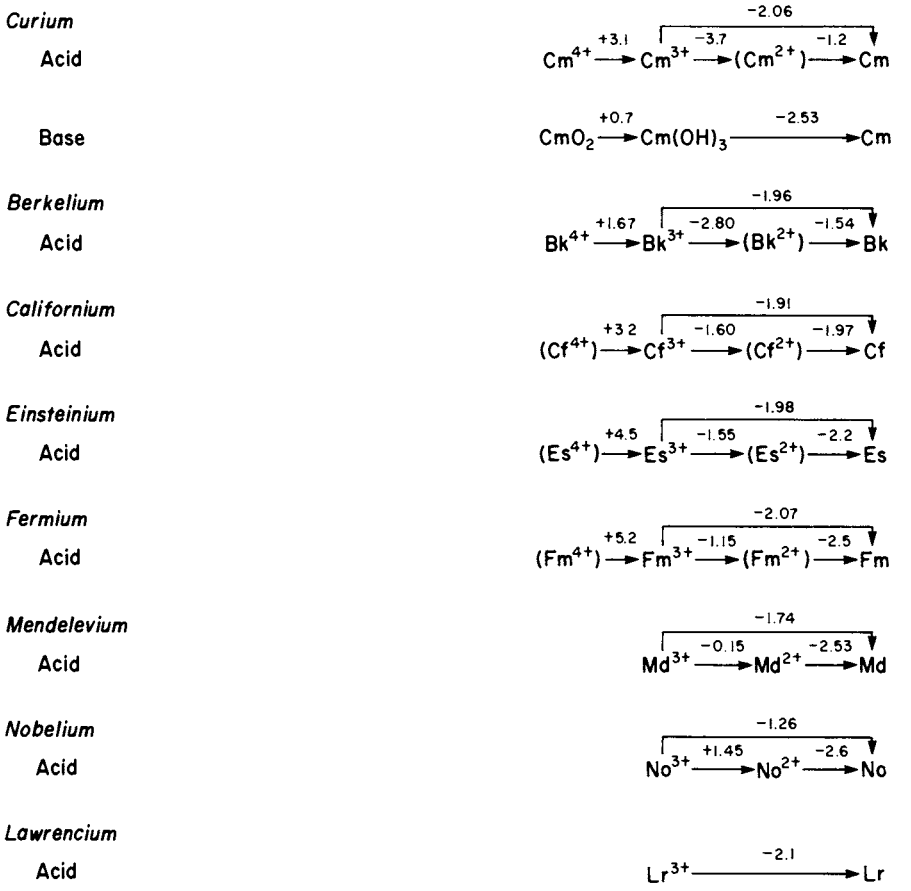

Fig. 14.6 *Standard (or formal) reduction potentials of actinium and the actinide ions in acidic (pH 0) and basic (pH 14) aqueous solutions (values are in volts vs standard hydrogen electrode).*

VI states occurs in water. Once the uranyl, neptunyl, and plutonyl ions are formed, the only practical way to remove the coordinated oxygen atoms is by reduction to the IV state. Although uranyl nitrate can be obtained as an anhydrous compound, in this form it is coordinatively unsaturated, and it is usually encountered as the hexahydrate or coordinated to equivalent ligands.

It is well-known that aquo cations of heavy elements in the III oxidation state or higher readily lose protons to form hydroxo complexes. Subsequent condensation reactions between the hydroxo complexes can then form polynuclear species in which the metal ions are linked through hydroxo (M–OH–M) or oxo (M–O–M) bridges. For the formation of polynuclear species, the pH range is critical; at too low a pH the ion will exist as the simple aquocation, and at too high a pH the hydrous oxide or hydroxide precipitates. The actinide ions with oxidation number IV are particularly prone to hydrolysis and polymerization, but the V and VI oxo

Table 14.6 *Stability of actinide ions in aqueous solution.*

Ion	*Stability*
Md^{2+}	stable to water, but readily oxidized
No^{2+}	stable
Ac^{3+}	stable
U^{3+}	aqueous solutions evolve hydrogen on standing
Np^{3+}	stable to water, but readily oxidized by air to Np^{4+}
Pu^{3+}	stable to water and air, but easily oxidized to Pu^{4+}; oxidizes slightly under the action of its own α radiation (in form of ^{239}Pu)
Am^{3+}	stable; difficult to oxidize
Cm^{3+}	stable
Bk^{3+}	stable; can be oxidized to Bk^{4+}
Cf^{3+}	stable
Es^{3+}	stable
Fm^{3+}	stable
Md^{3+}	stable, but rather easily reduced to Md^{2+}
No^{3+}	easily reduced to No^{2+}
Lr^{3+}	stable
Th^{4+}	stable
Pa^{4+}	stable to water, but readily oxidized
U^{4+}	stable to water, but slowly oxidized by air to UO_2^{2+}
Np^{4+}	stable to water, but slowly oxidized by air to NpO_2^+
Pu^{4+}	stable in concentrated acid, e.g. 6 M HNO_3, but disproportionates to Pu^{3+} and PuO_2^{2+} at lower acidities
Am^{4+}	known in solution only as complex fluoride ion
Cm^{4+}	known in solution only as complex fluoride ion
Bk^{4+}	marginally stable; easily reduced to Bk^{3+}
Pa^{5+}	stable, hydrolyses readily
UO_2^+	disproportionates to U^{4+} and UO_2^{2+}; most nearly stable at pH 2–4
NpO_2^+	stable; disproportionates only at high acidities
PuO_2^+	tends to disproportionate to Pu^{4+} and PuO_2^{2+} (ultimate products); most nearly stable at very low acidities
AmO_2^+	disproportionates in strong acid to Am^{3+} and AmO_2^{2+}; reduces fairly rapidly under the action of its own α radiation at lower acidities (in form of ^{241}Am)
UO_2^{2+}	stable; difficult to reduce
NpO_2^{2+}	stable; easy to reduce
PuO_2^{2+}	stable; easy to reduce; reduces slowly under the action of its own α radiation (in form of ^{239}Pu)
AmO_2^{2+}	easy to reduce; reduces fairly rapidly under the action of its own α radiation (in form of ^{241}Am)
NpO_5^{3-}	observed only in alkaline solution
PuO_5^{3-}	observed only in alkaline solution; oxidizes water

cations are also known to have considerable tendencies toward polynuclear ion formation. Among the 4+ cations, thorium(IV), uranium(IV), and especially plutonium(IV) form polymeric species. Thorium(IV) has a very complicated solution chemistry and, except in strong acid solutions, polynuclear species are easily generated in which Th atoms are crosslinked by hydroxo bridges. Similarly, uranium(IV) forms polynuclear aggregates that may contain both hydroxo and oxo bridges. The $U(OH)^{3+}$ ion, which predominates in very acid solutions and low uranium concentrations, rapidly undergoes polymerization in solutions of moderate or low acidity. Two hexameric species, $U_6(OH)_{15}^{9+}$ and $U_6O_4(OH)_4^{12+}$, have been characterized. The formation of very large polymers occurs with U(IV) at much lower ligand numbers than is the case for Th(IV). The hydrolytic behavior of the neptunium(IV) ion is similar to that of U^{4+}, although Np^{4+} is an appreciably weaker acid. The hydrated plutonium(IV) ion is about as strong an acid as is the U(IV) ion, but it appears to be exceptionally prone to polymer formation. As hydrolysis proceeds and before actual precipitation occurs, positively charged polymers of colloidal dimensions with molecular weights as high as 10^{10} have been observed. Although all of the polynuclear species of the actinide ions are of scientific interest, the polymers of plutonium(IV) have attracted the most attention because of practical considerations. The effect of concentration, acidity, temperature, and ionic strength on polymer formation are ill-defined, and, as the plutonium(IV) polymers are very stable and depolymerization is not at all easily effected, the erratic behavior of plutonium(IV) solutions can pose major problems and create potentially serious hazards in nuclear fuel processing.

The actinyl ions MO_2^+ and MO_2^{2+} are considerably less acidic than are the IV state monomeric ions, and therefore have a smaller tendency to undergo hydrolysis. Hydrolysis decreases in the order $M^{4+} > MO_2^{2+} > M^{3+} > MO_2^+$. If, as is generally supposed, the ratio of charge to ion size is the determining factor in hydrolysis, then the diminished tendency of the actinyl(VI) ions to hydrolyze is not surprising. There must be important factors other than the size/charge ratio, however, that supervene. Thus, the order of acidity for the 4+ species is $U^{4+} \approx Pu^{4+} > Np^{4+}$. The decrease in the extent of hydrolysis of Np^{4+} is unexpected, and the reversal in the order of hydrolysis at plutonium cannot be understood simply in terms of charge-to-size considerations. On the basis of increasing charge and decreasing ionic size, it could be expected that the degree of hydrolysis for a series of ions of any charge in the actinide series would increase with atomic number. For the actinyl(V) and actinyl(VI) ions, however, the degree of hydrolysis decreases with increasing atomic number. This and the anomalous hydrolytic behavior of Np(IV) strongly imply that additional, and as yet unidentified, factors make important contributions to the interaction of the actinide ions with water.

The actinyl(V) ions, which carry the low charge of 1+, are weak acids, with the singular exception of protactinium(V). The protactinyl(V) ion is a much stronger

acid than either its predecessors or successors in the actinide series. In both its IV and V oxidation states, protactinium shows a phenomenal tendency to hydrolyze. Indeed, it is questionable whether monomeric protactinium species are ever encountered in the real world. Experience with protactinium chemistry on the tracer scale suggests that even in these extremely dilute solutions protactinium is already extensively hydrolyzed. The chemical investigation of protactinium at any level is rendered extremely difficult by the formation of intractable polymers. Efforts to prevent hydrolysis by the use of complexing agents such as fluoride ion are useful expedients but fall short of fully satisfactory solutions to the problem.

The actinyl(VI) ions all undergo hydrolysis to an appreciable extent. Hydrolysis of UO_2^{2+} even in dilute solution results in almost total conversion to polynuclear species. These are small entities, containing fewer than five uranium atoms. The tendency to form polymers of colloidal dimensions thus appears to be much diminished in the actinyl(VI) ions relative to the actinyl(IV) ions. Precipitation occurs early on after relatively small polymeric aggregates of actinyl ions form in the solution. The strong inclination to form insoluble precipitates after only a small amount of hydrolysis makes characterization of the water-soluble polymers of the actinyl ions a difficult matter.

14.5.4 Complex-ion formation

The tendency to form complex ions in solution is to a considerable extent an expression of the same forces that lead to hydrolysis. The high positive charge on a bare 3+ or 4+ ion provides a strong driving force for interaction with nucleophiles. Water is only one example of such a nucleophilic ligand. Other nucleophiles that may be present in a solution can compete for coordination to the electrophilic cation, to form complex ions. In most cases of complex formation, water molecules directly bound to the metal cation are displaced by the entering ligand to form an inner-sphere complex that may or may not contain water still bound to the metal ion. Alternatively, ligands may be attached to water molecules of the outer hydrate shell to form outer-sphere complexes. Strong complexes are for the most part of the inner-sphere type. For inorganic anions, the complexing power of the actinide cations is in the order fluoride > nitrate > chloride > perchlorate for the singly charged anions, and carbonate > oxalate > sulfate for doubly charged anions. The stability of the complexes for a given ligand follows the order $M^{4+} > MO_2^{2+} = M^{3+} > MO_2^{+}$. For ions of the same charge, the stability of the complex increases with decreasing ionic radius at the beginning of the actinide series. Many irregularities are encountered in the latter part of the series, just as there are discontinuities in the hydrolytic behavior of neptunium and plutonium. Overall, however, the stability of the actinide complexes increases as the ratio of effective charge to ionic radius increases. As a general rule, the actinide ions form somewhat more stable complexes than do the homologous lanthanide ions.

The phosphate anion PO_4^{3-} and organic phosphates are powerful complexing agents for actinide ions. The phosphate anion acts as a bridge between metal ions to form aggregates that are insoluble in water. The M^{4+} and MO_2^{2+} ions form complexes with many organic phosphates, either neutral or anionic, that are preferentially soluble in non-polar aliphatic hydrocarbons. Typical of such ligands are tributyl phosphate (TBP) and dibutyl phosphate (DBP). Phosphine oxides are also potent coordinating ligands. Oxygen-containing donor compounds such as the ketones, di-isopropyl ketone or methyl isobutyl ketone, and the ethers, diethyl ether, ethyleneglycol diethyl ether or diethyleneglycol dibutyl ether, act likewise and are good complexing agents for actinide ions. All of these ligands have oxygen atoms with lone electron pairs not otherwise engaged in chemical bonding that can act as electron donors in coordination interactions. Complexes with such reagents have been used on a very large scale in the extraction and separation of the actinide elements by liquid–liquid partition.

Chelating ligands form strong complexes with actinide ions. Examples of such are the β-diketones, the tropolones, 8-hydroxyquinoline and its derivatives, and ethylenediaminetetraacetic acid (EDTA), among many others. In its enol form, acetylacetone, a typical diketone, forms very strong metal complexes with M^{4+} ions. Even though these complexes have significant water solubility, they are easily and completely extracted by benzene, carbon tetrachloride or similar non-polar solvents. The acetylacetone complexes of the MO_2^{2+} actinyl ions form weaker complexes that show little preference for a non-polar organic phase. The structure of the diketone can be modified to enhance the preferential solubility of the metal complex for the organic phase. The most important of such modified β-diketone chelating agents is 2-thenoyltrifluoroacetone ($C_4H_3COCH_2COCF_3$), which has been widely used to extract plutonium from aqueous solutions into non-polar solvents. Tropolone is a seven-membered cyclic carbon compound containing a keto carbonyl function and a weakly acid hydroxyl group, which are able to form strong complexes with highly charged metal cations. A tropolone derivative containing an isopropyl group, β-thujaplicin, is a particularly useful chelating agent for actinide ions because its metal complexes show a strong preference for the organic phase in liquid–liquid partitions. Ethylenediaminetetraacetic acid (EDTA) is an effective sequestering agent for the actinide ions in aqueous solutions. The strongest complexes are formed by M^{4+}; the Np^{4+} complexes are weaker than those of U^{4+} and Pu^{4+}. The strength of the EDTA complexes with M^{3+} ions increases steadily from Pu^{3+} to Cf^{3+}. Possibly for steric reasons, EDTA interacts in a different way with actinyl(VI) ions; in these systems EDTA is a bridging ligand, and gives rise to linear polynuclear complexes.

There is a great deal more to be said about the actinide ions in solution, about hydrolytic phenomena, and about complex-ion formation. For a comprehensive and authoritative treatment of these important subjects, the reader is referred to Chapter 21 of this work.

14.6 THE METALLIC STATE

The actinide metals pose some of the most interesting problems in actinide research. Many actinide compounds behave in a perfectly conventional way (except for radioactivity), and have properties that can be safely inferred from lanthanide chemistry or the chemistry of similar compounds of well-studied elements. For no category of materials is this less true than for the actinide metals. The actinide elements in their elemental state are unique. They have metallurgical properties that are unprecedented in conventional metals, and their properties cannot be accounted for by conventional theories of the metallic state. The theoretical framework of the metallic state has had to be broadened to accommodate this group of unusual metals, and this has led to a better understanding of the metallic state in general [25].

14.6.1 Preparation

The actinide metals are highly electropositive and react with water vapor, oxygen, and, in finely divided form, with nitrogen of the air [26]. The alpha activity of the actinides makes confinement in atmosphere-controlled glove boxes compulsory. For some of the heavier actinide metals, shielding is required because of neutrons released by spontaneous fission. The actinide elements form very stable oxides and fluorides, and vigorous reducing agents and high temperatures are necessary for reduction to the metal. The earliest preparations of the actinide metals involved reduction of the anhydrous actinide tri- or tetrafluoride with lithium or barium metal at high temperature. For submilligram amounts this is still the method of choice. Alternatively, the actinide oxide is reduced at high temperature with lanthanum or thorium metal. All of the starting materials must be as pure as possible to assure a pure product. The actinide metal can be obtained from the reaction mixture in reasonable purity by volatilization of the metal. Reduction of the oxide is the preferred route to milligram-to-gram amounts of Ac, Am, Cm, Bk, Cf, and Es [27]. Uranium, thorium, and plutonium metals are obtained from normal industrial-scale operations.

Much modern research on the metallic state requires very pure metals. Depending on the nature of the impurities, the actinide metals can be purified by volatilization of the impurities in a very high vacuum, by volatilization of the metal itself to form films of very pure metal, or by electrodeposition from molten-salt baths. Very pure metals can be obtained by the Van Arkel process, which consists of converting the crude metal to the volatile iodide by reaction with elemental iodine at an elevated temperature, and decomposing the gaseous metal iodide on a hot filament [28–30]. This process produces exceptionally pure metals, which have been used for such demanding purposes as superconductivity measurements that require metals of the highest purity.

14.6.2 Crystal structures

The crystal structures, phase transformations, and metallic radii of the actinide metals are listed in Table 14.7, together with melting points, densities, and enthalpies of vaporization. The crystal structures of metallic protactinium, uranium, neptunium, and plutonium are complex, have no counterparts among the lanthanide metals, and resemble the 3d transition metals more closely than the lanthanides. The lanthanide metals show a generally uniform hexagonal close-packed (hcp) or face-centered cubic (fcc) crystal structure pattern at low temperatures, and body-centered cubic (bcc) structure at high temperatures. The lighter actinide elements have a bcc structure at the melting point, which changes to fcc in the elements after plutonium. For the actinide elements americium through einsteinium, the characteristic crystal structures at all temperatures below the melting point are the fcc and double hexagonal close-packed (dhcp) structures. In uranium, neptunium and plutonium, complex crystal structures are observed at low temperatures.

The differences between the actinide and lanthanide metals can be rationalized by a consideration of the differences between the 4f- and 5f-electron shells [25]. In the 4f series, all the 4f electrons (added after cerium) are buried in the interior of the electron cloud. The 4f electrons are thus confined to the core of the atom, and experience relatively little interaction with electrons in the 5d shell. The maxima in the radial charge density occur well inside the usual interatomic distances in solids, and consequently the 4f electron properties of the free atoms are retained in the metallic as well as ionic lanthanide solids. Cerium is the only 4f metal that does not conform to this generalization, presumably because its 4f-electron shell is not yet fully stabilized. The actinide 5f electrons behave quite differently. For the early members of the actinide series, the 5f electrons have a greater radial distribution than do their 4f homologs. The first few 5f electrons are not confined to the core of the atom, and they can therefore interact or mix with the other valence electrons to affect interatomic interactions in the solid state. Beyond plutonium, all the 5f electrons are localized within the atomic core, and the resemblance between the f-block elements becomes closer. Americium is the first actinide metal whose crystal structure resembles that of the lanthanide metals. In the transcurium metals, the resemblance to the lanthanide metals becomes increasingly stronger. The room-temperature crystal structure for the elements for Am to Cf is dhcp, just as it is in the light lanthanides.

A natural consequence of the increase in nuclear charge along the actinide series for a given oxidation state is an increasing tendency for the 6d and 7s electrons to experience less shielding from the nuclear charge, and this leads to a contraction of the atomic radius. Shielding of the valence electrons from the nucleus is also diminished by delocalization of the 5f electrons in the early part of the actinide series. In the metals, the atomic radius expands significantly when the 5f electrons are localized in the core, which occurs at americium and curium. The

Table 14.7 *Properties of actinides metals*

Element	*Melting point* (°C)	*Enthalpy of vaporization at 25°C* (kJ mol^{-1})	*Lattice symmetry*	*Temp. range of stability* (°C)	*Lattice constants* a_0 (Å)	b_0 (Å)	c_0 (Å)	β (deg)	*X-ray density* (g cm^{-3})	*Atoms per unit cell*	*Metallic radius, CN12*[a] (Å)
actinium	1050	418	fcc		5.315 ± 5				10.01	4	1.878
thorium		598	α, fcc	< ~1360	5.0842 (25°C)				11.724	4	1.798
	1750		β, bcc	~1360–1750	4.11 (1450°C)				11.10	2	1.80
protactinium		660	α, bc tetrag.	below 1165	3.929		3.241		15.37	2	1.642
	1572		β, bcc	1165–1572	3.81 (1186°C)				13.87	2	1.775
uranium		536	α, orthorhombic	below 668	2.8478 (25°C)	5.8580	4.9455		19.16	4	1.542
			β, tetragonal	668–775	10.763 ± 5 (720°C)[b]		5.652 ± 5		18.11	30	1.548
	1133		γ, bcc	775–1133	3.524 ± 2 (805°C)				18.06	2	1.548
neptunium		465	α, orthorhombic	below 280	6.663 ± 3	4.723 ± 1	4.887 ± 2		20.45	8	1.503
			β, tegragonal	280–576	4.897 ± 2 (313°C)		3.388 ± 2		19.36	4	1.511
	637		γ, bcc	576–637	3.518 (600°C)				18.04	2	1.53
plutonium		342	α, monoclinic	below 122	6.183 (21°C)	4.822	10.963	101.79	19.86	16	1.523
			β, monoclinic	122–207	9.284 (190°C)	10.463	7.859	92.13	17.70	34	1.571
			γ, orthorhombic	207–315	3.159 (235°C)	5.768	10.162		17.14	8	1.588
			δ, fcc	315–457	4.637 (320°C)				15.92	4	1.640
			δ', bc tetrag.	457–479	3.34 (465°C)		4.44		16.00	2	1.640
	640		ε, bcc	479–640	3.636 (490°C)				16.51	2	1.592
americium		284	α, dhcp	below 658	3.468 (20°C)		11.241		13.6	4	1.730
			β, fcc	793–1004	4.894 ± 5				13.65	4	1.730
	1173		γ, ?	~1050–1173							
curium		387	α, dhcp	below ~1277	3.496		11.33		13.5	4	1.743
	1345		β, fcc	~1277–1345	5.039				12.9	4	1.782
berkelium		310	α, dhcp	below 930	3.416 ± 3		11.069		14.79	4	1.704
	1050		β, fcc	930–986	4.997 ± 4				13.24	4	1.767
californium		196	α, dhcp	below 900	3.384		11.040		15.10	4	1.694
	900		β, fcc		5.74				8.74	4	2.030
einsteinium		133	α, dhcp	below 860	?		?		?	4	
			β, fcc		5.75				8.84	4	2.03

[a] Radii are corrected to coordination number 12 (see ref. 95, Chapters 10–12 and Table 20.8). [b] Errors in the final digits of the lattice constants are given in the form 10.763 ± 5.

transition from delocalized to localized f-electron behavior at americium is clearly reflected in the chemical and physical properties of the actinide series. Uranium, neptunium, and plutonium metals in the crossover region of the actinide series exhibit particularly complex behavior because they have a mixture of properties that are present in pure form at either end of the actinide series.

14.6.3 Polymorphic transformations

Protactinium, uranium, neptunium, and plutonium metal have complex structures unlike anything encountered in the lanthanide metals. For example, plutonium metal has no fewer than six allotropic modifications between room temperature and its melting point at 639.5°C. A remarkable contraction occurs at the transition between the δ and the δ' phases. As the temperature increases, the density of the metal increases significantly. For no two of the plutonium metal phases do both the coefficient of thermal expansion and the temperature coefficient of resistivity have the same sign, for the electrical resistance decreases when the unit cell of the phase expands on heating. An immense effort has been expended to map the phase transformations in uranium and plutonium metals and their alloys because of their great importance in nuclear technology. Details of the metallurgy and other matters related to the actinide metals can be found in Chapter 19 of this work and in refs 30 and 31.

14.6.4 Electronic structures

We have noted in Sections 14.6.1 and 14.6.2 the effects of localized and delocalized 5f electrons on the crystal structures and phase transformations of the actinide metals. These effects are observed in many contexts, but perhaps most clearly in the actinide metals. The basis for the differences observed for localized and delocalized 5f electrons has been discussed briefly in Section 14.4, but because of their importance in the metallic state some additional discussion of the electronic state in the actinide metals seems appropriate. The classical d-electron or d-block transition series and the f-block elements have as a principal feature of their electronic architecture the filling of the 3d, 4d, and 5d electron shells for the classical transition series, and the 4f and 5f energy levels in the lanthanide and actinide series. The f electrons occupy energy levels or orbitals closer to the nucleus of the atom than do the outer s and p valence electrons. In the lanthanide elements beyond cerium, the 4f levels are highly localized and, since overlap between the levels is minimal, these energy levels are not broadened to any appreciable extent by 4f–4f interactions. Nor do the 4f electrons tend to mix with the d, s or p valence electrons. In the d-block metals, the d-electron levels have significant overlap with other d electrons; the d electrons also mix or hybridize with s and p levels. The extensive mixing of the d, s, and p orbitals in d-block elements generates broad energy bands whose existence is reflected in the magnetic and electrical properties of the d-block transition metals.

The electronic properties of the 5f elements are intermediate between the d-block elements and the 4f elements. At the beginning of the actinide series, the 5f electrons interact strongly with each other, and the band character of the delocalized 5f electrons is inhibitory to the development of magnetism. As the 5f shell is filled, the 5f electrons become increasingly localized and the energy levels fall so that they are well below the Fermi band level. The band nature of the 5f electrons diminishes and the Fermi level energy is lowered. The transition from delocalized to localized 5f electrons takes place in the vicinity of plutonium, as shown in schematic fashion in Fig. 14.7 [32]. In the crossover region, which extends from uranium to americium and perhaps beyond, the electronic behavior is especially complicated because the energy differences between localized and delocalized 5f electrons is small. Comparatively small perturbations can convert the immobilized 5f electrons into mobile electrons with a band structure, or the reverse. This delicate balance near the middle of the actinide series gives rise to unusual crystal structures, unusual thermodynamic and mechanical properties, multiple oxidation states, and collective phenomena such as magnetism, superconductivity, and valence fluctuations. So complex are the phenomena near the middle of the actinide series that modern theories of the metallic state have serious difficulties in dealing with them, a situation that has been largely rectified and may well turn out to be not the least valuable contribution that the study of the actinide elements will have made to the understanding of the solid state.

One of the most powerful techniques for the elucidation of the electronic states of the actinide elements is the application of high pressure [33]. Pressures as high as several tens of gigapascals (GPa) have been used in these experiments. Under

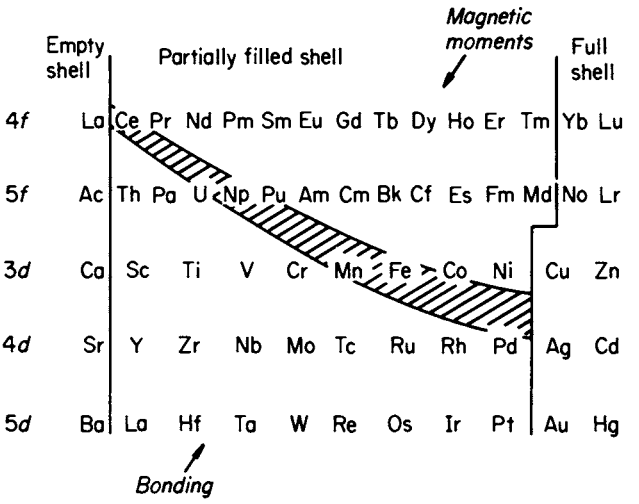

Fig. 14.7 *Transition metals (f and d series) showing the crossover from delocalized (bonding) to localized (magnetic moments) f- and d-electron behavior (from ref. 32 with permission).*

high pressure, which facilitates f–f overlap, the highly symmetrical cubic and orthorhombic structures of plutonium, which are antagonistic to f-electron bonding, change to the monoclinic β phase and the liquid phase, both of which are considered to facilitate f-electron bonding. In americium, the 5f electrons are already localized in the core, and low-symmetry structures associated with delocalized 5f electrons are not observed at ordinary pressures. Under high pressure (16.1 GPa), the core 5f electrons are brought closer together, and the 5f electrons now resemble the (partially) delocalized 5f electrons present in uranium, neptunium, and plutonium at atmospheric pressure. Americium then assumes an orthorhombic structure that characteristically occurs in uranium metal [34]. Pressure also affects the superconducting transition temperature and the magnetic properties of the actinide metals. Similarly, large pressure effects have been observed in actinide pnictides, chalcogenides, and intermetallic compounds [33].

14.6.5 Superconductivity

Superconductivity in the actinide metals is closely related to the degree of delocalization of the 5f electrons. Highly localized 5f electrons, which are characteristic of the latter portion of the actinide series, are associated with temperature-dependent paramagnetism and the absence of superconductivity. Delocalized 5f electrons participate in chemical bonding, show small temperature-independent magnetic moments, and are conducive to superconductivity. Protactinium metal becomes superconducting at 0.42 K [35] and americium metal at 0.79 K [36]. Uranium metal is also a superconductor. These three elements are considered from other lines of evidence to have delocalized (itinerant) 5f electrons. Neptunium and plutonium, especially the latter, are anomalous. The 5f electrons in americium behave as if they are localized, but americium metal is superconductive, because for various reasons its magnetic moments at low temperatures are identically zero. The heavier actinide metals all contain strongly localized 5f electrons, are not superconductors, and have large magnetic moments at low temperatures. Plutonium is not superconducting, but at the same time it does not have the magnetic properties that the absence of superconductivity would imply [37]. A serious problem that must be faced in resolving the anomalous behavior of neptunium and plutonium is the paucity of data on the behavior of actinide metals and compounds at very low temperatures. The radioactivity of the actinides causes heating that makes superconductivity measurements very difficult. Another severe problem is purity, as impurities in metals can inhibit superconductive behavior. Some of the actinide metals have been obtained in a state of very high purity, and improvements in cryogenic techniques may resolve some of these fascinating puzzles.

14.7 SOLID COMPOUNDS

14.7.1 Introductory remarks

Thousands of compounds of the actinide elements have been prepared [38–40]. Compounds that have special scientific or technological importance are described in the preceding chapters on the chemistry of the individual actinide elements, and in a systematic way in Chapter 20. In the past few years there have been important additions to the roster of actinide compounds and new chemical phenomena that are particularly characteristic of, although perhaps not entirely confined to, the chemical behavior of the actinide compounds, and these are commented on here.

14.7.2 Binary compounds

Table 14.8 lists the binary hydrides, oxides, and halides of the actinide elements along with their melting points, color, and crystal structure parameters. The properties of the hydrides and oxides included in Table 14.8 are for compounds that come close to the indicated stoichiometric composition. The methods of preparation of the compounds in Table 14.8 are essentially classical procedures adapted to a micro- or semi-microscale and to the radioactivity of the actinide elements [41]. There are claims in the literature for the synthesis of actinide halides in which the actinide element is in an unusually high or low oxidation state. Reports of the synthesis of the higher-valent actinide fluorides PuF_5, EsF_4, CmF_6, and AmF_6 have not been confirmed. Since the discovery of the dihalides $NdCl_2$ and $TmCl_2$, the dichlorides, dibromides, and di-iodides of Am and Cf have been prepared [42].

14.7.3 Other compounds

The actinide M^{3+} ions in aqueous solution resemble the tripositive lanthanide ions in their precipitation reactions, allowing for differences in the redox properties of early members of the actinide series. The chloride, bromide, nitrate, bromate, and perchlorate anions form water-soluble salts, which can be isolated as hydrated solids by evaporation. The acetates, iodates, and iodides are somewhat less soluble in water. The sulfates are sparingly soluble in hot solutions, somewhat more soluble in the cold. Insoluble precipitates are formed with hydroxide, fluoride, carbonate, oxalate, and phosphate anions. Precipitates formed from aqueous solution are usually hydrated, and the preparation of anhydrous salts from the hydrates without formation of hydrolyzed species can only be accomplished with difficulty. The actinide(IV) ions resemble Ce(IV) in forming fluorides and oxalates insoluble even in acid solution. The nitrates, sulfates, perchlorates, and sulfides are all water-soluble. The IV state actinide ions form insoluble iodates and arsenates even in rather strong acid solution. The

Table 14.8 *Properties and crystal structure data for some important actinide binary compounds.*

Compound	*Color*	*Melting point* (°C)	*Symmetry*	*Space group or structure type*	*Lattice parameters* a_0 (Å)	b_0 (Å)	c_0 (Å)	*Angle* (deg)	*Density* (g cm^{-3})
AcH_2	black		cubic	fluorite ($Fm3m$)	5.670				8.35
ThH_2	black		tetragonal	$F4/mmm$	5.735		4.971		9.50
Th_4H_{15}	black		cubic	$I4\bar{3}d$	9.11				8.25
α-PaH_3	gray		cubic	$Pm3n$	4.150				10.87
β-PaH_3	black		cubic	β-W	6.648				10.58
α-UH_3	?		cubic	$Pm3n$	4.160				11.12
β-UH_3	black		cubic	β-W ($Pm3n$)	6.645				10.92
NpH_2	black		cubic	fluorite	5.343				10.41
NpH_3	black		trigonal	$P\bar{3}c1$	6.51		6.72		9.64
PuH_2	black		cubic	fluorite	5.359				10.40
PuH_3	black		trigonal	$P\bar{3}c1$	6.55		6.76		9.61
AmH_2	black		cubic	fluorite	5.348				10.64
AmH_3	black		trigonal	$P\bar{3}c1$	6.53		6.75		9.76
CmH_2	black		cubic	fluorite	5.322				10.84
CmH_3	black		trigonal	$P\bar{3}c1$	6.528		6.732		10.06
BkH_2	black		cubic	fluorite	5.248				11.57
BkH_3	black		trigonal	$P\bar{3}c1$	6.454		6.663		10.44
Ac_2O_3	white		hexagonal	La_2O_3 ($P\bar{3}m1$)	4.07		6.29		9.19
Pu_2O_3	?		cubic	$Ia3$ (Mn_2O_3)	11.03				10.20
Pu_2O_3	black	2085	hexagonal	La_2O_3	3.841		5.958		11.47
Am_2O_3	tan		hexagonal	La_2O_3	3.817		5.971		11.77
Am_2O_3	reddish brown		cubic	$Ia3$	11.03				10.57
Cm_2O_3	white to faint tan	2260	hexagonal	La_2O_3	3.792		5.985		12.17
Cm_2O_3			monoclinic	$C2/m$ (Sm_2O_3)	14.282	3.641	8.883	$\beta = 100.29$	11.90
Cm_2O_3	white		cubic	$Ia3$	11.002				10.80
Bk_2O_3	light green		hexagonal	La_2O_3	3.754		5.958		12.47

Table 14.8 (*Contd.*)

Compound	*Color*	*Melting point* (°C)	*Symmetry*	*Space group or structure type*	*Lattice parameters*				*Density* ($g\ cm^{-3}$)
					a_0 (Å)	b_0 (Å)	c_0 (Å)	*Angle* (deg)	
Bk_2O_3	yellow-green		monoclinic	$C2/m$	14.197	3.606	8.846	$\beta = 100.23$	12.20
Bk_2O_3	yellowish brown		cubic	$Ia3$	10.887				11.66
Cf_2O_3	pale green		hexagonal	La_2O_3	3.72		5.96		12.69
Cf_2O_3	lime green		monoclinic	$C2/m$	14.121	3.592	8.809	$\beta = 100.34$	12.37
Cf_2O_3	pale green		cubic	$Ia3$	10.83				11.39
Es_2O_3	white		hexagonal	La_2O_3	3.7		6.0		12.7
Es_2O_3	white		monoclinic	$C2/m$	14.1	3.59	8.80	$\beta = 100$	12.4
Es_2O_3	white		cubic	$Ia3$	10.766				11.79
ThO_2	white	~3050	cubic	fluorite	5.597				10.00
PaO_2	black		cubic	fluorite	5.509				10.45
UO_2	brown to black	2875	cubic	fluorite	5.471				10.95
NpO_2	apple green		cubic	fluorite	5.425				11.14
PuO_2	yellow-green to brown	2400	cubic	fluorite	5.3960				11.46
AmO_2	black		cubic	fluorite	5.374				11.68
CmO_2	black		cubic	fluorite	5.358				11.92
BkO_2	yellowish-brown		cubic	fluorite	5.332				12.31
CfO_2	black		cubic	fluorite	5.310				12.46
Pa_2O_5	white		cubic	fluorite-related	5.446 or 5.492				11.14
Np_2O_5	dark brown		monoclinic	$P2_1/c$	4.183	6.584	4.086	$\beta = 90.32$	8.18
α-U_3O_8	black-green	1150 (dec)	orthorhombic	$C2mm$	6.716	11.960	4.147		8.39
β-U_3O_8	black-green		orthorhombic	$Cmcm$	7.069	11.445	8.303		8.32
γ-UO_3	orange	650 (dec)	orthorhombic	$Fddd$	9.81	19.93	9.71		7.80

$AmCl_2$	black		orthorhombic	$Pbnm$ ($PbCl_2$)	8.963	7.573	4.532		6.78
$CfCl_2$	red-amber		?						
$AmBr_2$	black		tetragonal	$SrBr_2$ ($P4/n$)	11.592		7.121		7.00
$CfBr_2$	amber		tetragonal	$SrBr_2$	11.500		7.109		7.22
ThI_2	gold		hexagonal	$P6_3/mmc$	3.97		31.75		7.45
AmI_2	black	~ 700	monoclinic	EuI_2 ($P2_1/c$)	7.677	8.311	7.925	$\beta = 98.46$	6.60
CfI_2	violet		hexagonal	CdI_2 ($P\bar{3}m1$)	4.56		6.99		6.63
CfI_2	violet		rhombohedral	$CdCl_2$ ($R\bar{3}m$)	7.43			$\alpha = 36$	6.58
AcF_3	white		trigonal	LaF_3 ($P\bar{3}c1$)	7.41		7.53		7.88
UF_3	black	> 1140 (dec)	trigonal	LaF_3	7.18		7.348		8.95
NpF_3	purple		trigonal	LaF_3	7.129		7.288		9.12
PuF_3	purple	1425	trigonal	LaF_3	7.092		7.254		9.33
AmF_3	pink	1393	trigonal	LaF_3	7.044		7.225		9.53
CmF_3	white	1406	trigonal	LaF_3	7.014		7.194		9.85
BkF_3	yellow-green		orthorhombic	YF_3 ($Pnma$)	6.70	7.09	4.41		9.70
BkF_3	yellow-green		trigonal	LaF_3	6.97		7.14		10.15
CfF_3	light green		orthorhombic	YF_3	6.653	7.039	4.393		9.88
CfF_3	light green		trigonal	LaF_3	6.945		7.101		10.28
$AcCl_3$	white		hexagonal	UCl_3 ($P6_3/m$)	7.62		4.55		4.81
UCl_3	green	835	hexagonal	$P6_3/m$	7.443		4.321		5.50
$NpCl_3$	green	~ 800	hexagonal	UCl_3	7.413		4.282		5.60
$PuCl_3$	emerald green	760	hexagonal	UCl_3	7.394		4.243		5.71
$AmCl_3$	pink or yellow	715	hexagonal	UCl_3	7.382		4.214		5.87
$CmCl_3$	white	695	hexagonal	UCl_3	7.374		4.185		5.95
$BkCl_3$	green	603	hexagonal	UCl_3	7.382		4.127		6.02
α-$CfCl_3$	green	545	orthorhombic	$TbCl_3$ ($Cmcm$)	3.859	11.748	8.561		6.07
β-$CfCl_3$	green		hexagonal	UCl_3	7.379		4.090		6.12
$EsCl_3$	white to orange		hexagonal	UCl_3	7.40		4.07		6.20
$AcBr_3$	white		hexagonal	UBr_3 ($P6_3/m$)	8.06		4.68		5.85
UBr_3	red	730	hexagonal	$P6_3/m$	7.936		4.438		6.55
$NpBr_3$	green		hexagonal	UBr_3	7.916		4.390		6.65
$NpBr_3$	green		orthorhombic	$TbCl_3$ ($Cmcm$)	4.109	12.618	9.153		6.67

Table 14.8 (*Contd.*)

Compound	*Color*	*Melting point* (°C)	*Symmetry*	*Space group or structure type*	*Lattice parameters*				*Density* ($g\ cm^{-3}$)
					a_0 (Å)	b_0 (Å)	c_0 (Å)	*Angle* (deg)	
$PuBr_3$	green	681	orthorhombic	$TbCl_3$	4.097	12.617	9.147		6.72
$AmBr_3$	white to pale yellow		orthorhombic	$TbCl_3$	4.064	12.661	9.144		6.85
$CmBr_3$	pale yellow-green	625 ± 5	orthorhombic	$TbCl_3$	4.041	12.700	9.135		6.85
$BkBr_3$	light green		monoclinic	$AlCl_3$ (C2/*m*)	7.23	12.53	6.83	$\beta = 110.6$	5.604
$BkBr_3$	light green		orthorhombic	$TbCl_3$	4.03	12.71	9.12		6.95
$BkBr_3$	yellow green		rhombohedral	$FeCl_3$ ($R\bar{3}$)	7.66			$\alpha = 56.6$	5.54
$CfBr_3$	green		monoclinic	$AlCl_3$	7.214	12.423	6.825	$\beta = 110.7$	5.673
$CfBr_3$	green		rhombohedral	$FeCl_3$	7.58			$\alpha = 56.2$	5.77
$EsBr_3$	straw		monoclinic	$AlCl_3$	7.27	12.59	6.81	$\beta = 110.8$	5.62
PaI_3	black		orthorhombic	$TbCl_3$ (*Cmcm*)	4.33	14.0	10.02		6.69
UI_3	black		orthorhombic	$TbCl_3$	4.328	13.996	9.984		6.76
NpI_3	brown		orthorhombic	$TbCl_3$	4.30	14.03	9.95		6.82
PuI_3	green		orthorhombic	$TbCl_3$	4.326	13.962	9.974		6.92
AmI_3	pale yellow	$\sim$ 950	hexagonal	BiI_3 ($R\bar{3}$)	7.42		20.55		6.35
AmI_3	yellow		orthorhombic	$PuBr_3$	4.28	13.94	9.974		6.95
CmI_3	white		hexagonal	BiI_3	7.44		20.40		6.40
BkI_3	yellow		hexagonal	BiI_3	7.584		20.87		6.02
CfI_3	red-orange		hexagonal	BiI_3	7.587		20.81		6.05
EsI_3	amber to light yellow		hexagonal	BiI_3	7.53		20.84		6.18
ThF_4	white	1068	monoclinic	UF_4 (C2/*c*)	13.00	10.99	8.60	$\beta = 126.4$	6.20
PaF_4	reddish-brown		monoclinic	UF_4	12.88	10.88	8.49	$\beta = 126.4$	6.38

UF_4	green	960	monoclinic	$C2/c$	12.803	10.792	8.372	$\beta = 126.3$	6.73
NpF_4	green		monoclinic	UF_4	12.68	10.66	8.34	$\beta = 126.3$	6.86
PuF_4	brown	1037	monoclinic	UF_4	12.60	10.57	8.28	$\beta = 126.3$	7.05
AmF_4	tan		monoclinic	UF_4	12.56	10.58	8.25	$\beta = 125.9$	7.23
CmF_4	light gray-green		monoclinic	UF_4	12.50	10.49	8.18	$\beta = 126.1$	7.36
BkF_4	pale yellow-green		monoclinic	UF_4	12.396	10.466	8.118	$\beta = 126.3$	7.55
CfF_4	light green		monoclinic	UF_4	12.327	10.402	8.113	$\beta = 126.4$	7.57
α-$ThCl_4$	white		orthorhombic		11.18	5.93	9.09		4.12
β-$ThCl_4$	white	770	tetragonal	UCl_4 ($I4_1/amd$)	8.473		7.468		4.60
$PaCl_4$	greenish-yellow		tetragonal	UCl_4	8.377		7.481		4.72
UCl_4	green	590	tetragonal	$I4_1/amd$	8.296		7.481		4.89
$NpCl_4$	red-brown	518	tetragonal	UCl_4	8.266		7.475		4.96
α-$ThBr_4$	white		tetragonal	$I4_1/a$	6.737		13.601		5.94
β-$ThBr_4$	white		tetragonal	UCl_4	8.931		7.963		5.77
$PaBr_4$	orange-red		tetragonal	UCl_4	8.824		7.957		5.90
UBr_4	brown	519	monoclinic	$2/c$–/–	10.92	8.69	7.05	$\beta = 93.15$	
$NpBr_4$	dark red	464	monoclinic	$2/c$–/–	10.89	8.74	7.05	$\beta = 94.19$	
ThI_4	yellow	556	monoclinic	$P2_1/n$	13.216	8.068	7.766	$\beta = 98.68$	6.00
PaI_4	black								
UI_4	black								
PaF_5	white		tetragonal	$I\bar{4}2d$	11.53		5.19		
α-UF_5	grayish white		tetragonal	$I4/m$	6.512		4.463		5.81
β-UF_5	pale yellow		tetragonal	$I\bar{4}2d$	11.456		5.196		6.47
NpF_5			tetragonal	$I4/m$	6.53		4.45		
$PaCl_5$	yellow	306	monoclinic	$C2/c$	8.00	11.42	8.43	$\beta = 106.4$	
α-UCl_5	brown		monoclinic	$P2_1/n$	7.99	10.69	8.48	$\beta = 91.5$	3.81

Table 14.8 (*Contd.*)

Compound	*Color*	*Melting point* (°C)	*Symmetry*	*Space group or structure type*	*Lattice parameters*				*Density* ($g\ cm^{-3}$)
					a_0 (Å)	b_0 (Å)	c_0 (Å)	*Angle* (deg)	
β-UCl_5	red-brown		triclinic	$P\bar{1}$	7.07	9.65	6.35	$\alpha = 89.10$ $\beta = 117.36$ $\gamma = 108.54$	
α-$PaBr_5$			monoclinic	$P2_1/c$	12.64	12.82	9.92	$\beta = 108$	
β-$PaBr_5$	orange-brown		monoclinic	$P2_1/n$	9.385	12.205	8.95	$\beta = 91.1$	
UBr_5	brown		monoclinic	$P2_1/n$					
PaI_5	black		orthorhombic		6.98	2.160	21.30		
UF_6	white	64.02 at 151.6 kPa	orthorhombic	*Pnma*	9.900	8.962	5.207		5.060
NpF_6	orange	55	orthorhombic	*Pnma*	9.909	8.997	5.202		5.026
PuF_6	reddish-brown	52	orthorhombic	*Pnma*	9.95	9.02	5.26		4.86
UCl_6	dark green	178	hexagonal	$P\bar{3}m1$	10.9		6.03		3.62

actinyl(v) ions can be precipitated as the insoluble potassium salts from concentrated carbonate solutions. Actinyl(vi) ions in solutions containing high concentrations of acetate ions form an insoluble crystalline double salt, $NaMO_2(O_2CCH_3)_3$. The hydroxides or hydrous oxides of any of the actinide ions in all oxidation states are insoluble in water. From solutions containing the UO_2^{2+} ion, compounds of the type $Na_2U_2O_7$ can be precipitated from alkaline solution. The ions NpO_5^{3-} and PuO_5^{3-}, in which neptunium and plutonium are in the vii oxidation state, exist in alkaline solution, from which they can be precipitated by several di- and tripositive cations. Actinide(iv) ions form insoluble peroxy compounds with hydrogen peroxide in moderately acid solution. The solid peroxy compounds incorporate inorganic anions such as sulfate, nitrate or chloride that may be present in the solution. Phosphates, arsenates, cyanides, cyanates, thiocyanates, selenocyanates, sulfites, selenates, selenites, tellurates, and tellurites of the actinide elements have all been prepared, but have been little studied.

14.7.4 Non-stoichiometric systems

There are many inorganic compounds whose composition is not necessarily expressible as the ratio of small whole numbers. Instead, they exist over a range of compositions. Compounds of variable composition often have electrical, magnetic, and thermal conductivity properties that are exceedingly sensitive to the exact composition. Non-stoichiometry is purely a solid-state phenomenon, which is associated with vacancies in cation or anion sites in a crystal lattice [43]. An element that can readily undergo oxidation or reduction must be present in either the anion or cation. Electrical neutrality in the crystal must of course be maintained, and deviations from exact stoichiometry can only exist if compensated by a change in the oxidation state of another constituent of the crystal. Non-stoichiometry is therefore encountered in binary and ternary compounds of transition elements with hydrogen, oxygen, chalcogens, pnictogens, carbon, silicon, and boron. The presence of a metallic ion in more than one oxidation state in a crystal endows non-stoichiometric compounds with a variety of interesting properties: they may be highly colored; they may show metallic electrical conduction, or they may be semiconductors; they frequently show marked catalytic activity; and they may differ significantly in chemical reactivity from the stoichiometric compounds of the same elements. Non-stoichiometric compounds are important as transistors, thermistors, rectifiers, ionic electrical conductors, thermoelectric generators, photodetectors, and other electronic and optical devices. The actinide elements, because of the multiplicity of oxidation states that they can assume, are particularly prone to the formation of non-stoichiometric systems. This is especially true for the elements uranium through curium.

The oxide systems illustrate many of the salient features of non-stoichiometry in actinide element chemistry. Table 14.9 shows the composition and thermochemical properties of the well-characterized binary actinide oxides as a function

Table 14.9 *Well-characterized binary actinide oxides. Measured enthalpies of formation* (kJ mol^{-1}) *and standard entropies* (J K^{-1} mol^{-1}) *are shown beneath corresponding formulas* (Table 17.14).

An(III)		An(IV)		An(V)		An(VI)
$AcO_{1.5}$		ThO_2 -1226.4 ± 3.5 65.23 ± 0.20				
		PaO_2		$PaO_{2.5}$		
		UO_2 -1085.0 ± 1.0 77.03 ± 0.20	$UO_{2.25}$ -1127.6 ± 1.2 83.53 ± 0.18	$UO_{2.33}$ -1142.4 ± 0.9 83.51	$UO_{2.67}$ -1191.6 ± 0.8 94.18 ± 0.17	$UO_3(\gamma)$ -1223.8 ± 2.0 96.11 ± 0.40
		NpO_2 -1074.0 ± 2.5 80.3 ± 0.4		$NpO_{2.5}$		
$PuO_{1.5}$ -828 ± 10 81.51 ± 0.32	$PuO_{1.61}$ -884.5 ± 16.7	PuO_2 -1056.2 ± 0.7 66.13 ± 0.26				
$AmO_{1.5}$ -845 ± 8	$AmO_{1.6}$(?)	AmO_2 -932.2 ± 2.7				
$CmO_{1.5}$ -841.5 ± 6.0	$CmO_{1.714}$	CmO_2 -911 ± 6				
$BkO_{1.5}$	$BkO_{1.8}$	BkO_2				
$CfO_{1.5}$ -826.5 ± 5.0	$CfO_{1.714}$	CfO_2				

of oxidation state and the location of the element in the actinide series [44]. The first of the actinide elements to form non-stoichiometric oxides is protactinium. It is also the first of the actinide elements to have two readily accessible oxidation states. The black dioxide PaO_2 is obtained by reduction of Pa_2O_5 with hydrogen or carbon. Intermediate phases with the composition $PaO_{2.18-2.20}$, $PaO_{2.33}$, $PaO_{2.40-2.42}$, and $PaO_{2.42-2.44}$ have been detected by x-ray crystallography. Pa_2O_5 itself occurs in several crystal modifications determined by the method and temperature of preparation.

The complexity of the uranium–oxygen system is awesome. In the composition range UO_2 to UO_3 there are close to a dozen phases, many of which exist in several crystal modifications. UO_3 itself occurs in six polymorphs. The complex phase relationships result from the easy change in oxidation state of the uranium as additional oxygen is introduced into the UO_2 lattice. The additional oxygen incorporated in hyperstoichiometric uranium dioxide is distributed at random into vacant lattice sites. The original fluorite structure is distorted, but remains recognizably the same phase over a range of compositions. The stoichiometry range of a phase is a measure, at a particular temperature and oxygen pressure, of its ability to accommodate randomly distributed oxygen without change in the long-range order of a crystal. When random incorporation is no longer possible, additional oxygen is ordered in a superlattice structure, and a new phase appears, possibly also of variable composition. In the uranium–oxygen system such an abrupt transformation occurs at the composition $UO_{2.4}$. Six more phases occur between $UO_{2.4}$ and UO_3, the compositions of some of which are shown in Table 14.9.

Only two neptunium oxide phases with compositions ranging from NpO_2 to $NpO_{2.5}$ are known. The composition of the latter oxide is consistent with the well-known stability of the neptunium(v) state. Plutonium has two oxides corresponding to the oxidation states III and IV, and an oxide of intermediate composition, $PuO_{1.61}$. Despite the existence of stable VI states for both neptunium and plutonium, no binary oxide corresponding to the VI oxidation state is known for either of these elements. For the transplutonium elements through fermium, the III oxidation state is the stable one, and the elements subsequent to plutonium have oxides of the composition An_2O_3. All of the transplutonium elements to californium also form oxides in which the actinide elements have the formal oxidation state IV, which is consistent with the known ability of these elements to assume oxidation states higher than III. The relative ease of formation of the transplutonium dioxides is in the order $BkO_2 > AmO_2 > CmO_2 > CfO_2$. Curium and californium are also reported to form intermediate oxides of the composition $CmO_{1.714}$ and $CfO_{1.714}$. In the case of $CfO_{1.714}$, this is the highest oxide that can be prepared in air or in oxygen at 1 atm pressure. The oxide systems of the transcalifornium elements still remain to be explored. By comparison, the non-stoichiometric compounds of the actinides elements with the chalcogenides and pnictides have only received a modest amount of study.

14.7.5 Crystal structures and ionic radii

The vast accumulation of crystal structure data has provided the basis for the determination of the ionic radii, for coordination number 6, presented in Table 14.10 [38]. Ionic radii for the lanthanide series are listed for comparison. For both the 3+ and 4+ ions of the actinide series, the ionic radii decrease with increasing atomic number, indicative of decreased shielding by f electrons of the outer valence electrons from the increasing nuclear charge. The actinide contraction is very similar to the corresponding lanthanide contraction. As a consequence of the ionic character of most actinide compounds, and the similarity of the ionic radii for a given oxidation state, analogous compounds are generally isostructural. In the series UBr_3, $NpBr_3$, $PuBr_3$, and $AmBr_3$, the structural type changes with increasing atomic number, which is consistent with the contraction in ionic radius. The extraordinary stability of the fluorite-type MO_2 structure is responsible for the existence of such compounds as PaO_2, AmO_2, CmO_2, and CfO_2, despite the instability of the IV oxidation state of these elements in solution. The actinide contraction and the isostructural relationship of the compounds are particularly convincing evidence for the actinide elements as a 5f transition series.

14.7.6 Organometallic compounds

When the first edition of this book was in preparation, the prospects of an organoactinide chemistry, especially for compounds containing a metal–carbon bond, were judged to be very dim. At this time of writing, the situation is very different. A rich organometallic chemistry of the actinide elements has come into existence in the last two decades, so luxuriant in fact that presenting a concise summary that does justice to the subject becomes a problem. This field of inquiry is one of the most vigorous and important in current actinide element research. Not only are new organoactinide compounds with remarkable properties appearing at a rapid rate, but studies of their structure and physical properties by the use of nuclear magnetic resonance, optical and vibrational spectroscopy, photoelectron spectroscopy, and many other physical and chemical techniques are contributing valuable information on the electronic structure and the nature of chemical bonding in the 5f elements, subjects that are of great importance in every aspect of actinide element chemistry.

The first stable covalent organometallic compound of a transition metal was synthesized in 1951 [45]. The regular (non-transition) elements were well-known to form compounds in which covalent metal–carbon bonds were formed, but transition metals were widely regarded as incapable of forming stable bonds of this kind. The first stable transition-metal organometallic compounds were derivatives of cyclopentadiene, C_5H_6. This compound has aromatic characteristics, and its cyclopentadienide ion (Cp^-) possesses π electrons in two conjugated double bonds capable of coordination to vacant d orbitals on the

Table 14.10 *Ionic radii of lanthanides and actinides (CN 6).*

No. of 4f or 5f electrons	*Lanthanide series*						*Actinide series*					
	2+ *ion*	*Radius* (Å)	3+ *ion*	*Radius* (Å)	4+ *ion*	*Radius* (Å)	2+ *ion*	*Radius* (Å)	3+ *ion*	*Radius* (Å)	4+ *ion*	*Radius* (Å)
0			La^{3+}	1.032	Ce^{4+}	0.87			Ac^{3+}	1.12	Th^{4+}	0.94
1			Ce^{3+}	1.01	Pr^{4+}	0.85			Th^{3+}		Pa^{4+}	0.90
2			Pr^{3+}	0.99					Pa^{3+}	1.04	U^{4+}	0.89
3			Nd^{3+}	0.983					U^{3+}	1.025	Np^{4+}	0.87
4	Nd^{2+}	1.21	Pm^{3+}	0.97					Np^{3+}	1.01	Pu^{4+}	0.86
5			Sm^{3+}	0.958					Pu^{3+}	1.00	Am^{4+}	0.85
6	Sm^{2+}	1.19	Eu^{3+}	0.947					Am^{3+}	0.98	Cm^{4+}	0.84
7	Eu^{2+}	1.17	Gd^{3+}	0.938	Tb^{4+}	0.76	Am^{2+}	1.19	Cm^{3+}	0.97	Bk^{4+}	0.83
8			Tb^{3+}	0.923					Bk^{3+}	0.96	Cf^{4+}	0.821
9			Dy^{3+}	0.912					Cf^{3+}	0.95	Es^{4+}	0.81
10	Dy^{2+}	1.07	Ho^{3+}	0.901			Cf^{2+}	1.12	Es^{3+}	0.94		
11			Er^{3+}	0.890								
12			Tm^{3+}	0.880								
13	Tm^{2+}	1.03	Yb^{3+}	0.868								
14	Yb^{2+}	1.02	Lu^{3+}	0.861			No^{2+}	1.05				

transition metal. In 1956, uranium, newly recognized as a member of a transition element series, became the first of the actinide elements to yield a stable covalent cyclopentadienyl (Cp) compound, tris(cyclopentadienyl)uranium chloride, Cp_3UCl [46]. A decade was to pass before the first transuranium organometallic derivative, tris(cyclopentadienyl)neptunium chloride, was prepared [47]. Since then, several hundred organometallic derivatives of the actinide metals have been prepared. Among these are compounds containing other π donor ligands, such as indenyl and cyclo-octatetraenyl groups. The chemical bonds in the organoactinide compounds of these ligands range from ionic to purely covalent σ bonds, and thus provide an excellent environment for the study of chemical bonding in the f-block elements [48].

Cyclopentadienyl organometallic compounds can be prepared by a variety of reactions [49, 50]. The general method for actinides in the III and IV oxidation states is by reaction of potassium or sodium cyclopentadienide with the anhydrous actinide halide (AnX_n) in an organic solvent such as tetrahydrofuran (THF), benzene, or diethyl ether:

$$AnX_4 + 4KCp \rightarrow AnCp_4 + 4KX$$
$$AnX_4 + 3KCp \rightarrow Cp_3AnX + 3KX$$
$$AnX_3 + 3KCp \rightarrow AnCp_3 + 3KX$$
$$AnX_3 + 2KCp \rightarrow Cp_2AnX + 2KX$$

The actinide compounds are recovered from the reaction mixture by extraction with an appropriate organic solvent, and further purified by sublimation in a good vacuum when the volatility of the compound permits. The actinide cyclopentadienylides can also be prepared by metathesis in the molten phase by heating the actinide halide with beryllium or magnesium cyclopentadienides. In the uranium tris(cyclopentadienyl) halides the anion can be exchanged by double decomposition reactions in aqueous solutions. A list of representative actinide(III) and (IV) cyclopentadienyl complexes is shown in Table 14.11 [51]. The tris(cyclopentadienyl) compounds are strong Lewis acids and form adducts with many Lewis bases. They are highly ionic substances, although the bonding has more of a covalent character than in the corresponding lanthanide compounds. All of the actinide(III) compounds, with the exception of the uranium compound, are soluble in organic solvents, are reasonably stable, and are appreciably volatile, but all are sensitive to air. The tetrakis (cyclopentadienyl) complexes are soluble in organic solvents and moderately stable to air; they are not, however, appreciably volatile.

Compounds of the type MCp_3X, where M is an actinide element in the IV oxidation state and X is an anion, have been prepared in large numbers and with a great variety of anions. Evidence has been adduced that the uranium tris(cyclopentadienyl) chloride ionizes in water to form the UCp_3^+ and Cl^- ions. Replacement of anions can readily be effected in such solutions. Anions that can be introduced include not only the common halides, sulfate, perchlorate, nitrate,

Table 14.11 *Some representative actinide cyclopentadienyl complexes.*

Compound	*Color*	*Melting point*[a] (°C)	*Sublimation temperature*[b] (°C)
$Th(C_5H_5)_3$	green		
$Th(C_5H_5)_3Cl$	colorless		
$Th(C_5H_5)_4$	colorless	170 d	250–290
$Pa(C_5H_5)_4$	orange-yellow	220 d	220 d
$U(C_5H_5)_3$	brown	> 200	
$U(C_5H_5)_3Cl$	red-brown	260	260
$U(C_5H_5)_4$	red	250 d	200–220 d
$Np(C_5H_5)_3Cl$	brown		
$Np(C_5H_5)_4$	red-brown	220 d	200–220 d
$Pu(C_5H_5)_3$	green	180 d	140–165
$Am(C_5H_5)_3$	flesh	330 d	160–200
$Cm(C_5H_5)_3$	colorless		180
$Bk(C_5H_5)_3$	amber		135–165
$Cf(C_5H_5)_3$	red		135–320

[a] d indicates decomposition.
[b] At a pressure of 10^{-3} to 10^{-4} torr.

thiocyanate, etc., but also more exotic anions such as BH_4^-, BPh_3CN^-, $Co_3(CO)_{10}^-$, and OR^- (where R is an alkyl or other organic radical). These compounds have been subjected to structural analysis as well as to examination by modern spectroscopic techniques. Nuclear magnetic resonance spectroscopy has shown that the hydrogen atoms in the borohydride derivatives are all equivalent. The crystal structure indicates that in the BH_4^- anion there are two distinct structural categories of hydrogen atoms, bridge atoms and terminal atoms. The equivalence of the hydrogen atoms in the BH_4^- anion on the NMR timescale demonstrates the existence of a rapid internal dynamic exchange process. The NMR studies have not only revealed unusual features of the structure of the organoactinide compounds but have also contributed to the theory of NMR paramagnetic chemical shifts by virtue of the magnetic properties of the 5f electrons in the compounds.

π-Donor ligands other than cyclopentadiene also interact with the actinide elements to form analogs of the cyclopentadienyl compounds. Indene, ring-bridged cyclopentadienyl compounds, and peralkylated cyclopentadienes all form organometallic compounds with structures and chemical properties similar to the tris(cyclopentadienyl) actinide compounds. Tris(indenyl) actinide halides can be prepared by metathesis of MX_4 with $K(C_9H_7)$. The steric requirements of the indenyl group are expected to be more stringent than for the cyclopentadienyl moiety, and this is confirmed by differences in the structures of corresponding compounds of the two ligands. Bridged cyclopentadienes can be readily prepared; the bridge can be $-CH_2-$, or a longer alkyl chain, or groups such as $(CH_3)_2Si$.

Bridged cyclopentadienyl donor molecules can occupy two of the ligand sites around the metal atom. The crystal structure of UCp_2X_2 (the two Cp molecules are linked by a $-CH_2-$ bridge) has been determined for the compound $Li^+U_2(THF)_2[X(C_5H_4CH_2C_5H_4)_2]_2Cl_5^-$ and is found to have an unusual dimeric structure. Thorium and uranium bis(pentamethylcyclopentadienyl) dichlorides have been obtained by reaction with the peralkylated pentamethylcyclopentadiene. It has not been possible, however, to introduce more than two of these ligands into MX_4, no doubt because of the larger steric requirements of the peralkylated ligands. The pentamethylcyclopentadienyl uranium(III) monochloride has been the starting point for much new chemistry of trivalent uranium. Similar studies have not as yet been made on the transuranium elements, but it is likely that such compounds will be added to the already long list of organoactinide compounds.

The discovery in 1968 by Streitwieser and Müller-Westerhoff [52, 53] that the dianion of cyclo-octatetraene, $C_8H_8^{2-}$, can act as a ligand to the actinide elements signaled an important new development in organoactinide chemistry. The first compound of this class was uranocene, prepared by reaction of UCl_4 with the potassium salt of cyclo-octatetraene (COT):

$$UCl_4 + 2K_2(COT) \rightarrow U(COT)_2 + 4KCl$$

Subsequently, the corresponding compounds of Th, Pa, Np, and Pu have been prepared. All have a sandwich structure in which two planar COT rings enclose a metal atom. Uranocene is the most intensively studied of these compounds. It is exceedingly reactive toward oxygen, but it reacts only slowly with water or acetic acid. Unlike the cyclopentadienyl sandwich compounds of the actinides, all reactions with strong electrophiles completely decompose uranocene. The nature of the bonding in the actinide bis(cyclo-octatetraene) compounds has naturally attracted much interest. From crystal structure data ionic bonding seems plausible, but photoelectron, NMR, and Mössbauer spectroscopy all suggest substantial covalence. Numerous derivatives of cyclo-octatetraene also function as donors. Alkyl-substituted cyclo-octatetraenes yield actinide element compounds that closely resemble the unsubstituted derivatives. Benzocyclo-octatetraene, however, forms adducts that have significantly different properties (for example, electronic transition spectra) because the aromatic benzene ring can accommodate a substantial fraction of the spin density of the compound. NMR has been especially useful in studying ligand-exchange reactions, in mapping the electron spin distribution, and in the exploration of dynamic processes in these compounds.

Attempts to prepare organometallic compounds that contain a direct metal–carbon bond were made in the very early days of the Manhattan Project, with the objective of producing compounds sufficiently volatile to be useful in isotope separation by diffusion or electromagnetic separation methods. All products prepared by the reactions then available for the synthesis of (σ) metal–carbon bonds gave products that were unstable at room temperature. The

first cyclopentadienyl compound containing a true σ metal–carbon bond was obtained by alkylation of tris(cyclopentadienyl) uranium(IV) chloride [54–56]:

$$UCp_3Cl + RLi \rightarrow UCp_3\text{–}R + LiCl$$

where R = methyl and many other straight- and branched-chain alkyl groups, unsaturated alkenes such as allyl and vinyl, aromatic radicals such as phenyl, tolyl, or benzyl, and many others. Analogous compounds of thorium but not of the other actinide elements have also been reported. The structure of the UCp_3R compounds is basically that of a distorted tetrahedron with the three cyclopentadienyl rings at three of the corners, and the covalently linked alkyl group at the fourth corner on the three-fold axis of rotation of the molecule. The NMR spectra are very informative about the structure, the spin delocalization of the uranium(IV), and the structural dynamics of the molecule. At room temperature the three cyclopentadienyl rings are magnetically equivalent, but at low temperature the equivalence vanishes because of restricted rotation about the uranium–carbon σ bond.

The chemistry of the actinide–carbon σ bond has been studied intensively. The MCp_3R compounds are extremely sensitive to air, have high thermal stability, and completely lack any tendency to β-hydride elimination from the alkyl moiety. Hydrogen elimination is a common process in organometallic compounds, and its complete suppression in the actinide hydrocarbyl derivatives is noteworthy. The most reactive of the actinide hydrocarbyls so far prepared are derived from pentamethylcyclopentadiene. Uranium and thorium(IV) bis(pentamethylcyclopentadienyl) dichlorides can be readily alkylated with lithium reagents in diethyl ether solutions to yield the air-sensitive but thermally stable bis(pentamethylcyclopentadienyl) actinide dialkyls. These actinide hydrocarbyls are highly reactive. Hydrogenolysis yields organoactinide hydrides; this constituted the first preparation of a member of this class of compounds. The dihydrocarbyls also show remarkable reactivity with carbon monoxide at low temperatures to form metal–oxygen and carbon–carbon double bonds, reactions that are of interest in catalysis. The comprehensive review by Marks (in whose laboratory much of the research described in this section was first carried out) and Ernst [49] may be consulted for a full description of the many interesting features of these and other organoactinide compounds. Chapter 22 of this volume, a contribution from the laboratory in which uranocene was first discovered, describes the organoactinide derivatives of cyclo-octatetraene in considerable detail.

14.8 ENVIRONMENTAL ASPECTS OF THE ACTINIDE ELEMENTS

The development of a large-scale nuclear power industry and the detonation of nuclear weapons in the atmosphere have created world-wide anxiety about the long-term consequences arising from the introduction of transuranium elements

into the atmosphere, the hydrosphere, and the biosphere. The radioactive nature of the transuranium elements, and the relatively long half-lives of many of these radionuclides, provide ample reasons for concern. In this section, a concise summary of the distribution and dissemination of the actinide elements in the environment is presented. In the preparation of this discussion we have made extensive use of a number of reviews [57–60]. A summary of the environmental research on the transuranium elements conducted under the auspices of the US Department of Energy to 1980 provides a very useful, comprehensive, and authoritative guide to the voluminous literature on the subject [61].

14.8.1 Actinide elements of natural origin

Several of the actinide elements are natural constituents of the Earth's crust. Of these, thorium and uranium are relatively common and, in the aggregate, occur in enormous quantities in the lithosphere. Uranium and thorium, in fact, are present in the Earth's crust to a larger extent than such familiar elements as mercury, bismuth, tin, cadmium, and silver, and in about the same concentration as lead. The uranium concentration is estimated at 1–10 $\mu g\ g^{-1}$ in the igneous rocks of the Earth's crust; some sedimentary rocks contain much more, as also do some granites. The concentration of thorium in igneous rock is somewhat higher than that of uranium, in the range 5–20 $\mu g\ g^{-1}$. The uranium content of sea water is 0.01–10 $\mu g\ l^{-1}$, and, as the uranium content varies with salinity, may reach 500 $\mu g\ l^{-1}$ in particularly saline waters. Thorium concentrations in water are generally below the microgram per litre level. Estimates of about 10^{14} tons for the uranium content of the Earth's crust (to a depth of 20 km) have been made, and about 10^{10} tons of uranium may be contained in the Earth's oceans. Other naturally occurring radioactive elements are present in the lithosphere and the oceans to much smaller extents: protactinium and radium have an abundance of about 10^{-12} wt%, and the remaining radioactive isotopes perhaps as little as several orders of magnitude less. The concentration of radioactive nuclides in secular equilibrium with the progenitors of the natural uranium and thorium decay series is determined by the half-lives of the daughter radionuclides, and, unless concentrated by some geochemical process, they will be present in very small amounts. Radioactivity is a primeval endowment of the world we inhabit.

Neptunium and plutonium are found in nature in minute amounts, formed by neutron reactions in uranium. The $^{239}Pu/^{238}U$ ratio is about 3×10^{-12}. Longer-lived ^{244}Pu, which may be primordial in origin, is present in the rare-earth mineral bastnasite to the extent of 1 part in 10^{18} [62]. The amounts of the naturally occurring plutonium isotopes are so small that for all practical purposes any of the actinide elements other than thorium and uranium encountered in the environment must be taken as man-made.

There is convincing evidence that some uranium ores have in past geological epochs sustained natural chain reactions. Some samples of pitchblende, U_3O_8, from the Oklo Mine in Gabon, Africa, have a ^{235}U content distinctly lower than

the natural average of 0.72 %. Some samples contained less than 0.5 % ^{235}U, and other elements in these samples had isotopic compositions that varied considerably from the norm. For example, some of the pitchblende from the Oklo Mine had an unusually high content of ^{143}Nd, and an equally unusually low content of ^{142}Nd. Fission-product neodymium contains a high percentage of ^{143}Nd, whereas ^{142}Nd is not formed in the fission of ^{235}U. A high ^{143}Nd content is found in ore that has a low ^{235}U content. These observations suggest that in some remote bygone age, ^{235}U had undergone fission, a conclusion supported by the unusual isotopic compositions of elements in the ore, indicating they were produced by fission. It is not likely that similar natural 'reactors' are in operation today. Fissile ^{235}U has a much shorter half-life than ^{238}U. In the early days of the Earth, the ^{235}U content of uranium minerals relative to ^{238}U was therefore higher. The age of the Oklo deposit has been established at 1.74×10^9 years. Calculation indicates that the ^{235}U content of the Oklo pitchblende 1.74×10^9 years ago was about 3 %. At this concentration of fissile material, water suffusing the ore deposit could have brought regions of the deposit to criticality, and a slow or intermittent chain reaction could have ensued. It is believed that other concentrated uranium ore deposits could have achieved supercriticality in the presence of water as a neutron moderator $(2–3) \times 10^9$ years ago. Such chain reactions conceivably played an important part in early geological events. It is interesting to note that the fission products produced at Oklo over an estimated period of 10^6 years are still retained in the rock in which they were formed more than a billion years ago [63].

14.8.2 Man-made actinides

In terms of amount, by far the most significant of the synthetic actinide elements is plutonium. Nuclear power production by fission in uranium produces as a by-product approximately 50 tons per year world-wide of a mixture of plutonium isotopes. About 250 tons of plutonium is estimated to be in the world plutonium inventory, some still in unprocessed spent fuel assemblies from nuclear reactors. World inventory of plutonium by the year 2000 has been estimated at 2400 tons [57]. Plutonium produced for nuclear weapons is mainly ^{239}Pu, but plutonium produced as a by-product of energy production contains substantial amounts of ^{240}Pu, ^{241}Pu, and ^{242}Pu and small amounts of ^{238}Pu [64]. The plutonium in the environment is due, in decreasing order of importance, to the testing of nuclear weapons in the atmosphere, the re-entry into the atmosphere and disintegration of satellites equipped with ^{238}Pu power sources, and the processing of irradiated uranium fuel from nuclear reactors.

During the period 1950–63, when testing nuclear weapons in the atmosphere was regarded as acceptable practice by the USSR and the USA, 4.2 tons of a mixture of ^{239}Pu and ^{240}Pu were injected into the atmosphere [57], mostly as plutonium oxide. Around 90 % of this has by now been redeposited on Earth. Of the original 12.8 PBq (3.5×10^5 Ci) of plutonium originally present in the

atmosphere of the Northern Hemisphere, about 37 TBq (1000 Ci) remain, a decrease by a factor of 350. Another 1.4 tons of plutonium have been deposited in the ground in the course of surface and subsurface testing of nuclear devices [57]. The ^{238}Pu in the atmosphere is largely the result of the disintegration over the Indian Ocean in 1964 of a satellite carrying a nuclear power source [65]. The amount of plutonium in the environment resulting from nuclear reactors and fuel reprocessing operations is regarded as small. Measurements in the waters of the Seine Bay (taken near the LaHague fuel reprocessing plant) indicate a plutonium concentration about 10 000 times less than the concentration of natural uranium [65].

What complicates the environmental situation is that plutonium is not the only transuranium element produced in nuclear reactors. Curium and americium are also formed by multiple neutron capture (see Fig. 14.1). The amounts of long-lived actinides in spent fuel as a function of time after removal from a reactor are shown in Table 14.12. The elements americium and curium formed in the reactor undergo radioactive decay to produce radioactive daughter species [57]:

$$^{245}Cm \rightarrow {}^{241}Pu \rightarrow {}^{241}Am \rightarrow {}^{237}Np \rightarrow {}^{233}U \rightarrow {}^{229}Th$$

$$^{242}Am \rightarrow {}^{242}Cm \rightarrow {}^{238}Pu \rightarrow {}^{234}U \rightarrow {}^{230}Th \rightarrow {}^{226}Ra$$

$$^{243}Am \rightarrow {}^{239}Pu \rightarrow {}^{235}U \rightarrow {}^{231}Pa \rightarrow {}^{227}Ac$$

The effect of radioactive decay of the americium and curium is an increase in the intensity of radioactivity with time after removal from the reactor. For a period

Table 14.12 *Long-lived actinides in spent fuel*[a] [57].

Nuclide	*Half-life* (yr)	*Activity* (GBq/t U) *after* 40 yr	100 yr	1000 yr
^{229}Th	7.3×10^3	–	–	0.006
^{230}Th	8.0×10^4	0.018	0.048	0.74
^{231}Pa	3.28×10^4	0.001	0.002	0.011
^{232}U	72	0.78	0.44	–
^{233}U	1.59×10^5	0.003	0.007	0.15
^{234}U	2.45×10^5	52	67	89
^{235}U	7.04×10^8	0.52	0.52	0.52
^{236}U	2.34×10^7	10	10	10
^{238}U	4.47×10^9	12	12	12
^{237}Np	2.14×10^6	16	19	48
^{239}Pu	2.41×10^4	1.1×10^4	1.1×10^4	1.1×10^4
^{240}Pu	6.57×10^3	1.4×10^4	1.4×10^4	1.3×10^4
^{241}Pu	14.4	9.3×10^5	5.2×10^4	12
^{242}Pu	3.76×10^5	110	110	110
^{241}Am	433	1.8×10^5	1.9×10^5	4.4×10^4
^{243}Am	7.38×10^3	0.0012	0.0012	0.0011

[a] PWR, 38 000 MWd/t U.

from 10 to 10^3–10^4 years after discharge from the reactor, the environmental hazards will be preponderantly due to ^{241}Am; from 10^4–10^5 years the nuclides ^{239}Pu, ^{240}Pu, and ^{243}Am will be the principal actinides present; and for the period after 10^6 years, ^{237}Np and ^{229}Th will be responsible for the greatest amount of radioactivity. The chemical properties of uranium, neptunium, plutonium, americium, and curium, then, determine the mode and extent of dispersion of radioactivity introduced into the environment from nuclear operations. Table 14.13 indicates the amounts of transuranium elements released into the atmosphere as of 1980. The disposal of low-level waste streams from nuclear fuel reprocessing in the sea is estimated to add considerably less than 0.1 kg per year (0.3 TBq per year) of plutonium to the environmental inventory [57].

14.8.3 Actinides in the hydrosphere

From the discussion of ions in solution and their redox and hydrolytic properties in Section 14.5, it can be inferred that the transuranium elements in a marine environment will tend to form insoluble compounds. Under the redox conditions that obtain in the ocean, the stable oxidation states of plutonium, americium, and curium are expected to be Pu(IV), Am(III), and Cm(III). Under reducing conditions, neptunium is expected to be in the Np(IV) state, and to behave much as does plutonium(IV). Under oxidizing conditions, however, the actinyl(V) ion, NpO_2^+, will be the stable species; this ionic species has a smaller tendency to undergo hydrolysis or to form strong complexes than do the IV state ions or other actinyl ions in the V or VI oxidation state. Plutonium and the other transplutonium elements in the III and IV oxidation states readily undergo hydrolysis at the normal pH of marine waters to form hydroxides and oxides that are essentially insoluble in water. However, these ions tend to form strong complexes with oxygen-

Table 14.13 *Transuranium elements released to the atmosphere* [57].

Nuclide	*Amount* (TBq)
^{238}Pu[a]	890[b]
^{239}Pu	5.7×10^3
^{240}Pu	7.7×10^3
^{241}Pu	3.6×10^5[c]
^{241}Am	1.2×10^4[d]

[a] Half-life 87.7 yr.
[b] Including 590 TBq from a SNAP 9A radionuclide battery in a satellite that vaporized upon re-entering the atmosphere.
[c] Largely decayed to ^{241}Am.
[d] Largely from ^{241}Pu.

containing ligands, which may change their redox potentials significantly, and this may render them oxidizable. The overall effect of the formation of higher oxidation states and complex ions is to produce actinide ions that are more soluble in water. The carbonate ion in particular is important because it is present in natural waters, it forms complexes that stabilize the higher oxidation states of Np, Pu, and Am, and it forms carbonate complexes of these actinide elements that are water-soluble. Allard *et al.* [57] have made a detailed analysis of the interaction of the transuranium elements with natural complexing agents as a function of concentration and pH, and have calculated solubilities in water that may be expected for these elements under various conditions. Since natural conditions vary a great deal, it is difficult to make precise generalizations, but general trends can be discerned without too much difficulty. The transuranium actinides under most conditions form insoluble species that result in actinide enrichment in bottom sediments. The tendency to form strong complexes with water-insoluble oxygen-containing ligands (e.g. the exoskeletons of marine organisms) is another route for the removal of the transuranium actinides from the water column to the bottom sediments. The nature of the chemical forms in which the actinide elements occur in marine sediments is almost totally unknown.

The availability of ocean transuranium elements to marine organisms has received attention. Plutonium is accumulated quite efficiently by benthic (sea-bottom) algae and invertebrates and by plankton. While it is a fairly straightforward matter to determine the plutonium content of harvested organisms, it is not so simple to decide the route by which the plutonium entered or just where in the organism the plutonium is retained. Transfer of plutonium in the water to starfish can take place via ingested food, but is can also occur by adsorption on the surface of the organism. The high concentration of plutonium in starfish appears to be due largely to the strong affinity of polymeric plutonium hydrosols or simple plutonium ions for the mucus sheath that coats the organism. Neptunium, as the NpO_2^+ ion, is rapidly accumulated and excreted by marine zooplankton, but appears, on the basis of limited observations, to be less available than either plutonium or americium.

The transfer rate of americium from sediments containing it in insoluble form is low, and it appears for the most part to be adsorbed on the exterior of bivalve molluscs, Polychaeta (marine worms), and isopods (crustaceans). In the presence of higher concentrations of carbonate (Atlantic sediments containing 83% carbonate as compared to Pacific sediments containing only 8% carbonate), the transfer of americium to living organisms increased several fold [59]. Experiments in which the marine environment was simulated show that the accumulation of ^{241}Am by tiny crustaceans (krill) occurred mainly by adsorption on the exoskeleton, and that only a small amount of americium was retained by the krill after molting. Americium sorbed on diatoms ingested by krill was not assimilated and was excreted in a short time.

Based on a limited amount of data acquired in the Irish Sea near the reprocessing plant at Sellafield, UK, invertebrates and algae accumulate higher

concentrations of curium than do the edible parts of fish. The behavior of californium has been studied in a preliminary way in sea water, sediments, and plankton [59]. Californium(III) is rapidly adsorbed by particulate matter and sediments with distribution coefficients of 10^4–10^5. It is also taken up rapidly by marine zooplankton. The relative order of uptake by krill is Cf(III) > Am(III) > Pu(V + VI) > Np(V). Assimilation and incorporation of Cf(III) by the zooplankton in the internal tissues is extremely low in these organisms, and take-up is most likely due to adsorption on the surface of the organisms. Surface-adsorbed actinides, however, provide a mechanism for the introduction of transuranium elements into the food chain even though the actinides are not actually incorporated into the internal tissues of the organisms.

14.8.4 Actinide sorption and mobility

Polymeric actinide ions carry a positive charge, and are easily scavenged by negatively charged surfaces. As depolymerization is a very slow process even in strong acid solution, the plutonium(IV) polymer is an attractive candidate for an explanation of the ease with which it is removed and the tenacity with which it is retained by clays or soils. Many minerals, especially clays, have ion-exchange properties. Ion exchange would firmly bind the simple actinide ions in the III and IV oxidation states; binding of the actinyl ions in the V and VI states would be considerably weaker. Plutonium is strongly sorbed on most minerals in the pH range normally encountered in the environment under both oxidizing and reducing conditions.

The overall effect of ion exchange and other sorption processes by solid phases is to remove actinides at tracer concentrations from an aqueous phase. The uptake on solids is in the same sequence as the order of hydrolysis: Pu(IV) > Am(III) > U(VI) > Np(V). Assimilation in plants commonly declines in the order: Np(V) > U(VI) > Am(III) > Pu(IV), Np(IV). Both phenomena are evidently contingent on the species formed by hydrolysis: the easily immobilized species are also assimilated with difficulty by plants. The uptake of actinides by living organisms from solid phases is minor, and this is also the case for actinide elements immobilized on food. Of the 4.2 tons of plutonium that came to Earth after atmospheric testing of nuclear weapons, the total amount fixed in the world population is estimated to be less than 1 g [57]. Allard *et al.* [57] conclude from the available evidence that plutonium in the environment is not concentrated in the food chain. The enrichment of actinides in the food chain to humans is minimized by discrimination against the absorption of actinides by organisms at higher levels in the food chain. Thus, it is unlikely that the concentration of plutonium in a human being will significantly exceed the concentration in natural waters, regardless of the mode of ingestion.

Organic and inorganic particles or colloids to which actinide elements are attached constitute a major mode of dissemination of the actinide elements in the environment. Natural waters contain particulate silt and organic matter, which

may or may not be living. Transport of actinide elements adsorbed on particulate matter will then depend on particle size, water flow, and factors other than the chemical properties of the actinide species themselves. Living organisms can also act as carriers even if the actinide elements are not actually incorporated into the tissues of the organism.

14.8.5 Nuclear waste disposal

The fate of actinide elements introduced into the environment is of course not merely a scientific issue. The disposal of the by-products of the nuclear power industry has become a matter of public concern. For each 1000 kg of uranium fuel irradiated in a typical nuclear reactor for a three-year period, about 50 kg of uranium are consumed. In addition to a large amount of energy evolved as heat, 35 kg of radioactive fission products and 15 kg of plutonium and transplutonium elements are produced. Many of the fission-product nuclides are stable, but others are highly radioactive. All of the fission products are isotopes of elements whose chemical properties are well-understood. The transuranium elements produced in the reactor by neutron capture, however, have unique chemical properties, which are reasonably well-understood but are not always easily inferred by extrapolation from the chemistry of the classical elements. Plutonium is fissile and can be recycled as a nuclear fuel in conventional or breeder reactors, but the transplutonium elements are not fissile to the extent of supporting a nuclear chain reaction, and in any event they are produced in amounts too small to be of interest for large-scale uses. The transplutonium elements must therefore be secured and stored.

The exact form in which fission products and heavy elements are extracted from spent fuel elements is determined by the chemical process used to treat the spent fuel. In the past, most fuel processing has been by solvent extraction, and it is probable that solvent extraction will continue to be the most widely used processing procedure, at least until new reactor types are introduced. Solvent extraction is efficient in separating uranium, fission products, and transuranium elements, but large volumes of liquid waste streams with rather low but not negligible levels of radioactivity are generated in the process. The plutonium is generally separated from the transplutonium elements, leaving a complex mixture of fission products and americium, curium, and transcurium elements, which as they decay form isotopes of neptunium, uranium, and radioisotopes of natural radioactive elements. These must be immobilized and stored in a way and in places where no geological or man-made catastrophe will release the radioactive material into the environment, even over an enormously long timespan.

Many schemes have been considered for disposal of both fission products and actinide elements. A succinct and informative discussion of these proposals has been given by Choppin and Rydberg [66]. Nuclear incineration is one possibility. For the actinide elements, which are the predominant source of radioactivity after about 600 years, prolonged neutron irradiation in an ordinary nuclear reactor, or

preferably in a fast breeder reactor, will transmute americium and curium to short-lived radioactive or stable isotopes faster than they will be formed from the plutonium fuel in the reactor. The actinide elements subjected to nuclear incineration must be free of lanthanide fission products, as some of these have very large cross-sections for neutron capture and thus could adversely affect the neutron economy of a nuclear reactor. Although neutron incineration does not appear to be a practical possibility at the time of writing for technical, economic, and political reasons, it is an alternative that must be kept in mind, for it is a way to remove permanently, if not all, at least a large part of the inventory of transplutonium elements that will accumulate. Sending actinide waste into space has also been considered. The technology for doing this exists, but the hazards associated with take-off may pose unacceptable risks.

Immobilization and disposal in appropriate geological formations has received the most attention. The first step in immobilization is to convert the liquid waste streams from fuel processing into dry solids by evaporation or some other drying process. The dry residue is calcined to convert the radioactive mix to metal oxides. In this form the calcined oxides are leachable and can easily become airborne. Their thermal conductivity is low, and good heat conductivity is essential to dissipate the heat liberated by radioactive decay. A great variety of glassy and crystalline matrices have been explored. Prime requirements are stability to radiation and to chemical attack by or to solubility in water, since exposure to ground water is a possibility that must be guarded against in any subterranean repository. Borosilicate and phosphate glasses are the preferred glassy matrices, with borosilicate regarded as the more satisfactory of the two. Additional encapsulation of the solidified waste is generally considered mandatory, and for this purpose corrosion-resistant materials such as graphite, titanium, lead, gold or ceramics have been explored.

The requirements for a geological repository are quite stringent. The repository must be sited in a region of high geological stability, free of earthquakes and volcanic activity. The chosen stratum must be free of vents to the surface, and it must have little or no ground water circulation. It is important that the geological formation have good heat conduction properties to enable heat evolved by radioactive decay, which is very substantial, to be conducted away rapidly enough to prevent destruction of the containment by high temperature. Rock salt, granite, and clay all have their proponents. Disposal in the Arctic ice caps and burial in deep seabeds also have been considered. Rock salt formations, at least in France, the Federal Republic of Germany, the Netherlands, and the USA, appear to be the geological stratum of choice. Unaltered rock salt formations of great age and of unquestionable seismic stability are known. Rock salt has exceptionally good heat transfer properties. Extremely dry salt domes that have existed for more than 100 million years without appreciable alteration exist in many places. Salt is plastic, and holes and fractures in the salt bed will self-seal. Granted that the surface layers are not breached by drilling, rock salt domes appear to have most of the features required for a secure repository. Clays

likewise have desirable properties. The migration rate of fission products and actinides through clay is very slow and, once adsorbed in such a matrix, the transuranium elements are effectively immobilized. However, clay deposits frequently are percolated by water, and it is difficult to guarantee that even a bed dry for geological epochs will remain that way. Still, even radionuclides that enter underground water are readily removed and immobilized by ion exchange on clays and other minerals. A very good example of efficient and extraordinarily effective immobilization of radioactive fission products by natural processes is found in the Oklo mineral formation, where the products of a natural chain reaction have remained in close proximity to their point of origin although the rock formation has been suffused repeatedly by water in the past billion years (see Section 14.8.1). Clay certainly has its uses but reservations have been expressed about its use as a primary barrier. Although there are unanswered questions about nuclear repositories, there is every reason to suppose that the technical problems in nuclear waste disposal can be solved satisfactorily. Indeed, most of the necessary technology has been in existence for some time, and a high level of technical sophistication already exists [67]. It seems likely that interim or monitored retrieval storage will be the method of choice for the storage of nuclear waste. Storage of this kind is easier to prove safe and could be useful for a century or more.

14.9 BIOLOGICAL BEHAVIOR OF THE ACTINIDE ELEMENTS

14.9.1 General considerations

In the preparation of this section we have made extensive use of several authoritative reviews [65, 68, 71] that emphasize chemical aspects of importance in the biological behavior of the actinide elements. None of the elements heavier than iodine (atomic number 53) is, so far as is known, essential to life, and an intrusion by any of them into living organisms is generally regarded as a noxious event best avoided. Studies on the heavier elements tend to be sparse or fragmentary except where special circumstances apply, i.e. mercury or lead for example. Were it not for the long-lived radioactivity of the actinide elements, it is likely that they too would attract little interest. Plutonium, americium, and curium have been regarded as the major health hazards among the actinide elements, and thus have been the focus of research activity. Recently, interest in the biological properties of neptunium has reawakened [69]. Neptunium(v) appears to be the most readily assimilated of the actinide ionic species. This, coupled with the realization that long-lived ^{237}Np formed by the radioactive decay of ^{241}Pu in nuclear waste could make ^{237}Np the major contributor to the radioactivity of nuclear waste at times greater than 10^5 years, has stimulated new interest in the biological properties of neptunium.

14.9.2 State of actinide elements in body fluids

The forms in which plutonium, americium, and curium occur in blood and urine are continuing topics of major concern, for they are intimately involved in transport in the body after ingestion and in subsequent excretion. In 1965, it was found that plutonium injected intravenously into the rat was bound in the blood serum to transferrin, a protein produced in the liver that transports iron between tissues and bone marrow. Plutonium(IV) in the blood is rapidly and firmly bound to transferrin. By far the greater part of the plutonium is captured by transferrin, but small amounts are believed to be complexed by citrate ion or low-molecular-weight carbohydrates or peptides. This may reflect a complex equilibrium situation, or may be an indication that more than one ionic species of plutonium in more than one oxidation state is present. The binding of plutonium to transferrin is strong, but Fe(III) can displace it, and plutonium is not bound by iron-saturated transferrin. Bicarbonate ion is required to bind iron to transferrin, and this is also the case for plutonium. The half-life for the removal of transferrin-bound iron and plutonium from the circulation is the same. The exact nature of the binding sites remains unknown, and whether the same site is used for binding iron and plutonium is unsettled. Transferrin contains a sialic acid component (an oligo- or polysaccharide containing an acidic sugar, *N*-acetylneuraminic acid), which is an excellent complexing agent for metal ions. However, destruction of the polysaccharide moiety inhibits the binding of Pu(IV) but not of Fe(III), suggesting a more complicated binding site situation than at first anticipated. Pu(IV) shows remarkable similarity to Fe(III) in its coordination behavior, attributed by Raymond *et al.* [72] to similar ratios of charge to ionic radius for Pu(IV) ($4.6e/\text{Å}$) and Fe(III) ($4.2e/\text{Å}$). The 3+ ions of americium, curium, and the transcurium elements bind very weakly, if at all, to transferrin. Instead, the actinide(III) ions present in biological fluids are weakly associated with various plasma proteins. Uranium, present as the dipositive uranyl ion, which has a much diminished tendency to form complex ions as compared to uranium in lower oxidation states, is found in the blood in roughly equal amounts associated with protein and as uranyl carbonate complex ions. Uranium(IV), however, binds strongly to protein and is excreted very slowly.

Such studies as are available indicate that plutonium, americium, and curium are cleared through the kidneys and excreted in the urine as citrate complexes, whereas uranyl ion is excreted as a bicarbonate complex. Although there is by now a considerable body of information on the rate of excretion of plutonium in the urine as influenced by a variety of additives and presumptive therapeutic agents, much remains to be learned about the chemistry of the elimination of the actinide elements through the kidney.

Plutonium, americium, and curium are cleared from the liver through bile, and this is the principal source of these elements in feces. The clearance of the actinide elements through the feces, however, constitutes only a very small fraction of the radioactivity transported in the organism. Transport of the actinide elements also

appears to take place in lymph fluid. This mode of transportation presumably is involved in plutonium introduced in a wound. Plutonium as a simple ion in the lymphatic system moves with the fluid flow, but plutonium as a colloid or as particulate matter is transported in lymphocytes whose function it is to scavenge ingested particulate matter. Plutonium in the fluid phase of the lymph migrates as a transferrin complex. The behavior of plutonium and the transplutonium elements in the lymphatic system may well have an important bearing on the decorporation of ingested actinide elements, but too little information is available to make any definitive declarations on this point.

14.9.3 Uptake of actinide elements in the liver

Actinide elements are rapidly cleared from the body fluids. As is usual in the removal of xenobiotics, the first repository is the liver. According to Bulman [68], the mechanism by which plutonium, americium, and curium are removed from the blood and trapped in the liver is not well-understood. The actinide elements bound by transferrin are transferred in the liver to ferritin, an iron storage protein, but nothing is known about the transfer process. It might be expected that actinide element colloids would be taken up by endocytosis, the process of cellular uptake or internalization by which particles, macromolecules, and fluid droplets are removed from the bloodstream and incorporated into living cells. However, the literature does not support this view. Endocytosis (or pinocytosis as it is also known) is not considered to play an important part in the incorporation of actinide elements into liver cells [73]. What seems well-established is the critical role of phospholipids in the take-up of the actinide elements by the liver. Actinide(III) and (IV) ions are complexed strongly by phosphates in simple aqueous systems. Thorium(IV) likewise interacts strongly with phospholipids [70, 74]. Such behavior for other actinides ions in the III and IV oxidation states would not be unexpected. Phospholipids could thus act as ionophores in the concentration of the actinide elements in the liver. The evidence in support of this hypothesis is mostly indirect. Based on the behavior of Fe(III) and the uptake of plutonium in animals treated so as to have a much higher than normal concentration of phospholipids in the liver, there is reason to suppose that phospholipids are involved in the concentration of plutonium by the liver. Thioacetamide characteristically increases the accumulation of acidic phospholipids in the liver, and this compound is found to cause a 2.5-fold increase in the uptake of Pu(IV) by the liver. The effect of various phospholipids on the liquid–liquid partition of Pu(IV), Am(III), and Cm(III) between water and water-immiscible organic solvents provides additional evidence of the ionophore capabilities of phospholipids. Nevertheless, the exact nature of the receptors involved in actinide uptake (if indeed there are specific receptors) remains to be established.

Several research groups have provided evidence that plutonium, americium, and curium are taken up by lysosomes in the liver. Lysosomes are specialized

parts of cells or organelles in which an important part of the cellular metabolism is carried out. The lysosome is surrounded by a single membrane and contains a complex mixture of hydrolytic enzymes; together these enzymes are able to dismantle proteins, nucleic acids, polysaccharides, and lipids to their component parts. The actinide elements not translocated from the liver remain associated with the lysosomes, possibly bound to the iron storage proteins ferritin and hemosiderin. Lysosomes are associated with endocytosis and at least a fraction of the lysosomes are formed by endocytosis. If the main part of the actinide uptake is really associated with liver lysosomes, then it may be premature to exclude endocytosis as a primary event in liver uptake of actinide ions. A substantial association of the cellular actinide content with mitochondria is also probable.

A body of evidence indicates that, within three days of administration, considerable amounts of plutonium are bound to lysosomal ferritin, and similar findings have been reported for americium and curium administered as monomeric citrates [75]. Americium has been reported to associate with lysosomal ferritin and lipofuscin, a yellow-brown pigment that accumulates in aging cells. Lipofuscin contains phospholipids and is known to bind metal ions.

14.9.4 Uptake of actinides by bone

The ultimate fate of plutonium that is not excreted promptly after administration or ingestion is deposition in the bone and other mineralized tissues. Whether the mineralization is phosphate- or carbonate-based appears to be immaterial. In cartilaginous fish, plutonium is concentrated in the skeleton to a significant extent, and in fish with a bony skeleton, the plutonium concentration in the soft tissues may be less than 1% of that in the skeleton. The uptake of actinide elements from the body fluids by bone is a slow process, because of the strong binding of plutonium by transferrin. Autoradiography of bone shows quite different patterns of deposition for plutonium and americium compared to the deposition of radioactive calcium. Calcium deposition is uniform, whereas actinide deposition is irregular. The lack of uniformity in the distribution of the actinides deposited in bone may be related to variations in the pH of the bone surface, or to different concentrations of citrate ion at different locations on the bone surface.

Glycoprotein has been suggested as the important agent in the fixation of plutonium, but less so for americium or curium [76]. Glycoproteins that have a high acidic amino acid content bind plutonium *in vitro*. Calcium ion is required for plutonium fixation, which suggests that calcium nucleation sites are necessary for plutonium uptake. Phospholipids have also been implicated in the process, and a lysosome–inositol triphosphatide complex that plays an important part in a model of bone calcification is known to complex Pu(IV), Am(III), and Cm(III) from citrate solutions or plasma [77]. Eventually the plutonium in bone accumulates in immobilized deposits of hemosiderin, which, unlike the iron storage protein ferritin, is insoluble in aqueous media. Hemosiderin contains a large core of iron

hydroxides and phosphates, and is the repository of the iron content of heme liberated by the catabolism of hemoglobin. Hemosiderin deposits are located close to the surfaces of the bone in the reticuloendothelial cells of the bone marrow [78]. Once plutonium is incorporated into bone, it is not totally immobilized, but the rate at which it leaves the bone is slow and the process by which it is released is unknown. The half-time for the spontaneous removal of plutonium from bone has been estimated as 65–130 years. Release of plutonium from hemosiderin should not be taken to imply that the mobile plutonium will be excreted through the kidney. More probably, it will be bound to transferrin and recycled into the liver and bone.

14.10 TOXICOLOGY OF THE ACTINIDE ELEMENTS

The toxic properties of plutonium have attracted interest to such an extent that it has become one of the best understood toxic substances known. Although plutonium has been known since 1940 and has been manufactured and handled on a large scale, 'no unquestionable direct relationship, 40 years later has been established between its toxicity and human death' [65]. Everything known about the toxicity of plutonium has been learned from animal experimentation, as there is no known case of ingestion by a human of a sufficiently large amount of plutonium to produce symptoms of acute toxicity. The application of information acquired in this way to humans can only be by extrapolation, which raises questions of species specificity that cannot be answered at this time. The information available about the other actinide elements is fragmentary and much less abundant, and generalizations must be accepted with reservations.

14.10.1 Ingestion

Any of the actinide elements in the environment can obtain entry to the human body by ingestion with food, by inhalation of particulate matter, by passage through the skin, or by accidents accompanied by forcible introduction of the actinide into the body. Absorption through the intestinal tract appears to be one of the least important routes for the incorporation of plutonium and the transplutonium elements. Plutonium is not concentrated in the food chain (cf. Section 14.8.4), nor does it at all readily pass through the intestinal wall. The unbroken skin likewise presents an essentially impermeable barrier to the passage of actinide ions. The fate of plutonium deposited in an open wound depends largely on the chemical state of the plutonium. If the plutonium is in a soluble form such as a citrate complex, it will rapidly reach the circulation and form a transferrin complex. If it is deposited in a wound as an insoluble compound, translocation is likely to be very slow. By far the most important (and serious) mode of entry for plutonium into the body is inhalation of insoluble particulate matter into the lungs. What happens then and how fast depends on the exact particle size and the solubility properties of the particulate.

Where particulate matter ingested by inhalation is deposited in the lung is determined by the size distribution of the particles and the breathing characteristics of the individual. The smaller the particle size, the more likely the particles will be deposited deep in the lung. The fraction of the lung irradiated by a radioactive substance is closely related to the particle size. Thus, for $^{239}PuO_2$ particles 0.1 μm in size, approximately 30% of the lung may be irradiated by the alpha decay of the plutonium, whereas for particles 1.0 μm in diameter, only 0.03% of the lung will be subject to alpha radiation. Water-soluble compounds such as plutonium nitrate or complexes with small ligands are more uniformly distributed, resulting in a more uniform irradiation of the lung than is likely to occur from particulate matter.

Clearance of plutonium from the lung is also dependent on the size and chemical characteristics of the ingested particles. Extremely small particles (1 nm in diameter) of PuO_2 are quickly absorbed from the lung and enter the circulation as low-molecular-weight complexes. Large particles (0.025–0.22 μm) clear very slowly [68]. AmO_2 made by calcination of americium oxalate at 600°C was observed to be removed so rapidly from the lung as to raise questions whether the compound should continue to be considered insoluble. Large particles of AmO_2 cleared more rapidly than did small particles for fresh preparations, but the order was reversed when aged suspensions in water were used. It is possible that the americium dioxide preparation was actually americium hydroxide polymer, and it may be that small deviations from stoichiometry could have a considerable effect on the rate of dissolution and removal from the lung. Variations in stoichiometry are expected to be much more prominent in plutonium than in americium, and this may be responsible for the surprising differences in the behavior of the oxides of these two actinide elements. Curium dioxide behaves quite similarly to americium dioxide, but there is at least one important and puzzling difference between the two. While americium dioxide does not bind to protein, curium dioxide does. In the absence of information about the stoichiometry of the actinide oxide preparations used in the experiments, it is difficult to ascertain whether it is particle size or deviations from stoichiometry that are responsible for the biological properties of the actinide oxides. Many questions about the behavior of actinide particulates in the lung still remain, the answers to which could have implications for other lung pathologies. It should also be noted that $^{238}PuO_2$ is reported to clear the lung much faster than does $^{239}PuO_2$ [68]. The magnitude of the difference is clearly beyond the range of ordinary isotope effects, and must be attributed to the increased radiation damage incurred by the oxide particles from the more energetic alpha particles emitted by the shorter-lived radionuclide ^{238}Pu.

14.10.2 Acute toxicity of plutonium

There is general agreement that the toxicity of plutonium is caused by its alpha radioactivity [65, 68]. Raymond [71], on the basis of very old work on animals [79], considers the acute chemical toxicity of $^{239}Pu^{4+}$ to be about the same as

strychnine, which is to say among the most toxic chemicals known. This makes plutonium out to be a much more acutely toxic substance than mercury or any other heavy element. No experimental evidence is available that bears on this point in humans, as there is no known instance where any human being has ingested as much as a milligram of plutonium, let alone any amount considered likely to result in an acute toxic response. Consequently all data on the chemical toxicity of plutonium are derived from animal experiments. Neptunium-237 injected into rats intravenously at $3\ mg\ kg^{-1}$ induces short-term subacute changes in the liver, but is nowhere near as toxic as strychnine. On the assumption that ions of similar size and charge will have similar toxicological properties, which is a reasonable assumption in this situation, to produce a similar change in an adult human liver would require the intravenous injection of about 200 mg of plutonium. We believe that the weight of the evidence is in favor of the view that the chemical toxicity of plutonium is comparable to that of neptunium, and that plutonium is not an extraordinarily virulent chemical poison. The toxic manifestations of plutonium are due to long-term effects of radiation damage from its radioactive decay.

The acute toxicity of uranium in the form of the uranyl ion varies considerably with the experimental animal; the acute dose in the rabbit and guinea-pig is in the range 0.1–0.3 $mg\ kg^{-1}$, and in mice it may be as much as 20–25 $mg\ kg^{-1}$ [68]. Differences in toxicity in different species have been attributed to differences in diet that result in the excretion of urine of widely differing pH. Herbivores excrete very acidic urine, which interferes with the formation of carbonate and citrate complexes of uranyl ion. These are the forms in which uranium is cleared through the kidneys. Under conditions that lower the carbonate and citrate concentrations, uranium clears the organism more slowly, and a given dose of uranium in a herbivore appears to have a higher toxicity than in an organism that can eliminate uranium more rapidly. Acute toxic symptoms produced in yeast by uranyl salts appear to be a result of the suppression of glucose metabolism by interaction of the uranyl ion with the cell surface. Reagents such as phosphate that complex uranyl ion strongly reverse the inhibition of respiratory activity.

14.10.3 Long-term effects of ingested plutonium

The maximum allowed dose of plutonium in humans is set at 1480 Bq [65]. A population of 26 individuals who acquired plutonium body burdens between 260 and 8510 Bq during World War II has been followed for 37 years, and no serious deleterious effects have been observed. No cases of cancer were observed except in three subjects with a history of skin cancer [80]. In subjects who have both lung and other body burdens of plutonium, chromosomal aberrations of lymphocytes were observed, but subjects who had the same total amount of plutonium but fixed only in the lung showed no such abnormalities [65]. Because no serious consequences such as a shortening of the lifespan or malignancies were seen in humans who ingested amounts of plutonium in excess of the permissible levels,

the available information on the results of long-term exposure to immobilized plutonium *in vivo* is derived entirely from animal experiments.

Low doses of radiation in the lungs of rats produces three types of cancer: sarcomas (10%), bronchoalveolar cancers (40%), and bronchogenic cancers (50%). The lowest dose at which a significant increase in lung cancers occurs is 37 Bq g^{-1} of lung tissue for inhaled insoluble plutonium compounds. The mode of distribution of plutonium in the lung has a large effect, and whether the plutonium was acquired in a single exposure or by multiple exposures is also a factor that is important in subsequent pathology. In the dose range 0.06–37 kBq kg^{-1} of bone, an osteosarcoma incidence from 31% to 100% has been observed in dogs. Organisms experiencing rapid bone growth are more sensitive to osteosarcomas from plutonium than are adults. Liver appears to be less sensitive to alpha radiation than either lung or bone. The effects of ingested plutonium on the blood are largely due to irradiation of the hematopoietic tissues where blood cells are formed. No leukemia has ever been detected in dogs. In humans exposed to plutonium, stable chromosomal aberrations in the blood have been seen. Finally, no hereditary diseases have been observed in the progeny of animals whose bodies contained plutonium [65].

14.10.4 Removal of actinide elements from the body

Once plutonium has gained access to the bloodstream, there is no normal physiological process that will eliminate it rapidly from the body. Foreign chemicals that gain entry are converted in the liver by oxidation and conjugation into compounds that can be excreted, but for heavy metals deposited in insoluble form or strongly complexed to body constituents no such pathway exists. Plutonium retention is not absolute, but the excretion rate is so slow that in a normal lifespan only a fraction of the deposited actinide will be removed from the body. Early attempts to increase the rate of plutonium excretion were based on competitive displacement by innocuous metal ions of a size and charge that would enable them to compete successfully with Pu(IV) for binding sites or crystal lattice sites. Zirconyl(IV) citrate was found to accelerate considerably the excretion of injected plutonium, but only if the zirconium was administered within a very short time after the plutonium. Zirconyl citrate appears to be reasonably effective in displacing plutonium(IV) from the bloodstream but not from body tissues. Other hydrous metal oxides such as those of thorium or aluminum minimize deposition of plutonium in bone, but increase the amount of plutonium deposited in the liver. Therapeutic approaches along these lines have therefore fallen into disuse.

The strategy for the removal of immobilized plutonium that has received the most attention is based on the use of chelating agents to form water-soluble complexes of plutonium. Citrate and ascorbate are effective complexing agents to a degree, but are metabolized too rapidly to be of practical utility. Useful therapeutic agents have therefore been sought among the numerous chelating

agents that have been synthesized for ion sequestration purposes, particularly derivatives and analogs of ethylenediaminetetraacetic acid (EDTA). EDTA itself is quite effective in accelerating the excretion of plutonium, provided it is administered within a short time after plutonium ingestion, but it is much less effective when the interval between ingestion and therapy is of the order of weeks [81–83]. Of the considerable number of derivatives and analogs of EDTA that have received attention, perhaps the most successful agent is diethylenetriamine-pentaacetic acid (DTPA). This compound has one carboxyl group more available for chelation than EDTA, which significantly enhances the stability of its complex with plutonium(IV). DTPA administered promptly in a single dose after plutonium ingestion causes the excretion of about 90% of the plutonium in the following six days as compared to less than 5% excretion in controls; the experimental animal in these experiments was the pig [84]. To achieve such good results, DTPA must be administered within 30 min after plutonium administration to beagles. Delay the administration of DTPA for as little as 2 h, and only 15% of the injected plutonium is excreted during the first day. Delayed treatment with multiple doses of DTPA is effective in removing moderate amounts of plutonium from the pig. In these experiments it was observed that the principal source of the excreted plutonium was the soft tissues, and that removal of plutonium from the bone did not proceed to the point where the number of bone tumors formed was significantly reduced [85]. Additional details on the use of DTPA can be found elsewhere [81, 82, 86, 87]. Many other chelating agents related in structure to EDTA and DTPA have been studied, but none of these are significantly better performers. Increasing the number of carboxyl groups does not improve their decorporation properties, and the replacement of oxygen functions by sulfur or phosphorus analogs degrades their performance.

The *in vivo* situation of chelating agents is infinitely more complicated than sequestration of alkaline-earth ions in a detergent solution, not to say laboratory systems arranged for the measurements of complexation constants. It has been recognized for some time [83] that, because the calcium-ion concentration in serum is much greater than that of other metal ions, unless a chelating agent has a much lower affinity for calcium ion than for another metal ion, the chelating agent will exist predominantly as the calcium complex in the circulatory system. The apparent efficacy of a chelating agent is thus increased by a low affinity for calcium ion as well as by an enhanced affinity for plutonium. A foreign metal ion will be partitioned between natural chelators engaged in the transport or metabolic activities of metal ions and any chelating agents that may be introduced for therapeutic purposes. The naturally occurring iron sequestering agent desferrioxamine (DFOA) is a very much weaker complexing agent for calcium ion than is DTPA, and even though it does not bind much more strongly to Fe(III) than does DTPA, it nevertheless is much more effective in removing iron from the body, presumably because of its lower affinity for calcium ion. Whereas DFOA is more efficient in plutonium removal than DTPA, provided it is administered within an hour after injection of plutonium, its efficacy decreases more rapidly

than that of DTPA as the time interval between plutonium incorporation and therapy increases. Combined use of DTPA and DFOA appears to remove the greatest amount of plutonium. The presumption is that plutonium ion liberated from the Pu(IV)–DFOA complex is recomplexed and excreted as the DTPA complex before irreversible deposition of the plutonium can occur. Once plutonium has been deposited in insoluble form, no known therapeutic approach is efficacious. Inhalation of insoluble plutonium can only be countered by repeated pulmonary lavage with isotonic saline solution [65].

Conventional chelating agents have received by far the most attention in the search for effective removal of ingested plutonium. Raymond and his co-workers have undertaken a search for chelating agents that would bind strongly to and be specific for actinide ions [71, 72, 88]. They have adopted a biomimetic approach in which compounds are modeled after the powerful and highly specific siderophores, the natural iron sequestering agents used by micro-organisms to acquire Fe(III) from the environment [89]. The siderophores contain hydroxamate or catechol groups that are arranged to form an octahedral cavity of exactly the size of a ferric ion. Catechol (1,2-dihydroxybenzene) is a very weak acid whose conjugate base binds very strongly to Fe(III) and Pu(IV). By introducing several catechol functional groups, enough binding sites on the ligand are provided to occupy all of the coordination sites on the metal ion. The metal ion is then encapsulated, so to speak, by the chelating agent. A variety of biomimetic chelate compounds have been prepared, one of which is shown in Fig. 14.8. These new chelating agents bind plutonium *in vivo* and promote excretion [90, 91]. The excretion of americium(III) in dogs surprisingly enough is distinctly accelerated, even though in the laboratory the ligands do not appear to bind strongly to Am(III).

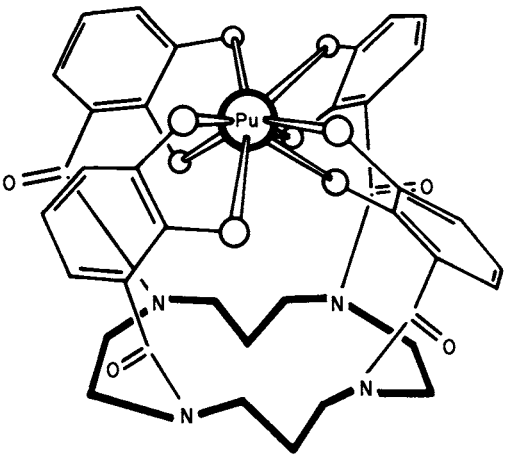

Fig. 14.8 *An example of a tetracatechol chelating agent for the decorporation of plutonium (from Raymond and Smith* [71] *with permission of Springer-Verlag).*

14.11 PRACTICAL APPLICATIONS OF THE ACTINIDE ELEMENTS

The principal application of the actinide elements is in the production of nuclear energy. Although this is by far the most important use for any of the actinide elements, a surprising number of other uses have been found. These include the use of short-lived actinide isotopes as portable power supplies for satellites; in ionization smoke detectors; in the therapy of cancer; in neutron radiography; in mineral prospecting and oil-well logging; as neutron sources in nuclear reactor start-up; and as neutron sources in a variety of analytical procedures, the most important of which are neutron activation analysis and heavy-ion desorption mass spectroscopy.

14.11.1 Nuclear power

The practical importance of the actinide elements derives from the discovery of fission by Hahn and Strassman in 1939. Atoms of the naturally occurring isotope of uranium, ^{235}U, split into two approximately equal fragments by the capture of a neutron, an event that releases an enormous amount of energy. Approximately 2.5 neutrons are released in each fission event, making it possible to initiate an explosive chain reaction in the pure fissile isotope; alternatively, controlled fission in a nuclear reactor can be used to provide heat to generate electricity. The plutonium isotope ^{239}Pu is produced in chain-reacting nuclear reactors by capture of excess neutrons in non-fissionable ^{238}U. Plutonium-239 itself is also fissionable with slow (essentially zero-energy) neutrons. The naturally occurring thorium isotope ^{232}Th, which does not undergo fission, can be converted by neutron capture to ^{233}U, which is a fissionable nuclide. The complete utilization of non-fissionable ^{238}U (through conversion to fissionable ^{239}Pu) and non-fissionable ^{232}Th (through conversion to fissionable ^{233}U) can be accomplished by breeder reactors. The fissile isotopes ^{233}U, ^{235}U, and ^{239}Pu constitute an enormous, in principle inexhaustible, energy resource. The future of nuclear power, however, is clouded by technological and social problems. The technical problems relate to the safety of nuclear reactors, to the ability to prevent access of radioactive substances to the environment, and to the prevention of the diversion of plutonium for the clandestine manufacture of nuclear weapons. We adhere to the school of thought that believes the technological problems of safe nuclear energy and environmental contamination are soluble problems. Indeed, many of these problems have already been solved, and those that remain do not require the discovery of new or unheard of scientific principles for their solution. The social, economic, and political problems are another matter. The fully justified fear of nuclear war is projected onto nuclear power, as if nuclear power and nuclear war were synonymous, and as if the fear of nuclear war could be exorcised by abolishing nuclear power. Prevention of nuclear war and the proliferation of nuclear weapons can only be accomplished by international statesmanship, not by a refusal to make use of the limitless energy that can be supplied by fission.

Some countries (France is a notable example) have embraced nuclear power, with the probable result that they will have a future economic advantage in world trade from the cheaper electric power that nuclear energy can provide. Nuclear power promises a more prosperous future, but whether the promise becomes a reality in many additional countries will depend on the solution of the social, economic, and international problems that enmesh the issue of nuclear energy.

14.11.2 Portable power sources

Radioactive decay is accompanied by the evolution of heat, and radioactive nuclides can therefore be used as portable heat sources. One gram of ^{238}Pu produces about 0.56 W of thermal power, primarily from alpha decay, and this isotope of plutonium has found use in space vehicles to drive small thermoelectric power units. Several satellites with ^{238}Pu generators that produce 25 W have been deployed in space, and the Apollo spacecraft carried a ^{238}Pu generator with a total weight of 14 kg that produced 50 W of power. A 73 W power supply fueled with 2.6 kg of ^{238}Pu in the form of PuO_2 produced the electrical power to run the scientific experiments of the Apollo lunar expedition. The satellite that sent the amazing photographs of Jupiter and the outer planets back to Earth used a 50 W ^{238}Pu power supply for this purpose.

14.11.3 Neutron sources

The radionuclide americium-241 emits alpha particles, which produce neutrons by an (α,n) nuclear reaction with light elements. A mixture of americium-241 with beryllium produces 1.0×10^7 neutrons per second per gram of ^{241}Am. A large number of ^{241}Am–Be sources are in daily use world-wide in oil-well logging operations to measure the amount of oil produced in a given period of time. These sources have also been used to measure the water content of soils, and to monitor process streams in industrial plants. ^{241}Am itself has extensive uses in dissipating static electrical charges and in smoke detectors, where it functions to ionize air.

The radioactive decay of the nuclide californium-252 is largely by alpha emission, but part of the decay is by spontaneous fission. ^{252}Cf thus provides an intense neutron source: 1 g emits 2.4×10^{12} neutrons per second. ^{252}Cf is the only commercially available nuclide that can be fabricated into small neutron sources that produce an intense neutron flux over a useful period of time. The physical size of these sources is considerably smaller than α- or γ-neutron sources, and less space must be provided in the ^{252}Cf sources to accommodate gaseous products. Since ^{252}Cf neutron sources became available in 1975, a surprising variety of industrial and scientific uses have been developed for them.

One of the largest uses of these sources is in reactor start-up operations. Prior to achieving criticality, a neutron source is inserted into the reactor to allow instrument calibration and observation of the approach to criticality. ^{252}Cf sources are used in reactor start-up all over the world because of the high neutron

flux that can be obtained and their small size ($< 1\,cm^3$), which is very advantageous in the start-up procedure. ^{252}Cf neutron sources are used in the nuclear power industry as fuel-rod scanners, a procedure in which the amount and uniformity of the fissile material in the fuel rod is measured. This is the second largest industrial application of californium neutron sources.

Applications to neutron activation analysis constitute another important use of ^{252}Cf neutron sources. Neutron capture in many elements forms radioactive species that then decay with highly characteristic gamma-ray emissions. This analytical procedure is very sensitive and specific, and is widely used for the analysis of trace elements. Neutron activation finds use in uranium borehole logging to make accurate determinations of the uranium concentrations in boreholes; as little as 100 parts per million of U_3O_8 can be detected by this procedure. Other industrial uses for ^{252}Cf sources are in the continuous monitoring of the sulfur and ash content of coal on a moving conveyor belt at the rate of 50 tons per hour. Batch analysis of the vanadium content of crude oil is still another application of neutron activation analysis.

A use for ^{252}Cf that is assuming increasing importance is in the mass spectroscopy of non-volatile substances of high molecular weight. The spontaneous fission process in ^{252}Cf yields not only neutrons but fission fragments as well. The fission fragments are emitted with enormous energy derived from the fission process. Heavy ions traveling at high speed can impart sufficient energy while traversing a thin film to desorb ions, which can then be accelerated down a flight tube. An accurate measurement of the time of flight for a fixed distance then translates into the molecular weight of the desorbed ion. The fission fragments turn out to be ideal for this purpose. The spontaneous fission of ^{252}Cf atoms produces ions of elements in the middle of the periodic table with energies of the order of 100 MeV per atom. These energetic particles are allowed either to pass through a thin film or to hit the surface of the substance under investigation, desorbing ions of the sample. Fig. 14.9 shows the apparatus for determining the molecular weight by time of flight. This mass spectrometric technique has been named californium-252 plasma desorption mass spectroscopy (^{252}Cf PDMS) by Macfarlane, its discoverer [92]. The method can be applied to materials that are thermally unstable or totally non-volatile, in contradistinction to conventional mass spectrometric techniques, which require materials that can be volatilized in the source. ^{252}Cf PDMS (for reasons that are far from clear) produces molecular ions with molecular weights unprecedented in any other form of mass spectroscopy. Molecular ions of proteins greater than 50 000 atomic mass units have been recorded, and these form biopolymers that are non-volatile and very sensitive to heat. ^{252}Cf PDMS is finding many applications and is one of the most unexpected and useful applications that has been found for californium [93].

14.11.4 Medical applications

Americium-241 has found use in the diagnosis of thyroid disorders. Miniature power generators using ^{238}Pu have been developed for use in heart pacemakers.

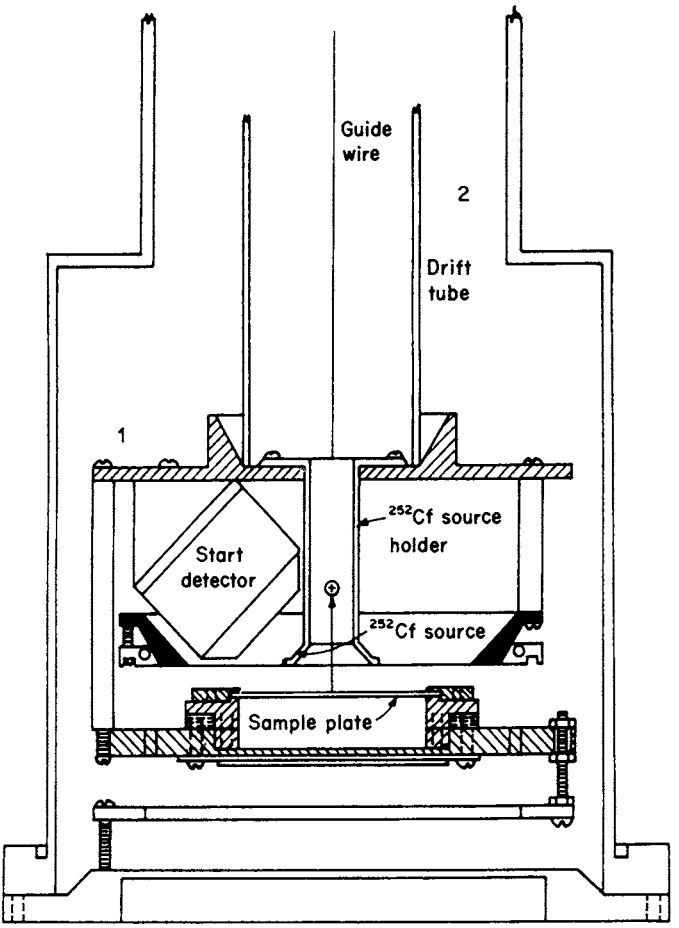

Fig. 14.9 *The ^{252}Cf PDMS mass spectrometer at Argonne National Laboratory. The ^{252}Cf fission fragment source is located in front of the sample film. An accelerating potential of 10 kV is maintained between the sample plate and grid located 3 mm from the sample plate. Region 1 houses the primary ion source, acceleration region, and start detector. Region 2 houses a time-of-flight guide wire, drift tube, and stop (secondary-ion) detector. Both regions are maintained at a pressure of less than 1×10^{-6} mmHg.*

The pacemaker itself is a device planted in the chest and connected to the heart muscles; a programmed electrical pulse is periodically administered, which assures regularity in the heart beat. Heart pacemakers that operate from chemical batteries have a limited life, and must be replaced periodically by a surgical procedure. A nuclear power source increases the time between repowering the pacemaker by a factor of at least 5. A typical nuclear-powered heart pacemaker contains about 160 mg of ^{238}Pu encased in a tantalum–iridium–platinum alloy. Several thousand such devices are in use world-wide.

Californium-252 attracted early attention as a possible therapeutic agent in cancer treatment. The general impression formed from early work was that neutron therapy was inferior to x-ray therapy. More recent studies, however, indicate that neutron irradiation may have advantages over x-rays or γ-rays in certain situations. In the period 1976–82, several hundred cancer cases were treated by neutron irradiation supplied by ^{252}Cf [94]. Although not a cure, ^{252}Cf neutron therapy appears to have promise in the treatment of pelvic cancer and in brachytherapy (short exposure therapy). Neutrons appear to have particular utility in tumors whose oxygen supply is impaired, and which, as a consequence, are relatively insensitive to x-rays or γ-rays. While the applications of neutrons in the treatment of cancer are still experimental, there is a possibility that further clinical studies may well find a use for the neutron-emitting californium isotopes in therapy.

ACKNOWLEDGEMENT

The work reported herein was performed under the auspices of the Office of Basic Energy Sciences, Division of Chemical Sciences, US Department of Energy under Contract W-31-109-ENG-38.

REFERENCES

1. Martin, D. (1985) *The New York Times*, March 3, p. 4f.
2. Hyde, E. K., Perlman, I., and Seaborg, G. T. (1964) *Nuclear Properties of the Heavy Elements*, vol. II, *Detailed Radioactivity Properties*, Prentice-Hall, Englewood Cliffs, NJ.
3. Seaborg, G. T. (ed.) (1978) *Transuranium Elements. Benchmark Papers in Physical Chemistry and Chemical Physics*, vol. 1, Dowden, Hutchinson & Ross, Stroudsburg, PA.
4. Seaborg, G. T. (1963) *Man-Made Transuranium Elements*, Prentice-Hall, Englewood Cliffs, NJ.
5. Choppin, G. R. and Rydberg, J. (1980) *Nuclear Chemistry*, Pergamon Press, Oxford, p. 249.
6. Keller, O. L., Jr, Hoffman, D. C., Penneman, R. A., and Choppin, G. R. (1984) *Phys. Today*, March, 35–41.
7. National Research Council (1983) *Opportunities and Challenges in Research with Transplutonium Elements*, National Research Council, Washington, DC.
8. Ghiorso, A. (1982) in *Actinides in Perspective* (ed. N. M. Edelstein), Pergamon Press, Oxford, pp. 23–56.
9. Ref. 5, pp. 347–64.
10. *Gmelin Handbuch der Anorganischen Chemie*, Suppl. Ser., *Transurane*, Verlag Chemie, Weinheim, part A2, The Elements (1973).
11. Benes, P. and Majer, V. (1980) *Tracer Chemistry of Aqueous Solutions*, Elsevier, Amsterdam.

12. National Academy of Sciences (1959–74) *Series on Radiochemistry*: Stevenson, P. C. and Nervik, W. E. (1961) *Actinium*, NAS-NS-3020; Hyde, E. (1960) *Thorium*, NAS-NS-3004; Kirby, H. W. (1959) *Protactinium*, NAS-NS-3016; Gindler, J. (1961) *Uranium*, NAS-NS-3050; Burney, G. A. and Harbour, R. M. (1974) *Neptunium*, NAS-NS-3060; Roleman, G. H. and Hoff, R. W. (1965) *Plutonium*, NAS-NS-3058; Penneman, R. A. and Keenan, R. K. (1960) *Americium and Curium*, NAS-NS-3006; Higgins, G. H. (1960) *The Transcurium Elements*, NAS-NS-3031.
13. *Gmelin Handbuch der Anorganischen Chemie*, Suppl. Ser., *Transurane*, Verlag Chemie, Weinheim, Springer-Verlag, Berlin, Heidelberg & New York, parts D1 and D2, Chemistry in Solution (1974, 1975).
14. Seaborg, G. T. and Katz, J. J. (eds) (1954) *The Actinide Elements*, Natl Nucl. En. Ser., Div. IV, 14A, McGraw-Hill, New York.
15. Seaborg, G. T., Katz, J. J., and Manning, W. M. (eds) (1949) *The Transuranium Elements: Research Papers*, Natl Nucl. En. Ser., Div. IV, 14B, McGraw-Hill, New York.
16. Ref. 7, p. 81.
17. Sullivan, J. C., Gordon, S., Mulac, W. A., Schmidt, K. H., Cohen, D., and Sjoblom, R. (1976) *Inorg. Chem. Lett.*, **12**, 599–601.
18. Sullivan, J. C., Gordon, S., Cohen, D., Mulac, W., and Schmidt, K. H. (1976) *J. Phys. Chem.*, **80**, 1684–6.
19. Gordon, S., Mulac, W., Schmidt, K. H., Sjoblom, R. K., and Sullivan, J. C. (1978) *Inorg. Chem.*, **17**, 294–6.
20. Sullivan, J. C., Morss, L. R., Schmidt, K. H., Mulac, W. A., and Gordon, S. (1982) *Inorg. Chem.*, **22**, 2338–9.
21. Mikheev, N. B. (1984) *Inorg. Chim. Acta*, **94**, 241–8.
22. Newton, T. W. (1975) *The Kinetics of Oxidation–Reduction Reactions of Uranium, Neptunium, Plutonium and Americium in Aqueous Solution*, TID-26506.
23. Baes, C. F. and Mesmer, R. E. (1976) *The Hydrolysis of Cations*, Wiley, New York.
24. Burgess, J. (1978) *Metal Ions in Solution*, Wiley, New York.
25. Freeman, A. J. and Darby, J. B., Jr (eds) (1974) *The Actinides: Electronic Structure and Related Properties*, vols I and II, Academic Press, New York.
26. Keller, C. (1971) *The Chemistry of the Transuranium Elements*, Verlag Chemie, Weinheim.
27. Haire, R. G. in ref. 8, pp. 309–42.
28. Brown, D., Tso, T. C., and Whittaker, B. (1977) *J. Chem. Soc., Dalton Trans.*, 2291–6.
29. Spirlet, J. C. (1979) *J. Phys. Colloq. C4*, **40**, 87–94.
30. Spirlet, J. C. in Ref. 8, pp. 361–80.
31. Lam, D. J., Darby, J. B., Jr, and Nevitt, M. V. in Ref. 25, vol. II, pp. 119–84.
32. Smith, J. L. and Kmetko, E. A. (1983) *J. Less Common Metals*, **90**, 83–8.
33. Benedict, U. (1984) *J. Less Common Metals*, **100**, 153–70.
34. Roof, R. B. (1982) *Z. Kristallogr.*, **158**, 307–12.
35. Smith, J. L., Spirlet, J. C., and Müller, W. (1979) *Science*, **205**, 188–90.
36. Smith, J. L. and Haire, R. G. (1978) *Science*, **200**, 535–7.
37. Smith, J. L., Fisk, Z., Willis, J. D., and Haire, R. G. (1982) Los Alamos National Laboratory Report LA-UP-82-2624.
38. Shannon, R. D. (1976) *Acta Crystallogr. A*, **32**, 751–67 (see also Chapters 17 and 20).
39. Müller, W. and Lindner, R. (eds) (1975) *Transplutonium* 1975, *Proc. 4th Int. Transplutonium Symp.*, Baden-Baden, Sept. 13–17, 1975, North-Holland, Amsterdam;

Müller, W. and Blank, H. (eds) (1975) *Heavy Element Properties, Proc. Joint Session Transplutonium Element Symp.* and *5th Int. Conf. on Plutonium and Other Actinides*, Baden-Baden, Sept. 13, 1975, North-Holland, Amsterdam & Oxford, American Elsevier, New York.
40. *Gmelin Handbuch der Anorganischen Chemie*, Suppl. Ser., *Transurane*, Springer-Verlag, Berlin, part C, The Compounds (1972).
41. Müller, W. (1983) *Chem. Z.*, **106**, 105–12.
42. Morss, L. R. and Edelstein, N. (1984) *J. Less Common Metals*, **100**, 15–28.
43. Anderson, J. S. (1970) in *Modern Aspects of Solid State Chemistry* (ed. C. N. R. Rao), Plenum, New York, pp. 29–105.
44. Morss, L. R. in Ref. 8, pp. 381–407.
45. Keally, T. J. and Pauson, P. L. (1951) *Nature*, **168**, 1039–40.
46. Reynolds, L. T. and Wilkinson, G. (1956) *J. Inorg. Nucl. Chem.*, **2**, 246–53.
47. Baumgärtner, F., Fischer, E. O., and Laubereau, P. (1965) *Naturwissenschaften*, **52**, 560.
48. Marks, T. J. and Fischer, R. D. (eds) (1979) *Organometallics of the f-Elements*, Reidel, Dordrecht.
49. Marks, T. J. and Ernst, R. D. (1982) *Comprehensive Organometallic Chemistry*, vol. 3, Pergamon Press, Oxford, pp. 173–270.
50. Kanellakopulos, B. (1979) in *Organometallics of the f-Elements* (eds T. J. Marks and R. D. Fischer), Reidel, Dordrecht, pp. 1–35.
51. Marks, T. J. (1982) *Science*, **217**, 989–97.
52. Streitwieser, A., Jr, and Müller-Westerhoff, U. (1968) *J. Am. Chem. Soc.*, **90**, 7364.
53. Streitwieser, A., Jr, in Ref. 48, pp. 149–77.
54. Marks, T. J., Seyam, A. M., and Kolb, J. R. (1973) *J. Am. Chem. Soc.*, **95**, 5529–39.
55. Brandi, G., Brunelli, M., Lugli, G., and Mazzei, A. (1973) *Inorg. Chim. Acta*, **7**, 319–22.
56. Gebala, A. E. and Tsutsui, M. (1973) *J. Am. Chem. Soc.*, **95**, 91–3.
57. Allard, B., Olofsson, V., and Torstenfelt, B. (1984) *Inorg. Chim. Acta*, **94**, 205–21.
58. Bidoglio, G., DePlano, A., Avogadro, A., and Murray, C. N. (1984) *Inorg. Chim. Acta*, **95**, 1–3.
59. Scoppa, P. (1984) *Inorg. Chim. Acta*, **95**, 23–27.
60. Walters, R. L., Hakonson, T. E., and Lane, L. J. (1983) *Radiochim. Acta*, **32**, 89–103.
61. Hanson, W. C. (ed.) (1980) *Transuranic Elements in the Environment*, DOE/TIC-22800.
62. Hoffman, D. C., Lawrence, F. D., Mewherter, J. L., and Rourke, F. M. (1971) *Nature*, **234**, 132–4.
63. Maurette, M. (1976) *Annu. Rev. Nucl. Sci.*, **26**, 319–50.
64. Choppin and Rydberg, in ref. 5, pp. 456–60.
65. Nenot, J. C. and Metivier, H. (1984) *Inorg. Chim. Acta*, **94**, 165–70.
66. In ref. 5, pp. 502–59.
67. Topp, S. V. (ed.) (1982) *Scientific Basis for Nuclear Waste Management, Materials Research Society Symp. Proc.*, vol. 6, Elsevier, Amsterdam.
68. Bulman, R. A. (1980) *Coord. Chem. Rev.*, **31**, 221–50.
69. Thompson, R. C. (1982) *Radiat. Res.*, **90**, 1–32.
70. Boocock, G. and Popplewell, D. S. (1965) *Nature*, **208**, 282–3.
71. Raymond, K. N. and Smith, W. L. (1981) *Struct. Bonding (Berlin)*, **43**, 159–86.
72. Raymond, K. N., Freeman, G. E., and Kappel, M. J. (1984) *Inorg. Chim. Acta*, **94**, 193–204.
73. Taylor, D. M. (1972) *Health Phys.*, **22**, 575–81.

74. Barton, P. G. (1968) *J. Biol. Chem.*, **243**, 3884–90.
75. Boocock, G., Danpure, C. J., Popplewell, D. S., and Taylor, D. M. (1976) *Radiat. Res.*, **42**, 381–96.
76. Mahlum, D. D. (1967) *Toxicol. Appl. Pharmacol.*, **11**, 264–71.
77. Bulman, R. A. and Griffin, R. G. (1980) *Metab. Bone Dis. Relat. Res.*, **2**, 281–3.
78. Durbin, P. W. (1975) *Health Phys.*, **29**, 495–510.
79. Finkle, R. (1940) University of Chicago Metallurgical Laboratory Report CH-3783 (MDDC-1140).
80. Voelz, G. L., Grier, R. S., and Hempelmann, L. H. (1985) *Health Phys.*, **48**, 249–59.
81. Durbin, P. W. (1973) *Handb. Exp. Pharmacol.*, **36**, 739–896.
82. Vaughn, J., Bleany, B., and Taylor, D. M. (1973) *Handb. Exp. Pharmacol.*, **36**, 349–502.
83. Schubert, J. (1955) *Annu. Rev. Nucl. Sci.*, **5**, 369–412.
84. Taylor, G. N. (1978) *Health Phys.*, **35**, 201–10.
85. James, A. C. and Taylor, D. M. (1971) *Health Phys.*, **21**, 31–9.
86. Rosenthal, M. W. and Lindenbaum, A. (1967) *Radiat. Res.*, **31**, 506–21.
87. Smith, V. H. (1972) *Health Phys.*, **22**, 765–78.
88. Raymond, K. N., Koppel, M. J., Pecoraro, V. L., Harris, W. R., Carrano, C. J., Weill, F. L., and Durbin, P. W. (1982) in ref. 8, pp. 491–507.
89. Raymond, K. N. and Carrano, C. J. (1979) *Acc. Chem. Res.*, **12**, 183–90.
90. Durbin, P. W., Jones, E. S., Raymond, K. N., and Weitl, F. L. (1980) *Radiat. Res.*, **81**, 170–87.
91. Weitl, F. L., Raymond, K. N., and Durbin, P. W. (1981) *J. Med. Chem.*, **24**, 203–6.
92. Macfarlane, R. D. and Torgerson, D. F. (1976) *Science*, **191**, 985–91.
93. Hunt, J. E., Schaber, P. M., Michalski, T. J., Dougherty, R. C., and Katz, J. J. (1983) *Int. J. Mass Spectrom. Ion Phys.*, **53**, 45–58.
94. Murayama, Y., in ref. 7, pp. 339–52.
95. Zachariasen, W. H. (1971) *J. Inorg. Nucl. Chem.*, **35**, 3487–97.

CHAPTER FIFTEEN

SPECTRA AND ELECTRONIC STRUCTURE OF FREE ACTINIDE ATOMS AND IONS

Mark S. Fred

with revisions by Jean Blaise

15.1 INTRODUCTION

This chapter deals with the electronic properties of isolated actinide atoms and ions, observed in the vapor phase at low density. The free atoms have all or most of the valence electrons present, and the spectra are due essentially to changes in the quantum numbers of the valence electrons. This is in contrast to the spectra of actinides in crystals or in solution, where the spectra are largely due to transitions within the 5f shell. In both cases, the energy level structure is dominated by the structure of the 5f shell, but in different ways. In crystals, the actinide ions are exposed to the electric field of the surrounding ions, which produces a Stark effect on the levels. The magnitude of the effect is relatively small because the field has high symmetry and, moreover, the 5f electrons are shielded from it by the 6s and

6p electrons. The result is a mild perturbation in which each 5f level is split into a number of close components. In free atoms, on the other hand, the valence electrons, which now have to be considered, interact strongly with the 5f electrons and also with each other. Hence each 5f level gives rise to many daughter levels, which are more widely split than the parent separations and have large angular momentum contributions from the parent. The result in this case is a great number of levels whose structure is not simply related to the structure of the 5f levels or to the structure of the valence-electron levels by themselves. It is evident that the 5f level structure can be deduced more directly from crystal spectra but the properties of the valence electrons (in particular, the chemical properties) must be deduced from the free-atom spectra.

Historically, the correlation between actinide chemistry and spectroscopy was anticipated before much experimental information was available in either field. There was therefore interest in actinide spectroscopy as an aid to predicting actinide chemistry, in the expectation that smaller quantities of these elements would be required. In practice, the chemistry developed first as soon as sufficient amounts were produced, while the spectroscopy encountered difficulties because the complexities were underestimated. The difficulty was not so much the enormous total number of levels, which could be counted readily, but the extent to which the levels interacted so as to preclude simplification.

The interaction implies that each level is a mixture of various pure states labeled by quantum numbers for the 5f shell and also by quantum numbers for each valence-electron shell. Different levels have different mixtures, and the composition of each level cannot be deduced by inspection because of the large number of quantum numbers, with a different energy dependence for each. Hence the compositions must be derived by comparison with theoretical calculations. The calculations are difficult to perform even with a large computer, and because of the mixing the results do not give a simple picture of the way in which the energy of an actinide atom depends on the valence-electron configuration. This complexity is, of course, inherent in atoms with 5f electrons, and the chemistry is correspondingly more difficult to predict. Nevertheless, it is clearly desirable to attempt it.

We shall begin with a resumé of the experimental data, then present an outline of the theory, and finally try to interpret the data.

15.2 EXPERIMENTAL SPECTROSCOPY OF FREE ACTINIDE ATOMS AND IONS

The main interest in the spectra is in the analysis, which provides the relative energies of various electron configurations for each actinide and the way the strength of interaction between different kinds of electrons varies along the actinide series. The first step in this process is a complete description of the spectra.

In each actinide spectrum, tens of thousands of spectral lines can be observed and many more are possible but weak. No order is apparent. The determination of the energy levels from the lines is based on the search for a recurrent difference between the wavenumbers of various pairs of lines, indicating pairs of transitions to a given pair of levels from levels of opposite parity. The level structure can be derived in principle by establishing a number of such level pairs. For actinide spectra, however, a purely numerical approach is hopeless: (1) the large line density yields many more fortuitous recurrences than real ones; (2) the real recurrences due to transitions involving a given pair of levels are limited to a relatively small number by selection rules; and (3) the strong lines are often paired with weak lines. Hence one needs (1) wavelengths of as many lines as possible, measured with the highest accuracy and resolution (as opposed to spectrochemical analysis, for which only a relatively small number of strong lines are required) and (2) corroborative information, i.e. Zeeman data, isotope shifts, hyperfine structure, vapor absorption, etc.

Experimental techniques are now adequate for the production of neutral and first-ion spectra, in spite of the limitations of available sample size and radioactivity, of all the actinides through einsteinium ($Z = 99$). The usual light source is an electrodeless discharge made of quartz tubing about 7 mm in diameter and 25 mm long into which the sample (~ 0.1 mg as iodide) is sublimed and the tube sealed off under vacuum [1, 2]. A microwave discharge supplies the heat to volatilize the sample, to dissociate the molecules, and to excite the atomic spectrum. This source is sensitive, confines the radioactivity, gives sharp lines, can be run in a magnetic field, and can differentiate lines of the neutral spectrum from those of the first ion by varying the power. A comparable source for the higher ions is unfortunately not yet available. Analyses of most of the actinide spectra are based on exposures made on the Argonne 30 ft Paschen–Runge spectrograph, which covers a large wavelength range at high resolving power with a single exposure. A Fourier transform spectrometer with comparable resolving power has been operational at the Laboratoire Aimé Cotton, Orsay, since 1970. Built initially for the infrared region, it now covers the region 4 μm–400 nm, and a second spectrometer covers the visible and ultraviolet regions down to 300 nm. More recently, another Fourier transform spectrometer has been built at the Kitt Peak National Observatory, and all the actinide spectra from Th to Cf have now been recorded with these instruments. Observation of the infrared spectrum with high resolving power is specially important for the term analysis of the lanthanide and actinide spectra because of the large number of low levels which give transitions in that region.

The present status of the term analyses of actinide spectra varies from essentially complete for the even-Z elements (Th, U, Pu, Cm) to only just beginning. In the first category, all the strong and moderate-intensity lines have been classified and only weak lines remain (however, these are a considerable fraction of the total number). The limitation is manpower availability, not only for accumulating the data and classifying the lines but also for entering the data in

the line list. Because of the labor involved, because the data in the line list show a slow but continual growth, and because conventional publication of so much data is impracticable, this information is at present available only in the laboratory doing the work. Nevertheless, wavelengths of the strongest emission lines of all the actinides from actinium through californium have been tabulated according to stage of ionization [3–5]. More or less extensive lists of classified lines have also been published for several elements, and references will be given in Table 15.6, which summarizes the main features of each spectrum investigated.

15.3 EMPIRICAL ANALYSIS OF ACTINIDE SPECTRA

A neutral actinide has typically a thousand experimental levels, a first ion somewhat fewer. The levels are organized by the half-dozen into terms, some dozens of terms form a configuration, and there are a dozen or more configurations for a given stage of ionization. The order in this hierarchy, however, is not evident: there is considerable overlapping of different terms and of different configurations, the terms are not pure in any coupling scheme but must be described as mixtures to account for their properties, and there is often mixing of configurations. The only way most levels can be identified is by comparison with theoretical calculations using appropriate parameters.

There are, however, several fortunate circumstances which make it possible to identify the lowest terms of each configuration and thereby the relative energies of the configurations. In SL coupling the lowest term of a configuration is usually found to be fairly pure and follows Hund's rule, i.e. this term has maximum multiplicity and maximum orbital angular momentum. Fig. 15.1 shows, as an example of Hund's rule, the lowest term of a number of configurations in neutral plutonium.

Corroborative evidence can be obtained from isotope shifts. In the heavy elements the difference in energy of an atomic level from one isotope to another is due to the difference in nuclear volume. For an electron very near the center of the atom, the Coulomb attraction is decreased from that for a point nucleus. The effect is larger for heavier (larger) isotopes and is also larger for electron configurations with more s electrons since these are the only type (non-relativistically) with a finite electron density at the nucleus. The isotope shift is therefore larger for $5f^N7s^2$ than for $5f^N7s7p$, say, but not directly proportional to the number of 7s electrons because the total s-electron density at the nucleus is modified by mutual shielding among the electrons. If two 7s electrons are present, the inner electron density of one of them to some extent shields the outer density of the other from the nuclear attraction, and consequently the $7s^2$ central density is less than twice that for $7s^1$. The presence of an inner electron (5f or, somewhat less so, 6d) also shields a 7s electron, and so converting a 5f to a 6d electron reduces the shielding of 7s by inner s electrons and increases the isotope shift. Non-relativistic Hartree–Fock calculations [6] gave the result that, in converting

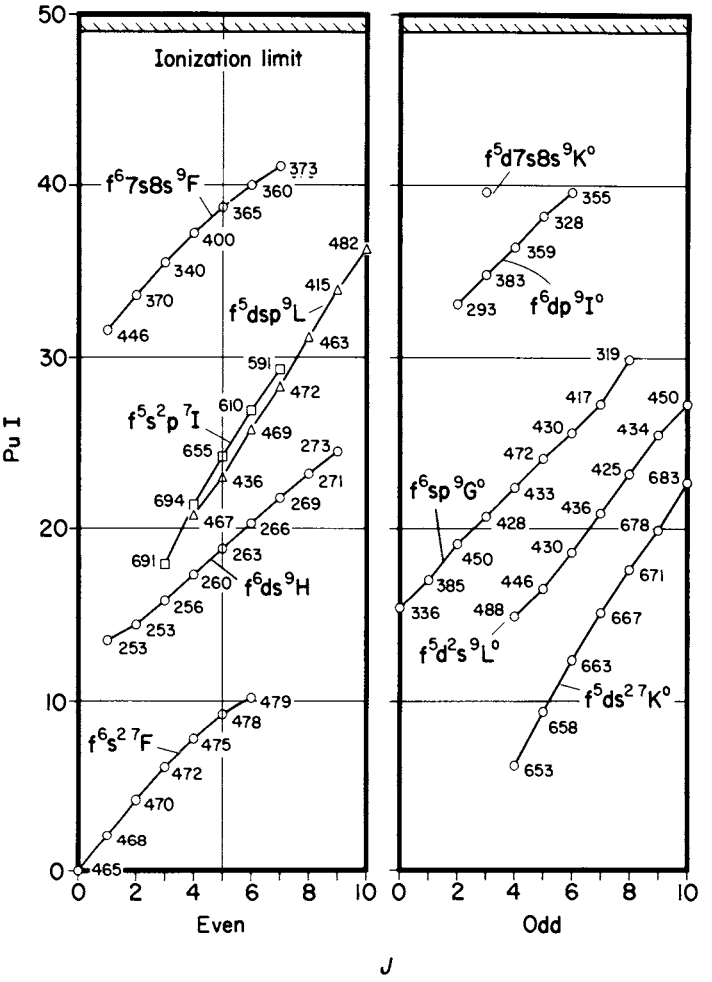

Fig. 15.1 *Hund's rule multiplet of various electron configurations of neutral plutonium, Pu I. The numbers opposite each fine-structure level are the observed isotope shifts* (^{240}Pu–^{239}Pu) *in* $10^{-3}\ cm^{-1}$.

one type of valence electron to another, the 5s and 6s electron densities also changed appreciably and had to be considered since it is the total density of all the s electrons that is responsible for the isotope shift. Relativistic Hartree–Fock calculations [7], on the other hand, ascribe the shift to changes in the shielding of just the 7s electron. Fig. 15.2 shows the experimental shifts and calculated densities at the nucleus for a number of Pu I configurations, illustrating the linear relationship. The experimental shifts are also given for the fine-structure levels of the terms plotted in Fig. 15.1, showing that there is a sensibly constant shift within each set of levels. They are, in fact, fairly constant not only within the lowest term

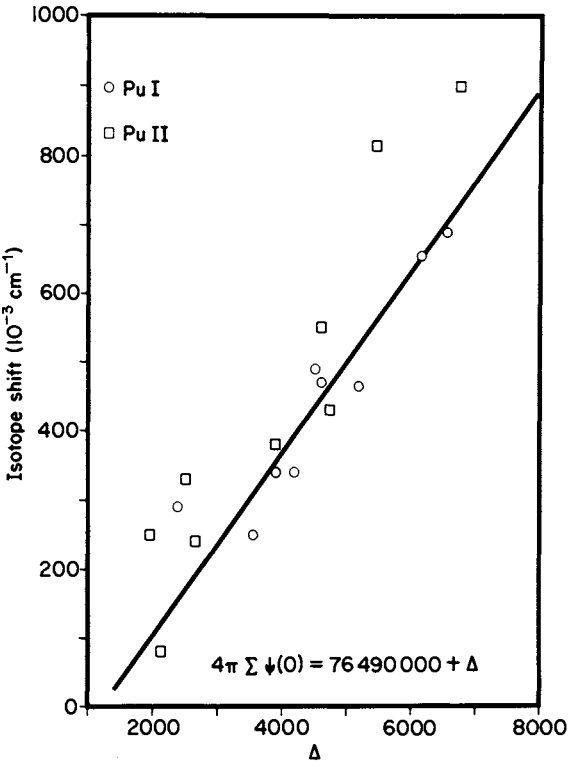

Fig. 15.2 *Isotope shifts of configurations of Pu I and Pu II as a function of electron density at the nucleus.*

but also for all the levels of a configuration. The fluctuation is evidently due to varying amounts of configuration interaction, which mixes different configurations and hence mixes the shifts in proportion. The isotope shifts thus make it possible to assign most experimental levels to a definite configuration, which is a very valuable property even though it says nothing about the assignment of term quantum numbers to individual levels within a configuration.

15.4 SYSTEMATICS OF ACTINIDE CONFIGURATIONS

Electron configurations analogous to the Pu configurations shown in Fig. 15.1 occur in the other actinide elements, i.e. configurations with the same combination of valence electrons but with the number of 5f electrons changing as Z changes. These can be generalized into various series, e.g. $5f^N7s^2$, $5f^{N-1}6d7s^2$, etc., where for the neutral atom $N = Z - 88$. Within a series, the S and L of the Hund's rule term change from series member to member because of the changing

contribution from the 5f shell. There are also corresponding series for the ions, e.g. $5f^N7s$.

The usefulness of the series concept comes from the regularity in energy of the lowest term: the relative energies of different series change with Z but the change is systematic. This is illustrated in Fig. 15.3(a) and (b) for the neutral atoms; the data are given in Tables 15.1 and 15.6. The absolute binding energies increase with Z (become more negative) but the quantity of interest is usually the relative energy between series, and in Fig. 15.3(a) the zero energy for each element has been taken arbitrarily as the configuration $5f^{N-1}6d7s^2$ (the lowest with three valence electrons; trivalent) and in Fig. 15.3(b) as the configuration $5f^N7s^2$. The regularity provides independent evidence of the correct assignment of levels to the various series in the individual actinide elements, except for the irregular behavior near the middle of the 5f shell.

The irregularity is due mainly to the fact that the overall spread in energy of the f^N configurations is greatest for the half-closed shell, $N = 7$. (Each f^N configuration consists of a number of SL terms due to 5f–5f repulsions, and these terms have quite different energies.) Fig. 15.4 shows the approximate position of the lowest term of each f^N configuration with respect to the weighted average of the configuration, and also with respect to the lowest term of f^{N-1}. When f^N is compared with $f^{N-1}d$ (the $7s^2$ electrons do not contribute to the structure), the irregularity is reduced because the f–d electrostatic interaction changes sign at $N = 8$, and also slope.

Inspection of Fig. 15.3(a) shows three families of series based on f^N, f^{N-1}, and f^{N-2}, having respectively negative, roughly zero, and positive slope. The relative positions of different series characterized by various configurations of outer electrons tend to repeat for each family, and consequently the existence of families is clearly due to the properties of the 5f electrons. For simplicity, Fig. 15.5 presents the lowest series of each family, those configurations with $7s^2$. Now Hartree–Fock calculations show that most of the energy in actinide configurations comes from the electrostatic attraction between the individual 5f electrons and the nucleus. This attraction increases with Z (the actinide contraction) and the total 5f attraction energy is proportional to the number of 5f electrons. The $7s^2$ energy is nearly constant with Z and so does not affect the trend of the series. The 6d energy is also nearly constant but gives an additional (almost constant) contribution to $5f^{N-1}ds^2$ and twice as much to $5f^{N-2}6d^27s^2$; it affects the absolute positions of the three series but not the slopes. The three series have roughly equal energies for atomic numbers around that of uranium ($Z = 92$). For smaller Z the 6d binding energy is more important than 5f, but for larger Z the 5f becomes increasingly more stable due to increase with both Z and N.

The electron–nucleus attraction energy is related by the virial theorem to the mean value of r (the electron–nucleus separation) for the different kinds of electrons. Fig. 15.6 shows (non-relativistic) Hartree–Fock solutions for the radial distribution $P(r)$ for plutonium as a typical actinide. The abscissa is chosen as $r^{1/2}$ (in atomic units) in order to show more detail at small r and less at large r. The

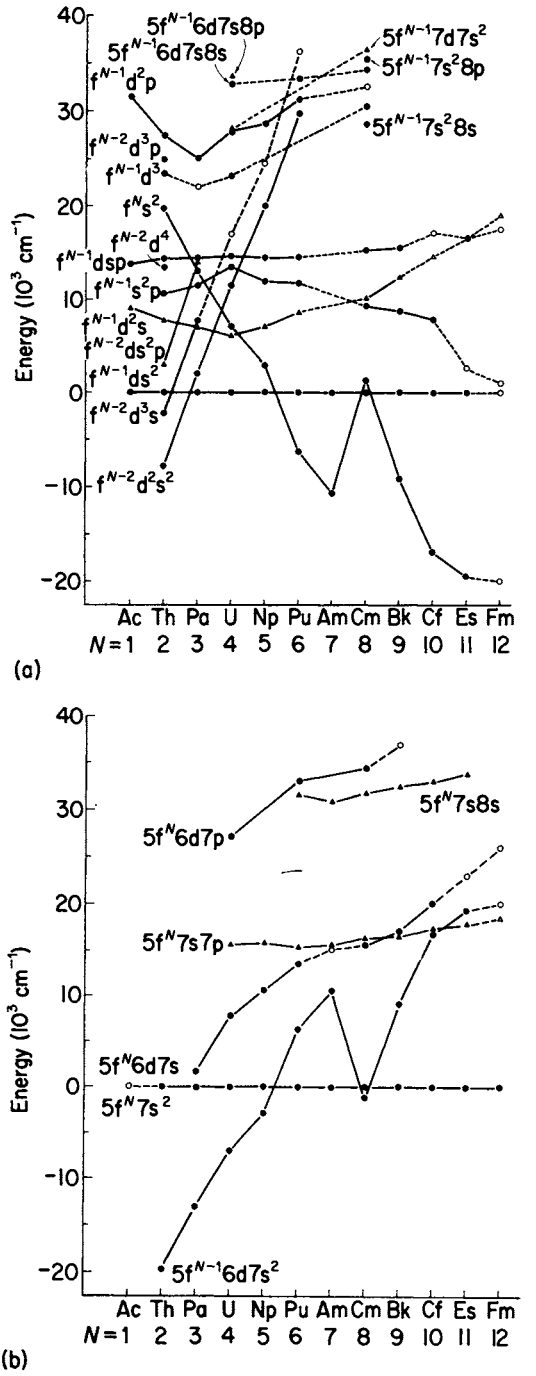

Fig. 15.3 *Energies of various series of configurations in the neutral actinides compared to* $5f^{N-1}\,6d\,7s^2$ *(a) and* $5f^N7s^2$ *(b). The open symbols indicate estimates from Brewer* [8].

Table 15.1 *Lowest levels of neutral actinide configurations*.*

	Ac	*Th*	*Pa*	*U*	*Np*	*Pu*	*Am*	*Cm*	*Bk*	*Cf*	*Es*	*Fm*	*Md*
	$Z = 89$	90	91	92	93	94	95	96	97	98	99	100	101
	$N = 1$	2	3	4	5	6	7	8	9	10	11	12	13
$5f^{N-1}6d7s^2$	0	7795	0	0	0	6314	10684	0	9141	16910	19368	(20000)	(30000)
$5f^{N-1}6d^27s$	9217	15619	7000	6249	7112	14912	(21000)	10145	21506	(31500)	(36000)	(39000)	(51000)
$5f^{N-1}7s^27p$	(9500)	18432	11445	13463	11940	17898	(22000)	9263	17778	24728	(22000)	(21000)	(28000)
$5f^{N-1}6d7s7p$	13713	22098	14393	14644	14339	20828	(25500)	15253	24652	33952	(36000)	(37500)	(48000)
$5f^N7s^2$	(30000)	27496	13019	7021	2831	0	0	1214	0	0	0	0	
$5f^N6d7s$	(42000)	(39000)	14693	14840	13384	13528	15136	16933	17182	20044	(23000)	(26000)	(28000)
$5f^N6d^2$	(59000)	(57000)	(39000)	(34000)	(27000)	31711	(36000)	(41000)	(45000)	(50000)	(54000)	(58000)	(62000)
$5f^N7s7p$	(43000)	(42000)	(25600)	22792	18655	15449	15608	17657	16914	17459	17803	18500)	(19000)
$5f^{N-2}6d^27s^2$		0	1978	11503	20050	36050	(51000)	(50000)					
$5f^{N-2}6d^37s$		5563	7585	(16930)	(24500)	(42500)							

* Values in parentheses are estimates taken from Brewer [8].

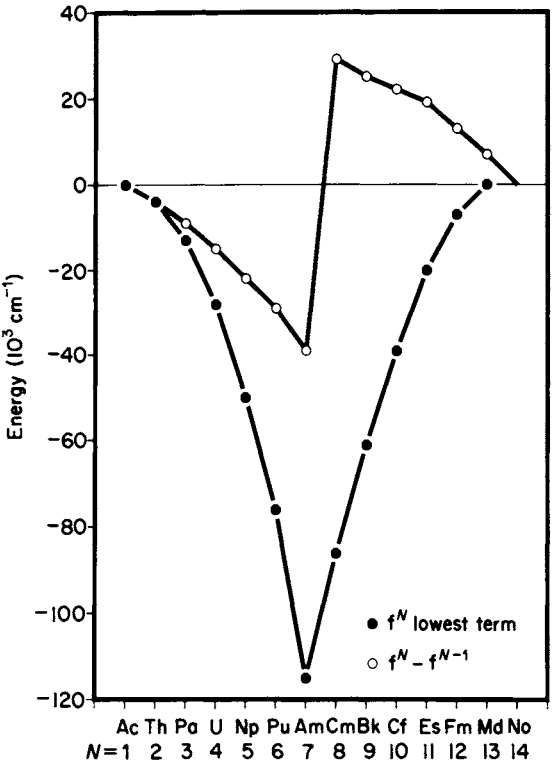

Fig. 15.4 *Approximate energy of the lowest term of f^N relative to the weighted average of f^N and of f^{N-1}.*

figure also shows the total electron density due to the first 86 electrons in the radon core, plotted to a reduced ordinate scale. At the bottom of the figure is Z^*, the effective Z, which describes how the nuclear charge seen by an electron at separation r is reduced by the shielding due to the electron density between zero and r. The 5f electrons clearly see a larger Z^* than do 6d or 7p, and the 5f Coulomb energy $-Z^*e^2/\langle r \rangle$ is more negative ($\langle r \rangle$ is the expectation value of r, i.e. r averaged over the radial density distribution). The total energy also includes a centrifugal term $+l(l+1)/r^2$, which tends to equalize the 5f, 6d, and 7p Coulomb energies, and the details vary along the actinide series as first shown by Goeppert Mayer [9].

It will be seen that the 7s radial function has its main contribution well outside the radon core, the 6d not quite so much, while the 5f electron is completely inside the core. The 5f is an inner electron and not much affected by the environment outside the core.

There are clear implications for actinide chemistry in the relative energies and radial distributions of the last $(Z-86)$ electrons of a neutral actinide atom. For a typical actinide, the 6d and $7s^2$ electrons extend beyond the radon core and are

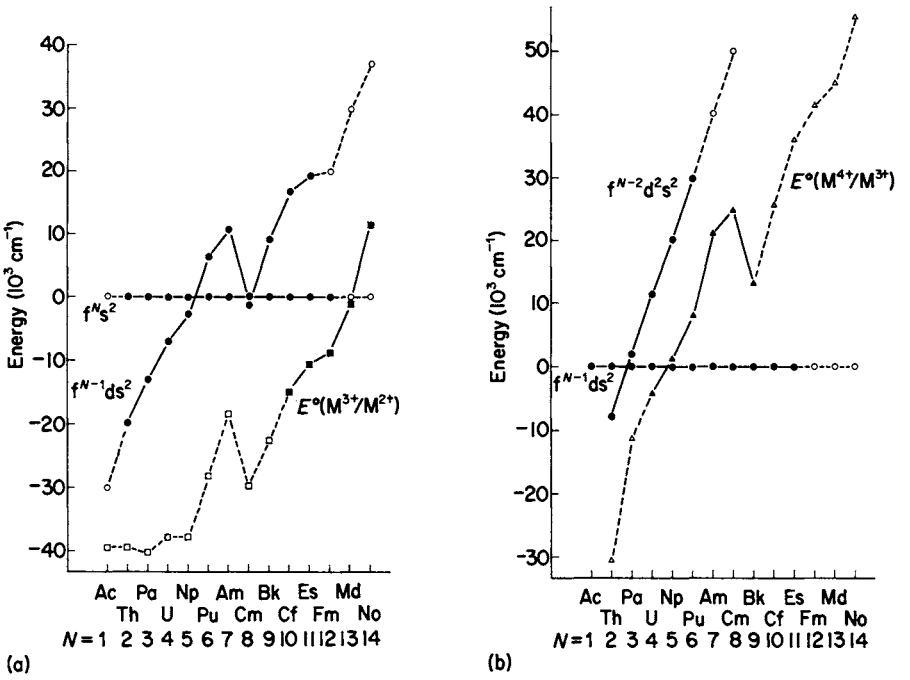

Fig. 15.5 *Comparison of actinide standard oxidation–reduction potentials and the relative energies of series on converting a 5f to a 6d electron.*

available for forming chemical bonds, i.e. a typical actinide should be trivalent. At the beginning of the series, however, the 5f electron is not so firmly bound and has a larger $\langle r \rangle$, which reduces the shielding of the nuclear charge seen by the 6d electron. Hence for thorium, 6d is favored over 5f because of its larger Z^* and smaller centrifugal loss, and the ground state is $6d^2 7s^2$, resulting in a neutral atom with four external electrons (quadrivalent). At the other end of the actinide series, however, the 5f becomes increasingly bound compared with 6d and it is more favorable to convert the 6d to another 5f, producing $5f^N 7s^2$ as the ground state (divalent). This change in valency along the series is reduced in the lanthanides because $4f^{N-1}5d6s^2$ is about 10 000 cm^{-1} higher than $4f^N 6s^2$ compared with the corresponding actinide configurations.

These qualitative considerations are compared with solution chemistry in Fig. 15.5(a) and (b). The standard oxidation–reduction potentials $E°(M^{(n+1)+}/M^{n+})$, converted from volts to cm^{-1}, are plotted for comparison with the energies of f → d transitions in free atoms. The full symbols are experimental values (see Table 17.3); the open symbols were calculated by Nugent [10]. The similarity in shape of the two sets of curves is evident. There are approximate shifts of about 30 000 cm^{-1} for the (III)/(II) potentials (Fig. 15.5(a)) and about 20 000 cm^{-1} for (IV)/(III) (Fig. 15.5(b)) in the same direction, i.e. less energy is required for f → d conversion in solution than in the free neutral atom.

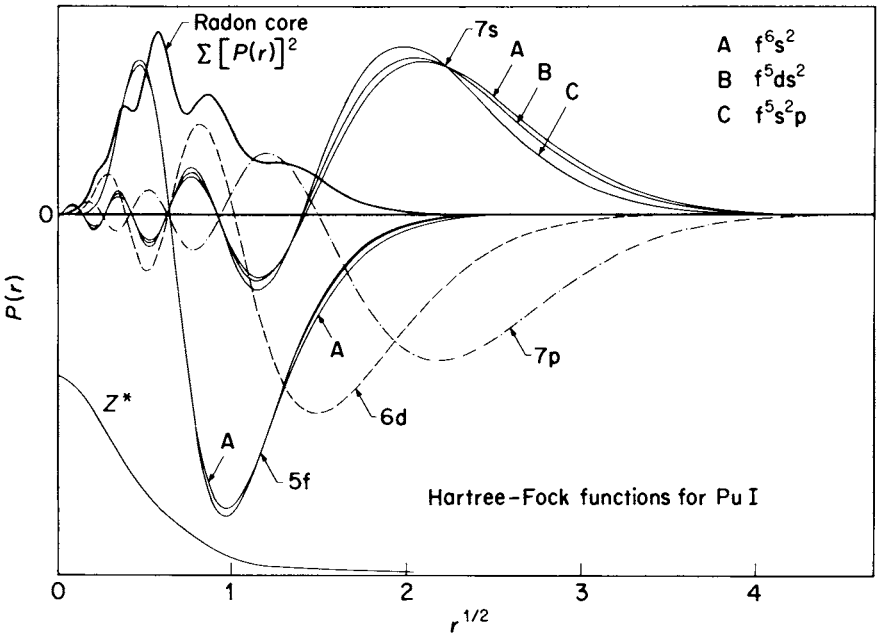

Fig. 15.6 *Radial distribution functions for valence electrons in neutral plutonium.*

15.5 THEORETICAL TERM STRUCTURE OF THE FREE ACTINIDES

15.5.1 Electrostatic interactions of open-shell electrons*

The energy of a given level is calculated as a sum of various interactions [11, 12]. There is first of all the Coulomb attraction between the nucleus and the individual electrons. Next in importance are the Coulomb repulsions between all pairs of electrons. This is the many-body problem; it cannot be solved exactly and yet the total repulsion energy is too large to be treated as a perturbation of the Coulomb attraction energy. For optical spectroscopy, however, the repulsion energy defined completely is unnecessarily detailed and can be replaced by the central-field model: for the core electrons there is substituted a spherically symmetric continuous distribution of negative charge. The distribution is chosen so that the potential energy $U(r)$ so generated yields attraction energies for the individual core electrons which agree as well as possible with observed x-ray term energies. By this approximation the core electrons are made independent of each other.

The total wavefunction for independent core electrons is a product of individual one-electron wavefunctions, each a solution of the one-electron wave

* Electrons not in closed shells.

equation for quantum numbers nlm and potential energy $U(r)$ instead of $-Ze^2/r$:

$$\Psi_0 = \psi(n^1 l^1 m_l^1)\psi(n^2 l^2 m_l^2)\psi(n^3 l^3 m_l^3) \ldots \psi(n^{86} l^{86} m_l^{86})$$

Since the field is assumed to be central, i.e. a function of r only, the angular parts of the ψ are spherical harmonics $\Theta(lm_l)\Phi(m_l)$ just as in hydrogen, and are exact. The radial parts $R(nl)$, however, depend on the shape assumed for $U(r)$ and must be evaluated by numerical integration, and hence the eigenvalues are only approximations to the observed x-ray energies. The fit can be improved by iteration (the Hartree–Fock self-consistent field method). It remains approximate because of the simplifying assumptions, but for present purposes it is good enough since the core electrons remain constant independent of outer-electron excitation, i.e. the same for all final terms.

By the device of a central potential, most of the electron–electron repulsions have been eliminated and the remaining repulsion energy is now small enough to be treated as a perturbation. This comes from the N open-shell electrons and to first order is evaluated as

$$W_1 = \int \bar{\Psi}_0^* \left(\sum_{i>j=1}^{N} \frac{e^2}{r_{ij}} \right) \Psi_0 \, \mathrm{d}v$$

where Ψ_0 (the zeroth approximation eigenfunction) is now a product of the N independent one-electron solutions $\psi(n^t l^t m_l^t)$ for the nuclear attraction $U(r)$. Each of these is of the form of a radial factor $R(n^t l^t)$ times a spherical harmonic $\Theta(l^t m_l^t)\Phi(m_l^t)$ times a factor m_s^t indicating spin-up or spin-down, and

$$W_1 = \sum_{t^*=1}^{N} \sum_{t=1}^{N} \sum_{i>j=1}^{N} \int \psi^*(n^{t^*} l^{t^*} m_l^{t^*})(e^2/r_{ij})\psi(n^t l^t m_l^t)\, \mathrm{d}v$$

Since each repulsion term involves only two electrons, Ψ_0^* and Ψ_0 can differ in at most two electrons, the remaining sets of quantum numbers being identical and giving a factor unity. Each pair of electrons (or set of quantum numbers) contributes a quantity

$$\begin{aligned} &\int R_1(n^a l^a)\Theta_1(l^a m_l^a)\Phi_1^*(m_l^a) R_2(n^b l^b)\Theta_2(l^b m_l^b)\Phi_2^*(m_l^b)(e^2/r_{12}) \\ &\quad \times R_1(n^c l^c)\Theta_1(l^c m_l^c)\Phi_1(m_l^c) R_2(n^d l^d)\Theta_2(l^d m_l^d)\Phi_2(m_l^d)\mathrm{d}v \end{aligned}$$

The conversion of the two-electron repulsion potential e^2/r_{12} to a form involving each electron separately is accomplished by expansion in a series of Legendre polynomials $P_k(\cos\omega)$ where ω is the angle subtended by the two electrons. Each P_k can be expressed in turn in a series of products of spherical harmonics by the spherical harmonic addition theorem:

$$\begin{aligned} 1/r_{12} &= (r_1^2 + r_2^2 - r_1 r_2 \cos\omega)^{-1/2} \\ &= \sum_{k=0}^{\infty} \frac{r_<^k}{r_>^{k+1}} P_k(\cos\omega) \\ &= \sum_{k=0}^{\infty} \frac{r_<^k}{r_>^{k+1}} \frac{4\pi}{2k+1} \sum_{m=-k}^{k} \Theta_1(km)\Theta_2(km)\Phi_1(m)\Phi_2^*(m) \end{aligned}$$

where $r_<$ and $r_>$ are the smaller and larger of r_1 and r_2. Thus

$$W_1(ab, cd) = l^2 \sum_{k=0}^{\infty} \int\int \frac{r_<^k}{r_>^{k+1}} R_1(n^a l^a) R_2(n^b l^b) R_1(n^c l^c) R_2(n^d l^d)\, \mathrm{d}r_1\, \mathrm{d}r_2$$

$$\times \frac{4\pi}{2k+1} \sum_{m=-k}^{k} \int_0^{\pi} \Theta_1(km)\, \Theta_1(l^a m_l^a)\, \Theta_1(l^c m_l^c) \sin\theta_1\, \mathrm{d}\theta_1$$

$$\times \int_0^{2\pi} \Phi_1(m)\, \Phi_1^*(m_l^a)\, \Phi_1(m_l^c)\, \mathrm{d}\phi_1$$

$$\times \int_0^{\pi} \Theta_2(km)\, \Theta_2(l^b m_l^b)\, \Theta_2(l^d m_l^d) \sin\theta_2\, \mathrm{d}\theta_2$$

$$\times \int_0^{2\pi} \Phi_2(m)\, \Phi_2^*(m_l^b)\, \Phi_2(m_l^d)\, \mathrm{d}\phi_2$$

The two integrals involving ϕ give acceptable solutions (single-valued for $\phi \to \phi + 2\pi$) only if $m = m_l^a - m_l^c = -m_l^b + m_l^d$, in which case each integral is equal to $1/\sqrt{(2\pi)}$; otherwise they give zero. Note that the value of m can never become large because it is limited by the dependence on the m_l, and the value of k is likewise limited by the second summation to the maximum value of m. Hence the formal expansion of $1/r_{12}$ in an infinite series is limited in practice to a small number of terms. The numerical value as a function of l and m comes from the integrals over θ, which can be evaluated by Gaunt's formula [13] or Racah's formula [14]. Both formulas involve summations over factorials of k and l; that of Racah is based on his tensor operator techniques and shows the selection rules directly from its explicit dependence on the $3j$ symbol*: the integrals are zero unless k, l^a, l^c and k, l^b, l^d obey the triangular sum rule with even integral sum. The result for each integral over θ and ϕ is designated $c^k(lm_l, l'm_l')$; the usual cases are listed in table 1[6] of ref. 11. The combined radial integrals are commonly designated $R^k(ab, cd)$. The repulsion contribution of electrons 1 and 2 with initial quantum numbers a and b and final quantum numbers c and d is hence

$$\sum_k c^k(l^a m_l^a, l^c m_l^c)\, c^k(l^d m_l^d, l^b m_l^b)\, R^k(n^a l^a n^b l^b, n^c l^c n^d l^d)$$

Note that m_s has been ignored because e^2/r_{12} does not involve the electron spin, and m_s must be the same throughout, i.e. it appears as delta functions $\delta(m_s^a, m_s^c)$ and $\delta(m_s^b, m_s^d)$, where

$$\delta(x, y) = \begin{cases} 1 & \text{if } x = y \\ 0 & \text{if } x \neq y \end{cases}$$

* The $3j$, $6j$, and $9j$ symbols are coupling (transformation) coefficients, defined e.g. in ref. 18 in terms of sums of products of factorials of the quantum numbers. They are best evaluated by computer.

Some frequently occurring two-electron radial integrals are given special names, as listed in Table 15.2.

The above description of the electrostatic interaction between a given pair of electrons assumes that it is possible to assign a definite set of quantum numbers to each in both the initial and final states. In a typical actinide, however, the 5f electrons are better described as all coupled to form states with a definite value of total spin S and total orbital angular momentum L (SL coupling). These states have magnetic quantum numbers M_S and M_L, made up of appropriate combinations of the individual m_s and m_l; i.e. the coupling process removes the property of being able to assign definite m_s and m_l values to each electron. A similar kind of ambiguity arises in configurations with several open shells, i.e. the interaction a–b is influenced by the interactions a–c and b–c, etc. Hence the angular coefficients $c^k(l^a m_l^a, l^b m_l^b)$ must be modified to take into account the coupling of electrons a and b with the other open-shell electrons of the configuration. This is accomplished by an uncoupling procedure, which can be formulated in terms of Racah's tensor algebra [15–19] and furnishes a coupling coefficient between the pair and the remaining electrons specified by intermediate quantum numbers. For example, the d–s interaction in f^5ds is part of the chain $f^5(\alpha S_1 L_1)d(S_2 L_2)s\,SL$, so the d–s contribution $c^2(ds)c^2(sd)G^2(ds)$ must be multiplied by a factor involving an nj symbol in order to separate $S_2 L_2$ from $\alpha S_1 L_1$ and SL (α is a label that distinguishes the individual f^5 states which occur multiply, i.e. having the same $S_1 L_1$; e.g. there are four different ^{4}G terms in f^5). For other types of electron pairs, it may be necessary to change the order in the chain to put the pair concerned at the end of the chain (another nj symbol). In addition, for the f–d or f–s interaction in f^5ds, it is necessary to uncouple one f

Table 15.2 *Two-electron radial integrals* $R^k(n^a l^a n^b l^b, n^c l^c n^d l^d)$.

*Condition**	*Name*	*Examples*
$a = b = c = d$	$F^k(n^a l^a, n^a l^a)$ diagonal	d^2: F^2(dd), F^4(dd) f^2: F^2(ff), F^4(ff), F^6(ff)
$a = c$, $b = d$	$F^k(n^a l^a, n^b l^b) =$ $R^k(ab, ab)$ direct integral	fd: F^2(fd), F^4(fd)
$a = d$, $b = c$	$G^k(n^a l^a, n^b l^b) =$ $R^k(ab, ba)$ exchange integral	fd: G^1(fd), G^3(fd), G^5(fd)
$a, b \neq c, d$ parity conserved	$R^k(n^a l^a n^b l^b, n^c l^c n^d l^d)$ configuration interaction	(d^2, ds): R^2(dd, ds) (f^2, ds): R^3(ff, ds), R^3 (fd, sf) (fp, ds): R^1(fp, ds), R^1(fs, dp), R^3(fp, sd), R^3(fd, sp)

* Triangular conditions: $\Delta(k, l^a, l^c)$ and also $\Delta(k, l^b, l^d)$; $(k + l^a + l^c)$ and also $(k + l^b + l^d)$ even.

electron from f^5, which requires a summation over the states of f^4 multiplied by coefficients of fractional parentage [20] to keep all the f electrons indistinguishable. For the f–d interaction there are five different radial integrals – namely $F^2(fd)$, $F^4(fd)$, $G^1(fd)$, $G^3(fd)$, and $G^5(fd)$ – separate angular coefficients for each, and separate uncoupling factors. Finally there is the f–f interaction, which is the same in f^5ds as in f^5, involving $F^2(ff)$, $F^4(ff)$, and $F^6(ff)$. The final result for the electron repulsion energy of one state SL in f^5ds is the sum of all 10 (i.e. for ds, fs, fd, and ff) products of the coefficients, factors, and the corresponding radial integrals.

We have indicated how the electrostatic repulsion energy can be calculated for one state of the configuration f^5ds. There are, however, in general a number of states with the same final quantum numbers S and L but different intermediate quantum numbers and these states interact, so the above calculation is incomplete. A more useful approach is to consider the totality of states for the configuration as forming a large square array, a matrix with each element given by an expression involving, for f^5ds say, the 10 radial integrals combined with the proper angular coefficients. When numerical values are inserted for the coefficients and the R^k integrals, the resulting matrix represents the first-order perturbation of the complete configuration due to the open-shell electron repulsions acting on the degenerate system in which only the nuclear attractions are considered. The numerical energy matrix **H** is thus an eigenvalue–eigenvector problem: the eigenvector **A** is the matrix that transforms **H** into a diagonal matrix by $\mathbf{A}^{-1}\mathbf{HA}$, and the eigenvalues are the (diagonal) elements of the transformed matrix, i.e. the first-order energies when the open-shell electrostatic repulsions are included.

For the actinides the matrices are of large dimensions, equal to the number of terms in the configuration. For f^5 by itself there are 73 different terms, for f^5ds there are 1166. Table 15.3 shows how these are distributed according to spin multiplicity and L value. Note that most final SL values occur multiply; the individual f^5 terms with the same SL (in general written αSL) are distinguished by a serial number following the term symbol, e.g. ^{4}G1, ^{4}G2, ^{4}G3, ^{4}G4, defined in ref. 20. Each row or column of the matrix is identified with one of these terms. When the terms are arranged in a systematic order (usually the Nielson and Koster [20] order), the matrix shows considerable symmetry: the non-zero elements are grouped in square blocks along the diagonal, the size of the block being given by the number of terms with a given SL. A portion of the matrix for f^5 is shown schematically in Fig. 15.7, illustrating the selection rule given at the bottom of Table 15.3: off-diagonal matrix elements occur only within each block between different terms with the same SL. For f^5ds the matrix is much bigger (higher rank) because for each f^5 term S_1L_1 the interaction with ds S_2L_2 can produce five different final L values (unless limited by low L_1) and four different S values (unless limited). The individual terms in each SL block are here distinguished by the intermediate quantum numbers αS_1L_1 and S_2L_2. Fig. 15.8 illustrates the further selection rules for the coefficients of $F^k(fd)$ and $G^k(fd)$. The

Table 15.3 *Term distribution for* f^5 *SL and* f^5 $(\alpha S_1 L_1)d(S_2 L_2)s$ *SL.*

	f^5			f^5ds			
L	*Sextets*	*Quartets*	*Doublets*	*Octets*	*Sextets*	*Quartets*	*Doublets*
S		1			3	11	13
P	1	2	4	2	13	36	41
D		3	5	2	18	52	58
F	1	4	7	3	22	64	74
G		4	6	2	21	66	77
H	1	3	7	2	20	64	76
I		3	5	1	15	53	65
K		2	5	1	12	43	54
L		1	3		7	30	39
M		1	2		4	20	28
N			1		2	11	16
O			1		1	6	9
Q						2	4
R						1	2
	3	24	46	13	138	459	556
Total		73				1166	
Independent matrices		24				47	
Selection rules	F^k(ff): $\delta(SL)$			F^k(ff): $\delta(SL)$ F^k(fd): $\delta(SL)$, $\delta(S_1, S_1')$, $\delta(S_2, S_2')$, $\Delta(L_1, k, L_1')$ G^k(fd): $\delta(SL)$, $\Delta(L_1, k, L_1')$			

block structure reduces the diagonalization problem from one large matrix to a number of small independent matrices.

Each row and column of the eigenvector matrix **A** is also identified by the same terms as **H**. For a given term the eigenvector is a column vector that gives the composition of the term in the diagonalized matrix as a linear combination of the original terms (the basis states), restricted to those in the block. For example, in Fig. 15.7 the energy matrix elements of the ^{4}P terms occur in a 2×2 block and then so will the eigenvector elements:

$$\begin{array}{cccccccc} & & {}^4\mathrm{P}1 & {}^4\mathrm{P}2 & {}^4\mathrm{P}1 & {}^4\mathrm{P}2 & {}^4\mathrm{P}A & {}^4\mathrm{P}B \\ \left|\begin{array}{cc} a & b \\ -b & a \end{array}\right| & \left|\begin{array}{cc} H_{11} & H_{12} \\ H_{12} & H_{22} \end{array}\right| & \left|\begin{array}{cc} a & -b \\ b & a \end{array}\right| & = & \left|\begin{array}{cc} H_{11}+\Delta E & 0 \\ 0 & H_{22}-\Delta E \end{array}\right| & & \\ \mathbf{A}^{-1} & \mathbf{H} & \mathbf{A} & & & & & \end{array}$$

Here a and b are chosen to make the triple matrix product diagonal, subject to $a^2 + b^2 = 1$. Then $b/a = \Delta E/H_{12}$. If for convenience we write the eigenvectors as

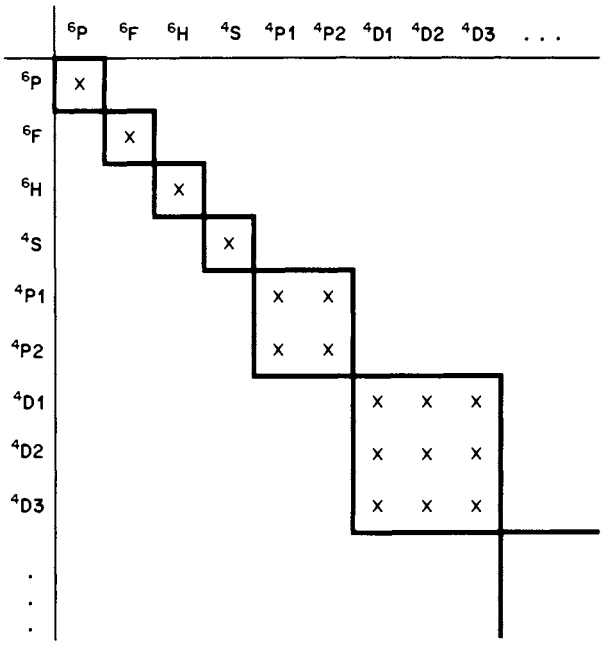

Fig. 15.7 *Portion of the electrostatic energy matrix for f^5.*

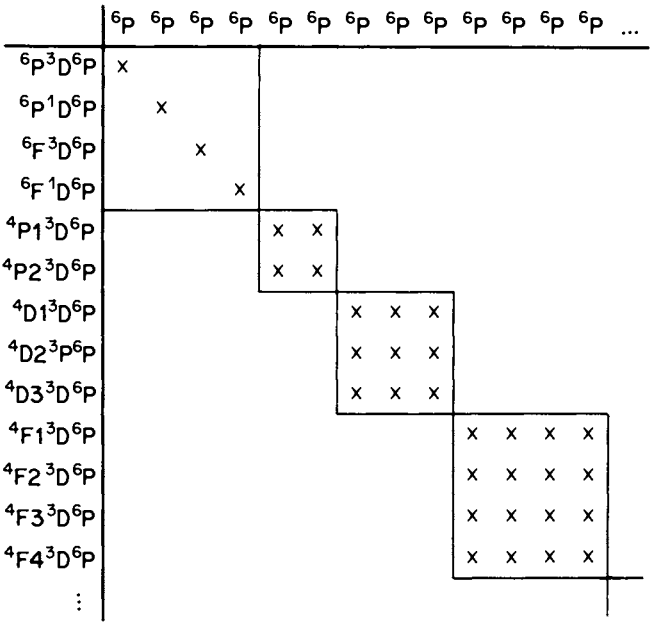

Fig. 15.8 *Portion of the electrostatic energy matrix for f^5 ds.*

rows instead of columns, we have the orthonormal combinations

$$^4\mathrm{P}A = \quad a^4\mathrm{P1} + b^4\mathrm{P2}$$

$$^4\mathrm{P}B = -b^4\mathrm{P1} + a^4\mathrm{P2}$$

Since b/a is related to $H_{12}/(H_{11} - H_{22})$ and these quantities are comparable in the actinides, the multiply occurring terms can be well mixed (for Pu II $f^5ds\ ^4P$, $b/a = 0.66$). This will not affect the g-values, since all components have the same Landé g-factor, but it can affect other properties such as the coupling for f–d interactions.

For blocks larger than 2×2, the eigenvector can be determined by a succession of off-diagonal eliminations, considering each H_{ij}, H_{ii}, and H_{jj} as a 2×2 block, but in present practice it is much better to use standard computer eigenvalue programs.

15.5.2 Spin–orbit interaction and coupling schemes

Spin–orbit interaction is more important in the actinides than in atoms with simpler spectra because of the large number of off-diagonal matrix elements. The selection rules here are $\Delta S = 0, \pm 1, \Delta L = 0, \pm 1$, and $\Delta J = 0$. They are thus more liberal than for the electrostatic coefficients (where $\Delta S = \Delta L = \Delta J = 0$) and more terms are connected, including many relatively close together. Consequently, although the spin–orbit interaction is an order of magnitude weaker than the electrostatic interaction, for close levels H_{ij} can be comparable to $(H_{ii} - H_{jj})$; hence there can be appreciable mixing even though ΔE, the energy perturbation, is small. Moreover the large number of spin–orbit H_{ij} can lead to a far-reaching effect by a chain reaction involving also the electrostatic H_{ij}, so that a low level can be repelled by high levels even though there is no matrix element directly connecting them.

The effect of spin–orbit interaction is to remove some of the degeneracy of the SL states by producing a different energy for each value of the total angular momentum J. The allowed J values run from a maximum of $S + L$ to a minimum of $|S - L|$, decreasing in steps of one unit. Each *level* of the SL *term* is still degenerate in the quantum number M_J ($2J + 1$ sublevels) as long as spherical symmetry is preserved (no external magnetic or electric field). For describing the energies of the term structure, the M_J degeneracy is not important. Removal of the degeneracy by an external magnetic field (the Zeeman effect) does, however, provide very useful information for identifying a particular experimental level with a given calculated $^{(2S+1)}L_J$ level. The electric field of a crystal lattice or ligand environment also removes the M degeneracy somewhat.

For spherical symmetry with spin–orbit included there are many more separate states to be considered. For f^5 the number increases from 73 SL states to 198 SLJ states; for f^5ds the numbers are 1166 and 3707. Table 15.4 shows the J distribution for these two configurations, with the selection rules for the spin–orbit coefficients. Because there are off-diagonal ζ matrix elements between adjacent S and L values, there is mixing between the states and S and L are no

Table 15.4 *Level distribution for* f^5 *SL and* $f^5(\alpha S_1 L_1)$ ds *SL.*

	Total levels	
J	f^5	f^5ds
1/2	10	187
3/2	21	345
5/2	28	459
7/2	30	519
9/2	29	521
11/2	26	475
13/2	20	397
15/2	16	305
17/2	9	216
19/2	5	139
21/2	3	79
23/2	1	40
25/2		18
27/2		6
29/2		1
Total	198	3707
Matrices	12	15
Selection rules		
ζ_f	$\Delta S, \Delta L = 0, \pm 1$	$\Delta S, \Delta L = 0, \pm 1$ $\Delta S_1, \Delta L_1 = 0, \pm 1$
ζ_d		$\Delta S, \Delta L = 0, \pm 1$ $\Delta\alpha, \Delta S_1, \Delta L_1 = 0$

longer good (well defined) quantum numbers. One cannot, therefore, factor the complete matrix into a series of *SL* blocks. The quantum number *J* remains a good (no-field) quantum number, and the matrix can be factored into a succession of *J* blocks. The total number of independent *J* blocks to be diagonalized is thus much smaller than for the purely electrostatic case, but each has a much higher rank (for f^5ds the maximum rank is 521, for $J = 9/2$). Since the computer effort increases as something like the cube of the rank, the advantage of having fewer matrices is far more than offset by the difficulty due to the increase in rank.

The radial part of the spin–orbit interaction, which determines ζ, is proportional to $(1/r)\,(\partial U/\partial r)$, where U is the central potential. For hydrogenic atoms, $U = -Ze^2/r$ and the radial integral is a factor times $Z^4/[n^3 l(l+\frac{1}{2})(l+1)]$, giving $\zeta(5f):\zeta(6d):\zeta(7p) = 1:1.6:5.1$. For the actinides, U is given by replacing Z by Z^* of Fig. 15.6, which increases $\zeta(5f)$ relatively by a factor of about 3; the factor increases across the actinide series, but the electrostatic radial integrals also increase so that $\zeta(5f)/F^k(ff)$ stays approximately constant and likewise the effect of the off-diagonal spin–orbit terms. Also $\zeta(6d)$ is about two-thirds of $\zeta(5f)$ at the middle of the series and stays more nearly constant. The biggest spin–orbit energy is with $\zeta(7p)$ and is quite constant because the 7p radial function is almost entirely

outside the radon core and has $Z^* = 1$; moreover, there is very little overlap of the 7p function with the 5f function and the electrostatic 5f–7p radial integrals are small. Hence for the $f^N p$ configuration (of $f^N s^2 p$) the ratio $H_{ij}/(H_{ii} - H_{jj})$ is large and a pair of SLJ states has $b/a \sim 1$. In this case SL coupling is a poor description of each level since it is far from SLJ (i) or $S'L'J'$ (j). A much better description is to use SL coupling for f^N and sl coupling for the p electron, writing a state $f^N S_1 L_1 J_1 p_{1/2} J$ or $f^N S_1 L_1 J_1 p_{3/2} J$, where $J = J_1 \pm \frac{1}{2}$ in the first case, and $J = J_1 \pm \frac{3}{2}, J_1 \pm \frac{1}{2}$ for the second. With no f–p electrostatic interaction we then have two levels, one doubly degenerate and one quadruply degenerate, separated by $\frac{3}{2}\zeta_p$. Introducing now the electrostatic interaction (assumed small compared with ζ_p) produces two sets of relatively close levels consisting of a pair for the lower and a quadruplet for the upper. The advantage of $J_1 j$ coupling over SL coupling for $f^N p$ is that the composition is much purer, which means that the properties of the levels are closer to those of the diagonal states. For example the $J_1 j$ g-values are nearly those given by the formula

$$g(J_1 jJ) = g(S_1 L_1 J_1)[J(J+1) + J_1(J_1+1) - j(j+1)]/2J(J+1)$$
$$+ g(slj)[J(J+1) - J_1(J_1+1) + j(j+1)]/2J(J+1)$$

whereas for SL coupling the g-value is given by the sum of the squares of the eigenvector components each multiplied by the Landé g-factor for the SL basis states

$$g = 1 + [J(J+1) - L(L+1) + S(S+1)]/2J(J+1)$$

Another advantage is that the $J_1 j$ level structure is directly related to the f^N structure, i.e. added to each $S_1 L_1 J_1$ level is the simple p-electron structure, whereas for the SL designation the levels do not follow an evident term structure and the assignments of the experimental levels are uncertain.

A similar form of $J_1 j$ structure is shown by $f^N s$, a low configuration in the first ion. There is no s-electron structure, of course, only spin, and there is only the electrostatic interaction $G^3(fs)$, which is weak. Hence to each J_1 level is associated a pair of levels with $J = J_1 \pm \frac{1}{2}$ separated by $\pm g_3 G^3$; in the SL designation, by contrast, there is a pair of SL terms, $S = S_1 \pm \frac{1}{2}$, which are well mixed.

15.6 PARAMETER FITTING

We have outlined in general terms a description of the term structure of an actinide configuration as given by the eigenvalues and eigenvectors of the energy matrix **H**. To obtain quantitative information it is necessary to provide numerical values for the matrix elements

$$H_{ij} = E_{av}\delta(i,j) + \sum_{ijkab} [f_k(ijab)F^k(l^a l^b) + g_k(ijab)G^k(l^a l^b)] + \sum_{ija} d(ija)\zeta(l^a)$$

and then to diagonalize the matrix. The problem thus divides naturally into three

stages: evaluating the angular coefficients f_k, g_k, and d; providing values for the radial integrals F^k, G^k, and ζ; diagonalization.

Recall that the coefficients are well defined quantities that can be evaluated exactly in terms of nj symbols, fractional parentage coefficients, and other functions of the quantum numbers. Each coefficient could be evaluated in principle by hand computation, but the computation is tedious and errors are to be expected. The main difficulty for the actinides is the large number of coefficients, of the order of 10^5 in a typical case. The obvious solution is to use a large computer. The first attempts at writing a computer program [21, 22] required considerable input information, which was time-consuming and subject to error. A nearly automatic code was developed by Cowan [23], requiring only the number of electrons in each open shell, a deck of fractional parentage coefficients, and a list of terms for each shell. The code then determined the final terms, evaluated the coefficients, and wrote them on magnetic tape. This program has been modified from time to time, and adapted to other computers by Wilson [24] and Crosswhite [25].

Each computer installation now includes in its library of standard mathematical programs an eigenvalue–eigenvector subroutine, requiring essentially no effort by the user. Hence with the tape of coefficients and a list of values to be used for the radial integrals, the energy matrix can readily be evaluated. The problem now is to choose values for the radial integrals so that the eigenvalues agree as well as possible with the observed level energies. The standard procedure is to treat the radial integrals as adjustable parameters to be derived by least-squares fitting. One begins with estimated values, modifies these by least squares, and repeats the process in successive iterations until convergence.

For the actinides, the fitting process rarely gives an automatic 'best fit' for a number of reasons. Theory nearly always predicts more levels than are observed experimentally because of weak intensity or too low excitation in the light source, and hence a decision must be made as to which eigenvalues are missing experimentally and must be ignored in the fit. Another observational problem is to select from all the experimental levels those which in fact belong to the configuration of interest; this choice is greatly aided by supplementary observations of g-values, isotope shifts, etc. Besides these observational uncertainties, there is the problem of deficiencies in the theory which preclude an exact fit: (a) truncation errors, (b) configuration interaction (CI), and (c) the weak interactions.

(a) Truncation errors

The complete matrix for the configuration is often of too high rank to be diagonalized conveniently by the eigenvalue subroutine. A maximum rank of 200 is a reasonable limit for the IBM 370/195; a much higher rank is possible but requires much more time and fast storage and so is impracticable for repeated iterations, further configurations, etc. But Table 15.4 gives a maximum rank of 521 for $f^5ds\,J = 9/2$. Since the number of observed levels with this J is perhaps 15,

near the lower end of the matrix, it might be assumed that truncating the matrices to a maximum rank of 200 by discarding the upper portion would not have too harmful an effect on the low eigenvalues. Unfortunately it has been found that the error due to truncation can be considerable, doubtless due to the intricate chain of off-diagonal matrix elements. The truncation error can be determined exactly for configurations that can be treated completely, such as f^4d which has a maximum rank of 146. Using the same parameters for the complete and truncated matrices gives sets of eigenvalues which can differ by more than 10^3 cm^{-1}; moreover, the differences vary from term to term in an irregular fashion so that least-squares fitting with the truncated matrices leads to a poor fit and distorted parameters.

One is thus faced with a dilemma: the matrices are often too large to handle, yet truncation introduces appreciable errors. One solution investigated by Crosswhite and Crowwhite [26] is first to diagonalize the f^N part of an actinide configuration using $F^k(ff)$ close to the final values, and then to use the resulting eigenvectors to transform the matrices U^k and V^{1k} [27]. The diagonalization eliminates the large electrostatic matrix elements between the f^N states, which can then be truncated; the transformation nevertheless includes the missing $S_1 L_1$ states in the calculation of the interaction with other open shells, thereby reducing the truncation error.

(b) Configuration interaction

CI is produced by off-diagonal matrix elements which connect two different configurations. These can be due to both electrostatic or (effectively) spin–orbit interactions, like the off-diagonal elements within a configuration, with analogous selection rules plus the requirement that both configurations have the same parity (odd or even according as the sum of the number of electrons in each open shell times the l value of the shell). The magnitudes of the CI matrix elements are also similar to those of the single configurations except for highly excited electrons which have very little overlap with the valence electrons, but the energy perturbation for each is in general less because the diagonal elements are further apart. On the other hand the total effect can be large because many configurations can contribute. This also aggravates the truncation problem because the total rank now is the sum of all the separate ranks to be diagonalized together. Moreover the number of parameters is increased by another set for each configuration plus the R^k integrals between pairs of configurations, and some configurations may not have very many observed terms. Clearly a complete CI parameter fit is usually impracticable.

The effect is that, as in the case of off-diagonal matrix elements within a configuration, one can distinguish between the large electrostatic CI matrix elements connecting well separated diagonal elements and the small spin–orbit elements connecting relatively close diagonal elements. The intermixing can be appreciable in both cases but observationally it is often easier to recognize the smaller energy perturbations than the large, because a single configuration fit

sometimes results in a relatively large fitting error for some levels, or involves levels with anomalous isotope shift or g-value. The large perturbations are more serious for the higher levels because there are more of them, the angular coefficients tend to be larger because of the low spin multiplicity, and the levels of different configurations become closer. This is quite evident on inspection of the level isotope shifts: low levels usually have essentially the pure configuration shifts with a considerable spread between configurations; high levels tend toward all having an average shift with a small spread. The same is true of the g-values, which tend toward unity. Thus, as with the truncation problem, the effects of CI are evident but a quantitative treatment is difficult.

(c) The weak interactions

These are of several kinds. First, there are higher-order spin–orbit interactions which appear in a more exact treatment, involving the mutual magnetic interaction of pairs of electrons: spin–spin (the spin of one electron with the spin of the other); spin–other orbit (the spin of one with the orbital motion of the other); orbit–orbit. While the magnitude of the effects is small, including them as additional parameters with appropriate coefficients leads to an appreciable improvement in fitting the fine-structure levels, especially for the low terms which are more or less isolated.

Secondly, there is CI with very high configurations, too numerous and experimentally too poorly known to include in a simultaneous diagonalization. On the assumption that the energy difference ΔE between the high and low configurations is large compared with the width of each, the energy perturbation appears as terms added to the diagonal elements. These terms are known as effective interactions, composed of radial parts (parameters) and angular coefficients which here represent a summation over all high SL terms that can interact with each low diagonal SL term. To second order the perturbation is $-H^2/\Delta E$. Here H is due mainly to H_1 (electrostatic repulsion) plus H_2 (spin–orbit interaction), so H^2 consists of $H_1 H_1$ (effective electrostatic interaction) plus $H_1 H_2 + H_2 H_1$ (effective electrostatic–spin–orbit interaction) plus $H_2 H_2$ (which can be absorbed in the usual spin–orbit interaction). Rajnak and Wybourne [28] have given formulas for different general classes of interacting configurations. $H_1 H_1$ of course has the biggest effect. For perturbing configurations that differ from the low configuration by two electrons (two-body interactions), the effect for f^N can be represented by the introduction of three new diagonal parameters α, β, and γ, where the coefficient of α is $L(L+1)$ and is most important; the other two coefficients are given by group theory. Three-body interactions require six more parameters and are usually not well determined by fitting except in crystal spectra where many different kinds of terms are found. The effective electrostatic–magnetic interaction $H_1 H_2 + H_2 H_1$ can be represented by the coefficient product of $\zeta_f F^k$. If we go to two open shells $f^N l'$ there are additional effective parameters corresponding to the ordinary $F^k(ll')$ and $G^k(ll')$.

Crosswhite [29] has shown that these can be derived by using values of k ordinarily forbidden; e.g. for $f^N d$ we have also $F^1(fd)$, $F^3(fd)$, $G^2(fd)$, and $G^4(fd)$.

There is one more reason why the fitting process often does not lead to a 'best fit', in addition to the observational and theoretical deficiencies: the least-squares normal equations may be ill conditioned because there are more parameters to be determined than there are different types of terms observed. Thus, there are seven electrostatic parameters for f^N ($E_{av}, F^k, \alpha, \beta, \gamma$), requiring at least seven different terms (terms, not levels), but for the example of $f^5 ds$ all terms below 25 000 cm^{-1} are built on f^5 ^6H or f^5 ^6F; the higher f^5 terms appear in some of the small components of the eigenvectors but these have only a second-order effect on the eigenvalues. Moreover, almost all of the lower terms are octets or sextets, but there are three $G^k(fd)$ parameters which determine the octet–sextet separations; hence some quartet terms are required, but these are higher and more likely to be perturbed by CI.

15.7 ACTINIDE PARAMETERS

It is not possible at present to derive systematic actinide parameters because of the difficulties discussed above. The early actinides are more completely known but have more close configurations, and so the parameter values derived are sensitive to how much CI is included. The middle actinides have larger configuration separations but more terms in each, and so the parameters have large truncation errors. The late actinides are less completely known and so the parameters are not well determined. In no case can the parameters be determined precisely; the values obtained depend on the assumptions made in defining the energy matrix and these vary from case to case and cannot be compared reliably.

On the other hand there are constraints on the uncertainties. We know that the radial integrals represented by the parameters must change in a regular way with atomic number, ion number, and change in valence electrons, since the radial functions are derived from the potential, which is a slowly varying function of these quantities. We can therefore expect similar trends in the experimental parameters.

Consider first the theoretical values. Fig. 15.9(a) shows relativistic Hartree–Fock (HF) calculations [30] for various cases, which certainly show regularities. The integrals $F^k(ff)$ all increase with atomic number, the increase approaching linearity for the second half of the series. The ratios of the limiting slopes are $F^2:F^4:F^6 = 1:0.643:0.464$. The numerical values of the integrals for $f^N s^2$ are for Th 49 704:31 366:22 660 = 1:0.631:0.456, and for Fm 90 499:58 914:43 210 = 1:0.651:0.477. For hydrogenic-shaped 5f radial functions, the ratios are 1:0.688:0.527. The similarity to hydrogen evidently means that, over the range in r which includes most of the HF 5f radial function, the potential does not change greatly from that for a fairly constant effective nuclear

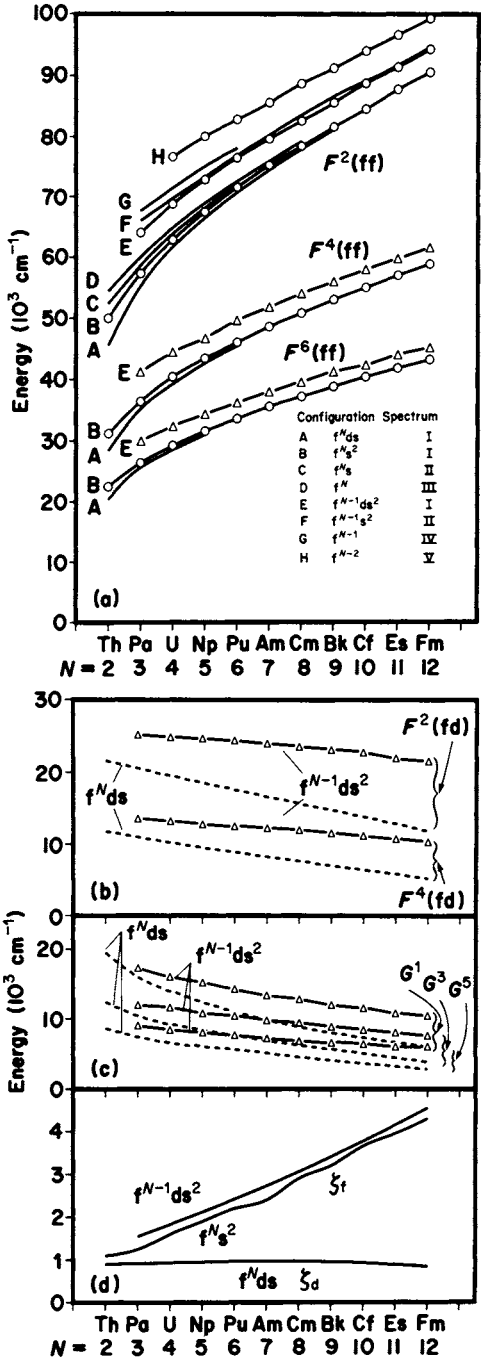

Fig. 15.9 *Relativistic Hartree–Fock calculations of some actinide radial integrals: (a) $F^k(ff)$; (b) $F^k(fd)$; (c) $G^k(fd)$; (d) ζ_f and ζ_d.*

charge Z^* (Fig. 15.6). The increase in the integral with Z corresponds to the actinide contraction; the ratios of the F^k are approximately constant.

Fig. 15.9(a) shows that the HF values of F^k(ff) are only mildly affected by changes in the outer electrons and for each k converge toward the same limit with increasing Z, independent also of ionic charge. The change in the integral for constant Z but varying number of 5f electrons is much greater and amounts to a constant shift, preserving the same slope (not converging). All these effects are in the direction expected for changes in the shielding of the 5f electrons.

The HF overlap integrals F^k(fd) and G^k(fd) in Fig. 15.9(b) show the opposite effect: they decrease with Z, because the 5f functions contract while the 6d functions remain more constant, and they are more sensitive to the number of 7s electrons, which affects their relative shielding. The one-electron integrals ζ_f increase with Z, being proportional to $\langle 1/r^3 \rangle$, and are affected by changes in the numbers of electrons in the direction expected by changes in shielding.

Now consider the experimental parameters and the comparison with theory. We cannot expect the comparison to be close because of the fitting difficulties (truncation error, CI, ill-conditioned matrices, etc.), which moreover vary from element to element. The HF values are also subject to some error because they are usually based on a single-configuration center of gravity. The experimental parameters must be derived from the observed levels, which are almost exclusively built on the lowest terms of the f^N or f^{N-1} core, i.e. on the core terms of highest multiplicity. These terms have separations that are a function of only one parameter, the Racah parameter $E^3 = (1/135)F^2 + (2/1089)F^4 - (175/42\,471)F^6$. Hence the individual F^k cannot be determined from those diagonal elements of the energy matrix which correspond to the observed levels, but only a linear combination of the F^k. But other core terms of lower multiplicity interact with terms of highest multiplicity through electrostatic off-diagonal matrix elements involving the other open-shell electrons (F^k(fd) and G^k(fd) for example) and also through off-diagonal spin–orbit matrix elements; the other core terms thus mix to a small extent involving the energy difference, which requires specification of all three F^k(ff) but only to second order. Hence the least-squares fit does yield values of all the F^k(ff) but with rather large statistical errors.

Table 15.5 presents some experimental values of F^k(ff) parameters, the corresponding HF radial integrals, and several ways of comparing them. The experimental parameters are all smaller than the calculated integrals, which is an almost universal characteristic throughout the periodic table except for p-electron parameters. The ratio (experiment/HF) is roughly 2/3 with irregular variations. Another ratio is F^k/F^2, which can be formed independently for experiment and for HF. A third possibility is the difference (experiment – HF), which Crosswhite [31] found to be nearly constant for each F^k for the tripositive lanthanide ions in an LaF_3 host. The different comparisons have different applications.

In parameter fitting of a set of observed actinide levels it is almost never possible to let all the parameters vary freely because of the difficulties discussed in the previous section. One chooses starting parameters which appear reasonable

Table 15.5 *Approximate values of some F^k(ff) parameters.*

Configuration	Element	Parameter	Experiment	Hartree–Fock	F^k/F^2 Expt	F^k/F^2 HF	Expt/HF	HF – Expt	Ref.
$5f^47s^2$	U I	F^2	36505	62891	1.0	1.0	0.580	26386	59
		F^4	28474	40290	0.780	0.641	0.707	11816	
		F^6	20808	29304	0.570	0.466	0.710	8496	
$5f^57s^2$	Np I	F^2	39797	67452	1.0	1.0	0.590	27655	30
		F^4	31017	43381	0.779	0.643	0.715	12364	
		F^6	23044	31611	0.579	0.469	0.729	8567	
$5f^67s^2$	Pu I	F^2	42935	71461	1.0	1.0	0.601	28526	30
		F^4	33472	46094	0.780	0.645	0.726	12622	
		F^6	24959	33638	0.580	0.471	0.742	8679	
$5f^87s^2$	Cm I	F^2	51025	78531	1.0	1.0	0.650	27506	30
		F^4	39133	50868	0.767	0.648	0.769	13883	
		F^6	30579	37204	0.599	0.474	0.822	8229	
$5f^36d7s^2$	U I	F^2	43915	68684	1.0	1.0	0.639	24769	59
		F^4	31929	44396	0.727	0.646	0.719	12467	
		F^6	27126	32417	0.618	0.472	0.837	5291	
$5f^46d7s^2$	Np I	F^2	43317	72662	1.0	1.0	0.596	29345	30
		F^4	37170	47094	0.858	0.648	0.789	9924	
		F^6	23286	34436	0.538	0.474	0.676	11150	
$5f^56d7s^2$	Pu I	F^2	43787	76279	1.0	1.0	0.574	32492	30
		F^4	38445	49543	0.878	0.649	0.776	11098	
		F^6	24191	36268	0.552	0.475	0.667	12077	

and proposes to improve them by successive least-squares iterations. For the F^k(ff) one expects the final ratios to be approximately 1:0.7:0.5, but if all three are free the second iteration may give something like $1:-0.2:1.5$, which is clearly impossible and further iteration will only make it worse. The difficulty may be in the other starting parameters of the configuration, in the choice of levels, etc. The usual procedure is to constrain the three F^k(ff) to vary in the expected ratio and try to deduce the other sources of difficulty. There remains, however, the problem of choosing a good starting value for F^2(ff) and also for all the other parameters. The HF values can give an indication through the ratios (expt/HF) or the differences (expt – HF) if these quantities are known for similar configurations or neighboring elements. Clearly it is helpful to have as many comparison cases as possible. At the present time the situation is very unsatisfactory.

15.8 SUMMARY OF ACTINIDE CONFIGURATIONS

Table 15.6 lists the lowest level of all known actinide configurations. Thousands of higher levels are known, but for this survey we are more interested in

Table 15.6 *Lowest levels of identified configurations, with isotope shifts and hyperfine structure widths.*
(Widths are negative for inverted HFS splittings.)

Spectrum measured isotopes	*Configuration*	*Parity*	*Term*	*Level* (cm^{-1})	g_{obs}	g_{SL}	*IS* (10^{-3} cm^{-1})	*HFS* (10^{-3} cm^{-1})	*Refs*
Ac III	7s	E	$^2S_{1/2}$	0.0					32
	6d	E	$^2D_{3/2}$	801.0					
	5f	O	$^2F^o_{5/2}$	23 454.5					
	7p	O	$^2P^o_{1/2}$	29 465.9					
Ac II	$7s^2$	E	$^1S_0$	0.00					32
	6d7s	E	$^3D_1$	4 739.63					
	$6d^2$	E	$^3F_2$	13 236.46					
	7s7p	O	$^3P^o_0$	20 956.40					
	6d7p	O	$^3P^o_2$	26 446.96					
	5f7s	O	$^3F^o_2$	31 878.87					
	5f6d	O	$^3H^o_4$	39 807.14					
	7s8s	E	$^3S_1$	51 680.55					
	5f7p	E	$^3F_2$	54 633.05					
Ac I	$6d7s^2$	E	$^2D_{3/2}$	0.00					32
	$6d^27s$	E	$^4F_{3/2}$	9 217.28					
	$7s^27p$	O	$^2P^o_{1/2}$	?					
	6d7s7p	O	$^4F^o_{3/2}$	13 712.90					
	$6d^27p$	O	$^4G^o_{5/2}$	31 494.68					
Th IV	5f	O	$^2F^o_{5/2}$	0.00					33
	6d	E	$^2D_{3/2}$	9 192.84					
	7s	E	$^2S_{1/2}$	23 130.2					
	7p	O	$^2P^o_{1/2}$	60 238.9					
Th III	5f6d	O	$^3H^o_4$	0.000	0.89	0.800			34–39
	$6d^2$	E	$^3F_2$	63.267	0.744	0.666			
	5f7s	O	$^3F^o_3$	2 527.095	1.071	1.084			
	6d7s	E	$^3D_1$	5 523.881	0.50	0.499			
	$7s^2$	E	$^1S_0$	11 961.133	–	–			
	$5f^2$	E	$^3H_4$	15 148.519	0.81	0.800			
	5f7p	E	$^3G_3$	33 562.349	0.849	0.749			
	6d7p	O	$^3F^o_2$	37 280.229	0.793	0.666			
	7s7p	O	$^3P^o_0$	42 259.714	–	–			
	5f8s	O	$J = 2$	74 644.27					
	5f7d	O	$J = 3$	78 327.71					
	6d8s	E	$^3D_1$	81 706.37					
	6d7d	E	$J = 1$	83 358.66					
	5f8p	E	$J = 3$	86 086.37					
	5f6f	E	$J = 5$	86 933.97					
	6d6f	O	$J = 4$	94 657.94					
Th II	$6d^27s$	E	$^4F_{3/2}$	0.000	0.639	0.399	0	−141	38,
IS	$6d7s^2$	E	$^2D_{3/2}$	1 859.938	0.586	0.800	34	−102	40–42,
232–230	$5f7s^2$	O	$^2F^o_{5/2}$	4 490.256	0.856	0.857	−54	+17	94
HFS	5f6d7s	O	$^4H^o_{7/2}$	6 168.351	0.718	0.666	−371		

Table 15.6 (*Contd.*)

Spectrum measured isotopes	*Configuration*	*Parity*	*Term*	*Level* (cm^{-1})	g_{obs}	g_{SL}	*IS* (10^{-3} cm^{-1})	*HFS* (10^{-3} cm^{-1})	*Refs*
229	$6d^3$	E	$^4F_{3/2}$	7001.425	0.800	0.399	−422		
	$5f6d^2$	O	$^4H^o_{7/2}$	12485.688	0.855	0.666	−680		
	6d7s7p	O	$^4F^o_{3/2}$	23372.582	1.067	0.399	−554		
	$5f^27s$	E	$^4H_{7/2}$	24381.802	0.70	0.666	−590		
	5f7s7p	E	$^4G_{5/2}$	26488.644	0.776	0.570	−305	(?)	
	$6d^27p$	O	$^4G^o_{5/2}$	28243.812	0.922	0.570	−421		
	5f6d7p	E	$^4I_{9/2}$	30452.723	1.035	0.727	−640		
	$7s^27p$	O	$^2P^o_{1/2}$	31625.680	0.344	0.666	−139		
	$5f^26d$	E	$^4K_{11/2}$	32620.859	0.826	0.769	−948		
Th I	$6d^27s^2$	E	$^3F_2$	0.000	0.736	0.666	0		38, 39,
IS	$6d^37s$	E	$^5F_1$	5563.143	0.065	−0.002	−328		43, 44
232–230	$5f6d7s^2$	O	$^3H^o_4$	7795.270	0.863	0.800	−244		
	$6d7s^27p$	O	$^3F^o_2$	10783.153	0.732	0.666	−33		
	$6d^27s7p$	O	$^5G^o_2$	14465.220	0.810	0.332	−209		
	$5f6d^27s$	O	$^5H^o_3$	15618.985	0.600	0.499	−535		
	$5f7s^27p$	E	$^3G_3$	18431.685		0.749	−162		
	$6d^4$	E	$^5D_0$	21176.012	–	–	−655		
	5f6d7s7p	E	$^5I_4$	22098.187	0.742	0.599	−485		
	$5f^27s^2$	E	$^3H_4$	27495.589	1.005	0.800	−396		
	$5f6d^3$	O	$^5I^o_4$	31194.705	0.735	0.599	−789		
	$6d^37p$	O	$^5G^o_2$	32575.421	0.720	0.332	−672		
	$5f6d^27p$	E	$^5K_5$	35300.914	0.875	0.666	−671		
Pa II	$5f^27s^2$	E	$^3H_4$	0.000	0.821	0.800		0	45, 46
HFS	$5f^26d7s$	E	$^5K_5$	823.265		0.666		−1410	
231	$5f6d^27s$	O	$^5I^o_4$	4751.660		0.599		−1065	
	$5f^26d^2$	E	$^5L_6$	7454.030	0.77	0.714		205	
	$5f^36d$	O	$^5L^o_6$?	19162.305		0.714		315	
	$5f^27s7p$	O	$^5I^o_4$	22549.535		0.599		−680	
Pa I	$5f^26d7s^2$	E	$^4K_{11/2}$	0.000	0.820	0.769		0	46–48
HFS	$5f6d^27s^2$	O	$^4H^o_{7/2}$	1978.220	0.790	0.666		−130	95
231	$5f^26d^27s$	E	$^6L_{11/2}$	7000.290		0.614		−1030	
	$5f6d^37s$	O	$^6I^o_{7/2}$	7585.025		0.443		−585	
	$5f^27s^27p$	O	$^4I^o_{9/2}$	11444.705	0.88	0.727		145	
	$5f^37s^2$	O	$^4I^o_{9/2}$	13018.610	0.81	0.727		−100	
	$5f^26d7s7p$	O	$^6L^o_{11/2}$	14393.410	0.675	0.614		−745	
	$5f6d^27s7p$	E	$^6I_{7/2}$	15061.150				−705	
	$5f^26d^27p$	O	$^6M^o_{13/2}$	25106.985	0.980	0.666		−310	
U VI	5f	O	$^2F^o_{5/2}$	0.0					49
	6d	E	$^2D_{3/2}$	90999.6					
	7s	E	$^2S_{1/2}$	141447.5					
	7p	O	$^2P^o_{1/2}$	193340.2					
U V	$6p^65f^2$	E	$^3H_4$	0.00					50
	$6p^65f6d$	O	$^3H^o_4$	59183.36					
	$6p^65f7s$	O	$^3F^o_2$	94069.53					

Table 15.6 (*Contd.*)

Spectrum measured isotopes	*Configuration*	*Parity*	*Term*	*Level* (cm^{-1})	g_{obs}	g_{SL}	*IS* (10^{-3} cm^{-1})	*HFS* (10^{-3} cm^{-1})	*Refs*
	$6p^6 6d^2$	E	$^3F_2$	137 608.14					
	$6p^6 5f\,7p$	E	$^3G_3$	139 140.96					
	$6p^5 5f^3$	E	$J = 4$	145 870.70					
U III	$5f^4$	E	$^5I_4$	0.000			0		93
IS	$5f^3 6d$	O	$^5L^o_6$	210.265			291		
238–235	$5f^3 6s$	O	$^5I^o_4$	3 743.963			1340		
	$5f^2 6d^2$	E	$^5L_6$	19 416.772			719		
U II	$5f^3 7s^2$	O	$^4I^o_{9/2}$	0.000	0.765	0.727	0		51–55
IS	$5f^3 6d7s$	O	$^6L^o_{11/2}$	289.040	0.655	0.614	−788		
238–235	$5f^3 6d^2$	O	$^6M^o_{13/2}$	4 585.434	0.785	0.667	−1286		
	$5f^4 7s$	E	$^6I_{7/2}$	4 663.803	0.480	0.443			
	$5f^4 6d$	E	$^6L_{11/2}$	12 513.885	0.680	0.614			
	$5f^2 6d^2 7s$	E	$^6L_{11/2}$	13 783.030	0.685	0.614			
	$5f^2 6d7s^2$	E	$^4K_{11/2}$	16 706.304	0.790	0.769			
	$5f^2 6d^3$	E	$^6L_{13/2}$	20 702.037	0.990	0.969	−1375		
	$5f^3 7s7p$	E	$^6K_{9/2}$	23 315.090	0.880	0.544	−636		
	$5f^3 6d7p$	E	$^6M_{13/2}$	26 191.309	0.890	0.666	−1124		
	$5f^4 7p$	O	$^6K^o_{9/2}$	30 599.179	0.900	0.545			
U I	$5f^3 6d7s^2$	O	$^5L^o_6$	0.000	0.750	0.714	0	−112	53–59
IS	$5f^3 6d^2 7s$	O	$^7M^o_6$	6 249.029	0.625	0.570	−565		
238–235	$5f^4 7s^2$	E	$^5I_4$	7 020.710	0.660	0.599	−310		
HFS	$5f^2 6d^2 7s^2$	E	$^5L_6$	11 502.624	0.775	0.714	450		
235	$5f^3 7s^2 7p$	E	$^5K_5$	13 463.392	0.675	0.666	100		
	$5f^3 6d7s7p$	E	$^7M_6$	14 643.867	0.675	0.570	−380		
	$5f^4 6d7s$	E	$^7L_5$	14 839.736	0.565	0.499	−380		
	$5f^4 7s7p$	O	$^7K^o_4$	22 792.372	0.645	0.399	−665		
	$5f^3 6d^3$	O	$^7M^o_6$	23 084.307	0.825	0.570	−699		
	$5f^2 6d^2 7s7p$	O	$^7M^o_?$?	27 576.161	0.99	0.804	−170		
	$5f^3 6d^2 7p$	E	$^7N_7$	27 886.992	0.850	0.624	−580		
	$5f^3 7d7s^2$	O	$^5L^o_6$	27 920.942	0.835	0.714	40		
	$5f^3 6d7s8s$	O	$^7L^o_5$	32 857.449	0.760	0.499	−360		
	$5f^3 6d7s8p$	E	$^7M_6$	33 639.562	0.820	0.570	−420		
	$5f^4 6d7p$	O	$^7M^o_6$	34 160.569	0.890	0.570	−770		
Np II	$5f^4 6d7s$	E	$^7L_5$	0.000		0.499		−1722	53,
HFS	$5f^4 7s^2$	E	$^5H_4$	24.270	0.650	0.599		776	60–62
237	$5f^5 7s$	O	$^7H^o_2$	83.490		−0.002		−1585	
	$5f^5 6d$	O	$^7K^o_4$	9 446.880	0.485	0.399		936	
	$5f^4 7s7p$	O	$J = 4$	21 922.530				−528	
	$5f^5 7p$	E	$J = 4$	22 720.500				670	
Np I	$5f^4 6d7s^2$	E	$^6L_{11/2}$	0.000	0.655	0.614		777	53,
HFS	$5f^5 7s^2$	O	$^6H^o_{5/2}$	2 831.140	0.43	0.284		534	62, 63
237	$5f^4 6d^2 7s$	E	$^8M_{11/2}$	7 112.430	0.48	0.460		−924	
	$5f^4 7s^2 7p$	O	$^6K^o_{9/2}$	11 940.075	0.625	0.544		976	
	$5f^5 6d7s$	O	$^8K^o_{7/2}$	13 384.205		0.220		−1008	

Table 15.6 (*Contd.*)

Spectrum measured isotopes	*Configuration*	*Parity*	*Term*	*Level* (cm^{-1})	g_{obs}	g_{SL}	*IS* (10^{-3} cm^{-1})	*HFS* (10^{-3} cm^{-1})	*Refs*
	$5f^46d7s7p$	O	$^8M^o_{11/2}$	14 338.880		0.460		−661	
	$5f^57s7p$	E	$^8I_{5/2}$	18 654.895	0.71	−0.002		75	
	$5f^36d^27s^2$	O	$^6M^o_{13/2}$	20 050.905	0.780	0.666		842	
	$5f^46d^27p$	O	$^8N^o_{13/2}$	28 551.035	0.940	0.532		1183	
Pu II	$5f^67s$	E	$^8F_{1/2}$	0.000	3.150	4.007	381		53,
IS	$5f^57s^2$	O	$^6H^o_{5/2}$	8 198.665	0.414	0.284	896		64–68
240–239	$5f^56d7s$	O	$^8K^o_{7/2}$	8 709.640	0.308	0.220	555		
HFS	$5f^66d$	E	$^8H_{3/2}$	12 007.503	−0.019	−0.403	77		
239	$5f^56d^2$	O	$^8L^o_{9/2}$	17 296.880	0.494	0.363	242		
	$5f^67p$	O	$^8G^o_{1/2}$	22 038.950	0.345	−1.339	287	40	
	$5f^57s7p$	E	$^8I_{5/2}$	30 956.355	0.646	−0.002	424		
	$5f^56d7p$	E	$^8L_{9/2}$	33 793.295	0.800	0.362	208		
	$5f^46d^27s$	E	$^8M_{11/2}$	37 640.775	0.70	0.460	813		
Pu I	$5f^67s^2$	E	$^7F_0$	0.000	–	–	465		53,
IS	$5f^56d7s^2$	O	$^7K^o_4$	6 313.866	0.487	0.399	653		67–71
240–239	$5f^66d7s$	E	$^9H^o_1$	13 528.246	−0.59	−1.005	253		
	$5f^56d^27s$	O	$^9L^o_4$	14 912.011	0.496	0.198	488		
	$5f^67s7p$	O	$^9G^o_0$	15 449.475	–	–	336		
	$5f^57s^27s$	E	$^7I_3$	17 897.917	0.450	0.248	691		
	$5f^56d7s7p$	E	$^9L_4$	20 828.475	0.352	0.198	467		
	$5f^77s$	O	$^9S^o_4$	25 192.231	1.768	2.002	273		
	$5f^67s8s$	E	$^9F_1$	31 572.610	2.403	3.506	446		
	$5f^66d^2$	E	$^9I_2$	31 710.912	0.200	−0.336	115		
	$5f^66d7p$	O	$^9I_2$	33 070.577	0.673	−0.336	293		
	$5f^46d^27s^2$	E	$^7M_6$	36 050.520	0.850	0.570	535		
	$5f^56d^27p$	E	$^9M_5$	37 415.495	0.980	0.332	403		
	$5f^56d7s8s$	O	$^9K^o_3$	39 618.178	0.27	−0.002	503		
Am II	$5f^77s$	O	$^9S^o_4$	0.00			400	1726	72
IS	$5f^76d$	O	$^9D^o_3$	14 222.21			−17	−260	
243–241									
HFS 241	$5f^66d7s$	E	$J = 2$	20 501.00			547	−929	
Am I	$5f^77s^2$	O	$^8S^o_{7/2}$	0.000	1.937	2.002	0	−20	53, 72
IS	$5f^66d7s^2$	E	$^8H_{3/2}$	10 683.568		−0.403	268	83	92, 96
243–241	$5f^76d7s$	O	$^{10}D^o_{5/2}$	14 506.922		2.575	−269	1021	
HFS	$5f^77s7p$	E	$^{10}P_{7/2}$	15 608.260	1.382	2.225	−210	933	
241	$5f^77s8s$	O	$^{10}S^o_{9/2}$	30 884.895		2.002	−130	1859	
	$5f^77s7d$	O	$^{10}D^o_{7/2}$	35 092.332	1.753	2.098	−217	478	
Cm II	$5f^77s^2$	O	$^8S^o_{7/2}$	0.000	1.935	2.002	0		73–76
IS	$5f^87s$	E	$^8F_{13/2}$	2 093.870	1.500	1.540	−738		97
246–244	$5f^76d7s$	O	$^{10}D^o_{5/2}$	4 010.645	2.492	2.575	−496		
	$5f^76d^2$	O	$^{10}F^o_{3/2}$	14 830.150	3.009	3.205	−962		
	$5f^86d$	E	$^8G_{13/2}$	17 150.790	1.415	1.457	−1177		
	$5f^77s7p$	E	$^{10}P_{7/2}$	24 046.385	2.098	2.225	−403		

Table 15.6 (*Contd.*)

Spectrum measured isotopes	*Configuration*	*Parity*	*Term*	*Level* (cm^{-1})	g_{obs}	g_{SL}	*IS* (10^{-3} cm^{-1})	*HFS* (10^{-3} cm^{-1})	*Refs*
	$5f^87p$	O	$^8F^o_{11/2}$	27065.085	1.51	1.554	−972		
	$5f^76d7p$	E	$^{10}F_{3/2}$	32034.430	2.933	3.205	−923		
Cm I	$5f^76d7s^2$	O	$^9D^o_2$	0.000	2.563	2.671	0		53,
IS	$5f^87s^2$	E	$^7F_6$	1214.203	1.452	1.501	−275		74, 75,
246–244	$5f^77s^27p$	E	$^9P_3$	9263.374	2.112	2.253	118		77, 78
	$5f^76d^27s$	O	$^{11}F^o_2$	10144.927	2.873	3.005	−339		
	$5f^76d7s7p$	E	$^{11}F_2$	15252.710	2.835	3.005	−269		
	$5f^86d7s$	E	$^9G_7$	16932.750	1.466	1.501	−586		
	$5f^87s7p$	O	$^9D^o_6$	17656.657	1.621	1.668	−463		
	$5f^77s^28s$	O	$^9S^o_4$	28635.020	1.731	2.002	−126		
	$5f^76d^3$	O	$^{11}F^o_2$	30443.915	2.53	3.005	−619		
	$5f^87s8s$	E	$^9F_7$	33013.035	1.54	1.573	−450		
	$5f^76d7s8s$	O	$^{11}D^o_3$	34255.170	2.064	2.503	−220		
	$5f^77s^28p$	E	$^9P_3$	35540.695	2.00	2.253	135		
	$5f^86d7p$	O	$J = 7$	35694.690	1.358		−677		
	$5f^76d^27p$	E	$^{11}F_2$	36128.790	2.733	3.005	−628		
	$5f^77d7s^2$	O	$^9D^o_2$	36481.435	2.373	2.671	105		
Bk II	$5f^97s$	O	$^7H^o_8$	0.00				6195	53,
HFS	$5f^87s^2$	E	$^7F_6$	7040.98				820	79–81
249	$5f^86d7s$	E	$J = 8$	12340.96				8678	
	$5f^96d$	O	$J = 8$	16360.00				670	
	$5f^97p$	E	$J = 7$	26938.26				2050	
	$5f^87s7p$	O	$J = 6$	32025.72				3445	
Bk I	$5f^97s^2$	O	$^6H^o_{15/2}$	0.000	1.28	1.334		1150	53,
HFS	$5f^86d7s^2$	E	$^8G_{13/2}$	9141.115	1.415	1.457		836	79–81
249	$5f^97s7p$	E	$J = 15/2$	16913.770				3168	
	$5f^96d7s$	O	$J = 17/2$	17182.482				4472	
	$5f^87s^27p$	O	$J = 11/2$	17777.808				157	
	$5f^86d^27s$	E	$^{10}G_{13/2}$	21506.406		1.550		3596	
	$5f^86d7s7p$	O	$J = 13/2$	24652.405	1.38			1157	
	$4f^97s8s$	O	$^8H^o_{17/2}$	32488.850		1.413		6306	
	$4f^96d7p$	E	$J = 17/2$	36952.610				1800	
Cf II	$5f^{10}7s$	E	$^6I_{17/2}$	0.00	1.280	1.295		0	53,
HFS	$5f^{10}6d$	E	$J = 15/2$	19359.06				500	82, 83
249	$5f^{10}7p$	O	$J = 15/2$	26858.90	1.26			520	
Cf I	$5f^{10}7s^2$	E	$^5I_8$	0.000	1.213	1.251		0	53,
HFS	$5f^96d7s^2$	O	$J = 8$	16909.535	1.301			−40	82–84
249	$5f^{10}7s7p$	O	$J = 8$	17459.210	1.277			−140	
	$5f^{10}6d7s$	E	$J = 8$	20043.930				−210	
	$5f^97s^27p$	E	$J = 7$	24727.600				60	
	$5f^{10}7s8s$	E	$^7I_9$	32983.180	1.300	1.334		−490	
	$5f^96d7s7p$	E	$J = 8$	33952.135				−200	
	$5f^{10}7s8p$	O	$J = 8$	38225.945				−410	

Table 15.6 (*Contd.*)

Spectrum measured isotopes	*Configuration*	*Parity*	*Term*	*Level* (cm^{-1})	g_{obs}	g_{SL}	*IS* (10^{-3} cm^{-1})	*HFS* (10^{-3} cm^{-1})	*Refs*
Es II	$5f^{11}7s$	O	$^5I^o_8$	0.00				7086	53, 85
HFS	$5f^{11}7p$	E	$J = 7$	27751.12				442	
253	$5f^{10}6d7s$	E	$J = 8?$	32632.50			–	1250	
Es I	$5f^{11}7s^2$	O	$^4I^o_{15/2}$	0.00	1.185138	1.200264		1542	53,
HFS	$5f^{11}7s7p$	E	$J = 15/2$	17802.89				3835	85, 86
253	$5f^{10}6d7s^2$	E	$J = 17/2$	19367.93				−229	
	$5f^{11}7s8s$	O	$^6I^o_{17/2}$	33829.35				6252	
Fm I	$5f^{12}7s^2$	E	$^3H_6$	0	1.16052	1.16705			87

generalities than in details. The trend of analogous configurations as a function of atomic number in the neutral atoms has been shown in Fig. 15.3(a) and (b). The relative energies as a function of ionization stage are given in Table 15.7 for Th I–IV 5f, 6d, 7s, and 7p, showing that 5f becomes increasingly more stable as outer electrons are removed (5f gains 17000 cm^{-1} over 6d in going from Th I to Th IV). The change in 5f energy with increase in atomic number corresponds to the actinide contraction, which increases the effective nuclear charge Z^*. Increasing ionization also increases Z^* by reducing the shielding of 5f from the nucleus as outer electrons are removed, and the effect on the 5f energy is thus in the same direction as increasing Z. The outer electrons 7s and 7p are more nearly hydrogenic and have energies that become more negative as approximately the square of the ionic charge (about the same for all Z); hence the 7s–7p difference increases with ionic charge.

The term structure of Th III was treated by Racah [35] in a classic paper on least-squares parameter fitting in intermediate coupling with configuration interaction. With these off-diagonal matrix elements included, the calculated

Table 15.7 *Comparison of thorium configurations in four stages of ionization.*

Th IV (Th^{3+})		Th III (Th^{2+})		Th II (Th^{+})		Th I (Th^0)	
Configuration	*T* (cm^{-1})	*Configuration*	*T* (cm^{-1})	*Configuration*	*T* (cm^{-1})	*Configuration*	*T* (cm^{-1})
5f	0	5f7s	2527	$5f7s^2$	4490	$5f7s^27p$	18432
6d	9193	6d7s	5524	$6d7s^2$	4113	$6d7s^27p$	10783
Δ(5f − 6d)	−9193		−2997		337		7649
7s	23130	$7s^2$	11961	$6d7s^2$	4113	$6d^27s^2$	0
7p	60239	7s7p	42260	6d7s7p	23373	$6d^27s7p$	14465
Δ(7s − 7p)	−37109		−30299		−19260		−14465

energies were in much better agreement with observation, and in addition the calculated g-values were also in better agreement than the pure SL Landé g-factors. This has been the general experience in fitting spectra with more than two electrons: the better the energy fit, the better the g-value fit; it also applies to other properties such as isotope shift, hyperfine structure, and relative intensities of transitions, and thus lends confidence to the calculation. Attempts to make the g-value fit more exact by trying to fit the energies and g-values simultaneously have not been successful, however, because these are not independent quantities. If the calculated g-values are not more or less in agreement with observation, it is an indication that some interactions are missing from the energy matrix. Since parameter fits in the general case are not exact and are in a state of flux, no attempt has been made in Table 15.6 to try to include calculated g-values and other calculated properties; comparison with the column of SL g-values serves as an indication of how much intermediate coupling and configuration interaction are present (and not that the assignment is in doubt).

Table 15.6 shows that, in moving toward the middle of the actinide series, the multiplicity increases in accordance with Hund's rule. Thus in Pa I (the first true actinide with a 5f electron in the ground state) there are quartets and sextets (and also doublets in the higher states), whereas in Am I there are octets and decets (and also sextets, quartets, and doublets). This has a profound effect on the intensity distribution of the observed spectral lines. In pure SL coupling there is a selection rule $\Delta S = 0$ (octet terms have transitions only to octets, etc.). In intermediate coupling, as obtains in the actinides, there are off-diagonal spin–orbit matrix elements between terms of adjacent multiplicity ($\Delta S = 0, \pm 1$; Table 15.4), which means that octet terms, for example, will also have some decet and sextet eigenvector components, and therefore transitions to decet and sextet terms. There will be, however, no transitions to quartet and doublet terms. The strong lines (those involving the low terms) will therefore consist of transitions between terms of high multiplicity, which are comparatively few in number. There will also be transitions among the terms of low multiplicity, of course, but these will be very numerous and weak. The observed Am I spectrum thus consists of a relatively small number of strong lines superimposed on a weak complex background. The strong lines are easy to classify into a transition array, the weak lines are not. To determine the G^k parameters, however, requires knowledge of terms of all multiplicity, not obtainable from just the strong lines. At the beginning of the actinide series, by contrast, the multiplicities are all low and the ΔS selection rule is not so restrictive, and hence the range in intensity is not so great. Pa I, in fact, appears at first sight to have the most complex spectrum of all the actinides because of the comparatively uniform intensities, despite fewer expected terms. The Pa spectrum is further complicated by the presence of hyperfine structure (HFS): many transitions have four HFS components, which moreover have a large degradation in intensity because of the low nuclear spin and low J values, so they often cannot be distinguished from neighboring weak lines (in Am there are six HFS components, in Bk eight, with less degradation so

they usually stand out from the background). Hence the analysis and interpretation of a spectrum like Pa is no easier than for later elements with larger multiplicities.

Another characteristic of the actinide series is the fact that the L values for f^N go through a maximum not at the half-filled shell, as in the case of the S values, but at the one-fourth- and three-fourths-filled shell. Thus the ground state of Np I f^4ds^2 is $^6L_{11/2\text{-}21/2}$; for Np I f^4d^2s it is $^8M_{11/2\text{-}25/2}$. These high J values are poorly excited by electron collision in the light source and so transitions to the highest J levels are weak and hard to find, in contrast to multiplets at the beginning of the actinides. For the three-fourths-filled f^N shell the multiplets are inverted and not so much of a problem. The high L values for Np have a considerable effect on the hyperfine structure because the large orbital angular momentum produces a high magnetic field at the nucleus, which increases the orbital contribution. The Np I ground state has a total width of 0.777 cm^{-1} in spite of having no unpaired s electron, the usual source of large hyperfine structure. Bk I and Es I have even larger widths due to larger nuclear spin, larger J value, and larger Z. The ability to measure HFS splittings to better than 1 part in 1000 is a great help in the empirical analysis of these spectra. Moreover, the quantum numbers of the various levels can be obtained by comparing the relative widths with those calculated by standard HFS theory.

Ionization energies of the neutral atoms, derived by Sugar [88] by interpolation of the series properties of the $5f^N$ 7s8s configurations, are given in Table 17.4. Rydberg series have been observed by laser spectroscopy techniques for U I [89, 90] and for Np I [91] and very accurate values of the ionization limit have been obtained: $49\,958.4 \pm 0.5$ and $50\,536 \pm 4$ cm^{-1}. These values are respectively 2% and 1% larger than Sugar's estimates.

To summarize, the spectroscopic properties of all the actinide elements have now been investigated experimentally and theoretically. The present status is satisfactory as a first approximation in that most of the information of interest for chemistry is available. Much more work is required to provide details.

REFERENCES

1. Tomkins, F. S. and Fred, M. (1957) *J. Opt. Soc. Am.*, **47**, 1087–91.
2. Worden, E. F., Gutmacher, R. G., and Conway, J. G. (1963) *Appl. Opt.*, **2**, 707–13.
3. Reader, J. and Corliss, C. H. (1980) *Wavelengths and Transition Probabilities for Atoms and Atomic Ions*, Part I, *Wavelengths*, NSRDS-NBS 68, National Bureau of Standards, Washington DC.
4. Korostyleva, L. A. and Dontsov, Yu. P. (1978) *Tables of Spectral Lines of Neutral and Ionized Atoms of Uranium*, Academy of Science USSR, Moscow (in Russian); Engl. transl. Shalimoff, G. V. (1980) Lawrence Berkeley Laboratory.
5. Lobikov, E. A., Odintsova, N. K., and Striganov, A. R. (1979) *Emission Spectrum of Curium*, Rep. IAE-3210, Moscow (in Russian); Engl. transl. Shalimoff, G. V. (1980) Lawrence Berkeley Laboratory.
6. Wilson, M. (1968) *Phys. Rev.*, **176**, 58–63.

7. Rajnak, K. and Fred, M. (1977) *J. Opt. Soc. Am.*, **67**, 1314–23.
8. Brewer, L. (1971) *J. Opt. Soc. Am.*, **61**, 1101–11; (1984) *High Temp. Sci.*, **17**, 1–30.
9. Goeppert Mayer, M. (1941) *Phys. Rev.*, **60**, 184–7.
10. Nugent, L. J. (1975) *MTP International Review of Science, Inorganic Chemistry*, ser. 2, vol. 7, Butterworths, London, pp. 195–219.
11. Condon, E. U. and Shortley, G. H. (1935) *The Theory of Atomic Spectra*, Cambridge University Press, Cambridge, ch. VI.
12. Slater, J. C. (1960) *Quantum Theory of Atomic Structure*, vol. I, McGraw-Hill, New York, ch. 8.
13. Ref. 11, equation $8^6(11)$, p. 176.
14. Ref. 15, equation (50).
15. Racah, G. (1942) *Phys. Rev.*, **62**, 438–62.
16. Racah, G. (1943) *Phys. Rev.*, **63**, 367–82.
17. Racah, G. (1949) *Phys. Rev.*, **76**, 1352–65.
18. Judd, B. R. (1963) *Operator Techniques in Atomic Spectroscopy*, Interscience, New York.
19. Wybourne, B. G. (1965) *Spectroscopic Properties of Rare Earths*, Wiley, New York.
20. Nielson, C. W. and Koster, G. F. (1964) *Spectroscopic Coefficients for p^n, d^n, and f^n Configurations*, MIT Press, Cambridge Ma.
21. Racah, G. (1959) *Bull. Res. Counc. Isr.*, **8F**, 1–14.
22. Bordarier, Y. (1970) Thesis, University of Paris.
23. Cowan, R. D. (1968) *J. Opt. Soc. Am.*, **58**, 808–18.
24. Wilson, M., private communication.
25. Crosswhite, H., private communication.
26. Crosswhite, H. M. and Crosswhite, H., private communication.
27. Ref. 19, equation (2–99).
28. Rajnak, K. and Wybourne, B. G. (1964) *Phys. Rev. A*, **134**, 596–600.
29. Crosswhite, H. M. (1971) *Phys. Rev. A*, **4**, 485–9.
30. Crosswhite, H. M., private communication.
31. Carnall, W. T., Crosswhite, H., and Crosswhite, H. M. (1978) *Energy Level Structure and Transition Probabilities of the Trivalent Lanthanides in LaF_3*, Argonne National Laboratory Report ANL-78-
32. Meggers, W. F., Fred, M., and Tomkins, F. S. (1957) *J. Res. NBS*, **58**, 297–315.
33. Klinkenberg, P. F. A. and Lang, R. G. (1949) *Physica*, **15**, 774–88.
34. Klinkenberg, P. F. A. (1950) *Physica*, **16**, 618–50.
35. Racah, G. (1950) *Physica*, **16**, 651–66.
36. Litzén, U. (1974) *Phys. Scr.*, **10**, 103–4.
37. Wyart, J. F. and Kaufman, V. (1981) *Phys. Scr.*, **24**, 941–52.
38. Palmer, B. A. and Engleman, R. (1983) *Atlas of the Thorium Spectrum*, Los Alamos National Laboratory Report LA-9615.
39. Blaise, J., Wyart, J. F., Engleman, R., and Palmer, B. A. (1983) *15th EGAS Conf.*, Madrid, Europhys. Conf. Abstr. 7C, no. 101.
40. Zalubas, R. and Corliss, C. H. (1974) *J. Res. NBS*, **78A**, 163–246.
41. Giacchetti, A., Blaise, J., Corliss, C. H., and Zalubas, R. J. (1974) *J. Res. NBS*, **78A**, 247–81.
42. Gerstenkorn, S., Luc, P., Vergès, J., Englekemeir, D. W., Gindler, J. E., and Tomkins, F. S. (1974) *J. Physique*, **35**, 483–95.
43. Zalubas, R. (1975) *J. Res. NBS*, **80A**, 221–358.

44. Engleman, R., Jr and Palmer, B. A. (1983) *J. Opt. Soc. Am.*, **73**, 694–701.
45. Giacchetti, A. (1967) *J. Opt. Soc. Am.*, **57**, 728–33.
46. Blaise, J. (1983) unpublished results.
47. Giacchetti, A. (1966) *J. Opt. Soc. Am.*, **56**, 653–7.
48. Giacchetti, A. and Blaise, J. (1970) *2nd EGAS Conf.*, Hanover.
49. Kaufman, V. and Radziemski, L. J., Jr (1976) *J. Opt. Soc. Am.*, **66**, 599–600.
50. Wyart, J. F., Kaufman, V., and Sugar, J. (1980) *Phys. Scr.*, **22**, 389–96.
51. Steinhaus, D. W., Radziemski, L. J., Jr, Cowan, R. D., Blaise, J., Guelachvili, G., Ben Osman, Z., and Vergès, J. (1971) Los Alamos Scientific Laboratory Report LA-4501.
52. Blaise, J. and Radziemski, L. J., Jr (1975) unpublished results.
53. Blaise, J., Wyart, J. F., Conway, J. G., and Worden, E. F. (1980) *Phys. Scr.*, **22**, 224–30.
54. Palmer, B. A., Keller, R. A., and Engleman, R., Jr (1980) Los Alamos Scientific Laboratory Report LA-8251-MS.
55. Conway, J. G., Worden, E. F., Brault, J. W., Hubbard, R. P., and Wagner, J. J. (1983) Lawrence Berkeley Laboratory Preprint LBL-15764; (1984) *Atom. Data Nucl. Data Tables*, **31**, 299–358.
56. Blaise, J. and Radziemski, L. J., Jr (1976) *J. Opt. Soc. Am.*, **66**, 644–59.
57. Engleman, R., Jr and Palmer, B. A. (1980) *J. Opt. Soc. Am.*, **70**, 308–17.
58. Childs, W. J., Poulsen, O., and Goodman, L. S. (1979) *Opt. Lett.*, **4**, 35–7.
59. Rajnak, K. (1979) private communication.
60. Blaise, J., Luc, P., and Vergès, J. (1977) *9th EGAS Conf.*, Cracow.
61. Blaise, J. and Fred, M. (1977) unpublished results.
62. Fred, M., Tomkins, F. S., Blaise, J., Camus, P., and Vergès, J. (1976) Argonne National Laboratory Report ANL-76-68.
63. Fred, M., Tomkins, F. S., Blaise, J., Camus, P., and Vergès J. (1977) *J. Opt. Soc. Am.*, **67**, 7–23.
64. McNally, J. R., Jr and Griffin, P. M. (1959) *J. Opt. Soc. Am.*, **49**, 162–6.
65. Bauche, J., Blaise, J., and Fred, M. (1963) *C. R. Acad. Sci. Paris*, **256**, 5091–3.
66. Bauche-Arnoult, C., Gerstenkorn, S., Vergès, J., and Tomkins, F. S. (1973) *J. Opt. Soc. Am.*, **63**, 1199–203.
67. Blaise, J., Fred, M., Carnall, W. T., Crosswhite, H. M., and Crosswhite, H. (1983) *Plutonium Chemistry* (*ACS Symp. Ser. no.* 216) American Chemical Society, Washington DC, pp. 173–98.
68. Blaise, J., Fred, M., and Gutmacher, R. G. (1984) Argonne National Laboratory Report ANL-83-95.
69. Blaise, J., Fred, M., Gerstenkorn, S., and Judd, B. R. (1962) *C. R. Acad. Sci. Paris*, **255**, 2403–5.
70. Bauche, J., Blaise, J., and Fred, M. (1963) *C. R. Acad. Sci. Paris*, **257**, 2260–3.
71. Striganov, A. R. (1983) *Atomic Spectrum and Energy Levels of the Neutral Atom of Plutonium*, Energoatomisdat, Moscow (in Russian).
72. Fred, M. and Tomkins, F. S. (1957) *J. Opt. Soc. Am.*, **47**, 1076–87.
73. Worden, E. F. and Conway, J. G. (1967) *Physica*, **33**, 274.
74. Conway, J. G., Blaise, J., and Vergès, J. (1976) *Spectrochim. Acta B*, **31**, 31–47.
75. Worden, E. F., Hulet, E. K., Gutmacher, R. G., and Conway, J. G. (1976) *Atom. Data Nucl. Data Tables*, **18**, 459–95.
76. Blaise, J., Vergès, J., Wyart, J. F., Conway, J. G., and Worden, E. F. (1981) *Eur. Conf. on Atomic Physics*, Heidelberg, vol. 5A, part I, pp. 102–3.
77. Worden, E. F. and Conway, J. G. (1976) *J. Opt. Soc. Am.*, **66**, 109–21.

78. Lobikov, E. A., Striganov, A. R., Labozin, V. P., Odintsova, N. K., and Pomytkin, V. F. (1976) *Opt. Spektrosk.*, **46**, 1054–60; *Opt. Spectrosc.*, **46**, 596–9.
79. Conway, J. G., Worden, E. F., Blaise, J., Camus, P., and Vergès, J. (1977) *Spectrochim. Acta*, **32B**, 101–6.
80. Worden, E. F. and Conway, J. G. (1978) *Atom. Data Nucl. Data Tables*, **22**, 326–66.
81. Blaise, J., Luc, P., Vergès, J., Wyart, J. F., Conway, J. G., and Worden, E. F. (1980) *12th EGAS Conf.*, Pisa, Europhys. Conf. Abstr. 4E, no. 3.
82. Worden, E. F. and Conway, J. G. (1970) *J. Opt. Soc. Am.*, **60**, 1144–5.
83. Blaise, J., Vergès, J., Wyart, J. F., Conway, J. G., and Worden, E. F. (1978) *10th EGAS Conf.*, Garching.
84. Conway, J. G., Worden, E. F., Blaise, J., and Vergès, J. (1977) *Spectrochim. Acta*, **32B**, 97–9.
85. Worden, E. F., Lougheed, R. W., Gutmacher, R. G., and Conway, J. G. (1974) *J. Opt. Soc. Am.*, **64**, 77–85.
86. Goodman, L. S., Diamond, H., and Stanton, H. E. (1975) *Phys. Rev. A*, **11**, 499–504.
87. Goodman, L. S., Diamond, H., Stanton, H. E., and Fred, M. (1971) *Phys. Rev. A*, **4**, 473–5.
88. Sugar, J. (1974) *J. Chem. Phys.*, **60**, 4103.
89. Solarz, R. W., May, C. A., Carlson, L. R., Worden, E. F., Johnson, S. A., Paisner, J. A., and Radziemski, L. J., Jr (1976) *Phys. Rev. A*, **14**, 1129–36.
90. Coste, A., Avril, R., Blancard, J., Chatelet, J., Lambert, D., Legre, J., Liberman, S., and Pinard, J. (1982) *J. Opt. Soc. Am.*, **72**, 103–9.
91. Worden, E. F. and Conway, J. G. (1979) *J. Opt. Soc. Am.*, **69**, 733–8.
92. Pulliam, B. V. (1983) private communication.
93. Blaise, J., Wyart, J. F., Palmer, B. A., and Engleman, R. (1984) *16th EGAS Conf., London.*
94. Engleman, R. Jr. and Palmer, B. A. (1984) *J. Opt. Soc. Am. B*, **1**, 782–7.
95. Blaise, J., Ginibre, A. and Wyart, J. F. (1985) *Z. Phys. A. Atoms and Nuclei*, **321**, 61–3.
96. Pulliam, B. V. (1985) private communication to J. Blaise.
97. Worden, E. F., Conway, J. G., and Blaise, J. (1985) Lawrence Berkeley Laboratory preprint LBL-20691.

CHAPTER SIXTEEN

OPTICAL SPECTRA AND ELECTRONIC STRUCTURE OF ACTINIDE IONS IN COMPOUNDS AND IN SOLUTION*

W.T. Carnall and H.M. Crosswhite

16.1 INTRODUCTION

One of the features that sets actinide and lanthanide spectra apart from those of other elements in the periodic table is that the f orbitals can be considered both as containing the optically active electrons and as belonging to the core of filled shells. As a result of this dominant characteristic, the spectra of these elements, particularly of the lower valence states, are moderately insensitive to changes in the ionic environment. This relative insensitivity of core electrons to external circumstances also means that for these elements there is a close connection between energy levels in compounds and those in gaseous free atoms and ions.

For the actinide valence states of most interest to chemists, 1+ through 7+, very few gaseous free-ion spectra have been sufficiently analyzed to provide a

* This chapter is an abbreviated version of a more extensive ANL report [1]. The work reported was performed under the auspices of the Office of Basic Energy Sciences, Division of Chemical Sciences, US Department of Energy [2].

basis for guiding theoretical interpretation. With the experimental techniques used, highly excited states belonging to many different configurations are produced simultaneously, making interpretation difficult and resulting in fragmentary analyses. This situation is responsible for the fact that most of our structural information for the f^N states comes from observation of forced electric dipole absorption and fluorescence transitions in optically clear crystals. The latter analysis is much simplified by the fact that only transitions between nominal f^N levels are involved. These transitions are normally forbidden by the parity selection rule, but in crystals such as $LaCl_3$, that have no center of symmetry, enough of the character of opposite-parity configurations can be mixed in to induce such transitions [3]. At the same time, the admixture (of the order of 0.1 %) is small enough that the f character of the levels is preserved and level calculations can be made on the assumption of a pure f^N configuration.

The stability of f orbitals against changes in the ionic environment results in energy levels of various compounds being closely correlated among themselves as well as with those of the free ion, where known. *Ab initio* free-ion calculations have therefore proven to be very useful for interpreting the crystal levels, and a parametric model based on these calculations has been developed. This model can be applied in a consistent way to ions of both the actinide and lanthanide series [4], and it is used here to help systematize our overall view of actinide spectra.

A major complicating factor in the theoretical interpretation of 5f spectra is the extensive interconfiguration mixing, or configuration interaction [3, 5–7]. This effect of mixing the character of other configurations into the $5f^N$ states involves not only competing configurations with large overlaps but also cumulative interactions with infinitely many distant electronic configurations. That this is a serious problem is demonstrated by analysis of isotope shifts and hyperfine structure in actinide free-ion spectra [8, 9]. The parameters that describe the energy level structure for a configuration would show less variation if the independent-particle model were better justified. The effects of configuration interaction are partially compensated by the use of effective operators in the atomic Hamiltonian for f^N shells [5, 7, 10–15].

16.2 RELATIVE ENERGIES OF ACTINIDE ELECTRONIC CONFIGURATIONS

In order to emphasize the systematic correlations found in the energy level structure of actinide ions both as a function of atomic number Z and for configurations with the same number of f electrons but different charge states, we begin by considering the types of interactions that have been used successfully to account for the structure. In the discussion of atomic spectra, attention is focused on identification of the ground (lowest-energy) and excited electronic configurations of neutral as well as ionized species. The relative energies of the various

electronic configurations thus established provide the basis for extending the interpretation of spectra (and thus electronic structure) to condensed media. In free neutral or ionic species, the energy level structure is attributed primarily to the interaction between electrons in unfilled shells. In condensed media, there is superimposed the additional effect of the ligand field. Several summaries of the actinide atomic spectra literature have been published [9, 16–18].

The progenitor of the actinide (5f) series is actinium; it is comparable to lanthanum in the corresponding lanthanide (4f) series. The electronic structure of zero-valent actinium (Ac I)* is represented as three electrons ($6d7s^2$) outside the radon core. This can be written [Rn]($6d7s^2$), but in the subsequent discussion the core symbol [Rn] will be omitted from the notation. All of the actinide atomic and ionic species are built on the radon core, but the nature of the electronic structure beyond the core is a function of excitation energy, atomic number Z, and state of ionization [19–21]. Thus, within the energy range indicated in Fig. 16.1, in addition to configurations involving 6d and 7s electrons, there are those containing 7p and 5f electrons.

Fig. 16.1 is to be interpreted in the following manner. In Ac I the lowest-energy electron states result from the coupling of two 7s electrons and one 6d. Further,

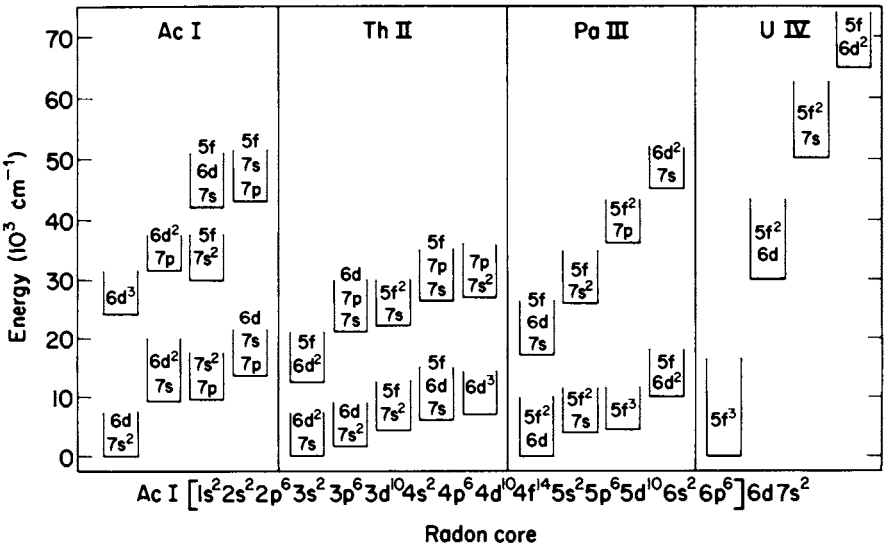

Fig. 16.1 *Three-electron configurations beyond the radon core.*

* The conventional spectroscopic notation for zero-valent actinium is Ac I. Similarly, the singly ionized species is Ac II, and the doubly charged, Ac III. The chemical notation for the latter is Ac^{2+} or Ac(II). When referring to free-ion spectra we will use the spectroscopic notation. When indicating the valence state of an ionic species in a condensed phase we will use the chemical notation. We use the symbol An to represent any actinide element, and Ln as the general symbol for the lanthanides.

an energy equivalent to about 9000 cm^{-1} is sufficient to promote a ground-state 7s electron to the 6d shell, thus forming the lowest level of the excited configuration ($6d^27s$). Essentially the same energy is required to promote a ground-state 6d electron to the 7p shell, giving the excited configuration ($7s^27p$). Only the lowest-energy state (relative to the ground state) for each configuration is indicated in the figure. In most cases large numbers of excited states exist within each of the configurations, so that the density of levels from overlapping configurations increases appreciably with excitation energy. However, since the coupling of two 7s electrons results in a filled subshell, we find that the ground configuration in Ac I ($6d7s^2$) is simple in structure, involving only the states of a single 6d electron, $^2D_{3/2}$ and $^2D_{5/2}$. Such states, written in terms of the quantum numbers S, L, and J, are subsequently referred to as free-ion states.

In Th II, the ground state belongs to $6d^27s$, but again Fig. 16.1 indicates that the spectrum at lower energies is very complex because of the number of electronic configurations with nearly the same energy relative to the ground state. In Pa III, the three electrons beyond the Rn core in the ground state belong to the $5f^26d$ configuration. In U IV further stabilization of the 5f orbital has taken place and excited configurations occur at much higher energies relative to the ground state than was the case in Pa III, Th II, and Ac I. Thus in U IV, the only electronic transitions observed in absorption in the range up to approximately 30 000 cm^{-1} are those *within* the $5f^3$ configuration.

Experimentally, free-ion spectra (both neutral and ionic species) are usually observed in emission, and the energy level structure is deduced from coincidences of energy differences of pairs of spectral lines, subject to verification by isotope shift, hyperfine structure and magnetic g-factor tests. In condensed phases, spectra are more commonly measured in absorption. Relative intensities associated with 'parity-allowed' and 'forbidden' transitions are reflected in the nature of two processes: transitions in which the initial and final states belong to electronic configurations of different parity (parity-allowed transitions, e.g. $5f^3 \rightarrow 5f^26d$); and those in which both states belong to the same configuration (parity-forbidden transitions, e.g. $5f^3 \rightarrow 5f^3$). The latter are weak and sharp. The former are much more intense and are associated with broader absorption bands. Both types of transitions are apparent in Fig. 16.2, which shows the aqueous solution absorption spectra of the trivalent actinides.

16.2.1 Free-ion $5f^N$ states in condensed media

For the trivalent actinides, as for the trivalent lanthanides, ligand field effects are relatively small. In a number of instances, isolated bands in Fig. 16.2 can be interpreted as envelopes which constitute a sum over transitions to all the crystal field components of discrete SLJ states within the $5f^N$ configuration. The effect of the environment is to remove the degeneracy of the free-ion state, but the resulting crystal field components exhibit an energy spread of only about 200–300 cm^{-1}. The center of gravity of such absorption bands is often referred to

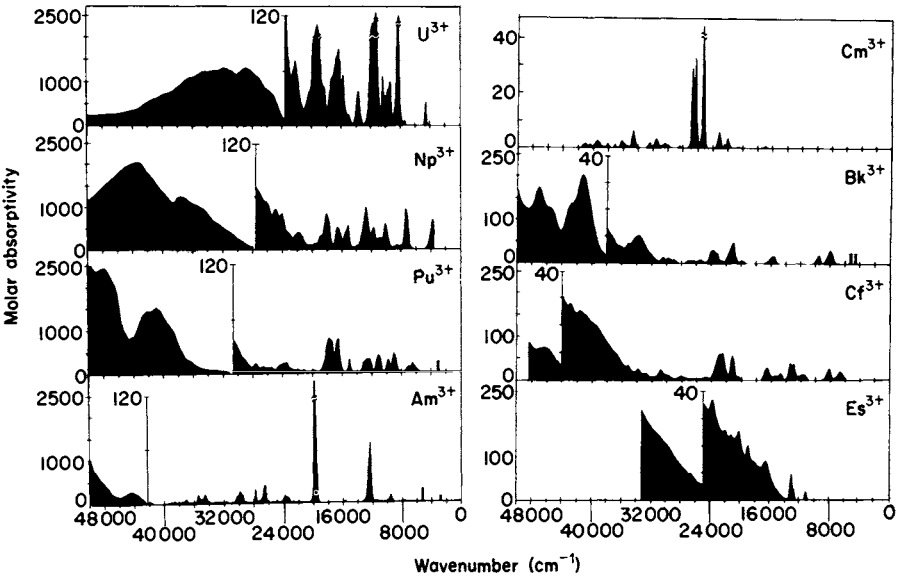

Fig. 16.2 *Absorption spectra of the trivalent actinide ions in dilute acid solution.*

as the 'free-ion state' energy in that particular medium. The energies of these so-called free-ion states shift from one medium to another; the total splitting of the crystal field components that make up such states also varies.

16.2.2 Media effects on the free-ion states in excited configurations

In Fig. 16.1 the energy of the lowest state in the (excited) $5f^2 6d$ configuration of U IV relative to that of the ground state ($^4I_{9/2}$ of $5f^3$) is estimated to be approximately 30 000 cm^{-1}, whereas in Fig. 16.2 the onset of intense transitions in U^{3+}(aquo) is nearer to 24 000 cm^{-1}. This energy difference ($\sim$ 6000 cm^{-1}) is due to the influence of the solvation energy of U^{3+}(aquo) [22] on the relative energies of the 6d and 5f electrons. A similar ΔE is found for the couple Np IV–Np^{3+}(aquo), but the energy of the lowest f → d transition is greater in Np IV than in U IV.

From the regularities revealed in Fig. 16.1 we can generalize. With increasing state of ionization beyond U IV, a concomitant increase in the energy gap between the ground states of the f^N and higher-lying configurations is expected. It is apparent from Fig. 16.2 that this energy gap also increases with atomic number Z across a series of ions of the same charge state. However, there are half-filled-shell effects, since beyond Cm^{3+} ($5f^7$) the pattern of increasing energy of the f → d transitions is repeated. The actual correlations have been tabulated by Brewer [19, 20]. Other regularities, such as the apparent decrease in intensity of f → f transitions for the 3 + actinide ions with increasing Z, will be discussed in Section 16.3.8.

16.3 INTERPRETATION OF OBSERVED SPECTRA OF TRIVALENT ACTINIDES

A great deal of progress had been made in interpreting condensed-phase spectra of the trivalent lanthanide ions in terms of a physical model before much was known about the transuranium elements [3]. Since, except for Th and Pa, each member of the actinide series also exhibits a well characterized trivalent state, it is not surprising that the model developed in treating lanthanide spectra has served as the basis for interpretation of trivalent actinide spectra as well.

In what follows, we summarize the results of modeling high-resolution spectra of An^{3+} in terms of the energy level structure for the An^{3+} ions. Regularities in the values of electronic structure parameters that can be shown to exist for the 3+ actinides are then explored for other valence states.

16.3.1 Free-ion models

There are two complementary aspects of theoretical modeling of atomic electron systems, involving the radial parts of the atomic electron wavefunctions on the one hand and angular parts on the other. Because the angular parts can be treated exactly, clear structural relationships can be demonstrated for various parts of the Hamiltonian. The work of B. R. Judd in particular [12, 14, 15] has defined complete sets of generalized operators which can be included individually as needed to describe a particular atomic system. On the other hand, since by their nature these generalized parameters absorb a wide variety of distinct effects, the physical content of the resulting parameters is not obvious, and it is useful to relate them to *ab initio* calculations of specific effects, as given by less exact but more physically meaningful integrals over the radial wavefunctions. A single-configuration Hartree–Fock method gives valuable insight without undue computing requirements or loss of accuracy. The final parametric determination comes from a least-squares fitting of the more general parametric Hamiltonian variables to the experimental data.

The dominant interactions are (1) electrostatic repulsion between pairs of electrons and (2) the mutual interactions of the magnetic moments generated by the spin and orbital angular momenta. We begin with the Schrödinger equation for the steady state of a many-electron atomic system:

$$H\Psi = E\Psi \tag{16.1}$$

The actual form of the Hamiltonian H assumes that the nucleus can be treated as a point charge. Since exact solutions, i.e. those based on an explicit form of the Coulomb interaction, are only known in the one-electron cases, some method of approximation must be utilized. This is usually the central-field approximation. Each electron is assumed to move independently in the field of the nucleus and an additional central field composed of the spherically averaged potential fields of each of the other electrons in the system. In other words, each electron is treated

as if it moved independently in a spherically symmetric potential. Variables are separated as in the solution of the Schrödinger equation for the hydrogen atom, and the angular parts of the interaction are evaluated explicitly. The total Hamiltonian can be written:

$$H = H_0 + H_e + H_{so} + H_{corr} \tag{16.2}$$

where H_0 involves the kinetic energy of the electrons and their interaction with the nucleus, H_e is the electron–electron electrostatic term, H_{so} is the sum of spin–orbit interactions, and H_{corr} represents higher-order interactions including approximations of configuration interactions and miscellaneous magnetic effects. More specifically,

$$H_e = \sum_{k=0}^{6} F^k(nf, nf) f_k \qquad (k \text{ even}) \tag{16.3}$$

and

$$H_{so} = \sum_{\text{electrons}} \zeta_{nf} A \tag{16.4}$$

in which f_k and A are coefficients for angular-momentum-dependent interactions. The $F^k(nf, nf)$ are Slater radial integrals, and ζ_{nf} corresponds to the Thomas–Frenkel expression [7, 111] for the spin–orbit interaction radial integral with $n = 5$ for cases of primary interest here.

If it is assumed that the difference in energy between the mean, E_p, of all levels of perturbing configurations and that of any level i of the f^N configuration, $E_i(f^N)$, is very large such that $E_p - E_i(f^N)$ is effectively constant for all states i, then the closure theorem is valid and the effects of configuration interaction can be represented [23] by

(1) changes in F^k and ζ,
(2) additional N-body (effective) operators operating within the f^N configuration.

Within the above context, the F^k parameters are not to be identified as the $F^k(nf, nf)$ integrals of the Hartree–Fock (HF) model; as parameters they also absorb some of the effects of configuration interaction. This partially accounts for the large differences between the parametric and HF values of F^k and gives an estimate of the magnitudes of the corrections needed to the basic model.

A model that only includes the electrostatic interaction in terms of the Slater integrals $F^k(nf, nf)$ and the spin–orbit interaction ζ_{nf} results in correlations between observed and calculated free-ion states that are only approximate. The higher-order correction terms must be added to achieve good agreement with experiment. The nature of the corrections that refine the model suggests that the problem can be treated as if the f electrons spent some time in higher-lying configurations where they move in larger orbits and interact less with each other, but in a manner related to the particular class of configurations occupied. These higher-order corrections to the simple model account in large part for the effects of configuration interaction.

16.3.2 A predictive model for trivalent f-element spectra

When the results of a Hartree–Fock calculation are compared to those of a parametric analysis of experimentally identified levels for a given element, the magnitudes of the computed energies, particularly those for F^k, are generally found to be too high. For a more realistic Hamiltonian, using the parametric approach, one can apply subtractive corrections to the estimates derived from *ab initio* calculations. These corrections turn out to be essentially constant over the series and in fact almost identical for both $4f^N$ and $5f^N$ shells [24]. The significance of this is that mixing with high configurations can be taken as essentially a fixed contribution to a global parametric model [4, 24].

Qualitatively, the radial wavefunctions for lanthanides and actinides are very similar in that the f shell is inside already filled s and p shells of one-higher principal quantum number, which partially shield it from external influences. A comparison of the Nd^{3+} and U^{3+} analogs is shown in Fig. 16.3, where the f-electron radial functions are multiplied by an arbitrary factor for emphasis. Notice that for U^{3+} the f^N peak is considerably displaced toward greater r values with respect to the shielding s and p shells, and the relative magnitude of the f-electron tail at large r with respect to the rest of the core function is larger and more exposed.

Because of the greater extension of the 5f radial wavefunctions with respect to those of the shielding 7s and 7p shells, they are more sensitive to changes in the valence-electron situation than for the corresponding lanthanide cores. Nevertheless, their rigidity is remarkable as compared to that for the valence electrons themselves. This can be seen quantitatively in the plots for the Slater electrostatic interaction integrals F^k (5f, 5f) and spin–orbit radial integral ζ_{5f}, which dominate the atomic Hamiltonian for all cases of interest to us here.

We have seen in Fig. 16.1 that there is competition between 5f, 6d, and 7s orbitals for occupancy of low actinide configurations for lower ionization states. However, if we confine our attention to the configurations of the elements beyond thorium, we can limit the types to $5f^{Z-89}6d7s^2$ or $5f^{Z-88}7s^2$ for first spectra, $5f^{Z-89}\,7s^2$ or $5f^{Z-88}\,7s$ for second, $5f^{Z-89}\,6d$ or $5f^{Z-88}$ for third, and $5f^{Z-89}$ for fourth spectra and higher. Fig. 16.4 shows the results of *ab initio* calculations of F^k (5f, 5f) for $k = 2$. Similar calculations were reported by Varga *et al.* [25]. The filled circles of Fig. 16.4 represent configurations that are lowest for those particular ions; open circles represent selected competing (next-lowest) configurations. For instance, the ground configuration for neutral atoms is $5f^{Z-89}6d7s^2$ for Pa I through Np I, $5f^{Z-88}7s^2$ for Pu I and Am I, $5f^{Z-89}6d7s^2$ for Cm I, and $5f^{Z-88}7s^2$ for Bk I through Fm I. These calculations were made using a version of a Hartree–Fock program written by Fischer [26] but containing an approximate correction for relativistic contraction of s-electron orbitals [24, 27]. For second spectra there is similar competition, this time between 5f and 7s orbitals, giving $5f^{Z-88}7s^2$ as the lowest configuration of Pa, U, and the half-filled-shell case of Cm.

Inspection of Fig. 16.4 shows that the addition of a valence-shell electron

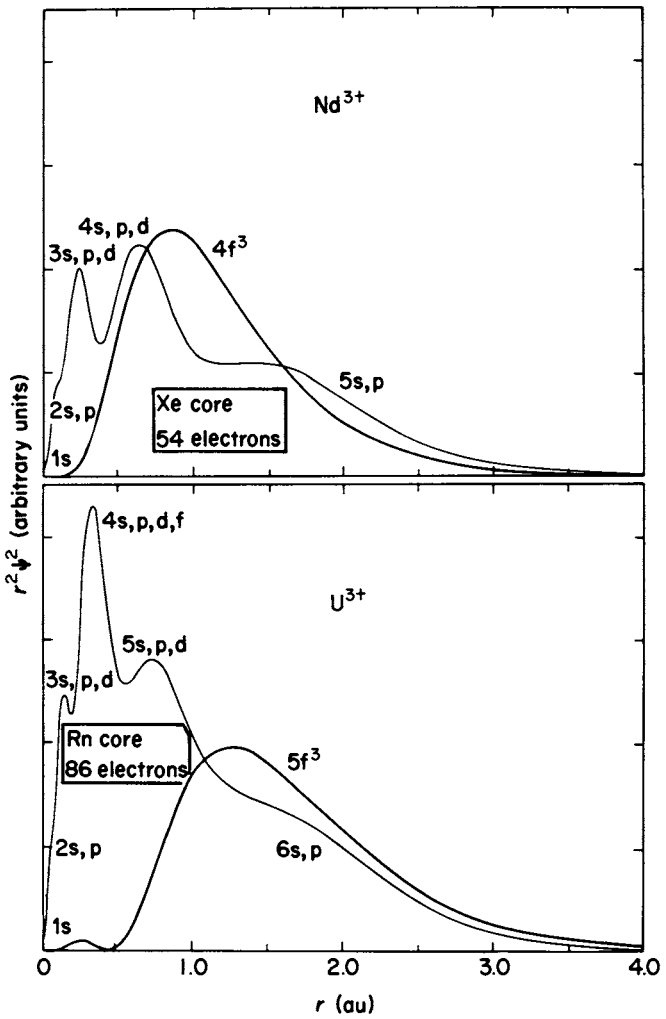

Fig. 16.3 *Comparison of the overlap of $4f^3$–5s,p configurations and those of $5f^3$–6s,p configurations for Nd^{3+} and U^{3+}, respectively.*

diminishes the Slater integrals for the $5f^N$ core slightly but not seriously, and that the effects are additive: $5f^{Z-88}$ III values are enhanced twice as much compared to $5f^{Z-88}7s^2$ I as compared to $5f^{Z-88}7s$ II (and nearly the same as the difference between $5f^{Z-89}$ IV and $5f^{Z-89}7s^2$ II). The $5f^{Z-89}$ IV–$5f^{Z-89}6d$ III difference is the same as that for $5f^{Z-89}7s^2$ II–$5f^{Z-89}6d7s^2$ I. Similar results are found for the other Slater and spin–orbit interaction integrals which combine to dominate the atomic Hamiltonian. As a first approximation they can be taken to depend only on the population of the 5f shell itself and to be independent of the distribution over valence-electron shells.

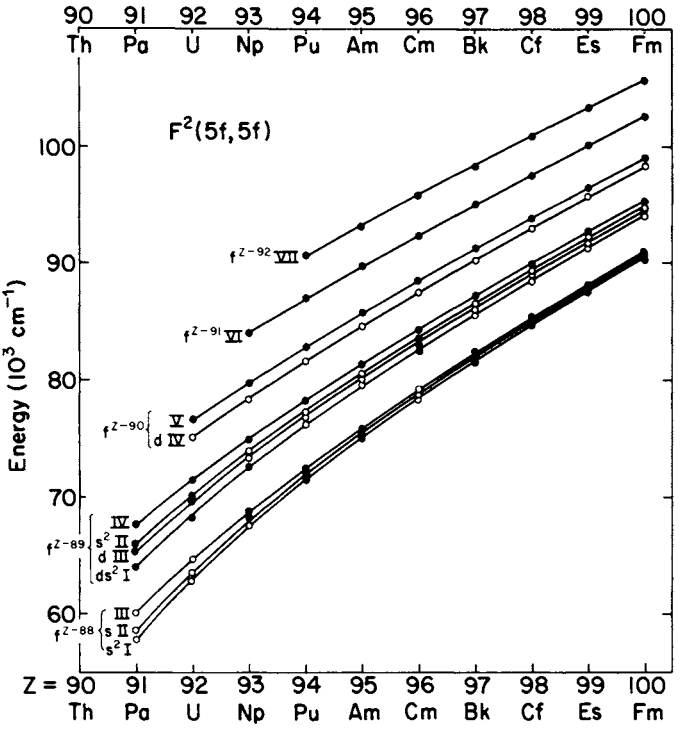

Fig. 16.4 *Variation of Hartree–Fock* [27] $F^2(nf,nf)$ *values with Z.*

16.3.3 Effective operators

The *ab initio* radial wavefunction calculations are in error partly because of the assumption of a single-configuration model. Multiconfiguration calculations, which take configuration interactions into account, are more accurate, but they are much too time-consuming for general application to the many situations encountered in the analyses. However, a very useful result comes out of the calculations that have been made, namely that the energy level shifts induced by these interactions can be mimicked by effective operators acting only within the f^N configuration itself.

The most common convention for defining the additional two-body effective operators referred to in Section 16.3.1 uses the interactions

$$\alpha L(L+1), \qquad \beta G(G_2) \qquad \text{and} \qquad \gamma G(R_7) \tag{16.5}$$

where $G(G_2)$ and $G(R_7)$ are Casimir operators [5, 28], and α, β, and γ are adjustable parameters.

Multiconfiguration calculations have shown that similar values of these effective-operator parameters are to be expected at both ends of the lanthanide

sequence [29], and empirical evaluations are in agreement with this for both the lanthanides and actinides.

For three (or 11) electrons, similar arguments show the need for additional (three-body) operators in order to parametrize the electrostatic interactions completely. If consideration is limited to the interactions arising from second-order perturbation theory, only six new operators are needed [11, 15], and their experimental evaluation is consistent with results expected from first-principles calculations [13].

Similar arguments hold for corrections to the spin–orbit interaction, as well as additional interactions of relativistic origin such as spin–other orbit and spin–spin. Hartree–Fock calculations give good estimates of the Marvin radial integrals M^k ($k = 0, 2, 4$) associated with spin–other orbit and spin–spin interactions. Experimental investigations are needed for evaluation of the magnetic corrections associated with configuration interactions, but experience has shown that a single set of parameters P^k ($k = 2, 4, 6$, with $P^4 = 0.75P^2$ and $P^6 = 0.50P^2$) accounts for a large part of this class of corrections [12]. Use of sets of all of the foregoing parameters has been explored in detail for all of the trivalent ions from U^{3+} through Es^{3+}, and values are shown in Table 16.1 for $An^{3+}:LaCl_3$.

16.3.4 The crystal field Hamiltonian

When a lanthanide or actinide ion occurs in a condensed-phase medium, it retains a large part of its 'free-ion' character, but energy levels are shifted to a greater or lesser degree, depending on the nature and strength of the interaction with the environment. A good part of this interaction can be absorbed by the nominal 'free-ion' parameters themselves, and a measure of this contribution would give clues as to the nature of the interactions. Unfortunately, mainly because of the different methods by which the free-ion and condensed-phase levels are determined, there are very few cases in which both sets of parameters are known well enough for meaningful comparisons to be drawn. Some of the more useful of these and the means by which they can be incorporated into a predictive model will be discussed in Section 16.3.5.

In addition to modifications of the atomic parameters, there are medium-related effects which must be taken into account explicitly. The broken spherical symmetry that normally results when an isolated free gaseous ion is placed in a ligand field gives rise to a splitting of the free-ion level into a maximum of $(2J + 1)$ components. A single-particle crystal field model has had remarkable success for lanthanides and somewhat qualified, but nevertheless satisfactory, success for the trivalent actinides in providing an interpretation of the data [3, 6, 24]. The additional splitting induced by the crystal field can be described by the expression:

$$E_{\mathrm{cf}} = \sum_{k,q,i} B_q^k (C_q^k)_i \tag{16.6}$$

Table 16.1 *Energy level parameters* (cm^{-1}) *for* $An^{3+}:LaCl_3$[a,b].

Parameter	$U^{3+}:LaCl_3$	$Np^{3+}:LaCl_3$	$Pu^{3+}:LaCl_3$	$Am^{3+}:LaCl_3$[c]	$Cm^{3+}:LaCl_3$	$BkCl_3$	$CfCl_3$	$Es^{3+}:LaCl_3$
E_{ave}	19 544	29 989	39 631	53 667	64 125	54 953	49 530	44 709
F^2	39 715 (218)	44 907 (161)	48 670 (154)	51 800	55 109 (129)	57 015 (120)	61 014 (223)	62 766 (273)
F^4	33 537 (302)	36 918 (245)	39 188 (294)	41 440	43 803 (328)	45 698 (165)	44 483 (517)	48 003 (200)
F^6	23 670 (211)	25 766 (221)	27 493 (153)	30 050	32 610 (168)	33 552 (154)	36 168 (323)	35 309 (326)
α	27.6 (0.9)	31.5 (0.3)	29.7 (0.4)	29.0	28.4 (0.8)	29.9 (0.4)	27.7 (0.8)	[20.9]
β	−722 (33)	−740 (18)	−671 (15)	−660	[−650]	[−674]	−681 (41)	[−500]
γ	[1 000]	899 (70)	1 067 (79)	1 000	935 (107)	[913]	1 082 (137)	[700]
ζ	1623(4)	1938(2)	2241(2)	2580	2903(4)	3216(6)	3568(3)	3962(6)
T^2	217 (90)	278 (22)	186 (11)	200	200	200	[300]	[200]
T^3	63 (13)	44 (7)	48 (13)	50	50	40	86 (23)	[50]
T^4	255 (23)	65 (7)	38 (21)	40	40	65 (63)	54 (32)	[50]
T^6	−107 (49)	−361 (18)	−364 (22)	−360	−360	−326 (50)	−350 (57)	[−360]
T^7	617 (78)	434 (22)	364 (15)	390	390	442 (40)	281 (40)	[400]
T^8	[350]	353 (17)	332 (18)	340	340	380	364 (27)	[340]
M^{0}[d]	[0.67]	0.68 (0.17)	0.95 (0.21)	0.99	1.09	1.19	1.3	[1.0]
P^{2}[e]	1 276 (104)	894 (14)	822 (44)	850	922 (37)	523 (73)	578 (60)	825 (184)
B_0^2	260 (64)	163 (26)	226 (25)	230	244 (42)	[250]	476 (36)	363 (101)
B_0^4	−532 (139)	−632 (48)	−543 (48)	−610	−710 (84)	−922 (82)	−1 108 (73)	−1 264 (249)
B_0^6	−1 438 (113)	−1 625 (52)	−1 695 (45)	−1 590	−1 383 (113)	−1 324 (76)	−1 367 (79)	−1 466 (167)
B_6^6	1 025 (88)	1 028 (35)	1 000 (40)	980	929 (77)	910 (44)	963 (63)	749 (124)
No. of levels	51	150	155	–	88	60	90	36
σ[f]	26	20	18	–	27	22	28	33

[a] The data for U^{3+} through Cm^{3+} were obtained in absorption and fluorescence using doped single crystals of $LaCl_3$; while those for Bk^{3+} and Cf^{3+} were measured in absorption with thin films of the pure halide. Preliminary data for Es^{3+} were obtained from excitation spectra of doped single-crystal $LaCl_3$.
[b] Values in square brackets were assigned and were not varied; values in parentheses are the root mean square errors. Data from Ref. 1.
[c] The parameters for Am^{3+} were obtained by extrapolation.
[d] In establishing values for M^0, M^2, and M^4, the following ratios were maintained, $M^2/M^0 = 0.56$ and $M^4/M^0 = 0.38$. When M^0 was varied, the established ratios were maintained constant.
[e] The procedure for establishing values of P^k, $k = 2,4,6$, was identical to that cited above: $P^4/P^2 = 0.75$ and $P^6/P^2 = 0.5$.
[f] σ = mean error (see footnote f of Table 16.4).

where the B_q^k are radial integrals treated as parameters, the C_q^k are tensor operators dependent on the symmetry of the crystal lattice, and the sum over i represents the sum over the electrons. The most extensive investigations of actinide spectra have been carried out for the 3+ actinide ions doped into single-crystal $LaCl_3$, since $LaCl_3$ is a well characterized crystalline matrix in which polarized spectra can be measured. Such investigations, supplemented by Zeeman-effect studies of the influence of applied magnetic fields on the energy levels, provide the basis for experimental characterization of the observed transitions in terms of the free-ion SLJ and crystal field quantum numbers.

The relative energies of some of the low-lying states in U^{3+}:$LaCl_3$ are shown in Fig. 16.5 [30]. As indicated, each free-ion state is split by the crystal electric field. When viewed at the temperature of liquid He (~ 4 K), only transitions from the lowest state (taken as the zero of energy and having a crystal field quantum number $\mu = 5/2$ in this case) are observed. Absorption bands, which are

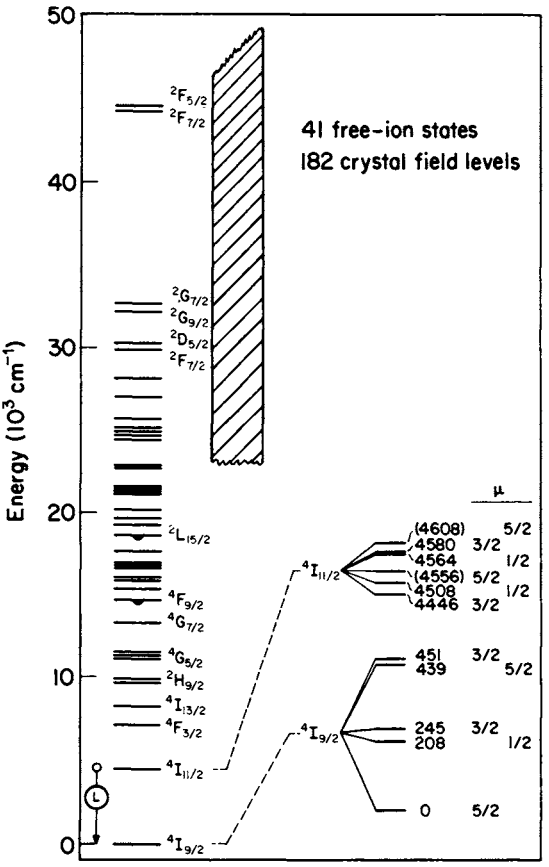

Fig. 16.5 *Energy level structure for* U^{3+}: $LaCl_3$.

interpreted as arising from transitions between the $^4I_{9/2}$ (ground) and $^4I_{11/2}$ excited states, are shown in Fig. 16.6 as obtained at ~ 4 K in moderate resolution. Most of the experimental results that have been reported were photographed using high-resolution grating spectrographs. Transitions to only three levels of $^4I_{11/2}$ were readily observed in absorption; that to a $\mu = 1/2$ state (found by other techniques near 4580 cm^{-1}) was too weak to be apparent. Electric dipole selection rules in this case forbid transitions between the ground ($\mu = 5/2$) and excited ($\mu = 5/2$) states, so levels that would have corresponded to transitions at 4556 and 4608 cm^{-1} had to be established by other experimental methods (fluorescence).

As the energies of the components of various groups are established experimentally, the model free-ion and crystal field parameters that reproduce the splitting can be computed by a suitable (least-squares) fitting procedure. The computed values are then used to predict the splitting patterns in other groups where not all the allowed components can be observed. Thus in the analysis of such spectral data there is a continual interplay between theory and experiment. When large numbers of levels have been experimentally confirmed, most (in some cases, all) of the parameters of the model can be varied simultaneously to establish the final values (Table 16.1).

In typical analyses of actinide and lanthanide spectra in condensed phases, the range of observation may extend well into the near-ultraviolet to 30 000–40 000 cm^{-1}. The number of assignments made to different multiplets and states is usually sufficient to determine most of the energy level parameters. However, as indicated in Figs 16.7 and 16.8, the observations may be limited to less than 50% of the total extent of the f^N configuration. The accuracy of

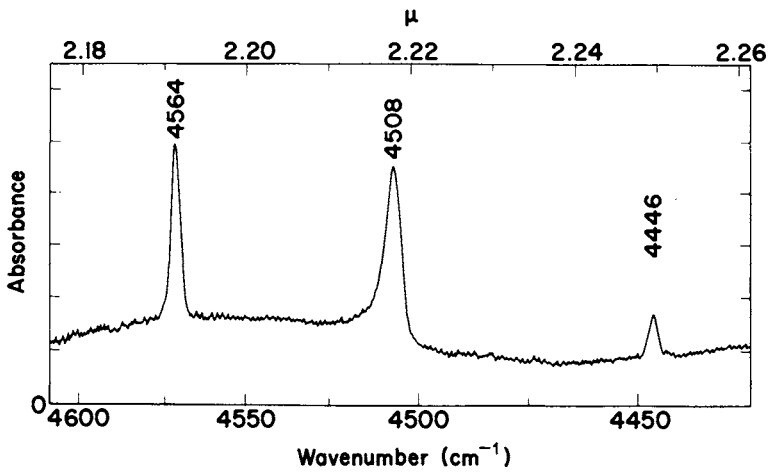

Fig. 16.6 *Observed spectrum of* U^{3+}: $LaCl_3$ *in the range* 4600–4440 cm^{-1} *at* ~ 4 *K.*

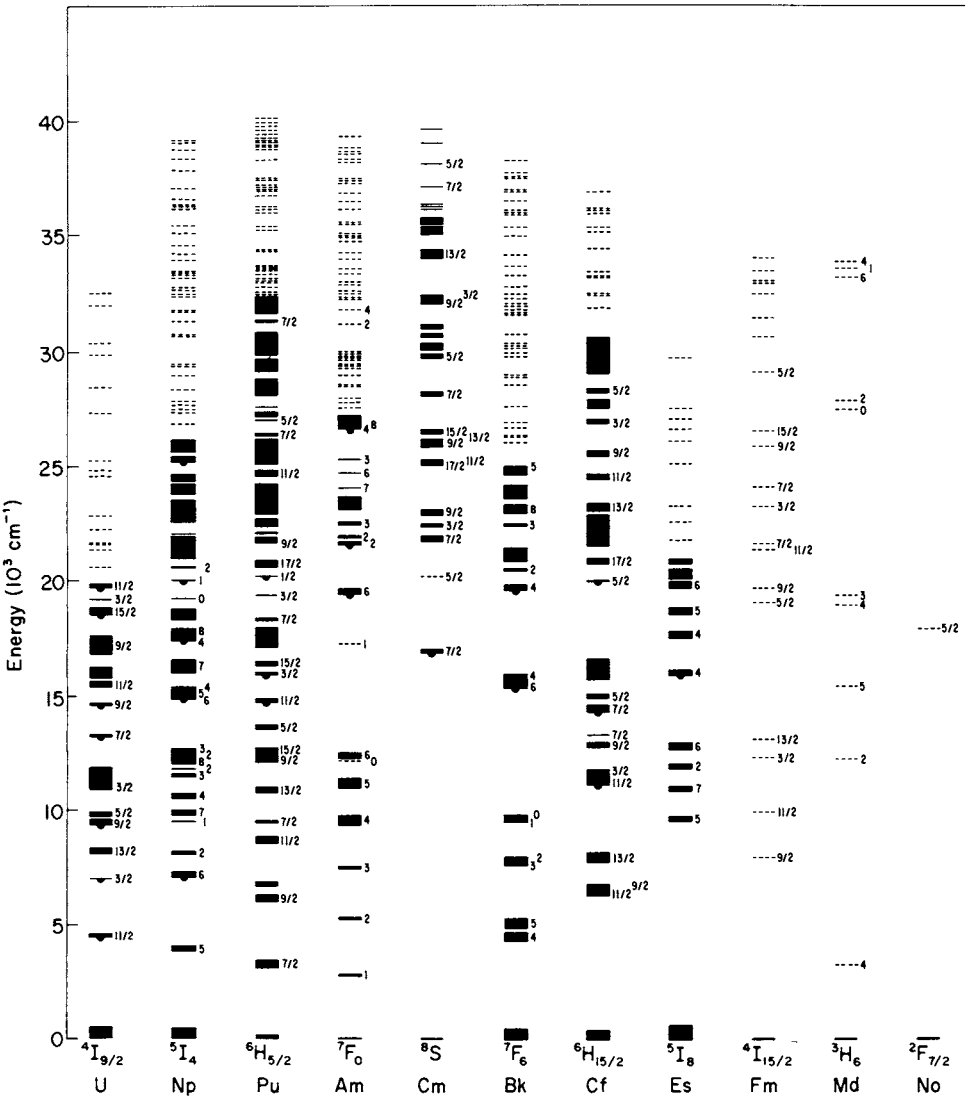

Fig. 16.7 *Free-ion energy level structure for An^{3+}. The approximate extent of the crystal field splitting for certain low-lying levels is indicated.*

predicted level energies in the ultraviolet range clearly remains to be thoroughly tested; however, it was possible to show for $Gd^{3+}:CaF_2$ that parameters based on assignments below 50 000 cm^{-1} predicted very adequately the levels later observed in the vacuum-ultraviolet range above 50 000 cm^{-1} [31].

The reduction in the overall range of energy for transitions characteristic of the $5f^N$ configurations in An^{3+} compared to the $4f^N$ configurations in Ln^{3+} is also

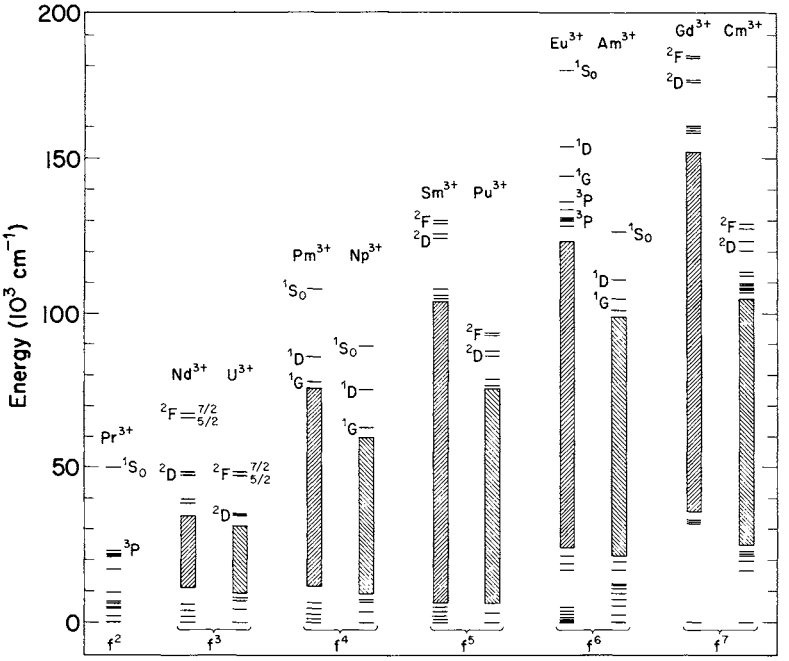

Fig. 16.8 *The computed energy range for the complete $4f^N$ and $5f^N$ configurations for $N = 2$–7.*

indicated in Fig. 16.8. The Slater parameters in An^{3+} are typically only two-thirds as large as those of the Ln^{3+}, but ζ_{5f} is a factor of 2 larger than ζ_{4f}; so while the energy range of the $5f^N$ configurations is reduced, the states are significantly more mixed in character because of the increased spin–orbit interaction.

In discussing Fig. 16.5 it was pointed out that each free-ion state is split by crystal field interactions into a number of components. Assigning energies corresponding to the centers of gravity of these components, thus defining the 'free-ion' levels for the ion in a particular medium, yields the energy level scheme indicated at the left in Fig. 16.5. While the levels are shifted to somewhat lower energies than those of the true gaseous free-ion states, the basic structure appears to be preserved and is usually only moderately changed from medium to medium for trivalent lanthanides and actinides. For example, the center of gravity of the $^4I_{11/2}$ state in U^{3+}: $LaCl_3$ in Fig. 16.6 is $\sim 4544\ cm^{-1}$. An isolated band in U^{3+} (aquo) (Fig. 16.2) near this same energy can be identified similarly. The 'free-ion' states deduced for the 3+ actinides in $LaCl_3$ are shown in Fig. 16.7 with the extent of the observed crystal field splitting indicated where experimental measurements have been made.

While the spectra of several organometallic 3+ actinides (and lanthanides), such as plutonium tricyclopentadienide, have been measured, the analysis of data is still quite incomplete. Nevertheless, it seems apparent that at present the energy

level parameters for such systems can at least be approximated by those characteristic of the actinides in the $LaCl_3$ host [32].

16.3.5 Correlation of free-ion and condensed-phase energy level structures

It was pointed out earlier that, because of the different techniques used in studying condensed-phase and free-ion spectra, the configurations available for direct comparison in the two cases have very little overlap. When crystals or solutions are cooled to near 4 K so that only the lowest (ground) electronic state is populated, the resultant absorption spectrum is directly interpretable in terms of energy levels, and, except for complications of superimposed vibronic bands and the added perturbations of crystal field effects themselves, the analysis can proceed to the study of atomic parameter variations. In free-ion emission studies, on the other hand, many overlapping transition arrays between the multiple configurations displayed in Fig. 16.1 are obtained simultaneously, and one must first disentangle these. This can only be done with the aid of additional tags on the energy levels such as isotope shift, hyperfine structure or Landé g-factor information, which requires in fact that multiple experiments be carried out. Of the many configurational analyses that finally result, most are too heavily involved with s, p and d orbitals for easy comparison with the f-shell cases with which we are concerned here. Nevertheless, with some assistance from theory, cases are available from which a beginning can be made on constructing a useful interpretative and predictive model.

We consider first the analogous lanthanide situation. Nearly all $4f^2$ atomic states are known for the free-ion Pr IV [33, 34], $LaCl_3$-host [35, 36], and LaF_3-host [37–39] Pr^{3+} cases. The corresponding parametric results are given in Table 16.2. This is the only example yet available in either the lanthanides or actinides for which this direct comparison can be made. For this reason we will look at this case a little more closely. Columns 2 (free ion) and 3 ($LaCl_3$ crystal) in the upper part of the table give the parametric results from the approximation we are using in our working model. Comparing the two cases line by line, significant differences can be seen for the major parameters F^k and ζ, and lesser ones for α and β. Any possible differences in the M^k and P^k values are masked by the statistical uncertainties. The parameter shifts attributed to the Pr^{3+} environment are given in column 4 and the relative change of the crystal values, compared to those of the free ion, in column 5. Note that the most important change, nearly 5%, occurs for F^2, and about half of this for F^4, F^6 and ζ. Also α is in the same range, but with less certainty. The most striking change seems to be for β, which shows an *increase* in magnitude of some 10–15%.

The $5f^2$ free-ion configurations are completely known for both Th III [40] and U V [41, 42], but the Th^{2+} condensed-phase analog is not known, and analyzed data for U^{4+} are limited in scope. The $4f^3$ Pr III configuration is nearly completely known [43], but there is no corresponding divalent crystal case for comparison. On the other hand, both the $Nd^{3+}:LaCl_3$ [44] and $U^{3+}:LaCl_3$ [30]

Table 16.2 *Parameter shifts for trivalent ions in $LaCl_3$.*

	Pr IV (cm^{-1})	Pr^{3+}:$LaCl_3$ (cm^{-1})	*Medium shift* (cm^{-1})	*Relative change* (%)
F^2	71822 (41)	68498 (20)	−3324	−4.63 ± 0.08
F^4	51829 (112)	50317 (50)	−1512	−2.92 ± 0.33
F^6	33889 (72)	33127 (38)	−762	−2.25 ± 0.32
α	23939 (322)	22866 (173)	−1073	−4.5 ± 2.1
β	−599 (19)	−678 (9)	−79	+13 ± 5
ζ	766 (3)	749 (1)	−17	−2.0 ± 0.5
M^0	2.0 (0.4)	1.7 (0.2)	0	-
P^2	168 (58)	248 (32)	0	-

	Pu II $5f^5 7s^2$ (*exp.*) (cm^{-1})	Pu IV $5f^5$ (*est.*) (cm^{-1})	Pu^{3+}:$LaCl_3$ (*exp.*) (cm^{-1})	*Medium shift* (cm^{-1})	*Relative change* (%)
F^2	49066 (770)	50015	48670 (154)	−1345 (924)	−2.7 ± 1.8
F^4	39640 (719)	40322	39188 (294)	−1134 (1013)	−2.8 ± 2.5
F^6	26946 (785)	27466	27493 (153)	+27 (938)	+0.1 ± 3.4
ζ	2275 (27)	2305	2241 (2)	−64 (29)	−2.8 ± 1.3

spectra are very well documented, but experimental work for Nd IV and U IV are both incomplete. In fact, except for thorium, there are no doubly or triply ionized actinide free-ion analyses known.

Nevertheless, a few scattered examples exist. Although the parametric analyses are incomplete, enough free-ion data are available in these cases to permit a determination of all or most of the major parameters F^k and ζ. For the actinides, these are all first (neutral) and second (singly ionized) cases, for which, again, no condensed-phase analogs are available. These are U I $5f^4 7s^2$, U II $5f^3 7s^2$, Pu I $5f^6 7s^2$, Pu II $5f^5 7s^2$, and Cf I $5f^{10} 7s^2$, all of which contain the closed shell $7s^2$. If we use the Hartree–Fock [27] results to make corrections for removal of the $7s^2$ shells, we can then infer values for the divalent U III, Pu III, and Cf III, and trivalent U IV and Pu IV. The best example of this is for Pu IV. Comparison of estimated free-ion parameters with the Pu^{3+}:$LaCl_3$ results is also given in Table 16.2. Although the statistical uncertainties are large, the relative changes are consistent with those for Pr^{3+} for the same host.

Since the shifts due to the crystalline environment and those due to the addition of the $7s^2$ shell are nearly the same, it has turned out that, for initial identifications, the crystal absorption lines can be related directly to the free-ion spectral lines themselves, at least in those cases for which the crystal field can be treated in the weak-field approximation.

16.3.6 Luminescence spectra

Several excited states from which luminescence can be observed at low temperatures can be found in most crystal lattices into which the 3+ actinides have been doped. Prominent emitting states for $An^{3+}:LaCl_3$ are indicated in Fig. 16.7 by pendant semicircles. The crystal field structures of the ground state and most of the excited states which occur in the far-infrared range are usually defined via fluorescence measurements.

16.3.7 Actinide lasers

Laser action from an actinide ion, U^{3+}, was reported in 1960, the same year that the first ruby (Cr^{3+} in Al_2O_3) laser was described. Stimulated emission from $U^{3+}:CaF_2$ at 4016 cm^{-1} could be detected even at 25°C [45]. The corresponding transition is indicated in Fig. 16.5. Since that time, a huge literature describing different lasing ions and media has grown up. In the area of solid-state lasers, the rare earths are the dominant activators used; no further successful experiments with actinide ions have been reported. Nevertheless, the similarities in electronic structure of the 3+ lanthanides and actinides suggests that analogies to the demonstrated lasing properties of U^{3+} can probably be found.

The f → d transitions in the 3+ actinides occur at lower energies than in the lanthanides and the 6d appreciably overlaps the 5f configuration. In principle, this should make it possible to pump the intense f → d band with the expectation of rapid non-radiative transfer of energy to the 5f states. However, the presence of strong absorption bands in the ultraviolet range and in some cases low-lying charge-transfer bands increases the probability that intense excited-state absorption with non-radiative relaxation may occur. The net effect is the probable restriction of potential lasing transitions in the 3+ actinides to the infrared region of the spectrum [46].

16.3.8 Intensity calculations for trivalent actinide spectra

A systematic understanding of the energy level structure for An^{3+} serves as a foundation upon which to base the interpretation of other physical measurements. Considerable success has now been achieved in developing a parametrized model of f → f transition intensities.

The intensity of an absorption band can be defined in terms of the area under the band envelope as normalized for concentration of the absorbing ion and the path length of light in the absorbing medium. A proportional quantity, oscillator strength P, has been tabulated for trivalent actinide-ion absorption bands in aqueous solution. The experimentally determined oscillator strengths of transitions can in turn be related to the mechanisms by which light is absorbed [47]:

$$P = \frac{8\pi^2 mc\sigma}{3he^2(2J+1)}(\chi\bar{F}^2 + n\bar{M}^2) \tag{16.7}$$

where $\bar{F}$ and $\bar{M}$ are respectively the matrix elements of the electric dipole and magnetic dipole operators joining the initial state J to a final state J', $\chi = (n^2+2)^2/9n$ and n is the refractive index, σ is the energy of the transition (cm^{-1}), and the other symbols have their usual meaning.

Only a few transitions observed for the 3+ actinides have any significant magnetic dipole character; however, the matrix elements of $\bar{M}^2$ can be evaluated directly from the knowledge of the eigenvectors of the initial (ψJ) and final ($\psi' J'$) states. The Judd–Ofelt theory [48, 49] has successfully addressed the problem of computing the matrix elements of $\bar{F}^2$, and can be written in the form:

$$\bar{F}^2 = e^2 \sum_{k=2,4,6} \Omega_k (\psi J \| \mathbf{U}^{(k)} \| \psi' J')^2 \tag{16.8}$$

where $\mathbf{U}^{(k)}$ is a unit tensor operator of rank k, the sum running over the three values $k = 2, 4, 6$, and Ω_k are three parameters which in practice are evaluated from measured band intensities. These parameters involve the radial parts of the f^N wavefunctions, the wavefunctions of perturbing configurations such as $5f^{N-1}6d$, and the interaction between the central ion and the immediate environment.

Judd was able to show both that the theory could successfully reproduce the observed intensities of bands throughout the optical range for Nd^{3+} (aquo) and Er^{3+} (aquo), and that intensity parameters Ω_k computed from first principles were consistent with those derived in fitting experimental data [48]. Later systematic treatments of the intensities observed in the spectra of all Ln^{3+} (aquo) ions have confirmed and extended the original correlation [50, 51]. Recently it was found that a similar systematic treatment of band intensities for An^{3+} (aquo) spectra could be successfully carried out with only Ω_4 and Ω_6 treated as variables [52]. The emphasis on aquo-ion spectra stems from the ability to identify many relatively isolated bands with single or very limited numbers of SLJ states, the corresponding unambiguous quantitative nature of the oscillator-strength calculation, and the wide range of data available, i.e. most members of the 4f and 5f series can be readily obtained as trivalent aquo ions in dilute acid solution. Intensity correlations for Ln^{3+} in a great many different host crystals, as well as in vapor complexes, have been developed. For the actinides, systematic and quantitative examination of transition intensities is presently restricted to An^{3+} (aquo).

Examination of Figs 16.2 and 16.7 shows that, particularly for U^{3+}, Np^{3+}, and Pu^{3+}, the density of states is high and few of the observed aquo-ion bands can be uniquely identified. Both the relative intensities of observed transitions and the density of states decrease in magnitude with increasing atomic number. Starting with Cm^{3+} (aquo), the heavy-actinide aquo-ion spectra are all amenable to intensity analysis with excellent correlation found between observed oscillator strengths and intensities computed using the Judd parametrization [53]. While the oscillator strengths of An^{3+} (aquo) bands tend to be a factor of 10–100 greater than those observed for the lanthanides, one of the most striking features in

Fig. 16.2 is the change in intensity across the actinide series. Starting with Bk^{3+} (aquo), there is an apparent transition to a heavy-lanthanide-like character in the spectra, with no bands being disproportionately intense. Analysis reveals that the trends in the intensity parameter values over the series can be correlated with the extent to which higher-lying opposite-parity configurations like $f^{N-1}d$ are mixed into the f^N configuration. There is much less mixing of $f^{N-1}d$ states into $5f^8$ (Bk^{3+}) than in $5f^3$ (U^{3+}) even though the proximity of the $f^{N-1}d$ to the f^N configuration is very similar in these two cases. An example of the type of correlation obtained between experiment and theory for An^{3+} (aquo) is given for Cm^{3+} (aquo) in Fig. 16.9 [54].

16.3.9 Fluorescence lifetimes

One reason for the interest in computing absorption intensity correlations is that, once the parameters of the Judd–Ofelt theory are evaluated, they can be used to compute the radiative lifetime of any excited state of interest via the Einstein expression

$$A(\psi J, \psi' J') = \frac{64\pi^2\sigma^3}{3h(2J+1)}(\chi' \bar{F}^2 + n^3 \bar{M}^2) \tag{16.9}$$

where $|\psi J\rangle$ and $|\psi' J'\rangle$ are the initial and final states, A is the rate of relaxation of ΨJ by radiative processes, and $\bar{F}^2$ and $\bar{M}^2$ are the terms defined in equation (16.7). The observed lifetime of a particular excited state, τ_T, is usually determined by *non*-radiative rather than radiative relaxation mechanisms. Thus we write

$$(\tau_T)^{-1} = A_T(\psi J) + W(\psi J) \tag{16.10}$$

where $A_T(\psi J)$ is the total *radiative* relaxation rate from state $|\psi J\rangle$, that is, the sum of the rates of radiative decay to all states with energy less than that of $|\psi J\rangle$. If τ_R(calc) is the (computed) total *radiative* lifetime of $|\psi J\rangle$, then $\tau_R(\text{calc}) = [A(\psi J)]^{-1}$. Similarly, $W_T(\psi J)$ is a total rate summed over all *non-radiative* relaxation processes. The magnitude of the energy gap between a fluorescing state and the next lower-energy state appears to play a major role in determining the non-radiative lifetime of that state; shorter lifetimes are correlated with narrower gaps.

On the basis of the existence of relatively large energy gaps in the spectra of some of the heavier actinides (Fig. 16.7), experiments were initiated and fluorescence lifetimes were successfully measured in solution for excited states in Bk^{3+} and Es^{3+} [55], as well as Cm^{3+} (aquo) [56]. As indicated in Fig. 16.10, which shows the lower energy level structure for the heavier An^{3+} (aquo) ions, only in the case of Cm^{3+} (aquo) does the observed lifetime of 0.94 ms in D_2O compare well with the computed radiative lifetime, $\tau_R = 1.3$ ms. With smaller energy gaps, the non-radiative relaxation rate clearly becomes rate-determining. Inability to observe a fluorescing state for Cf^{3+} (aquo) in preliminary experiments suggests that lifetimes may be in the nanosecond time range [55].

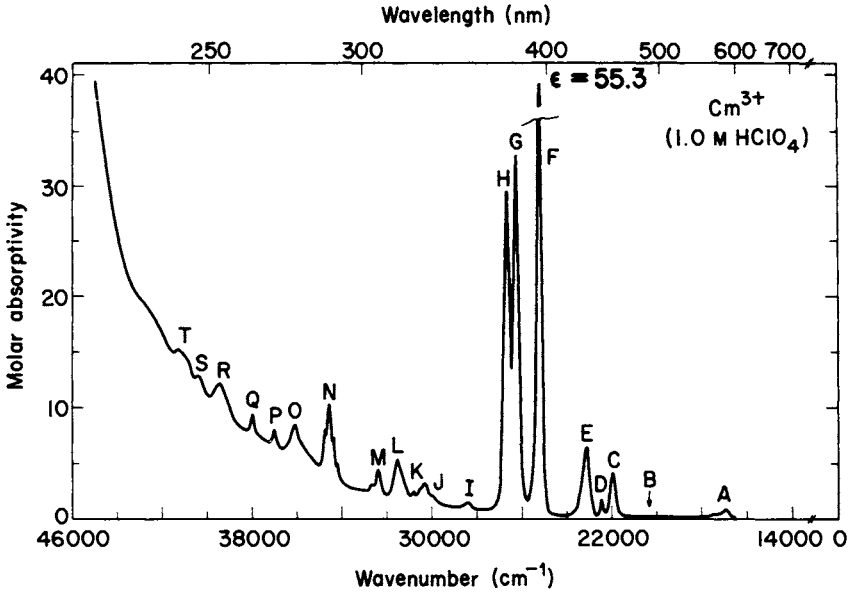

Band	$2J$	$E(cm^{-1})$ Center	$P \times 10^6$ (Obs.)	$P \times 10^6$ (Calc.)	Band	$2J$	$E(cm^{-1})$ Center	$P \times 10^6$ (Obs.)	$P \times 10^6$ (Calc.)
A	7	17095	1.6	2.0 E D 0.2 M D	N	13	34540	12	8.4
B	5	20350	0.4	0.6 E D 0.2 M D	O	17 7 11 9 13 1	35800	4.0	6.0
C	7	21955	5.7	4.7					
D	3	22435	0.7	0.01					
E	9	23120	11	10	P	7	37010	1.2	0.3
F	17 11	25250	49	52	Q	5	37995	2.0	0.6
G	9 13	26225	40	37	R	15 3 13 5 9	39400	~ 10	5.1
H	15	26630	35	34					
I	7	28370	1.0	2.0					
J	5	30030	1.1	1.1	S	11 7	40300	~ 1.6	0.44
K	7 5 3	30550	3.6	4.3	T	5 9 15 11	41100	~ 10	1.8
L	11	31500	8.2	9.5					
M	9 3	32500	3.2	5.3	R.M.S. deviation = 1.9×10^{-6}				

Fig. 16.9 *Absorption spectrum and intensity analysis for* Cm^{3+} *(aquo), Ref. 54. (ED = electric dipole; HD = magnetic dipole.)*

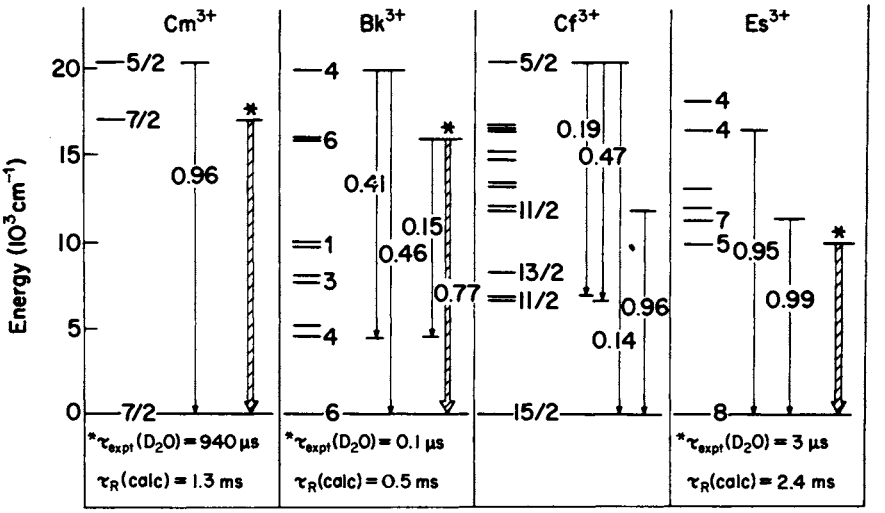

Fig. 16.10 *Energy level schemes and selected branching ratios for radiative relaxation for* Cm^{3+} *through* Es^{3+}.

In addition to computing radiative lifetimes, it is instructive to establish the most probable pathway for fluorescence from a given state. Thus the branching ratio, β_R, from a given relaxing state to a particular final state is

$$\beta_R(\psi J, \psi' J') = \frac{A(\psi J, \psi' J')}{A_T(\psi J)} \tag{16.11}$$

As indicated in Fig. 16.10 for Cf^{3+}, $\beta_R = 0.47$ for emission from an excited ($J = 5/2$) state to a lower-lying ($J = 11/2$) state, while $\beta_R = 0.14$ for emission to the ground state. In the case of the $J = 5/2$ state, it would be appropriate to monitor for fluorescence near 13 000 cm^{-1} as well as near 20 000 cm^{-1}.

The identification of the mechanisms of non-radiative relaxation of actinide ions in solution as well as in solids [57] remains an important area for research. Extensive experimental results for lanthanide systems are available for comparison with those obtained for actinide ions. It should be possible to explore sensitively bonding differences between selected actinides and lanthanides by examining their excited-state relaxation behavior.

16.4 SPECTRA AND ELECTRONIC STRUCTURE IN THE 2+, 4+, AND HIGHER VALENCE STATES OF THE ACTINIDES

While spectra of actinide compounds and solutions exhibiting other than the 3+ valence state are well known, systematic analyses of the electronic structure in other valence states are very tentative at present. Extensive experimental analysis

is limited to a few isolated cases. However, tabulations of electrostatic [25] and spin–orbit integrals [58], computed using *ab initio* methods, have been published, and the relative energies of electronic configurations occurring within the usual spectral range of interest to chemists have been estimated from free-ion spectra [20].

The electrostatic and spin–orbit interactions in any given valence state are expected to vary systematically across the series. However, in the trivalent series it was necessary to introduce effective operators to screen explicitly for the effects of configuration interaction in order to obtain good correlation with experiment. In the absence of these correction terms the values of the Slater integrals obtained in fitting data exhibited a much more erratic behavior when plotted as a function of Z. As we consider the 2+, 4+, and higher-valent actinides, the role of second-order correction terms has not been studied in detail. What is clear is that the importance both of spin–orbit coupling and of the crystal field interaction relative to the electrostatic interaction increases with increasing valence.

One of the reasons for introducing the theoretical interpretation of trivalent spectra in some detail was to provide the basis for discussing models appropriate to other valence states. While detailed models are yet to be constructed, and may lead to revision of some of the values given here, it is felt advantageous to introduce a generalizing element into the discussion and relate available spectra to this central theme rather than approach each different actinide ion as a unique entity.

In outline, the theoretical model that has been introduced has the following form (similar to equation (16.2)):

$$H' = H_e + H_{corr} + H_{so} + H_{cf} = H_{ec} + H_{so} + H_{cf} \tag{16.12}$$

where $H_{ec} \equiv H_e + H_{corr}$, H_{cf} represents the crystal field interaction, and other terms are defined in equation (16.2). For An^{3+} it was shown that $E_{ec} > E_{so} \gg E_{cf}$. It will be shown that for An^{2+} the interactions appear to be of the same relative magnitude as for An^{3+}; however for An^{4+} and An^{5+} the crystal field interaction becomes, relatively, much more important, and extraction of well defined parameters for the interactions contained in the three parts E_{ec}, E_{so}, and E_{cf} becomes more difficult. In An^{3+} spectra the correction terms H_{corr} act mainly on H_e, although some provision for second-order magnetic effects is included. We assume that it is not necessary to modify the magnitudes of the terms associated with H_{corr} in treating other valence states. Since E_{cf} is computed using a single-particle model, corrections to E_{cf} may be required as the relative magnitude of the crystal field increases.

16.4.1 Model calculation of atomic parameters

In early attempts to develop a systematic interpretation of trivalent actinide and lanthanide spectra, initial sets of F^k and ζ_{nf} for some members of the series had to be estimated. This was done by linear extrapolation based on the fitted

parameters that were available from the analyses of other individual spectra. As more extensive data and improved modeling yielded better determined and more consistent F^k and ζ_{nf} values for the 3+ actinides (and lanthanides), it became apparent that the variation in the parameters was non-linear, as indicated for $F^2(5f, 5f)$ in Fig. 16.11. This non-linearity could also be observed in the parameter values of the *ab initio* calculations. The difference between the *ab initio* and fitted values of parameters (ΔP) appears to exhibit a much more linear variation with Z than the parameter values themselves. Consequently, ΔP has been adopted as the basis for a useful predictive model [4, 24].

For the trivalent actinides the values of ΔP are not constant over the series, but use of a single average value over a group of four or five elements is not an unreasonable approximation. Thus, in developing a predictive model for the F^k and ζ_{nf} parameters, an attempt is made to establish average values of ΔP for a particular valence state and type of crystal field interaction. The energy level structure computation based on the predicted parameters can be compared to that observed, and then appropriate modifications sought by a fitting procedure where necessary.

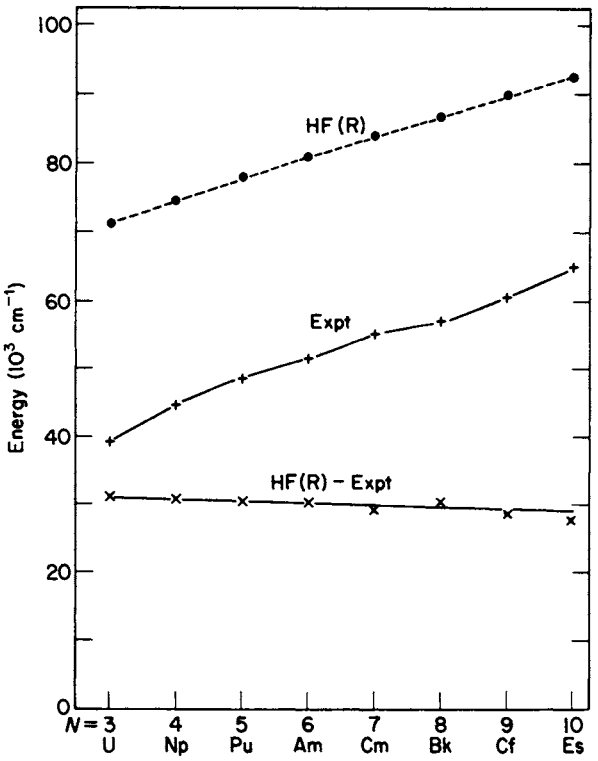

Fig. 16.11 *Comparison of F^2 calculated by HFR method, F^2 found by fitting to experimental data, and their difference, ΔE, for An^{3+}.*

16.4.2 Divalent actinide-ion spectra

Efforts to prepare divalent actinide compounds and analyze their spectra have been less successful than was the case for the lanthanides, where the divalent ion for each member of the series could be stabilized in CaF_2 [59]. In both $Am^{2+}:CaF_2$ and $Es^{2+}:CaF_2$ [60–63], intense absorption bands were observed. They could be attributed to either $f \rightarrow d$ or charge-transfer transitions. The presence of divalent actinide ions in these cases was established by measurements of the electron paramagnetic resonance spectra, not on the basis of the observed optical spectra. In contrast to the more intense absorption bands reported for $Es^{2+}:CaF_2$, weak absorption bands consistent with the intensities expected for $f \rightarrow f$ transitions were identified in the 10 000–20 000 cm^{-1} region in both $EsCl_2$ and $Es^{2+}:LaCl_3$ [64]. The relatively narrow band structure exhibited by the Es^{2+} halides was also found to be characteristic of the Cf^{2+} halides [65, 66].

While it was not possible to stabilize Cm^{2+} in CaF_2 under the same conditions that yielded evidence for Am^{2+} and Es^{2+}, evidence for the formation of both Am^{2+} and Cm^{2+} has been obtained in solution in pulse radiolysis studies; however, as in the spectrum of $Am^{2+}:CaF_2$, the absorption bands were broad and intense. The nature of the absorption process is therefore not clear. A charge-transfer process cannot be excluded [67].

Since the available spectroscopic results for divalent actinides are fragmentary, we adopt a consistent interpretation which accounts for all observations and predicts the energies of other bands that might be accessible to observation. The basic aspects of the required tentative model can be deduced in part from available data for divalent lanthanide spectra.

The free-ion spectra of Ce III and Pr IV are known. Initial estimates of F^k and ζ_{4f} values appropriate to Ln^{2+} in condensed phases can be made by assuming that the change observed in these parameters for iso-f-electron couples such as Ce III/Pr IV (both $4f^2$) will also be characteristic of the couple Ce^{2+}/Pr^{3+} in condensed phases. This suggests a reduction of 20–30 % in comparing values of F^k and ζ_{4f} for divalent compared to isoelectronic trivalent-ion cases. If we compare the results for $Eu^{2+}:CaF_2$ [68] with those for $Gd^{3+}:LaF_3$ [69], the parameters for Eu^{2+} ($4f^7$) are about 82–86 % of those for Gd^{3+} ($4f^7$). The little information available on divalent lanthanide-ion crystal field splitting [3] suggested that the crystal field interaction was even smaller than for the trivalent case. This was also suggested in the recent analysis of Eu^{2+} [68].

Based on the small crystal field splitting indicated for the divalent lanthanides, it is reasonable to assume as a first approximation that corresponding actinide crystal field splitting will be small. Although fragmentary, spectroscopic data available for An^{2+} appear to be consistent with this estimate. The initial model can consequently be limited to free-ion considerations. The initial F^k and ζ_{5f} parameters for An^{2+} may be estimated to be 85–90 % of those for the iso-f-electronic $An^{3+}:LaCl_3$ ion. The effects of configuration interaction for An^{3+} can be taken to approximate those for An^{2+}. The resulting model energy level

schemes for An^{2+} are plotted in Fig. 16.12 where the overlap of the $5f^{N-1}6d$ and $5f^N$ configurations [20] is also indicated.

Examining the range of energies in which f → f transitions might be observed, we see from the figure that the largest 'optical windows' are expected in Am^{2+}, Cf^{2+}, and Es^{2+}. In Np^{2+}, Pu^{2+}, Cm^{2+}, and Bk^{2+}, it is probable that f → f transitions will only be observed in the infrared range. This of course assumes that the $5f^N$ is consistently the ground configuration. Transitions resulting from the promotion f → d would be expected to result in intense (allowed) absorption bands such as those observed in Ln^{2+} spectra [59]. The much weaker f → f transitions occurring in the same energy range as the allowed transitions would be masked, so the optical windows correspond to the energy range below the first allowed transition. As in the An^{3+} spectra, the first allowed transition for An^{2+} in a condensed phase would be expected to occur at an energy somewhat lower than that for the gaseous free-ion f → d transition energies indicated in Fig. 16.12 [20]. The computed level structures for Cf^{2+} and Es^{2+} are in agreement with the experimental results, but indicate the existence of bands not yet reported.

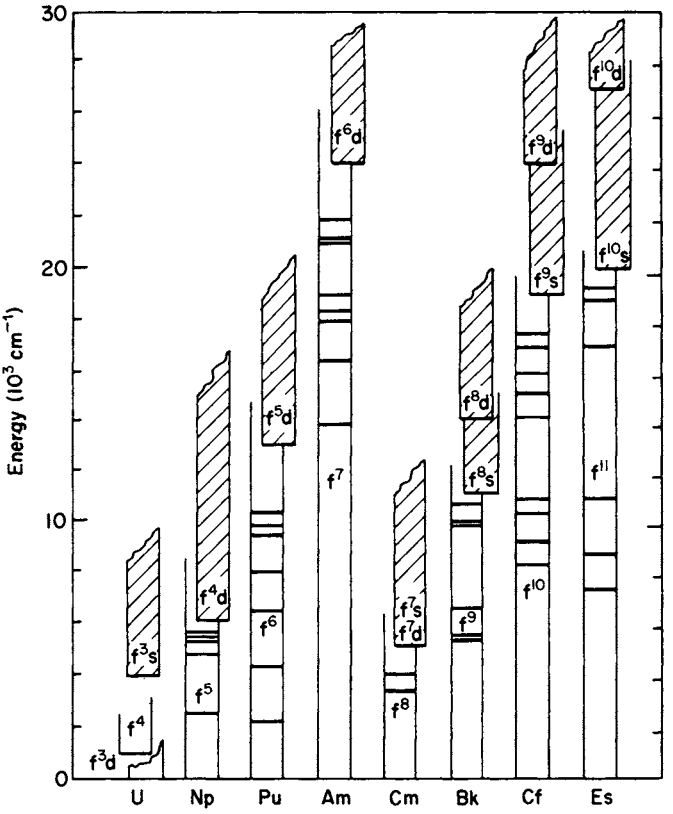

Fig. 16.12 *Estimated ranges of energies in which 5f → 5f transitions in An^{2+} may be experimentally observed.*

Systematic energy level calculations are of considerable importance in predicting the energies at which fluorescence might be observed. In general, the longest-lived fluorescence will originate in a state with the largest energy gap between it and the next lower-energy state. Based on the computed large energy gap between the ground ($^8S_{7/2}$) and first excited ($^6P_{7/2}$) states in Am^{2+} ($5f^7$), isolated Am^{2+} sites would be expected to exhibit fluorescence near 14 000 cm^{-1}.

16.4.3 Quadrivalent actinide-ion spectra

The absorption spectra of tetravalent actinides in a number of different solvents as well as in solid compounds have been reported. Structure characteristic of $f \rightarrow f$ transitions has been observed throughout the optical range. The observations are consistent with trends indicated in Fig. 16.1 which suggest that transitions to the $f^{N-1}d$ configurations in An V will lie even higher in energy relative to the lowest-energy f^N state than in the corresponding transitions for An IV. The lowest $f \rightarrow d$ transition in the atomic spectrum of U V was placed at 59 183 cm^{-1} [41]. Consequently, broad intense band structure in the spectra of An(IV) compounds beginning near 40 000–45 000 cm^{-1} would be consistent with the onset of $f \rightarrow d$ transitions. The energy level structure of the U V ($5f^2$) configuration provides a valuable basis for comparison in developing the analysis of An^{4+} spectra in solids.

Analyses of the spectra of U^{4+} in both high-symmetry (O_h) and relatively low-symmetry (D_{2d} and D_2) sites have been published. Somewhat in contrast to observations made with trivalent ions, the magnitude of the crystal field splitting in the two cases differs significantly. An example of the high-symmetry case is that of U^{4+} in Cs_2UCl_6 [70, 71]. The low-symmetry (D_{2d}) case is illustrated in the analysis of $U^{4+}:ThBr_4$ [72]. The crystal field splitting in the Cs_2UCl_6 is over twice as large as that in $U^{4+}:ThBr_4$. As a result, a much more complex structure with states of different J values in close proximity occurs within a given energy range in Cs_2UCl_6 compared to the $U^{4+}:ThBr_4$ case.

The extensive analysis of the data for $U^{4+}:ThBr_4$ and the similar crystal field parameters deduced for $Pa^{4+}:ThCl_4$ [73] have provided a new basis for examining other An^{4+} spectra. As Auzel and co-workers have shown [74], band intensities in the spectrum of U^{4+} (aquo) can now be understood in terms of crystal-field-split SLJ levels similar to those deduced for $U^{4+}:ThBr_4$, whereas such an analysis would not be consistent with the larger crystal field splitting deduced for U^{4+} in Cs_2UCl_6. Comparison of U(IV) spectra in aqueous solution and in molten LiCl–KCl eutectic with that for single crystals of Cs_2UCl_6 had earlier led Gruen and McBeth [75] to suggest a change from eight-fold to six-fold coordination as the basis for the contrasting spectroscopic results.

If we examine the spectra of U^{3+} (aquo) and Np^{4+} (aquo), both $5f^3$ ions (Fig. 16.13), we can interpret the apparent similarities in the band structure based on the analysis of U^{4+}(aquo) cited above. If the crystal field splitting in both cases is relatively small, then the apparent shift of corresponding band structure to higher

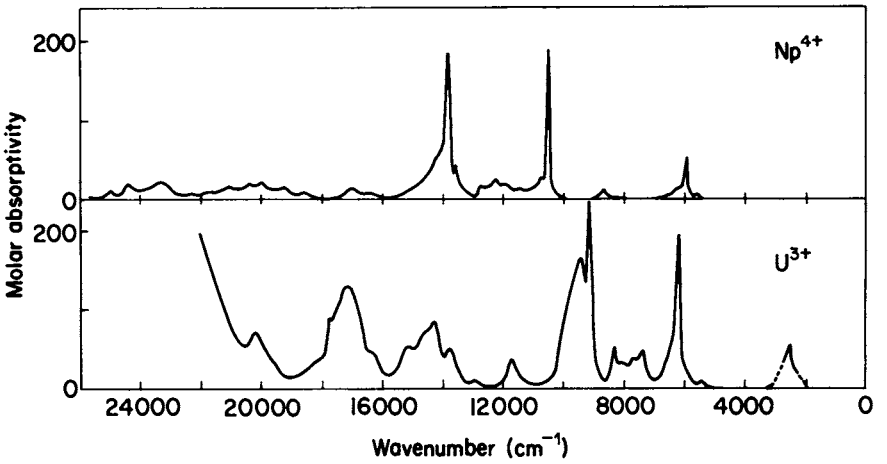

Fig. 16.13 *Solution absorption spectra of* Np^{4+} *(aquo) and* U^{3+} *(aquo).*

energies in Np^{4+} (aquo) compared to U^{3+}(aquo) is consistent with an expected greater electrostatic and spin–orbit interaction in the Np^{4+} case. Using the method of extrapolation discussed in Section 16.4.1, energy level parameters that are consistent with those for Pa^{4+}:$ThCl_4$ and U^{4+}:$ThBr_4$ can be extrapolated to obtain a set for Np^{4+}, and we find a good correlation between this energy level structure and the band structure observed for Np^{4+} (aquo). That the apparent correlation between band structure observed for iso-f-electronic An^{4+} (aquo) and An^{3+}(aquo) ions continues along the series is evident in comparing the spectra of Pu^{4+}(aquo) and Np^{3+} (aquo) (Fig. 16.14). Jørgensen called attention to this apparent correlation in the band structure observed for iso-f-electronic An^{3+} and

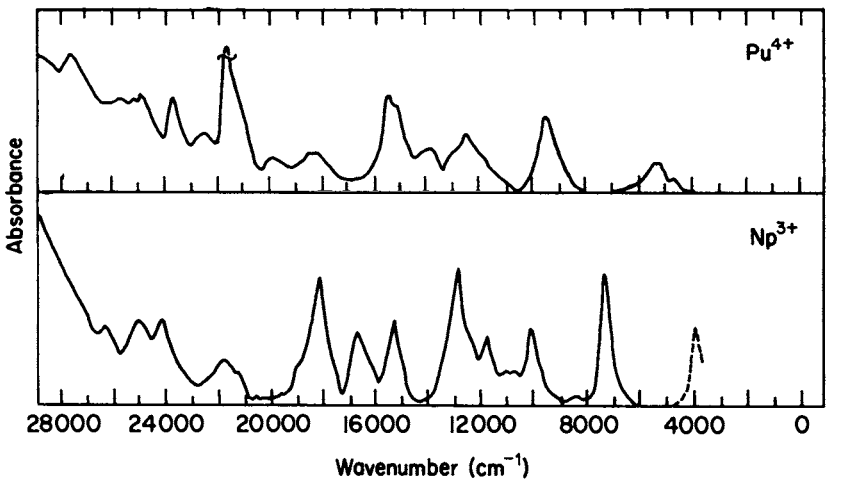

Fig. 16.14 *Solution absorption spectra of* Pu^{4+} *(aquo) and* Np^{3+} *(aquo).*

An^{4+} spectra at a time when little was known about the extent of the ligand fields involved [76]. Concern that the data for An^{4+} (aquo) should be interpreted in terms of large ligand field splitting characteristic of Cs_2UCl_6 instead of a weaker-field case may have been partially responsible for the slow pace in exploration of Jørgensen's insight. Of course, development of this An^{3+}/An^{4+} spectral correlation also required an understanding of the energy level structures in An^{3+}, which was not well understood in 1959. If we adopt the electrostatic and spin–orbit parameters for $U^{4+}:ThBr_4$ as a basis for estimating parameters for the An^{4+} ions, the general character of the spectra of all of the An^{4+} ions indicated in Fig. 16.15 can be interpreted. For an earlier estimate see Conway [77].

In solid compounds such as Cs_2UCl_6, where the 4+ ions occupy sites of inversion symmetry, the observed structure is almost exclusively vibronic in character, as contrasted with the electronic transitions characteristic of 3+ compounds. The electronic origins were deduced from progressions in the vibronic structure, since the electronic transitions themselves were symmetry-forbidden. An analysis of the intensities of vibronic bands has been reported [78, 79]. Other extensive analyses of the spectra of U^{4+} in crystalline hosts include those for $U^{4+}:ZrSiO_4$ [80, 81]. It is remarkable that in studies of the 4+ actinides, fluorescence from a U^{4+} compound has only been established for U^{4+} in the $ThBr_4$ host [82]. The fluorescence of Np^{4+} in both $ThCl_4$ and $ThBr_4$ has also been reported [83].

16.4.4 Spectra of actinide ions in the V, VI, and VII valence states

The actinide ions with well defined valence states greater than IV are confined to the light half of the 5f series. A large number of stable compounds are known, and spectra have been recorded in solutions, in solids, and in the gas phase. However, there have been relatively few attempts to develop detailed energy level analyses.

While Hartree–Fock type calculations of F^k and ζ_{5f} can be carried out for any arbitrary state of ionization of an actinide ion, the relative importance of the ligand (or crystal) field must also be established in order to develop a correlation to experimentally observed transition energies. *Ab initio* models of the ligand field are characteristically very crude. The spectra of penta- and higher-valent actinides are strong-crystal-field cases and the development of correction terms for the first-order crystal field model may well be essential to any detailed analysis.

Two types of ionic structure are normally encountered in the higher-valent species: the actinyl ions AnO_2^+ and AnO_2^{2+}, and halides such as UCl_5, $CsUF_6$, and PuF_6. Mixed oxohalide complexes are also known. In the actinyl ions (An=U, Np, Pu, Am) the axial field imposed by the two nearest-neighbor (-yl) oxygen atoms plays a dominant role in determining the observed energy level structure [84, 85]. The analysis of spectra of higher-valent actinide halides is also based on a strong ligand field interaction, but the symmetry is frequently found to be octahedral or distorted octahedral [86–89].

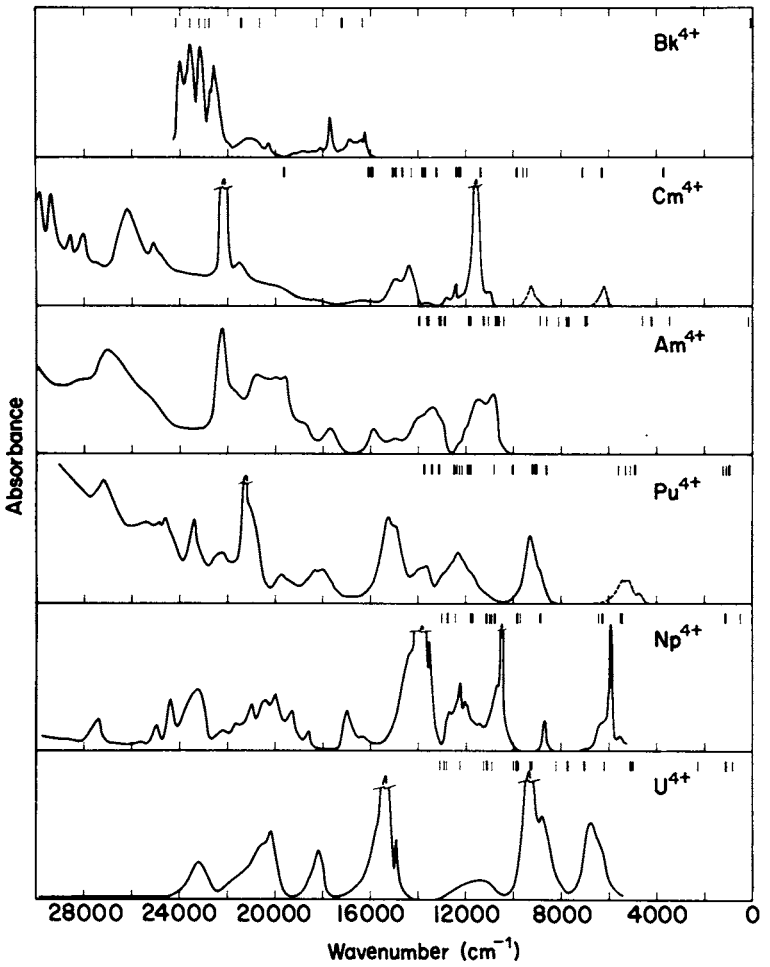

Fig. 16.15 *Absorption spectra of the quadrivalent actinide ions. Aquo-ion spectra are indicated for* U^{4+}, Np^{4+}, *and* Pu^{4+}, *while the spectra of* Am^{4+}, Cm^{4+}, *and* Bk^{4+} *are of solid* AnF_4 *samples* [112]. *Estimated free-ion energy level structure is shown for first few excited states. (See discussion in Section* 16.4.3.)

Typical iso-f-electronic penta- and higher-valent actinide species are shown in Table 16.3, where X is a halide ion.

Aqueous-solution spectra characteristic of the NpO_2^+ and PuO_2^{2+} ions, both having the $5f^2$ electronic structure, are shown in Fig. 16.16. Some qualitative similarities in band patterns for these iso-f-electronic ions appear to exist, but detailed analysis of the observed structure in terms of a predictive model is tentative. Electron-transfer bands for NpO_2^+, PuO_2^+, and AmO_2^+ apparently lie at such high energies that they have not been reported, but this type of transition in NpO_2^{2+} (20 800 cm^{-1}), PuO_2^{2+} (19 000 cm^{-1}), and AmO_2^{2+} ($\sim$ 18 000 cm^{-1})

Table 16.3 *Some iso-f-electronic penta- and higher-valent actinide species.*[a]

Number of 5f electrons =	0	1	2	3	4
	UO_2^{2+} Np(VII) UF_6 UCl_6	UO_2^{+} NpO_2^{2+} Pu(VII) NpF_6 UX_6^{-} UF_5	PuO_2^{2+} NpO_2^{+} PuF_6 NpX_6^{-}	AmO_2^{2+} PuO_2^{+} PuX_6^{-}	AmO_2^{+}

[a] X = halide ion.

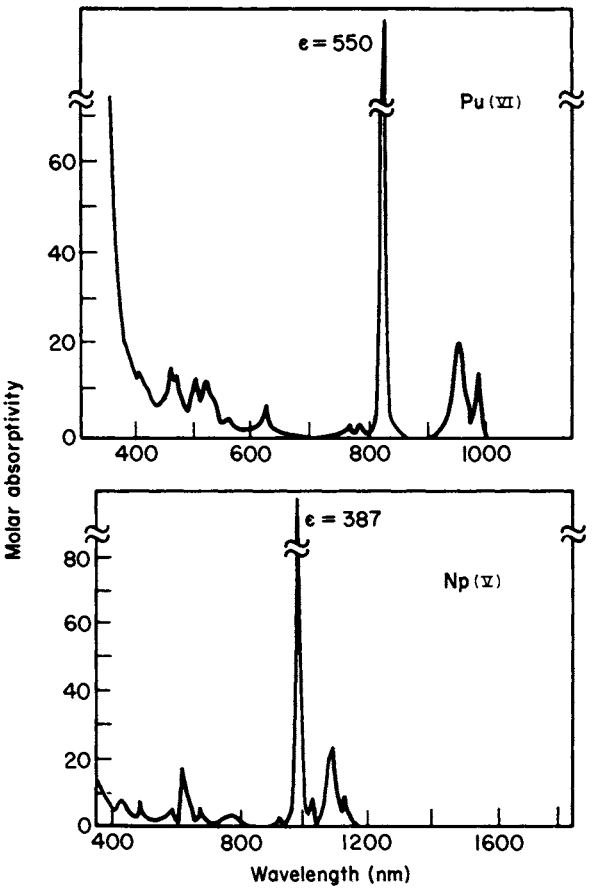

Fig. 16.16 *Aqueous solution absorption spectra of* PuO_2^{2+} *(Pu(VI)) and* NpO_2^{+} *(Np(V)).*

has been identified [90]. Spectra of all of the actinyl ions and the molar absorptivities of the more intense bands in aqueous solution have been tabulated [16].

Attempts to interpret the spectra of the penta- and hexahalides of the actinides have been published, but the results should be considered preliminary; only U(v) and Np(vi), both $5f^1$, have been analyzed in any detail. The magnitude of the spin–orbit interaction is known for U VI. Its free-ion spectrum has been interpreted in terms of a coupling constant, $\zeta_{5f} = 2173.9\,cm^{-1}$, based on a $^2F_{5/2} \rightarrow {}^2F_{7/2}$ energy difference of $7608.6\,cm^{-1}$ [91].

The spectra of a number of complex U(v) halide compounds appear in the literature and, based on representative crystallographic determinations, the site symmetry is usually shown to be approximately octahedral. The combined effect of the spin–orbit and octahedral ligand field interactions is to split the parent ^2F state into five components whose irreducible double group labels are indicated in Fig. 16.17.

The energy level structures of several actinide(iv), (v), and (vi) compounds with the $5f^1$ configuration are compared in Table 16.4. The ligand field parameters in such analyses are sometimes reported in terms of Δ and Θ, linear combinations of the normal fourth- and sixth-degree crystal field potential terms B_0^4 and B_0^6, together with the so-called orbital reduction factors k and k' [84, 92]. The orbital reduction factors provide a basis for discussing the covalency of the bonding. As indicated in Table 16.4, the fitting of parameters to spectra for several U(v) compounds has resulted in a spin–orbit parameter of approximately $2200\,cm^{-1}$, consistent with the free-ion results for U VI. However, there has been considerable variation in the ligand field parameters deduced by different investigators from absorption spectra in which the energies of observed features are surprisingly consistent. Attempts have been made to analyze the spectra using

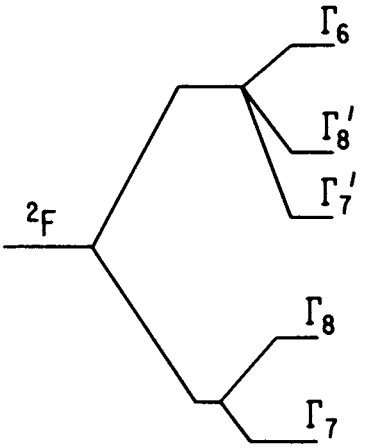

Fig. 16.17 *Energy level diagram for a $5f^1$ configuration in an octahedral crystal field.*

Table 16.4 *Energy level structures and parameters (cm^{-1}) for An(IV), (V), and (VI) compounds.*

	$(5f^1)$ $(NEt_4)_2PaCl_6$[a]		$(5f^1)$ $(NEt_4)UCl_6$[a,b]		$(5f^1)$ $(NEt_4)UBr_6$[b,c]	
	Exp.	*Calc.*	*Exp.*	*Calc.*	*Exp.*	*Calc.*
Γ_7	0	0	0	0	0	0
Γ_8	(1730)	1799	–	3649	3670	3715
$\Gamma_{7'}$	5330	5434	6801	7157	6831	7022
$\Gamma_{8'}$	7022	7026	9950 10450 (10190)	10154	9435 9805 (9668)	9627
Γ_6	8011	8079	11470	11742	10605	10736
ζ		1554 (15)	1913[a]	(1913)	2197[c]	1761 (31)
Δ[d]			2936[a]		51[c]	
Θ[d]			3371[a]		5676[c]	
k					0.79[c]	
k'					0.32[c]	
B_0^4[e]		6503 (169)		12209 (710)		10953 (350)
B_0^6		480.8 (188)		39 (776)		−1058 (274)
σ[f]		60		266		123

	$(5f^1)$ UCl_5[g]			$(5f^1)$ $CsUF_6$[h,i]		
	Obs.		*Calc.* (O_h)[e]	*Calc.* (O_h)[e]	*Obs.*	*Calc.* (D_{3d})[j]
Γ_7	0		0	0	0	0
Γ_8	4300		4174	5151	5150 (5105 5206)	5086 5212
$\Gamma_{7'}$	6643		6413	7399	7399	7390
$\Gamma_{8'}$	8970 9772	9371	9643	13122	13128 (12850 13405)	12865 13370
Γ_6	11665		11218	15807	15798	15840
ζ			1559 (115)	1914.6 (2)		1910.2 (13)
B_0^2						534.2 (139)
B_0^4			13479 (1125)	21292 (17)		−14866 (66)
B_0^6			−158.6 (745)	2265 (10)		3305 (78)
σ[f]			370	57		33

	$(5f^1)$ NpF_6[k]		$(5f^2)$	$(5f^3)$
	Obs.	*Calc.* (O_h)[e]	$CsNpF_6$[i]	$CsPuF_6$[i]
Γ_7	0	−18		
Γ_8	7711	7690		
Γ'_7	9515	9563		
Γ'_8	23548	23500		
Γ_6	28000	27912		

Table 16.4 (*Contd.*)

	$(5f^1)$ NpF_6 [k]		$(5f^2)$ $CsNpF_6$ [i]	$(5f^3)$ $CsPuF_6$ [i]
	Obs.	*Calc.* (O_h)[e]		
F^2			48920	51760
F^4			42300	44200
F^6			27700	29120
ζ		2448.4 (33)	2200	2510
α			30000	30000
β			−660	−660
γ			700	700
B_0^2			534.2	543.2
B_0^4		44553 (211)	−14866	−14866
B_0^6		7992 (105)	3305	3305
σ [f]		73		

[a] Ref. 92. The Γ_8 state was assigned at 1730 cm^{-1} based on estimates from other studies.
[b] Ref. 99.
[c] Ref. 89.
[d] $\Theta = \frac{8}{33}(B_0^4 + \frac{35}{13}B_0^6)$ $\Delta = \frac{2}{33}(5B_0^4 - \frac{210}{13}B_0^6)$.
[e] Crystal field parameters in O_h symmetry were computed with the ratios $B_4^4/B_0^4 = 0.598$, $B_4^6/B_0^6 = -1.870$ fixed.
[f] Deviation $\sigma = \Sigma(\Delta i^2/n-p)^{1/2}$ where Δi is the difference between observed and calculated energies, n is the number of levels used in the fitting procedure, and p is the number of parameters freely varied.
[g] Ref. 94.
[h] Experimental results from present study differ from those of ref. 96; see ref. 99.
[i] Estimated parameters cited in text. In addition to those parameters tabulated, the following were included: $P^2 = 500$, $P^4 = P^6 = 0$ (for both $CsNpF_6$ and $CsPuF_6$); $T^2 = 200$, $T^3 = 50$, $T^4 = 100$, $T^6 = -300$, $T^7 = 400$, $T^8 = 350$ for $CsPuF_6$ only.
[j] Crystal field parameters in D_{3d} symmetry referred to the C_3 axis: $B_0^4(C_3 \text{ axis}) = -\frac{7}{9}B_0^4(C_4 \text{ axis})$, $B_0^6(C_3 \text{ axis}) = \frac{16}{9}B_0^6(C_4 \text{ axis})$. Thus, referred to the C_4 axis, the parameters for $CsUF_6$ would be: $B_0^2 = 534.2$, $B_0^4 = 22299$, $B_0^6 = 1859$. The fixed ratios for D_{3d} were $B_3^4/B_0^4 = 1.125$, $B_3^6/B_0^6 = -1.0$, $B_6^6/B_0^6 = 0.704$.
[k] Ref. 86.

a lower-symmetry (D_{3d}, C_{2v}) ligand field, but the increase in the number of adjustable parameters makes it necessary to introduce other approximations.

The case of UCl_5, which has a dimeric structure that gives rise to approximate octahedral U(v) sites, is particularly interesting because the spectra of solutions (UCl_5 in $SOCl_2$) [93], of single crystals [94], and of the vapor phase, $(UCl_5)_2$ or $UCl_5 \cdot AlCl_3$ [95], all give absorption features that are very similar in both the relative intensities of the transitions and their energies. The absorption spectrum of $UCl_5 \cdot AlCl_3$ in the vapor phase at 596 K [95] is shown in Fig. 16.18, and can be compared with the computed levels for UCl_5 (Table 16.4). The importance of the nearest-neighbor coordination sphere in determining the spectra, essentially to the exclusion of the effects of long-range order, is consistent with the behavior expected for strong octahedral bonding. However, more evidence is needed to

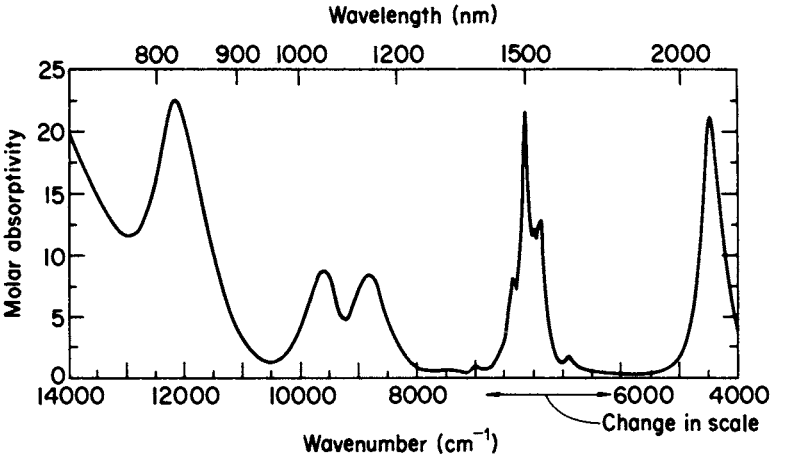

Fig. 16.18 *Absorption spectrum of the $UCl_5 \cdot AlCl_3$ vapor complex at 596 K, from ref. 95.*

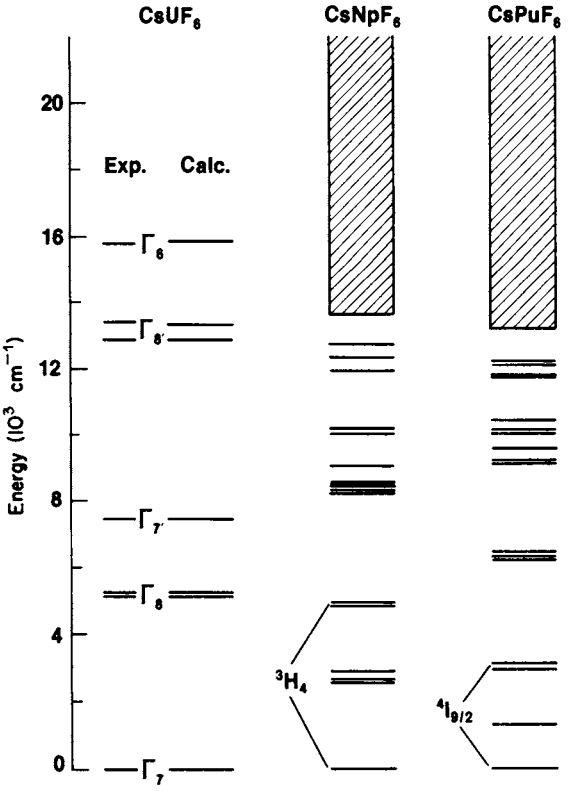

Fig. 16.19 *Computed energy level schemes for $CsUF_6$, $CsNpF_6$, and $CsPuF_6$. Experimental results for $CsUF_6$ from Table 16.4. The cross-hatched areas indicate that a relatively dense energy structure is predicted.*

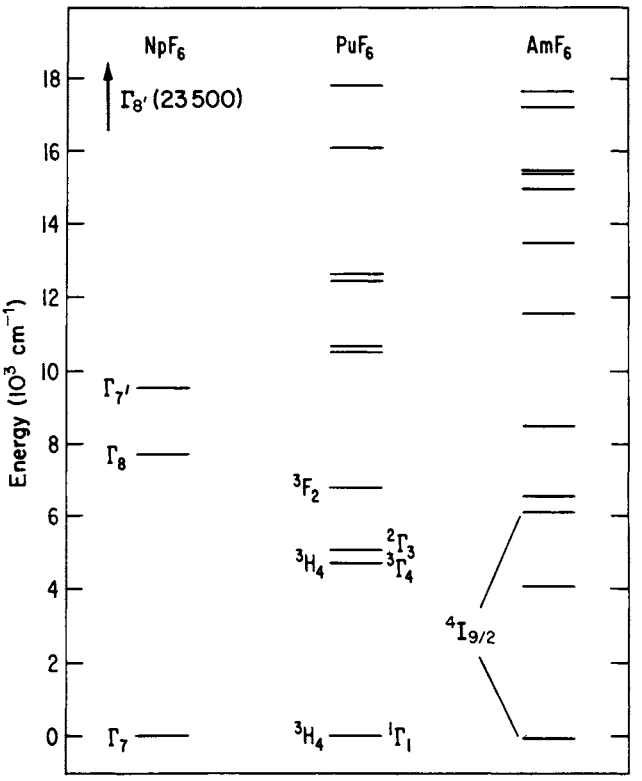

Fig. 16.20 *Computed energy level schemes for NpF_6, PuF_6, and AmF_6.*

justify the assignments and to establish uniquely the limits within which the ligand field parameters may vary.

The spectra of $CsUF_6$ [96] and $CsNpF_6$ [97] have been reported and analyzed, and that of $CsPuF_6$ has been measured [98]. However, the treatment of $CsUF_6$, which has been considered to be a model for other cases of distorted octahedral symmetry, has been questioned both on experimental [99] and theoretical grounds. Both Leung [100] and Soulie [101] have pointed out that there is actually a very significant distortion of the O_h symmetry originally assumed for $CsUF_6$ [96], with a D_{3d} symmetry providing the basis for a much improved interpretation. If we use electrostatic interaction parameters of the same order of magnitude as those suggested by Poon and Newman [102] for $CsNpF_6$, together with D_{3d} ligand field parameters for $CsUF_6$, and further extrapolate these results to provide values for the $CsPuF_6$ case, the resulting energy level structure is that indicated in Fig. 16.19. The general aspects of this predicted structure appear to be consistent with available experimental data. Aside from the structure of the ground state, we expect to observe a relatively isolated $^3F_2$ state in $CsNpF_6$. However, with the exception of this $^3F_2$ state, neither the spectrum of $CsNpF_6$ nor that of $CsPuF_6$ is expected to exhibit any extensive, easily recognizable band

structure. A relatively high density of excited states is predicted and detailed analysis can be expected to be difficult.

The actinide hexafluorides, UF_6, NpF_6, and PuF_6, form a unique group of volatile molecular species. They are not regarded as strongly bonded since the metal–fluorine distances tend to be rather large ($\sim$ 1.98 Å) [103]. The combination of well characterized spectroscopic [86] and magnetic [104] results for NpF_6 has served to establish a reasonable basis for the energy level analysis in octahedral symmetry summarized in Table 16.4. A consistent set of F^k and ζ 5f parameters can be combined with the crystal field for NpF_6 to yield an estimate of the parameter sets for PuF_6 and AmF_6. The energies of some of the lower-lying states in NpF_6, PuF_6, and AmF_6 computed with estimated parameters are shown in Fig. 16.20. The indicated structure is consistent with the principal features in the absorption spectrum of PuF_6 [88] (Fig. 16.21). Detection of fluorescence in the selective excitation of NpF_6 and PuF_6 and at energies in agreement with the energy gaps between the predicted ground and first excited states in both spectra was recently reported [105].

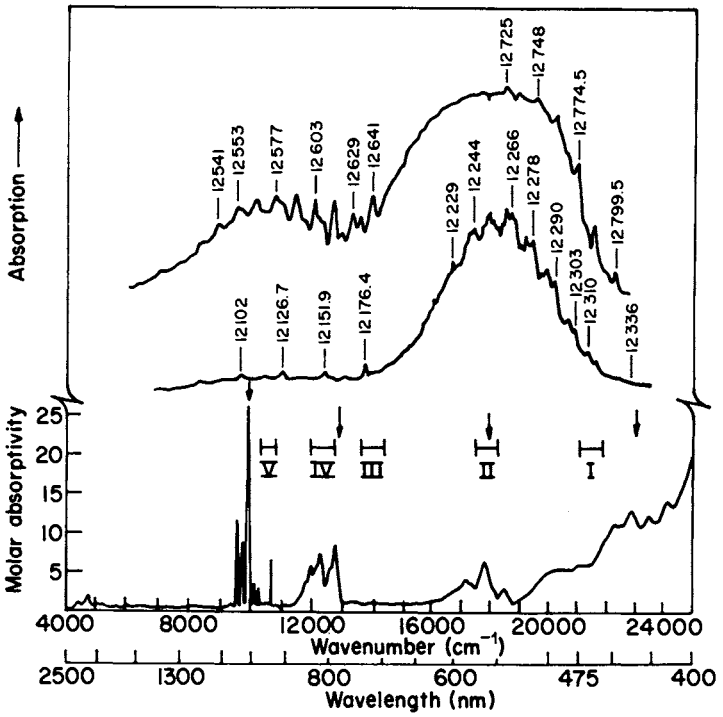

Fig. 16.21 *The absorption spectrum of* PuF_6 *(g). Arrows indicate regions reported to show vibrational structure. Bars indicate regions examined by intracavity laser absorption: I,* 455–470*; II,* 550–574*; III,* 697–729*; IV,* 786–845*; V,* 918–971 *nm. At the top is a densitometer trace of the high-resolution absorption spectrum of* PuF_6 *in the* 781–830 *nm region obtained in multipass experiments. Data from ref.* 88.

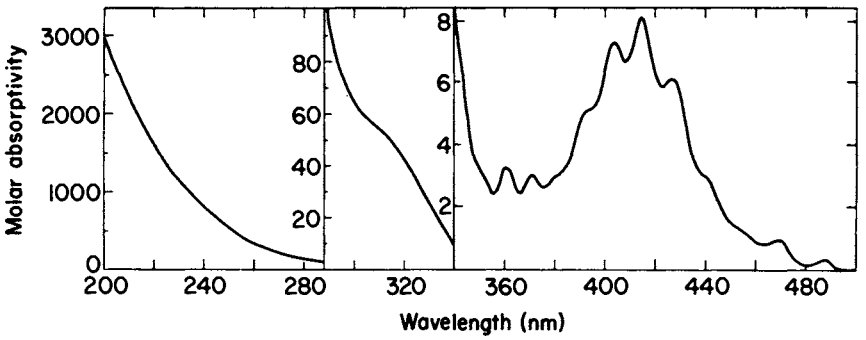

Fig. 16.22 *The absorption spectrum of* UO_2^{2+} *in* 1 M $HClO_4$.

The spectra of UO_2^{2+}, UF_6, and Np(VII) are atypical of the actinide series since, in contrast to the transitions between states within the f^N configuration which characterize most of the actinide spectra discussed in previous sections, the above species contain no f electrons in open shells. Yet spectra of UO_2^{2+} compounds with a characteristic structure limited to the visible–ultraviolet range below 400 nm (Fig. 16.22) are probably more extensively reported than those of any other actinide species. The transitions in this class of spectra are interpreted in terms of molecular-orbital states, and extensive analyses of crystal spectra such as that for $Cs_2UO_2Cl_4$ are now available [106]. For the closely related case of NpO_2^{2+} doped into single-crystal $Cs_2UO_2Cl_4$, detailed spectroscopic studies have identified a single electronic transition belonging to the $5f^1$ configuration, but the other structure observed is similar in origin to that reported for U(VI), i.e. transitions to molecular-orbital states [107–109]. Extensive analyses of the absorption and fluorescence spectra of UF_6 have been published, and are covered in a recent review [110]. In the visible–near-ultraviolet range, the character of the spectrum is similar to that of UO_2^{2+}.

REFERENCES

1. Carnall, W. T. and Crosswhite, H. M. (1985) Argonne National Laboratory Report ANL- 84–90.
2. Contract number W-31-109-ENG-38.
3. Dieke, G. H. (1968) in *Spectra and Energy Levels of Rare Earth Ions in Crystals* (ed. H. M. Crosswhite and H. Crosswhite), Wiley, New York.
4. Crosswhite, H. M. and Crosswhite, H. (1984) *J. Opt. Soc. Am. B*, **1**, 246–54.
5. Wybourne, B. G. (1965) *Spectroscopic Properties of the Rare Earths*, Interscience, New York.
6. Hüfner, S. (1978) *Optical Spectra of Transparent Rare Earth Compounds*, Academic Press, New York.
7. Goldschmidt, Z. B. (1978) in *Handbook on the Physics and Chemistry of Rare Earths*, vol. 1 (eds K. A. Gschneidner Jr and L. Eyring), North-Holland, New York, pp. 1–171.

8. Fred, M. (1967) *Lanthanide/Actinide Chemistry* (ACS Adv. Chem. Ser. no. 71), American Chemical Society, Washington DC, pp. 180–202.
9. Fred, M. and Blaise, J. (1986) this volume, ch. 15.
10. Trees, R. E. (1964) *J. Opt. Soc. Am.*, **54**, 651–7.
11. Judd, B. R. (1966) *Phys. Rev.*, **141**, 4–15.
12. Judd, B. R., Crosswhite, H. M., and Crosswhite, H. (1968) *Phys. Rev.*, **169**, 130–8.
13. Poon, Y. M. and Newman, D. J. (1983) *J. Phys. B: At. Mol. Phys.*, **16**, 2093–101.
14. Judd, B. R. and Crosswhite, H. (1984) *J. Opt. Soc. Am. B*, **1**, 255–60.
15. Judd, B. R. and Suskin, M. A. (1984) *J. Opt. Soc. Am. B*, **1**, 261–5.
16. Carnall, W. T. (1971) in *Gmelin Handbuch der Anorganischen Chemie*, vol. **71**, Gmelin Institute, p. 120.
17. Crosswhite, H. M. (1982) in *Gmelin Handbuch der Anorganischen Chemie*, 8th edn, *Uranium Supplement*, vol. A5, Springer-Verlag, New York, pp. 1–68.
18. Blaise, J., Fred, M. S., Carnall, W. T., Crosswhite, H. M., and Crosswhite, H. (1983) *Plutonium Chemistry* (ACS Symp. Ser. no. 216), American Chemical Society, Washington DC, pp. 173–98.
19. Brewer, L. (1971) *J. Opt. Soc. Am.*, **61**, 1101–11.
20. Brewer, L. (1971) *J. Opt. Soc. Am.*, **61**, 1666–82.
21. Brewer, L. (1983) in *Systematics and the Properties of the Lanthanides*, NATO ASI Series (ed. S. P. Sinha), Reidel, Boston, pp. 17–63.
22. Jørgensen, C. K. (1962) *Absorption Spectra and Chemical Bonding in Complexes*, Pergamon Press, London.
23. Rajnak, K. and Wybourne, B. G. (1963) *Phys. Rev.*, **132**, 280–90.
24. Crosswhite, H. M. (1977) *Colloq. Int. CNRS, Spectroscopie des Elements de Transition et des Elements Lourds dans les Solides*, 28 June–3 July 1976, Editions du CNRS, Paris, pp. 65–69.
25. Varga, L. P., Brown, J. D., Reisfeld, M. J., and Cowan, R. D. (1970) *J. Chem. Phys.*, **52**, 4233–41.
26. Fischer, C. F. (1969) *Comput. Phys. Commun.*, **1**, 151–66.
27. Cowan, R. D. and Griffin, C. D. (1976) *J. Opt. Soc. Am.*, **66**, 1010–14.
28. Casimir, H. (1931) *Proc. K. Akad. Wet. Amsterdam*, **34**, 844.
29. Morrison, J. C. (1972) *Phys. Rev. A*, **6**, 643–50.
30. Crosswhite, H. M., Crosswhite, H., Carnall, W. T., and Paszek, A. P. (1980) *J. Chem. Phys.*, **72**, 5103–17.
31. Crosswhite, H. M., Schwiesow, R. L., and Carnall, W. T. (1969) *J. Chem. Phys.*, **50**, 5032–3.
32. Carnall, W. T. (1979) in *Organometallics of the f-Elements* (eds T. J. Marks and R. D. Fischer), Reidel, Boston.
33. Sugar, J. (1965) *Phys. Rev. Lett.*, **14**, 731–2; *J. Opt. Soc. Am.*, **55**, 1058–61.
34. Crosswhite, H. M, Dieke, G. H., and Carter, W. J. (1965) *J. Chem. Phys.*, **43**, 2047–54.
35. Rana, R. S. and Kaseta, F. W. (1983) *J. Chem. Phys.*, **79**, 5280.
36. Rana, R. S., Cordero-Montalvo, C. D., and Bloembergen, N. (1984) *J. Chem. Phys.*, **81**, 2951–2.
37. Carnall, W. T., Fields, P. R., and Sarup, R. (1969) *J. Chem. Phys.*, **51**, 2587.
38. Yen, W. M., Levey, C. G., Shikua Huang, and Shui T. Lai (1981) *J. Lumin.*, **24/25**, 6597.
39. Cordero-Montalvo, C. D. and Bloembergen, N. (1984) *Phys. Rev. B, Rapid Commun.*, **31**, 613.

40. deBruin, T. L., Klinkenberg, P. F. A., and Schuutmans, Ph. (1941) *Z. Phys.*, **118**, 58–87.
41. Wyart, J. F., Kaufman, V., and Sugar, J. (1980) *Phys. Scr.*, **22**, 389–96.
42. Van Deurzen, C. H. H., Rajnak, K., and Conway, J. G. (1984) *J. Opt. Soc. Am. B*, **1**, 45–7.
43. Sugar, J. (1963) *J. Opt. Soc. Am.*, **53**, 831–5.
44. Crosswhite, H. M., Crosswhite, H., Kaseta, F. W., and Sarup, R. (1976) *J. Chem. Phys.*, **64**, 1981–5.
45. Sorokin, P. P. and Stevenson, M. J. (1960) *Phys. Rev. Lett.*, **5**, 557–9.
46. Weber, M. J. (1980) *Lanthanide and Actinide Chemistry and Spectroscopy* (ACS Symp. Ser. no. 131), American Chemical Society, Washington DC, pp. 275–311.
47. Condon, E. U. and Shortley, G. H. (1963) *The Theory of Atomic Spectra*, Cambridge University Press, Cambridge.
48. Judd, B. R. (1962) *Phys. Rev.*, **127**, 750.
49. Ofelt, G. S. (1962) *J. Chem. Phys.*, **37**, 511.
50. Carnall, W. T., Fields, P. R., and Rajnak, K. (1968) *J. Chem. Phys.*, **49**, 4412.
51. Carnall, W. T. (1979) in *Handbook on the Physics and Chemistry of Rare Earths*, vol. 3 (eds K. A. Gschneidner Jr and L. Eyring), North-Holland, New York.
52. Carnall, W. T., Beitz, J. V., and Crosswhite, H. (1984) *J. Chem. Phys.*, **80**, 2301–8.
53. Carnall, W. T., Beitz, J. V., Crosswhite, H., Rajnak, K., and Mann, J. B. (1983) in *Systematics and the Properties of the Lanthanides*, NATO ASI Series (ed. S. P. Sinha), Reidel, Boston, pp. 389–448.
54. Carnall, W. T. and Rajnak, K. (1975) *J. Chem. Phys.*, **63**, 3510–14.
55. Beitz, J. V., Carnall, W. T., and Wester, D. W. (1981) Lawrence Berkeley Laboratory Report LBL-12441, pp. 108–10.
56. Beitz, J. V. and Hessler, J. P. (1980) *Nucl. Technol.*, **51**, 169–77.
57. Hessler, J. P., Brundage, R. T., Hegarty, J., and Yen, W. M. (1980) *Opt. Lett.*, **5**, 348–50.
58. Lewis, W. B., Mann, J. B., Liberman, D. A., and Cromer, D. T. (1970) *J. Chem. Phys.*, **53**, 809–20.
59. McClure, D. S. and Kiss, Z. (1963) *J. Chem. Phys.*, **39**, 3251–7.
60. Edelstein, N., Easley, W., and McLaughlin, R. (1966) *J. Chem. Phys.*, **44**, 3130–4.
61. Edelstein, N., Easley, W., and McLaughlin, R. (1967) *Lanthanide/Actinide Chemistry* (ACS Adv. Chem. Ser. no. 71), American Chemical Society, Washington DC, pp. 203–10.
62. Baybarz, R. D., Asprey, L. B., Strouse, C. E., and Fukushima, E. (1972) *J. Inorg. Nucl. Chem.*, **34**, 3427–31.
63. Edelstein, N., Conway, J. G., Fujita, D., Kolbe, W., and McLaughlin, R. (1970) *J. Chem. Phys.*, **52**, 6425–6.
64. Fellows, R. L., Peterson, J. R., Young, J. P., and Haire, R. G. (1978) *The Rare Earths in Modern Science and Technology* (eds G. J. McCarthy and J. J. Ryne), Plenum, New York, pp. 493–9.
65. Peterson, J. R., Fellows, R. L., Young, J. P., and Haire, R. G. (1977) *Radiochem. Radioanal. Lett.*, **31**, 277–82.
66. Wild, J. F., Hulet, E. K., Lougheed, R. W., Hayes, W. N., Peterson, J. R., Fellows, R. L., and Young, J. P. (1978) *J. Inorg. Nucl. Chem.*, **40**, 811–16.
67. Sullivan, J. C., Gordon, S., Mulac, W. A., Schmidt, K. H., Cohen, D., and Sjoblom, R. (1976) *Inorg. Nucl. Chem. Lett.*, **12**, 599–601.

68. Downer, M. C., Cordero-Montalvo, C. D., and Crosswhite, H. (1983) *Phys. Rev. B*, **28**, 4931–43.
69. Carnall, W. T., Fields, P. R., and Sarup, R. (1971) *J. Chem. Phys.*, **54**, 1476.
70. Johnston, D. R., Satten, R. A., Schreiber, C. L., and Wong, E. Y. (1966) *J. Chem. Phys.*, **44**, 3141–3.
71. Johnston, D. R., Satten, R. A., and Wong, E. (1966) *J. Chem. Phys.*, **44**, 687–91.
72. Delamoye, P., Rajnak, K., Genet, M., and Edelstein, N. (1983) *Phys. Rev. B*, **28**, 4923.
73. Krupa, J. C., Hubert, S., Foyentin, M., Gamp, E., and Edelstein, N. (1983) *J. Chem. Phys.*, **78**, 2175–9.
74. Auzel, F., Hubert, S., Delamoye, P., and Hussonnois, M. (1982) *J. Lumin.*, **26**, 251–62.
75. Gruen, D. M. and McBeth, R. L. (1959) *J. Inorg. Nucl. Chem.*, **9**, 290–301.
76. Jørgensen, C. K. (1959) *Mol. Phys.*, **2**, 96–108.
77. Conway, J. G. (1964) *J. Chem. Phys.*, **41**, 904–5.
78. Satten, R. A., Schreiber, C. L., and Wong, E. Y. (1983) *J. Chem. Phys.*, **78**, 79–87.
79. Reid, M. F. and Richardson, F. S. (1984) *Mol. Phys.*, **51**, 1077.
80. Richman, I., Kisliuk, P., and Wong, E. Y. (1967) *Phys. Rev.*, **155**, 262–7.
81. Mackey, D. J., Runciman, W. A., and Vance, E. R. (1975) *Phys. Rev. B*, **11**, 211–18.
82. Delamoye, P., Hubert, S., Hussonnois, M., Krupa, J. C., Genet, M., Guillaumont, R., Naud, C., and Parrot, R. (1979) *J. Lumin.*, **18/19**, 76–80.
83. Gruber, J. B. and Menzel, E. R. (1969) *J. Chem. Phys.*, **50**, 3772–4.
84. Eisenstein, J. C. and Pryce, M. H. L. (1966) *J. Res. NBS*, **70A**, 165–76.
85. Bell, J. T. (1969) *J. Inorg. Nucl. Chem.*, **31**, 703–10.
86. Goodman, G. L. and Fred, M. (1959) *J. Chem. Phys.*, **30**, 849–50.
87. Eisenstein, J. C. and Pryce, M. H. L. (1960) *Proc. R. Soc. A*, **255**, 181–98.
88. Kugel, R., Williams, C., Fred, M., Malm, J. G., Carnall, W. T., Hindman, J. C., Childs, W. J., and Goodman, L. S. (1976) *J. Chem. Phys.*, **65**, 3486–92.
89. Eichberger, K. and Lux, F. (1980) *Ber. Bunsenges. Phys. Chem.*, **84**, 800–7.
90. Jørgensen, C. K. (1970) *Prog. Inorg. Chem.*, **12**, 101–52.
91. Kaufman, V. and Radziemski, L. J. (1976) *J. Opt. Soc. Am.*, **66**, 599–601.
92. Edelstein, N., Brown, D., and Whittaker, B. (1974) *Inorg. Chem.*, **13**, 563.
93. Karraker, D. G. (1964) *Inorg. Chem.*, **3**, 1618–22.
94. Leung, A. F. and Poon, Y.-M. (1977) *Can. J. Phys.*, **55**, 937–42.
95. Gruen, D. M. and McBeth, R. L. (1969) *Inorg. Chem.*, **8**, 2625.
96. Reisfeld, M. J. and Crosby, G. A. (1965) *Inorg. Chem.*, **4**, 65–70.
97. Hecht, H. G., Varga, L. P., Lewis, W. B., and Boring, A. M. (1979) *J. Chem. Phys.*, **70**, 101–8.
98. Morss, L. R., Williams, C. W., and Carnall, W. T. (1983) *Plutonium Chemistry* (ACS Symp. Ser. no. 216), American Chemical Society, Washington DC, pp. 199–210.
99. Ryan, J. L. (1971) *J. Inorg. Nucl. Chem.*, **33**, 153–77.
100. Leung, A. F. (1977) *J. Phys. Chem. Solids*, **38**, 529–32.
101. Soulie, E. (1978) *J. Phys. Chem. Solids*, **39**, 695–8.
102. Poon, Y. M. and Newman, D. J. (1982) *J. Chem. Phys.*, **77**, 1077–9.
103. Claassen, H. H. (1959) *J. Chem. Phys.*, **30**, 968–9.
104. Hutchison, C. A. and Weinstock, B. (1960) *J. Chem. Phys.*, **32**, 56–61.
105. Beitz, J. V., Williams, C. W., and Carnall, W. T. (1982) *J. Chem. Phys.*, **76**, 2756–7.
106. Denning, R. G., Norris, J. O. W., Short, I. G., Snellgrove, T. R., and Woodwark, D. R. (1980) *Lanthanide and Actinide Chemistry and Spectroscopy* (ACS Symp. Ser. no. 131), American Chemical Society, Washington DC, pp. 313–30.

107. Stafsudd, O. M., Leung, A. F., and Wong, E. Y. (1969) *Phys. Rev.*, **180**, 339–43.
108. Jørgensen, C. K. (1982) *Chem. Phys. Lett.*, **89**, 455–8.
109. DeKock, R. L., Baerends, E. J., Boerrigter, P. M., and Snijders, J. G. (1985) *Chem. Phys. Lett.*, **105**, 308–16.
110. Carnall, W. T. (1982) in *Gmelin Handbuch der Anorganischen Chemie*, 8th edn, *Uranium Supplement*, vol. A5, Springer-Verlag, New York, pp. 69–161.
111. Thomas, L. H. (1926) *Nature*, **117**, 514; Frenkel, J. (1926) *Z. Phys.*, **37**, 243–4.
112. Asprey, L. B., and Keenan, T. K. (1958) *J. Inorg. Nucl. Chem.*, **7**, 27–31; Ensor, D. D., Peterson, J. R., Haire, R. G., and Young, J. P. (1981) *J. Inorg. Nucl. Chem.*, **43**, 1001–3.

CHAPTER SEVENTEEN

THERMODYNAMIC PROPERTIES

Lester R. Morss

17.1 INTRODUCTION

The necessity of obtaining accurate thermodynamic quantities for the actinide elements and their compounds was recognized at the outset of the Manhattan Project, when a dedicated team of scientists and engineers initiated the program to exploit nuclear energy for military purposes. Since the end of World War II, both fundamental and applied objectives have motivated a great deal of further study of actinide thermodynamics. This chapter brings together many research papers and critical reviews on this subject. It also seeks to assess, to systematize, and to predict important properties of the actinide elements, ions, and compounds, especially for species in which there is significant interest and for which there is experimental basis for the prediction.

Many experimental and theoretical studies of thermochemical and thermophysical properties of thorium, uranium, and plutonium species were undertaken by Manhattan Project investigators. Some of these reports appeared in the National Nuclear Energy Series [1]. These papers, and others in the literature through 1956, formed the basis for Table 11.11 'Summary of thermodynamic data for the actinide elements' of the first edition of this book. That table, completed by J. D. Axe and E. F. Westrum Jr, listed 126 species, of which the properties of 40 were estimates. A fair measure of the progress in actinide thermodynamics is the number of subsequent research papers and reviews; another measure is the 731 species included in Table 17.14 of this chapter, few of which are estimates.

Until recently, the reviews of actinide thermodynamics lagged behind the reports of these measurements themselves. In 1952 two monumental works

appeared: the US National Bureau of Standards Circular no. 500 [2] included all known data through uranium, and Latimer's *Oxidation Potentials* [3] included oxidation–reduction data on all actinides through americium. Following the publication of the first edition of this work, with its thermodynamic summary in Table 11.11, the only major reviews of actinide thermodynamics during the decade 1960–69 were the monograph of Rand and Kubaschewski [4] on uranium, the IAEA panel reports on oxides [5, 6] and carbides [7], and long reviews by Rand [8] and Oetting [9].

Critical efforts to compile and to assess actinide thermodynamic properties have improved in more recent years. Krestov [10] prepared an extensive compilation of rare-earth and actinide thermochemical properties. Rand [11] comprehensively and critically reviewed thorium thermodynamics, and the thermodynamics group of the US National Bureau of Standards [12] published the final volume of the Technical Note 270 series, which included the elements actinium through uranium. At nearly the same time the parallel compendium of Glushko *et al.* [13] was published in the USSR. The most contemporary and thoroughly annotated compilation is the fourteen-part series issued under the auspices of the International Atomic Energy Agency, *The Chemical Thermodynamics of Actinide Elements and Compounds*, of which nine volumes [14–21, 354] have been published as of the time of writing.

17.2 ELEMENTS AND ALLOYS

Thermodynamic measurements that have been made on the actinide metals are low- and high-temperature heat capacities, properties of phase transitions, and vapor pressures. At least one of these measurements has been made on each element through einsteinium; unfortunately, however, none has been made on actinium, so that even its enthalpy of vaporization must be estimated. As of the time of writing (February 1986) vapor-pressure measurements have been made through einsteinium [22] and low-temperature heat-capacity measurements through americium [23] by innovative microscale methods.
innovative microscale methods have been applied to determine vapor pressures and very low-temperature heat capacities of transplutonium actinides.

From these measured properties, thermodynamic state functions (enthalpies of sublimation, entropies, and free-energy functions) have been derived. For several actinides, these properties have been critically reviewed by Hultgren *et al.* [24] and more recently by Oetting, Rand, and Ackermann [14]. The latter compilation includes properties for the metallic state and for ideal gas to 5000 K for the elements Th through Cm. Sublimation enthalpies (determined from measured vaporization behavior for Th through Es) and standard entropies (determined from measured heat capacities for Th through Am) of the actinide metals are compiled in Table 17.1. Sublimation enthalpies have been correlated with metal structures and electronic energy levels [27, 28].

Table 17.1 *Thermodynamic properties of actinide metals and aqueous ions at 25°C.*

			An^{2+}			An^{3+}			An^{4+}		
An	$S°$(An) ($J K^{-1} mol^{-1}$)	$\Delta H_f°$(An(g)) ($kJ mol^{-1}$)	$\Delta H_f°$ ($kJ mol^{-1}$)	$S°$ ($J K^{-1} mol^{-1}$)	$\Delta G_f°$ ($kJ mol^{-1}$)	$\Delta H_f°$ ($kJ mol^{-1}$)	$S°$ ($J K^{-1} mol^{-1}$)	$\Delta G_f°$ ($kJ mol^{-1}$)	$\Delta H_f°$ ($kJ mol^{-1}$)	$S°$ ($J K^{-1} mol^{-1}$)	$\Delta G_f°$ ($kJ mol^{-1}$)
Ac	(62)	(418)	(−118)	(+12)	(−142)	(−628)	(−180)	(−615)			
Th	53.4	598	(+161)	(+15)	(+134)	(−347)	(−173)	(−339)	−769	−424	−705
Pa	55	570	(+50)	(+17)	(+22)	(−439)	(−172)	(−431)	−620	(−397)	(−564)
U	50	536	(+3)	(+14)	(−28)	−489	(−175)	−481	−591	−414	−531
Np	51	465	(−39)	(+3)	(−64)	−527	(−179)	−517	−556	−389	−503
Pu	56	342	(−224)	(−16)	(−241)	−592	−184	−579	−536	−389	−482
Am	55	284	(−355)	(−1)	−377	−617	(−201)	−599	(−406)	(−408)	(−347)
Cm	(72)	387	(−222)	(−1)	−239	−615	(−194)	−593	(−379)	(−426)	(−295)
Bk	(78)	310	(−294)	(−2)	−309	−601	(−194)	(−578)	(−483)	(−413)	(−417)
Cf	(81)	196	(−385)	(−5)	−398	−577	(−197)	(−553)	(−313)	(−412)	(−244)
Es	(90)	130	(−415)	(−8)	−425	(−603)	(−206)	(−573)	(−211)	(−414)	(−139)
Fm	(91)	(130)	(−474)	(−13)	−482	(−632)	(−215)	(−599)	(−170)	(−415)	(−97)
Md	(87)	(128)	(−481)	(−20)	−488	(−538)	(−224)	(−504)		(−419)	(+38)
No	(65)	(126)	(−494)	(−39)	−502	(−395)	(−231)	(−365)		(−423)	(+284)
Lr	(55)	(341)				(−630)	(−255)	(−596)		(−430)	(+165)
Refs	14, 22, Table 17.14	Table 17.14	calc.	Table 17.2	25–27, 123, Table 17.14, Fig. 17.2	15, Table 17.14	15, 25, 27	15, 25, 48	15	Table 17.2	15, 26, 28, Table 17.14, Fig. 17.2

( ) Estimated values.

For the actinides beyond einsteinium, radiochemical (tracer) methods only are available to the experimentalist. Predictions of ΔH_{subl} for these elements were made by correlating energetics of divalent and trivalent lanthanides and actinides [29] or by correlating electronic configuration with metallic radius, melting temperature, and enthalpy of sublimation [30]. A more reliable series of sublimation properties was generated by David *et al.* [25, 27], who included experimental radioelectrochemical measurements in their correlation. An independent method of estimation of sublimation properties is that of thermochromatography, which has been utilized effectively for the elements [31]. The best estimates are cited in Table 17.1 and are plotted in Fig. 17.1.

The entropies of the metals heavier than americium have been estimated by Ward and his colleagues [22, 32–37] from those of the lighter actinide metals by correlation with metallic radius, atomic weight, and magnetic entropy. These entropies have been accepted by David [25, 27] and by Ward [38] and are also listed in Table 17.1.

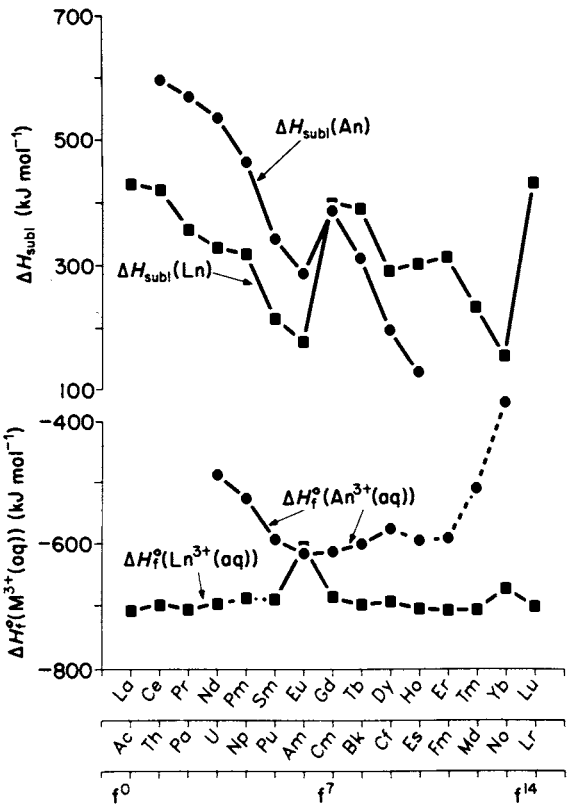

Fig. 17.1 *Enthalpies of sublimation of lanthanide and actinide metals and enthalpies of formation of lanthanide(III) and actinide(III) aquo ions at 298 K.*

Thermodynamic properties of alloys containing one or more actinide elements have been critically assessed by Chiotti *et al.* [18]. This latter monograph includes phase diagrams, structures, and thermodynamic properties, and is not included in the summary tables of this chapter.

17.3 AQUEOUS IONS

17.3.1 Enthalpies of formation

For all of the transuranium elements, the enthalpy of formation of aquo ions was the first thermochemical property of the elements to be determined. One reason was that the measurement of the 'heat of solution' of metals was an appropriate step in the determination of enthalpies of formation of compounds. A more fundamental reason is that the enthalpy of formation of an aquo ion establishes a fundamental property of that ion and references all stability studies of compounds of that ion. Since *solution* microcalorimetry is more readily done than *combustion* microcalorimetry, milligram-scale enthalpy-of-formation studies of aquo ions have been possible whereas such studies of oxides and halides by combustion calorimetry have not. In fact, microcalorimetry studies of transuranics have been carried out for nearly 40 years, with barely an order of magnitude improvement in sensitivity in all that time!

Selected values of actinide aquo-ion enthalpies of formation of actinium through berkelium (except for any Pu(VII) species) were assessed by Fuger and Oetting [15]; their values have been adopted here in Tables 17.1 and 17.14. For berkelium and californium, new measurements have provided the tabulated enthalpies of formation. All An^{3+} values are plotted in Fig. 17.1. For heavier actinides, Nugent *et al.* [29] estimated enthalpies of formation systematically; David *et al.* [25, 27] applied more elaborate systematics and electrochemical measurements to estimate aquo-ion enthalpies of formation. David's predictions for $\Delta H_f^\circ(Bk^{3+})$ and $\Delta H_f^\circ(Cf^{3+})$ have been borne out by experiments. Some enthalpies of formation of tetravalent and higher ions have been calculated from free energies (EMF measurements) and entropies (estimates) [15]. Enthalpies of formation of the tetravalent ions Am^{4+}, Cm^{4+} and Cf^{4+} have been estimated from enthalpies of formation and solution of the dioxides [39–41]. A correlation function $P(M)$ is discussed in Section 17.5.2.

17.3.2 Entropies

Entropies of aqueous ions can be determined directly by measuring the enthalpy of solution of the metal to form the aquo ion and the free energy of solution of a salt of the ion. Upon correction to standard state, these data yield standard enthalpy and free energy of formation of the ion, from which its standard entropy

of formation can be calculated:

$$\Delta S_f^\circ = (\Delta H_f^\circ - \Delta G_f^\circ)/T \tag{17.1}$$

The absolute entropy of the ion is then calculated from the equation representing ΔS_f°:

$$\mathrm{M(c)} + n\mathrm{H^+(aq)} = \mathrm{M^{n+}(aq)} + (n/2)\mathrm{H_2(g)} \tag{17.2}$$

Standard-state entropies of aqueous ions are by convention referenced to $S^\circ(\mathrm{H^+(aq)}) = 0$. Alternatively, the temperature coefficient of the electromotive force of an equilibrium reaction involving the ion can be used to calculate the entropy of the reaction, and from the reaction entropy as well as necessary auxiliary data the entropy of formation of the ion can be calculated. Four actinide aquo-ion entropies (Th^{4+}, Pu^{3+}, UO_2^{2+}, and NpO_2^{2+}) have been determined by the former method. The other aquo-ion entropies of uranium, neptunium, and plutonium have been connected by the latter method.

Fuger and Oetting [15] summarized all experimental data and selected or estimated entropies of the aquo ions of Th through Bk. We have adopted their values. For the important trivalent aquo ions beyond Pu, only estimated entropies are available. These estimates are fairly trustworthy since they depend only upon the ion charges, the ionic radii, and the magnetic degeneracy of the ground states.

Several semiempirical equations have been proposed to fit entropies of aquo ions to the above parameters, for example [42, 43]:

$$S^\circ(\mathrm{M^{2+}}) = \tfrac{3}{2}R\ln(\text{at. wt}) + R\ln(2J+1) + 256.8 - 32.84\frac{(|z|+3)^2}{r+c} \tag{17.3}$$

where $R = 8.314\ \mathrm{J\,K^{-1}\,mol^{-1}}$, J is the total angular momentum quantum number of the ion, z is the ionic charge, r is the ionic radius for coordination number 6 taken from Shannon [44] (except that coordination number 8 is used for $z = 4$), and c is a term added to the radius to represent the inner hydration sphere: $c = 1.20$ Å for cations and $c = 0.40$ Å for anions. Recently David [25] has proposed the equation

$$S^\circ(\mathrm{M^{2+}}) = \tfrac{3}{2}R\ln(\text{at. wt}) + R\ln(2J+1) + Sc(r) \tag{17.4}$$

where $Sc(r)$ is a structural entropy term, dependent for a given z only on the hydrated-ion structure. Equation (17.4) was devised by David to take into account the change in inner-sphere hydration number from 9 to 8 between Sm and Tb in the Ln^{3+} ions and between Cm and Es in the An^{3+} ions, and we accept David's estimates of the heavy An^{3+} ion entropies. Equation (17.3) is more general and has been used for divalent and tetravalent ions (Table 17.2). The necessary ionic radii for equation (17.3) (Table 17.2) were estimated by comparison of isoelectronic 4f and 5f ions as well as by Shannon-type plots of unit-cell volumes of dihalides and dioxides against r^3. Other predictive equations give fairly consistent entropy estimates [25, 45] even though ionic radii as small as 1.0 Å for No^{2+} have been estimated [25, 46].

Table 17.2 *Entropies of aqueous actinide ions at 25°C.*

		An^{2+}			An^{3+}			An^{4+}		
An	*At. wt*	*Degen.*[a]	IR[b] (Å)	$\bar{S}°$ ($J\,K^{-1}\,mol^{-1}$)	*Degen.*[a]	IR[b] (Å)	$\bar{S}°$ ($J\,K^{-1}\,mol^{-1}$)	*Degen.*[a]	IR[c] (Å)	$\bar{S}°$ ($J\,K^{-1}\,mol^{-1}$)
Ac	227	2	(1.38)	(+12)	1	1.12	(−180)			
Th	232	5	(1.34)	(+15)	6		(−173)	1	1.05	−424
Pa	231	12	(1.30)	(+17)	9	1.04	(−172)	6	1.01	(−389)
U	238	13	(1.27)	(+14)	10	1.025	(−175)	9	1.00	−414
Np	237	6	(1.24)	(+3)	9	1.01	(−179)	10	0.98	−389
Pu	239	1	(1.21)	(−16)	6	1.00	−184	9	0.96	−389
Am	243	8	1.19	(−1)	1	0.98	(−201)	6	0.95	(−408)
Cm	248	13	(1.16)	(−1)	8	0.972	(−194)	1	0.94	(−426)
Bk	249	16	(1.14)	(−2)	13	0.958	(−194)	8	0.93	(−413)
Cf	249	17	1.12	(−5)	16	0.946	(−197)	13	0.92	(−412)
Es	254	16	(1.10)	(−8)	17	(0.934)	(−206)	16	(0.91)	(−414)
Fm	255	13	(1.08)	(−13)	16	(0.924)	(−215)	17	(0.905)	(−415)
Md	258	8	(1.06)	(−20)	13	(0.914)	(−224)	16	(0.895)	(−419)
No	255	1	(1.05)	(−39)	8	(0.904)	(−231)	13	(0.89)	(−423)
Lr	256				1	(0.898)	(−255)	8	(0.88)	(−430)
Refs			25, 46	eqn (17.3)		25, 44	15, 25		25, 44[d]	eqn (17.3)

[a] Degeneracy of electronic ground state, taken as $2J+1$ with J assumed the same as that for the free ion.
[b] Coordination number 6.
[c] Coordination number 8.
[d] Or extrapolated from isoelectronic ions.

17.3.3 Free energies of formation: electrode potentials

(a) Acid solution

Free energies of formation of the aquo ions of actinium through berkelium in acid solution (with the important exception of Np(VII)) were calculated and assessed by Fuger and Oetting [15]. Free energies of formation of trivalent ions were calculated from enthalpies of formation and standard entropies, as were free energies of formation of UO_2^{2+}(aq), NpO_2^{2+}(aq), and PuO^{2+}(aq). The free energy of formation of PuO_2^{2+}(aq) was determined from the equilibrium constant of the Pu^{4+} disproportionation and the $E°(Pu^{4+}/Pu^{3+})$.

Fuger and Oetting also assessed the reversible cell EMF and polarographic data that allowed them to calculate free-energy differences between many aquo-ion pairs. By this means they were able to connect all aquo ions and to tabulate free energies of formation of all actinide aquo ions in acid solution.

Comprehensive summaries of reduction-potential literature values have been assembled [47, 170]. In a later and more critical review, Martinot and Fuger [48] have presented reduction potentials in acid solution for all of these elements. More recent calorimetric measurements on Bk^{3+}(aq) and Cf^{3+}(aq) allowed them to estimate reduction potentials for the Bk^{3+}/Bk and Cf^{3+}/Cf couples.

The heavier actinide ions present especially challenging problems. These elements have short-lived isotopes with available amounts ranging between micrograms and single atoms. They also have accessible divalent states. To achieve meaningful experimental measurements on these ions, Maly [49–51], David [25], and their co-workers developed radioelectrochemical tracer methods, and Mikheev [52] and his co-workers developed co-crystallization systematics. Judicious application of radiopolarography, radiocoulometry, amalgamation energies, and co-crystallization has yielded $E°$ for An^{3+}/An^{2+}, An^{2+}/An, and An^{3+}/An couples [25] and has provided free energies of formation for Es^{3+}, Md^{3+}, and No^{3+}. The best free energies of formation of Fm^{3+} and Lr^{3+} have actually been calculated from estimates of enthalpies of sublimation, promotion energies P(M) (see Section 17.5.2), and entropies [25].

The recommended values of Fuger and Oetting [15], Martinot and Fuger [48], and David [25] have been utilized in Tables 17.1 and 17.14. Fig. 17.2 summarizes reduction potentials in acid solution that are consistent with these free energies of formation. Because of the necessity of making EMF measurements in strongly acidic solution, and the impossibility of making measurements approaching standard state (nearly neutral solution), both the free energies of formation and reduction potentials refer to formal potentials rather than standard potentials (unit concentration rather than unit activity of hydrogen ion).

The reduction potentials in Fig. 17.2 are 'Latimer' diagrams [3] showing the potentials of half-reactions in which the left-hand species is reduced to the right-hand species with the appropriate number of electrons, H^+, and H_2O to balance the half-reaction. (Species not found in aqueous solution, but whose

(a) Acid

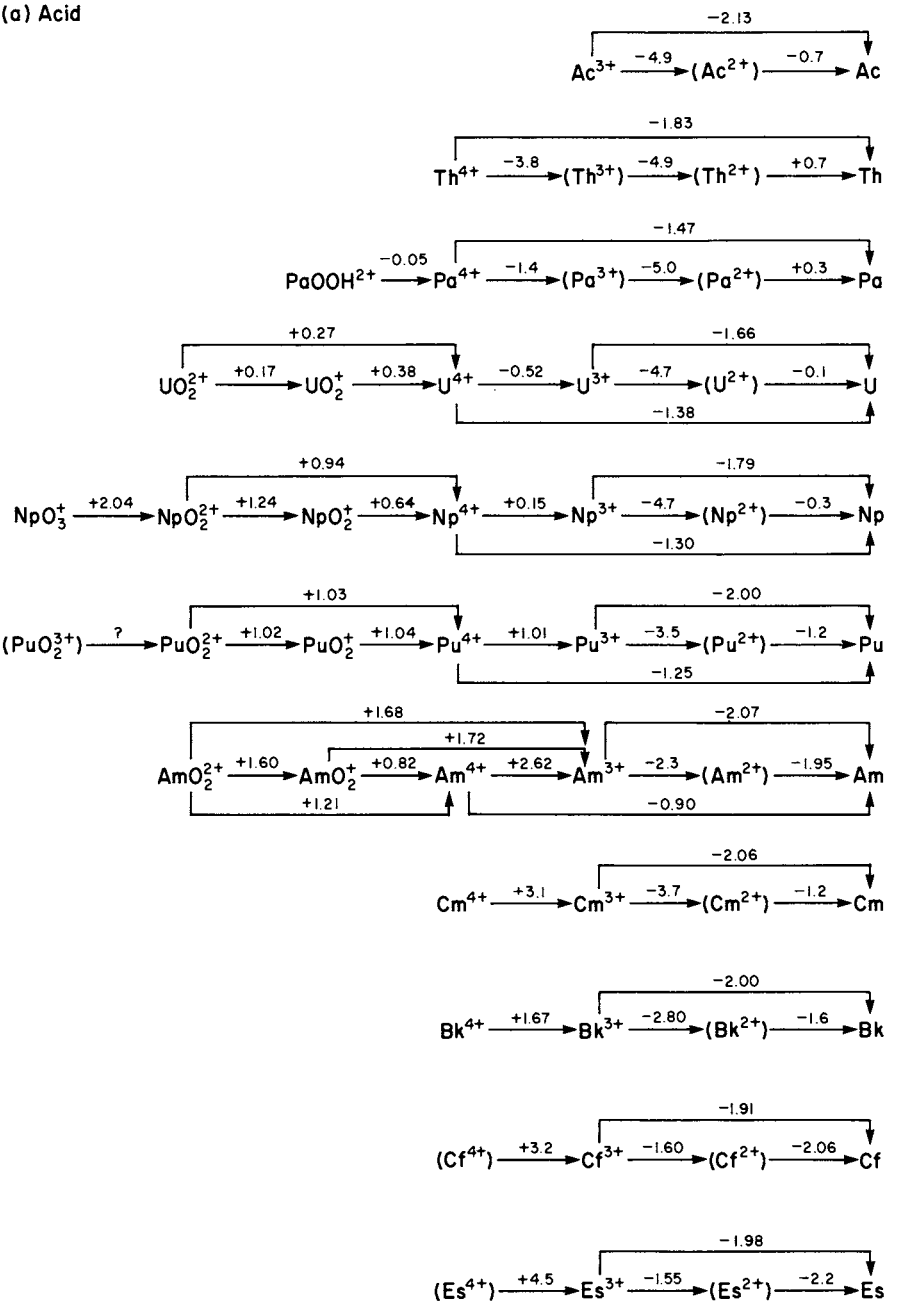
−2.13
Ac3+ −4.9 (Ac2+) −0.7 Ac
−1.83
Th4+ −3.8 (Th3+) −4.9 (Th2+) +0.7 Th
−1.47
PaOOH2+ −0.05 Pa4+ −1.4 (Pa3+) −5.0 (Pa2+) +0.3 Pa
+0.27
−1.66
UO22+ +0.17 UO2+ +0.38 U4+ −0.52 U3+ −4.7 (U2+) −0.1 U
−1.38
+0.94
−1.79
NpO3+ +2.04 NpO22+ +1.24 NpO2+ +0.64 Np4+ +0.15 Np3+ −4.7 (Np2+) −0.3 Np
−1.30
+1.03
−2.00
(PuO23+) ? PuO22+ +1.02 PuO2+ +1.04 Pu4+ +1.01 Pu3+ −3.5 (Pu2+) −1.2 Pu
−1.25
+1.68
+1.72
−2.07
AmO22+ +1.60 AmO2+ +0.82 Am4+ +2.62 Am3+ −2.3 (Am2+) −1.95 Am
+1.21
−0.90
−2.06
Cm4+ +3.1 Cm3+ −3.7 (Cm2+) −1.2 Cm
−2.00
Bk4+ +1.67 Bk3+ −2.80 (Bk2+) −1.6 Bk
−1.91
(Cf4+) +3.2 Cf3+ −1.60 (Cf2+) −2.06 Cf
−1.98
(Es4+) +4.5 Es3+ −1.55 (Es2+) −2.2 Es

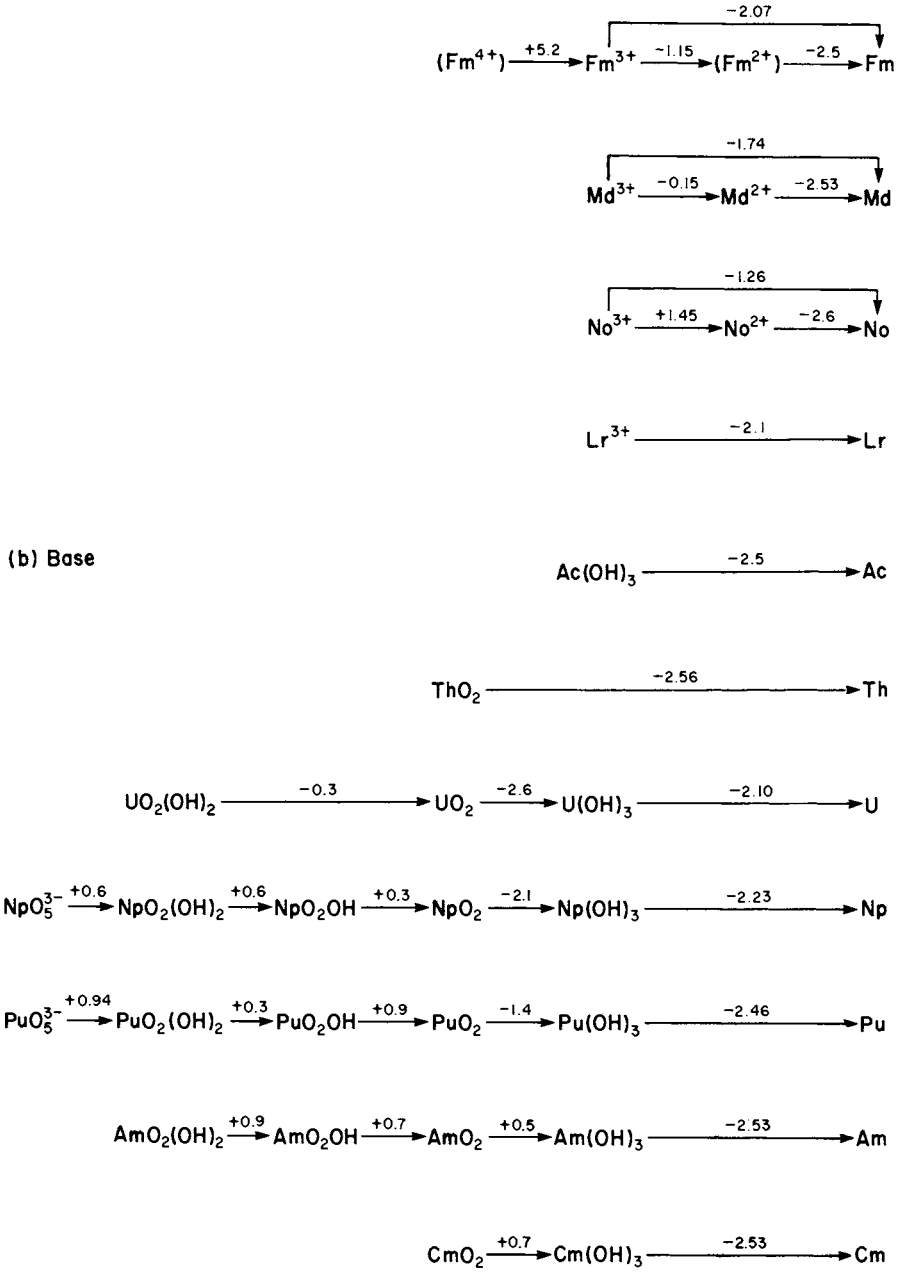

Fig. 17.2 *Standard (or formal) reduction potential diagrams for the actinide ions in (a) acidic (pH 0) and (b) basic (pH 14) solutions. (Values in volts versus standard hydrogen electrode.) Note that the solubility of* $PuO_2(OH)_2$ *increases from 1 M KOH to 10 M KOH solution [57]. Thus there is evidence for amphoteric behavior of* $PuO_2(OH)_2$ *by forming* $PuO_2(OH)_3^-$ *in strong base.*

thermodynamic properties have been estimated, are indicated in parentheses.) The potentials are summarized in Fig. 17.3 as $nE°$ (n is the oxidation state), a property proportional to ΔG_f°, so that the lowest-lying species for each element is the one most stable in equilibrium with the H^+/H_2 couple.

(b) Basic solution

E_B values should represent unit activities of all species including OH^-, i.e. pH 14. Under such basic conditions, all actinide ions precipitate as hydroxides or hydrated oxides. Very few of these precipitates have been thoroughly characterized; interpolations, extrapolations, and approximations are usually necessary. Latimer [3] estimated the solubility products K_{sp} of actinide(III) hydroxides, $An(OH)_3$, from corresponding values for freshly precipitated hydroxides of the lanthanides. It is well known that, as these gelatinous precipitates age, their crystallinity increases and their K_{sp} decreases, so that the aged precipitates more nearly reflect equilibrium conditions. Rai *et al.* [53], however, found that both $^{241}Am^{3+}$ and $^{243}Am^{3+}$ hydroxides reached equilibrium from over- and undersaturation within 7 days, with

$$\log K_a = 3 \log K_w + \log K_{s10} = 3(-14.0) + (17.3 \pm 0.3) = -24.5 \pm 0.3$$

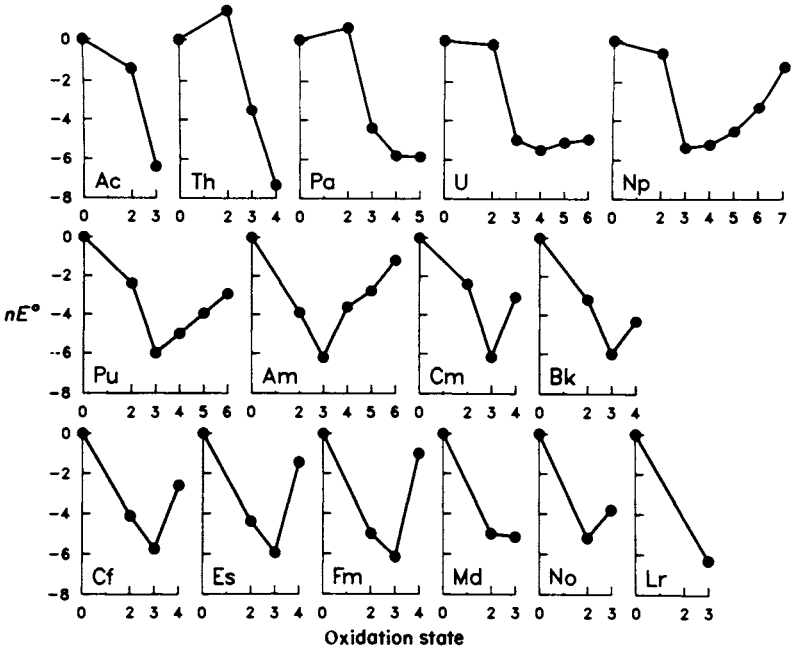

Fig. 17.3 *Comparative stability of actinide aquo ions (relative to the $H^+(aq)/H_2(g)$ couple).*

(K_{s10} refers to the equilibrium $Am(OH)_3 + 3H^+ = Am^{3+} + 3H_2O$.) Baes and Mesmer [57] have exhaustively surveyed the literature and have evaluated heterogeneous equilibria for lanthanide and actinide hydroxides and hydrated oxides. The thermodynamic activity products K_a (recommended by this author) to calculate free energies and E_b in basic solution are listed in Table 17.3. In general, the values selected by Baes and Mesmer have been adopted; however, in some cases more recent results have been selected or averaged [53, 60]. These more recent results yield a monotonic relation between $Ln(OH)_3$ unit-cell volumes and K_a. For tetravalent ions, no hydroxides have been characterized and we assume that the dioxides are in equilibrium with hydrated dioxides, if any exist. Hence K_a values refer to reactions such as the following (see [361]):

$$MO_2(c) + 2H_2O(l) = MO_2 \cdot 2H_2O(c) \tag{17.5}$$

$$MO_2 \cdot 2H_2O(c) = M^{4+}(aq) + 4OH^-(aq) \tag{17.6}$$

For reaction (17.5) we assume $\Delta G^\circ = 0$. Equilibrium cannot of course be observed for reaction (17.6) but, since standard free energies are known for

Table 17.3 *Activity products K_a of actinide hydroxides at 25°C:* $K_a = [M^{n+}][OH^-]^n \gamma_\pm^{n+1}$.

Ln	*IR* (M^{3+}) (Å)	*Unit-cell volume,* $M(OH)_3$ (Å^3)	$-\log K_a$ ($M(OH)_3$)	*An*	*IR* (M^{3+}) (Å)	*Unit-cell volume,* $M(OH)_3$ (Å^3)	$-\log K_a$ ($M(OH)_3$)	$-\log K_a$ (MO_2)
La	1.032	141.8	21.7	Ac	1.12		20.9	
Ce	1.01	139.8	22.1[a]	Th				49.4
Pr	0.99	135.9	22.1	Pa	1.04			
Nd	0.983	133.6	23.1	U	1.025		22.2[a,b]	57.8[c,d]
Pm	0.97	130.1	(24)	Np	1.01		22.4[b]	60.0[c,d]
Sm	0.958	129.3	25.2	Pu	1.00		22.6[b]	63.3[c,d]
Eu	0.947	127.8	26.5	Am	0.9		24.0	64[b,d]
Gd	0.938	126.0	26.9	Cm	0.97		24.0[b]	64[b]
Tb	0.923	124.1	26.3	Bk	0.9		25.0[b]	65[b]
Dy	0.912	122.2	25.9	Cf	0.9		25.5[b]	65[b]
Ho	0.901	120.5	26.5	Es	0.93		26.0[b]	
Er	0.890	119.2	26.6					
Tm	0.880	117.8	26.6					
Yb	0.868	117.3	26.6					
Lu	0.861		27.0					
Refs	44	54, 55	55–57	44,	Table 17.2		53, 57, 58	57

[a] For CeO_2, $\log K_a = -64.1$ [57]. For UO_2, see Garisto and Garisto [361].
[b] Estimated by author, this chapter.
[c] Calculated from ΔG° for reaction $MO_2 + 2H_2O \rightarrow M^{4+} + 4OH^-$.
[d] For U–Am: $MO_2OH \rightleftharpoons MO_2^+ + OH^-$, $\log K_a \simeq -10$ [57].

$MO_2(OH)_2 \rightleftharpoons MO_2^{2+} + 2OH^-$, $\log K_a \simeq -22$ [57].

For Np: activity product of $NpO_3 \cdot H_2O$ is $K_a = 8 \times 10^{-23}$ [59].

MO_2(c) (Table 17.14) and aqueous species, we can calculate ΔG° for reaction (17.6) and hence its K_a. These K_a values were then used to estimate E_b values. For example, from $E^\circ(AmO_2^+/Am^{4+}) = 0.82$ V, $\Delta G^\circ = -79$ kJ mol^{-1}, and

$$4H^+(aq) + AmO_2^+(aq) + e^- \rightarrow Am^{4+}(aq) + 2H_2O(l) \quad -\log K_a \simeq -10, \quad \Delta G^\circ = -79 \text{ kJ mol}^{-1}$$

$$AmO_2OH(c) \rightarrow AmO_2^+(aq) + OH^-(aq) \quad \log K_a \simeq -10, \quad \Delta G^\circ \simeq 57 \text{ kJ mol}^{-1}$$

$$Am^{4+}(aq) + 4OH^-(aq) \rightarrow AmO_2(c) + 2H_2O(l) \quad -\log K_a \simeq +64, \quad \Delta G^\circ = -365 \text{ kJ mol}^{-1}$$

$$4H_2O(l) \rightarrow 4H^+(aq) + 4OH^-(aq) \quad 4 \log K_w = -56, \quad \Delta G^\circ = 320 \text{ kJ mol}^{-1}$$

we can obtain

$$AmO_2OH(c) + e^- \rightarrow AmO_2(c) + OH^-(aq) \qquad \Delta G^\circ = -67 \text{ kJ mol}^{-1}, \; E_b^\circ = +0.69 \text{ V}$$

All of these E_b values are cited as basic potentials (pH 14) in Fig. 17.2. From estimated activity products (e.g. for $Ac(OH)_3$) and appropriate cycles, the free energies of formation of the crystalline hydroxides and of Np(VII) aquo ions were calculated (Table 17.14).

Potential–pH 'Pourbaix' and potential–concentration diagrams for the important actinides have been prepared by several authors [61–65, 361]. These diagrams are useful in identifying predominant species under given conditions, but must be used with caution since they are often based upon estimated free-energy values.

(c) Other media

Electrochemical measurements have been made of actinide ions in complexed aqueous media, especially carbonate–bicarbonate systems [66–68]. Such measurements are particularly useful in establishing the actinide oxidation states and species present in natural water and biological systems. Complexes such as fluoride, chloride, carbonate, and phosphotungstate are stronger with tetravalent than with trivalent cations, so they significantly stabilize the higher oxidation state.

Electrochemistry of actinides in molten salts has been pursued by many authors. There are thorough recent reviews [47, 69, 70]. In some cases, high oxidation states are stabilized, while in others the use of strong Lewis-acid molten salts stabilizes lower oxidation states. Co-precipitation of lanthanide tri- and dichlorides and oxychlorides with trace amounts of some actinides has yielded some An^{3+}/An^{2+} E° values as mentioned in Section 17.3.3(a) and has produced evidence (unconfirmed by other methods) of divalent Pu, Cm, and Bk [52].

17.3.4 Heat capacities and high-temperature properties

Heat capacities, as well as entropies, of aqueous ions are the fundamental thermodynamic properties that reflect their structure and hydration. Heat capacities are also necessary for calculation of other thermodynamic properties at

temperatures other than 298 K. For the actinides, high-temperature (at least to 473 K) properties are essential for calculation of redox, complexation, and heterogeneous equilibria, which are useful in separation and waste-management technologies.

The most thorough treatment of uranium and plutonium aquo-ion equilibria over extended temperatures is that of Lemire and Tremaine [71]. This paper uses the systematic relationships developed by Criss and Cobble [72], which relate aquo-ion entropies, heat capacities, and their high-temperature behavior. Although the experimental determination of aquo-ion heat capacities has been dramatically advanced by the development of flow microcalorimeters [73, 74], the only measurements of f-block aquo-ion heat capacities were made before this innovation [75, 76]. Therefore, Lemire and Tremaine had to rely on estimated heat capacities for almost all of their calculations, and most of their equilibrium constants are uncertain by two or more orders of magnitude. Lemire [77] has also written a report on neptunium aquo-ion equilibria over extended temperatures.

Theoretical equations, based upon extended Debye–Hückel parameters or equations of state, have been advanced by Pitzer [78] and Helgeson [79] to predict the behavior of electrolyte solutions over a wide range of temperature, concentration, and pressure. Experimental heat-capacity data are still needed for trivalent and tetravalent ions. Nevertheless, databases have been established that use the scarce experimental measurements and the tenuous theoretical formalisms to predict high-temperature equilibria [80].

17.3.5 Complex ions

A substantial number of recent studies have measured the electrochemical behavior of complexed actinides in aqueous solution. Complexation of f-block ions by ligands such as carbonate and polyphosphotungstate has allowed otherwise unstable species such as Am(IV) and U(V) to be studied electrochemically [66, 67, 81, 82]. Carbonate and bicarbonate stabilize acidic cations at relatively high pH (typical of environmental and biological systems); the many actinide–carbonate studies have been reviewed recently [83, 84].

Ions that are stabilized as complexes can be utilized to determine standard redox potentials. The $E°(Am^{4+}/Am^{3+})$ measured by cyclic voltammetry in 2 M $Na_2CO_3/NaHCO_3$ at pH 9.7, namely 0.92 ± 0.01 V, could be corrected for the preferred complexation of Am(IV) in this medium by 1.7 V to yield $E°(Am^{4+}/Am^{3+}) = 2.6 \pm 0.1$ V [66], in good agreement with the accepted (Fig. 17.2) thermochemical value of 2.62 ± 0.09 V [39].

Polyphosphotungstate appears to be able to complex Cm(IV) and Cf(IV) sufficiently well to stabilize these ions in aqueous solution [81]. Since the An^{4+}/An^{3+} potential shift of 1.7 V in carbonate is more favourable for stabilization of An^{4+} than is the shift of 1.0 V in polyphosphotungstate [82], it was expected that Cm(IV) and Cf(IV) would be readily produced in carbonate. Such was not found to be the case, however [67].

17.4 GASEOUS ATOMS AND IONS

Brewer [353] has systemized the energy levels of many configurations of gaseous atoms and ions; see also Chapter 15. Because of the complexity of the atomic spectra of the f-block elements, the derivation of ionization energies has been very difficult for spectroscopists. A complete set of I_1 values was calculated by Sugar [85] and was included in a major compilation of f-element ionization potentials [86]. At that time there were few other known actinide ionization potentials, although several sets of lanthanide potentials (I_1 through I_4) had already been published. Sugar's values for I_1 and I_2 are given in Table 17.4 (with more recent values of I_1 for U and Np). High-temperature properties of An^+ ions have been calculated [354].

Among efforts to calculate actinide ionization potentials from first principles, the set of Carlson *et al.* [87] is often cited. However, their I_1 values are about 10% smaller than Sugar's [85] and we have chosen to adjust them (see below).

A number of efforts have been made to calculate ionization-potential sums from thermochemical data and appropriate Born–Haber cycles. When an isostructural set of compounds is used, and covalence/repulsion corrections are made from a systematic lanthanide–actinide comparison, such sums can be quite reliable, as has been repeatedly demonstrated for the trivalent lanthanides [88]. For example, Morss [89] was able to estimate the sum of the first three ionization energies ($I_1 + I_2 + I_3$) for Pu as

$$Pu(g) = Pu^{3+}(g) + 3e^- \tag{17.7}$$

Using more recent auxiliary data, Goldman and Morss [90] estimated ($I_1 + I_2 + I_3$) for the elements U through Bk. From these estimates, and from comparable calculations for the lanthanides, they calculated $\Delta H_{hyd}(An^{3+})$:

$$An^{3+}(g) = An^{3+}(aq) \qquad \Delta H = \Delta H_{hyd} \tag{17.8}$$

All of these results are quoted in Table 17.4. Although other authors have made similar calculations, they do not differ significantly (e.g. those of Kiselev [91]) or have not yet been published [92] and thus are not cited in Table 17.4.

Quite recently, Sugar [93] derived new actinide I_2 values that are cited in Table 17.4. As of the date of writing, the only independent I_3 values are those of Carlson *et al.* [87], but since we note that Carlson's individual I_n values are consistently smaller than spectroscopic values or thermochemical sums, the I_3 entries in Table 17.4 are Carlson's values multiplied by a 'normalizing' factor 1.055. A new set of actinide ionization potentials, especially for the interesting higher potentials, is included in Table 17.4 [346].

17.5 OXIDES AND COMPLEX OXIDES

17.5.1 Monoxides

Monoxides of Th and of U through Am have been reported as surface layers on

Table 17.4 *Hydration enthalpies and ionization energies.*

		$(I_1+I_2+I_3)_{BH}$ (eV)						I_3 (eV)				
M	ΔH^0_{hyd} (M^{3+}) (kJ mol^{-1})	*Hydration cycle*	*Oxide cycle*	*Complex chloride cycle*	*Born–Haber average*	I_1 (eV)	I_2 (eV)	*Thermal*[a]	*Calc.*	*Syst. Diff.*		I_4 (eV)
Ac	−3266	36.7			36.7	5.17	11.87	19.7		18.9		
Th	−3268					6.08	11.89			20.0[d]		28.75
Pa	−3289					5.89	11.7		18.8	20.0		31.0
U	−3326	37.5	38.2	37.8	37.8	6.194	11.9	19.7	19.1	20.0		32.6
Np	−3406	38.7	39.0	38.5	38.7	6.266	11.7	20.7	19.4	20.7		33.6
Pu	−3400	39.2	39.7	39.2	39.4	6.062	11.7	21.6	21.8	21.8		34.6
Am	−3439	40.0	40.3	40.0	40.1	5.993	12.0	22.1	19.9	22.4		36.2
Cm	−3477	39.5	39.4	39.2	39.4	6.021	12.4	21.0	20.0	21.2		36.8
Bk	−3510	41.2	40.8	40.4	40.8	6.229	12.3	22.3	20.4	22.3		35.6
Cf	−3533	42.2	42.5	42.1	42.3	6.298	12.5	23.5	23.5	23.6		37.3
Es	−3567	43.0	43.4		43.2	6.422	12.6	24.2	24.6	24.1		38.7
Fm	−3604	43.4	44.0		43.7	6.50	12.7	24.5	25.7	24.4		39.3
Md	−3642	44.7	45.2		45.0	6.58	12.8	25.6	26.7	25.4		39.8
No	−3681	46.6	47.3		47.0	6.65	13.0	27.4	27.7	27.0		41.0
Lr	−3721	42.1	42.9		42.5	4.6[b]	14.8[b]	23.1	22.8	23.0		42.6
104										24.0		33.0
Refs	90	90	42[c]	42[c]		85, 95, 96, 354	93, 354	[a]	87[b]	346	94	346

[a] I_3 (thermal) $= (I_1+I_2+I_3)_{BH,ave} - I_1 - I_2$.
[b] Since all ionization energies of Carlson *et al.* [87] are smaller than those of Sugar [93], and also smaller than those calculated from thermal cycles, these entries are those of Carlson *et al.* adjusted by multiplying by 1.055.
[c] Extended for actinides.
[d] Spectroscopic [86, 94].

the metals, as the reduction product of PuO_2 with Pu or C, as the product of reaction of Am with HgO, or in the gas phase. Only the gas-phase monoxides are well-established species; all the solid monoxides are highly suspect for the reasons cited below.

Among the reported lanthanide monoxides, only EuO is well-characterized, impure YbO can be prepared with difficulty, and 'metallic' (trivalent) monoxides of La, Ce, Pr, Nd, and Sm can be synthesized at high temperature and pressure. Earlier reports of lanthanide monoxides as surface phases are believed to be oxynitrides, oxycarbides, or hydrides [40]. Similarly, earlier reports of 'PuO' are now believed to have been an oxide carbide [97].

Thermodynamic calculations have shown how marginally stable the few lanthanide monoxides are, even under the exotic conditions of their preparation, and that classical (divalent) CfO should be unstable with respect to disproportionation [40]. Thus the only hope of synthesis of actinide monoxides would appear to be the high-pressure route for AmO and CfO, an extremely demanding synthetic procedure.

17.5.2 Sesquioxides

Unlike the 4f elements, for which sesquioxides are ubiquitous, only the sesquioxides of Ac and Pu through Es have been prepared. Sesquioxides of Th through Np are clearly thermodynamically unstable with respect to disproportionation to the metals and the much more stable dioxides. (Those of heavier actinides would be obtainable if their half-lives were much longer and nuclear yields more favorable.) An overview of known actinide oxides, and their enthalpies of formation and standard entropies, was given earlier in Table 14.9; although most of the actinide sesquioxides have been known since before 1970 (Am_2O_3 since before 1950), only in the past decade have thermophysical [98] and thermochemical [99] properties been determined. Since the optimum solvent for solution calorimetry of these sesquioxides is moderately concentrated hydrochloric acid, a systematic approach to the prediction of the enthalpies of formation of other sesquioxides is to devise a cycle yielding the enthalpy of solution in infinitely dilute acid:

$$An_2O_3(c) + 6HCl(n\ \text{M}) \rightarrow 2AnCl_3\ (\text{in } n\ \text{M HCl}) + 3H_2O\ (\text{in } n\ \text{M HCl})$$

$$2AnCl_3\ (\text{in } n\ \text{M HCl}) \rightarrow 2AnCl_3(c)$$

$$2AnCl_3(c) \rightarrow 2AnCl_3\ (\text{in } H_2O)$$

$$6HCl\ (\text{in } H_2O) \rightarrow 6HCl\ (n\ \text{M})$$

$$3H_2O\ (\text{in } n\ \text{M HCl}) \rightarrow 3H_2O(l)$$

which can be summarized as:

$$An_2O_3(c) + 6HCl\ (\text{in } H_2O) \rightarrow 2AnCl_3\ (\text{in } H_2O) + 3H_2O(l)$$

or

$$An_2O_3(c) + 6H^+(aq) \rightarrow 2An^{3+}(aq) + 3H_2O(l) \qquad \Delta H^\circ_{soln}(An_2O_3)$$

Thus, we obtain

$$\Delta H^\circ_{soln}(An_2O_3) = 2\Delta H^\circ_f(An^{3+}(aq)) + 3\Delta H^\circ_f(H_2O(l)) - \Delta H^\circ_f(An_2O_3(c)) \quad (17.9)$$

The enthalpy of solution represents the difference between the lattice enthalpy of the crystalline sesquioxide and the enthalpy of hydration of its ionic components. Both of these properties are difficult to calculate and change substantially as a function of ionic properties, whereas their difference (the enthalpy of solution) should change slowly and smoothly as a function of ionic size.

The enthalpy of solution of lanthanide and actinide sesquioxides is plotted as a function of molar volume in Fig. 17.4. Molar volume was chosen as a parameter because there are three different sesquioxide structures with different coordination numbers and numbers of molecules per unit cell; the plot is referenced to one mole of M ($MO_{1.5}$ rather than M_2O_3) because trichloride data are shown on a similar plot and will be discussed below. Ionic radii [44] could have been used, since these are tabulated as a function of coordination number, but often they are reliable to only two significant figures. It is evident that, for all three structure types, the enthalpies of solution of actinide sesquioxides are significantly less exothermic than for structurally similar lanthanide sesquioxides.

For predictive purposes, the enthalpies of solution of the other known sesquioxides (Pu_2O_3 and Bk_2O_3) were estimated from Fig. 17.4. Enthalpies of solution and molar volumes of expected structural types of neighboring actinide sesquioxides were also estimated. Table 17.5 shows these estimates and also the

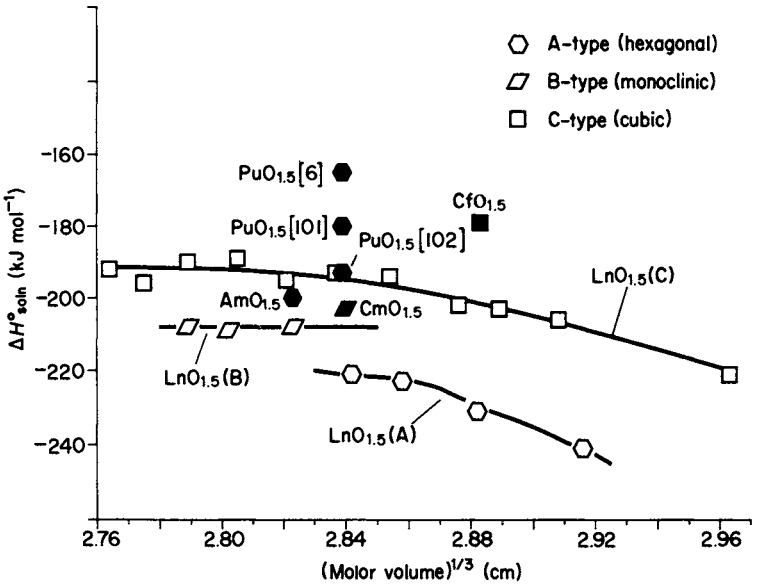

Fig. 17.4 *Enthalpies of solution of f-element sesquioxides.*

Table 17.5 *Enthalpies of solution and formation of lanthanide and actinide sesquioxides.*

Ln	$2\Delta H_f^\circ(Ln^{3+}(aq))$ (kJ mol^{-1})	$\Delta H_{soln}^\circ(Ln_2O_3(c))$ (kJ mol^{-1})	*Unit-cell volume* (Å^3)	$\Delta H_f^\circ(Ln_2O_3(c))$ (kJ mol^{-1})	An	$2\Delta H_f^\circ(An^{3+}(aq))$ (kJ mol^{-1})	$\Delta H_{soln}^\circ(An_2O_3(c))$ (kJ mol^{-1})	*Unit-cell volume* (Å^3)	$\Delta H_f^\circ(An_2O_3(c))$ (kJ mol^{-1})
La	−1419	−482[a]	165[a]	−1794[a]	Ac	(−1256)	(−357)[a]	180[a]	(−1756)[a]
Ce	−1401	−462[a]	159[a]	−1796[a]	Th				
Pr	−1412	−442[a]	155[a]	−1823[a]	Pa				
		−446	1387	−1828					
Nd	−1393	−442[a]	152[a]	−1808[a]	U	−978	(−379)[a]	(159)[a]	(−1456)[a]
Pm	−1376	(−420)	1327	(−1813)	Np	−1054	(−389)[a]	(155)[a]	(−1522)[a]
Sm	−1382	−416	149[b]	−1824[b]	Pu	−1184	(−385)[a]	152[a]	(−1656)[a]
		−411	1307	−1828					
Eu	−1211	−418	146[b]	−1651[b]	Am	−1233	−400[a]	150[a]	−1690[a]
		−406	1281	−1663					
Gd	−1374	−416	144[b]	−1816[b]	Cm	−1230	−406[b]	152[b]	−1682[b]
		−404	1264	−1827					
Tb	−1396	−388	1235	−1865	Bk	−1202	(−366)	1290	(−1694)
Dy	−1392	−386	1213	−1863	Cf	(−1154)	−358	1273	−1653
Ho	−1414	−390	1193	−1881	Es	(−1192)	(−353)	1248	(−1696)
Er	−1416	−378	1173	−1898	Fm	(−1184)	(−347)	(1228)	(−1694)
Tm	−1410	−380	1153	−1889	Md	(−1020)	(−342)	(1208)	(−1535)
Yb	−1349	−392	1136	−1815	No	(−740)	(−337)	(1190)	(−1260)
Lu	−1405	−384	1122	−1878	Lr	(−1246)	(−337)	(1175)	(−1766)
Refs	100	calc.	60	40		Tables 17.1, 17.14	calc.	Table 14.8	Tables 17.14, or calc.

[a] Hexagonal sesquioxide.
[b] Monoclinic sesquioxide.
( ) Estimated values.

predicted enthalpies of formation derived from the estimated enthalpies of solution:

$$\Delta H_f^\circ(An_2O_3) = 2\Delta H_f^\circ(An^{3+}(aq)) + 3\Delta H_f^\circ(H_2O(l)) - \Delta H_{soln}^\circ(An_2O_3) \qquad (17.10)$$

Simple calculations confirm that the sesquioxides of uranium and neptunium are significantly unstable with respect to disproportionation into metal and dioxide, e.g. using enthalpies of formation from Tables 17.5 and 17.14 and estimated entropies,

$$2Np_2O_3(c) = 3NpO_2(c) + Np(c) \qquad \Delta G^\circ = -170\ kJ\ mol^{-1} \qquad (17.11)$$

The corresponding U reaction has $\Delta G^\circ = -331\ kJ\ mol^{-1}$.

The case of Pu_2O_3 deserves special mention. Its enthalpy of formation has been estimated as $-1710 \pm 13\ kJ\ mol^{-1}$ [6] from high-temperature EMF measurements, as $-1685 \pm 21\ kJ\ mol^{-1}$ [101] from high-temperature calorimetry, and as $-1656\ kJ\ mol^{-1}$ [102] from earlier measurements and more recent heat-capacity values. The last value is in excellent agreement with the systematics of Fig. 17.4 and has been adopted in this chapter. Since there is an experimentally derived standard entropy of Pu_2O_3, we can calculate its free energy of solution, $-290\ kJ\ mol^{-1}$, for comparison with that of the structurally similar Nd_2O_3, $-338\ kJ\ mol^{-1}$. Actinide sesquioxides appear to be more stable than structurally similar lanthanide sesquioxides in comparison with the corresponding aqueous solutions, so that nuclear waste oxide matrices that accept lanthanide ions should bind corresponding trivalent actinides (Pu^{3+}, Am^{3+}) even more strongly. The reason for this behavior is not clear; a rationalization is that the 5f covalence is stronger to oxygen in solid oxides than in hydrated ions.

An important correlation between trivalent f-block ions and their 'trivalent' atoms ($f^n ds^2$) is the $P(M)$ function proposed by Nugent *et al.* [29]. This function has been utilized for predicting enthalpies of sublimation of metals and enthalpies of formation of aqueous ions. David *et al.* [27] used heavy-actinide thermodynamic properties to establish a $P(M)$ function relating all of the actinide metals and their 3 + aquo ions. Morss and Sonnenberger [103] used newer data to refine this $P(M)$ and to develop similar $P(M)$ plots relating f-block metals and their sesquioxides and trichlorides (Figs 17.5 and 17.6).

There are, as of the time of writing, no thermochemical data on complex oxides containing trivalent actinides (e.g. $AmAlO_3$ or $SrAm_2O_4$). Indeed, such measurements are still lacking for the lanthanides.

17.5.3 Dioxides

Table 14.9 showed that all the dioxides from ThO_2 through CfO_2 are known, but that several have not been studied thermodynamically. Morss and Fuger [39–41, 157] have established an enthalpy-of-solution plot (Fig. 17.7) for f-block dioxides that is similar in principle to that discussed above for sesquioxides but shows no shift between 4f and 5f elements. (If greater covalence of 5f ions than 4f ions with

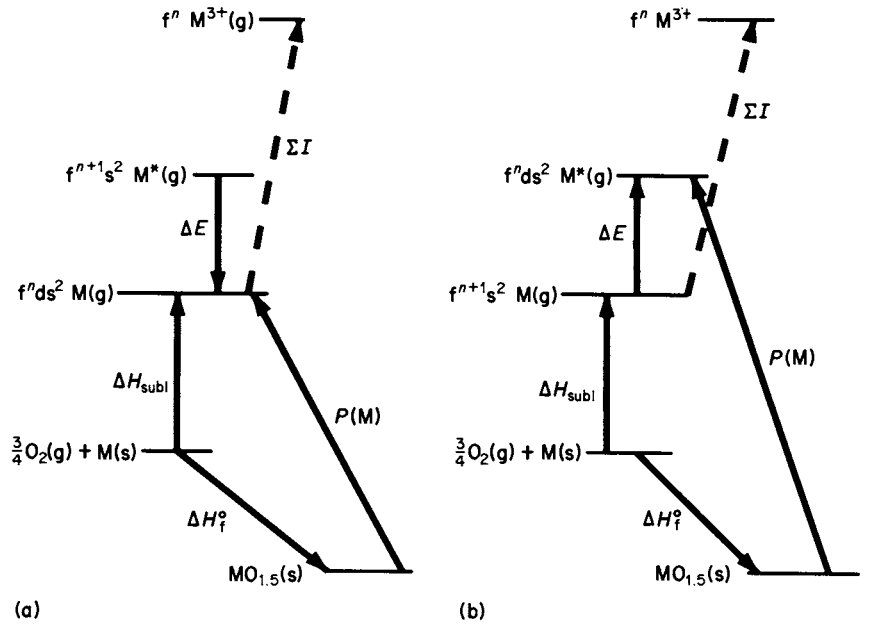

Fig. 17.5 *P* (M) *diagrams for trivalent species: (a) for* M = *La, Ce, Gd, Lu, Ac–Np, and Cm; (b) for other lanthanides, and Pu, Am, and Bk–No.*

oxides were postulated, then the An^{4+} ions should show a greater shift than the An^{3+} ions compared to the corresponding lanthanide ions.)

Fig. 17.7 can be used to estimate enthalpies of solution of other actinide dioxides and to calculate their enthalpies of formation. The relevant data are shown in Table 17.6. A tetravalent *P*(M) function has also been conceived and plotted [40] but its component terms have large error limits and there are few reliable data points, so that the tetravalent *P*(M) function is not useful to explain metallic behavior or to predict dioxide thermodynamics.

17.5.4 Higher oxides and complex oxides

Although a number of binary uranium oxides with O/U > 2.00 are known, along with many of their thermodynamic properties, there are no comparable properties of heavier actinide oxides with which to compare them. (The only transuranium binary oxide with O/An > 2.00 is Np_2O_5 and none of its thermodynamic properties have been measured.) To compare thermodynamic properties of actinide oxides in high oxidation states, scientists have studied complex oxides.

One class of complex oxides containing tetravalent f ions has been studied thermochemically, the perovskites $BaMO_3$. Only the thermodynamic properties of two actinide(IV) perovskites have been determined, $BaUO_3$ and $BaPuO_3$ [104, 355]. A general trend is that the perovskites are increasingly stabilized (with

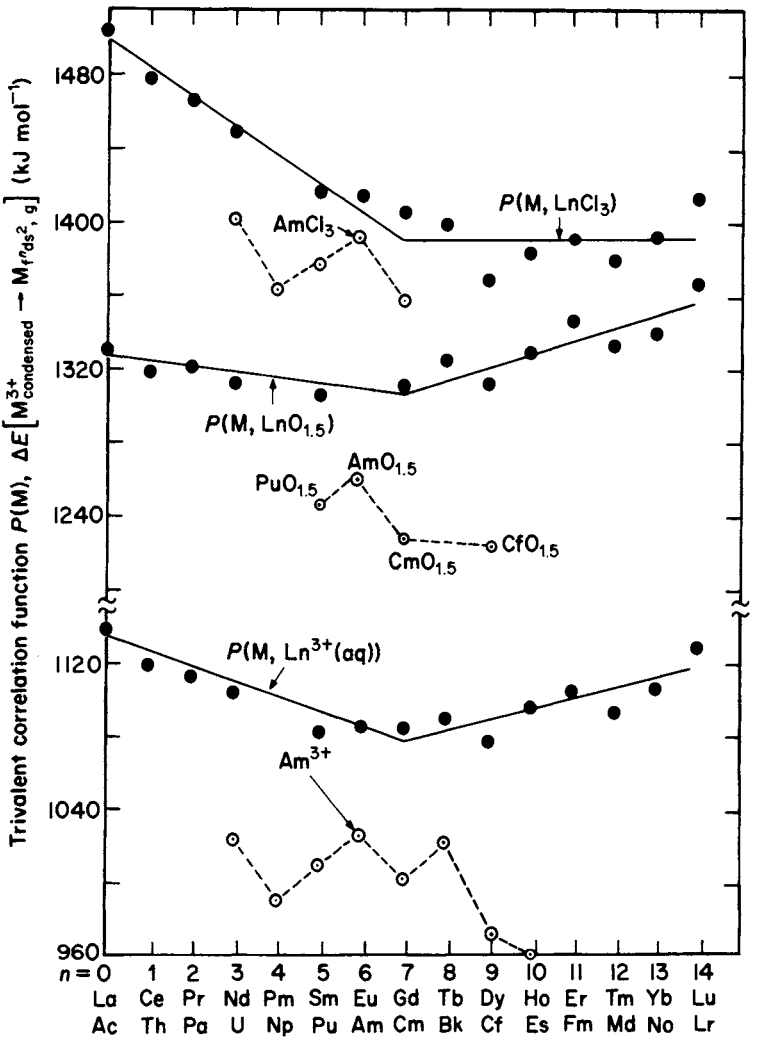

Fig. 17.6 *P* (M) *function for f-element trichlorides, sesquioxides, and aquo ions.*

respect to the parent oxides) as the tolerance factor t approaches unity [40, 104]. This trend leads to the conclusion that an exciting compound like $BaEsO_3$ might exist as the first macroscopic Es(IV) compound, but this compound has not been reported.

Three types of complex oxides containing pentavalent uranium ($LiUO_3$, $BaUO_{3.5}$, and Na_3UO_4 are examples) have been studied thermochemically [105, 106, 265]. Several classes of complex oxides containing hexavalent uranium, a few classes containing hexavalent Np and Pu, and one class (the ordered perovskites) containing hexavalent U, Np, and Pu have been studied. Lindemer *et al.* [363] and Fuger [265] have reviewed the results on all of these complex oxides.

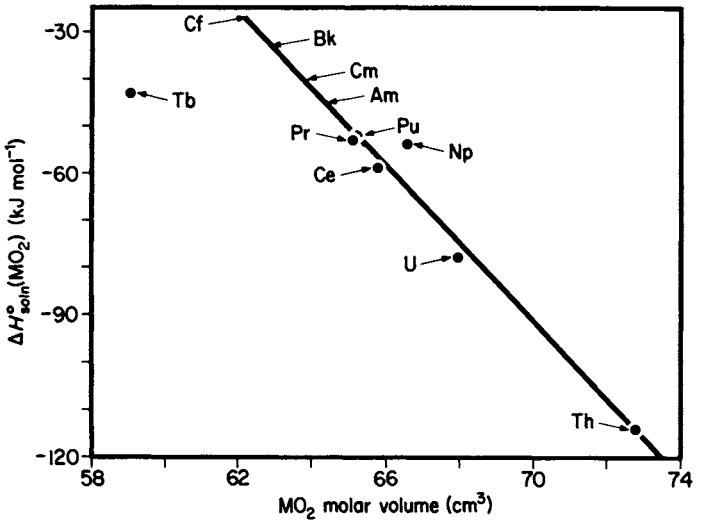

Fig. 17.7 *Enthalpies of solution of f-element dioxides.*

Table 17.7 and Figs 17.8 and 17.9 summarize these results. Enthalpies of solution represent the stability of these oxides in comparison with the aquo ions. Enthalpies of complexation indicate their stability with respect to the parent binary oxides, and represent a mixture of structural-packing (ionic) stabilization energies and acidic oxide–basic oxide (covalent) energies.

Enthalpies of complexation cannot be calculated for complex Np(VI) oxides or for complex Pu(VI) oxides, because NpO_3(c) and PuO_3(c) are unknown. Therefore Fig. 17.9 utilizes as an initial actinide(VI) species the aquo ion AnO_2^{2+} and shows the enthalpies of reactions such as

$$3SrO(c) + UO_2^{2+}(aq) + H_2O(l) = Sr_3UO_6(c) \qquad (17.12)$$

The most exothermic enthalpy effect of the reactions indicated in Fig. 17.9, for Na_4NpO_5, implies that this matrix stabilizes An(VI) ions particularly well. Of course, the instabilities and basicities of the alkali-metal oxides and alkaline-earth oxides are also implicitly included in these enthalpies of complexation (Table 17.7) and the enthalpies represented by equation (17.12) (Fig. 17.9).

Figure 17.8 represents the ΔH_f° of some +4 to +6 uranium oxides. The slopes of the curve represent partial molal enthalpies with respect to oxygen, becoming more negative in the sequence UO_{2+x} > (Li, Na, K, Sr) UO_{3+x} > $BaUO_{3+x}$ and confirming the stabilization effect of Ba on hexavalent actinide oxides.

Table 17.6 *Enthalpies of solution and formation of lanthanide and actinide dioxides.*

Ln	$\Delta H_f^\circ(Ln^{4+}(aq))$ (kJ mol^{-1})	$\Delta H^\circ_{soln}(LnO_2(c))$ (kJ mol^{-1})	*Unit-cell volume* (Å^3)	$\Delta H_f^\circ(LnO_2(c))$ (kJ mol^{-1})	An	$\Delta H_f^\circ(An^{4+}(aq))$ (kJ mol^{-1})	$\Delta H^\circ_{soln}(AnO_2(c))$ (kJ mol^{-1})	*Unit-cell volume* (Å^3)	$\Delta H_f^\circ(AnO_2(c))$ (kJ mol^{-1})
Ce	−580	−63	158.4	−1089	Th	−769	−115	175.2	−1226
Pr	(−439)[a]	−62	156.9		Pa	−622	(−85)	166.8	(−1109)
		−53		−958	U	−591	−78	163.7	−1085
					Np	−556	−54	160.5	−1074
					Pu	−536	−52	157.1	−1056
					Am	(−406)	(−46)	155.4	−932
					Cm	(−379)	(−41)	153.9	−911
Tb	(−443)	−43	141.7	−972	Bk	(−483)	(−36)	151.8	(−1021)
					Cf	(−313)	(−27)	149.7	(−858)
					Es	(−211)	(−20)	(−148)	(−763)
Refs	100	calc.	60	100		Tables 17.1, 17.14	calc. (Fig. 17.7)	111, Table 14.8	Table 17.14, or calc.

[a] Calculated from $E^\circ(Pr^{4+}/Pr^{3+})$ [26] and ΔS°.
( ) Estimated values.

Table 17.7 *Enthalpies of solution, formation, and complexation of some complex actinide oxides* [16, 104–106, 265].

	ΔH°_{soln} (1 M HCl) (kJ mol^{-1})			ΔH°_f (kJ mol^{-1})			ΔH°_{cplx} (kJ mol^{-1}) (*binary oxides* → *complex oxide*)		
Compound	*U*	*Np*	*Pu*	*U*	*Np*	*Pu*	*U*	*Np*	*Pu*
tetravalent									
$BaAnO_3$	−290			−1690	●	−1656	−57		
pentavalent									
$LiAnO_3$				−1522			−53[a]		
$NaAnO_3$				−1495			−118[a]		
$KAnO_3$				−1523			−172[a]		
$RbAnO_3$				−1521			−182[a]		
Na_3AnO_4				−2025	●	●	−234[a]		
hexavalent									
Li_2AnO_4				−1962	●		−150		
α-Na_2AnO_4				−1889	●		−259		
β-Na_2AnO_4				−1879	●		−248		
K_2AnO_4				−1911	●	●	−336		
Rb_2AnO_4				−1913	●	●	−350		
Cs_2AnO_4				−1922	●	●	−359		
Li_4AnO_5				−2460	●	●	−221		
β-Na_4AnO_5				−2451	●	●	−399		
$MgAnO_4$				−1857			−32		
$CaAnO_4$				−2002	●		−143		
α-$SrAnO_4$				−1989	●	●	−175		
β-$SrAnO_4$				−1990					
$BaAnO_4$				−1997	●		−225		
Ba_2MgAnO_6	−451	−442	−504	−3245	−3096	−2994	−324	(−328)[b]	
Ba_2CaAnO_6	−478	−456	−509	−3296	−3159	−3068	−341	(−358)[b]	
Ba_2SrAnO_6	−524	−501	−562	−3257	−3123	−3024	−347	(−366)[b]	
Ca_3AnO_6	−483			−3301			−173		
Sr_3AnO_6	−550	−530	−576	−3263	−3125	−3042	−267	(−284)[b]	
Ba_3AnO_6	−555	−522	−572	−3211	−3086	−2998	−343	(−372)[b]	
$LiAnO_{3.5}$	−117			−1607			−84		
$NaAnO_{3.5}$	−86	−83		−1602	−1447		−171	(−170)[b]	
$KAnO_{3.5}$	−74	−75		−1625	−1466		−220	(−215)[b]	
$RbAnO_{3.5}$	−83	−83		−1616	−1457		−223	(−218)[b]	
β-$CsAnO_{3.5}$	−94			−1613			−216		

● Compound known but no thermodynamic data.
[a] Assumes $\Delta H^\circ_f(UO_{2.5}(c)) = -1170$ kJ mol^{-1}.
[b] Assumes $\Delta H^\circ_f(NpO_3(c)) = -1070$ kJ mol^{-1}.

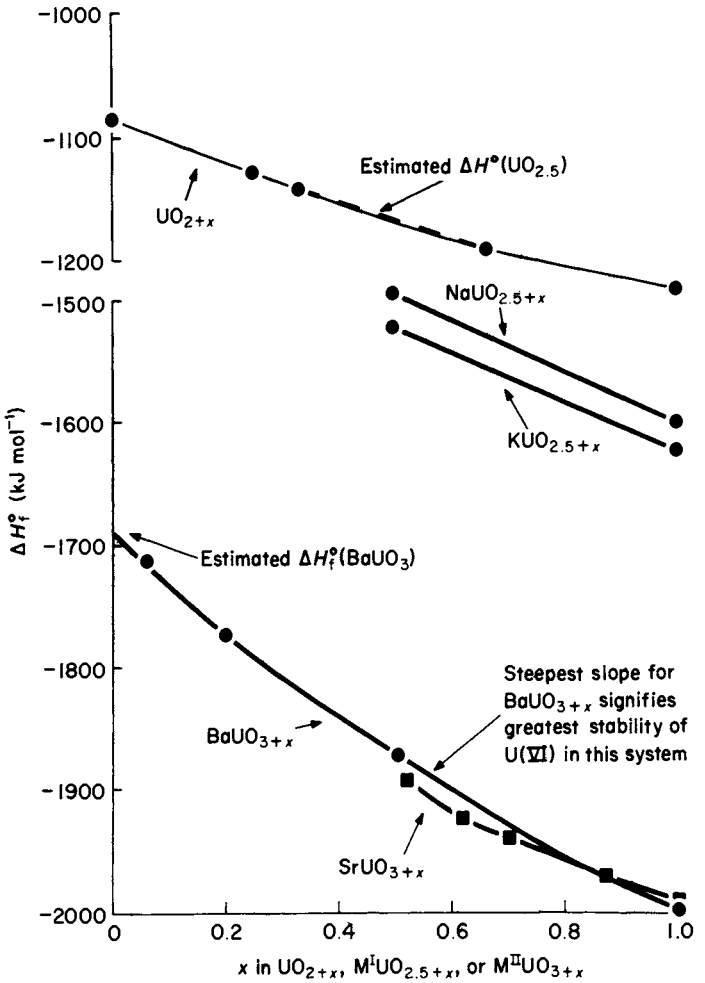

Fig. 17.8 *Comparison of enthalpies of formation of uranium(V) oxides* [105] *with uranium(IV) and (VI) oxides.*

17.6 HALIDES

Because of the fundamental and applied interest in the many actinide halides, their thermodynamic properties have received much attention. The recent authoritative assessment by Fuger *et al.* [20] is cited throughout Table 17.14 for most actinide halides. The discussion that follows will be limited to systematic properties of halide families and areas needing further study. Thermodynamic properties of many gaseous actinide halides and their ions have been assessed by Hildenbrand *et al.* [354] and by Kleinschmidt and Ward [362]; only properties of halide species are included in Table 17.14.

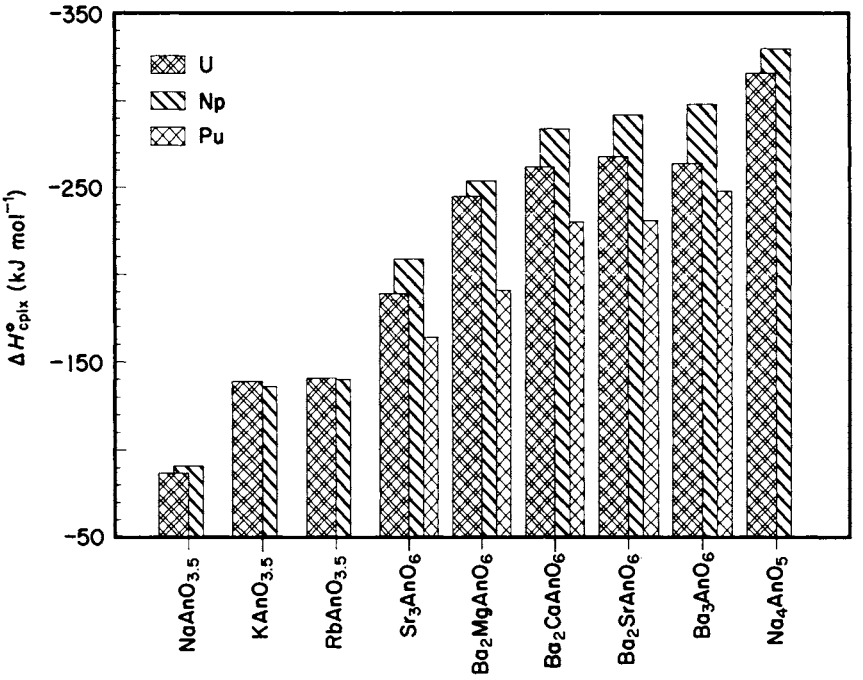

Fig. 17.9 *Enthalpies of complexation of complex actinide(VI) oxides (see equation* (17.12)).

17.6.1 Dihalides

The dichlorides, dibromides, and di-iodides of Am and Cf have been reported. No thermochemical data are available. Since these dihalides parallel lanthanide dihalides of similar M^{2+} ionic radii, it is possible to estimate their enthalpies of formation by a method similar to that used by Morss and Fahey [107]. The data for this estimation, and the resulting predicted enthalpies of formation, are shown in Table 17.8. The enthalpies of the reactions

$$Am(c) + 2AmCl_3(c) = 3AmCl_2(c) \qquad \Delta H = -6\,kJ\,mol^{-1} \qquad (17.13)$$

and

$$Cf(c) + 2CfCl_3(c) = 3CfCl_2(c) \qquad \Delta H = -77\,kJ\,mol^{-1} \qquad (17.14)$$

illustrate the relative difficulty and ease of preparing the dihalides of americium and californium respectively.

17.6.2 Trifluorides

Trigonal trifluorides are known for all the actinides Ac and U–Cf. Surprisingly, for only UF_3 and PuF_3 have thermodynamic measurements been performed; even more surprising is the unsatisfactory situation regarding even these two trifluorides. Fuger *et al.* [20] have elaborated all of the experimental results and

Table 17.8 *Enthalpies of solution and formation of lanthanide and actinide dichlorides.*

Ln	$\Delta H_f^\circ(LnCl_2(aq))$ (kJ mol^{-1})	ΔH°_{soln} (kJ mol^{-1})	IR(Ln^{2+}) (Å)	$\Delta H_f^\circ(LnCl_2(c))$ (kJ mol^{-1})	An	$\Delta H_f^\circ(AnCl_3(aq))$ (kJ mol^{-1})	ΔH°_{soln} (kJ mol^{-1})	IR(An^{2+}) (Å)	$\Delta H_f^\circ(AnCl_2)$ (kJ mol^{-1})
Pr									
Nd	(−736)	(−29)	1.22	−707					
Pm	(−724)	(−33)	(1.19)	−691					
Sm	(−838)	(−36)	1.18	−802	Pu	(−558)	(−30)	(1.21)	(−528)
Eu	−862	−38	1.17	−824	Am	(−689)	(−35)	1.19	(−654)
					Cm	(−556)	(−40)	(1.16)	(−516)
					Bk	(−629)	(−45)	(1.14)	(−584)
Dy	(−752)	(−59)	1.09	−693	Cf	(−719)	(−50)	1.12	(−669)
					Es	(−749)	(−55)	(1.10)	(−694)
					Fm	(−808)	(−60)	(1.08)	(−748)
Tm	(−776)	(−67)	1.04	−709	Md	(−815)	(−63)	(1.06)	(−752)
Yb	(−871)	(−71)	1.03	−800	No	(−828)	(−65)	(1.05)	(−763)
Refs	100, 107	calc. (107)	107	100, 107		Table 17.1	est.	Table 17.2	calc.

( ) Estimated values.

Table 17.9 *Enthalpies of solution and formation of lanthanide and actinide trifluorides.*

Ln	$\Delta H_f^\circ(LnF_3(aq))$ (kJ mol^{-1})	ΔH_{soln}° (kJ mol^{-1})	*Unit-cell volume* (Å^3)	$\Delta H_f^\circ(LnF_3(c))$ (kJ mol^{-1})	An	$\Delta H_f^\circ(AnF_3(aq))$ (kJ mol^{-1})	ΔH_{soln}° (kJ mol^{-1})	*Unit-cell volume* (Å^3)	$\Delta H_f^\circ(AnF_3(c))$ (kJ mol^{-1})
La	−1715	−16	328.7[a]	−1699 ± 2	Ac	(−1634)	(+25)	359.3[a]	(−1659)
Ce	−1706	−3	318.8[a]	−1703					
Pr	−1712	−23	313.9[a]	−1689 ± 3					
Nd	−1703	−24	308.1[a]	−1679 ± 2	U	−1495	+7	328.2[a]	−1502
Pm	(−1694)	(−26)	302.5[a]	(−1668)	Np	−1533	(−4)	320.8[a]	(−1529)
Sm	−1697	−28	298.2[a]	−1669 ± 5	Pu	−1598	−12	316.1[a]	−1586
Eu	−1612	−41	293.8[a]	−1571	Am	−1623	(−18)	310.5[a]	(−1605)
Gd	−1693	+6	201.4[b]	−1699 ± 2	Cm	−1621	(−22)	304.6[a]	(−1599)
Tb	−1704	+3	198.3[b]	−1707	Bk	−1607	(−26)	300.4[a]	(−1581)
Dy	−1701	−9	195.4[b]	−1692 ± 2	Cf	(−1583)	(−30)	296.6[a]	(−1553)
Ho	−1713	−15	192.7[b]	−1698 ± 2	Es	(−1609)	(−34)	unknown	(−1575)
Er	−1715	−21	190.4[b]	−1694 ± 2	Fm				
Tm	−1711	−55	188.6[b]	−1656	Md				
Yb	−1680	−110	187.0[b]	−1570	No				
Lu	−1709	−8	185.8[b]	−1701	Lr				
Refs	42, 100, 112	calc.	60	60, 109, 110		Table 17.14, 15, 112	calc. (Fig. 17.10)	111, Table 14.8	Table 17.14, 20, calc.

( ) Estimated values.
[a] LaF_3 (trigonal) structure.
[b] YF_3 (orthorhombic) structure.

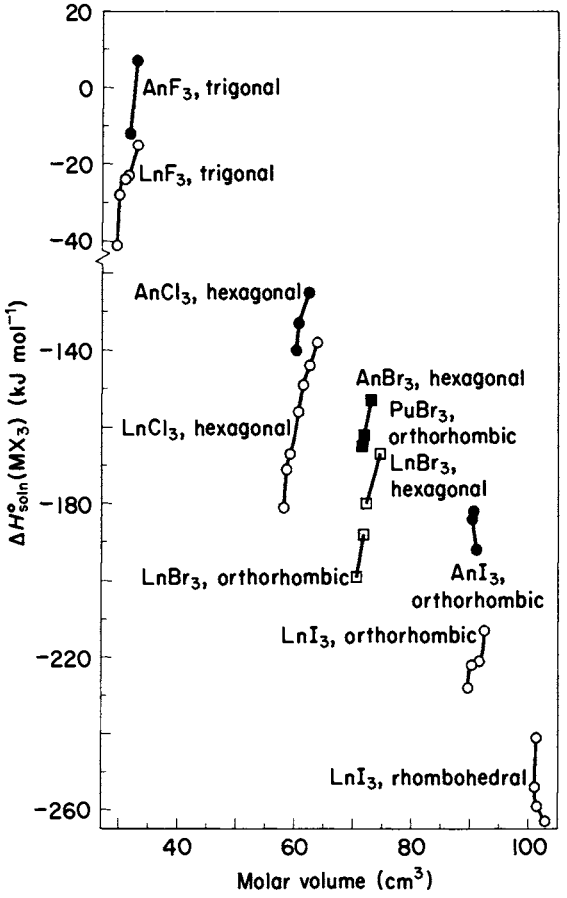

Fig. 17.10 *Enthalpies of solution of f-element trihalides.*

their unresolved questions. For UF_3 several independent thermochemical pathways have been used, yielding unresolvable inconsistencies with a variety of uranium species; sample impurities plagued the fluorine combustion measurements and complex thermochemical cycles, involving many species, obfuscate the solution calorimetry measurements. For PuF_3 the one measurement [108] is uncertain primarily because it was a reaction to an unanalyzed trifluoride precipitate assumed to be anhydrous but probably $PuF_3 \cdot 0.4H_2O$. Nevertheless, these two data points must be used to compare and to predict the properties of all f-element trifluorides.

Fortunately, there are enthalpy-of-formation data on almost all lanthanide trifluorides. Table 17.9 and Fig. 17.10 present these data along with structural data that permit an enthalpy-of-solution correlation similar to that done above on sesquioxides. It can be seen that there is scatter among the calculated enthalpies of solution of neighboring lanthanide trifluorides, so that the

correlation will have limited value until better lanthanide and actinide trifluoride enthalpy measurements are made. Still, the two actinide trifluorides correlate well with the enthalpies of solution of LaF_3 and PrF_3; as was the case for sesquioxides, the enthalpies of solution of actinide trifluorides are less exothermic than for structurally similar lanthanide trifluorides. Our prediction for NpF_3 yields $\Delta H_f^\circ = -1529$ kJ mol^{-1}, identical to that estimated by Fuger *et al.* [20].

AmF_3 has a similar unit-cell volume to NdF_3, but the enthalpies of solution of NdF_3 through EuF_3 do not change smoothly enough to permit direct lanthanide-to-actinide comparisons. Reasonable estimates have been made of enthalpies of solution for AmF_3 through CfF_3 (Table 17.9) to derive their enthalpies of formation. Fuger *et al.* [20] estimated only $\Delta H_f^\circ(AmF_3(c)) = -1588 \pm 13$ kJ mol^{-1}, disagreeing from the estimate in Table 17.9 probably because they used a slightly different systematic procedure and extrapolation (without use of lanthanide data) on the basis of ionic radii only. Since AmF_3 is a compound easily prepared, its enthalpy of formation (as well as that of AmF_4) ought to be determined.

Low-temperature heat capacities of UF_3 and PuF_3 have been measured. From these and high-temperature data on UF_3, Fuger *et al.* [20] calculated thermal functions up to high temperature for UF_3, NpF_3, and PuF_3.

17.6.3 Other trihalides

Trichlorides, tribromides, and tri-iodides of all elements from uranium through einsteinium are known. Solution-calorimetry enthalpies of formation are known for these trihalides of uranium through plutonium, although that of $NpCl_3$ requires an estimate of its heat of solution [20]. The enthalpy of formation of $AmCl_3$ is known from solution calorimetry; that of other americium trihalides as well as heavier trihalides must be estimated.

As was the case for oxides, the enthalpy of formation of trihalides can be estimated by a correlation of their enthalpies of solution versus molar volume for isostructural compounds. Such data sets are shown in Tables 17.10 through 17.12 with corresponding data plotted in Fig. 17.10. The resultant enthalpies of formation have been incorporated in Table 17.14.

17.6.4 Tetrafluorides and other tetrahalides

Knowledge of actinide tetrafluoride enthalpies of formation is little better than that for trifluorides. Even for ThF_4 there are discordant values: for UF_4, Fuger *et al.* [20] show 14 experimental efforts with scatter of 36 kJ mol^{-1}; for PuF_4, there are only estimates from high-temperature equilibria. There are no lanthanide thermochemical comparisons, not even for CeF_4. We have accepted the assessed values of Fuger *et al.* [20] and have attempted to incorporate estimates of tetrafluoride thermochemistry with those of other tetravalent compounds. Vaporization properties of ThF_4 and UF_4 are well established [20, 360].

There are two other well-studied classes of tetravalent actinide compounds.

Table 17.10 *Enthalpies of solution and formation of lanthanide and actinide trichlorides.*

Ln	$\Delta H_f^\circ(LnCl_3(aq))$ (kJ mol^{-1})	ΔH°_{soln} (kJ mol^{-1})	*Unit-cell volume* (Å^3)	$\Delta H_f^\circ(LnCl_3(c))$ (kJ mol^{-1})	An	$\Delta H_f^\circ(AnCl_3(aq))$ (kJ mol^{-1})	ΔH°_{soln} (kJ mol^{-1})	*Unit-cell volume* (Å^3)	$\Delta H_f^\circ(AnCl_3(c))$ (kJ mol^{-1})
La	−1211	−138	211.8	−1073	Ac	(−1154)	(−105)	230.5	(−1049)
Ce	−1202	−144	207.4	−1058	Th				
Pr	−1207	−148	203.9	−1059	Pa				
Nd	−1198	−156	201.1	−1042	U	−990	−124	207.3	−866
Pm	(−1189)	(−160)	199.5	(−1029)	Np	−1028	(−130)	204.2	(−898)
Sm	−1192	−166	196.6	−1026	Pu	−1093	−133	201.1	−960
Eu	−1107	−171	194.6	−936	Am	−1118	−140	200.0	−978
Gd	−1188	−180	192.9	−1008	Cm	−1116	(−142)	197.4	−974
Tb	−1199	−192	383.3[a]	−1007	Bk	−1102	(−150)	194.7	(−952)
Dy	−1197	−208	493.5[b]	−989	Cf	(−1078)	(−153)	193.6	(−925)
							(−170)	389.2[a]	(−908)[a]
Ho	−1208	−213	484.9[b]	−995	Es	(−1104)	(−154)	193.5	(−950)
Er	−1210	−215	479.2[b]	−995	Fm	(−1133)	(−170)[c]		(−963)[c]
Tm	−1206	−215	473.6[b]	−991	Md	(−1039)	(−175)[c]		(−864)[c]
Yb	−1176	−216	468.8[b]	−960	No	(−896)	(−180)[c]		(−716)[c]
Lu	−1204	−218	466.9[b]	−986	Lr	(−1131)	(−185)[c]		(−946)[c]
Refs	42, 100, 112	calc.	113, 114	42, 100		15, 112, Table 17.14	calc. (Fig. 17.10)	111, Table 14.8	20, Table 17.14, calc.

[a] Orthorhombic ($PuBr_3$).
[b] Monoclinic ($AlCl_3$).
[c] Assumes crystal structure change (cf. $TbCl_3$ or $DyCl_3$).
( ) Estimated values.

Table 17.11 *Enthalpies of solution and formation of lanthanide and actinide tribromides.*

Ln	$\Delta H_f^\circ(LnBr_3(aq))$ (kJ mol^{-1})	ΔH_{soln}° (kJ mol^{-1})	*Unit-cell volume* (Å^3)	$\Delta H_f^\circ(LnBr_3(c))$ (kJ mol^{-1})	An	$\Delta H_f^\circ(AnBr_3(aq))$ (kJ mol^{-1})	ΔH_{soln}° (kJ mol^{-1})	*Unit-cell volume* (Å^3)	$\Delta H_f^\circ(AnBr_3(c))$ (kJ mol^{-1})
La	−1074	−167	247.9[a]	−907	Ac	(−993)			
Ce	−1065	(−175)	243.4[a]	(−890)	Th	(−712)			
Pr	−1071	−180	240[a]	−891	Pa	(−804)			
Nd	−1061	−188	477[b]	−873	U	−854	−155	242.5[a]	−699
Pm	(−1053)	(−195)	471[b]	(−858)	Np	−892	−162	238.5[a] 479[b]	−730
Sm	−1056	−199	469[b]	−857	Pu	−957	−164	475[b]	−793
Eu	−971	−192	466[b]	−779	Am	−981	(−170)	470[b]	(−810)
Gd	−1052	−223	865[c]	−829	Cm	−980	(−172)	468[b]	(−808)
Tb	−1063	(−225)	851[c]	(−838)	Bk	−966	(−172)	469[b]	(−794)
Dy	−1060	−226	838[c]	−834	Cf	−968	(−200)	843[c]	(−768)
Ho	−1072	(−230)	829[c]	(−842)	Es				
Er	−1073	−234	823[c]	−839	Fm				
Tm	−1070	(−235)	811[c]	(−835)	Md				
Yb	−1040	(−235)	807[c]	(−805)	No				
Lu	−1068	(−240)	799[c]	(−828)	Lr				
Refs	42, 100, 112	calc.	114	100, 115		Table 17.14, 15, 112	calc., Fig. 17.10	Table 14.8, 111	20, 115

[a] UBr_3 (hexagonal) structure.
[b] $PrBr_3$ (orthorhombic) structure.
[c] $FeCl_3$ (hexagonal) structure.

Table 17.12 *Enthalpies of solution and formation of lanthanide and actinide tri-iodides.*

Ln	$\Delta H_f^\circ(LnI_3(aq))$ (kJ mol^{-1})	ΔH°_{soln} (kJ mol^{-1})	*Unit-cell volume* (Å^3)	$\Delta H_f^\circ(LnI_3(c))$ (kJ mol^{-1})	An	$\Delta H_f^\circ(AnI_3(aq))$ (kJ mol^{-1})	ΔH°_{soln} (kJ mol^{-1})	*Unit-cell volume* (Å^3)	$\Delta H_f^\circ(AnI_3(c))$ (kJ mol^{-1})
La	−880	−213	614.7[a]	−667	Ac				
Ce	−871	−221	608.7[a]	−650	Th				
Pr	−877	−222	599.9[a]	−654	Pa				
Nd	−867	−228	595.7[a]	−639	U	−659	−192	604.8[a]	−467
Pm					Np	−697	−184	600.3[a]	−513
Sm	−862	−241	1010.5[b]	−620	Pu	−762	−182	601.6[a]	−580
Eu					Am	−787	(−175)	595.1	
									(−612)
								979.8[b]	
Gd	−857	−263	1025.3[b]	−594	Cm	−785		977.9[b]	
Tb					Bk	−771		993.8[b]	
Dy	−866	−259	1011.6[b]	−607	Cf	−747		1037[b]	
Ho	−877	−254	1007.1[b]	−623	Es	−773			
Er	−878	−266	999.1[b]	−613					
Tm	−876	−274	989.5[b]	−602					
Yb	−844	(−275)	−992[b]	(−569)					
Lu	−873	−325	980.8[b]	−548					
Refs	42, 100, 112	calc.	113, 114	100, 114		Table 17.14, 15, 112	calc.	Table 14.8, 111	Table 17.14, 20

[a] $PuBr_3$ structure (orthorhombic *Ccmm*).
[b] BiI_3 structure (rhombohedral $R\bar{3}$).

Table 17.13 *Enthalpies of formation of actinide(IV) species* (kJ mol^{-1}).

An	AnF_4 (s)	$AnCl_4$ (s)	$AnBr_4$ (s)	AnI_4 (s)	AnO_2 (s)	An^{4+} (aq)
Th	−2098	−1186	−964	−671	−1226	−769
Pa	(−1946)	−1044	−826	−524	(−1109)	−622
U	−1914	−1022	−802	−519	−1085	−591
Np	(−1874)	−984	−771	(−484)[a]	−1074	−556
Pu	(−1846)	(−964)			−1056	−536
Am	(−1720)				−932	(−406)[a]
Cm	(−1689)				−911	(−379)[a]
Bk	(−1793)				(−1021)	(−483)
Cf	(−1623)				(−858)	(−313)[a]
Es	(−1521)[a]				(−763)[a]	(−211)[a]

[a] Believed to be unstable.

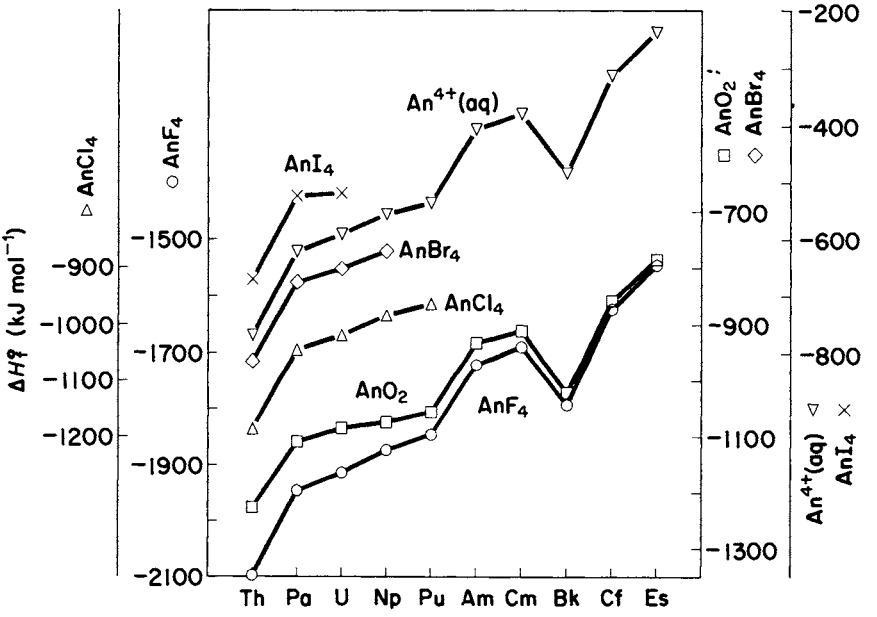

Fig. 17.11 *Comparison of enthalpies of formation of actinide(IV) species.*

One, the dioxides, has already been treated in this chapter (Section 17.5.3). The other is the tetrahalides of thorium, protactinium, uranium, and neptunium (excluding PaF_4, NpF_4, and NpI_4). In addition to the discordant values for the enthalpies of formation of the tetrafluorides (previous paragraph), there are discordant values for UCl_4 clustering around −1019 and −1045 kJ mol^{-1} [20]. Fortunately, enthalpies of formation of other thorium, protactinium, uranium, and neptunium tetrahalides appear to be well-established. In all cases we have accepted the recommended values of Fuger *et al.* [20], except that O'Hare's [347] consistent value for $\Delta H_f^\circ(UCl_4\ (c))$ is recommended.

Table 17.13 lists and Fig. 17.11 plots the enthalpies of formation of all known tetravalent actinide compounds and the aquo ions as a function of Z. The enthalpy scale has been compressed to facilitate comparison. Data were taken from Table 17.14. Interpolations can be made, using the best-fit curves shown, since each set of tetravalent compounds is isostructural, and other enthalpies of formation have thereby been estimated. The differences between the values thus calculated and those predicted by Fuger *et al.* [20] are relatively small.

An interesting but unstable compound is $PuCl_4$. It has been seen in the gas phase [317] and was believed to have been synthesized in a dilute solution of UF_4 [116]. Nevertheless, by comparison of other tetrahalides and complex chlorides, its enthalpy of formation is predictable within narrow error limits [20] and has been included in Fig. 17.11.

17.6.5 Pentahalides and hexahalides

We classify these compounds into three categories: those with modern, well-established thermochemistries; those with classical but usable thermochemistries; and those that have (or have not) been prepared and have not even estimated thermochemical properties.

Fuger *et al.* [20] accept the enthalpies of formation of $PaCl_5$, $PaBr_5$, and UF_5 (as well as some intermediate uranium fluorides) to be well-established, based upon single recent thermochemical studies. The enthalpy of formation of UF_6 is well-established, based upon an assessment of Parker [117] and confirmed by direct fluorine combustion calorimetry [118].

Thermochemical properties of UCl_5 and UCl_6 are based largely upon older (World War II) calorimetry. Properties of UBr_5 and PuF_6 are based upon high-temperature heterogeneous equilibria and have large uncertainties. The other higher halides (PaF_5, NpF_5, and NpF_6) have not been studied thermochemically and their properties cannot yet be estimated because of insufficient experimental data. See also [354 and 362].

Estimates of enthalpies of formation of a large group of higher actinide halides and oxyhalides have also been made by the Orsay thermochromatography group [119]. We have not accepted their values because they represent tracer-level phenomena that hypothesize a number of compounds not seen on the macroscopic level or that decompose at temperatures alleged for their thermochromatographic deposition temperatures.

17.6.6 Oxyhalides

There are many oxyhalides of actinide oxidation states 3+ through 6+. In general these are more stable than a mixture of oxide and halide, e.g.

$$UF_6(c) + 2UO_3(c,\gamma) = 3UO_2F_2(c) \qquad \Delta G^\circ = -316\ \text{kJ mol}^{-1} \quad (17.15)$$

reflecting the acid-based nature of reactions such as equation (17.10). In some cases, however, e.g.

$$2UF_6(c) + UO_3(c,\gamma) = 3UOF_4(c) \qquad \Delta H^\circ = -156\ \text{kJ mol}^{-1} \quad (17.16)$$

the reactions are almost thermoneutral, and the chemical properties of such oxyhalides reflect their weak bonding. In Table 17.14 we have accepted the assessed values of Fuger *et al.* [20] from calorimetric and vapor–solid hydrolysis equilibria. We have not attempted to predict the thermodynamic properties of any oxyhalides.

17.6.7 Complex halides and complex oxyhalides

Very many complex halides of thorium and uranium have been prepared for crystallographic, magnetic, and spectroscopic studies. Preparative conditions suggested that these compounds are more stable than the parent (binary) halides. For example, UF_5 is difficult to prepare but complex halides such as $CsUF_6$ are relatively stable. Among the transuranium elements, fewer high-valent binary

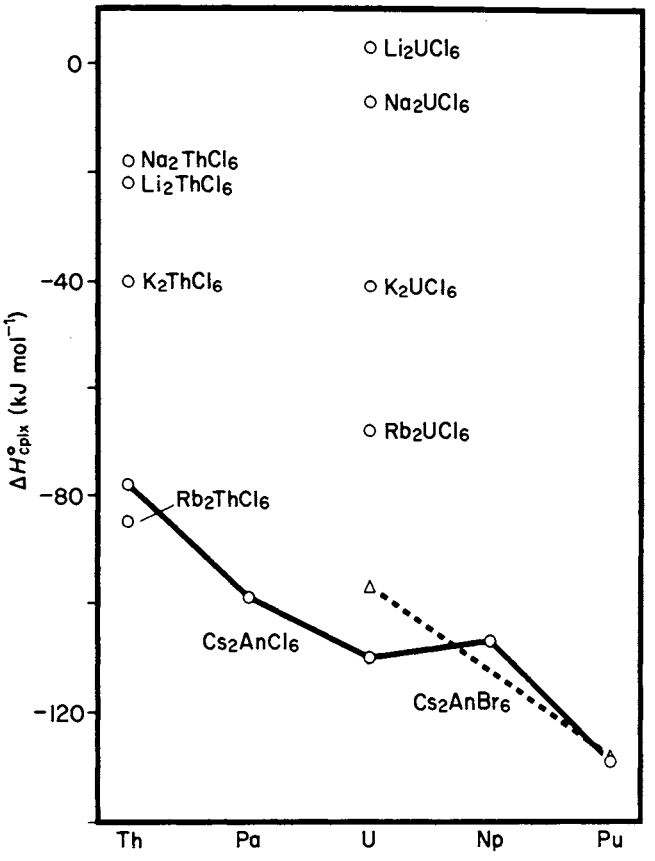

Fig. 17.12 *Enthalpies of complexation of complex actinide(IV) halides.*

Table 17.14 *Summary of thermodynamic properties (see text, p. 1347).*

Species	*State*	ΔH_f° (kJ mol^{-1})	*Refs*	ΔG_f° (kJ mol^{-1})	*Refs*	S° (J K^{-1} mol^{-1})	*Refs*	C_p° (J K^{-1} mol^{-1})	*Refs*	*Thermal data refs*	
										Low temp.	*High temp.*
Ac	c	0		0		(62 ± 1)	38				
Ac	g	(418 ± 13)	12, 27, 29								122
Ac^{2+}	aq	(−118)	calc.	(−142)	27, 123	(12)	Table 17.2				
Ac^{3+}	aq	(−628 ± 29)	27	(−617 ± 33)	27	(−180 ± 17)	15, 27				
Ac_2O_3	c	(−1756 ± 80)	Table 17.5			(67)	124				
$Ac(OH)_3$	c			(−1207)	calc.	(96)	125				
AcF_3	c	(−1659 ± 45)	Table 17.9								
$AcCl_3$	c	(−1049 ± 40)	Table 17.10	(−973)	calc.	(144)	est.				
Th	c	0		0		52.64	126	26.24	126	14, 126	11, 14, 126
Th	g	598 ± 6	127, 128	556.4	14	189.3	11, 126, 128	20.79	14	11, 14	11, 14
Th^{2+}	aq	(161)	calc.	(134)	27, 123	(10)	Table 17.2				
Th^{3+}	aq	(−347)	calc.	(−339 ± 29)	27	(−173)	27				
Th^{4+}	aq	−769.0 ± 2.5	15	−705 ± 5	15	−424 ± 4	15, 43	−1 ± 11	15, 43		
ThO	g	−28 ± 2	11			240.0	11, 12				11, 129–132
ThO_2	c	−1226.4 ± 3.5	128	−1168.7	calc.	65.23 ± 0.20	128	61.76 ± 0.07	133	242	134, 181
ThO_2	g	−497 ± 3	12			65.22	11, 12	47.35	12		11, 129, 132, 365

Table 17.14 (*Contd.*)

Species	*State*	ΔH_f° (kJ mol^{-1})	*Refs*	ΔG_f° (kJ mol^{-1})	*Refs*	S° (J K^{-1} mol^{-1})	*Refs*	C_p° (J K^{-1} mol^{-1})	*Refs*	*Thermal data refs*	
										Low temp.	*High temp.*
ThH_2	c	-145.1 ± 1.0	21, 135	-105.6 ± 1.0	21	50.73 ± 0.10	21, 136	36.71 ± 0.07	21, 136	21, 136	21, 135, 136
ThD_2	c	(-147.1 ± 1.1)	21	(-104.9 ± 1.1)	21	(55.7 ± 0.6)	21	(47.7 ± 0.5)	21		
ThT_2	c	(-147.6 ± 1.2)	21	(104.2 ± 1.2)	21	(60.5 ± 0.6)	21	(54.3 ± 0.5)	21		
$ThH_{3.75}$	c	-215.8 ± 4.4	21	-143.3 ± 4.4	21	54.42 ± 0.11	21, 136	51.32 ± 0.10	21, 136	21, 136	21, 136
$ThD_{3.75}$	c	(-220.3 ± 4.5)	21	(-142.7 ± 4.5)	21	(64.0 ± 0.6)	21	(69.7 ± 0.7)	21	21	21
$ThT_{3.75}$	c	(-221.4 ± 4.5)	21	(-141.7 ± 4.5)	21	(72.6 ± 0.7)	21	(81.5 ± 0.8)	21	21	21
ThF	g	19 ± 10	354			257.2	12, 354	34.7	12, 354	354	354
ThF_2	g	-605 ± 13	354	-617	calc.	295.1	12, 20, 354	52.4	12, 20, 354	354	20, 354
ThF_3	g	-1179 ± 15	20	-1184	calc.	339.2	12, 20, 354	73.3	12, 20, 354	354	20, 354
ThF_4	c	-2098 ± 8	20	-2004	20	142.0	20, 136	110.7	20, 136	136	20
ThF_4	g	-1759 ± 11	20	-1724	20	342	20	93.0	12, 20		20
$ThF_4\cdot2.5H_2O$	c	-2854 ± 10	12	-2614 ± 10	12	234 ± 9	12				
$ThOF_2$	c	-1669 ± 11	12, 20	-1593 ± 11	12, 20	101 ± 9	101	86	101		20
ThCl	g	258 ± 13	354			269.1	12	36.5	12	354	354
$ThCl_2$	g	-148 ± 15	354			317.0	12	55.3	12	354	354
$ThCl_3$	g	-529 ± 15	354			369.6	12	78.0	12	354	354
$ThCl_4$	c	-1186.1 ± 1.7	20	-1095 ± 3	20	(190)	20	120	12, 20		20
$ThCl_4$	g	964 ± 20	20	-932 ± 3	20	390.7	20	107.6	20		20
$ThCl_4\cdot2H_2O$	c	-1836 ± 8	20								
$ThCl_4\cdot4H_2O$	c	-2470 ± 8	20								
$ThCl_4\cdot7H_2O$	c	-3376 ± 8	20								
$ThCl_4\cdot8H_2O$	c	-3675 ± 8	20								
$ThOCl_2$	c	-1232 ± 8	20	-1170 ± 3	20	115	20	91	20		20
ThBr	g	274 ± 25	354			281.0	12	37.5	12	354	354
$ThBr_2$	g	-96 ± 25	354			338.9	12	56.7	12	354	354
$ThBr_3$	g	-415 ± 25	354			405.1	12	80.8	12	354	354

$ThBr_4$	c, β	-964.4 ± 2.0	20	-926 ± 4	20	(228)	12, 20	125	12, 20		20
$ThBr_4$	g	-762 ± 20	20	-783	20	430	20	104.9	12, 20		20
$ThBr_4\cdot7H_2O$	c	-3168 ± 4	12								
$ThBr_4\cdot10H_2O$	c	-4080 ± 4	12								
$ThBr_4\cdot12H_2O$	c	-4684 ± 4	12								
$ThOBr_2$	c	-1130	20	-1076	20	130	20	93	20		20
ThI	g	348 ± 25	354			228.5		37.6			
ThI_2	c	(-352)	11								
ThI_2	g	-62 ± 25	354			355.5	12	57.4	12		
ThI_3	c	(-515)	11								
ThI_3	g	-187 ± 25	354			429.8	12, 354	81.8	12, 354	354	354
ThI_4	c	-670.7 ± 3.8	20	-662	20	255	12, 20	126.6	12, 20		20
ThI_4	g	-466 ± 8	20	-521	20	469	20	106	20		20, 137
$ThOI_2$	c	-997	20	-959	20	145	20	94	20		20
ThS	c	-399 ± 4	17	-395 ± 4	17	69.81 ± 0.35	17	47.72 ± 0.24	17		17, 139
$ThS_{1.03}$	c	-405 ± 4	138								
ThS_2	c	-627 ± 40	17	-621 ± 40	17	96.2 ± 0.8	17	70.3 ± 0.3	17		17, 139
Th_2S_3	c	-1083	17	-1077 ± 13	17	180 ± 8	17				17
Th_2S_5	c	-1272 ± 40	17			(215)	17				
Th_7S_{12}	c	-4138 ± 53	11			641	17				139
$Th(SO_4)_2$	c	-2536 ± 21	16	-2310 ± 5	12	158 ± 10	12				16
ThN	c	-389 ± 5	12	-361 ± 5	12	56.1 ± 0.8	12			140	11
ThN	g	-485 ± 25	11	-512	calc.	241	11				11
Th_3N_4	c	-1315 ± 10	12	-1208	calc.	183	11				
Th_2N_2O	c	-1289	11	-1206	calc.	124	11				
$Th(NO_3)_4$	c	-1446 ± 13	16	-1049 ± 14	calc.	335 ± 13	12				
$Th(NO_3)_4\cdot4H_2O$	c	-2707 ± 13	16								
$Th(NO_3)_4\cdot5H_2O$	c	-3007.9 ± 4.2	12, 16, 43	-2325 ± 4	calc.	543.1 ± 2.0	141	480.8	141	141	
ThP	c									142	
$ThC_{0.75}$	c	-69.5 ± 6.7	143							142	
$ThC_{0.97}$	c	-125.5	143	-125.5	calc.	59.0 ± 0.8	11	45.2 ± 0.4	11		
ThC	c	-125 ± 6	19	-126	12, 19	58.0 ± 0.8	144	45.1 ± 0.5	144	144	145, 146
$ThC_{1.5}$	c										146

Table 17.14 (*Contd.*)

Species	*State*	ΔH_f° (kJ mol^{-1})	*Refs*	ΔG_f° (kJ mol^{-1})	*Refs*	S° (J K^{-1} mol^{-1})	*Refs*	C_p° (J K^{-1} mol^{-1})	*Refs*	*Thermal data refs*	
										Low temp.	*High temp.*
$ThC_{1.9}$	c	-125 ± 7	19	-126 ± 7	12, 19	68.4	147	56.7	147	147	147
ThC_2	c, α	-117 ± 8	11	-118	145	70.3	11	56.7 ± 0.6	145		145
ThC_2	g	720	12, 19	663	19	257	11, 19	44.6	19		19
$ThC_{0.6}N_{0.4}$	c									142	
Th–C–O system	c										148
$Th(C_2O_4)_2$	c	-1339 ± 42	16								
$Th(C_2O_4)_2\cdot6H_2O$	c			-3618 ± 10	12						149
$Th(CH_3COO)_2(OH)_2$	c	-1151 ± 46	16								16
ThSi	c	-121 ± 13	12	-117	calc.	58	11				150
$ThSi_2$	c	-165 ± 13	12	-162	calc.	82	11				150
Th_3Si_2	c	-271 ± 13	12	-261	calc.	163	11				150
Th_3Si_5	c	-463 ± 13	12	-451	calc.	213	11				150
ThGe	c	79 ± 13	12								150
$ThGe_2$	c	-117 ± 13	12								150
$ThGe_3$	c	-141 ± 13	12								150
Th_3Ge	c	-109 ± 13	12								150
Th_3Ge_2	c	-199 ± 13	12								150
Th_3Ge_5	c	-318 ± 13	12								150
$ThSn_3$	c	-41	151								
ThPb	c										152
$ThPb_2$	c										152
$ThPb_3$	c	-29	151								152
$ThPb_4$	c										152
$ThAl_3$	c										152
$ThIn_3$	c	-38	151								
$ThTl_3$	c	-104	12								152

$ThZn_2$	c	(94)	152					152
$ThZn_4$	c	(141)	152					152
$ThZn_{8.5}$	c	(203)	152					152
Th_2Zn	c	(56)	152					152
ThHg	c							152
$ThHg_2$	c							152
$ThHg_3$	c							152
$ThNi_2$	c	-129 ± 7	12	-126 ± 7	12, 153	103 ± 2	12	152, 153
$ThNi_5$	c	-260 ± 7	12	-247 ± 8	12, 153	160 ± 2	12	153
Th_2Ni_{17}	c	-471 ± 21	12	-461 ± 21	12, 153	579 ± 7	12	153
ThCo	c	-94 ± 7	12	-85 ± 7	12, 153	55 ± 2	12	153
$ThCo_5$	c	-179 ± 7	12	-163 ± 7	12, 153	151 ± 2	12	153
Th_2Co_7	c	-376 ± 12	12	-337 ± 12	12, 153	189 ± 4	12	153
Th_2Co_{17}	c	-313 ± 21	12	-294 ± 21	12, 153	554 ± 7	12	153
Th_7Co_3	c	-302 ± 47	12	-292 ± 48	12, 153	431 ± 14	12	153
$ThMg_2$	c							152
$LiThCl_5$	c	-1620	20					
$LiThCl_5\cdot8H_2O$	c	-4063	20					
Li_2ThCl_6	c	-2039	20					
$NaThCl_5\cdot10H_2O$	c	-4726	20					
Na_2ThCl_6	c	-2041	20					
$KThCl_5\cdot9H_2O$	c	-4415	20					
K_2ThCl_6	c	-2111	20, 358					
Rb_2ThCl_6	c	-2157	20					
$Rb_2ThCl_6\cdot9H_2O$	c	-4842	20					
Rb_4ThCl_8	c	-3064	20					
Cs_2ThCl_6	c	-2148	20, 358					
$Cs_2ThCl_6\cdot8H_2O$	c	-4562	20					
Cs_4ThCl_8	c	-3053	20					
NH_4ThCl_5	c	-1570	20					
$(NH_4)_2ThCl_6\cdot10H_2O$	c	-4911	20					

Table 17.14 (*Contd.*)

Species	*State*	ΔH_f° (kJ mol^{-1})	*Refs*	ΔG_f° (kJ mol^{-1})	*Refs*	S° (J K^{-1} mol^{-1})	*Refs*	C_p° (J K^{-1} mol^{-1})	*Refs*	*Thermal data refs*	
										Low temp.	*High temp.*
K_2ThBr_6	c	358									
Cs_2ThBr_6	c	358									
Pa	c	0		0		55±1	154	34±1	154	154	14
Pa	g	570±26	155, 362	527	calc.	197.9	14	22.9	14	14	14
Pa^{2+}	aq	(49)	calc.	(22)	Table 17.1	(22)	Table 17.2				
Pa^{3+}	aq	(−439)	calc.	(−431)	27	(−172)	27				
Pa^{4+}	aq, 1 M HCl	−622±14	15, 156	(−567±17)	15, 156	−397±40	15				
Pa^{5+}	aq, 12 M HCl/ 0.05 M HF	−677±14	156								
$PaOOH^{2+}$	aq, 1 M HCl	−1113±17	15	−1050±17	15	(−21±16)					
PaO_2	c	(−1109)	157, Table 17.6	(−1044)	158	(77)	124				158
Pa_2O_5	c					(88)	124				
PaF_4	c	(−1946±20)	20	(−1853)	20	(147)	20	(115)	20		20
$PaCl_4$	c	−1044±13	20	(−954)	20	(194)	20	(121)	20		20
$PaCl_5$	c	−1143±15	20	(−1032)	20	(238)	20	(156)	20		20
$PaBr_4$	c	−826±13	20	(−790)	20	(233)	20	(127)	20		20
$PaOBr_2$	c	−1001.2±17	20								
$PaBr_5$	c	−862±16	20	(−819)	20	289	20	162	20		20
PaI_4	c	−524±15	20	(−516)	20	(259)	20	(134)	20		20
PaC	c	(−113±16)	19	(−113±16)	19						
PaC_2	c	(−100±16)	19	(−105±16)	19						

Cs_2PaCl_6	c	-2029 ± 1	20								
U	c, α	0		0		50.2 ± 0.20	12, 14, 128	27.66 ± 0.05	12, 14, 126	14, 154	14, 126
U	c, β										14, 126
U	c, γ										14
U	g	536	12	491	12	199.7	12, 14, 24	23.69	12, 14	14	14, 159
U^{2+}	aq	(3)	calc.	(−28)	Table 17.1	(+14)	Table 17.2				
U^{3+}	aq	-489.1 ± 3.8	15	-480.7 ± 4.6	15	-174.9 ± 6.4	15				
U^{4+}	aq, 0.1 M $HClO_4$	-591.2 ± 3.3	12, 15	-530.9 ± 2.1	12, 15	-414 ± 21	15				
UO_2^+	aq	-1033 ± 6	15	-969 ± 5	15	-26 ± 8	15				
UO_2^{2+}	aq	-1019.2 ± 2.5	15, 128	-952.7 ± 2.1	15	-98.3 ± 4.0	15, 128	108	75		
UO	c					(68)	124				160
UO	g	21	12								
UO_{2-x}	c										161–164, 348, 356
UO_2	c	-1085.0 ± 1.0	12, 128, 165	−1031.8	calc., 12	77.03 ± 0.20	12, 128, 166	63.60 ± 0.03	12, 166	166	167–173, 361
UO_2	g	−467	12, 128, 132			261.99	174	53.15	174	174	132, 162, 170, 174–176
UO_{2+x}	c										4, 5, 162, 163, 177–179, 349, 356 180–182, 365
$(U_yTh_{1-y})O_{2+x}$	c										
UO_3 (brown)	c, α	-1217.5 ± 1.3	12, 183	-1140.6 ± 1.3	12, 183	99.4 ± 0.4	12, 183	81.83	12, 183		
UO_3 (orange)	c, β	-1220.3 ± 1.3	12, 183	-1142.2 ± 1.3	12, 183	96.3 ± 0.4	12, 183	81.3 ± 0.1	12, 183		
UO_3 (yellow)	c, γ	-1223.8 ± 2.0	12, 128, 183	-1145.8 ± 2.0	12, 183	96.11 ± 0.40	12, 128, 183, 184	81.7 ± 0.1	12, 183, 184	184	185, 186

Table 17.14 (*Contd.*)

Species	*State*	ΔH_f° (kJ mol^{-1})	*Refs*	ΔG_f° (kJ mol^{-1})	*Refs*	S° (J K^{-1} mol^{-1})	*Refs*	C_p° (J K^{-1} mol^{-1})	*Refs*	*Thermal data refs*	
										Low temp.	*High temp.*
UO_3 (red)	c, δ	-1219.6 ± 2.1	12, 183								185
UO_3 (brick red)	c, ε	-1217.5 ± 1.3	12, 183								
UO_3 (orange)	amorph.	$-1208.1 + 1.3$	12, 183								
UO_3	g	-816	12, 183								131, 132, 162, 187
U_2O_3	c	(-1456 ± 20)	41, Table 17.5, Fig. 17.8	(-1382)	est.	(160)	est.				131
U_2O_5	c	(-2340)	calc.								
U_3O_7	c, α					247.7	12, 183	71.25	12, 183	188	
U_3O_7	c, β			-3240 ± 12	183	250.54 ± 0.2	12, 183	71.84 ± 0.2	12, 183	188	
U_3O_8 (fc orthorhombic)	c, α	-3574.8 ± 2.5	12, 128, 183	-3370 ± 3	12, 183	282.55 ± 0.50	12, 128, 183, 189	237.9 ± 0.2	12, 128, 183, 189	189	185, 190–192
U_4O_9	c, α	-4510 ± 4	12, 183	-4275	12, 183	334.1 ± 0.7	183, 193	293.3 ± 0.6	193	193	192
$U(OH)_3$	c	(-1056)	calc.								
$UO_{2.86} \cdot 0.5H_2O$	c	-1367 ± 4	12, 16								
$UO_{2.86} \cdot 1.5H_2O$ ('U_3O_8 hydrate')	c	-1666 ± 2	12, 16								16
$UO_3 \cdot 0.5H_2O$	c	-1380 ± 3	16								
$UO_3 \cdot 0.85H_2O$	c, α	-1492 ± 2	16								
$UO_3 \cdot H_2O$ (orthorhombic, II)	c, β	-1533 ± 2	12, 16, 183	-1397 ± 2	183	(134)	16				194

$UO_3 \cdot H_2O$ (monoclinic)	c, ε	-1531 ± 2	16								194
$UO_3 \cdot 2H_2O$	c	-1827 ± 2	12, 16, 183			(176)	16				195
$UO_4 \cdot 2H_2O$	c	-1782 ± 4	16								
$UO_4 \cdot 4H_2O$	c	-2384 ± 2	16								
UH_3	c, β	-126.99 ± 0.12	12, 21	-72.61 ± 0.13	12, 21	63.67 ± 0.13	12, 21	49.3 ± 0.1	21	21	21
UD_3	c	-129.79 ± 0.13	21	-71.43 ± 0.14	21	71.76 ± 0.14	21	64.98 ± 0.06	21	21	21
UT_3	c	(-130.29 ± 0.21)	21	(-70.37 ± 0.32)	21	(79.08 ± 0.79)	21	(74.43 ± 0.74)	21	21	21
UF	g	-42 ± 14	20, 354	-72	20	252	20, 354	37.9	20, 354	354	20, 196, 354
UF_2	g	-531 ± 15	20, 354		calc.	316	20	56	354	354	196, 354
UF_3	c	-1502	20	-1433	20	123.4 ± 0.4	20	95.1 ± 0.4	20		20, 197
UF_3	g	-1059 ± 10	20, 196, 354		calc.	347	20	76	354	354	196, 354
UF_4	c	-1910	20, 357	-1820	20, 357	151.7	20	116.0	20	198, 199	20, 360
UF_4	g	-1599 ± 8	20, 196, 354	-1573	137, 196	363	137, 354	101	354	354	20, 137, 196, 354
UF_5	c, α	-2075 ± 7	12, 20	-1969	12, 20	(200)	12, 20	132	20		20
UF_5 (low temp.)	c, β	-2083 ± 6	12, 20	-1971	12, 20	(180)	12	132	20		20, 185
UF_5	g	-1937 ± 13	20, 354, 359	-1887	20	386	354	111	354	354	20, 350, 354
UF_6	c	-2197.0 ± 1.8	12, 20, 118	-2068.6	20	227.8	12, 20	166.8	12, 20	200	20
UF_6	g	-2147.4 ± 2.0	20, 354	-2063.8	20	377.8	20, 354	129.6	20, 354		20, 354
U_2F_9	c	-4016 ± 8	12, 20	-3812	12, 20	(329.6)	20	251.0	20		20
U_2F_{10}	g	-4042 ± 27	354								
U_4F_{17}	c	-7849 ± 12	12, 20	-7464	12, 20	(631)	4, 20	485	20		20
UOF	g	-544 ± 100	354								
UOF_2	c	-1504.6	20	-1434	20	(119 ± 4)	20				
UOF_2	g	-1117 ± 100	354			336	354	79	354	354	354
$UOF_2 \cdot H_2O$	c	-1802	20	-1675 ± 5	20	(161 ± 8)	20				

Table 17.14 (*Contd.*)

Species	*State*	ΔH_f° (kJ mol^{-1})	*Refs*	ΔG_f° (kJ mol^{-1})	*Refs*	S° (J K^{-1} mol^{-1})	*Refs*	C_p° (J K^{-1} mol^{-1})	*Refs*	*Thermal data refs*	
										Low temp.	*High temp.*
UOF_3	g	-1510 ± 100	354			353	354	89	354	354	354
$(H_3O^+)(UF_6^-)$	c	-2634	201								
UOF_4	c	-1924.6 ± 2.4	202								
UOF_4	g	-1734 ± 10	350			363	354	108	354	354	354
UO_2F	g	-996 ± 100	354			329	354	68	354	354	354
UO_2F_2	c	-1653.5 ± 1.2	12, 202	-1557.3	20	135.6	20	103.2	20		20
UO_2F_2	g	-1351.0 ± 6.3	350			-349	350	86	350	350	350
$UO_2F_2\cdot3H_2O$	c	-2534.7 ± 4.2	20								
$U_3O_5F_8$	c	-5203 ± 5	202								
$UO_2(OH)F\cdot H_2O$	c	-1894 ± 8	20	-1722 ± 8	20	180 ± 13	20				
$UO_2(OH)F\cdot2H_2O$	c	-2192 ± 12	20	-1961 ± 8	20	(222 ± 17)	20				
UCl	g	213 ± 13	203, 354			266	354	43	354	354	354
UCl_2	g	-146 ± 13	203, 354			339	354	60	354	354	354
UOCl	c	-834 ± 4	204			(103)	205		205		
UCl_3	c	-866.1 ± 4.2	20	-798.7	20	159.1	20	102.5	20	206	20, 206
UCl_3	g	-510 ± 13	354			380	354	82	354	354	205, 354
UCl_4	c	-1022 ± 4	20, 347	-933 ± 3	20, 347	197.1	12, 20	122.0	12, 20	206	20
UCl_4	g	-809 ± 3	20	-786	20	403	354	108	354	354	205, 354
UCl_5	c	-1041.5 ± 1.9	204	-933	204	243	12, 20	151	20		
UCl_5	g	-897	354			439	354	124	354	354	354
U_2Cl_{10}	g	-1975	20	-1816	20	686	20				
UCl_6	c	-1068.3 ± 1.9	204	-938	204	285.6	12, 20	175.7	12, 20	206	20, 205, 206
UCl_6	g	-1013	20	-928	20	433	20				205
$UOCl_2$	c	-1067	20	-996	20	138.3	20, 207	95.1	20, 207	207	20, 205
$UOCl_3$	c	-1163 ± 20	20	-1069	20	172 ± 10	20	117	20		20, 205
UO_2Cl_2	c	-1243.5 ± 1.3	20	-1146.0	20	150.5	20, 208	107.9	20, 208	208	20

UO_2Cl_2	g	-979 ± 13	20			372	205				205
$UO_2Cl_2\cdot H_2O$	c	-1559.8 ± 2.1	20	-1405 ± 3	20	192 ± 8	20				
$UO_2Cl_2\cdot 3H_2O$	c	-2164.8 ± 1.7	20	-1895 ± 3	20	272 ± 8	20				
$(UO_2)_2Cl_3$	c	-2404.5 ± 1.7	20								
$UO_2(OH)Cl\cdot 2H_2O$	c	-2010.4 ± 1.7	20								
UBr	g	268 ± 13	354			278	354	44	354	354	354
UBr_2	g	-54 ± 13	354			341	354	57	354	354	354
UBr_3	c	-699 ± 4	20	-673 ± 5	20	(192)	20	109	20		20
UBr_3	g	-392 ± 6	20			392	354	81	354	354	354
UBr_4	c	-802.1 ± 2.5	20	-767 ± 4	20	(238 ± 8)	20	128	20		20
UBr_4	g	-593 ± 3	20, 209			465 ± 8	20, 209	105	354	354	354
UBr_5	c	-810 ± 8	20	-769	20	293	20	161	20		20
$UOBr_2$	c	-974 ± 8	20	-930 ± 8	20	157.6	20, 207	98.0	20, 207	207	20
$UOBr_3$	c	-954 ± 21	20	-901	20	205	20	121	20		20
UO_2Br_2	c	-1137.4 ± 1.0	20	-1066	20	169	20	116	20		20
$UO_2Br_2\cdot H_2O$	c	-1456 ± 2	20								
$UO_2Br_2\cdot 3H_2O$	c			-2058 ± 2	20						
$UO_2(OH)Br\cdot 2H_2O$	c	-1958 ± 2	20								
UCl_2Br	c	-812	20								
$UClBr_2$	c	-751	20								
UCl_3Br	c	-967	20								
UCl_2Br_2	c	-908	20								
$UClBr_3$	c	-852	20								
UI	g	341 ± 25	354			286	354	44	354	354	354
UI_2	g	100 ± 25	354			358	354	57	354	354	354
UI_3	c	-467 ± 4	20	-466 ± 5	20	(222 ± 8)	20	112	20		20
UI_3	g	-140 ± 25	354			420	354	82	354	354	354
UI_4	c	-519 ± 3	20	-513 ± 4	20	(264 ± 8)	20	126	20		20
UI_4	g	-308 ± 9	20	-372 ± 10	20	480	354	106	354	354	354
UO_2I_2	c	(-1000 ± 4)	210								
UCl_3I	c	-898	20	-830	20	213 ± 8	20				
UBr_3I	c	-728	20								

Table 17.14 (*Contd.*)

Species	*State*	ΔH_f° (kJ mol^{-1})	*Refs*	ΔG_f° (kJ mol^{-1})	*Refs*	S° (J K^{-1} mol^{-1})	*Refs*	C_p° (J K^{-1} mol^{-1})	*Refs*	*Thermal data refs*	
										Low temp.	*High temp.*
US	c	-322 ± 11	17	-321	17	78.0 ± 0.2	17,211	50.5 ± 0.1	17,211	211	17,211
US	g	310 ± 15	17	257 ± 13	17	(262 ± 5)	17	(35 ± 2)	17		17
$US_{1.9}$	c	-514 ± 21	17	-514 ± 21	17	109.7 ± 0.2	17,212	74.0	17,212	212	
US_2	c, β	-521 ± 8	213	-519 ± 8	213	110.4 ± 0.2	17	74.6 ± 0.1	17,214	214	17
US_3	c	-544 ± 13	17	-542	17	138.5 ± 0.2	17,214	95.6 ± 0.3	17,214	214	17
U_2S_3	c	-879 ± 67	17	-879 ± 67	17	199.1	17	141.7	17		17
$U(SO_4)_2$	c	-2310 ± 13	16			(180)	16				
$U(SO_4)_2\cdot4H_2O$	c	-3483 ± 6	12, 16								
$U(SO_4)_2\cdot8H_2O$	c	-4662 ± 6	12, 16								
UO_2SO_4	c, β	-1845 ± 1	16								16
$UO_2SO_4\cdot2.5H_2O$	c	-2608 ± 1	16								
$UO_2SO_2\cdot3H_2O$	c	-2749 ± 4	16								
$UO_2SO_4\cdot3.5H_2O$	c	-2902 ± 1	16								
USe	c	-276 ± 15	17	-277 ± 15	17	96.5 ± 0.2	17,215	54.8 ± 0.1	17,215	215	17
USe_2	c, α	(-427 ± 42)	17	(-427 ± 42)	17	135.0 ± 0.3	17,212	79.2	17,212	212,215	17
U_2Se_3	c	(-711 ± 75)	17	(-724 ± 75)	17	261 ± 1	17	168 ± 3	17		17
U_3Se_4	c	-983 ± 85	17								
UO_2SeO_3	c	-1522.1 ± 0.9	216								
UO_2SeO_4	c	-1539 ± 3	16,216								
UTe	c	-182 ± 11	17			(109)	17			124	
UTe_3	c					214 ± 2	17	117 ± 3			
U_3Te_4	c	-684 ± 142	17								
UOTe	c					116.7	217	80.6	217		
$UOTe_3$	c					214.3	217	117.2	217		

UN	c	−290.8	12	−266	12	62.63	218, 219	47.82	218, 219	218, 219	185, 220
U_2N_3 (hexagonal)	c, β	−736	12								220
$UN_{1.54}$ (bcc)	c, α					65.0	218	54.2	218		220
U–N–O system											221
$2UO_3 \cdot NH_3 \cdot 3H_2O$	c	-3483 ± 2	16								
$3UO_3 \cdot NH_3 \cdot 5H_2O$	c	-5311 ± 3	16								
$3UO_3 \cdot 2NH_3 \cdot 4H_2O$	c	-5117 ± 3	16								
$NOUF_6$	c	−2268	222								
$UO_2(NO_3)_2$	c	−1349	12	−1105	12	243	12				
$UO_2(NO_3)_2 \cdot H_2O$	c	−1664	12	−1363	12	284	12				
$UO_2(NO_3)_2 \cdot 2H_2O$	c	−1980	12	−1622	12	329	12	278 ± 4	12, 75		
$UO_2(NO_3)_2 \cdot 3H_2O$	c	−2281	12	−1866	12	362	16				
$UO_2(NO_3)_2 \cdot 6H_2O$	c	-3168 ± 2	12, 16	−2585.8	12	505.6	16, 223	468.6	16, 223	223	
$(NH_4)_3UO_2F_5$	c	-3130 ± 3	20	-2698 ± 6	20	377 ± 21	20				
$NH_4(UO_2)_2F_5$	c	-3829 ± 4	20	-3526 ± 6	20	360 ± 21	20				
$NH_4(UO_2)_2F_5 \cdot 3H_2O$	c	−4719	20	−4246	20	485	20				
$NH_4(UO_2)_2F_5 \cdot 4H_2O$	c	−5012	20	−4485	20	527	20				
UP	c	−268	12	−264	12	78.3	12, 224	49.6	224	224	225
UP_2	c	−305	12	−297	12	99.6	217	77.5	217		
U_3P_4	c	−837	12	−820	12	259	12, 224, 226	175	12, 224, 226	224, 226	225
U–P–S system										227	
UAs	c	-234 ± 8	12			97.54	217	57.91	217		
UAs_2	c					127.96	217	85.90	217		
U_3As_4	c	−720	12	−724	12	309.1 ± 0.3	12, 228	187.5	12, 228	228	228

Table 17.14 (*Contd.*)

Species	*State*	ΔH_f° (kJ mol^{-1})	*Refs*	ΔG_f° (kJ mol^{-1})	*Refs*	S° (J K^{-1} mol^{-1})	*Refs*	C_p° (J K^{-1} mol^{-1})	*Refs*	*Thermal data refs*	
										Low temp.	*High temp.*
$(UO_2)_3(AsO_4)_2$	c	-4689 ± 3	229								
$(UO_2)_2As_2O_7$	c	-3426 ± 2	229								
$UO_2(AsO_3)_2$	c	-2157 ± 2	229								
UAsS	c					114.5	217	80.9	217		
UAsSe	c					131.7	217	83.5	217		
UAsTe	c					139.8	217	81.3	217		
USb	c	-138 ± 7	12								
USb_2	c	-176 ± 11	12	-176	12	144.1	217	80.87	217		
U_3Sb_4	c	-452	12	-456	12	349.8 ± 0.4	12, 228	188.2 ± 0.2	12, 228	228	228
UBi	c	-117	12	-105	4	63.2	4				18
UBi_2	c	-109	12	-97	4	121.8	4				18
U_3Bi_4	c	-385	12	-344	4	244.8	4				18
UC	c	-97.9 ± 2.1	19	-98.9	19	59.0	19	50.0	19	230, 231	19, 145, 171, 232, 233
UC	g	793	234								234
$UC_{1.9}$	c	-85.2 ± 3.0	235	-87.3	calc.	68.1	230, 231	60.6	230, 231, 236	230, 231	145, 232, 236
$UC_{1.93-1.94}$	c	-85.8 ± 4.2	145	-88.7 ± 4.2	145	68.32	145	60.75	145, 237		238, 239
UC_2 (bc tetragonal)	c, α	-85.3	19	-87.5	19	68.3	19	60.7	19	230, 231	19, 237, 238, 240
UC_2	g	691	234								
UC_3	g	800	234								
UC_4	g	834	234								

UC_5	g	971	234									
UC_6	g	1010	234									
U_2C_3	c	-183 ± 8	19	-204	19	137.8	19, 230, 241	107.4		19, 230, 241	230, 241	19, 145, 232, 240
UO_2CO_3	c	-1690 ± 8	16	-1562 ± 4	16	140 ± 17	16					
$UO_2C_2O_4$	c	-1796.7 ± 2.5	242									
$UO_2C_2O_4\cdot H_2O$	c	-2111.8 ± 2.4	242									
$UO_2C_2O_4\cdot 3H_2O$	c	-2715.3 ± 2.4	242									
$U(C_2O_4)_2$	c	-1351 ± 42	16									
$U(C_2O_4)_2\cdot 2H_2O$	c											149
$U(C_2O_4)_2\cdot 6H_2O$	c											149
$UO_2(HCOO)_2$	c	-1851 ± 1	16									
$U(CH_3COO)_4$	c	-2492 ± 5	243									
$UO_2(HCOO)_2\cdot H_2O$	c	-2158 ± 1	16									
$UO_2(CH_3COO)_2$	c	-1957.7 ± 1.1	242									
$UO_2(CH_3COO)_2\cdot 2H_2O$	c	-2557.3 ± 1.1	242									
$UO_2NH_4(CH_3COO)_3\cdot 6H_2O$	c	-4343 ± 8	16									
U–C–O system												148, 160, 221
U–C–N system											140	221, 244
U–Th–C–O system												148
USi	c	-80.3 ± 1.2	12, 245			(67)	4					18, 152
USi_2	c, α	-130.1 ± 1.2	12, 245			(82)	4					18, 150
USi_3	c	-132.2 ± 0.4	12, 245			(106.3)	4					18, 150
U_3Si	c	-134	12	-134	12	174	12	108		12		
U_3Si_2	c	-170.3 ± 2.1	12, 245			(197)	4					18
U_3Si_5	c	-354	4			(231)	4					18, 246
UGe	c	-62 ± 4	4	-73 ± 4	calc.	90 ± 3	4					18, 246
UGe_2	c	-87 ± 6	4	-109 ± 7	calc.	131 ± 5	4					18, 246
UGe_3	c	-107 ± 8	4	-179 ± 8	calc.	301 ± 8	4					18, 246
U_3Ge_5	c	-240 ± 17	4	-296 ± 18	calc.	352 ± 13	4					246
U_5Ge_3	c	-235 ± 17	4	-269 ± 18	calc.	375 ± 13	4					246
USn_3	c	-91	12			202 ± 8	4					18, 246
U_3Sn_2	c	-136 ± 10	4	-134 ± 10	calc.	247 ± 8	4					18, 246

Table 17.14 (*Contd.*)

Species	*State*	ΔH_f° (kJ mol^{-1})	*Refs*	ΔG_f° (kJ mol^{-1})	*Refs*	S° (J K^{-1} mol^{-1})	*Refs*	C_p° (J K^{-1} mol^{-1})	*Refs*	*Thermal data refs*	
										Low temp.	*High temp.*
U_3Sn_5	c	-218 ± 17	4	-214 ± 18	calc.	398 ± 17	4				18, 246
UPb	c	-59	18	-50	18	88	18				18, 246
UPb_3	c	-73	18	-68 ± 10	18	230	18				18, 246
UB_2 (MW 259.4348)	c	-164 ± 17	247	-162 ± 17	247	55.12 ± 0.12	12, 247	55.37 ± 0.12	12, 247	247	18
UB_4	c	-159	12								18
UB_{12}	c	-314	12								18
UAl_2	c	-92	12, 18, 248								18, 248
UAl_3	c	-105	12, 18, 248								18, 248
UAl_4	c	-130	12, 18, 248								18, 248
UGa	c	-35.8	12	-37.7	12	96	12				18, 150
UGa_2	c	-72.8	12	-74.5	12	138	12				18, 150
UGa_3	c	-102.1	12	-103.3	12	176	12				18, 150
UIn_3	c	-63.6	12								18, 150, 249
UTl_3	c	-59	12								18, 249
UZn_{12}	c										18, 249
U_2Zn_{17}	c	(341)	152								18
UCd_{11}	c	50 ± 8	4								18, 249, 250

UHg_2	c	−0.4	4								18, 251
UHg_3	c	−2.3	4								18, 252
UHg_4	c	−6.7	4								18
$AgUF_6$	c	−2353.3 ± 8.3	253								
$NiUO_4$	c										16
NiU_2O_6	c	−2556	254			202.9	254				
NiU_3O_{10}	c	−3942	254			358	254				
UFe_2	c	−32.2 ± 2.1	12, 18, 152								18
$MnUO_4$	c										16
UBe_3	c	−164 ± 15	18								18
$MgO–UO_{2\pm x}$ system	c										255, 256
$MgUO_4$	c	−1856.9 ± 1.3	16	−1749.3 ± 13	16	131.92	16, 257	128.07	16, 257	257	16
MgU_3O_{10}	c					338.6	16	305.6	16		
$CaUO_4$	c	−2001.6 ± 21	16	−1894.9 ± 3.3	calc.	123.8	257	123.3	257	257	16, 258
CaU_2O_6	c	−3210	258								
CaU_2O_7	c	−3335	258								
Ca_3UO_6	c	−3301	259								
$SrUO_4$	c, α	−1985 ± 2	16								260
$SrUO_4$	c, β	−1987 ± 2	16			153.1	257	130.5	257	257	
Sr_2UO_5	c	−2626 ± 2	16								
$Sr_2U_3O_{11}$	c	−5234 ± 3	16								
Sr_3UO_6	c	−3263 ± 4	16, 259								
$BaUO_3$	c	−1690 ± 10	104								
$BaUO_4$	c	−1997.1 ± 2.1	261	−1887. ± 2.1	261	153.97 ± 0.31	261	125.27 ± 0.25	261	257, 261	16, 257, 261
Ba_3UO_6	c	−3210.7 ± 5.8	259								
Ba_2MgUO_6	c	−3245.3 ± 4.8	262								
Ba_2CaUO_6	c	−3295.6 ± 5.3	263								
Ba_2SrUO_6	c	−3257.5 ± 4.4	263								
$LiUO_3$	c	−1522.1 ± 1.7	264								
Li_2UO_4	c, α	−1972	12								

Table 17.14 (*Contd.*)

Species	*State*	ΔH_f° (kJ mol^{-1})	*Refs*	ΔG_f° (kJ mol^{-1})	*Refs*	S° (J K^{-1} mol^{-1})	*Refs*	C_p° (J K^{-1} mol^{-1})	*Refs*	*Thermal data refs*	
										Low temp.	*High temp.*
Li_4UO_5	c	−2641	12								
$Li_2U_2O_7$	c	−3213.3 ± 5.1	265								
Li_2UCl_6	c	−1831 ± 4	20								
Li_2UBr_6	c										266
$NaUO_3$	c	−1494.6 ± 1.6	264	−1412.3 ± 1.6	calc.	132.8 ± 0.1	267	108.9 ± 0.1	267	267	268
Na_2UO_4	c, α	−1897 ± 4	16, 265, 268	−1779 ± 2	calc.	166.0 ± 0.3	16	146.6 ± 0.3	16	269	16
Na_2UO_4	c, β	−1886 ± 4	16, 265								
Na_4UO_5	c	−2451 ± 2	16								
$Na_2U_2O_7$	c	−3203.8 ± 4.4	265	−3002	268	275.9 ± 0.8	268	227.3 ± 0.7	268	268	268
Na_3UO_4	c	−2022 ± 3	16	−1898 ± 2	16	198.2 ± 0.4	16	173.0 ± 0.4	16	16	270
$Na_6U_7O_{24}$	c	−1135.5 ± 8	16								
$NaUF_6$	c, α	−2694 ± 13	20								
$NaUF_6$	c, β	−2708 ± 5	20								
$NaUF_7$	c	−2803 ± 10	20			272 ± 13	20				
Na_3UF_8	c	−3874	271								
Na_2UF_8	c	−3389 ± 13	20			331	20				
$Na_3UO_2F_5$	c	−3415 ± 3	20								
$Na(UO_2)_2F_5$	c	−3918 ± 3	20								
$NaUCl_6$	c, α	−1472 ± 3	20								
$NaUCl_6$	c, β	−1473 ± 2	20								
Na_2UCl_6	c	−1848 ± 2	20								
Na_2UBr_6	c	−1530 ± 2	20								
KUO_3	c	−1522.9 ± 1.6	264								
K_2UO_4	c	−1911 ± 2	16								
$K_2U_2O_7$	c	−3250.7 ± 4.5	265								
KUF_6	c	−2731 ± 5	20								
K_2UF_7	c	−3310	271								

K_3UF_8	c	−3955	271								
K_4UF_9	c	−4532	271								
$K_3UO_2F_5$	c	−3484±3	20								
$K(UO_2)_2F_5$	c	−3955±3	20								
$K_5(UO_2)_2F_9$	c	−6377±6	20								
$KUCl_5$	c	−1481±3	20								
$KUCl_6$	c	−1525±3	20								
$NaKUCl_6$	c	−1892±4	20								
K_2UCl_6	c	−1932±2	20								
K_2NaUCl_6	c	−2174	272								
K_2UBr_5	c	−1515±5	20								
K_2UBr_6	c	−1633±3	20								
K_2NaUBr_6	c	−1872	272								
$RbUO_3$	c	−1520.9±1.7	264								
Rb_2UO_4	c	−1913±2	16								
$Rb_2U_2O_7$	c	−3231.7±4.3	265								
$RbUF_6$	c	−2741±6	20								
Rb_2UF_7	c	−3334	271								
Rb_3UF_7	c	−3735±3	20								
Rb_3UF_8	c	−3955	271								
Rb_4UF_9	c	−4536	271								
$Rb_3UO_2F_5$	c	−3472±7	20								
$Rb(UO_2)_2F_5$	c	−3965±4	20								
$Rb_5(UO_2)_2F_9$	c	−6374±8	20								
$RbUCl_5$	c	−1498±4	20								
$RbUCl_6$	c	−1554±3	20								
Rb_2UCl_6	c	−1956±4	20								
Rb_2NaUCl_6	c	−2173	272								
Rb_4UCl_8	c	−2828±4	20								
Rb_2UBr_5	c	−1528±5	20								
Rb_2UBr_6	c	−1653±2	20								
Cs_2UO_4	c	−1926±4	16	−1804±4	16	219.7±0.4	16	152.8±0.3	16	273	16
$Cs_2U_2O_7$	c, β	−3226.6±4.5	265			327.8±0.7	274	231.2±0.5	274	274	
$Cs_2U_4O_{12}$	c, α	−5574±6	275	−5253±6	275	526.4±0.5	275	384.0±0.3	275	275	275, 276
$CsUF_6$	c	−2756±5	20								
Cs_2UF_6	c	−3156±4	20								

Table 17.14 (*Contd.*)

Species	*State*	ΔH_f° (kJ mol^{-1})	*Refs*	ΔG_f° (kJ mol^{-1})	*Refs*	S° (J K^{-1} mol^{-1})	*Refs*	C_p° (J K^{-1} mol^{-1})	*Refs*	*Thermal data refs*	
										Low temp.	*High temp.*
Cs_2UF_7	c, α	-3365	271								
Cs_2UF_7	c, β	-3353	271								
Cs_3UF_8	c	-4002	271								
$Cs_3UO_2F_5$	c	-3469 ± 7	20								
$Cs(UO_2)_2F_5$	c	-3978 ± 4	20								
$Cs_5(UO_2)_2F_9$	c	-6375 ± 11	20								
$CsUCl_5$	c	-1518 ± 4	20								
Cs_2UCl_6	c	-2011 ± 4	20								
$CsUCl_6$	c	-1574 ± 3	20								
CsU_2Cl_9	c	-2535 ± 8	20								
Cs_2NaUCl_6	c	-2181	277								
$Cs_2UO_2Cl_4$	c	-2204.5 ± 1.3	20								
Cs_2UBr_5	c	-1553 ± 5	20								
Cs_2UBr_6	c	-1710 ± 3	20								
Cs_3UBr_6	c	-2004	272								
Cs_2NaUBr_6	c	-1919	272								
$Cs_2UO_2Br_4$	c	-2009 ± 2	20								
Np	c	0		0		50.3	14	29.62	14	14, 154	14
Np	g	465	14	421	14	197.6	14	20.82	14	14	14
Np^{2+}	aq	(-39)	calc.	(-64)	Table 17.1	($+3$)	Table 17.2				
Np^{3+}	aq	-527.2 ± 2.1	15	-517.1 ± 3.3	15	-179.1 ± 6.4	15				
Np^{4+}	aq	-556.1 ± 4.2	15	-502.9 ± 7.5	15	-389 ± 21	15				
NpO_2^+	aq	-978 ± 5	15	-915 ± 5	15	-21 ± 8	15				
NpO_2^{2+}	aq	-861 ± 5	15	-796 ± 5	15	-94 ± 8	15				

NpO_3^+	aq, 1 M H^+			−836	48, 278						
NpO_5^{3-}	aq, 1 M NaOH			−1065	48, 279						
NpO	c					(69)	124				
NpO	g										131, 280, 281
NpO_2	c	−1074 ± 3	282	−1022 ± 3	calc.	80.3 ± 0.4	283, 284	66.2 ± 0.3	284	284	281, 285
NpO_2	g		280								
NpO_3	c	(−1070 ± 6)	262								
Np_2O_3	c	(−1522)	41, Table 17.5	(−1448)	calc.	(160)	est.				9
$Np(OH)_3$	c			(−1093)	calc.						
$NpO_3 \cdot H_2O$ (orthorhombic, II)	c	−1379 ± 5	16	−1247 ± 8	16	146 ± 33	16				
NpH_2	c	(−126 ± 19)	21	(−91)	21	(66 ± 10)	21	(47 ± 7)	21		286, 287
NpF_3	c	(−1529 ± 5)	20, Table 17.9	(−1460)	20	(125)	20	(98)	20		20
NpF_4	c	(−1874)	20	(−1784)	20	(153)	20	(116)	20		20
NpF_6	c					229.1 ± 0.5	288	167.4 ± 0.3	288	288	20
NpF_6	g					377 ± 1	288	129.1	288	288	20, 288
$NpCl_3$	c	(−898 ± 5)	20, Table 17.10	(−832)	20	(162)	20	(104)	20		20
$NpCl_4$	c	−984.1	20	(−896)	20	(202)	20	(120)	20		20
$NpOCl_2$	c	−1038 ± 13	20			(141)	20				
$NpBr_3$	c	−730.5 ± 2.3	20	−706	20	(197)	20	(109)	20		20
$NpBr_4$	c	−771.2 ± 1.8	20	−738	20	(243)	20	(129)	20		20
$NpOBr_2$	c	(−946 ± 13)	20			(158)	20				
NpI_3	c	−512.8 ± 2.1	20	−513	20	(226)	20				

Table 17.14 (*Contd.*)

Species	*State*	ΔH_f° (kJ mol^{-1})	*Refs*	ΔG_f° (kJ mol^{-1})	*Refs*	S° (J K^{-1} mol^{-1})	*Refs*	C_p° (J K^{-1} mol^{-1})	*Refs*	*Thermal data refs*	
										Low temp.	*High temp.*
NpN	c	< −255	289								289
$NpO_2(NO_3)_2$	c	(−1190)	est.								
$NpO_2(NO_3)_2 \cdot H_2O$	c	(−1505)	est.								
$NpO_2(NO_3)_2 \cdot 2H_2O$	c	(−1821)	est.								
$NpO_2(NO_3)_2 \cdot 3H_2O$	c	(−2122)	est.								
$NpO_2(NO_3)_2 \cdot 6H_2O$		−3009.1 ± 5.0	16	(2429 ± 6)	16	(516 ± 10)	16				
$NpC_{0.91}$	c	−71 ± 6	19, 290	−75	19, 290	69.7	290	50.0	290	290	
$NpC_{1.5}$	c	−94 ± 10	19	−96 ± 12	19						
$Np(C_2O_4)_2 \cdot 6H_2O$	c										149
$NpCd_6$	c										18
$NpCd_{11}$	c										18
Sr_3NpO_6	c	−3125.3 ± 5.8	262								
Ba_3NpO_6	c	−3086.0 ± 7.7	259								
Ba_2MgNpO_6	c	−3096.4 ± 6.5	262								
Ba_2CaNpO_6	c	−3159.2 ± 6.7	263								
Ba_2SrNpO_6	c	−3122.6 ± 6.7	263								
$Na_2Np_2O_7$	c	−2893.5 ± 9.9	265								
Na_3NpF_8	c					375		288, 291			
$K_2Np_2O_7$	c	−2932.5 ± 9.9	265								
$Rb_2Np_2O_7$	c	−2914 ± 11	265								
Cs_2NpCl_6	c	−1977.4 ± 1.7	20								
$Cs_2NpO_2Cl_4$	c	−2056 ± 5	20								
$Cs_2NpO_2Cl_4$	c	−2450 ± 5	20								
$Cs_2NaNpCl_6$	c	−2220	277								
Cs_2NpBr_6	c	−1682.4 ± 1.9	20								

Pu	c	0		0		54.46	292	31.19	292	14, 292	14, 352
Pu	g	342±2	293	305	calc.	177.1	14, 24	20.85	14	14	14, 159, 293
Pu^{2+}	aq	(−224)	calc.	(−241)	Table 17.1, Fig. 17.2	(−16)	Table 17.2				
Pu^{3+}	aq	−592±2	15	−579±3	15	−184±8	15				
Pu^{4+}	aq	−536±3	15	−482±3	15	−389±20	15				
PuO_2^+	aq	−915±6	15	−850±8	15	−21±8	15				
PuO_2^{2+}	aq	−822±7	15	−756±7	15	−92±8	15				
PuO_5^{3-}	aq				294						
PuO	c	(565)	9			(71±6)	9, 124	(51.3)	9		6, 9, 295
PuO	g	−92	210	−119	calc.	249	210				6, 131
$PuO_{1.515}$ (bcc)	c, α	(−836±11)	6, 41	(−795)	6, 41	75.7	6				6
$PuO_{1.61}$ (bcc)	c, α^1	−884±17	101								
PuO_2	c	−1056.2±0.7	296, 297	−998.0±0.7	297	66.13±0.26	297	66.25±0.26	297	297, 298	6, 9, 131, 298, 299
PuO_2	g	−422	132								131, 132, 300
Pu_2O_3 (hexagonal)	c, β	(−1656)	41, 102	(−1580)	calc.	163.0±0.6	98	117.0±0.5	98	98	6
$(Pu_yTh_{1-y})O_{2-x}$	c										180
$(Pu_xU_{1-x})O_{2\pm x}$	c										6, 172, 177, 270, 301–303, 364
$Pu(OH)_3$	c			(−1157)	est.						
'$Pu(OH)_4$'	amorph.			−1430	46						
$PuH_{1.9}$	c					72.7±0.4	21	43.04±0.20	21	21, 304	
PuH_2	c	−164	21	−130	21	72.8±0.7	21, 304	43.5±0.4	21, 304	304	9, 21, 304, 305
PuH_{2+x}	c		306								305, 307
PuD_2	c					(68±4)	9	(47.4)	9		9
PuH_3 (cubic)	c	−211	21	−158±13	21	(70±4)	21	(43.2)	9		9, 305

Table 17.14 (*Contd.*)

Species	*State*	ΔH_f° (kJ mol^{-1})	*Refs*	ΔG_f° (kJ mol^{-1})	*Refs*	S° (J K^{-1} mol^{-1})	*Refs*	C_p° (J K^{-1} mol^{-1})	*Refs*	*Thermal data refs*	
										Low temp.	*High temp.*
PuF	g	-116 ± 23	308, 354			250	354	33	354	354	354
PuF_2	g	-615 ± 17	308, 354			297	354	51	354	354	354
PuF_3	c	-1585.7 ± 4.2	20	-1516.4	20	126.11 ± 0.36	20	92.64 ± 0.28	20	309	20
PuF_3	g	-1163 ± 13	20	-1158	calc.	336	354	72	354	354	308, 354
PuF_4	c	(-1846 ± 21)	20	(-1753 ± 21)	20	147.25 ± 0.37	20	116.19 ± 0.29	20	310	8, 9, 20, 311
PuF_4	g	-1443	8, 9	-1416	calc.	368	8, 9, 310				
PuF_6	c	-1862 ± 29	20	-1728	20	222 ± 21	20, 310	167	9		8, 9
PuF_6	g	-1813 ± 20	20, 310	-1724	20	369.1	20, 310	129.4	20, 310		20, 310, 312
PuOF	c	-1139 ± 20	313			(92 ± 8)	9				9
$PuCl_2$	c	(-528)	Table 17.8								
$PuCl_3$	c	-959.8 ± 1.7	20	-892	20	(164)	20	103	9, 20		9, 20, 314–316
$PuCl_3$	g	-652 ± 4	20, 210			363	210				318
$PuCl_3\cdot6H_2O$	c	-2773.6 ± 2.1	20	-2365	calc.	420 ± 6	20				
$PuCl_4$	c	(-964 ± 8)	20								
$PuCl_4$	g	(-792 ± 3)	20	-765	20	412 ± 10	20				317
PuOCl	c	-931 ± 2	20	-882	20	104 ± 5	20	84	9		9
$PuBr_3$	c	-792.9 ± 2.1	20	-768	20	201	20	(108)	9		9
$PuBr_3$	g	-479.5 ± 4.2	20	-526	20	(439)	20				318
PuOBr	c	-870 ± 5	20, 210, 313, 319	(-832)	calc.	(117 ± 8)	9, 210	(87)	9		9
PuI_3	c	-579.8 ± 2.7	20	(-575 ± 7)	calc.	(230 ± 21)	20	112	9		9
PuOI	c	(-803 ± 20)	313			(137 ± 21)		(92)	9		9
PuS	c	(-364 ± 38)	17	(-360 ± 42)	17	(75 ± 8)	17	61	320		9, 320

PuS_2	c	(-529 ± 54)	17	(-523 ± 59)	17	(107 ± 13)	17				
Pu_2S_3	c	(-987 ± 100)	17	(-979 ± 108)	17	(188 ± 17)	17	(130)	9		9
$Pu(SO_4)_2$	c	(-2238 ± 42)	16	(-2013 ± 42)	16	(184 ± 21)	16	(182)	9		
PuN	c	-299.2 ± 2.6	296	-291	calc.	64.8	321	49.6	321	321	316, 322
Pu–N–O system											
PuP	c							62.1	320		320
$PuBi_2$	c	-188	18								18
$PuC_{0.67}$	c, ζ	-37.6	19	-40.6	19	(70)	19, 323, 324	(46)	19, 323, 324	323, 324	19
$PuC_{0.84}$ ('PuC')	c	-45.2	19	-49.3	19	74.8	19	47.1	19		7, 19, 232, 240, 316, 325, 326
$PuC_{1.5}$	c	-74.7 ± 4.2	19	-77.7	19	75.0	19, 323	57.0	19, 323	323	7, 19, 232, 316, 326, 327
PuC_2	c	-4	9	-10	9	(86)	9	(55)	9		9, 232
$Pu(C_{12}O_4)_2 \cdot 6H_2O$	c										149
$PuO_2(C_2O_4) \cdot 3H_2O$	c										149
$Pu_2(C_2O_4)_3 \cdot 10H_2O$											149
Pu–C–O system											221, 295
Pu–C–N system											221
$PuSn_3$	c	-220 ± 11	18								
Pu_3Sn	c	-209 ± 42	18								
$PuAl_2$	c	-142 ± 6	18, 152								18
$PuAl_3$	c	-181 ± 6	18, 152								18
$PuAl_4$	c	-181 ± 7	18, 152								18
$PuGa_2$	c	-190	18								
$PuGa_6$	c	-238	18								
Pu_3Ga	c	-158	18								
$PuZn_{12}$	c										18, 152
Pu_2Zn_{17}	c	-481	18								
$PuCd_6$	c	-117	18								18, 152

Table 17.14 (*Contd.*)

Species	*State*	ΔH_f° (kJ mol^{-1})	*Refs*	ΔG_f° (kJ mol^{-1})	*Refs*	S° (J K^{-1} mol^{-1})	*Refs*	C_p° (J K^{-1} mol^{-1})	*Refs*	*Thermal data refs* *Low temp.*	*High temp.*
$PuCd_{11}$	c	−113	18								18
$PuFe_2$	c	−27 ± 3	18, 152								
Pu_6Fe	c	(−14)	18								18
Pu_2Ni_{17}	c										
$PuBe_{13}$	c	−149 ± 15	18, 152								
Sr_3PuO_6	c	−3042 ± 9	263								
$BaPuO_3$	c	−1656 ± 6	355								
Ba_3PuO_6	c	−2998 ± 9	263								
Ba_2MgPuO_6	c	−2994 ± 8	263								
Ba_2CaPuO_6	c	−3068 ± 9	263								
Ba_2SrPuO_6	c	−3024 ± 8	263								
Cs_2PuO_4	c										276
$CsCl$–$PuCl_3$ system											315, 328
Cs_2PuCl_6	c	−1978.6 ± 8.4	20								
$Cs_2NaPuCl_6$	c	−2294.9 ± 2.5	20								
Cs_2PuBr_6	c	−1694.1 ± 4.2	20								
Am	c	0		0		55.4 ± 2	38, 329	25.5 ± 1	329	329–331	14
Am	g	284 ± 4	14, 35, 38	242	14	194.4	14	20.79	14	122	14, 35, 122
Am^{2+}	aq	(−355)	calc.	−377	Table 17.1	(−1)	Table 17.2				
Am^{3+}	aq	−616.7 ± 1.3	15	−599 ± 4	15	(−201 ± 13)	15				
Am^{4+}	aq	−406 ± 6	39	−347 ± 9	39, 66	(−408)	39				
AmO_2^+	aq	−805 ± 5	15	−741 ± 5	15	−21 ± 8	15				
AmO_2^{2+}	aq	−652 ± 2	15	−587 ± 3	15	−88 ± 8	15				

AmO	g										131
AmO_2	c	-932.2 ± 2.7	39			(86)	124				131, 333
Am_2O_3	c	-1692 ± 15	103			(158)	124				131, 333
$Am(OH)_3$	c			(−1168)	calc.						
AmH_2	c	(-184 ± 15)	21	(−143)	21	(48 ± 4)	21	(38 ± 3)	21		332
AmF_3	c	(-1588 ± 13)	20, Table 17.9			(128 ± 4)	20				
AmF_4	c	(-1720 ± 29)	20, Table 17.13			(149 ± 4)					334
$AmCl_2$	c	(−654)	Table 17.8								
$AmCl_3$	c	-977.8 ± 1.3	20	−911	20	(165)	20				
AmOCl	c	-953.5 ± 2.5	20	−901	20	103 ± 7	20				
$AmBr_3$	c	(-810 ± 7)	20, Table 17.11	(−787)	20	(205 ± 17)	20				
AmOBr	c	-890 ± 7	20, 319	(−860)	20, 319	(117 ± 17)	20				
AmI_3	c	(-612 ± 7)	20, Table 17.12	(−614)	20	(234 ± 21)	20				
$Cs_2NaAmCl_6$	c	−2313	277								
Cm	c	0		0		(72 ± 1)	14, 33, 38			14	14
Cm	g	387.4 ± 2.1	14, 32, 38, 39	350 ± 2	14	197.3	14, 32			14	14, 32, 36
Cm^{2+}	aq	(−222)	Table 17.1	(−239)	calc.	(−1)	Table 17.2				
Cm^{3+}	aq	-615 ± 5	15, 335	(−594)	15	(−194)	15				
Cm^{4+}	aq	(-379 ± 9)	41	-295 ± 25	Table 17.1	(−426)	Table 17.2				
CmO_2	c	-911 ± 6	41, 157			(87)	124				336
Cm_2O_3	c	-1682 ± 12	99			(161)	124				337
$Cm(OH)_3$	c			(−1166)	est.						

Table 17.14 (*Contd.*)

Species	*State*	ΔH_f° (kJ mol^{-1})	*Refs*	ΔG_f° (kJ mol^{-1})	*Refs*	S° (J K^{-1} mol^{-1})	*Refs*	C_p° (J K^{-1} mol^{-1})	*Refs*	*Thermal data refs*	
										Low temp.	*High temp.*
CmF_3	c	(-1599 ± 18)	Table 17.9								
CmF_4	c	(-1689)	Table 17.13								
$CmCl_2$	c	(-516)	Table 17.8								
$CmCl_3$	c	(-974 ± 8)	20	(-897)	calc.	(166 ± 8)	20				
CmOCl	c	-963 ± 7	20	-911	calc.	105 ± 21	20				
$CmBr_3$	c	(-808 ± 15)	Table 17.11								
Bk	c	0		0		(78 ± 1)	38				37
Bk	g	(310 ± 6)	37			200.6	37, 122	20.79	37	122	37, 122
Bk^{2+}	aq	(-294)	Table 17.1	(-309)	Table 17.1	(-2)	Table 17.2				
Bk^{3+}	aq	-601 ± 5	338	-578 ± 7	338	(-194 ± 17)	15				
Bk^{4+}	aq	(-483 ± 29)	15, 338, Table 17.1	-417 ± 25	Table 17.1	(-412 ± 20)	Table 17.2				
BkO_2	c	(-1021)	Table 17.6			(89)	124				
Bk_2O_3	c	(-1694)	41, Table 17.5								
BkF_3	c	(-1581)	Table 17.9								

BkF_4	c	(−1793)	Table 17.13								
$BkCl_2$	c	(−584)	Table 17.8								
$BkCl_3$	c	(−952 ± 15)	Table 17.12	(−878)	calc.						
$BkBr_3$	c	(−794)	Table 17.11								
Cf	c	0		0		(81 ± 1)	36, 38	28.0	34		36
Cf	g	196 ± 1	34, 36, 38				122			122	36, 122
Cf^{2+}	aq	(−385)	Table 17.1	(−398)	26, Fig. 17.2	(−5)	Table 17.2				
Cf^{3+}	aq	−577 ± 5	339	(−552)	25, 27, 339, 340	(−197)	25, 27				
Cf^{4+}	aq	(−313)	Table 17.1	−243	Table 17.1	(−412)	Table 17.2				
CfO_2	c	(−858)	Table 17.6			(87)	124				
Cf_2O_3	c	−1653 ± 10	353								
CfF_3	c	(−1553 ± 35)	Table 17.9								
CfF_4	c	(−1623)	Table 17.13								
$CfCl_2$	c	(−669)	Table 17.8								
$CfCl_3$	c	(−965 ± 23)	Table 17.10								
$Cs_2NaCfCl_6$	c	−2292	277								
$CfBr_3$	c	(−768)	Table 17.11								

Table 17.14 (*Contd.*)

Species	*State*	ΔH_f° (kJ mol^{-1})	*Refs*	ΔG_f° (kJ mol^{-1})	*Refs*	S° (J K^{-1} mol^{-1})	*Refs*	C_p° (J K^{-1} mol^{-1})	*Refs*	*Thermal data refs*	
										Low temp.	*High temp.*
Es	c	0		0		(89)	341				
Es	g	133	341				122			122	122
Es^{2+}	aq	(−415)	Table 17.1	(−425)	26, 342, Fig. 17.2	(−8)	Table 17.2				
Es^{3+}	aq	(−603 ± 21)	25, 27, Table 17.1	(−573 ± 17)	25, 27, 340	(−206)	25, 27				
Es^{4+}	aq	(−211)	Table 17.1	(−139)	Table 17.1	(−414)	Table 17.2				
Es_2O_3	c	(−1696)	Table 17.5								
EsO_2	c	(763)	Table 17.6								
EsF_3	c	(−1575 ± 40)	Table 17.9								
EsF_4	c	(−1521)	Table 17.13								
$EsCl_2$	c	(−694 ± 30)	Table 17.8								
$EsCl_3$	c	(−950 ± 24)	Table 17.10								

Fm	c	0		0		(91)	33		
Fm	g	(130)	25				122	122	122
Fm^{2+}	aq	(−474)	Table 17.1	−482	25, 26, 343	(−13)	Table 17.2		
Fm^{3+}	aq	(−632 ± 42)	Table 17.1	(−599 ± 38)	100, 343	(−215)	27		
Fm^{4+}	aq	(−170)	Table 17.1	(−97)	Table 17.1	(−415)	Table 17.2		
Fm_2O_3	c	(−1694 ± 86)	Table 17.5						
$FmCl_2$	c	(−748)	Table 17.8						
$FmCl_3$	c	(−963 ± 44)	Table 17.10						
Md	c	0		0		(87)	33		
Md	g	(128 ± 8)	25				122		
Md^{2+}	aq	(−481)	Table 17.1	−488	344	(−20)	Table 17.2		
Md^{3+}	aq	(−538)	25, 27	(−504)	25, 27	(−224)	25		
Md_2O_3	c	(−1535)	Table 17.5						
$MdCl_2$	c	(−752)	Table 17.8						
$MdCl_3$	c	(−864)	Table 17.10						

Table 17.14 (*Contd.*)

Species	*State*	ΔH_f° (kJ mol^{-1})	*Refs*	ΔG_f° (kJ mol^{-1})	*Refs*	S° (J K^{-1} mol^{-1})	*Refs*	C_p° (J K^{-1} mol^{-1})	*Refs*	*Thermal data refs*	
										Low temp.	*High temp.*
No	c	0		0		(65)	33				
No	g	(126)	25				122				
No^{2+}	aq	(−494)	Table 17.1	(−502)	345	(−39)	Table 17.2				
No^{3+}	aq	(−395)	25,27	(−365)	25,27	(−231)	25				
No_2O_3	c	(−1260)	Table 17.5								
$NoCl_2$	c	(−763)	Table 17.8								
$NoCl_3$	c	(−716)	Table 17.10								
Lr	c	0		0		(55)	33				
Lr	g	(341)	25								
Lr^{3+}	aq	(−630)	25,27	(−596)	25,27	(−255)	25				
Lr_2O_3	c	(−1766)	Table 17.5								
$LrCl_3$	c	(−946)	Table 17.10								

halides are known, but complex halides (e.g. Cs_2PuCl_6 and $CsPuF_6$) are known where the binary actinide halides ($PuCl_4$ and PuF_5) have been sought without success. Some of these complex halides have been exploited in separation schemes for the actinides [120]. Their thermodynamic properties have been of interest since the first years of this century [20].

Fuger [121] surveyed these compounds in a review article and Fuger *et al.* [20] assessed all of their thermodynamic properties more recently. Fig. 17.12 displays the enthalpies of complexation, e.g.

$$2CsCl(c) + UCl_4(c) = Cs_2UCl_6(c) \qquad \Delta H = \Delta H_{cplx} \tag{17.17}$$

of some of these compounds. Interpolation and extrapolation of ΔH_{cplx} along with enthalpies of formation of the binary compounds provide the values necessary to predict the enthalpies of formation of several of these complex halides. Note that ΔH_{cplx} becomes more favorable (exothermic) as the alkali-metal ion A^+ becomes larger and, to a lesser extent, as the actinide ion An^{4+} becomes smaller. As with complex oxides, these are both structural-packing (ionic) and acid–base (covalent) effects.

17.7 SUMMARY TABULATION

Table 17.14 represents a listing of all actinide compounds and other species for which measured or estimated thermodynamic properties are available. The sequence of species is by actinide element, with subordinate elements following the US National Bureau of Standards standard order of arrangement. Original literature references have been cited, unless there is an authoritative review or assessment. Error limits are given wherever possible. This tabulation attempts to be self-consistent with the CODATA [128] thermodynamic compilations, and in general accepts IAEA assessments [14–21], which are consistent with CODATA–IUPAC selected data. In many cases for thorium and uranium compounds the NBS [12] tabulations were accepted; it should be pointed out that the NBS compilation is self-consistent but not always contemporary and not in exact agreement with CODATA key values. Estimated values of thermodynamic properties are shown in parentheses.

ACKNOWLEDGMENTS

The work reported herein was performed under the auspices of the Office of Basic Energy Sciences, Division of Chemical Sciences, US Department of Energy, under Contract no. W-31-109-ENG-38. The author thanks many colleagues, especially J. Fuger, P. A. G. O. Hare, G. K. Johnson, V. B. Parker and W. B. Hubbard for guidance.

REFERENCES

1. Seaborg, G. T., Katz, J. J., and Manning, W. M. (eds) (1949) *The Transuranium Elements: Research Papers*, Natl Nucl. En. Ser., Div. IV, 14B, McGraw-Hill, New York.
2. Rossini. F. D., Wagman, D. D., Evans, W. H., Levine, S., and Jaffe, I. (1952) *Selected Values of Chemical Thermodynamic Properties*, US Natl Bur. Stand. Circ. 500, US Govt Printing Office, Washington, DC.
3. Latimer, W. M. (1952) *Oxidation Potentials*, 2nd edn, Prentice-Hall, New York.
4. Rand, M. H. and Kubaschewski, O. (1963) *The Thermochemical Properties of Uranium Compounds*, Interscience, New York.
5. IAEA (1965) *Thermodynamic and Transport Properties of Uranium Dioxide and Related Phases*, Technical Reports Series no. 39, International Atomic Energy Agency, Vienna.
6. IAEA (1967) *The Plutonium–Oxygen and Uranium–Plutonium–Oxygen Systems: A Thermochemical Assessment*, Technical Reports Series no. 79, International Atomic Energy Agency, Vienna.
7. Rand, M. H. (1968) *Technical Panel on Uranium and Plutonium Carbides*, International Atomic Energy Agency, Vienna.
8. Rand, M. H. (1966) *At. Energy Rev.*, **4**, Spec. Issue no. 1, 7–51.
9. Oetting, F. L. (1967) *Chem. Rev.*, **67**, 261–97.
10. Krestov, G. A. (1972) *Thermochemistry of Compounds of Rare-Earth and Actinide Elements*, Atomizdat, Moscow (English translation: AEC-tr-7505, National Technical Information Service, Springfield. VA 22151).
11. Rand, M. H. (1975) *At. Energy Rev.*, Spec. Issue no. 5, 7–85.
12. Wagman, D. D., Evans, W. H., Parker, V. B., Schumm, R. H., and Nuttall, R. L. (1981) US. Natl. Bur. Stand. Tech. Note 270-8, US Govt Printing Office, Washington, DC; (1982) *J. Phys. Chem. Ref. Data*, **11**, Suppl. 2.
13. Glushko, V. P., Medvedev, V. A., Bergman, G. A., Gurvich, L. W., Vorob'ev, A. F., Vasil'ev, V. P., Kolesov, V. P., Yungman, V. S., Reznutskij, L. R., Baibuz, V. F., Gal'chenko, G. L., and Yatzimirskij, K. B. (1978) *Thermodynamic Constants of Substances*, Academy of Science Publishing House, Moscow.
14. Oetting, F. L., Rand, M. H., and Ackermann, R. J. (1976) *The Chemical Thermodynamics of Actinide Elements and Compounds*, part 1, *The Actinide Elements*, STI/PUB/424/1, International Atomic Energy Agency, Vienna.
15. Fuger, J. and Oetting, F. L. (1976) *The Chemical Thermodynamics of Actinide Elements and Compounds*, part 2, *The Actinide Aqueous Ions*, STI/PUB/424/2, International Atomic Energy Agency, Vienna.
16. Cordfunke, E. H. P. and O'Hare, P. A. G. (1978) *The Chemical Thermodynamics of Actinide Elements and Compounds*, part 3, *Miscellaneous Actinide Compounds*, STI/PUB/424/3, International Atomic Energy Agency, Vienna.
17. Gronvold, F., Drowart, J., and Westrum, E. F., Jr (1984) *The Chemical Thermodynamics of Actinide Elements and Compounds*, part 4, *The Actinide Chalcogenides (Excluding Oxides)*, STI/PUB/424/4. International Atomic Energy Agency, Vienna.
18. Chiotti, P., Akhachinskij, V. V., Ansara, I., and Rand, M. H. (1981) *The Chemical Thermodynamics of Actinide Elements and Compounds*, part 5, *The Actinide Binary Alloys*, STI/PUB/424/5, International Atomic Energy Agency, Vienna.

19. Holley, C. E., Rand, M. H., and Storms, E. K. (1984) *The Chemical Thermodynamics of Actinide Elements and Compounds*, part 6, *The Actinide Carbides*, STI/PUB/424/6, International Atomic Energy Agency, Vienna.
20. Fuger, J., Parker, V. B., Hubbard, W. N., and Oetting, F. L. (1983) *The Chemical Thermodynamics of Actinide Elements and Compounds*, part 8, *The Actinide Halides*, STI/PUB/424/8, International Atomic Energy Agency, Vienna.
21. Flotow, H. E., Haschke, J. M., and Yamauchi, S. (1984) *The Chemical Thermodynamics of Actinide Elements and Compounds*, part 9, *The Actinide Hydrides*, STI/PUB/424/9, International Atomic Energy Agency, Vienna.
22. Kleinschmidt, P. D., Ward, J. W., and Haire, R. G. (1983) *Proc. II Symp. on High Temperature Materials Chemistry* (eds Z. Munir and D. Cubiciotti), Electrochemical Society, Pennington, NJ, pp. 23–31.
23. Stewart, G. R. (1983) *Rev. Sci. Instrum.*, **54**, 1–11.
24. Hultgren, R., Desai, P. D., Hawkins, D. T., Gleiser, M., Kelley, K. K., and Wagman, D. D. (1973) *Selected Values of the Thermodynamic Properties of the Elements*, American Society for Metals, Metals Park, Ohio.
25. David, F. (1984) in *Handbook of the Chemistry of the Actinides* (ed. C. Keller), in press.
26. Nugent, L. J. (1975) *J. Inorg. Nucl. Chem.*, **37**, 1767–70.
27. David, F., Samhoun, K., Guillaumont, R., and Edelstein, N. (1978) *J. Inorg. Nucl. Chem.*, **40**, 69–74.
28. Nugent, L. J., Baybarz, R. D., Burnett, J. L., and Ryan, J. L. (1973) *J. Phys. Chem.*, **77**, 1528–39.
29. Nugent, L. J., Burnett, J. L., and Morss, L. R. (1973) *J. Chem. Thermodyn.*, **5**, 665–78.
30. Fournier, J. M. (1976) *J. Phys. Chem. Solids*, **37**, 235–44.
31. Hubener, S. and Zvara, I. (1982) *Radiochim. Acta*, **31**, 89–94.
32. Ward, J. W., Ohse, R. W., and Reul, R. (1975) *J. Chem. Phys.*, **62**, 2366–72.
33. Ward, J. W. and Hill, H. H. (1976) in *Heavy Element Properties* (eds W. Muller and H. Blank), North-Holland, Amsterdam , pp. 65–79.
34. Ward, J. W., Kleinschmidt, P. D., and Haire, R. G. (1979) *J. Physique*, **40**, Colloq. C4. 233–5.
35. Ward, J. W., Kleinschmidt, P. D., and Haire, R. G. (1979) *J. Chem. Phys.*, **71**, 3920–5.
36. Ward, J. W., Kleinschmidt, P. D., Haire, R. G., and Brown, D. (1980) in *Lanthanide and Actinide Chemistry and Spectroscopy* (ed. N. Edelstein), American Chemical Society, Washington, DC, pp. 199–220.
37. Ward, J. W., Kleinschmidt, P. D., and Haire, R. G. (1982) *J. Chem. Phys.*, **77**, 1464–8.
38. Ward, J. W. (1983) *J. Less Common Metals*, **93**, 279–92.
39. Morss, L. R. and Fuger, J. (1981) *J. Inorg. Nucl. Chem.*, **43**, 2059–64.
40. Morss, L. R. (1983) *J. Less Common Metals*, **93**, 301–21.
41. Morss, L. R. (1985) in *Americium and Curium Chemistry and Technology* (ed. N. Edelstein), in press.
42. Morss, L. R. (1976) *Chem. Rev.*, **76**, 827–41.
43. Morss, L. R. and McCue, M. C. (1976) *J. Chem. Eng. Data*, **21**, 337–41.
44. Shannon, R. D. (1976) *Acta Crystallogr. A*, **32**, 751–67.
45. Lebedev, I. A. (1981) *Radiokhimiya*, **23**, 12–14.
46. Silva, R. J., McDowell, W. J., Keller, O. L., Jr, and Tarrant, J. R. (1974) *Inorg. Chem.*, **13**, 2233–7.
47. Martinot, L. (1978) in *Encyclopedia of Electrochemistry of the Elements*, vol. VIII (ed. A. J. Bard), Marcel Dekker, New York, pp. 149–206.

48. Martinot, L. and Fuger, J. (1985) in *Standard Potentials in Aqueous Solution* (eds A. J. Bard, R. Parsons, and J. Jordan), Marcel Dekker, New York, chap. 21.
49. Maly, J. (1967) *Inorg. Nucl. Chem. Lett.*, **3**, 373–81.
50. Maly, J. and Cunningham, B. B. (1967) *Inorg. Nucl. Chem. Lett.*, **3**, 445–51.
51. Maly, J., Sikkeland, T., Silva, R., and Ghiorso, A. (1968) *Science*, **160**, 1114–15.
52. Mikheev, N. B. (1983) *Radiochim. Acta*, **32**, 69–80.
53. Rai, D., Strickert, R. G., Moore, D. A., and Ryan, J. L. (1983) *Radiochim. Acta*, **33**, 201–6.
54. Dillin, D. R., Milligan, W. O., and Williams, R. J. (1973) *J. Appl. Crystallogr.*, **6**, 492–4.
55. *Gmelin Handbuch der Anorganischen Chemie*, Verlag Chemie, Weinheim, System-Nummer 39, Seltenerdelemente, part C2 (1974).
56. Aksel'rud, N. V. (1963) *Russ. Chem. Rev.*, **32**, 353–66.
57. Baes, C. F., Jr and Mesmer, R. E. (1976) *The Hydrolysis of Cations*, Wiley-Interscience, New York.
58. Ziv, D. M. and Shestakova, I. A. (1965) *Radiokhimiya*, **7**, 175–87.
59. Moskvin, A. I. (1971) *Radiokhimiya*, **13**, 293–5.
60. In ref. 55, part C3 (1976).
61. Ahrland, S., Liljenzin, J., and Rydberg, J. (1973) in *Comprehensive Inorganic Chemistry*, vol. V (ed. A. F. Trotman-Dickinson), Pergamon, New York, pp. 465–635.
62. Allard, B. (1982) in *Actinides in Perspective* (ed. N. Edelstein), Pergamon, Oxford, pp. 553–80.
63. Allard, B. and Rydberg, J. (1984) in *Plutonium Chemistry* (eds W. T. Carnall and G. R. Choppin), (Am. Chem. Soc. Symp. Ser. no. 216), American Chemical Society, Washington DC, pp. 275–95.
64. Allard, B., Olofsson, U., and Torstenfelt, B. (1984) *Inorg. Chim. Acta*, **94**, 205–21.
65. Silver, G. L. (1981) *J. Inorg. Nucl. Chem.*, **43**, 2997–9.
66. Hobart, D. E., Samhoun, K., and Peterson, J. R. (1982) *Radiochim. Acta*, **31**, 139–45.
67. Hobart, D. E., Varlashkin, P. G., Samhoun, K., Haire, R. G., and Peterson, J. R. (1983) *Rev. Chim. Minér.*, **20**, 817–27.
68. Wester, D. W. and Sullivan, J. C. (1980) *Inorg. Chem.*, **19**, 2838–40; (1981) *J. Inorg. Nucl. Chem.*, **43**, 2919–23; (1983) *Radiochim. Radioanal. Lett.*, **57**, 35–42.
69. Gruen, D. M. (1976) *Proc. Int. Symp. on Molten Salts*, Washington DC, pp. 204ff.
70. *Gmelin Handbuch der Anorganischen Chemie*, Suppl. Ser., *Uran*, Springer Verlag, Berlin, part D1 (1984), chaps 2 and 4.
71. Lemire, R. J. and Tremaine, P. R. (1980) *J. Chem. Eng. Data*, **25**, 361–70.
72. Criss, C. M. and Cobble, R. W. (1964) *J. Am. Chem. Soc.*, **86**, 5385–90, 5390–93.
73. Mayrath, J. E. and Wood, R. H. (1982) *J. Chem. Thermodyn.*, **14**, 15–26.
74. Busey, R. H., Holmes, H. F., and Mesmer, R. E. (1984) *J. Chem. Thermodyn.*, **16**, 343–72.
75. Jekel, E. C., Criss, C. M., and Cobble, J. W. (1964) *J. Am. Chem. Soc.*, **86**, 5404–7.
76. Morss, L. R. (1972) unpublished.
77. Lemire, R. J. (1984) Atomic Energy of Canada Ltd Report AECL-7817, Whiteshell Nuclear Research Establishment.
78. Pitzer, K. S. (1977) *Acc. Chem. Res.*, **10**, 371–7.
79. Helgeson, H. C. (1982) in *Chemistry and Geochemistry of Solutions at High Temperatures and Pressures* (eds D. Rickard and F. E. Wickman), Pergamon, Oxford; (1985) *Pure Appl. Chem.*, **57**, 31–44.
80. Phillips, S. L. (1984) Lawrence Berkeley Laboratory Report LBL-17886.

81. Kosyakov, V. N., Timofeev, G. A., Erin, I. A., Kopytov, V. V., and Andreev, V. J. (1977) *Radiokhimiya*, **19**, 82–4.
82. Volkov, Yu. F., Visyashcheva, G. I., Tomilin, S. V., Kapshukov, I. I., and Rykov, A. G. (1981) *Radiokhimiya*, **23**, 243–7.
83. Cleveland, J. M. (1979) in *Chemical Modeling in Aqueous Systems* (ed. E. A. Jenne), (Am. Chem. Soc. Symp. Ser. 93), Washington, DC, pp. 321–38.
84. Newton, T. W. and Sullivan, J. C. (1985) in *Handbook on the Chemistry of the Actinides*, vol. 2 (eds A. J. Freeman, G. L. Lander, and C. Keller), in press.
85. Sugar, J. (1973) *J. Chem. Phys.*, **59**, 788–91; (1974) *J. Chem. Phys.*, **60**, 4103.
86. Martin, W. C., Hagan, L., Reader, J., and Sugar, J. (1974) *J. Phys. Chem. Ref. Data*, **3**, 771–80.
87. Carlson, T. A., Nestor, C. W., Wasserman, N., and McDowell, J. D. (1970) Oak Ridge National Laboratory Report ORNL-4562.
88. Johnson, D. A. (1969) *J. Chem. Soc. A*, 1525–28.
89. Morss, L. R. (1971) *J. Chem. Phys.*, **75**, 392–9.
90. Goldman, S. and Morss, L. R. (1975) *Can. J. Chem.*, **53**, 2695–700.
91. Kiselev, Yu. M. (1984) *Radiokhimiya*, **25**, 463–8.
92. Schoebrechts, J.-P., Fuger, J., and Morss, L. R. (1985) *Proc. 189th American Chemical Society Meeting*, Miami Beach, FL, April, NUCL-23.
93. Sugar, J. (1983) personal communication.
94. Moore, C. B. (1970) US. Natl Bur. Stand. Report NSRDS–NBS 34, National Bureau of Standards, Washington, DC.
95. Worden, E. F. and Conway, J. G. (1980) in *Lanthanide and Actinide Chemistry and Spectroscopy* (ed. N. Edelstein), (Am. Chem. Soc. Symp. Ser. 131), American Chemical Society, Washington, DC, pp. 381–425.
96. Rajnak, K. and Shore, B. W. (1978) *J. Opt. Soc. Am.*, **68**, 360–7.
97. Larson, D. T. and Haschke, J. M. (1981) *Inorg. Chem.*, **20**, 1945–50.
98. Flotow, H. E. and Tetenbaum, M. (1981) *J. Chem. Phys.*, **74**, 5269–77.
99. Morss, L. R., Fuger, J., Goffart, J., and Haire, R. G. (1983) *Inorg. Chem.*, **22**, 1993–6.
100. Morss, L. R. (1985) in *Oxidation–Reduction Potentials in Aqueous Solution* (eds A. J. Bard, J. Jordan, and R. Parsons), Marcel Dekker, New York, in press.
101. Chereau, P., Dean, G., DeFranco, M., and Gerdanian, P. (1977) *J. Chem. Thermodyn.*, **9**, 211–19.
102. Besmann, T. M. and Lindemer, T. B. (1983) *J. Am. Ceram. Soc.*, **66**, 782–5.
103. Morss, L. R. and Sonnenberger, D. C. (1985) *J. Nucl. Mater.*, **130**, 266–72.
104. Williams, C. W., Morss, L. R., and Choi, I.-K. (1984) in *Geochemical Behavior of Disposed Radioactive Waste* (eds G. S. Barney, J. D. Navratil, and W. W. Schulz), (Am. Chem. Soc. Symp. Ser. 246), American Chemical Society, Washington, DC, pp. 323–34.
105. Fujino, T. and Morss, L. R. (1986) *Inorg. Chim. Acta*, submitted.
106. Morss, L. R. (1982) in *Actinides in Perspective* (ed. N. M. Edelstein), Pergamon, Oxford, pp. 381–407.
107. Morss, L. R. and Fahey, J. A. (1976) *Proc. 12th Rare Earth Res. Conf.*, vol. 1, Denver Research Institute, Denver, CO, pp. 443–50.
108. Westrum, E. F., Jr and Eyring, L. (1949) in *The Transuranium Elements* (eds G. T. Seaborg, J. J. Katz, and W. M. Manning), Natl Nucl. En. Ser., Div. IV, 14B, McGraw-Hill, New York, paper 6.52.
109. Johnson, G. K., Pennell, R. G., Kim, K.-Y., and Hubbard, W. N. (1980) *J. Chem. Thermodyn.*, **12**, 125–36.

110. Kim, Y.-C., Oishi, J., and Kang, S.-H. (1977) *J. Chem. Thermodyn.*, **9**, 973–7; *idem.* (1978) *J. Chem. Thermodyn.*, **10**, 975–81; Kim, Y.-C., Misumi, M., Yano, H., and Oishi, J. (1979) *J. Chem. Thermodyn.*, **11**, 657–62.
111. *Gmelin Handbuch der Anorganischen Chemie*, Suppl. Ser., *Transurane*, Verlag Chemie, Weinheim, vol. 4, part C, Compounds (1972).
112. Parker, V. B., Wagman, D. D., and Garvin, D. (1976) US Natl Bur. Stand. Report, NBSIR 75–968.
113. Brown, D. (1968) *Halides of the Lanthanides and Actinides*, Wiley-Interscience, London.
114. *Gmelin Handbuch der Anorganischen Chemie*, Verlag Chemie, Weinheim, System-Nummer 39, Seltenerdelemente, part C4a/b (1982), part 6 (1978).
115. Hurtgen, C., Fuger, J., and Brown, D. (1980) *J. Chem. Soc., Dalton Trans.*, 70–5.
116. Fried, S. (1981) personal communication.
117. Parker, V. B. (1980) US Natl Bur. Stand. Report, NBSIR 80–2029.
118. Johnson, G. K. (1979) *J. Chem. Thermodyn.*, **11**, 483–90.
119. Jouniaux, B., Legoux, Y., Merinis, J., and Bouissieres, G. (1979) *Radiochem. Radioanal. Lett.*, **39**, 129–40.
120. ANL (1967) Argonne Natl Lab., Chem. Eng. Div. Report, ANL-7375; Schmets, J. J. (1973) in *Gmelin Handbuch der Anorganischen Chemie*, Suppl. Ser., *Transurane*, Verlag Chemie, Weinheim, vol. A1, part II, pp. 251–65.
121. Fuger, J. (1979) *J. Physique*, **40**, Colloq. C4, 207–13.
122. Feber, R. C. and Herrick, C. C. (1965) *Ideal Gas Thermodynamic Functions of Lanthanide and Actinide Elements*, Los Alamos Scientific Laboratory Report LA-3184.
123. Nugent, L. J. (1975) in *MTP International Review of Science, Inorganic Chemistry*, ser. 2, vol. 7, Butterworths, London, pp. 195–219.
124. Westrum, E. F., Jr and Grønvold, F. (1962) *Thermodynamics of Nuclear Materials, Proc. Symp. 1962*, International Atomic Energy Agency, Vienna, pp. 3–37.
125. Moskvin, A. I. (1973) *Radiokhimiya*, **15**, 353–62.
126. Nakamura, J., Takahashi, Y., Izumi, S., and Kanno, M. (1980) *J. Nucl. Mater.*, **88**, 64–72.
127. Ackermann, R. J. and Rauh, E. G. (1972) *J. Chem. Thermodyn.*, **4**, 521–32.
128. CODATA (1977) *CODATA Recommended Key Values for Thermodynamics*, CODATA Bulletin no. 28, CODATA, Paris.
129. Ackermann, R. J., and Rauh, E. G. (1973) *High Temp. Sci.*, **5**, 463–73.
130. Ackermann, R. J. and Rauh, E. G. (1974) *J. Chem. Phys.*, **60**, 2266–71.
131. Ackermann, R. J. and Chandrasekharaiah, M. S. (1975) *Thermodynamics of Nuclear Materials, Proc. Symp. 1974*, International Atomic Energy Agency, Vienna, pp. 3–26.
132. Green, D. W. (1980) *J. Nucl. Mater.*, **88**, 51–63.
133. Osborne, D. W. and Westrum, E. F., Jr (1953) *J. Chem. Phys.*, **21**, 1884–7.
134. Ackermann, R. J. and Tetenbaum, M. (1980) *High Temp. Sci.*, **13**, 91–105.
135. Picard, C. and Kleppa, O. J. (1980) *High Temp. Sci.*, **12**, 89–98.
136. Lohr, H. R., Osborne, D. W., and Westrum, E. F., Jr (1964) *J. Am. Chem. Soc.*, **76**, 3837–9.
137. Rajendra Prasad, Nagarajan, K., Singh, Z., Bhupathy, M., Venugopal, V., and Sood, D. D. (1980) *Thermodynamics of Nuclear Materials, Proc. Symp. 1979*, vol. I, International Atomic Energy Agency, Vienna, pp. 45–59.

138. O'Hare, P. A. G., Ader, M., Hubbard, W. N., Johnson, G. K., and Settle, J. L. (1975) *Thermodynamics of Nuclear Materials, Proc. Symp. 1974*, vol. II, International Atomic Energy Agency, Vienna, pp. 439–53.
139. Aronson, S. (1967) *J. Inorg. Nucl. Chem.*, **29**, 1611–17.
140. DeNovion, C.-H. and Costa, P. (1972) *J. Physique*, **33**, 257–71.
141. Cheda, J. A. R., Westrum, E. F., Jr and Morss, L. R. (1976) *J. Chem. Thermodyn.*, **8**, 25–59.
142. Maurice, V., Boutard, J. L., and Abbe, D. (1979) *J. Physique*, **40**, Colloq. C4, 140–1.
143. Huber, E. J., Jr, Holley, C. E., Jr, and Krikorian, N. H. (1968) *J. Chem. Eng. Data*, **13**, 253–6.
144. Danan, J. (1975) *J. Nucl. Mater.*, **57**, 280–2.
145. Holley, C. E., Jr and Storms, E. K. (1968) *Thermodynamics of Nuclear Materials, Proc. Symp. 1967*, International Atomic Energy Agency, Vienna, pp. 397–426.
146. Potter, P. E. (1969) *J. Inorg. Nucl. Chem.*, **31**, 1821–9.
147. Westrum, E. F., Jr, Takahashi, Y., and Stout, N. D. (1965) *J. Phys. Chem.*, **69**, 1520–4.
148. Besmann, T. M. and Beahm, E. C. (1979) *Thermodynamics of Nuclear Materials, Proc. Symp. 1979*, International Atomic Energy Agency, Vienna.
149. Subramanian, M. S., Singh, R. N., and Sharma, H. D. (1969) *J. Inorg. Nucl. Chem.*, **31**, 3789–95.
150. Alcock, C. B., Cornish, J. B., and Grieveson, P. (1966) *Thermodynamics, Proc. Symp. 1965*, vol. I, International Atomic Energy Agency, Vienna, pp. 211–30.
151. Palenzona, A. and Cirafici, S. (1975) *Thermochim. Acta*, **13**, 357–60.
152. Kubaschewski, O. (1967) *Thermodynamics of Nuclear Materials, Proc. Symp. 1967*, International Atomic Energy Agency, Vienna, pp. 685–98.
153. Skelton, W. H., Magnani, N. J., and Smith, J. F. (1970) *Metall Trans.*, **1**, 1833–7.
154. Mortimer, M. J. (1979) *J. Physique*, **40**, Colloq. C4, 124–9, and personal communication.
155. Bradbury, M. H. (1981) *J. Less Common Metals*, **78**, 207–18.
156. Fuger, J., Bohet, J., Müller, W., Whittacker, B., and Brown, D. (1978) *Inorg. Nucl. Chem. Lett.*, **14**, 11–13.
157. Fuger, J. (1982) in *Actinides in Perspective* (ed. N. Edelstein), Pergamon, Oxford, pp. 409–31.
158. Lorenz, R. and Scherff, H. L. (1971) *Third Int. Protactinium Conf.*, Schloss Elmau, 1969, Inst. Radiochemie, Tech. Univ. Munich, paper 15.
159. Rand, M. H. (1979) *Thermodynamics of Nuclear Materials, Proc. Symp. 1979*, vol. I, International Atomic Energy Agency, Vienna, pp. 197–217.
160. Steele, B. C. H., Javed, N. A., and Alcock, C. B. (1970) *J. Nucl. Mater.*, **35**, 1–13.
161. Green, D. W. and Leibowitz, L. (1981) Argonne National Laboratory Report ANL-CEN-RSD-81-1.
162. Blackburn, P. E. (1973) *J. Nucl. Mater.*, **46**, 244–52.
163. Markin, T. L., Wheeler, V. J., and Bones, R. J. (1968) *J. Inorg. Nucl. Chem.*, **30**, 807–17.
164. Tetenbaum, M. and Hunt, P. D. (1969) *J. Chem. Phys.*, **49**, 4739–44.
165. Huber, E. J., Jr and Holley, C. E., Jr (1969) *J. Chem. Thermodyn.*, **1**, 267–72.
166. Huntzicker, J. J. and Westrum, E. F., Jr (1971) *J. Chem. Thermodyn.*, **3**, 61–76.
167. Fink, J. K., Chasanov, M. G., and Leibowitz, M. G. (1981) *J. Nucl. Mater.*, **102**, 17–25.

168. Long, K. A., Babelot, J. F., Magill, J., and Ohse, R. W. (1980) *High Temp. High Press.*, **12**, 515–36.
169. MacInnes, D. A. (1978) *J. Nucl. Mater.*, **78**, 225–7.
170. Ohse, R. W., Babelot, J. F., Cercignani, C., Kinsman, P. R., Long, K. A., Magill, J., and Scott, A. (1979) *J. Nucl. Mater.*, **80**, 232–48.
171. Ohse, R. W., Babelot, J. F., Frezotti, A., Long, K. A., and Magill, J. (1980) *High Temp. Sci.*, **13**, 35–78.
172. Ohse, R. W., Babelot, J. F., Brumme, G. D., and Kinsman, P. R. (1978) *Rev. Int. Hautes Temp. Refract.*, **15**, 319–32.
173. Thorn, R. J., Winslow, J. S., and Ziomek, J. S. (1979) *J. Nucl. Mater.*, **87**, 416–18.
174. Ackermann, R. H., Rauh, E. G., and Rand, M. H. (1979) *Thermodynamics of Nuclear Materials, Proc. Symp. 1979*, International Atomic Energy Agency, Vienna.
175. Reedy, G. T. and Chasanov, M. G. (1972) *J. Nucl. Mater.*, **42**, 341–4.
176. Tetenbaum, M. and Hunt, P. D. (197) *J. Nucl. Mater.*, **34**, 86–91.
177. Affortit, C. and Marcon, J. P. (1970) *Rev. Hautes Temp. Refract.*, **7**, 236–41.
178. Hoch, M. (1972) *High Temp. High Press.*, **4**, 493–5.
179. Picard, C. and Gerdanian, P. (1981) *J. Nucl. Mater.*, **99**, 184–9.
180. Woodley, R. E. and Adamson, M. G. (1979) *Thermodynamics of Nuclear Materials, Proc. Symp. 1979*, International Atomic Energy Agency, Vienna, pp. 333–55.
181. Fischer, D. F., Fink, J. K., and Leibowitz, M. G. (1981) *J. Nucl. Mater.*, **102**, 220–2.
182. Fischer, D. F., Fink, J. K., and Leibowitz, M. G. (1983) *J. Nucl. Mater.*, **118**, 342–8.
183. Fuger, J. (1983) in *Gmelin Handbuch der Anorganischen Chemie*, Suppl. Ser., *Uran*, Verlag Chemie, Weinheim, part A6, pp. 165–92.
184. Westrum, E. F., Jr (1966) *Thermodynamics, Proc. Symp. 1965*, vol. 2, International Atomic Energy Agency, Vienna, pp. 495–510.
185. Cordfunke, E. H. P. and Aling, P. (1965) *Trans. Faraday Soc.*, **61**, 50–3.
186. Moore, G. E. and Kelley, K. K. (1947) *J. Am. Chem. Soc.*, **69**, 2105–7 (UO_3 used in this study was not characterized structurally).
187. Ackermann, R. J. and Chang, A. T. (1973) *J. Chem. Thermodyn.*, **5**, 873–90.
188. Westrum, E. F., Jr and Grønvold, F. (1962) *J. Phys. Chem. Solids*, **23**, 39–53.
189. Westrum, E. F., Jr and Grønvold, F. (1959) *J. Am. Chem. Soc.*, **81**, 1777–80.
190. Aronson, S. and Belle, J. (1958) *J. Chem. Phys.*, **29**, 151–8.
191. Girdhar, H. L. and Westrum, E. F., Jr (1968) *J. Chem. Eng. Data*, **13**, 531–3.
192. Roberts, L. E. J. and Walter, A. J. (1961) *J. Inorg. Nucl. Chem.*, **22**, 213–29.
193. Flotow, H. E., Osborne, D. W., and Westrum, E. F., Jr (1968) *J. Chem. Phys.*, **49**, 2438–42.
194. Dharwadkar, S. R., Tripathi, S. N., Karkhanavala, M. D., and Chandrasekharaiah, M. S. (1975) *Thermodynamics of Nuclear Materials, Proc. Symp. 1974*, International Atomic Energy Agency, Vienna, pp. 455–65.
195. Pattoret, A., Drowart, J., and Smoes, S. (1968) *Thermodynamics, Proc. Symp. 1967*, International Atomic Energy Agency, Vienna, pp. 613–36.
196. Lau, K. H. and Hildebrand, D. L. (1982) *J. Chem. Phys.*, **76**, 2646–52.
197. Ferris, L. M., Mailen, J. C., and Smith, F. J. (1971) *J. Inorg. Nucl. Chem.*, **38**, 1325–33.
198. Burns, J. H., Osborne, D. W., and Westrum, E. F., Jr (1960) *J. Chem. Phys.*, **33**, 387–94.
199. Osborne, D. W., Westrum, E. F., Jr, and Lohr, H. R. (1955) *J. Am. Chem. Soc.*, **77**, 2737–9.

200. Brickwedde, F. G., Hoge, H. J., and Scott, R. B. (1948) *J. Chem. Phys.*, **16**, 429–36.
201. Masson, J. P., Desmoulin, J. P., Charpin, P., and Bougon, R. (1976) *Inorg. Chem.*, **15**, 2529–31 (corrected).
202. O'Hare, P. A. G. and Malm, J. G. (1982) *J. Chem. Thermodyn.*, **14**, 331–6.
203. Lau, K. H. and Hildebrand, D. L. (1984) *J. Chem. Phys.*, **80**, 1312–17.
204. Cordfunke, E. H. P., Ouweltjes, W., Prins, G., and van Vlaanderen, P. (1983) *J. Chem. Thermodyn.*, **15**, 1103–4.
205. Cordfunke, E. H. P. and Kubaschewski, O. (1984) *Thermochim. Acta*, **74**, 235–45.
206. Katz, J. J. and Rabinowitch, E. (1951) *The Chemistry of Uranium*, McGraw-Hill, New York.
207. Greenberg, E. and Westrum, E. F., Jr (1956) *J. Am. Chem. Soc.*, **78**, 5144–7.
208. Greenberg, E. and Westrum, E. F., Jr (1956) *J. Am. Chem. Soc.*, **78**, 4526–8.
209. Singh, Z., Prasad, R., Venugopal, V., Roy, K. N., and Sood, D. D. (1981) *J. Chem. Thermodyn.*, **13**, 485–90.
210. Prins, G., Cordfunke, E. H. P., and Ouweltjes, W. (1978) *J. Chem. Thermodyn.*, **10**, 1003–10.
211. Westrum, E. F., Jr, Walters, R. R., Flotow, H. E., and Osborne, D. W. (1968) *J. Chem. Phys.*, **48**, 155–61.
212. Westrum, E. F., Jr and Grønvold, F. (1970) *J. Inorg. Nucl. Chem.*, **32**, 2169–77.
213. Settle, J. L. and O'Hare, P. A. G. (1984) *J. Chem. Thermodyn.*, **16**, 1175–80.
214. Grønvold, F. and Westrum, E. F., Jr (1968) *J. Inorg. Nucl. Chem.*, **30**, 2127–33.
215. Takahashi, Y. and Westrum, E. F., Jr (1965) *J. Phys. Chem.*, **69**, 3618–21.
216. Cordfunke, E. H. P. and Ouweltjes, W. (1977) *J. Chem. Thermodyn.*, **9**, 1057–62.
217. Blaise, A. (1979) *J. Physique*, **40**, Colloq. C4, 49–61.
218. Counsell, F. J., Dell, R. M., and Martin, J. F. (1966) *Trans. Faraday Soc.*, **62**, 1736–47.
219. Westrum, E. F., Jr and Barber, C. M. (1966) *J. Chem. Phys.*, **45**, 635–9.
220. Potter, P. E., Mills, K. C., and Takahashi, Y. (1986) *The Chemical Thermodynamics of Actinide Elements and Compounds*, part 7, *The Actinide Pnictides*, STI/PUB/424/7, International Atomic Energy Agency, Vienna, in preparation.
221. Potter, P. E. and Spear, K. E. (1979) *Thermodynamics of Nuclear Materials, Proc. Symp. 1979*, vol. II, International Atomic Energy Agency, Vienna, pp. 195–227.
222. Plurien, P, Chatelet, J., Luce, M., and Rigny, P. (1973) *Proc. 7th Int. Symp. on Fluorine Chemistry*, Santa Cruz, CA.
223. Coulter, L. V., Pitzer, K. S., and Latimer, W. M. (1940) *J. Am. Chem. Soc.*, **62**, 2845–51.
224. Counsell, F. J., Dell, R. M., Junkison, A. R., and Martin, J. F. (1959) *Trans. Faraday Soc.*, **63**, 72–9.
225. Ono, F., Kanno, M., and Mukaibo, T. (1973) *J. Nucl. Sci. Technol.*, **10**, 764–5.
226. Stalinsky, B., Bieganski, Z., and Troc, R. (1966) *Phys. Status Solids*, **17**, 837–41.
227. Counsell, J. F., Martin, J. F., Dell, R. M., and Junkison, A. R. (1968) *Thermodynamics of Nuclear Materials, Proc. Symp. 1967*, International Atomic Energy Agency, Vienna, pp. 385–94.
228. Alles, A., Falk, B. G., Westrum, E. F., Jr, Grønvold, F., and Zaki, M. R. (1977) *J. Inorg. Nucl. Chem.*, **39**, 1993–2000.
229. Cordfunke, E. H. P., Ouweltjes, W., and Barten, H. (1982) *J. Chem. Thermodyn.*, **14**, 883–6.

230. Andon, R. J. L., Counsell, J. F., Martin, J. F., and Hedger, H. J. (1964) *Trans. Faraday Soc.*, **60**, 1030–7.
231. Westrum, E. F., Jr, Suits, E., and Lonsdale, H. K. (1965) *Advances in Thermophysical Properties at Extreme Temperatures and Pressures*, American Society of Mechanical Engineers, New York, pp. 156–61.
232. Ackermann, R. J., Oetting, F. L., Potter, P. E., Rand, M. W., and Storms, E. K. (1979) IAEA Technical Panel Series, International Atomic Energy Agency, Vienna.
233. Oetting, F. L., Navratil, J. D., and Storms, E. K. (1972–73) *J. Nucl. Mater.*, **45**, 271–83.
234. Gupta, S. K. and Gingerich, K. A. (1979) *J. Chem. Phys.*, **71**, 3072–80.
235. Huber, E. J., Jr, Head, E. L., and Holley, C. E., Jr (1963) *J. Phys. Chem.*, **67**, 1730–1.
236. MacLeod, A. C. and Hopkins, S. W. J. (1967) *Proc. Br. Ceram. Soc.*, **8**, 15–30.
237. MacLeod, A. C. (1969) *J. Inorg. Nucl. Chem.*, **31**, 715–25.
238. Storms, E. K. (1966) *Thermodynamics, Proc. Symp. 1965*, vol. I, International Atomic Energy Agency, Vienna, pp. 309–43.
239. Storms, E. K. (1967) *The Refractory Carbides*, Academic Press, New York, pp. 171–213.
240. Holley, C. E., Jr (1973) *Thermodynamic Properties of Actinide Carbides*, Los Alamos Scientific Laboratory Report LA-UR-73-847.
241. Farr, J. D., Witteman, W. G., Stone, P. L., and Westrum, E. F., Jr (1965) *Advances in Thermophysical Properties at Extreme Temperatures and Pressures*, American Society of Mechanical Engineers, New York, pp. 162–6.
242. O'Hare, P. A. G. (1977) *J. Chem. Thermodyn.*, **9**, 1077–86.
243. Thakur, L., Prasad, R., Thakur, A. K., and Ahmad, M. F. (1979) *Indian J. Chem.*, **18A**, 258–9.
244. Prins, G., Cordfunke, E. H. P., and Depaus, R. (1980) *J. Nucl. Mater.*, **89**, 221–8.
245. Gross, P., Hayman, C., and Clayton, H. (1963) *Thermodynamics of Nuclear Materials, Proc. Symp. 1962*, International Atomic Energy Agency, Vienna, pp. 653–65.
246. Alcock, C. B. and Grieveson, P. (1961) *J. Inst. Metals*, **90**, 304–10.
247. Flotow, H. E., Osborne, D. W., O'Hare, P. A. G., Settle, J. L., Mrazek, F. C., and Hubbard, W. N. (1969) *J. Chem. Phys.*, **51**, 583–92 (C_p° and S° refer to $UB_{1.979}$).
248. Chiotti, P. and Kateley, J. A. (1969) *J. Nucl. Mater.*, **32**, 135–45.
249. Johnson, I. and Feder, H. M. (1962) *Thermodynamics of Nuclear Materials, Proc. Symp. 1962*, International Atomic Energy Agency, Vienna, pp. 319–29.
250. Johnson, I. and Feder, H. M. (1962) *Trans. Metall. Soc. AIME*, **224**, 468–73.
251. Forsberg, H. C. (1960) Oak Ridge National Laboratory Report ORNL-2885.
252. Johnson, I. (1964) *Proc. Symp. on Compounds of Interest in Nuclear Reactor Technology*, AIME, New York; *Nucl. Metall*, **10**, 171.
253. O'Hare, P. A. G. and Malm, J. G. (1984) *J. Chem. Thermodyn.*, **16**, 753–9.
254. Dewally, D. and Perrot, P. (1976) *Rev. Chim. Minér.*, **13**, 605–13.
255. Fujino T., Tateno, J., and Tagawa, H. (1979) *J. Solid State Chem.*, **24**, 11–19.
256. Tateno, J., Fujino, T., and Tagawa, H. (1979) *J. Solid State Chem.*, **30**, 265–73.
257. Westrum, E. F., Jr, Zainel, H. A., and Jakes, D. (1979) *Thermodynamics of Nuclear Materials, Proc. Symp. 1979*, vol. II, International Atomic Energy Agency, Vienna, pp. 143–54.

258. Gol'tsev, V. P., Tret'yakov, A. A., Kerko, P. F., Barinov, V. I., and Malevich, V. M. (1981) *Vestsi Akad. Nauk BSSR, Ser. Fiz.-Energ. Navuk.*, 24–9 (*Chem. Abstr.*, **94**, 128546r).
259. Morss, L. R., Williams, C. W., Choi, I.-K., Gens, R., and Fuger, J. (1983) *J. Chem. Thermodyn.*, **15**, 1093–102.
260. Tagawa, H. and Fujino, T. (1978) *J. Inorg. Nucl. Chem.*, **40**, 2033–6.
261. O'Hare, P. A. G., Flotow, H. E., and Hoekstra, H. R. (1980) *J. Chem. Thermodyn.*, 1003–8.
262. Morss, L. R., Fuger, J., and Jenkina, H. D. B. (1982) *J. Chem. Thermodyn.*, **14**, 377–84.
263. Gens, R., Fuger, J., Morss, L. R., and Williams, C. W. (1985) *J. Chem. Thermodyn.*, **17**, 561–73.
264. Cordfunke, E. H. P., and Ouweltjes, W. (1981) *J. Chem. Thermodyn.*, **13**, 187–92.
265. Fuger, J. (1985) *J. Nucl. Mater.*, **130**, 253–65.
266. Bogacz, A., Szczepaniak, W., Bros, J.-P., Fouque, Y., and Gaune-Escard, M. (1984) *J. Chem. Soc., Faraday Trans.*, **180**, 2935–41.
267. Lyon, W. G., Osborne, D. W., Flotow, H. E., and Hoekstra, H. R. (1977) *J. Chem. Thermodyn.*, **9**, 201–10.
268. Cordfunke, E. H. P., Muis, R. P., Ouweltjes, W., Flotow, H. E., and O'Hare, P. A. G. (1982) *J. Chem. Thermodyn.*, **14**, 313–22.
269. Osborne, D. W., Flotow, H. E., Dallinger, R. P., and Hoekstra, H. R. (1974) *J. Chem. Thermodyn.*, **6**, 751–6.
270. Adamson, M. G., Aitken, E. A., Caputi, R. W., Potter, P. E., and Mignanelli, M. A. (1979) *Thermodynamics of Nuclear Materials, Proc. Symp. 1979*, vol. I, International Atomic Energy Agency, Vienna, pp. 503–38.
271. Suglobova, I. G., Fedorov, V. L., and Chirkst, D. E. (1981) *Izv. Akad. Nauk SSSR, Neorg. Mater.*, **17**, 712–17 (corrected with accepted binary fluoride ΔH_f° values).
272. Aurov, N. A. and Chirkst, D. E. (1983) *Sov. Radiochem.*, **25**, 445–9; (1983) *Radiokhimiya*, **25**, 468–73.
273. Osborne, D. W., Brletic, P. A., Hoekstra, H. R., and Flotow, H. E. (1976) *J. Chem. Thermodyn.*, **8**, 361.
274. O'Hare, P. A. G., Flotow, H. E., and Hoekstra, H. R. (1981) *J. Chem. Thermodyn.*, **13**, 1075–80.
275. Cordfunke, E. H. P. and Westrum, E. F., Jr (1979) *Thermodynamics of Nuclear Materials, Proc. Symp. 1979*, vol. II, International Atomic Energy Agency, Vienna, pp. 125–41.
276. Lorenzelli, R., LaDudal, R., and Atabeck, R. (1979) *Thermodynamics of Nuclear Materials, Proc. Symp. 1979*, vol. I, International Atomic Energy Agency, Vienna, pp. 539–64.
277. Morss, L. R., Fuger, J., Goffart, J., Endlestein, N., and Shalimoff, G. M. (1986) *J. Less-Common Metals*, submitted.
278. Musikas, C., Couffin, F., and Marteau, M. (1974) *J. Chim. Phys.*, **71**, 641–8.
279. Zielen, A. J. and Cohen, D. (1970) *J. Phys. Chem.*, **74**, 394–405.
280. Ackermann, R. J., Faircloth, R. L., Rauh, E. G., and Thorn, R. J. (1968) *J. Inorg. Nucl. Chem.*, **28**, 111–18.
281. Ackermann, R. J. and Rauh, E. G. (1975) *J. Chem. Phys.*, **62**, 108–12.
282. Huber, E. J., Jr and Holley, C. E., Jr (1968) *J. Chem. Eng. Data*, **13**, 545–6.
283. Osborne, D. W. and Westrum, E. F., Jr (1953) *J. Chem. Phys.*, **21**, 1884–7.

284. Westrum, E. F., Jr, Hatcher, J. B., and Osborne, D. W. (1953) *J. Chem. Phys.*, **21**, 419–23.
285. Arkhipov, V. A., Gutina, E. A., Dabretsov, V. N., and Ustinov, V. A. (1974) *Radiokhimiya*, **16**, 123–5.
286. Mulford, R. N. R. and Wiewandt, T. A. (1965) *J. Phys. Chem.*, **69**, 1641–4.
287. Mintz, M. H., Hadari, Z., and Bixon, M. (1976) *J. Less Common Metals*, **48**, 183–6.
288. Osborne, D. W., Weinstock, B., and Burns, J. A. (1970) *J. Chem. Phys.*, **52**, 1803–10.
289. Olson, W. M. and Mulford, R. N. R. (1966) *J. Phys. Chem.*, **70**, 2932–4.
290. Sandenaw, T. A., Gibney, R. B., and Holley, C. E., Jr (1973) *J. Chem. Thermodyn.*, **5**, 41–7.
291. Trevorrow, L. E., Gerding, T. J., and Steindler, M. J. (1968) *Inorg. Chem.*, **7**, 2226–9.
292. Gordon, J. E., Hall, R. O. A., Lee, J. A., and Mortimer, M. J. (1976) *Proc. R. Soc. Lond. A*, **351**, 179–96.
293. Bradbury, M. H. and Ohse, R. W. (1979) *J. Chem. Phys.*, **70**, 2310–14.
294. Musikas, C. (1975) in *Gmelin Handbuch der Anorganischen Chemie*, Suppl. Ser., *Transurane*, Verlag Chemie, Weinheim, vol. 20, part D1.
295. Potter, P. E. (1968) *Thermodynamics of Nuclear Materials, Proc. Symp. 1967*, International Atomic Energy Agency, Vienna, pp. 337–69.
296. Johnson, G. K., Van Deventer, E. H., Kruger, O. L., and Hubbard, W. N. (1969) *J. Chem. Thermodyn.*, **1**, 89–98.
297. Flotow, H. E., Osborne, D. W., Fried, S. M., and Malm, J. G. (1975) *J. Chem. Phys.*, **65**, 1124–9.
298. Kruger, O. L. and Savage, H. (1968) *J. Chem. Phys.*, **49**, 4540–4.
299. Ogard, A. E. (1970) in *Plutonium 1970 and Other Actinides, Proc. 4th Int. Conf. on Plutonium and Other Actinides*, Santa Fe, NM, vol. I (ed. W. N. Miner), Metallurgical Society, New York, pp. 78–83.
300. Green, D. W. (1980) Argonne National Laboratory Report ANL-CEN-RSD-80-2.
301. Chilton, G. R. and Edwards, J. (1979) *Thermodynamics of Nuclear Materials, Proc Symp. 1979*, vol. I, International Atomic Energy Agency, Vienna, pp. 357–68.
302. Rand, M. H. and Roberts, L. E. J. (1966) *Thermodynamics, Proc. Symp. 1965*, vol. I, International Atomic Energy Agency, Vienna, pp. 3–31.
303. Woodley, R. E. and Adamson, M. G. (1979) *J. Nucl. Mater.*, **82**, 65–75.
304. Oetting, F. L., Hodges, A. E., Haschke, J. M., and Flotow, H. E. (1984) *J. Chem. Thermodyn.*, **16**, 1089–102.
305. Haschke, J. M., Hodges, A. E., Smith, C. M., and Oetting, F. L. (1980) *J. Less Common Metals*, **73**, 41–8.
306. Smith, C. M., Hodges, A. E., Haschke, J. M., and Oetting, F. L. (1982) *J. Chem. Thermodyn.*, **14**, 115–24.
307. Haschke, J. M. (1980) US Dept of Energy Report RFP-3099.
308. Kent, R. A. (1968) *J. Am. Chem. Soc.*, **90**, 5657–9.
309. Osborne, D. W., Flotow, H. E., Fried, S. M., and Malm, J. G. (1974) *J. Chem. Phys.*, **61**, 1463–8.
310. Osborne, D. W., Flotow, H. E., Fried, S. M., and Malm, J. G. (1975) *J. Chem. Phys.*, **63**, 4613–17.
311. Chudinov, E. G. and Choporov, D. Ya. (1970) *At. Energy (USSR)*, **28**, 151–3.
312. Weinstock, B., Weaver, E. E., and Malm, J. G. (1959) *J. Inorg. Nucl. Chem.*, **17**, 104–14.

313. Fuger, J. (1983) in *Plutonium Chemistry* (eds W. T. Carnall and G. R. Choppin), (Am. Chem. Soc. Symp. Ser. 216), American Chemical Society, Washington, DC, ch. 6.
314. Belyaev, Yu. I., Dobretsov, V. N., and Ustinov, V. A. (1979) *Sov. Radiochem.*, **21**, 386–7; (1979) *Radiokhimiya*, **21**, 450–1.
315. Benz, R. (1961) *J. Chem. Phys.*, **65**, 81–4.
316. Campbell, G. M., Mullins, L. J., and Leary, J. A. (1968) *Thermodynamics of Nuclear Materials, Proc. Symp. 1967*, International Atomic Energy Agency, Vienna, pp. 75–88.
317. Gruen, D. M. and DeKock, C. W. (1967) *J. Inorg. Nucl. Chem.*, **29**, 2569–75.
318. Phipps, T. E., Sears, G. W., Seifert, R. L., and Simpson, O. C. (1950) *J. Chem. Phys.*, **18**, 713–23.
319. Weigel, F., Wishnevsky, V., and Güldner, R. (1982) *J. Less Common Metals*, **84**, 147–55.
320. Moser, J. B. and Kruger, O. L. (1968) *J. Am. Ceram. Soc.*, **51**, 369–72.
321. Hall, R. O. A., Lee, J. A., Martin, D. J., and Sutcliffe, P. W. (1978) *J. Chem. Thermodyn.*, **10**, 935–40.
322. Oetting, F. L. (1978) *J. Chem. Thermodyn.*, **10**, 941–8.
323. Haines, H. R., Hall, R. O. A., Lee, J. A., Mortimer, M. J., and McElroy, D. (1980) *J. Nucl. Mater.*, **88**, 261–4.
324. Sandenaw, T. A. and Gibney, R. B. (1970) in *Plutonium 1970 and Other Actinides, Proc. 4th Int. Conf. on Plutonium and Other Actinides*, Santa Fe, NM, vol. 1 (ed. W. N. Miner), Metallurgical Society, New York, pp. 104–12.
325. Kruger, O. L. and Savage, H. (1964) *J. Chem. Phys.*, **40**, 3324–8.
326. Olson, W. M. and Mulford, R. N. R. (1968) *Thermodynamics of Nuclear Materials, Proc. Symp. 1967*, International Atomic Energy Agency, Vienna, pp. 467–79.
327. Oetting, F. L. (1980) *J. Nucl. Mater.*, **88**, 265–72.
328. Benz, R. and Leary, J. A. (1961) *J. Phys. Chem.*, **65**, 1056–8.
329. Hall, R. O. A., Lee, J. A., Mortimer, M. J., McElroy, D. L., Müller, W., and Spirlet, J. C. (1980) *J. Low Temp. Phys.*, **41**, 397–404.
330. Müller, W., Schenkel, R., Schmidt, H. E., Spirlet, J. E., McElroy, D. L., Hall, R. O. A., and Mortimer, M. J. (1978) *J. Low Temp. Phys.*, **30**, 561–78.
331. Smith, J. L., Stewart, G. R., Huang, C. Y., and Haire, R. G. (1979) *J. Physique*, **40**, Colloq. C4, 138–9.
332. Olson, W. M. and Mulford, R. N. R. (1966) *J. Phys. Chem.*, **70**, 2934–7.
333. Chikalla, T. D. and Eyring, L. (1967) *J. Inorg. Nucl. Chem.*, **29**, 2281–93.
334. Chudinov, E. G. and Choporov, D. Ya. (1970) *At. Energiya*, **28**, 62–4; (1970) *Sov. J. At. Energy*, **28**, 71.
335. Raschella, D. L., Fellows, R. L., and Peterson, J. R. (1981) *J. Chem. Thermodyn.*, **13**, 303–12.
336. Turcotte, R. P., Chikalla, T. D., and Eyring, L. (1973) *J. Inorg. Nucl. Chem.*, **35**, 809–16.
337. Smith, P. K. and Peterson, D. E. (1970) *J. Chem. Phys.*, **52**, 4963–72.
338. Fuger, J., Haire, R. G., and Peterson, J. R. (1981) *J. Inorg. Nucl. Chem.*, **43**, 3209–12.
339. Fuger, J., Haire, R. G., and Peterson, J. R. (1984) *J. Less Common Metals*, **98**, 315–21.
340. Samhoun, K. and David, F. (1979) *J. Inorg. Nucl. Chem.*, **41**, 357–63.

341. Kleinschmidt, P. D., Ward, J. W., Matlack, G. M., and Haire, R. G. (1984) *J. Chem. Phys.*, **81**, 473–7.
342. Mikheev, N. B., Spitsyn, V. I., Kamenskaya, A. N., Rozenkevich, N. A., Rumer, I. A., and Auerman, L. N. (1972) *Radiokhimiya*, **14**, 486–7; (1972) *Sov. Radiochem.*, **14**, 494–5.
343. Mikheev, N. B., Spitsyn, V. I., Kamenskaya, A. N., Konovalova, N. A., Rumer, I. A., Auerman, L. N., and Podorozhnyi, A. M. (1977) *Inorg. Nucl. Chem. Lett.*, **13**, 651–6.
344. Hulet, E. K. (1980) in *Lanthanide and Actinide Chemistry and Spectroscopy* (ed. N. Edelstein), (Am. Chem. Soc. Symp. Ser. 131), American Chemical Society, Washington, DC.
345. Meyer, R. E., McDowell, W. J., Dittner, P. F., Silva, R. J., and Tarrant, J. R. (1976) *J. Inorg. Nucl. Chem.*, **38**, 1171–3.
346. Bratsch, S. G. and Lagowski, J. J. (1986) *J. Phys. Chem.*, 307–12.
347. O'Hare, P. A. G. (1985) *J. Chem. Thermodyn.*, **17**, 611–22.
348. Storms, E. K. (1985) *J. Nucl. Mater.*, **132**, 231–43.
349. Matsui, T. and Naito, K. (1985) *J. Nucl. Mater.*, **132**, 212–21.
350. Lau, K. H., Brittain, R. D., and Hildenbrand, D. L. (1985) *J. Phys. Chem.*, **89**, 4369–73.
351. Fouque, Y., Bros, J. P., Gaune-Escard, M., Wisniowski, M., and Bogacz, A. (1985) *Ber. Bunsenges. Phys. Chem.*, **89**, 777–9.
352. Oetting, F. L. and Adams, R. O. (1983) *J. Chem. Thermodyn.*, **15**, 537–54.
353. Brewer, L. (1971) *J. Opt. Soc. Am.*, **61**, 1101–11, 1106–81; (1984) *High-Temp. Sci.*, **17**, 1–30.
354. Hildenbrand, D. L., Gurvich, L. V., and Yungman, V. S. (1985) *The Chemical Thermodynamics of Actinide Elements and Compounds*, part 13, *The Gaseous Actinide Ions*, STI/PUB/424/13, International Atomic Energy Agency, Vienna.
355. Morss, L. R. (1986) to be published.
356. Lindemer, T. B. and Besmann, T. M. (1985) *J. Nucl. Mater.*, **130**, 473–88.
357. Johnson, G. K. (1985) *J. Nucl. Mater.*, **130**, 102–8.
358. Westland, A. D. and Tarafder, M. T. H. (1983) *Can. J. Chem.*, **61**, 1573–7.
359. Pyatenko, A. T., Gusarov, A. V., and Gorokhov, L. N. (1984) *Zh. Fiz. Khim.*, **58**, 1280–1.
360. Leitnaker, J. M. (1983) *High-Temp. Sci.*, **16**, 239–40.
361. Garisto, F. and Garisto, N. C. (1985) *Nucl. Sci. Eng.*, **90**, 103–10.
362. Kleinschmidt, P. D. and Ward, J. W. (1986) *J. Less-Common Metals*, in press.
363. Lindemer, T. B., Besmann, T. M., and Johnson, C. E. (1981) *J. Nucl. Mater.*, **100**, 178–226.
364. Besmann, T. M. and Lindemer, T. B. (1985) *J. Nucl. Mater.*, **130**, 489–504.
365. Belle, J. and Berman, R. M., eds. (1984) *Thorium Dioxide: Properties and Nuclear Applications*, U.S. Dept. of Energy, Washington, D.C., DOE/NE-0060, chapter 5.

CHAPTER EIGHTEEN

MAGNETIC PROPERTIES

Norman M. Edelstein and Jean Goffart

18.1 INTRODUCTION

The magnetic properties of actinide ions and compounds arise from the spin and orbital angular momenta of the unpaired electrons. The theoretical basis for understanding these properties was provided by Van Vleck in 1932 in his classic work *The Theory of Electric and Magnetic Susceptibilities* [1]. The Van Vleck equation is expressed as follows:

$$\chi_M = \frac{N \sum_i [(E_i^{(1)})^2/kT - 2E_i^{(2)}] \exp(-E_i^\circ/kT)}{\sum_i \exp(-E_i^\circ/kT)} \tag{18.1}$$

where χ_M is the molar susceptibility and E_i the energy of the ith energy level, which can be expanded as a power series in the magnetic field H:

$$E_i = E_i^\circ + E_i^{(1)}H + E_i^{(2)}H^2 + \ldots \tag{18.2}$$

The material can possess no residual moment in the absence of a magnetic field, so that:

$$\sum_i E_i^{(1)} \exp(-E_i^\circ/kT) = 0 \tag{18.3}$$

The term in equation (18.1) involving $E^{(1)}$ is the first-order Zeeman interaction and the term involving $E^{(2)}$ is the second-order Zeeman interaction. If the ground

crystal field state is a singlet and the next state is greater than kT away in a particular temperature range, the first-order term will be zero and only the second-order term will contribute to the paramagnetic susceptibility, which will be independent of temperature (temperature-independent paramagnetism, TIP).

If enough information is available about an ion or molecule (i.e. from optical spectroscopy) such that the properties of the energy levels in a magnetic field can be calculated, magnetic susceptibility measurements provide a good test for the wavefunctions. Conversely, magnetic data can be used to determine information about energy levels and their wavefunctions. Magnetic measurements usually are performed in the temperature range 2–300 K (energy range $\sim$ 1.5–200 cm^{-1}). From optical data, the crystal or ligand field splittings of the ground state of some $5f^1$ hexahalo compounds are shown in the second column of Table 18.1 and vary from 1730 cm^{-1} in Pa^{4+} to about 7500 cm^{-1} for Np^{6+}. For $5f^2$ U^{4+} compounds, the total crystal field splitting of the ground $^3H_4$ term is about 2240 cm^{-1} in Cs_2UCl_6 [2], about 2000 cm^{-1} in Cs_2UBr_6 [2], about 2400 cm^{-1} in $U(C_5H_5)_4$ [3], and about 1800 cm^{-1} for $U(BH_4)_4$ diluted in $Zr(BH_4)_4$ [4]. For the $5f^3$ ion, U^{3+} diluted in $LaCl_3$, the total crystal field splitting of the ground term is 451 cm^{-1} [5], while for the $5f^4$ ion, Np^{3+} diluted in $LaCl_3$ and in $LaBr_3$, the total splittings of the ground terms are 465 and 401 cm^{-1} [6], respectively. From the above data, it is clear that temperature-dependent magnetic susceptibility measurements provide information only about the ground crystal field state and possibly a few lower-lying states. Most susceptibility measurements are performed on polycrystalline samples which give only the average susceptibility.

Electron paramagnetic resonance (EPR) measurements for actinide ions are usually made at liquid-helium temperatures in order to lengthen the spin–lattice relaxation time (T_1) so the resonance may be observed [7, 8]. Consequently information is obtained only about the ground crystal field state and possibly the first excited state. The spectra are interpreted in terms of an effective spin Hamiltonian:

$$H = \mu_B(g_x H_x S_x + g_y H_y S_y + g_z H_z S_z) \tag{18.4}$$

where μ_B is the Bohr magneton, and g_i, H_i, and S_i ($i = x, y, z$) are the components

Table 18.1 *Optical transitions, g-values, and the best-fit parameters to the Eisenstein–Pryce theory for some $5f^1$ hexahalo compounds* [35].

	Electronic transitions					*Best-fit parameters*				
Compound	$\Gamma_7 \rightarrow \Gamma_8$ (cm^{-1})	$\Gamma_7 \rightarrow \Gamma_7'$ (cm^{-1})	$\Gamma_7 \rightarrow \Gamma_8'$ (cm^{-1})	$\Gamma_7 \rightarrow \Gamma_6$ (cm^{-1})	$\lvert g \rvert$	ζ (cm^{-1})	Δ (cm^{-1})	Θ (cm^{-1})	k	k'
$((C_2H_5)_4N)_2$ $PaCl_6$	1730	5330	7140	8011	1.18	1689	600	3525	0.83	0.46
$CsUF_6$	5363	7400	13800	15900	0.708	2206	3335	8050	0.84	0.61
$RbUCl_6$	3800	6794	10137	11520	1.12	2219	826	5794	0.78	0.45
$CsUBr_6$	3700	6830	9761	10706	1.21	2190	99	5746	0.79	0.32
NpF_6	7543	9348	24000	27000	0.605	2697	4775	16921	0.85	0.60

of the g-tensor, the magnetic field, and the spin operator along the principal axes of the crystal field. For a crystal or molecule with the highest-symmetry rotation axis (the z-axis by definition) of three-fold symmetry or greater, $g_x = g_y = g_\perp$ and $g_z = g_\parallel$. For T_d or O_h symmetry the g-value is isotropic (except for a Γ_8 state being lowest). For the purpose of this review hyperfine and quadrupole effects are not considered.

An electron configuration with an odd number of electrons ($f^1, f^3, \ldots$, etc.) has a Kramers degeneracy that can be lifted by a magnetic field but not by a crystal field. However, it is possible that the pair of states which lies lowest will not have an EPR signal because the selection rule $\Delta J_z = \pm 1$ will be violated. For example, consider a $J = 5/2$ term in a purely axial crystal field. This term will be split into three doublets, $J_z = \pm 1/2, \pm 3/2, \pm 5/2$. If the crystal field is such that the $J_z = \pm 3/2$ or $J_z = \pm 5/2$ state is lowest, there will be no EPR transitions allowed.

An electron configuration with an even number of electrons ($f^2, f^4, \ldots$, etc.) is called a non-Kramers ion. If the highest-symmetry axis is a C_2 axis, the crystal field will split an integer J term into $2J + 1$ singlets, and EPR will not be observed. If the highest-symmetry axis is C_3 or higher, a doubly or triply degenerate crystal field state could be lowest and EPR might be observed. However EPR has been reported only for the non-Kramers ion $U^{4+}(^3H_4)$ in the actinide series. Non-Kramers ions are discussed in detail by Abragam and Bleaney [7].

For an f^n configuration the electrostatic interaction between two f electrons results in a series of terms that can be classified by the total orbital and spin angular momenta, L and S, defined as

$$\mathbf{L} = \sum_i^n \mathbf{l}_i \qquad \mathbf{S} = \sum_i^n \mathbf{s}_i \tag{18.5}$$

where $\mathbf{l}_i$ and $\mathbf{s}_i$ are the orbital and spin angular momenta of the ith electron. The eigenstates are then labeled by the quantum numbers (or symbols) ^{2S+1}L. This classification is called Russell–Saunders coupling. Inclusion of the spin–orbit interaction will cause mixing of the spin and orbital angular momenta and requires the use of J, the total angular momentum, defined as

$$\mathbf{J} = \mathbf{L} + \mathbf{S} \tag{18.6}$$

The ^{2S+1}L multiplet is split into levels labeled by their J eigenvalues, $J = L+S$, $L+S-1, \ldots, L-S$, where each J level has a $2J+1$ degeneracy. It is this J degeneracy which is split by the crystal field [9, 10]. Usually, the lowest J level is relatively isolated, the ligand field splittings are approximately 100–1000 cm^{-1}, and only the lowest few crystal field states as indicated above provide the main contribution to the measured magnetic susceptibility. The effects of the various interactions are shown in Fig. 18.1 for the f^2 configuration.

A large number of magnetic susceptibility and EPR measurements have been made on actinide ions in crystal fields of O_h or T_d symmetry. In these symmetries the ordering of the energy levels of a J term depends only on the ratio of two

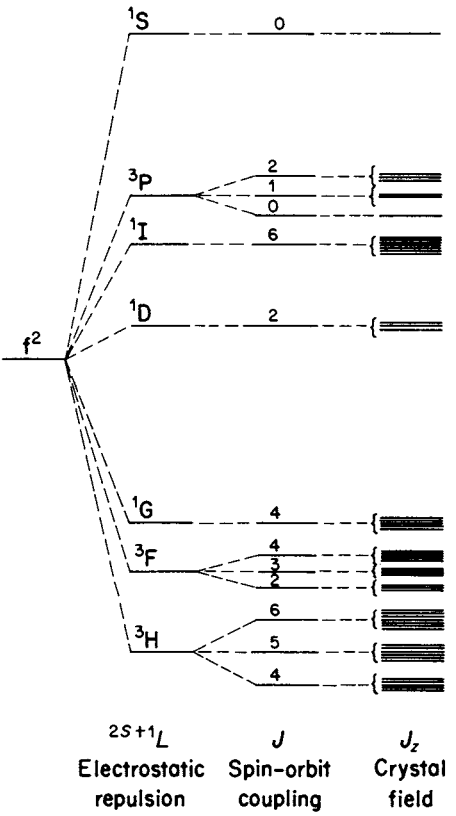

Fig. 18.1 *The effects of the electrostatic, spin–orbit, and crystal field interactions on the f^2 configuration.*

crystal field parameters, the fourth-order term and the sixth-order term. From magnetic data the ground crystal field state may be determined, which in turn can set a limit on the ratio of the fourth- to the sixth-order term. Lea, Leask, and Wolf [11] have tabulated the results in reduced coordinates for all J levels of interest and their nomenclature is widely used. An illustration of the application of the Lea, Leask, and Wolf method (plus the effects of mixing other J states by the crystal field) is given in the study of Hendricks *et al.* [98] on the temperature dependence of the magnetic susceptibility of the isostructural series, Cs_2NaMCl_6, M = U^{3+}, Np^{3+}, Pu^{3+}, Am^{3+}, Cm^{3+}, and Bk^{3+}. The data are shown in Table 18.2. From a consideration of these data, limits were placed on the possible values of the fourth- and sixth-order crystal field parameters B_0^4 and B_0^6 (defined as described by Wybourne [9]). The crystal field splittings calculated from these limits for the ground term of the trivalent actinide ions are shown in Fig. 18.2.

Magnetic susceptibility data are usually represented by a plot of $1/\chi_M$ vs T. This plot is linear over a particular range of temperatures, and the data are fitted to the

Table 18.2 *Magnetic data for octahedral actinide(III) chlorides* [98].

Compound	T[a] (K)	μ_{eff} (μ_B)	θ (K)	χ_{TIP}[b] (10^{-6} emu mol^{-1})
Cs_2NaUCl_6	4–20	2.49 ± 0.06	-0.53	–
	25–50	2.92 ± 0.06	-9.6	–
$Cs_2NaNpCl_6$	3–50	1.92 ± 0.05	-0.47	–
$Cs_2NaPuCl_6$	3–21	0.97 ± 0.05	-1.3	–
	25–50	1.16 ± 0.08	-12.4	–
$Cs_2NaAmCl_6$	40–300	–	–	660 ± 40[d]
$Cs_2NaCmCl_6$[c]	7.5–25	7.90 ± 0.10	-3.87	–
	25–45	7.48 ± 0.50	-1.15	–
$Cs_2NaBkCl_6$[c]	10–40	–	–	$19\,2000 \pm 30\,000$

[a] Region exhibiting Curie–Weiss behavior.
[b] Temperature-independent paramagnetic susceptibility.
[c] Diluted into $Cs_2NaLuCl_6$.
[d] Ref. 123.

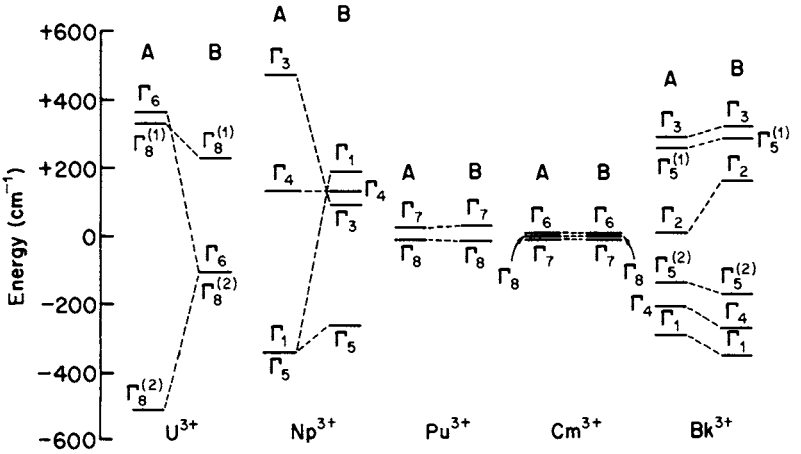

Fig. 18.2 *Crystal field splittings for the ground terms of the trivalent actinide ions in Cs_2NaMCl_6 calculated for the two limiting cases* [98].

Case	B_0^4 (cm^{-1})	B_0^6 (cm^{-1})	B_0^6/B_0^4
A	2420	1490	0.616
B	3015	204	0.0676

Curie–Weiss law:

$$\chi_M = C/(T-\theta) \tag{18.7}$$

where χ_M is the molar magnetic susceptibility (expressed in cgs units in cm^3 mol^{-1} or emu mol^{-1}), T and θ (the Weiss constant) are expressed in kelvin,

and C is the Curie constant. Note that equation (18.7) uses $(T-\theta)$ in the denominator. Some authors use $(T+\theta)$ and this is a point of great confusion. All data quoted in this chapter using the Curie–Weiss law will use the form in equation (18.7). Another common way of representing data is to use the effective moment, μ_{eff} (in units of the Bohr magneton μ_B):

$$\mu_{\text{eff}} = 2.828C^{1/2} = 2.828\,[\chi_M(T-\theta)]^{1/2} \tag{18.8}$$

or

$$\mu_{\text{eff}}^2 = 8.0\chi_M(T-\theta) \tag{18.9}$$

If the data do not follow the Curie–Weiss law, μ_{eff} is commonly defined as:

$$\mu_{\text{eff}} = 2.828\,(\chi_M T)^{1/2} \tag{18.10}$$

If we consider a temperature range where only the ground crystal field state is populated and there is no second-order Zeeman effect, the molar susceptibility in the z-direction may be written as:

$$\chi_z = \frac{N\mu_B^2 g_z^2}{4kT} \tag{18.11}$$

with similar equations for the x- and y-directions. Since $\chi_{\text{ave}} = \frac{1}{3}(\chi_x + \chi_y + \chi_z)$, so:

$$\chi_{\text{ave}} = \frac{N\mu_B^2(g_x^2 + g_y^2 + g_z^2)}{12kT} \tag{18.12}$$

The g_x, g_y, and g_z in equation (18.12) are the same g-values obtained from EPR measurements on the ground crystal field state. Magnetic susceptibility measurements and units are discussed in detail by Myers [12] and Boudreaux and Mulay [13]. All data quoted in this chapter will be in cgs units (see equation (18.7)).

This review is limited in scope and will cover only selected topics, with the emphasis on recent measurements. Earlier reviews cover the $5f^0$, $5f^1$, and some selected data for $5f^2$ and higher configurations [14]. The two volumes edited by Freeman and Darby [15] contain a wealth of information about the magnetic properties of various actinide materials, including a review by Lam and Chan [16] on actinide salts, carbides, chalcogenides, pnictides (group V), and various intermetallic compounds, plus another review by Nellis and Brodsky [17] on the pure metals and alloys. See also Section 19.7 of this volume. Some magnetic data are given in the review by Keller [99] on lanthanide and actinide mixed oxides and by Dell and Bridger [100] in their review of actinide chalcogenides and pnictides. The review article by Boatner and Abraham [8] summarizes all the EPR data on actinide ions published through 1976. Kanellakopulos [101] has recently reviewed the magnetic properties of cyclopentadienyl compounds of the trivalent and tetravalent actinides. A number of very interesting magnetic measurements have been reported in the 'Proceedings of the International Conference on the Physics of Actinides and Related 4f Materials' [18]. Some of these papers are individually referenced later.

18.2 $5f^0$ $^1S_0$; Th^{4+}, Pa^{5+}, U^{6+}, UO_2^{2+}

For a closed-shell configuration, compounds formed with these ions should be diamagnetic. This is found to be true for Th^{4+} and Pa^{5+}, but uranyl compounds and UF_6 exhibit temperature-independent paramagnetism (TIP). The weak paramagnetism for UF_6 has been attributed by Eisenstein and Pryce [19] to the coupling of higher-energy states into the ground configuration by the magnetic field. From an analysis of the observed susceptibility they concluded that the bonding in the actinide hexafluorides is at least partially covalent. A similar model was also proposed by Eisenstein and Pryce [20] and later by McGlynn and Smith [21] to explain the weak paramagnetism of uranyl salts. Recent work by Denning and co-workers [22, 23] on the high-resolution spectral characteristics, including Zeeman-effect measurements of the uranyl ion in tetragonal and trigonal equatorial fields (perpendicular to O–U–O bond axis), has resulted in the determination of paramagnetic magnetic moments for some excited states and a consistent description of the bonding within the uranyl group.

18.3 $5f^1$ $^2F_{5/2}$; Th^{3+}, Pa^{4+}, U^{5+}, Np^{6+}, Pu^{7+}

The $5f^1$ ions are good examples for the interpretation of magnetic data because electron repulsion is absent and at most six transitions are allowed in the optical spectrum. A purple trivalent thorium complex, formulated as $Th(C_5H_5)_3$, has been reported by Kanellakopulos *et al.* [102], with a room-temperature magnetic moment of 0.403 μ_B. A second compound, also formulated as $Th(C_5H_5)_3$ but green in color, has been prepared by Kalina *et al.* [24], who have reported a magnetic moment of 2.10 μ_B. Trisindenylthorium(III) has been prepared by Goffart and also has a very low magnetic moment [18].

The magnetic susceptibility of protactinium tetrachloride has been measured between 3.2 and 296 K [25], as shown in Table 18.3, and exhibits a ferromagnetic transition at 182 ± 2 K. A high degree of covalency has been suggested to explain this relatively high transition temperature. The magnetic susceptibility of protactinium tetraformate [26] has been measured from 80 to 300 K and follows

Table 18.3 *Magnetic data for some tetravalent actinide chlorides* [25].

Compound	*Principal ground-state configuration*	T[a] (K)	θ (K)	μ_{eff} (μ_B)	T_C[b] (K)
$PaCl_4$	$5f^1$ $^2F_{5/2}$	182–210	+158	1.04 ± 0.06	182 ± 2
UCl_4	$5f^2$ $^3H_4$	90–551	−65	3.29	–
$NpCl_4$	$5f^3$ $^4I_{9/2}$	7–43	+6.9	3.08	6.7 ± 0.1

[a] Region exhibiting Curie–Weiss behavior.
[b] Ferromagnetic transition temperature.

the Curie–Weiss law with $\mu_{eff} = 1.23\ \mu_B$ and $\theta = -3$ K. The crystal structure of this compound and its Np analog are reported to have the M^{4+} ion at the center of a nearly undistorted cube of eight oxygen atoms. However, the U analog is stated to have lower symmetry, which appears inconsistent. By assuming that the $J = 5/2$, Γ_7 state is lowest and is the only one that contributes to the measured susceptibility, a value of $\mu_{eff} = 1.24\ \mu_B$ (with $g_J = 6/7$) is calculated from the wavefunctions given by Lea, Leask, and Wolf [11], in good agreement with the experimental value.

The susceptibility of tetrakis(cyclopentadienyl)protactinium has been measured between 4.2 and 300 K [18]. Above 90 K the magnetic susceptibility obeys the Curie–Weiss law with $\theta = -8.6$ K, and the magnetic moment at room temperature is $0.725\ \mu_B$. A $J = 5/2$ state will split into at most three Kramers doublet levels, and in this compound it is reported that the first two levels are separated by approximately 15–30 cm^{-1} and that the third level is at about 600 cm^{-1}. J mixing cannot explain the low magnitude of the magnetic moment.

The magnetic susceptibilities and EPR spectra of pure MUO_3 (M = Li, Na, K, and Rb) with distorted perovskite structures have been reported by Miyake and co-workers [27, 28], who find values of χ_M quite different from those reported by Keller [99]. In the temperature range 16–32 K a sharp spike appeared for all compounds in the susceptibility vs temperature curve. In the case of $NaUO_3$ this spike occurs at the same temperature, 32 K, as a lambda-type anomaly observed in the heat capacity–temperature curve and has been attributed to a magnetic ordering. However, Kanellakopulos and co-workers [29] have remeasured the magnetic susceptibilities of some of these compounds and obtained different results. They suggest that the unusual magnetic behavior reported for these uranate compounds is spurious. The g-values determined by EPR [27] and reported to be in the range 2–4 appear incorrect as they conflict with the magnetic susceptibility results and the g-values of about 0.7 reported by Lewis and co-workers [30] for U^{5+} diluted in $LiNbO_3$, $LiTaO_3$, and $BiNbO_4$. These latter authors also could not find any verifiable EPR spectra due to U^{5+} in a number of magnetically concentrated crystals including $NaUO_3$ and $LiUO_3$. In the eight-fold cubic coordination of Na_3UF_8, they measured a g-value of 1.2 at 7 K.

The magnetic susceptibilities of M_3UF_8 (M = Na, Cs, Rb, and NH_4) have been measured from 8 to 300 K [31]. The experimental data were fitted very satisfactorily with a model that assumed a trigonal (D_{3d}) distortion to the eight-fold cubic coordination of the fluorine atoms.

A very careful study of the magnetic susceptibility of NpF_6 and NpF_6 diluted in UF_6 (approximately O_h symmetry) in the temperature range 4.2–336.9 K has been reported by Hutchison and co-workers [32]. The g-value extrapolated to infinite dilution was found to be 0.605 ± 0.004. The g-value was found to vary as a function of the mole fraction of NpF_6 (six different samples of varying mole fractions were measured), with a maximum value of 0.694 ± 0.011 at a mole fraction of 0.34. No explanation has been given for these observations. The magnetic measurements agree with EPR measurements of NpF_6 diluted in UF_6

[33] and with the calculations of Eisenstein and Pryce [19]. Analysis of the fluorine superhyperfine structure measured by electron nuclear double resonance (ENDOR) in single crystals of NpF_6 diluted in UF_6 [34] indicates that 5f-orbital covalency effects are approximately an order of magnitude larger in NpF_6 than in 4f complexes. This is consistent with the larger radial extension of 5f orbitals as compared to 4f orbitals.

Some EPR and optical measurements have been reported for NpF_6, UX_6^- (X = F, Cl, Br) [35], and PaX_6^{2-} (X = F, Cl, Br, I) [36] (see Table 18.1). For a $5f^1$ ion, the energy level diagram of Fig. 18.3 may be used.* For one electron, the ^2F Russell–Saunders state breaks up into two J states, $J = 5/2$ and $J = 7/2$, when the effect of spin–orbit coupling (where ζ is the spin–orbit coupling constant) is

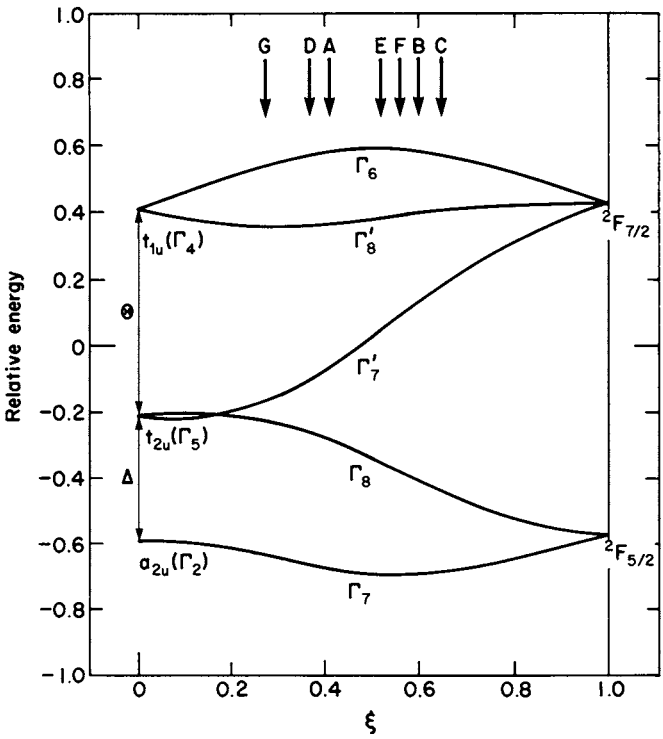

Fig. 18.3 *Relative energy splittings of an f^1 electron as the relative magnitudes of the crystal field and spin–orbit coupling interactions change (O_h symmetry) (see footnote to text). The arrows at the top of the figure represent the approximate values of: A, $(NEt_4)_2PaF_6$; B, $(NEt_4)_2PaCl_6$; C, $(NEt_4)_2PaBr_6$; D, $(NEt_4)UF_6$; E, $(NEt_4)UCl_6$; F, $(NEt_4)UBr_6$; and G, NpF_6. The data are taken from ref.* 36.

* The ordinate in the figure is defined as Relative energy $= E[(\Delta+\Theta)^2 + (7\zeta/2)^2]^{1/2}$ and the abscissa can be determined from the relationship $(1-\xi)/\xi = (\Delta+\Theta)/(7\zeta/2)$. This figure is drawn for the ratio of the crystal field splittings, $\Theta/\Delta = 13/8$.

included. If we assume octahedral symmetry for the above hexahalogenated actinide ions, the $J = 5/2$ state breaks up into a doubly degenerate Γ_7 state and a four-fold degenerate Γ_8 state. The higher-lying $J = 7/2$ state breaks up into two doubly degenerate states, Γ_6 and Γ'_7, and one four-fold degenerate Γ'_8 state. The ground state in this symmetry is the $J = 5/2$, Γ_7 state. The parameters Θ and Δ represent the splittings of the f orbitals for O_h symmetry when the spin–orbit interaction is zero. This is represented at the far left side of Fig. 18.3. As the relative strengths of the crystal field and spin–orbit interactions become comparable, the relative energy splittings change as shown in the center of Fig. 18.3. The far right side of Fig. 18.3 shows the splitting ($7\zeta/2$) in the limit of strong spin–orbit coupling and no crystal field.

If the ground state were a pure $J = 5/2$ state, the measured g-value could easily be calculated. However, the crystal field interaction is not small as compared to the spin–orbit coupling interaction so the excited $J = 7/2$, Γ'_7 state is mixed into the ground $J = 5/2$, Γ_7 state via this interaction. The resulting expression for the ground-state g-value is given by [37]:

$$g = -2\left(\frac{5}{7}\cos^2\phi - \frac{4\sqrt{3}}{21}\sin 2\phi - \frac{12}{7}\sin 2\phi\right)$$

and

$$\Gamma_7^{(1)} = |^2F_{5/2}\,\Gamma_7\rangle\cos\phi - |^2F_{7/2}\,\Gamma'_7\rangle\sin\phi$$

There are four electronic transitions (O_h symmetry) which should be observed in these systems, and three optical and/or near-infrared transitions between the $J = 5/2$ and $J = 7/2$ states have been reported for all the above complexes. In some cases the Γ_7–Γ_8 transition of the $J = 5/2$ state which occurs in the infrared or near-infrared region has also been observed. These electronic absorption data plus the EPR data on the ground state allow the parameters (including orbital reduction factors) of the Eisenstein–Pryce model [19, 35, 38] for an octahedral f^1 system to be evaluated as shown in Table 18.1.

Kanellakopulos and co-workers [29] have reported optical and magnetic susceptibility data for a number of uranates (U^{5+}), neptunates (Np^{6+}), and one plutonate (Pu^{7+}), Li_5PuO_6. The data have been fitted to the Eisenstein–Pryce model with an additional parameter δ to account for a tetragonal component of the crystal field. This additional term breaks the degeneracies of the Γ_8 and Γ'_8 states and shifts the energies of each of the states to different extents. In addition the ground state and the temperature-independent susceptibility become magnetically anisotropic. An empirical TIP term was necessary in order to obtain satisfactory fits of the magnetic data as a function of temperature. Some of the results are shown in Table 18.4. These parameter values can be compared with those found for the $5f^1$ hexahalides shown in Table 18.1.

It is rather surprising that the spin–orbit coupling constant ζ appears approximately constant in Table 18.4 for U^{5+}, Np^{6+}, and Pu^{7+}, and in fact with a value different from that found for U^{5+} in the hexahalides. Hartree–Fock calculations show that the spin–orbit coupling constant does increase markedly

Table 18.4 *Values of the parameters of the modified Eisenstein–Pryce theory fit to the optical spectra and magnetism of some uranates (U^{5+}), neptunates (Np^{6+}), and a plutonate (Pu^{7+}) [29].*

Compound	ζ (cm^{-1})	Δ (cm^{-1})	Θ (cm^{-1})	δ (cm^{-1})	k	k'	χ_{TIP} [a] (10^{-6} emu mol^{-1})
Li_7UO_6	1870	4604	7099	−145	1.0	0.85	10
Li_3UO_4	1780	4353	3507	−100	1.0	0.90	0
$LiUO_3$	1800	4574	4039	−165	0.95	0.80	210
$NaUO_3$	1800	4348	4405	−190	1.0	0.80	180
KUO_3	1850	4152	4055	−200	1.0	0.70	250
Ba_3NpO_6	1810	8421	4325	0	0.70	1.0	125
Li_4NpO_5	1800	9141	3527	−800	0.80	1.0	125
Na_2NpO_4	1800	8509	1246	+750	0.70	0.65	140
Li_5PuO_6	1900	8967	4201	−625	0.80	1.0	120

[a] Empirical parameter.

with higher atomic number and higher charge on the ion. This trend is found in the hexahalide data. The orbital reduction constants for the actinide hexahalides suggest that NpF_6 and $CsUF_6$ are the most ionic of the listed compounds ($k = k' = 1$ results in a pure crystal field model). This interpretation is in conflict with the $X\alpha$ calculations for octahedral $5f^1$ complexes [103] which showed NpF_6 to be the most covalent compound. The main conclusion of these calculations was that the f-orbital splittings were dominated by ionic effects with a lesser contribution from covalent bonding. Other effects, such as the orbital–lattice interaction or the Jahn–Teller effect [39], could also affect the measured magnetic properties and have not been considered in the analysis. The data for the hexahalide compounds have also been discussed by Warren [104] in terms of the angular-overlap model.

The magnetic susceptibility of UCl_5 (a dimeric compound with an octahedral array of chlorine atoms, two of which are bridging) as a function of temperature was first reported by Handler and Hutchison [105] and later by Fuji, Miyake, and Imoto [106]. The latter authors have also reported the g-value as measured by EPR [107]. They have combined the magnetic data with optical measurements by Leung and Poon [108] and fitted all the data with a crystal field model based on a weak C_{2v} distortion of the predominantly octahedral (O_h) crystal field. However, they calculated an isotropic g-value on the basis of octahedral symmetry when in fact their model predicts an anisotropic g-tensor. Soulie and Edelstein [109] have adopted a different point of view by noting the large difference in distances between the two bridging chlorines (U–Cl $\simeq -2.68$ Å) and the four non-bridging chlorines (U–Cl $\simeq 2.43$ Å) in the crystal structure. They used the Newman superposition model [110] and fitted the optical and magnetic data. Their best fit gave $g_x = 0.226$ and $g_y \simeq g_z \simeq 1.186$, as observed. This g_x-value would not be experimentally observed because of the large magnetic field necessary to do so, but the derived spin–orbit coupling constant of 1196 cm^{-1} is much smaller than

that observed in any U^{5+} compounds. Furthermore the calculated $\mu_{eff} \sim 0.85\ \mu_B$ is lower than the measured value of $1.08\ \mu_B$.

18.4 $5f^2\ {}^3H_4$; U^{4+}, Np^{5+}, Pu^{6+}

Uranium(IV) compounds have been widely studied. The total crystal field splitting for the $^3H_4$ ground term of the $5f^2$ configuration is expected to be of the same order as or greater than $200\ cm^{-1}$ (kT at room temperature). Thus only the ground crystal field state or perhaps the two or three lowest-lying states will provide first-order contributions to the observed magnetic susceptibility. Measurements over as wide a temperature range as possible are clearly desirable. Since very little optical data are available for any compound of U^{4+}, magnetic data are usually interpreted by considering only the ground $^3H_4$ term, determining the crystal field splittings for a particular point symmetry group (usually from crystallographic data), choosing a ground state either empirically or by calculation (i.e. point-charge or molecular-orbital model), and then calculating the susceptibility. A $J = 4$ state in a point group symmetry lower than tetragonal will split into nine singlet states. In higher symmetries there will be some singlet states and some doubly and/or triply degenerate states. If a singlet state lies lowest there will be a range of temperature for which the compound will exhibit only temperature-independent paramagnetism. Some examples from the voluminous literature follow.

Early work on the magnetic susceptibilities of solid solutions of UO_2 in ThO_2 (cubic symmetry) was interpreted as showing 'spin only' behavior for the d^2 configuration on extrapolation to infinite dilution. Subsequently Hutchison and Candela [40] showed that a model based on the $5f^2$ configuration with a strong spin–orbit interaction and the ratio of the crystal field parameters such that the Γ_5 (O_h) triplet state is lowest would also fit the observed magnetism. UO_2 undergoes a first-order phase transition from the paramagnetic to the antiferromagnetic state at 30.8 K [111, 112]. Blume, assuming the electronic structure of U^{4+} consisted of a non-magnetic singlet ground state with a low-lying magnetic triplet state and also bilinear isotropic exchange interactions, was able to account semiquantitatively for the magnetic phase transition with this model [113]. Allen has proposed a strong spin–lattice interaction as the driving force for the first-order phase transition [114]. Rahman and Runciman [115] calculated the ground state of UO_2 to be a Γ_5 (O_h) triplet separated by about $1400\ cm^{-1}$ from the higher-lying Γ_3 (O_h) doublet. Faber and Lander [116] have interpreted the results of a single-crystal neutron diffraction study of UO_2 (face-centered cubic, fluorite structure) in terms of an inhomogeneous deformation that causes a shift of the oxygen atoms from the ideal fluorite structure. The dominance of this deformation mode suggested the presence of a non-collinear magnetic structure in UO_2. Recent magnetic measurements [117] on UO_2 diluted in ThO_2 were qualitatively explained on the basis of a model with a non-magnetic singlet

ground state and a first excited state that is populated between 10 and 20 K.

Anisotropic magnetic susceptibility measurements have been reported on a single crystal of UCl_4 [124] which supersede earlier work [41–43]. Using the available optical data [44–46, 124] a fair fit was obtained between the calculated single crystal susceptibilities and the experimental values. The fit could easily have been improved with only minor changes in the crystal field parameter set or the introduction of orbital reduction factors. However the authors believed a better parameter set should be based on an improved fit to the optical data rather than relying on susceptibility data which is sensitive only to the low-lying crystal field levels.

Optical and magnetic studies on $U(NCS)_8(NEt_4)_4$ ($Et = C_2H_5$) have also been published by several groups [43, 45, 47, 48]. In this compound the uranium ion is at a site of cubic symmetry in the first coordination sphere surrounded by eight nitrogen atoms from the thiocyanate groups. By fitting the measured magnetic susceptibility in the temperature range 4.2–290 K, Soulie and co-workers [48] evaluated the appropriate free-ion and crystal field parameters. They found good agreement above 30 K with the measured susceptibility but with significant deviations below this temperature. These deviations were attributed to a slight D_{4h} distortion of the cubic symmetry (confirmed by Raman spectra) which was not taken into account in their calculations. Subsequently Kanellakopulos and co-workers [43, 45] determined another set of empirical parameters using cubic crystal field parameters obtained from the assignment of the optical spectrum. They then took into account the lower symmetry by using perturbation theory to split the ground triplet state in cubic symmetry into a singlet state and a higher-lying doublet state. The use of this model and the introduction of an orbital reduction factor resulted in satisfactory agreement between the calculated and experimental susceptibility data.

The temperature dependence of the magnetic susceptibility of three U^{4+} sulfates, $U(SO_4)_2 \cdot 4H_2O$, $U_6O_4(OH)_4(SO_4)_6$, and $U(OH)_2SO_4$, in the temperature range 4.2–300 K has been reported by Mulak [49]. These three compounds have a similar antiprismatic coordination about the U^{4+} ion by oxygen anions with almost the same U–O distances. Using a simplified model of the U^{4+} ion with a $^3H_4$ ground term, $J = 4$ as a good quantum number in a D_{4d} crystal field, and only the energy splittings between the two lowest crystal field states as empirical parameters, the temperature dependence of the magnetic susceptibility was fitted. A further low-symmetry distortion had to be introduced (which split the energy levels that were doubly degenerate in D_{4d} symmetry) in order to obtain satisfactory agreement. Despite the very similar coordination environment about the U ion in the three compounds, there are significant differences in the low-temperature magnetic behavior. In particular, the magnetic susceptibility for $U(OH)_2SO_4$ from 4.2 to 21 K is approximately constant while above 21 K the susceptibility decreases with a temperature dependence typical of a paramagnetic compound with a degenerate ground state. This low-temperature behavior is attributed to a crystallographic transition induced by the cooperative Jahn–Teller

effect. Hinatsu and co-workers [50] have reported the temperature dependence from 1.8 to 300 K of a new crystalline uranium(IV) sulfate which showed a broad maximum in the susceptibility at 21.5 K. They assumed a one-dimensional chain structure with U atoms linked by hydroxyl groups (or possibly oxygen atoms) and fitted their data to an exchange interaction between uranium atoms along this one-dimensional chain.

The synthesis of the organometallic 'sandwich' compound uranocene, $U(C_8H_8)_2$, by Müller-Westerhoff and Streitwieser [51] has led to a renaissance in the organometallic chemistry of the actinide series [52]. Magnetic susceptibility measurements have played an important role in the discussions of the electronic structure of these types of compounds. Karraker *et al.* [53] initially reported the temperature-dependent susceptibility of $U(C_8H_8)_2$ and interpreted the data on the basis of a crystal field of C_{8h} symmetry acting on the $^3H_4$ ground term. The data were fitted with a $J_z = \pm 4$ ground state and the inclusion of an orbital reduction factor to account for covalency. This model also fitted the experimental results for $Np(C_8H_8)_2$ and $Pu(C_8H_8)_2$. Hayes and Edelstein [54] then proceeded actually to calculate the necessary crystal field parameters using molecular-orbital theory and the Wolfsberg–Helmholz approximation. From the calculated crystal field parameters and published free-ion parameters they found the ground crystal field state to be the $J_z = \pm 3$ level. More careful measurements by Karraker [55] had shown that the susceptibility of $U(C_8H_8)_2$ at low temperature became temperature independent and was attributed by Hayes and Edelstein as being due to a possible low-temperature crystal structure phase transition causing the U^{4+} ion to be at a symmetry site lower than C_{8h}. This model was disputed by Amberger *et al.* [56]. They recalculated the crystal field parameters for uranocene in three ways: using the purely electrostatic approach, the angular-overlap model, and a molecular-orbital model. Assuming rigorous D_{8h} symmetry they found that a crystal field splitting with a singlet ground state ($J_z = 0$) and an excited doublet state at 17 cm^{-1} ($J_z = \pm 1$) gave the best agreement with their molecular-orbital calculation and the experimental data. Subsequently, Edelstein *et al.* [57] showed that some uranocene-type molecules with alkyl or phenyl groups attached to the cyclooctatetraene rings showed the temperature-dependent behavior expected for a degenerate ground state down to 4.2 K. This behavior is inconsistent with the Amberger *et al.* model. Warren [58] has discussed the magnetic properties of uranocene-type compounds in his extensive review on ligand field theory of f-orbital sandwich complexes.

Another class of organometallic uranium(IV) compounds that have been thoroughly studied is tetrakis(cyclopentadienyl)uranium(IV), UCp_4, and its tris(cyclopentadienyl) derivatives, Cp_3UR, where R = BH_4, BF_4, OR, F, Cl, Br, I, etc. [18]. These compounds have been divided into two categories: those showing a small dipole moment and a small range of temperature-independent susceptibilities; and a second category exhibiting larger dipole moments and a more extended range of temperature-independent susceptibilities. These differences have been attributed to an increasing trigonal distortion in the second category of

compounds. Amberger *et al.* [59] have used three different semiempirical calculations to estimate the two crystal field parameters needed for the assumed T_d symmetry of UCp_4. The temperature-dependent magnetic susceptibility of UCp_4 was then fitted assuming a weak crystal field of lower symmetry which split the tetrahedral energy levels. The tetrahedral wavefunctions were used for the calculations and the energy differences of four levels plus one scaling parameter were varied. Satisfactory agreement with the experimental data was obtained. Amberger later analyzed optical spectra of UCp_4 and Cp_3UCl assuming T_d symmetry [60, 61]. He further analyzed the fine structure of the spectrum and determined the crystal field splitting of the ground $^3H_4$ term. Using tetrahedral wavefunctions and the crystal field splitting of the ground term he was able satisfactorily to fit the observed susceptibility using only one scaling parameter. Magnetic data for a number of Cp_3UR compounds have been given by Aderhold and co-workers [42].

Magnetic exchange phenomena have been reported for two amide complexes of UCl_4, i.e. $UCl_4 \cdot 3DMBA$ and $UCl_4 \cdot 3MAA$ (DMBA = *N*,*N*′-dimethylbenzamide; MAA = *N*-methylacetanilide) [62]. Unfortunately, the crystal structures of these compounds are not known. However, the authors assume dimeric structures for the compounds and interpret the measured susceptibilities in terms of the Heisenberg spin–spin interaction between two U ions:

$$E = 2J_{ex}\mathbf{s}_1 \cdot \mathbf{s}_2$$

with $2J_{ex} = -94\,cm^{-1}$ and $-99\,cm^{-1}$ for $UCl_4 \cdot 3DMBA$ and $UCl_4 \cdot 3MAA$ respectively. The occurrence of the exchange phenomenon depended on the substituents on the amide groups, which suggested that the amide groups act as bridging ligands.

18.5 $5f^3\ {}^4I_{9/2}$; U^{3+}, Np^{4+}, Pu^{5+}

The magnetic properties of the uranium(III) halides have been reported [63, 64] and are listed in Table 18.5. UF_3 followed the Curie–Weiss law down to about 125 K, below which temperature the susceptibility increased more rapidly than expected from the higher-temperature data [63]. UH_3 has been reported to have a ferromagnetic transition at approximately 172 K and a saturation magnetic moment in the temperature range 63–196 K of approximately 1 μ_B [65]. EPR measurements have been reported for surprisingly few U^{3+} compounds and are discussed by Boatner and Abraham [8]. Crosswhite *et al.* [5], from their analysis of the optical spectrum of U^{3+} diluted in $LaCl_3$, have calculated $g_{\|} = -4.17$, which agrees well with the magnetic resonance value of $|g_{\|}| = 4.153$ [66]. Magnetic susceptibility data for Cs_2NaUCl_6 [98] as a function of temperature are given in Table 18.5. Calculations indicate that the ground state is probably a slightly distorted Γ_8 (O_h) state.

$NpCl_4$ (Table 18.3) is reported to have a ferromagnetic transition at 6.7 K [67]. Kanellakopulos and co-workers [43] have reported recently the

Table 18.5 *Magnetic data for some trivalent actinide halides* [63,64].

Compound	T[a] (K)	θ (K)	μ_{eff} (μ_B)	T_N (K)	χ_{TIP} (10^{-6} emu mol^{-1})
UF_3	125–293	-110 ± 5	3.67 ± 0.06	–	
UCl_3	25–117	−89	3.70 ± 0.08	22.0 ± 1.0	–
UBr_3	25–76	−54	3.57 ± 0.08	15.0 ± 0.5	–
UI_3	5–14	−9.1	2.67 ± 0.10	3.4 ± 0.2	–
	25–200	−34	3.65 ± 0.05	–	–
$NpCl_3$	3.5–50	–	–	–	6400 ± 100
	75–240	−83.5	2.81 ± 0.09	–	–
α-$NpBr_3$[b]	10–30	–	–	–	10850 ± 320
	50–125	−86	3.26 ± 0.40	–	–
NpI_3[c]	3–15	–	–	–	17000 ± 7000
	25–60	−42	3.17 ± 0.40	–	–
$PuCl_3$	5–100	−7.9	1.11 ± 0.04	4.5 ± 0.5	–
$PuBr_3$	2.2–20	−0.55	0.81 ± 0.08	–	–
	25–60	−10.5	1.01 ± 0.10	–	–
PuI_3	5–50	+4.15	0.88 ± 0.08	4.75 ± 0.10[d]	–

[a] Region exhibiting Curie–Weiss behavior.
[b] Contains $NpOBr_2$ impurity.
[c] Estimated to contain 5% $NpOI_2$ impurity.
[d] T_C listed for ferromagnetic PuI_3.

temperature dependence of the magnetic susceptibility for $NpCl_4$ and $((C_2H_5)_2N)_4Np(Cp(NCS)_8)$ and interpreted these data in a similar fashion as for the analogous U compounds. Dornberger *et al.* [68] have measured the optical spectra and magnetic susceptibilities of Cp_4Np and Cp_3NpX where X = Cl, Br, and I. On the basis of theory described by Amberger [61] they were able to fit the magnetic susceptibility data with the use of a large orbital reduction factor.

From magnetic susceptibility measurements [69] and EPR measurements [70] of hexachloro complexes of Np^{4+}, the ground state of the $^4I_{9/2}$ term is shown to be a $^4\Gamma_8(O_h)$. Limits on the ratios of the fourth- to the sixth-order crystal field parameters have been determined, and these limits are consistent in the isostructural series MCl_6^{2-}, M = Pa^{4+}, U^{4+}, Np^{4+}. Depending on the cation involved, the Γ_8 state may be split by 5–10 cm^{-1} due to small deviations from O_h symmetry. The free-ion g-value (~ 0.6) for Np^{4+} deduced from the data is much reduced from the value of 0.77 obtained from optical data. EPR data obtained at liquid-helium temperatures for $Np(BH_4)_4$ and $Np(BD_4)_4$ diluted in the corresponding $Zr(BH_4)_4$ and $Zr(BD_4)_4$ hosts show that the $^2\Gamma_6$ state (T_d) of the $^4I_{9/2}$ term is lowest [71]. Again the free-ion g-value (0.515) is much lower than expected. Richardson and Gruber [72] have claimed that they observed the EPR spectrum of Np^{4+} diluted in ThO_2.

$SrNpO_3$ and $BaNpO_3$ show magnetic transitions at 31 and 48 K respectively [73]. A sharp increase in magnetization was observed below the transition temperature, which suggested a complicated magnetic structure.

Neptunium dioxide crystallizes in the cubic fluorite structure and magnetic measurements have been reported from 4 to 300 K [16, 74, 75]. There is a magnetic transition at 25.4 K. Above 60 K, the susceptibility follows the Curie–Weiss law ($\mu_{eff} = 2.95$–$3.00\ \mu_B$, $\theta = -22$ K). Below 10–12 K, the magnetic susceptibility becomes independent of temperature ($\chi_M = 8.4 \times 10^{-3}$ emu mol^{-1}). Different models have been suggested to explain the magnetic behavior of NpO_2, including the possibility of a $5f^4$ configuration [75]. The form factor derived from polarized neutron diffraction data obtained on a single crystal of NpO_2 can be satisfactorily fitted with a theoretical calculation using relativistic wavefunctions for Np^{4+}. A magnetic moment of 0.07 μ_B was induced by an applied field of 4.6 T at 4.2 K [76].

18.6 $5f^4\ {}^5I_4$; Np^{3+}, Pu^{4+}

The magnetic susceptibility and magnetization of NpH_x ($x = 2.04, 2.67, 3$) have been measured in the temperature range 4–700 K [77]. The dihydride data could be fitted with a crystal field model based on cubic symmetry (O_h) for the Np^{3+}, $5f^4$ configuration, with a nominal $^5I_4$ ground state split into a ground Γ_3 doublet and a Γ_4 and a Γ_5 triplet at 512 and 549 cm^{-1} respectively. The Γ_1 singlet is calculated to be at 1851 cm^{-1} above the Γ_5 state. Magnetic data for $Cs_2NaNpCl_6$ [98] are shown in Table 18.2 and were assigned as due to the magnetic properties of the Γ_5 (O_h) ground state. The magnetic properties of NpX_3 (X = Cl, Br, I) are given in Table 18.5 [63].

Magnetic susceptibilities from 2.5 to 50 K for Pu^{4+} in three hexachloro complexes were reported by Karraker [78]. Surprisingly, one of the compounds, Cs_2PuCl_6, had a temperature-dependent paramagnetism at low temperatures, which means a non-Kramers doublet is the lowest state. The other two $PuCl_6^{2-}$ complexes had temperature-independent susceptibilities at the lowest temperatures, which arises from a singlet state being the ground state. These data have been interpreted on the basis of a model based on the distorted O_h symmetry of the $PuCl_6^{2+}$ octahedron. PuO_2 exhibits TIP between 4 and 1000 K [79]. Assuming cubic symmetry (O_h) with the Γ_1 state lowest, the first excited state Γ_4 is calculated to be at 2990 cm^{-1}.

Magnetic susceptibility measurements have been reported for $Pu(C_8H_8)_2$ and $Pu(C_8H_7R)_2$, where R is an alkyl group [55]. Earlier work showed these compounds to be diamagnetic. The susceptibility was expected to be small for the $^5I_4$ state in C_{8h} symmetry if the $J_z = 0$ state was lowest. However, there should be a temperature-independent moment. Recent magnetic susceptibility measurements [80] and proton NMR shifts [81] for $Pu(C_8H_8)_2$ suggest that $(PuC_8H_7R)_2$ complexes are indeed paramagnetic.

18.7 $5f^5\ {}^6H_{5/2}$; Pu^{3+}, Am^{4+}

The magnetic properties of PuH_x ($2.0 \leqslant x \leqslant 3$) have been measured between 4 and 700 K [77]. The cubic PuH_2 appears to order antiferromagnetically at 30 K. Cubic Pu compounds with higher hydrogen concentrations order ferromagnetically with higher transition temperatures as x increases. A maximum is reached at $T = 66$ K and $x = 2.7$. Hexagonal PuH_3 becomes ferromagnetic at 101 K. The temperature dependence of the magnetic susceptibility indicates that the ground-state configuration is Pu^{3+}, $5f^5$. The magnetic properties of PuX_3 (X = Cl, Br, I) [63] are given in Table 18.5. $PuCl_3$ shows an antiferromagnetic transition at 4.5 K while PuI_3 has a ferromagnetic transition at 4.75 K. For $PuCl_3$, magnetic susceptibility calculations using wavefunctions obtained from optical data on Pu^{3+} diluted in $LaCl_3$ reproduce the observed susceptibility. Magnetic data for the octahedral complex $Cs_2NaPuCl_3$ [98] are given in Table 18.2.

Magnetic susceptibility measurements ($T = 4$–300 K) indicate that hexagonal β-Pu_2O_3 becomes antiferromagnetic at $T \sim 19$ K [82]. The magnetic structure obtained from neutron diffraction measurements at 13 K consists of Pu moments in the basal plane which vary along the c-direction in a pseudospiral way. At 4 K a spin rotation occurs so the magnetic moment becomes parallel to the crystallographic c-axis.

EPR measurements on Pu^{3+} and Am^{4+} at liquid-helium temperatures in various cubic hosts have been summarized by Boatner and Abraham [8]. For both Pu^{3+} and Am^{4+} with a nominally ${}^6H_{5/2}$ ground state, strong intermediate-coupling effects cause the Γ_7 state (O_h) to be the ground crystal field state, rather than the $\Gamma_8(O_h)$ state as expected for pure Russell–Saunders coupling [83]. Crystal field mixing between the ground state and the excited J states makes the measured g-value a very sensitive indicator of the magnitude of the crystal field [84]. $^{243}AmO_2$ shows an antiferromagnetic transition at 8.5 ± 0.5 K [85]. Above 15 K two regions of temperature-dependent paramagnetism were observed. The ground state was determined to be a Γ_7 (O_h) but the derived g-value of 1.51 is 17% larger than the EPR value of 1.286 found for Am^{4+} diluted in ThO_2. The excited Γ_8 state (O_h) is at about 35 cm^{-1}. A neutron diffraction study on $^{243}AmO_2$ at 20 K and at 6.5 K showed no difference in the two diffraction patterns. Also no magnetic hyperfine field was detected for AmO_2 by the Mössbauer effect [118]. As a consequence of these results, only the magnetic susceptibility measurements indicate an antiferromagnetic transition at 8.5 K [85].

18.8 $5f^6\ {}^7F_0$; Am^{3+}, Cm^{4+}

Very few data exist for these ions. Karraker *et al.* have measured the magnetic susceptibility of $Cs_2NaAmCl_6$ [98] as shown in Table 18.2. The susceptibility was temperature independent, as expected for a $J = 0$ ground state, but the

magnitude found was much larger than that calculated considering only the second-order Zeeman effect to the $J = 1$ state at 2720 cm^{-1}, as found from optical data. New measurements on $Cs_2NaAmCl_6$ and Am_2O_3 agree much better with the calculated value [123]. Am metal is found to exhibit temperature-independent paramagnetism, suggesting a localized $5f^6$ configuration plus conduction electrons [17]. The susceptibility of CmO_2 should also be temperature independent but exhibits Curie–Weiss behavior [86, 125]. This anomaly is not understood but might be caused by non-stoichiometry of the CmO_2. The magnetic properties of Am metal and compounds have recently been reviewed [126].

18.9 $5f^7$ $^8S_{7/2}$; Am^{2+}, Cm^{3+}, Bk^{4+}

The $5f^7$ configuration in Russell–Saunders coupling has an $^8S_{7/2}$ ground state. For a pure $^8S_{7/2}$ term the crystal field should not split the $J = 7/2$ state. For the $4f^7$ ion, Gd^{3+}, it is indeed found that crystal field splittings of the $J = 7/2$ state are of the order of about 0.2 cm^{-1}. However, the ground term for Cm^{3+} is only 87% $^8S_{7/2}$ because intermediate-coupling effects mix in substantial amounts of the $^6P_{7/2}$, $^6D_{7/2}$, and higher terms which result in crystal field splittings of about 5–100 cm^{-1}. Studies of this sort by EPR have been reviewed by Boatner and Abraham [8]. Am^{2+} ions have approximately the same magnetic properties as Cm^{3+}, and it was this fact that was used for the first identification of Am^{2+} as a chemically stable oxidation state [87]. Magnetic susceptibility measurements of Cm^{3+} diluted in $Cs_2NaLuCl_6$ (Table 18.2) suggest a crystal field splitting of 5–10 cm^{-1}. Above 7.5 K there is reasonably good agreement with the calculated free-ion moment of 7.64 μ_B. A recent review of the magnetic properties of Cm and its compounds has been published [126]. The temperature-dependent magnetic susceptibility of BkO_2 diluted in ThO_2 showed the ground state to be a $\Gamma_6(O_h)$ and the excited $\Gamma_8(O_h)$ state to be at about 80 cm^{-1} [88]. The g-value of the ground state was 5.04, about 10% higher than the more accurate value of 4.488 $\pm$ 0.004 measured by EPR [89]. The total overall splitting of the ground $J = 7/2$ state was estimated to be about 300 cm^{-1}. A possible antiferromagnetic transition at 3 K has been suggested to account for the anomalous magnetic behavior of these samples below 10 K. This transition would require segregation of the BkO_2 in the host ThO_2 matrix. Nave *et al.* [119] have measured the magnetic susceptibility of a 56.6 μg sample of BkO_2 (containing a 3% Cf impurity at the time of the measurement) and find Curie–Weiss behavior from 4.2 to 300 K with $\mu_{eff} = 7.92\ \mu_B$ and $\theta = -250$ K. Their value agrees with the calculated value for an $^8S_{7/2}$ state. However, it does conflict with the EPR results and Karraker's results which indicate a considerable splitting of the ground $J = 7/2$ term. A number of magnetic susceptibility measurements have been reported for Cm metal but reports by various investigators do not agree with one another [90, 91, 120].

18.10 $5f^8\ {}^7F_6$; Bk^{3+}

The magnetic data for Bk^{3+} diluted in $Cs_2NaLuCl_6$ are given in Table 18.2 [98]. The magnetic susceptibility is temperature independent, which shows that a singlet state is the ground state. From the systematics of the crystal field parameters for the host crystal the ground state is assigned as a Γ_1 (O_h) state, and from the magnitude of the susceptibility the first excited state is calculated to be a triplet Γ_4 (O_h) state at about 85 cm^{-1}. The magnetic susceptibility of Bk^{3+} adsorbed on an ion-exchange bead [92] has been measured from 9.3 to 298 K (Fig. 18.4). Approximately 1 μg of the ^{249}Bk ($\tau_{1/2}$ = 314 days) was used with a high-sensitivity Faraday balance based on the design of Cunningham. The data followed the Curie–Weiss law with $\mu_{eff} = 9.40 \pm 0.06\ \mu_B$ and $\theta = 11.0 \pm 1.9$ K. Based on the assumption that crystal field splittings are small or negligible for actinide ions adsorbed on an ion-exchange bead, the free-ion g-value of 1.452 $\pm$ 0.008 calculated from the data agrees well with the value of 1.446 obtained from spectroscopic data [93]. Nave *et al.* [119] have reported the magnetic susceptibility for 143.5 μg of $^{249}BkF_3$ which followed the Curie–Weiss law from 4.2 to 300 K with $\mu_{eff} = 9.38\ \mu_B$ and $\theta = -77.9$ K. The magnetic susceptibility of Bk metal has also been reported by Nave *et al.* [119, 120] and by Fujita [92] and the results are presented in Table 18.6. Clearly these very difficult measurements need to be repeated.

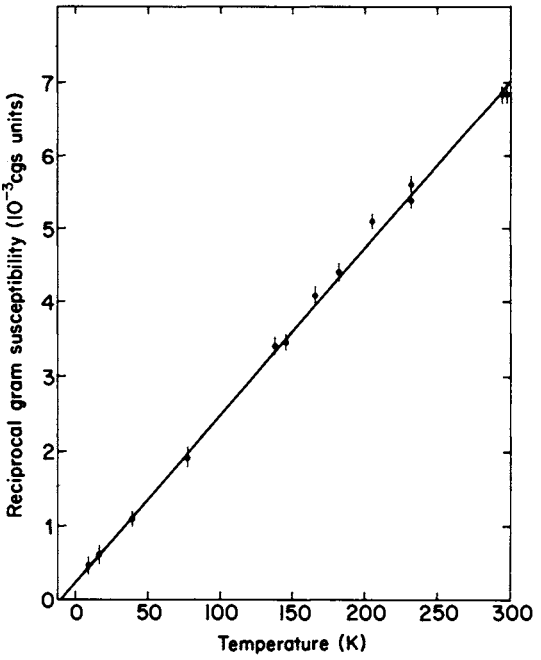

Fig. 18.4 *$1/\chi_g$ vs temperature for about 1 μg of Bk^{3+} adsorbed on one or two ion-exchange beads* [92].

Table 18.6 *Magnetic data for* ^{249}Bk *metal samples.*

Sample	*Mass* (μg)	μ_{eff} (μ_B)	θ (K)	T[a] (K)	T_C (K)	Cf[b] (%)	*Ref.*	*Comments*
^{249}Bk metal	338.7	9.67[c]	−183	4.2–300	22	2	119	
^{249}Bk metal 4	21.0	9.69[c]	−101.6	4.2–300		12	120	pure dhcp
^{249}Bk metal 4	21.0	8.6[c]	−243.6	4.2–300		27	120	pure dhcp
^{249}Bk metal 5	19.0	8.82[c]	−84.4	4.2–300		16.5	120	pure dhcp
^{249}Bk metal 6	126.0	8.98[c]	−79.2	4.2–300		20	120	pure dhcp
^{249}Bk metal II	1.67	8.23	−64.4	170–350	140 ± 15?	~20	92	predominantly fcc; dull gray-black in appearance; ferromagnetic, due to contamination?
^{249}Bk metal III	5.63	8.52	−72.7	50–298	35.3	~16	92	predominantly dhcp; minor component fcc; silvery; antiferromagnetic
^{249}Bk metal V–I	1.73	8.83	−33	100–298	–	1.7	92	mixture fcc, dhcp; silvery; susceptibility lower than calculated from Curie–Weiss law below 100 K

[a] Temperature range of Curie–Weiss behavior, except for the first five entries which cover the entire range of measurements.
[b] Percentage ^{249}Cf at time of measurement.
[c] High-temperature moment.

18.11 $5f^9\ {}^6H_{15/2}; Cf^{3+}$

The magnetic susceptibility of about 1 μg of Cf^{3+} adsorbed on an ion-exchange bead [92] has been measured from 77 to 297 K on a high-sensitivity Faraday balance. The data followed the Curie–Weiss law with $\mu_{eff} = 9.14 \pm 0.66\ \mu_B$ and $\theta = 5.6 \pm 3.2$ K. With the same assumption as discussed for Bk^{3+}, a free-ion g-value of 1.144 ± 0.007 was obtained for the ${}^6H_{15/2}$ ground term. The EPR spectrum of Cf^{3+} in $Cs_2NaLuCl_6$ powder has been observed at 4.2 K [94]. From the measured isotropic g-value of 6.273 the ground crystal field was identified as the Γ_6 (O_h) state and a free-ion g-value of 1.279 for the nominally ${}^6H_{15/2}$ term was determined. For the $4f^9$ analog, Dy^{3+}, the free-ion g-value is 1.333. The magnetic susceptibility of ${}^{249}Cf^{3+}$ (~ 2.4 mg) diluted into octahedral Cs_2NaYCl_6 has been reported in the temperature range from 2.2 to 100 K. From an analysis of the data the Γ_6 state was determined to be the ground state, in agreement with EPR measurements, with a $\Gamma_8^{(1)}$ level as the first excited level at about 50 cm^{-1}. The total crystal field splitting was calculated to be about 860 cm^{-1}. Limits were set for the ratio of B_0^4/B_0^6 which were consistent with those determined previously for the trivalent actinide compounds Cs_2NaMCl_6 ($M = U^{3+}, \ldots, Bk^{3+}$) [121].

Fujita and co-workers [122] have reported the magnetic susceptibility of two samples of fcc ${}^{249}Cf$ metal of mass 8.85 and 5.64 μg. These samples followed the Curie–Weiss law in the temperature range of approximately 25–298 K with $\mu_{eff} = 9.84$ and 9.67 μ_B and $\theta = 3.24$ and -3.00 K, respectively. Nave *et al.* [120] have reported magnetic measurements on an fcc ${}^{249}Cf$ metal sample of mass 14.69 ± 0.15 μg which showed a ferro- or ferrimagnetic transition at about 56 K. At high temperature μ_{eff} is reported to be 9.93 μ_B with $\theta = +55.7$ K. If Cf were divalent in Cf metal, the ground term would be a $J = 8$, $\mu_{eff} = 10.22\ \mu_B$; while for a trivalent ion, $J = 15/2$, $\mu_{eff} = 10.18\ \mu_B$. Unfortunately, magnetic measurements will not be able to distinguish between these two configurations.

18.12 $5f^{11}\ {}^4I_{15/2}; Es^{2+}$

The EPR spectrum at 4.2 K of Es^{2+} diluted in CaF_2 was reported Edelstein *et al.* [95] and used to identify the stabilization of this oxidation state. The measured g-value of 5.809 ± 0.005 identified the ground state as a Γ_6 (O_h) state. Subsequently, Boatner *et al.* [96] found that the ground state of Es^{2+} diluted in $SrCl_2$ had a g-value of 6.658 ± 0.003, which was assigned to the Γ_7 (O_h) state. Thus, the ratio of the crystal field parameters changed on going from CaF_2 to $SrCl_2$, causing the ground state to switch. Analogous behavior had been found for the $4f^{11}$ ion, Ho^{2+}, in the same host crystals. The magnitude of the measured g-values is smaller than expected, and has been attributed primarily to covalency effects [96, 97]. Subsequently Nave *et al.* [127] reported $\mu_{eff} = 1.07 \pm 0.2\ \mu_B$ and $\mu_{eff} = 9.7 \pm 0.2\ \mu_B$ for the high temperature moment of dhcp ${}^{249}Cf$ metal.

ACKNOWLEDGMENTS

This work was supported in part by the Director, Office of Energy Research, Office of Basic Energy Sciences, Chemical Sciences Division of the US Department of Energy under Contract No. DE-ACO3-76SF00098. One of us (JG) is Chercheur Qualifié, at IISN (Brussels).

REFERENCES

1. Van Vleck, J. H. (1932) *The Theory of Electric and Magnetic Susceptibilities*, Oxford University Press, London.
2. Johnston, D. A., Satten, R. A., Schreiber, C. L., and Wong, E. Y. (1966) *J. Chem. Phys.*, **44**, 3141–3.
3. Amberger, H. D. (1976) *J. Organomet. Chem.*, **110**, 59–66.
4. Bernstein, E. R. and Keiderling, T. A. (1973) *J. Chem. Phys.*, **59**, 2105–22.
5. Crosswhite, H. M., Crosswhite, H., Carnall, W. T., and Pasze, A. P. (1980) *J. Chem. Phys.*, **72**, 5103–17.
6. Carnall, W. T., Crosswhite, H., Crosswhite, H. M., Hessler, J. P., Edelstein, N., Conway, J. G., Shalimoff, G. V., and Sarup, R. (1980) *J. Chem. Phys.*, **72**, 5089–102.
7. For a comprehensive treatise on electron paramagnetic resonance including f transition elements, see Abragam, A. and Bleaney, B. (1970) *Electron Paramagnetic Resonance of Transition Ions*, Oxford University Press, London.
8. For a specialized review of electron paramagnetic resonance of actinide ions, see Boatner, L. A. and Abraham, M. M. (1978) *Rep. Prog. Phys.*, **41**, 87–155.
9. See Wybourne, B. G. (1965) *Spectroscopic Properties of Rare Earths*, Wiley, New York; and see ref. 10 for detailed discussions of the atomic theory of f electron systems.
10. Judd, B. R. (1963) *Operator Techniques in Atomic Spectroscopy*, McGraw-Hill, New York.
11. Lea, K. R., Leask, J. M., and Wolf, W. P. (1962) *J. Phys. Chem. Solids*, **23**, 1381–405.
12. Myers, R. J. (1973) *Molecular Magnetism and Magnetic Resonance Spectroscopy*, Prentice-Hall, Englewood Cliffs, NJ.
13. Boudreaux, E. A. and Mulay, L. N. (eds) (1976) *Theory and Applications of Molecular Paramagnetism*, Wiley-Interscience, New York.
14. Sidall, T. H., III (1976) in ref. 13, pp. 317–48.
15. Freeman, A. J. and Darby, J. B. Jr (eds) (1974) *The Actinides: Electronic Structure and Related Properties*, vols I and II, Academic Press, New York.
16. Lam, D. J. and Aldred, A. T. (1974) in ref. 15, vol. I, pp. 109–79.
17. Nellis, W. J. and Brodsky, M. B. (1974) in ref. 15, vol. II, pp. 265–88.
18. Wachter, P. (ed.) (1980) *Proc. Int. Conf. on the Physics of Actinides and Related 4f Materials*; *Physica*, **102B/C**, 1–400.
19. Eisenstein, J. C. and Pryce, M. H. L. (1960) *Proc. R. Soc. A*, **255**, 181–98.
20. Eisenstein, J. C. and Pryce, M. H. L. (1955) *Proc. R. Soc. A*, **229**, 20–38.
21. McGlynn, S. P. and Smith, J. K. (1962) *J. Mol. Spectrosc.*, **6**, 164.
22. Denning, R. G., Norris, J. O. W., Short, I. G., Snellgrove, T. R., and Woodmark, D. R. (1980) in *Lanthanide and Actinide Chemistry and Spectroscopy* (ed. N. M.

Edelstein), (ACS Symp. Ser. 131), American Chemical Society, Washington DC, pp. 313–30.
23. Denning, R. G., Snellgrove, T. R., and Woodmark, D. R. (1979) *Mol. Phys.*, **37**, 1109–43.
24. Kalina, D. G., Marks, T. J., and Wachter, W. A. (1977) *J. Am. Chem. Soc.*, **99**, 3877–9.
25. Hendricks, M. E., Jones, E. R. Jr, Stone, J. A., and Karraker, D. G. (1971) *J. Chem. Phys.*, **55**, 2993–7.
26. Schenk, H. J., Bohres, E. W., and Schwochau, K. (1975) *Inorg. Nucl. Chem. Lett.*, **11**, 201–6.
27. Miyake, C., Fuji, K., and Imoto, S. (1979) *Chem. Phys. Lett.*, **61**, 124–6.
28. Miyake, C., Fuji, K., and Imoto, S. (1977) *Chem. Phys. Lett.*, **46**, 349–50.
29. Kanellakopulos, B., Hendrich, E., Keller, C., Baumgartner, F., Konig, E., and Desai, V. P. (1980) *Chem. Phys.*, **53**, 197–213.
30. Lewis, W. B., Hecht, H. G., and Eastman, M. P. (1973) *Inorg. Chem.*, **12**, 1634–9.
31. Rigny, P., Dianoux, A. J., and Plurien, P. (1971) *J. Phys. Chem. Solids*, **32**, 1901–8.
32. Hutchison, C. A. Jr, Tsang, T., and Weinstock, B. (1962) *J. Chem. Phys.*, **37**, 555–62.
33. Hutchison, C. A. Jr and Weinstock, B. (1960) *J. Chem. Phys.*, **32**, 56–61.
34. Butler, J. E. and Hutchison, C. A. Jr (1981) *J. Chem. Phys.*, **74**, 3102–19.
35. Eichberger, K. and Lux, F. (1980) *Ber. Bunsenges. Phys. Chem.*, **84**, 800–7.
36. Brown, D., Lidster, P., Whittaker, B., and Edelstein, N. (1976) *Inorg. Chem.*, **15**, 511–14.
37. Axe, J. D. (1960) University of California Radiation Laboratory Report UCRL-9293.
38. Edelstein, N. (1977) *Rev. Chim. Minér.*, **14**, 149–59.
39. Judd, B. R. (1977) in *Proc. 2nd Int. Conf. on the Electronic Structure of the Actinides* (eds J. Mulak, W. Suski, and R. Troc), Polish Academy of Sciences, Warsaw, pp. 93–103.
40. Hutchison, C. A. Jr and Candela, G. A. (1957) *J. Chem. Phys.*, **27**, 707–10.
41. Hendricks, M. E. (1971) PhD Thesis, University of South Carolina; Savannah River Laboratory Report DP-MS-71-46, Aiken, SC.
42. Aderhold, C., Baumgartner, F., Dornberger, E., and Kanellakopulos, B. (1978) *Z. Naturf.*, **33a**, 1268–80.
43. Kanellakopulos, B., Klenze, R., and Stollenwerk, A. (1980) in *Proc. 10ème Journees des Actinides* (eds B. Johansson and A. Rosengren), Stockholm, pp. 217–31.
44. Hecht, H. G. and Gruber, J. B. (1974) *J. Chem. Phys.*, **60**, 4872–9; Erratum (1975) *J. Chem. Phys.*, **63**, 2773–4.
45. Carnall, W. T., Kanellakopulos, B., Klenze, R., and Stollenwerk, A. (1980) in *Proc. 10ème Journees des Actinides* (eds B. Johansson and A. Rosengren), Stockholm, pp. 201–16.
46. Gruber, J. B. and Hecht, H. G. (1974) *J. Chem. Phys.*, **60**, 1352–4; Erratum (1975) *J. Chem. Phys.*, **62**, 311–12.
47. Folcher, G., Marquet-Ellis, H., Rigny, P., Soulie, E., and Goodman, G. (1976) *J. Inorg. Nucl. Chem.*, **38**, 747–53.
48. Soulie, E. and Goodman, G. (1976) *Theor. Chim. Acta*, **41**, 17–36; Erratum (1979) *Theor. Chim. Acta*, **51**, 259–60.
49. Mulak, J. (1978) *J. Solid State Chem.*, **25**, 355–66.
50. Hinatsu, Y., Miyake, C., and Imoto, S. (1981) *J. Nucl. Sci. Tech.*, **18**, 349–54.

51. Müller-Westerhoff, U. and Streitwieser, A. Jr (1968) *J. Am. Chem. Soc.*, **90**, 7364–5.
52. Hayes, R. G. and Thomas, J. L. (1971) *Organomet. Rev. A*, **7**, 1–50.
53. Karraker, D. G., Stone, J. A., Jones, E. R., and Edelstein, N. (1970) *J. Am. Chem. Soc.*, **92**, 4841–5.
54. Hayes, R. G. and Edelstein, N. (1972) *J. Am. Chem. Soc.*, **94**, 8688–91.
55. Karraker, D. G. (1973) *Inorg. Chem.*, **12**, 1105–8.
56. Amberger, H. D., Fischer, R. D., and Kanellakopulos, B. (1975) *Theor. Chim. Acta*, **37**, 105–27.
57. Edelstein, N., Streitwieser, A. Jr, Morrell, D. G., and Walker, R. (1976) *Inorg. Chem.*, **15**, 1397–8.
58. Warren, K. D. (1977) *Struct. Bonding*, **33**, 97–138.
59. Amberger, H. D., Fischer, R. D., and Kanellakopulos, B. (1976) *Z. Naturf.*, **31b**, 12–21.
60. Amberger, H. D. (1976) *J. Organomet. Chem.*, **110**, 59–66.
61. Amberger, H. D. (1976) *J. Organomet. Chem.*, **116**, 219–29.
62. Miyake, C., Hinatsu, Y., and Imoto, S. (1979) *Chem. Phys. Lett.*, **63**, 529–30.
63. Jones, E. R. Jr, Hendricks, M. E., Stone, J. A., and Karraker, D. G. (1974) *J. Chem. Phys.*, **60**, 2088–94.
64. Berger, M. and Sienko, M. J. (1967) *Inorg. Chem.*, **6**, 324–6.
65. Green, D. M. (1955) *J. Chem. Phys.*, **23**, 1708–10.
66. Hutchison, C. A. Jr, Llewellyn, P. M., Wong, E., and Dorain, P. (1956) *Phys. Rev.*, **102**, 292.
67. Stone, J. A. and Jones, E. R. Jr (1971) *J. Chem. Phys.*, **54**, 1713–18.
68. Dornberger, E., Kanellakopulos, B., Klenze, R., and Stollenwerk, A. H. (1980) in *Proc. 10ème Journees des Actinides* (eds B. Johansson and A. Rosengren), Stockholm, pp. 58–73.
69. Karraker, D. G. and Stone, J. A. (1980) *Phys. Rev. B*, **22**, 111–14.
70. Edelstein, N., Kolbe, W., and Bray, J. E. (1980) *Phys. Rev. B*, **21**, 338–42.
71. Banks, R. H. and Edelstein, N. (1980) in *Lanthanide and Actinide Chemistry and Spectroscopy* (ed. N. M. Edelstein), (ACS Symp. Ser. 131), American Chemical Society, Washington DC, pp. 331–48.
72. Richardson, R. P. and Gruber, J. B. (1972) *J. Chem. Phys.*, **56**, 256–60.
73. Kanellakopulos, B., Keller, C., Klenze, R., and Stollenwerk, A. H. (1980) *Physica*, **102B**, 221–5.
74. Ross, J. W. and Lam, D. J. (1967) *J. Appl. Phys.*, **38**, 1451–3.
75. Erdos, P., Solt, G., Zolnierek, Z., Blaise, A., and Fournier, J. M. (1980) *Physica*, **102B**, 164–70.
76. Delapalme, A., Forte, M., Fournier, J. M., Rebizant, J., and Spirlet, J. C. (1980) *Physica*, **102B**, 171–3.
77. Aldred, A. T., Cinader, G., Lam, D. J., and Weber, L. W. (1979) *Phys. Rev. B*, **19**, 300–5.
78. Karraker, D. G. (1971) *Inorg. Chem.*, **10**, 1564–6.
79. Raphael, G. and Lallement, R. (1968) *Solid State Commun.*, **6**, 383–5.
80. Kanellakopulos, B. (1981) unpublished work.
81. Solar, J. P., Streitwieser, A. Jr, and Edelstein, N. (1980) unpublished work.
82. McCart, B., Lander, G. H., and Aldred, A. T. (1981) *J. Chem. Phys.*, **74**, 5263–8.
83. Edelstein, N. M., Easley, W. C., and Mehlhorn, R. J. (1969) *J. Chem. Phys.*, **51**, 3281–5.

84. Lam, D. J. and Chan, S. K. (1974) *Phys. Rev. B*, **9**, 808–14.
85. Karraker, D. G. (1975) *J. Chem. Phys.*, **63**, 3174–5.
86. Morss, L. R., Fuger, J., and Goffart, J. (1981) in *Actinides–1981*, Abstracts, Lawrence Berkeley Lab. Report LBL-12441, p. 263.
87. Edelstein, N., Easley, W., and McLaughlin, R. (1968) *J. Chem. Phys.*, **44**, 3130–1.
88. Karraker, D. G. (1975) *J. Chem. Phys.*, **62**, 1444–6.
89. Boatner, L. A., Reynolds, R. W., Finch, C. B., and Abraham, M. M. (1972) *Phys. Lett. A*, **42**, 93.
90. Fournier, J. M., Blaise, A., Muller, W., and Spirlet, J. C. (1977) *Physica*, **86–88B**, 30–1.
91. Huray, P. G., Nave, S. E., Peterson, J. R., and Haire, R. G. (1980) *Physica*, **102B**, 217–20.
92. Fujita, D. K. (1969) University of California Radiation Laboratory Report UCRL-19507.
93. Crosswhite, H. and Carnall, W. T. (1982) private communication.
94. Edelstein, N. and Karraker, D. G. (1975) *J. Chem. Phys.*, **62**, 938–40.
95. Edelstein, N., Conway, J. G., Fujita, D., Kolbe, W., and McLaughlin, R. (1970) *J. Chem. Phys.*, **52**, 6425–6.
96. Boatner, L. A., Reynolds, R. W., Finch, C. B., and Abraham, M. M. (1976) *Phys. Rev. B*, **13**, 953–8.
97. Edelstein, N. (1971) *J. Chem. Phys.*, **54**, 2488–91.
98. Hendricks, M. E., Jones, E. R. Jr, Stone, J. A., and Karraker, D. G. (1974) *J. Chem. Phys.*, **60**, 2095–103.
99. Keller, C. (1972) in *MTP International Review of Science*, Inorganic Chemistry, ser. I, vol. 7, *Lanthanides and Actinides* (ed. K. W. Bagnall), Butterworths, London, pp. 47–85.
100. Dell, R. M. and Bridger, N. J. (1972) in ref. 99, pp. 211–74.
101. Kanellakopulos, B. (1979) in *Organometallics of the f-Elements* (eds T. J. Marks and R. D. Fischer), Reidel, Dordrecht, pp. 1–35.
102. Kanellakopulos, B., Dornberger, E., and Baumgartner, F. (1974) *Inorg. Nucl. Chem. Lett.*, **10**, 155–60.
103. Thornton, G., Rosch, N., and Edelstein, N. (1980) *Inorg. Chem.*, **19**, 1304–7.
104. Warren, K. D. (1977) *Inorg. Chem.*, **16**, 2008–11.
105. Handler, P. and Hutchison, C. A. Jr (1956) *J. Chem. Phys.*, **25**, 1210–13.
106. Fuji, K., Miyake, C., and Imoto, S. (1979) *J. Nucl. Sci. Tech.*, **16**, 207–13.
107. Miyake, C., Fuji, K., and Imoto, S. (1977) *Inorg. Nucl. Chem. Lett.*, **13**, 53–5.
108. Leung, A. F. and Poon, Y. (1977) *Can. J. Phys.*, **55**, 937–42.
109. Soulie, E. and Edelstein, N. (1980) *Physica*, **102B**, 93–9.
110. Newman, D. J. (1971) *Adv. Phys.*, **20**, 197–256.
111. Frazer, B. C., Shirane, G., Cox, D. E., and Olsen, C. E. (1965) *Phys. Rev. A*, **140**, 1448–52.
112. Allessandri, U. A., Cracknel, A. P., and Prgystawa, J. (1976) *Comm. Phys.*, **1**, 51–5.
113. Blume, M. (1966) *Phys. Rev.*, **141**, 517–24.
114. Allen, S. J. (1968) *Phys. Rev.*, **167**, 492–6.
115. Rahman, H. U. and Runciman, W. A. (1966) *J. Phys. Chem. Solids*, **27**, 1833–5.
116. Faber, J. Jr and Lander, G. H. (1976) *Phys. Rev. B*, **14**, 1151–64.
117. Soulie, E., deNovion, C., and Blaise, A. (1981) *Proc. 11ème Journees des Actinides* (eds G. Bombieri, G. de Paoli, and P. Zanella), Padova, pp. 138–40.

118. Boeuf, A., Fournier, J. M., Gueugnon, J. F., Manes, L., Rebizant, J., and Rustichelli, F. (1979) *J. Phys. Lett.*, **40**, 335–8.
119. Nave, S. E., Haire, R. G., and Huray, P. G. (1981) in *Actinides–1981*, Abstracts, Lawrence Berkeley Lab. Report LBL-12441, pp. 144–6.
120. Nave, S. E., Huray, P. G., Haire, R. G., and Peterson, J. R. (1980) Oak Ridge National Lab. Report ORNL-5665, pp. 74–6.
121. Karraker, D. G. and Dunlap, B. D. (1976) *J. Chem. Phys.*, **65**, 2032–3.
122. Fujita, D. K., Parsons, T. C., Edelstein, N., Noe, M., and Peterson, J. R. (1976) in *Transplutonium Elements* (eds W. Müller and R. Linder), North-Holland, Amsterdam, pp. 173–8.
123. Soderholm, L., Edelstein, N., Morss, L. R., and Shalimoff, G. V. (1986) *J. Mag. Magn. Mat.*, **54–57**, 597–8.
124. Gamp, E., Edelstein, N., Khan Malek, C., Hubert, S., and Genet, M. (1983) *J. Chem. Phys.*, **79**, 2023–6.
125. Nave, S., Haire, R. G., and Huray, P. G. (1983) *Phys. Rev. B*, **28**, 2317–27.
126. Edelstein, N. (1985) in *Americium and Curium Chemistry and Technology*, (eds N. Edelstein, J. D. Navratil, and W. W. Schulz) D. Reidel, Dordrecht, pp. 193–211.
127. Nave, S. E., Moore, J. R., Spaar, M. T., Haire, R. G., and Huray, P. G. (1985) *Physica*, **130B**, 225–7.

CHAPTER NINETEEN

THE METALLIC STATE

M.V. Nevitt and M.B. Brodsky

19.1 INTRODUCTION

A number of the properties covered in this chapter are also given elsewhere in this volume. In this presentation, the properties of the actinide elements are taken as a whole and attempts are made to compare them with the properties of metallic elements occurring in other parts of the periodic table. The actinide metals are often thought to be *exotic*, because they tend to have properties that are difficult to explain by simple theoretical approaches that have been useful for simple metals. The properties of the actinide metals do in fact represent a severe test to the theoretical solid-state scientist, as do the other transition-metal series. But, like other metals, they are lustrous and may be malleable; they have, among their several crystalline structures, some simple atomic arrangements; and they have relatively low electrical resistivities and high thermal conductivities.

One may ask whether these elements are properly called 'actinides' or 'thorides' in the metallic state, that is, whether the 5f electrons become stabilized after actinium or after thorium. This matter will arise indirectly in Section 19.3, but will be addressed here to introduce the nature of the series. Are the 5f-electron energies for Th lower than the highest energy associated with an occupied state, the Fermi energy (E_F)? It is known from many experimental observations of properties that depend on the stability of 5f electrons (including magnetic susceptibility, electrical resistivity, and specific heat) and from theoretical calculations that there are no known metallic systems involving thorium for which the 5f-electron energy is below E_F. On the other hand, energy band calculations, and perhaps photoelectron spectroscopy measurements for α-Th, show that the results cannot be explained properly unless the presence of the 5f electrons immediately above E_F are factored into the model. Thus, in the metallic

state the series may be properly called the thorides, but is also a *virtual* actinide series, and the term 'actinide series' is satisfactory.

This chapter will deal with pure actinide metals, disordered alloy systems, and atomically ordered intermetallic compounds. The latter have been very useful in understanding properties related to the electronic structure of the pure metals; the very large number of actinide intermetallic compounds yields several whose electronic structure is such that their properties are totally explained by well-understood phenomena. It then becomes possible to understand systems with more complicated properties as modifications of the well-understood materials.

19.2 ATOMIC STRUCTURE

19.2.1 Crystal structure

The general crystal structure pattern of the actinide series fails to show a strong similarity to that of the rare-earth series but, rather, resembles that of the 3d transition elements. This is true in three particular respects:

(1) The crystal structure that exists at the melting point is body-centered cubic (bcc) through the light actinide metals and changes after Pu to face-centered cubic (fcc). A similar change occurs between Fe and Co in the 3d elements.
(2) The latter part of the series, Am through Es, is characterized by the occurrence of the fcc and double hexagonal close-packed (dhcp) structures at all temperatures below the melting point; the occurrence of the hexagonal close-packed (hcp) and/or fcc structures is also characteristic of Co, Ni, and Cu.
(3) In the middle of the series – at U, Np, and Pu – one or more complex crystal structures intervene as low-temperature forms, in analogy to the complex crystal structures that Mn assumes at low temperatures.

The lanthanide series, in contrast, exhibits a generally uniform crystal structure pattern of hcp or fcc at low temperatures and bcc at high temperatures.*

The occurrence of complex crystal structures as the low-temperature polymorphic forms of U, Np, and Pu, together with several more that characterize intermediate phases in binary systems of these elements is believed to be due to the participation of f-like electronic charge in the bonding; f-electron ligands favor these low-symmetry structures over the typically metallic crystal structures (fcc and hcp) and, concomitantly, greater packing density is achieved [1–6]. This effect is overcome at higher temperatures by the large vibrational contribution to the entropy that is made by the bcc structure [7]. For detailed information on phase diagrams, several compilations should be consulted [8–11].

* The crystal structure characteristics of the lanthanide and actinide series are similar in one respect: the hcp structure has a doubled *c*-axis in the actinide elements Am through Es, as it does in the lanthanide series for La through Pm.

19.2.2 Melting points

In the actinide metals the pattern of melting points and the relationship to crystal structure also resemble those observed in the 3d elements. The temperature of solidification (Table 19.1) rises to a maximum in the region where the bcc structure exists at the melting point, falls to a minimum at Np and Pu, then rises to a second, lesser, maximum later in the series where the fcc and hcp structures occur.

Fig. 19.1, due to Smith and Kmetko [3], illustrates in a schematic and approximate way the crystal structure and melting-point trends described above. The diagram has some speculative features, e.g. the occurrence of the bcc structure at the melting point beyond Pu. It is intended to convey only gross features. Participation by f electrons in bonding is thought to favor the liquid state and thus to be the source of the melting-point suppression centered at Np–Pu [12]. A full listing of the crystallographic data for the polymorphic forms of the actinides at ambient pressure [10, 13] is given in Table 19.1 (see also Chapters 2–12).

19.2.3 Pressure effects

The actinide metals respond to pressure by undergoing transformations of a kind that sheds light on the extent of participation of f electrons in bonding. Pressure, which favors f–f overlap, extinguishes the high-symmetry cubic and orthorhombic structures of Pu that are not favorable for f-electron bonding, and at modest levels (3 GPa) brings into equilibrium the monoclinic β phase and the liquid phase, both of which are believed to permit enhanced f-electron bonding [12]. In the case of Am the contraction of the f shell into the core precludes the presence of delocalized f-like bonding and, as a result, the low-symmetry structures characteristic of f-electron bonding in U, Np, and Pu are not observed at atmospheric pressure. But at about 15 GPa pressure the normally unexposed f electrons are brought closer together and the 5f electron participation in bonding resembles that found in U, Np, and Pu at 1 atm. In this condition Am transforms from the high-symmetry fcc structure to the orthorhombic α-U structure [4] or to a monoclinic structure based on a distorted α-U structure [5]. Pressure-induced transformation that can be associated in a consistent way with f–f overlaps are also observed in Cm, Bk, and Cf (6). All of these elements undergo a transformation to an α-U type structure: Cm 18 GPa; Bk 25 GPa; Cf 41 GPa.

19.3 ELECTRONIC STRUCTURE

19.3.1 Character of 5f electrons

It is well-known that the rare-earth series and the several transition-metal series are characterized by the stabilization and filling-up of 4f or 3d, 4d, and 5d energy

Table 19.1 *Polymorphic modifications, transformation temperatures, and structural data for the actinide metals.*

Element	*Melting point* (°C)	*Lattice symmetry*	*Temperature range of stability* (°C)	*Lattice constants* a_0 (Å)	b_0 (Å)	c_0 (Å)	β (deg)	*X-ray density* (g cm^{-3})	*Atoms per unit cell*
actinium		fcc	–	5.315±5	–	–	–	10.07	4
thorium		α, fcc	< ~1360	5.0843(25°C)	–	–	–	11.724	4
	1750	β, bcc	< ~1360–1750	4.11 (1450°C)	–	–	–	11.10	2
protactinium		α, bct	<1165	3.929	–	3.241	–	15.37	2
	1572	β, bcc	1165–1572	3.81 (1186°C)	–	–	–	13.87	2
uranium		α, orthorhombic	<668	2.8478 (25°C)	5.8580	4.9455	–	19.16	4
		β, tetragonal	668–775	10.763±5(720°C)	–	5.652±5	–	18.11	30
	1133	γ, bcc	775–1133	3.524±2 (805°C)	–	–	–	18.06	2
neptunium		α, orthorhombic	<280	6.663±3	4.723±1	4.887±2	–	20.45	8
		β, tetragonal	280–576	4.897±2 (313°C)	–	3.388±2	–	19.36	4
	639	γ, bcc	576–639	3.518 (600°C)	–	–	–	18.04	2
plutonium		α, monoclinic	<122	6.183 (21°C)	4.822	10.963	101.79	19.86	16
		β, monoclinic	122–207	9.284 (190°C)	10.463	7.859	92.13	17.70	34
		γ, orthorhombic	207–315	3.159 (235°C)	5.768	10.162	–	17.14	8
		δ, fcc	315–457	4.6371 (320°C)	–	–	–	15.92	4
		δ', bct	457–479	3.34 (465°C)	–	4.44	–	16.00	2
	640	ε, bcc	479–640	3.636 (490°C)	–	–	–	16.51	2
americium		α, dhcp	<658	3.468 (20°C)	–	11.241	–	13.6	4
		β, fcc	793–1004	4.894±5	–	–	–	13.65	4
	1173	γ, ?	~1050–1173						
curium		α, dhcp	< ~1277	3.496	–	11.33	–	13.5	4
	1345	β, fcc	~1277–1345	5.039	–	–	–	12.9	4
berkelium		α, dhcp	<930	3.416±3	–	11.069	–	14.79	4
	1050	β, fcc	930–986	4.997±4	–	–	–	13.24	4
californium		α, dhcp		3.384	–	11.040	–	15.10	4
	900	β, fcc	< 900	5.74	–	–	–	8.74	4
einsteinium		α, dhcp		?	–	?	–	?	4
		β, fcc	<860	5.75	–	–	–	8.84	4

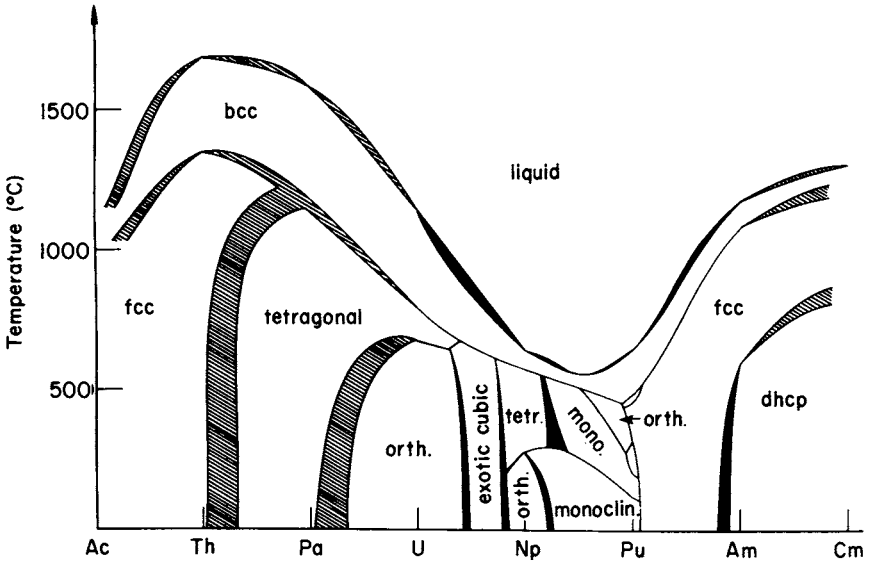

Fig. 19.1 *Schematic binary phase diagram of the actinide metals. (After Smith and Kmetko* [3].)

levels, respectively, which are closer to the nucleus than the outer or valence s and p electrons. In the case of the rare-earth metals (beyond cerium), electrons of the 4f energy levels are very localized, and in real space there is no appreciable overlap in wavefunction between atomic sites. Thus, these levels are not broadened by 4f–4f interactions and, furthermore, they do not tend to mix, or hybridize, with energy levels of differing orbital quantum numbers. For the transition metals, however, the d-electron wavefunctions have significant overlap among atomic sites, and d-electron wavefunctions hybridize with s and p wavefunctions. This overlap causes the energy levels to broaden into energy bands. In discussions related to electronic properties, including magnetism, the band nature of the d electrons is more difficult to treat exactly than are localized 4f electrons.

The electronic structure of the actinide metals falls between those of the various d and the 4f series [14]. At the beginning of the actinide series the 5f wavefunctions overlap strongly and the non-local, band character of the 5f electrons retards the occurrence of magnetism. This is shown in Fig. 19.2, where the average 5f-electron radial extent is seen to be larger than that of the 3d transition metal, iron, for α-phase actinides up to, and including, Pu [14]. The 5f bands in the first half of the series have energies close to E_F. Consequently, there is a high density of electronic states at the Fermi level (designated as $N(E_F)$). Th, Pa, and U exhibit superconductivity because of their high $N(E_F)$ values, which are not high enough for the spin fluctuations to destroy the superconductivity as for Np and Pu. A high value of $N(E_F)$ has strong effects on the magnitude and thermal dependence of many properties, such as electrical resistivity,

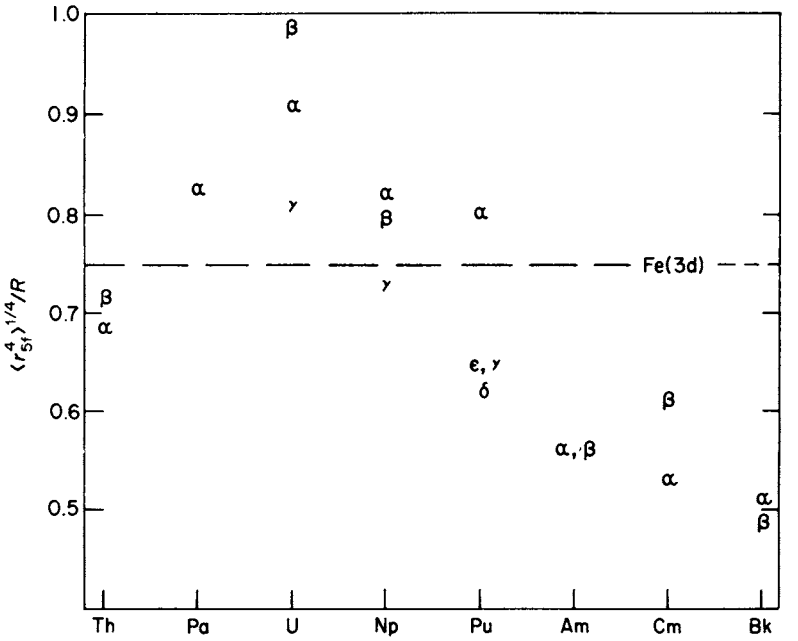

Fig. 19.2 *Ratio of average 5f radial extension to interatomic spacing for various crystallographic phases of actinide metals. The value for Fe is shown by the broken line. (After Freeman and Koelling* [14].)

thermoelectric power, specific heat, and magnetization. Table 19.2 lists a number of properties of pure actinides related to $N(E_F)$. It is seen that the resistivity and electronic specific-heat coefficient are largest for Np and Pu.

As the actinide series is traversed, two effects occur simultaneously. The radial extent of the 5f-electron wavefunctions decreases (see Fig. 19.2) and the greater stability of the 5f electrons places their energies well below E_F. These effects lead to a lessening of the band nature of the 5f electrons and a decrease in $N(E_F)$ for the heavy actinides (Am and beyond). For Am, the localized 5f electrons do not lead to magnetism due to the f^6 configuration, and the relatively high $N(E_F)$ allows superconductivity to occur [15]. A maximum value for $N(E_F)$ occurs near Np and Pu, leading to greatest complexity in the properties of these metals, their alloys, and compounds. A very large $N(E_F)$ or, more particularly, the existence of values of $U_0/W \simeq 1$ (see Table 19.2) is a very difficult problem to treat theoretically within a band model because of strong correlation effects, but is equally difficult to treat within a localized model because of the band nature of the 5f electrons near E_F. Of course, the density of states is not sufficient to describe the 5f bands fully; their dispersion, i.e. dependence on momentum, must also be considered.

Table 19.2 *Properties related to $N(E_F)$ for α-phase actinide metals.*

Metal	$\rho_{300}-\rho_4$[a] ($\mu\Omega$ cm)	χ_{300}[b] (10^4 emu mol^{-1})	γ[c] (mJ K^{-2} mol^{-1})	n[d]	U_0/W[e]	*Magnetic/ superconductor*[f]
Th	14	0.8	4.3	3	0.3	S
Pa	18	2.7	–	2.8	(0.4)	S
U	31	3.9	9.1	1–4[g]	0.6	S
Np	123	5.5	12.4	2	0.7	–
Pu	138	5.1	17.0	2	1.8	–
Am	67	7.8	6.0	5	50	S
Cm	86	119.0	–	2	>50	M
Bk	–	–	–	–	>50	M
Cf	–	–	–	–	>50	M

[a] Electrical resistivity: difference in values at 300 and 4 K $\propto N(E_F)$.
[b] Magnetic susceptibility at room temperature.
[c] Coefficient of the electronic term in the specific heat, $\gamma \propto N(E_F)$.
[d] Low-temperature value in: $\rho-\rho_0 = aT^n$.
[e] Ratio of polar state formation energy to bandwidth (for $U_0/W \lesssim 1$, bands are formed).
[f] M = orders magnetically; S = superconductor.
[g] A function of crystallographic direction.

19.3.2 5f-Electron bands and magnetism

In an effort to correlate the magnetic properties and the electronic structure of the actinides, Hill [16] showed that there were no magnetic cerium or uranium compounds in which interactinide distances (r_i) are smaller than the critical values of 0.34 and 0.35 nm, respectively. He attributed this phenomenon to f-band formation occurring as the result of 4f–4f or 5f–5f wavefunction overlap. The rule applies to most compounds of U, Np, and Pu. A plot of magnetic ordering temperature vs r_i for Np compounds is shown in Fig. 19.3. Actinide compounds in which r_i is only slightly larger than the critical value exhibit band ferromagnetism similar to that of Ni. For many compounds of the early actinides with large values of r_i, the 5f electrons do not form bands and they have local-moment magnetism. However, hybridization may interfere with magnetism in an intermetallic compound with a large value of r_i. Many cases are known where the hybridization of 5f electrons with p and d electrons leads to magnetic properties similar to those of transition metals having no local moment (see, for example, Freeman and Darby [17] and Brodsky [18]).

A further consequence of 5f–5f overlap and hybridization in metallic actinides is a reduction of the importance of valence as a useful concept. In most of the light actinide metallic materials there is no clear separation between 5f electrons and bonding electrons. Unlike 4f electrons, the 5f electrons may enter into the bonding. There are, however, cases where the concept of actinide valence is useful, particularly when the magnetism has a local-moment character. Many properties of each system must be examined and reconciled before simplifying concepts such as localized magnetism and valence can be used correctly. Chan and Lam [19]

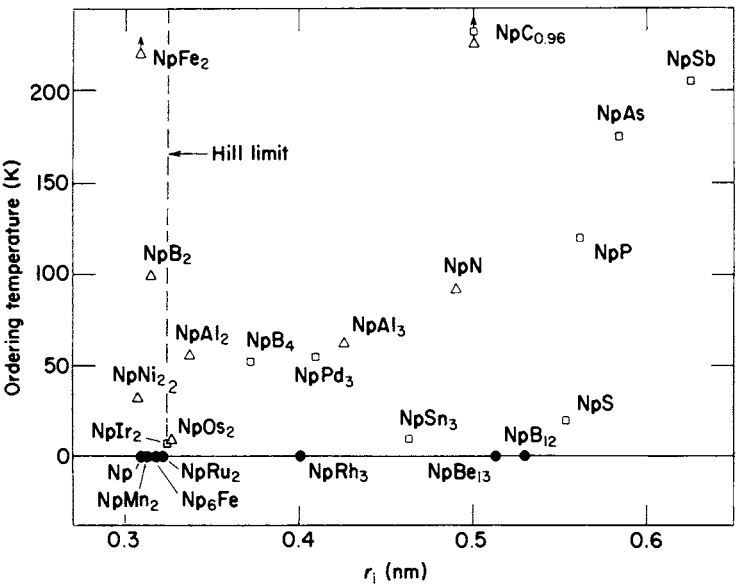

Fig. 19.3 *Magnetic ordering temperatures of Np intermetallics plotted against interactinide spacing:* □, T_N; △, T_C; ●, *no ordering. (After Brodsky* [18].)

have shown that when the full j-manifold is considered, the resultant J is a good quantum number.

The electronic structures of a number of actinide systems have been determined in detail by microscopic experiments and detailed calculations. For example, Fig. 19.4 shows experimental results of an x-ray photoelectron study [20] of several U systems, where the narrow 5f band at, or near, E_F is clearly seen. Recent studies with various energies of incident photons have made it possible to separate the contributions to valence-region spectra into the component orbital-angular-momentum contributions [21]. Recent discussions of the theoretical and experimental details of actinide electronic structure are available [22–26].

19.4 THERMODYNAMIC PROPERTIES

Experimental difficulties and the complexity of actinide bonding have combined to retard the acquisition of reliable thermodynamic values for the metals and the development of an understanding of their thermodynamic properties. However, considerable progress has been made recently, particularly in estimating, measuring, and interpreting heats of sublimation and crystal entropies. Currently accepted values are given in Table 19.3. The heat of sublimation, which is a direct measure of cohesive energy when the electronic structure of the vapor species is identical to that of the solid phase [27, 28], declines steadily from U through Am as progressive f-band narrowing occurs and f electrons withdraw from metallic

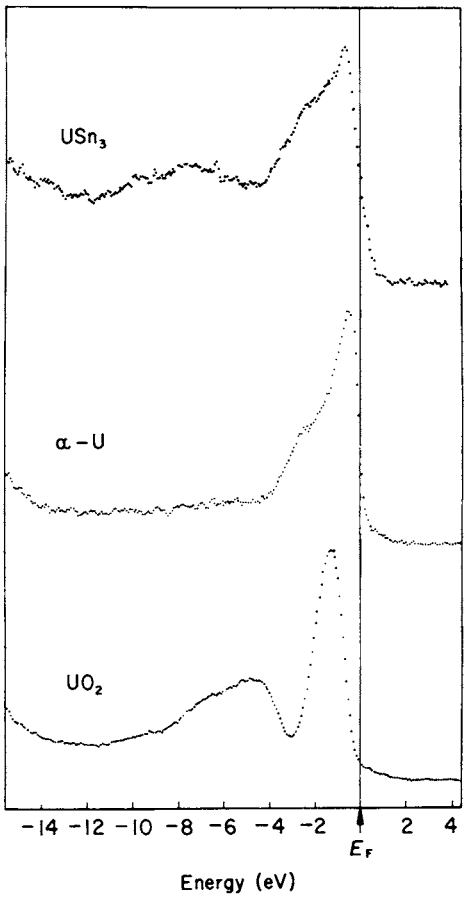

Fig. 19.4 *X-ray photoelectron spectra of USn_3, α-U, and UO_2. (After Lander et al. [20].)*

Table 19.3 *Heats of sublimation and crystal entropies of actinide metals (see Chapter 17 for complete listings of thermodynamic data).*

Element	ΔH°_{298} (kJ mol^{-1})	ΔS°_{298} (J K^{-1} mol^{-1})
Ac	(418)	(62)
Th	598	53.39
Pa	570	55.3[a]
U	536	50.2
Np	465	50.5
Pu	342	56.5
Am	284	55.2
Cm	387	(72)
Bk	310	(78)
Cf	196	(81)

[a] Tentative value. ( ) Estimate.

bonding. Crystal entropies remain relatively constant in this part of the period. Beyond Am the sublimation enthalpy rises again, having gained an additional contribution through the $G = H - TS$ relation because the vapor phase has an electronic configuration different from that of the solid. This shows up clearly as an abrupt increase in the crystal entropy associated with a magnetic contribution that is not present earlier in the period. More detailed treatments of thermodynamic relationships can be found in several reviews [10, 11, 27–30]. Overall systematics of actinide-metal thermodynamics are developed in Chapter 17.

19.5 ALLOYING RELATIONSHIPS

19.5.1 Solid solutions

In the first half of the series, where the bcc structure exists, there is high mutual solid solubility between the actinide elements at high temperatures. The bcc forms of Th, U, Np, and Pu are completely or extensively soluble in each other. Extensive solubility exists as well between Th, U, (probably Np), and Pu and the group IV elements Zr and Hf. Chiotti *et al.* [11] have assessed phase relationships of actinide binary alloys.

Similarly, there is high mutual solid solubility between U, Np, and Pu when they occur in their complex crystalline forms at low temperatures. Solid miscibility gaps of only a few atomic percent separate α-Np and β-Np from α-Pu and β-Pu, although the terminal solid solutions have different crystal structures. The same may be said of the extent of solid solubility between the low-temperature forms in the systems U–Np and U–Pu, provided that the broadly stable intermediate phases that occur are considered to be transitional extensions of the terminal solid solution phases. Fig. 19.5 shows schematically that regions of single-phase solid solution exist over virtually the entire compositional region at low temperatures in the neighboring binary systems U–Np and Np–Pu [31].*

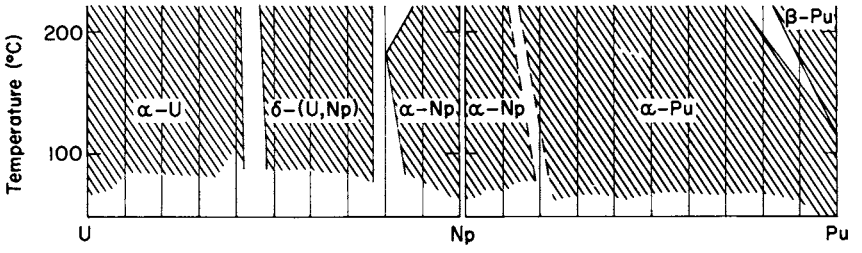

Fig. 19.5 *Regions of single-phase solid solution in the neighboring binary systems U–Np and Np–Pu. (After Elliott* [31].)

* The U–Np δ phase is isostructural with the U–Pu ζ phase, which is reported to have a complex crystal structure with cubic symmetry at room temperature and 58 atoms per unit cell [32, 33]. An isostructural intermediate phase also occurs in the Np–Pu system.

No other elements, irrespective of atomic size or valence, show any appreciable solubility in these low-symmetry complex phases. Unique bonding conditions apparently exist, involving participation by f-like electronic charge, which are satisfied only by actinides.

Little is known about solid solubility relationships for the actinide fcc and dhcp phases, which begin at mid-series, apart from the observation that Am is extensively soluble in fcc Pu, as are the non-actinide elements Al, Ce, Ga, Sc, and Zr.

19.5.2 Intermetallic compounds

A large number of intermetallic compounds are known to occur that include actinide elements with 3d, 4d, and 5d elements and with elements of the aluminum and silicon groups. All have metallic properties.

At AnX_3 stoichiometry there are four families of binary intermetallic compounds, which represent different stacking schemes of the close-packed layer shown in Fig. 19.6(a) [34]. All stacking variants yield crystal structures in which a CN 12 polyhedron consists entirely of X atoms surrounding the An atom. The structures that occur are the $AuCu_3$, $TiNi_3$, $MgCd_3$, and $PuAl_3$ types. The $AuCu_3$-type structure, ordered fcc, is the most prevalent, occurring particularly when the actinides combine with Rh and Pd; the other three structure types are ordered variants of the hcp structure.

The stacking of close-packed layers in various close-packed sequences is expected to be the favored arrangement when the An atom and its X partner have similar atomic radii, since optimum space filling is achieved under this condition. But, in fact, CN 12 radii derived from the structures of the pure An and X metals differ by 30%, leading one to believe that the effective atomic radii displayed by the An atom and its partner in an AnX_3 intermetallic compound may differ appreciably from the pure-metal radii.

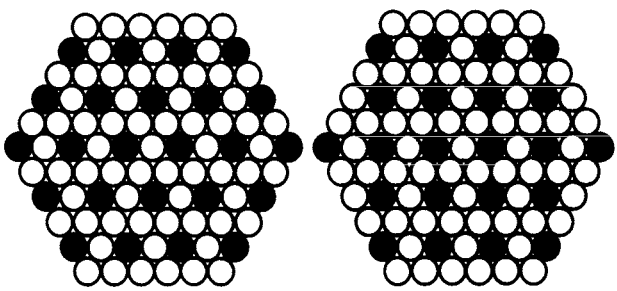

Fig. 19.6 *Close-packed ordered layers in AB_3 phases. (a) Layer occurs in phases of the $AuCu_3$, $TiNi_3$, $MgCd_3$, and $PuAl_3$ types. (b) Layer occurs in $TlCu_3$ and $TiAl_3$ types. (After Saito and Beck* [34].)

At the stoichiometries AnX_2 and AnX_5, intermetallic compounds having related crystal structures occur widely. At AnX_2 are found the familiar Laves phases, having the $MgCu_2$-, $MgZn_2$-, and $MgNi_2$-type structures. The first of these is cubic, the others hexagonal. Closely related $AuBe_5$- and $CaCu_5$-type structures, cubic and hexagonal, respectively, are found at AnX_5.

Many actinide systems contain $MgCu_2$-type or $MgZn_2$-type Laves phases, especially when the partner is an Fe- or Ni-group transition metal. This tendency is also observed in systems with the lanthanide elements. The rationale for the widespread occurrence of actinide Laves phases is based on the stabilizing influence of efficient space filling. The ideal radius ratio for optimum space filling by rigid spheres is 1.225 in the Laves phase structure, wherein there occurs a CN 16 polyhedron with the An atom at its center. The enveloping polyhedron is composed of twelve X atoms and four An atoms.

By replacing the four An atoms in the CN 16 polyhedron of the $MgCu_2$-type structure with an equal number of X atoms, the $AuBe_5$-type structure is generated. This structure preserves the favorable space-filling configuration while accommodating a higher concentration of X. A similar X-for-An substitution, together with a translation of certain atomic sites, transforms the $MgZn_2$-type structure to the $CaCu_5$-type structure.

A large number of metallic compounds with the NaCl-type structure are found at the AnX stoichiometry. These form when X is a chalcogenide, a pnictide or carbon. An_3X_4 compounds having the cubic Th_3P_4-type structure frequently coexist with the NaCl-type compounds in systems of the actinides with the chalcogenides and pnictides.

A comprehensive review of the structures of actinide intermetallic compounds [13] should be consulted for more information.

19.6 METALLURGY

19.6.1 Materials preparation

It is now possible to carry out bulk-property measurements, at varying levels of precision and sophistication, on the elements through Cf; some preliminary measurements are being made on Es. Therefore, emphasis will be placed here on methods and techniques applicable to samples in the milligram to gram range. No attention will be given to the production of actinide metals on an industrial scale.

While the quantity of material available is always a significant factor in sample preparation, other characteristics also have important influences. Alpha activity occurring throughout the series imposes glove-box confinement as a routine requirement beyond U. In addition, shielding is frequently required because of gamma activity and, beginning at mid-series, because of neutrons generated by spontaneous fission. The high chemical reactivity of the actinides has a generally adverse effect on sample purity and this problem is exacerbated by small sample

size and by radioactive self-heating. Contamination by grown-in daughter products causes a further deterioration of sample purity.

For Th, U, and Pu the starting materials for research samples are often metals prepared external to the laboratory by larger-scale processing. On the other hand, for the transplutonium elements, and Pa and Np, laboratory-scale preparation predominates, and the major preparation routes involve pyrometallurgy combined with vapor transport.

The two most widely used processing options for the transplutonium elements are these:

(1) The actinide oxide is reduced with La or Th and the resulting actinide metal is distilled from the reactant–reductant mixture and collected. The vapor pressure of the reductant metal must be several orders of magnitude less than the vapor pressure of the actinide metal.
(2) Previously prepared actinide fluoride is reacted with Li metal and the resulting lithium fluoride and unreacted Li are separated from the reactant–reductant mixture by vaporization. The actinide fluoride must be free of non-volatile impurities, particularly oxides.

The oxide reduction method is feasible for Ac, Am, Cm, Bk, Cf, and Es, and is generally the favored process for producing thin-film or globular multi-milligram and multigram samples. On the other hand, when only multi-microgram quantities are to be recovered and favorable vapor pressures obtain (Bk and Cf), the Li reduction–vaporization method produces a more attractive bulk sample form.

With Ta as the reductant, the actinide starting material may instead be the carbide, previously prepared by the carbo-reduction of the oxide. This process is an attractive alternative for producing Pu and Cm because in the preparation of the carbide from the oxide a large number of impurities are eliminated by vaporization. Table 19.4 presents a brief summary of commonly used preparation methods.

Purification methods vary in complexity with the chemical and physical characteristics of the actinide metal and with the quantity of material being processed. The principal refining processes, and their applicability, can be summarized as follows:

(1) Levitation melting in ultra-high vacuum (10^{-9} torr) eliminates volatile impurities by evaporation. In this way residual iodides are removed from Van Arkel-produced metals and excess halides are removed from metals produced by halide reduction.
(2) The impure metals are selectively evaporated in a 10^{-6} torr or better vacuum and the vapor captured as a solid-state condensate; impurity-rich residuals are left behind. The process may be repeated several times, ultimately yielding a condensate with impurity levels reduced by a factor of 100.

Table 19.4 *Laboratory methods for preparing actinide metals.*

Metal	*Favored method*	*Typical batch*	*Alternative method*
Ac	Th reduction of oxide	–	–
Th	Van Arkel processing of carbide	multigram	Van Arkel processing of metal
Pa	Van Arkel processing of carbide	1–2 g	Ba reduction of fluoride
U	Ca or Mg reduction of fluoride	multigram	–
Np	Ca or Mg reduction of fluoride	1–5 g	–
Pu	Ca or Mg reduction of fluoride	multigram	Th reduction of oxide
Am	La reduction of oxide	multi-milligram to gram	Th reduction of oxide
Cm	Th reduction of oxide	gram	Li reduction of fluoride (for multi-milligram batch)
Bk	Li reduction of fluoride	milligram	–
Cf	La reduction of oxide	milligram	–
Es	La reduction of oxide	multi-microgram	–

(3) Th, U, and Pu in the form of anodes are electrolytically dissolved in a LiCl–KCl eutectic bath and redeposited as cathode metals whose total metallic and non-metallic impurity levels have been reduced from about 10 000 atomic ppm to below 2000.

(4) Repetitive passage of a molten zone along a bar of the impure actinide metal (zone melting), particularly when followed by the induced migration of impurities in the solid by an impressed electric field (electrotransport), can be used to reduce the impurity level in Pu from 200 ppm to 20 ppm.

The preparation of actinide single crystals, generally difficult because of the nature of the materials, is made more complicated by the multiple phase transformations that occur in the solid state. Many techniques are employed, of which the following are examples. Single crystals of α-U are prepared by a special grain-coarsening method that requires the generation and control of a dispersion of grain-growth-inhibiting inclusions. The preparation of α-Pu single crystals takes advantage of the effect of pressure in reducing the number of polymorphic forms; single crystals result from a liquid $\rightarrow \beta \rightarrow \alpha$ transformation sequence in a strain-free, high-pressure environment. Single crystals of Am and Cm have been produced by direct condensation from the metallic vapor phase and, similarly, Th and Pa crystals can be grown from the gaseous iodide phase. Finally, clusters of actinide single crystals can also be prepared by electrolytic dissolution and redeposition in a molten LiCl–KCl eutectic bath. Preparation, purification, and characterization techniques are described in more detail in several papers [27, 35–39, 74].

19.6.2 Transformations

In the metallic actinides, particularly in U, Np, and Pu, the subject of transformations from one polymorphic form to another is a complicated one, because of the unique crystallographic relationships and because of the large number of polymorphic forms that exist in a relatively narrow range of temperature. The transformations and their products have characteristics that depend on temperature, on the rate of change of temperature, on composition, and on initial structure.

Although the situation is generally complex, the transformation mechanisms and the conditions under which they occur are generally the same as those observed in metals elsewhere in the periodic table. At high temperatures – where the mobility of individual atoms is high – transformations occur by a thermally activated process involving diffusion, nucleation, and growth. At low temperatures–where individual atom movements are restricted–transformations are most commonly martensitic in character, i.e. they occur by the cooperative, shear-dependent movement of many atoms, assisted by the movement of dislocations. Martensitic transformations exhibit a specific orientation relationship between the original and transformed crystal lattices, a relationship that is lacking in transformations, which occur by diffusion, nucleation, and growth. The presence of alloying elements, even in minor concentrations, can have a significant influence, as can other variables such as grain size and applied stress.

The largest amount of information on this subject exists for U and Pu. The following discussion will place emphasis on these two metals in their pure and dilutely alloyed states.

(a) Uranium

In the transformation $\gamma \rightleftarrows \beta$ in pure U, nucleation and growth are generally observed. The temperature of the $\gamma \rightarrow \beta$ transformation can be depressed by rapid cooling, but the formation of the β product cannot be suppressed, even by drastic quenching. Alloyed γ-U behaves quite differently on being quenched, forming normal or distorted α directly or, when alloy concentration is sufficiently high, retaining the γ structure in normal or distorted form. All of the decomposition products of alloyed γ-U are thought to be formed by shear. The α-U $\rightleftarrows$ β-U transformation occurring during slow cooling at or near the equilibrium temperature is controlled by diffusion, nucleation, and growth. When pure β-U is rapidly cooled, α-U forms by a diffusionless shear transformation at a temperature about 50°C below the equilibrium temperature, but the $\beta \rightarrow \alpha$ transformation cannot be circumvented even when cooling rates well in excess of 1000°C per second are employed. In contrast, alloyed β-U can be retained metastably at temperatures several hundred degrees below the equilibrium temperature by rapid cooling. In the upper-temperature portion of this zone of metastable β-U, the retained reactant transforms isothermally and eutectoidally to α-U and a

second phase by diffusion, nucleation, and growth. As the retained β-U is held at progressively lower temperatures, non-equilibrium products form by nucleation and growth and, finally, at still lower temperature (300°C) the retained β-U transforms to a martensitic product supersaturated with respect to the alloying element. α-U undergoes a transformation at 42 K to an α' structure, a modulation of the α structure in which there are small sinusoidal displacements of atoms in all three crystallographic directions. These lattice distortions are believed to be induced by a charge-density wave.

(b) Plutonium

The α, β, and γ phases of Pu, about which most of the information on transformations is available, all exist under equilibrium conditions at 315°C and below. Transformations occurring in such a low-temperature regime between phases having such complex crystallographic relationships are understandably sluggish, hysteretic, and sensitive to prior treatment and alloying. Several features will be discussed to exemplify some of these characteristics. By rapid quenching, the $\beta \rightleftarrows \alpha$ transformation can be suppressed so that β can be retained at temperatures as low as -100°C. By holding retained metastable β isothermally at various low temperatures, time–temperature–transformation relationships (TTT curves) can be established which, together with structural studies, indicate that a transformation controlled by nucleation and growth gives way to a shear transformation when the pure β-Pu phase is held at a temperature more than 50°C below the equilibrium $\beta \rightleftarrows \alpha$ temperature. However, the kinetics of the transformation are so sensitive to the initial structure, to prior thermal history, and to applied stress that valid generalizations are difficult to make. When Pu is alloyed with Al, Ga, In, Ce or Am there are drastic effects on transformations. For example, 2 at % Al dissolved in the δ phase of Pu permits retention of this phase to room temperature. The retained δ phase can be converted in a diffusionless transformation to the α' phase by cooling below room temperature, or by deformation or by applying pressure.

(c) Other actinides

The transformation in Th is strictly diffusional in character, while Np transformations, to the extent that they have been observed, resemble those of U and Pu. No conclusive information is yet available on transformation mechanisms in Am and in the elements beyond. More detailed treatments of the subject may be found in refs 40–46.

19.6.3 Mechanical properties

Strength, ductility, and hardness are structure-sensitive bulk properties, the measurement of which requires relatively massive samples. Moreover, these

properties are highly dependent upon purity and prior metallurgical history. Only Th, U, and Pu have been available in sufficient purity and in quantities and forms that permit extensive studies. This brief treatment can only address typical values and give several generalizations.

Thorium, in the form of the pure, polycrystalline fcc metal, has mechanical properties at room temperature that are not unlike those of other ductile, fcc metals with comparable melting temperatures, such as Ni (see Table 19.5). Plastic deformation at room temperature occurs by slip on (111) planes in the [110] direction, as in other fcc metals.

The mechanical properties of U metal are strongly dependent on purity and structure. Because of the low crystallographic symmetry of α-U, a high degree of anisotropy may be observed in the mechanical properties, even for polycrystalline material. When α-U is deformed at room temperature, the predominant deformation mechanism is twinning, with the (130) twin system being the most active. As the temperature increases, deformation by slip becomes more important. The most active slip system is (010)–[100]. Slip on (010) does not interrupt the strong covalent bonds that occur in certain crystallographic directions in α-U. The other two polymorphic forms, β-U and γ-U, also show extensive ductility when deformed at a high temperature.

The mechanical properties of Pu metal are highly variable because of the dominant influences of structure and deformation mechanism, which can be significantly altered by thermal and mechanical treatments. The α, β, and γ forms of Pu, having crystal structures with low symmetry, are hard and strong, and lack ductility. When the mechanism for plastic deformation is restricted to slip, ductility is poor because the extent of slip is very limited in these polymorphic

Table 19.5 *Typical plastic properties of pure actinide metals (measured at room temperature on high- or commercial-purity polycrystalline material after prior plastic deformation and annealing).*

Metal	*Tensile strength* (10^7 dyn cm^{-2})	*Yield strength* (10^7 dyn cm^{-2})	*Elongation* (% in 50 mm)	*Diamond pyramid hardness*
Th[a]	120	48	36	150
U[b]	585	240	10	220
Np[c]	–	–	–	346
Pu[d]	525	300	8	250
for comparison				
Ni[e]	315	60	30	70

[a] Iodide (high-purity) grade; forged, hot and cold rolled, annealed at 850°C.
[b] Mg-reduced (commercial-purity) grade; hot rolled as an α phase, annealed β phase region, water-quenched.
[c] Electrolytic (high-purity) grade.
[d] Electrolytic (high-purity) grade; prior treatment consisted of extrusion at 108°C without subsequent annealing.
[e] Electrolytic grade; cold rolled, annealed at 550°C.

forms. In monoclinic α-Pu, slip appears to occur in small amounts on a number of planes, including (112). It may be noted in Table 19.5 that Pu has higher yield strength and lower ductility at room temperature than Th or U.

However, when polycrystalline α-Pu is thermally and mechanically treated in a way that develops a fine grain (crystallite) size, a drastic increase in ductility and an equally significant loss in strength occur because deformation also occurs by grain-boundary sliding, frequently accompanied by recrystallization. Thus, fine-grained α-Pu exhibits exceptionally high ductility at a temperature around 100°C; an elongation in excess of 200% is observed. The mechanical properties of β-Pu are even more dramatically affected by the grain structure produced by prior thermal treatment. When formed on heating from α-Pu, the β-Pu phase is fine-grained and extraordinarily ductile ('superplastic') when deformed at about 100°C; elongation reaches 700% before fracture.

The detailed mechanical behavior of neptunium metal has not been determined. α-Np twins profusely during plastic deformation at room temperature, indicating that few slip systems exist, and that a high resolved shear stress is required for yielding by slip.

The elastic properties, like the plastic properties just described, are influenced by the thermal and mechanical history of the samples. The values given in Table 19.6 are typical, but significant variations are observed.

A more extensive treatment of the mechanical properties of the actinide metals may be obtained through a review of refs 47–53.

19.7 MAGNETISM AND RELATED PROPERTIES

The discussion in Section 19.3 on electronic structure correctly infers that nearly all of the types of magnetism found in transition metals and rare earths can be found in the actinides. A number of these are described below. Current work in this area tends to concentrate on mechanisms of magnetic ordering, making use of data from single crystals and continued discussion of localized vs itinerant magnetism. In many cases, the understanding of the magnetic properties of some actinide materials was only possible after many related properties had been measured. These include the magnetic susceptibility, electrical resistivity, specific

Table 19.6 *Typical elastic properties of pure actinide metals.*

Metal	*Shear modulus* (10^{11} dyn cm^{-2})	*Modulus of elasticity* (10^{11} dyn cm^{-2})	*Poisson's ratio*
Th	2.8	7.4	0.27
U	8.4	20	0.25
Np	8	–	–
Pu	4.5	9.9	0.2

heat [18], and Mössbauer effect [54]. The very powerful tool of neutron scattering has been used in those cases where suitable samples were available [26].

19.7.1 Local-moment magnetism

Fig. 19.7 shows the magnetic susceptibility (χ) of Cm and PuSb plotted as $1/\chi$ versus temperature. In both cases, the susceptibility essentially follows the Curie–Weiss law, $\chi = C/(T-\theta)$, which is expected for this simple case of local-moment magnetism. Both of these materials are ferromagnets, although there is also evidence for antiferromagnetism and even ferrimagnetism in some samples of Cm [55]. The curvature in the data of PuSb is explained as the effect of the crystalline field acting on the localized 5f electrons in a Pu^{3+} valence state. The data in Fig. 19.7 yield an effective moment per Cm of 8 μ_B (Russell–Saunders coupling gives 7.7 μ_B for $5f^7$) and 1.0 μ_B per Pu in PuSb.

Neutron diffraction and magnetization measurements on the local-moment ferromagnet PuP show that conduction-electron polarization modifies the ordered moment. Thus, an ordered moment of 0.77 μ_B is found in bulk-magnetization measurements, whereas the effective moment is 1.1 μ_B. In general, attempts to find crystal field levels in metallic actinide systems by neutron inelastic scattering with single crystals have not been successful, although such levels are easily found with rare earths and the effects of crystalline fields on

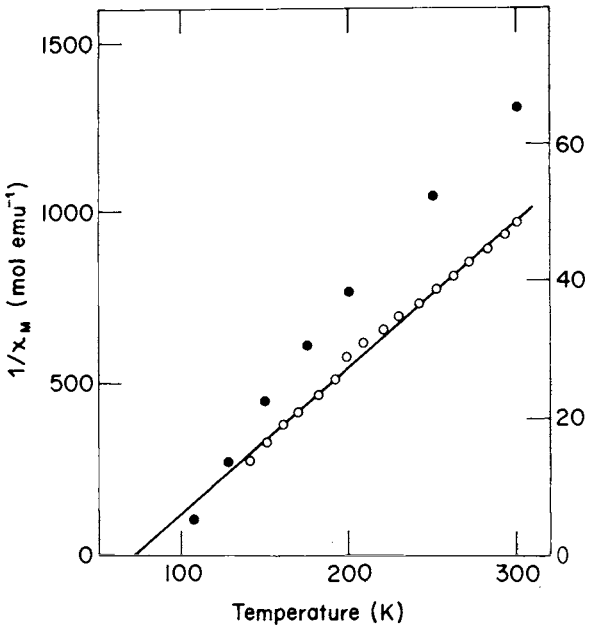

Fig. 19.7 *Reciprocal molar susceptibility of two local-moment systems: ●, PuSb, left-hand scale; ○, Cm, right-hand scale.*

magnetic properties are well-documented [19] as for PuSb in Fig. 19.7. Very recently, well-defined crystal field levels have been observed for UPd_3 in a $5f^2$ configuration [56].

19.7.2 Band magnetism

Metals with high $N(E_F)$ may reach the Stoner condition for band ferromagnetism, $[1 - N(E_F)I]^{-1} \geqslant 1$, due to exchange splitting of spin-up and spin-down bands; I is the effective exchange parameter. This behavior is found for Ni and $ZrZn_2$ as well as for the actinides $NpOs_2$, $NpIr_2$, and $NpMn_2$. In these cases, very small ordered magnetic moments are observed (0.4, 0.6, and 0.33 μ_B for $NpOs_2$, $NpIr_2$, and $NpMn_2$, respectively), while the effective paramagnetic moment may be much larger, e.g. 3.3 μ_B for $NpOs_2$.

A very interesting example of band magnetism is found in $NpSn_3$, which is a band *anti*ferromagnet [57]. Examples of this type of magnetism are rare, otherwise occurring only in Cr and some of its compounds. Fig. 19.8 shows the low-temperature electronic specific heat plotted as C_E/T vs T. The sharp λ-type anomaly is consistent with a second-order magnetic transition. The magnetic susceptibility has a rounded maximum above T_N and the antiferromagnetic

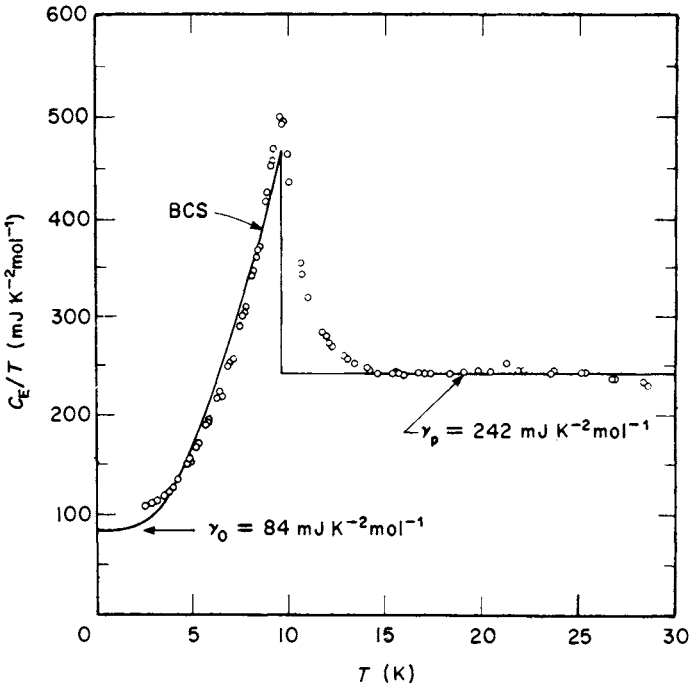

Fig. 19.8 *Electronic specific heat as C_E/T against T for $NpSn_3$. The full curve is the mean field-theoretical prediction. (After Trainor et al. [57].)*

nature of the transition is supported by Mössbauer-effect results, which show a two-site character for the Sn atoms. The gap-like nature of the transition (which is also the driving force for the transition in Cr) is seen by the good fit to the BCS gap equation.

19.7.3 Spin fluctuations

Just above the magnetic ordering temperature of a band ferromagnet, e.g. Ni, the spins may align briefly. These spin fluctuations may exist for sufficiently long times, 10^{-14} s, to be observed by neutron scattering. In nearly magnetic systems, e.g. Pd and Pu, the spin fluctuations may also scatter conduction electrons and provide a strong low-temperature electrical resistivity component, $\rho \propto T^2$, although they do not persist long enough to yield magnetic ordering. The spin fluctuations also have a strong effect on the specific heat of the system, which is discernible if the so-called spin-fluctuation temperature, T_{sf}, lies in the vicinity of 5–30 K. UAl_2 is such a material with $T_{sf} = 25$ K; an initial drop in the specific heat, plotted as C/T, has been shown to fit the theory (Fig. 19.9). In order to show unequivocally that the effects in Fig. 19.9 are due to spin fluctuations and not to magnetic clusters, it was necessary to make the specific-heat measurements in applied magnetic fields up to 43 kOe [58]. The model is also supported by electrical resistivity, magnetic susceptibility, and photoemission measurements on UAl_2. Conceptually, UAl_2 and other spin-fluctuation materials have magnetic

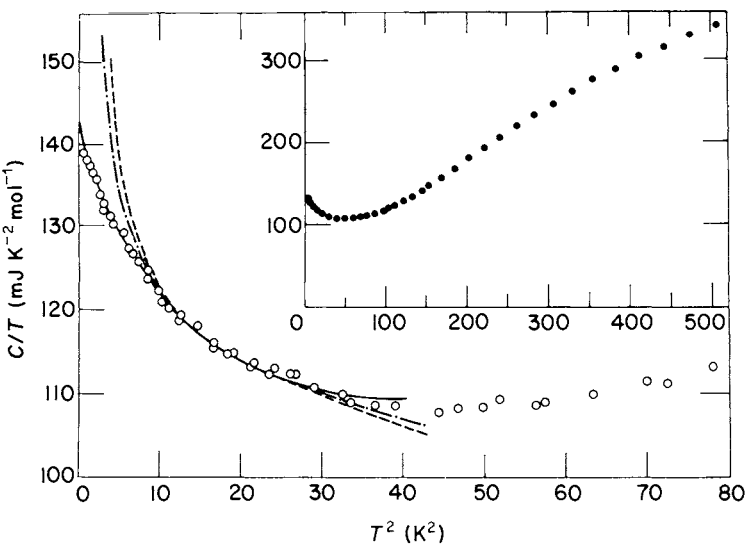

Fig. 19.9 *Specific heat of UAl_2 plotted as C/T vs T^2. Fits of the data above 3 K were made for a possible Schottky anomaly* (– – –), *magnetic clusters* (–·–·–), *and spin fluctuations* (———). (*After Trainor et al.* [58].)

ordering temperatures below 0 K, i.e. they do not truly order magnetically. Many actinide systems have been proposed to be spin-fluctuation materials. It is believed that the very complex resistivity–temperature curves for α-Np, and α-, β-, and δ-Pu are also due to spin fluctuations.

19.7.4 Non-magnetic behavior

If the hybridized 5f bands are very broad in energy and $N(E_F)$ is relatively small, i.e. is of the same magnitude as that of non-magnetic transition metals, an actinide compound may be expected to be non-magnetic. Thus, the 5f electrons are not localized, local-moment behavior is not expected, and the small $N(E_F)$ prevents the Stoner criterion for band magnetism from being fulfilled. Examples of this behavior include URh_3, $NpRh_3$, and UIr_3. In the case of UIr_3, the low-temperature electrical resistivity is found to be proportional to T^3, as is found for non-magnetic transition metals. The lack of a temperature-dependent susceptibility does not preclude magnetism (in the broadest sense) in an actinide system, as this also is to be expected in a system with a high T_{sf}. Such a case is UIr_2, where a T_{sf} of 200 K is proposed.

Fuller discussions of the rich variety of magnetic properties of the actinides may be found elsewhere [17, 18, 59, 60].

19.7.5 Heavy fermion superconductivity

As was seen in Table 19.2, those actinide elements with a specific heat coefficient, γ, below 10 mJ K^{-2} mol^{-1} become superconductors in at least one of their allotropes. This is not surprising, since similar γ values are measured for non-magnetic d-transition-element superconductors ($\gamma = 7.80$ mJ K^{-2} mol^{-1}) for the highest superconducting-temperature metal Nb, with $T_c = 9.25$ K). The discussion in Sections 19.7.2 and 19.7.3 give satisfactory explanations for the lack of superconductivity when γ is large because of the presence of band magnetism or spin fluctuations, both of which tend to destroy superconductivity.

Recently, however, new actinide-compound superconductors have been found, which have extremely large γ-values. These are UBe_{13} [61], UPt_3 [62] and URu_2Si_2 [63]. Similar behavior is observed for the rare-earth compound $CeCu_2Si_2$ [64]. The data in Table 19.7 show that these low-T_c materials ($T_c \approx 0.5$–0.95 K) have extraordinarily high γ-values (up to 1100 mJ K^{-2} mol^{-1}). This astonishing result has led to wide-spread experimental and theoretical studies, world-wide. See, for example, refs. 61–72.

The above discussions concentrated on the $N(E_F)$ values derived from specific heat data. However, there is an alternative way of thinking about the properties. The key equation is $m^* = 3\hbar^2\gamma[\Omega/(3\pi^2 Z)]^{1/3}/k_B^2$, where m^* is the effective electron mass, Ω the volume per unit cell, and Z the number of electrons per unit cell [72]. This equation is valid in the nearly-free-electron-mass approximation, i.e., when $m^* \approx m_0$ and $N(E_F)$ is approximately the value derived if all of the

valence electrons contribute to $N(E_F)$. Typically, the expression for γ can be applied to metals such as Cu, Ag and Au, with m^*/m_0 values of 1.44, 1.02 and 1.16, respectively, when $N(E_F)$ is assumed to be due to one electron per atom. (Note: The effective masses of energy bands can be determined experimentally by deHaas-van Alphen measurements. Although these measurements become very difficult for systems with large γ-values, and are limited by sample quality [66], ratios of m^*/m_0 up to 8.0 have been observed for U_3As_4.) Thus, the electronic specific heat may be discussed in terms of m^*, which is $\sim 100\, m_0$ for $CeCu_2Si_2$; the electrons in such systems are said to be 'heavy fermions', since the m^* values are so large.

Figure 19.10 shows the low temperature specific heat data for UPt_3, which has the $MgCd_3$-type, hexagonal structure discussed in Section 19.5.2. The superconducting transition temperature, 0.54 K, corresponds to the initial rise of the C/T curve shown in the figure [62]. The broadened peak is due to the effects of impurities and lattice imperfections on the properties of all of the heavy fermion materials. These data may be compared to those of Figure 19.8, for the itinerant antiferromagnetic transition in $NpSn_3$. These are both for second-order transitions and should both have λ-type, sharp peaks. The $NpSn_3$ data are also broadened but not as severely as those for UPt_3. The extrapolation of the data for UPt_3 to zero temperature leads to a γ-value of 420. However, above T_c, the data fit

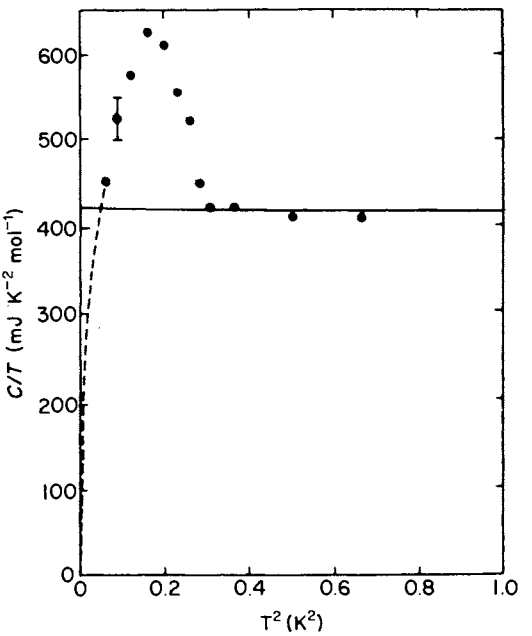

Fig. 19.10 *Specific heat data for a flux-grown single crystal of* UPt_3 [*after Stewart et al.* (62)].

well to equations which include the spin-fluctuation term, as for UAl_2 (see Figure 19.9). This approach modifies γ to a value of 452 mJ K^{-2} mol^{-1} and the effective masses of the superconducting electrons are of the order of 100–200 m_o.

Thus, at least for UPt_3, there is a coexistence of superconductivity and spin fluctuations. This is contrary to the singlet-state, electron-electron coupling of the BCS model for superconductivity, but not for a triplet ground-state [65, 67]. This type of fermion pairing is seen in superfluid ^3He, but nowhere else in condensed-matter systems. The existence of spin fluctuations in the other heavy fermion superconductors is not confirmed. The strongest evidence for triplet-pairing occurs in UBe_{13} and UPt_3 [68].

Although a full discussion of the theoretical models used to explain heavy fermion superconductivity is beyond the scope of this work, some mention of their range seems worthwhile. The problem is as stated in Section 19.3.1; viz., the difficulty of handling systems with $U_0/W \approx 1$. The models applied to the heavy fermion superconductors generally are extrapolations from local magnetic impurity arguments (e.g., a lattice of non-magnetic – Kondo-like impurities – the so-called Kondo/Anderson lattice [69]) and one-electron band models (e.g., based on f electron hybridization [70, 71]). Thus, these models continue the controversy that has existed for some time about the nature of f electrons – localized vs. itinerant – in conducting actinide materials [18]. Figure 19.11 shows the electronic and magnetic properties of UX_3 compounds, where X is indicated

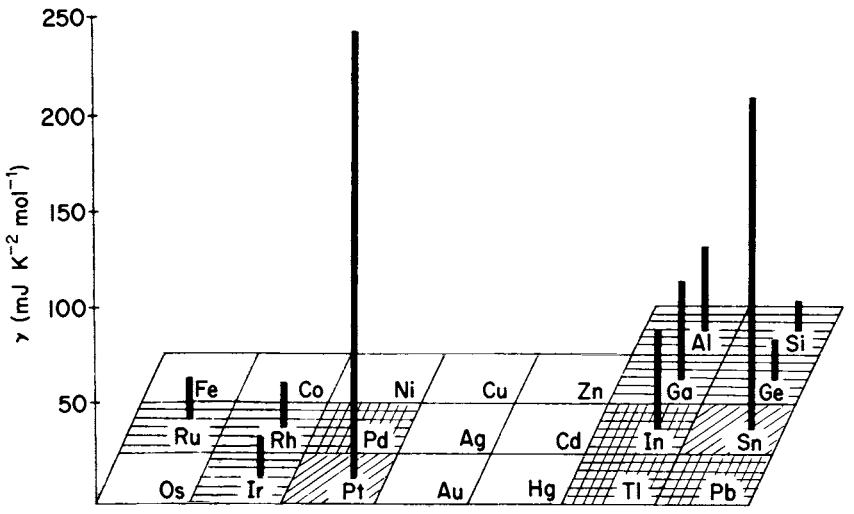

Fig. 19.11 *Overview of the electronic and magnetic properties of UX_3 compounds, where X is indicated on the figure. Vertical bars show the value of the electronic specific-heat coefficient γ. Magnetic behavior is shown as follows: horizontal hatching–Pauli paramagnetism; diagonal hatching–spin fluctuations; cross-hatching–local moments [after Koelling et al. (70)].*

in the caption [70]. This figure, which emphasizes the cross-over from localized to itinerant f-electron behavior in a compound series, is being used to help predict which pseudo-binary compounds may have heavy-fermion behavior. Other phenomenological approaches to understanding and predicting heavy fermion behavior include emphasis on relationships between γ and the exchange enhancement [72].

A requirement of all theories for heavy fermion compounds is the existence of a large $N(E_F)$ due to the f electrons. Figure 19.12 shows the low-temperature ultraviolet photoemission spectra from UBe_{13} and UPt_3 [73]. The high $N(E_F)$, narrow f-peak is definitely observed with bandwidths of about 0.15 eV. Further analysis of the data yields a true bandwidth of 0.075 eV, which is extremely narrow, but much broader than the ~ 0.001 eV needed to explain the enormous γ-values. In order to find the expected narrower bands, and/or to observe a theoretically predicted Kondo temperature of 10–20 K, data of this type must be

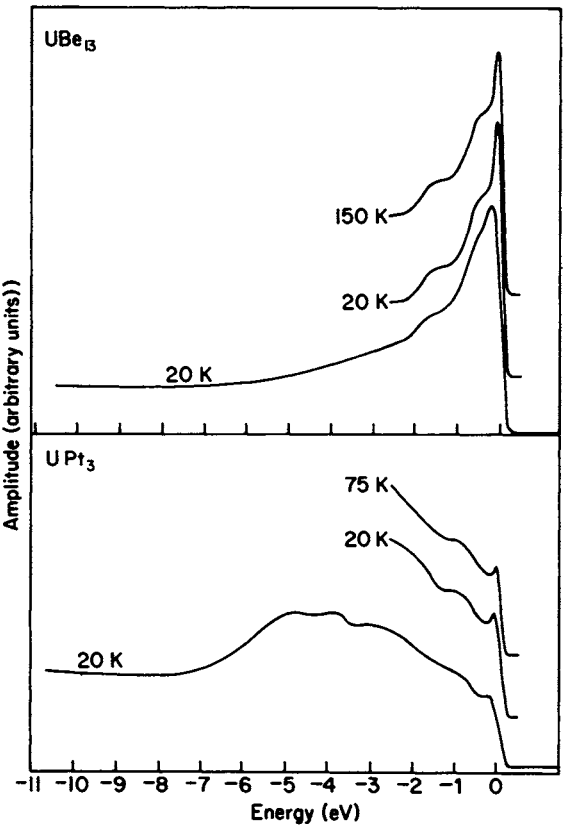

Fig. 19.12 *Energy distribution curves for UBe_{13} and UPt_3 at 40-eV photon energy. The long scans are at 20 K and 0.3-eV resolution. The short scans are at 0.13-eV resolution at the temperatures indicated [after Arko et al. (73)].*

Table 19.7 *Properties of heavy fermion actinide (and rare-earth) compounds*

Compound	γ (mJ K^{-2} mol^{-1})	*Ground state properties*
$CeCu_6$	1600	non-magnetic, Kondo lattice (?)
$CeAl_3$	1620	non-magnetic
$CeCu_2Si_2$	1600	superconductor
UBe_{13}	1100	superconductor
$NpBe_{13}$	900	antiferromagnetic, itinerant (?)
UCd_{11}	840	antiferromagnetic
U_2Zn_{17}	535	antiferromagnetic
UPt_3	450	superconductor
$NpSn_3$	242	itinerant antiferromagnet
$NpOs_2$	200	itinerant ferromagnet
UAl_2	142	spin fluctuations
U_6Fe	150	superconductor

taken with even greater resolution and at still lower temperatures. Nevertheless, this study already shows the nature of the hybridization and orbital-character of the observed energy bands.

Since it would be somewhat arbitrary to limit this presentation only to the superconducting heavy fermion materials, or even only to heavy-effective-mass materials, Table 19.7 lists related properties of many interesting narrow-band f-electron compounds. The inclusion of Ce compounds in the Table is intended to show how closely related these are to those of the early members of the actinide series due to their narrow-band-like nature. Clearly, the early members of the actinide (and rare-earth) series continue to reveal physical properties which are fascinating, but very difficult to explain on a first-principles, theoretical basis. Thus, they will remain a challenge to experimentalists and theoreticians for some time.

ACKNOWLEDGMENT

The work reported herein has been supported by the US Department of Energy.

REFERENCES

1. Friedel, J. (1958) *J. Phys. Rad.*, **19**, 573–81.
2. Matthias, B. T., Zachariasen, W. H., Webb, G. W., and Engelhardt, J. J. (1967) *Phys. Rev. Lett.*, **18**, 781–4.
3. Smith, J. L. and Kmetko, E. A. (1983) *J. Less-Common Metals*, **90**, pp. 83–8.
4. Roof, R. B., Haire, R. G., Schiferl, D., Schwalbe, L. A., Kmetko, E. A., and Smith, J. L. (1980) *Science*, **207**, 1353–5; Roof, R. B. (1981) in *Actinides–1981* (ed. N. M. Edelstein), Lawrence Berkeley Laboratory Rep. LBL-12441, pp. 213–5.

5. Smith, G. S., Akella, J., Reichlin, R., Johnson, Q., Shock, R. N., and Schwab, M. (1981) *Actinides–1981* (ed. N. M. Edelstein), Lawrence Berkeley Lab. Report LBL-12441, Abstracts, pp. 218–20.
6. Benedict, U. (1984) *J. Less-Common Metals*, **100**, 153–70. (Many additional references in this review article. See also Benedict, U. (1984) *J. Phys. Colloq.*, **8**, 145–8).
7. Zener, C. (1955) *Phys. Rev.*, **77**, 846–56.
8. Moffatt, W. G. (1981) *The Handbook of Binary Phase Diagrams*, General Electric Co.
9. Rose, R. L., Kelley, R. E., and Lesuer, D. R. (1979) *J. Nucl. Mater.*, **79**, 414–6.
10. Oetting, F. L., Rand, M. H., and Ackermann, R. J. (1976) *The Chemical Thermodynamics of Actinide Elements and Compounds*, part 1, *The Actinide Elements*, IAEA, Vienna.
11. Chiotti, P., Akhachinskii, V. V., Ansara, I., and Rand, M. H. (1981) *The Chemical Thermodynamics of Actinide Elements and Compounds*, part 5, *The Actinide Binary Alloys*, IAEA, Vienna.
12. Kmetko, E. A. and Hill, H. H. (1976) *J. Phys. F: Metal Phys.*, **6**, 1025–37.
13. Lam, D. J., Darby, J. B. Jr, and Nevitt, M. V. (1974) in *The Actinides: Electronic Structure and Related Properties* (eds A. J. Freeman and J. B. Darby Jr), Academic Press, New York, pp. 119–84.
14. Freeman, A. J. and Koelling, D. D. (1974) in ref. 13, pp. 51–108.
15. Smith, J. L. and Haire, R. G. (1978) *Science*, **200**, 535–7.
16. Hill, H. H. (1970) in *Plutonium 1970 and Other Actinides* (ed. W. N. Miner), Metallurgical Society, AIME, New York, pp. 2–19.
17. Freeman, A. J. and Darby, J. B. Jr (eds) (1974) *The Actinides: Electronic Structure and Related Properties*, Academic Press, New York.
18. Brodsky, M. B. (1978) *Rep. Prog. Phys.*, **41**, 1547–608.
19. Chan, S. K. and Lam, D. J. (1974) in *The Actinides: Electronic Structure and Related Properties* (eds A. J. Freeman and J. B. Darby Jr), Academic Press, New York, pp. 1–49.
20. Lander, G. H., Brun, T. O., Veal, B. W., and Lam, D. J. (1974) *Proc. 1st Conf. on Crystalline Electric Field Effects in Metals and Alloys*, University of Montreal, pp. 480–93.
21. Reihl, B., Martensson, N., Heimann, P., and Eastman, D. E. (1981) *Phys. Rev. Lett.*, **46**, 1480.
22. Freeman, A. J. (1980) *Physica*, **102B/C**, 3–11.
23. Johansson, B., Skriver, H. L., Martensson, N., Andersen, O. K., and Glötzel, D. (1980) *Physica*, **102B/C**, 12–21.
24. Schirber, J. E. and Arko, A. J. (1980) *Physica*, **102B/C**, 287–90.
25. Arko, A. J. and Koelling, D. D. (1978) *Phys. Rev. B*, **17**, 3104–14.
26. Lander, G. H. (1978) in *Rare Earths and Actinides* 1977 (eds W. D. Corner and B. K. Tanner), (Inst. Phys. Conf. Ser. 37), Institute of Physics, London and Bristol, ch. 7, pp. 173–83.
27. Muller, W. (1980) in *Lanthanide and Actinide Chemistry and Spectroscopy* (ed. N. M. Edelstein), (ACS Symp. Ser. 131), American Chemical Society, Washington DC, pp. 183–98.
28. Ward, J. W., Kleinschmidt, P. D., Haire, R. G., and Brown, D. (1980) in ref. 28, pp. 199–220.
29. Nugent, L. J., Burnett, J. L., and Morss, L. R. (1973) *J. Chem. Thermodyn.*, **5**, 665–78.
30. David, F., Samhoun, K., Guillaumont, R., and Edelstein, N. M. (1978) *J. Nucl. Chem.*, **40**, 69–74.

31. Elliott, R. P. (1965) *Constitution of Binary Alloys*, 1st Suppl., McGraw-Hill, New York.
32. Mardon, P. G. and Pearce, J. H. (1959) *J. Less-Common Metals*, **1**, 467–75.
33. Ellinger, F. H., Elliot, R. O., and Cramer, E. M. (1959) *J. Nucl. Mater.*, **1**, 233–43.
34. Saito, S. and Beck, P. A. (1959) *Trans. AIME*, **215**, 938–41.
35. Spirlet, J. C. (1981) *Actinides*–1981 (ed. N. M. Edelstein), Lawrence Berkeley Lab. Report LBL-12441, Abstracts, pp. 51–4.
36. Haire, R. G. (1981) in ref. 35, pp. 34–6.
37. Brown, D. (1981) in ref. 35, pp. 22–4.
38. Fisher, E. S. (1957) *Trans. AIME*, **209**, 882–8.
39. Liptai, R. G. and Friddle, R. J. (1967) *J. Nucl. Mater.*, **24**, 316–22.
40. Goldberg, A. and Massalski, T. B. (1970) in *Plutonium* 1970 *and Other Actinides* (ed. W. N. Miner), Metallurgical Society, AIME, New York, pp. 875–973.
41. Faiers, M. E. (1975) in *Plutonium* 1975 *and Other Actinides* (eds H. Blank and R. Lindner), North-Holland, Amsterdam, pp. 739–48.
42. Robinson, A. C. and Stacey, R. J. (1975) in ref. 41, pp. 749–55.
43. Allen, R. P. and Arrowsmith, H. W. (1975) in ref. 41, pp. 775–85.
44. Rechtien, J. J. and Nelson, R. D. (1973) *Metal. Trans.*, **4**, 2755–65.
45. Zukas, E. G., Hecker, S. S., and Pereyra, R. A. (1983) *J. Nucl. Mater.*, **115**, 63–8.
46. Lander, G. H. (1982) *J. Magn. Magn. Mater.*, **29**, 271–281.
47. Grisson, E., Lord, W. P. H., and Fowler, R. D. (1960) *Second Int. Conf. on Plutonium Metallurgy*, Cleaver-Hume, London, pp. 499–583.
48. Kittel, J. H., *et al.* (1971) *Nucl. Eng. Design*, **15**, 373–440.
49. Merz, M. D. and Nelson, R. D. (1970) in *Plutonium* 1970 *and Other Actinides* (ed. W. N. Miner), Metallurgical Society, AIME, New York, pp. 387–405.
50. ASM (1979) *Metals Handbook*, vol. 2, pp. 785, 809–10, 822.
51. Fisher, E. S. (1974) in *The Actinides: Electronic Structure and Related Properties* (eds A. J. Freeman and J. B. Darby Jr), Academic Press, New York, pp. 289–342.
52. Merz, M. D. and Kjarmo, H. E. (1975) in *Plutonium* 1975 *and Other Actinides* (eds H. Blank and R. Lindner), North-Holland, Amsterdam, pp. 679–85.
53. Hecker, S. S. and Morgan, J. R. (1975) in ref. 52, pp. 697–709.
54. Dunlap, B. D. and Lander, G. H. (1974) *Phys. Rev. Lett.*, **33**, 1046–8.
55. Huray, P. G., Nave, S. E., Peterson, J. R., and Haire, R. G. (1980) *Physica*, **102B/C**, 217–30; see also Fournier, J. M., Blaise, A., Muller, W., and Spirlet, J. C. (1977) *Physica*, **86**, 30–1.
56. Murray, A. F. and Buyers, W. J. L. (1980) in *Proc. Int. Conf. on Crystalline Field and Structural Effects in f-Electron Systems* (eds J. E. Crow, R. P. Guertin, and T. W. Mihalisin), Academic Press, New York, pp. 257–67.
57. Trainor, R. J., Brodsky, M. B., Dunlap, B. D., and Shenoy, G. K. (1976) *Phys. Rev. Lett.*, **37**, 1511–4.
58. Trainor, R. J., Brodsky, M. B., and Culbert, H. V. (1975) *Phys. Rev. Lett.*, **34**, 1019–22.
59. Wachter, P. (ed.) (1980) *Proc. Int. Conf. on the Physics of Actinides and Related 4f Materials*; *Physica*, **102B/C**, 1–400.
60. Freeman, A. J. and Lander, G. H. (eds) (1985) *Handbook on the Physics and Chemistry of the Actinides*, North Holland, Amsterdam.
61. Ott, H. R., Rudigier, H., Fisk, Z., and Smith, J. L. (1983) *Phys. Rev. Lett.*, **50**, 1595–8.
62. Stewart, G. R., Fisk, Z., Willis, J. O., and Smith, J. L. (1984) *Phys. Rev. Lett.*, **52**, 679–82.
63. Palstra, T. T. M., Menovsky, A. A., van den Berg, J., Dirkmaat, A. J., Kes, P. H., Nieuwenhuys, G. J., and Mydosh, J. A. (1985) *Phys. Rev. Lett.*, **55**, 2727–30.

64. Franz, W., Griessel, A., Steglich, F., and Wohleben, D. (1978) *Z. Phys. B*, **31**, 7–17, and Steglich, F., Aarts, J., Bredl, C. D., Lieke, W., Meschede, D., Franz, W., and Schäfer, J. (1979) *Phys. Rev. Lett.*, **43**, 1892–6.
65. Stewart, G. R. (1984) *Rev. Mod. Phys.*, **56**, 755–87.
66. Henkie, Z., Johanson, W. R., Arko, A. J., Crabtree, G. W., and Bazan, C. (1983) *Phys. Rev. B*, **28**, 4198–203.
67. Anderson, P. W. (1984) *Phys. Rev. B*, **30**, 1549–50, and 4000–2; and Varma, C. M. (1985) *Comments Solid State Phys.*, **11**, 221–43.
68. Golding, B., Bishop, D. J., Batlogg, B., Haemmerle, W. H., Fisk, Z., Smith, J. L., and Ott, H. R. (1985) *Phys. Rev. Lett.*, **55**, 2479–82.
69. Tachiki, M. and Maekawa, S. (1984) *Phys. Rev. B*, **29**, 2497–502.
70. Koelling, D. D., Dunlap, B. D., and Crabtree, G. W. (1985) *Phys. Rev. B*, **31**, 4966–71.
71. Oguchi, T. and Freeman, A. J. (1985) *J. Magn. Magn. Mater.*, **52**, 174–8.
72. DeLong, L. E., Guertin, R. P., Hasanain, S., and Fariss, T. (1985) *Phys. Rev. B*, **31**, 7059–76.
73. Arko, A. J., Olson, C. G., Wieliczka, D. M., Fisk, Z., and Smith, J. L. (1984) *Phys. Rev. Lett.*, **53**, 2050–3.
74. Reavis, J. G., Bowersox, D. F., Christensen, D. C., and Mullins, L. J. (1985) *Radiochim. Acta*, **38**, 135–9.

CHAPTER TWENTY

STRUCTURAL CHEMISTRY

John H. Burns

20.1 INTRODUCTION

This chapter deals with the structural chemistry of compounds of the actinide elements from Ac to Es as elucidated mainly by the methods of x-ray and neutron diffraction. Metals, intermetallic compounds, and alloys are not considered here (see Chapter 19 and the review by Lam *et al.* [250]).

While the ultimate objective in the study of the solid state is an understanding of the electronic energy states of the elements involved and the combinations of these states which lead to chemical bonding, an important first step toward this goal is to obtain a detailed knowledge of the crystal and/or molecular structure of the substances of interest. In some cases this alone provides a basis for conclusions about the bonding, e.g. the covalence of the actinyl entity O=M=O, the filling of the 5f shell as reflected in the actinide contraction, and metallic bonding in the silicides as seen in the short U–U distances; but in other cases, e.g. organometallic compounds, other physical measurements and theoretical correlations are needed for an understanding of the bonding. The following survey is primarily descriptive but includes references to the conclusions that may be drawn from these structures where appropriate.

During the last 25 years significant improvements in experimental techniques for the study of crystal structures have been made, and many of them have added to our ability to make quantitative studies of the actinide elements and their compounds. As a result, the inherent inaccuracies caused by the disparity in scattering of x-rays by these heavy elements and by most of the elements with which they form compounds have been considerably reduced. The development of neutron diffraction, in which the scattering cross-sections of elements of widely differing atomic number are often of comparable size (and independent of scattering angle), and the use of counter detectors and computer-controlled diffractometers in x-ray diffraction have improved the precision of the data used in structure determination. Use of high-speed, large-capacity computers for calculation of absorption corrections has also improved the accuracy with which actinide structures can be determined, and the refinement of structural parameters by least-squares methods has been advantageous here as well as elsewhere.

As the data collection techniques have become more automatic and the problem of light vs heavy atoms ameliorated, single-crystal diffraction methods have been used to determine many complicated structures of actinide compounds, e.g. organometallics, β-diketone and Schiff-base complexes, and phthalocyanines, to name a few. Also, the availablility of microgram and milligram quantities of the relatively long-lived isotopes ^{248}Cm, ^{249}Bk, and ^{249}Cf has made possible the growth of single crystals of compounds containing these elements and their study by x-ray diffraction. The α radiation from ^{253}Es is so intense that crystal structures containing this element do not survive long enough to allow their study by other than the powder method, and the heavier elements have not been produced in sufficient quantities for solid-state studies.

The following discussion is organized on the basis of compounds having similar chemical properties, in order to facilitate comparisons among substances that are expected to have similar chemical bonds in the solid state.

20.2 OXIDES

Because of their refractory nature, most actinide oxides have not been obtained in the form of large crystals; consequently most solid-state studies have been made using powder methods. This has imposed limitations on the amount of detailed information obtained about coordination and bonding in many instances, but in some cases rather detailed models have been proposed and made to agree with powder diffraction data. The following discussion will be limited mainly to those compounds for which some details of the structure are known beyond the crystal system. Non-stoichiometric phases, solid solutions, and other aspects of the phase diagrams will not be covered here.

The largest number of crystalline phases among the actinide oxides exists for uranium. This results, in part, from the variability of the valence of this element

and the existence in solid compounds of more than one valence state simultaneously. Only the major structure types are discussed, namely those of UO_2, U_4O_9, U_3O_8, and UO_3. See also Section 5.7.2.

Uranium dioxide crystallizes in the face-centered cubic, fluorite-type structure shown in Fig. 20.1; in fact all the actinide elements from Th to Cf form isostructural dioxides [1, 2]. In this rather open structure there are four large interstices V surrounding each anion. This openness allows the anions to move toward the holes and causes the oxygen atoms to vibrate in an anharmonic fashion even though occupying a point of cubic symmetry [3]. Another consequence of the adoption of this open structure is that additional oxygen atoms can be added to the holes (accompanied by an increase in valence of some of the uranium atoms) without changing the basic structure. This occurs as the stoichiometry varies from UO_2 to UO_{2+x}, x increasing up to 0.25. Precisely how the interstitial oxygen atoms are distributed is not known, although there have been many careful studies by x-ray [4], neutron [5], and electron [6] diffraction. At $x = 0.25$ an ordering of the oxygen atoms occurs and the U_4O_9 structure is formed. Its body-centered cubic lattice has a unit-cell edge equal to four times that of UO_2 (eight times according to a neutron diffraction study [7]), and several models of the ordering have been proposed to account for this superstructure.

The next higher oxide exists in either of two forms at room temperature: α-U_3O_8 and β-U_3O_8 (Fig. 20.2). While most methods of preparation yield α-U_3O_8,

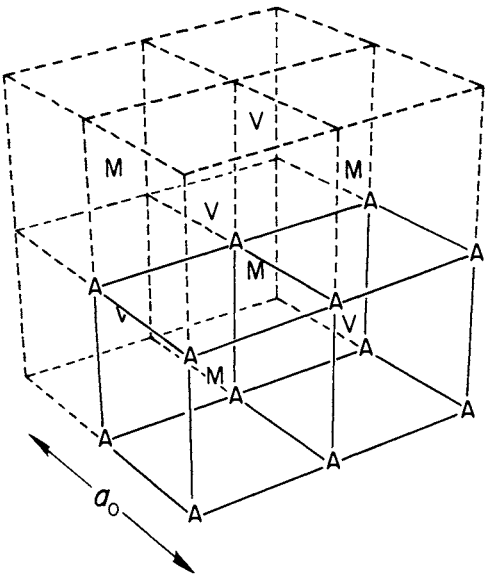

Fig. 20.1 *The fluorite-type structure with cubic unit-cell dimension a_0. Each unit cell contains eight small cubes with anions, A, at their corners and their centers alternately filled (with metal ions, M) and vacant, V.*

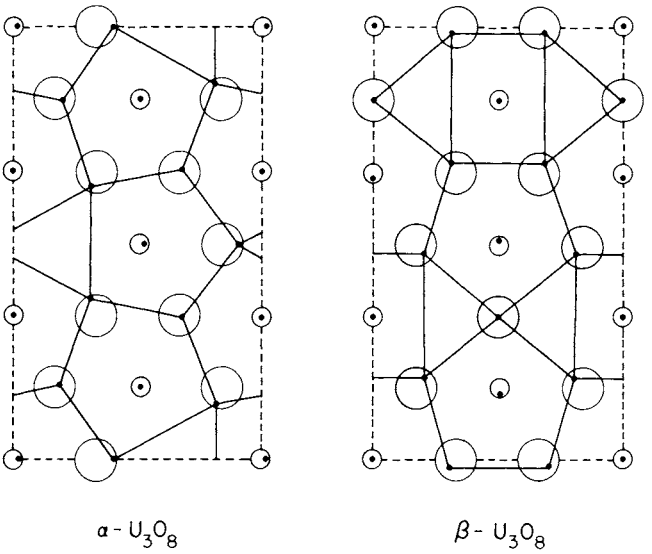

Fig. 20.2 *Sections perpendicular to the c-axis showing the relationship between the two forms of U_3O_8. Small circles represent U atoms, large circles O atoms in the ideal UO_3 structure from which U_3O_8 is derived. Actual atomic sites in U_3O_8 are shown as dots. (After Loopstra* [8, 9].)

the β form is obtained by extended heating above 1000°C followed by slow cooling. Neither form has been made as single crystals, and several early attempts at determination of their structure from x-ray powder diffraction data yielded descriptions that had to be revised as other data became available. Currently, the best picture is that of Loopstra [8, 9] who used neutron powder diffraction. In his models both phases are orthorhombic and have essentially the same distribution of uranium atoms in U–O–U–O chains along the *c*-axis. The oxygen coordination number is 6 or 7 for each uranium atom, but these octahedra and pentagonal bipyramids are quite irregular. This fact, plus the wide and continuous variation in bond lengths, makes an assignment of coordination numbers rather arbitrary. Although the uranium valences are thought to be 5, 5, and 6, only in the β-U_3O_8 structure is there good evidence of a uranyl group (with U–O bond length of 1.89 Å). The orthorhombic lattice parameters of α-U_3O_8 were observed by Siegel [10] to change in a smooth way when the substance is heated up to about 400°C, at which point the b/a axial ratio is such that the lattice can be called trigonal; and a phase change was thought to occur there. However, from neutron diffraction data at 500°C, Herak [11] concluded that at this temperature the orthorhombic symmetry and the space group of α-U_3O_8 persist, but that there are significantly different oxygen positions, and suggested that the transition is second order. (For β-U_3O_8 also the b/a ratio diverges from the trigonal approximation but in the opposite way from α-U_3O_8.)

Uranium trioxide has been prepared in six crystalline forms [12], but the details of atomic arrangement are known for only three of them: high-pressure UO_3, α-UO_3, and γ-UO_3. For the first of these, an analysis [13] using a single crystal made at 30 kbar provided one of the few unequivocal structural descriptions available in the uranium–oxygen system. The hexavalent uranium atom forms a uranyl group with two of its seven oxygen neighbors (at 1.80 and 1.85 Å), and the other five oxygen atoms comprise a puckered pentagon perpendicular to it. All oxygen atoms are shared between uranium atoms and the pentagonal bipyramids are extensively crosslinked. The structure of α-UO_3, however, has been the subject of several studies, each adding further modifications to the description of it. The latest [14] is a neutron and electron diffraction investigation from which a structure is proposed based on that of α-U_3O_8 but with a random deficiency of uranium atoms and the formation of some uranyl-like bonds in the U–O–U–O chains. Superstructure reflections are also observed and indicate an even more complex structure based on 11 of the original unit cells. The degree to which these small perturbations of the gross structure can be deduced with certainty is clearly limited by lack of single-crystal data. The γ-UO_3 phase was studied [15] by x-ray powder diffraction and a structure derived consisting of UO_6 octahedra sharing edges and corners in a three-dimensional network. There is the possibility of some uranyl groups in this form also, but the evidence is not very definitive.

Several hydrates of UO_3 are known. Some occur as minerals with composition near $UO_3 \cdot 2H_2O$. While studies have been made to characterize these [16] and also synthetic analogs [17] of them, no detailed structures have been established. Indeed it may be asked whether they actually contain water of hydration since two 'hydrates' that have been elucidated do not. One of these is $UO_3 \cdot H_2O$, whose crystal structure [18] indicates that it is best described as uranyl dihydroxide; in it there are distinct uranyl groups aligned perpendicular to a square of hydroxide ions (Fig. 20.3). The other is $UO_3 \cdot \frac{1}{3} H_2O$, which was shown by x-ray [19] and neutron [20] diffraction to be in fact hydrogen triuranate. Both octahedra and pentagonal bipyramids comprise the coordination of various uranium atoms, and the presence of hydrogen atoms attached to some of the oxygens was established by neutron diffraction with deuterated samples.

Oxides of the lighter actinides include Ac_2O_3, which exists only in the A-type sesquioxide form (discussed later), ThO_2, which has the fluorite structure, and Pa_2O_5, which has five crystal modifications [2], none of which have been elucidated in detail. This last compound can be reduced to PaO_2 having the fluorite arrangement.

The established oxides of neptunium include NpO_2 (fluorite), monoclinic Np_2O_5 [21, 22], $NpO_3 \cdot H_2O$ [23], which is isostructural with β-$UO_2(OH)_2$, and $NpO_2 \cdot 2H_2O$ [23], which is similar to $UO_2 \cdot 2H_2O$ in structure. Only NpO_2 has been prepared as large crystals [24].

In addition to formation of PuO_2 (fluorite-type) and Pu_2O_3 (hexagonal A-type), plutonium forms non-stoichiometric oxides by losing oxygen from the

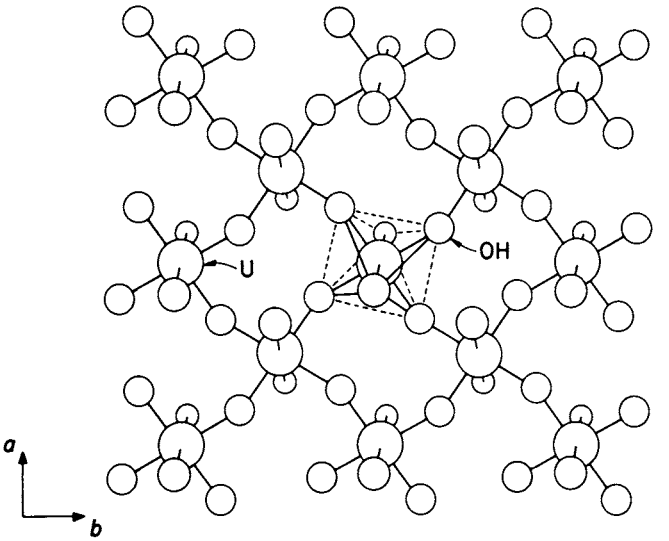

Fig. 20.3 *The structure of one layer of β-$UO_2(OH)_2$. Large circles are U atoms, small ones are O atoms. Uranyl O atoms are above and below the plane of the figure, and the remaining O atoms belong to hydroxyl ions. (After Roof, Cromer, and Larson* [18].)

former and by oxidation of the latter [25]. On addition of a small amount of oxygen to Pu_2O_3 it adopts the C-type structure, which it retains up to $PuO_{1.69}$. Precisely how the oxygen atoms enter or leave the basic structures has not been determined. There is, however, a relationship between the fluorite structure and the C-type (bixbyite [26]) structures which may facilitate transformation from one to the other under suitable oxidation–reduction conditions. In the former each metal ion is at the center of a cube of oxygen atoms, while in the latter a similar configuration exists, but two oxygen atoms of each cube are missing and small shifts of the other oxygens have occurred.

The sesquioxides already mentioned, as well as those of the transplutonium elements through einsteinium, crystallize in one or more of three structure types designated A (hexagonal [27]), B (monoclinic [28]), and C (cubic). They are distributed among these as follows (See Table 14.8):

Type A	Ac_2O_2	... Pu_2O_3	Am_2O_3	Cm_2O_3	Bk_2O_3 [29]	Cf_2O_3 [29]	Es_2O_3
Type B	–	... –	Am_2O_3	Cm_2O_3	Bk_2O_3 [29]	Cf_2O_3	Es_2O_3
Type C	–	... Pu_2O_3	Am_2O_3 [30]	Cm_2O_3 [31]	Bk_2O_3 [32]	Cf_2O_3 [33]	Es_2O_3 [34]

None of the actinide sesquioxides have been analyzed by single-crystal methods; consequently the exact locations of the oxygen atoms in each modification are not known, and the metal–oxygen bond lengths are known only by estimation. In none of these structures, shown in Fig. 20.4, is the configuration of oxygen atoms about the metal very symmetric, nor in structures A or B is the delineation of nearest neighbors very distinct. The general trend, however, is for

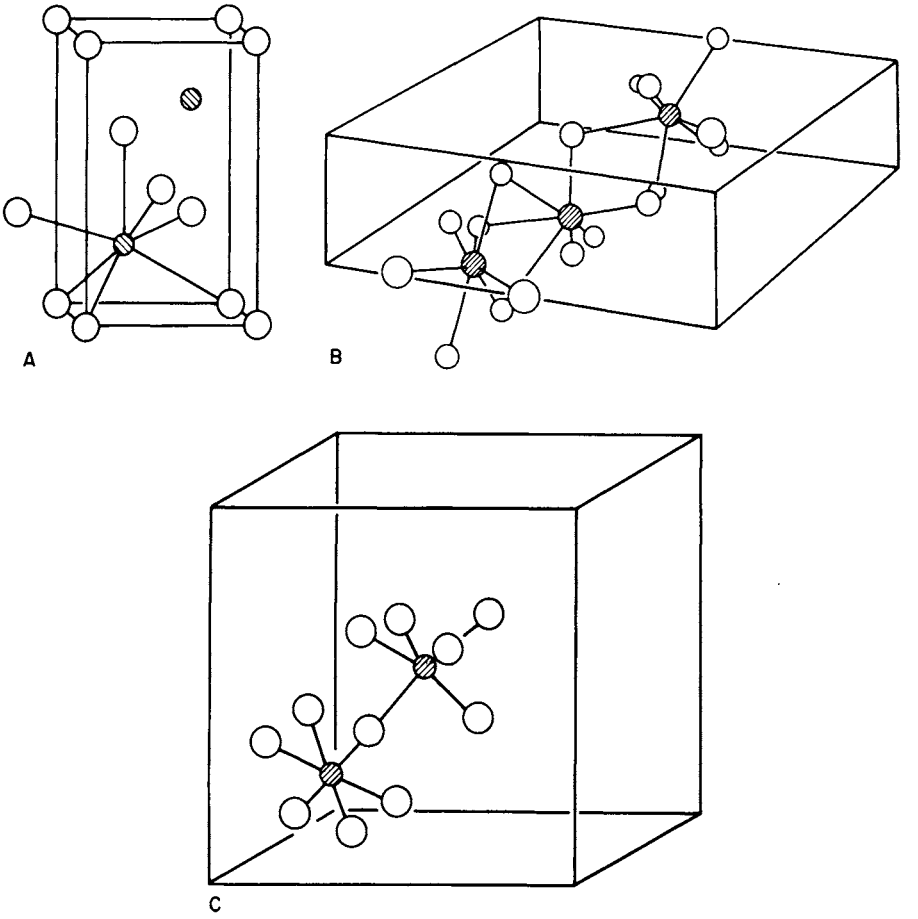

Fig. 20.4 *Unit cells of the three forms of actinide sesquioxides: A, hexagonal; B, monoclinic; and C, cubic. Only those atoms are included which are needed to show the coordination of the metal ions in each instance.*

the coordination number in type A to be 7, in type B to be 6 or 7, and in type C to be 6. The smaller actinide ions favor the C-type structure. Two different rhombohedral structures have been suggested for intermediate phases CmO_x [31] and CfO_x [33], with $1.5 < x < 2.0$, but no details have been obtained.

Several monoxides of the actinides have been reported with the NaCl-type structure. These include PaO [35], NpO [36], PuO [36], and AmO [37]. They may, however, be oxycarbides [536].

In addition to the binary oxides of the actinides there are many compounds that are made by reaction of these with oxides of alkali metals, transition metals, alkaline earths, and some other elements. Comprehensive surveys of these by Keller [38] and Morss [540] provide lists of known compounds and organize the available crystallographic data to show the isostructural series that exist. They

also point out the many instances in which these compounds were found to belong to known structural types. Few of these substances have been prepared as single crystals, but many powder diffraction analyses have been performed. In those cases where the structural details have been reasonably well-established, the actinide atom is usually seen to be coordinated by an octahedron of oxygen atoms, irrespective of the valence state of the actinide. Precise bond lengths are not available for such compounds in which the actinide valence is 4 or 5, but several studies with hexavalent uranium have been precise enough to allow some conclusion to be drawn regarding the bonding.

Three types of octahedra may be identified, although in many cases the variation in bond lengths is so continuous as to make a clear distinction impossible. In the first case, typified by copper monouranate ($CuUO_4$) [39] and barium diuranate (BaU_2O_7) [40], two of the oxygen atoms form a collinear UO_2^{2+} group with the uranium at U–O distances of 1.8–1.9 Å, and the other four form a square around its equator at U–O distances of about 2.2 Å. The opposite distribution of bond lengths occurs in the second type, e.g. Na_4MO_5 (M = U [41] to Am [42]), in which there are four short M–O bonds and two long ones. The majority of the compounds studied, however, seem to be in the third category in which all six oxygen atoms are at about equal distances from the metal. Some well-established structures of this form include Pb_3UO_6 [43], Cd_2UO_5 [44], Ca_3UO_6 [45], Li_2UO_4 [46], and Li_6UO_6 [541]. The structures of a large number of alkali polyuranates are known [47–51] to varying degrees of completeness; these all contain uranyl groups with four or five O atoms around their equators.

20.3 ACTINYL COMPLEXES

The structures of uranyl compounds were among the first of the actinides to be studied, and there continues to be a wide interest in determining such structures. The linear arrangement of the O=U=O atoms was deduced from the space group symmetry of sodium uranyl acetate in 1935 [52]; among the 200 or so structures containing actinyl groups that have been elucidated since then, there has rarely been found to be a significant deviation from linearity. Although most of the precise studies of the geometry of the actinyl ion have dealt with the case of uranium, a few single-crystal analyses and numerous powder diffraction measurements with transuranic actinyls have been made. Evidence from vibrational spectra has been reviewed [542]. It has been established that the MO_2^{2+} (M = Np, Pu, Am) ions are isostructural with the UO_2^{2+} prototype, and that the MO_2^{+} (M = Np, Pu, Am) ion is a symmetric, linear entity also, see Section 7.8.

The difficulty in stating the dimensions of the uranyl ion with accuracy lies in the fact that most of the structural analyses have been made with x-ray diffraction data. The large discrepancy in scattering power between uranium and oxygen plus the high absorption coefficient of uranium make the U=O bond length

inherently difficult to measure accurately. A few of the known structures have been determined by neutron diffraction methods, in which the above difficulties are greatly reduced. This technique is usable only when the structure is simple enough to be analyzed by powder diffraction or when multi-milligram crystals can be grown. In those instances where the latter applies, the more precise bond lengths have been found.

The lengths of the M=O bonds in various compounds range from 1.7 to 2.0 Å and are influenced by several factors. Sometimes the two M=O bonds in a single ion show apparent differences which can be correlated with the different environments provided by the rest of the structure [53], but usually these differences are not greater than the assigned errors of the determination. The MO_2^{2+} and MO_2^{+} ions exhibit the actinide contraction, as do actinides in other valence states, and it amounts to about 0.01 Å for each increment in atomic number. This effect was found in unit-cell measurements of powder samples of KMO_2CO_3 [54, 55], $RbMO_2F_2$ [56] (M = Np(v), Pu(v), Am(v)), and $NaMO_2(CH_3CO_2)_3$ [57] (M = U(VI), Np(VI), Pu(VI), Am(VI)). This was also verified by determination of bond lengths in single crystals of $Na_4UO_2(O_2)_3 \cdot 9H_2O$ and $Na_4NpO_2(O_2)_3 \cdot 9H_2O$ [58, 59]. Another influence on bond lengths is, of course, the valence state of the actinide; and changing from VI to V results in a lengthening of about 0.14 Å [60]. This implies a weakening of the bond and is attributable to the additional non-bonding electron in each MO_2^{+} ion compared to its corresponding MO_2^{2+} ion.

The factor that contributes most to the M=O bond-length variations (other than valence changes) is the bonding of other ligands to the M atom in a plane through it and perpendicular to the MO_2 axis. The number of such equatorial (or secondary) bonds ranges from four to six in known structures. Zachariasen noted in 1954 [57] that the primary U=O bond lengths in uranyl compounds vary from one compound to another and he correlated bond lengths with bond strengths using data available at that time. Later he revised and extended this relationship; it now covers secondary bonds to elements other than oxygen [61]. Atoms forming the secondary bonds to the actinide element generally lie in a plane when they are four or five in number, but form a puckered hexagon if six. For bidentate radicals, such as peroxide, carbonate, nitrate, or sulfate, six O atoms can be coplanar and all attached to the actinide atom, because bonding within the radicals causes short O–O distances. Dentition can be higher, and values of 3, 4, and 5 from a single ligand are known. Examples of the highest of these are uranyl saldien ($UO_2C_{18}H_{19}O_2N_3$) [62] and uranyl 'superphthalocyanine' [63] (Fig. 20.5). In addition to oxygen, secondary bonds to F, Cl, Br, N, and S have been found in various compounds.

The most common polyhedra involving the actinyl group, pentagonal and hexagonal bipyramids, are often isolated units in crystals, but there are examples in which parts of the polyhedra are shared. This sharing ranges from a common pentagonal vertex as in $K_5(UO_2)_2F_9$ [64], to one vertex plus one edge in $K_3(UO_2)_2F_7 \cdot 2H_2O$ [65] (Fig. 20.6(a)), to shared F–F edges in

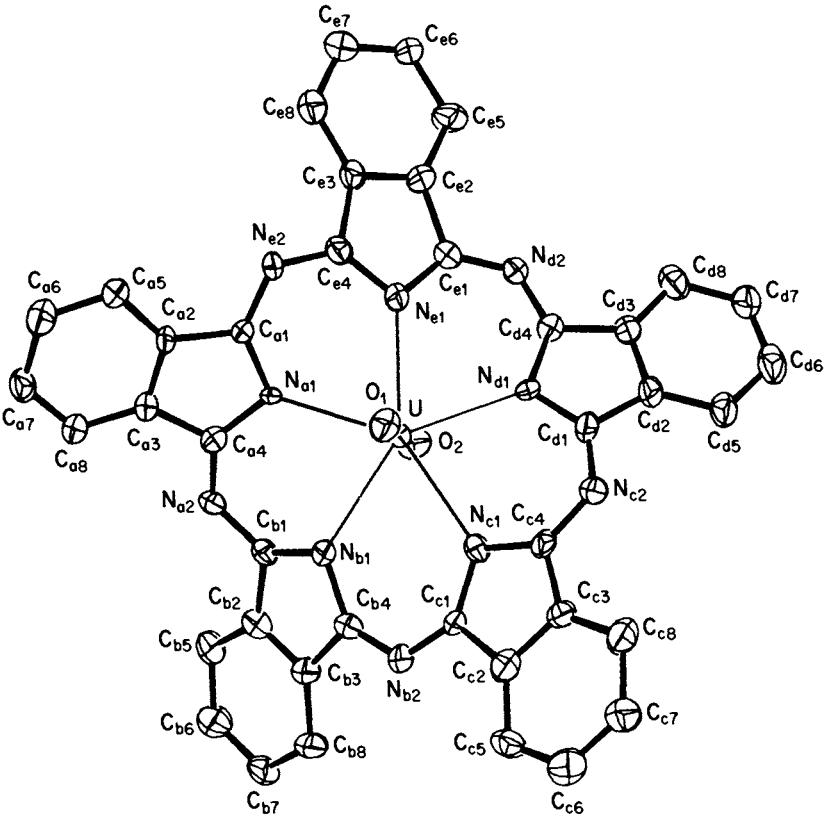

Fig. 20.5 *The molecular structure of uranyl 'superphthalocyanine'. (Reproduced, with permission, from ref. 63. Copyright by the American Chemical Society.)*

$Cs_4(UO_2)_2F_8 \cdot 2H_2O$ [66] (Fig. 20.6(b)) and $Ni(NH_4)_2(UO_2)_2F_8 \cdot 6H_2O$ [67], and to sharing of all hexagonal edges in the bipyramids of UO_2F_2 [68].

In Table 20.1 are listed most of the actinyl compounds whose structures have been determined by analysis with single-crystal data or have been shown by powder diffraction to be isostructural with one of the known structures. Reviews have been written about uranyl complexes with chelating agents [69, 70] and with carboxylic acids [71].

20.4 HYDRIDES, BORIDES, CARBIDES, AND SILICIDES

Six different crystal structures are known for the actinide hydrides. The two best characterized are those of α-UH_3 [215] and β-UH_3 [216]; in the latter, hydrogen atoms were located by neutron diffraction studies. In these two distinct cubic modifications, each U atom is bonded to 12 hydrogen atoms at 2.32 Å, and each

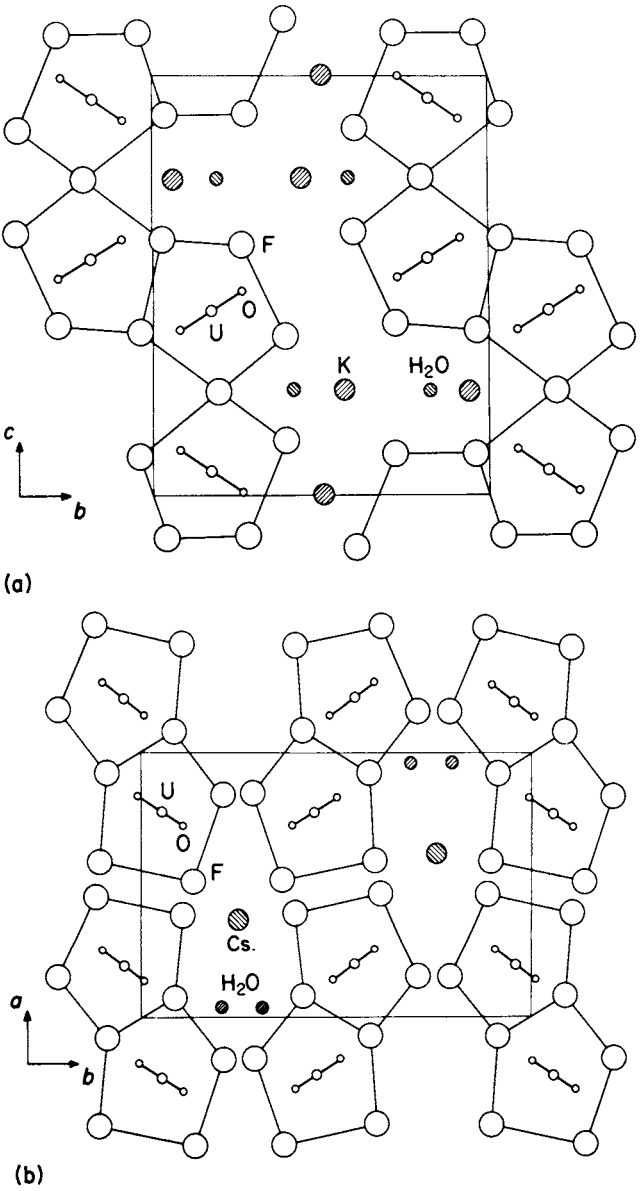

Fig. 20.6 *A portion of two structures, (a)* $K_3(UO_2)_2F_7 \cdot 2H_2O$ *and (b)* $Cs_4(UO_2)_2F_8 \cdot 2H_2O$*, to illustrate the sharing of polyhedral edges.*

H atom is tetrahedrally surrounded by U atoms. The β-UH_3 structure is also found [217] for PaH_3. Thorium forms two hydrides: ThH_2, which has a tetragonally distorted fluorite-like structure [218], and Th_4H_{15}, which is cubic [219] and has each Th atom bonded to nine H atoms at distances of 2.29 and

Table 20.1 *Actinyl compounds whose structures have been determined.*

Compound	*Ref.*
four equatorial bonds	
$MgUO_2O_2$	72
$BaUO_2O_2$	73
β-$UO_2(OH)_2$	18
$NpO_2(OH)_2$	23
$HUO_2PO_4 \cdot 4H_2O$	74
$Cs_2UO_2Cl_4$	75
$Cs_3NpO_2Cl_4$	76
$Cs_3PuO_2Cl_4$	76
$Cs_3AmO_2Cl_4$	76
$Cs_2UO_2Br_4$	77
$[(CH_3)_4N]_2UO_2Cl_4$	78
$[(CH_3)_4N]_2UO_2Br_4$	79
$[(C_2H_5)_3NH]_2UO_2Cl_4$	80
$(C_2H_5)_4NUO_2Cl_4$	81
$[(C_3H_7)_4N]_2UO_2Cl_4$	82
$[(C_3H_7)_4N]_2UO_2Br_4$	83
$[(C_4H_9)_4N]_2UO_2Cl_4$	84
$[(C_4H_9)_4N]_2UO_2Br_4$	85
$(C_3N_2H_5)_2UO_2Cl_4$	86
$(C_{20}H_{18}N_4S_2)UO_2Cl_4$	87
$(C_7H_{16}NO_2)UO_2Br_4$	88
$(C_6H_{18}N_3PO)_2UO_2Cl_2$	89
$(C_6H_{18}N_3PO)_4UO_2(ClO_4)_2$	90
$[(C_6H_5)_3PO]_2UO_2Cl_2$	91
$(C_{12}H_{18}N_4ClOS)_2UO_2Cl_4$	92
$(C_{42}H_{44}N_{10})UO_2Cl_4 \cdot CH_3CN$	93
$Na_2(C_{28}H_{40}O_{10})UO_2Cl_4$	94
five equatorial bonds	
UO_2Cl_2	95
$UO_2Cl_2 \cdot H_2O$	96
$(UO_2)_2(OH)_2Cl_2 \cdot 4H_2O$	97
$[(UO_2)_4Cl_2O_2(OH)_2(H_2O)_6] \cdot 4H_2O$	98
$[(UO_2)_3O(OH)_3(H_2O)_6]NO_3 \cdot 4H_2O$	99
$K_2(UO_2)_4O_2(OH)_2Cl_4(H_2O)_6$	100
$[(C_6H_5CH_2)N]_4[Cl_3UO_2{-}O_2{-}UO_2Cl_3]$	101
$CuUO_2(OH)_4$	102
$K_3UO_2F_5$	103
$K_3NpO_2F_5$	104
$K_3(UO_2)_2F_7 \cdot 2H_2O$	65
$K_5(UO_2)_2F_9$	64
$Ni(NH_4)_2(UO_2)_2F_8 \cdot 6H_2O$	67
$Cs_xUO_2OCl_x (x \sim 0.9)$	105
$K_xUO_2OCl_x (x \sim 0.9)$	105
$K_xUO_2OBr_x (x \sim 0.9)$	105
$Rb_xUO_2OCl_x (x \sim 0.9)$	105

Table 20.1 (*Contd.*)

Compounds	*Ref.*
$Cs_2UO_2F_4 \cdot H_2O$	66
$Cs_3UO_2(NCS)_5$	106
$Ca(H_3O)_2(UO_2)_2(SiO_4)_2 \cdot 3H_2O$	107
$Cs_2(UO_2)_2V_2O_8$	108
$Cs_2(UO_2)_2(SO_4)_3$	109
$Cu(UO_2)_2(SO_4)_2(OH)_2 \cdot 6H_2O$	110
$K_2UO_2(SO_4)_2 \cdot 2H_2O$	111
$(NH_4)_2UO_2(SO_4)_2 \cdot 2H_2O$	112
$K_2UO_2(SO_4)F_2 \cdot H_2O$	113
β-UO_2SO_4	114
UO_2SeO_4	114
$UO_2SO_4 \cdot 2.5H_2O$	115
α-$UO_2SO_4 \cdot 3.5H_2O$	116
β-$UO_2SO_4 \cdot 3.5H_2O$	117
UO_2SeO_3	118
UO_2TeO_3	119, 118
$UO_2(ClO_4)_2 \cdot 7H_2O$	120
$UO_2(HCOO)_2 \cdot H_2O$	121
$UO_2(HCOO)(OH) \cdot H_2O$	122
$NaUO_2(HCOO)_3 \cdot H_2O$	123
$(NH_4)_2UO_2(HCOO)_4$	124
$SrUO_2(HCOO)_4 \cdot (1+x)H_2O$	125
$UO_2(CH_3COO)_2 \cdot 2H_2O$	126
$UO_2(CH_2OHCOO)_2$	127
$UO_2(CH_2COO)_2 \cdot H_2O$	128
$UO_2(CO_2CH_2OCH_2CO_2)$	129
$\{[(C_6H_5)_3PO]UO_2(CH_3COO)_2\}_2$	130
$\{[(C_6H_5)_3AsO]UO_2(CH_3COO)_2\}_2$	131
$(NH_4)_2UO_2(C_3H_2O_4)_2 \cdot H_2O$	132
$UO_2(C_2O_4) \cdot 3H_2O$	133
$(NH_4)_2UO_2(C_2O_4)_2$	134
$(NH_4)_2(UO_2)_2(C_2O_4)_3$	135
$(C_5H_7O_2)UO_2 \cdot H_2O$	136
$(C_5H_7O_2)_2(C_5H_8O_2)UO_2$	137
$(C_5H_7O_2)_2UO_2(C_5H_9ON)$	138
$(C_5H_7O_2)_2UO_2(C_6H_{11}ON)$	139
$(C_5H_7O_2)_2UO_2(C_7H_{13}ON)$	140
$(C_5H_7O_2)_2UO_2(C_8H_{15}ON)$	141
$[(C_5F_6HO_2)_2UO_2]_3$	142
$(C_5F_6HO_2)_2UO_2 \cdot NH_3$	143
$(C_5F_6HO_2)_2UO_2 \cdot (C_4H_8O)$	144
α-$(C_5F_6HO_2)_2UO_2 \cdot [(OCH_3)_3PO]$	145
β-$(C_5F_6HO_2)_2UO_2 \cdot [(OCH_3)_3PO]$	146
$[(C_2H_5)_4N]UO_2[(C_6H_5)_2C_3HO_2]_2NO_3$	147
$(C_7H_5O_2)_2UO_2(C_5H_5N)$	148
$(C_7H_5O_2)_2UO_2(C_2H_5OH)$	149
$(C_7H_3NO_5)UO_2 \cdot 3H_2O$	150

Table 20.1 (*Contd.*)

Compounds	*Ref.*
$(C_7H_3NO_4)UO_2 \cdot H_2O$	151
$(C_8H_4N_2)_5UO_2$	63
$(C_4H_5NO_4)UO_2$	152
$(C_{16}H_{14}N_2O_4)UO_2(CH_3OH)$	153
$(C_{20}H_{26}N_2O_2)UO_2(C_2H_5OH)$	154
α,β-$(C_{25}H_{23}N_5O_4)UO_2$	155
$(C_{18}H_{18}N_2O_3)UO_2 \cdot CHCl_3$	156
α,β-$(C_{18}H_{18}N_2O_3)UO_2$	157
$(C_{18}H_{19}N_3O_2)UO_2$	62
$(C_{14}H_{10}N_2O_2)UO_2 \cdot H_2O$	158
$(C_{22}H_{30}N_2O_4)UO_2$	159
$(C_{14}H_{12}N_2O_3)UO_2$	160
$(C_{17}H_{26}N_2O_5)UO_2$	161
$(C_9H_6NO)_2UO_2(C_9H_7NO) \cdot CHCl_3$	162
$(C_{14}H_{22}N_4O_4Cl_2)UO_2$	163
$(C_{20}H_{32}N_2OCl_3)UO_2$	164
$(C_{12}H_{22}SO_2Cl_2)UO_2$	165
$UO_2(CH_3SO_3)_2 \cdot H_2O$	166
$(CH_3)_2UO_2SOF_2$	167
$[(NH_2)_2CO]_3UO_2SO_4$	168
$[(NH_2)_2CO]_5UO_2(NO_3)_2$	169
$[(NH_2)_2CO]_4UO_2(NO_3)_2 \cdot H_2O$	170
$[(NH_2)_2CO]_3UO_2(OH)I_4$	171
$[(NH_2)_3C]_2UO_2(SO_4)_2 \cdot 3H_2O$	172
$[(CH_2)_5CHNO]_4UO_2(ClO_4)_2 \cdot H_2O$	173
$[(C_2H_5)_2NH_2]UO_2[(C_2H_5)_2NCOS]_2OC_2H_5$	174
$[(C_2H_5)_2NCS_2]_2UO_2(C_6H_5)_3AsO$	175
$[(C_2H_5)_2NCS_2]_2UO_2(C_6H_5)_3PO$	175
$(C_2H_3S_2)_2UO_2(C_6H_5)_3PO$	176
$UO_2(NCS)_2[(C_6H_5)_3PO]_4 \cdot CH_3COCH_3$	177
$(C_8H_4O_2SF_3)_2UO_2(C_8H_{17})_3PO$	178
$[UO_2Cl_3(OH)(H_2O)][UCl_3(C_{12}H_{24}O_6)]_2CH_3NO_2$	179
six equatorial bonds	
UO_2F_2	68
NPO_2F_2	180
PuO_2F_2	181
AmO_2F_2	182
UO_2CO_3	183
α-$UO_2(OH)_2$	184
$[UO_2(OH)_2UO_2](NO_3)_2 \cdot (H_2O)_3 \cdot (H_2O)$	185
$UO_2(NO_3)_2 \cdot 2H_2O$	186
$UO_2(NO_3)_2 \cdot 3H_2O$	187
$UO_2(NO_3)_2 \cdot 6H_2O$	188
$NpO_2(NO_3)_2 \cdot 6H_2O$	189
$UO_2(NO_3)_2(C_4H_8O)_2$	190

Table 20.1 (*Contd.*)

Compounds	*Ref.*
$UO_2(NO_3)_2[(C_6H_5)_3AsO]_2$	191
$[UO_2(NO_3)_2 \cdot H_2O]_2(C_3H_4N_2)_2$	192
$UO_2(C_6H_{14}N_4O_{10})$	193
$CaUO_2O_2$	194
$SrUO_2O_2$	194
$UO_2Te_3O_7$	195
$RbUO_2(NO_3)_3$	196
$CsUO_2(NO_3)_3$	197
$(NH_4)_2UO_2(NO_3)_4$	198
$Rb_2UO_2(NO_3)_4$	198
$Cs_2UO_2(NO_3)_4$	198
$NaUO_2(CH_3COO)_3$	57
$NaNpO_2(CH_3COO)_3$	57
$NaPuO_2(CH_3COO)_3$	57
$NaAmO_2(CH_3COO)_3$	57
$BaNpO_2(CH_3COO)_3 \cdot 2H_2O$	60
$Na_2UO_2(CO_2CH_2OCH_2CO_2)_2 \cdot 2H_2O$	199
$Li(C_5H_6O_4)(C_5H_7O_4)UO_2 \cdot 4H_2O$	200
$(NH_4)_4UO_2(C_2O_4)_3$	201
$(NH_4)_4UO_2(CO_3)_3$	58
$K_4UO_2(CO_3)_3$	202
$K_4NpO_2(CO_3)_3$	59
$Na_4NpO_2(O_2)_3 \cdot 9H_2O$	59
$Na_4UO_2(O_2)_3 \cdot 9H_2O$	203, 59
$(CH_3)_4NUO_2[(C_2H_5)_2NCS_2]_3$	204
$KNpO_2F_2$	104
$RbNpO_2F_2$	56
$RbPuO_2F_2$	56
$NH_4PuO_2F_2$	56
$KAmO_2F_2$	205
$RbAmO_2F_2$	56
$KNpO_2CO_3$	54
$KPuO_2CO_3$	55
$NH_4PuO_2CO_3$	55
$KAmO_2CO_3$	54
$RbAmO_2CO_3$	55
$CsAmO_2CO_3$	56
$UO_2(NH_2O)_2(NH_2OH)_2 \cdot 2H_2O$	206
$UO_2(NH_2O)(HOCH_2CH_2OH)$	207
α-$UO_2(NH_2O)_2 \cdot 4H_2O$	208
$UO_2(NH_2O)_2 \cdot 3H_2O$	209
$(C_4H_6O_4N)_2UO_2$	210
$(C_{15}H_9O_2)_2UO_2(H_2O)_2(C_4H_8O)_3$	211
$(C_8H_{16}O_4)UO_2(NO_3)_2 \cdot 2H_2O$	212
$(C_{12}H_{24}O_6)UO_2(NO_3)_2 \cdot 2H_2O$	213
$[(C_6H_5)_4As]_2UO_2(C_{14}H_6N_2O_8) \cdot 6H_2O$	214

2.46 Å. The transuranium elements, Np [220], Pu [221], Am [222], Cm [223], and Bk [224], form dihydrides having the fluorite structure; in most cases the ratio of H to metal is variable from 2.0 to 2.7. Presumably the excess H atoms enter the octahedral holes in the structure. It has been noted that the cubic lattice parameters of this series of hydrides do not show the expected contraction with atomic number, but no explanation for this has been offered. Hexagonal trihydrides [220–222] are formed by Np, Pu, and Am; the structure for these phases remains in doubt. (See footnote to Table 7.56.)

The nature of the hydrogen and its bonding to the metal in these hydrides is not clear. Chemically the behavior of these compounds is between that of the metals and that of the salt-like alkali hydrides. A model for bonding has been presented by Libowitz and Gibb [225], who suggested that the hydrogen is anionic and that the metal atoms are ionically bonded to it and have weak metallic bonds to each other. A survey of these and other metallic hydrides is available in a book by Mueller *et al.* [226].

The structure of a complex hydride, $HU\{N[Si(CH_3)_3]_2\}_3$, has been established, but the H atoms were not located [227]. The borohydride analog, $BH_4U\{N[Si(CH_3)_3]_2\}_3$, has the B atom triply hydrogen-bridged to the U atom [228].

Uranium borohydride itself, $U(BH_4)_4$ [229], and its adducts with dimethyl and diethyl ether [230], with diisopropyl ether [231], and with tetrahydrofuran [232] contain double and triple hydrogen bridges between uranium and boron. Usually the U atom achieves coordination 14, mostly with H atoms but including up to two O atoms. Polymers are common since BH_4 molecules are frequently bridged to two U atoms. The average U–H bond length (from neutron diffraction) in $U(BH_4)_4$ is 2.38 Å, close to that in UH_3.

The actinide borides (Table 20.2) all contain either two- or three-dimensional networks of covalent B–B linkages of from 1.72 to 1.83 Å in length, and the metal atoms are contained between layers of B atoms or within the networks. Metal-to-boron bond lengths vary considerably from one structure type to another even for the same metal; they seem to adjust to the more rigid covalent framework of B atoms. In the structure of the diborides [235] each B atom is bonded to three others to form triangular nets which alternate with similar layers of actinide atoms in a simple hexagonal stacking sequence. Each metal atom has 12 B neighbors. The hexaborides [236], shown in Fig. 20.7(a), have each B atom bonded to five others, forming a cubic array of crosslinked B_6 octahedra. The metal atom is at the cube center (a CsCl arrangement) and has a B coordination of 24. The structure of the tetraborides [237] contains some geometrical elements of both the di- and hexaboride structures, and each metal atom has 18 B atoms around it. In the dodecaborides [236] (Fig. 20.7(b)) all B atoms are bonded to five others and form icosahedra. These polyhedra alternate with metal atoms in a cubic array of the NaCl type. Each metal atom has 24 bonds to B atoms.

Three metal-to-carbon (M/C) ratios are found among the actinide carbides: MC, M_2C_3, and MC_2. The structures that these exhibit are distributed among six

Table 20.2 *Structures of actinide borides, carbides, and silicides.*

Structure type	*Compounds*				
AlB_2	–	UB_2	NpB_2 [233]	PuB_2 [234]	–
UB_4	ThB_4	UB_4	NpB_4	PuB_4	AmB_4
CaB_6	ThB_6	–	NpB_6	PuB_6	AmB_6
ZrB_{12}	–	UB_{12}	NpB_{12}	PuB_{12}	–
NaCl	ThC	UC	NpC	PuC	
Pu_2C_3	–	U_2C_3	Np_2C_3	Pu_2C_3 [238]	Am_2C_3 [239]
CaC_2	–	α-UC_2	NpC_2	α-PuC_2	
KCN	γ-ThC_2	β-UC_2		β-PuC_2	
β-ThC_2	β-ThC_2				
α-ThC_2	α-ThC_2				
U_3Si	–	U_3Si [244]	–		
W_5Si_3	–	–	–	Pu_5Si_3 [245]	
U_3Si_2	Th_3Si_2	U_3Si_2	Np_3Si_2	Pu_3Si_2 [246]	
FeB	ThSi	USi	–	PuSi [246]	
AlB_2	β-$ThSi_2$ [247]	β-USi_2	–	Pu_3Si_5 (defect) [246]	
α-$ThSi_2$	α-$ThSi_2$ [247]	α-USi_2	$NpSi_2$ [244]	$PuSi_2$ [244]	

different types as listed in Table 20.2. All of these structures were determined by x-ray diffraction except for ThC_2 and UC_2 for which neutron diffraction [240, 241] was used. In these latter compounds the positions of the C atoms were directly determined, while, in the others, reasonable deductions were made as to their placement. The existence of the C_2 group, with a C–C bond length of about 1.3 Å, has been clearly established in several structures and is assumed to exist in all the others except the monocarbides, which have the NaCl arrangement of M and C atoms. The nature of the carbon in these (sometimes substoichiometric) monocarbides is not known; it is curious that these compounds can form solid solutions [241] with cubic *di*carbides which are known to contain C_2 groups.

The structures of the three ThC_2 phases are closely related [240]. In the highest-temperature form, cubic γ-ThC_2, the C_2 groups are randomly oriented in three dimensions; at somewhat lower temperatures, a tetragonal species (β-ThC_2) exists in which the C_2 disorder has been reduced to two dimensions; and the room-temperature monoclinic α-ThC_2 has the orientation of the C_2 fixed. The tetragonal β-ThC_2 is different from the tetragonal CaC_2 structure adopted by

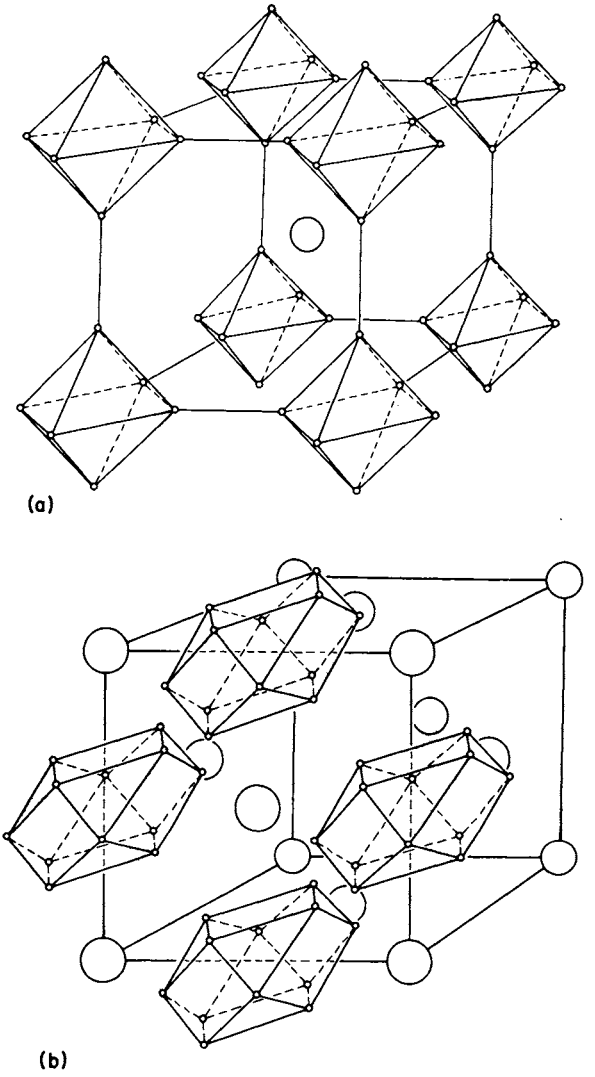

Fig. 20.7 *Unit cells of (a) the actinide hexaborides and (b) the actinide dodecaborides. Small circles represent B atoms, large ones actinide atoms. (After Blum and Bertaut* [236].)

α-UC_2, NpC_2, and PuC_2 [242]; but the cubic γ-ThC_2 has an analog in β-UC_2. A different cubic structure is found [243] for Pu_2C_3, and an arrangement of C_2 groups around each Pu atom is proposed, but this has not been experimentally verified. (See Sections 3.7.2, 5.7.3, 6.6.5 and 7.7.2.)

The silicides of the actinide elements can be grouped according to structure type as in Table 20.2. One compound, Pu_5Si_3, was studied by single-crystal methods [245], while all the others were analyzed by powder techniques. In most

cases the data indicate isomorphism with well-established structural types, which adds confidence to the conclusions that, at least, the qualitative aspects of the proposed structures are correct.

By comparing these silicide structures it is seen that, as the ratio of Si to metal increases, the role of the Si changes from that of isolated Si atoms, as in U_3Si and Pu_5Si_3, to the case where more and more Si–Si bonds are present and extensive crosslinkages occur. In U_3Si_2 these are diatomic Si_2 groups, in USi these are Si–Si–Si zigzag chains, in β-USi_2 hexagonal layers of Si atoms interleave layers of metal atoms, and in α-USi_2 there exists a three-dimensional network of Si–Si bonds. On the other hand, the distances between metal atoms (2.7–3.3 Å) are small enough to indicate metal–metal bonding in the metal-rich compounds U_3Si, Pu_5Si_3, and U_3Si_2, but are considerably longer in the other compounds in which the actinide atoms are more dilute.

20.5 PNICTIDES AND CHALCOGENIDES

Actinide elements form compounds with N, P, As, Sb, Bi, S, Se, and Te having a variety of stoichiometric ratios. Most of these have been studied by x-ray powder diffraction methods to the extent of measurement of lattice parameters and identification of the structure type adopted by each compound. Little in the way of structure determination using single crystals has been done, although suitably large specimens have been produced in several cases [248, 249], e.g. US_2, USe_2, UTe_2, USe_3, UTe_3, U_3P_4, and U_3As_4. In some instances carefully measured powder diffraction intensities were used to ascertain atomic positions. A summary of structure types exhibited by this class of compounds has been published by Lam, Darby, and Nevitt [250], and a review discussing structures and also chemical properties has been presented by Dell and Bridger [251]. Subsequently, Damien and co-workers [252–258] have characterized the pnictides and chalcogenides of many transuranic elements in detail, including a single-crystal study of $AmTe_{1.73}$ [259] (Fig. 20.8). Those structure types for which an appreciable number of examples have been identified are listed in Table 20.3; for other possibilities refs 250 and 251 should be consulted.

The nature of the bonding in these compounds is not completely understood but it is generally agreed that it is semimetallic. The subgroup exhibiting the NaCl-type structure has received the most attention from theorists, and a discussion of the band structure theory for them has been given by Davis [260], who concludes that the 5f electrons participate in the conduction at least in the early part of the actinide series. Allbutt and Dell [261] have considered the lattice parameters for many pnictides and chalcogenides having this structure and derived a set of ionic radii for the Th, U, and Pu atoms in these compounds. From these radii they deduced the charges on the ions and suggested that the remaining electrons are in conduction bands.

The atomic arrangements of the other structures listed in Table 20.3 are

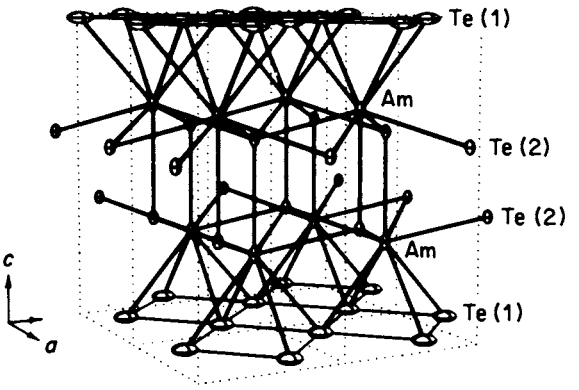

Fig. 20.8 *The layered structure of* $AmTe_{1.73}$. *(Reproduced, with permission, from ref.* 259.)

described briefly in the following, but no conclusions regarding the nature of the bonding will be attempted. The Th_3P_4 structure is cubic, and each metal atom is coordinated by a dodecahedron ($\bar{4}$ symmetry) of atoms of the other element. The Ce_2S_3 structure, exhibited only by chalcogenides, is identical to that of Th_3P_4 except that there is a random deficiency of atoms at the metal site. Some of the sesquichalcogenides prefer to crystallize in the layer-type Sb_2S_3 structure in which the metal has seven neighbors. In both the $PbCl_2$ and PbFCl structure types the metal atoms have nine nearest neighbors, but the distances vary considerably among the bonds in each compound. Among the compounds adopting the U_2N_2Sb and Ce_2O_2S structures, those containing the larger Sb, Bi, or Te atoms have the former type and those with P, As, S, or Se have the latter [262]. See Sections 3.7.3, 5.7.4, 5.7.5, 7.7.3 and 7.7.4.

20.6 HALIDES, OXYHALIDES, AND HALO COMPLEXES

The actinide halides are the most widely studied compounds of these elements from the point of view of structure determination. Indeed, along with the oxides, the halides have always been the first compounds to be prepared as new members of this series were discovered. The simplicity of the structures as well as the usually long isostructural series make it possible to obtain much information from powder diffraction data alone. Many structures were in fact deduced from such data by Zachariasen, who did not have single-crystal specimens available. Building on his original suggested structure types, extensive isomorphous series were in many cases delineated by later workers as the heavier elements became available. Eventually some, but not all, of these structures were described more quantitatively using single-crystal methods.

A comprehensive review of actinide halides and oxyhalides is found in a book

Table 20.3 *Some pnictides and chalcogenides with known structures.*

*NaCl**		*Th_3P_4**		*U_2N_2Sb**		*Ce_2S_3**	*Ce_2O_2S**	
ThN		Th_3P_4		Th_2N_2Sb	Th_2N_2Te	Ac_2S_3	$Th_2(N, O)P$	Th_2N_2S
ThP	ThS	Th_3As_4		$Th_2(N, O)_2Sb$		γ-Np_2S_3	$Th_2(N, O)As$	Th_2N_2Se
ThAs	ThSe	Th_3Sb_4		Th_2N_2Bi		γ-Pu_2Se_3	U_2N_2P	U_2N_2S
ThSb		Th_3Bi_4		$Th_2(N, O)_2Bi$		γ-Pu_2Te_3	U_2N_2As	U_2N_2Se
UN		U_3P_4				γ-Am_2S_3		Pu_2O_2S
UP	US	U_3As_4	U_3Se_4	U_2N_2Sb		γ-Am_2S_3		Pu_2O_2Se
UAs	USe	U_3Sb_4	U_3Te_4	U_2N_2Bi		γ-Am_2Te_3		Am_2O_2S
USb	UTe	U_3Bi_4			U_2N_2Te	γ-Cm_2S_3		Cm_2O_2S
UBi						γ-Cm_2Se_3		Cm_2O_2Te
NpN			Np_3S_4			Bk_2S_3		Cf_2O_2S
NpP			Np_3Se_4					
NpAs	NpS					Cf_2S_3		
NpSb		Np_3Sb_4	Np_3Te_4					
NpBi								
PuN			Pu_3S_4					
PuP	PuS		Pu_3Se_4					
PuAs	PuSe	Pu_3Sb_4	Pu_3Te_4					
PuSb	PuTe							
PuBi			Am_3Se_4					
			Am_3Te_4					
AmN								
AmP	AmS							
AmAs								
AmSb								
AmBi								
CmN	CmAs							
CmP	CmSb							
BkN	BkAs							
BkP	BkSb							
	CfAs							
	CfSb							

Table 20.3 *(Contd.)*

*Sb_2S_3**	*$NdTe_3$**	*$PbCl_2$**	*PbFCl**		*Fe_2As**		*La_2O_2Te**	
Th_2S_3	$NpTe_3$	ThS_2	$ThAs_2$	ThOS	$NpTe_2$		Pu_2O_2Sb	Am_2O_2Bi
Th_2Se_3	$PuTe_3$	$ThSe_2$	$ThSb_2$	ThOSe		$PuS_{1.9}$	Cm_2O_2Sb	Cm_2O_2Bi
	$AmTe_3$		$ThBi_2$	ThOTe		$PuSe_{1.8}$		
U_2S_3	$CmTe_3$	β-US_2				$PuTe_{1.8}$		
U_2Se_3		β-USe_2						
Np_2S_3			UP_2	UOS		AmS_{2-x}		
Np_2Se_3			UAs_2			$AmSe_{2-x}$		
η-Np_2Te_3			USb_2	UTe_2		$AmTe_{2-x}$		
			UBi_2					
Pu_2Se_3				NpOS		CmS_{2-x}		
η-Pu_2Te_3						$CmSe_{2-x}$		
η-Am_2Te_3						$CmTe_{2-x}$		
η-Cm_2Te_3								

* Structural prototypes are marked with an asterisk.

by Brown [263] and in a review by Taylor [264] that includes illustrations of many structural types. A very complete survey of the structures of fluoride complexes was made by Penneman, Ryan, and Rosenzweig [265]. In the following discussion, the emphasis will be on well-characterized structural prototypes in most cases; further details about similar compounds can be found in one of these references.

For nearly all the binary halides that have been prepared, the structure is known, and those compounds for which this is true are listed in Table 20.4. Also listed there are the references to either the latest study on each compound or else the best analysis of the prototype of that particular structure. In some instances, e.g. the $PuBr_3$ type, an isomorphous compound, $CfCl_3$, has been more precisely analyzed than the prototype. Occasionally, two different prototypic names have evolved for what is actually the same structure, e.g. $AlCl_3$ and YCl_3, $FeCl_3$ and BiI_3. In such cases a somewhat arbitrary choice has been made for the purpose of the table.

While many of the early structure determinations by x-ray powder methods have been improved by single-crystal studies, improvements in the values of unit-cell parameters alone have also been made for a number of isostructural series. Although the volumes of the unit cells in a particular series show a decrease with increasing atomic number of the actinide involved, from this fact alone it cannot be ascertained whether the contraction is isotropic or even uniform. Only in the case of the transuranic trichlorides (UCl_3 type, Fig. 20.9) has a series been studied [284–288] using single crystals in order to detect changes in atomic positions within the unit cell; here the change is definitely anisotropic (see Section 20.7).

Because the halides are highly ionic compounds, directional bonding plays little if any role in the structures that these substances assume in the solid state. The primary influences are charge and ionic size, and the coordination polyhedra are diverse. In the binary halides these factors nearly always result in the sharing of the halide ions between two or more actinide cations. This is due to the fact that the actinide ions are relatively large and require six or more anions to fill the space around them, while the cationic charge is usually less than 6. Indeed, only for the hexafluorides and hexachlorides are structures found consisting of independent octahedral molecules. Moreover, the packing of MF_6 molecules in the solid state [277] distorts them slightly from the regular octahedra found in the gas [316]. In UCl_5 there are dimeric molecules in which each U(v) has octahedral coordination and, in all the other binary halides, chains, layers or more extensive forms of crosslinking occur.

Changes in structure type that occur for a particular halide across the series of actinides are correlated with the actinide contraction and the requirement of a smaller coordination number with increasing atomic number. These may be seen in Table 20.4 and have been discussed by Brown *et al.* for the trihalides [317].

In addition to the anhydrous halides there are some adducts with well-established structures. The hexahydrates of $PuCl_3$, $AmCl_3$, $BkCl_3$, UBr_3, $NpBr_3$, $PuBr_3$, and $AmBr_3$ are isomorphous [317, 318]; all the structural details were

Table 20.4 *Binary halides with known structures.**

Ac	Th	Pa	U	Np	Pu	Am	Cm	Bk	Cf	Es
AcF_3[a] [266]			UF_3[a] [266]	NpF_3[a] [266]	PuF_3[a] [266]	AmF_3[a] [267]	CmF_3[a] [267]	BkF_3[a, b] [268]	CfF_3[a, b] [269]	
	ThF_4[c] [270]	PaF_4[c] [270]	UF_4[c] [271]	NpF_4[c] [270]	PuF_4[c] [270]	AmF_4[c] [270]	CmF_4[c] [270]	BkF_4[c] [270]	CfF_4[c] [270]	
		Pa_2F_9[d] [272]	U_2F_9[d] [273]							
			α-UF_5[e] [273]	α-NpF_5[e] [274]						
		PaF_5[f] [275]	β-UF_5[f] [276]	[276]						
			UF_6[g] [277]	NpF_6[g] [278]	PuF_6[g] [279]					
						$AmCl_2$[h] [280]				
$AcCl_3$[i] [281]			UCl_3[i] [282]	$NpCl_3$[i] [283]	$PuCl_3$[i] [284]	$AmCl_3$[i] [285]	$CmCl_3$[i] [286]	$BkCl_3$[i] [287]	$CfCl_3$[i, j] [288]	$EsCl_3$[i] [289]
	α-$ThCl_4$[k] [290]	$PaCl_4$[l] [291]	UCl_4[l] [292]	$NpCl_4$[l] [291]						
	β-$ThCl_4$[l] [293]	$PaCl_5$[m] [294]	α-UCl_5[n] [295]							
			β-UCl_5[o] [296]							
			UCl_6[p] [297]							
						$AmBr_2$[q] [280]			$CfBr_2$[r] [298]	

$AcBr_3$[i] [281]			UBr_3[i] [282]	α-$NpBr_3$[i] [283]						
	α-$ThBr_4$[k] [299]			β-$NpBr_3$[j] [283]	$PuBr_3$[j] [283]	$AmBr_3$[j] [267]	$CmBr_3$[j] [284]	$BkBr_3$[j,s] [284]	$CfBr_3$[s,t] [284]	$EsBr_3$[s] [300]
	β-$ThBr_4$[l] [291]	$PaBr_4$[l] [301]	UBr_4[u] [302]	$NpBr_4$[u] [303]						
		β-$PaBr_5$[n] [304]	UBr_5[o] [305]							
		γ-$PaBr_5$[o] [306]								
	ThI_2[v] [307]					AmI_2[w] [308]			CfI_2[x] [309]	
		PaI_3[j] [310]	UI_3[j] [311]	NpI_3[j] [283]	PuI_3[j] [283]	AmI_3[t] [267]	CmI_3[t] [267]	BkI_3[t] [312]	CfI_3[t] [313]	
	ThI_4[y] [314]		UI_4[z] [315]							

* Superior letters refer to the structure type exhibited, as follows: [a]LaF_3, [b]YF_3, [c]UF_4, [d]U_2F_9, [e]α-UF_5, [f]β-UF_5, [g]UF_6, [h]$PbCl_2$, [i]UCl_3, [j]$PuBr_3$, [k]α-$ThCl_4$, [l]UCl_4, [m]$PaCl_5$, [n]α-UCl_5, [o]β-UCl_5, [p]UCl_6, [q]$EuBr_2$, [r]$SrBr_2$, [s]$AlCl_3$, [t]$FeCl_3$, [u]UBr_4, [v]ThI_2, [w]EuI_2, [x]CdI_2, [y]ThI_4, [z]UI_4. Lattice parameters are listed in Table 14.8.

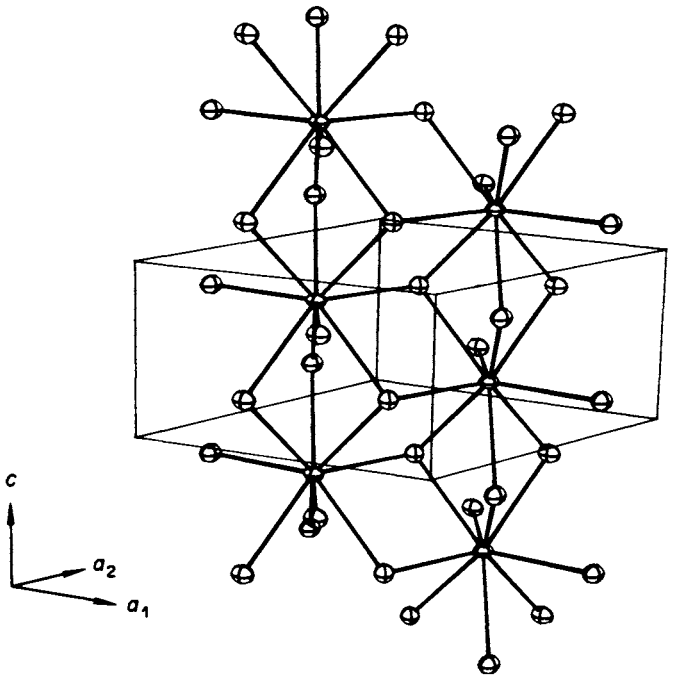

Fig. 20.9 *A portion of the structure of the UCl_3 type. Each actinide ion, M, is bonded to nine Cl ions. (Reproduced, with permission, from ref.* 285.)

established [318] for $AmCl_3 \cdot 6H_2O$. Its structure consists of $AmCl_2(H_2O)_6^+$ and $Cl(H_2O)_6^-$ ions linked by hydrogen bonds. Another case in which water replaces the halide ion in the coordination sphere of the actinide is that of $UF_4 \cdot 2.5H_2O$ [319], in which one U atom has nine F atom neighbors and another has five F atoms and four water molecules. Yet another structure having uranium in two kinds of environments is $UCl_4 \cdot 3(CH_3)_2SO$, in which one U atom has a dodecahedron of O atoms and another has an octahedron of Cl atoms [320]. In the structure of $ThCl_4 \cdot 4(C_6H_5)_2SO$, however, all Th atoms have the same eight-fold coordination, four Cl atoms and four O atoms from the diphenylsulfoxide [321]. Some adducts of UCl_4 with oxygen and nitrogen donor molecules have a planar UCl_4 group with donor atoms *trans* to it. Examples of these are $UCl_4\{[(CH_3)_2N]_3PO\}_2$, $UBr_4\{[(CH_3)_2N]_3PO\}_2$ [322], $UCl_4\{[(CH_3)_2NC_6H_5]PO\}_2$ [323], and $UCl_4[OAs(C_2H_5)_3]_2$ [324]. A quite different (seven-fold) coordination exists in $UCl_4[(CH_3)_3PO]_6$ where there are $UCl[(CH_3)_3PO]_6^{3+}$ and Cl^- ions [325]. In the case of $UCl_4[(C_6H_5)_3PO]_2$ the neutral molecules are *cis* on the UCl_4O_2 octahedron [326], while in the similar $UCl_4[(C_6H_5)_3PO]$ one of the neutral molecules is replaced by a Cl^- ion since the uranium is pentavalent [327]. A similar octahedral grouping occurs in the UCl_5O^- ion of $[(C_6H_5)_4P]UCl_5O$ [328]. Symmetrical octahedral ions are also found in the phosphonium hexahalo salts of U(IV) and U(VI); among

these are $[(C_6H_5)_3C_7H_7P]UCl_6$ [329], $[(C_6H_5)_3C_2H_5]_2UCl_6$, and $[(C_6H_5)_3C_2H_5]_2UBr_6$ [330].

Many of the simple oxyhalides have been characterized as to structure type by x-ray powder methods, but only a few complete structural analyses have been done. Table 20.5 summarizes the actinide oxyhalides whose structures are known. A wide variety of compounds adopt the PbFCl arrangement in which the metal atom has as neighbors four oxygen and five halide atoms. It is surprising that cations ranging in size from Ac^{3+} down to Es^{3+} and anions from Cl^- to I^- can all exist in this configuration. The variation in M–O distances that may accompany these wide changes in ionic sizes is not known, because two-thirds of the atoms in the structure type have variable positional parameters, and none of them have ever been ascertained. Probably the bonds to oxygen are similar to those in $PaOCl_2$, which has been determined, and its analogs.

A careful analysis of $PaOCl_2$ has been made, and it was found to exhibit a complicated polymeric network. In it, three different coordinations for the metal atom are found containing, respectively, seven, eight, and nine anions (Fig. 20.10(a)). Observation of this feature led to the suggestion that different valences might be involved, but the later discovery of other compounds with this same structure, especially $ThOCl_2$, $ThOBr_2$, and $ThOI_2$, is evidence to the contrary.

Two oxyhalide compounds of pentavalent Pa have been elucidated (Fig. 20.10(b) and (c)). In $PaOBr_3$, chains of Pa atoms are linked by bridging Br atoms and crosslinked by O atoms similarly to the Pa–O bonding in $PaOCl_2$. But in

Table 20.5 *Structures of oxyhalides.*

Compound	*Prototype*	*Ref.*	*Compound*	*Prototype*	*Ref.*
AcOCl	PbFCl	266	$ThOF_2$	LaF_3	266
AcOBr	PbFCl	266	$ThOCl_2$	$PaOCl_2$	337
NpOCl	PbFCl	283	$PaOCl_2$	$PaOCl_2$	338
NpOBr	PbFCl	283	$UOCl_2$	$PaOCl_2$	339
NpOI	PbFCl	283	$NpOCl_2$	$PaOCl_2$	337
PuOCl	PbFCl	266	$ThOBr_2$	$PaOCl_2$	337
PuOBr	PbFCl	266	$PaOBr_2$	$PaOCl_2$	337
PuOI	PbFCl	266	$UOBr_2$	$PaOCl_2$	337
AmOCl	PbFCl	331	$NpOBr_2$	$PaOCl_2$	337
CmOCl	PbFCl	332	$ThOI_2$	$PaOCl_2$	337
BkOCl	PbFCl	333	$PaOI_2$	$PaOCl_2$	337
CfOCl	PbFCl	334	UOI_2	$PaOCl_2$	337
EsOCl	PbFCl	335	$NpOI_2$	$PaOCl_2$	337
BkOBr	PbFCl	312	$NpOF_3$	NpO_2F_2	340
CfOBr	PbFCl	313	$PaOBr_3$	$PaOBr_3$	304
BkOI	PbFCl	312	Pa_2OF_8	U_2F_9	341
CfOI	PbFCl	313	Pa_3O_7F	hex-U_3O_8	341
AcOF	CaF_2	266	α-UOF_4	UOF_4	342
PuOF	CaF_2	266	β-UOF_4	β-UF_5	343
CfOF	CaF_2	336	UO_2Br	UO_2Br	344

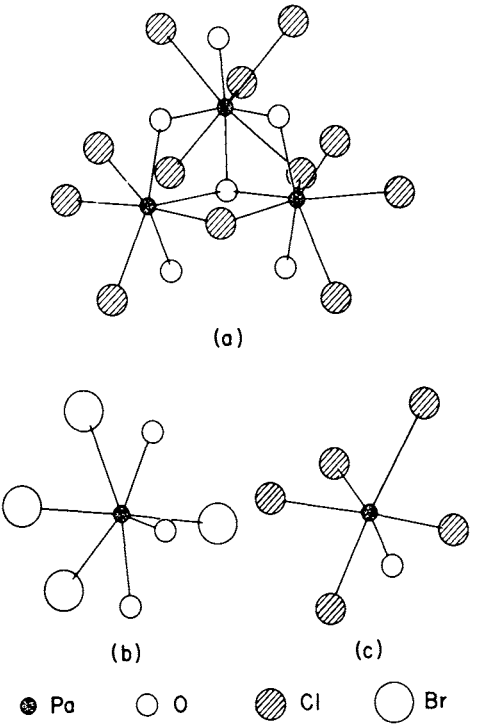

Fig. 20.10 *Different coordination geometries of three oxyhalide compounds of protactinium:* (*a*) $PaOCl_2$, (*b*) $PaOBr_3$, *and* (*c*) $[(C_2H_5)_4N]_2PaOCl_5$. (*After refs* 337, 304, *and* 345.)

$(C_2H_5N)_2PaOCl_5$ [345], in which the Pa is octahedrally coordinated by five Cl atoms and one O atom, the short Pa–O bond (1.74 Å) is suggestive of a double bond. Another oxyhalide in which there is a single, short bond to oxygen is UOF_4; there the U–O distance is about 1.78 Å [342].

A large number of complexes involving the actinide and alkali halides have been prepared and many studies of structure have been made. The majority of these are with fluoride and a comprehensive listing of these and their structures, where known, has been made by Penneman *et al.* [265]. These authors have also given some empirical principles that govern the type of structure achieved under various conditions of ionic size, charge, and stoichiometry. Coordination numbers of fluoride ions for the various actinides in these complexes range from 6 to 10. Selected examples illustrative of each number and configuration are given in the following, using well-characterized structures.

In $CsUF_6$ [346], $CsNpF_6$ [347], and $CsPuF_6$ [348] the actinide atoms are symmetrically surrounded by octahedra of fluorine atoms slightly elongated about a three-fold axis [265]. These octahedra are shared by each Cs atom to give it coordination 12. Octahedra containing U(v) also exist in complexes with Na

and Li, i.e. $LiUF_6$ [349] and α-$NaUF_6$ [350]. In these, the arrangement is such as to give these small alkali atoms coordination 6 (the $LiSbF_6$ structure type [351]). Actinide ions of lower valence are all sufficiently larger as to require greater coordination numbers.

Coordination 7 of actinide ions by fluoride ions appears in two forms. One is the trigonal prism with one of its rectangular faces capped by an additional atom; it is epitomized by the ion in the K_2NbF_7 structure, which was refined using neutron diffraction by Brown and Walker [352]. The compounds having this structure and containing pentavalent actinides are K_2UF_7, Rb_2UF_7, $(NH_4)_2UF_7$, Cs_2UF_7 [349], Rb_2PuF_7 [348], and Rb_2NpF_7 [347]. The other form assumed by seven fluoride ions is the pentagonal bipyramid; it is found in K_3UF_7 [353].

The coordination polyhedra formed by eight ligands are generally one of three types: cube, antiprism, and dodecahedron. For a particular ligand and a given radius of the central atom, the cube is the least stable configuration on electrostatic grounds, while the antiprism and dodecahedron are of approximately equal stability [354]. Because in crystals the polyhedra are not isolated but subject to influences of neighbors, these ideal polyhedra are usually only an approximation to the real configuration. Some quantitative criteria have been derived [355] for assigning the proper name when distortions from ideality are large, but usually the name is assigned only for descriptive convenience and has no intrinsic significance.

Examples of dodecahedral coordination are found in K_5ThF_9 [356], in which these polyhedra are isolated (i.e. they do not share fluorine atoms with other dodecahedra containing Th atoms), and in Rb_2UF_6 [357] and $RbPaF_6$ [358], in which dodecahedra share edges to form chains. In $(NH_4)_4UF_8$ are found [359] isolated polyhedra that are intermediate between the dodecahedron and the antiprism. The ease with which a particular coordination 8, for example UF_8, can adopt either of these two configurations is illustrated by comparison of the structure of α-$(NH_4)_2UF_6$ [360], which contains chains of antiprisms, with that of Rb_2UF_6 mentioned above. Yet another structure in which the actinide atoms are surrounded by antiprisms of fluorine atoms is that typified by $Na_7Zr_6F_{31}$ [361] and $K_7Th_6F_{31}$ [362] and adopted by various complexes of NaF, KF, RbF, and NH_4F with tetravalent actinides ranging from Th to Cf (see ref. 361 for a partial list). In this unusual arrangement, six antiprisms share corners to form a cuboctahedral cavity in which a lone (disordered) fluorine atom is situated. This atom plus an alkali atom in another cavity give rise to the deviation of the MF_4:XF ratio from 1:1.

For actinide ions having a radius in the range of 0.9–1.0 Å, coordination by nine fluoride ions is quite common. A number of structures in which this is true are listed in Table 20.6. Because ionic size is the important factor in yielding this coordination number, valences can range from 3 to 5, and the actinide elements involved can range from Pa to Am. In Li_3ThF_7 the F ions form a square antiprism with a pyramid on one face, but in all the other crystals listed the nine F neighbors

Table 20.6 *Structures having nine-fold fluoride coordination.*

Compound	*Ref.*	*Compound*	*Ref.*
pentavalent		$NaKThF_6$	372
K_2PaF_7	363	Li_3ThF_7	373
Cs_2PaF_7	364	$(NH_4)_4ThF_8$	374
		Li_4UF_8	375
tetravalent			
$LiUF_5$	365	$NH_4U_3F_{13}$	376
$TlUF_5$	366	CsU_6F_{25}	377
β-NH_4UF_5	367	α-KTh_6F_{25}	378
δ-Na_2UF_6	368	$Na_3BeTh_{10}F_{45}$	379
KU_2F_9	369	$CdTh(MoO_4)_3$	380
CsU_2F_9	370	$Na_3ZnTh_6F_{29}$	381
$CaMF_6$	371		
		trivalent	
(M = Th, U, Np, Pu)		$NaPuF_4$	382

of each actinide ion comprise a trigonal prism capped on its rectangular faces. In four of these compounds, $NaPuF_4$, $NaAmF_4$, β_1-K_2UF_6, and $NaKThF_6$, the actinide ion is at a site in the crystal whose point symmetry requires the tricapped trigonal prism to be regular, but in the others this idealized polyhedron is only an approximation. It is curious that the U ions in CsU_2F_9 and in KU_2F_9 have this same polyhedron of F ions even though (1) the structures are entirely different because of different sizes in the Cs and K ions, and (2) in the former structure this shape is achieved only by the existence of half-occupied F sites. Of course when the coordination becomes high and the demands of crystal symmetry are low (isotropic environment in the limit), the description in terms of an idealized polyhedron becomes less meaningful.

There is at present one well-established 10-coordinate fluoro complex of Th. It is $(NH_4)_7Th_2F_{15}\cdot H_2O$ [383] and contains a large dimeric unit containing two Th atoms triply bridged by F atoms. Six other F atoms are attached to each Th atom, and the tenth site is occupied by a water molecule on one Th atom and an NH_4 group on the other.

There are three well-established crystal structures of complexes involving actinide chlorides and cesium chloride, yet in each the actinide ion has an octahedral chloride ion environment and the cesium ion has 12 chloride neighbors. Zachariasen was the first to elucidate one of these, and he observed [384] that Cs_2PuCl_6 has the same structure as K_2GeF_6. Subsequently several other complexes containing tetravalent actinides in this same configuration were prepared; these are Cs_2PaCl_6 [385], Cs_2ThCl_6 [386], Cs_2UCl_6 [386], and Cs_2NpCl_6 [387]. The hexachlorometallate ion is not perfectly regular in these trigonal crystals but has a small axial distortion. A different crystalline arrangement of Cs^+ and MCl_6^- ions exists in Cs_2BkCl_6 [388], which adopts the hexagonal Rb_2MnF_6 type of structure. Trivalent actinides also exhibit the MCl_6

configuration as is seen in $Cs_2NaPuCl_6$ [389], $Cs_2NaAmCl_6$ [390], and $Cs_2NaBkCl_6$ [388], all of which crystallize in the cubic K_2NaCrF_6 type of structure [389, 391]. In this case both the Na^+ and M^{3+} ions are at sites of O_h symmetry, making the chloride octahedra truly regular. $CsUCl_6$ also appears to have O_h symmetry [543].

A series of crystalline compounds of substituted ammonium hexachloro- and hexabromoprotactinates(IV), thorates(IV), uranates(IV), plutonates(IV), and neptunates(IV) have been prepared and examined by x-ray powder diffraction methods, for which some structural details are available [392], as well as for Cs_2UBr_6 and Cs_2NpBr_6, which are cubic [393].

20.7 IONIC AND METALLIC RADII

The ionic radius is a useful parameter with which to correlate numerous physical and thermodynamic properties of the actinide elements. Its usefulness for this purpose is not usually dependent on how it is defined or on the absolute values that are used when comparing members of the series. Nevertheless, the term 'radii' implies spherical ions, and the modes of deriving such radii from crystallographic data usually assume that these spheres are in contact with spherical anions. When this assumption is not true, as in most real crystals, the derived radii depend on the method of calculation and are somewhat arbitrary. Consequently, there have been published for the actinide elements several tables of radii which differ both in absolute values and in the slope of the curve obtained when they are plotted against atomic number. All of these sets of radii have in common, however, two qualitative features: a contraction of the radius with increasing atomic number and a cusp at the half-filled 5f-electron shell. Additional perturbations of the curve at the one-fourth- and three-fourths-filled shells have not been established for the actinides, although slight effects were shown to exist for the lanthanides [394]. Detection of this 'tetrad effect' may be impossible for the actinides, because the interelectronic-repulsion-stabilization energy to which the effect is attributed [395] is smaller for the 5f than for the 4f elements.

In Table 20.7 are listed radii of trivalent actinide ions (coordination number CN 6) derived from measurements on trichlorides by the method of Burns, Peterson, and Baybarz [288]. Determinations of M–Cl distances have been made for M = U, Pu, Am, Cm, and Cf; the other values were estimated by use of unit-cell data and curve fitting. All these radii are relative to the trivalent lanthanide radii of Templeton and Dauben [396], who employed data from cubic sesquioxides and assumed atomic positions to establish M–O distances. Also included in Table 20.7 are radii of tetravalent actinide ions obtained from the M–O distances calculated from unit-cell parameters of the dioxides [1] by subtracting 1.38 Å for oxygen (the value used [396] for the sesquioxides). For comparison, Shannon's ionic radii, derived from oxides and fluorides, and Peterson's tetravalent radii, derived from dioxides, are shown [537, 538]. As

Table 20.7 *Ionic radii.*

	Radius (M^{3+}) (CN 6) (Å)		*Radius* (M^{4+}) (CN 8) (Å)		
M	*Ref.* 288	*Ref.* 537	*Ref.* 1[a]	*Ref.* 537	*Ref.* 538
Ac	1.119	1.12	–	–	–
Th	–	–	0.972	1.05	0.985
Pa	–	–	0.935	1.01	0.945
U	1.041	1.025	0.918	1.00	0.930
Np	1.017	1.01	0.903	0.98	0.915
Pu	0.997	1.00	0.887	0.96	0.895
Am	0.982	0.975	0.878	0.95	0.89
Cm	0.970	0.97	0.871	0.95	0.88
Bk	0.949	0.96	0.860	0.93	0.87
Cf	0.934	0.95	0.851	0.92	0.86
Es	0.925	–	–	–	–

[a] See text.

expected, different sets of radii (for the same oxidation state and coordination number) differ only by a constant.

For actinide valences of 5 and 6, there are not many measurements of bond lengths available other than for uranyl compounds. The structures of several complex fluorides of Pa(v) have been well-determined, but in them the symmetries of the coordination polyhedra are low and assignment of a radius to Pa(v) is not reasonable. One exception is Na_3PaF_8 [397], in which the Pa atom has a cubic environment of F atoms at a bond distance of 2.21 Å. In isomorphous Na_3UF_8 and Na_3NpF_8 the U–F and Np–F distances are estimated to be 2.21 and 2.19 Å, respectively. If the ionic radius of fluorine is subtracted, a radius for the pentavalent cation, for example U(v), of 0.77 Å is obtained. Applying the same type of calculation using measured bond lengths for the octahedra in $CsUF_6$ [346] and in UF_6 [277], radii of U(v) and U(vi) of 0.70 and 0.62 Å are obtained. There is a significant and variable amount of covalent bonding with these higher valence states, as is seen in their tendency to form actinyls, and the concept of ionic radii loses its applicability to these compounds. Hence the greatly different radii derived above for U(v). The only bond length available for a heptavalent actinide is that in the $[NpO_4(OH)_2]^{3-}$ group (Fig. 20.11) where Np–O distances of 1.85 and 1.96 Å were reported [398]; these are believed to be as covalent as the familiar actinyl bonds.

Because the trivalent state exists for all the lanthanides and most of the actinides, variations in chemical properties with ionic radius are often compared for the two series. In general, those changes in crystal structure or other properties that depend on ionic size occur two elements earlier in the 4f series than in the 5f series. This is because the trivalent ion with a particular number of 5f electrons is larger, by about 0.03 Å in the transuranic region, than the trivalent ion with an equal number of 4f electrons.

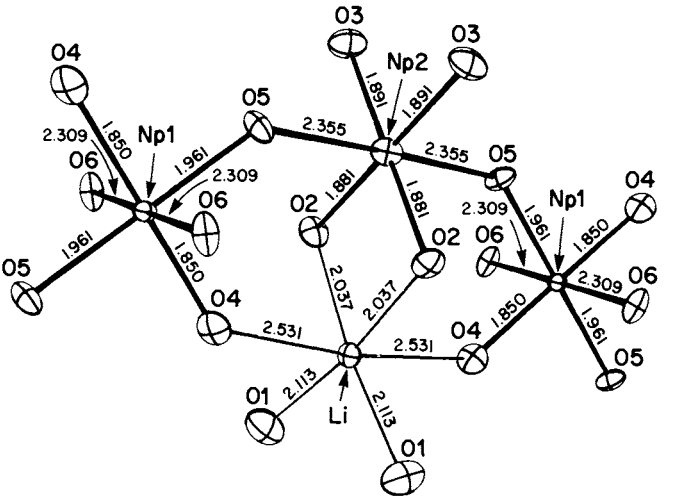

Fig. 20.11 *Shared* $[NpO_4(OH)_2]^{3-}$ *ions in the structure of* $LiCo(NH_2)_6Np_2O_8(OH)_2 \cdot 2H_2O$. *(Reproduced, with permission, from ref.* 398, *copyright by the American Chemical Society.)*

The metallic radius is defined as one-half the bond length in the first coordination sphere of the metal structure. Because the radius varies with the number of nearest neighbors, the measured values are usually adjusted to the CN 12 of closest-packed structures. In cases where the symmetry is low and bond lengths vary over a range, a radius can be derived by use of atomic volumes instead of individual bond lengths. Zachariasen [399] has used this method in deriving the set of metallic radii in Table 20.8 from crystallographic data on actinide metals. There is disagreement as to the metallic valences that are to be inferred from these radii; this has been discussed elsewhere [399, 400].

20.8 CARBONATES, NITRATES, PHOSPHATES, ARSENATES, AND SULFATES

The common structural feature of these compounds is that the anions all provide oxygen atoms which surround the actinide cation in each case. The number of such coordinating oxygen atoms ranges from eight to 12 for Th(IV) and is usually eight or nine for the heavier elements, although it is as low as six in a few structures containing the uranyl group. The relatively large coordination numbers usually involve bidentate ligation with the pair of oxygen atoms close together because of being bonded to a common atom of the anion, as in NO_3^- or PO_4^{3-}.

Few structures of actinide carbonates have been determined and all of these contain the actinyl group, MO_2. This linear, triatomic group in each case forms

Table 20.8 *Metallic radii* [399].

Element	*Radius* (Å)	*Element*	*Radius* (Å)	*Element*	*Radius* (Å)
Ac	(1.878)	α-Np	1.503	α-Am	1.730
		β-Np	1.511	β-Am	1.730
α-Th	1.798	γ-Np	1.53		
β-Th	1.80			α-Cm	1.743
		α-Pu	1.523	β-Cm	1.782
α-Pa	1.642	β-Pu	1.571		
β-Pa	1.775	γ-Pu	1.588	α-Bk	1.703
		δ-Pu	1.640	β-Bk	1.767
α-U	1.542	δ'-Pu	1.640		
β-U	1.548	ε-Pu	1.592	α-Cf	1.69[a]
γ-U	1.548			β-Cf	1.75[a]
				γ-Cf	2.03[a]

[a] From ref. 401.

the axis of a hexagonal bipyramid in which oxygen atoms of CO_3^{2-} ions are arrayed about the equator. In the structure typified by $KPuO_2CO_3$ [54, 55] and $K_4NpO_2(CO_3)_3$ [59, 202, 402] (Fig. 20.12), three CO_3^{2-} ions act as bidentate ligands, and in UO_2CO_3 [403, 183] the hexagon involves two bidentate CO_3^{2-} ions and two that are monodentate. The length of the M=O actinyl bond has been found to have widely differing values in UO_2CO_3, where it is 1.67(9) Å, and in $(NH_4)_4UO_2(CO_3)_3$, [58] where it is 1.79 Å. Because the hexagonal–bipyramidal environment of the U atom in these two structures is quite similar, it is unlikely that the bond lengths really differ by that much. Interatomic distances between actinides and light atoms, when determined by x-ray diffraction, are often subject to systematic errors and are not necessarily reliable unless done with counter diffractometer methods and adequate attention to absorption effects. In the case of $K_4NpO_2(CO_3)_3$ such techniques were used, and the Np=O bond length was determined [59] to be 1.776(5) Å.

The actinide nitrates whose structures are known are listed in Table 20.9, and a review of actinide complexes has been published by Casellato *et al.* [413]. These are limited mainly to tetravalent Th and to uranyl complexes. In the Th(IV) and Pu(IV) compounds the NO_3^- ions are bidentate, which allows for large coordination numbers compared to the usual eight-fold coordination of these ions with monodentate ligands. In the uranyl complexes the two close actinyl oxygen atoms limit the available space for other bonded atoms, and the maximum number of equatorial oxygen atoms is six, even for bidentate NO_3^- ions. In $Cs_2UO_2(NO_3)_4$ all four NO_3^- ions are attached to the U atom even though space allows only two of them to be bidentate.

In Table 20.10 are listed the actinide phosphate and arsenate compounds whose structures have been determined. All of these structures involve the tetrahedral XO_4^{3-} ion in mono- and bidentate linkages to actinide ions.

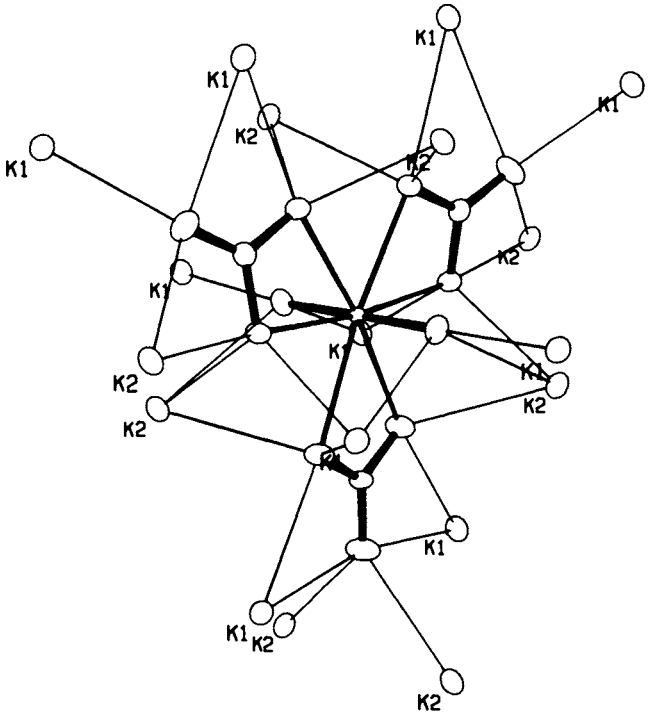

Fig. 20.12 *Structure of $K_4NpO_2(CO_3)_3$ showing three CO_3^{2-} ligands around the equator of an NpO_2^+ ion.*

In the series of compounds of the type $MPO_4 \cdot (0–0.5)H_2O$, there are four monodentate and two bidentate tetrahedra linked to the metal, forming a hexagonal network with open, oxygen-lined channels that hold zeolitic water. When this water is driven out by high temperature, a different, more dense, structure is obtained which is isomorphous with the mineral monazite. The metal atom retains its same oxygen coordination number.

Pyrophosphates form two modifications: the orthorhombic β form is not known in detail, but the cubic α-UP_2O_7 has been elucidated. In it the tetravalent actinide is bonded to six oxygens of the ditetrahedral $P_2O_7^{4-}$ ion.

A number of uranyl complexes of phosphates and arsenates are found as minerals. These comprise the torbernite and metatorbernite groups, in which the latter has a much lower water content. The general composition is $A(UO_2)_2(XO_4)_2 \cdot nH_2O$, in which A is Cu, Ca, Ba, or Mg and X is P or As. The structure of autunite, $Ca(UO_2)_2(PO_4)_2 \cdot (10–12)H_2O$, was determined and the other members of the torbernite group are isomorphous with it. The linear UO_2 portion has an equatorial square of oxygen atoms belonging to four different PO_4 tetrahedra.

In $KTh_2(PO_4)_3$ and isomorphous $NaTh_2(PO_4)_3$ an arrangement of nine

Table 20.9 *Actinide nitrates.*

Compound	*Number of oxygen atoms coordinated to the actinide*	*Ref.*
$MTh(NO_3)_6 \cdot 8H_2O$ (M = Mg, Co, Ni, Zn)	12	404
$[(C_6H_5)_4P]Th(NO_3)_5 \cdot [(CH_3)_3PO]_2$	12	405
$Th(NO_3)_4 \cdot 5H_2O$	11	406, 407
$Pu(NO_3)_4 \cdot 5H_2O$	11	408
$Th_2(NO_3)_6(OH)_2 \cdot 8H_2O$	11	409
$Th(NO_3)_4 \cdot 2.67[(CH_3)_3PO]$	10, 12	405
$Th(NO_3)_4 \cdot [(C_6H_5)_3PO]_2$	10	410
$UO_2(NO_3)_2 \cdot 2H_2O$	8	186
$UO_2(NO_3)_2 \cdot 3H_2O$	8	187
$UO_2(NO_3)_2 \cdot 6H_2O$	8	188
$NpO_2(NO_3)_2 \cdot 6H_2O$	8	189
$UO_2(NO_3)_2 \cdot (C_4H_8O)_2$	8	190
$[UO_2(NO_3)_2 \cdot H_2O]_2 \cdot (C_3H_4N_2)_2$	8	192
$RbUO_2(NO_3)_3$	8	196
$CsUO_2(NO_3)_3$	8	197
$M_2UO_2(NO_3)_4$ (M = $(C_2H_5)_3N$, NH_4, Rb, Cs)	8	198
$UO_2(NO_3)_2 \cdot [(C_2H_5O)_3PO]_2$	8	411
$UO_2(NO_3)_2 \cdot [(C_6H_5)_3XO]_2$ (X = P, As)	8	191
$(C_2H_5NH_2CO_2)_2UO_2(NO_3)_2$	8	412
$UO_2(NO_3)_2[CO(NH_2)_2]_4 \cdot H_2O$	7	170
$[(NH_2)_2CO]_5UO_2(NO_3)_2$	7	169
$[(C_2H_5)_4N]UO_2[(C_6H_5)_2C_3HO_2]_2NO_3$	7	147

oxygen atoms of low symmetry involves three PO_4 edges and three PO_4 corners. Dimeric ions are formed by the sharing of two PO_4 tetrahedra in a 2:1 fashion.

Several sulfates of tetravalent Th and U have been analyzed crystallographically. Since the size of these actinide ions is such as to require a coordination of eight or nine oxygen atoms, the number of tetrahedral sulfate ions available stoichiometrically can only partly fill this need; additional oxygen atoms in the form of water or hydroxyl ions are usually present in the structure. A square antiprism of oxygen atoms, from four monodentate sulfate ions and four water molecules or hydroxyl ions, is the common coordination polyhedron about Th^{4+} and U^{4+} ions in these compounds: $Th(OH)_2SO_4$ [428], $U(OH)_2SO_4$ [429], $U(SO_4)_2 \cdot 4H_2O$ [430], and $U_6O_4(OH)_4(SO_4)_6$ [431]. In the last of these, six uranium atoms and their antiprisms of oxygen atoms form a cuboctahedron. These large cations are linked together by sharing oxygen atoms of the exterior sulfate groups. The cuboctahedral arrangement is identical to that in $Na_7U_6F_{31}$ [361], in which an additional F ion occupies the cavity within the cuboctahedron. Whether an extra ion is present in the sulfate compound cannot be determined from the data used. In $K_4Th(SO_4)_4 \cdot 2H_2O$ [432] the inner coordination sphere

Table 20.10 *Actinide phosphates and arsenates.*

Compound	*Number of oxygen atoms coordinated to the actinide*	*Ref.*
$AcPO_4 \cdot (0–0.5)H_2O$	8	414, 415
$PuPO_4 \cdot (0–0.5)H_2O$	8	415, 416
$AmPO_4 \cdot (0–0.5)H_2O$	8	415, 417
$PuPO_4$	8	416, 418
$AmPO_4$	8	417
α-ThP_2O_7	6	419
α-UP_2O_7	6	420
α-NpP_2O_7	6	417
α-PuP_2O_7	6	416
torbernite minerals:		
$A(UO_2)_2(XO_4)_2 \cdot nH_2O$, A = Cu, Ca, Ba, Mg; X = P, As; n = approx. 8–12	6	421, 422
metatorbernite minerals:		
$n = 2\frac{1}{2}$–8	6	421
synthetic torbernites:		
A = H, Li, Na, K, NH_4, Mg, Ca, Ba, Sr	6	423, 424
$ANpO_2XO_4 \cdot nH_2O$, A = H, Li, Na, K, NH_4; X = P, As; n = 3–4.	6	425
$A(NpO_2XO_4)_2 \cdot nH_2O$, A = Mg, Ca, Sr, Ba; X = P, As; n = 6–10	6	425
$NH_4AmO_2PO_4 \cdot 3H_2O$	6	426
$KTh_2(PO_4)_3$	9	427
$NaTh_2(PO_4)_3$	9	427
$PuAsO_4$	8	417
$AmAsO_4$	8	417

contains nine oxygen atoms; seven belong to sulfate ions, one of which is bidentate, and two to water molecules.

Among the uranyl complexes listed in Table 20.1 there are about a dozen containing the sulfate ion. In each of these the central configuration is a pentagonal bipyramid in which those SO_4^{2-} ions involved are always monodentate. Frequently, however, these tetrahedral ions link two or three bipyramids together, forming layers or chains. An unusual feature of the β-UO_2SO_4 structure is that one of the apical uranyl O atoms is also an equatorial ligand in an adjacent bipyramid.

The only transplutonium sulfate complex elucidated thus far is $Am_2(SO_4)_3 \cdot 8H_2O$ [433]. Since the Am^{3+} ion is about the same size as the Th^{4+} and U^{4+} ions, it is not surprising that it has the same eight-fold coordination as the hydrated and basic sulfates discussed above (Fig. 20.13). In this compound the Am^{3+} ion is coordinated by four sulfate oxygen atoms and four water molecules. The same structure exists for a range of lanthanide elements from Pr to Sm. A different structure, involving nine-fold coordination of the metal, is

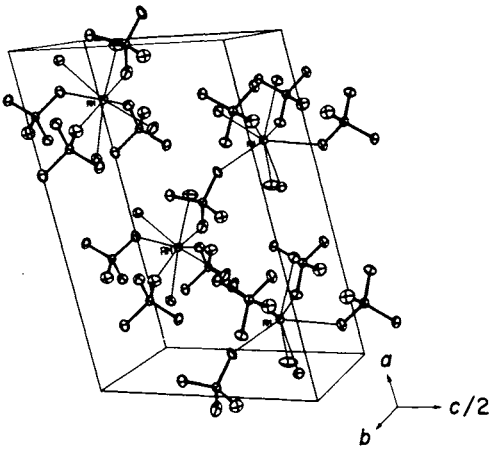

Fig. 20.13 *One unit cell of the structure of* $Am_2(SO_4)_3 \cdot 8H_2O$. *The tetrahedral groups are* SO_4^{2-} *ions and the separate atoms linked to the Am atom are O atoms of water molecules. (Reproduced, with permission, from ref.* 433, *copyright by the American Chemical Society.)*

exhibited by the larger lanthanides (La–Tb) and by U(III); it is typified by $(NH_4)U(SO_4)_2 \cdot 4H_2O$ [434]. Here the U atom is surrounded by two bidentate and two monodentate SO_4^{2-} ions plus three H_2O molecules.

20.9 CARBOXYLATES AND THIOCARBAMATES

In addition to the carboxylates discussed in Section 20.3 on actinyl complexes there have been structural analyses of a number of carboxylates of trivalent and tetravalent actinides. Thorium and uranium tetraacetates are isostructural [435]. A single-crystal structure determination [436] of the latter has shown it to be polymeric and to have the metal atom coordinated by 10 oxygen atoms arranged as a square antiprism capped on the square faces. A somewhat more regular bicapped square antiprism is found [437] in $K_4Th(C_2O_4)_4 \cdot 4H_2O$. Here, even though H_2O molecules are present, the 10-fold coordination is made up entirely of oxalate groups, two of which are quadridentate. The H_2O molecules play only the secondary role of linking together chains of antiprisms. In the glycollate of U(IV), however, discrete molecules of $U(C_2H_3O_2)_4 \cdot 2H_2O$ have two water molecules as an integral part of the bicapped square antiprism [438].

Oxalates of the trivalent actinides are important in separation chemistry, and their structures have received some attention. X-ray powder diffraction studies of the oxalates of Pu [439] and Am [440] have shown them to be isomorphous with the lanthanide analogs, while the oxalate of Cm that was made did not give useful diffraction patterns [441]. All of these oxalates have the nominal composition $M_2(C_2O_4)_3 \cdot 10H_2O$ (M = lanthanide or actinide element), but the degree of hydration has been shown to vary somewhat depending on the method of

preparation. This variability results from the manner in which some of the water molecules are held in clathrate cages formed by other fixed H_2O molecules of the crystal [442, 443]. The trivalent metals are themselves nine-coordinated by three water molecules and three bidentate oxalate groups. These oxygen atoms form a trigonal prism capped on its rectangular faces.

The salicylate complex $(C_7H_5O_3)_3Am \cdot H_2O$ has each Am^{3+} ion bonded to O atoms from six salicylato ions plus a water molecule to achieve a nine-fold coordination [444]. There are no discrete molecules but extensive crosslinking through phenolic and carboxylic O atoms.

Bonding between sulfur and the actinide elements is found in diethylthiocarbamate (DTC) complexes. Bagnall *et al.* [445] prepared $Th(DTC)_4$, $U(DTC)_4$, $Np(DTC)_4$, and $Pu(DTC)_4$ and found them isomorphous, after which Brown *et al.* [446] determined the structure of $Th(DTC)_4$ in detail. In it the thorium atom is coordinated by eight sulfur atoms in a configuration between an ideal antiprism and an ideal dodecahedron. In a study of $[(C_2H_5)_4N]Np(DTC)_4$ by Brown *et al.* [447], the trivalent neptunium atom was found also to be eight-coordinated by sulfur atoms; in this case the configuration is described as a highly distorted dodecahedron. The one diethylcarbamato complex of U(IV) that has been studied forms a tetramer, $U_4O_2[O_2CN(C_2H_5)_2]_{12}$, in which the U atoms are eight-coordinated [448].

The uranyl ion also can be bonded to the sulfur atoms of the DTC group. In $[(CH_3)_4N]UO_2(DTC)_3$ [204] the six sulfur atoms are linked equatorially to the UO_2^{2+} group; and in two isomorphous complexes, $UO_2(DTC)_2 \cdot (C_6H_5)_3AsO$ and $UO_2(DTC)_2 \cdot (C_6H_5)_3PO$, the equatorial position is occupied by four sulfur atoms from two DTC groups and one oxygen of the adduct ligand [175]. In a structurally analogous compound of the diethylmonothiocarbamate, $(C_2H_5)_2NH_2\{UO_2[(C_2H_5)_2NCOS]_2OC_2H_5\}$, two S atoms are replaced by O atoms and the adduct ligand is ethoxy [174].

20.10 CHELATES AND MOLECULAR COMPLEXES

The chelate complexes formed by acetylacetone (pentane-2,4-dione, PD) with tetravalent actinides crystallize in two modifications [449]. In the α form, which is exhibited by the $Th(PD)_4$ and $U(PD)_4$, the eight ketonic O atoms form a dodecahedron around the metal atom; and in the β form, also adopted by these compounds and by $Pa(PD)_4$ [450], $Np(PD)_4$, and $Pu(PD)_4$, the arrangement of O atoms is antiprismatic. In each modification there are discrete $M(PD)_4$ molecules, and the four PD ligands are each planar and attached in a bidentate fashion to the metal. The same arrangement is adopted in $Th(PD)_4 \cdot \frac{1}{2}(C_6H_6)$ [451], but in the trifluorinated species, $Th(CF_3C_4H_4O_2)_4 \cdot H_2O$, the water is included to make coordination 9 [452].

Several PD chelates with the uranyl ion have been made. In these, two PD ligands are attached equatorially in a bidentate fashion, and a fifth equatorial site

contains an O atom from either H_2O [136], another (monodentate) PD molecule [137], or any of several ketoamines [138–141].

The bulkier ligand 1,3-diphenylpropane-1,3-dione (DPPD) also forms chelates with Th, U [453], and Pa [450] in which the metal is bonded to eight O atoms. The polyhedron that they comprise is described as a bisdisphenoid. Studies of the proton magnetic resonance of $Th(DPPD)_4$ and $U(DPPD)_4$ led to the conclusion [454] that the f orbitals of these actinides are involved to a small extent in the bonding. This same ligand also can be attached to a uranyl ion. A pentagon of O atoms from two DPPD ligands and a monodentate nitrate ion surrounds the uranyl equator in $[(C_2H_5)_4N]UO_2(DPPD)_2(NO_3)$ [147].

Chelates also have been made with phenyltrifluoroacetylacetone, $U(C_{10}H_6F_3O_2)_4$ [455], and with salicylaldehyde, $Th(C_7H_5O_2)_4$ [456]. These have similar dodecahedral configurations about the tetravalent ions.

Little is known about compounds of the type $M(PD)_3$, where M is a trivalent actinide, except for the unit cell of $Pu(PD)_3$ [450]; but similar compounds in which the PD has all its terminal H atoms replaced have been characterized. One such case is $Am(THD)_3$, where THD is 2,2,6,6-tetramethylheptane-3,5-dione. It was shown [457] to be isomorphous with $Pr(THD)_3$ for which the structure is known [458]. The metal atoms in these structures have a rather low coordination number of 7. This is achieved by formation of dimeric molecules in which one O atom of each of two THD groups is shared between two metal atoms. Further sharing or polymerization is prevented by the bulky organic ligands, the presence of which accounts also for the volatility of these substances.

Another β-diketone that reacts with Am(III) to produce a volatile chelate complex is PD with all its terminal H atoms replaced by fluorine: 1,1,1,5,5,5-hexafluoropentane-2,4-dione(HFPD) (Fig. 20.14). In this case a molecular anion, $[Am(HFPD)_4]^-$, is formed and the cation is Cs^+ [459].

No structural data are available on the volatile chelates of tetravalent actinides [460], but three volatile HFPD chelates with the uranyl ion have been characterized. In each, the central configuration is the same as in the uranyl PD chelates discussed above; two HFPD molecules are bidentate, and a fifth equatorial ligand is furnished by either OC_4H_8 [144], $(OCH_3)_3PO$ [145, 146], or NH_3 [143]. A highly reactive trimer of $UO_2(HFPD)_2$ also exists and exhibits a rare configuration in which one of the five equatorial uranyl sites is occupied by an *apical* O atom of another UO_2^{2+} ion [142] (see also β-UO_2SO_4).

Structural analysis [461] of the chelate complex $ThT_4 \cdot DMF$ (where T = tropolonate ion and DMF = dimethylformamide) showed that the α-diketone O atoms of the four $(T)^-$ ions plus the formamide O atom form a singly capped square antiprism about the Th^{4+} ion. The same geometry is exhibited by $ThT_4 \cdot H_2O$ [462] and $Th(IPT)_4 \cdot H_2O$ [463] with the water molecule providing the ninth O atom (IPT = isopropyltropolonato ion). In two uranyl complexes, UO_2T_2X, a pentagon is formed around the equator of the UO_2^{2+} by two T^- ions and X, which is either ethanol [149] or pyridine [148]. Another type of coordination 9, a tricapped trigonal prism, exists for Th(IV) in $Th(TTA)_4 \cdot TOPO$

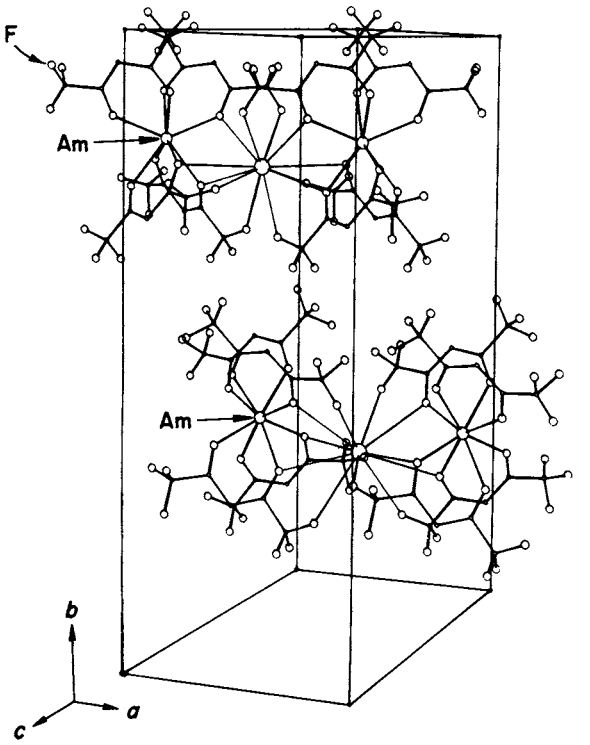

Fig. 20.14 *One unit cell of the crystal structure of $CsAm(HFPD)_4$. The largest circles represent Cs^+ ions. (Reproduced, with permission, from ref. 459, copyright by the American Chemical Society.)*

(where TTA = 1,1,1-trifluorothenoylacetone and TOPO = tri-n-octylphosphine oxide) [464]. Without the TOPO, $Th(TTA)_4$ is eight-fold coordinated [465]. The uranyl ion forms a complex, $UO_2(TTA)_2 \cdot TOPO$, in which the O atoms are arranged as a pentagonal bipyramid [178].

Phthalocyanine (PC) forms complexes with actinide elements; in these, N atoms from the organic ligand are bonded to the metal. The series of complexes $Th(PC)_2$, $Pa(PC)_2$, $U(PC)_2$, $Np(PC)_2$, and $Pu(PC)_2$ are isomorphous [466], and structural analyses have been completed on crystals of $Th(PC)_2$ [467] and $U(PC)_2$ [468]. In these crystals the metal atom is sandwiched between two disc-shaped PC molecules having their convex sides inward. Four N atoms from each PC ligand surround the actinide atom with a distorted antiprism. The uranyl ion, with its strong preference for ligands around its equator, reacts to form a 'superphthalocyanine' in which the UO_2^{2+} is inserted in a ring of five N atoms from a single organic molecule [63] (Fig. 20.5).

Attempts to put U(IV) and UO_2^{2+} ions into the ring of the polyether called 18-crown-6 (1,4,7,10,13,16-hexaoxacyclooctadecane) has yielded mixed results. The U atom is located elsewhere in the crystal in two cases,

$U(SCN)_4(18\text{-crown-}6)_{1.5}(H_2O)_7(C_6H_{12}O)$ [469] and $UO_2(NO_3)_2$ (18-crown-6)·$4H_2O$ [470], but when accompanied by three Cl atoms the U(IV) atom does fit into the ring and is bonded to all six ether O atoms. Two examples of this arrangement are $[UCl_3(18\text{-crown-}6)]_2[UO_2Cl_3(OH)(H_2O)]CH_3NO_2$ [179] and $[UCl_3(DCC)]_2UCl_6$ (DCC = dicyclohexyl-18-crown-6) [471]. The 15-crown-5 ring is also too large for the UO_2^{2+} ion; it occupies another site in the structure of $[Na(benzo\text{-}15\text{-crown-}5)]_2UO_2Cl_4$ [94]. The claim that the uranyl ion is in the crown in $UO_2(12\text{-crown-}4)(NO_3)_2\cdot 2H_2O$ [212] was shown to be incorrect; it is merely linked to the crown by hydrogen bonds [539].

The structures of a variety of other molecular complexes in which nitrogen is bonded to actinides are known. Those forming discrete molecules include $Th(C_6H_3ON_2F_6)_4$ and $U(C_6H_3ON_2F_6)_4$, in which O and N atoms form a dodecahedron around the actinide atom [472]. Discrete ions and molecules in which the actinide atom is eight-fold coordinated by N atoms only are found in $Cs_4U(NCS)_8$, $Cs_4Pu(NCS)_8$ [473], $U(NCS)_4[(C_6H_5)_3PO]_4$ [474], and $U(NCS)_4[(CH_3)_4PO]_4$ [475], in which the N atoms form an antiprism, and in $(C_2H_5)_4NM(NCS)_8$ (M = Th, Pa, U, Np, Pu) [476, 477], $(C_2H_5)_4NM(NCSe)_8$, (M = Pa, U), and $U(C_{10}H_8N_2)_4$ [478], in which the N atoms form a cube. The coordination in the related molecule $Th(NCS)_4\{[(CH_3)_2N]_2CO\}_4$ is dodecahedral [479]. Six-fold N-atom coordination is found in the trimeric and tetrameric clusters $(CH_3NCH_2CH_2NCH_3)_6U_3$ [480] and $(CH_3NCH_2CH_2NCH_3)_8U_4$ [481]. Still lower coordination is present in the dimeric molecule $\{[(C_2H_5)_2N]_4U\}_2$ with five N atoms around each U atom [482] and the $\{UO[(C_6H_5)_2N]_3LiO(C_2H_5)_2\}_2$ dimer with the U atom surrounded by four N atoms and one O atom [483]. Finally, an unusually low value of 4 for U(IV) coordination appears in the diphenylamido complex $U[(C_6H_5)_2N]_4$ [483].

20.11 ORGANOMETALLIC COMPOUNDS

The first stable actinide organometallic compound was made in 1956. Structural studies in the subsequent years have contributed greatly to the understanding of the chemistry of actinide organometallics, and the information obtained has often served as a guide for later work. Two reviews [484, 485] summarize the structural analyses available through 1975, and the implications that these have for the modes of bonding were discussed in 1980 [486]. Organoactinide chemistry is surveyed in Chapters 22 and 23 of this volume.

From the first, somewhat qualitative, structure determination of an actinide(IV) cyclopentadienide, namely $U(C_5H_5)_3Cl$ [487], was found the shape adopted by all the compounds of this general composition. The three pentagonal rings are η^5 (pentahapto)-bonded to the uranium atom, and about it the chlorine atom plus the centroids of the three rings form an irregular tetrahedron. Subsequent precise structural analyses of a variety of compounds in which the chlorine atom is replaced by other entities have not only found this same molecular arrangement

but also established that the rings are aromatic and that the U–C bonds are essentially equivalent in length.

The first of these compounds for which such precision was attained [488] is $U(C_9H_7)_3Cl$, shown in Fig. 20.15, in which C_9H_7 is the fused five- and six-membered ring system, indenyl. In the five-ring portion of the system, which is η^5-bonded to the uranium atom, the U–C bonds average about 0.14 Å longer on one side than the other; but this is adequately explained, not as localization of the electrons, but as due to contacts between the six-membered rings and the chlorine atom. Closely related is tris(benzylcyclopentadienide)uranium(IV) chloride; in this molecule the values of the U–C bond lengths were found [489] to scatter by about the same amount but in a random manner. Here too is η^5-bonding but, because of different stereochemistry, it is unperturbed by the presence of the chlorine atom. A fourth compound in this category is $U(C_5H_5)_3F$, which was reported [490] to be dimeric in benzene solution and thus was expected to be fluorine-bridged in the crystal. Structural analysis [491] showed it not to be, however, but to consist of monomers having C_{3v} symmetry, a configuration approximated by the molecules discussed above. Thus, in all known examples, the $(C_5H_5)_3U^+$ group, or its derivative containing ring substituents, is the same shape; the C–C bond lengths average about 1.39 Å and the U–C bonds about 2.74 Å.

Numerous compounds in which the fourth site around the uranium atom is occupied by a σ-bonded alkyl or aryl group also have been prepared [492], and structures of some of them have been reported. In them, the configuration is the same as for the chlorides above with the chloride position being occupied by either ethynyl [493], phenylethynyl [494], *p*-methylbenzyl, n-butyl [495] or pyrazolate [496] ligands. The U–C bond length to the σ-bonded carbon atom is

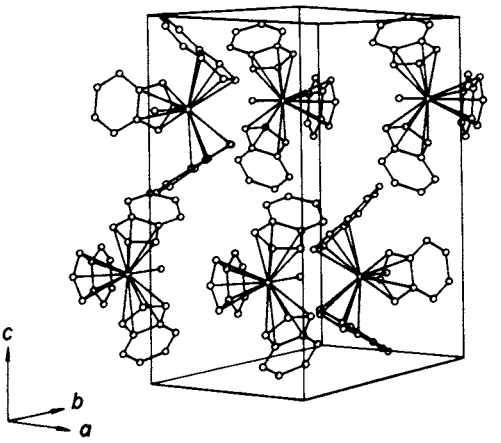

Fig. 20.15 *One unit cell of the structure of tris(indenyl)uranium chloride. Uranium atoms are at the center of each molecule; the lone atom attached to uranium is a chlorine. (Reproduced, with permission, from ref.* 488, *copyright by the American Chemical Society.)*

about 2.3 Å. One instance has been found in which a fifth (neutral) ligand can be added; in $(C_5H_5)_3U(NCS)(CH_3CN)$ [497] the C_5H_5 ligands are around the equator of a trigonal bipyramid. No stable compounds of the actinides have been made having solely alkyl ligands.

Studies [498] of allyl as a ligand for uranium(IV) have shown that in tetraallyl compounds the bonding is of the symmetrical π-allyl type, but crystallographic studies [499] on the compound tris(cyclopentadienyl)-(2-methylallyl)uranium(IV) ascertained that it has the same general configuration as the $(C_5H_5)_3X$ and $(C_5H_5)_3R$ molecules, and that the methylallyl ligand is σ-bonded to the uranium atom at a distance of 2.48 Å. An η^1-bond between allyl and uranium is also found in $[U(C_3H_5)_2(OC_3H_7)_2]_2$, where the C_3H_5 ligands are on the equator of a pentagonal bipyramid along with one OC_3H_7 molecule [500].

Tetracyclopentadienyl complexes of several actinide elements (Th, Pa, U, and Np) have been made. Infrared data suggest that these all have similar molecular structures, and x-ray powder diffraction [501] was used to show the isomorphism of the compounds of Th, U, and Np. A single-crystal structural analysis [502] of $U(C_5H_5)_4$ revealed that the molecules are tetrahedral and that all four cyclopentadienyl rings are η^5-bonded to the metal atom. Because of the higher coordination that this produces, the average U–C bond length (2.81 Å) is longer than in the previously discussed structures.

The proclivity for forming tetrahedral arrays often results in binuclear molecules in which each metal atom has two terminal cyclopentadienyl ligands forming a 'bent sandwich' plus bridging atoms or groups to complete each tetrahedron. Such molecules as these include $\{[(CH_3)_5C_5]_2ThH(\mu\text{–}H)\}_2$ [503], $[(C_5H_5)_2Th(C_5H_4)]_2$ [504], $\{[(CH_3)_5C_5]_2Th[\mu\text{–}O_2C_2(CH_3)_2]\}_2$ [505], $\{[(CH_3)_5C_5]_2Th[\mu\text{–}CO(CH_2C(CH_3)_3)CO]Cl\}_2$ [506], and $[(C_5H_5)_2U(\mu\text{–}CH)CH_2P(C_6H_5)_2]_2\cdot 0.5(C_2H_5)_2O$ [507]. A triangle of $[(CH_3)_5C_5]_2U^+$ 'bent sandwiches' is connected in $\{[(CH_3)_5C_5]_2U(\mu\text{–}Cl)\}_3$ by Cl bridges between each U atom and two others [508]. This sharing balances the charge on the *trivalent* uranium as well as giving it tetrahedral coordination. The only other bis(cyclopentadienyl)monochloride of a trivalent actinide known is $(C_5H_5)_2BkCl$. Although its crystal structure has not been determined, the presence of dimeric molecules has been deduced [509] from mass-spectrometric data. Structural analyses of similar, though not isomorphous, compounds, $(C_5H_5)_2ScCl$ [510], $(C_5H_5)_2YbCl$ [511], and $(CH_3C_5H_4)_2YbCl$ [512], have revealed chlorine-bridged dimers, thereby adding credence to the suggested $[(C_5H_5)_2BkCl]_2$ formulation.

Attempts to prepare $(C_5H_5)_2UCl_2$ have not succeeded, but one product obtained [513] in trying to make this substance was $(CH_3C_5H_4)UCl_3\cdot(OC_4H_8)_2$, which consists of molecules in which the U(IV) is pseudo-octahedrally coordinated by two O atoms, three Cl atoms, and one η^5-$(CH_3C_5H_4)$ ligand. The same kind of coordination appears in $(C_5H_5)UCl_3[(C_6H_5)_3PO]_2\cdot(OC_4H_8)$; in this case the (OC_4H_8) is not involved in the coordination [514]. A stable dichloride can be made, however, when the bulkier dicarbollide ion is used [515];

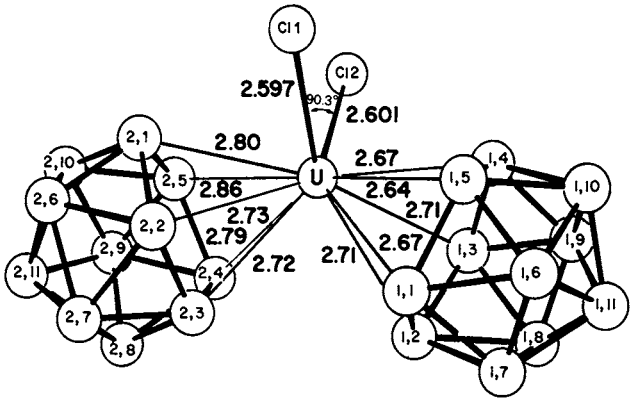

Fig. 20.16 *The* $[U(C_2B_9H_{11})_2Cl_2]^{2-}$ *ion. The C and B atoms were indistinguishable from the x-ray data. (Reproduced, with permission, from ref.* 515, *copyright by the American Chemical Society.)*

in $[Li(C_4H_8O)_4]_2[(C_2B_9H_{11})_2UCl_2]$ the pentagonal face of each of two $[C_2B_9H_{11}]^{2-}$ ions and two Cl^- ions are tetrahedrally attached to a central U(IV) ion (Fig. 20.16). A more complex chloride is formed when two C_5H_5 rings are linked together by a methylene group and used as a ligand; in the compound $Li\{[CH_2(C_5H_4)_2]_2UCl_5\}$ $(C_4H_8O)_2$ the two U atoms are each bonded to a linked pair of cyclopentadienyl rings but also share three bridging Cl atoms and have one terminal Cl atom each [516].

Tricyclopentadienides have been synthesized for all the lanthanide metals and for a wide range of actinides including Th, U, Pu, Am, Cm, Bk, and Cf. Studies of single crystals and powders have established the isomorphism of the lanthanide complexes ranging from Pr to Gd, at least, and of the actinide complexes including Th [517] and Pu to Cf [518]. A determination of the structure of the crystals (for the case of $Sm(C_5H_5)_3$) has been reported [519], but it is not very useful. A disordered model involving at least three types of metal–carbon bonds was proposed to describe the structure. Since twinning is a problem inherent with this particular structure, the data used for $Sm(C_5H_5)_3$ may be from a twinned crystal. Later a study [520] of the structure of neodymium tris(methylcyclopentadienide) was made in order to get away from the $Sm(C_5H_5)_3$ structure type and still be able to examine the interaction of trivalent metal ions and the cyclopentadienide ion. The structure achieved appears to result from simple packing of ions about the central metal. Analogous actinide compounds have not been synthesized, but should be isostructural.

Cyclopentadienides of trivalent lanthanides and actinides show Lewis-acid character, and adducts with several Lewis bases have been made. The only one for which the structure is known [521] contains cyclohexylisonitrile as the base. In this case, $(C_5H_5)_3PrCNC_6H_{11}$, the isonitrile carbon atom forms an electron-donor bond to the Pr atom, and the three C_5H_5 rings are trigonally arrayed about

it, in similar fashion to the tetravalent actinide cyclopentadienides. One complex of a trivalent actinide, $(C_5H_5)_3UCNC_6H_{11}$, has been shown [522] to have this structure and several others that have been made (with Np, Pu, Am) probably do also.

A most satisfying sequence of applications of theoretical, synthetic, and structural chemistry resulted in the synthesis and characterization of uranocene, $U(C_8H_8)_2$, in which the uranium ion is sandwiched between two cyclooctatetraene dianions. Since the motivation for making this substance was the prediction that it would be analogous to ferrocene [523], one of the first measurements made was x-ray diffraction [524] to determine the molecular shape. A crystal structure was found containing molecules of the π-sandwich type having D_{8h} symmetry (Fig. 20.17). Subsequent analyses of single crystals of $Th(C_8H_8)_2$ [525] and powder samples of $Pa(C_8H_8)_2$ [526], $Np(C_8H_8)_2$ [527], and $Pu(C_8H_8)_2$ [527] showed them to be isostructural with uranocene. The U–C bond lengths in uranocene are equal within experimental error and average about 2.647 Å, while in thoracene the average is 2.701 Å. The two rings of the sandwich are eclipsed in this structure, but this is not required to maximize f-orbital overlap; in the (tetra)methyl-substituted compound, $U[C_8H_4(CH_3)_4]_2$, there are two varieties of molecular structure – one with the methyl groups nearly eclipsed and one with them nearly staggered. The U–C bond lengths are not significantly longer than in the unsubstituted compound. Apparently there is little resistance to rotation of the rings, and the conformation attained results from differing degrees of

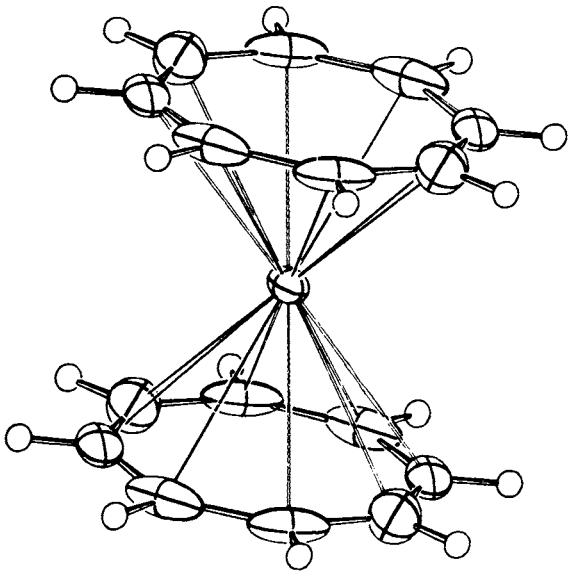

Fig. 20.17 *The uranocene molecule with uranium at its center. (Reproduced, with permission, from ref. 524, copyright by the American Chemical Society.)*

intermolecular contact of the methyl groups. In octaphenyluranocene, $U[C_8H_4(C_6H_5)_4]_2$, the rings are nearly eclipsed [528] (Fig. 22.17) and in dicyclobutenouranocene, $U(C_{10}H_{10})_2$, the rings are exactly eclipsed [529]. In addition to thoracene, Th forms a compound having only one $(C_8H_8)^{2-}$ ion: $C_8H_8ThCl_2(OC_4H_8)_2$. On one side of the Th atom it is symmetrically bonded to the $(C_8H_8)^{2-}$ ion and on the other to two Cl^- ions and two OC_4H_8 molecules [530].

The extent to which there is f-orbital participation in the U–C bonding is not evident from the structures found, since the sandwich is a good ionic model also, but many other physical and chemical observations have been interpreted as indicating some covalency. Baker *et al.* [485] have summarized the studies and conclusions that have been made thus far.

Trivalent actinides also have been reacted with the cyclooctatetraene dianion, yielding $KNp(C_8H_8)_2$ and $KPu(C_8H_8)_2$ solvated with either tetrahydrofuran or diglyme, $(CH_3OCH_2)_2O$. X-ray powder diffraction data on $KPu(C_9H_8)_2 \cdot$diglyme was interpreted [531] to mean that this compound is isostructural with its Ce analog, which is known [532] to have the Ce atom sandwiched between two C_8H_8 rings. These compounds are believed to be more ionic in nature than those with tetravalent actinides.

One π-arene compound of uranium has been prepared and its structure determined [533]: $U(AlCl_4)_3 \cdot C_6H_6$. The molecule contains three $AlCl_4$ tetrahedra, each sharing two chlorine atoms with the uranium, and a benzene ring π-bonded to the uranium. The mean U–C distance to the ring is 2.91 Å, indicating that the bonding is rather weak.

A stable aryl actinide, tetrabenzylthorium(IV), has been synthesized [534] and studied by NMR and infrared spectroscopy. It may be isostructural with the zirconium and titanium [535] analogs in which the metal is tetrahedrally surrounded by benzyl groups σ-bonded to it through the methylene carbon atoms.

ACKNOWLEDGMENTS

This work was sponsored by the Division of Basic Energy Sciences of the US Department of Energy under Contract W-7405-Eng-26 with the Union Carbide Corporation.

REFERENCES

1. Fahey, J. A., Turcotte, R. P., and Chikalla, T. D. (1974) *Inorg. Nucl. Chem. Lett.*, **10**, 459–65.
2. Muxart, R., Guillaumont, R., and Bouissieres, G. (1969) *Actinide Rev.*, **1**, 223–74.
3. Rouse, K. D., Willis, B. T. M., and Pryor, A. W. (1968) *Acta Crystallogr. B*, **24**, 117–22.
4. Belbeoch, B., Piekarski, C., and Perio, P. (1961) *Acta Crystallogr.*, **14**, 837–43.

5. Willis, B. T. M. (1978) *Acta Crystallogr. A*, **34**, 88–90.
6. Blank, H. and Ronchi, C. (1968) *Acta Crystallogr. A*, **24**, 657–66.
7. Masaki, N. and Doi, K. (1972) *Acta Crystallogr. B*, **28**, 785–91.
8. Loopstra, B. O. (1964) *Acta Crystallogr.*, **17**, 651–4.
9. Loopstra, B. O. (1970) *Acta Crystallogr. B*, **26**, 656–7.
10. Siegel, S. (1955) *Acta Crystallogr.*, **8**, 617–19.
11. Herak, R. (1969) *Acta Crystallogr. B*, **25**, 2505–8.
12. Hoekstra, H. R. and Siegel, S. (1961) *J. Inorg. Nucl. Chem.*, **18**, 154–65.
13. Siegel, S., Hoekstra, H., and Sherry, E. (1965) *Acta Crystallogr.*, **20**, 292–5.
14. Greaves, C. and Fender, B. E. F. (1972) *Acta Crystallogr. B*, **28**, 3609–14.
15. Engmann, R. and de Wolff, P. M. (1963) *Acta Crystallogr.*, **16**, 993–6.
16. Christ, C. L. and Clark, J. R. (1960) *Am. Minerol.*, **45**, 1026–61.
17. Sobry, R. (1973) *J. Inorg. Nucl. Chem.*, **35**, 1515–24.
18. Roof, R. B., Cromer, D. T., and Larson, A. C. (1964) *Acta Crystallogr.*, **17**, 701–5; Bannister, M. J. and Taylor, J. C. (1970) *Acta Crystallogr. B*, **26**, 1775–81.
19. Siegel, S., Viste, A., Hoekstra, H. R., and Tani, B. (1972) *Acta Crystallogr. B*, **28**, 117–21.
20. Taylor, J. C. and Wilson, P. W. (1974) *Acta Crystallogr. B*, **30**, 151–4.
21. Cohen, D. and Walter, A. J. (1964) *J. Chem. Soc. A*, 2696–9.
22. Fahey, J. A., Turcotte, R. P., and Chikalla, T. D. (1976) *J. Inorg. Nucl. Chem.*, **38**, 495–500.
23. Bagnall, K. W. and Laidler, J. B. (1964) *J. Chem. Soc. A*, 2693–6.
24. Finch, C. B. and Clark, G. W. (1969) *J. Cryst. Growth*, **5**, 219–21.
25. Gardner, E. R., Markin, T. L., and Strut, R. S. (1965) *J. Inorg. Nucl. Chem.*, **27**, 541–51.
26. Pauling, L. and Schappell, M. D. (1930) *Z. Krist.*, **75**, 128–42.
27. Koehler, W. C. and Wollan, E. O. (1953) *Acta Crystallogr.*, **6**, 741–2.
28. Cromer, D. T. (1957) *J. Phys. Chem.*, **61**, 753–5.
29. Baybarz, R. D. (1973) *J. Inorg. Nucl. Chem.*, **35**, 4149–58.
30. Chikalla, T. D. (1968) *J. Inorg. Nucl. Chem.*, **30**, 133–45.
31. Chikalla, T. D. and Eyring, L. (1969) *J. Inorg. Nucl. Chem.*, **31**, 85–93; Noe, M., Fuger, J., and Duyckaerts, G. (1970) *Inorg. Nucl. Chem. Lett.*, **6**, 111–19.
32. Peterson, J. R. and Cunningham, B. B. (1967) *Inorg. Nucl. Chem. Lett.*, **3**, 327–36; Baybarz, R. D. (1968) *J. Inorg. Nucl. Chem.*, **30**, 1769–73.
33. Baybarz, R. D., Haire, R. G., and Fahey, J. A. (1972) *J. Inorg. Nucl. Chem.*, **34**, 557–65.
34. Haire, R. G. and Baybarz, R. D. (1973) *J. Inorg. Nucl. Chem.*, **35**, 489–96.
35. Zachariasen, W. H. (1952) *Acta Crystallogr.*, **5**, 19–21.
36. Zachariasen W. H. (1949) *Acta Crystallogr.*, **2**, 388–90.
37. Akimoto, Y. (1967) *J. Inorg. Nucl. Chem.*, **29**, 2650–2.
38. Keller, C. (1971) in *MTP International Review of Science, Inorganic Chemistry*, ser. 1, vol. 7, *Lanthanides and Actinides*, (ed. K. W. Bagnall), Butterworths, London, p. 47ff.
39. Siegel, S. and Hoekstra, H. R. (1968) *Acta Crystallogr. B*, **24**, 967–70.
40. Allpress, J. G. (1965) *J. Inorg. Nucl. Chem.*, **27**, 1521–7.
41. Hoekstra, H. R. and Siegel, S. (1964) *J. Inorg. Nucl. Chem.*, **26**, 693–700.
42. Keller, C., Koch, L., and Walter, K. H. (1965) *J. Inorg. Nucl. Chem.*, **27**, 1205–23.
43. Sterns, M. (1967) *Acta Crystallogr.*, **23**, 264–72.
44. Sterns, M. and Sawyer, J. O. (1964) *J. Inorg. Nucl. Chem.*, **26**, 2291–6.
45. Loopstra, B. O. and Rietveld, H. M. (1969) *Acta Crystallogr. B*, **25**, 787–91.

46. Gebert, E., Hoekstra, H. R., Reis, A. H., and Peterson, S. W. (1978) *J. Inorg. Nucl. Chem.*, **40**, 65–8.
47. Van Egmond, A. B. (1975) *J. Inorg. Nucl. Chem.*, **37**, 1929–31; (1976) *ibid.*, **38**, 1645–7; *ibid.*, **38**, 1649–51; *ibid.*, **38**, 2105–7.
48. Van Egmond, A. B. and Cordfunke, E. H. P. (1976) *J. Inorg. Nucl. Chem.*, **38**, 2245–7.
49. Cordfunke, E. H. P., Van Egmond, A. B., and Van Voorst, G. (1975) *J. Inorg. Nucl. Chem.*, **37**, 1433–6.
50. Kovba, L. M. and Trunova, V. I. (1971) *Sov. Radiochem.*, **13**, 796–7.
51. Kovba, L. M. (1972) *Sov. Radiochem.*, **14**, 746–9; (1972) *J. Struct. Chem.*, **13**, 235–7.
52. Fankuchen, I. (1935) *Z. Krist.*, **91**, 473–9.
53. Taylor, J. C., Ekstrom, A., and Randall, C. H. (1978) *Inorg. Chem.*, **17**, 3285–9.
54. Keenan, T. K. and Kruse, F. H. (1964) *Inorg. Chem.*, **3**, 1231–2.
55. Ellinger, F. H. and Zachariasen, W. H. (1954) *J. Phys. Chem.*, **58**, 405–8.
56. Keenan, T. K. (1965) *Inorg. Chem.*, **4**, 1500–1.
57. Zachariasen, W. H. (1954) *Acta Crystallogr.*, **7**, 795–9; Zachariasen, W. H. and Plettinger, H. A. (1959) *Acta Crystallogr.*, **12**, 526–30.
58. Graziani, R., Bombieri, G., and Forsellini, E. (1972) *J. Chem. Soc. Dalton Trans.*, 2059–61.
59. Musikas, C. and Burns, J. H. (1976) in *Transplutonium* 1975 (eds W. Müller and R. Lindner), North-Holland, Amsterdam, pp. 237–45.
60. Burns, J. H. and Musikas, C. (1977) *Inorg. Chem.*, **16**, 1619–22.
61. Zachariasen, W. H. (1976) in *Heavy Element Properties* (eds W. Müller and H. Blank), North-Holland, Amsterdan, pp. 91–6.
62. Benetolo, F., Bombieri, G., and Smith, A. J. (1979) *Acta Crystallogr. B*, **35**, 3091–3.
63. Day, V. W., Marks, T. J., and Wachter, W. A. (1975) *J. Am. Chem. Soc.*, **97**, 4519–27.
64. Mikhailov, Yu. N., Udovenko, A. A., Kuznetsov, V. G., and Davidovich, R. L. (1972) *J. Struct. Chem.*, **13**, 694; Brusset, H., Dao, N. Q., and Chourou, S. (1974) *Acta Crystallogr. B*, **30**, 768–73.
65. Mikhailov, Yu. N., Udovenko, A. A., Kuznetsov, V. G., and Davidovich, R. L. (1972) *J. Struct. Chem.*, **13**, 879–80.
66. Dao, N. Q. (1972) *Acta Crystallogr. B*, **28**, 2011–15.
67. Mikhailov, Yu. N., Udovenko, A. A., Kuznetsov, V. G., Butman, L. A., and Kokh, L. A. (1973) *J. Struct. Chem.*, **14**, 154.
68. Zachariasen, W. H. (1948) *Acta Crystallogr.*, **1**, 277–81; Atoji, M. (1970) *Acta Crystallogr. B*, **26**, 1540–4.
69. Casellato, U., Vidali, M., and Vigato, P. A. (1979) *Coord. Chem. Rev.*, **28**, 231–77.
70. Casellato, U., Vidali, M., and Vigato, P. A. (1976) *Inorg. Chim. Acta*, **18**, 77–112.
71. Casellato, U., Vigatto, P. A., and Vidali, M. (1978) *Coord. Chem. Rev.*, **26**, 85–159.
72. Zachariasen, W. H. (1954) *Acta Crystallogr.*, **7**, 788–92.
73. Reis, A. H., Jr., Hoekstra, H. R., Gebert, E., and Peterson, S. W. (1976) *J. Inorg. Nucl. Chem.*, **38**, 1481–5.
74. Morosin, B. (1978) *Acta Crystallogr. B*, **34**, 3732–4.
75. Hall, D., Rae, A. D., and Waters, T. N. (1966) *Acta Crystallogr.*, **20**, 160–2.
76. Vodovatov, V. A., Ladugin, I. N., Luchev, A. A., Mashirov, L. G., and Suglobov, D. N. (1975) *Sov. Radiochem.*, **17**, 771–5.
77. Mikhailov, Yu. N. and Kuznetsov, V. G. (1971) *Russ. J. Inorg. Chem.*, **16**, 1340–2.
78. DiSipio, L., Tondello, E., Pelizzi, G., Ingeletto, G., and Montenero, A. (1974) *Cryst. Struct. Commun.*, **3**, 297–300.

79. Jensen, W., Dickerson, D., and Johnson, Q. (1974) *Acta Crystallogr. B*, **30**, 840–1.
80. Bois, C., Dao, N. Q., and Rodier, N. (1976) *J. Inorg. Nucl. Chem.*, **38**, 755–7.
81. Bois, C., Dao, N. Q., and Rodier, N. (1976) *Acta Crystallogr. B*, **32**, 1541–4.
82. DiSipio, L., Tondello, E., Pelizzi, G., Ingeletto, G., and Montenero, A. (1974) *Cryst. Struct. Commun.*, **3**, 731–4.
83. DiSipio, L., Tondello, E., Pelizzi, G., Ingeletto, G., and Montenero, A. (1974) *Cryst. Struct. Commun.*, **3**, 301–3.
84. DiSipio, L., Tondello, E., Pelizzi, G., Ingeletto, G., and Montenero, A. (1974) *Cryst. Struct. Commun.*, **3**, 527–30.
85. DiSipio, L., Tondello, E., Pelizzi, G., Ingletto, G., and Montenero, A. (1977) *Cryst. Struct. Commun.*, **6**, 723–6.
86. Perry, D. L., Freyberg, D. P., and Zalkin, A. (1980) *J. Inorg. Nucl. Chem.*, **42**, 243–5.
87. Bombieri, G., Forsellini, E., and Graziani, R. (1978) *Acta Crystallogr. B*, **34**, 2622–4.
88. Marzotto, A., Graziani, R., Bombieri, G., and Forsellini, E. (1974) *J. Cryst. Mol. Struct.*, **4**, 253–62.
89. Russell, J. C., duPlessis, M. P., Nassimbeni, L. R., duPreez, J. G. H., and Gallatly, B. J. (1977) *Acta Crystallogr. B*, **33**, 2062–5; Julien, R., Rodier, N., and Khodadad, P. (1977) *ibid*, 2411–14.
90. Nassimbeni, L. R. and Rodgers, A. L. (1976) *Cryst. Struct. Commun.*, **5**, 301–8.
91. Bombieri, G., Forsellini, E., Day, J. P., and Azeez, W. I. (1978) *J. Chem. Soc. Dalton Trans.*, 677–80.
92. Marzotto, A., Bandoli, G., Clemente, D. A., Benetollo, F., and Galzigna, L. (1973) *J. Inorg. Nucl. Chem.*, **35**, 2769–74.
93. Graziani, R., Bombieri, G., Forsellini, E., and Paolucci, G. (1975) *J. Cryst. Mol. Struct.*, **5**, 1–14.
94. Moody, D. C. and Ryan, R. R. (1979) *Cryst. Struct. Commun.*, **8**, 933–6.
95. Taylor, J. C. and Wilson, P. W. (1973) *Acta Crystallogr. B*, **29**, 1073–6.
96. Taylor, J. C. and Wilson, P. W. (1974) *Acta Crystallogr. B*, **30**, 169–75.
97. Aberg, M. (1969) *Acta Chem. Scand.*, **23A**, 791–810.
98. Aberg, M. (1976) *Acta Chem. Scand.*, **30A**, 507–14.
99. Aberg, M. (1978) *Acta Chem. Scand.*, **32A**, 101–7.
100. Perrin, A. and LeMarouille (1977) *Acta Crystallogr. B*, **33**, 2477–81.
101. Haegele, R. and Boeyens, J. C. A. (1977) *J. Chem. Soc. Dalton Trans.*, 648–50.
102. Rosenzweig, A. and Ryan, R. R. (1977) *Cryst. Struct. Commun.*, **6**, 53–6.
103. Zachariasen, W. H. (1954) *Acta Crystallogr.*, **7**, 783–7.
104. Thalmayer, C. E. and Cohen, D. (1967) in *Lanthanide/Actinide Chemistry* (eds P. R. Fields and T. Moeller), (ACS Adv. Chem. Ser. 71), American Chemical Society, Washington DC, p. 256.
105. Allpress, J. G. and Wadsley, A. D. (1964) *Acta Crystallogr.*, **17**, 41–6.
106. Arutyunyan, E. G. and Porai-Koshits, M. A. (1963) *J. Struct. Chem.*, **4**, 96–7.
107. Smith, D. K., Gruner, J. W., and Lipscomb, W. N. (1957) *Am. Minl.*, **42**, 594–618.
108. Appleman, D. E. and Evans, H. T. (1957) *Acta Crystallogr.*, **10**, 765.
109. Ross, M. and Evans, H. T. (1960) *J. Inorg. Nucl. Chem.*, **15**, 338–51.
110. Appleman, D. E. (1960) *Geol. Soc. Am. Bull.*, **68**, 1696–8.
111. Niinisto, L., Toivonen, J., and Valkonen, J. (1979) *Acta Chem. Scand.*, **33A**, 621–4.
112. Niinisto, L., Toivonen, J., and Valkonen, J. (1978) *Acta Chem. Scand.*, **32A**, 647–51.
113. Alcock, N. W., Roberts, M. M., and Chakravorti, M. C. (1980) *Acta Crystallogr. B*, **36**, 687–90.

114. Brandenburg, N. P. and Loopstra, B. O. (1978) *Acta Crystallogr. B*, **34**, 3734–6.
115. van der Putten, N. and Loopstra, B. O. (1974) *Cryst. Struct. Commun.*, **3**, 377–80.
116. Zalkin, A., Ruben, H., and Templeton, D. H. (1978) *Inorg. Chem.*, **17**, 3701–2.
117. Brandenburg, N. P. and Loopstra, B. O. (1973) *Cryst. Struct. Commun.*, **2**, 243–6.
118. Loopstra, B. O. and Brandenburg, N. P. (1978) *Acta Crystallogr. B*, **34**, 1335–7.
119. Meunier, G. and Galy, G. (1973) *Acta Crystallogr. B*, **29**, 1251–5.
120. Alcock, N. W. and Esperas, S. (1977) *J. Chem. Soc. Dalton Trans.*, 893–6.
121. Mentzen, B. F., Puaux, J.-P., and Loiseleur, H. (1976) *Acta Crystallogr. B*, **32**, 1848–51.
122. LeRoux, S. D., van Tets, A., and Adrain, H. W. W. (1979) *Acta Crystallogr. B*, **35**, 3056–7.
123. Mentzen, B. F. (1977) *Acta Crystallogr. B*, **33**, 2546–9.
124. Mentzen, B. F., Puaux, J.-P., and Sautereau, H. (1978) *Acta Crystallogr. B*, **34**, 1846–9.
125. Mentzen, B. F., Puaux, J.-P., and Sautereau, H. (1978) *Acta Crystallogr. B*, **34**, 2707–11.
126. Howatson, J., Grev, D. M., and Morosin, B. (1975) *J. Inorg. Nucl. Chem.*, **37**, 1933–5.
127. Mentzen, B. F. and Santereau, H. (1980) *Acta Crystallogr. B*, **36**, 2051–3.
128. Bombieri, G., Benetollo, F., del Pra, A., and Rojas, R. (1979) *J. Inorg. Nucl. Chem.*, **41**, 201–3.
129. Bombieri, G., Croatto, U., Graziani, R., Forsellini, E., and Magon, L. (1974) *Acta Crystallogr. B*, **30**, 407–11.
130. Panattoni, C., Graziani, R., Bandoli, G., Zarli, B., and Bombieri, G. (1969) *Inorg. Chem.*, **8**, 320–5.
131. Bandoli, G., Graziani, R., and Zarli, B. (1968) *Acta Crystallogr. B*, **24**, 1129–30.
132. Rojas, R., del Pra, A., Bombieri, G., and Benetollo, F. (1979) *J. Inorg. Nucl. Chem.*, **41**, 541–5.
133. Jayadevan, N. C. and Chakraburtty, D. M. (1972) *Acta Crystallogr. B*, **28**, 3178–82.
134. Alcock, N. W. (1973) *J. Chem. Soc. Dalton Trans.*, 1614–15.
135. Alcock, N. W. (1973) *J. Chem. Soc. Dalton Trans.*, 1616–20.
136. Fransson, E., Bombieri, G., and Panattoni, C. (1966) *Coord. Chem. Rev.*, **1**, 145–50.
137. Lenner, M. (1979) *Acta Crystallogr. B*, **35**, 2396–8.
138. Rodgers, A. L., Nassimbeni, L. R., Paupit, R. A., Orpen, G., and Haigh, J. M. (1977) *Acta Crystallogr. B*, **33**, 3110–13.
139. Haigh, J. M., Nassimbeni, L. R., Paupit, R. A., Rodgers, A. L., and Sheldrick, G. M. (1976) *Acta Crystallogr. B*, **32**, 1398–401.
140. Nassimbeni, L. R., Orpen, G., Paupit, R., Rodgers, A. L., and Haigh, J. M. (1977) *Acta Crystallogr. B*, **33**, 959–62.
141. Rodgers, A. L., Nassimbeni, L. R., and Haigh, J. M. (1977) *Acta Crystallogr. B*, **33**, 1176–9.
142. Taylor, J. C., Ekstrom, A., and Randall, C. H. (1978) *Inorg. Chem.*, **17**, 3285–9.
143. Johnson, D. A., Taylor, J. C., and Waugh, A. B. (1979) *J. Inorg. Nucl. Chem.*, **41**, 827–31.
144. Kramer, G. M., Dines, M. B., Hall, R. B., Kalder, A., Jacobson, A. J., and Scanlon, J. C. (1980) *Inorg. Chem.*, **19**, 1340–7.
145. Taylor, J. C. and Waugh, A. B. (1977) *J. Chem. Soc. Dalton Trans.*, 1630–6.
146. Taylor, J. C. and Waugh, A. B. (1977) *J. Chem. Soc. Dalton Trans.*, 1636–40.
147. Graziani, R., Marangoni, G., Paolucci, G., and Forsellini, E. (1978) *J. Chem. Soc. Dalton Trans.*, 818–21.

148. Bombieri, G., Degetto, S., Marangoni, G. P., Graziani, R., and Forsellini, E. (1973) *Inorg. Nucl. Chem. Lett.*, **9**, 233–6.
149. Clemente, D. A., Bandoli, G., Vidali, M., Vigato, P. A., Portanova, R., and Magon, L. (1973) *J. Cryst. Mol. Struct.*, **3**, 221–33.
150. Bombieri, G., Degetto, S., Forsellini, E., Marangoni, G., and Immirzi, A. (1977) *Cryst. Struct. Commun.*, **6**, 115–18.
151. Immirzi, A., Bombieri, G., Degetto, S., and Marangoni, G. (1975) *Acta Crystallogr. B*, **31**, 1023–8.
152. Battiston, G. A., Sbrignadello, G., Bandoli, G., Clemente, D. A., and Tomat, G. (1979) *J. Chem. Soc. Dalton Trans.*, 1965–71.
153. Bandoli, G., Clemente, D. A., Croatto, U., Vidali, M., and Vigato, P. A. (1973) *J. Chem. Soc. Dalton Trans.*, 2331–5.
154. Bandoli, G., Clemente, D. A., Croatto, U., Vidali, M., and Vigato, P. A. (1971) *J. Chem. Soc. Chem. Commun.*, 1330–1.
155. Paolucci, G., Marangoni, G., Bandoli, G., and Clemente, D. A. (1979) *J. Chem. Soc. Dalton Trans.*, 1304–11.
156. Bombieri, G., Forsellini, E., Benetollo, F., and Fenton, D. E. (1979) *J. Inorg. Nucl. Chem.*, **41**, 1437–41.
157. Brock, A. M., Cook, D. H., Fenton, D. E., Bombieri, G., Forsellini, E., and Benetollo, F. (1978) *J. Inorg. Nucl. Chem.*, **40**, 1551–9.
158. Bandoli, G. and Clemente, D. A. (1975) *J. Chem. Soc. Dalton Trans.*, 612–15.
159. Clemente, D. A., Bandoli, G., Benetollo, F., Vidali, M., Vigato, P. A., and Casellato, U. (1974) *J. Inorg. Nucl. Chem.*, **36**, 1999–2013.
160. Bandoli, G., Cattalini, L., Clemente, D. A., Vidali, M., and Vigato, P. A. (1972) *J. Chem. Soc. Chem. Commun.*, 344–5.
161. Graziani, R., Vidali, M., Casellato, U., and Vigato, P. A. (1976) *Acta Crystallogr. B*, **32**, 1681–6.
162. Hall, D., Rae, A. D., and Waters, T. N. (1967) *Acta Crystallogr.*, **22**, 258–68.
163. Bandoli, G., Clemente, D. A., and Cingi, M. B. (1975) *J. Inorg. Nucl. Chem.*, **37**, 1709–14.
164. Boeyens, J. C. A. and Haegele, R. (1976) *Inorg. Chim. Acta*, **20**, L7.
165. Baracco, L., Bombieri, G., Degetto, S., Forsellini, E., Marangoni, G., Paolucci, G., and Graziani, R. (1975) *J. Chem. Soc. Dalton Trans.*, 2161–4.
166. Wilson, A. S. (1978) *Acta Crystallogr. B*, **34**, 2302–3.
167. Dewan, J. C., Edwards, A. J., Slim, D. R., Guerchais, J. E., and Kergoat, R. (1975) *J. Chem. Soc. Dalton Trans.*, 2171–4.
168. Ruben, H., Spencer, B., Templeton, D. H., and Zalkin, A. (1980) *Inorg. Chem.*, **19**, 776–7.
169. Zalkin, A., Ruben, H., and Templeton, D. H. (1979) *Inorg. Chem.*, **18**, 519–21.
170. Dalley, N. K., Mueller, M. H., and Simonsen, S. H. (1972) *Inorg. Chem.*, **11**, 1840–5.
171. Mikhailov, Yu. N., Kuznetsov, V. G., and Kovaleva, E. S. (1969) *J. Struct. Chem.*, **9**, 620–1.
172. Baggio, R. F., deBenyacar, M. A. R., Perazzo, B. O., and Perazzo, P. K. (1977) *Acta Crystallogr. B*, **33**, 3495–9.
173. Honan, G. A., Kepert, D. C., Lincoln, S. F., Patrick, J. M., and White, A. H. (1980) *Aust. J. Chem.*, **33**, 69–75.
174. Perry, D. L., Templeton, D. H., and Zalkin, A. (1978) *Inorg. Chem.*, **17**, 3699–701.
175. Graziani, R., Zarli, B., Cassol, A., Bombieri, G., Forsellini, E., and Tondello, E. (1970) *Inorg. Chem.*, **9**, 2116–24.

176. Bombieri, G., Croatto, U., Forsellini, E., Zarli, B., and Graziani, R. (1972) *J. Chem. Soc. Dalton Trans.*, 560–4.
177. Bombieri, G., Forsellini, E., dePaoli, G., Brown, D., and Tso, T. C. (1979) *J. Chem. Soc. Dalton Trans.*, 2042–6.
178. Lu, T. H., Lee, T. J., Lee, T. Y., and Wong, C. (1977) *Inorg. Nucl. Chem. Lett.*, **13**, 363–5.
179. Bombieri, G., dePaoli, G., and Immirzi, A. (1978) *J. Inorg. Nucl. Chem.*, **40**, 1889–94.
180. Zachariasen, W. H. (1949) *Acta Crystallogr.*, **2**, 388–90.
181. Alenchikova, I. F., Zeitseva, L. L., Lipis, L. V., Nikolayev, N. S., Fomin, V. V., and Chebotarev, N. T. (1958) *Russ. J. Inorg. Chem.*, **3** (4), 178–87.
182. Keenan, T. K. (1968) *Inorg. Nucl. Chem. Lett.*, **4**, 381–4.
183. Cromer, D. T. and Harper, P. E. (1955) *Acta Crystallogr.*, **8**, 847–8.
184. Taylor, J. C. (1971) *Acta Crystallogr. B*, **27**, 1088–91; Taylor, J. C. and Hurst, H. J. (1971) *Acta Crystallogr. B*, **27**, 2018–22.
185. Perrin, A. (1976) *Acta Crystallogr. B*, **32**, 1658–61.
186. Dalley, N. K., Mueller, M. H., and Simonsen, S. H. (1971) *Inorg. Chem.*, **10**, 323–8.
187. Vdovenko, V. M., Stroganov, E. V., and Sokolov, A. P. (1963) *Sov. Radiochem.*, **5**, 83–8.
188. Hall, D. A., Rae, A. D., and Waters, T. N. (1965) *Acta Crystallogr.*, **19**, 389–95; Taylor, J. C. and Mueller, M. H. (1965) *Acta Crystallogr.*, **19**, 536–43.
189. Laidler, J. B. (1966) *J. Chem. Soc. A*, 780–4.
190. Reynolds, J. G., Zalkin, A., and Templeton, D. H. (1977) *Inorg. Chem.*, **16**, 3357–9.
191. Panattoni, C., Graziani, R., Croatto, U., Zarli, B., and Bombieri, G. (1968) *Inorg. Chim. Acta*, **2**, 43–8.
192. Perry, D. L., Ruben, H., Templeton, D. H., and Zalkin, A. (1980) *Inorg. Chem.*, **19**, 1067–9.
193. Graziani, R., Bombieri, G., Forsellini, E., Degetto, S., and Marangoni, G. (1973) *J. Chem. Soc. Dalton Trans.*, 451–4.
194. Zachariasen, W. H. (1948) *Acta Crystallogr.*, **1**, 281–5.
195. Galy, J. and Meunier, G. (1971) *Acta Crystallogr. B*, **27**, 608–16.
196. Barclay, G. A., Sabine, T. M., and Taylor, J. C. (1965) *Acta Crystallogr.*, **19**, 205–9.
197. Zivadinovic, M. S. (1967) *Bull. Inst. Nucl. Sci. 'Boris Kidrich', Phys.*, **18**, 1.
198. Kapshukov, I. I., Volkov, Yu. F., Moskvichev, E. P., Lebedev, I. A., and Yakolev, G. N. (1971) *J. Struct. Chem.*, **12**, 77–80.
199. Bombieri, G., Graziani, R., and Forsellini, E. (1973) *Inorg. Nucl. Chem. Lett.*, **9**, 551–7.
200. Benetollo, F., Bombieri, G., Herrero, J. A., and Rojas, R. M. (1979) *J. Inorg. Nucl. Chem.*, **41**, 195–9.
201. Alcock, N. W. (1973) *J. Chem. Soc. Dalton Trans.*, 1610–13.
202. Malcic, S. S. (1958) *Bull. Inst. Nucl. Sci. 'Boris Kidrich'*, **8**, 99.
203. Alcock, N. W. (1968) *J. Chem. Soc. A*, 1588–94.
204. Bowman, K. and Dori, Z. (1968) *J. Chem. Soc. Chem. Commun.* 636.
205. Asprey, L. B., Ellinger, F. H., and Zachariasen, W. H. (1954) *J. Am. Chem. Soc.*, **76**, 5235–7.
206. Adrian, H. W. W. and van Tets, A. (1979) *Acta Crystallogr. B*, **35**, 153–5.
207. Adrian, H. W. W. and van Tets, A. (1978) *Acta Crystallogr. B*, **34**, 2632–4.
208. Adrian, H. W. W. and van Tets, A. (1978) *Acta Crystallogr. B*, **34**, 80–90.
209. Adrian, H. W. W. and van Tets, A. (1977) *Acta Crystallogr. B*, **33**, 2997–3000.
210. Bombieri, G., Forsellini, E., Tomat, G., Magnon, L., and Graziani, R. (1974) *Acta Crystallogr. B*, **30**, 2659–63.

211. Albano, V. G., Braga, D., Concilio, C., and Roveri, N. (1978) *Cryst. Struct. Commun.*, 7, 133–8.
212. Armagan, N. (1977) *Acta Crystallogr. B*, **33**, 2281–4.
213. Bombieri, G., dePaoli, G., and Immirzi, A. (1978) *J. Inorg. Nucl. Chem.*, **40**, 799–802.
214. Marangoni, G., Degetto, S., Graziani, R., Bombieri, G., and Forsellini, E. (1974) *J. Inorg. Nucl. Chem.*, **36**, 1787–94.
215. Mulford, R. N. R., Ellinger, F. H., and Zachariasen, W. H. (1954) *J. Am. Chem. Soc.*, **76**, 297–300.
216. Rundle, R. E. (1951) *J. Am. Chem. Soc.*, **73**, 4172–4. See also Section 5.7.1.
217. Sellers, P. A., Fried, S., Elson, R. E., and Zachariasen, W. H. (1954) *J. Am. Chem. Soc.*, **76**, 5935–8.
218. Rundle, R. E., Shull, C. G., and Wollan, E. O. (1952) *Acta Crystallogr.*, **5**, 22–6.
219. Zachariasen, W. H. (1953) *Acta Crystallogr.*, **6**, 393–5.
220. Mulford, R. N. R. and Wiewandt, T. A. (1965) *J. Phys. Chem.*, **69**, 1641–4.
221. Ellinger, F. H. (1961) in *The Metal Plutonium* (eds A. S. Coffinberry and W. N. Miner), The University of Chicago Press, Chicago, p. 291.
222. Olson, W. M. and Mulford, R. N. R. (1966) *J. Phys. Chem.*, **70**, 2934–7.
223. Bansal, B. M. and Damien, D. (1970) *Inorg. Nucl. Chem. Lett.*, **6**, 603–6.
224. Fahey, J. A., Peterson, J. R., and Baybarz, R. D. (1972) *Inorg. Nucl. Chem. Lett.*, **8**, 101–7.
225. Libowitz, G. G. and Gibb, T. R. P. (1956) *J. Phys. Chem.*, **60**, 510–11.
226. Mueller, W. M., Blackledge, J. P., and Libowitz, G. G. (eds) (1968) *Metal Hydrides*, Academic Press, New York.
227. Anderson, R. A., Zalkin, A., and Templeton, D. H. (1981) *Inorg. Chem.*, **20**, 622–3.
228. Turner, H. W., Anderson, R. A., Zalkin, A., and Templeton, D. H. (1979) *Inorg. Chem.*, **18**, 1221–4.
229. Bernstein, E. R., Hamilton, W. C., Keiderling, T. A., LaPlaca, S. J., Lippard, S. J., and Mayerle, J. J. (1972) *Inorg. Chem.*, **11**, 3009–16.
230. Rietz, R. R., Zalkin, A., Templeton, D. H., Edelstein, N., and Templeton, L. K. (1978) *Inorg. Chem.*, **17**, 653–8.
231. Zalkin, A., Rietz, R. R., Templeton, D. H., and Edelstein, N. M. (1978) *Inorg. Chem.*, **17**, 661–3.
232. Rietz, R. R., Edelstein, N. M., Ruben, H. W., Templeton, D. H., and Zalkin, A. (1978) *Inorg. Chem.*, **17**, 658–60.
233. Eick, H. A. and Mulford, R. N. R. (1969) *J. Inorg. Nucl. Chem.*, **31**, 371–5.
234. Eick, H. A. (1966) *Inorg. Chem.*, **4**, 1237–9.
235. Post, B., Glaser, F. W., and Moskowitz, D. (1954) *Acta Met.*, **2**, 20–5.
236. Blum, P. and Bertaut, F. (1954) *Acta Crystallogr.*, **7**, 81–6.
237. Zalkin, A. and Templeton, D. H. (1950) *J. Chem. Phys.*, **18**, 391.
238. Mulford, R. N. R., Ellinger, P. H., Hendrix, G. S., and Albrecht, E. D. (1961) in *Plutonium* 1960 (ed. E. Grison), Cleaver-Hume, London, p. 301.
239. Mitchell, A. W. and Lam, D. J. (1970) *J. Nucl. Mater.*, **37**, 349–52.
240. Bowman, A. L., Krikorian, N. H., Arnold, G. P., Wallace, T. C., and Nereson, N. G. (1968) *Acta Crystallogr. B*, **24**, 1121–3.
241. Bowman, A. L., Arnold, G. P., Wittman, W. G., Wallace, T. C., and Nereson, N. G. (1966) *Acta Crystallogr.*, **21**, 670–1.
242. Chackraburrty, D. M. and Jayadevan, N. C. (1965) *Acta Crystallogr.*, **18**, 811–12.
243. Zachariasen, W. H. (1952) *Acta Crystallogr.*, **5**, 17–19.

244. Zachariasen, W. H. (1949) *Acta Crystallogr.*, **2**, 94–9.
245. Cromer, D. T., Larson, A. C., and Roof, R. B. (1964) *Acta Crystallogr.*, **17**, 947–50.
246. Land, C. C., Johnson, K. A., and Ellinger, F. H. (1965) *J. Nucl. Mater.*, **15**, 23–32.
247. Brown, A. (1961) *Acta Crystallogr.*, **14**, 860–5.
248. Slovyanskikh, V. K., Ellert, G. V., Yarembash, E. I., and Korsakova, M. D. (1966) *Inorg. Mater. (USSR)*, **2**, 827–9.
249. Buhrer, C. F. (1969) *J. Phys. Chem. Solids*, **30**, 1273–6.
250. Lam, D. J., Darby, J. B., and Nevitt, M. V. (1974) in *The Actinides, Electronic Structure and Related Properties*, vol. 2 (eds A. J. Freeman and J. B. Darby), Academic Press, New York, p. 119ff.
251. Dell, R. M. and Bridger, N. J. (1972) in *MTP International Review of Science, Inorganic Chemistry*, ser. 1, vol. 7, *Lanthanides and Actinides* (ed. K. W. Bagnall), Butterworths, London, p. 211ff.
252. Charvillat, J. P. and Damien, D. (1973) *Inorg. Nucl. Chem. Lett.*, **9**, 559–63.
253. Damien, D., Charvillat, J. P., and Müller, W. (1975) *Inorg. Nucl. Chem. Lett.*, **11**, 451–7 and references therein.
254. Damien, D., Wojakowski, A., and Müller, W. (1976) *Inorg. Nucl. Chem. Lett.*, **12**, 441–9 and references therein.
255. Damien, D. and Wojakowski, A. (1976) *Inorg. Nucl. Chem. Lett.*, **12**, 533–8 and references therein.
256. Damien, D., Haire, R. G., and Peterson, J. R. (1980) *Inorg. Nucl. Chem. Lett.*, **16**, 537–41. Damien, D. and de Novion, C. H. (1981) *J. Nucl. Mater.*, **100**, 167–77.
257. Charvillat, J. P. and Zachariasen, W. H. (1977) *Inorg. Nucl. Chem. Lett.*, **13**, 161–4.
258. Damien, D., Haire, R. G., and Peterson, J. R. (1980) *J. Inorg. Nucl. Chem.*, **42**, 995–8.
259. Burns, J. H., Damien, D., and Haire, R. G. (1979) *Acta Crystallogr. B*, **35**, 143–4.
260. Davis, H. L. (1974) in *The Actinides, Electronic Structure and Related Properties*, vol. 2 (eds A. J. Freeman and J. B. Darby), Academic Press, New York, p. 1ff.
261. Allbutt, M. and Dell, R. M. (1968) *J. Inorg. Nucl. Chem.*, **30**, 705–10.
262. Benz, R. and Zachariasen, W. H. (1970) *Acta Crystallogr. B*, **26**, 823–7.
263. Brown, D. (1968) *Halides of the Lanthanides and Actinides*, Wiley, London.
264. Taylor, J. C. (1976) *Coord. Chem. Rev.*, **20**, 197–273.
265. Penneman, R. A., Ryan, R. R., and Rosenzweig, A. (1973) *Struct. Bonding*, **13**, 1–52.
266. Zachariasen, W. H. (1949) *Acta Crystallogr.*, **2**, 388–90.
267. Asprey, L. B., Keenan, T. K., and Kruse, F. H. (1965) *Inorg. Chem.*, **4**, 985–6.
268. Peterson, J. R. and Cunningham, B. B. (1968) *J. Inorg. Nucl. Chem.*, **32**, 1775–84.
269. Stevenson, J. N. and Peterson, J. R. (1973) *J. Inorg. Nucl. Chem.*, **35**, 3481–6.
270. Asprey, L. B. and Haire, R. G. (1973) *Inorg. Nucl. Chem. Lett.*, **9**, 1121–8.
271. Larson, A. C., Roof, R. B., and Cromer, D. T. (1964) *Acta Crystallogr.*, **17**, 555–8.
272. Zachariasen, W. H. (1949) *Acta Crystallogr.*, **2**, 390–3.
273. Eller, P. G., Larson, A. C., Peterson, J. R., Ensor, D. D., and Young, J. P. (1979) *Inorg. Chim. Acta*, **37**, 129–33.
274. Baluka, M., Yeh, S., Banks, R., and Edelstein, N. (1980) *Inorg. Nucl. Chem. Lett.*, **16**, 75–7.
275. Zachariasen, W. H. (1949) *Acta Crystallogr.*, **2**, 296–8.
276. Ryan, R. R., Penneman, R. A., Asprey, L. B., and Paine, R. T. (1976) *Acta Crystallogr. B*, **32**, 3311–13.
277. Levy, J. H., Taylor, J. C., and Wilson, P. W. (1976) *J. Chem. Soc. Dalton Trans.*, 219–24.

278. Malm, J. G., Weinstock, B., and Weaver, E. E. (1958) *J. Phys. Chem.*, **62**, 1506–8.
279. Weinstock, B. and Malm, J. G. (1956) *J. Inorg. Nucl. Chem.*, **2**, 380–94.
280. Baybarz, R. D. (1973) *J. Inorg. Nucl. Chem.*, **35**, 483–7.
281. Zachariasen, W. H. (1948) *Acta Crystallogr.*, **1**, 265–8.
282. Taylor, J. C. and Wilson, P. W. (1974) *Acta Crystallogr. B*, **30**, 2803–5.
283. Brown, D. and Edwards, J. (1972) *J. Chem. Soc. Dalton Trans.*, 1757–62.
284. Burns, J. H., Peterson, J. R., and Stevenson, J. N. (1975) *J. Inorg. Nucl. Chem.*, **37**, 743–9.
285. Burns, J. H. and Peterson, J. R. (1970) *Acta Crystallogr. B*, **26**, 1885–7.
286. Peterson, J. R. and Burns, J. H. (1973) *J. Inorg. Nucl. Chem.*, **35**, 1525–30.
287. Peterson, J. R. and Cunningham, B. B. (1968) *J. Inorg. Nucl. Chem.*, **30**, 823–8.
288. Burns, J. H., Peterson, J. R., and Baybarz, R. D. (1973) *J. Inorg. Nucl. Chem.*, **35**, 1171–7.
289. Fujita, D. K., Cunningham, B. B., and Parsons, T. C. (1969) *Inorg. Nucl. Chem. Lett.*, **5**, 307–13.
290. Mason, J. T., Jha, M. C., and Chiotti, P. (1974) *J. Less Common Metals*, **34**, 143–51.
291. Brown, D., Hall, T. L., and Moseley, P. T. (1973) *J. Chem. Soc. Dalton Trans.*, 686–91.
292. Taylor, J. C. and Wilson, P. W. (1973) *Acta Crystallogr. B*, **29**, 1942–4.
293. Mucker, K., Smith, G. S., Johnson, Q., and Elson, R. E. (1969) *Acta Crystallogr. B*, **25**, 2362–5.
294. Dodge, R. P., Smith, G. S., Johnson, Q., and Elson, R. E. (1967) *Acta Crystallogr.*, **22**, 85–9.
295. Smith, G. S., Johnson, Q., and Elson, R. E. (1967) *Acta Crystallogr.*, **22**, 300–3.
296. Muller, U. and Kolitsch, W. (1974) *Z. Anorg. Allg. Chem.*, **410**, 32–8.
297. Taylor, J. C. and Wilson, P. W. (1974) *Acta Crystallogr. B*, **30**, 1481–4.
298. Peterson, J. R. and Baybarz, R. D. (1972) *Inorg. Nucl. Chem. Lett.*, **8**, 423–31.
299. Mason, J. T., Jha, M. C., Bailey, D. M., and Chiotti, P. (1974) *J. Less Common Metals*, **35**, 331–8.
300. Fellows, R. L., Peterson, J. R., Noe, M., Young, J. P., and Haire, R. G. (1975) *Inorg. Nucl. Chem. Lett.*, **11**, 737–42.
301. Brown, D., Petcher, T. J., and Smith, A. J. (1971) *J. Chem. Soc. A*, 908–10.
302. Taylor, J. C. and Wilson, P. W. (1974) *Acta Crystallogr. B*, **30**, 2664–7.
303. Brown, D., Hill, J., and Rickard, C. E. F. (1970) *J. Chem. Soc. A*, 476–80.
304. Brown, D., Petcher, T. J., and Smith, A. J. (1975) *Acta Crystallogr. B*, **31**, 1382–5.
305. Levy, J. H., Taylor, J. C., and Wilson, P. W. (1978) *J. Inorg. Nucl. Chem.*, **40**, 1055–7.
306. Brown, D. (1979) *Inorg. Nucl. Chem. Lett.*, **15**, 219–23.
307. Guggenberger, L. J. and Jacobson, R. A. (1968) *Inorg. Chem.*, **7**, 2257–60.
308. Baybarz, R. D., Asprey, L. B., Strouse, C. E., and Fukushima, E. (1972) *J. Inorg. Nucl. Chem.*, **34**, 3427–31.
309. Hulet, E. K., Wild, J. F., Lougheed, R. W., and Hayes, W. N. (1976) *Proc. Moscow Symp. on the Chemistry of Transuranium Elements* (eds V. Spitsyn and J. J. Katz), Pergamon Press, New York, pp. 33–5.
310. Scherrer, V., Weigel, F., and Van Ghemen, M. (1967) *Inorg. Nucl. Chem. Lett.*, **3**, 589–95.
311. Levy, J. H., Taylor, J. C., and Wilson, P. W. (1975) *Acta Crystallogr. B*, **31**, 880–2.
312. Cohen, D., Fried, S., Siegel, S., and Tani, B. (1968) *Inorg. Nucl. Chem. Lett.*, **4**, 257–60.
313. Fried, S., Cohen, D., Siegel, S., and Tani, B. (1968) *Inorg. Nucl. Chem. Lett.*, **4**, 495–8.
314. Zalkin, A., Forrester, J. D., and Templeton, D. H. (1964) *Inorg. Chem.*, **3**, 639–41.

315. Levy, J. H., Taylor, J. C., and Wilson, P. W. (1980) *Inorg. Chem.*, **19**, 672–4.
316. Kimura, M., Schomaker, V., Smith, D. W., and Weinstock, B. (1968) *J. Chem. Phys.*, **49**, 5135–7.
317. Brown, D., Fletcher, S., and Holah, D. G. (1968) *J. Chem. Soc. A*, 1889–94.
318. Burns, J. H. and Peterson, J. R. (1971) *Inorg. Chem.*, **10**, 147–51.
319. Zadneprovskii, G. M. and Borisov, S. V. (1971) *J. Struct. Chem.*, **12**, 761–9.
320. Bombieri, G. and Bagnall, K. W. (1975) *J. Chem. Soc. Chem. Commun.*, 188–9.
321. Rickard, C. E. F. and Woolard, D. C. (1980) *Acta Crystallogr. B*, **36**, 292–4.
322. duPreez, J. G. H., Gallatly, B. J., Jackson, G., Nassimbeni, L. R., and Rogers, A. L. (1978) *Inorg. Chim. Acta*, **27**, 181–4.
323. Caira, M. R. and Nassimbeni, L. R. (1977) *J. Inorg. Nucl. Chem.*, **39**, 455–7.
324. Sommerville, P. and Laing, M. (1976) *Acta Crystallogr. B*, **32**, 1551–2.
325. Bombieri, G., Forsellini, E., Brown, D., and Whittaker, B. (1976) *J. Chem. Soc. Dalton Trans.*, 735–738.
326. Bombieri, G., Brown, D., and Graziani, R. (1975) *J. Chem. Soc. Dalton Trans.*, 1873–6.
327. Bombieri, G., Brown, D., and Mealli, C. (1976) *J. Chem. Soc. Dalton Trans.*, 2025–9.
328. de Wet, J. F. and duPreez, J. G. H. (1978) *J. Chem. Soc. Dalton Trans.*, 592–7.
329. de Wet, J. F., Caira, M. R., and Gallatly, B. J. (1978) *Acta Crystallogr. B*, **34**, 1121–4.
330. Caira, M. R., de Wet, J. F., duPreez, J. G. H., and Gallatly, B. J. (1978) *Acta Crystallogr. B*, **34**, 1116–20.
331. Templeton, D. H. and Dauben, C. H. (1953) *J. Am. Chem. Soc.*, **75**, 4560–2.
332. Peterson, J. R. (1972) *J. Inorg. Nucl. Chem.*, **34**, 1603–7.
333. Peterson, J. R. and Cunningham, B. B. (1967) *Inorg. Nucl. Chem. Lett.*, **3**, 579–83.
334. Copeland, J. C. and Cunningham, B. B. (1969) *J. Inorg. Nucl. Chem.*, **31**, 733–40.
335. Fujita, D. K., Cunningham, B. B., and Parsons, T. C. (1969) *Inorg. Nucl. Chem. Lett.*, **5**, 307–13.
336. Peterson, J. R. and Burns, J. H. (1968) *J. Inorg. Nucl. Chem.*, **30**, 2955–8.
337. Bagnall, K. W., Brown, D., and Easey, J. F. (1968) *J. Chem. Soc. A*, 288–91.
338. Dodge, R. P., Smith, G. S., Johnson, Q., and Elson, R. F. (1968) *Acta Crystallogr. B*, **24**, 304–12.
339. Taylor, J. C. and Wilson, P. W. (1974) *Acta Crystallogr. B*, **30**, 175–7.
340. Bagnall, K. W., Brown, D., and Easey, J. F. (1968) *J. Chem. Soc. A*, 2223–7.
341. Brown, D. and Easey, J. F. (1970) *J. Chem. Soc. A*, 3378–81.
342. Levy, J. H., Taylor, J. C., and Wilson, P. W. (1977) *J. Inorg. Nucl. Chem.*, **39**, 1989–91.
343. Taylor, J. C. and Wilson, P. W. (1974) *J. Chem. Soc. Chem. Commun.*, 232–3.
344. Levet, J.-C., Potel, M., and leMarouille, J.-Y. (1977) *Acta Crystallogr. B*, **33**, 2542–6.
345. Brown, D., Reynolds, C. T., and Moseley, P. T. (1972) *J. Chem. Soc. Dalton Trans.*, 857–9.
346. Rosenzweig, A. and Cromer, D. T. (1967) *Acta Crystallogr.*, **23**, 865–7.
347. Asprey, L. B., Keenan, T. K., Penneman, R. A., and Sturgeon, G. D. (1966) *Inorg. Nucl. Chem. Lett.*, **2**, 19–21.
348. Penneman, R. A., Sturgeon, G. D., Asprey, L. B., and Kruse, F. H. (1965) *J. Am. Chem. Soc.*, **87**, 5803–4.
349. Penneman, R. A., Sturgeon, G. D., and Asprey, L. B. (1964) *Inorg. Chem.*, **3**, 126–9; Suglobova, I. G., Fedorov, V. L., and Chirkst, D. E. (1980) *Inorg. Mater.*, **16**, 452–9.
350. Sturgeon, G. D., Penneman, R. A., Kruse, F. H., and Asprey, L. B. (1965) *Inorg. Chem.*, **4**, 748–50.
351. Burns, J. H. (1962) *Acta Crystallogr.*, **15**, 1098–101.

352. Brown, G. M. and Walker, L. A. (1966) *Acta Crystallogr.*, **20**, 220–9.
353. Zachariasen, W. H. (1954) *Acta Crystallogr.*, **7**, 792–4.
354. Hoard, J. L. and Silverton, J. V. (1963) *Inorg. Chem.*, **2**, 235–43.
355. Lippard, S. J. and Russ, B. J. (1968) *Inorg. Chem.*, **7**, 1686–8.
356. Ryan, R. R. and Penneman, R. A. (1971) *Acta Crystallogr. B*, **27**, 829–33.
357. Kruse, F. H. (1971) *J. Inorg. Nucl. Chem.*, **33**, 1625–7.
358. Burns, J. H., Levy, H. A., and Keller, O. L. (1968) *Acta Crystallogr. B*, **24**, 1675–80.
359. Rosenzweig, A. and Cromer, D. T. (1970) *Acta Crystallogr. B*, **26**, 38–44.
360. Ryan, R. R., Larson, A. C., and Kruse, F. H. (1969) *Inorg. Chem.*, **8**, 33–6.
361. Burns, J. H., Ellison, R. D., and Levy, H. A. (1968) *Acta Crystallogr. B*, **24**, 230–7.
362. Brunton, G. (1971) *Acta Crystallogr. B*, **27**, 2290–2.
363. Brown, D., Kettle, S. F. A., and Smith, A. J. (1967) *J. Chem. Soc. A*, 1429–34.
364. Brown, D., Easey, J. F., and Holah, D. G. (1967) *J. Chem. Soc. A*, 1979–80.
365. Brunton, G. (1966) *Acta Crystallogr.*, **21**, 814–17.
366. Avignant, D., Mansouri, I., and Sabatier, R. (1980) *Acta Crystallogr. B*, **36**, 664–6.
367. Penneman, R. A., Ryan, R. R., and Rosenzweig, A. (1974) *Acta Crystallogr. B*, **30**, 1966–70.
368. Cousson, A., Tabuteau, A., Pages, M., and Gasperin, M. (1979) *Acta Crystallogr. B*, **35**, 1198–200.
369. Brunton, G. (1969) *Acta Crystallogr. B*, **25**, 1919–21.
370. Rosenzweig, A., Ryan, R. R., and Cromer, D. T. (1973) *Acta Crystallogr. B*, **29**, 460–2.
371. Keller, C. and Salzer, M. (1967) *J. Inorg. Nucl. Chem.*, **29**, 2925–34.
372. Brunton, G. (1970) *Acta Crystallogr. B*, **26**, 1185–7.
373. Cousson, A., Pages, M., and Chevalier, R. (1978) *Acta Crystallogr. B*, **34**, 1776–8.
374. Ryan, R. R., Penneman, R. A., and Rosenzweig, A. (1969) *Acta Crystallogr. B*, **25**, 1958–62.
375. Brunton, G. (1967) *J. Inorg. Nucl. Chem.*, **29**, 1631–6.
376. Abazli, H., Cousson, A., Tabuteau, A., Pages, M., and Gasperin, M. (1980) *Acta Crystallogr. B*, **36**, 2765–6.
377. Brunton, G. (1971) *Acta Crystallogr. B*, **27**, 245–7.
378. Brunton, G. (1972) *Acta Crystallogr. B*, **28**, 144–7.
379. Brunton, G. (1973) *Acta Crystallogr. B*, **29**, 2976–8.
380. Launay, S. and Rimsky, A. (1980) *Acta Crystallogr. B*, **36**, 910–12.
381. Cousson, A., Tabuteau, A., Pages, M., and Gasperin, M. (1979) *Acta Crystallogr. B*, **35**, 2674–6.
382. Keller, C. and Smutz, H. (1964) *Z. Naturf.*, **19b**, 1080; Burns, J. H. (1965) *Inorg. Chem.*, **4**, 881–6.
383. Penneman, R. A. and Ryan, R. R. (1973) *J. Chem. Soc. Chem. Commun.*, 69.
384. Zachariasen, W. H. (1948) *Acta Crystallogr.*, **1**, 268–9.
385. Brown, D. and Jones, P. J. (1967) *J. Chem. Soc. A*, 243–6.
386. Siegel, S. (1956) *Acta Crystallogr.*, **9**, 827.
387. Bagnall, K. W. and Laidler, J. B. (1966) *J. Chem. Soc. A*, 516–20.
388. Morss, L. R. and Fuger, J. (1969) *Inorg. Chem.*, **8**, 1433–9.
389. Morss, L. R., Siegal, M., Stenger, L., and Edelstein, N. (1970) *Inorg. Chem.*, **9**, 1771–5.
390. Bagnall, K. W., Laidler, J. B., and Stewart, M. A. A. (1968) *J. Chem. Soc. A*, 133–6.
391. Morss, L. R. and Robinson, W. R. (1972) *Acta Crystallogr. B*, **28**, 653–4.
392. Brown, D. (1966) *J. Chem. Soc. A*, 766–9.
393. Magette, M. and Fuger, J. (1977) *Inorg. Nucl. Chem. Lett.*, **13**, 529–36.

394. Siekierski, S. (1971) *J. Inorg. Nucl. Chem.*, **33**, 377–86.
395. Nugent, L. J. (1970) *J. Inorg. Nucl. Chem.*, **32**, 3485–91.
396. Templeton, D. H. and Dauben, C. H. (1954) *J. Am. Chem. Soc.*, **76**, 5237–9.
397. Brown, D., Easey, J. F., and Rickard, C. E. F. (1969) *J. Chem. Soc. A*, 1161–4.
398. Burns, J. H., Baldwin, W. H., and Stokely, J. R. (1973) *Inorg. Chem.*, **12**, 466–9.
399. Zachariasen, W. H. (1973) *J. Inorg. Nucl. Chem.*, **35**, 3487–97.
400. Cunningham, B. B. and Wallmann, J. C. (1964) *J. Inorg. Nucl. Chem.*, **26**, 271–5.
401. Noé, M. and Peterson, J. R. (1976) in *Transplutonium* 1975 (eds W. Müller and R. Lindner), North-Holland, Amsterdam, pp. 69–77.
402. Gorbenko-Germanov, D. S. and Klimov, V. C. (1966) *Russ. J. Inorg. Chem.*, **11**, 280–2.
403. Christ, C. L., Clark, J. R., and Evans, H. T. (1955) *Science*, **121**, 472–3.
404. Scavnicar, S. and Prodic, B. (1965) *Acta Crystallogr.*, **18**, 698–702.
405. Alcock, N. W., Esperas, S., Bagnall, K. W., and Hsian-Yun, W. (1978) *J. Chem. Soc. Dalton Trans.*, 638–46.
406. Ueki, T., Zalkin, A., and Templeton, D. H. (1966) *Acta Crystallogr.*, **20**, 836–41.
407. Taylor, J. C., Mueller, M. H., and Hitterman, R. L. (1966) *Acta Crystallogr.*, **20**, 842–51.
408. Staritzky, E. (1956) *Anal. Chem.*, **28**, 2021–2.
409. Johansson, G. (1968) *Acta Chem. Scand.*, **22**, 389–98.
410. Haque, M.-U., Caughlan, C. N., Hart, F. A., and Van Nice, R. (1971) *Inorg. Chem.*, **10**, 115–22.
411. Fleming, J. E. and Lynton, H. (1960) *Chem. Ind.*, 1415–16.
412. Graziani, R., Bombieri, G., Forsellini, E., Degetto, S., and Marangoni, G. (1973) *J. Chem. Soc. Dalton Trans.*, 451–4.
413. Casellato, U., Vigato, P. A., and Vidali, M. (1981) *Coord. Chem. Rev.*, **36**, 183–265.
414. Fried, S., Hagemann, F., and Zachariasen, W. H. (1950) *J. Am. Chem. Soc.*, **72**, 771–5.
415. Mooney, R. C. L. (1950) *Acta Crystallogr.*, **3**, 337–40.
416. Bjorklund, C. W. (1958) *J. Am. Chem. Soc.*, **79**, 6347–50.
417. Keller, C. and Walter, K. H. (1965) *J. Inorg. Nucl. Chem.*, **27**, 1253–60.
418. Mooney, R. C. L. (1948) *J. Chem. Phys.*, **16**, 1003.
419. Burdese, A. and Borlera, M. L. (1963) *Ann. Chim.*, **53**, 333–43.
420. Peyronel, G. (1936) *Z. Krist.*, **94**, 311–13; Levi, G. R. and Peyronel, G. (1935) *Z. Krist.*, **92**, 190–209.
421. Palache, C., Berman, H., and Frondel, C. (1951) *The System of Mineralogy*, 7th edn, vol. 2, Wiley, New York, p. 980ff.
422. Beintema, J. (1938) *Rec. Trav. Pays-Bas*, **57**, 155–74.
423. Fairchild, J. G. (1929) *Am. Min.*, **14**, 265–75; Weiss, A., Hartl, K., and Hofmann, U. (1957) *Z. Naturf.*, **12b**, 669–71.
424. Weigel, F. and Hoffmann, G. (1976) *J. Less Common Metals*, **44**, 99–123.
425. Weigel, F. and Hoffmann, G. (1976) *J. Less Common Metals*, **44**, 125–32.
426. Weigel, F. and Hoffmann, G. (1976) *J. Less Common Metals*, **44**, 133–6.
427. Matkovic, B., Prodic, B., Sljukiv, M., and Peterson, S. W. (1968) *Croat. Chem. Acta*, **40**, 147–61.
428. Lundgren, G. (1950) *Arkiv. Kemi*, **2**, 535–49.
429. Lundgren, G. (1952) *Arkiv. Kemi*, **4**, 421–8.
430. Kierkegaard, P. (1956) *Acta Chem. Scand.*, **10**, 599–616.
431. Lundgren, G. (1953) *Arkiv. Kemi*, **5**, 349–63.

432. Arutyunyan, E. G., Porai-Koshits, M. A., and Molodkin, A. K. (1966) *J. Struct. Chem.*, **7**, 683–6.
433. Burns, J. H. and Baybarz, R. D. (1972) *Inorg. Chem.*, **11**, 2233–7.
434. Bullock, J. I., Ladd, M. F. C., Povey, D. C., and Storey, A. E. (1980) *Inorg. Chim. Acta*, **43**, 101–8.
435. Eliseev, A. A., Molodkin, A. K., and Ivanova, O. M. (1967) *Russ. J. Inorg. Chem.*, **12**, 1507–8.
436. Jelenić, I., Grdenić, D., and Bezjak, A. (1964) *Acta Crystallogr.*, **17**, 758–9.
437. Akhtar, M. M. and Smith, A. J. (1969) *J. Chem. Soc. Chem. Commun.*, 705–6.
438. Alcock, N. W., Kemp, T. J., Sostero, S., and Traverso, O. (1980) *J. Chem. Soc. Dalton Trans.*, 1182–5.
439. Chackraburtty, D. M. (1963) *Acta Crystallogr.*, **16**, 834.
440. Weigel, F. and ter Meer, N. (1967) *Inorg. Nucl. Chem. Lett.*, **3**, 403–8.
441. Scherer, V. and Fochler, M. (1968) *J. Inorg. Nucl. Chem.*, **30**, 1433–7.
442. Hansson, E. (1970) *Acta Chem. Scand.*, **24**, 2969–82.
443. Ollendorff, W. and Weigel, F. (1969) *Inorg. Nucl. Chem. Lett.*, **5**, 263–9.
444. Burns, J. H. and Baldwin, W. H. (1977) *Inorg. Chem.*, **16**, 289–94.
445. Bagnall, K. W., Brown, D., and Holah, D. G. (1968) *J. Chem. Soc. A*, 1149–53.
446. Brown, D., Holah, D. G., Rickard, C. E. F., and Moseley, P. T. (1970) *J. Chem. Soc. A*, 423–5.
447. Brown, D., Holah, D. G., and Rickard, C. E. F. (1970) *J. Chem. Soc. A*, 786–90.
448. Calderazzo, F., dellAmico, G., Pasquali, M., and Perego, G. (1978) *Inorg Chem.*, **17**, 474–9.
449. Allard, B. (1976) *J. Inorg. Nucl. Chem.*, **38**, 2109–15.
450. Brown, D., Whittaker, B., and Tacon, J. (1975) *J. Chem. Soc. Dalton Trans.*, 34–9.
451. Lenner, M. (1978) *Acta Crystallogr. B*, **34**, 3770–2.
452. Hambley, T. W., Kepert, D. L., Raston, C. L., and White, A. H. (1978) *Aust. J. Chem.*, **31**, 2635–40.
453. Wolf, L. and Bärnighausen, H. (1960) *Acta Crystallogr.*, **13**, 778–85.
454. Wiedenheft, C. (1969) *Inorg. Chem.*, **8**, 1174–9.
455. Navaza, A., deRango, C., and Charpin, P. (1980) *Acta Crystallogr. B*, **36**, 696–7.
456. Hill, R. J. and Rickard, C. E. F. (1977) *J. Inorg. Nucl. Chem.*, **39**, 1593–6.
457. Danford, M. D., Burns, J. H., Higgins, C. E., Stokely, J. R., and Baldwin, W. H. (1970) *Inorg. Chem.*, **9**, 1953–5.
458. Erasmus, C. S. and Boeyens, J. C. A. (1970) *Acta Crystallogr. B*, **26**, 1843–54.
459. Burns, J. H. and Danford, M. D. (1969) *Inorg. Chem.*, **8**, 1780–4.
460. Swain, H. A. and Karraker, D. G. (1970) *Inorg. Chem.*, **9**, 1766–9.
461. Day, V. W. and Hoard, J. L. (1970) *J. Am. Chem. Soc.*, **92**, 3626–35.
462. Hill, R. J. and Rickard, C. E. F. (1975) *J. Inorg. Nucl. Chem.*, **37**, 2481–5.
463. Huber-Buser, E. (1975) *Cryst. Struct. Commun.*, **4**, 731–5.
464. Leipoldt, J. G., Wessels, G. F. S., and Bok, L. D. C. (1975) *J. Inorg. Nucl. Chem.*, **37**, 2487–90.
465. Lenner, M. and Lindquist, O. (1979) *Acta Crystallogr. B*, **35**, 600–3.
466. Geiren, A. (1973) quoted by F. Lux (1973) *Proc. Tenth Rare Earth Research Conf.*, CONF-730402-P2, USAEC, Oak Ridge, Tenn., p. 871.
467. Kirin, I. S., Kolyadin, A. B., and Lychev, A. A. (1974) *J. Struct. Chem.*, **15**, 415–18.
468. Geiren, A. and Hoppe, W. (1971) *J. Chem. Soc. Chem. Commun.*, 413–14.
469. Charpin, P., Costes, R. M., Folcher, G., Plurein, P., Navaza, A., and deRango, C. (1977) *Inorg. Nucl. Chem. Lett.*, **13**, 341–7

470. Eller, P. G. and Penneman, R. A. (1976) *Inorg. Chem.*, **15**, 2439–42.
471. deVillardi, G. C., Charpin, P., Costes, R. M., Folcher, G., Plurien, P., Rigny, P., and deRango, C. (1978) *J. Chem. Soc. Chem. Commun.*, 90–2.
472. Volz, K., Zalkin, A., and Templeton, D. H. (1976) *Inorg. Chem.*, **15**, 1827–31.
473. Bombieri, G., Moseley, P. T., and Brown, D. (1975) *J. Chem. Soc. Dalton Trans.*, 1520–3.
474. Bombieri, G., dePaoli, G., Forsellini, E., and Brown, D. (1979) *J. Inorg. Nucl. Chem.*, **41**, 827–31.
475. Rickard, C. E. F. and Woolard, D. C. (1979) *Aust. J. Chem.*, **32**, 2181–5.
476. Countryman, R. and McDonald, W. S. (1971) *J. Inorg. Nucl. Chem.*, **33**, 2213–20.
477. Al-Kazzaz, Z. M. S., Bagnall, K. W., Brown, D., and Whittaker, B. (1972) *J. Chem. Soc. Dalton Trans.*, 2273–7.
478. Del Piero, G., Perego, G., Zazzetta, A., and Brandi, G. (1975) *Cryst. Struct. Commun.*, **4**, 521–6.
479. Rickard, C. E. F. and Woolard, D. C. (1980) *Aust. J. Chem.*, **33**, 1161–5.
480. Reynolds, J. G., Zalkin, A., Templeton, D. H., and Edelstein, N. M. (1977) *Inorg. Chem.*, **16**, 599–603.
481. Reynolds, J. G., Zalkin, A., Templeton, D. H., and Edelstein, N. M. (1977) *Inorg. Chem.*, **16**, 1858–61.
482. Reynolds, J. G., Zalkin, A., Templeton, D. H., Edelstein, N. M., and Templeton, L. K. (1976) *Inorg. Chem.*, **15**, 2498–502.
483. Reynolds, J. C., Zalkin, A., Templeton, D. H., and Edelstein, N. (1977) *Inorg. Chem.*, **16**, 1090–6.
484. Cernia, E. and Mazzei, A. (1974) *Inorg. Chim. Acta*, **10**, 239–52.
485. Baker, E. C., Halstead, G. W., and Raymond, K. N. (1976) *Struct. Bonding*, **25**, 23–68.
486. Raymond, K. N. and Eigenbrot, C. W. (1980) *Acc. Chem. Res.*, **13**, 275–83.
487. Wong, C. H., Yen, T., and Lee, T. (1965) *Acta Crystallogr.*, **18**, 340–4.
488. Burns, J. H. and Laubereau, P. G. (1971) *Inorg. Chem.*, **10**, 2789–92.
489. Leong, J., Hodgson, K. O., and Raymond, K. N. (1973) *Inorg. Chem.*, **12**, 1329–35.
490. Fischer, R. D., von Ammon, R., and Kanellakopulos, B. (1970) *J. Organometal. Chem.*, **25**, 123–37.
491. Ryan, R. R., Penneman, R. A., and Kanellakopulos, B. (1975) *J. Am. Chem. Soc.*, **97**, 4258–60.
492. Brandi, G., Brunelli, M., Lugli, G., and Mazzei, A. (1973) *Inorg. Chim. Acta*, **7**, 319–22; Gebala, A. E. and Tsutsui, M. (1973) *J. Am. Chem. Soc.*, **95**, 91–3; Marks, T. J. and Seyam, A. M. (1972) *J. Am. Chem. Soc.*, **94**, 6545–6.
493. Atwood, J. L., Tsutsui, M., Ely, N., and Gebala, A. E. (1976) *J. Coord. Chem.*, **5**, 209–15.
494. Atwood, J. L., Hains, C. F., Tsutsui, M., and Gebala, A. E. (1973) *J. Chem. Soc. Chem. Commun.*, 452–3.
495. Perego, G., Cesari, M., Farina, F., and Lugli, G. (1976) *Acta Crystallogr. B*, **32**, 3034–9.
496. Eigenbrot, C. W. and Raymond, K. N. (1981) *Inorg. Chem.*, **20**, 1553–6.
497. Fischer, R. D., Klahne, E., and Kopf, J. (1978) *Z. Naturf. B*, **33**, 1393.
498. Brunelli, M., Lugli, G., and Giacometti, G. (1973) *J. Magn. Reson.*, **9**, 247–54.
499. Halstead, G. W., Baker, E. C., and Raymond, K. N. (1975) *J. Am. Chem. Soc.*, **97**, 3049–52.
500. Brunelli, M., Perego, G., Lugli, G., and Massei, A. (1979) *J. Chem. Soc. Dalton Trans.*, 861–8.

501. Kanellakopulos, B. (1972) in *MTP International Review of Science, Inorganic Chemistry*, ser. 1, vol. 7, *Lanthanides and Actinides* (ed. K. W. Bagnall), Butterworths, London, p. 308; Karraker, D. G. and Stone, J. A. (1972) *Inorg. Chem.*, **11**, 1742–6.
502. Burns, J. H. (1974) *J. Organometal. Chem.*, **69**, 225–33.
503. Broach, R. W., Schultz, A. J., Williams, J. M., Brown, G. M., Manriquez, J. M., Fagan, P. J., and Marks, T. J. (1979) *Science*, **203**, 172–4.
504. Baker, E. C., Raymond, K. N., Marks, T. J., and Wachter, W. A. (1974) *J. Am. Chem. Soc.*, **96**, 7586–8.
505. Manriquez, J. M., Fagan, P. J., Marks, T. J., Day, C. S., and Day, V. W. (1978) *J. Am. Chem. Soc.*, **100**, 7112–14.
506. Fagan, P. J., Manriquez, J. M., Marks, T. J., Day, V. W., Vollmer, S. H., and Day, C. S. (1980) *J. Am. Chem. Soc.*, **102**, 5393–6.
507. Cramer, R. E., Maynard, R. B., and Gilje, J. W. (1980) *Inorg. Chem.*, **19**, 2564–9.
508. Manriquez, J. M., Fagan, P. J., Marks, T. F., Vollmer, S. H., Day, C. S., and Day, V. W. (1979) *J. Am. Chem. Soc.*, **101**, 5075–8.
509. Laubereau, P. G. (1970) *Inorg. Nucl. Chem. Lett.*, **6**, 611–16.
510. Atwood, J. L. and Smith, K. D. (1973) *J. Chem. Soc. Dalton Trans.*, 2487–90.
511. Burns, J. H. and Laubereau, P. G., unpublished results.
512. Baker, E. C., Brown, L. D., and Raymond, K. N. (1975) *Inorg. Chem.*, **14**, 1376–9.
513. Ernst, R. D., Kennelly, W. J., Day, C. S., Day, V. W., and Marks, T. J. (1979) *J. Am. Chem. Soc.*, **101**, 2656–64.
514. Bombieri, G., de Paoli, G., Del Pra, A., and Bagnall, K. W. (1978) *Inorg. Nucl. Chem. Lett.*, **14**, 359–61.
515. Fronczek, F. R., Halstead, G. W., and Raymond, K. N. (1977) *J. Am. Chem. Soc.*, **99**, 1769–75.
516. Secaur, C. A., Day, V. W., Ernst, R. D., Kennelly, W. J., and Marks, T. J. (1976) *J. Am. Chem. Soc.*, **98**, 3713–15.
517. Kanellakopulos, B., Dornberger, E., and Baumgärtner, F. (1974) *Inorg. Nucl. Chem. Lett.*, **10**, 155–60.
518. Laubereau, P. G. and Burns, J. H. (1970) *Inorg. Chem.*, **9**, 1091–5; Laubereau, P. G. and Burns, J. H. (1970) *Inorg. Nucl. Chem. Lett.*, **6**, 59–63.
519. Wong, C. H., Lee, T., and Lee, Y. (1969) *Acta Crystallogr. B*, **25**, 2580–7.
520. Burns, J. H., Baldwin, W. H., and Fink, F. H. (1974) *Inorg. Chem.*, **13**, 1916–20.
521. Burns, J. H. and Baldwin, W. H. (1976) *J. Organometal. Chem.*, **120**, 361–8.
522. Kanellakopulos, B. and Aderhold, C. (1973) *XXIVth IUPAC Congress*, Hamburg, Abstracts, p. 632.
523. Streitwieser, A. and Müller-Westerhoff, U. (1968) *J. Am. Chem. Soc.*, **90**, 7364.
524. Zalkin, A. and Raymond, K. N. (1969) *J. Am. Chem. Soc.*, **91**, 5667–8.
525. Avdeef, A., Raymond, K. N., Hodgson, K. O., and Zalkin, A. (1972) *Inorg. Chem.*, **11**, 1083–8.
526. Starks, D. F., Parsons, T. C., Streitwieser, A., and Edelstein, N. (1974) *Inorg. Chem.*, **13**, 1307–8.
527. Karraker, D. G., Stone, J. A., Jones, E. R., and Edelstein, N. (1970) *J. Am. Chem. Soc.*, **92**, 4841–5.
528. Templeton, L. K., Templeton, D. H., and Walker, R. (1977) *Inorg. Chem.*, **15**, 3000–3.
529. Zalkin, A., Templeton, D. H., Berryhill, S. R., and Luke, W. D. (1979) *Inorg. Chem.*, **18**, 2287–9.

530. Zalkin, A., Templeton, D. H., leVanda, C., and Streitweiser, A. (1980) *Inorg. Chem.*, **19**, 2560–3.
531. Karraker, D. G. and Stone, J. A. (1974) *J. Am. Chem. Soc.*, **96**, 6885–8.
532. Hodgson, K. O. and Raymond, K. N. (1972) *Inorg. Chem.*, **11**, 3030–5.
533. Cesari, M., Pedretti, U., Zazzetta, A., Lugli, G., and Marconi, W. (1971) *Inorg. Chim. Acta*, **5**, 439–44.
534. Köhler, E., Brüser, W., and Thiele, K. H. (1974) *J. Organometal. Chem.*, **76**, 235–40.
535. Davies, G. R., Jarvis, J. A. T., and Kilbourn, B. T. (1971) *J. Chem. Soc. Chem. Commun.*, 1511–12.
536. Larson, D. T. and Haschke, J. M. (1981) *Inorg. Chem.*, **20**, 1945–50.
537. Shannon, R. D. (1976) *Acta Crystallogr. A*, **32**, 751–67.
538. Peterson, J. R. and Fuger, J. (1971) *J. Inorg. Nucl. Chem.*, **33**, 4111–17.
539. Ritger, P. L., Burns, J. H., and Bombieri, G. (1983) *Inorg. Chim. Acta*, 77, L217–9.
540. Morss, L. R. (1982) in *Actinides in Perspective* (ed. N. M. Edelstein), Pergamon, Oxford. pp. 381–407.
541. Wolf, R. and Hopper, R. (1985) *Z. Anorg. Allg. Chem.*, **528**, 129–37.
542. Hoekstra, H. R. (1982) in *Gmelin Handbook of Inorg. Chem.*, Uranium, Suppl. **A5**, Springer-Verlag, Berlin. pp. 211–240.
543. Kudryashov, V. L., Suglobova, I. G., and Chirkst, D. E. (1978) *Radiokhimiya*, **20**, 366–72.

CHAPTER TWENTY ONE

SOLUTION CHEMISTRY AND KINETICS OF IONIC REACTIONS

Sten Ahrland

21.1 IONS FORMED IN NON-COMPLEX AQUEOUS SOLUTIONS

In sufficiently acid aqueous solutions containing no complex-forming ligands, actinides in oxidation states II to VI exist as hydrated M^{2+}, M^{3+}, M^{4+}, MO_2^+, and MO_2^{2+} ions. As is generally the case with metal-ion hydrates, those of the actinides act as acids, splitting off protons from the water molecules of the hydration shell. Their strength as acids increases strongly with the charge on the central atom. The divalent ions are probably very weak acids. On account of their large radii, the trivalent actinide ions are much weaker acids than are most other metal ions of this charge. The charge of the tetravalent ions is, however, high enough to turn their hydrates into quite strong acids, in spite of the large radii. Hydrates of penta- and hexavalent ions are too acidic to exist in aqueous solution. Even at extremely high acidities, these ions are hydrolyzed to actinyl(V) and actinyl(VI) ions, respectively, with the exception of protactinium(V) which forms a less hydrolyzed species, as discussed below. The charge on the central atom of these rod-shaped ions is considerably higher than the net ionic charge. In the case of MO_2^+, the charge is nevertheless not high enough to make the hydrate a very strong acid. The acid properties of the MO_2^{2+} ions are, on the other hand, quite significant.

The only divalent ions able to exist in aqueous solution seem to be Md^{2+} and No^{2+} [1–7]. In the case of nobelium, the divalent state is even the most stable one, evidently on account of its filled f shell. The standard potential of the No^{3+}/No^{2+} couple vs the standard hydrogen electrode is nearly 1.5 V, making No^{3+} a strong oxidizing agent [4]. The tendency to complete the f shell is thus much stronger for nobelium than for the homologous lanthanide ytterbium. A value of -1.15 V has been found for the standard potential of the Yb^{3+}/Yb^{2+} couple, implying that Yb^{2+} is a strong reducing agent [8].

On the other hand, Am^{2+} does not exist as a stable species in aqueous solution in spite of the possibility of a half-filled f shell. The ion can be produced by pulse radiolysis but its half-life is extremely short, about 5 μs [7]. The tendency to complete a half-filled f shell is evidently much stronger for the homologous lanthanide europium. The Eu^{2+} ion is only a moderately strong reducing agent, the standard potential of the Eu^{3+}/Eu^{2+} couple being -0.35 V [9].

In ethanol solution, californium, einsteinium, and fermium can also be reduced to the divalent state by Sm(II) or Yb(II) even if the solutions contain 15% water [223, 224]. Attempts to reduce mendelevium further to the monovalent state, which would correspond to a filled f shell, appear to have failed, although this matter remains controversial [224] (see also Chapter 13).

M^{3+} ions are formed in aqueous solution by all actinides except protactinium and thorium. In the case of uranium, the rather strong reducing properties of U^{3+} have made its investigation difficult. Np^{3+} is already fairly stable to oxidation, however, and Pu^{3+} is an easily formed state of this element. For the other actinides, the trivalent state is the predominant one, with the exception of nobelium, mentioned above.

All actinides from thorium to californium form tetravalent oxidation states. For the three elements of highest atomic number, however, viz. americium, curium, and berkelium, the hydrated M^{4+} ions are too strongly oxidizing to be stable in aqueous solution [7, 10]. Their rates of reduction nevertheless vary widely, in the order $Bk^{4+} < Am^{4+} < Cm^{4+} < Cf^{4+}$, with Bk^{4+} being by far the most resistant species. This is also the order of thermodynamic stability, as indicated by the oxidation potentials of the M^{4+}/M^{3+} couples [11]. Americium(IV) is also very prone to disproportionation into the trivalent and pentavalent, or even hexavalent, states (see Chapter 8). Americium(IV) can be stabilized [12] by the fluoride ion, a strongly complexing agent preferring the tetravalent state, as will be discussed further below (Section 21.4.2).

In the case of thorium, on the other hand, the tetravalent state is the only one existing in solution. The hydrated Th^{4+} ion is, moreover, by far the least acidic of the actinide M^{4+} ions. In contrast to this, the neighbor Pa^{4+} is by far the most acidic, extensively hydrolyzed even in strongly acid solutions. The acidities of U^{4+}, Np^{4+}, and Pu^{4+} are intermediate. These ions all play an important part in the solution chemistries of the respective elements, though U^{4+} especially is fairly easily oxidized.

MO_2^+ ions are formed by all elements from protactinium to americium. For protactinium, the pentavalent oxidation state is in fact the most stable one [13]. The protactinyl(v) ion takes up a proton much more readily than do other actinyl(v) ions, so it should perhaps be formulated as $PaO(OH)_2^+$ rather than as PaO_2^+ [14]. The former formula also accounts for the marked resistance of the last oxygen against further addition of protons. Also, for neptunium, the pentavalent state is very important, though NpO_2^+ has a perceptible tendency to disproportionate. For UO_2^+, PuO_2^+, and AmO_2^+ this tendency is very marked. It is not possible to obtain aqueous solutions which in equilibrium contain exclusively the pentavalent state. Under special conditions, however, a sizable proportion of the total metal concentration may well be present as MO_2^+ (see, for example, ref. 15 for UO_2^+, and ref. 16 for PuO_2^+). On account of the slow reduction of plutonium(v), fairly pure solutions of PuO_2^+ can be prepared that are kinetically reasonably stable [17] and at pH $\sim$ 8 may even predominate in seawater under oxidizing conditions. Complex formation with carbonate ions strongly stabilizes MO_2^+, especially in the form of many solid carbonato complexes [18].

MO_2^{2+} ions are formed by the four elements from uranium to americium. For uranium, the hexavalent oxidation state is the most stable one. Though easily reduced, it is also prominent in the chemistries of neptunium and plutonium. Americium(VI) is a very strong oxidizing agent. As the americium isotopes available are quite radioactive, a steady radiation-induced reduction of AmO_2^{2+} occurs in aqueous solution, as soon as a strongly oxidizing system is not present [19].

Neptunium and plutonium also form heptavalent oxidation states [20, 21]. In acid aqueous solutions, these are strong oxidizing agents. Neptunium(VII) is reduced by water in a short while, and plutonium(VII) almost at once. The rapid reduction has precluded any direct determination of the formulas of the ionic species present. In alkaline solutions, on the other hand, both neptunium(VII) and plutonium(VII) are reasonably stable, though a slow reduction still takes place, again more rapidly in the case of plutonium(VII). The elements are present as analogous anions, most probably of charge 3−. The simplest formula is thus MO_5^{3-}. On reduction of neptunium to the hexavalent state, an anion of charge 2− is formed, most simply formulated as MO_4^{2-}. The ready reversibility of the Np(VII)/Np(VI) couple indicates, however, that no markedly covalent Np–O bonds are likely to be broken in the electrode reaction, which would be the case if the anions had the formulas stated. Much more probable compositions are $NpO_2(OH)_6^{3-}$ and $NpO_2(OH)_4(H_2O)_2^{2-}$, respectively, where the reduction is accompanied only by simple protonations [22]. These formulas are also supported by the composition of the hexaammine cobalt(III) salt of neptunium(VII) anion, which corresponds to the formula $Co(NH_3)_6[NpO_2(OH)_6)]$. The anions would then contain the entity MO_2^{3+}, corresponding to MO_2^{2+} and MO_2^+ formed by the hexa- and pentavalent states. In acid solutions the hydrated MO_2^{3+}, and/or more or less hydrolyzed forms of this ion, would be the strong oxidizing species present.

21.2 ACIDIC PROPERTIES OF ION HYDRATES

21.2.1 Divalent ions

The divalent ions Md^{2+} and No^{2+} are available only in extremely minute amounts. The numbers of atoms used in a single experiment have been [1, 2, 23] at most approximately 10^5 for the more easily synthesized mendelevium (as the isotope ^{256}Md; $t_{1/2} = 77$ min) and approximately 10^3 for nobelium (as ^{255}No; $t_{1/2} = 223$ s). The opportunity to study the chemical behavior of Md^{2+} and No^{2+} is therefore restricted and no investigations of their hydrolytic reactions have so far been made. As already mentioned, they must in any case be extremely weak acids. From the affinities of No^{2+} toward carboxylate ions (Section 21.4.4), it might be concluded that their hydrolytic behavior is much the same as that of Ca^{2+} or Sr^{2+} [23].

21.2.2 Trivalent ions

Surprisingly little is known about the hydrolysis of the trivalent actinide ions M^{3+}. On account of their large radii they are, as already mentioned, quite weak acids. In the case of the easily oxidized U^{3+} and Np^{3+}, traces of the tetravalent states are difficult to avoid. As these are much stronger acids, reliable determinations of the acidities of the trivalent ions are difficult. For Pu^{3+}, the constant β_{11}^*, referring to simple mononuclear dissociation:

$$Pu^{3+} + H_2O \rightleftharpoons PuOH^{2+} + H_3O^+$$

was determined in the early days of plutonium solution chemistry [24]. A value of $p\beta_{11}^* = 6.95$ was found, but in this case the result may also be affected by oxidation to plutonium(IV) and by precipitation reactions. The result should therefore be regarded as a lower limit for $p\beta_{11}^*$. That the value should in fact be higher also looks reasonable by comparison with the lanthanides, where the values of $p\beta_{11}^*$ vary between 8.5 (La^{3+}) and 7.6 (Lu^{3+}), and with Y^{3+}, where $p\beta_{11}^* = 7.7$ (table 7.2 of ref. 25). As the actinide ions have larger radii, they should be weaker acids than Y^{3+} and the lanthanide ions, i.e. their values of $p\beta_{11}^*$ should be higher. In view of this, the even lower value of 5.54 (at an ionic strength $I = 1$ M) is rather surprising [238]. Even more so are the very low values found by a solvent extraction method for Pu^{3+}, Am^{3+}, Cm^{3+}, Bk^{3+}, Cf^{3+}, Es^{3+}, and Fm^{3+} ($p\beta_{11}^* = 3.80$ for Pu^{3+} [239]; $p\beta_{11}^*$ decreasing between Am^{3+} and Fm^{3+} from 5.92 to 3.8 [26–28]). The suspicion that this method gives much too low values of $p\beta_{11}^*$ is strengthened by the fact that $p\beta_{11}^*$ values for the lanthanide ions determined in this way are indeed much lower than those found by direct measurements of pH [25, 29]. Very recent measurements of $p\beta^*$ for Am^{3+} yield expected values of 7.5 [266, 267].

21.2.3 Tetravalent ions

The strongly acidic properties of the tetravalent actinide ions M^{4+} have been subject to many investigations. This applies especially to thorium, where the tetravalent oxidation state is of unique importance as the only one existing in solution. The stability of tetravalent thorium, and its easy availability, also allow very thorough studies without the expenditure of an excessive amount of time and effort. The Th^{4+} ion is therefore suitable to use as a model for other tetravalent actinide ions, though it should be remembered that, as the first member of the series, Th^{4+} presents certain specific features.

The hydrolysis of Th^{4+} involves extensive formation of polynuclear complexes. In the earlier stages of the hydrolysis in perchlorate media, when the number of hydroxide ions per thorium atom in the complexes (i.e. the ligand number $\bar{n}$) is $\bar{n} \lesssim 2$, the hydrolytic reactions are fully reversible and equilibrium is quickly reached [30–32]. The first extensive measurements [30] were interpreted as indicating the formation of an infinite series of 'core + links' complexes, $Th((OH)_3Th)_n^{4+n}$. Other measurements at widely varying pH and central-ion concentration, C_M, could, however, be satisfactorily fitted by only three polymers, viz. $Th_2(OH)_2^{6+}$, $Th_4(OH)_8^{8+}$, and $Th_6(OH)_{15}^{9+}$, besides the two monomers $ThOH^{3+}$ and $Th(OH)_2^{2+}$ [31, 32]. In Table 21.1 the constants β_{mn}^* are listed, referring to the equilibrium (asterisk refers to hydrolysis reaction):

$$m\mathrm{Th}^{4+} + n\mathrm{H_2O} \rightleftharpoons \mathrm{Th}_m(\mathrm{OH})_n^{4m-n} + n\mathrm{H}^+.$$

At 25°C, and even more so at 0°C, mononuclear complexes are of minor importance, except in extremely dilute solutions. As the temperature increases they become more prominent, however. These conditions are illustrated by the distribution diagrams for 0 and 95°C in Fig. 21.1 [32]. From the temperature dependence of the constants, values of the standard enthalpy and entropy changes, ΔH_{mn}° and ΔS_{mn}°, have been calculated, as will be discussed further below. Of the complexes mentioned, $Th_2(OH)_2^{6+}$ certainly plays an important part also in chloride media [25, 33, 259]. Rather than $Th_4(OH)_8^{8+}$ and $Th_6(OH)_{15}^{9+}$, the complexes $Th_2(OH)_3^{5+}$ and $Th_6(OH)_{14}^{10+}$ seem to be formed in chloride media, however (Table 21.1). In nitrate medium, the complexes $Th_2(OH)_2^{6+}$ and $Th_6(OH)_{15}^{9+}$ are again found, along with $Th_3(OH)_5^{7+}$, not found in the other media [240]. Constants for corresponding complexes are somewhat smaller throughout in chloride and nitrate media. This is expected as formation of chloride and nitrate complexes, markedly suppressing hydrolysis, certainly takes place at the high ionic concentration (3 M) employed (Section 21.4.2).

For values $\bar{n} \gtrsim 2$, equilibrium is no longer rapidly established. Slow reactions occur resulting in the formation of very large polymers before precipitation finally takes place. The formation of these large aggregates is best investigated by methods such as ultracentrifugation and light scattering, which measure the particle size. For the present system, both methods indicate a very rapid increase

Table 21.1 *Hydrolysis of thorium (IV) and uranium (IV) in solutions of various ionic strengths I and temperatures t. Medium (Na,H)ClO_4, if not otherwise stated. Constants $p\beta^*_{mn}$ listed refer to the acid dissociation equilibria* $mM^{4+} + nH_2O \rightleftharpoons M_m(OH)_n^{(4m-n)+} + nH^+$.

	m,n	$t = 0°C$[a] $I = 1$ M	25°C 1 M	95°C 1 M	25°C 3 M[b]	25°C 3 M[c]
Th^{4+}	1,1	4.31	4.23	2.25		
	1,2	8.46	7.69	4.51		
	2,2	5.59	4.61	2.59	4.69	5.19
	2,3				8.73	
	4,8	22.80	19.16	10.44		
	6,14				36.37	
	6,15	43.81	37.02	20.61		42.3
	Ref.	32	31	32	25	240
	m,n	$t = 10°C$ $I = 0.5$ M	25°C 0.5 M	43°C 0.5 M	25°C 3 M[d]	25°C 3 M[e]
U^{4+}	1,1	1.90	1.47	1.00	2.00	2.1
	6,15				18.2	16.9
	Ref.		40		42	25

[a] The constants referring to these temperatures are on the molality scale.
[b] Medium (Na,H)Cl. Recalculation of data from ref. 33.
[c] Medium (Na,H)NO_3. Complex $Th_3(OH)_5^{7+}$ also suggested, $p\beta^*_{35} = 14.23$.
[d] Series of 'core + links' complexes suggested.
[e] Recalculation of data from ref. 42, considering only the two complexes listed here.

of the average degree of polymerization in perchlorate solutions once $\bar{n}$ has exceeded 2 (Fig. 21.2) [34, 35]. For $\bar{n} = 3$, the aggregates contain on average well over 100 thorium atoms. For $\bar{n} \lesssim 2.4$, the particle size found agrees fairly well with that calculated from pH measurements. In chloride solutions, the polymerization is even more extensive, and also much slower; already at $\bar{n} \simeq 2$, equilibrium is not established even after several months [35].

Direct structure determinations by x-ray diffraction on hydrolyzed thorium nitrate solutions of $\bar{n} \simeq 0.7$ have confirmed the existence of the dimer $Th_2(OH)_2^{6+}$ [36]. The Th–Th distance is 3.99 Å, i.e. exactly the same as in the solid $Th_2(OH)_2(NO_3)_6(H_2O)_8$ which contains dimers joined by double hydroxo bridges [36]. Most likely, therefore, the same type of bridging occurs in the solution. As the hydrolysis proceeds, complexes of higher nuclearity become prominent, though the Th–Th distance stays much the same, approximately 3.94 Å. At $\bar{n} = 2.4$, the average number of thorium atoms in the complexes is at least 4, possibly as high as 6, which agrees fairly well with the values found by other methods (Fig. 21.2). The scattering data do not allow a unique interpretation of the structures of these complexes, since more than one structural model is

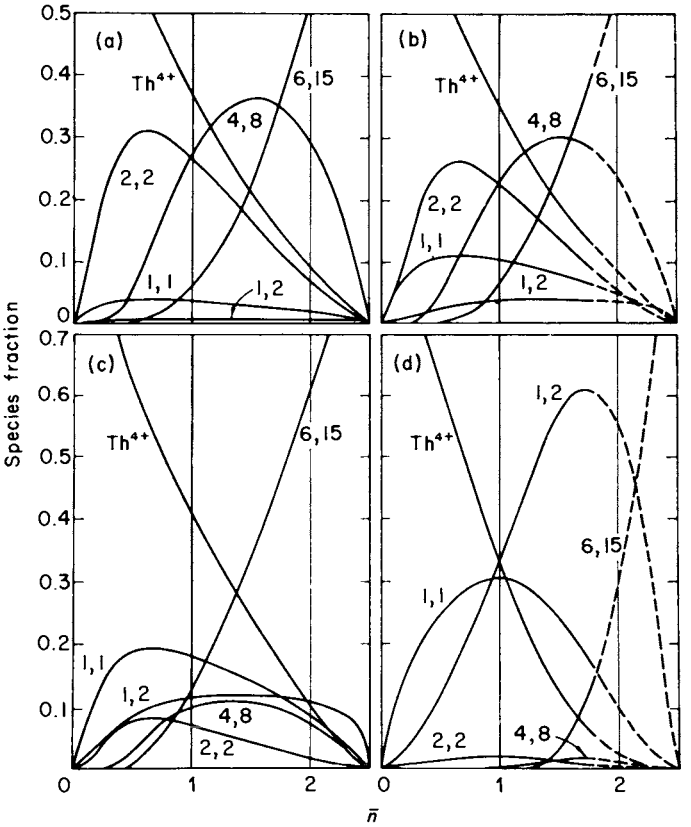

Fig. 21.1 *Species fractions in hydrolyzed thorium(IV) solutions as a function of the ligand number $\bar{n}$ for two highly different values of the thorium concentration, at 0 and 95°C* [32]. *The concentrations are expressed in molalities, m. Medium* 1 M *(Na,H)ClO_4. (a)* 0°C, 0.1 *m; (b)* 95°C, 0.1 *m; (c)* 0°C, 0.001 *m; (d)* 95°C, 0.001 *m.*

in approximate agreement with the data. The hydrolytic complexes formed in concentrated nitrate solutions also contain nitrate ligands, coordinated as bidentates. As expected, the number of nitrate ions coordinated per thorium decreases as hydrolysis becomes more extensive. Diffraction measurements on hydrolyzed solutions of thorium perchlorate and chloride give the same Th–Th distance of 3.94 Å, implying that the same type of hydroxo-bridged complexes are also formed in these media [36].

The evidence is still scarce and conflicting on the hydrolysis of Pa^{4+}. Values of $p\beta^*_{11} = 0.14$ and $p\beta^*_{12} = 0.52$ have been found for the first two mononuclear complexes in a 3 M $(Li,H)ClO_4$ medium, by means of a solvent extraction method [37]. This would mean that about 50% of the protactinium is present as Pa^{4+} in 1 M perchloric acid. Other extraction measurements indicate, however, that a divalent ion, i.e. $Pa(OH)_2^{2+}$ or PaO^{2+}, is still the predominant species in 1 M acid

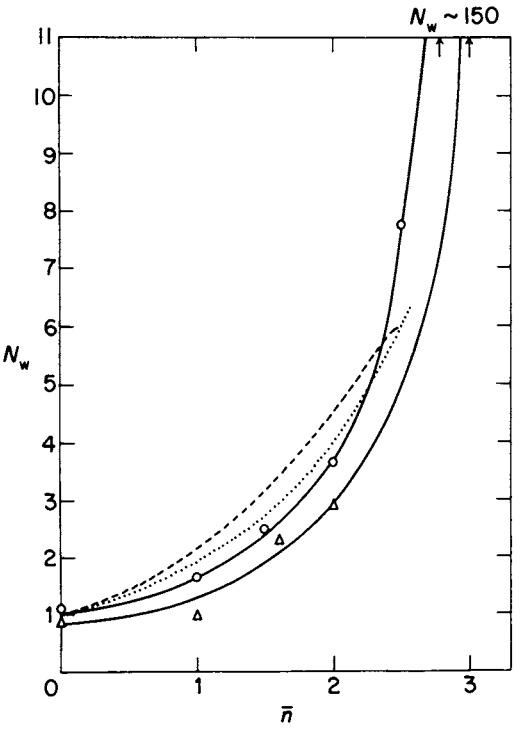

Fig. 21.2 *Weight-average degree of polymerization, N_w, of hydrolyzed thorium(IV) solutions as a function of the ligand number $\bar{n}$, at 25°C* [35]*: equilibrium centrifugation in* 1 M *(Na,H)ClO_4* [35], ○——; *light scattering in* 1 M *(Na,H)ClO_4* [34], △——; *calculated from $p[H^+]$ measurements in* 1 M *(Na,H)ClO_4* [32], ...; *and calculated from $p[H^+]$ measurements in* 3 M *(Na,H)Cl* [33], – – – –.

[38]. The latter study admittedly refers to a 1 M (Na,H)ClO_4 medium, but the difference in medium is hardly large enough to account for such a large difference in the degree of hydrolysis. The reason for the discrepancy is therefore still obscure. The mononuclear complexes predominate only in extremely dilute solutions. Polymers become prominent at protactinium concentrations as low as 10^{-5} M [37].

The hydrolysis of U^{4+} has been investigated fairly thoroughly [260]. Though U^{4+} is readily hydrolyzed, it does exist as a hydrated ion in strongly acid solutions [39]. As hydrolysis changes the light absorption very markedly, and because precise potentiometric studies are difficult at high acidities, it was natural to use spectrophotometric methods in the first investigations of the hydrolysis [39–41]. At low uranium concentrations and high acidities, where the first mononuclear species UOH^{3+} predominates, such methods work well. At lower acidities, polynuclear complexes exist, however, and for their investigation potentiometric measurements have been performed [42]. Values of $p\beta^*_{11}$ are listed in Table 21.2.

Table 21.2 *Hydrolysis of tetravalent actinide ions. Constants* $p\beta^*_{11}$ *listed refer to formation of the first mononuclear complex in solutions of various ionic strengths I in light and heavy water, at 25°C. Medium (Na,H)ClO₄, if not otherwise stated.*

M_z^+	$I = 0.11$ M	0.5 M	1 M	2 M	3 M	2 M[a]	*Ref.*
Th^{4+}			4.23		5.0[b]		31, 33
Pa^{4+}					0.14[c]		37
U^{4+}	1.23	1.47	1.56	1.68	2.00	1.74	39–42
U^{4+}	1.35[b]	1.60[b]	1.73[b]	1.82[b]			39
Np^{4+}				2.30		2.50	41
Pu^{4+}		1.60	1.51	1.73		1.94	39, 45, 46

[a] In heavy water [41,46].
[b] Medium (Na,H)Cl.
[c] Medium (Li,H)ClO_4.

In both perchlorate and chloride media, the acidity of U^{4+} decreases with ionic strength, from $I = 0.11$ M upward. The values of $p\beta^*_{11}$ are throughout lower in chloride medium where the formation of chloride complexes markedly suppresses hydrolysis.

The acidity of U^{4+} increases rapidly with temperature [40], as is evident from the values of $p\beta^*_{11}$ listed in Table 21.1. As might be expected, uranium(IV) behaves in this respect much like throium(IV) (Table 21.1). From the temperature dependence of β^*_{11}, values of ΔH°_{11} and ΔS°_{11} have been calculated, which will be discussed in Section 21.3.

In the potentiometric study [42], both the acidity and the uranium concentration C_M were varied within wide limits, and both $[H^+]$ and $[U^{4+}]$ were measured, the latter via the UO_2^{2+}/U^{4+} couple. The existence of the mononuclear UOH^{3+} was confirmed. Polynuclear complexes predominate in the later stages of the hydrolysis, the more so the higher the value of C_M. A series of 'core + links' complexes $U((OH)_3U)_n^{4+n}$ was presumed [42]. It has since been pointed out, however, that the 'core + links' hypothesis has been discredited in several other cases, among them the closely related Th^{4+} [25]. Except for the highest ligand numbers, the data may in fact be described by the monomer UOH^{3+} and only one of the polymers previously postulated, viz. the hexamer $U_6(OH)_{15}^{9+}$. Finally, complexes of even higher nuclearity are no doubt formed. There is no need, however, to assume any complexes containing two, three, four or five uranium atoms. The hexamer is a very important species also in thorium hydrolysis, but the dimer and tetramer which are also prominent in that system do not seem to be favored at all by uranium(IV). In Table 21.1, the value of $p\beta^*_{6,15}$ calculated originally [42] is given, as well as the value calculated on the assumption that the hexamer is the only polymer of low nuclearity formed [25].

The formation of very large polymers, and the ensuing precipitation, takes place at much lower ligand numbers for uranium(IV) than for thorium(IV). It is therefore much more difficult to study the structures of the hydroxo complexes of uranium(IV) in solution. Polynuclear complexes are formed, with U–U distances

equal to 4.0 Å, which indicates that the uranium atoms are joined by double hydroxo bridges, i.e. the arrangement is the same as in thorium complexes [43]. The formulas of the complexes cannot be deduced, however. Among the hydrolyzed uranium(IV) compounds whose structures are known, $U_6O_4(OH)_4(SO_4)_6$ seems to be the only one containing a discrete complex, viz. $U_6O_4(OH)_4^{12+}$. It might be significant that this complex is indeed a hexamer. The uranium atoms are at the corners of an almost regular octahedron [44]. They are joined by oxohydroxo bridges, at a U–U distance of 3.85 Å, i.e. somewhat shorter than for the double hydroxo bridges postulated to exist in solution.

The hydrolysis of Np^{4+} appears to be very similar to that of U^{4+}, though Np^{4+} is an appreciably weaker acid [41] (Table 21.2). From the actinide contraction (see, for example, ref. 261, p. 466) the opposite trend would rather be expected. This unexpected relation between the stabilities of corresponding uranium and neptunium complexes is a general feature, found for both the tetravalent and hexavalent states. Evidently, the strength of the complex formation is not governed exclusively by simple electrostatic interaction.

The acidity of Pu^{4+} is again stronger, though hardly stronger than that of U^{4+} [39, 45, 46]. Also for Pu^{4+}, and Np^{4+}, polymers become prominent as hydrolysis proceeds. Before they precipitate, these polymers have grown to colloidal dimensions. In the case of plutonium(IV), the colloids have attracted much attention, on account of their practical importance for the reprocessing of nuclear fuels where the somewhat capricious behavior constitutes a potential hazard. The slow adjustment to equilibrium also makes it diffucult to ascertain the nature and concentration of species present at a certain moment.

The constants β_{11}^* of U^{4+}, Np^{4+}, and Pu^{4+} have also been measured in heavy water [41, 46]. In all cases, a slight decrease of the acidity is found, as compared with ordinary water.

21.2.4 Actinyl(V) ions

The acidities of the actinyl(v) ions, of low net charge 1, are quite weak, with the marked exception of protactinium. For the dissociation reactions:

$$MO_2^+ + H_2O \rightleftharpoons MO_2OH + H^+$$

values of $p\beta_{11}^* = 8.9$ and 9.7 have been found for NpO_2^+ and PuO_2^+, respectively, and there is no reason to believe that UO_2^+, or AmO_2^+, would behave very differently [47]. The protactinyl(v) ion is a much stronger acid with $p\beta_{11}^* = 4.5$ in 3 M (Li,H)ClO_4 [48]. In both the tetravalent and pentavalent state, protactinium thus hydrolyzes much more readily than do the other actinides. As mentioned above (Section 21.1), the protactinyl(v) ion acts as a base even in moderately concentrated acids, which would indicate a structure different from the other actinyl(v) ions, viz. $PaO(OH)_2^+$, with only one strongly covalent M–O bond [14]. For the equilibrium:

$$PaO(OH)^{2+} + H_2O \rightleftharpoons PaO(OH)_2^+ + H^+$$

a constant $pK_1 = 1.05$ has been found in 3 M $(Li,H)ClO_4$, implying that the protonated form $PaO(OH)^{2+}$ is already the predominant species in 1 M acid [49]. Only in extremely dilute solutions of fairly high acidity do the monomers formed seem to be thermodynamically stable. As the acidity decreases and the concentration of protactinium increases, polymerization takes place at increasing rates, finally resulting in very large aggregates [48, 49].

21.2.5 Actinyl(VI) ions

The hydrated uranyl(VI) ion present in the solid perchlorate heptahydrate is $UO_2(H_2O)_5^{2+}$, with the five water oxygens pentagonally arranged in the equatorial plane of the uranyl ion [225]. The U–O distances in the uranyl group are 1.71 Å, a normal bond length for uranyl compounds [62, 255], while the U–OH_2 distances are, as expected, considerably longer, 2.45 Å. A recent x-ray and proton NMR study shows that the same species exists also in solution, with bond distances very close to those found for the solid phase, viz. U–O 1.70 Å and U–OH_2 2.42 Å [256]. A more accurate value of the hydration number can be obtained by NMR than is possible from diffraction data. The signals for bound water and bulk water are separated, however, only if the temperature is kept low, around 190 K. This means that acetone has to be added to the aqueous solution in order to prevent freezing. There are good reasons to believe, however, that the hydration number of 5 found will be the same in pure water at room temperature, i.e. under the conditions of the x-ray study. In previous NMR investigations, a hydration number of 4 has been found [226, 227], presumably because only a low water/uranyl ratio was used in these measurements.

Also in several other solvents, e.g. dimethylsulfoxide, dimethylformamide, and dimethylacetamide [227], UO_2^{2+} exists as a pentasolvate, most probably with the solvent molecules coordinated in the equatorial plane, as in water.

It is to be assumed that other actinide ions MO_2^{2+} are solvated in the same manner as UO_2^{2+}.

The central part played by the UO_2^{2+} ion in the chemistry of uranium prompted strong interest in its reactions in aqueous solution at an early stage. Among these, hydrolysis is especially important. As the equilibria involved are fairly complicated, numerous investigations have been necessary in order to arrive at a reasonably reliable picture [260]. Not until fairly recently have analogous investigations of the hydrolysis of NpO_2^{2+} and PuO_2^{2+} been performed.

Even in very dilute solutions, the hydrolysis of UO_2^{2+} results almost exclusively in polynuclear species. This is immediately evident from the marked dependence of the degree of hydrolysis on the uranyl concentration, C_M, even at fairly low values of C_M (Fig. 21.3(a)). Within wide ranges of pH and C_M, the predominant complex is the dimer $(UO_2)_2(OH)_2^{2+}$ in all the media studied (Table 21.3). The dimer does not dissociate very readily, so the monomer UO_2OH^+ is formed in appreciable amounts only in very dilute solutions, $C_M \lesssim 1$ mM. For higher values

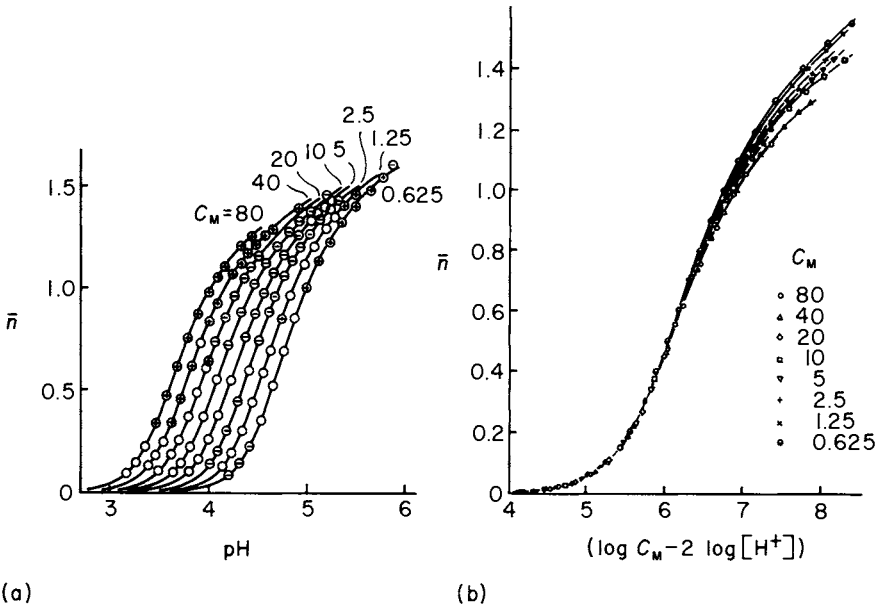

Fig. 21.3 *Hydrolysis of uranyl(VI) in 3 M (Na)Cl medium at 25°C* [50]. *(a) The ligand number as a function of pH for values of C_M varying from 0.625 to 80 mM. Circles denote experimental data, curves are calculated from the constants found (listed in Table 21.3). Signs in circles indicate the sign of the difference between calculated and experimental values of $\bar{n}$. (b) If all the polynuclear complexes $(UO_2)_m(OH)_n^{2m-n}$ had had $n = 2(m-1)$, as have $(UO_2)_2(OH)_2^{2+}$, $(UO_2)_3(OH)_4^{2+}$, and $(UO_2)_4(OH)_6^{2+}$, the curves $\bar{n}$ (log $C_M - 2\log[H^+]$) would have coincided. They do in their lower parts where such complexes (especially $(UO_2)_2(OH)_2^{2+}$) predominate but not in their upper parts where $(UO_2)_3(OH)_5^+$ and possibly also $(UO_2)_4(OH)_7^+$, not belonging to this series, become important.*

of pH, the trimer $(UO_2)_3(OH)_5^+$ becomes prominent (Table 21.3 and Fig. 21.3(b)). In chloride solutions especially, a more protonated trimer, $(UO_2)_3(OH)_4^{2+}$, is also formed. In concentrated solutions at low pH, $(UO_2)_2OH^{3+}$ is present. Other complexes claimed to exist are $(UO_2)_4(OH)_6^{2+}$ and, in isolated cases, $(UO_2)_4(OH)_7^+$ and $(UO_2)_5(OH)_8^{2+}$ (Table 21.3).

For a given cation concentration, the hydrolysis is throughout less extensive in chloride than in perchlorate media, as has already been noted for U^{4+} (cf. Table 21.2). The reason is evidently the same, viz. that the hydrolysis is to some extent suppressed by the formation of chloride complexes. A similar, though smaller, effect is also found for nitrate media. In sulfate media, on the other hand, the effect is much larger, owing to the much stronger affinity of UO_2^{2+} for the medium anion (cf. Tables 21.6 and 21.8). For media of a given anion concentration, the dissociation is throughout less extensive for divalent cations (Mg^{2+}, Ca^{2+}) than for the monovalent Na^+.

Table 21.3 *Hydrolysis of uranyl (VI) in various aqueous media*[a], *at 25°C except when stated otherwise. Constants* $p\beta^*_{mn}$ *listed refer to the acid dissociation equilibria* $mUO_2^{2+} + nH_2O \rightleftharpoons (UO_2)_m(OH)_n^{2m-n} + nH^+$.

	$(M,H)ClO_4$						(Na,H)Cl	
m,n	M = Na C_A = 0.5 M	Na 1 M	Na 3 M	Mg 3 M	Ca 3 M	Na[b] 3 M	1 M	3 M
1,1			6.1				5.6	
2,1	3.81			3.81	3.96			
2,2	6.03	5.94	6.04	6.25	6.20	6.80	6.20	6.64
3,4	13.17		13.2	13.3	13.4	14.0	12.33	12.54
3,5	16.78	16.41	16.53	17.18	16.91	18.63	16.93	18.07
4,6	18.91			20.2				20.0
4,7								24.9
Ref.	241	51	52	52	52	53	54	52

	$(M,H)NO_3$						$(Na,H)SO_4$
m,n	M = K C_A = 0.5 M	K 1 M	Na 3 M	Mg 3 M	Mg 5 M	K[c] 0.5 M	1.5 M
1,1	5.7			5.4	5.5	4.19	
2,1		4.2					
2,2	5.92	5.96	6.13	6.34	6.52	4.51	8.20
3,4		12.8					16.21
3,5	16.22	16.21	16.65	17.37	17.76	12.74	22.13
4,6							24.56
5,8							32.30
Ref.	55	52	242	56	56	55	52

[a] The total concentrations of medium anions, C_A, have been kept constant in all the investigations at the values denoted, except in ref. 55 where a constant ionic strength has been maintained (on the molality scale). For a 1,1 electrolyte as KNO_3 used here, the difference is not very important. For a complete list of data concerning the hydrolysis of uranyl(VI), up to 1980, see ref. 260.
[b] In heavy water.
[c] At 94°C.

In heavy water, the acidity of UO_2^{2+} is markedly lower than in light water (Table 21.3). The change is thus in the same direction as for U^{4+}, Np^{4+}, and Pu^{4+} (Table 21.2), but considerably larger.

The hydrolytic reactions of NpO_2^{2+} and PuO_2^{2+} follow much the same pattern as for UO_2^{2+} (Table 21.4). The dimers $(MO_2)_2(OH)_2^{2+}$ are the predominant species. Higher polymers also undoubtably exist in both systems. These species have been identified as the trimers $(MO_2)_3(OH)_5^+$, i.e. as analogs of the well-established $(UO_2)_3(OH)_5^+$ [57, 59]. One investigation of the PuO_2^{2+} system identifies the higher polymer as $(PuO_2)_4(OH)_7^+$, however [60]. The difference in medium is hardly large enough to account for this discrepancy, which presently remains unresolved. The monomers MO_2OH^+ are more prominent than the

Table 21.4 *Hydrolysis of neptunyl(VI) and plutonyl(VI) in aqueous sodium perchlorate media at 25°C. Values of* $p\beta^*_{mn}$ *are listed (cf Table 21.3).*

	NpO_2^{2+}	PuO_2^{2+}		
m,n	$C_A = 1$ M	1 M	1 M	3 M
1,1	5.17	5.71	5.97	
2,2	6.68		8.51	8.23
3,5	18.25		22.16	
4,7				29.13
Ref.	57	58	59	60

corresponding uranyl(VI) species. This is especially true in the case of NpO_2OH^+ [57]. The values of C_M applied in ref. 60 are hardly low enough to allow the detection of the monomer PuO_2OH^+.

The acidities of the actinyl(VI) ions decrease in the order $UO_2^{2+} > NpO_2^{2+} > PuO_2^{2+}$, with the larger difference between NpO_2^{2+} and PuO_2^{2+} (Table 21.3 and 21.4). Considering the actinide contraction, the opposite trend would be expected. The behavior is also different from that found for the actinide(IV) ions where the order of acidities is $U^{4+} > Np^{4+} < Pu^{4+}$. For these ions, the unexpected decrease between U^{4+} and Np^{4+} is followed by a marked reversal at Pu^{4+} (Table 21.2).

The tendency to form high polymers of colloidal dimensions before precipitation occurs is evidently much smaller for MO_2^{2+} than for M^{4+} ions. This has also been verified by equilibrium ultracentrifugation of hydrolyzed uranyl(VI) solutions [54]. Even in solutions on the verge of precipitation, the average degree of polymerization does not exceed 3 (Fig. 21.4). Also in this case, a few complexes of low nuclearity give a better fit than an unlimited series of 'core + links' complexes.

The existence of the dimer $(UO_2)_2(OH)_2^{2+}$ has been confirmed by direct determination of the species present in hydrolyzed uranyl(VI) chloride solutions [61]. Even in the concentrated solutions ($C_M = 3$ M) that have to be used in these diffraction studies, the dimer is an important species at the lower ligand number investigated, viz. $\bar{n} = 0.58$. The average U–U distance in this solution is 3.88 Å, which is close to the distance 3.94 Å found in the solids $[(UO_2)_2(OH)_2Cl_2(H_2O)_4]$ and $[(UO_2)_2(OH)_2(NO_3)_2(H_2O)_3]H_2O$ [62, 63]. In these compounds, the U atoms are joined by double hydroxo bridges, as depicted in Fig. 21.5 which shows the chloride compound. Most probably the same arrangement also exists in solution. In compounds where the U atoms are joined by single hydroxo bridges, the U–U distances are much larger, e.g. 4.22 Å in β-$UO_2(OH)_2$ [64]. At the high chloride concentrations used, chloride ions are certainly also coordinated, most probably in terminal positions as found in the solid dimer [62].

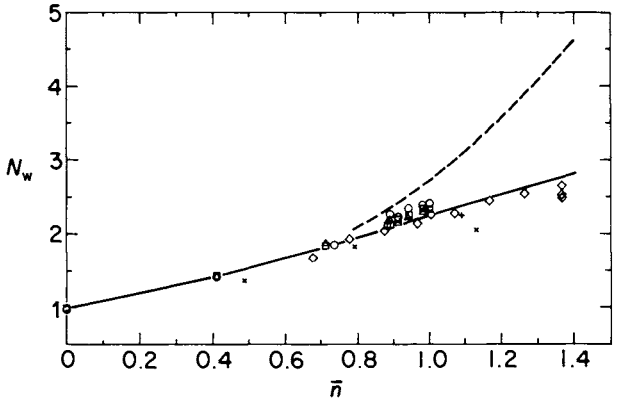

Fig. 21.4 *Weight-average degree of polymerization, N_w, of hydrolyzed uranyl(VI) solutions as a function of the ligand number $\bar{n}$, at 25°C* [54]. *Equilibrium centrifugation in 1 M (Na,H)Cl, at values of C_M (mM):* 100, ○; 50, △; 25, □; 10, ◇; *in 1 M (Na,H)ClO_4, C_M = 10 mM,* ×; *in 0.5 M (K,H)NO_3, C_M = 10 mM,* +. *Full curve calculated from the values of β^*_{22}, β^*_{34}, and β^*_{35} found from pH measurements in 1 M (Na,H)Cl* [54]. *Broken curve calculated from the 'core + links' scheme proposed earlier to account for pH measurements in 1 M (Na,H)ClO_4.*

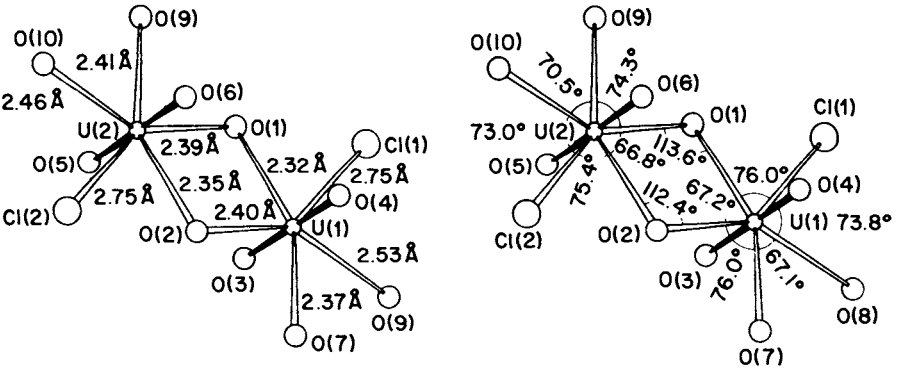

Fig. 21.5 *Structures of the dimer $[(UO_2)_2(OH)_2Cl_2(H_2O)_4]$ present in crystalline phase* [61] *and most probably also in hydrolyzed solutions of high chloride concentrations* [62]. *Distances are given to the left, angles to the right. The U–U distance is* 3.94 Å.

In the more hydrolyzed solution, of $\bar{n} = 1.11$, a trimeric complex predominates [61]. The average U–U distance in this solution is 3.84 Å. The absence of any U–U interactions at larger distances excludes all complexes except a trinuclear one with the U atoms at the corners of an equilateral triangle. Such an arrangement has been found in the solid $[(UO_2)_3O(OH)_3(H_2O)_6]NO_3 \cdot 4H_2O$ [65], where the hydrolyzed uranyl entity is equivalent to the trimer $(UO_2)_3(OH)_5^+$, well-established in nitrate solutions, for example (Table 21.3). In this solid, the U atoms are joined by one hydroxo and one oxo bridge, the latter

common to the three U atoms. The average U–U distance is 3.81 Å, while in the hydrolyzed chloride solution of $\bar{n} = 1.11$ the distance is 3.84 Å [61]. In spite of this close agreement, the bridging arrangement may well be different in the chloride solution. Provided that the stability constants determined in ref. 50 are also at least approximately valid at the high values of C_M used in the diffraction experiments, the predominant trimer in the chloride solutions should be $(UO_2)_3(OH)_4^{2+}$ rather than $(UO_2)_3(OH)_5^{+}$ [61]. The exact arrangement of the bridges in this complex is still unknown. In any case, structural investigation of the hydrolyzed solutions fully confirms the predominant formation of dimeric and trimeric species.

An entity corresponding to the tetramer $(UO_2)_4(OH)_6^{2+}$, claimed to exist especially in chloride and sulfate solutions (Table 21.3), has been found in the solid $[(UO_2)_4O_2(OH)_2Cl_2(H_2O)_6]\cdot 4H_2O$ [262]. The four U atoms are at the corners of two approximately equilateral and coplanar triangles sharing one side. The existence of this discrete tetramer in a solid certainly supports the claims founded on pH^+ measurements that such a complex also exists in solution.

21.3 THERMODYNAMICS OF HYDROLYTIC REACTIONS

For three actinide ions, viz. Th^{4+}, U^{4+}, and UO_2^{2+}, the enthalpy changes ΔH° accompanying the hydrolytic reactions have also been determined. In two of these investigations, pertaining to Th^{4+} [259] and UO_2^{2+} [66], the values of ΔH° have been measured calorimetrically. In all other cases [32, 40, 55, 67] the values have been calculated from the temperature coefficient of the equilibrium constant, a method that is generally less accurate. Perchlorate media have been used, except for one study of Th^{4+} [259] and one of UO_2^{2+} [55] which refer to chloride and nitrate media, respectively.

From the measurements in perchlorate and nitrate media, a fairly coherent picture of the thermodynamics of the hydrolytic reactions emerges (Table 21.5). Though fairly acidic, the actinide ions still have acid dissociation constants below 1 on the molar scale. The standard free-energy changes are therefore positive. Nevertheless, they are smaller than the corresponding values of ΔH°; the reactions are all strongly endothermic. Consequently, the entropy changes ΔS° are all positive, generally very strongly so. The entropy term therefore always favors dissociation, in many cases to a considerable extent, while the endothermic enthalpy term counteracts it.

For the polynuclear complexes formed by Th^{4+} and UO_2^{2+}, the values of both ΔH° and ΔS° per proton split off are strikingly constant for each of the acceptors. Both quantities, especially $\Delta S^\circ/n$, are much higher for Th^{4+} than for UO_2^{2+}, reflecting a much larger desolvation entropy for the more highly charged ion. The formation of mononuclear complexes of Th^{4+} involves lower values of both $\Delta H^\circ/n$ and, particularly, $\Delta S^\circ/n$ than the formation of polynuclear complexes of the same acceptor.

Table 21.5 *Thermodynamics of the protolytic reactions* $mM^{z+} + nH_2O \rightleftharpoons M_m(OH)_n^{(mz-n)+} + nH^+$ *for actinide ions at 25°C; medium (Na,H)ClO₄, if not otherwise stated.*

M^{z+}	m,n	I (M)	ΔG° (kJ mol^{-1})	ΔH° (kJ mol^{-1})	ΔS° (J K^{-1} mol^{-1})	$\Delta H^\circ/n$	$\Delta S^\circ/n$	*Ref.*
Th^{4+}	1,1		23.4	24.7	3.8	24.7	3.8	
	1,2		44.7	58.2	46.0	29.1	23.0	
	2,2	1	26.4	61.9	118.8	30.9	59.4	32
	4,8		108.4	241.4	446.0	30.2	55.8	
	6,15		209.6	454.0	819	30.3	54.7	
U^{4+}	1,1	0.5	8.4	46.9	130			40
		0.19	6.7	44.8	172			67
		0	3.9	49.0	151			40
UO_2^{2+}	2,2	3	34.3	39.7	18.0	19.8	9.0	66
	3,5		94.6	102.1	25	20.4	5	
	2,2	0.5[a]	33.8	42.6	29.7	21.3	14.9	55
	3,5		92.5	105.9	42	21.0	8	

[a] Medium 0.5 M $(K)NO_3$, cf. Table 21.3, note a.

Between Th^{4+} and U^{4+}, the values of ΔH°_{11} and ΔS°_{11} both become much more positive. Evidently, the dissociation of a proton from the smaller U^{4+} takes more energy, hence the more endothermic enthalpy change. On the other hand, U^{4+} also has the stronger ordering influence upon the solvent. The partial neutralization of its charge will therefore result in a larger entropy gain than for Th^{4+}. This entropy term is in fact large enough to make U^{4+} a much stronger acid, in spite of its much less favorable dissociation enthalpy.

The positive values of ΔG° indicate that hydrolysis is far from complete in the presence of no stronger base than H_2O. This even applies to the stronger acid U^{4+} if its concentration is not extremely low. In the presence of stronger bases, e.g. OH^-, the hydrolysis easily proceeds to completion, as is evident from the strongly negative values of ΔG° found for the reactions:

$$mM^{z+} + nOH^- \rightleftharpoons M_mOH_n^{(mz-n)+}$$

The thermodynamics of these reactions can easily be found by combining the values found for the dissociation reactions (Table 21.5) with the well-established values for the dissociation of water. Complex formation is favored both by highly positive values of ΔS° and, moreover, by negative values of ΔH°. The contributions from the enthalpy and entropy terms to the decrease of the free energy are in fact of the same order of magnitude except for the formation of UOH^{3+} where the entropy term is still very predominant. The constancy of $\Delta H^\circ/n$ and $\Delta S^\circ/n$ observed for the formation of the polynuclear complexes by acid dissociation reactions naturally remains when the hydrolyses are looked upon as reactions with hydroxide ions.

The stability of the complex $Th_2(OH)_2^{6+}$, and hence the value of ΔG°, does not

differ much between perchlorate and chloride media [32, 259]. The dissociation reaction is considerably more endothermic in chloride medium; consequently the entropy change is also much more positive. Both ΔH° and ΔS° further become more positive with increasing ionic strength. Remarkably enough, ΔH° and ΔS° decrease with ionic strength when $Th_2(OH)_3^{5+}$ is formed [259].

The hydrolysis thermodynamics of uranium and plutonium ions as a function of temperature have been assessed and predicted by Lemire and Tremaine [263].

21.4 COMPLEX FORMATION OF ACTINIDE IONS

21.4.1 General characteristics

Like other ion hydrates formed in aqueous solution, the actinide ions are able to form complexes with various ligands. In most cases, complex formation certainly involves an exchange in the hydrate shell of water molecules for ligands, i.e. inner-sphere complexes are formed. Until the final number of ligands has been coordinated, both ligands and water molecules are, as a rule, directly bonded to the central metal ion. Examples of such complexes have been quoted already in the discussion of hydrolysis. In other cases, the ligands may be attached via the water molecules of the hydrate shell, i.e. outer-sphere complexes are formed. Strong complexes are always of the inner-sphere type. In the case of weak complexes, an equilibrium is often set up between inner- and outer-sphere complexes. However, these equilibria have been investigated only in fairly few cases [68].

A necessary condition for the formation of a strong complex is evidently that the ligand has an affinity for the actinide central ion strong enough to compete with that of the coordinated water. As will be demonstrated in the following sections, such strong affinities are exhibited by the fluoride ion and by a wide variety of ions coordinating via oxygen. Only very weak complexes, if any, are formed with the heavier halides or with ligands coordinating via the heavier chalcogens. The heavy donor atoms of the nitrogen group are not coordinated even though a relatively strong affinity is found for nitrogen.

For a given ligand, e.g. F^-, the stability of the complexes increases in the order $MO_2^+ < M^{3+} \simeq MO_2^{2+} < M^{4+}$, i.e. with the order of the effective charge on the acceptor atom. For ions of the same charge, the stability increases with decreasing radius, at least at the beginning of the actinide series. Later the trend is often reversed, as has already been pointed out in the case of the hydrolytic complexes formed by neptunium and plutonium (Section 21.3). In spite of these irregularities, however, it is clear that the stability of actinide complexes generally increases as the ratio of effective charge to radius becomes larger.

These features are characteristic of metal ions (or acceptors generally) classified as hard or (a) acceptors while their counterparts, the soft or (b) acceptors, possess just the opposite characteristics [69–71]. From the behavior of the hard acceptors, it is immediately evident that the electrostatic attraction between the central ion and the ligand is of crucial importance in their formation, while

covalent interactions are subordinate. For the soft acceptors, the opposite must be true [71–74].

The stabilities of complexes formed by hard acceptors are always very much due to the favorable entropy terms. The enthalpy changes are as a rule either rather endothermic, thus appreciably counteracting the reactions, or quite small and therefore of little significance for the position of the equilibrium [72]. Only the coordination of highly charged anions is generally markedly exothermic, especially in the later steps [74]. The actinide ions behave as typically hard acceptors in these respects also, as will be demonstrated below.

21.4.2 Complexes formed with halide ions

The equilibria between actinide ions of various types and halide ions have been extensively investigated. A representative selection of results is presented in Table 21.6. In order to avoid the complications due to hydrolysis, the measurements have often been performed in strongly acid solutions. This applies especially to investigations involving the easily hydrolyzed M^{4+} ions. Under such conditions, the fluoride ligand is present as the undissociated hydrofluoric acid, HF. The constants listed in the original papers therefore often refer to equilibria where HF, and not F^-, is regarded as the ligand, e.g. overall equilibria:

$$M^{4+} + nHF \rightleftharpoons MF_n^{4-n} + nH^+$$

or stepwise equilibria:

$$MF_{n-1}^{5-n} + HF \rightleftharpoons MF_n^{4-n} + H^+$$

Table 21.6 *Stability of actinide halide complexes in aqueous solution. The values refer to perchlorate media and 25°C, if not otherwise stated*[a].

M^{z+}	I (M)	*Fluoride*				*Ref.*
		$\log K_1$	$\log K_2$	$\log K_3$	$\log K_4$	
Am^{3+}	0.1	2.59	2.17			268
	0.5	3.39	2.72	2.89		79
	1	2.93				
Cm^{3+}	0.5	3.34	2.83	2.90		79
Cm^{3+}	1	2.99				
Cf^{3+}	1	2.99				
Th^{4+}	0.5[b]	7.56	5.72	4.42		80
	4[c]	8.11	6.34			81
Pa^{4+}	3	7.87	6.67			
U^{4+}	4[c]	8.96	6.64	5.41		81
Np^{4+}	4[d]	8.26	6.13	5.78	4.7	76
Pu^{4+}	0	8.4	7.0			269
Pu^{4+}	2	7.75	6.09			244
UO_2^{2+}	1	4.54	3.43	2.45	1.46	82, 276
NpO_2^{2+}	1[d]	4.27	3.11			76, 276
PuO_2^{2+}	1[e]	4.22	4.99	4.88	3.17	83, 276

Table 21.6 (*Contd.*)

M^{z+}	I (M)	*Chloride* $\log K_1$	*Chloride* $\log K_2$	*Bromide* $\log K_1$	*Ref.*
Ac^{3+}	1	−0.10	−0.52	−0.25	
Pu^{3+}	1[f]	0.0			84
Am^{3+}	0.5[f]	0.24			84
	1[g]	−0.01	−0.37		85
	4	−0.15	−0.54		
Cm^{3+}	0.5	0.18			
Bk^{3+}	1[h]	−0.02			245
Cf^{3+}	1	0.14			246
Th^{4+}	1	0.18			
U^{4+}	1[d]	0.30		0.18	
Np^{4+}	1[d]	−0.04			
Pu^{4+}	1	0.14			
Pu^{4+}	2	0.15	−0.6		244
UO_2^{2+}	1[d]	−0.10		−0.30	
	2	−0.06			
NpO_2^{2+}	2	−0.21			
PuO_2^{2+}	4	0.02			

[a] For this table, as well as for the following ones, the values have to a great extent been selected from the compilations of Sillén and Martell [77] and from reviews of Jones and Choppin [78] and of Fuger [243]. The latter two contain specifically stability constants and enthalpy changes pertaining to the formation of actinide complexes. For values not to be found in any of these compilations (as a rule from investigations too recent to be included) special references are given.

[b] Calculated from the values of K_n^* reported with $\log K_1(H) = 2.91$ [74].

[c] Involves a recalculation of 25°C of values of K_n^* determined earlier (1969) at 20°C, by means of a calorimetric determination of ΔH_n° (of Table 21.7).

[d] Temperature 20°C.

[e] Calculated from the values of K_n^* reported with $\log K_1$ (H) = 2.95 and 3.11, for I = 1 and 2 M, respectively [75].

[f] In pure hydrochloric acid medium.

[g] Na^+ medium; also measurements in H^+, Li^+, and NH_4^+ media.

[h] Temperature 30°C.

characterized by constants β_n^* and K_n^*, respectively. A fair comparison between the affinities of the actinide acceptors for various halide donors presumes, however, that constants of analogous reactions are considered. The constants β_n^* and K_n^* have therefore been recalculated as β_n and K_n, pertaining to the equilibria:

$$M^{4+} + nF^- \rightleftharpoons MF_n^{4-n}$$

and

$$MF_{n-1}^{5-n} + F^- \rightleftharpoons MF_n^{4-n}$$

respectively. This is possible when the constant $K_1(H)$ for the equilibrium:

$$H^+ + F^- \rightleftharpoons HF$$

is known for the actual medium and temperature. For the compilation of Table 21.6, the pertinent values of K_1(H) have been taken from refs 75 and 76. Iodide complexes have not been measured, owing to their low stability and to the ready oxidation of I^- by many actinide ions, e.g. all MO_2^{2+}.

The high stabilities of the fluoride complexes, and the very low stabilities of the complexes formed by the heavier halides, are evident. So also are the very high stabilities of fluoride complexes of M^{4+} ions relative to those of MO_2^{2+} and M^{3+} ions. Just as found for their hydrolytic reactions, Np^{4+} and NpO_2^{2+} do not follow the expected trend. In spite of the actinide contraction, their complexes are less stable than those formed by U^{4+} and UO_2^{2+}, respectively. That even lower values are found for Pu^{4+} than for Np^{4+} is possibly due to the lower value of $I = 2$ M used in this case; at $I = 4$ M, $\log K_1(Pu^{4+})$ is presumably around 8.5. Between the various M^{3+} ions, the fluoride complexes do not differ much in stability. On the whole, however, halide complex formation characterizes the actinide ions as very typical hard acceptors.

The simple fluorides MF_3 and MF_4 are relatively insoluble compounds. Few determinations of their solubility products have been carried out, however, and the values published have often been calculated without due consideration for the complexes formed in solution. For ThF_4, however, a reliable determination of the equilibrium constant for the reaction:

$$ThF_4 \cdot 4H_2O(s) + 2H^+ \rightleftharpoons ThF_2^{2+} + 2HF + 4H_2O.$$

has been performed [80]. Combination of this constant with K_1 and K_2 determined in the same investigation and K_1(H) from ref. 75 yields solubility product K_{so} for the reaction:

$$ThF_4 \cdot 4H_2O(s) \rightleftharpoons Th^{4+} + 4F^- + 4H_2O.$$

In a perchlorate medium of $I = 0.5$ M, $pK_{so} = 26.3$ at 25°C.

For a neutral complex such as ThF_4 or UF_4, the concentration in solution in equilibrium with a solid phase of the same stoichiometry has to be constant, independent of the concentration of ligand present. Nor does the solubility depend much on I, as the activity coefficient of a neutral species does not change very much with the ionic medium.

For UF_4, the solubility in a 0.12 M perchlorate medium at 25°C has been found to be 1.09×10^{-4} M [86]. For the calculation of K_{so}, the constants K_1 to K_4 are needed. Of these, only K_3 and K_4 have been determined in the actual medium, while K_1 and K_2 values are known only for $I = 4$ M (in Table 21.6). These constants vary considerably with the medium, and the use of the present values therefore implies a rather crude approximation. If they are applied nevertheless, a value of $pK_{so} \simeq 28$ results, i.e. a somewhat higher value than that found for ThF_4. This result seems very reasonable, in view of the higher affinity for F^- displayed by U^{4+}, as compared with Th^{4+} (Table 21.6).

Fluorides of the actinyl ions are very soluble in water, as are the heavier halides of all oxidation states of the actinides. For these, however, hydrolytic reactions

are always prone to occur when the solutions are not sufficiently acidic (Section 21.2.4). The fluoride solutions are, on the other hand, relatively well-protected against hydrolysis by the strong complex formation occurring. Even at fairly high ligand concentrations, no more than four F^- can be coordinated to UO_2^{2+} or PuO_2^{2+} [82, 83] while the solid $K_3UO_2F_5$ contains discrete ions $UO_2F_5^{3-}$, with the ligands arranged pentagonally in the equatorial plane of the uranyl ion [228]. As discussed above, such a difference does not seem to exist between uranyl(VI) solvates in solution and solid phase (Section 21.2.5).

For the fluoride complexes of Th^{4+}, U^{4+}, and UO_2^{2+}, reliable determinations of the changes of enthalpy and entropy accompanying complex formation are also available (Table 21.7). Evidently, the high stabilities of the complexes are due to the highly positive values of ΔS_n°. The values of ΔH_n° are all small, either slightly negative or slightly positive. As mentioned in Section 21.4.1, these features are typical for the formation of complexes of hard acceptors in general. They will be discussed more fully in Section 21.4.7.

21.4.3 Complexes formed with inorganic ligands coordinating via oxygen

Prominent among the complexes coordinating via oxygen are the hydrates and the hydroxo complexes. On account of the fundamental importance of these

Table 21.7 *Thermodynamics of the stepwise formation of actinide fluoride complexes*[a], *at 25°C.*

M^{z+}	n	I (M)	ΔG_n° (kJ mol^{-1})	ΔH_n° (kJ mol^{-1})	ΔS_n° (J K^{-1} mol^{-1})	*Ref.*
Th^{4+}	1	4[c]	−46.27	−2.0	148	81
	2		−36.2	−1.0	117	
	1	→0	−48.2	−5.0	145	87[b]
	2		−37.8	−3.3	115	
	3		−27.1	−3.3	80	
	4		−19.4	−3.8	52	
U^{4+}	1	4[c]	−51.14	−5.4	154	81
	2		−37.9	2.4	135	
	3		−30.9	5	120	
UO_2^{2+}	1	1[d]	−25.89	1.70	92.5	82
	2		−19.65	0.4	67	
	3		−13.91	0.3	48	
	4		−8.4	−2.1	21	

[a] Calorimetric determinations except in ref. 87 where the values of ΔH_n° have been determined from the temperature coefficients of K_n between 0 and 45°C.
[b] Values of ΔS_n° recalculated by the present author from the values of K_n and ΔH_n° given in the original paper.
[c] Medium $HClO_4$.
[d] Medium $NaClO_4$.

complexes in the chemistry of the actinides in aqueous solution, they have been treated separately in Section 21.2. As shown by the high enthalpies of solvation [78], strong bonding forces operate between the actinide ions and the oxygen donor atom of the water molecule. As just discussed, the water molecules are nevertheless readily displaced by fluoride ions but not by the heavier halides. The question now arises to what extent the hydrate water may be replaced by ligands coordinating via donor atoms belonging to the chalcogen and nitrogen groups. In the first place, the affinity of ligands coordinating via oxygen should be considered.

An important difference exists between halogen donor atoms and those belonging to the other groups. The former are present in aqueous solutions as monatomic ions, while the latter are not (except S^{2-} and its homologs in strongly alkaline media). The chalcogen and nitrogen donors are generally part of a polyatomic ligand, the composition of which extensively influences the coordinating properties of the donor atoms. This must, of course, always be remembered when the affinities of various donor atoms are compared. Such comparisons are only valid between structurally similar ligands.

When donor atoms are built into a more or less complicated molecule or ion, two or more may be present in the same species. These donor atoms may, or may not, be of the same kind. They may coordinate to the same actinide ion, forming chelates, or to different ions, forming bridged complexes whose polynuclearity might vary widely.

The common inorganic anions NO_3^-, SO_4^{2-}, CO_3^{2-}, and PO_4^{3-}, all coordinating via oxygen, possess very different affinities for actinide ions. The complexes formed by NO_3^- are as unstable as those formed by the heavier halides. Even with the highly charged U^{4+}, extensive complex formation occurs only at high nitrate concentrations [88]. Much stronger complexes are formed by SO_4^{2-}, mainly because of its higher charge. The stabilities decrease with the effective charge of the acceptor, i.e. in the sequence $M^{4+} > M^{3+} \simeq MO_2^{2+}$. For all types of ions, the complexes generally become more stable as the ionic radius decreases, but exceptions occur, notably for the neptunium ions (Table 21.8). On the whole, the trends are very similar to those found for the fluoride complexes.

For several sulfate systems, the enthalpy and entropy changes have also been determined (Table 21.9). The entropy changes are positive and of the same order of magnitude as for the fluoride complexes. The enthalpy changes are much more endothermic, however, so the sulfate complexes are considerably less stable. The thermodynamic characteristics of a typically hard–hard interaction are thus very marked in the case of the actinide sulfate systems.

Addition of the strong base CO_3^{2-} first causes hydrolysis, with the formation of precipitates. Their exact nature is not known but as CO_3^{2-}, like OH^- or O^{2-}, may act as a bridging ligand, mixed hydroxocarbonato or oxocarbonato complexes are most likely formed. At higher concentrations of CO_3^{2-}, depolymerization takes place and soluble carbonato complexes are formed, most readily by the MO_2^{2+} ions. In uranyl(VI) solutions, carbonato complexes exist also in solutions of low pH, pH 3 to 4.8 [231]. In this acidity range, introduction of CO_2 into the

Table 21.8 *Stability of actinide sulfate and nitrate complexes in aqueous solution. The values refer to perchlorate media and 25°C, if not otherwise stated.*

		Sulfate		*Nitrate*
M^{z+}	I (M)	$\log K_1$	$\log K_2$	$\log K_1$
Ac^{3+}	1	1.20	0.65	0.12
Pu^{3+}	1	1.73[a,b]	1.66	
	2	1.65[a,b]	1.64	
Am^{3+}	0.5	1.85	0.99	
	1	1.57[b]	1.09	0.26[f]
	2	1.43[b]	0.42	
Cm^{3+}	0.5	1.86	0.89	
	2	1.34[b]	0.52	
Cf^{3+}	2	1.36	0.71	
Th^{4+}	2	3.30[c]	2.42	
U^{4+}	2	3.65[c]	2.43	0.06
Np^{4+}	2	3.51[c]	2.12	
Pu^{4+}	2	3.82[c]	2.76	
	2	3.84[g]		
UO_2^{2+}	1	1.81[d]	0.95	−0.30
NpO_2^{2+}	1	1.80[e]	0.77	

[a] Ref. 229.
[b] For Pu^{3+}, Am^{3+}, and Cm^{3+}, slightly different values are reported in ref. 230, the values of $\log K_1$ being $\simeq 0.2$ units higher than those listed in the table.
[c] For these sulfate systems, values of K_n^* have been determined: Th^{4+} [89], U^{4+} [90], Np^{4+} [91], and Pu^{4+} [92]. These values have been converted to K_n by means of the value of $\log K_1(H) = 1.08$, determined in ref. 93.
[d] Ref. 94.
[e] Temperature 21°C. Values of K_n^* determined in ref. 76, converted to K_n by means of $\log K_1(H) = 1.01$. This value has been calculated from $\log K_1(H) = 1.06$ and $\Delta H_1^\circ(H) = 23.47\ kJ\ mol^{-1}$ determined for $I = 1$ M and 25°C in ref. 94.
[f] Ref. 85; Na^+ medium; also measurements in H^+, Li^+, and NH_4^+ media.
[g] Ref. 275.

Table 21.9 *Thermodynamics of the stepwise formation of actinide sulfate complexes in perchlorate media, at 25°C. Values of ΔH_n° determined calorimetrically in refs 89 and 94, and by temperature coefficient method in refs 78 and 91 (see notes).*

M^{z+}	I (M)	ΔG_1° (kJ mol^{-1})	ΔH_1° (kJ mol^{-1})	ΔS_1° (J K^{-1} mol^{-1})	ΔG_2° (kJ mol^{-1})	ΔH_2° (kJ mol^{-1})	ΔS_2° (J K^{-1} mol^{-1})	*Ref.*
Am^{3+}	2	−8.4	18.4[a]	90				78
Cm^{3+}	2	−7.5	17.2[a]	83				78
Cf^{3+}	2	−7.9	18.8[a]	90				78
Th^{4+}	2	−18.8	20.9	133	−13.8	19.5	112	89
Np^{4+}	2	−20.0	18.3[b]	128				91
UO_2^{2+}	1	−10.3	18.2	96	−5.4	16.9	75	94

[a] From K_1, 0–55°C.
[b] From K_1^*, 10–35°C, combined with $K_1(H)$ from ref. 89.

solutions results in the formation of UO_2CO_3 and $(UO_2)_3(OH)_3CO_3^+$. These exist besides the hydrolytic species $(UO_2)_2(OH)_2^{2+}$ and $(UO_2)_3(OH)_5^+$ discussed above (Section 21.2.5). The final complex formed with increasing carbonate concentration in alkaline solutions of actinyl(VI) ions is no doubt $MO_2(CO_3)_3^{4-}$. This has been definitely proved for M = U [95–97, 232] and is also strongly indicated for M = Pu [233]. For $UO_2(CO_3)_3^{4-}$, a value of $\log \beta_3 = 21.54$, valid in 0.1 M $NaNO_3$ and at 20°C, has been found by solvent extraction measurements [96]. This value is of the same order of magnitude as that determined earlier in 0.2 M NH_4NO_3 by solubility measurements, viz. $\log \beta_3 = 20.7$ [77]. Recent solubility measurements yield values of $\log \beta_3 = 22.6, 21.5$, and 21.3 for the media 3 M $NaClO_4$, 0.5 M $NaClO_4$, and pure water, respectively [247]. At lower carbonate concentrations, not only is the monomer $UO_2(CO_3)_2^{2-}$ formed, but also the trimer $(UO_2)_3(CO_3)_6^{6-}$ [232, 247]. The trimerization is especially extensive in media of high ionic strength; in 3 M (Na)ClO_4, the trimer predominates completely over the monomer even at a total uranyl(VI) concentration of 0.1 M [247]. At lower carbonate concentrations, solid UO_2CO_3 is precipitated if the concentration of uranyl(VI) is not very low. In pure water, the solubility of this complex is only about 10^{-5} M; in 3 M (Na)ClO_4 it is even lower, about $10^{-5.6}$ [247].

Solid phases containing discrete tricarbonato complexes are also well-known [98, 234]. In these, the ligands are coordinated as bidentates, with six equidistant oxygens in the equatorial plane of the uranyl(VI) ion. The same structure certainly also exists in solution. As to the trimer, its structure in solution has recently been determined [235] by X-ray diffraction and ^{13}C NMR, and confirmed [270] by Raman spectroscopy. The uranium atoms are at the corners of an equilateral triangle, joined by carbonato bridges. The remaining three carbonate ions are coordinated one to each uranium, as bidentates. The whole arrangement is planar, with the U–O bonds of the uranyl groups perpendicular to the plane.

In uranyl(V) solutions, an analogous tricarbonato complex, $UO_2(CO_3)_3^{5-}$, is formed, differing only in one unit of charge from the uranyl(VI) complex [248]. As might be expected from the lower charge of the central ion, the stability is much lower, however, $\log \beta_3 = 13.3$. Any formation of a trinuclear complex $(UO_2)_3(CO_3)_6^{9-}$ is precluded by the disproportionation of uranyl(V) in the carbonate concentration range where such a complex might exist.

The carbonato complex formation of uranium(IV) in alkaline solution has also recently been quantitatively investigated. In this case, $U(CO_3)_5^{6-}$ is finally formed, with $\log \beta_5 \simeq 40$ [249].

Carbonato complexes analogous to those found for the various oxidation states of uranium are to be expected for other actinides. Their stabilities certainly depend mainly upon the oxidation state and hence do not differ very much from what has been found for the analogous uranium complexes [248]. Maya [272] and Wester and Sullivan [274] determined the Np(VI)/Np(V) and Pu(VI)/Pu(V) potentials respectively in carbonate media. Electrochemistry, equilibria, and kinetics of actinide carbonate complexes have been critically reviewed [271].

At the oxidation potential prevailing in sea water, uranium is present

exclusively in the hexavalent state. The carbonate concentration and the pH are high enough to ensure that soluble uranyl(VI) carbonato complexes are formed. Though the value of K_3 has not been determined in sea water, it seems safe to assume that the tricarbonato complex will be the predominant species at the actual value of $p[CO_3^{2-}] = 4.25$. Owing to the existence of these soluble complexes, the concentration of uranium in sea water is quite high, approximately 10^{-8} M, in comparison to that of most other heavy elements [99, 100]. The concentration is in fact so high that sea water has been seriously considered as a possible source of uranium [100, 101]. In contrast to this, thorium, which at the actual oxidation potential is tetravalent, is present in amounts too small to determine. In this case, the carbonate concentration is too low for the formation of soluble complexes, so under the prevailing conditions the stable form of thorium is extremely insoluble hydroxide. The same is presumably true also for plutonium. At the fairly high pH value of about 8 for sea water, Pu(IV) is stable, especially when sorbed on particulates, because of its hydrolysis and its very insoluble hydroxide (section 21.2.3), although Pu(V) predominates in solution under nonequilibrium conditions [265].

The PO_4^{3-} ion acts preferably as a bridge, forming slightly soluble precipitates with the actinide ions. Generally several different phases may be formed, each one stable between certain limits of phosphate concentration and acidity of the supernatant solution. Thus, for U(IV), $U(HPO_4)_2 \cdot 6H_2O$ is stable in contact with phosphoric acid at a concentration below 9.8 M, while for acid concentrations above 9.8 M, $U(HPO_4)_2 \cdot H_3PO_4 \cdot H_2O$ is formed. For U(VI) three phases have been identified, viz. $(UO_2)_3(PO_4)_2 \cdot 6H_2O$, $UO_2HPO_4 \cdot 4H_2O$, and $UO_2(H_2PO_4)_2 \cdot 3H_2O$, stable in equilibrium with low (< 0.014 M), intermediate, and high (> 6.1 M) phosphoric acid concentrations, respectively [102].

These phosphates generally possess structures which are open enough to allow migration of ions from solution into the solid phase. If cations thus entering the solid phase have a sufficiently high affinity for phosphate, they will displace the hydrogen ions attached to the phosphate groups [104, 105]. Insoluble phosphates of this type will thus act as ion exchangers. The actual composition of the solid phase will then evidently depend upon the concentrations of sorbable cations in the solution. Any extensive displacement of hydrogen ions is, moreover, likely to involve a change of structure of the solid phase. When high-valency ions are taken up, drastic changes occur even at low loads. After such a change, the compound does not generally revert to the original structure even if exclusively loaded with hydrogen ions.

With increasing acidity, hydrogen ions become more and more efficient competitors for the oxygen donor atoms of the phosphate ions. The bridging properties of the ligand therefore decline and, instead of large polymers, monomeric protonated complexes are formed. These are more or less easily soluble. Thus, for U(VI), a maximum solubility of not less than about 2 M is reached in 6.1 M phosphoric acid. For U(IV), solubilities of the same order of magnitude are reached at high concentrations of phosphoric acid [102].

The M^{4+} and MO_2^{2+} actinide ions are also apt to coordinate organic phosphates

both neutral and anionic ones, as exemplified by tributyl phosphate (TBP) and dibutyl phosphate (DBP), respectively. Also, phosphine oxides and other organophosphorus compounds with oxygen donor atoms are readily coordinated. These ligands, and even more the complexes formed, prefer organic solvents of low, or zero, polarity to aqueous solutions [103]. They have therefore been utilized on a very large scale for the extraction and separation of actinides, as will be discussed further in Sections 21.5.2 and 21.5.3.

21.4.4 Complexes formed with carboxylate ligands

Carboxylate ligands form stronger complexes than sulfate but weaker than carbonate. The affinity thus increases with the basicity of the ligand, as will be discussed further below. Unlike carbonate, carboxylates are generally not basic enough to precipitate slightly soluble hydrolytic products. Very strong complexes are formed if the ligand contains several carboxylate groups and hence is able to form chelates. This is evident from Table 21.10 where the stabilities of the actinide complexes formed by some representative carboxylate ligands are listed. For comparison, the values of the proton association constants are also given.

Even data pertaining to a divalent ion, viz. No^{2+}, have recently been obtained, by means of a solvent extraction method [23]. This is indeed remarkable, considering the short half-life of the ^{255}No nuclide used ($t_{1/2} = 223$ s) and the extremely low concentrations of nobelium reached ($\simeq 10^{-18}$ M). The distribution equilibria between the aqueous phase and an organic phase containing the complexing agent di(2-ethylhexyl)phosphoric acid in n-octane were measured by α counting. The α energy of the short-lived ^{255}No (8.11 MeV) is well above that of the only nuclide of importance that could possibly interfere, viz. ^{250}Fm ($t_{1/2} = 30$ min; α energy 7.44 MeV), which makes possible a rapid determination without previous separation steps.

As to carboxylate ligands, complexes of all types of actinide ions have thus been investigated. The stability order is clearly $M^{2+} < MO_2^+ < MO_2^{2+} \simeq M^{3+} < M^{4+}$, i.e., the order of increasing effective charge on the central ions (cf Section 21.4.1). This is also in keeping with the behavior of the other ligands so far discussed. Also, in solutions containing carboxylates, the tetravalent oxidation state is much stabilized relative to both the higher and the lower states.

The higher acetate complexes are formed much more readily for MO_2^{2+} ions than for M^{3+} ions, however. For the former ions, they are in fact so strong that, even at rather modest concentrations of free ligand, practically all of the central ion is present as the coordinatively saturated triacetato complex. Such complexes form crystalline salts with many cations, e.g. $Na[UO_2(OOCCH_3)_3]$. In this salt, the acetate ion acts as a bidentate ligand, the six oxygens forming a plane hexagon around the uranyl group [124]. The arrangement is thus analogous to that found for the tricarbonato complexes. No doubt it also persists in solution.

The propionate ion forms somewhat stronger complexes than the acetate ion with Th^{4+}, MO_2^{2+}, and H^+, while the opposite is true for monochloroacetate (Table 21.10). For ligands containing just one carboxylate group, an almost linear

Table 21.10 *Stability of actinide carboxylate complexes in aqueous perchlorate media, compared with the basicity of the ligands. These are expressed by log $K_1(H)$, determined in the same investigations as K_n. Temperature 20 or 25°C*[a].

	M^{z+}	I (M)	log K_1	log K_2	log K_3	log K_1 (H)	*Ref.*
acetate	No^{2+}	0.5[b]	v. small				23
	Pu^{3+}	2	2.02	1.32		4.80	106
	Am^{3+}	0.5	1.99	1.28			107
		2[a]	1.96			4.80	108
	Cm^{3+}	0.5	2.06	1.04			107
		2[a]	2.03				108
	Bk^{3+}	2[a]	2.05				108
	Cf^{3+}	2[a]	2.12				108
	Th^{4+}	1	3.88	3.03	2.14	4.59	109
	UO_2^{2+}	1	2.38	1.98	1.98	4.59	110
	NpO_2^{2+}	1	2.31	1.92	1.77	4.61	111
	PuO_2^{2+}	1	2.05	1.49	1.42	4.63	110
		0.1[a]	2.31	1.49			112
propionate	Th^{4+}	1	3.94	3.31	2.19[c]	4.73	109
	UO_2^{2+}	1	2.53	2.15	1.64		113
	NpO_2^{2+}	1	2.44	2.02	2.04	4.72	100
monochloro-	Th^{4+}	1	2.77	1.87	1.11[d]	2.66	109
acetate	UO_2^{2+}	1	1.44	0.85	0.51	2.66	110
	NpO_2^{2+}	1	1.33	0.77			110
	PuO_2^{2+}	1	1.16	0.45			110
glycolate	Am^{3+}	0.5	2.82	2.04			107
	Cm^{3+}	0.5	2.85	1.90			107
	Th^{4+}	1	3.98	3.38	2.59[e]	3.62	114
	UO_2^{2+}	1	2.42	1.54	1.24	3.60	115
	NpO_2^{2+}	1	2.37	1.58	1.05		111
	PuO_2^{2+}	1	2.16	1.29	0.82	3.63	116
		0.1[a]	2.43	1.36		3.65	117
thioglycolate	Th^{4+}	1[a]	3.21	2.47	1.51[f]	3.53	118
	UO_2^{2+}	1[a]	1.89	1.31	1.3		118
oxalate	No^{2+}	0.5[b]	1.7				105
	Am^{3+}	0.5[a]	4.82	3.78			119
		1[a]	4.63	3.72	2.80	3.54[h]	120
	Cm^{3+}	0.5[a]	4.80	3.82			119
	Th^{4+}	1[a]	8.23	8.54	6.00[g]		121
	Np^{4+}	1[a]	7.47	6.22	5.68		122
	NpO_2^{+}	1	3.74	2.57		3.60[i]	123
	UO_2^{2+}	1	4.63	4.05	3.31		113

[a] Investigations performed at 25°C, all other data refer to 20°C.
[b] Nitrate medium.
[c] Log $K_4 = 1.76$.
[d] Log $K_4 = 1.04$.
[e] Log $K_4 = 2.00$.
[f] Log $K_4 = 1.33$.
[g] Log $K_4 = 4.4$.
[h] Log $K_2(H) = 1.0$.
[i] Log $K_2(H) = 1.13$.

relation in fact exists between $\log K_1$ and $\log K_1(\mathrm{H})$ for both Th^{4+} and UO_2^{2+} (Fig. 21.6). The values of K_1 of the hydroxycarboxylate complexes are all above the lines, indicating increased stability relative to the corresponding acid. This is most probably due to chelate formation. The thioglycolate complexes are on the lines, however. Evidently, no chelates are formed involving the sulfur atom. This is to be expected for the typically hard actinide acceptors.

The effect of a hydroxy group is small compared to that brought about by further carboxylate groups (Fig. 21.6). As may be expected, especially stable complexes result if five- or six-membered rings can be formed.

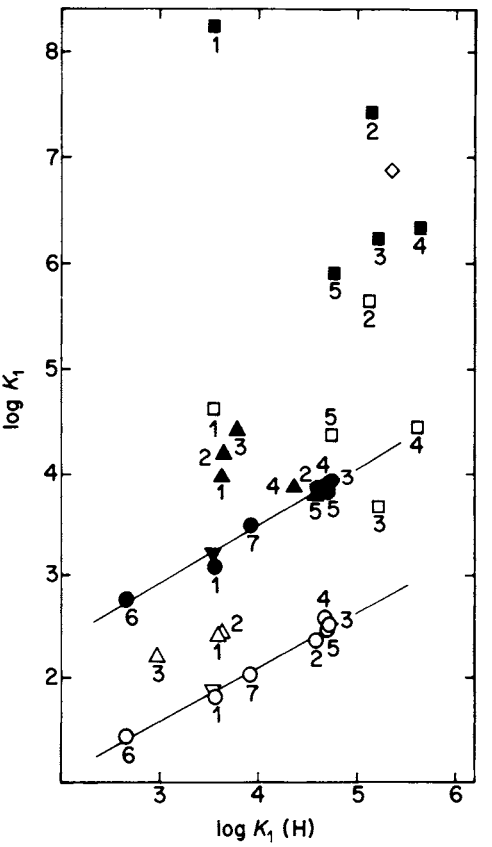

Fig. 21.6 *The relation between the stabilities of the first complexes of thorium(IV) (filled signs) and uranyl(VI) (open signs) and the basicities of the carboxylate ligands, expressed by the constants K_1 (H). Monocarboxylates (●, ○): formate, 1; acetate, 2; propionate, 3; butyrate, 4; isobutyrate, 5; chloroacetate, 6; β-chloropropionate, 7. Oxycarboxylates (▲, △): glycolate, 1; lactate, 2; thorium α-, β-, γ-hydroxybutyrate, 3, 4, 5; uranyl salicylate, 3. Dicarboxylates (■, □): oxalate, 1; malonate, 2; succinate, 3; maleate, 4; phthalate, 5. Tricarboxylate (◇): uranyl(VI) citrate. Thorium and uranyl thioglycolates (▼, ▽). Data from Table 21.10 and, for the additional ligands selected, from refs 77, 125, 128 and 129.*

With M^{3+} ions, glycolate forms much stronger complexes than does acetate, in spite of its considerably lower basicity. The chelate effect is thus considerable. With MO_2^{2+} ions, the first complex formed is of about the same strength for both ligands, while the higher complexes are stronger in the case of acetate. Though still marked, the chelate effect is evidently much smaller for MO_2^{2+} than for M^{3+}. This is to be expected as MO_2^{2+} ions form chelate complexes also with the acetate ion whereas M^{3+} ions do not [126, 127]. A more versatile chelating ligand should therefore have a larger effect on M^{3+} ions than on MO_2^{2+} ions.

As soon as more than one carboxylate group is present, polynuclear complexes are easily formed. In the case of oxalate and other simple dicarboxylates, highly polynuclear complexes tend to precipitate, seemingly without the intermediate formation of soluble polymers of low nuclearity [77, 128, 129]. In keeping with this, the solid uranyl(VI) oxalates investigated contain either discrete mononuclear trioxalato ions or endless chains [130]. On the other hand, di- and tricarboxylates also containing hydroxy groups, e.g. malate, tartrate, and citrate, do form polymers of low nuclearity, at least with UO_2^{2+}. For the dimerizations (protons of both carboxylate and hydroxy groups considered free to dissociate):

$$2UO_2L^- \rightleftarrows (UO_2L)_2^{2-} \qquad \text{for malate}$$

$$2UO_2HL^- \rightleftarrows (UO_2HL)_2^{2-} \qquad \text{for tartrate}$$

and

$$2UO_2HL^- \rightleftarrows (UO_2HL)_2^{2-} \qquad \text{for citrate}$$

the constants $\log K_d = 3.35$, 3.24, and 3.95, respectively, have been found in 1 M KNO_3 at 25°C [128]. This means that the dimer dominates over the monomer except in very dilute solutions.

Also the carboxylate complexes are highly entropy-stabilized (Table 21.11). The enthalpy changes are either fairly endothermic or quite small. Again, the general features of hard–hard acceptor–donor interactions are evident. The general increase of stability relative to the sulfate complexes is due to much less unfavorable enthalpy changes which more than compensate the somewhat less favorable entropy terms (Tables 21.9 and 21.11). The formation of a chelate bond via the hydroxy group, postulated to take place in the glycolate complex, is mainly reflected in enthalpy changes. Chelate formation should be most important in the first steps, where the competition for the coordination sites from further ligands is least. Both for UO_2^{2+} and, even more, for Th^{4+}, the enthalpy changes of these steps are less endothermic for glycolate than for thioglycolate and acetate.

Hydroxycarboxylates have been extensively utilized as eluting agents in ion-exchange processes used for the identification and separation of actinides (Section 21.6.1).

21.4.5 Some typical chelate complexes

Strong complexes with actinide ions are formed by several typical chelating ligands. Representative among these are the β-diketones, the tropolones, the

Table 21.11 *Thermodynamics of the stepwise formation of actinide carboxylate complexes in perchlorate media, at 25°C. Values of* ΔH_n° *determined calorimetrically for* Th^{4+} *and* UO_2^{2+}*, and by temperature coefficient method*[a] *for* M^{3+}.

	M^{z+}	I (M)	ΔG_1° (kJ mol^{-1})	ΔH_1° (kJ mol^{-1})	ΔS_1° (J K^{-1} mol^{-1})	ΔG_2° (kJ mol^{-1})	ΔH_2° (kJ mol^{-1})	ΔS_2° (J K mol^{-1})	ΔG_3° (kJ mol^{-1})	ΔH_3° (kJ mol^{-1})	ΔS_3° (J K^{-1} mol^{-1})	*Ref.*
acetate	Am^{3+}	2	−11.2	18.0	98							108
	Cm^{3+}	2	−11.7	18.0	100							108
	Bk^{3+}	2	−11.7	18.4	101							108
	Cf^{3+}	2	−12.0	15.9	94							108
	Th^{4+}	1	−22.0	11.3	112	−17.8	4.5	74	−11.2	13.7	84[b]	131
	UO_2^{2+}	1	−13.8	10.5	82	−11.4	9.7	71	−11.3	−4.0	25	94
glycolate												
	Th^{4+}	1	−23.5	2.1	86	−19.0	−0.8	61	−15.5	−3.0	42[c]	118
	UO_2^{2+}	1	−13.4	5.4	63	−9.3	7.5	56	−6.8	−0.8	20	132
thioglycolate	Th^{4+}	1	−18.4	10.2	96	−14.1	8.0	74	−8.7	10.9	66[d]	118
	UO_2^{2+}	1	−10.8	8.6	65	−7.5	10.6	61	−7.4	0.0	25	118

[a] 0–55°C (0–40°C for Bk^{3+}).
[b] $\Delta G_4^\circ = -7.8$, $\Delta H_4^\circ = 5.2$, $\Delta S_4^\circ = 43$, also fifth complex claimed.
[c] $\Delta G_4^\circ = -10.3$, $\Delta H_4^\circ = -3.9$, $\Delta S_4^\circ = 21$, also fifth complex claimed.
[d] $\Delta G_4^\circ = -7.6$, $\Delta H_4^\circ = 3.3$, $\Delta S_4^\circ = 37$.

8-hydroxyquinolines (oxines), ethylenediaminetetraacetic acid (EDTA), and other complexones.

In their enolic forms, the β-diketones form six-membered chelate complexes, with the replacement of the enol proton. The simplest compound of this class, acetylacetone, $CH_3C(O)CH_2C(O)CH_3$ (HAA), is fairly soluble in water ($\simeq$ 1.7 M). Even metal ions forming rather weak complexes might thus be effectively sequestered in aqueous solution, though the possibilities are restricted by the low solubilities of the neutral acetylacetonates. On the other hand, these are soluble in many organic solvents of low, or zero, polarity, notably benzene, alkylbenzenes, carbon tetrachloride, and chloroform [133, 134]. Also, pure acetylacetone can be used as an extractant, being a liquid at ordinary temperatures (m.p. -23°C, b.p. 139°C). Especially the complexes formed by the M^{4+} actinide ions are very strong (Table 21.12). Moreover, the Nernst distribution constant K_{D4} between organic solvents and aqueous solutions of the neutral complexes ML_4 are so high that complete extraction is easily feasible. Also PaO^{3+}, where the effective charge on the protactinium atom is certainly high, has a strong affinity for acetylacetone. In this system, however, the neutral third complex rather prefers the aqueous phase, as is evident from the low value of its distribution constant K_{D3}. The same is true for the neutral first complex of the more hydrolyzed form PaO_2^+, with distribution constant K_{D1}. The complexes formed by this ion in aqueous solution are also much less stable, as may be expected from its lower charge. The divalent UO_2^{2+} is presumably extracted in two forms, $UO_2(AA)_2$ and $UO_2(AA)_2HAA$ [139]. None of these is very strongly preferred by the organic phase, however (Table 21.12). The ML_4 complexes represent an optimum of extractability, evidently due to their combination of zero charge and coordinative saturation in a highly symmetrical structure.

Table 21.12 *Stability of acetylacetonate complexes in aqueous solution*[a] *and the distribution constants* $K_{D\lambda}$ *of the neutral complexes* $M(AA)_\lambda$ *between benzene or chloroform, and the aqueous phase. The values refer to perchlorate media and 25°C.*

M^{z+}	I (M)	$\log K_1$	$\log K_2$	$\log K_3$	$\log K_4$	$\log K_{D4}$ *benz.*	$\log K_{D4}$ *chlor.*	*Ref.*
Th^{4+}	0.1	8.00	7.48	6.00	5.30	2.52	2.55	135
U^{4+}	0.1	9.02	8.26	6.52	5.60	3.64	4.0	135, 136
Np^{4+}	1	8.58	8.65	6.71	6.28	3.45		136
Pu^{4+}	0.1	10.5	9.2	8.4	5.91	2.54	2.6	135, 136
PaO^{3+}	3	10.75[b]				$\log K_{D3} = -0.06$[c]		137, 138
PaO_2^+	3	6.60[b]	4.08[b]			$\log K_{D1} = 0.02$[c]		137
UO_2^{2+}	0.1	6.8	6.3			$\log K_{D2} = 0.25$[d]		139

[a] For the protonation constant K_1(H) and the distribution of HAA, see Table 21.18.
[b] Calculated by combining constants reported in refs 137 and 138.
[c] Between xylene and aqueous phase.
[d] Between benzene and aqueous phase. For the protonated complex $UO_2(AA)_2HAA$, $\log K_{D3} = 1.52$ [139].

By suitable modifications of the structure, β-diketones can be obtained which very much prefer the organic phase. Metal complex formation will then take place mainly in this phase. As the neutral complexes favor the organic phase even more markedly than does the protonated ligand, extraction becomes almost complete once these complexes have been formed.

By far the most used of these modified β-diketones is 2-thenoyltrifluoroacetone (HTTA) [133, 134]:

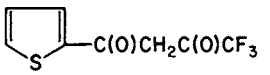

This compound is solid at ordinary temperature (m.p. 43°C) and cannot, therefore, be used as a pure extract. For all solvents investigated, however, the distribution constants are much higher than those found in the case of acetylacetone (see Table 21.18). On account of the low solubility in water of both HTTA and the metal chelates, complex formation in water is incompletely known, and anyhow of limited interest. The extraction equilibria are, on the other hand, very important and will be discussed more fully in Section 21.5.2. Other β-diketones used for the extraction of actinides are benzoylacetone, $PhC(O)CH_2C(O)CH_3$, and dibenzoylmethane, these have properties between those of HAA and HTTA [134] (cf. also Table 21.18).

The tropolones contain a seven-membered ring of carbon atoms, formally with one oxo and one hydroxo group on adjacent carbons. The ring has a largely aromatic character, however. The proton on the hydroxy group is therefore easily replaced by suitable metal ions. In this process, five-membered chelate complexes are formed, where the two oxygen donor atoms are indistinguishable. As the unsubstituted tropolone is not a very stable compound, and moreover is difficult to prepare, the stable and easily available β-isopropyl derivative (β-thujaplicin, denoted HIPT) is generally preferred as a practical chelating ligand [133, 134, 140]. Like HTTA, both HITP and its metal chelates strongly prefer the organic solvents to water. For the actinide ions, only extraction equilibria have therefore been determined (see Section 21.5.2 and Table 21.18).

The simple 8-hydroxyquinoline (Ox) is used far more than any of its derivatives. The oxines all form five-membered chelate rings, with one oxygen and one nitrogen as donor atoms. These complexes also much prefer the organic phase, being only slightly soluble in water [134]. As a rule, only extraction equilibria have therefore been determined (see Section 21.5.2 and Table 21.18).

For the sequestering of actinide ions in aqueous solution, EDTA is a most effective ligand. Only the first complex, presumably a hexadentate, is formed, coordinating via four oxygens and two nitrogens. As usual, the strongest complexes are formed by the M^{4+} ions, again with the complex of Np^{4+} weaker than that of U^{4+}. The strength of M^{3+} complexes increases steadily from Pu^{3+} to Cf^{3+}. The stereochemistry of the MO_2^{2+} ions is certainly not very favorable for EDTA. For a ligand of this structure, it must be almost impossible to conform to

the plane or somewhat puckered hexagons preferred by these acceptors [98]. Thus, EDTA will tend to act as a bridging ligand with such ions, giving rise to polynuclear complexes. The monomers formed are readily protonated, indicating that the chelate is coordinated via less than six donor atoms [77, 78]. Also the EDTA complexes are strongly entropy-stabilized. For the two systems measured (Table 21.13), complex formation is admittedly exothermic but the enthalpy change contributes only a minor part of the total decrease of free energy.

An even higher affinity for both M^{3+} and M^{4+} actinide ions is displayed by DTPA (diethylenetriaminepentaacetic acid), evidently because the high coordination numbers of the actinide ions are better satisfied with this ligand. For these ions, K_1 increases by about four orders of magnitude relative to EDTA [77, 250, 251]. As the increase is much smaller for divalent ions (practically zero for Ca^{2+}), DTPA has become the reagent of choice for the treatment of actinide poisoning [252].

Still more efficient in this respect, however, are chelating agents coordinating via phenolic oxygens [252]. The most efficient arrangement so far found is an array of four catechols (which have two adjacent phenol groups) properly spaced by connecting chains of suitable length. In this manner the right number of most attractive groups can be offered in the most favorable steric positions, thus forming a ligand of really formidable affinity. As the M^{3+} and M^{4+} ions have fairly specific requirements in these respects, the reagents are also selective. The most efficient removal of plutonium from living animals so far achieved is by the linear sulfonated catechoylamide denoted 3,4,3-LICAMS [252].

Table 21.13 *Stability of EDTA complexes in aqueous solution, and thermodynamics of the formation of the Pu^{3+} and Am^{3+} complexes, in perchlorate media at 25°C, if not otherwise stated*[a].

M^{z+}	I (M)	$\log K$	$\Delta G°$ (kJ mol^{-1})	$\Delta H°$ (kJ mol^{-1})	$\Delta S°$ (J K^{-1} mol^{-1})	*Ref.*
Pu^{3+}	0.1[b]	18.07	−103.1	−17.7	287	141
Am^{3+}	0.1	18.16	−103.6	−19.5	282	141, 142
Cm^{3+}	0.1	18.45				142
Bk^{3+}	0.1	18.88				142
Cf^{3+}	0.1	19.09				142
Th^{4+}	0.1	25.3				143
U^{4+}	0.1	25.83				144
Np^{4+}	1	24.55				145
Pu^{4+}	0.1	25.6				146
PuO_2^{2+}	0.1[b,c]	16.39				147

[a] A critical review of these complexes has been written by Anderegg [251].
[b] Chloride medium.
[c] 20°C.

21.4.6 Complexes formed with ligands coordinating via nitrogen

When present in chelating ligands together with oxygen donors, nitrogen donor atoms are evidently able to participate in chelate formation, as shown by the formation of oxinate and EDTA complexes. Most ligands coordinating only via nitrogen, on the other hand, have low affinities for actinide ions. Generally they cannot displace the hydrate water to any measurable degree. Moreover, the nitrogen donors are often so basic that they coordinate the protons of the hydrate water instead of the actinide ion, thus causing the formation of hydrolyzed species. This happens, for example, on addition of ammonia or amines. Only for nitrogen ligands of unusually low basicity, such as SCN^- (with a value of $\log K_1$(H) probably rather much less than 0) and N_3^- (with $\log K_1$(H) = 4.44 in 1 M sodium perchlorate at 25°C), have actinide complexes been found. In the latter case, they have been claimed only for UO_2^{2+}, however. The more numerous and more reliable data refer to SCN^- (Table 21.14).

It should be pointed out that the linear species SCN^- may coordinate via either the S or N atom. There is no doubt, however, that coordination to all the hard actinide acceptors takes place via the harder N rather than via the softer S. This has also been proved conclusively by measurements of the infrared absorption of the complexes [148, 149].

The thiocyanate complexes are all weaker than the corresponding carboxylate or sulfate complexes. The pattern found for the affinity to actinide ions of different charge types is very similar to that found for the ligands discussed previously.

Values of $\Delta H°$ and $\Delta S°$ have been determined only for the UO_2^{2+} system [94] (Table 21.15). For the coordination of the softer nitrogen, different conditions prevail than for the coordination of the harder oxygen. The first two thiocyanate complexes are enthalpy-stabilized while the entropy term is either small ($\Delta S_1°$) or strongly counteracting ($\Delta S_2°$). These complexes thus represent a trend toward a softer donor–acceptor interaction, though, as pointed out, UO_2^{2+} is not soft enough to prefer sulfur to nitrogen. Remarkably enough, the third complex is again entropy-stabilized.

Table 21.14 *Stability of actinide thiocyanate complexes in aqueous perchlorate media, at 25°C (mainly from refs 77 and 78).*

M^{z+}	I (M)	$\log K_1$	$\log K_2$	$\log K_3$	*Ref.*
Pu^{3+}	1	0.46	0.29		
Am^{3+}	1	0.50	0.34		
Cm^{3+}	1	0.43	0.41		
Cf^{3+}	1	0.48			
Th^{4+}	1	1.08			
U^{4+}	1	1.49	0.62		
Np^{4+}	2	1.49	0.56	0.47	150
UO_2^{2+}	1	0.75	−0.03	0.5	94

Table 21.15 *Thermodynamics of uranyl thiocyanate formation in* 1 M $NaClO_4$, *at* 25°C [94].

n	ΔG_n° (kJ mol^{-1})	ΔH_n° (kJ mol^{-1})	ΔS_n° (J K^{-1} mol^{-1})
1	−4.27	−3.22	3.5
2	0.2	−5.7	−20
3	−2.6	2.9	18

21.4.7 Concluding remarks on complex formation in aqueous solution

In the preceding discussions of the complexes formed by actinide ions with various classes of ligands, it has been stressed that the electrostatic interactions are no doubt paramount, as is generally the case with typically hard acceptors. For covalent interactions to be important, acceptors have seemingly to combine a high polarizability with a large number of d electrons in the outer shell [151]. This condition is evidently not fulfilled by the actinide ions.

Perhaps surprisingly, the strong electrostatic interactions are not reflected in exothermic values of $\Delta H°$, but rather in very positive values of $\Delta S°$. This is due to the fact that these hard acceptors are, on account of their high charges, very strongly solvated. Also, the hard ligand atoms they prefer have a fairly high charge/radius ratio and are therefore relatively strongly solvated. Complex formation means that water molecules move from the well-ordered acceptor and donor hydrates to the less ordered structure of bulk water. The neutralization of charges taking place at the coordination of anionic ligands means moreover that the water molecules remaining on the complex are less tightly held, and hence possess a larger degree of freedom than they had in the original metal-ion hydrate. These structural changes consequently imply a large decrease of order, and hence a large entropy gain, which is not compensated for very much by the entropy loss due to the new acceptor-to-donor bond. As more ligands are coordinated, solvation of the complexes thus becomes weaker. Consequently, the entropy to be gained should generally decrease for each consecutive step, as is in fact found (Tables 21.7, 21.9, and 21.11). If a change of coordination number occurs at a certain step, this monotonic decrease may be interrupted. Such changes are not common in the case of typically hard acceptors, however [152].

On the other hand, the breaking of the strong solvate bonds takes much energy. For most systems, this energy is not fully compensated by the energy gained on formation of the new bond to the ligand, at least not for the first steps. These are therefore endothermic as a rule. In some cases, however, notably for EDTA, ligand bond formation does in fact provide more enthalpy than is used up for dehydration, which results in an exothermic reaction. The entropy gain nevertheless yields the largest contribution by far to the stability for these systems also (Table 21.13).

The low affinity for actinide ions of the heavier chalcogens relative to oxygen is clearly demonstrated by a comparison of the stabilities of the oxydiacetate and thiodiacetate complexes of UO_2^{2+} and Th^{4+} (Tables 21.16 and 21.17). In spite of the higher basicity of the thiodiacetate ion, its complexes are considerably less stable than those of the oxydiacetate ion. For Th^{4+}, it has been found that the difference is mainly due to a more unfavorable value of ΔH_1°, indicating that the total strengths of the coordinate bonds are much smaller for this ligand. Evidently, the intermediate oxygen donor atom does coordinate to actinide ions, which the sulphur atom does only weakly, or perhaps not at all. Tridentate oxydiacetate coordination is also found in the solid uranyl complex that can be crystallized from aqueous solution, though this compound is a polymer in which every ligand is shared between three uranium atoms [154].

From a comparison of the oxydiacetate and iminodiacetate complexes, it is also evident that, for a given basicity of ligand, oxygen has a higher affinity than nitrogen for actinide ions. The basicity of the imino group is indeed high relative to that of oxo groups, as seen from the large difference between the values of $\log K_1$(H) (Table 21.16). Consequently, iminodiacetate complexes of the MO_2^{2+} ions are also much more stable than oxydiacetate complexes. But while for the oxy ligand all the values of $\log K_1$ are higher than the values of $\log K_1$ (H), this is not true for the imino ligand. Relative to the basicity, the affinity of O for MO_2^{2+} is thus stronger than that of N.

The same applies to Th^{4+}, as is evident from a comparison between the values of ΔG_1° for the oxy- and iminodiacetate complexes formed by Th^{4+} and H^+ (Table 21.17). For H^+, the N complex is much more stable; for Th^{4+}, only slightly so.

21.5 SOLVENT EXTRACTION EQUILIBRIA

21.5.1 Scope of extraction processes and types of extractants

Solvent extraction is defined as the transfer of solutes between two immiscible or only partly miscible liquid phases. As a rule, an aqueous phase is brought into

Table 21.16 *Stability of complexes of actinide MO_2^{2+} ions with dicarboxylates containing other donor atoms, compared with the basicity of the ligands. Medium* 1 *M* $(Na,H)ClO_4$, *temperature* 20°C. *Data from ref.* 153.

	$\log K_1$			$\log K_1$(H)	$\log K_2$(H)
	UO_2^{2+}	NpO_2^{2+}	PuO_2^{2+}	H^+	H^+
oxydiacetate	5.11	5.16	4.97	3.75	2.82
thiodiacetate	3.16			4.04	3.14
iminodiacetate	8.66	8.72	8.50	9.33	2.52

Table 21.17 *Thermodynamics of complex formation of Th^{4+} and H^+ with dicarboxylates containing other donor atoms. Medium 1 M (Na, H)ClO_4 (Th^{4+}) and 0.1 M (Na,H)ClO_4 (H^+), temperature 25°C. Data from ref. 253 (Th^{4+}) and adapted from ref. 254 (H^+).*

	Th^{4+}			H^+		
	ΔG_1° (kJ mol^{-1})	ΔH_1° (kJ mol^{-1})	ΔS_1° (J K^{-1} mol^{-1})	ΔG_1° (kJ mol^{-1})	ΔH_1° (kJ mol^{-1})	ΔS_1° (J K^{-1} mol^{-1})
oxydiacetate	−46.5	8.4	184	−22.3	6.2	96
thiodiacetate	−32.0	20.5	176	−23.5	2.8	88
iminodiacetate	−55.3	6.5	207	−53.1	−32.3	70

contact with a non-polar, or slightly polar, organic phase. Already in Section 21.4.5, benzene and various alkylbenzenes, carbon tetrachloride, and chloroform have been mentioned as suitable organic phases for the extraction of metal chelates. Other solvents used for this purpose include methyl isobutyl ketone (hexone) and other ketones, and a great variety of esters, alcohols, and ethers [133, 134]. Solvents of this type, possessing functional groups, may also serve as extractants in their own right (see below).

The chelating agents are coordinated to the metal ions as anions. They thus act as anionic extractants. Also, a number of organophosphorus compounds are efficient anionic extractants. Besides alkyl- and aryl-substituted phosphates, as exemplified by dibutyl phosphate (DBP) mentioned earlier in Section 21.4.3, phosphinates and phosphonates have also been used [103, 155]. Like the chelates discussed previously, these agents are always added as the corresponding acids, and extraction thus always involves a transfer of protons to the aqueous phase. Whether the organophosphorus extractants act as chelates is an open question. Evidently the common five- and six-membered rings cannot be formed. On the other hand, discrete chelate complexes are formed, at least in the solid state, e.g. by Th^{4+} with nitrate [156] and by UO_2^{2+} with carbonate, acetate, and nitrate [98, 124, 157]. In all these complexes, the rings are only four-membered, as would be the case in the chelates possibly formed by the organophosphorus anions.

Also, neutral and cationic species act as extractants, however. Among the neutral ones, alcohols, ethers, and ketones have long been known to be good solvents for actinide salts. The classical example is the high solubility of uranyl nitrate in diethyl ether, which allows extensive extraction of this salt from aqueous solutions [158]. Another ether which acquired considerable importance in the early days of nuclear waste processing was bis(2-butoxyethyl) ether (dibutylcarbitol, Butex), used in the Butex process [159]. Owing to the large alkyl groups, this compound is much less miscible with water than diethyl ether. Methyl isobutyl ketone was also used as an extractant on a large scale at that time, in the Redox process [160]. In these processes, the actinides are extracted as nitrates, and the charge of the actinide ions was compensated in the organic phase by the coordination of nitrate ions.

Organophosphorus compounds have since become the most-used neutral extractants. The ester tributyl phosphate (TBP) especially has become very important as the extractant of the Purex process, used almost exclusively in all modern reprocessing of spent nuclear fuels. Also, with these extractants, the actinides are generally extracted as nitrates [161, 162].

Amines constitute a third group of neutral extractants. They differ markedly from the two previous groups, however, by being quite strong bases. Consequently, acids are extensively extracted from the aqueous phase, with the formation of undissociated ammonium compounds in the organic phase. Also the metal complexes formed by extraction into this phase are always protonated. The amines are not coordinated in the base form but as ammonium ions. By ion pairing with the anions present, a neutral entity is finally formed. The amines thus in fact act as cationic extractants. In analogy with this, quarternary ammonium salts are also good extractants for actinide ions of various oxidation states [163–165].

Extraction by means of tertiary amines is very important technologically. Most of the uranium presently produced is separated by such a process, working with a mixture of long-chain tertiary amines [166]. Also, extraction by tertiary amines is generally applied for the separation of transplutonium elements on a large scale [167].

21.5.2 Extraction by anions

The extraction properties of the typical chelating agents discussed in Section 21.4.5 are well-illustrated by the equilibrium constants listed in Table 21.18. As to the β-diketones, the extraction always increases in the sequence AA < Benz A < TTA, generally quite strongly. The tropolone ITP is an even better extractant than TTA, especially in the case of Th^{4+}, which is remarkably poorly extracted by the β-diketones as compared with other M^{4+} ions. Nor is oxine a good extractant for Th^{4+}. This ligand extracts UO_2^{2+} relatively well, however.

In Table 21.18, the distribution constants of the acids and their association constants in the aqueous phase are also listed. All the acids are quite weak, and all except HAA more or less strongly prefer the organic phase. Though these properties of the acids obviously influence the extraction equilibrium, there is no immediate correlation between the values of K_D, or $K_1(H)$, and those of K_{ex}. The specific interaction between ligand and metal ion is the paramount factor.

Extraction by means of oxine is illustrated in Fig. 21.7. The percentage extracted is given as a function of pH. The value of pH is commensurate with log[AA] as long as [HAA] is practically constant ($pH - \log[AA] = \log K_1 - \log[HAA]$). Protactinium(v) and neptunium(iv) are strongly preferred to the trivalent actinides (and even more to radium(ii)). At high values of pH (i.e. [AA]), anionic complexes of protactinium(v) are formed in the aqueous phase, resulting in a steep decrease in extraction.

Table 21.18 *Constants K_{ex} of the extraction $M^{z+}(aq)+zHL(org)\rightleftharpoons ML_z(org)+zH^+(aq)$, K_D of the distribution $HL(aq)\rightleftharpoons HL(org)$, and $K_1(H)$ of the protonation $H^+ + L^- \rightleftharpoons HL$ in the aqueous phase. Organic phase benzene, temperature 25°C, if not otherwise stated. Perchlorate medium in the aqueous phase, of ionic strength I stated. Data from ref.* 134.

	log K_{ex}				
M^{z+}	L = AA	BenzA	TTA	ITP	Ox
Am^{3+}		−18.45[e]	−7.92[a,f,m]	−7.20[a,g]	
Th^{4+}	−12.16[a]	−7.68[a,j]	1.3[c]	4.66[b,g]	4.12[a,g]
U^{4+}	−5.3[a,i]		5.3[c]		
Np^{4+}	−4.97[b]		5.6[c]		1.2[a,g]
Pu^{4+}	−1.8[a,i]		6.85[b]	7.33[h]	
PaO^{3+}	−0.4[d]				
PaO_2^+	−2.1[d]				
UO_2^{2+}	−5.85[c]	−5.50[c,k,l]	−2.0[c]	1	−2.42[a,g,l]
log K_D[a]	0.77	3.14	1.62	3.37[g]	2.32
log K_1(H)[a]	8.82	8.96	6.46	7.04	9.66

[a] $I = 0.1$ M.
[b] $I = 1$ M.
[c] $I = 2$ M.
[d] $I = 3$ M; organic phase xylene.
[e] $I = 0.5$ M; organic phase chloroform.
[f] K_{ex} of the same order of magnitude for Cm^{3+}, Bk^{3+}, Cf^{3+}, Es^{3+}, and Fm^{3+}.
[g] Organic phase chloroform.
[h] I varies: 1–3 M.
[i] With chloroform: −7.4 for U^{4+}; −4.2 for Pu^{4+}.
[j] 20°C.
[k] 30°C.
[l] For $UO_2^{2+}(aq)+3HL(org)\rightleftharpoons UO_2L_2HL(org)+2H^+(aq)$: −4.68 (BenzA, 20°C); 2.63 (ITP, 25°C); −1.60 (Ox in chloroform, 20°C).
[m] With chloroform: −9.20.

Though these chelating agents allow practically complete extraction of actinides in one single step, they are not used for large-scale processes. The distribution constant of the uncharged complex is admittedly very high, but its solubility in the organic phase is nevertheless fairly low. Only limited amounts can be extracted and the chelating agents are therefore mostly used for fundamental investigations and for analytical purposes [169].

The metal complexes formed by the anionic organophosphorus extractants are, on the other hand, very soluble in organic solvents. Such compounds have therefore been used for various technical processes. Most important is the monobasic diethylhexylphosphoric acid (HDEHP), but dibutylphosphoric acid (DBP) has also been widely applied [103, 155]. Some data illustrating the properties of these extractants are collected in Table 21.19.

In contrast to the chelating agents of Table 21.18, these acids are quite strong. Moreover, DBP especially dimerizes extensively in the organic phase. Consequently, the ligands strongly prefer this phase, in spite of the low values of

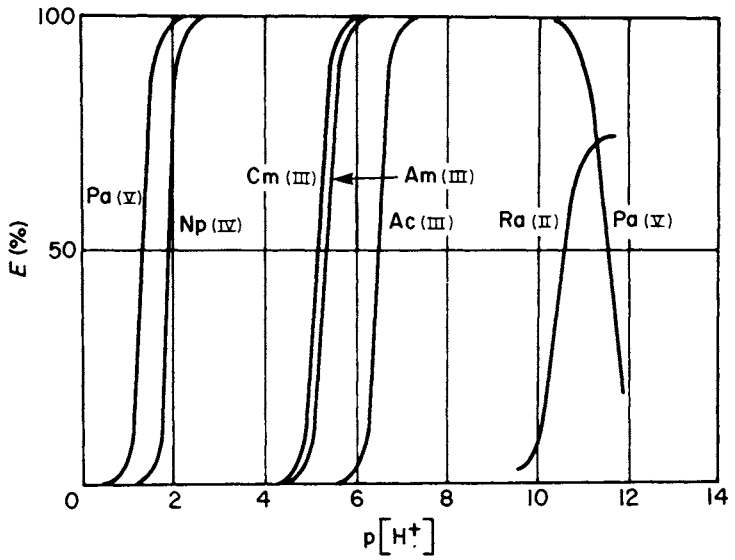

Fig. 21.7 *The extraction E of tracer amounts of actinides in various oxidation states, and of radium(II), by* 0.1 M *(for Ra(II)* 1 M*)* 8*-hydroxyquinoline in chloroform, as a function of pH, at* 25°C [168]. *Aqueous medium* 0.1 M $(Na,NH_4,H)ClO_4$.

Table 21.19 *Extraction by organophosphorus compounds. Constants* K_{ex} *of the extraction* $M^{z+}(aq)+z(HL)_2\ (org) \rightleftharpoons M(HL)_zL_z\ (org) + zH^+(aq)$, K_D *of the distribution* $HL(aq) \rightleftharpoons HL(org)$, K_{II} *of the dimerization* $2HL \rightleftharpoons (HL)_2$ *in the organic phase, and* $K_1(H)$ *of the protonation in the aqueous phase. Perchlorate medium* 25°C, *data from ref.* 103, *if not stated otherwise.*

	$\log K_{ex}$		
M^{z+}	*DBP*	*DEHP*	*Solvent*
Eu^{3+}	1.73	−0.50	toluene
Gd^{3+}		0.20	toluene
Am^{3+}		−1.53	toluene
Cm^{3+}		−1.40	toluene
UO_2^{2+}	4.56	2.98[d]	toluene
	3.58		chloroform
NpO_2^{2+}	4.28[a]	4.36[d]	[e]
$\log K_D$	−0.91[b]	1.22	carbon tetrachloride
$\log K_{II}$	5.33[b]	2.0	carbon tetrachloride
$\log K_1(H)$	1.00[c]	1.4[d]	

[a] 21°C; ref. 76.
[b] Nitric acid medium.
[c] Ref. 170.
[d] 20–23°C.
[e] Carbon tetrachloride for DBP; toluene for DEHP.

the distribution constants of the monomers. The complexes formed by M^{3+} and MO_2^{2+} ions generally keep half of the protons originally attached to the ligand. In the case of M^{4+} ions, anions from the aqueous solution are often incorporated in the complex so that the number of protons transferred to the aqueous solution is less than 4 [103].

The MO_2^{2+} ions are extensively extracted. This was utilized in the first large-scale extraction process (Dapex) developed for the recovery of uranium from ores where HDEHP was applied [171]. The M^{4+} ions are also readily extracted while M^{3+} ions have rather low values of K_{ex} (Table 21.19). This difference is utilized in the processing of irradiated ^{242}Pu for transplutonium elements. The unchanged plutonium is kept tetravalent while all the transplutonium elements are in their trivalent states. Plutonium is completely extracted from the mixture by HDEHP dissolved in diethylbenzene, while the trivalent elements remain in the aqueous phase (Pubex process) [172].

The actinide(III) ions are also extracted more poorly than the corresponding lanthanide(III) ions (Table 21.19), but the difference is smaller than between M^{3+} and M^{4+}, or MO_2^{2+}. Complete separation can be achieved, however, by adding diethylenediaminepentaacetic acid and lactic acid to the aqueous phase. These preferentially sequester the actinide(III) ions so that complete separation from the lanthanides can be obtained by extracting the latter by HDEHP in diisopropylbenzene [173].

21.5.3 Extraction by neutral compounds

For extractions with neutral or cationic extractants, the properties and concentrations of the anions present in the aqueous phase are obviously very important. Efficient extraction is possible only if the anion is able to participate in the formation of mixed complexes which are readily accepted by the organic phase. Generally, extraction is a rather complicated function of the anion concentration. This is, for example, the case in the Purex process, where tetra- and hexavalent actinides are extracted by means of TBP. This compound is a high-boiling liquid, too viscous at ordinary temperatures to be used in a practical extraction process. It is therefore diluted by an inert solvent. In the present technology for the reprocessing of irradiated nuclear fuels, a 30% solution of TBP in a fairly high-boiling hydrocarbon is generally used. As might be expected, however, the choice of diluent does not influence the extraction very much. In practice, extraction always takes place from nitric acid solutions. The conditions are therefore not very different from those applied in the fundamental study illustrated by Fig. 21.8 [174].

The reactions taking place can be written:

$$M^{4+}(aq) + 4NO_3^-(aq) + 2TBP(org) \rightleftharpoons M(NO_3)_4(TBP)_2(org)$$

and

$$MO_2^{2+}(aq) + 2NO_3^-(aq) + 2TBP(org) \rightleftharpoons MO_2(NO_3)_2(TBP)_2(org)$$

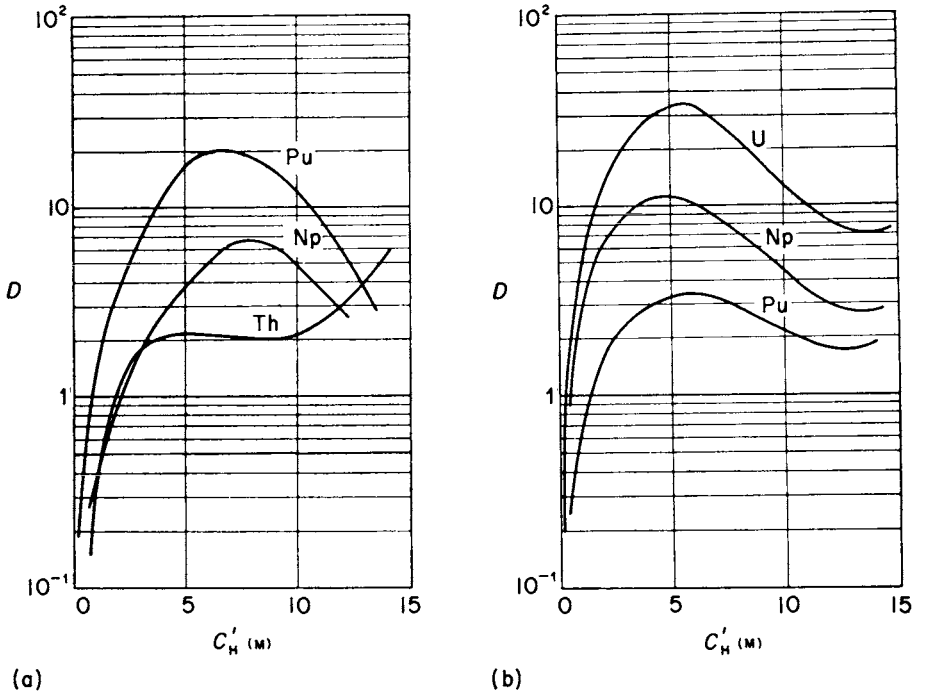

Fig. 21.8 *Extraction of (a) tetravalent and (b) hexavalent actinide nitrates at low concentrations (< 10 mM) by 19% tributyl phosphate in kerosene, at 25°C [174]. The curves give the distribution ratios $D = C_M(org)/C_M(aq)$ as a function of the (initial) nitric acid concentration in the aqueous phase, C'_H.*

respectively. To start with, the extraction increases rapidly with nitric acid concentration in the aqueous phase, as might be expected (Fig. 21.8). By and by, however, the curves become less steep, and at a concentration of about 5 M, or somewhat higher, a maximum is reached, followed by a decrease which in most cases becomes fairly steep. This is probably due to a combination of two effects. The most important of these is presumably the competing extraction of nitric acid, with the formation of $HNO_3 \cdot TBP$ in the organic phase which becomes extensive at high acid concentrations [175]. This means a decrease of the free-ligand ion concentration [TBP] and hence of actinide extraction. Also, at high acid concentrations, anionic nitrate complexes may be formed in the aqueous phase. These compete with the mixed nitrate–TBP complexes for the actinide ions, thereby decreasing the extraction. In media where strong actinide complexes are formed, e.g. sulfuric acid (cf. Section 21.4.3), extraction may be severely suppressed even at fairly low concentrations of the coordinating ligand [176]. At very high nitric acid concentrations, the extraction tends to increase again, notably for thorium(IV) (Fig. 21.8). This is presumably due to extensive changes of hydration of the species in the aqueous phase.

A very low extraction is found when the anions in the aqueous phase are reluctant to form complexes. Thus the extraction of, for example, plutonium(IV) from perchloric acid solutions, is poor even at fairly high perchlorate concentrations [176].

The phosphine oxides are powerful extractants. Tri-n-octylphosphine oxide (TOPO) is the most thoroughly investigated of these compounds, but the properties of tributylphosphine oxide (TBPO) are also fairly well-known [103, 176]. The values of $\log K_{ex}$ for the extraction with carbon tetrachloride:

$$UO_2^{2+}(aq) + 2NO_3^-(aq) + 2L(org) \rightleftharpoons UO_2(NO_3)_2L_2(org)$$

where L = TOPO or TBPO, are much higher than for the analogous extraction with TBP [103], viz. approximately 7 for the phosphine oxides as against approximately 2 for TBP. The character of the organic diluent is moreover not very important, as has already been pointed out. Much the same values are found for cyclohexane or kerosene, for example.

The ketones and ethers used in the early extraction processes served as both solvent and extractant. Their extracting power is generally fairly low, however. Extraction often increases with nitric acid concentration in the aqueous phase up to at least 10 M acid. The extraction of acid is seemingly less extensive in these solvents than in TBP solution. Still better extractability can be achieved, however, by the addition of non-extractable nitrates instead of nitric acid ('salting out') [177]. The distribution ratios of tetra- and hexavalent plutonium between some extractants of these types and an aqueous solution are given in Table 21.20. The nitrate concentration in the aqueous phase is high, which means that the extraction conditions are quite favorable. Still, the distribution ratios are mostly low. For plutonium(IV), Butex, with three ether oxygens, has the highest value of D, comparable to that found for TBP at maximum extraction (Fig. 21.8). For plutonium(VI), methyl isobutyl ketone is the most efficient extractant. As to the other ethers, even modest modifications of the alkyl groups bring about vast changes in extracting power, as is evident from a comparison between the diethyl,

Table 21.20 *The distribution ratio D for tetra- and hexavalent plutonium between various organic solvents and an aqueous solution, containing* 1 M *nitric acid and* 10 M *ammonium nitrate, if not otherwise stated* [176].

Extractant	*Pu(IV)*	*Pu(VI)*
Methyl isobutyl ketone	4.56	42.3[a]
Diethyl ether	0.47	1.0
Di-n-propyl ether	<0.01	0.05[b]
Diisopropyl ether	0.075	0.01
Ethyl n-butyl ether	0.032	0.14
Butex	13.3	10[b]

[a] Aqueous phase containing 6% nitric acid, 60% ammonium nitrate.
[b] Uncertain values.

di-n-propyl, diisopropyl, and ethyl n-butyl ethers. None of the ethers containing larger alkyl groups is nearly as efficient an extractant as the diethyl ether.

21.5.4 Extraction by alkylammonium extractants

Among the alkylammonium compounds, the tertiary amines are by far the most important actinide extractants, as has already been mentioned (Section 21.5.1). Extraction depends upon the nature and concentration of the anion in much the same manner as for neutral extractants (Section 21.5.2). A good example is the extraction of neptunyl(VI) by methyldioctylamine in chloroform from solutions containing increasing concentrations of sulfuric, hydrochloric, or nitric acids (Fig. 21.9) [178]. The value of D increases rapidly at low concentrations, and most rapidly for sulfuric acid, as the complexes formed by the sulfate ion are much stronger than those formed by chloride or nitrate. Consequently, extractable

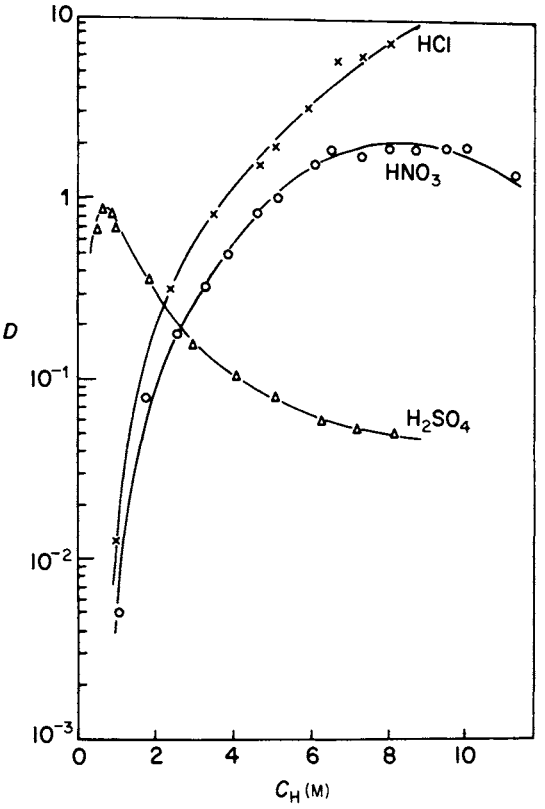

Fig. 21.9 *Extraction of neptunium(VI) by 0.4 M methyldioctylamine in chloroform from aqueous solutions of hydrochloric, nitric, and sulphuric acids, at 20°C* [178]. *Initial concentration of neptunium 0.45 mM. The curves give the distribution ratio D as a function of the equilibrium acid concentration in the aqueous phase,* C_H.

complexes are formed at much lower ligand concentrations in the sulfate system. On the other hand, the factors acting against extraction, i.e. the extraction of acid and the formation of anionic complexes in the aqueous phase, also become important sooner in this system. Consequently, maximum extraction already occurs at an acid concentration of about 0.7 M for sulfuric acid compared to about 8 M for nitric acid. For hydrochloric acid, the maximum has not been reached even at such a high concentration.

In order to act as efficient extractants, the tertiary amines must have fairly long carbon chains. On the other hand, if the chains are too long, or too heavily branched, the efficiency again decreases. The highest distribution ratios are often found for trioctylamine (TOA) or triisooctylamine (TIOA). This is the case, for example, when neptunium(IV) is extracted from a nitric acid or sodium nitrate solution (Fig. 21.10) [179].

The two families of curves in Fig. 21.10 also demonstrate very clearly the salting-out effect discussed in Section 21.5.2. The nitric acid curves display

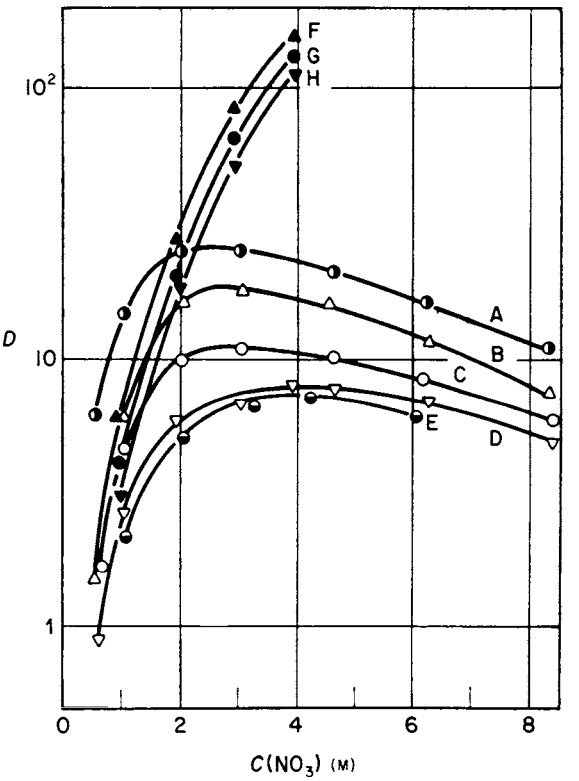

Fig. 21.10 *Extraction of neptunium(IV) by 0.1 M trialkylammonium nitrate solutions in xylene, as a function of the nitric acid (curves A–E) or sodium nitrate (curves F–H) concentrations* [179]. *The letters refer to: triisooctylamine (A); trioctylamine (B,F); triheptylamine (C,G); tridecylamine (D,H); trilaurylamine (E).*

maxima similar to those found for the TBP extraction of tetravalent actinides from nitric acid solutions (Fig. 21.8), while the sodium nitrate curves continue to rise steeply to the highest concentration used, 4 M.

The extraction of various actinide(IV) and actinyl(VI) ions from nitric acid solution by means of a xylene solution of TOA is shown in Fig. 21.11. Though the curves are similar in many respects to the TBP curves of Fig. 21.8, the differences are also marked. Thus, in the case of tetravalent ions, the high extractabilities of plutonium(IV) and neptunium(IV), and the slight extractability of thorium(IV), are striking. In the case of the actinyl(VI) ions, UO_2^{2+} is extracted much less readily than NpO_2^{2+} or PuO_2^{2+} by TOA but more readily by TBP. In the case of TOA, NpO_2^{2+} and PuO_2^{2+} behave in much the same manner.

21.6 ION EXCHANGE

21.6.1 Cation exchange

The uptake of actinides by cation exchangers varies greatly between ions of different types and charges, in the sequence $MO_2^+ < M^{2+} < MO_2^{2+} < M^{3+} < M^{4+}$ [181, 182]. M^{4+} ions are very strongly sorbed, even from acid solutions. The sorption of M^{3+} is considerably weaker though nevertheless still quite strong. MO_2^{2+} ions are more readily sorbed than divalent M^{2+} ions of spherical

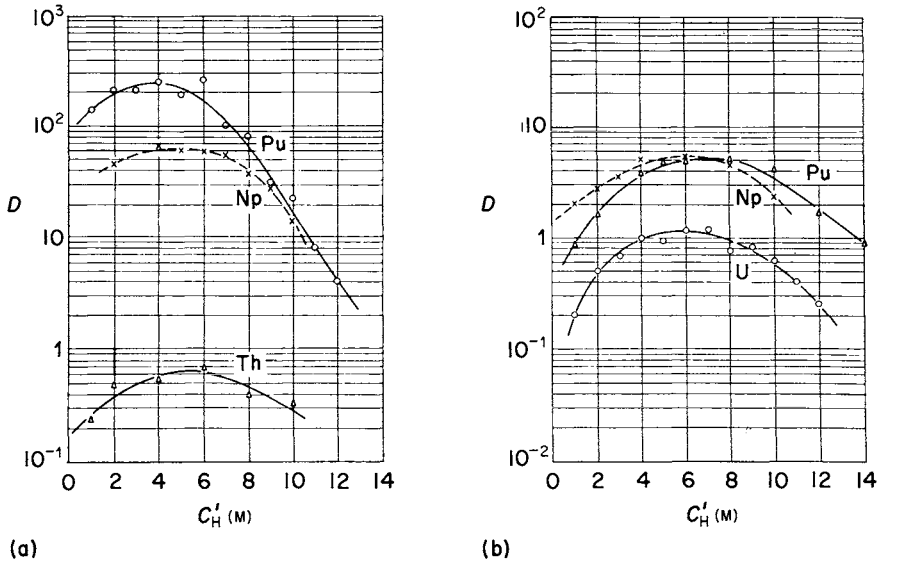

Fig. 21.11 *Extraction of (a) tetravalent and (b) hexavalent actinide nitrates by* 10% *trioctylamine in xylene, at* 25°C [180]. *The curves give the distribution ratios D as a function of the (initial) nitric acid concentration in the aqueous phase,* C'_H.

symmetry, evidently on account of a higher charge on the central metal ion. The monovalent MO_2^+, finally, is only weakly sorbed. The affinity differences between ions of different types are so large that their separation by cation exchange is an easy matter.

Cation-exchange techniques have nevertheless been the most widely used for the separation of ions of the same charge. Mixtures of closely related trivalent ions especially have been successfully handled in this way. The sorption coefficients admittedly do not differ widely. They decrease slightly with decreasing ionic radius of M^{3+} [182, 183], i.e. contrary to what would be expected from the simplest electrostatic argument. The reversal is due to the fact that hydration becomes more extensive as the ionic radius decreases. This means that the radius of the hydrated ion increases, with a consequent decrease of the sorbability.

The separation effect can be much enhanced, however, by the use of selective eluting agents. These are solutions of chelating ligands, most often oxycarboxylates, with an affinity for M^{3+} which increases as the ionic radius decreases. This technique was first introduced in order to achieve separations of the trivalent lanthanide ions, with citrate as eluting agent [184, 185]. The process provided the first really satisfactory solution to a long-standing and extremely difficult separation problem. The technique has since proved as successful for the separation of the various transplutonium elements from mixtures obtained by the irradiation processes used in their production. As these nuclides are often very short-lived, and moreover obtained only in minute amounts, the separation procedure has to be both very fast and very efficient. Ion exchange has fulfilled these demands better than any other conceivable method.

During the irradiation used for the production of transplutonium elements, lanthanides are formed as fission products. As the lanthanide(III) and actinide(III) ions are eluted together from the ion exchanger by the procedure described above, the lanthanides have to be removed prior to that treatment. This can be achieved by another cation-exchange procedure. The trivalent actinides and lanthanides are sorbed together on the ion exchanger. On account of their stronger tendency to form chloride complexes, the actinides can then be eluted as a group, well in advance of the lanthanides, by means of concentrated hydrochloric acid [186, 187]. Even better separation is achieved by 20% ethanol saturated with hydrochloric acid, which means a concentration of acid equal to 12.5 M [188].

The citrate ion was the eluting agent used in the first isolation of berkelium and californium [189, 190]. Soon afterwards, however, the lactate and tartrate ions were found to give considerably improved separations between americium(III) and curium(III) [191]. Lactate elution also proved superior to the classic citrate elution for the first isolation of einsteinium and fermium [188]. Later on, an even more selective eluant for actinide(III) ions has been found in the α-hydroxyisobutyrate ion [192]. With this ligand, very clean separations of the heavy actinide(III) ions can be achieved, as illustrated in Fig. 21.12. The first isolation of mendelevium was achieved by this procedure [193].

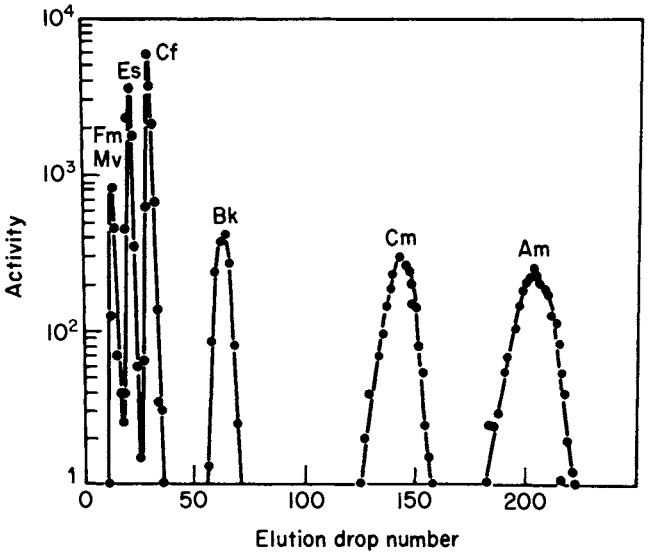

Fig. 21.12 *Separation of the trivalent oxidation states of the transplutonium elements Am–Md by elution from the cation-exchange resin Dowex* 50 *(sulfonated polystyrene;* 12% *crosslinked) with a* 0.4 M *ammonium α-hydroxyisobutyrate solution at* 87°C [192].

Organic cation-exchange resins have been invaluable for the isolation and characterization of the transplutonium elements. As far as the transcurium elements are concerned, it might even be held that their isolation would have been impossible by any other method. On the other hand, organic ion exchangers are of limited utility when large activities are involved, on account of their sensitivity to radiation [194]. For technical or preparative purposes, involving separation of actinides and fission products on a large scale, they are therefore not suitable.

For such purposes, inorganic ion exchangers might prove to be more advantageous, as they are extremely resistant to radiation. Even doses as high as 3×10^9 rad do not cause any perceptible deterioration of their exchange properties [194, 195]. Especially zirconium phosphate (ZrP) ion exchangers of various compositions have been studied rather extensively, as they combine high radiation resistance with large capacity and a strong affinity for both actinide ions and many important fission products. Like the organic ion-exchange resins, they do not, however, discriminate between actinide(III) and lanthanide(III) ions (Fig. 21.13) [196]. But contrary to the organic resins, the affinity increases in each group with decreasing ionic radius. For this type of ion exchanger, the sorbability is evidently determined by the radius of the naked ion, not by the radius of the hydrate. Another difference is that ZrP prefers UO_2^{2+} to M^{3+}. The strongest affinities for both ZrP and organic resins are displayed by M^{4+} ions, however [196, 197]. These are in fact never sorbed in a true ion-exchange process but rather enter the phosphate matrix in reactions which are not readily reversible [197].

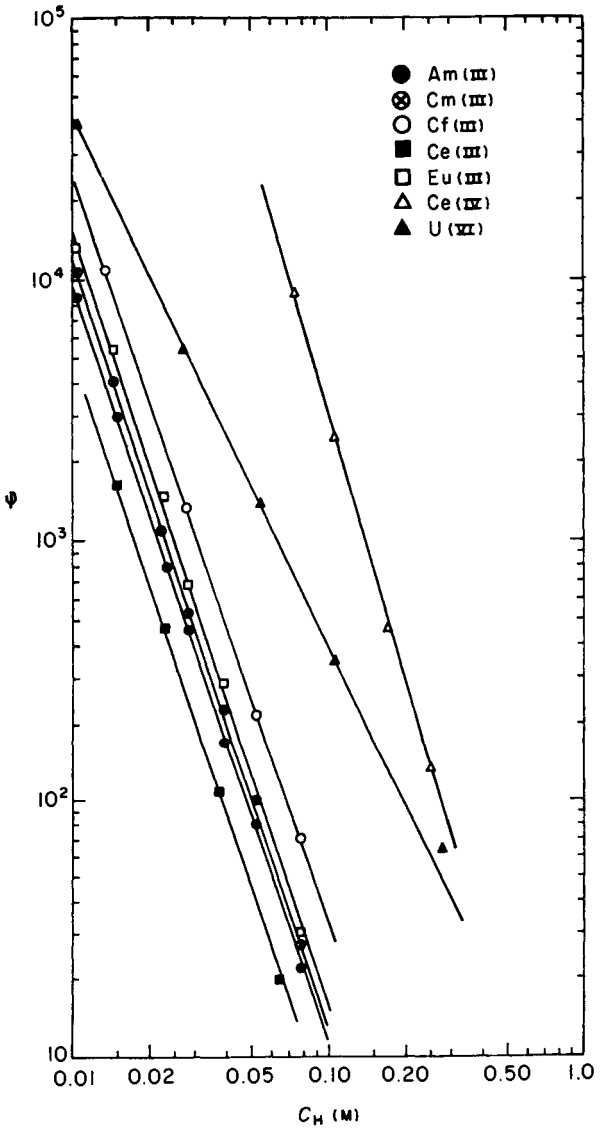

Fig. 21.13 *Sorption of tracer concentrations of actinides and lanthanides on amorphous zirconium phosphate of phosphate/zirconium ratio of* 1.34 [196]. *The distribution ratio* $\varphi(ml\,g^{-1}) = C_M(ZrP)/C_M(aq)$ *is plotted as a function of the nitric acid concentration,* C_H. *Temperature* 75°C.

21.6.2 Anion exchange

Though anion exchangers have been used much less than cation exchangers for the isolation and characterization of the actinide elements, they have nevertheless been applied in several interesting separation processes. An exhaustive survey [198] of the sorption of the important oxidation states of most elements from chloride solutions shows that the distribution ratio varies with the anion concentration in a very characteristic manner. First a steep rise is observed which levels off until a maximum is reached. The sorption then decreases, generally less steeply than it originally rose. Similar patterns are found also for other anions, e.g. bromide, iodide [199], and carboxylates [200]. The maximum occurs when the concentration of the neutral complex in the outer solution reaches its maximum value, i.e. when the ligand number $\bar{n} = z$ for solutions containing cations M^{z+} [199, 200]. It might seem paradoxical that the sorption then decreases with increasing anion concentration, in spite of the steady increase of the fraction of anionic complexes in the outer solution. The explanation is that the concentration of free anions increases even more. The anionic complexes are in fact forced out of the anion exchanger by their own ligands. It should also be pointed out that within the ion-exchanger, the ligand concentration is very high as the resin is generally saturated with the proper anions before being used. The metal ions sorbed are therefore almost exclusively present as anionic complexes [200]. The amount of metal ions sorbed thus depends upon the ligand concentration in the solution, but the composition of the species present in the anion exchanger depends upon the ligand concentration in that phase.

Anion exchange from chloride solutions may be used for group separation of trivalent actinides and lanthanides. Actinide(III) ions form much more stable chloride complexes than do lanthanide(III) ions. They are therefore sorbed on anion-exchange resins from concentrated (13 M) hydrochloric acid, while the lanthanides are not [188]. The smaller the ionic radius of the actinide ion, the more stable are the complexes. The ions are consequently more strongly sorbed, the higher the atomic number of the element. On elution, the lightest element will leave the column first and the heaviest one last, i.e. in the reverse order to that found by elution from a cation-exchange column (Section 21.6.1). The separation is poorer, however, than that achieved by elution with concentrated hydrochloric acid from a cation-exchange column [188]. Once the lanthanides have been removed, the best separation is in any case obtained by elution with α-hydroxyisobutyrate from a cation-exchange column (Fig. 21.12).

The formation of thiocyanate complexes of actinide(III) ions (Section 21.4.6) has also been successfully utilized for the separation of actinides from lanthanides by means of anion exchange [188, 201]. From a 5 M ammonium thiocyanate solution, americium (III) is strongly sorbed on an anion-exchange column while the lanthanides pass through [201]. In this way, americium (III) can be almost completely separated from lanthanides present even in very large amounts.

On a technical scale, anion exchange has been used extensively for the processing of uranium ores (cf. Chapter 5). The solutions obtained by sulfuric acid leaching especially are amenable to such an intermediate purification step. Carbonate leaching solutions may also be treated in this way.

For the first purification of plutonium in the processing of irradiated nuclear fuels, an anion-exchange process has been widely used [202]. In this process, complex formation of plutonium(IV) with nitrate is utilized in order to remove the last traces of uranium (present as uranyl(VI)) and fission products (primarily lanthanides). In this system, the maximum sorption of plutonium(IV) occurs at a nitric acid concentration of 7.2 M. The process is run at 60°C. At lower temperatures, the sorption is too slow; at higher temperatures, the distribution ratio becomes more unfavorable and the resin is more liable to deteriorate. Under the conditions chosen, neither uranyl(VI) nor lanthanides are sorbed. The elution of plutonium(IV) is readily achieved by dilute ($\simeq$ 0.7 M) nitric acid. The weak point of the process is the limited resistance of organic ion exchangers to chemical attack and to high doses of radiation, already discussed in Section 21.6.1. These difficulties can be overcome, at least partly, by careful selection of the resin to be used.

21.7 KINETICS OF REACTIONS IN SOLUTION

21.7.1 Acid–base reactions

The various acid–base reactions discussed in Sections 21.2–21.4 are generally very fast processes. Important exceptions, however, are the later stages of hydrolysis of M^{4+} ions (Section 21.2.3). The kinetics of these reactions are complicated. Thus, in the case of thorium(IV), not only the size of the aggregates but also their rate of formation depend very much upon the anions present (Fig. 21.2). In chloride solutions, the aggregates are not only larger than in perchlorate solutions, but they also continue to grow during extended periods of time [35].

On account of its large practical importance, polymer formation in hydrolyzed plutonium(IV) solutions has attracted much interest [203]. This polymer is formed fairly rapidly [204, 205]. The reaction is faster, and more extensive, the higher the temperature. As long as ionic plutonium(IV) is present in detectable amounts, the rate of polymerization is proportional to the concentration of this component, and inversely proportional to the square of the acidity. When the ionic plutonium(IV) has been consumed, the rate depends in a rather complicated manner upon the concentration of other oxidation states present [205]. If the polymer is allowed to age, depolymerization becomes very slow even if the concentration of acid is fairly high [204]. The colloid behaves very differently from ionic plutonium(IV) in the extraction and ion-exchange procedures used in the processing of plutonium, and is also apt to transform into a precipitate. The conditions should therefore be chosen so that the formation of the colloid is

avoided. If it has nevertheless accidentally been formed, depolymerization must be effected without delay.

21.7.2 Oxidation–reduction reactions

In processes involving oxidation and reduction of actinide species, slow kinetics are quite common. Generally, reactions that involve the formation or rupture of the strongly covalent metal-to-oxygen bonds in the ions MO_2^{2+} and MO_2^{+} are slow. On the other hand, reactions involving only an electron transfer, besides relatively minor adjustments of the hydration shells, are apt to be fast and readily reversible. As is often found in kinetic measurements, however, the rates may differ widely between reactions which are seemingly analogous.

As examples of reactions where the M–O bonds in the actinyl ions are not broken, processes

$$M^{3+}(1) + MO_2^{2+}(2) \rightarrow M^{4+}(1) + MO_2^{+}(2)$$

will be considered. Generally, (1) and (2) denote ions formed by different elements, but in special cases M may be the same in all ions. A number of such reactions, involving uranium, neptunium, and plutonium as reductants and oxidants, have been carefully studied (Table 21.21) [206, 207]. Though these processes are, as expected, all fast, the rates nevertheless vary within wide limits. The oxidations of U^{3+} and Np^{3+} by UO_2^{2+} and NpO_2^{2+}, respectively, are extremely fast. The oxidations of Np^{3+} by UO_2^{2+} and of Pu^{3+} by NpO_2^{2+} are both much slower. The difference is not due to the circumstance that the later reactions involve different actinides, as is obvious from the fact that the oxidation of Pu^{3+} by PuO_2^{2+} is even slower.

The rates of reaction are closely connected with the free energies, enthalpies, and entropies of activation (ΔG^*, ΔH^*, and ΔS^*). These have been determined from the temperature dependence of the rate constants. Also, the thermodynamic equilibrium parameters ΔG°, ΔH°, and ΔS° (generally determined via EMF measurements; cf. Chapter 17) are of interest in this connection. All the quantities mentioned have therefore been entered in Table 21.21.

As to the equilibrium parameters, the entropy changes are practically the same in all the reactions. This is rather to be expected as the hydration of each type of ion must be fairly independent of the element involved. The values of ΔS° are very negative, implying that the formation of strongly hydrated M^{4+} ions brings about a considerable net increase of order in the solutions. The values of ΔH°, and consequently the values of ΔG°, on the other hand, differ considerably between the various systems, and moreover in such a way that the two fastest reactions are also by far the most exothermic ones. The values of k do not decrease monotonically as the reactions become less exothermic, however.

Naturally enough, the activation parameters are more informative about the reason for the large differences in the reaction rates. The three reactions $U^{3+} + UO_2^{2+}$, $Np^{3+} + NpO_2^{2+}$, and $Pu^{3+} + PuO_2^{2+}$ are all first order in each of

Table 21.21 *Reactions not involving breaking of M–O bonds: rate constants ($M^{-1}\,s^{-1}$), activation parameters, and thermodynamic equilibrium parameters for reactions $M^{3+}(1)+MO_2^{2+}(2) \rightarrow M^{4+}(1)+MO_2^{+}(2)$. Medium 1 M $HClO_4$; 25°C* [206].

Reaction	*k*	ΔG^* (kJ mol^{-1})	ΔH^* (kJ mol^{-1})	ΔS^* (J K^{-1} mol^{-1})	ΔG° (kJ mol^{-1})	ΔH° (kJ mol^{-1})	ΔS° (J K^{-1} mol^{-1})
$U^{3+}+UO_2^{2+}$	5.5×10^4	46.0	18.1	−93	−67	−112	−151
$Np^{3+}+NpO_2^{2+}$	1.05×10^5	44.4	4.2	−134	−95	−141	−159
$Pu^{3+}+PuO_2^{2+}$	2.7	70.5	20.2	−169.0	6.3	−40	−151
$Np^{3+}+UO_2^{2+}$	39	64.4	10.9	−178	8.6	−36	−151
$Pu^{3+}+NpO_2^{2+}$	35.5	64.2	14.6	−166.2	−15	−61	−153

Table 21.22 *Reactions involving breaking of M–O bonds*[a]*: rate constants*[b]*, activation parameters, and thermodynamic equilibrium parameters for reactions $M^{4+}(1)+MO_2^{2+}+2H_2O \rightarrow MO_2^{+}(1)+MO_2^{+}(2)+4H^+$. Perchlorate media of ionic strength I stated. Temperature 25°C and, for $Np^{4+}+PuO_2^{2+}$, 30°C.*

Reaction	*I*	n[c]	k[b]	ΔG^* (kJ mol^{-1})	ΔH^* (kJ mol^{-1})	ΔS^* (J K^{-1} mol^{-1})	ΔG° (kJ mol^{-1})	ΔH° (kJ mol^{-1})	ΔS° (J K^{-1} mol^{-1})	*Ref.*
$U^{4+}+UO_2^{2+}$	2	−3	4×10^{-7}	111	157	152	51.4	111	198	201, 211
$U^{4+}+NpO_2^{2+}$	2	−1	22	66.9	76.1	31	−54.0	7.1	205	212
$U^{4+}+PuO_2^{2+}$	2	−1(−2)	3.1	69.5	73.6	14	−32.6	28.9	205	
$Np^{4+}+NpO_2^{2+}$	2	−2(−1)	5×10^{-2}	80.8	102.9	74	−38.5	31.4	234	213
$Np^{4+}+PuO_2^{2+}$	1	−2(−3)	7.5×10^{-4}[d]	93	129	125	−17.2			214
$Pu^{4+}+PuO_2^{2+}$	1	−3	2×10^{-7}[d]	111	158	159	24.3	79.5	184	215

[a] Data from ref. 209 and from the original papers quoted in the last column.
[b] Rate constants k refer to 1 M acid. They are thus apparent second-order constants ($M^{-1}\,s^{-1}$).
[c] Order of hydrogen-ion dependence. In cases where more than one reaction path has been found, the order of the less important one is given within parentheses.
[d] Values extrapolated, or calculated, by the present author.

the reactants and independent of H^+ in the range of acidities measured (0.04–0.6 M, 0.01–0.1 M, and 0.1–1 M perchloric acid, respectively, at constant ionic strength) [16, 207]. This implies that the reaction proceeds via an activated complex $\{M \cdot MO_2^{5+}\}^*$. As to the reaction $Pu^{3+} + NpO_2^{2+}$, the formation of this complex still provides the main route. In this case, however, the rate also depends upon the acidity (varied in the range 0.03–1 M). To account for this, a subsidiary alternative route via a hydrolyzed complex $\{Pu \cdot OH \cdot NpO_2^{4+}\}^*$ has been postulated [206]. In the case of $Np^{3+} + UO_2^{2+}$, the conditions are complicated by the parallel subsequent reactions [208]:

$$Np^{3+} + UO_2^+ + 4H^+ \rightarrow Np^{4+} + U^{4+} + 2H_2O$$

and

$$2UO_2^+ + 4H^+ \rightarrow UO_2^{2+} + U^{4+} + 2H_2O$$

Especially at high acidities, these are quite fast, in spite of the breaking of the U–O bonds in UO_2^+. In 1 M acid, uranyl(v) soon reaches a maximum concentration and then declines, while the concentration of uranium(IV) steadily increases after a slow beginning (Fig. 21.14). The parameters applying to the activated complex $\{Np \cdot UO_2^{5+}\}^*$ of the first step can nevertheless be determined accurately. The

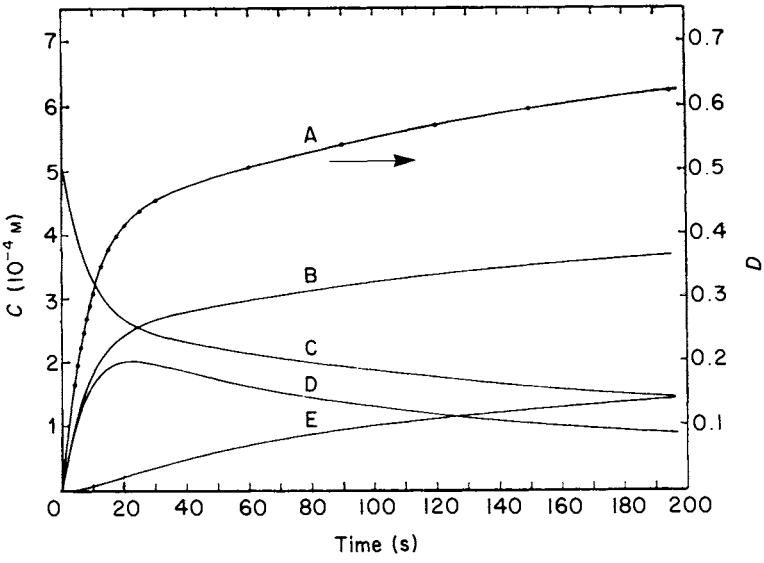

Fig. 21.14 *The rapid reaction* $Np^{3+} + UO_2^{2+} \rightarrow Np^{4+} + UO_2^+$ *followed by the parallel reactions* $Np^{3+} + UO_2^+ + 4H^+ \rightarrow Np^{4+} + U^{4+} + 2H_2O$ *and* $2UO_2^+ + 4H^+ \rightarrow UO_2^{2+} + U^{4+} + 2H_2O$. *The kinetics are determined by measuring the increase of the absorbance D of* Np^{4+} *with time at 723 nm for various acidities and temperatures. The run refers to 1 M perchloric acid and 0.6°C; curve A refers to absorbance D. From the rate laws deduced, the concentrations C (in* 10^{-4} M*) of the species involved have been calculated as functions of time: for* $[Np^{4+}]$, *curve B;* $[Np^{3+}]$, *curve C;* $[UO_2^+]$, *curve D; and* $[U^{4+}]$, *curve E.*

activation parameters listed in Table 21.21 thus all refer to analogous activated complexes $\{M \cdot MO_2^{5+}\}^*$.

Perhaps surprisingly, the very high rates of the two fastest reactions are mainly due to different causes. For $U^{3+} + UO_2^{2+}$, the activation entropy is especially favorable; for $Np^{3+} + NpO_2^{2+}$, the activation enthalpy is favorable. The values of ΔH^* are in fact not very different for $U^{3+} + UO_2^{2+}$ and $Pu^{3+} + PuO_2^{2+}$, but the values of ΔS^* are indeed different. The faster rates of the mixed systems $Np^{3+} + UO_2^{2+}$ and $Pu^{3+} + NpO_2^{2+}$ compared to $Pu^{3+} + PuO_2^{2+}$ are on the whole due to more favorable values of ΔH^*.

As examples of reactions where M–O bonds are broken, processes

$$M^{4+}(1) + MO_2^{2+}(2) + 2H_2O \rightarrow MO_2^{+}(1) + MO_2^{+}(2) + 4H^+$$

will be considered (Table 21.22). Analogous to the oxidations of M^{3+} (Table 21.21), the rates are always first order in each of the actinide reactants. As might be expected, however, the rates of the M^{4+} oxidations also depend upon the acidity, though the rate law is by no means the same for all the processes, in spite of the analogy with the total process. The order of hydrogen dependence varies between -1 and -3. For three of the reactions, a non-integral exponent is found, indicating alternative paths with different orders of acidity dependence (Table 21.22). The apparent second-order rate constants k referring to 1 M acid are, as expected, generally much smaller than the rate constants of the M^{3+} oxidations (Table 21.21). The slowest of these reactions run at about the same rate as the fastest of the M^{4+} oxidations, and the latter are often much slower. Not unexpectedly, the reaction rate in 1 M acid is slower, the larger the negative exponent of the acidity dependence. With decreasing acidity, the actual rates thus become less different than in 1 M acid. The strong tendency for hydrolysis of M^{4+} sets a lower limit on the acidity of the solutions to be investigated, viz. 0.2 M for U^{4+} and Pu^{4+} and 0.04 M for Np^{4+}.

Inverse cubic acidity dependence is displayed by the reactions $U^{4+} + UO_2^{2+}$ and $Pu^{4+} + PuO_2^{2+}$. Moreover, these have the same slow rates, and practically the same activation parameters. Evidently they proceed along analogous paths. As a contrast, $U^{4+} + NpO_2^{2+}$ and $U^{4+} + PuO_2^{2+}$, with an inverse linear acidity dependence, are the fastest of the reactions concerned. Also, for these latter reactions, the activation parameters are very similar. The very large increase in rate depends solely on much more favorable values of ΔH^*. The values of ΔS^* are much less favorable than for the inverse cubic systems; about half of the gain due to the change of ΔH^* is in fact lost by the change of ΔS^*. The two inverse square systems $Np^{4+} + NpO_2^{2+}$ and $Np^{4+} + PuO_2^{2+}$ are, as expected, in an intermediate position with respect to both the reaction rates and the activation enthalpies and entropies.

Generally, the slow rates of the M^{4+} oxidation depend upon very unfavorable values of ΔH^*. Positive values of ΔS^* favor the process but not enough to compensate for the influence of ΔH^*. In both respects, the M^{4+} oxidations differ strikingly from the M^{3+} oxidations (Table 21.21).

These trends become even more marked in the thermodynamic equilibrium parameters of the two types of reaction (Tables 21.21 and 21.22). The values of ΔS° are much the same for all M^{4+} oxidations, just as they are for all M^{3+} oxidations. But while the values of ΔS° are very negative in the latter reactions, on account of the formation of strongly solvated M^{4+} ions, they are very positive in the former ones, on account of the disappearance of M^{4+} ions. These very favorable changes of ΔS° are strongly counteracted, however, by unfavorable changes of ΔH°. The M^{3+} oxidations are all exothermic, the M^{4+} oxidations all endothermic. On balance, these conditions create a mixture of large and small, negative and positive, values of ΔG° in both types of reactions. This of course illustrates the intricate oxidation–reduction pattern of the actinide elements, also reflected in their oxidation potentials (Chapter 17).

The disproportionation of actinyl(v) ions MO_2^+ is the reverse of the oxidation–reduction reactions $M^{4+} + MO_2^{2+}$. In Table 21.23, the rates and activation parameters of the disproportionation of UO_2^+, NpO_2^+, and PuO_2^+ have been listed. The rates again vary within very wide limits, with UO_2^+ reacting quite rapidly and NpO_2^+ extremely slowly. The fast rate of UO_2^+ is mainly due to a low value of ΔH^*, the slow rate of NpO_2^+ mainly to a very negative value of ΔS^*.

For both the oxidation–reduction and disproportionation reactions, ΔS^* becomes more favorable, the lower the charge of the activated complex. For the formation of MO_2^+ ions, the values of ΔS^* are more positive, the more negative the exponent of the hydrogen dependence (Table 21.22). For the disproportionations, the values of ΔS^* are more negative, the more positive the exponent of the hydrogen dependence (Table 21.23).

All the ions MO_2^+ listed disproportionate at a somewhat faster rate in heavy water. The rate increase is not very spectacular, however [215, 216]. The reaction rates of MO_2^+ ions are often influenced by complex formation with cations produced in the reaction. The first complex of this type observed was $NpO_2^+ \cdot Cr^{3+}$ [217]. Later, the analogous $UO_2^+ \cdot Cr^{3+}$, $PuO_2^+ \cdot Cr^{3+}$ [218], and $NpO_2^+ \cdot Rh^{3+}$ [219] were found. Though the stability constants of these

Table 21.23 *Disproportionation of actinyl(v) ions according to* $2MO_2^+ + 4H^+ \rightarrow M^{4+} + MO_2^{2+} + 2H_2O$. *Rate constants*[a] *and activation parameters from the same references as quoted for the reverse reactions (Table* 21.22). *Perchlorate media of the ionic strength I stated;* 25°C.

	I	n	k	ΔG^* (kJ mol^{-1})	ΔH^* (kJ mol^{-1})	ΔS^* (J K^{-1} mol^{-1})
UO_2^+	2	1	4×10^2	60	46	−46
NpO_2^+	2	2	9×10^{-9}	119	72	−159
PuO_2^+	1	1	3.6×10^{-3}	87	79	−24

[a] Rate constants k are apparent second-order constants ($M^{-1}\,s^{-1}$) referring to 1 M acid. The acidity dependence n is also given in the table.

complexes are small (< 10 M^{-1}), the oxidations of MO_2^+ by several agents are markedly slowed down by their formation.

Related complexes are also formed between MO_2^+ and MO_2^{2+} ions, viz. $UO_2^+ \cdot UO_2^{2+}$, $NpO_2^+ \cdot UO_2^{2+}$, $AmO_2^+ \cdot UO_2^{2+}$, and $NpO_2^+ \cdot NpO_2^{2+}$ [211, 212, 236, 237]. The stabilities of the complexes containing UO_2^{2+} decrease in the sequence $UO_2^+ > NpO_2^+ > AmO_2^+$, with a value of $\beta = 16$ M^{-1} for the most stable, $UO_2^+ \cdot UO_2^{2+}$. The complexes $NpO_2^+ \cdot UO_2^{2+}$ and $NpO_2^+ \cdot NpO_2^{2+}$ have much the same stability [237]. The structures of these complexes are still unknown. Though recent Raman and x-ray studies of the complex $NpO_2^+ \cdot UO_2^{2+}$ certainly confirm its existence, they fail to give an unambiguous picture of its structure [257, 258]. As the complex $UO_2^+ \cdot UO_2^{2+}$ disproportionates at a much slower rate than UO_2^+, uranium(v) solutions are greatly stabilized in the presence of UO_2^{2+}.

Also, in reactions other than those involving only actinide ions, resulting in the rupture or formation of actinide–oxygen bonds, large differences in hydrogen dependence and rate of reaction are found between formally analogous processes. The reactions:

$$M^{4+} + Fe^{3+} + 2H_2O \rightarrow MO_2^+ + Fe^{2+} + 4H^+$$

where M = U or Np are both first order in M^{4+} and Fe^{3+}, but the exponent of $[H^+]$ is -1.81 for U and -3.0 for Np. As the reaction paths are obviously different, the rates are of course also likely to be different. The apparent second-order constants k in 1 M acid are 12.8 and 0.057 M^{-1} s^{-1}, respectively [209].

All reactions so far discussed take place between hydrated metal ions in virtually non-complexing perchlorate media. In the presence of complex-forming anions, the reaction rates generally increase considerably. This was noticed quite early for both chloride and sulfate solutions. Thus plutonium(IV) disproportionates about five times faster in hydrochloric acid than in perchloric acid of the same concentration [220]. A careful study of sulfate media containing Np(IV), Np(V), and Np(VI) revealed that the formation of neptunium(V) depends upon the concentration of the complexes $NpSO_4^{2+}$ and NpO_2SO_4, while disproportionation depends upon the concentration of HSO_4^- [221]. For both reactions, the rate laws are quite complicated. With increasing sulfate concentration, the rate of formation first increases to a maximum and then decreases again. The maximum coincides with the maximum concentration of $NpSO_4^{2+}$; the higher sulfate complexes do not have any catalytic effect. The rate of disproportionation, on the other hand, is a monotonic increasing function of the concentration of HSO_4^-. Also for the disproportionation of americium(V), analogous catalytic effects have been observed [222]. In perchloric acid, the reaction:

$$3AmO_2^+ + 4H^+ \rightarrow 2AmO_2^{2+} + Am^{3+} + 2H_2O$$

takes place, with an exponent for the hydrogen-ion dependence between 2 and 3. At 75.7°C and an acidity of 2 M, the rates in nitric, hydrochloric, and sulfuric acids are 4, 4.6, and 24 times as great as that in perchloric acid. Similar effects have also

been found for several other systems. It is in fact to be expected that the formation of complexes will always exert a more or less marked influence on the rates of oxidation–reduction reactions.

Extensive treatments of oxidation–reduction kinetics of the aqueous ions of uranium through americium are found in Chapters 5–8, in the critical monograph of Newton [264], and in a recent review [273].

REFERENCES

1. Hulet, E. K., Lougheed, R. W., Brady, J. D., Stone, R. E., and Coops, M. S. (1967) *Science*, **158**, 486–7.
2. Maly, J. and Cunningham, B. B. (1967) *Inorg. Nucl. Chem. Lett.*, **3**, 445–51.
3. Maly, J., Sikkeland, T., Silva, R., and Ghiorso, A. (1968) *Science*, **160**, 1114–15.
4. Silva, R. J., Sikkeland, T., Nurmia, M., Ghiorso, A., and Hulet, E. K. (1969) *J. Inorg. Nucl. Chem.*, **31**, 3405–9.
5. Nugent, L. J., Baybarz, R. D., Burnett, J. L., and Ryan, J. L. (1973) *J. Phys. Chem.*, **77**, 1528–39.
6. Friedman, H. A. and Stokeley, J. R. (1976) *Inorg. Nucl. Chem. Lett.*, **12**, 505–13.
7. Sullivan, J. C., Gordon, S., Mulac, W. A., Schmidt, K. H., Cohen, D., and Sjoblom, R. (1976) *Inorg. Nucl. Chem. Lett.*, **12**, 599–601.
8. Laitinen, H. A. (1942) *J. Am. Chem. Soc.*, **64**, 1133–35.
9. Rard, J. A. (1985) *Chem. Rev.*, **85**, 555–82.
10. Propst, R. C. and Hyder, L. (1970) *J. Inorg. Nucl. Chem.*, **32**, 2205–16.
11. Nugent, L. J., Baybarz, R. D., Burnett, J. L., and Ryan, J. L. (1971) *J. Inorg. Nucl. Chem.*, **33**, 2503–30. See also Ch. 17.
12. Asprey, L. B. and Penneman, R. A. (1961) *Inorg. Chem.*, **1**, 134–6.
13. Haissinsky, M. and Pluchet, E. (1962) *J. Chim. Phys.*, **59**, 608–10.
14. Guillaumont, R., Bouissières, G., and Muxart, R. (1968) *Actinides Rev.*, **1**, 135–63.
15. Nelson, F. and Kraus, K. A. (1951) *J. Am. Chem. Soc.*, **73**, 2157–61.
16. Rabideau, S. W. and Kline, R. J. (1958) *J. Phys. Chem.*, **62**, 617–20.
17. Cohen, D. (1961) *J. Inorg. Nucl. Chem.*, **18**, 207–10, 211–18.
18. Keenan, T. K. and Kruse, F. H. (1964) *Inorg. Chem.*, **3**, 1231–2.
19. Asprey, L. B. and Penneman, R. A. (1967) *Chem. Eng. News*, **45**, 75–91.
20. Spitsyn, V. I., Gelman, A. D., Krot, N. N., Mefodiyeva, M. P., Zacharova, F. A., Komkov, Ya. A., Shilov, V. P., and Smirnova, I. V. (1968) *J. Inorg. Nucl. Chem.*, **31**, 2733–45.
21. Sullivan, J. C. and Zielen, A. J. (1969) *Inorg. Nucl. Chem. Lett.*, **5**, 927–31.
22. Zielen, A. J. and Cohen, D. (1970) *J. Phys. Chem.*, **74**, 394–405.
23. McDowell, W. J., Keller, O. L. Jr, Dittner, P. E., Tarrant, J. R., and Case, G. N. (1976) *J. Inorg. Nucl. Chem.*, **38**, 1207–10.
24. Kraus, K. A. and Dam, J. R. (1949) in *The Transuranium Elements* (eds G. T. Seaborg, J. J. Katz, and W. M. Manning), Natl Nucl. En. Ser., Div. IV, 14B, McGraw-Hill, New York, pp. 466–77.
25. Baes, C. F. and Mesmer, R. E. (1976) *The Hydrolysis of Cations*, Wiley, New York.
26. Désiré, B., Hussonnois, M., and Guillaumont, R. (1969) *C. R. Acad. Sci. Paris*, **269C**, 448–51.

27. Hussonnois, H., Hubert, S., Aubin, L., Guillaumont, R., and Bouissières, G. (1972) *Radiochem. Radioanal. Lett.*, **10**, 231–8.
28. Hussonnois, H., Hubert, S., Brillard, L., and Guillaumont, R. (1973) *Radiochem. Radional. Lett.*, **15**, 47–56.
29. Guillaumont, R., Désiré, B., and Galin, M. (1971) *Radiochem. Radioanal. Lett.*, **8**, 189–98.
30. Hietanen, S. (1954) *Acta Chem. Scand.*, **8**, 1626–42.
31. Kraus, K. A. and Holmberg, R. W. (1954) *J. Phys. Chem.*, **58**, 325–30.
32. Baes, C. F. Jr, Meyer, N. J., and Roberts, C. E. (1965) *Inorg. Chem.*, **4**, 518–27.
33. Hietanen, S. and Sillén, L. G. (1968) *Acta Chem. Scand.*, **22**, 265–80.
34. Hentz, F. C. Jr and Tyree, S. Y. Jr (1965) *Inorg. Chem.*, **4**, 873–7.
35. Hentz, F. C. and Johnson, J. S. (1966) *Inorg. Chem.*, **5**, 1337–44.
36. Johansson, G. (1968) *Acta Chem. Scand.*, **22**, 389–98, 399–409.
37. Guillaumont, R. (1968) *Bull. Soc. Chim. Fr.*, 162–8.
38. Lundqvist, R. (1974) in *Proc. Int. Solvent Extraction Conf.*, Lyon, vol. 1, pp. 469–76.
39. Kraus, K. A. and Nelson, F. (1950) *J. Am. Chem. Soc.*, **72**, 3901–6.
40. Kraus, K. A. and Nelson, F. (1955) *J. Am. Chem. Soc.*, **77**, 3721–2.
41. Sullivan, J. C. and Hindman, J. C. (1959) *J. Phys. Chem.*, **63**, 1332–3.
42. Hietanen, S. (1956) *Acta Chem. Scand.*, **10**, 1531–46.
43. Pocev, S. and Johansson, G. (1973) *Acta Chem. Scand.*, **27**, 2146–60.
44. Lundgren, G. (1953) *Ark. Kemi*, **5**, 349–63.
45. Rabideau, S. W. and Lemons, J. F. (1951) *J. Am. Chem. Soc.*, **73**, 2895–9.
46. Rabideau, S. W. and Kline, R. J. (1959) *J. Phys. Chem.*, **64**, 680–2.
47. Kraus, K. A., Nelson, F., and Johnson, L. J. (1949) *J. Am. Chem. Soc.*, **71**, 2510–17.
48. Guillaumont, R. (1968) *Bull. Soc. Chim. Fr.*, 168–70.
49. Guillaumont, R. and Bouissières, G. (1964) *Bull. Soc. Chim. Fr.*, 2098–103.
50. Dunsmore, H. S. and Sillén, L. G. (1963) *Acta Chem. Scand.*, **17**, 2657–63.
51. Rush, R. M. and Johnson, J. S. (1963) *J. Phys. Chem.*, **67**, 821–5.
52. Dunsmore, H. S., Hietanen, S., and Sillén, L. G. (1963) *Acta Chem. Scand.*, **17**, 2644–56.
53. Maeda, M. and Kakihana, H. (1970) *Bull. Chem. Soc. Jap.*, **43**, 1097–100.
54. Rush, R. M., Johnson, J. S., and Kraus, K. A. (1962) *Inorg. Chem.*, **1**, 378–86.
55. Baes, C. F. Jr and Meyer, N. J. (1962) *Inorg. Chem.*, **1**, 780–9.
56. Schedin, U. and Frydman, M. (1968) *Acta Chem. Scand.*, **22**, 115–27.
57. Cassol, A., Magon, L., Tomat, G., and Portanova, R. (1972) *Inorg. Chem.*, **11**, 515–19.
58. Kraus, K. A. and Dam, J. R. (1949) in *The Transuranium Elements* (eds G. T. Seaborg, J. J. Katz, and W. M. Manning), Natl Nucl. En. Ser., Div. IV, 14B, McGraw-Hill, New York, pp. 528–49.
59. Cassol, A., Magon, L., Portanova, R., and Tondello, E. (1972) *Radiochim. Acta*, **17**, 28–32.
60. Schedin, U. (1975) *Acta Chem. Scand. A*, **29**, 333–44.
61. Åberg, M. (1970) *Acta Chem. Scand.*, **24**, 2901–15.
62. Åberg, M. (1969) *Acta Chem. Scand.*, **23**, 791–810.
63. Perrin, A. (1976) *Acta Crystallogr. B*, **22**, 1658–61.
64. Bergström, G. and Lundgren, G. (1956) *Acta Chem. Scand.*, **10**, 673–80.
65. Åberg, M. (1978) *Acta Chem. Scand. A*, **32**, 101–7.
66. Arnek, R. and Schlyter, K. (1968) *Acta Chem. Scand.*, **22**, 1331–3.
67. Betts, R. H. (1955) *Can. J. Chem.*, **33**, 1775–79.

68. Ahrland, S. (1972) *Coord. Chem. Rev.*, **8**, 21–9.
69. Ahrland, S., Chatt, J., and Davies, N. R. (1958) *Q. Rev. Chem. Soc.*, **12**, 265–76.
70. Pearson, R. G. (1968) *J. Chem. Educ.*, **45**, 581–7, 643–8.
71. Pearson, R. G. (ed.) (1973) *Hard and Soft Acids and Bases*, Dowden, Hutchinson and Ross, Stroudsburg, Penn.
72. Ahrland, S. (1967) *Helv. Chim. Acta*, **50**, 306–18; (1968) *Struct. Bonding (Berlin)*, **5**, 118–49.
73. Klopman, G. (1968) *J. Am. Chem. Soc.*, **90**, 223–34.
74. Schwarzenbach, G. (1970) *Pure Appl. Chem.*, **24**, 307–34.
75. Farrer, H. N. and Rossotti, F. J. C. (1964) *J. Inorg. Nucl. Chem.*, **26**, 1959–65.
76. Ahrland, S. and Brandt, L. (1968) *Acta Chem. Scand.*, **22**, 106–14, 1579–89.
77. Sillén, L. G. and Martell, A. E. (1964, 1971) *Stability Constants of Metal-Ion Complexes* and *Supplement No.* 1, Spec. Publ. Nos 17 and 25, The Chemical Society, London.
78. Jones, A. D. and Choppin, G. R. (1969) *Actinides Rev.*, **1**, 311–36.
79. Aziz, A. and Lyle, S. J. (1969) *J. Inorg. Nucl. Chem.*, **31**, 3471–80.
80. Dodgen, H. W. and Rollefsen, G. K. (1949) *J. Am. Chem. Soc.*, **71**, 2600–7.
81. Norén, B., personal communication; see also Norén, B. (1969) *Acta Chem. Scand.*, **23**, 931–42.
82. Ahrland, S. and Kullberg, L. (1971) *Acta Chem. Scand.*, **25**, 3457–70, 3471–83.
83. Krylov, V. N., Komarov, E. V., and Pushlenkov, M. F. (1968) *Radiokhimiya*, **10**, 719–22.
84. Ward, M. and Welch, G. A. (1956) *J. Inorg. Nucl. Chem.*, **2**, 395–402.
85. Khopkar, P. K. and Narayanankutty, P. (1971) *J. Inorg. Nucl. Chem.*, **33**, 495–502.
86. Savage, A. W. and Browne, J. C. (1960) *J. Am. Chem. Soc.*, **82**, 4817–21.
87. Baumann, E. W. (1970) *J. Inorg. Nucl. Chem.*, **32**, 3823–30.
88. McKay, H. A. C. and Woodhead, J. L. (1964) *J. Chem. Soc.*, 717–23.
89. Zielen, A. J. (1959) *J. Am. Chem. Soc.*, **81**, 5022–8.
90. Day, R. A. Jr, Wilhite, R. W., and Hamilton, F. D. (1955) *J. Am. Chem. Soc.*, **77**, 3180–2.
91. Sullivan, J. C. and Hindman, J. C. (1954) *J. Am. Chem. Soc.*, **76**, 5931–4.
92. Fardy, J. J. and Pearson, J. M. (1974) *J. Inorg. Nucl. Chem.*, **36**, 671–7.
93. Zebroski, E. L., Alter, H. W., and Heumann, F. K. (1951) *J. Am. Chem. Soc.*, **73**, 5646–70.
94. Ahrland, S. and Kullberg, L. (1971) *Acta Chem. Scand.*, **25**, 3677–91.
95. Scanlan, J. P. (1977) *J. Inorg. Nucl. Chem.*, **39**, 635–9.
96. Cinnéide, S. O., Scanlan, J. P., and Hynes, M. J. (1975) *J. Inorg. Nucl. Chem.*, **37**, 1013–18.
97. Babko, A. K. and Kodenskaya, V. S. (1960) *Russ. J. Inorg. Chem.*, **5**, 1241–4.
98. Evans, H. T. Jr (1963) *Science*, **141**, 154–8.
99. Dyrssen, D. (1969) in *Chemical Oceanography* (ed. R. Lange), Universitetsforlaget, Oslo, ch. 3.
100. Spence, R. (1968) *Talanta*, **15**, 1307–9.
101. Astheimer, L., Schenk, H. J., and Schwochau, K. (1977) *Chem. Z.*, **101**, 544–6; Schwochau, K., Astheimer, L., Schenk, H. J., and Schmitz, J. (1977) Berichte der Kernforschungsanlage Jülich 1415.
102. Schreyer, J. M. and Baes, C. F. Jr (1954) *J. Am. Chem. Soc.*, **76**, 354–7; Schreyer, J. M. (1955) *J. Am. Chem. Soc.*, **77**, 2972–4.

103. Marcus, Y., Kertes, A. S., and Yanir, E. (1974) *Equilibrium Constants of Liquid–Liquid Distribution Reactions*, Introduction and Part I, *Organophosphorus Extractants*, Butterworths, London; Marcus, Y. (1974) *Critical Evaluation of Some Equilibrium Constants Involving Organophosphorus Reagents*, Butterworths, London (IUPAC additional publ. to *Pure Appl. Chem.*).
104. Pekárek, V. and Benešová, M. (1964) *J. Inorg. Nucl. Chem.*, **26**, 1743–51.
105. Vesely, V. and Pekárek, V. (1965) *J. Inorg. Nucl. Chem.*, **27**, 1419–25.
106. Magon, L., Cassol, A., and Portanova, R. (1968) *Inorg. Chim. Acta*, **2**, 285–8.
107. Grenthe, I. (1962, 1963) *Acta Chem. Scand.*, **16**, 1695–712; **17**, 1814–15.
108. Choppin, G. R. and Schneider, J. K. (1970) *J. Inorg. Nucl. Chem.*, **32**, 3283–8.
109. Portanova, R., Tomat, G., Cassol, A., and Magon, L. (1972) *J. Inorg. Nucl. Chem.*, **34**, 1685–90.
110. Cassol, A., Magon, L., Tomat, G., and Portanova, R. (1969) *Inorg. Chim. Acta*, **3**, 639–43.
111. Portanova, R., Tomat, G., Magon, L., and Cassol, A. (1970, 1972) *J. Inorg. Nucl. Chem.*, **32**, 2343–8; **34**, 1768–70.
112. Eberle, S. H., Schaefer, J. B., and Brandau, E. (1968) *Radiochim. Acta*, **10**, 91–7.
113. Miyake, C. and Nürnberg, H. W. (1967) *J. Inorg. Nucl. Chem.*, **29**, 2411–29.
114. Magon, L., Bismondo, A., Maresca, L., Tomat, G., and Portanova, R. (1973) *J. Inorg. Nucl. Chem.*, **35**, 4237–43.
115. Ahrland, S. (1953) *Acta Chem. Scand.*, **7**, 485–94.
116. Portanova, R., Cassol, A., Magon, L., and Tomat, G. (1970) *J. Inorg. Nucl. Chem.*, **32**, 221–8.
117. Eberle, S. H. and Schaefer, J. B. (1968) *Inorg. Nucl. Chem. Lett.*, **4**, 283–7.
118. Di Bernardo, P., Roncari, E., Mazzi, U., and Cassol, A. (1978) *Thermochim. Acta*, **23**, 293–302.
119. Aziz, A., Lyle, S. J., and Naqvi, S. J. (1968) *J. Inorg. Nucl. Chem.*, **30**, 1013–18.
120. Sekine, T. (1964) *J. Inorg. Nucl. Chem.*, **26**, 1463–5.
121. Moskvin, A. I. and Essen, L. N. (1967) *Russ. J. Inorg. Chem.*, **12**, 359–62.
122. Bansal, B. M. L. and Sharma, H. D. (1964) *J. Inorg. Nucl. Chem.*, **26**, 799–805.
123. Magon, L., Bismondo, A., Tomat, G., and Cassol, A. (1972) *Radiochim. Acta*, **17**, 164–7.
124. Zachariasen, W. H. and Plettinger, H. A. (1959) *Acta Crystallogr.*, **12**, 526–30.
125. Magon, L., Portanova, R., Zarli, B., and Bismondo, A. (1972) *J. Inorg. Nucl. Chem.*, **34**, 1971–6.
126. Grenthe, I. (1969) *Acta Chem. Scand.*, **23**, 1752–62.
127. Albertsson, J. (1970) *Acta Chem. Scand.*, **24**, 3527–41.
128. Rajan, K. S. and Martell, A. E. (1964, 1965) *J. Inorg. Nucl. Chem.*, **26**, 1927–44; **29**, 523–9; (1967) *Inorg. Chem.*, **4**, 462–9.
129. Tomat, G., Magon, L., Portanova, R., and Cassol, A. (1972) *Z. Anorg. Allg. Chem.*, **393**, 184–92.
130. Alcock, N. W. (1973) *J. Chem. Soc. Dalton Trans.*, 1610–20.
131. Portanova, R., Di Bernardo, P., Traverso, O., Mazzochin, G. A., and Magon, L. (1974) *J. Inorg. Nucl. Chem.*, **37**, 2177–9.
132. Di Bernardo, P., Bismondo, A., Portanova, R., Traverso, O., and Magon, L. (1976) *Inorg. Chim. Acta*, **18**, 47–50.
133. Starý, J. (1964) *The Extraction of Metal Chelates*, Pergamon, Oxford.
134. Starý, J. and Freiser, H. (1978) *Equilibrium Constants of Liquid–Liquid Distribution*

Reactions, Part 4, *Chelating Extractants*, Pergamon, Oxford (IUPAC Chemical Data Series No. 18).
135. Rydberg, J. (1960) *Acta Chem. Scand.*, **14**, 157–79.
136. Liljenzin, J. O. and Starý, J. (1970) *J. Inorg. Nucl. Chem.*, **32**, 1357–63.
137. Liljenzin, J. O. (1970) *Acta Chem. Scand.*, **24**, 1655–61.
138. Sekine, T. and Ihara, N. (1971) *Bull. Chem. Soc. Jap.*, **44**, 2942–50.
139. Rydberg, J. (1955) *Ark. Kemi*, **8**, 113–40.
140. Sekine, T. and Dyrssen, D. (1967) *J. Inorg. Nucl. Chem.*, **29**, 1457–73.
141. Fuger, J. and Cunningham, B. B. (1965) *J. Inorg. Nucl. Chem.*, **27**, 1079–84.
142. Fuger, J. (1958, 1961) *J. Inorg. Nucl. Chem.*, **5**, 332–8; **18**, 263–9.
143. Bottari, E. and Anderegg, G. (1967) *Helv. Chim. Acta*, **50**, 2349–56.
144. Krot, N. N., Ermolaev, N. P., and Gelman, A. D. (1962) *Russ. J. Inorg. Chem.*, **7**, 1062–6.
145. Eberle, S. H. and Paul, M. T. (1971) *J. Inorg. Nucl. Chem.*, **33**, 3067–75.
146. Cauchetier, P. and Guichard, C. (1973) *Radiochim. Acta*, **19**, 137–46.
147. Foreman, J. K. and Smith, T. D. (1957) *J. Chem. Soc.*, 1752–62.
148. Fronaeus, S. and Larsson, R. (1962) *Acta Chem. Scand.*, **16**, 1447–54.
149. Burmeister, J. L., Patterson, S. D., and Deardorff, E. A. (1969) *Inorg. Chim. Acta*, **3**, 105–9.
150. Vasudeva Rao, P. R., Bagawde, S. V., Ramakrishna, V. V., and Patil, S. K. (1978) *J. Inorg. Nucl. Chem.*, **40**, 339–43.
151. Ahrland, S. (1966) *Struct. Bonding (Berlin)*, **1**, 207–20.
152. Ahrland, S. (1973) *Struct. Bonding (Berlin)*, **15**, 167–88.
153. Cassol, A., Di Bernardo, P., Portanova, R., and Magon, L. (1973) *Inorg. Chim. Acta*, **7**, 353–8.
154. Bombieri, G., Forsellini, E., Graziani, R., Tomat, G., and Magon, L. (1972) *Inorg. Nucl. Chem. Lett.*, **8**, 1003–7.
155. Duyckaerts, G. and zur Nedden, P. (1975) in *Gmelin Handbook of Inorganic Chemistry*, 8th edn, Suppl. Ser., *Transuranium*, Springer-Verlag, Berlin, part D2, pp. 249–311.
156. Ščavničar, S. and Prodic, B. (1964) *Acta Crystallogr.*, **18**, 698–702.
157. Barclay, G. A., Sabine, T. M., and Taylor, J. C. (1965) *Acta Crystallogr.*, **19**, 205–9.
158. Peligot, E. (1842) *Ann. Chim. Phys.*, **3**(5), 5.
159. Howells, G. R., Hughes, T. G., Mackey, D. R., and Saddington, K. (1958) *Proc. 2nd UN Int. Conf. on Peaceful Uses of Atomic Energy*, Geneva, pp. 3–24 (P/307).
160. Lawroski, S. and Levinson, M. (1958) *Prog. Nucl. Energy*, **3**(2), 258–78.
161. Cooper, V. R. and Walling, M. T. Jr (1958) *Proc. 2nd U N Int. Conf. on Peaceful Uses of Atomic Energy*, Geneva, pp. 291–323 (P/2409).
162. Awwal, M. A. and Carswell, D. J. (1966) *Chem. Rev.*, **66**, 279–95.
163. Kertes, A. S., Marcus, Y., and Yanir, E. (1974) *Equilibrium Constants of Liquid–Liquid Distribution Reactions*, Part 2, *Alkylammonium Salt Extractants*, Butterworths, London (IUPAC additional publ. to *Pure Appl. Chem.*).
164. Müller, W. (1967) *Actinides Rev.*, **1**, 71–119.
165. Eberle, S. H. and Ali, S. A. (1969) *Radiochim. Acta*, **11**, 149–53.
166. Andersson, S. O., Ashbrook, A., Flett, D. S., Ritcey, G. M., and Spink, D. R. (1971) *Solvent Extraction in Process Metallurgy*, University of Waterloo Press, Waterloo, Ont.
167. Leuze, R. E. and Lloyd, M. H. (1970) *Prog. Nucl. Energy*, **3**(4), 549–630.

168. Keller, C. and Mosdzelewski, K. (1967) *Radiochim. Acta*, **7**, 185–8.
169. Starý, J., Zolotov, Yu. A., and Petrukhin, O. M. (1979) *Critical Evaluation of Equilibrium Constants Involving 8-Hydroxyquinoline and Its Metal Complexes*, Pergamon, Oxford (IUPAC Chemical Data Series No. 24).
170. Dyrssen, D. (1957) *Acta Chem. Scand.*, **11**, 1771–86.
171. Brown, K. B. and Coleman, C. F. (1958) *Prog. Nucl. Energy*, **3**(2), 3–34.
172. Koch, G. (1974) in *Gmelin Handbook of Inorganic Chemistry*, 8th edn, Suppl. Ser., *Transuranium*, Springer-Verlag, Berlin, part A1, II, pp. 288–315.
173. Weaver, B. and Kappelmann, F. A. (1968) *J. Inorg. Nucl. Chem.*, **30**, 263–72.
174. Alcock, K., Best, G. F., Hesford, E., and McKay, H. A. C. (1958) *J. Inorg. Nucl. Chem.*, **6**, 328–33.
175. Alcock, K., Grimley, S. S., Healy, T. V., Kennedy, J., and McKay, H. A. C. (1956) *Trans. Faraday. Soc.*, **52**, 39–47.
176. McKay, H. A. C., Scargill, D., and Wain, A. G. (1975) in *Gmelin Handbook of Inorganic Chemistry*, 8th edn, Suppl. Ser., *Transuranium*, Springer-Verlag, Berlin, part D2, pp. 177–220.
177. Kolarik, Z. (1975) in *Gmelin Handbook of Inorganic Chemistry*, 8th edn, Suppl. Ser., *Transuranium*, Springer-Verlag, Berlin, part D2, pp. 220–34.
178. Bullock, J. I. and Tuck, D. G. (1971) *J. Inorg. Nucl. Chem.*, **33**, 3891–904.
179. Zakharkin, V. S., Zemlyanukin, V. I., and Shevchenko, V. B. (1970) *Radiokhimiya*, **12**, 577–84.
180. Keder, W. E., Sheppard, J. C., and Wilson, A. S. (1960) *J. Inorg. Nucl. Chem.*, **12**, 327–35.
181. Ryan, J. L. (1975) in *Gmelin Handbook of Inorganic Chemistry*, 8th edn, Suppl. Ser., *Transuranium*, Springer-Verlag, Berlin, part D2, pp. 373–437.
182. Nelson, F., Murase, T., and Kraus, K. A. (1964) *J. Chromatogr.*, **13**, 503–35.
183. Surls, J. P. Jr and Choppin, G. R. (1957) *J. Am. Chem. Soc.*, **79**, 855–9.
184. Johnson, W. C., Quill, L. L., and Daniels, F. (1947) *Chem. Eng. News*, **25**, 2494.
185. Spedding, F. H., Fulmer, E. I., Butler, T. A., Gladrow, E. M., Gobusch, M., Porter, P. E., Powell, J. E., and Wright, J. M. (1947) *J. Am. Chem. Soc.*, **69**, 2812–18.
186. Street, K. Jr and Seaborg, G. T. (1950) *J. Am. Chem. Soc.*, **72**, 2790–2.
187. Diamond, R. M., Street, K. Jr, and Seaborg, G. T. (1954) *J. Am. Chem. Soc.*, **76**, 1461–9.
188. Thompson, S. G., Harvey, B. G., Choppin, G. R., and Seaborg, G. T. (1954) *J. Am. Chem. Soc.*, **76**, 6229–36.
189. Thompson, S. G., Cunningham, B. B., and Seaborg, G. T. (1950) *J. Am. Chem. Soc.*, **72**, 2798–801.
190. Street, K., Thompson, S. G., and Seaborg, G. T. (1950) *J. Am. Chem. Soc.*, **72**, 4832–5.
191. Glass, R. A. (1955) *J. Am. Chem. Soc.*, **77**, 807–9.
192. Choppin, G. R., Harvey, B. G., and Thompson, S. G. (1956) *J. Inorg. Nucl. Chem.*, **2**, 66–8.
193. Ghiorso, A., Harvey, B. G., Choppin, G. R., Thompson, S. G., and Seaborg, G. T. (1955) *Phys. Rev.*, **98**, 1518–19.
194. Nater, K. A. (1958) *Proc. 2nd UN Int. Conf. on Peaceful Uses of Atomic Energy*, Geneva, pp. 238–45 (P/1476).
195. Ahrland, S. and Carleson, G. (1971) *J. Inorg. Nucl. Chem.*, **33**, 2229–46.
196. Horwitz, E. P. (1966) *J. Inorg. Nucl. Chem.*, **28**, 1469–78.
197. Ahrland, S. and Albertsson, J. (1964) *Acta Chem. Scand.*, **18**, 1861–78.

198. Kraus, K. A. and Nelson, F. (1956) *Proc. 1st UN Int. Conf. on Peaceful Uses of Atomic Energy*, Geneva, pp. 113–25 (P/837).
199. Fronaeus, S. (1953) *Svensk Kem. Tidskr.*, **65**, 1–8.
200. Lundqvist, I. (1964) *Acta Chem. Scand.*, **18**, 858–70, 1125–37.
201. Coleman, J. S., Penneman, R. A., Keenan, T. K., LaMar, L. E., Armstrong, D. E., and Asprey, L. B. (1956) *J. Inorg. Nucl. Chem.*, **3**, 327–8.
202. Ryan, J. L. and Wheelwright, E. J. (1958) *Proc. 2nd UN Int. Conf. on Peaceful Uses of Atomic Energy*, Geneva, pp. 137–44 (P/1915).
203. Toth, L. M. and Friedman, H. A. (1978) *J. Inorg. Nucl. Chem.*, **40**, 807–10, and references therein.
204. Ockenden, D. W. and Welch, G. A. (1956) *J. Chem. Soc.*, 3358–63.
205. Costanzo, D. A., Biggers, R. E., and Bell, J. T. (1973) *J. Inorg. Nucl. Chem.*, **35**, 609–28.
206. Fulton, R. B. and Newton, T. W. (1970) *J. Phys. Chem.*, **74**, 1661–9.
207. Newton, T. W. and Fulton, R. B. (1970) *J. Phys. Chem.*, **74**, 2797–801.
208. Newton, T. W. (1970) *J. Phys. Chem.*, **74**, 1655–61.
209. Newton, T. W. and Baker, F. B. (1967) in *Lanthanide/Actinide Chemistry* (ACS Adv. Chem. Ser. 71), American Chemical Society, Washington DC, pp. 268–95.
210. Masters, B. J. and Schwartz, L. L. (1961) *J. Am. Chem. Soc.*, **83**, 2620–4.
211. Newton, T. W. and Baker, F. B. (1965) *Inorg. Chem.*, **4**, 1166–70.
212. Sullivan, J. C., Zielen, A. J., and Hindman, J. C. (1960) *J. Am. Chem. Soc.*, **82**, 5288–92.
213. Hindman, J. C., Sullivan, J. C., and Cohen, D. (1954) *J. Am. Chem. Soc.*, **76**, 3278–80.
214. Newton, T. W. and Montag, T. (1976) *Inorg. Chem.*, **15**, 2856–61.
215. Rabideau, S. W. (1957) *J. Am. Chem. Soc.*, **79**, 6350–3.
216. Hindman, J. C., Sullivan, J. C., and Cohen, D. (1959) *J. Am. Chem. Soc.*, **81**, 2316–19.
217. Sullivan, J. C. (1964) *Inorg. Chem.*, **3**, 315–19.
218. Newton, T. W. and Burkhart, M. J. (1971) *Inorg. Chem.*, **10**, 2323–6.
219. Murmann, R. K. and Sullivan, J. C. (1967) *Inorg. Chem.*, **6**, 892–900.
220. Rabideau, S. W. and Cowan, H. D. (1955) *J. Am. Chem. Soc.*, **77**, 6145–8.
221. Sullivan, J. C., Cohen, D., and Hindman, J. C. (1957) *J. Am. Chem. Soc.*, **79**, 4029–34.
222. Coleman, J. S. (1963) *Inorg. Chem.*, **2**, 53–7.
223. Mikheev, N. B., Spitsyn, V. I., Kamenskaya, A. N., Konovalova, N. A., Rumer, I. A., Auerman, L. N., and Podorozhnyi, A. M. (1977) *Inorg. Nucl. Chem. Lett.*, **13**, 651–6, and references therein.
224. Hulet, E. K., Lougheed, R. W., Baisden, P. A., Landrum, J. H., Wild, J. F., and Lundqvist, R. F. D. (1979) *J. Inorg. Nucl. Chem.*, **41**, 1743–7.
225. Alcock, N. W. and Esperås, S. (1977) *J. Chem. Soc. Dalton Trans.*, 893–6.
226. Fratiello, A., Kubo, V., Lee, R. E., Peak, S., and Schuster, R. E. (1970) *J. Inorg. Nucl. Chem.*, **32**, 3114–16.
227. Honan, G. J., Lincoln, S. F., and Williams, E. H. (1978) *J. Solution Chem.*, **7**, 443–51.
228. Zachariasen, W. H. (1954) *Acta Crystallogr.*, **7**, 783–7.
229. Fardy, J. J. and Buchanan, J. M. (1976) *J. Inorg. Nucl. Chem.*, **38**, 579–83.
230. Rao, P. R. V., Bagawde, S. V., Ramakrishna, V. V., and Patil, S. K. (1978) *J. Inorg. Nucl. Chem.*, **40**, 123–7.
231. Ciavatta, L., Ferri, D., Grimaldi, M., Palombari, R., and Salvatore, F. (1979) *J. Inorg. Nucl. Chem.*, **41**, 1175–82.
232. Ciavatta, L., Ferri, D., Grenthe, I., and Salvatore, F. (1981) *Inorg. Chem.*, **20**, 463–7; Ferri, D., Grenthe, I., and Salvatore, F. (1981) *Acta Chem. Scand. A*, **35**, 165–8.
233. Woods, M., Mitchell, M. I., and Sullivan, J. C. (1978) *Inorg. Nucl. Chem. Lett.*, **14**, 465–7.

234. Graziani, R., Bombieri, G., and Forsellini, E. (1972) *J. Chem. Soc. Dalton Trans.*, 2059–61.
235. Åberg, M., Ferri, D., Glaser, J., and Grenthe, I. (1983) *Inorg. Chem.*, **22**, 3981–5.
236. Rykov, A. G. and Frolov, A. A. (1975) *Radiokhimiya*, **17**, 187–9.
237. Madic, C., Guillaume, B., Morisseau, J. C., and Moulin, J. P. (1979) *J. Inorg. Nucl. Chem.*, **41**, 1027–31.
238. Nair, G. M., Chander, K., and Joshi, J. K. (1982) *Radiochim. Acta*, **30**, 37–40.
239. Hubert, S., Hussonnois, M., and Guillaumont, R. (1975) *J. Inorg. Nucl. Chem.*, **37**, 1255–8.
240. Milic, N. B. and Suranji, T. M. (1982) *Can. J. Chem.*, **60**, 1298–303.
241. Lajunen, L. H. and Parhi, S. (1979) *Finn. Chem. Lett.*, 143–4.
242. Milic, N. B. and Suranji, T. M. (1982) *Z. Anorg. Allg. Chem.*, **489**, 197–203.
243. Fuger, J. (1983) *Plutonium Chemistry* (ACS Symp. Ser. 216) (eds W. T. Carnall and G. R. Choppin), American Chemical Society, Washington DC, pp. 75–98.
244. Bagawde, S. V., Ramakrishna, V. V., and Patil, S. K. (1976) *J. Inorg. Nucl. Chem.*, **38**, 1339–45.
245. Harmon, H. D., Peterson, J. R., and McDowell, W. J. (1972) *Inorg. Nucl. Chem. Lett.*, **8**, 57–63.
246. Khopkar, P. K. and Mathur, J. N. (1980) *J. Inorg. Nucl. Chem.*, **42**, 109–13.
247. Grenthe, I., Ferri, D., Salvatore, F., and Riccio, G. (1984) *J. Chem. Soc. Dalton Trans.*, 2439–43.
248. Ferri, D., Grenthe, I., and Salvatore, F. (1983) *Inorg. Chem.*, **22**, 3162–5.
249. Ciavatta, L., Ferri, D., Grenthe, I., Salvatore, F., and Spahiu, K. (1983) *Inorg. Chem.*, **22**, 2088–92.
250. Perrin, D. D. (1979) *Stability Constants of Metal–Ion Complexes*, Part B, *Organic Ligands* (Supplement to ref. 77) Pergamon, Oxford (IUPAC Chemical Data Series No. 22).
251. Anderegg, G. (1977) *Critical Survey of Stability Constants of EDTA Complexes*, Pergamon, Oxford (IUPAC Chemical Data Series No. 14).
252. Raymond, K. N. and Smith, W. L. (1981) *Struct. Bonding*, **43**, 159–86.
253. Di Bernardo, P., Cassol, A., Tomat, G., Bismondo, A., and Magon, L. (1983) *J. Chem. Soc. Dalton Trans.*, 733–5.
254. Cali, R., Rizzarelli, E., Sommartano, S., and Pettit, L. E. (1980) *Thermochim. Acta*, **35**, 169–79.
255. Wells, A. F. (1975) *Structural Inorganic Chemistry*, 4th edn, Clarendon, Oxford.
256. Åberg, M., Ferri, D., Glaser, J., and Grenthe, I. (1983) *Inorg. Chem.*, **22**, 3986–9.
257. Guillaume, B., Begun, G. M., and Hahn, R. L. (1982) *Inorg. Chem.*, **21**, 1159–66.
258. Guillaume, B., Hahn, R. L., and Narten, A. H. (1983) *Inorg. Chem.*, **22**, 109–11.
259. Milić, N. B. (1981) *J. Chem. Soc. Dalton Trans.*, 1445–9.
260. Ahrland, S. (1984) in *Gmelin Handbook of Inorganic Chemistry*, 8th Edn, Suppl. Ser., *Uranium*, Springer-Verlag, Berlin, part D1, pp. 93–111.
261. Ahrland, S., Liljenzin, J. O., and Rydberg, J. (1973) in *Comprehensive Inorganic Chemistry*, vol. 5 (eds J. C. Bailar, H. J. Emeleus, R. Nyholm and A. F. Trotman-Dickenson), Pergamon Press, New York, pp. 465–635.
262. Aberg, M. (1976) *Acta Chem. Scand.*, **A30**, 507–14.
263. Lemire, R. J. and Tremaine, P. R. (1980) *J. Chem. Eng. Data*, **25**, 361–70.
264. Newton, T. W. (1975) *The kinetics of the Oxidation–Reduction Reactions of Uranium, Neptunium, Plutonium, and Americium in Aqueous Solutions*, U.S. ERDA TID-26506.

265. Choppin, G. R. (1985) in *Environmental Inorganic Chemistry*, (eds K. J. Irgolic and A. E. Martell), VCH Publishers, Deerfield Beach, Florida, pp. 307–20.
266. Rai, D., Strickert, R. G., Moore, D. A., and Ryan, J. L. (1983) *Radiochim. Acta*, **33**, 201–6.
267. Caceci, M. S. and Choppin, G. R. (1983) *Radiochim. Acta*, **33**, 101–4.
268. Nash, K. L. and Cleveland, J. M. (1984) *Radiochim. Acta*, **37**, 19–24.
269. Nash, K. L. and Cleveland, J. M. (1984) *Radiochim. Acta*, **36**, 129–34.
270. Madic, C., Hobart, D. E., and Begun, G. M. (1983) *Inorg. Chem.*, **22**, 1494–503.
271. Newton, T. W. and Sullivan, J. C. (1985) in *Handbook on the Physics and Chemistry of the Actinides*, vol. 3 (eds A. J. Freeman and C. Keller), Elsevier, Amsterdam, pp. 387–406.
272. Maya, L. (1984) *Inorg. Chem.*, **23**, 3926–30.
273. Nash, K. L. and Sullivan, J. C. (1986) in *Inorg. and Bioinorg. Reaction Mechanisms*, vol. 4 (ed. A. G. Sykes), Academic Press, London, pp. 185–215.
274. Wester, D. W. and Sullivan, J. C. (1983) *Radiochim. Radioanal. Lett.*, **57**, 35–42.
275. Nash, K. L. and Cleveland, J. M. (1983) *Radiochim. Acta*, **33**, 105–111.
276. Choppin, G. R. and Rao, L. F. (1984) *Radiochim. Acta*, **37**, 143–6.

CHAPTER TWENTY TWO

ORGANOACTINIDE CHEMISTRY: PROPERTIES OF COMPOUNDS HAVING METAL–CARBON BONDS ONLY TO π-BONDED LIGANDS

Tobin J. Marks and Andrew Streitwieser, Jr

22.1 INTRODUCTION

The period since 1955 has witnessed a dramatic development of chemistry involving bonds between transition metals and hydrocarbon ligands. This burgeoning of d-block organometallic chemistry [1, 2] reflects the importance of the field in teaching us fundamental new things about molecular structure and bonding as well as in providing stoichiometric and catalytic reactivity patterns of considerable practical significance. In contrast, the corresponding development of actinide organometallic chemistry is a more recent phenomenon, and the most intense activity has taken place in the past decade. The delayed development of organic 5f chemistry reflects several factors. Unsuccessful attempts to synthesize uranium alkyls in the 1940s led Gilman [3] to conclude that alkyluranium compounds (desired at the time for their anticipated volatility) were thermally unstable if they had any existence at all. In addition, of the 14 actinide elements from thorium to lawrencium, 11 are synthetic, the products of relatively recent

nuclear chemistry and physics. The first actinide cyclopentadienyl complexes were prepared by the groups of Wilkinson (uranium, 1956) [4] and Fischer (thorium, uranium, 1962) [5, 6]. Nevertheless, the beginning of modern organoactinide chemistry can best be correlated with the synthesis of bis([8]annulene)uranium(IV) ('uranocene') in 1968 [7] and the first isolable uranium alkyls in 1972 [8–10].

The purpose of this chapter is to summarize actinide organometallic chemistry involving compounds having metal–carbon linkages *only* to π-bonded ligands. The organization of the presentation is by formal electron-donor capacity of the neutral, *fully bonded* ligand. Organoactinide complexes of this type illustrate many of the unique characteristics of organo-5f compounds and serve as important synthetic precursors for more elaborate molecules with metal–carbon, metal–hydrogen, and metal–metal σ bonds. These latter species are the subject of Chapter 23. The treatment in this chapter is necessarily compact and the reader is referred to recent review articles [11–13] and monographs [14, 15] for additional details and background material.

22.2 ALLYL COMPLEXES

Tetrakis(allyl) complexes of thorium [16] and uranium [17] have been synthesized via the reaction

$$MCl_4 + 4C_3H_5MgX \rightarrow M(C_3H_5)_4 + 4MgXCl \qquad (22.1)$$

The 2-methylallyluranium complexes can be prepared by an analogous approach [18]. None of these complexes is stable above 0°C for a significant period of time. Low-temperature nuclear magnetic resonance (NMR) spectroscopy reveals an A_2B_2X pattern characteristic of η^3-allyl ligation (e.g. structure (*1*)),

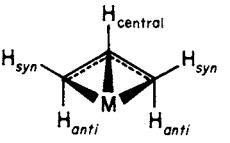

(*1*)

while variable-temperature studies of $Th(C_3H_5)_4$ reveal fluxional behavior at higher temperatures:

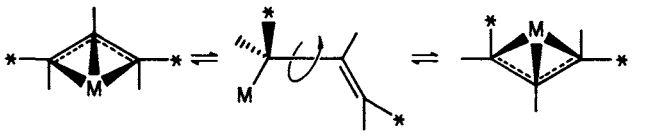

(22.2)

Tetrakis(allyl)uranium readily undergoes protonolysis with hydrogen halides and alcohols [19]

$$U(C_3H_5)_4 + 1HX \longrightarrow U(C_3H_5)_3X + C_3H_6 \qquad (22.3)$$
$$X = Cl, Br, I$$

$$U(C_3H_5)_4 + 2ROH \longrightarrow \tfrac{1}{2}[U(C_3H_5)_2(OR)]_2 + 2C_3H_6 \qquad (22.4)$$
$$R = C_2H_5, i\text{-}C_3H_7, t\text{-}C_4H_9$$

A stoichiometric excess of alcohol completely removes the allyl ligands [20]. The molecular structure of the t-butoxyallyl dimer is shown in Fig. 22.1. It consists

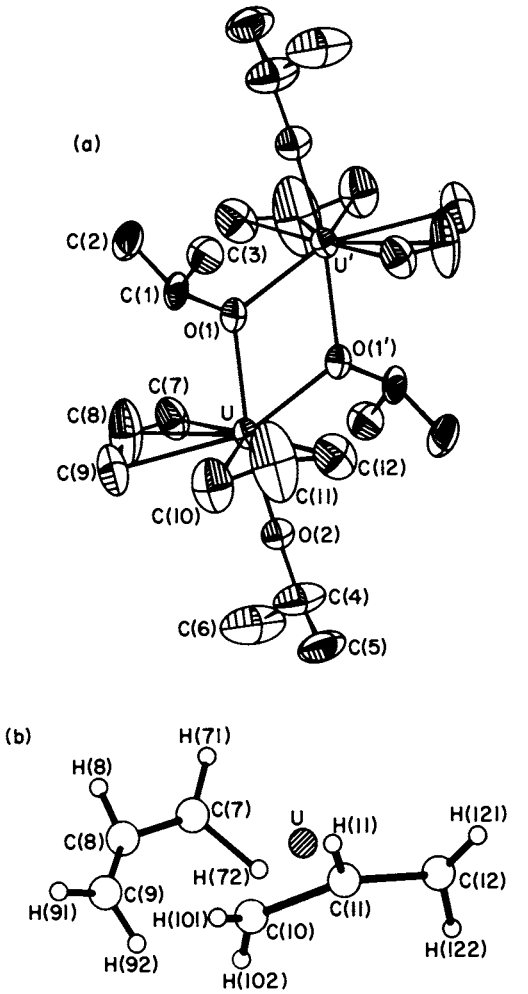

Fig. 22.1 *Molecular structure of* $\{U(C_3H_5)_2[OC(CH_3)_3]_2\}_2$ *showing (a) the entire dimer and (b) details of the allyl ligation* [20].

of a centrosymmetric, alkoxy-bridged dimer with trihapto-allyl ligands (U–C = 2.644(16)–2.736(18) Å).

The reaction of $U(C_5H_5)_4$ with excess 2,2′-bipyridyl yields a thermally stable product, '$U(2,2'\text{-bipy})_3(C_3H_5)_4$', in which two of the allyl groups have been transferred to one or two of the coordinated bipyridyl ligands [21]. The two remaining allyl ligands appear to be coordinated in a monohapto fashion.

Additional allyl complexes, stabilized by $(CH_3)_5C_5$ co-ligands, are discussed in Section 22.4.2.

22.3 CYCLOPENTADIENYL COMPLEXES

22.3.1 $M(C_5H_5)_3$ compounds

The trivalent uranium complex UCp_3 ($Cp = \eta^5\text{-}C_5H_5$) can be prepared via the following routes [22–24]:

$$UCl_3 + 3KCp \xrightarrow[\text{reflux}]{\text{benzene}} UCp_3 + 3KCl \tag{22.5}$$

$$UCp_4 + K \xrightarrow[\text{reflux}]{\text{benzene}} UCp_3 + KCp \tag{22.6}$$

$$U + 3UCp_4 \xrightarrow[\text{reflux}]{\text{benzene}} 4UCp_3 \tag{22.7}$$

$$Cp_3UCl + NaH \xrightarrow{\text{benzene}} UCp_3 + NaCl + \tfrac{1}{2}H_2 \tag{22.8}$$

$$U + 3C_5H_6 \xrightarrow{\text{benzene}} UCp_3 + \tfrac{3}{2}H_2 \tag{22.9}$$

It is a strong Lewis acid and forms adducts with a wide variety of donors [22]:

$$UCp_3 + L \longrightarrow Cp_3UL \tag{22.10}$$

L = THF, RNC, nicotine

The THF adduct can also be prepared via the routes [25–27]:

$$UCl_3 \cdot n\text{THF} + 3NaC_5H_5 \xrightarrow{\text{THF}} Cp_3U \cdot \text{THF} + 3NaCl \tag{22.11}$$

$$U[N(SiEt_3)_2]Cl_2 + 3NaC_5H_5 \xrightarrow{\text{THF}} Cp_3U \cdot \text{THF} + \text{other products} \tag{22.12}$$

$$Cp_3UCl + Na \xrightarrow[\text{THF}]{C_{10}H_8} Cp_3U \cdot \text{THF} + NaCl \tag{22.13}$$

Under electrochemical reduction conditions [28], the first product formed from UCp_3Cl is the stable complex UCp_3Cl^-.

The molecular structure of UCp_3THF (Fig. 22.2) features a distorted tetrahedral coordination geometry with U–C = 2.76(2)–2.82(2) Å and U–O = 2.55(1) Å [26]. A photochemical synthesis of this complex, which involves photoinduced β-hydride elimination,

$$Cp_3MCH(CH_3)_2 \xrightarrow[\text{benzene}]{h\nu} Cp_3MH + CH_2{=}CHCH_3 \qquad (22.14)$$

$$Cp_3MH + Cp_3MCH(CH_3)_2 \longrightarrow 2MCp_3 + CH_3CH_2CH_3 \qquad (22.15)$$
$$M = Th, U$$

has also been reported [29, 30]. Competing U–C σ-bond homolysis also yields $(C_5H_5)_3U \cdot THF$ [2, 10]. The relatively polar character of the U–C_5H_5 bonding is demonstrated by facile ring protonolysis [31]:

$$UCp_3 + HCN \xrightarrow{\text{benzene}} Cp_2UCN + C_5H_6 \qquad (22.16)$$

The reaction of $(CH_3C_5H_4)_3U \cdot THF$ with organic azides and with organic isocyanides yields uranium imido (equation (22.17)) and isocyanato (equation (22.18)) complexes [32]:

$$(CH_3C_5H_4)_3UTHF + RN_3 \longrightarrow (CH_3C_5H_4)_3UNR + N_2 + THF \qquad (22.17)$$
$$R = C_6H_5, Si(CH_3)_3$$

$$(CH_3C_5H_4)_3UTHF + RNCO \longrightarrow [(CH_3C_5H_4)_3U]_2(\eta^2\text{-}OCNR) + THF \qquad (22.18)$$
$$R = C_6H_5$$

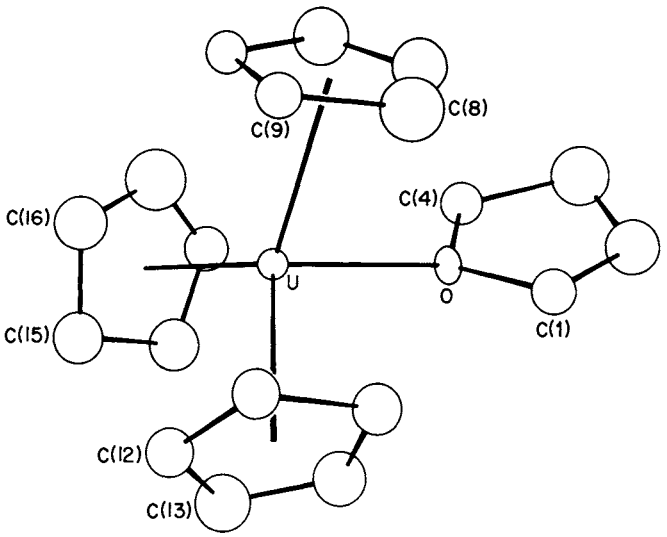

Fig. 22.2 *Molecular structure of* $(C_5H_5)_3U \cdot THF$ *in the solid state* [26].

X-ray diffraction studies suggest considerable U–N multiple bond character in the phenylimido complex (U–N bond length of 2.019(6) Å and U–N–C (phenyl *ipso*) angle of 167.4(6)°), while the isocyanate features a bridging C_6H_5NCO unit (*2*):

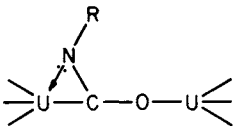

(*2*)

The trivalent thorium complex $Th(C_5H_5)_3$ has been prepared by sodium naphthalide reduction of $(C_5H_5)_3ThCl$ in tetrahydrofuran [33]:

$$Cp_3ThCl + Na \xrightarrow[THF]{C_{10}H_8} Cp_3Th \cdot THF + NaCl \qquad (22.19)$$

The intensely violet product can be isolated as a THF adduct. $Th(C_5H_5)_3$ was characterized by elemental analysis, several spectroscopic techniques, and magnetic susceptibility ($\mu_{eff} = 0.331\ \mu_B$). $ThCp_3$ is reported on the basis of x-ray powder diffraction to be isomorphous with other tris(cyclopentadienyls) of 4f and heavier 5f elements. As might be anticipated, Cp_3Th also forms an adduct with cyclohexyl isocyanide, formulated as $Cp_3ThCNC_6H_{11}$. It undergoes reaction with ammonium chloride according to the equation [33]:

$$ThCp_3 + NH_4Cl \xrightarrow{\text{benzene}} Cp_2ThCl + NH_3 + C_5H_6 \qquad (22.20)$$

A dark-green $ThCp_3$ complex, prepared from Cp_3Th(i-propyl) or Cp_3Th(n-butyl) via the photochemical β-hydride elimination sequence of equations (22.14) and (22.15) (M = Th and using benzene as the solvent), has also been reported [29, 30]. The mechanism of the photochemical process was supported by deuterium labeling studies and other experiments. Green $ThCp_3$ was characterized by a variety of analytical techniques and by chemical reactions. Thus, green $ThCp_3$ reacts with iodine to form the known tris(cyclopentadienyl) iodide (equation (22.21)) and with methanol to liberate 0.5 moles of H_2 (equation (22.22)):

$$ThCp_3 + \tfrac{1}{2}I_2 \xrightarrow{\text{benzene}} Cp_3ThI \qquad (22.21)$$

$$ThCp_3 + 4CH_3OH \longrightarrow Th(OCH_3)_4 + 3C_5H_6 + \tfrac{1}{2}H_2 \qquad (22.22)$$

At room temperature, $\mu_{eff} = 0.404\ \mu_B$.

A trivalent neptunium cyclopentadienyl has been synthesized by the following procedure [27]:

$$Cp_3NpCl + Na \xrightarrow[THF]{C_{10}H_8} Cp_3Np \cdot 3THF + NaCl \qquad (22.23)$$

The ^{237}Np Mössbauer spectrum of this compound indicates the presence of Np^{3+} and relatively ionic metal–ligand bonds.

Transplutonium tris(cyclopentadienyls) can be prepared on a microscale by the reaction of molten bis(cyclopentadienyl)beryllium with the corresponding metal chlorides [34–40]:

$$2MCl_3 + 3BeCp_2 \xrightarrow{65°C} 2MCp_3 + 3BeCl_2 \qquad (22.24)$$

$$M = Pu, Am, Cm, Bk, Cf$$

The actinide-containing products of these reactions were isolated by fractional sublimation. X-ray powder diffraction data reveal that the Cp_3 complexes are isostructural with early lanthanide tris(cyclopentadienyls), $LnCp_3$, Ln = Pr, Sm, and Gd [12, 41]. Analysis of the single-crystal optical and fluorescence spectra of $CmCp_3$ and $AmCp_3$ suggests that the metal–ligand bonding in these late actinide tris(cyclopentadienyls) is probably more covalent than in late lanthanide tris(cyclopentadienyls), but is considerably less covalent than in typical transition-metal cyclopentadienyls [42].

22.3.2 $M(C_5H_5)_2X$ compounds

Although trivalent complexes of the Cp_2MX stoichiometry are common for lanthanides [12], only a handful of actinide analogs have been prepared (equations (22.16) and (22.20)) [31, 33]. Radioactive bis(cyclopentadienyl)berkelium chloride has been synthesized on a microscale via the following approach [43]:

$$BkCl_3 + BeCp_2 \longrightarrow BeCl_2 + Cp_2BkCl \qquad (22.25)$$

and is thought to have structure (*3*):

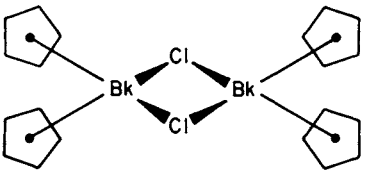

(*3*)

22.3.3 $M(C_5H_5)_4$ compounds

The actinide tetrakis(cyclopentadienyls), $ThCp_4$ [5] and UCp_4 [6], were prepared by Fischer and co-workers, using the approach:

$$MCl_4 + 4KCp \xrightarrow{\text{benzene}} MCp_4 + 4KCl \qquad (22.26)$$

$$M = Th, U$$

Alternatively, a solvent-free approach can also be used [44]:

$$MF_4 + 2MgCp_2 \longrightarrow MCp_4 + 2MgF_2 \qquad (22.27)$$

The molecular structure of UCp_4 (Fig. 22.3) features a nearly tetrahedral coordination geometry with four pentahapto-cyclopentadienyl ligands [45]. The average U–C distance is 2.81(2) Å, with a range of 2.79(2)–2.83(2) Å. Such U–C distances are somewhat longer than typically observed in other U(IV) cyclopentadienyl complexes (*vide infra*) and apparently reflect the pronounced crowding of the ligands about the metal ion. Because the NMR dipolar shift should be zero in a cubic complex, the room-temperature proton signal at 13.1 ppm above TMS (C_6D_6) ($\delta = -13.1$) in UCp_4 is an unambiguous measure of the pure contact shift, and hence of the distribution of unpaired 5f-electron spin density [46].

Electronic structure calculations on UCp_4 have been carried out at several levels of approximation [47] and have been used successfully to fit magnetic susceptibility and optical spectroscopic data [48]. It is found that $C_5H_5^-$ has a somewhat weaker ligand field strength than $C_8H_8^{2-}$, but one that is comparable to that of a tridentate BH_4^- ligand.

The U–C_5H_5 mean bond dissociation energy in UCp_4 has been estimated from thermochemical combustion data [49]. The measured value, 247 kJ mol^{-1}, is somewhat less than the corresponding value for ferrocene, 297 kJ mol^{-1} [50], and that in $U(C_8H_8)_2$ (Section 22.7.1), 347 kJ mol^{-1} [49].

The other known actinide tetrakis(cyclopentadienyls) are $PaCp_4$ [51] and $NpCp_4$ [52]. The protactinium compound was synthesized by the route of equation (22.28) while the neptunium compound is accessible via the more convenient procedure of equation (22.29):

$$Pa_2O_5 \xrightarrow[CCl_4]{Cl_2} PaCl_4 \xrightarrow{BeCp_2} PaCp_4 \qquad (22.28)$$

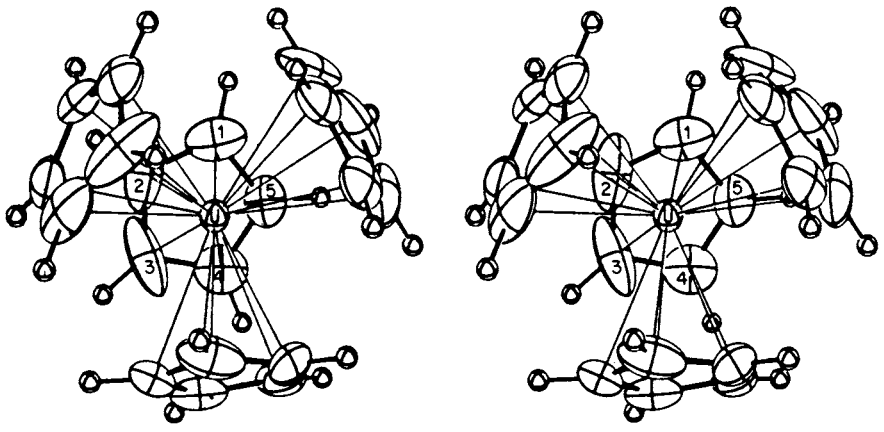

Fig. 22.3 *Stereoscopic view of the solid-state molecular structure of* $U(C_5H_5)_4$ [45].

$$NpCl_4 + 4KCp \xrightarrow{\text{benzene}} NpCp_4 + 4KCl \qquad (22.29)$$

From the ^{237}Np Mössbauer spectrum of $NpCp_4$, it was concluded that there is substantially greater shielding of the 6s shell in the tetrakis(cyclopentadienyl) than in $NpCl_4$, meaning enhanced metal–ligand bond covalence [27]. In contrast, the aforementioned compound $NpCp_3 \cdot 3THF$ exhibits an isomer shift almost identical to that of $NpCl_3$, suggesting considerably greater ionic character in the metal–ligand bonding. From the room-temperature ^1H NMR chemical shift of $NpCp_4$, the proton–electron hyperfine coupling constant was estimated to be about -1.7 MHz, compared to about -1.3 MHz in $NpCp_3Cl$ [53].

22.3.4 $M(C_5H_5)_3X$ compounds

The first organoactinide to be synthesized was red-brown Cp_3UCl, prepared from uranium tetrachloride and sodium cyclopentadienide [4]:

$$UCl_4 + 3NaCp \xrightarrow{\text{THF}} Cp_3UCl + 3NaCl \qquad (22.30)$$

A more convenient, higher-yield synthesis uses the air-stable cyclopentadienylating agent, TlCp, [54]:

$$UCl_4 + 3TlCp \xrightarrow{\text{DME}} Cp_3UCl + 3TlCl \qquad (22.31)$$

(DME = 1,2-dimethoxyethane). It was found that Cp_3UCl *does not* react with $FeCl_2$ to produce ferrocene [4]. This result is in contrast to the behavior of the tris(cyclopentadienyl)lanthanides [12] and suggests greater covalence in the U(IV)–$C_5H_5^-$ bonding. However, the chloride in Cp_3UCl is labile and this allows the synthesis of a great many other tris(cyclopentadienyl)uranium(IV) derivatives (*vide infra*). Indeed, there is now convincing evidence that Cp_3UCl undergoes ionization in aqueous solution to yield the $Cp_3U(H_2O)_2^+$ cation, which can be precipitated by a variety of anions [55]. An early x-ray diffraction study of Cp_3UCl revealed a distorted tetrahedral uranium coordination geometry (approximately C_{3v}), with η^5-C_5H_5 ligands and the U–Cl bond (2.559(16)Å) coincident with the molecular three-fold axis [56]. A more accurate description of this type of structure is provided by a diffraction study of tris(benzylcyclopentadienyl)uranium(IV) shown in Fig. 22.4 [57]. The average U–C(ring) distance is 2.733(1) Å, while the U–Cl distance is 2.627(2) Å. The coordination geometry about the uranium ion is approximately C_{3v}, with the Cl–U–ring centroid angles varying from 98.8° to 101.2°. This type of structure is essentially universal for UCp_3X derivatives (*vide infra*).

A number of synthetic approaches have been reported for UCp_3X compounds, some of which are shown below [34, 58, 59]:

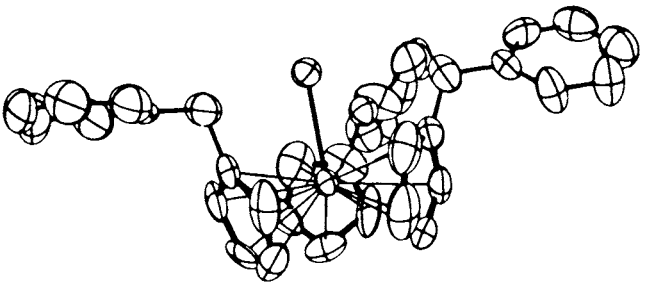

Fig. 22.4 *The crystal structure of* $(C_6H_5CH_2C_5H_4)_3UCl$ [57].

$$UX_4 + 3MCp \longrightarrow Cp_3UX + 3MX \qquad (22.32)$$
$$X^- = Cl^-, Br^-, I^-$$
$$M = K, Tl$$

$$Cp_3UCl + X^- \longrightarrow Cp_3UX + Cl^- \qquad (22.33)$$
$$X^- = F^-, SCN^-, OCN^-, BH_4^-, B(C_6H_5)_3CN^-,$$
$$\tfrac{1}{2}Ni(CN)_4^{2-}, \tfrac{1}{2}Pt(CN)_4^{2-},$$
$$Co_3(CO)_{10}^-, OR^-, C(CN)_3^-$$

$$UCp_4 + X_2 \longrightarrow Cp_3UX + C_5H_5X \qquad (22.34)$$
$$X = Br, I$$

$$UCp_4 + NH_4X \longrightarrow UCp_3X + NH_3 + C_5H_6 \qquad (22.35)$$
$$X^- = F^-, Cl^-, NO_3^-, ClO_4^-, ReO_4^-, B(C_6H_5)_4^-,$$
$$\tfrac{1}{2}SO_4^{2-}, \tfrac{1}{2}C_2O_4^{2-}, CN^-$$

The pseudo-tetrahedral solid-state molecular structure of $U(C_5H_5)_3F$ is similar to those of the aforementioned chlorides with an average ring centroid–U–F angle of 99.7(2)° and an average ring centroid–U–ring centroid angle of 117.21(1)° [60]. The U–F distance of 2.196(12) Å is the shortest U–F bond yet recorded for a U(IV) fluoride. The average U–C bonding contact is 2.74 Å.

The uranium thiocyanate of equation (22.33) forms adducts with Lewis bases such as CH_3CN and water. The molecular structure of $Cp_3UNCS(CH_3CN)$ (Fig. 22.5) [61] exhibits a pseudo-five-coordinate configuration with the three η^5-C_5H_5 ligands occupying the equatorial vertices of a trigonal bipyramid. The average ring centroid–U–ring centroid angle is 119.9°, while the average N(1)–U–ring centroid angle is 92.2°, and the average N(2)–U–ring centroid angle is 87.8°. The U–N(1) distance is 2.407(15) Å and the U–N(2) distance is 2.678(16) Å. In a similar vein, anionic $Cp_3MX_2^-$ complexes can be prepared as shown below for M = U, Np, Pu [62]:

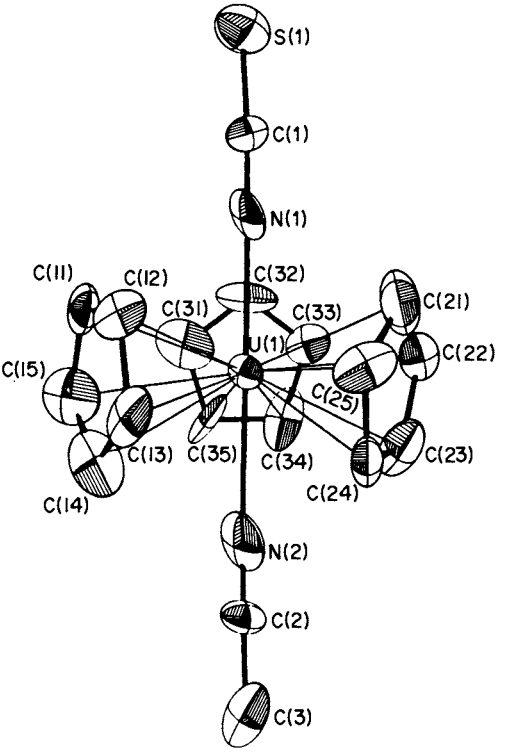

Fig. 22.5 *The solid-state molecular structure of* $(C_5H_5)_3UNCS(CH_3CN)$ [61].

$$Cp_3UNCS + ANCS \longrightarrow A^+Cp_3M(NCS)_2^- \qquad (22.36)$$

$$MCp_3NCS + AOCN \longrightarrow A^+MCp_3(NCS)(OCN)^- \qquad (22.37)$$

$$A^+ = AsPh_4^+,\ K^+,\ K^+(\text{crypt})$$

The molecular structure of $AsPh_4^+\ Cp_3U(NCS)_2^-$ [63] features a pseudo-trigonal bipyramidal uranium coordination geometry (*4*, cf. Fig. 22.5):

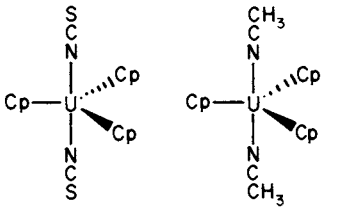

(4) (5)

with axial U–N distances of 2.46(1) and 2.50(1) Å. Treating Cp_3UCl in CH_3CN with butadiene containing traces of oxygen yields the complex

$Cp_3U(NCCH_3)_2^+ UO_2Cl_2^-$ [64]. The uranium coordination geometry is again a pseudo-trigonal bipyramid (*5*) with U–N = 2.61(2) and 2.58(2) Å [64].

Infrared and Raman spectroscopic studies of Cp_3UBH_4 and the ethyl-substituted derivative, prepared via the equation [65, 66]

$$Cp_3UBH_4 + R_3B \longrightarrow Cp_3UH_3BR + R_2BH \qquad (22.38)$$
$$R = C_2H_5, C_6H_5$$

indicate that both compounds have tridentate tetrahydroborate ligation (*6*) and (*7*). The structures of the related cyanoborohydrides involve coordination of the cyano functionality (*8*).

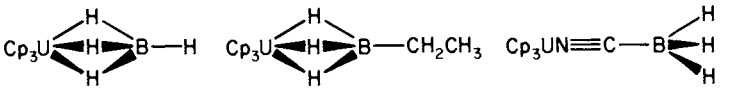

(*6*) (*7*) (*8*)

At room temperature, the bridge and terminal hydrogen atoms of the tetrahydroborate ligand in Cp_3UBH_4 are undergoing rapid interchange. However, the large H_b, H_t chemical shift difference imparted by the paramagnetic U(IV) center significantly alters the time resolution of the NMR experiment, and slowing of the exchange process can be observed at low temperatures [65].

In connection with the previously mentioned analysis of the UCp_4 optical spectrum, the spectrum of Cp_3UBH_4 has also been assigned [67]. The spectrum is simpler than those of most Cp_3UX compounds and closely resembles the spectrum of UCp_4. Using an energy matrix for an f^2 system in a tetrahedral environment, it is possible to fit the experimental data to crystal field parameters that show only a slight deviation from tetrahedral symmetry. That is, interestingly, $C_5H_5^-$ and tridentate BH_4^- have essentially the same crystal field strengths, and the effects of these ligands on the crystal field are additive. In contrast, Cp_3UCl is substantially distorted from a tetrahedral U(IV) environment [68].

A detailed analysis of the ^1H NMR spectra of a variety of Cp_3UOR complexes reveals that nearly all of the isotropic shifts conform to the $(3\cos^2\theta - 1)/r^3$ relationship expected for purely dipolar (pseudo-contact) isotropic shifts arising from the magnetic anisotropy of the complexes [69]. The only deviations are found for protons on the carbon directly bound to the oxygen atom. The deviation in the expected value by about 30 ppm was attributed to a contact interaction, i.e. distribution of unpaired 5f-electron spin density onto the α proton. The direction of the shift (downfield) can be taken as evidence for delocalization of negative spin density, possibly arising by a spin polarization mechanism. ^{13}C NMR studies of Cp_3UCl led to an estimate of the ring carbon contact shift of -309 ± 120 ppm at room temperature [70].

Ring-substituted tris(cyclopentadienyl)uranium(IV) complexes can be straightforwardly prepared from ring-substituted cyclopentadienylating reagents. Some examples are illustrated below [71, 72]:

$$UCl_4 + 3LiC_5H_4R \xrightarrow{THF} (C_5H_4R)_3UCl + 3LiCl \qquad (22.39)$$
$$R = CH_3,\ t\text{-}C_4H_9,\ i\text{-}C_3H_7,\ Si(CH_3)_3$$

$$(C_5H_4R)UCl_3 \cdot 2THF + 2LiCp \xrightarrow{THF} (C_5H_4R)Cp_2UCl + 2LiCl \qquad (22.40)$$

$$UCpCl_3 \cdot 2THF + 2LiC_5H_4R \xrightarrow{THF} Cp(C_5H_4R)_2UCl + 2LiCl \qquad (22.41)$$
$$R = i\text{-}C_3H_7$$

The organouranium compound of equation (22.39) is especially interesting since the $5f^2$ paramagnetism greatly enhances the anisochrony of the C_5H_4R ring and methyl protons.

Tris(cyclopentadienyl)uranium dialkylamides can be synthesized via partial amine displacement from tetrakis(diethylamido)uranium [73, 74]:

$$U[N(C_2H_5)_2]_4 + 3C_5H_6 \longrightarrow Cp_3UN(C_2H_5)_2 + 3HN(C_2H_5)_2 \qquad (22.42)$$

Tris(cyclopentadienyl) halides of thorium and neptunium have also been prepared. For thorium, the TlCp methodology is the most convenient synthetic approach [54]:

$$ThCl_4 + 3TlCp \xrightarrow{DME} Cp_3ThCl + 3TlCl \qquad (22.43)$$

X-ray powder diffraction data reveal that Cp_3UCl and Cp_3ThCl are isomorphous. Tris(cyclopentadienyl)thorium derivatives of other halides, alkoxides, tetrahydroborates, etc., can be prepared in a manner analogous to the uranium reaction above [58]. Tris(cyclopentadienyl)neptunium chloride, Cp_3NpCl, can be prepared either by a radiochemical synthesis [75]:

$$Cp_3{}^{239}UX \xrightarrow{\beta^-} Cp_3{}^{239}NpX \qquad (22.44)$$
$$X = Cl \text{ (also F)}$$

or chemically, using bis(cyclopentadienyl)beryllium [76] (equation (22.45)) or potassium cyclopentadienide [27] (equation (22.46)):

$$2NpCl_4 + 3BeCp_2 \xrightarrow{melt} 2Cp_3NpCl + 3BeCl_2 \qquad (22.45)$$

$$NpCl_4 + 3KCp \xrightarrow{THF} Cp_3NpCl + 3KCl \qquad (22.46)$$

Alkoxide and tetrahydroborate derivatives can be prepared using procedures similar to equation (22.33).

The ^{237}Np Mössbauer spectra of Cp_3NpCl, Cp_3NpOR ($R = i\text{-}C_3H_7$, $t\text{-}C_4H_9$, and $CH(CF_3)_2$), $(CH_3C_5H_4)_3NpBH_4$, $(CH_3C_5H_4)_3NpO(i\text{-}C_3H_7)$, and $Np(CH_3C_5H_4)_4$ indicate that the electron-donating power of X^- varies

approximately as $Cl^- \approx BH_4^- > OR^- > alkyl^- > C_5H_5^-$ [77]. The $C_5H_5^-$ result can be explained in terms of the expected increased metal–ring distances in $NpCp_4$. The magnetic susceptibility of a series of Cp_3NpX complexes (X = F, Cl, Br, I, $\frac{1}{2}SO_4$) also allows a qualitative ordering of the relative crystal field strengths of X [77].

Ultraviolet photoelectron spectra of Cp_3MCl and $(CH_3C_5H_4)_3MCl$ derivatives (M = Th and U) as well as those of $(CH_3C_5H_4)_3UBr$ and $(CH_3C_5H_4)_3UBH_4$ have been reported [78]. The uranium compounds exhibit weak $5f^2$ 'onset bands' at low energy (6.15–7.10 eV) which are absent in the thorium analogs. The energies of these bands are sensitive to the uranium ligation. The other transitions in the spectra can be explained with a qualitative molecular-orbital model.

22.3.5 $M(C_5H_5)_2X_2$ compounds

Although Cp_2MX_2 compounds are a cornerstone of early transition-metal organometallic chemistry, such species are rather unstable for the actinides. Thus, 'Cp_2UCl_2' prepared in 1,2-dimethoxyethane (DME) via the route below:

$$2TlCp + UCl_4 \xrightarrow{DME} \text{'}Cp_2UCl_2\text{'} + 2TlCl \qquad (22.47)$$

is actually a mixture of Cp_3UCl and $CpUCl_3(DME)$ (Section 22.3.6) [79]. Efforts to stabilize Cp_2UCl_2 against ligand redistribution by adding additional ligands have only been successful for $[Cp_2UCl_2L]_2$, where L is $(C_6H_5)_2P(O)CH_2CH_2P(O)(C_6H_5)_2$ [80] (see Section 22.4.3 for an alternate approach).

Despite the unsuitability of Cp_2UCl_2 as a synthetic precursor, other approaches to Cp_2UX_2 compounds are available. Thus, the diethylamide compound $U[N(C_2H_5)_2]_4$ undergoes reaction with two equivalents of cyclopentadiene [81]:

$$U[N(C_2H_5)_2]_4 + 2C_5H_6 \longrightarrow Cp_2U[N(C_2H_5)_2]_2 + 2HN(C_2H_5)_2 \qquad (22.48)$$

The diethylamido ligands in the bis(cyclopentadienyl) derivative can then be replaced by a variety of protonic or electrophilic reagents:

$$Cp_2U[N(C_2H_5)_2]_2 + RH_2 \longrightarrow [Cp_2UR]_2 + 2HN(C_2H_5)_2 \qquad (22.49)$$

RH_2 = *o*-mercaptophenol, toluene-3,4-dithiol, catechol, 1,2-ethanedithiol

$$Cp_2U[N(C_2H_5)_2]_2 + 2R'SH \longrightarrow Cp_2U(SR')_2 + 2HN(C_2H_5)_2 \qquad (22.50)$$

$R' = C_5H_5, C_6H_5, t\text{-}C_4H_9$

$$Cp_2U[N(C_2H_5)_2]_2 + 2CS_2 \longrightarrow Cp_2U[S_2CN(C_2H_5)_2]_2 \qquad (22.51)$$

Bis(cyclopentadienyl)uranium bis(tetrahydroborate) has been prepared as shown below [82]:

$$UCl_4 + 2NaBH_4 \xrightarrow[THF]{DME\ or} UCl_2(BH_4)_2 \qquad (22.52)$$

$$UCl_2(BH_4)_2 + 2TlCp \xrightarrow[THF]{DME\ or} Cp_2U(BH_4)_2 \qquad (22.53)$$

Vibrational spectra indicate that the tetrahydroborate ligation is tridentate. Preliminary x-ray diffraction results for $Cp_2U(BH_4)_2$ indicate U–B distances of 2.61(8) and 2.58(8) Å for one molecule in the unit cell, and 2.63(8) and 2.63(8) Å for the other [82].

The Cp_2UX_2 configuration has also been stabilized using the charged, multidentate acetylacetonate [83] and dihydrobis(pyrazolyl)borate or hydrotris(pyrazolyl)borate [84] ligands.

The synthesis

$$ThI_4 + \text{excess } MgCp_2 \longrightarrow Cp_2ThI_2 + MgI_2 \qquad (22.54)$$

is the only report of a $ThCp_2X_2$ compound [44].

22.3.6 $M(C_5H_5)X_3$ compounds

Compounds of the $MCpX_3 \cdot 2L$ type were first prepared by cyclopentadienylating uranium tetrachloride (M = U, X = Cl) in ethereal solvents [85, 86]:

$$MX_4 + TlCp \xrightarrow{DME} CpMX_3 \cdot DME + TlX \qquad (22.55)$$

$$MX_4 + TlCp \xrightarrow{THF} CpMX_3 \cdot 2THF + TlX \qquad (22.56)$$

M = Th, U
X = Cl, Br

Later reports describe the THF adducts of the uranium bromide as well as of the analogous thorium chloride and bromide [86, 87]. The molecular structure of $(CH_3C_5H_4)UCl_3 \cdot 2THF$ (prepared via the procedure of equation (22.56) using $Tl(CH_3C_5H_4)$) has been determined by single-crystal x-ray diffraction (Fig. 22.6) [79]. The coordination geometry about uranium approximates octahedral with angles C(11)–U–C(13) = 90.0(3)°, C(11)–U–O(1) = 78.8(3)°, C(11)–U–C(12) = 155.6(4)°, and C(11)–U–O(2) = 83.7(4)°. The average U–Cl distance is 2.620(9) Å, the average U–C(cyclopentadienyl) distance is 2.70(4) Å, and the average U–O distance is 2.44(2) Å. The disposition of the bulky THF ligands *cis* and *trans* to the cyclopentadienyl ring appears to be best to minimize intramolecular non-bonded repulsions. The crystal structures of $CpUCl_3[OP(C_6H_5)_3]_2$ [88] and $CpUCl_3\{OP[N(CH_3)_2]\}_2$ [89] are similar, with pseudo-octahedral uranium coordination geometries and occupation by the bulky ligands of one vertex *trans* to the η^5-C_5H_5 ligand and one *cis* (9):

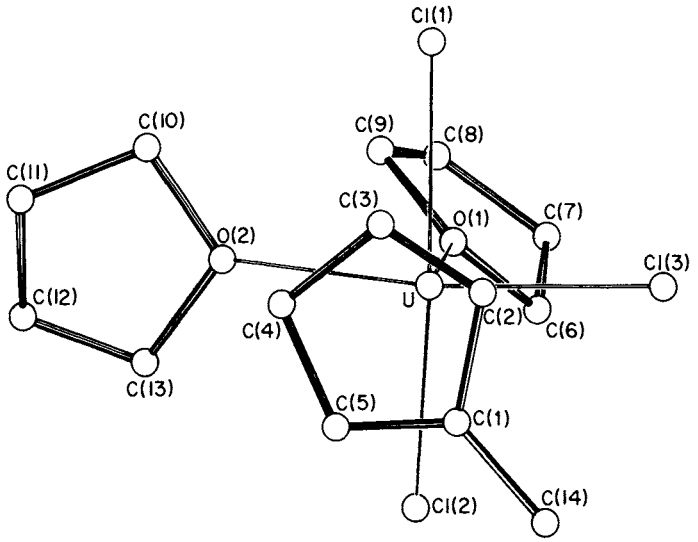

Fig. 22.6 *The molecular structure of* $(CH_3C_5H_4)UCl_3 \cdot 2THF$ *in the solid state* [79].

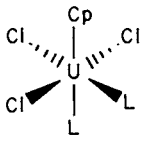

(9)

The other routes to $CpUX_3L_2$ compounds begin with the corresponding UX_4L_2 complexes [82]. Thus, a variety of (cyclopentadienyl)actinide acetylacetonates [85] and poly(pyrazolylborates) [84] can be synthesized via the following approaches:

$$UX_4L_2 + TlCp \xrightarrow{THF} CpUX_3L_2 + TlX \tag{22.57}$$

$$CpUCl_3(THF)_2 + Na(acac) \xrightarrow{THF} CpUCl_2(acac) + NaCl + 2THF \tag{22.58}$$

$$CpUCl_2(acac) + 2OP(C_6H_5)_3 \xrightarrow{THF} CpUCl_2(acac)[OP(C_6H_5)_3]_2 \tag{22.59}$$

$$CpUCl_3(THF)_2 + 2Na(acac) \xrightarrow{THF} CpUCl(acac)_2 + 2NaCl \tag{22.60}$$

$$UCl_2(acac)_2[OP(C_6H_5)_3]_2 + TlCp \xrightarrow{THF} CpUCl(acac)_2[OP(C_6H_5)_3]_2 + TlCl \quad (22.61)$$

$$CpMX_3L_2 + KHB(pz)_3 \xrightarrow{THF} CpMX_2[HB(pz)_3]L + KX + L \quad (22.62)$$

M = Th, U
X = Br, Cl
L = Lewis base

Such methods can be readily extended to $CH_3C_5H_4$ complexes.

A (cyclopentadienyl)neptunium trichloride can be prepared as shown:

$$NpCl_4 + Tl(CH_3C_5H_4) \longrightarrow (CH_3C_5H_4)NpCl_3 \cdot 2THF + TlCl \quad (22.63)$$

The ^{237}Np Mössbauer data have been interpreted in terms of η^1-$CH_3C_5H_4$ bonding [27].

22.4 MODIFIED CYCLOPENTADIENYL LIGAND COMPLEXES

22.4.1 Indenyl compounds

The indenide ligand (*10*)

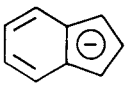

(*10*)

is formally analogous to the cyclopentadienide ligand, but differs significantly in electronic structure and other requirements. Tris(indenyl)actinide halides have been prepared as shown below [90–93]:

$$MX_4 + 3K(C_9H_7) \xrightarrow{THF} (C_9H_7)_3MX + 3KX \quad (22.64)$$

M = Th, U
X = Cl, Br, I

X-ray powder diffraction indicates that the thorium and uranium tris(indenyl) chlorides are isomorphous; they are not, however, isomorphous with the corresponding bromides. The molecular structure of $U(C_9H_7)_3UCl$ is shown in Fig. 22.7 [91]. The uranium coordination geometry is distorted tetrahedral with η^5-indenyl ligation. The average ring centroid–U–ring centroid angle is 112°, which can be compared to values of 117.2(1)° in $(C_5H_5)_3UF$ and 117.0° in

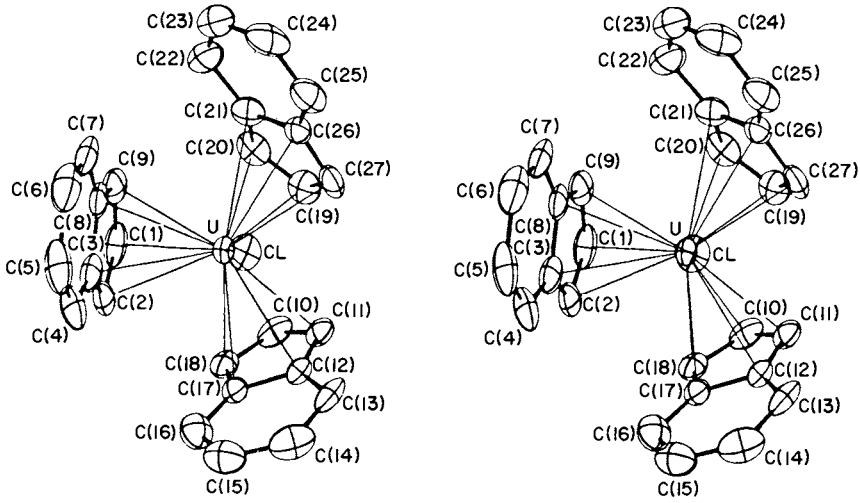

Fig. 22.7 *Stereoscopic view of the solid-state molecular structure of (indenyl)$_3$UCl* [91].

$(C_6H_5CH_2C_5H_4)_3UCl$ (*vide supra*). The average ring centroid–U–X angle is 106.7° in $(C_8H_7)_3UCl$ compared to 99.7° in $(C_5H_5)_3UF$ and 100.0° in $U(C_6H_5CH_2C_5H_4)_3Cl$. The tendency of the $(C_9H_7)_3UF$ parameters to be somewhat closer to an idealized tetrahedral geometry apparently reflects greater interligand non-bonded repulsions. The U–Cl distance in $(C_9H_7)_3UCl$ is 2.593(3) Å, and the average U–C(five-membered ring) distance is 2.78 Å, with a range of 2.67(1)–2.89(1) Å. The actinide $(C_9H_7)_3MX$ compounds can be converted to alkoxide and tetrahydroborate derivatives by simple metathesis chemistry (cf. equation (22.33)) [94, 95]. In the case of $(C_9H_7)_3UCl + NaBH_4$, reduction to the trivalent $(C_9H_7)_3U \cdot THF$ is reported to occur. Complexes similar to $(C_9H_7)_3MCl$ compounds have also been prepared and characterized with the substituted indenide ligands (*11*) and (*12*) [96, 97]:

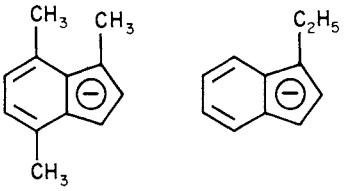

(*11*) (*12*)

The unusual compounds $M(C_9H_7)_3$, M = Th and U, have also been reported [98, 99], although full synthetic/spectroscopic details are lacking. However, the molecular structure of $U(C_9H_7)_3$ has been reported (Fig. 22.8) [98]. The uranium coordination geometry is approximately trigonal with U–C bond distances

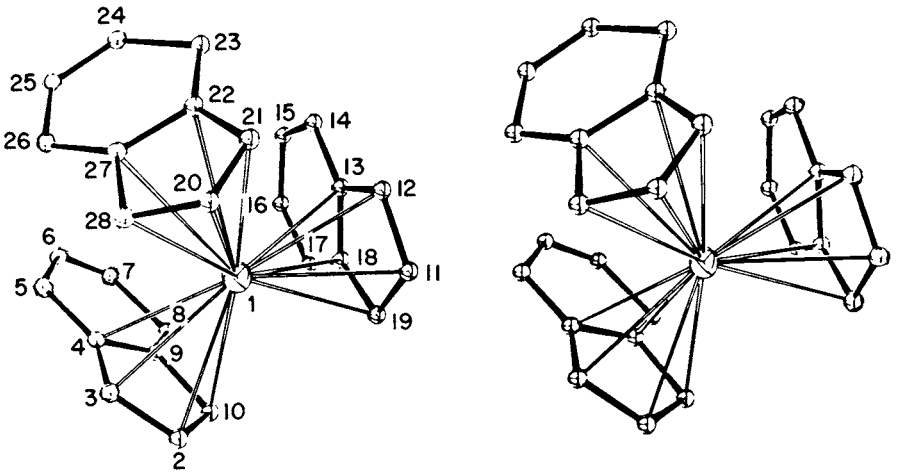

Fig. 22.8 *Stereoscopic view of the molecular structure of* $(indenyl)_3U$ [98].

ranging from about 2.75(2) Å for C(3) and C(10) to 2.81(2) Å for C(2), C(4), and C(9).

Indenyl complexes of the type $(C_9H_7)MX_3 \cdot L$ can be prepared as shown below [99–101]:

$$MX_4 + K(C_9H_7) \xrightarrow{THF} (C_9H_7)MX_3 \cdot THF + KX \tag{22.65}$$

$$(C_9H_7)MX_3 \cdot THF + (C_6H_5)_3PO \longrightarrow (C_9H_7)MX_3[OP(C_6H_5)_3] + THF$$
$$M = Th, U, Np \quad X = Cl, Br \tag{22.66}$$

$$(C_9H_7)_3UCl + 2UCl_4 \xrightarrow{THF} 3(C_9H_7)UCl_3 \cdot THF \tag{22.67}$$

22.4.2 Peralkylcyclopentadienyl complexes

Ring alkylation not only modifies the electronic and steric properties of η^5-C_5H_5 ligands but also greatly improves the solubility and crystallizability of the resulting actinide complexes. The first such compounds were prepared as follows [102–104]:

$$MCl_4 + 2Cp'MgBr \longrightarrow Cp'_2MCl_2 + 2MgClBr \tag{22.68}$$
$$M = Th, U \quad Cp' = \eta^5\text{-}(CH_3)_5C_5$$

$$UCl_4 + 2Bu_3Sn[(CH_3)_4(C_2H_5)C_5] \longrightarrow [(CH_3)_4(C_2H_5)C_5]_2UCl_2 + 2Bu_3SnCl \tag{22.69}$$

Preliminary crystallographic data are in accord with pseudo-tetrahedral 'bent sandwich' molecular structures for Cp'_2ThCl_2 and Cp'_2UCl_2 [105]. This evidence is reinforced by the molecular structure of $Cp'_2UCl_2 \cdot$pyrazole (Fig. 22.9) [106] with a ring centroid–U–ring centroid angle of 137.1°, a Cl–U–Cl angle of 148.29(8)°, and U–Cl = 2.696(2) Å, U–N = 2.607(8) Å, and U–C(ring) = 2.74(2) Å (average).

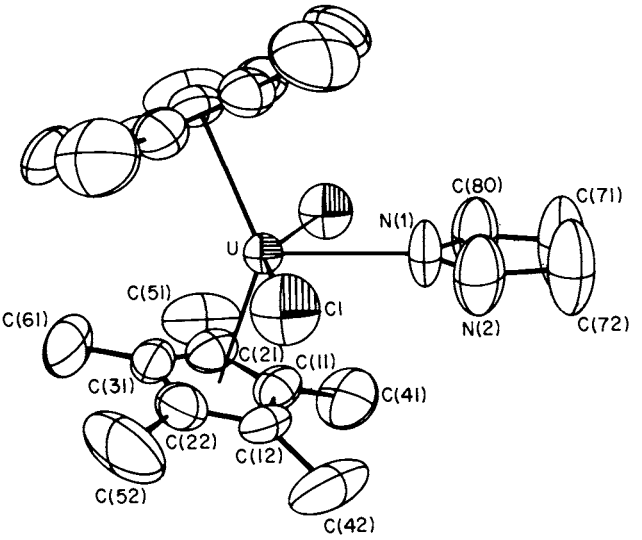

Fig. 22.9 *The molecular structure of* $[(CH_3)_5C_5]_2UCl_2 \cdot$*pyrazole* [106].

Straightforward metathesis chemistry can be used to prepare bis(pentamethylcyclopentadienyl)actinide alkoxides, amides, and bidentate [106] pyrazolates (pz^-) [106–108]:

$$Cp'_2MCl_2 + 2NaOCH_3 \longrightarrow Cp'_2M(OCH_3)_2 + 2NaCl \quad (22.70)$$
$$M = Th, U$$

$$Cp'_2MCl_2 + LiNR_2 \longrightarrow Cp'_2M(NR_2)Cl + LiCl \quad (22.71)$$
$$M = Th, U$$
$$R = CH_3, C_2H_5$$

$$Cp'_2MCl_2 + 2LiNR_2 \longrightarrow Cp'_2M(NR_2)_2 + 2LiCl \quad (22.72)$$
$$M = Th, U$$
$$R = CH_3$$

$$Cp'_2UCl_2 + Napz \longrightarrow Cp'_2U(\eta^2\text{-pz})Cl + NaCl \quad (22.73)$$

$$Cp'_2UCl_2 + 2Napz \longrightarrow Cp'_2(\eta^2\text{-pz})_2 + 2NaCl \quad (22.74)$$

Protolytic approaches to alkoxides, amides, and mercaptides [104, 108, 109] are also viable:

$$Cp'_2ThR_2 + R'OH \longrightarrow Cp'_2Th(R)OR' + RH \qquad (22.75)$$

R = alkyl group
R′ = $CH[C(CH_3)_3]_2$

$$Cp'_2MR_2 + R'_2NH \longrightarrow Cp'_2M(NR_2)_2 + 2RH \qquad (22.76)$$

M = Th, U
R = alkyl group
R′ = C_2H_5

$$Cp'_2ThR_2 + 2R'SH \longrightarrow Cp'_2Th(SR')_2 + 2RH \qquad (22.77)$$

R = alkyl group
R′ = n-C_3H_7

All products are formulated as monomeric 'bent-sandwich' Cp_2MX_2 molecules.

Electrochemical studies of Cp'_2UCl_2 [110, 111] reveal a reversible, one-electron reduction to $Cp'_2UCl_2^-$ ($E_{1/2} = -1.30$ V (CH_3CN), -1.22 V (THF) vs SCE). In contrast, Cp'_2ThCl_2 is not reduced at potentials as negative as -2.7 V vs SCE. For a series of group IV and actinide complexes, the relative ease of reduction is: $Cp_2TiCl_2 > Cp'_2UCl_2 > Cp_2ZrCl_2 \gg Cp'_2ThCl_2$.

The $Cp'_2M(NR_2)Cl$ and $Cp'_2M(NR_2)_2$ complexes exhibit a rich carbonylation chemistry in which migratory CO insertion occurs to yield dihapto-carbamoyls [107]:

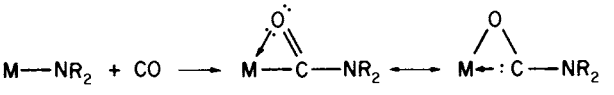

(22.78)

(*13*) (*14*)

As judged by spectroscopic and structural data, the contribution of carbene-like hybrid (*14*) is not as great as for the analogous acyls (see Chapter 23). This reflects the π-donor (N → C) tendencies of the nitrogen heteroatom [107]. An example of this type of compound is illustrated by the molecular structure of $Cp'_2U[\eta^2\text{-}CON(CH_3)_2]_2$ (Fig. 22.10). All heavy atoms in the η^2-$CON(CH_3)_2$ fragments are essentially coplanar.

Trivalent Cp'_2UX derivatives can be readily prepared via the following approach [112]:

$$3Cp_2U(R)Cl + \tfrac{3}{2}H_2 \longrightarrow [Cp'_2UCl]_3 + 3RH \qquad (22.79)$$

R = alkyl group

X-ray diffraction reveals the uranium monochloride to be a trimer (Fig. 22.11) with an approximately D_{3h} arrangement of Cp'_2U and bridging Cl groups. This

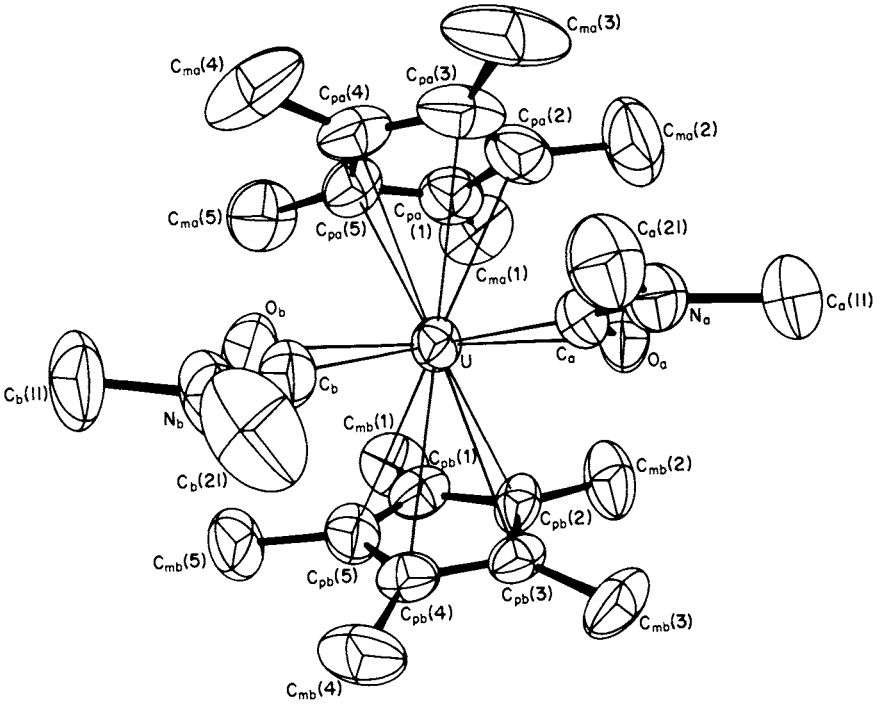

Fig. 22.10 *Solid-state structure* $[(CH_3)_5C_5]_2U[\eta^2\text{-}CON(CH_3)_2]_2$ [107].

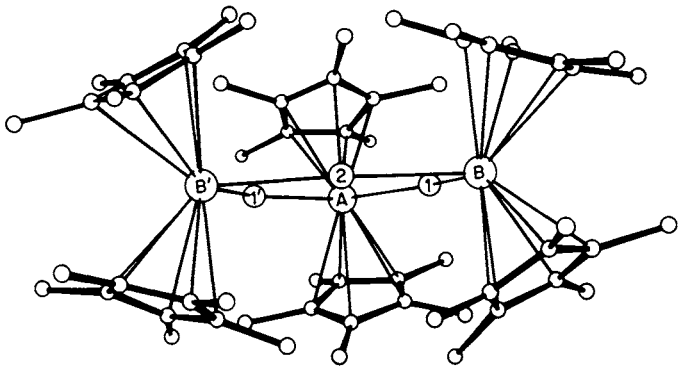

Fig. 22.11 *Molecular structure of* $\{[(CH_3)_5C_5]_2UCl\}_3$ [112].

compound forms adducts with Lewis bases and dialkylamides [112]:

$$(Cp'_2UCl)_3 + 3L \rightleftharpoons 3Cp'_2U(Cl)L \qquad (22.80)$$

L = pyridine, $P(CH_3)_3$, THF

$$(Cp'_2UCl)_3 + 3NaN[Si(CH_3)_3]_2 \longrightarrow 3Cp'_2UN[Si(CH_3)_3]_2 + 3NaCl \qquad (22.81)$$

The adduct $Cp'_2U(Cl)THF$ has been shown to be an extremely active halogen-atom abstractor from organic halides [177, 178].

Single-ring peralkylcyclopentadienyl actinide complexes can be prepared as follows [113, 87]:

$$MCl_4 + Cp'MgCl \xrightarrow{THF} Cp'MCl_3 \cdot 2THF + MgCl_2 \qquad (22.82)$$

M = Th, U

$$MCl_4L_2 + Li[(CH_3)_4(C_2H_5)C_5] \longrightarrow [(CH_3)_4(C_2H_5)C_5]MCl_3L_2 + LiCl \qquad (22.83)$$

M = Th, U
L = $OP(C_6H_5)_3$, $CH_3CON(CH_3)_2$, $(CH_3)_3CCON(CH_3)_2$

Spectroscopic data suggest pseudo-octahedral structure (*15*) for the L = THF complexes:

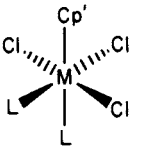

(*15*)

Tris(allyl) and tris(2-methylallyl) derivatives can then be prepared as shown below [114, 115]:

$$Cp'_2MCl_3 \cdot 2THF + RMgX \longrightarrow Cp'_2MR_3 + MgClX \qquad (22.84)$$

M = Th, R = allyl, X = Br
M = U, R = allyl, X = Br
M = U, R = 2-methylallyl, X = Cl

The molecular structure of $Cp'U(2\text{-methylallyl})_3$ [115] is shown in Fig. 22.12. The most interesting feature is the nature of the η^3-allyl ligation where U–C(terminal) = 2.66(1) Å (average) and U–C(central) = 2.80(1) Å (average). This trend is opposite to that observed for most transition-metal η^3-allyls, where the distance to the central allylic carbon atom is usually the shortest.

22.4.3 Chelating cyclopentadienyl compounds

Joining cyclopentadienyl ligands to form chelating ligands ((*16*), (*17*)) offers a potential means to 'open' an actinide co-ordination sphere and to prevent ligand redistribution processes. In the case of ligands (*16*), a variety of binuclear uranium halo complexes have been prepared [12, 116, 117]:

Table 21.11 *Thermodynamics of the stepwise formation of actinide carboxylate complexes in perchlorate media, at 25°C. Values of* ΔH_n° *determined calorimetrically for* Th^{4+} *and* UO_2^{2+}*, and by temperature coefficient method*[a] *for* M^{3+}.

	M^{z+}	I (M)	ΔG_1° (kJ mol^{-1})	ΔH_1° (kJ mol^{-1})	ΔS_1° (J K^{-1} mol^{-1})	ΔG_2° (kJ mol^{-1})	ΔH_2° (kJ mol^{-1})	ΔS_2° (J K mol^{-1})	ΔG_3° (kJ mol^{-1})	ΔH_3° (kJ mol^{-1})	ΔS_3° (J K^{-1} mol^{-1})	*Ref.*
acetate	Am^{3+}	2	−11.2	18.0	98							108
	Cm^{3+}	2	−11.7	18.0	100							108
	Bk^{3+}	2	−11.7	18.4	101							108
	Cf^{3+}	2	−12.0	15.9	94							108
	Th^{4+}	1	−22.0	11.3	112	−17.8	4.5	74	−11.2	13.7	84[b]	131
	UO_2^{2+}	1	−13.8	10.5	82	−11.4	9.7	71	−11.3	−4.0	25	94
glycolate												
	Th^{4+}	1	−23.5	2.1	86	−19.0	−0.8	61	−15.5	−3.0	42[c]	118
	UO_2^{2+}	1	−13.4	5.4	63	−9.3	7.5	56	−6.8	−0.8	20	132
thioglycolate	Th^{4+}	1	−18.4	10.2	96	−14.1	8.0	74	−8.7	10.9	66[d]	118
	UO_2^{2+}	1	−10.8	8.6	65	−7.5	10.6	61	−7.4	0.0	25	118

[a] 0–55°C (0–40°C for Bk^{3+}).
[b] $\Delta G_4^\circ = -7.8$, $\Delta H_4^\circ = 5.2$, $\Delta S_4^\circ = 43$, also fifth complex claimed.
[c] $\Delta G_4^\circ = -10.3$, $\Delta H_4^\circ = -3.9$, $\Delta S_4^\circ = 21$, also fifth complex claimed.
[d] $\Delta G_4^\circ = -7.6$, $\Delta H_4^\circ = 3.3$, $\Delta S_4^\circ = 37$.

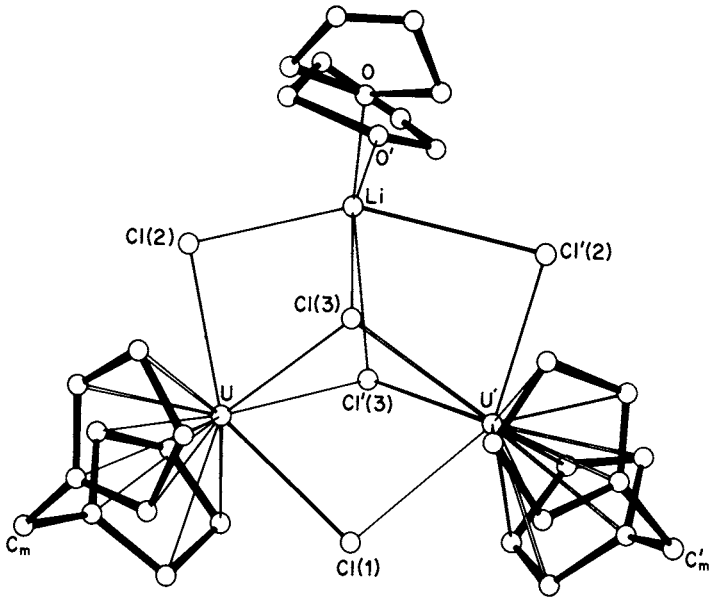

Fig. 22.13 *The crystal structure of* $Li^+(THF)_2[(C_5H_4)_2CH_2]_2U_2Cl_5^-$ [116].

bases (e.g. 2,2′-bipyridyl) as well as tetrahydroborate and alkyl compounds have been prepared [12, 13, 117]. Ligand (*17*) affords considerably more soluble organoactinide complexes [118, 119]:

$$(CH_3)_2Si[(CH_3)_4C_5]_2^{2-}(Li^+)_2 + ThCl_4 \longrightarrow Li^+\{(CH_3)_2Si[(CH_3)_4C_5]_2\}ThCl_3^- + LiCl \qquad (22.86)$$

and an extensive series of alkyl and aryl derivatives have been prepared (see Chapter 23) [118, 119].

22.5 PENTADIENYL COMPOUNDS

The 2,4-dimethylpentadienide ligand (*18*)

(*18*)

forms complexes with a variety of d- and f-block ions. In the case of trivalent uranium [120]:

$$UCl_3 \cdot n\text{THF} + 3K(2,4\text{-}C_7H_{11}) \longrightarrow U(2,4\text{-}C_7H_{11})_3 + 3KCl \qquad (22.87)$$

a tris(pentadienyl) complex is formed. It is likely to have a molecular structure with η^5 coordination, similar to that of $Nd(2,4\text{-}C_7H_{11})_3$ [121], structure (*19*):

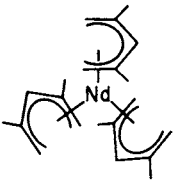

(*19*)

22.6 ARENE COMPLEXES

Reducing Friedel–Crafts reactions have been employed in the synthesis of U(III) (equation (22.88)) [122] and U(IV) (equation (22.89)) [123] arene complexes:

$$UCl_4 + AlCl_3 + Al \xrightarrow{C_6H_6} (C_6H_6)U(AlCl_4)_3 \qquad (22.88)$$

$$UCl_4 + AlCl_3 + Al \xrightarrow{(CH_3)_6C_6} [(CH_3)_6C_6]_2U_2Cl_7^+ AlCl_4^- \qquad (22.89)$$

The molecular structure of the binuclear hexamethylbenzene complex is illustrated in Fig. 22.14. The arene is bonded in an η^6 mode with a rather long

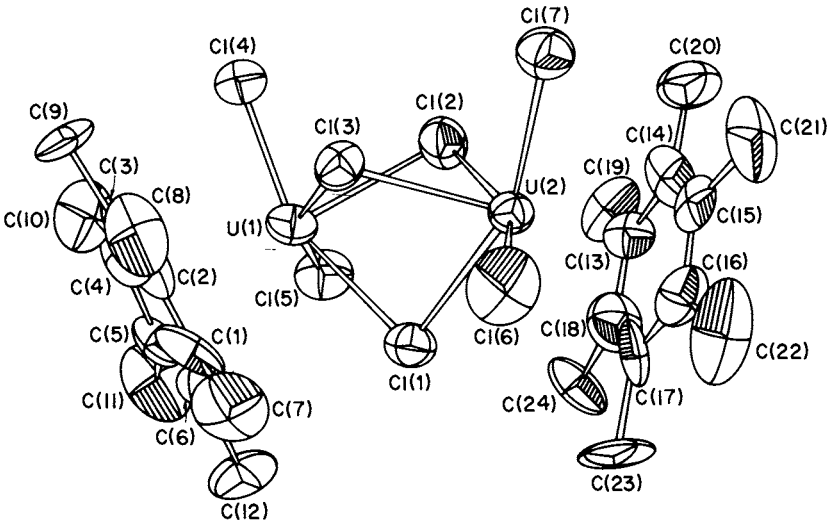

Fig. 22.14 *Molecular structure of* $[(CH_3)_6C_6]_2U_2^+Cl_7\,AlCl_4^-$ [123].

U–C(arene) distance of 2.92(4) Å (average), and U–U = 3.937(1) Å [123]. The coordinated arene ligands are readily displaced in both complexes.

22.7 CYCLO-OCTATETRAENE COMPLEXES

22.7.1 $M(C_8H_8)_2$ complexes

The Hückel $(4n+2)$ π-electron dianion of cyclo-octatetraene, $C_8H_8^{2-}$, forms complexes with a number of early transition-metal and actinide ions. The synthesis of the uranium sandwich complex, $U(C_8H_8)_2$ (bis([8]annulene)uranium(IV), known as 'uranocene'), was an important milestone in organoactinide chemistry. The green, pyrophoric compound was first prepared as shown below [7, 124]:

$$UCl_4 + 2K_2C_8H_8 \longrightarrow U(C_8H_8)_2 + 4KCl \qquad (22.90)$$

Uranocene can also be prepared by reacting cyclo-octatetraene with finely divided uranium, generated either electrolytically [125], by reducing UCl_4 with Na/K [126], or by the thermal decomposition of UH_3 [127] or '$U(n\text{-}C_4H_9)_4$' [128]. A solvent-free synthesis can be carried out with $Mg(C_8H_8)$ [129]:

$$UF_4 + Mg(C_8H_8) \longrightarrow U(C_8H_8)_2 + 2MgF_2 \qquad (22.91)$$

The molecular structure of uranocene has been determined by single-crystal x-ray diffraction and is shown in Fig. 22.15 [130, 131]. The molecule possesses rigorous D_{8h} symmetry with the eight-membered rings arranged in an eclipsed conformation. The mean U–C bond distance is 2.647(4) Å, and the mean C–C bond distance is 1.392(13) Å. The $C_8H_8^{2-}$ rings are planar to within experimental error.

'Thoracene', $Th(C_8H_8)_2$, can be prepared from thorium tetrachloride and cyclo-octatetraene dianion (cf. equation (22.90)) [124, 132]. Although the chemistry of this complex has not been as extensively investigated as that of uranocene, it appears to be more ionic. The structure of thoracene in the solid state is isomorphous with that of uranocene (Fig. 22.15) [130, 131]. The mean Th–C bond distance is 2.701(4) Å, and the mean C–C bond distance is 1.386(9)Å. The difference in metal–carbon bond lengths in $Th(C_8H_8)_2$ and $U(C_8H_8)_2$ is understandable on the basis of differences in ionic radii. No variations in bonding covalence or ionicity can be inferred from these structural data [131].

Bis(cyclo-octatetraene) derivatives are also known for neptunium, plutonium, and protactinium. $Np(C_8H_8)_2$ [133] and $Pu(C_8H_8)_2$ [133] can be prepared via the following equations:

$$NpCl_4 + 2K_2C_8H_8 \xrightarrow{THF} Np(C_8H_8)_2 + 4KCl \qquad (22.92)$$

$$[(C_2H_5)_4N]_2PuCl_6 + 2K_2C_8H_8 \longrightarrow Pu(C_8H_8)_2 + 4KCl + 2(C_2H_5)_4N^+Cl^- \qquad (22.93)$$

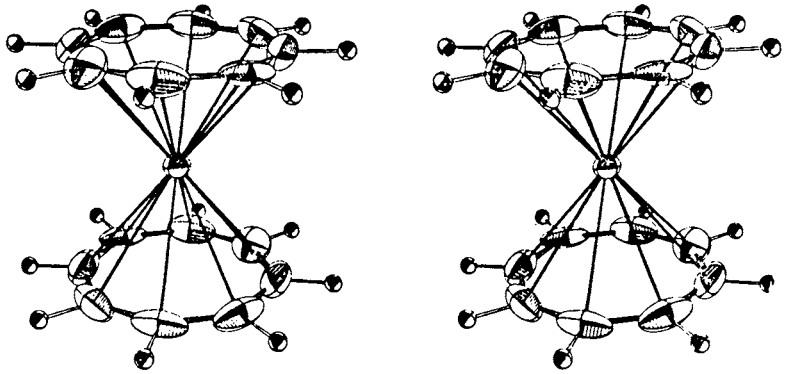

Fig. 22.15 *Stereoscopic view of the solid-state molecular structures of* $U(C_8H_8)_2$ *and* $Th(C_8H_8)_2$ [130, 131].

Alternatively, they can be prepared from cyclo-octatetraene and the finely divided metals [127]. X-ray powder diffraction data indicate that these complexes are isomorphous with uranocene. In a similar manner, bis(cyclo-octatetraene)protactinum has also been synthesized [134]:

$$PaCl_4 + 2K_2C_8H_8 \xrightarrow{THF} Pa(C_8H_8)_2 + 4KCl \qquad (22.94)$$

Infrared spectra and x-ray powder diffraction data suggest a molecular structure identical to uranocene.

A large number of 1,1'-disubstituted uranocenes have been prepared either from the corresponding substituted cyclo-octatetraenes [135–138]:

$$UCl_4 + 2K_2RC_8H_7 \longrightarrow U(RC_8H_7)_2 + 4KCl \qquad (22.95)$$

R = C_2H_5, n-C_4H_9, C_6H_5, $CH{=}CH_2$, OCH_3, $(CH_2)_3N(CH_3)_2$, C_8H_7, OC_2H_5, $OC(CH_3)_3$, $OCH_2CH{=}CH_2$, $N(CH_3)_2$, $CH_2N(CH_3)_2$, PR'_2 (R' = C_6H_5, t-C_4H_9, C_2H_5), *o*-tolyl, mesityl, *p*-$(CH_3)_2NC_6H_4$

or by carrying out transformations on substituted uranocenes [139]. Likewise, ring-substituted neptunium and plutonium complexes are also accessible [140]:

$$2K_2RC_8H_7 + NpCl_4 \xrightarrow{THF} Np(RC_8H_7)_2 + 4KCl \qquad (22.96)$$

$$2K_2RC_8H_7 + [(C_2H_5)_4N]_2PuCl_6 \longrightarrow Pu(RC_8H_7)_2 + 4KCl + 2[(C_2H_5)_4N]Cl \qquad (22.97)$$

R = C_2H_5, n-C_4H_9

Uranocenes with greater degrees of ring substitution have been prepared from the dianions of more highly substituted cyclo-octatetraenes. Thus,

1,3,5,7,1′,3′,5′,7′-octamethyl complexes can be prepared via the route below [139, 141–143]:

$$MCl_4 + 2K_2(CH_3)_4C_8H_4 \longrightarrow M[(CH_3)_4C_8H_4]_2 + 4KCl \quad (22.98)$$
$$M = Th, Pa, U, Np$$

An interesting feature of the solid-state structure of this complex is that two crystallographically independent rotamers are present in the unit cell [144] (Fig. 22.16). The methyl groups are nearly staggered in one rotamer and nearly eclipsed in the other. Metrical parameters for the two molecules are identical within experimental error with U–C (rotamer A) averaging 2.658(4) Å and U–C

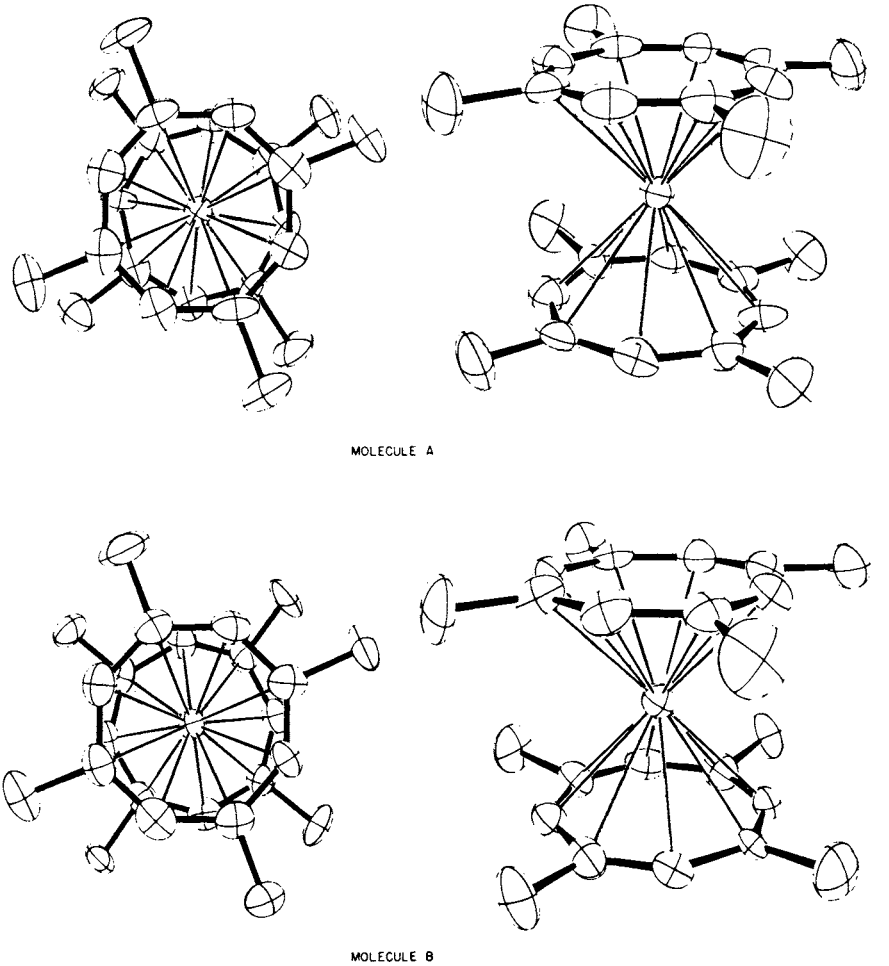

Fig. 22.16 *Stereoscopic view of the solid-state molecular structure of bis*(1,3,5,7-*tetramethylcyclo-octatetraene*)*uranium*(IV) [144]. *The two crystallographically unique molecules in the unit cell are shown.*

(rotamer B) averaging 2.657(6) Å. The ring methyl groups are tipped an average of 4.1° out of the C_8 plane toward the uranium. Other examples of highly substituted uranocenes are bis(cyclobutenocyclo-octatetraene)uranium(IV) [145], bis(benzocyclo-octatetraene)uranium(IV) [146], and other annulated uranocenes [147, 148] as well as bis(1,3,5,7-tetraphenylcyclooctatetraene)uranium(IV) [149, 150]. The latter complex is completely stable in air and sublimes unchanged at 400°C and 10^{-5} mm Hg. The molecular structure, viewed perpendicular to the ligand planes, is shown in Fig. 22.17. The planar cyclo-octatetraene ligands are essentially eclipsed, with the phenyl substituents in staggered positions, rotated an average of 42° out of the ligand plane. The average U–C(hydrogen-substituted) distance is 2.63(2) Å, and the average U–C(phenyl-substituted) distance is 2.68(1) Å.

With regard to chemical reactivity, all of the $M(C_8H_8)_2$ complexes are exceedingly sensitive to oxygen. Whereas thoracene is rapidly destroyed by protic agents, uranocene is hydrolyzed only slowly:

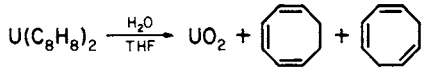

(22.99)

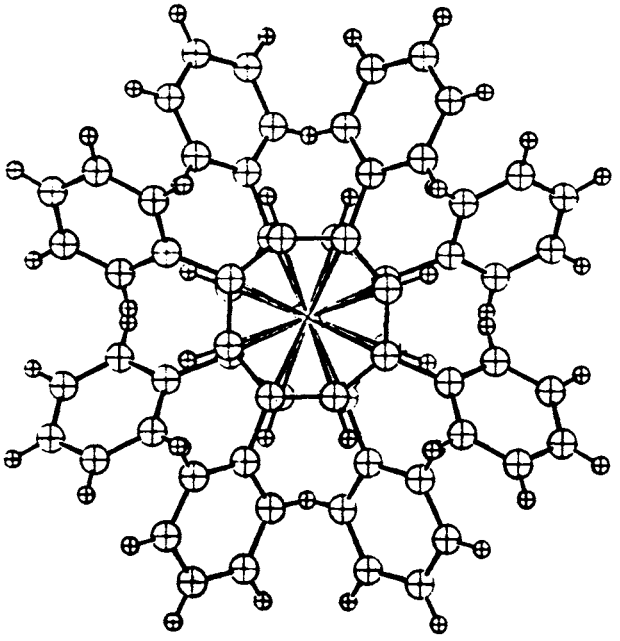

Fig. 22.17 *The molecular structure of bis*(1,3,5,7-*tetraphenylcyclo-octatetraene*)*uranium in the solid state* [150].

Mechanistic studies [138] indicate that electron-withdrawing ring substituents accelerate C_8H_8 cleavage, suggesting a rate-limiting ($k_{H_2O}/k_{D_2O} = 11.8$) proton transfer from a uranium-bound water molecule. Uranocene undergoes reaction with aromatic and aliphatic nitro compounds to produce the corresponding azo compounds in moderate to high yields [151]:

$$2U(C_8H_7R)_2 + 2RNO_2 \longrightarrow RN{=}NR' + 2UO_2 + 4C_8H_7R \quad (22.100)$$

In several cases the amine, RNH_2, is also produced in significant quantities; the source of the hydrogen atoms is apparently the solvent. The deoxygenation appears not to take place via free nitrene (R–N:) intermediates. Also, direct electron transfer to form a nitro radical anion ($R–NO_2\cdot$) can be reasonably ruled out. It thus appears that the initial step of the reaction involves direct attack by a nitro oxygen atom at the uranium. That nitrobenzene reacts more rapidly than 4-nitrotoluene (a Hammett ρ value of -1.7 is measured) argues that the nitro compound is being reduced in the transition state.

An electrochemical study of uranocene provides some evidence for a U(v) uranocene cation [152]. However, this species is unstable, and quasi-reversible cyclic voltammograms can only be observed at subambient temperatures.

The nature of the metal–ligand bonding in uranocene and other $M(C_8H_8)_2$ complexes has been the object of intense experimental and theoretical scrutiny. In terms of orbital symmetry, uranocene is an interesting f-orbital homolog of ferrocene [124]. Thus, the overlap of the $C_8H_8^{2-}$ highest occupied molecular orbitals (e_{2u} in D_{8h}) with the symmetry-appropriate f_{xyz} and $f_{z(x^2-y^2)}$ ($l_z = \pm 2$) uranium orbitals is reminiscent of the interaction of the e_{1g} $C_5H_5^-$ highest occupied molecular orbitals with the iron d_{xz} and d_{yz} orbitals (Fig. 22.18). However, the crucial issues have been the extent of metal–ligand bond covalence and the relative importance of 5f versus other actinide orbitals in the bonding. Experimental techniques that have been employed include magnetic susceptibility [153, 154], He I/He II photoelectron spectroscopy [155–157], electronic Raman spectroscopy [158], optical spectroscopy [135, 139], and ^{237}Np Mössbauer spectroscopy [159]. Theoretical studies have been carried out at the LCAO Wolfsberg–Helmholz level [153, 160, 161], at the non-relativistic SCF–$X\alpha$ scattered-wave level [162], and at the quasi-relativistic SCF–$X\alpha$ scattered-wave level [163, 164]. There is now reasonable agreement in the interpretation of most of these results. The picture emerging for uranocene is one in which there is significant metal–ligand bond covalence. While metal 5f orbitals are doubtless involved in the bonding, the role of 6d orbitals is probably comparable or greater. Furthermore, there is greater metal–ligand bond covalence in uranocene than in thoracene. Interestingly, the bonding in thoracene appears to be very similar to that in the lanthanide analog, cerocene ($Ce(C_8H_8)_2$) [157, 179].

The calorimetrically derived $U–C_8H_8$ mean bond dissociation energy in uranocene, 347 kJ mol^{-1}, is significantly greater than the $U–C_5H_5$ mean bond dissociation energy in $U(C_5H_5)_4$, 247 kJ mol^{-1} [49].

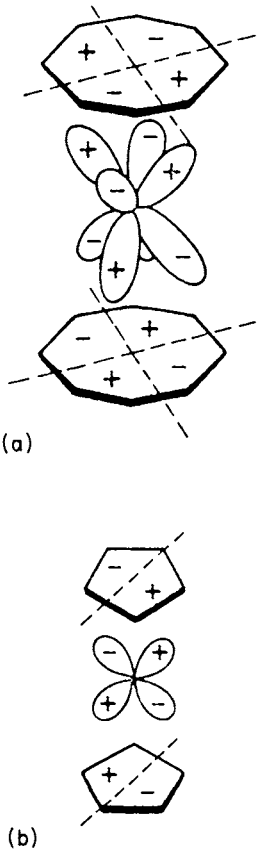

Fig. 22.18 *Illustration of the cognate metal–ligand orbital interactions in (a) uranocene and (b) ferrocene* [124].

NMR studies of uranocenes have focused upon separating contact (hyperfine) and pseudo-contact (dipolar) contributions to the paramagnetically shifted spectra [124, 138, 165, 166, 176] and upon analyzing conformational dynamics [138]. In regard to the former area, the synthesis and spectroscopic characterization of uranocenes with rigid ring substituents [146, 167] has greatly aided in quantifying the geometrically dependent dipolar shifts. The remaining contact shifts can be explained in terms of a spin polarization mechanism in which negative spin density remains in ligand π orbitals. Thus, the mechanism of unpaired spin distribution is similar to that in the $U(C_5H_5)_3R$ and related compounds [168]. The electron–ring proton hyperfine coupling constants in uranocene were estimated to be of the order of 1 MHz, again comparable to the $U(C_5H_5)_3R$ results. Variable-temperature NMR spectroscopy has identified two types of dynamic processes for substituted uranocenes: (i) hindered rotation about the ring-to-substituent C–C bond (e.g. 1,1′-dimesityluranocene) and (ii)

hindered rotation about the η^8 ring–metal bond (e.g. 1,1',4,4'-tetra-t-butyluranocene) [138].

Cyclo-octatetraene complexes of trivalent actinides have also been prepared. The synthesis of anionic neptunium and plutonium complexes is shown below [169]:

$$MX_3 + 2K_2(C_8H_8) \xrightarrow{THF} K(THF)_2^+ M(C_8H_8)^- + 3KX \qquad (22.101)$$
$$M = Np, Pu$$
$$X = Br, I$$

When diglyme was employed as a solvent in the synthesis of the plutonium derivative, the complex $K(diglyme)^+Pu(C_8H_8)_2^-$ was isolated. X-ray powder diffraction data indicate that the two $K(THF)_2^+ M(C_8H_8)_2^-$ compounds are isostructural. The x-ray powder pattern of the plutonium complex prepared in diglyme is similar to that of $K(diglyme)^+Ce(C_8H_8)_2^-$, which possesses a $Ce(C_8H_8)_2^-$ sandwich structure with the alkali-metal ion coordinated to one face of a C_8H_8 ring and to the three diglyme oxygen atoms [170]. Air oxidation converts the $M(C_8H_8)_2^-$ complexes to the known tetravalent $Np(C_8H_8)_2$ and $Pu(C_8H_8)_2$ organometallics. $K(THF)_2Np(C_8H_8)_2^-$ was found by ^{237}Np Mössbauer spectroscopy to exhibit the highest isomer shift ever reported for a Np(III) compound, $+3.92\ cm\ s^{-1}$ versus $NpAl_2$. Nevertheless, the increase in shift over that of $NpCl_3$ ($+3.54\ cm\ s^{-1}$) is not nearly so great as that exhibited by $Np(C_8H_8)_2$ ($+1.94\ cm\ s^{-1}$) compared to $NpCl_4$ ($-0.34\ cm\ s^{-1}$). These trends suggest that the covalence of the metal–ligand bonding is not as great in $Np(C_8H_8)_2^-$ as in $Np(C_8H_8)_2$. A bis(cyclo-octatetraene)americate(III) complex has been prepared as follows [171]:

$$AmI_3 + 2K_2(C_8H_8) \xrightarrow{THF} KAm(C_8H_8)_2 + 2KI \qquad (22.102)$$

The optical spectrum of this compound in THF solution exhibits red shifts of bands of the order of 250–450 cm^{-1} compared to the Am(III) ion in aqueous solution, suggesting a small degree of covalence in the metal–ligand bonding. Attempts to reduce $KAm(C_8H_8)_2$ to an Am(II) derivative have not been successful.

The reactions

$$U(C_8H_8)_2 + LiC_8H_{10} \xrightarrow{THF} Li^+U(C_8H_8)_2^- + C_8H_{10} \qquad (22.103)$$

$$UCl_3 \cdot n THF + 2K_2C_8H_8 \xrightarrow{THF} K^+U(C_8H_8)_2^- + 3KCl \qquad (22.104)$$

yield unstable products formulated as U(III) $(C_8H_8)_2^-$ complexes [172].

22.7.2 $M(C_8H_8)X_2$ compounds

'Half-sandwich' complexes of Th(IV) with cyclo-octatetraene and substituted cyclo-octatetraenes are accessible through the approaches [173]:

$$Th(RC_8H_7)_2 + ThCl_4 \xrightarrow{THF} 2(RC_8H_7)ThCl_2 \cdot 2THF \qquad (22.105)$$

$$Th(RC_8H_7)_2 + 2HCl \xrightarrow{THF} (RC_8H_7)ThCl_2 \cdot 2THF + C_8H_{10} \qquad (22.106)$$

$$Th[1,3,5,7\text{-}(CH_3)_4C_8H_4]_2 + ThCl_4 \xrightarrow{THF} 2[1,3,5,7\text{-}(CH_3)_4C_8H_4]ThCl_2 \cdot 2THF \qquad (22.107)$$

Analogous half-sandwich tetrahydroborate complexes can be prepared as shown [174, 175]:

$$ThCl_4 + 2LiBH_4 \xrightarrow{THF} 'ThCl_2(BH_4)_2' \qquad (22.108)$$

$$'ThCl_2(BH_4)_2' + K_2C_8H_8 \xrightarrow{THF} (C_8H_8)Th(BH_4)_2 \cdot 2THF \qquad (22.109)$$

$$Th(BH_4)_4 \cdot 2THF + Th(n\text{-}C_4H_9C_8H_7)_2 \xrightarrow{THF} 2Th(n\text{-}C_4H_9C_8H_7)(BH_4)_2 \cdot 2THF \qquad (22.110)$$

Infrared spectra indicate that the BH_4^- ligands are coordinated in a tridentate manner. The diffraction-derived molecular structure of $(C_8H_8)ThCl_2 \cdot 2THF$ (Fig. 22.19) confirms the half-sandwich structural proposal for two crystalline modifications [174]. The structure of the single molecule present in the α form is in good agreement with the two crystallographically non-equivalent molecules in the β form. The average Th–Cl distance is 2.686(6) Å, the average Th–O is 2.57(2) Å, and the average Th–C(ring) is 2.72(2) Å. The Cl–Th–Cl angles range from 99.0(3)° to 109.6(1)° and the O–Th–O angles from 130.6(2)° to 136.5(3)°.

ACKNOWLEDGMENTS

This work was supported at Northwestern University by the National Science Foundation (Grant CHE8306255) and the Department of Energy (Contract DEACO2-81ER11980), and at the Lawrence Berkeley Laboratory by the Director, Office of Energy Research, Office of Basic Energy Sciences, Chemical Sciences Division of the Department of Energy, under Contract DEACO3-76SF00098.

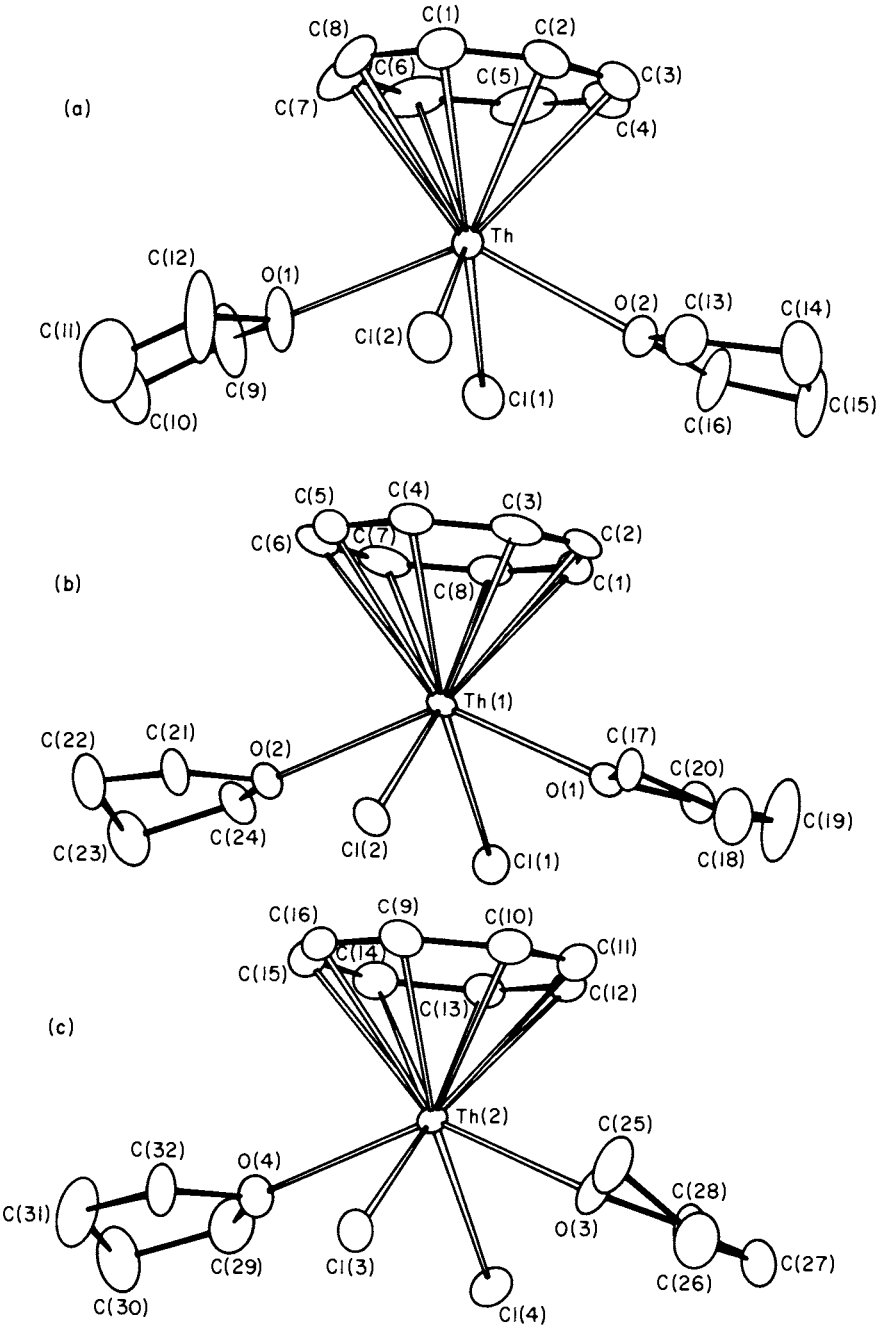

Fig. 22.19 *Molecular structures of* $(C_8H_8)ThCl_2 \cdot 2THF$ *in (a)* α*, (b)* β *and (c)* β *crystalline modifications* [174].

REFERENCES

1. Collman, J. P. and Hegedus, L. S. (1980) *Principles and Applications of Organotransition Metal Chemistry*, University Science Books, Mill Valley, CA.
2. Wilkinson, G., Stone, F. G. A., and Abel, E. W. (eds) (1982) *Comprehensive Organometallic Chemistry*, Pergamon Press, Oxford.
3. Gilman, H. (1968) *Advn. Organometal. Chem.*, **7**, 33.
4. Reynolds, L. T. and Wilkinson, G. (1956) *J. Inorg. Nucl. Chem.*, **2**, 246–53.
5. Fischer, E. O. and Triebner, A. (1962) *Z. Naturf. B*, **17**, 276–7.
6. Fischer, E. O. and Hristidu, Y. (1962) *Z. Naturf. B*, **17**, 275–6.
7. Streitwieser, A., Jr and Müller-Westerhoff, U. (1968) *J. Am. Chem. Soc.*, **90**, 7364.
8. Marks, T. J. and Seyam, A. M. (1972) *J. Am. Chem. Soc.*, **94**, 6545–6.
9. Brandi, G., Brunelli, M., Lugli, G., and Mazzei, A. (1973) *Inorg. Chim. Acta*, **7**, 319–22.
10. Gebala, A. E. and Tsutsui, M. (1973) *J. Am. Chem. Soc.*, **95**, 91–3.
11. Marks, T. J. (1982) *Science*, **217**, 989–97.
12. Marks, T. J. and Ernst, R. D. (1982) in ref. 2, ch. 21.
13. Fagan, P. J., Maatta, E. A., Manriquez, J. M., Moloy, K. G., Seyam, A. M., and Marks, T. J. (1982) in *Actinides in Perspective* (ed. N. Edelstein), Plenum Press, Oxford, pp. 433–52.
14. Marks, T. J. and Fischer, R. D. (eds) (1979) *Organometallics of the f-Elements*, Reidel, Dordrecht.
15. Marks, T. J. and Fragalà, I. L. (eds) (1985) *Fundamental and Technological Aspects of Organo-f-Element Chemistry*, Reidel, Dordrecht.
16. Wilke, G. *et al.* (1966) *Angew. Chem., Int. Edn*, **5**, 151–64.
17. Lugli, G., Marconi, W., Mazzei, A., Paladino, N., and Pedretti, U. (1969) *Inorg. Chim. Acta*, **3**, 253–4.
18. Brunelli, M., Lugli, G., and Giacometti, G. (1973) *J. Magn. Reson.*, **9**, 247–54.
19. Lugli, G., Mazzei, A., and Poggio, S. (1974) *Makromol. Chem.*, **175**, 2021.
20. Brunelli, M., Perego, G., Lugli, G., and Mazzei, A. (1979) *J. Chem. Soc., Dalton Trans.*, 861–8.
21. Vanderhooft, N. C. and Ernst, R. D. (1982) *J. Organomet. Chem.*, **233**, 313–19.
22. Kanellakopulos, B., Fischer, E. O., Dornberger, E., and Baumgärtner, F. (1980) *J. Organomet. Chem.*, **24**, 507–14.
23. Zanella, P., Rossetto, G., DePaoli, G., and Traverso, O. (1980) *Inorg. Chim. Acta*, **44**, L155–6.
24. Chang, C. C., Sung-Yu, N. K., Hseu, C. S., and Chang, C. T. (1979) *Inorg. Chem.*, **18**, 885–6.
25. Moody, D. C. and Odom, J. D. (1979) *J. Inorg. Nucl. Chem.*, **41**, 533–5.
26. Wasserman, H. J., Zozulin, A. J., Moody, D. C., Ryan, R. R., and Salazar, K. V. (1983) *J. Organomet. Chem.*, **254**, 305–11.
27. Karraker, D. G. and Stone, J. A. (1972) *Inorg. Chem.*, **11**, 1742–6.
28. Mugnier, Y., Dormand, A., and Laviron, E. (1982) *J. Chem. Soc., Chem. Commun.*, 257–8.
29. Kalina, D. G., Marks, T. J., and Wachter, W. A. (1977) *J. Am. Chem. Soc.*, **99**, 3877–9.
30. Bruno, J. W., Kalina, D. G., Mintz, E. A., and Marks, T. J. (1982) *J. Am. Chem. Soc.*, **104**, 1860–9.
31. Kanellakopulos, B., Dornberger, E., and Billich, H. (1974) *J. Organomet. Chem.*, **76**, C42–4.

32. Brennan, J. G. and Andersen, R. A. (1985) *J. Am. Chem. Soc.*, **107**, 514–16.
33. Kanellakopulos, B., Dornberger, E., and Baumgärtner, F. (1974) *Inorg. Nucl. Chem. Lett.*, **10**, 155–60.
34. Baumgärtner, F., Fischer, E. O., Kanellakopulos, B., and Laubereau, P. (1965) *Angew. Chem., Int. Edn*, **4**, 878.
35. Baumgärtner, F., Fischer, E. O., Kanellakopulos, B., and Laubereau, P. (1966) *Angew. Chem., Int. Edn*, **5**, 134.
36. Baumgärtner, F., Fischer, E. O., Billich, H., Dornberger, E., Kanellakopulos, B., Roth, W., and Steiglitz, L. (1970) *J. Organomet. Chem.*, **22**, C17–19.
37. Laubereau, P. and Burns, J. (1970) *Inorg. Nucl. Chem. Lett.*, **6**, 59–63.
38. Fischer, E. O. and Fischer, H. (1963) *J. Organomet. Chem.*, **6**, 141–50.
39. Laubereau, P. and Burns, J. H. (1970) *Inorg. Chem.*, **9**, 1091–5.
40. Baumgärtner, F., Fischer, E. O., and Laubereau, P. (1967) *Radiochim. Acta*, **7**, 188–97.
41. Fischer, E. O. and Fischer, H. (1966) *J. Organomet. Chem.*, **6**, 141–8.
42. Nugent, L. J., Laubereau, P. G., Werner, G. K., and van der Sluis, K. L. (1971) *J. Organomet. Chem.*, **27**, 365–72.
43. Laubereau, P. (1970) *Inorg. Nucl. Chem. Lett.*, **6**, 611–16.
44. Reid, A. F. and Wailes, R. D. (1966) *Inorg. Chem.*, **5**, 1213–16.
45. Burns, J. H. (1974) *J. Organomet. Chem.*, **69**, 235–43.
46. von Ammon, R., Kanellakopulos, B., and Fischer, R. D. (1968) *Chem. Phys. Lett.*, **2**, 513–15.
47. Amberger, H.-D., Fischer, R. D., and Kanellakopulos, B. (1976) *Z. Naturf.*, **31b**, 12–21.
48. Amberger, H.-D. (1976) *J. Organomet. Chem.*, **110**, 59–66.
49. Tel'noi, V. I., Rabinovich, I. B., Leonov, M. R., Solov'eva, G. V., and Gramoteeva, N. I. (1979) *Dokl. Akad. Nauk SSSR*, **245**, 1430–2.
50. Connor, J. A. (1977) *Topics Curr. Chem.*, **71**, 71–110.
51. Baumgärtner, F., Fischer, E. O., Kanellakopulos, B., and Laubereau, P. (1969) *Angew. Chem., Int. Edn*, **8**, 202.
52. Baumgärtner, F., Fischer, E. O., Kanellakopulos, B., and Laubereau, P. (1968) *Angew. Chem., Int. Edn*, **7**, 634.
53. Kanellakopulos, B., Klenze, R., Schilling, G., and Stollenwerk, A. H. (1980) *J. Chem. Phys.*, **72**, 6311–12.
54. Marks, T. J., Seyam, A. M., and Wachter, W. A. (1976) *Inorg. Synth.*, **XVI**, 147–51.
55. Fischer, R. D., Klähne, E., and Sienel, G. R. (1982) *J. Organomet. Chem.*, **238**, 99–111, and references therein.
56. Wong, C., Yen, T., and Lee, T. (1965) *Acta Crystallogr.*, **18**, 340–5.
57. Leong, J., Hodgson, K. O., and Raymond, K. N. (1973) *Inorg. Chem.*, **12**, 1329–35.
58. Kanellakopulos, B. (1979) in ref. 14, chap. 1.
59. von Ammon, R., Kanellakopulos, B., and Fischer, R. D. (1969) *Inorg. Nucl. Chem. Lett.*, **5**, 219–24.
60. Ryan, R. R., Penneman, R. A., and Kanellakopulos, B. (1975) *J. Am. Chem. Soc.*, **97**, 4258–60.
61. Fischer, R. D., Klähne, E., and Köpf, J. (1978) *Z. Naturf.*, **33b**, 1393–7.
62. Bagnall, K. W., Plews, M. J., Brown, D., Fischer, R. D., Klähne, E., Landgraf, G. W., and Sienel, G. R. (1982) *J. Chem. Soc., Dalton Trans.*, 1999–2007.
63. Bombieri, G., Benetollo, F., Bagnall, K. W., Plews, M. J., and Brown, D. (1983) *J. Chem. Soc., Dalton Trans.*, 45–9.

64. Bombieri, G., Benetollo, F., Klähne, E., and Fischer, R. D. (1983) *J. Chem. Soc., Dalton, Trans.*, 1115–21.
65. Marks, T. J. and Kolb, J. R. (1975) *J. Am. Chem. Soc.*, **97**, 27–33.
66. Marks, T. J. and Kolb, J. R. (1977) *Chem. Rev.*, **77**, 263–93.
67. Amberger, H.-D. and Sienel, G. R. (1976) *Z. Naturf.*, **31b**, 769–73.
68. Amberger, H.-D. (1976) *J. Organomet. Chem.*, **116**, 219–29.
69. von Ammon, R., Fischer, R. D., and Kanellakopulos, B. (1972) *Chem. Ber.*, **105**, 45–62.
70. Fukishima, E. and Larsen, S. D. (1976) *Chem. Phys. Lett.*, **44**, 285–8.
71. Dormond, A. and Duval, C. (1979) *J. Organomet. Chem.*, **178**, C5–7.
72. Dormond, A. (1983) *J. Organomet. Chem.*, **256**, 47–56.
73. Jamerson, J. D., Masino, A. P., and Takats, J. (1974) *J. Organomet. Chem.*, **65**, C33–6.
74. Takats, J. (1985) in ref. 15, ch. 5.
75. Baumgärtner, F., Fischer, E. O., and Laubereau, P. (1965) *Naturwissenschaften*, **52**, 560.
76. Fischer, E. O., Laubereau, P., Baumgärtner, F., and Kanellakopulos, B. (1966) *J. Organomet. Chem.*, **5**, 583–4.
77. Karraker, D. G. and Stone, J. A. (1979) *Inorg. Chem.*, **18**, 2205–7.
78. Fragalà, I., Ciliberto, E., Fischer, R. D., Sienel, G. R., and Zanella, P. (1976) *J. Organomet. Chem.*, **120**, C9–12.
79. Ernst, R. D., Kennelly, W. J., Day, C. S., Day, V. W., and Marks, T. J. (1979) *J. Am. Chem. Soc.*, **101**, 2656–64.
80. Bagnall, K. W., Edwards, J., and Tempest, A. C. (1978) *J. Chem. Soc., Dalton Trans.*, 295–8.
81. Jamerson, J. D. and Takats, J. (1974) *J. Organomet. Chem.*, **78**, C23–5.
82. Zanella, P., DePaoli, G., Bombieri, G., Zanotti, G., and Rossi, R. (1977) *J. Organomet. Chem.*, **142**, C21–4.
83. Bagnall, K. W., Edwards, J., Rickard, C. E. F., and Tempest, A. C. (1979) *J. Inorg. Nucl. Chem.*, **41**, 1321–3.
84. Bagnall, K. W., Beheshti, A., Edwards, J., Heatley, F., and Tempest, A. C. (1979) *J. Chem. Soc., Dalton Trans.*, 1241–5.
85. Doretti, L., Zanella, P., Faragalia, G., and Faleschini, S. (1972) *J. Organomet. Chem.*, **43**, 339–41.
86. Bagnall, K. W. and Edwards, J. (1974) *J. Organomet. Chem.*, **80**, C14–16.
87. Bagnall, K. W., Beheshti, A., and Heatley, F. (1978) *J. Less Common Metals*, **61**, 63–9.
88. Bombieri, G., DePaoli, G., DelPra, A., and Bagnall, K. W. (1978) *Inorg. Nucl. Chem. Lett.*, **14**, 359–61.
89. Benetollo, F., Bombieri, G., DePaoli, G., Zanella, P., and Bagnall, K. W. (1979) *Proc. 9th Int. Conf. on Organometallic Chemistry*, Dijon, France, September, Abstracts, p. 63.
90. Laubereau, P. G., Ganguly, L., Burns, J. H., Benjamin, B. M., Atwood, J. L., and Selbin, J. (1971) *Inorg. Chem.*, **10**, 2274–80.
91. Burns, J. H. and Laubereau, P. G. (1971) *Inorg. Chem.*, **10**, 2789–92.
92. Goffart, J., Fuger, J., Gilbert, B., Hocks, L., and Duyckaerts, G. (1975) *Inorg. Nucl. Chem. Lett.*, **11**, 569–83.
93. Goffart, J. and Duyckaerts, G. (1978) *Inorg. Nucl. Chem. Lett.*, **14**, 15–20.
94. Goffart, J., Gilbert, B., and Duyckaerts, G. (1977) *Inorg. Nucl. Chem. Lett.*, **13**, 189–96.

95. Goffart, J., Michel, G., Gilbert, B. P., and Duyckaerts, G. (1978) *Inorg. Nucl. Chem. Lett.*, **14**, 393–403.
96. Goffart, J., Desreux, J. F., Gilbert, B. P., Delsa, J. L., Renkin, J. M., and Duyckaerts, G. (1981) *J. Organomet. Chem.*, **209**, 281–96.
97. Spirlet, M. R., Rebizant, J., and Goffart, J. (1982) *Acta Crystallogr. B*, **38**, 2400–4.
98. Meunier-Piret, J., Declercq, J. P., German, G., and van Meersche, M. (1980) *Bull. Soc. Chim. Belg.*, **89**, 121–4.
99. Goffart, J. (1979) in ref. 14, ch. 15.
100. Goffart, J., Meunier-Piret, J., Duyckaerts, G. (1980) *Inorg. Nucl. Chem. Lett.*, **16**, 233–44.
101. Meunier-Piret, J., Germain, G., Declerq, J. P., and van Meersche, M. (1980) *Bull. Soc. Chim. Belg.*, **89**, 241–5.
102. Manriquez, J. M., Fagan, P. J., and Marks, T. J. (1978) *J. Am. Chem. Soc.*, **100**, 3939–41.
103. Green, J. C. and Watts, O. (1978) *J. Organomet. Chem.*, **153**, C40.
104. Fagan, P. J., Manriquez, J. M., Maatta, E. A., Seyam, A. M., and Marks, T. J. (1981) *J. Am. Chem. Soc.*, **103**, 6650–67.
105. Day, V. W. and Marks, T. J., unpublished results.
106. Eigenbrot, C. W., Jr and Raymond, K. N. (1982) *Inorg. Chem.*, **21**, 2653–60.
107. Fagan, P. J., Manriquez, J. M., Vollmer, S. H., Day, C. S., Day, V. W., and Marks, T. J. (1981) *J. Am. Chem. Soc.*, **103**, 2206–20.
108. Duttera, M. R., Day, V. W., and Marks, T. J. (1984) *J. Am. Chem. Soc.*, **106**, 2907–12.
109. Lin, Z., Brock, C. P., and Marks, T. J. (1986) submitted for publication.
110. Finke, R. G., Gaughan, G., and Voegeli, R. (1982) *J. Organomet. Chem.*, **229**, 179–84.
111. Reeb, P., Mugnier, Y., Dormond, A., and Laviron, E. (1982) *J. Organomet. Chem.*, **239**, C1–3.
112. Fagan, P. J., Manriquez, J. M., Marks, T. J., Day, C. S., Vollmer, S. H., and Day, V. W. (1982) *Organometallics*, **1**, 170–80.
113. Mintz, E. A., Moloy, K. G., Marks, T. J., and Day, V. W. (1982) *J. Am. Chem. Soc.*, **104**, 4692–5.
114. Sternal, R. S. and Marks, T. J. (1985) unpublished results.
115. Cymbaluk, T. H., Ernst, R. D., and Day, V. W. (1983) *Organometallics*, **2**, 963–8.
116. Secaur, C. A., Day, V. W., Ernst, R. D., Kennelly, W. F., and Marks, T. J. (1976) *J. Am. Chem. Soc.*, **98**, 3713–15.
117. Marks, T. J. (1977) in *Inorganic Compounds with Unusual Properties* (ACS Adv. Chem. Ser. no. 150), American Chemical Society, Washington DC, pp. 232–263.
118. Fendrick, C. M., Mintz, E. A., Schertz, L. D., Marks, T. J., and Day, V. W. (1984) *Organometallics*, **3**, 819–21.
119. Fendrick, C. M., Day, V. W., and Marks, T. J. (1986) submitted for publication.
120. Cymbaluk, T. H., Liu, J.-Z., and Ernst, R. D. (1983) *J. Organomet. Chem.*, **255**, 311–15.
121. Ernst, R. D. and Cymbaluk, T. H. (1982) *Organometallics*, **1**, 708–13.
122. Cesari, M., Pedretti, U., Lugli, G., and Marconi, W. (1971) *Inorg. Chim. Acta*, **5**, 439–44.
123. Cotton, F. A. and Schwotzer, W. (1985) *Organometallics*, **4**, 942–3.
124. Streitwieser, A., Jr (1979) in ref. 14, ch. 5.
125. Chang, C. C., Sung-Yu, N. K., Hseu, C. S., and Chang, C. T. (1979) *Inorg. Chem.*, **18**, 885–6.

126. Rieke, R. D. and Rhyne, L. D. (1979) *J. Org. Chem.*, **44**, 3445–6.
127. Starks, D. F. and Streitwieser, A., Jr (1973) *J. Am. Chem. Soc.*, **95**, 3423–4.
128. Cernia, E. and Mazzei, A. (1974) *Inorg. Chim. Acta*, **10**, 239–52.
129. Starks, D. F., Parson, T. C., Streitwieser, A., Jr, and Edelstein, N. (1974) *Inorg. Chem.*, **13**, 1307–8.
130. Avdeef, A., Raymond, K. N., Hodgson, K. O., and Zalkin, A. (1972) *Inorg. Chem.*, **11**, 1083–8.
131. Raymond, K. N. (1979) in ref. 14, ch. 8.
132. Streitwieser, A., Jr, and Yoshida, N. (1969) *J. Am. Chem. Soc.*, **91**, 7528.
133. Karraker, D. G., Stone, J. A., Jones, E. R., Jr, and Edelstein, N. (1970) *J. Am. Chem. Soc.*, **92**, 4841–5.
134. Goffart, J., Fuger, J., Brown, D., and Duyckaerts, G. (1974) *Inorg. Nucl. Chem. Lett.*, **10**, 413–19.
135. Harmon, C. A., Bauer, D. P., Berryhill, S. R., Hagiwara, K., and Streitwieser, A., Jr (1977) *Inorg. Chem.*, **16**, 2143–7.
136. Miller, J. T. and DeKock, C. W. (1979) *Inorg. Chem.*, **18**, 1305–6.
137. Spiegl, A. and Fischer, R. D. (1979) *Chem. Ber.*, **112**, 116.
138. Streitwieser, A., Jr and Kinsley, S. A. (1985) in ref. 15, ch. 3.
139. Streitwieser, A., Jr and Harmon, C. A. (1973) *Inorg. Chem.*, **12**, 1102–4.
140. Karraker, D. G. (1973) *Inorg. Chem.*, **12**, 1105–8.
141. Streitwieser, A., Jr, Dempf, D., LaMar, G. N., Karraker, D. G., and Edelstein, N. M. (1971) *J. Am. Chem. Soc.*, **93**, 7343–4.
142. LeVanda, C. and Streitwieser, A., Jr (1981) *Inorg. Chem.*, **20**, 656–9.
143. Solar, J. P., Burghard, H. P. G., Banks, R. H., Streitwieser, A., Jr, and Brown, D. (1980) *Inorg. Chem.*, **19**, 2186–8.
144. Hodgson, K. O. and Raymond, K. N. (1973) *Inorg. Chem.*, **12**, 458–66.
145. Zalkin, A., Templeton, D. H., Berryhill, S. R., and Luke, W. D. (1979) *Inorg. Chem.*, **18**, 2287–9.
146. Luke, W. D., Berryhill, S. R., and Streitwieser, A., Jr (1981) *Inorg. Chem.*, **20**, 3086–9.
147. Zalkin, A., Templeton, D. H., Luke, W. D., and Streitwieser, A., Jr (1982) *Organometallics*, **1**, 618–22.
148. Streitwieser, A., Jr, Kluttz, R. Z., Smith, K. A., and Luke, W. D. (1983) *Organometallics*, **2**, 1873–7.
149. Streitwieser, A., Jr and Walker, R. (1975) *J. Organomet. Chem.*, **97**, C41–2.
150. Templeton, L. K., Templeton, D. H., and Walker, R. (1976) *Inorg. Chem.*, **15**, 3000–3.
151. Grant, C. B. and Streitwieser, A., Jr (1978) *J. Am. Chem. Soc.*, **100**, 2433–40.
152. Butcher, J. A., Pagni, R. M., and Chambers, J. Q. (1980) *J. Organomet. Chem.*, **199**, 223–7.
153. Amberger, H.-D., Fischer, R. D., and Kanellakopulos, B. (1975) *Theor. Chim. Acta*, **37**, 105–27.
154. Edelstein, N., Streitwieser, A., Jr, Morrell, D. G., and Walker, R. (1976) *Inorg. Chem.*, **15**, 1397–8.
155. Fragalà, I., Condorelli, G., Zanella, P., and Tondello, E. (1976) *J. Organomet. Chem.*, **122**, 357–63.
156. Green, J. C., Payne, M. P., and Streitwieser, A., Jr (1983) *Organometallics*, **2**, 1707–10.
157. Fragalà, I. and Gulino, A. (1985) in ref. 15, ch. 9.
158. Dallinger, R. F., Stein, P., and Spiro, T. G. (1978) *J. Am. Chem. Soc.*, **100**, 7865–70.
159. Karraker, D. G. (1979) in ref. 14, ch. 13.

160. Hayes, R. G. and Edelstein, N. (1972) *J. Am. Chem. Soc.*, **94**, 8688–91.
161. Warren, K. D. (1977) *Struct. Bond.*, **33**, 98–138.
162. Rösch, N. and Streitwieser, A., Jr (1978) *J. Organomet. Chem.*, **145**, 195–200.
163. Rösch, N. and Streitwieser, A., Jr (1983) *J. Am. Chem. Soc.*, **105**, 7237–40.
164. Rösch, N. (1984) *Inorg. Chim. Acta*, **94**, 297–9.
165. Fischer, R. D. (1979) in ref. 14, ch. 11.
166. Fischer, R. D. (1985) in ref. 15, ch. 8.
167. Spiegl, A. W. and Fischer, R. D. (1979) *Chem. Ber.*, **112**, 116–27.
168. Marks, T. J., Seyam, A. M., and Kolb, J. R. (1973) *J. Am. Chem. Soc.*, **95**, 5529–39.
169. Karraker, D. G. and Stone, J. A. (1974) *J. Am. Chem. Soc.*, **96**, 6885–90.
170. Hodgson, K. O. and Raymond, K. N. (1972) *Inorg. Chem.*, **11**, 3030–5.
171. Karraker, D. G. (1977) *J. Inorg. Nucl. Chem.*, **39**, 87–9.
172. Billiau, F., Folcher, G., Marquet-Ellis, H., Rigny, P., and Saito, E. (1981) *J. Am. Chem. Soc.*, **103**, 5603–4.
173. LeVanda, C., Solar, J. P., and Streitwieser, A., Jr (1980) *J. Am. Chem. Soc.*, **102**, 2128–9.
174. Zalkin, A., Templeton, D. H., LeVanda, C., and Streitwieser, A., Jr (1980) *Inorg. Chem.*, **19**, 2560–3.
175. Solar, J. P., Streitwieser, A., Jr, and Edelstein, N. M. (1980) in *Lanthanide and Actinide Chemistry and Spectroscopy* (ACS Symp. Ser. no. 131), American Chemical Society, Washington DC, pp. 81–91.
176. Luke, W. D., and Streitwieser, A., Jr (1980) in *Lanthanide and Actinide Chemistry and Spectroscopy* (ACS Symp. Ser. no. 131), American Chemical Society, Washington DC, pp. 93–140.
177. Finke, R. G., Hirose, Y., and Gaughan, G. (1981) *J. Chem. Soc., Chem. Commun.*, 232–4.
178. Finke, R. G., Shiraldi, D. A., and Hirose, Y. (1981) *J. Am. Chem. Soc.*, **103**, 1873–6.
179. Streitwieser, A., Jr, Kinsley, S. A., Rigsbee, J. T., Fragalà, I. L., Ciliberto, E., Rösch, N. (1985) *J. Am. Chem. Soc.*, **107**, 7786–8.

CHAPTER TWENTY THREE

ORGANOACTINIDE CHEMISTRY: PROPERTIES OF COMPOUNDS WITH ACTINIDE–CARBON, ACTINIDE–HYDROGEN, AND ACTINIDE–TRANSITION-METAL σ BONDS

Tobin J. Marks

23.1 INTRODUCTION

In contrast to the relatively early flowering of organotransition-metal chemistry (1955 to the present), the corresponding development of actinide organometallic chemistry has taken place largely within the past 15 or so years. During this period, 5f organometallic science has blossomed, and it is now apparent that the actinides have a rich, intricate, and highly informative organometallic chemistry. Intriguing parallels to and sharp differences from the d-block elements have emerged. Several recent review articles [1–3] and two monographs [4, 5] attest to the broad and rapidly expanding scope of this field. They also offer a great deal of introductory information.

The purpose of this chapter is to survey and to analyze, in a necessarily brief and selective manner, actinide organometallic chemistry involving metal–carbon, metal–hydrogen, and metal–metal σ bonds. Such linkages are fundamental building blocks of modern organometallic chemistry and catalysis. The nature of actinide complexes based upon coordination to multihapto organic π-electron systems was surveyed in Chapter 22.

23.2 ACTINIDE CARBONYLS

23.2.1 Zero-valent carbonyls

Although stable, homoleptic, mononuclear and polynuclear complexes of carbon monoxide are known for almost every transition element, a number of experiments indicate that actinide carbonyls (e.g. $U(CO)_n$) are not stable at ambient temperature. However, uranium carbonyls can be prepared in cryogenic matrices [6, 7]. Co-condensation of uranium vapor with CO in a 4 K argon matrix yields species identifiable by infrared spectroscopy (in particular, ν_{CO}) as uranium carbonyls, $U(CO)_n$. Derived force constants suggest bonding patterns rather similar to those observed for zero-valent early transition-element and lanthanide carbonyls. However, decomposition of these actinide carbonyls occurs at temperatures above about 30 K.

23.2.2 Other carbonyls

In matrix experiments similar to those discussed above, Margrave and co-workers [8] found that the condensation of UF_4 and CO in an Ar matrix at 4 K yields products whose infrared spectra are indicative of metal carbonyls. The C–O stretching frequency of 2184 cm^{-1} indicates that U(IV) is a strong σ acceptor and poor π donor.

A number of organoactinide CO activation patterns also suggest the intermediacy of carbonyl complexes along the respective reaction coordinates (*vide infra*). Furthermore, extended Hückel molecular-orbital studies [9, 10] suggest that organoactinide carbonyls may be stable, although the bonding will be largely ligand-to-metal σ in character. Evidence for unstable $[(CH_3)_3SiC_5H_4]UCO$ has also been reported recently [105].

23.3 ACTINIDE–CARBON σ BONDS

23.3.1 Homoleptic compounds

The synthesis of isolable actinide complexes containing only alkyl, aryl, or alkenyl (hydrocarbyl) ligands has been an important goal since the early 1940s [11]. However, reactions such as

$$UCl_4 + 4RLi \xrightarrow[\text{or ether}]{\text{hydrocarbons}} \text{organic products} + U + 4LiCl \qquad (23.1)$$

are known to afford thermally unstable reaction mixtures. Marks and Seyam [12] showed that the products of equation (23.1), long assumed to be uranium tetraalkyls, readily undergo β-hydride elimination for R = n-butyl; for example

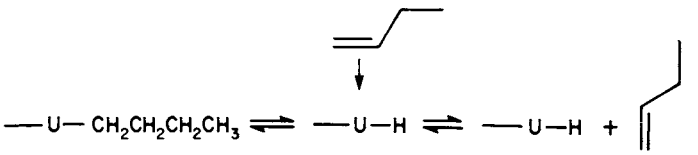

(23.2)

No effort was made to characterize the intermediate organometallic species of this rather complex, heterogeneous reaction, nor were specific structures or stoichiometries advanced. In later work, Evans and co-workers [13] reported that, for R = t-butyl in octane, the reaction did not proceed to completion. Whether the reasons were thermodynamic or kinetic was not resolved. Seyam [14] subsequently demonstrated that the results of Evans were largely an artifact of inadequate UCl_4 dispersion and reaction agitation. The reaction can be made to proceed to completion, and any assertion that it does not on thermodynamic grounds is unsupported.

In an effort to enhance thermal stability by saturating the metal coordination sphere, Sigurdson and Wilkinson [15] studied the reaction of UCl_4 with lithium reagents in stoichiometric excess:

$$UCl_4 + \text{excess } RLi \xrightarrow{S} Li_2UR_6 \cdot 8S + 4LiCl \qquad (23.3)$$

$R = CH_3, C_6H_5, CH_2Si(CH_3)_3$
$S =$ diethyl ether, THF

The products were formulated as hexaalkyl dianions, $[LiS_4]_2^{2+}UR_6^{2-}$. Although these compounds decompose thermally below room temperature, it proved possible partially to characterize them. Some of the spectroscopic and magnetic properties are rather unusual [2]. In reaction with tetramethylethylenediamine (TMEDA), the $Li_2UR_6 \cdot 8S$ complexes yield $Li_2UR_6 \cdot 7TMEDA$ derivatives. Sigurdson and Wilkinson [15] also investigated pentavalent uranium chemistry:

$$U_2(OC_2H_5)_{10} + \text{excess } RLi \longrightarrow 2Li_3UR_8 \cdot 3\text{dioxane} + 10LiOC_2H_5 \qquad (23.4)$$

$R = CH_3, CH_2Si(CH_3)_3, CH_2C(CH_3)_3$

Eight-coordinate UR_8^{3-} anions with $Li(\text{dioxane})^+$ cations capping the faces of the coordination polyhedra were proposed.

Investigations of presumed thorium tetraalkyls formed via

$$ThCl_4 + 4RLi \xrightarrow{\text{ether}} \text{products} \qquad (23.5)$$

revealed products of low thermal stability and β-hydride elimination products for R = n-butyl [16]. In contrast, Lauke, Swepston, and Marks [17] found that a crystalline heptamethylthorate complex could be prepared with excess methyllithium in the presence of TMEDA:

$$ThCl_4 + \text{excess } CH_3Li + \text{excess TMEDA} \xrightarrow[-78°C]{\text{ether}} [Li(TMEDA)]_3Th(CH_3)_7 \cdot TMEDA + 4LiCl \qquad (23.6)$$

The complex is stable at room temperature for many hours and can be characterized by standard methods. The molecular structure has been determined by x-ray diffraction and is illustrated in Fig. 23.1. The thorium ion is coordinated to seven methyl groups in a distorted monocapped trigonal prismatic pattern. Six of the methyl groups (Th–CH_3 = 2.667(8)–2.765(9) Å) are also coordinated pairwise to $Li(TMEDA)^+$ ions while the seventh (Th–CH_3 = 2.571(9) Å) is not. This complex reacts rapidly with H_2 and CO to yield hydride and migratory insertion products, respectively.

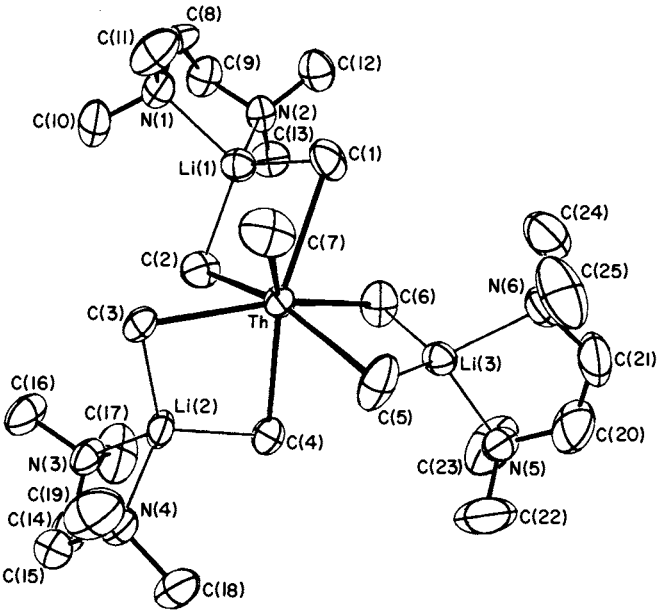

Fig. 23.1 *Perspective ORTEP drawing of the non-hydrogen atoms in* $[Li(TMEDA)]_3Th(CH_3)_7 \cdot TMEDA$ [17]. *Individual bond lengths* (Å) *and angles* (*deg*) *of interest include: Th–C*(1) = 2.698(8), *Th–C*(2) = 2.700(8), *Th–C*(3) = 2.655(8), *Th–C*(4) = 2.765(9), *Th–C*(5) = 2.667(8), *Th–C*(6) = 2.723(9), *Th–C*(7) = 2.571(9), *mean Li–C*(*methyl*) = 2.18(3), *mean Li–N* = 2.12(2); *C*(1)–*Th–C*(2) = 84.1(2), *C*(2)–*Th–C*(3) = 74.8(3), *C*(3)–*Th–C*(4) = 84.6(2), *C*(4)–*Th–C*(5) = 76.6(3), *C*(5)–*Th–C*(6) = 84.6(3), *C*(6)–*Th–C*(7) = 132.9(3).

Seyam [18] studied the reaction of lithium and Grignard reagents with uranyl chloride in ethereal and hydrocarbon media. The products of these reactions are thermally unstable; however, the nature of the organic decomposition products is informative. For R = phenyl, the major products are benzene and biphenyl (the latter could arise via reductive elimination in a 'UO_2R_2' intermediate). For R = CH_3 and vinyl, the predominant products are the corresponding RH molecules, while for R = i-C_3H_7, n-C_4H_9, and t-C_4H_9, the products are suggestive of β-hydride elimination processes.

There is some question as to whether homoleptic benzyls such as tetrabenzylthorium [19]

$$ThCl_4 + 4LiCH_2C_6H_5 \xrightarrow[-20°C]{THF} Th(CH_2C_6H_5)_4 + 4LiCl \qquad (23.7)$$

can legitimately be classified as monohapto-hydrocarbyls. Analogous group IV [20] and $Th[(CH_3)_5C_5]R_3$ (*vide infra*) complexes display significant multihapto coordination (*1*), which may well contribute to the thermal stability.

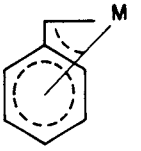

(*1*)

23.3.2 Cyclopentadienyl compounds

The general properties of cyclopentadienyl ligands are introduced in Chapter 22. Extensive classes of tris(cyclopentadienyl)thorium, uranium, and neptunium hydrocarbyls (Cp = η^5-C_5H_5) have been prepared since the mid-1970s:

$$Cp_3ThCl \xrightarrow{RMgX \text{ or } RLi} Cp_3ThR \qquad (23.8)$$

R = n-C_3H_7, i-C_3H_7, n-C_4H_9, neopentyl, cyclohexyl, allyl, 2-*cis*-2-butenyl, 2-*trans*-2-butenyl

$$Cp_3UCl \xrightarrow{RMgX \text{ or } RLi} Cp_3UR \qquad (23.9)$$

R = CH_3, n-C_3H_7, i-C_3H_7, n-C_4H_9, t-C_4H_9, neopentyl, ferrocenyl, allyl, 2-methylallyl, vinyl, C_6H_5, C_6F_5, *p*-$C_6H_4U(C_5H_5)_3$, C_2H, $C_2C_6H_5$, *p*-tolyl, benzyl, 2-*cis*-2-butenyl, 2-*trans*-2-butenyl, $(C_5H_4)Fe(C_5H_4)U(C_5H_5)_3$

$$Cp_3NpCl \xrightarrow{RLi} Cp_3NpR \qquad (23.10)$$

R = n-C_4H_9

The properties of these complexes have been reviewed in great detail [2, 21]. A representative structural study [22], illustrating the 'pseudo-tetrahedral' $M(C_5H_5)_3X$ coordination geometry, is shown in Fig. 23.2. Theoretical studies on the fictitious molecule $Cp_3UCH_3^{2+}$ [9] or on Cp_3UCH_3 [10] reveal rather small U–C(Cp) overlap populations, but large U–CH_3 overlap populations (comparable to those in typical transition-metal alkyls).

In thermochemical investigations, Sonnenberger, Morss, and Marks [23] have determined Cp_3ThR thorium–alkyl ligand bond disruption enthalpies

$$D(Cp_3Th\text{–}R) = \Delta H_f^\circ(Cp_3Th(g)) + \Delta H_f^\circ(R\cdot(g)) - \Delta H_f^\circ(Cp_3Th\text{–}R(g)) \quad (23.11)$$

for the gas-phase process

$$Cp_3ThR(g) \rightarrow Cp_3Th(g) + R\cdot(g) \quad (23.12)$$

for a variety of R ligands. The procedure involves the measurement of alcoholysis enthalpies

$$Cp_3Th\text{–}R + R'OH \rightarrow Cp_3Th\text{–}OR' + RH \quad (23.13)$$

by anaerobic batch titration calorimetry, and derived D(Th–R) value scales are 'anchored' to reasonable estimates of D(Th–OR'). In this sense, relative D(Th–R) parameters are highly accurate, while absolute values are subject to somewhat greater uncertainty. The results, derived for both the solution and gas phases, are set out in Table 23.1. Relative to other metal hydrocarbyls [24, 25], thorium–carbon σ bonds appear to be relatively 'strong'. Trends as a function of R are similar to some transition-metal and other organothorium systems (*vide infra*).

In the area of photochemistry, Marks and co-workers [26, 27] showed, on the basis of product yields, products, scavenging experiments, quantum yields, and

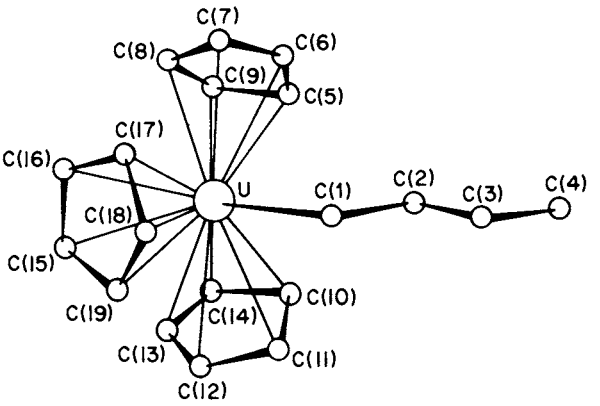

Fig. 23.2 *Perspective view of the non-hydrogen atoms in the molecule* $U(C_5H_5)_3(n\text{-}C_4H_9)$ [22]. *The U–C(1) distance is* 2.43(2) Å, *the mean U–C (ring) distance is* 2.73(1) Å, *and the U–C(1)–C(2) angle is* 129(2)°.

Table 23.1 *Experimental bond disruption enthalpies for Cp_3ThR complexes* (kJ mol^{-1})[a].

Compound	*D*(Th–R(gas))[b]	*D*(Th–R(soln))[b]
Cp_3ThCH_3	346.0 (4.6)	374.9 (4.6)
$Cp_3ThCH(CH_3)_2$	323.4 (11.3)	342.2 (10.9)
$Cp_3ThCH_2C(CH_3)_3$	325.9 (12.6)	333.0 (11.7)
$Cp_3ThCH_2Si(CH_3)_3$	360.2 (15.1)	367.8 (15.1)
$Cp_3ThCH_2C_6H_5$	325.9 (9.2)	315.1 (9.2)

[a] Quantities in parentheses are two standard deviations (2σ) for 6–10 determinations.
[b] Error limits do not include uncertainties that are constant throughout the series.

isotopic labeling, that $Th(C_5E_5)_3R$ complexes (E = H, D; R = i-C_3H_7, n-C_4H_9) undergo photoinduced β-hydride elimination:

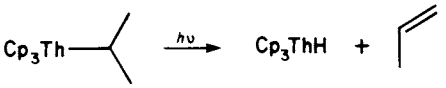

(23.14)

(23.15)

A secondary reaction pathway also involves hydrogen-atom abstraction from cyclopentadienyl ligands (as in the thermolysis pathway) or from the solvent. For Cp_3UR complexes in aromatic solvents, the same mechanistic tests reveal that photoinduced β-hydride elimination occurs, but is no longer the major pathway. Rather, hydrogen-atom abstraction from the cyclopentadienyl ligands predominates, with lesser abstraction also occurring from the solvent molecules. Photolysis in THF significantly increases the yield of Cp_3U.

Klähne *et al.* [28] studied the simultaneous photolysis and thermolysis of Cp_3UR compounds (R = CH_3, n-C_4H_9) generated *in situ* in THF at 60°C. Based on product identities in the gas phase and qualitative electron paramagnetic resonance (EPR) spin trapping experiments, it appears that part of the reaction can occur by a homolytic radical pathway. That β-hydride elimination is a minor pathway is in agreement with the above results of Marks *et al.* [27]. In further studies of Cp_3UR photochemistry (R = n-C_4H_9, i-C_4H_9, i-C_3H_7) by the same group, Burton *et al.* [29] again reported the absence of photochemical β-hydride elimination products. Hydrocarbon product identity as well as spin trapping experiments suggest a free-radical pathway. However, it was also noted that thermal reactions between Cp_3UR compounds and the spin traps occur readily.

Sonnenberger, Mintz, and Marks [30, 31] have studied the mechanistic aspects of migratory CO insertion for a series of Cp_3ThR complexes (R = i-C_3H_7, s-C_4H_9, neo-C_5H_{11}, n-C_4H_9, $CH_2Si(CH_3)_3$, CH_3, and $CH_2C_6H_5$). Under the conditions employed, insertion

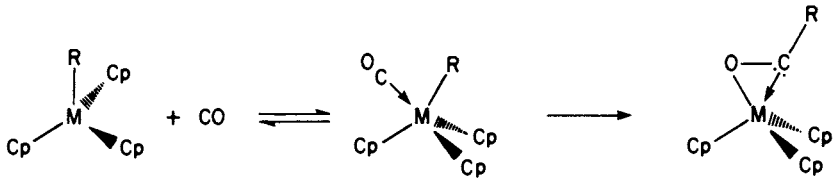

(23.16)

is first order in thorium complex and first order in CO. In the above order of R ligands, the relative rates of reaction are 42:18:1.3:1.0:0.02:0.01: < 0.01. In the case of R = CH_3, i-C_3H_7, n-C_4H_9, neo-C_5H_{11}, and s-C_4H_9, 'carbene-like' (i.e. resembling 'anchored' Fischer carbene complexes in spectroscopic and chemical properties) dihapto-acyl insertion products, $Th(C_5H_5)_3(\eta^2\text{-COR})$ ((*2*), (*3*)), could be isolated.

(*2*) (*3*)

However, for R = i-C_3H_7 and $CH_2Si(CH_3)_3$, only 1,2 rearrangement products could be isolated:

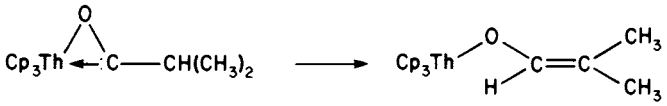

(23.17)

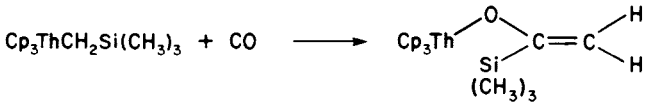

(23.18)

The relative rates of insertion appear to reflect steric as well as electronic factors, and there is a significant correlation with the Cp_3Th–R bond disruption enthalpies discussed above. It was also found that the rate of CO insertion could be significantly accelerated by photolysis. However, secondary reactions of the resulting acyl were noted. A comparative study of CO_2 migratory insertion to yield bidentate carboxylates:

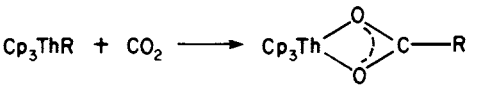

(23.19)

revealed that carboxylation is significantly slower than carbonylation (a factor of 50 for $Th(C_5H_5)_3CH_3$; a factor of 10^5 for $Th(C_5H_5)_3$ (i-C_3H_7)) and that, for the above two compounds, sensitivity of the rate to the nature of R is considerably altered relative to CO migratory insertion.

Paolucci *et al.* [32] have reported that Cp_3UR complexes also undergo migratory CO insertion. Interestingly, several of the reactions are reported to be reversible, and no indication of enolate-forming rearrangement reactions was found. Paolucci *et al.* [33] as well as Dormand, Elbouadili, and Moise [34] also discovered that isocyanides undergo similar insertion reactions to yield dihapto-iminoalkyls:

$$Cp_3UR + R'NC \longrightarrow Cp_3U[\eta^2\text{-}C(R)NR'] \qquad (23.20)$$

$R = CH_3$, $R' = C_6H_{11}$

$R = n\text{-}C_4H_9$, $R' = t\text{-}C_4H_9$, C_6H_{11}, $2,6\text{-}(CH_3)_2C_6H_3$

Variable-temperature NMR studies indicate restricted rotation of the iminoalkyl fragment (*4*) about the axis joining the C=N midpoint to uranium:

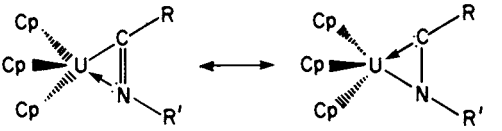

(*4*) (*4*)

Arnaudet, Folcher, and Marquet-Ellis [35] reported that Cp_3UR compounds also undergo insertion reactions with sulfur dioxide:

$$Cp_3UR + SO_2 \rightarrow Cp_3USO_2R \qquad (23.21)$$

$R = CH_3$, $n\text{-}C_4H_9$

Unfortunately, the products are only stable at low temperatures. For $R = CH_3$, the decomposition product is a species of composition '$U_2Cp_3(SO_2)_4(CH_3)_2$' where insertion into $U\text{–}C_5H_5$ bonds may have taken place.

Cramer, Gilje and co-workers [36] have prepared the first organoactinide with possible metal–carbon multiple bond (alkylidene) character. The compound, synthesized by the route

$$Cp_3UCl + Li(CH_2)(CH_2)P(CH_3)(C_6H_5) \longrightarrow Cp_3UCHP(CH_3)_2(C_6H_5) + LiCl \qquad (23.22)$$

has been characterized by single-crystal x-ray diffraction (Fig. 23.3). The short U–C(1) bond length of 2.29(3) Å can be compared to σ-bond distances of 2.33(2) Å in $Cp_3UC{\equiv}CC_6H_5$ [37] and 2.43(2) Å in $Cp_3U(n\text{-}C_4H_9)$ [22]. The U–C(1)–P angle of 142(1)° also argues for alkylidene character. Furthermore, theoretical calculations [10] at the extended Hückel level reveal an overlap population consistent with significant U–C multiple bonding. Most importantly, the chemistry of Cp_3UCHPR_3 compounds reveals a variety of new reaction patterns. For example, reaction with carbon monoxide yields a novel type of insertion product:

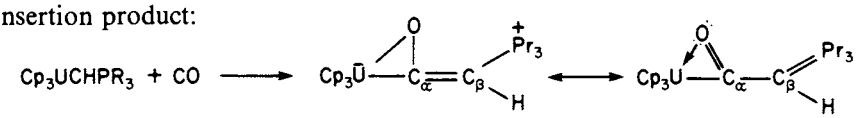

(23.23)

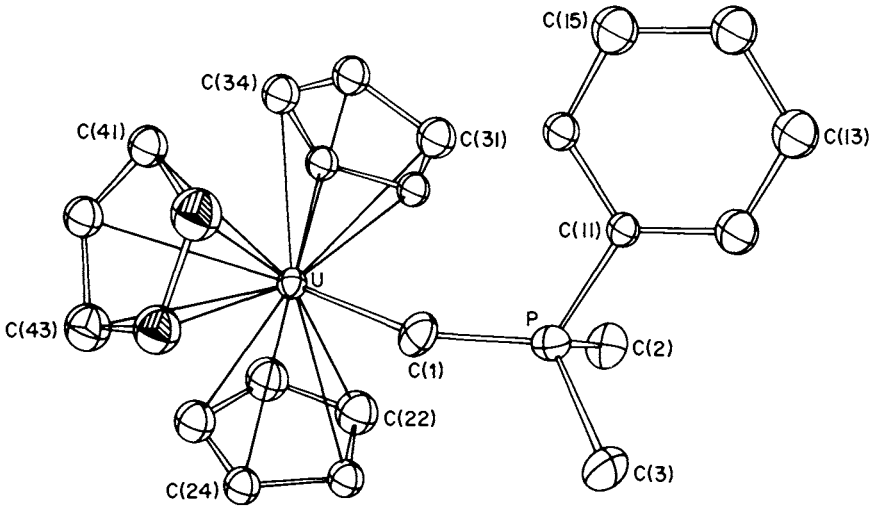

Fig. 23.3 *Perspective ORTEP drawing of the non-hydrogen atoms in* $U(C_5H_5)_3CHP(CH_3)_2(C_6H_5)$ [36].

The molecule $Cp_3U(OCCH)P(CH_3)(C_6H_5)_2$ [38] contains a U–O bond distance of 2.27(1) Å and a longer U–C_α distance of 2.37(2) Å. The C_α–O distance of 1.27(3) Å, the C_α–C_β distance of 1.37(3) Å, and the O–C_α–C_β angle of 128(2)° suggest significant ketene character.

The Cp_3UCHPR_3 complexes also undergo insertion into the C≡N bonds of nitriles and the C≡O bonds of metal carbonyls. Thus, Cramer *et al.* [39] reported that insertion reactions with acetonitrile yield uranium imido complexes:

$$Cp_3UCHP(CH_3)(C_6H_5)_2 + CH_3CN \rightarrow Cp_3UNC(CH_3)CHP(CH_3)(C_6H_5)_2 \tag{23.24}$$

Diffraction studies on the product reveal a U–N bond distance of 2.06(1) Å, significantly shorter than the value of 2.29(1) Å in the simple amide, $Cp_3UN(C_6H_5)_2$. This result and the U–N–C_α bond angle of 163(1)° imply possible uranium–nitrogen multiple bond character:

$$Cp_3U{\equiv}NC(CH_3){=}CHP(CH_3)(C_6H_5)_2 \leftrightarrow Cp_3U{=}\ddot{N}C(CH_3){=}CHP(CH_3)(C_6H_5)_2 \leftrightarrow Cp_3U{=}N{=}C(CH_3)CH{=}P(CH_3)(C_6H_5)_2$$

The reaction of the Cp_3UCHPR_3 compounds with $[CpFe(CO)_2]_2$ proceeds as follows [40]:

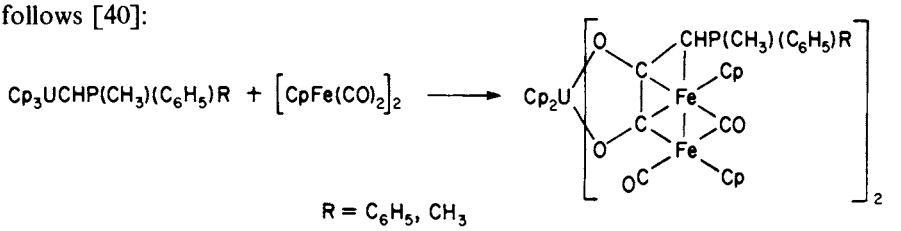

(23.25)

The structure of the polynuclear product has been established by x-ray diffraction and is formally derived from insertion of an iron-bound carbonyl ligand into the 'U=C' bond, followed by CO–CO coupling. Similar insertion chemistry is observed for $CpMn(CO)_3$:

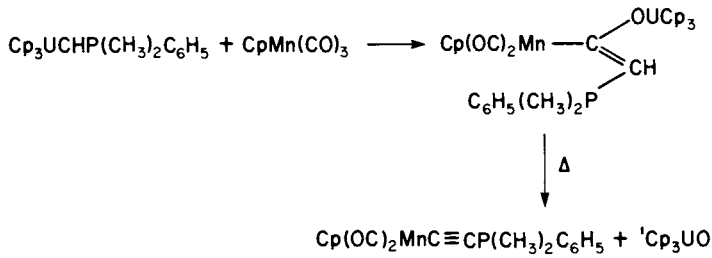

(23.26)

However, heating of the insertion product results in an unusual C–O cleavage process [41].

Arnaudet *et al.* [42] reported a number of Cp_3UR reduction reactions, which are formulated as shown below:

$$Cp_3UR + LiR \xrightarrow{THF} [Li(THF)_n^+][Cp_3UR^-] + RH + \text{other products}$$
$$R = CH_3,\ n\text{-}C_4H_9 \qquad (23.27)$$

The nature of the trivalent products was inferred *in situ* from NMR, optical spectroscopic, and EPR data as well as analysis of the organic reaction products. The crystal structure of $[Li(crypt)]^+ (C_5H_5)_3 U(n\text{-}C_4Hg)^-$ was also reported recently [106].

23.3.3 Bis(peralkylcyclopentadienyl) compounds

The general properties of peralkylcyclopentadienyl ligands are surveyed in Chapter 22. Probably the most reactive actinide hydrocarbyls prepared to date are stabilized by bis(pentamethylcyclopentadienyl) (Cp'_2) co-ligation. These complexes can, in general, be prepared as shown below for a wide range of R and R′ groups [43–45]:

$$2Cp'MgCl + MCl_4 \longrightarrow Cp'_2MCl_2 + 2MgCl_2 \qquad (23.28)$$

$$Cp'_2MCl_2 + R^- \longrightarrow Cp'_2M(Cl)R + Cl^- \qquad (23.29)$$

$$Cp'_2MCl_2 + 2R'^- \longrightarrow Cp'_2MR'_2 + 2Cl^- \qquad (23.30)$$

M = Th, R = CH_3, $CH_2Si(CH_3)_3$, $CH_2C(CH_3)_3$, $CH[Si(CH_3)_3]_2$, C_6H_5, $CH_2C_6H_5$

R′ = CH_3, $CH_2Si(CH_3)_3$, $CH_2C(CH_3)_3$, $CH_2C(CH_3)_2(C_2H_5)$, C_6H_5, $CH_2C_6H_5$, $\frac{1}{2}(CH_2CH=CHCH_2)$, $CH_2Si(CH_3)_2(C_6H_5)$, $CH_2C(CH_3)_2(C_6H_5)$

$$M = U, \quad R = CH_3, CH_2Si(CH_3)_3, CH_2C(CH_3)_3, CH[Si(CH_3)_3]_2, C_6H_5, CH_2C_6H_5$$
$$R' = CH_3, CH_2Si(CH_3)_3, CH_2C_6H_5, \tfrac{1}{2}(CH_2CH{=}CHCH_2)$$

The actinide – R bonds are significantly polar, and readily undergo protonolysis, addition to organic carbonyl groups, halogenolysis, and hydrogenolysis (to produce hydrides—*vide infra*).

The butadiene complexes shown in equation (23.30) [46] are interesting in that they test the tendency of the actinide ion to enter into divalent bonding, characteristic of transition-metal olefin complexes (*5*) as opposed to tetravalent σ^2,π-metallacyclopentene (*6*) or tetravalent η^4-butadienide (*7*) types of interactions. The conclusion drawn from spectroscopic data and the molecular structure of $Cp'_2Th(\eta^4\text{-}C_4H_6)$ (Fig. 23.4) is that the bonding involves tetravalent actinide ions ((*6*)↔(*7*)) in which the tetrahapto character reflects the high coordination numbers possible for $Cp'_2Th<$ and $Cp'_2U<$ fragments.

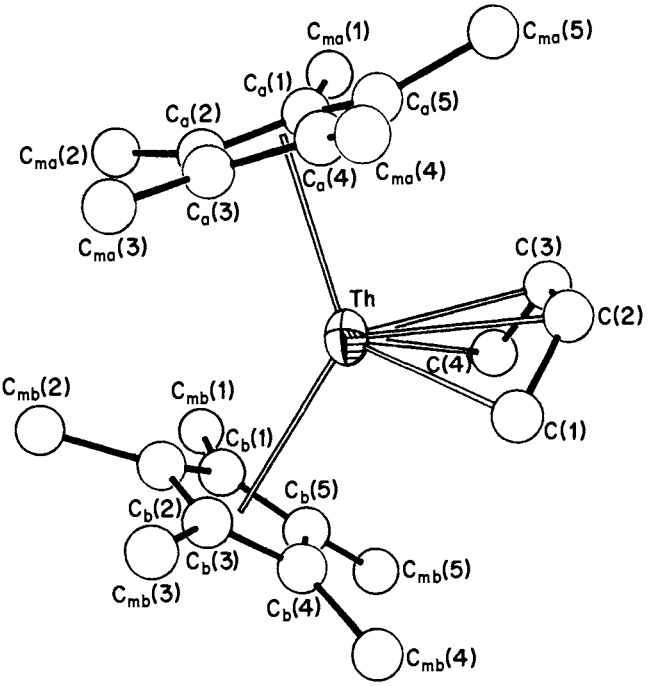

Fig. 23.4 *Perspective drawing of the non-hydrogen atoms in the molecule* $Th[(CH_3)_5C_5]_2(\eta^4\text{-}C_4H_6)$ [46]. *The average Th–C(1,4) distance is* 2.57(3) Å, *the average Th–C(2,3) distance is* 2.74(3) Å, *the average C(1)–C(2) and C(3)–C(4) distance is* 1.46(4) Å, *and C(2)–C(3)* = 1.44(3) Å.

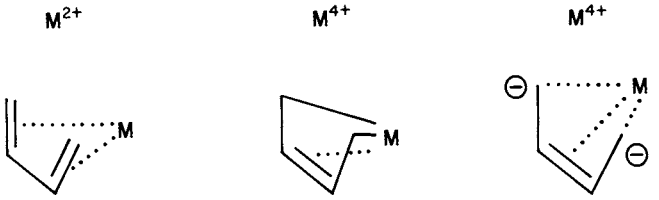

(5) (6) (7)

To study the bonding in the above types of compounds, a comparative gas-phase He I/He II photoelectron spectroscopic study of the series Cp'_2MCl_2 and $Cp'_2M(CH_3)_2$, M = Zr, Th, U, was performed [47]. It was found that the bonding in the early transition-metal and actinide complexes is surprisingly similar. The major differences between zirconium and the actinides could be ascribed to the involvement of 5f orbitals in the latter.

Trivalent uranium alkyls can be synthesized via the following approach [48, 49]:

$$\tfrac{1}{3}[Cp'_2UCl]_3 + RLi \longrightarrow Cp'_2UR + LiCl \qquad (23.31)$$

$$R = CH[Si(CH_3)_3]_2,\ C_6H_5,\ CH_2Si(CH_3)_3$$

Only for $R = CH[Si(CH_3)_3]_2$ is the product stable at room temperature for more than a brief period of time.

Bruno *et al.* [50, 51] have carried out extensive thermochemical studies of actinide–ligand bond disruption enthalpies, D (equations (23.11) and (23.12)), for Cp'_2ThR_2 and Cp'_2UR_2 complexes. Stepwise alcoholysis is observed for thorium:

$$Cp'_2ThR_2 + R'OH \longrightarrow Cp'_2Th(R)OR' + RH \qquad (23.32)$$

$$Cp'_2Th(R)OR' + R'OH \longrightarrow Cp'_2Th(OR')_2 + RH \qquad (23.33)$$

and it is possible to derive D(Th–R) values for both Cp'_2ThR_2 and $Cp'_2Th(OR')R$ complexes. These are given by the dual entries in Table 23.2. While the Th–R bonds in the Cp'_2ThR_2 series are rather 'strong', it is interesting to note that the observed D(Th–R) values are uniformly less than those for the Cp_3ThR series (Table 23.1). Within the Cp'_2ThR_2 series, it can be seen that alkoxide co-ligands slightly strengthen the Th–R bonds and halide ligands slightly weaken them. This effect can be rationalized in terms of the metal oxidation state changes accompanying homolytic bond disruption:

$$Th^{IV}\text{–}R \longrightarrow Th^{III}\cdot R \qquad (23.34)$$

and the comparative degree to which the supporting ligand stabilizes or destabilizes a particular thorium oxidation state. The conspicuously weak first bond disruption enthalpies of the metallacycles $Cp'_2Th(CH_2)_2C(CH_3)_2$ and $Cp'_2Th(CH_2)_2Si(CH_3)_2$ indicate strain in the four-membered rings, viz. about 67 and about 33 kJ mol^{-1}, respectively. This feature will be seen to have significant

Table 23.2 *Experimental bond disruption enthalpies for Cp'_2ThR_2 complexes* (kJ mol^{-1})[a].

Compound	D(Th–R(gas))[b]	D(Th–R(soln))[b]
$[(CH_3)_5C_5]_2Th(CH_3)_2$	323.0 (4.6) 331.8 (5.0)	339.7 (3.3) 350.6 (3.8)
$[(CH_3)_5C_5]_2Th(C_2H_5)_2$	294.6 (8.4) 305.0 (8.4)	307.5 (6.7) 319.2 (6.7)
$[(CH_3)_5C_5]_2Th(n\text{-}C_4H_9)_2$	299.6 (7.1) 309.2 (15.5)	299.6 (4.2) 307.9 (14.2)
$[(CH_3)_5C_5]_2Th(C_6H_5)_2$	377.8 (10.5) 397.9 (9.6)	372.0 (10.0) 386.6 (8.8)
$[(CH_3)_5C_5]_2Th[CH_2C(CH_3)_3]_2$	302.1 (16.3) 322.2 (16.3)	302.5 (15.9) 321.7 (15.5)
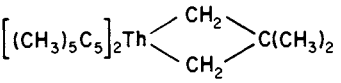	247.3 (10.0) 329.3 (12.1)	273.2 (9.6) 328.9 (10.9)
$[(CH_3)_5C_5]_2Th[CH_2Si(CH_3)_3]_2$	336.0 (14.2) 346.0 (13.8)	334.7 (13.0) 343.9 (13.0)
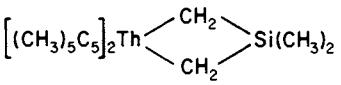	292.0 (13.8) 348.5 (15.5)	315.9 (13.4) 347.3 (14.2)
$[(CH_3)_5C_5]_2Th(\eta^4\text{-}C_4H_6)$	307.1 (11.3)[c]	318.4 (10.0)[c]
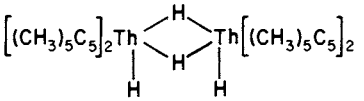	378.7(5.4)	407.9 (2.9)
$[(CH_3)_5C_5]_2Th(Cl)CH_2CH_3$	285.8 (8.4)	302.1 (7.5)
$[(CH_3)_5C_5]_2Th(Cl)CH_2C_6H_5$	299.2 (7.9)	285.3 (5.9)
$[(CH_3)_5C_5]_2Th(Cl)N(CH_3)_2$	379.9 (10.0)	373.2 (8.4)
$[(CH_3)_5C_5]_2Th[O\text{–}CH(t\text{-}Bu)_2]H$	367.4 (6.3)	390.4 (5.0)
$[(CH_3)_5C_5]_2Th[O\text{–}CH(t\text{-}Bu)_2](n\text{-}C_4H_9)$	341.0 (13.0)	339.7 (13.0)

[a] Quantities in parentheses are two standard deviations (2σ) for 6–10 determinations.
[b] Error limits do not include uncertainties that are constant throughout the series.
[c] Values are the average of those for the Cp'_2ThR_2 and $Cp'_2Th(R)OR'$ complexes.

chemical implications (*vide infra*). It is also evident that the Th–η^4-butadiene interaction enjoys no special stabilization, and that D(Th–H) – D(Th–C) is invariably less than 63 kJ mol^{-1} (cf. about 126 kJ mol^{-1} for middle and late first-row transition metals). The explanation for the alkyl/hydride trend plausibly resides in the high polarity of actinide–ligand bonds and the ineffectiveness of the non-polarizable hydride ligand in stabilizing negative charge:

$$\overset{\delta+\ \delta-}{M\text{–}H} \qquad \text{versus} \qquad \overset{\delta+\ \delta-}{M\text{–}CH_3}$$

This ordering means that β-hydride elimination (equation (23.2)) is considerably more endothermic than for middle and late 3*d* transition-element

complexes, and explains why, in the absence of unusual driving forces (e.g. follow-up reactions leading to a thermodynamic 'sink'), this reaction pattern is seldom observed in actinide (or lanthanide or early transition-metal) organometallic chemistry.

While Cp'_2ThR_2 alcoholysis was found to be stepwise, the reaction for the Cp'_2UR_2 analogs is not sufficiently selective to allow extraction of individual Cp'_2UR_2 and $Cp'_2U(R)OR'$ disruption enthalpies. Nevertheless, the averages of these quantities are highly informative and are set out in Table 23.3. While, for identical R ligands, trends in D(U–R) closely parallel those in D(Th–R) (cf. Fig. 23.5), the U–R bonds appear to be uniformly 'weaker'. This can be rationalized in terms of the energetically greater accessibility of the trivalent uranium oxidation state:

$$U^{IV}\text{–}R \longrightarrow U^{III}\cdot R \tag{23.35}$$

The Cp'_2ThR_2 complexes undergo a rich variety of thermally induced C–H activating cyclometallation processes [45, 52–54] (Fig. 23.6). Kinetic and labeling studies indicate that the reactions involve rate-limiting intramolecular abstraction of a γ-hydrogen atom. The thermochemical data indicate that these reactions are largely endothermic and are entropically driven ($T\Delta S > \Delta H > 0$; one particle → two particles) [50]. Steric crowding of the dialkyl ligands is evident in structural studies (e.g. Fig. 23.7) and no doubt makes a significant enthalpic contribution to the driving force for cyclometallation.

The reaction chemistry of thoracyclobutanes is particularly rich and can be predicted largely on the basis of thermochemical data. Fig. 23.8 illustrates some representative transformations. The facile activation of saturated hydrocarbons [55, 56] and prevalence of olefinic insertion over metathesis of C–H activation [56] are particularly fascinating.

The Cp'_2MR_2 organoactinides also display a rich CO migratory insertion chemistry [57, 58]. The key precursors in this chemistry are 'carbene-like' (i.e.

Table 23.3 *Experimental bond disruption enthalpies for Cp'_2UR_2 complexes* (kJ mol^{-1})[a].

Compound	D(U–R (gas))[b,c]	D(U–R (soln))[b,c]
$[(CH_3)_5C_5]_2U(CH_3)_2$	283.7 (14.6)	300.4 (13.8)
$[(CH_3)_5C_5]_2U(Cl)CH_3$	293.3 (7.1)	312.1 (6.7)
$[(CH_3)_5C_5]_2U(CH_2C_6H_5)_2$	258.6 (11.3)	243.9 (8.8)
$[(CH_3)_5C_5]_2U(Cl)CH_2C_6H_5$	276.6 (11.7)	263.6 (11.3)
$[(CH_3)_5C_5]_2U[CH_2Si(CH_3)_3]_2$	306.7 (13.8)	306.7 (13.0)
$[(CH_3)_5C_5]_2U(Cl)C_6H_5$	362.8 (10.9)	357.7 (10.9)
$[(CH_3)_5C_5]_2U(OR'')CH_3$[d]	302.9 (5.9)	318.0 (5.0)
$[(CH_3)_5C_5]_2U(OR'')H$[d]	319.7 (4.6)	344.8 (2.9)

[a] Quantities in parentheses are two standard deviations (2σ) for 6–10 determinations.
[b] Error limits do not include uncertainties that are constant throughout the series.
[c] Values are the average of those for the Cp'_2UR_2 and $Cp'_2U(OR')R$ complexes.
[d] $R'' = Si[C(CH_3)_3](CH_3)_2$.

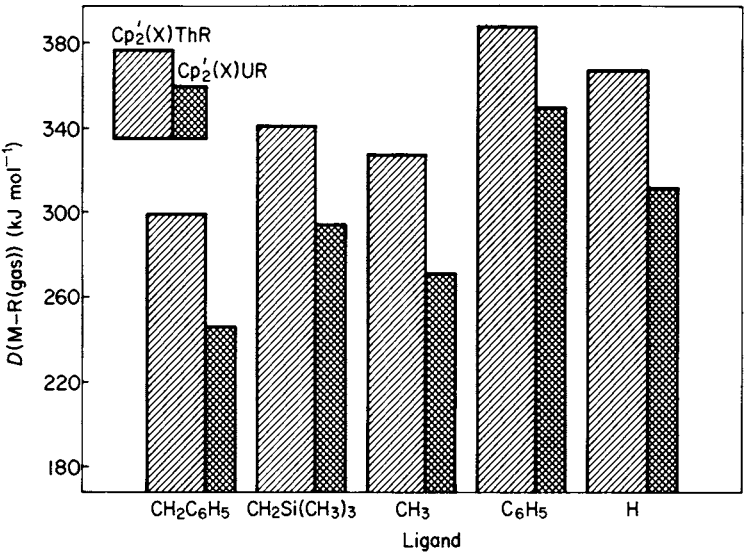

Fig. 23.5 *Comparison of gas-phase metal–ligand bond disruption enthalpies in corresponding* $Th[(CH_3)_5C_5]_2(X)R$ *and* $U[(CH_3)_5C_5]_2(X)R$ *complexes* [51].

behaving as 'anchored' Fischer carbene complexes) dihapto-acyl complexes ((*8*), (*9*)):

(*8*) (*9*)

Theoretical studies [59] indicate that the lowest unoccupied molecular orbital (LUMO) of such molecules is localized primarily on the acyl carbon atom, similarly to the situation in Fischer complexes. An example of such a compound is shown in Fig. 23.9, where the shortness of the Th–O_a distance (2.37(2) Å) relative to Th–C_a (2.44(2) Å) is unprecedented for a dihapto-acyl. A second example of an actinide dihapto-acyl is shown in Fig. 23.10. It should be noted that the orientation of the C–O vector is in the opposite direction from that in Fig. 23.9. The relative magnitudes of the Th–O and Th–C distances appear to reflect both the orientation of the C–O vector and conjugation with the arene π system. The intricate chemistry exhibited by actinide dihapto-acyls is summarized in Fig. 23.11. Important reactions include C–C coupling to form monomeric (*10*) or dimeric enediolates [57, 58, 60, 61], isomerization to yield enolates (*11*) [60, 62], catalytic hydrogenation to yield alkoxides (*12*) [63], CO tetramerization to form dionediolates (*13*) [62, 64], coupling with ketenes (*14*), coupling with CO and phosphines (*15*) [62, 64], and addition to isocyanides to yield ketenimines [62, 64] (*16*).

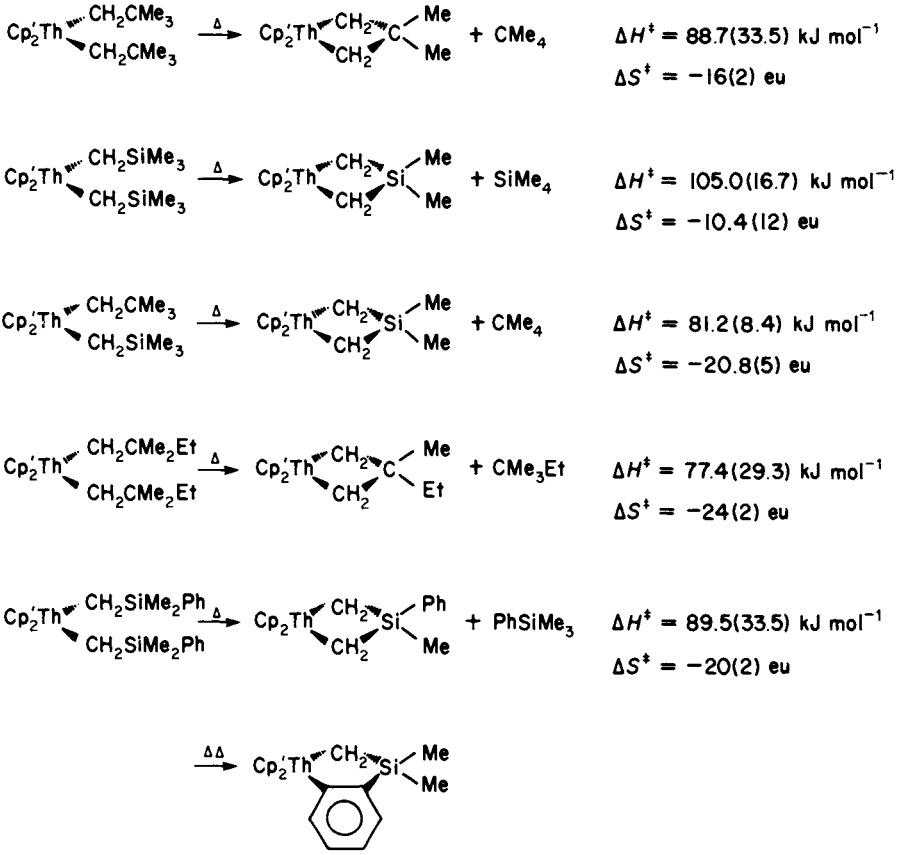

Fig. 23.6 *Scheme showing cyclometallation reactions of thorium complexes.*

Dormand, Elbouadili, and Moise [34] have also studied the insertion chemistry of (pentamethylcyclopentadienyl)uranium alkyls with isocyanides:

$$Cp'_2U(R)X + R'NC \longrightarrow Cp'_2U[C(R)NR']X \qquad (23.36)$$

$R = CH_3$, $X = CH_3$, $R' = t\text{-}C_4H_9$
$R = CH_3$, $X = Cl$, $R' = t\text{-}C_4H_9$
$R = n\text{-}C_4H_9$, $X = Cl$, $R' = t\text{-}C_4H_9$

As for the aforementioned Cp_3UR compounds, the products have been assigned a dihapto structure (*17*):

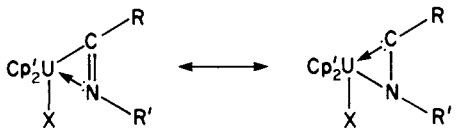

(*17*)

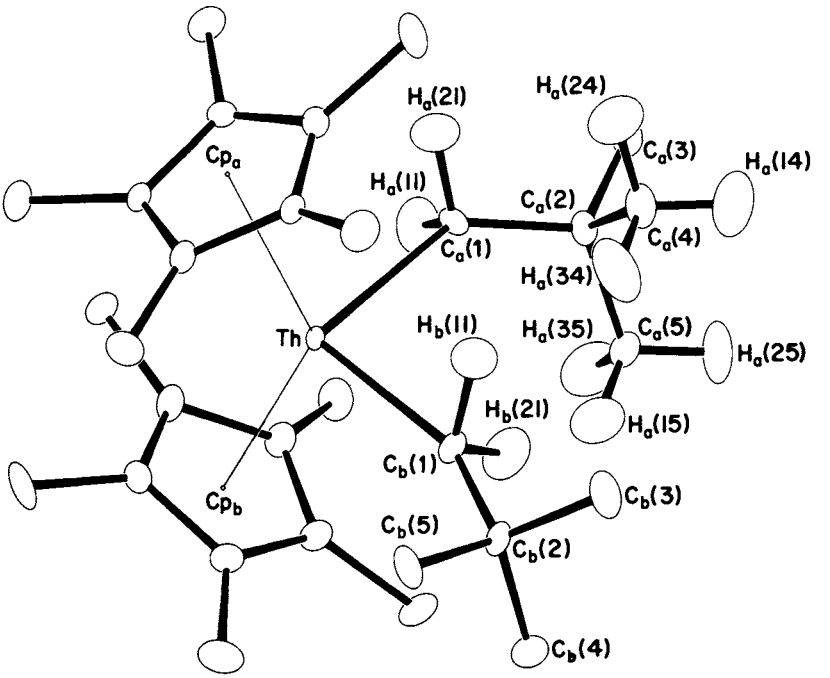

Fig. 23.7 *Solid-state structure of* $Th[(CH_3)_5C_5]_2[CH_2C(CH_3)_3]_2$ *by neutron diffraction* [45]. *Important bond lengths* (Å) *and angles* (*deg*) *for chemically distinct groups of atoms include:* $Th\text{–}C_a(1) = 2.546(4)$, $Th\text{–}C_b(1) = 2.478(4)$, $C_a(1)\text{–}C_a(2) = 1.549(5)$, $C_b(1)\text{–}C_b(2) = 1.537(6)$, $C_a(1)\text{–}H_a(11) = 1.087(11)$, $C_a(1)\text{–}H_a(21) = 1.094(8)$, $C_b(1)\text{–}H_b(11) = 1.112(9)$, $C_b(1)\text{–}H_b(21) = 1.130(8)$; $Th\text{–}C_a(1)\text{–}C_a(2) = 131.8(3)$, $Th\text{–}C_b(1)\text{–}C_b(2) = 158.6(3)$, $Th\text{–}C_b(1)\text{–}H_b(11) = 85.1(4)$, $Th\text{–}C_b(1)\text{–}H_b(21) = 87.5(4)$.

23.3.4 Mono(peralkylcyclopentadienyl) compounds

Less is known about single-ring organoactinides of the type $Cp'MR_3$, and thermal stability appears to be a sensitive function of R and M. The approach:

$$Cp'MCl_3 \cdot 2THF + 3RLi \longrightarrow CpMR_3 + 3LiCl \qquad (23.37)$$

M = Th, R = $CH_2C_6H_5$, $CH_2C(CH_3)_3$, *o*-$C_6H_4N(CH_3)_2$

M = U, R = $CH_2C_6H_5$

has yielded only a few isolable compounds despite a great deal of effort [65, 66]. The crystal structure of $Cp'Th(CH_2C_6H_5)_3$ (Fig. 23.12) reveals a multihapto mode of metal–benzyl interaction (*1*). This feature may account at least partially for the high thermal stability and bears an obvious analogy to the corresponding uranium [67] and thorium [66] $Cp'M(allyl)_3$ complexes. However, dispersion in Th–C(benzyl) metrical parameters and the NMR evidence for rapid $\eta^3 \rightleftharpoons \eta^1$ equilibration also suggest that the potential energy surface for various

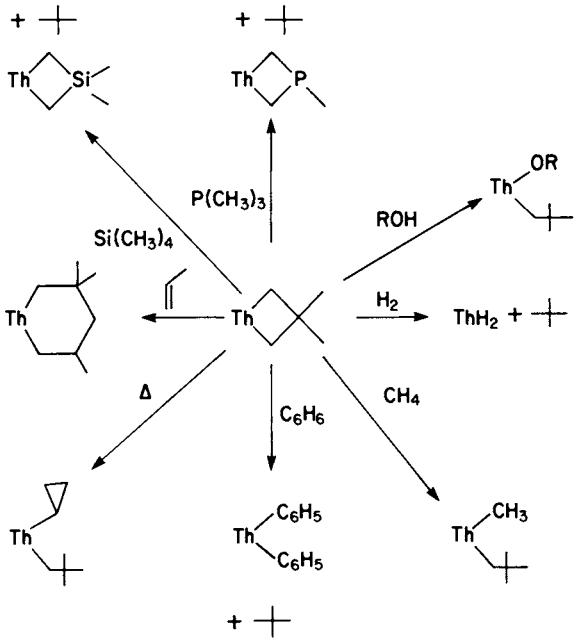

Fig. 23.8 *Scheme showing descriptive chemistry of thoracyclobutanes.*

actinide–benzyl bonding motifs is rather shallow. Enhanced electronic and steric saturation is also a likely factor in the stability of the *o*-$C_6H_4N(CH_3)_2$ compound. The situation is not so obvious for the tris(neopentyl) derivative; however, spectroscopic data provide no evidence for 'agostic' C–H . . . Th or any other unusual bonding interactions [66]. Purely steric saturation and consequent kinetic frustration of various decomposition processes seems most likely.

Little is known about the chemical reactivity of the actinide $Cp'MR_3$ compounds. The benzyl derivatives react rapidly with alcohols and formaldehyde. The M = U compound reacts rapidly with CO and H_2, while the M = Th compound is significantly more inert. In contrast, $Cp'Th[CH_2C(CH_3)_3]_3$ reacts in minutes with H_2 to form a mixture of several different pentamethylcyclopentadienyl hydrides and neopentane [66].

23.3.5 Phosphine-stabilized hydrocarbyls

Andersen has found that chelating phosphine ligands greatly enhance the thermal stability of certain actinide hydrocarbyls [68, 69]. Thus, both methyl and benzyl derivatives can be prepared by the reaction sequence shown below:

$$MCl_4 + 2dmpe \longrightarrow MCl_4(dmpe)_2 \qquad (23.38)$$

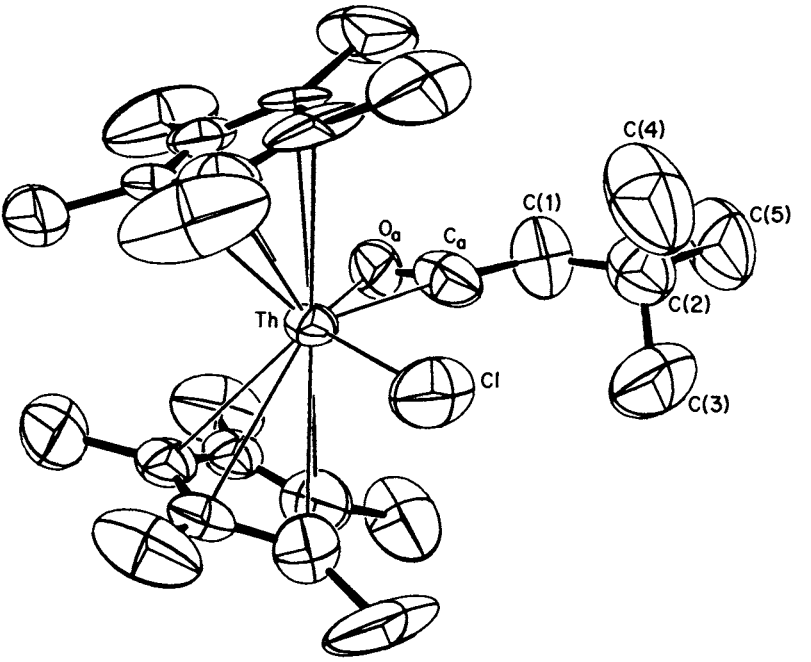

Fig. 23.9 *ORTEP drawing of the non-hydrogen atoms for the* $Th[(CH_3)_5C_5]_2[\eta^2\text{-}COCH_2C(CH_3)_3]Cl$ *molecule* [58]. *Important bond lengths* (Å) *and angles* (*deg*) *of chemically distinct bonds are the following:* $Th\text{–}Cl = 2.672(6)$, $Th\text{–}O_a = 2.37(2)$, $Th\text{–}C_a = 2.44(2)$, *Th–C(cyclopentadienyl)* = 2.80(2,2,3,10), $C_a\text{–}O_a = 1.18(3)$, $C_a\text{–}C(1) = 1.55(3)$; $Th\text{–}C_a\text{–}O_a = 73(1)$, $Th\text{–}C_a\text{–}C(1) = 169(2)$, $O_a\text{–}C_a\text{–}C(1) = 118(2)$.

$$MCl_4(dmpe)_2 + 4RLi \longrightarrow MR_4(dmpe)_2 \qquad (23.39)$$

M = Th, U

dmpe = $(CH_3)_2PCH_2CH_2P(CH_3)_2$

R = CH_3, $CH_2C_6H_5$

$$MCl_4(dmpe)_2 + 3C_6H_5CH_2Li + CH_3Li \rightarrow M(CH_3)(CH_2C_6H_5)_3(dmpe)_2 \qquad (23.40)$$

M = Th, U

In contrast, the products prepared with $R = CH_2C(CH_3)_3$, $CH_2C(C_6H_5)(CH_3)_2$, and $CH_2Si(CH_3)_3$ are reported to be thermally unstable above 0°C, and it was assumed that alkyls containing β-hydrogen atoms are also unstable. The solid-state molecular structure of $Th(CH_2C_6H_5)_4(dmpe)_2$ (Fig. 23.13) reveals three monohapto-benzyl ligands and one polyhapto ligand. In the latter ligand, the Th–C(8)–C(9) angle is 88(1)° and the Th–C(9) distance is 2.86(2) Å, with values of 90(1)° and 2.90(2) Å for the second independent molecule of the unit cell. The $Th\text{–}C_\alpha$ distances for the two polyhapto-benzyl ligands are 2.53(2) Å and 2.53(2) Å, respectively. The benzyl coordination in $U(CH_3)(CH_2C_6H_5)_3(dmpe)_2$ is also

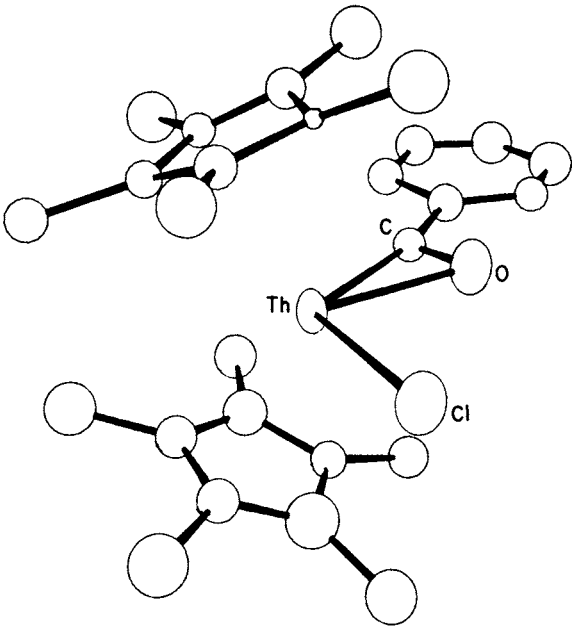

Fig. 23.10 *Molecular structure of the dihapto-acyl complex* $Th[(CH_3)_5C_5]_2$ $(\eta^2\text{-}COC_6H_5)Cl$ [104]. *At a preliminary stage of refinement, the following bond lengths* (Å) *can be given:* $Th\text{–}O = 2.43(1)$, $Th\text{–}C(acyl) = 2.41(2)$, $Th\text{–}Cl = 2.702(4)$.

unusual (Fig. 23.14), with two essentially monohapto ligands and one polyhapto ligand (U–C(15)–C(16) angle of 83.0(4)°, U–C(15) = 2.54(1) Å, U–C(16) = 2.758(5) Å, U–C(17) = 3.089(6) Å, U–C(21) = 3.450(7) Å). The three benzyl ligands are magnetically equivalent in the room-temperature ^1H NMR; however, the spectrum of the uranium derivative is very complex by $-60°C$.

23.3.6 Compounds with chelating peralkylcyclopentadienyl ligands

Chelating cyclopentadienyl ligands (*18*) offer an attractive means to modify $Cp_2M<$ coordination spheres and also to prevent ligand redistribution processes [70]. This chemistry has already been thoroughly reviewed for organoactinides [2, 21].

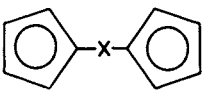

X = CH_2, $(CH_3)_2Si$, $CH_2CH_2CH_2$

(*18*)

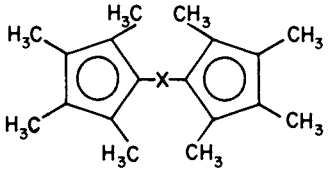

(*19*)

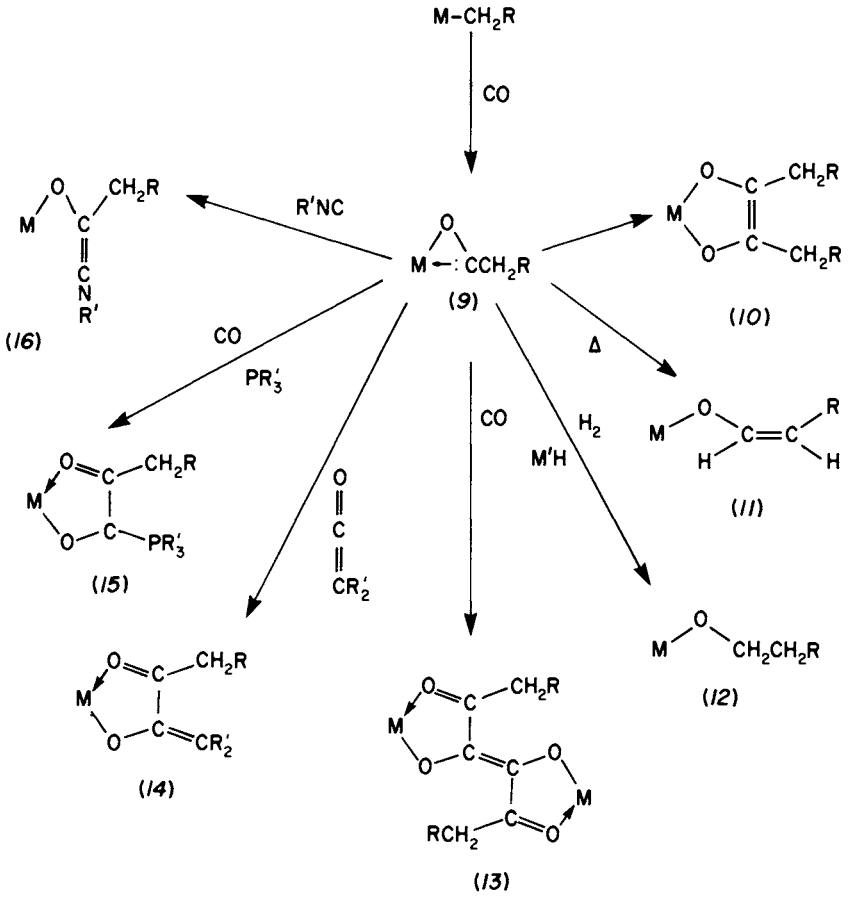

Fig. 23.11 *Scheme showing reaction patterns of actinide dihapto-acyls.*

While a number of interesting reactivity patterns have been observed, these systems suffer from poor solubility and decomposition via abstraction of cyclopentadienyl ring hydrogen atoms. Permethylation of the ligand (*19*) circumvents a number of these problems, and for X = $Si(CH_3)_2$ a new series of coordinatively unsaturated, thermally stable, and highly reactive actinide hydrocarbyls can be prepared [71, 72]:

$$(CH_3)_2SiCp''^{2-}_2 + ThCl_4 \xrightarrow{DME} \text{`}(CH_3)_2SiCp''_2ThCl_2\text{'} + 2Cl^- \quad (23.41)$$

$$(CH_3)_2SiCp''_2ThCl_2 + 2RLi \xrightarrow{DME} (CH_3)_2SiCp''_2ThR_2 + 2LiCl \quad (23.42)$$

R = n-C_4H_9, $CH_2C(CH_3)_3$, $CH_2Si(CH_3)_3$, $CH_2C_6H_5$, C_6H_5

Cp″ = $(CH_3)_4C_5$

DME = 1,2-dimethoxyethane

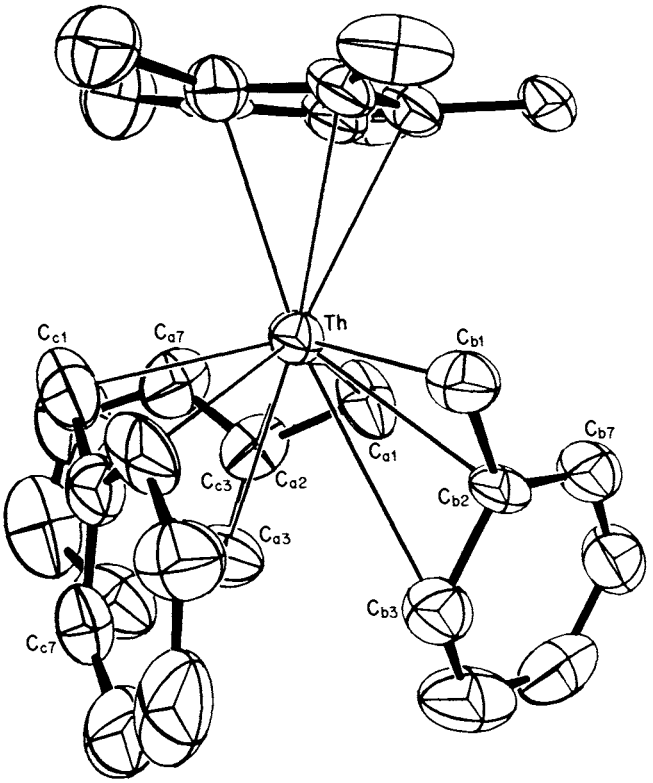

Fig. 23.12 *Perspective ORTEP drawing of the non-hydrogen atoms in* $Th[(CH_3)_5C_5](CH_2C_6H_5)_3$ [65]. *Important metal–ligand bond distances* (Å) *are:* $Th–C_a(1) = 2.581(19)$, $Th–C_b(1) = 2.579(17)$, $Th–C_c(1) = 2.578(21)$ (2.58(2,0,0,3) *average*); $Th–C_a(2) = 2.913(18)$, $Th–C_b(2) = 2.865(18)$, $Th–C_c(2) = 2.979(18)$ (2.92(2,4,6,3) *average*); $Th–C_a(3) = 3.413(21)$, $Th–C_b(3) = 3.352(19)$, $Th–C_c(3) = 3.325(18)$ (3.36(2,3,5,3) *average*); $Th–C_a(7) = 3.501(20)$, $Th–C_b(7) = 3.574(19)$, $Th–C_c(7) = 3.852(20)$; *Th–C(cyclopentadienyl)* = 2.79(2,2,4,5) *average. Important bond angles (deg) are:* $Th–C_a(1)–C_a(2) = 87(1)$, $Th–C_b(1)–C_b(2) = 86(1)$, $Th–C_c(1)–C_c(2) = 91(1)$, $C_a(1)–Th–C_b(1) = 112.6(6)$, $C_a(1)–Th–C_c(1) = 116.2(6)$, $C_b(1)–Th–C_c(1) = 117.3(6)$.

The molecular structure of the $R = CH_2Si(CH_3)_3$ derivative (Fig. 23.15) reveals a major 'pulling back' of the bis(cyclopentadienyl) coordination geometry versus that in Cp'_2ThR_2 complexes (*vide supra*). The (ring center of gravity)–Th–(ring center of gravity) angle has contracted from about 138° in Cp'_2Th complexes to 118° in the $(CH_3)_2SiCp''_2Th<$ compound. This contraction causes a large dispersion in the Th–C(ring) contacts for the latter compound and an alternation in the C(ring)–C(ring) distances. Interestingly, however, the distortion in the $Th[CH_2Si(CH_3)_3]_2$ fragment is nearly identical to that in the Cp'_2 analog [53]. This modification of the thorium Cp'_2 coordination sphere significantly enhances the catalytic activity of the corresponding hydride (*vide infra*).

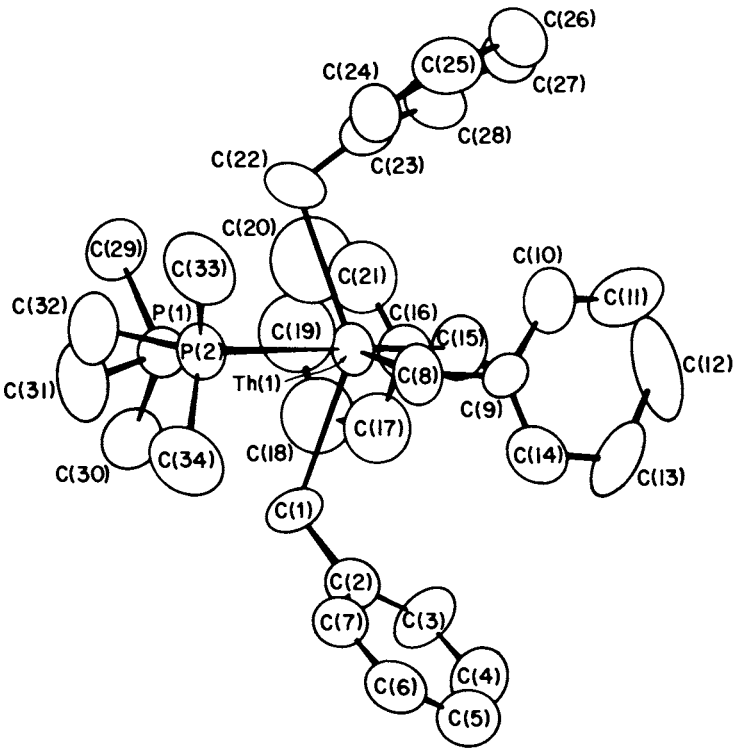

Fig. 23.13 *ORTEP drawing of the molecular structure of one (of two) independent molecules in the unit cell of Th* $(CH_2C_6H_5)_4$ *(dmpe)*$_2$ [69]. *The average Th–C σ-bond distance is* 2.55(2) Å *and the average Th–P distance is* 3.17(3) Å.

23.3.7 Amido-stabilized alkyls

Andersen has found that hydrocarbon-soluble, thermally stable actinide methyl compounds can be readily prepared via the approach below [73]:

$$MCl_4 + 3NaN[Si(CH_3)_3]_2 \longrightarrow M\{N[Si(CH_3)_3]_2\}_3Cl + 3NaCl \qquad (23.43)$$
$$M = Th, U$$

$$2Th\{N[Si(CH_3)_3]_2\}_3Cl + Mg(CH_3)_2 \xrightarrow{\text{ether}} 2Th\{N[Si(CH_3)_3]_2\}_3CH_3 + MgCl_2 \qquad (23.44)$$

$$U\{N[Si(CH_3)_3]_2\}_3Cl + LiCH_3 \xrightarrow{\text{ether}} U\{N[Si(CH_3)_3]_2\}_3CH_3 + LiCl \qquad (23.45)$$

From the diffraction-derived molecular structure of the analogous

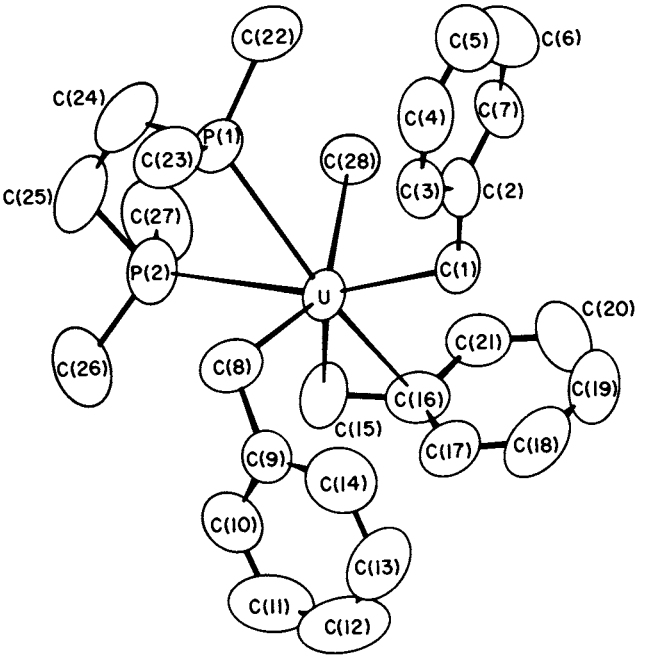

Fig. 23.14 *ORTEP drawing of the solid-state molecular structure of* $U(CH_3)(CH_2C_6H_5)_3(dmpe)_2$ [69]. *The U–C(methyl) distance is* 2.41(1) Å, *the average U–C(benzyl) is* 2.50(4) Å, *and the average U–P is* 3.015(5) Å.

tetrahydroborate, $Th\{N[Si(CH_3)_3]_2\}_3BH_4$, a pseudo-tetrahedral coordination geometry (*20*) has been put forward for these complexes:

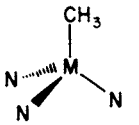

(*20*)

Thermolysis of either methyl compound proceeds by γ-hydrogen-atom elimination to produce a metallacycle (*21*) [74, 75]:

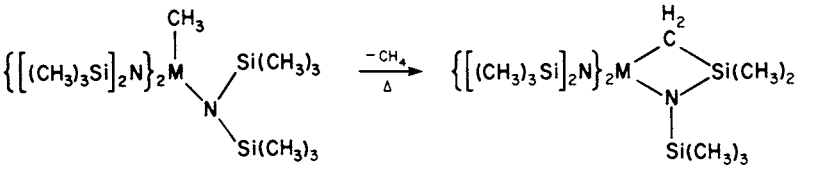

M = Th, U (*21*) (23.46)

Metallacycle (*21*) reacts with CO, t-C_4H_9NC, and t-C_4H_9CN as depicted in the following equations:

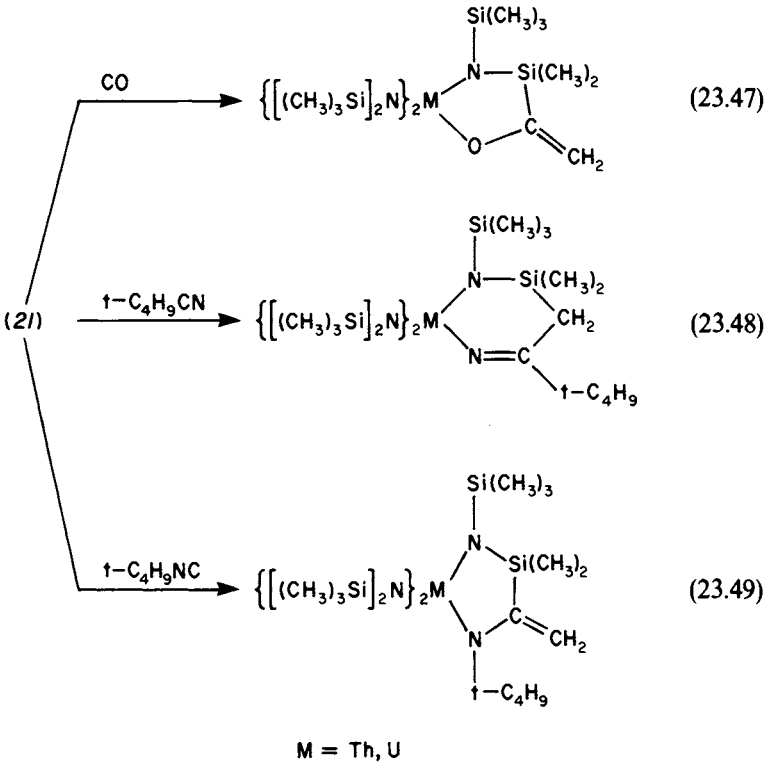

(23.47)

(23.48)

(23.49)

The products of equations (23.47) and (23.49) can be understood in terms of a migratory insertion to yield a 'carbene-like' acyl (cf. (*3*)) or iminoalkyl (cf. (*4*)), which then inserts into the neighboring C–Si bond:

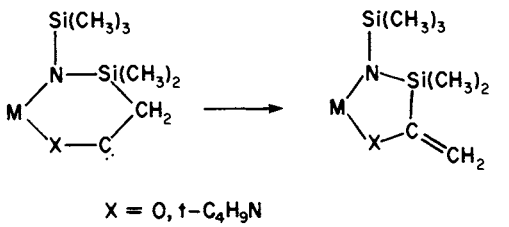

(23.50)

It will be seen that (*21*) undergoes hydrogenolysis to produce amido hydrides (*vide infra*).

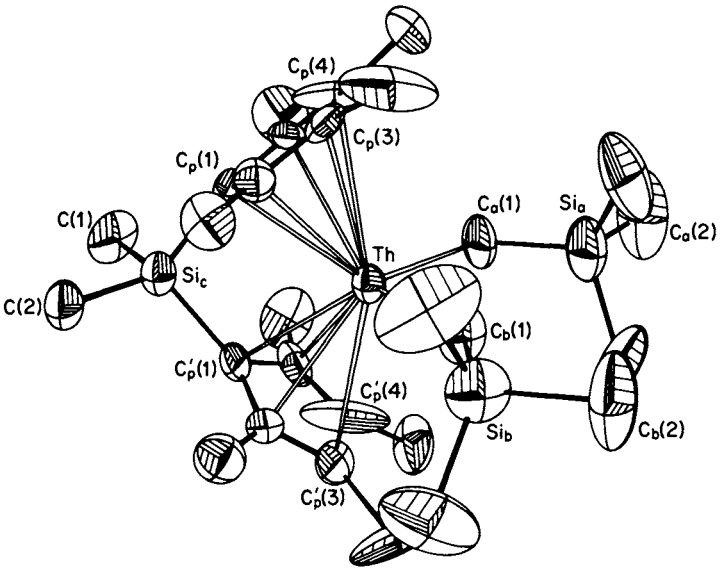

Fig. 23.15 *Perspective ORTEP drawing of the non-hydrogen atoms in* $(CH_3)_2Si[(CH_3)_4C_5]_2Th[CH_2Si(CH_3)_3]_2$ [71]. *Individual bond lengths* (Å) *and angles (deg) of interest include:* $Th–C_a(1) = 2.54(2)$, $Th–C_b(1) = 2.48(2)$; $Th–C_a(1)–Si_a = 124(1)$, $Th–C_b(1)–Si_b = 150(1)$; $Th–C_p(1) = 2.686(14)$, $Th–C_p(2) = 2.744(13)$, $Th–C_p(3) = 2.875(13)$, $Th–C_p(4) = 2.917(17)$, $Th–C_p(5) = 2.733(19)$, $C_p(1)–C_p(2) = 1.44(2)$, $C_p(1)–C_p(5) = 1.45(2)$, $C_p(1)–C_p(3) = 1.36(2)$, $C_p(3)–C_p(4) = 1.56(3)$, $C_p(4)–C_p(5) = 1.21(3)$, $Si_c–C_p(1) = 1.88(1)$, $Th \ldots Si_c = 3.465(6)$, $Si_a–C_a(1) = 1.81(3)$, $Si_b–C_b(1) = 1.90(3)$; $C_p(1)–Si–C_p'(1) = 100.6(9)$, $C_a(1)–Th–C_b(1) = 98.9(8)$.

23.4 ACTINIDE–HYDROGEN σ BONDS

23.4.1 Peralkylcyclopentadienyl hydrides

The first organoactinide hydrides were prepared by hydrogenolysis of the bis(pentamethylcyclopentadienyl) hydrocarbyls [1, 43]:

$$2Cp'_2MR_2 + 4H_2 \longrightarrow (Cp'_2MH_2)_2 + 4RH \qquad (23.51)$$
$$M = Th, U$$

$$2Cp'_2Th(R)Cl + 2H_2 \longrightarrow [Cp'_2Th(H)Cl]_2 + 2RH \qquad (23.52)$$

For $Cp'_2U(R)Cl$, hydrogenolysis yields the trivalent monochloride, $(Cp'_2UCl)_3$ [76]. The dimeric molecular structure of $(Cp'_2ThH_2)_2$, as determined by neutron diffraction, is presented in Fig. 23.16 [77]. The mean Th–H(terminal) and Th–H(bridge) distances are 2.03(1) Å and 2.29(3) Å, respectively. The former contact is approximately equal to the sum of the covalent radii for hydrogen and thorium. The H–Th–H angle is 58(1)° and the Th–H–Th angle is 122(4)°. These

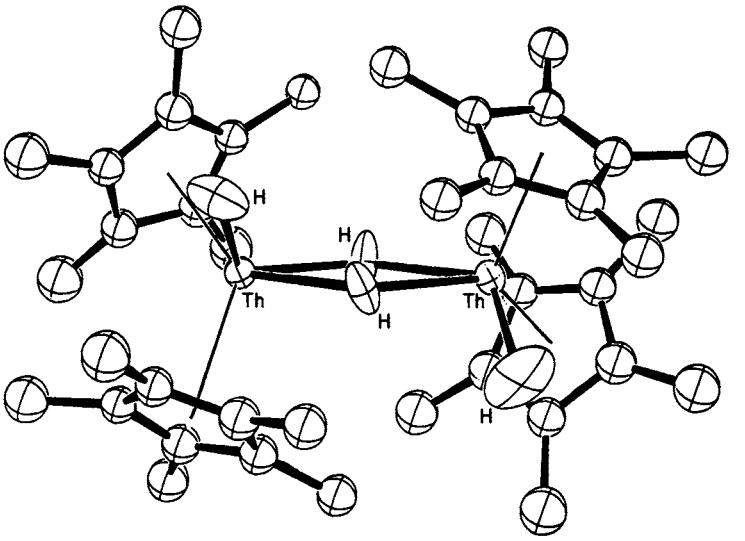

Fig. 23.16 *Perspective view of the hydride dimer* $\{Th[(CH_3)_5C_5]_2(H)(\mu\text{-}H)\}_2$ *by neutron diffraction* [77]. *Hydrogen atoms on the pentamethylcyclopentadienyl ligands have been deleted for clarity.*

parameters and the rather long Th–Th contact of 4.007(8) Å indicate minimal direct metal–metal interaction (Th–Th = 3.59 Å in thorium metal).

In solution, NMR studies indicate that the bridge and terminal hydride ligands of $(Cp'_2ThH_2)_2$ undergo rapid interchange. The hydride ligands also exchange rapidly with dissolved H_2. In contrast to thorium, the accessibility of the trivalent oxidation state is evident in the corresponding uranium hydride chemistry:

$$(n/2)(Cp'_2UH_2)_2 \rightleftharpoons (Cp'_2UH)_n + (n/2)H_2 \qquad (23.53)$$
$$n = \text{probably } 2$$

The actinide hydrides are rather 'hydridic' in nature and undergo rapid reaction with alcohols, ketones, and halocarbons:

$$M\text{–}H + RX \longrightarrow MX + RH \qquad (23.54)$$
$$X = Cl, Br, I$$

$$M\text{–}H + ROH \longrightarrow MOR + H_2 \qquad (23.55)$$

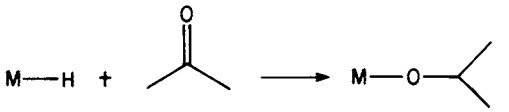

(23.56)

That rapid, quantitative addition to terminal olefins occurs, which is the reverse of β-hydride elimination,

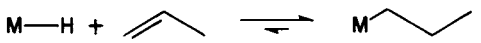

(23.57)

is consistent with the bond disruption enthalpy relationships discussed earlier. The hydride–olefin addition process can be coupled with metal–alkyl hydrogenolysis (equation (23.51)) to effect homogeneous olefin hydrogenation at respectable rates [43, 44, 78]. A plausible mechanism for α-olefin hydrogenation, based upon extensive studies of organolanthanide analogs [79], is shown in Fig. 23.17. For 1-hexene at 25°C and 1 atm H_2 pressure, N_t for $(Cp'_2UH_2)_2$-catalyzed hydrogenation exceeds 60 000 h^{-1} [78]. This same organouranium complex is also active for ethylene polymerization, presumably via migratory ethylene insertion. When adsorbed on high-surface-area dehydroxylated alumina, the bis(pentamethylcyclopentadienyl) organoactinide hydrides are potent heterogeneous catalysts for olefin hydrogenation (for propylene, they are comparable in activity to supported platinum) and ethylene polymerization [80–83].

The carbon monoxide chemistry of organoactinide hydrides provides a unique glimpse of a reaction pattern thought to be of key importance in catalytic CO reduction processes: migratory insertion of CO into a metal–hydrogen bond [84, 85]. At room temperature, the carbonylation of bis(pentamethylcyclopentadienyl)thorium alkoxyhydrides to yield *cis*-enediolates proceeds at rates that are inversely proportional to the steric bulk of R:

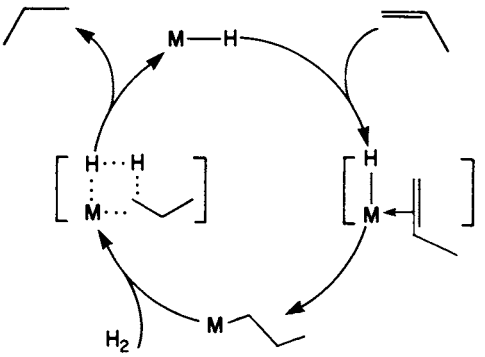

Fig. 23.17 *Scheme showing catalysis with f-element organometallics: homogeneous 1-hexene hydrogenation at 25°C and 1 atm H_2.*

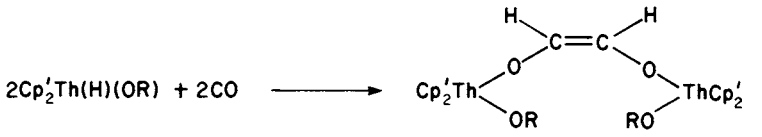

Rate as a function of R: t-Bu > $CH(t\text{-}Bu)_2$ > $2,6\text{-}(t\text{-}Bu)_2C_6H_3$

(23.58)

However, at low temperatures, all of these hydrides react rapidly (i.e. at a rate that is rapid on the NMR timescale by about −40°C) and reversibly with CO to yield bright-yellow complexes, which are formulated on the basis of spectroscopic data as dihapto-formyls [84, 85]:

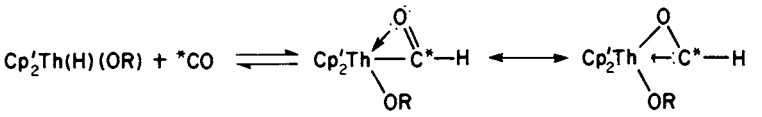

(23.59)

There is no spectroscopic evidence for actinide carbonyl complexes. For R = $CH(t\text{-}Bu)_2$, $\Delta H^\circ = -18.8(3.8)$ kJ mol^{-1}, $\Delta S = -11.7(4.3)$ eu; and for R = $2,6\text{-}(t\text{-}Bu)_2C_6H_3$, $\Delta H^\circ = 24.7(6.3)$ kJ mol^{-1}, $\Delta S = -23.9(7.4)$ eu.

NMR kinetic and crossover experiments indicate that equation (23.59) involves migratory insertion of CO into a Th–H bond in a process that is unimolecular in $Cp'_2Th(H)OR$ complex. Furthermore, a significant primary kinetic isotope effect, $(k_H/k_D)_{forward} = 2.8(4)$ (insertion) and $(k_H/k_D)_{reverse} = 4.1(5)$ (extrusion), argues that Th–H bond scission is rate-limiting. Insertion rate data for a series of $Cp'_2Th(OR)R$ alkyls show that the rate of hydride migration greatly exceeds that of alkyl migration. It is found that $k(H) \sim 5 \times 10^3 k(CH_2(CH_3)_3) \sim 7 \times 10^4 k(n\text{-}Bu) \sim 10^8 k(Me)$. The latter three rates partially reflect Th–C bond disruption enthalpy trends (Table 23.2). On the basis of these investigations, it is now possible to map out the free-energy surface for migratory insertion of CO into a Th–H bond *vis-à-vis* migratory insertion into a Th–alkyl bond. These relationships are shown in Fig. 23.18. While insertion into a Th–C bond is far more exothermic, it is also clear that hydride has a far greater migratory aptitude [85].

Kinetic investigations [86, 87] have also probed the pathway by which the enediolates of equation (23.58) are formed. The scheme shown below is in accord with the kinetic data:

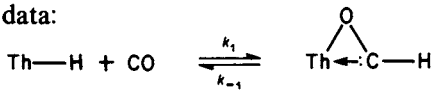

(23.60)

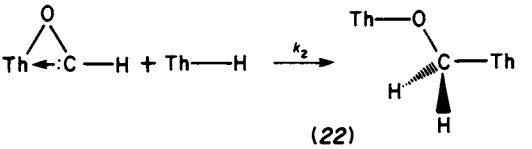

(23.61)

(22)

(23.62)

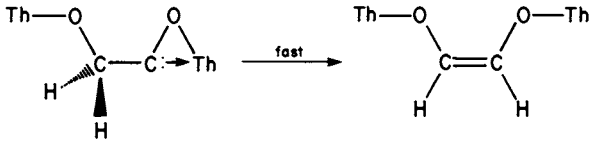

(23.63)

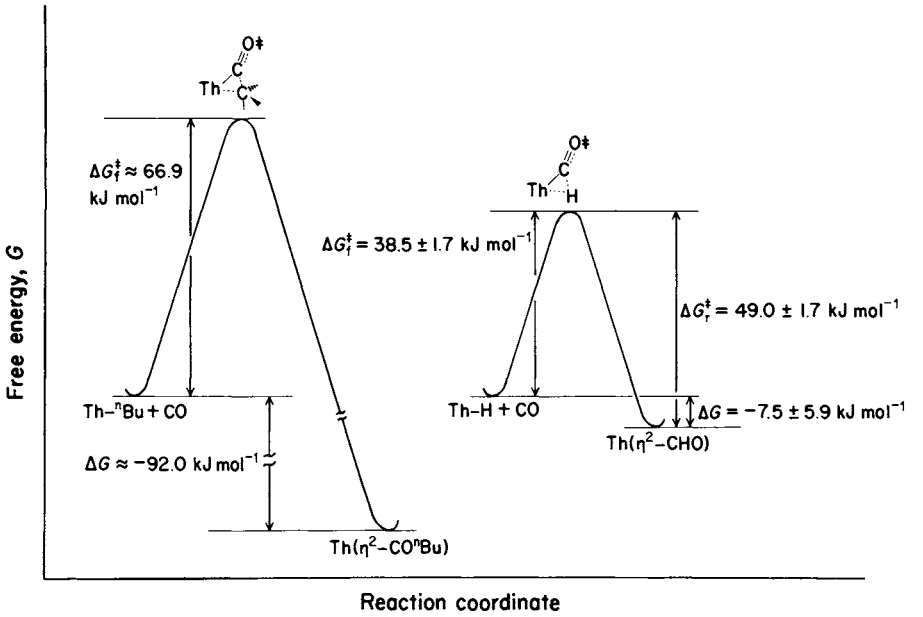

Fig. 23.18 *Free energy vs reaction coordinate diagrams for the insertion of CO into thorium alkyl and hydride bonds at about equal concentrations at −50°C and 1 atm CO pressure* [85]. *The positions of the reactants have been arbitrarily placed at the same energy level. Because it was not possible to determine the position of the presumed alkyl or hydride carbonyl intermediate (Th(CO)(R)), these pre-equilibria have been omitted from the energy profiles.*

Furthermore, as would be predicted by such a scenario, intermediate (*22*) can be hydrogenolytically intercepted to produce a methoxide:

$$Cp'_2Th(H)(OR) + CO + H_2 \longrightarrow Cp'_2Th(OCH_3)(OR) \qquad (23.64)$$

23.4.2 Other hydrides

The first organouranium phosphine hydride was synthesized via either of the routes shown below [88, 89]:

$$Cp'_2UR_2 + dmpe \xrightarrow{H_2} Cp'_2U(H)dmpe + 2RH \quad (23.65)$$

$$(Cp'_2UH_2)_2 + dmpe \xrightarrow{-H_2} 2Cp'_2U(H)dmpe + H_2 \quad (23.66)$$

$$dmpe = (CH_3)_2PCH_2CH_2P(CH_3)_2$$

The molecular structure of this compound was determined by x-ray diffraction and the result is illustrated in Fig. 23.19. Although the uranium-bound hydrogen atom could not be precisely located in the diffraction study, it is evident in the infrared spectrum ($\nu_{U-H} = 1219\ cm^{-1}$, $\nu_{U-D} = 870\ cm^{-1}$) and in low-temperature ^1H NMR spectra, which indicate instantaneous structure (*23*):

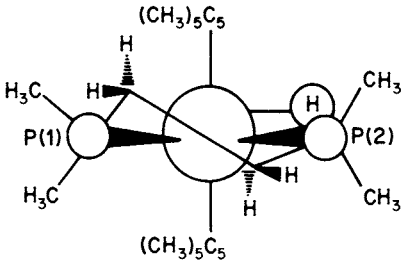

(*23*)

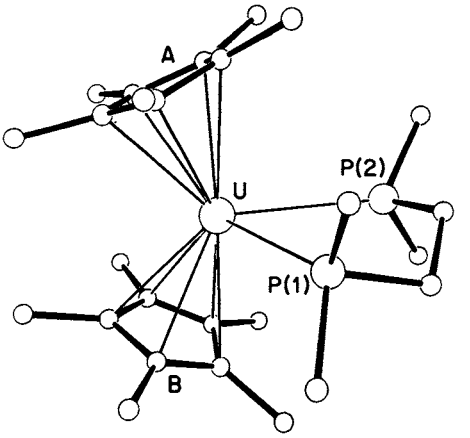

Fig. 23.19 *Perspective drawing of the non-hydrogen atoms in* $U[(CH_3)_5C_5]_2(H)[(CH_3)_2PCH_2CH_2P(CH_3)_2]$ [88]. *All atoms are represented by arbitrarily sized spheres for the purpose of clarity. Important bond lengths* (Å) *and angles* (deg) *for chemically distinct groups of atoms include: U–P*(1) = 3.211(8), *U–P*(2) = 3.092(8), *U–C*(*ring*) = 2.79(3) (*average*); *P*(1)–*U–P*(2) = 63.8(2), (*ring center of gravity*)–*U*–(*ring center of gravity*) = 136.2.

Variable-temperature NMR spectroscopy reveals at least two dynamic processes. An intramolecular exchange process interconverts magnetically nonequivalent Cp′ ligands and all dmpe CH_3 groups as the temperature is raised. This rearrangement presumably involves either spinning of the ligand about the local two-fold axis combined with inversion of the chelate ring, or stepwise dissociation and reassociation of the phosphorus atoms. In addition, magnetization transfer experiments indicate exchange of the coordinated dmpe with added free dmpe. Such lability is rather unusual for chelating phosphine ligands. Curiously, an analogous complex could not be prepared with the chelating amine donor $(CH_3)_2NCH_2CH_2N(CH_3)_2$ [90]. Instead, only the uranium hydride is obtained. Preliminary studies of $Cp'_2U(H)$ (dmpe) indicate that the phosphine ligand serves the function of solubilizing, but not interfering drastically with the reactivity of, the uranium hydride.

In contrast to the above results with phosphine donors, organoactinide hydrides do not form simple coordination complexes with phosphites. Rather, as exemplified by trimethyl phosphite

$$5(Cp'_2UH_2)_2 + 4P(OCH_3)_3 \xrightarrow[\text{toluene}]{25°C,\ 1\,h} 4[Cp'_2U(OCH_3)]_2PH + 2Cp'_2U(OCH_3)_2 + 8H_2 \tag{23.67}$$

$$5(Cp'_2ThH_2)_2 + 4P(OCH_3)_3 \xrightarrow[\text{toluene}]{25°C,\ 40\,h} 4[Cp'_2Th(OCH_3)]_2PH + 2Cp'_2Th(OCH_3)_2 + 8H_2 \tag{23.68}$$

the methoxy functionalities are rapidly and qualitatively cleaved [90]. The dinuclear phosphinidene products have been characterized by standard spectroscopic and chemical techniques as well as by x-ray diffraction for the uranium complex. As evident in Fig. 23.20, the U–P contacts are symmetrical and the U–O–C vectors are virtually linear.

Both $Th(CH_3)_7^{3-}$ (Section 23.3.1) [17] and $Cp'Th[CH_2C(CH_3)_3]_3$ (Section 23.3.4) [66] undergo reaction with H_2 to yield hydrides, as judged by NMR and/or vibrational spectroscopy. The nature of these hydrides is presently under investigation.

The ring-bridged $(CH_3)_2SiCp''_2ThR_2$ complexes described in Section 23.3.6 undergo rapid reaction with H_2 to liberate RH and to yield a hydride [71, 72]:

$$2(CH_3)_2SiCp''_2ThR_2 + 2H_2 \rightarrow 2[(CH_3)_2SiCp''_2ThH_2]_2 + 4RH \tag{23.69}$$

Diffraction studies indicate that the hydride is dimeric (Fig. 23.21) with a Th–Th distance 0.3 Å shorter than in $[Cp'_2Th(\mu\text{-}H)H]_2$ and comparable to that in thorium metal (3.59 Å). Interestingly, the infrared spectrum does not exhibit detectable terminal Th–H stretching modes, in contrast to $[Cp'_2Th(\mu\text{-}H)H]_2$. This strongly suggests a $Th(\mu\text{-}H)_4Th$ geometry (*24*):

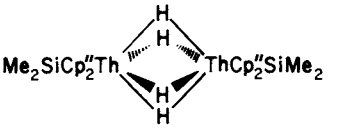

(24)

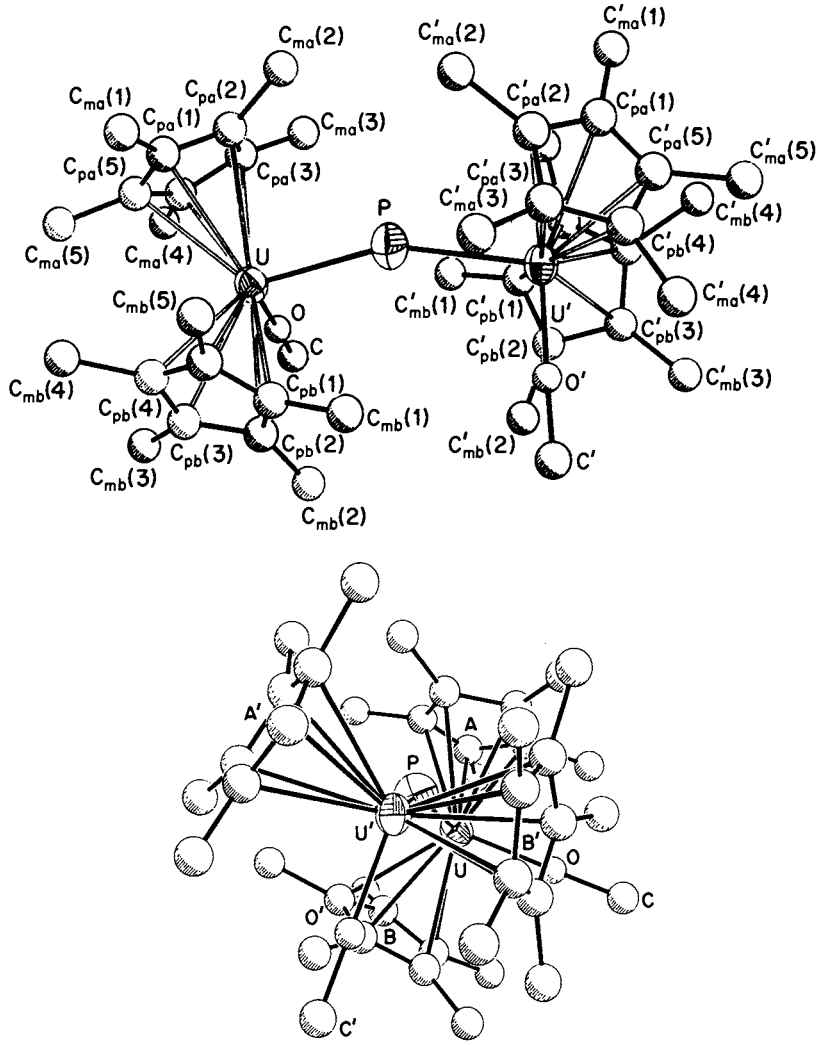

Fig. 23.20 *Two perspective views of the non-hydrogen atoms in* $[Cp_2U(OCH_3)]_2PH$ [90]. *Atoms labeled with primes are related to those labeled without primes by the crystallographic* C_2 *axis which passes through the phosphorus atom. Important bond lengths* (Å) *and angles (deg) for chemically distinct groups of atoms include:* $U–P = 2.743(1)$, $U–O = 2.046(14)$, $C–O = 1.44(3)$; $U–O–C = 178(1)$, $U–P–U = 157.4(3)$.

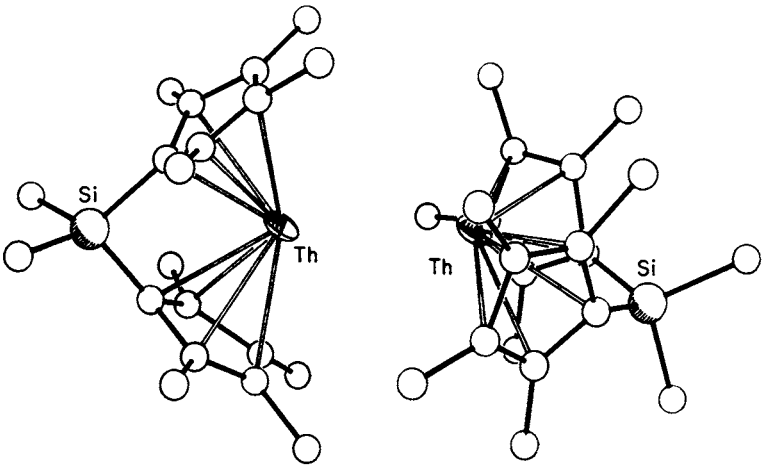

Fig. 23.21 *Molecular structure of the ring-bridged thorium hydride* $\{(CH_3)_2Si[(CH_3)_4C_5]_2ThH_2\}_2$ *by x-ray diffraction* [72]. *Relevant metrical parameters, bond lengths* (Å) *and angles* (*deg*), *are: Th–Th* = 3.628(1), *Th–Si* = 3.478(10) *and* 3.508(10); *(ring center of gravity)–Th–(ring center of gravity)* = 118.

With respect to catalytic olefin hydrogenation, the ring-bridged hydride is approximately 1000 times more active than $(Cp'_2ThH_2)_2$ for 1-hexene reduction [72].

Amido-substituted actinide hydrides [74, 91] can be synthesized as follows:

$$M\{N[Si(CH_3)_3]_2\}_3Cl + NaN[Si(CH_3)_3]_2 \xrightarrow{THF} M\{N[Si(CH_3)_3]_2\}_3H \quad M = Th, U \tag{23.70}$$

$$UCl_4 + 4NaN[Si(CH_3)_3]_2 \xrightarrow{THF} U\{N[Si(CH_3)_3]_2\}_3H \tag{23.71}$$

These compounds are both highly reactive and hydridic, as illustrated below:

$$M\{N[Si(CH_3)_3]_2\}_3H + CCl_4 \rightarrow M\{N[Si(CH_3)_3]_2\}_3Cl + HCCl_3 \tag{23.72}$$

$$M\{N[Si(CH_3)_3]_2\}_3H + BH_3 \cdot THF \rightarrow M\{N[Si(CH_3)_3]_2\}_3BH_4 \tag{23.73}$$

$$M\{N[Si(CH_3)_3]_2\}_3H \xrightarrow{D_2} M\{N[Si(CD_3)_3]_2\}_3D + HD \quad M = Th, U \tag{23.74}$$

They can be converted to the corresponding methyl derivatives via the unusual approach:

$$M\{N[Si(CH_3)_3]_2\}_3H \xrightarrow[(2)\ CH_3Br]{(1)\ n\text{-}C_4H_9Li} M\{N[Si(CH_3)_3]_2\}_3CH_3 \tag{23.75}$$

which also suggests some degree of protonic character for the hydrides.

23.5 ACTINIDE–TRANSITION-METAL σ BONDS

Although metal–metal bonding is an important facet of transition-metal chemistry, efforts to demonstrate metal–metal bonding involving actinides have, until recently, been largely unsuccessful or ambiguous in outcome. Thus, approaches employing metal carbonyl synthons have frequently resulted in isocarbonyl linkages to the oxophilic actinide centers ((*25*), $M'L_n$ = transition-metal fragment) [92–95] rather than in direct metal–metal bonds (*26*):

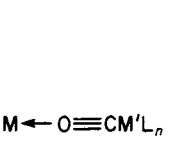

(*25*)

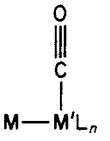

(*26*)

Possible examples involving phosphido ligands ((*27*), (*28*)) [96, 97]

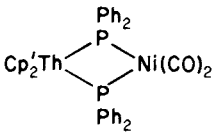

(*27*)

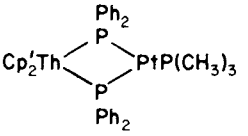

(*28*)

are complicated by the ambiguous significance of metal–metal distances in the presence of bridging ligands and by the necessarily dative character of any metal–metal bonding. A possible strategy to circumvent isocarbonyls would be to minimize crowding about the M–$M'L_n$(CO) bond and/or to select an $M'L_n$(CO) fragment with an appropriately directed, high-lying, metal-centered highest occupied molecular orbital (HOMO). Using $M'L_n$(CO) = $CpRu(CO)_2$ and M = $Cp'_2Th(X)$, X = Cl, I, as follows:

$$Cp'_2ThX_2 + CpRu(CO)_2Na \xrightarrow[25°C,\,2\,d]{\text{toluene}} Cp'_2Th(X)Ru(Cp)(CO)_2 + NaX \qquad X = Cl, I \tag{23.76}$$

it has recently proven possible to prepare the first complexes with direct, unsupported, actinide–transition-metal bonds [98]. The molecular structure of the X = I derivative is shown in Fig. 23.22. Both the Cp'_2ThI and $CpRu(CO)_2$ fragments are metrically unexceptional. The Th–Ru distance of 3.0277(6) Å can be compared to calculated Th–Ru distances of about 3.14 Å from metallic radii [99], about 3.23 Å from homobimetallic Ru–Ru and Th–Th (Fig. 23.21) compounds, about 3.12–3.15 Å from analogous Zr–Ru compounds [100] corrected for the Th(IV) ionic radius, and observed distances of about 2.87–3.24 Å in ThRu intermetallics [101–103]. Clearly, the Th–Ru distance in

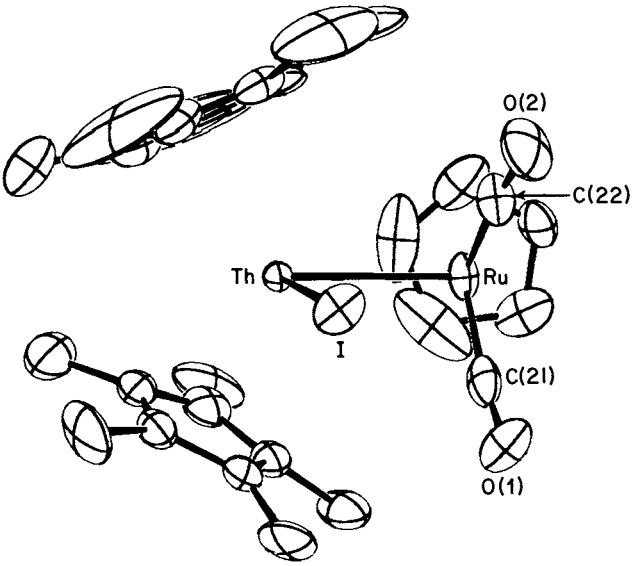

Fig. 23.22 *Perspective drawing of the molecular structure of* $Cp'_2Th(I)Ru(Cp)(CO)_2$ [98]. *Individual bond lengths* (Å) *and angles* (*deg*) *of interest include: Th–Ru* = 3.0277(6), *Th–I* = 3.0435(6), *Th–C*(*Cp' ring*) = 2.82(1,2,4,10), *Ru–C*(21) = 1.88(2), *Ru–C*(22) = 1.84(1), *Ru–C*(*Cp ring*) = 2.29(1,1,2,5); *Th–Ru–C*(21) = 83.8(2), *Th–Ru–C*(22) = 84.4(3), *C*(21)–*Ru–C*(22) = 88.3(5), *Th–Ru–Cp* (*centroid*) = 118.4.

$Cp'_2Th(I)Ru(Cp)(CO)_2$ is among the shortest of these values. In regard to reactivity, the Th–Ru bond undergoes rapid alcoholysis

$$Cp'_2Th(I)Ru(Cp)(CO)_2 + t\text{-}BuOH \rightarrow Cp'_2Th(I)(O\text{-}t\text{-}Bu) + CpRu(CO)_2H \quad (23.77)$$

implying highly polar character. Further studies of the chemistry of these and related heterobimetallic, actinide-containing complexes are in progress.

ACKNOWLEDGMENTS

The author thanks the National Science Foundation (Grant CHE8306255) and the Department of Energy (Contract DEAC 02-81ER10980) for support during the time in which this article was written.

REFERENCES

1. Marks, T. J. (1982) *Science*, **217**, 989–97.
2. Marks, T. J. and Ernst, R. D. (1982) in *Comprehensive Organometallic Chemistry* (eds G. Wilkinson, F. G. A. Stone, and E. W. Abel), Pergamon Press, Oxford, ch. 21.

3. Fagan, P. J., Matta, E. A., Manriquez, J. M., Moloy, K. G., Seyam, A. M., and Marks, T. J. (1982) in *Actinides in Perspective* (ed. N. M. Edelstein), Plenum Press, Oxford, pp. 433–52.
4. Marks, T. J. and Fischer, R. D. (eds) (1979) *Organometallics of the f-Elements*, Reidel, Dordrecht.
5. Marks, T. J. and Fragalà, I. L. (eds) (1985) *Fundamental and Technological Aspects of Organo-f-Element Chemistry*, Reidel, Dordrecht.
6. Ogden, A. J. (1976) in *Cryochemistry* (eds M. Moskovitz and G. A. Ozin), Wiley-Interscience, New York, ch. 7.
7. Sheline, R. K. and Slater, J. L. (1975) *Angew. Chem., Int. Edn*, **14**, 309–13.
8. Kunze, K. R., Hauge, R. H., Hamill, D., and Margrave, J. L. (1977) *J. Phys. Chem.*, **81**, 1664–7.
9. Tatsumi, K. and Hoffmann, R. (1984) *Inorg. Chem.*, **23**, 1633–4.
10. Tatsumi, K. and Nakamura, A. (1984) *J. Organomet. Chem.*, **272**, 141–54.
11. Gilman, H. (1968) *Adv. Organomet. Chem.*, **7**, 33.
12. Marks, T. J. and Seyam, A. M. (1974) *J. Organomet. Chem.*, **67**, 61–6.
13. Evans, W. J., Wink, D. J., and Stanley, D. R. (1982) *Inorg. Chem.*, **21**, 2565–73.
14. Seyam, A. M. (1983) *Inorg. Chim. Acta*, **77**, L123–L5.
15. Sigurdson, E. R. and Wilkinson, G. (1977) *J. Chem. Soc., Dalton Trans.*, 815–18.
16. Wachter, W. A. (1976) Ph.D. Thesis, Northwestern University.
17. Lauke, H., Swepston, P. N., and Marks, T. J. (1984) *J. Am. Chem. Soc.*, **106**, 6841–3.
18. Seyam, A. M. (1982) *Inorg. Chim. Acta*, **58**, 71–4.
19. Köhler, E., Brüser, W., and Thiele, K.-H. (1974) *J. Organomet. Chem.*, **76**, 235–40.
20. Davies, G. R., Jarvin, J. A., and Kilbourn, B. T. (1971) *Chem. Commun.*, 1511–12.
21. Marks, T. J. (1979) *Prog. Inorg. Chem.*, **25**, 224–333.
22. Perego, G., Cesari, M., Farina, F., and Lugli, G. (1976) *Acta Crystallogr. B*, **32**, 3034–9.
23. Sonnenberger, D. C., Morss, L. R., and Marks, T. J. (1985) *Organometallics*, **4**, 352–5.
24. Pilcher, G. and Skinner, J. A. (1982) in *The Chemistry of the Metal–Carbon Bond* (eds F. R. Hartley and S. Patai), Wiley, New York, pp. 43–90.
25. Connor, J. A. (1977) *Top. Curr. Chem.*, **71**, 71–110.
26. Kalina, D. G., Marks, T. J., and Wachter, W. A. (1977) *J. Am. Chem. Soc.*, **99**, 3877–9.
27. Bruno, J. W., Kalina, D. G., Mintz, E. A., and Marks, T. J. (1982) *J. Am. Chem. Soc.*, **104**, 1860–9.
28. Klähne, E., Giannotti, C., Marquet-Ellis, H., Folcher, G., and Fischer, R. D. (1980) *J. Organomet. Chem.*, **201**, 399–410.
29. Burton, M., Marquet-Ellis, H., Folcher, G., and Giannotti, C. (1982) *J. Organomet. Chem.*, **229**, 21–8.
30. Sonnenberger, D. C., Mintz, E. A., and Marks, T. J. (1981) *Proc. 10th Int. Conf. on Organometallic Chemistry*, Toronto, Abstracts 3D05.
31. Sonnenberger, D. C., Mintz, E. A., and Marks, T. J. (1984) *J. Am. Chem. Soc.*, **106**, 3484–91.
32. Paolucci, G., Rossetto, R., Zanella, R., Yünlü, K., and Fischer, R. D. (1984) *J. Organomet. Chem.*, **272**, 363–83.
33. Paolucci, G., Rossetto, R., Zanella, P., and Fischer, R. D., private communication.
34. Dormand, A., Elbouadili, A. A., and Moise, C. (1984). *J. Chem. Soc., Chem. Commun.*, 749–51.

35. Arnaudet, L., Folcher, G., and Marquet-Ellis, H. (1981) *J. Organomet. Chem.*, **214**, 215–20.
36. Cramer, R. E., Maynard, R. B., Paw, J. C., and Gilje, J. W. (1981) *J. Am. Chem. Soc.*, **103**, 3589–90.
37. Atwood, J. L., Haines, C. F., Tsutsui, M., and Gebala, A. E. (1973) *J. Chem. Soc., Chem. Commun.*, 452.
38. Cramer, R. E., Maynard, R. B., Paw, J. C., and Gilje, J. W. (1982) *Organometallics*, **1**, 869–71.
39. Cramer, R. E., Panchanatheswaran, K., and Gilje, J. W. (1984) *J. Am. Chem. Soc.*, **106**, 1853–4.
40. Cramer, R. E., Higa, K. T., Pruskin, S. L., and Gilje, J. W. (1983) *J. Am. Chem. Soc.*, **105**, 6749–50.
41. Cramer, R. E., Higa, K. T., and Gilje, J. W. (1985) *Organometallics*, **4**, 1140–1.
42. Arnaudet, L., Folcher, G., Marquet-Ellis, H., Klähne, E., Yünlü, K., and Fischer, R. D. (1983) *Organometallics*, **2**, 344–6.
43. Fagan, P. J., Manriquez, J. M., Maatta, E. A., Seyam, A. M., and Marks, T. J. (1981) *J. Am. Chem. Soc.*, **103**, 6650–7.
44. Duttera, M. R., Stecher, H. H., Suzuki, H., and Marks, T. J. (1985) submitted for publication.
45. Bruno, J. W., Smith, G. M., Fair, K., Schultz, A. J., Marks, T. J., and Williams, J. M. (1986) *J. Am. Chem. Soc.*, **108**, 40–56.
46. Smith, G. M., Suzuki, H., Sonnenberger, D. C., Day, V. W., and Marks, T. J. (1986) *Organometallics*, **5**, 549–61.
47. Ciliberto, E., Condorelli, G., Fagan, P. J., Manriquez, J. M., Fragalà, I., and Marks, T. J. (1981) *J. Am. Chem. Soc.*, **103**, 4755–69.
48. Fagan, P. J., Manriquez, J. M., Marks, T. J., Day, C. S., Vollmer, S. H., and Day, V. W. (1982) *Organometallics*, **1**, 170–80.
49. Suzuki, H. and Marks, T. J. (1984) unpublished results.
50. Bruno, J. W., Marks, T. J., and Morss, L. R. (1983) *J. Am. Chem. Soc.*, **105**, 6824–32.
51. Sonnenberger, D. C., Morss, L. R., and Marks, T. J. (1986) submitted for publication.
52. Bruno, J. W., Marks, T. J., and Day, V. W. (1982) *J. Am. Chem. Soc.*, **104**, 7357–60.
53. Bruno, J. W., Day, V. W., and Marks, T. J. (1983) *J. Organomet. Chem.*, **250**, 237–46.
54. Bruno, J. W., Duttera, M. R., Fendrick, C. M., Smith, G. M., and Marks, T. J. (1984) *Inorg. Chim. Acta*, **94**, 271–7.
55. Fendrick, C. M. and Marks, T. J. (1984) *J. Am. Chem. Soc.*, **106**, 2214–16.
56. Fendrick, C. M. and Marks, T. J. (1986) *J. Am. Chem. Soc.*, **108**, 425–37.
57. Fagan, P. J., Maatta, E. A., and Marks, T. J. (1981) in *Catalytic Activation of Carbon Monoxide* (ACS Symp. Ser. no. 152), American Chemical Society, Washington DC, pp. 53–78.
58. Marks, T. J., Manriquez, J. M., Fagan, P. J., Day, V. W., Day, C. S., and Vollmer, S. H. (1980) in *Lanthanide and Actinide Chemistry and Spectroscopy* (ACS Symp. Ser. no. 131), American Chemical Society, Washington DC, pp. 1–29.
59. Hofmann, P., Stauffert, P., Tatsumi, K., Nakamura, A., and Hoffmann, R. (1985) *Organometallics*, **4**, 404–6.
60. Manriquez, J. M., Fagan, P. J., Marks, T. J., Vollmer, S. H., Day, C. S., and Day, V. W. (1979) *J. Am. Chem. Soc.*, **101**, 5075–8.

61. Tatsumi, K., Nakamura, A., Hofmann, P., Hoffman, R., Moloy, K. G., and Marks, T. J. (1986) *J. Am. Chem. Soc.*, in press.
62. Moloy, K. G., Fagan, P. J., Manriquez, J. M., and Marks, T. J. (1986) *J. Am. Chem. Soc.*, **108**, 56–67.
63. Maatta, E. A. and Marks, T. J. (1981) *J. Am. Chem. Soc.*, **103**, 3576–8.
64. Moloy, K. G., Marks, T. J., and Day, V. W. (1983) *J. Am. Chem. Soc.*, **105**, 5696–8.
65. Mintz, E. A., Moloy, K. G., Marks, T. J., and Day, V. W. (1982) *J. Am. Chem. Soc.*, **104**, 4692–5.
66. Sternal, R. S. and Marks, T. J. (1984) unpublished results.
67. Cymbaluk, T. H., Ernst, R. E., and Day, V. W. (1983) *Organometallics*, **2**, 963–8.
68. Edwards, P. G., Andersen, R. A., and Zalkin, A. (1981) *J. Am. Chem. Soc.*, **103**, 7792–4.
69. Edwards, P. G., Andersen, R. A., and Zalkin, A. (1984) *Organometallics*, **3**, 293–8.
70. Secaur, C. A., Day, V. W., Ernst, R. D., Kennelly, W. J., and Marks, T. J. (1976) *J. Am. Chem. Soc.*, **98**, 3713–15.
71. Fendrick, C. M., Mintz, E. A., Schertz, L. D., Marks, T. J., and Day, V. W. (1984) *Organometallics*, **3**, 819–21.
72. Fendrick, C. M., Day, V. W., and Marks, T. J. (1986) submitted for publication.
73. Turner, J. W., Andersen, R. A., Zalkin, A., and Templeton, D. H. (1979) *Inorg. Chem.*, **18**, 1221–7.
74. Simpson, S, J., Turner, H. W., and Andersen, R. A. (1981) *Inorg. Chem.*, **20**, 2991–5.
75. Simpson, S. J. and Andersen, R. A. (1981) *J. Am. Chem. Soc.*, **103**, 4063–6.
76. Fagan, P. J., Manriquez, J. M., Marks, T. J., Day, V. W., Vollmer, S. H., and Day, C. S. (1980) *J. Am. Chem. Soc.*, **102**, 5396–8.
77. Broach, R., Schultz, A. J., Williams, J. M., Brown, G. M., Manriquez, J. M., Fagan, P. J., and Marks, T. J. (1979) *Science*, **203**, 172–4.
78. Duttera, M. R., Mauermann, H., and Marks, T. J. (1985) submitted for publication.
79. Jeske, G., Lauke, H., Mauermann, H., Schumann, H., and Marks, T. J. (1985) *J. Am. Chem. Soc.*, **107**, 8111–8.
80. Bowman, R. G., Nakamura, R., Fagan, P. J., Burwell, R. L., Jr, and Marks, T. J. (1981) *J. Chem. Soc., Chem. Commun.*, 257–8.
81. He, M.-Y., Burwell, R. L., Jr, and Marks, T. J. (1983) *Organometallics*, **2**, 566–9.
82. He, M.-Y., Xiong, G., Toscano, P. J., Burwell, R. L., Jr, and Marks, T. J. (1985) *J. Am. Chem. Soc.*, **107**, 641–52.
83. Toscano, P. J. and Marks, T. J. (1985) *J. Am. Chem. Soc.*, **107**, 653–9.
84. Fagan, P. J., Moloy, K. G., and Marks, T. J. (1981) *J. Am. Chem. Soc.*, **103**, 6959–62.
85. Moloy, K. G. and Marks, T. J. (1984) *J. Am. Chem. Soc.*, **106**, 7051–64.
86. Katahira, D. A., Moloy, K. G., and Marks, T. J. (1982) *Organometallics*, **1**, 1723–6.
87. Katahira, D. A., Moloy, K. G., and Marks, T. J. (1986) manuscript in preparation.
88. Duttera, M. R., Fagan, P. J., Marks, T. J., and Day, V. W. (1982) *J. Am. Chem. Soc.*, **104**, 865–7.
89. Duttera, M. R. and Marks, T. J. (1986) manuscript in preparation.
90. Duttera, M. R., Day, V. W., and Marks, T. J. (1984) *J. Am. Chem. Soc.*, **106**, 2907–12.
91. Simpson, S. J., Turner, H. W., and Andersen, R. A. (1979) *J. Am. Chem. Soc.*, **101**, 7728–9.
92. Marks, T. J., unpublished results.

93. Bennett, R. L., Bruce, M. I., and Stone, F. G. A. (1971) *J. Organomet. Chem.*, **26**, 355–6.
94. Fagan, P. J., Mintz, E. A., and Marks, T. J., unpublished results on $Cp_2U[MoCp(CO)_3]_2$ quoted in ref. 2, p. 261.
95. Dormand, A. and Moise, C. (1985) *Polyhedron*, **4**, 595–8.
96. Ritchey, J. M., Zozulin, A. J., Wrobleski, D. A., Ryan, R. R., Wassermann, H. J., Moody, C. D., and Paine, R. T. (1985) *J. Am. Chem. Soc.*, **107**, 501–3.
97. Hay, P. J., Ryan, R. R., Salazar, K. V., Worbleski, D. A., and Sattelberger, A. P. (1985) submitted for publication.
98. Sternal, R. S., Brock, C. P., and Marks, T. J. (1985) *J. Am. Chem. Soc.*, **107**, 8270–2.
99. Wells, A. F. (1984) *Structural Inorganic Chemistry*, 5th edn, Clarendon Press, Oxford, pp. 1286–8.
100. Casey, C. P., Jordon, R. F., and Rheingold, A. L. (1984) *Organometallics*, **3**, 604–5, and references therein.
101. Pearson, W. (ed.) (1961) *Structure Reports*, vol. 26, Oosthoek, Utrecht, pp. 236–7; (1962) vol. 27, p. 367.
102. Thomson, J. R. (1962) *Nature*, **194**, 465.
103. Thomson, J. R. (1963) *J. Less Common Metals*, **5**, 437–42.
104. Katahira, D. A., Liang, W.-B., Brock, C. P., Swepston, P. N., and Marks, T. J., unpublished results.
105. Brennan, J. G., Andersen, R. A., and Robbins, J. L. (1986) *J. Am. Chem. Soc.*, **108**, 335–6.
106. Arnaudette, L., Charpin, P., Folcher, G., Lance, M., Nierlich, M., and Vigner, D. (1986) *Organometallics*, **5**, 270–4.

CHAPTER TWENTY FOUR

FUTURE ELEMENTS

(including superheavy elements)

Glenn T. Seaborg and O. Lewin Keller, Jr

24.1 ELEMENTS NEAR PRESENT UPPER BOUNDARY

At the time of writing (1986), the heaviest known element is that with atomic number 109. Isotopes of elements in this uppermost region have half-lives in the millisecond range and are produced, as the result of heavy-ion bombardments, with extremely small yield (one atom per week of bombardment for element 109). Nevertheless it should perhaps be possible to synthesize and identify isotopes of elements 110 and 111, and additional isotopes of elements 107–109, using methods similar to those already employed, but this will be difficult and very time-consuming.

Because the half-lives and yields are becoming progressively smaller in this region at the upper boundary of the presently known elements, it might not be possible to proceed much further up the scale of atomic numbers unless some helpful factor intervenes. Fortunately there is general agreement that theoretical predictions define a range of superheavy elements (e.g. numbers 108–120) in an 'island of stability' with sufficient stability and yield to allow their study if they could be synthesized, but it cannot likewise be predicted whether there exist nuclear reactions for such syntheses in detectable amounts on Earth [1]. Synthesis reactions must be the result of bombardments with relatively high-Z heavy ions or massive prompt neutron capture and, if successful, should lead to the nearly simultaneous discovery of a number of such new elements. No

superheavy elements have been synthesized and identified at the time of writing (1986).

Decay by spontaneous fission becomes of greater relative importance soon beyond element 106. Alpha-particle decay permits detection through exploitation of genetic relationships with known alpha-particle-emitting daughters [2, 3] or coincident observation of K-series x-rays from daughter elements [4]. Isotopes with short half-lives which decay by spontaneous fission can be detected [5, 6], but assignment of atomic number is uncertain and difficult.

In line with the observation that the longest-lived alpha-particle-emitting isotope of each of the elements fermium (number 100), mendelevium (101), nobelium (102), lawrencium (103), rutherfordium (104), and hahnium (105) is one with 157 neutrons, it was found [7] as expected that $^{263}106$ is probably the longest-lived alpha-particle-emitting isotope of element 106. The anticipated large decrease in yield due to the competing fission reaction compounds the difficulties caused by decreasing half-lives in proceeding up the atomic-number scale; thus synthesis and identification for element 109 are orders of magnitude more difficult than for element 106.

The use of targets near the doubly magic ^{208}Pb allows the production of 'cold' compound systems in the transactinide region [8], which results in detectable yields of product nuclei. This 'cold fusion' route has led to the synthesis and identification of isotopes of elements 107, 108, and 109. An isotope of element 107, an approximately 5 ms alpha-particle-emitting $^{262}107$ (identified [3] via its alpha-particle-emitting descendants), was produced by the reaction ^{209}Bi(^{54}Cr, n). Element 109 was identified [9] as the result of the bombardment of ^{209}Bi with ^{58}Fe, according to the reaction ^{209}Bi(^{58}Fe, n); a single atom of $^{266}109$ (which decayed by alpha-particle emission after a time interval of 5 ms) was identified through observation of correlated alpha-particle and spontaneous-fission decays involving previously identified products. Three atoms of element 108 were identified [36] through the reaction ^{208}Pb(^{58}Fe, n)$^{265}108$, with a half-life for alpha-particle emission of 1.8 ms. The heaviest known elements, with atomic numbers 106, 107, 108, and 109, may represent an 'islet' of stability that may yet be extended. They have not been assigned names at the time of writing. We believe that the numerical (three-digit) atomic number should be used as the name and the chemical symbol for unnamed (e.g. 106) and undiscovered (e.g. 114) chemical elements.

Chemical identification is a desirable method for detection of a new element. Chemical identification of the elements immediately beyond hahnium (element 105) should be possible, but rapid chemical reactions will be required. Chemical properties can be predicted with the help of the periodic table shown in Fig. 24.1, which indicates that elements 106, 107, 108, etc., should be chemical homologs, respectively, of tungsten (W), rhenium (Re), osmium (Os), etc. The utilization of volatility properties perhaps offers the best possibility for very rapid chemical identification. The hexafluoride and hexacarbonyl of element 106 (eka-tungsten) should be quite volatile and the hexachloride, pentachloride, and oxychlorides

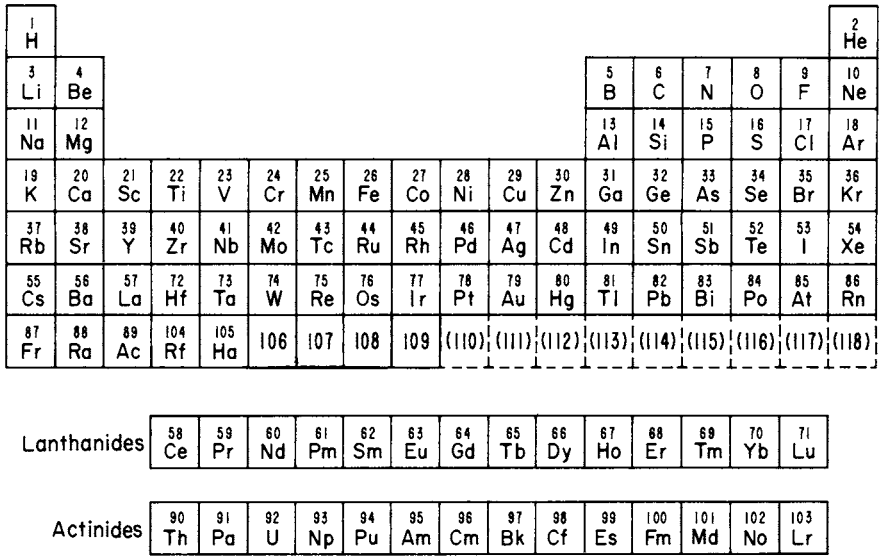

Fig. 24.1 *Periodic table of the elements. (Undiscovered elements are shown in parentheses.)*

should be moderately volatile. Element 107 should, similarly, be an eka-rhenium, with a volatile fluoride and oxyhalides. Element 108 should be an eka-osmium, and so have a volatile tetraoxide, which should be useful in designing experiments for its chemical identification.

These chemical predictions are based on the assumption that the filling of the electronic orbitals will continue on the basis of the 'aufbau' principle established for the lighter elements. Thus the periodic table of Fig. 24.1 shows elements 104 through 109 as homologs of hafnium through iridium, as would be expected on the basis of a 6d series following the actinides as a 5d series follows the lanthanides. The architecture of the periodic table thus depicted is confirmed by Dirac–Fock calculations (see Section 24.2). Experimental verification of these assumptions and calculations would be desirable to as high an atomic number as possible since some configurations may be close to each other in energy. For example, the electronic configuration of lawrencium might be expected to be $5f^{14}6d7s^2$ by analogy with lutecium. Brewer, however, made an early estimate that the ground-state configuration of lawrencium [10] should be $5f^{14}7s^27p_{1/2}$, and his result has since been confirmed by the multiconfigurational Dirac–Fock calculation of Desclaux and Fricke [11]. The latter authors give the configuration of the first excited state as $5f^{14}6d7s^2$. It is found to be separated from the ground state $5f^{14}7s^27p_{1/2}$ by only about $1500\,cm^{-1}$. Thus, the relative chemical influences of the $7p_{1/2}$ and 6d orbitals is difficult to predict in the transition region at the end of the actinide series and the beginning of the transactinide series. It is entirely possible that at least some of the elements in the 104–110 region will exhibit the character of 7p rather than 6d orbitals. Or, even more likely, the

orbitals may be close enough in energy and extension to give a mixed effect such as that which occurs for the 5f and 6d orbitals in the uranium–plutonium region.

A method is thus needed for distinguishing between p- and d-orbital character of metallic elements having half-lives as short as a few seconds which can be produced on as small a scale as one atom at a time. Perhaps such a method, applicable to elements 103–106 and possibly beyond, can be based on the large differences in the heats of sublimation between p and d elements. For example, the heats of sublimation of hafnium (611 kJ mol^{-1}), tantalum (782 kJ mol^{-1}), and tungsten (849 kJ mol^{-1}) are 3–4 times higher than those of thallium (180 kJ mol^{-1}), lead (197 kJ mol^{-1}), and bismuth (209 kJ mol^{-1}). These large differences, based on the different bond strengths associated with the p and d electrons, should carry over to the heats of adsorption of elements 103–106 in judiciously chosen gas–solid adsorption experiments. In particular, the thermochromatography approach developed by Zvara and co-workers at Dubna (USSR) should be applicable to differentiating between p- and d-electron configurations on the basis of differences in heats of sublimation as they correlate with adsorption. In thermochromatography, the gaseous atoms or molecules are passed down a column in which a linear temperature gradient is maintained. As would be expected, in general, atomic or molecular species that are relatively nonvolatile in the bulk condensed state deposit in the hotter regions of the tube, and those that are relatively volatile do not condense out until they reach the cooler portions of the tube. Deviations from this general trend can occur because the energetics in the adsorption of an atom on a surface differ from those in the macroscopic phase. Thus, for the metallic atoms of interest here, different metallic surfaces may also give different results, so that a series of experiments with, for example, titanium, vanadium, and molybdenum columns are necessary.

For example, Hubener and Zvara [12] applied the thermochromatographic technique using titanium columns to show that elemental californium, einsteinium, fermium, and mendelevium are divalent in the metallic vapor state and also adsorb on titanium in the divalent state. When they employed a molybdenum column, einsteinium, fermium, and mendelevium still adsorbed in the divalent position in the column, but californium deposited at a higher temperature thought to correspond to trivalent adsorption. These results suggest that it would be most interesting to determine using different metallic columns whether lawrencium behaves completely like a trivalent element, or possibly also has a monovalent form due to the tight binding of the $7s^2$ state. Since nobelium is most stable in the divalent state in aqueous solution, unlike the elements studied by Zvara, it should be included to serve as a confirmatory benchmark for completely divalent behavior in this region. Such investigations of the actinides would not only be important in increasing our understanding of the systematics of the 5f series but would also serve as a background for studies in the elements 104–106 and perhaps heavier transactinide region. In this region, where relativistic effects are so important, the 'aufbau' principle may be found to apply in a different way,

as pointed out above, in shaping the architecture of the periodic table than it does in the lighter elements.

A description of suitable criteria to establish the discovery of chemical elements is available [13]. The basic criterion must be proof that the atomic number (Z) of the new element is different from the atomic numbers of all previously known elements. Chemical identification constitutes an ideal proof. Also satisfactory is the identification of characteristic x-rays, the proof of a genetic relationship to a known nuclide through a decay chain, and, in the case of superheavy elements, the recognition of some anticipated distinctive radioactive decay properties. Even when these criteria are met, the name for a new element should not be proposed by the discoverers until the initial discovery is confirmed in another laboratory.

24.2 ELECTRONIC STRUCTURE OF SUPERHEAVY ELEMENTS

Although there are many schemes for the initial identification of these elements by purely physical methods, it is possible that chemical methods will be required for their initial identification and, in any case, these would be applied to their subsequent study.

Turning first to consideration of electronic structure, upon which chemical properties must be based, modern high-speed computers have made possible the calculation of such structures. Leading efforts took place in the USA at the Los Alamos Scientific Laboratory by Mann, Waber, and co-workers [14], and in Germany at the University of Frankfurt by Fricke and Greiner [15]. The calculations show that elements 104 through 112 are formed by filling the 6d subshell, which makes them, as expected, homologous in chemical properties with the elements hafnium (number 72) through mercury (80). Elements 113 through 118 result from the filling of the 7p subshell and are expected to be similar to the elements thallium (number 81) through radon (86). Thus, these calculations are consistent with the periodic table shown in Fig. 24.1 and are better illustrated in the periodic table shown in Fig. 24.2, which shows the filling of the electron subshells extending beyond element 118.

The calculations indicate that the 7s subshell should fill at elements 119 and 120, thus making these an alkali metal and alkaline-earth metal, respectively. Next the calculations point to the filling, after the addition of a 7d electron at element 121, of the inner 5g and 6f subshells, 32 places in all, which one of us [16] has termed the 'superactinide' elements and which terminates at element 153. This is followed by the filling of the 7d subshell (elements 154 through 162) and 8p subshell (elements 163 through 168).

Actually, more careful calculations have indicated that the picture is not this simple. The calculations indicate that other electrons (8p and 7d), in addition to those identified in the above discussion, enter the picture as early as element 121 (or 7p even in element 104), thus further complicating matters. These perturbations, caused by the spin–orbit splitting, become especially significant beyond

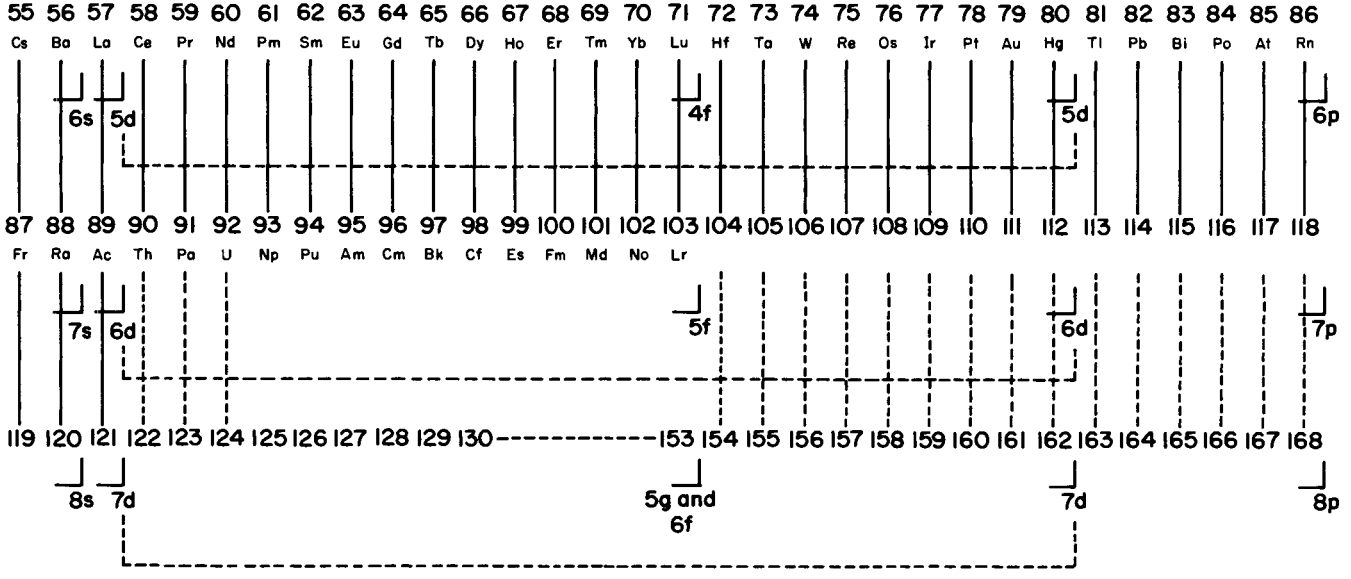

Fig. 24.2 *Modified form of periodic table showing known and predicted electron shells.*

the superactinide series, leading to predictions of chemical properties that are not consistent, element by element, with those suggested by Fig. 24.2. This, of course, is a region far beyond the region of expected nuclear stability – the only region where it might be possible to synthesize superheavy elements.

24.3 PREDICTIONS OF CHEMICAL PROPERTIES OF SUPERHEAVY ELEMENTS

Guided by a judicious combination of consideration of the calculated electronic structures, the periodic table (as shown in Figs 24.1 and 24.2), and various well-established qualitative chemical theories, scientists have been able to make some detailed predictions of the chemical properties of the superheavy elements. Of course, at first these elements will at best be produced 'one atom at a time', and they offer scant hope for ultimate production in the macroscopic quantities that would be required to verify some of these predictions. However, many of the predicted specific macroscopic properties, as well as the more general properties predicted for the other elements, will be useful in designing tracer experiments for the chemical identification of any of these elements that might be synthesized.

Few detailed predictions of the chemical properties of elements 109 (eka-iridium) and 110 (eka-platinum) have been made as yet. Their positions in the periodic table indicate that they should be noble metals. If the upper oxidation states are stable, volatile hexafluorides and octafluorides might be useful for chemical separation purposes. The predictions of the most stable oxidation states of elements 109 and 110 deviate widely. Penneman and Mann [17] give an oxidation state of I for 109 and 0 for 110. Cunningham preferred VI for both 109 and 110 [18].

Detailed predictions of the chemical properties of element 111 (eka-gold) have been made by Keller, Nestor, Carlson, and Fricke [19]. It appears that this noble metal will be most stable in the oxidation state III, and that it will be about as reactive as gold, with a chemistry similar to Au(III), but with more extensive complex-ion formation. The heat of sublimation is also expected to be similar to that of gold, although a direct extrapolation is not possible. Furthermore, the possibility exists that an ion with oxidation state -1 analogous to the auride ion will be stable. On the other hand, oxidation state $+1$ for element 111 should be much less important than for gold. If it exists, it will probably be in cyanide complexes. The oxidation state II will probably be unstable.

Similar detailed considerations concerning the chemical properties have not yet been made for element 112 (eka-mercury). More qualititative conjectures suggest that the most stable oxidation state might be the I state, but higher oxidation states will surely be important in aqueous solution and in compounds. It should be a distinctly noble metal, and there have even been suggestions, on the basis of its calculated high ionization potential and the relativistic effect on the closed $7s^2$ shell, that the interatomic attraction in the metallic state will be small,

possibly even leading to high volatility as in the noble gases [20]. A simple extrapolation of the volatility properties of its homologs, zinc, cadmium, and mercury, also suggests that metallic element 112 should be quite volatile. Again, it should have an extensive complex-ion chemistry. A number of these considerations suggest a chemistry noticeably different from its homolog, mercury.

Table 24.1 presents the predicted chemical properties of elements 104 through 112 as summarized in a review article by Keller and Seaborg [21].

A number of properties have been predicted by various workers for elements 113 through 120. The most conservative results are presented in Table 24.2, again taken from the review by Keller and Seaborg [21]. One of the most striking features of this table is the great decrease in boiling point predicted in going from element 113 (eka-thallium) to element 114 (eka-lead). This great decrease was predicted by Keller, Burnett, Carlson, and Nestor [22] on the basis of extrapolations of the heats of sublimation of the group III A and IV A elements versus row of the periodic system (Figs 24.3 and 24.4). The boiling points were then calculated using Trouton's rule. This predicted great decrease of almost 1000°C in boiling points in going from eka-thallium to eka-lead has been doubted by other workers in the field because the boiling point of lead is 1750°C, almost 300°C *higher* than that of thallium (1470°C). But this effect is a signal to us that something dramatic happens between elements 113 and 114 that does not happen between thallium and lead. And that something is a relativistic effect on the outermost electronic orbital.

To see the nature of what this relativistic effect may be, we should look into the periodic system of the known elements for a similar phenomenon. We find the same effect, indeed, in going from copper to zinc, or silver to cadmium, or gold to mercury (Table 24.3). The effect is obviously very dramatic, being 2350°C in the case of gold to mercury. What happens in each case to produce this great lowering of boiling points is the addition of an s electron to form an s^2 closed shell. In going from eka-thallium to eka-lead, a 7p electron is added to form a $7p^2$ configuration. In the lighter elements such a configuration would not be a closed shell but, because of relativistic effects, at element 114 it is. And this is the basis for the predicted different behavior in boiling points and many other differences in the region of element 114. Indeed, in the superheavy region, we would be studying relativity using test tubes.

In order to explain this important new effect on the periodic system, we need to see how relativistic effects change the properties of valence electrons in the region of element 114. In Fig. 24.5 we see the radii of the $p_{1/2}$ and $p_{3/2}$ valence electrons of antimony, bismuth, and element 115 (eka-bismuth). We pick element 115 for this discussion for the moment because the point is better made with it than with 114. In antimony the splitting between the p electrons of total angular momentum 1/2 and the p electrons with total angular momentum 3/2 is so small as to be of no importance. Also we just speak of a $5p^3$ configuration for antimony, and the designation of $p_{1/2}$ and $p_{3/2}$ is actually somewhat artificial from the point of view of its chemistry. This same story is almost, but not quite, true for bismuth. It is,

Table 24.1 *Predicted chemical properties of elements* 104–112 [21].

	Rf	Ha	106	107	108	109	110	111	112
stable oxidation states	III, IV	IV, V	IV, VI	III–VII	I–VIII	I–VI	I–VI	III(−1)	I, II
first ionization energy (eV)	5.1	6.6	7.6	6.9	7.8	8.7	9.6	10.5	11.4
standard electrode potential (V)	(4→0) −1.8	(5→0) −0.8	(4→0) −0.6	(5→0) +0.1	(4→0) +0.4	(3→0) +0.8	(2→0) +1.7	(3→0) +1.9	(2→0) +2.1
ionic radius (Å)	(+4) 0.71	(+5) 0.68	(+4) 0.86	(+5) 0.83	(+4) 0.80	(+3) 0.83	(+2) 0.80	(+3) 0.76	(+2) 0.75
atomic radius (Å)	1.50	1.39	1.32	1.28	1.26				
density (g cm^{-3})	23	29	35	37	41				
heat of sublimation (kJ mol^{-1})	694	795	858	753	628	594	481	335	29
boiling point (K)	5800								
melting point (K)	2400								

Table 24.2 *Predicted chemical properties of elements* 113–120 [21].

	113	114	115	116	117	118	119	120
stable oxidation states	I	II	I, III	II, IV	(−1), I, III, V	II, IV, VI, VIII	I, others	II
ionization energy (eV)								
I	7.4	8.5	5.2	6.6	7.6	8.7	4.8	6.0
II		16.8	18.1					
standard electrode potential (V)	(1→0) +0.6	(2→0) +0.9	(1→0) −1.5	(2→0) +0.1			(1→0) −2.7	(2→0) −3.0
ionic radius (Å)	(+1) 1.4	(+2) 1.2	(+1)1.5 (+3)1.0				(+1) 1.8	(+2) 1.6
atomic radius (Å)	1.7	1.6	2.0					
density (g cm^{-3})	18	22	11					
heat of sublimation (kJ mol^{-1})	142	42	142				42	138
boiling point (K)	1400	420	~1400			263		
melting point (K)	700	340	~700			258		

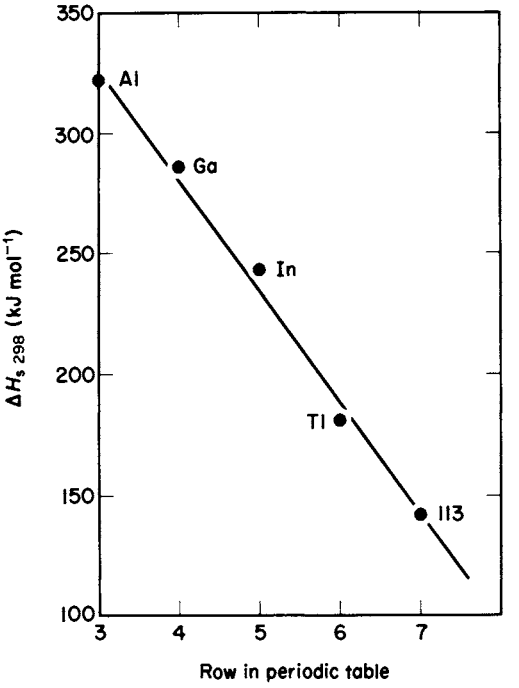

Fig. 24.3 *Heat of sublimation of element* 113.

interestingly enough, possible to make a chemical distinction under rather special conditions between the $6p_{3/2}$ electron and the two $6p_{1/2}$ electrons in bismuth. For example, the Bi^+ ion, in which the $6p_{3/2}$ electron has been removed leaving behind the $6p_{1/2}^2$ electrons, can be made in molten-salt media, as was discovered by Smith and co-workers [23] at Oak Ridge. But, in general, the p electrons in Bi appear to be indistinguishable. At 115, however, the relativistic effects are great enough to make the radius of the $7p_{3/2}$ electron very much larger than that of the $7p_{1/2}$ electrons. We might expect important differences in the chemistry between element 115 and bismuth because of this relativistic splitting of the $7p_{3/2}$ and $7p_{1/2}$ orbitals. Such a feeling is strengthened by looking at the energy splittings as well (Fig. 24.6). In antimony the splitting is quite small; in bismuth it is large enough to have some significance, as mentioned earlier; but in 115 the splitting is very large indeed. We must therefore take these relativistic effects into account when thinking about the chemistry of element 115.

In order to understand the differences between antimony, bismuth, and 115 still better, let us look at the wavefunctions for $p_{1/2}$ and $p_{3/2}$ electrons in the relativistic limit (Fig. 24.7). As can be seen, the $p_{1/2}$ wavefunction looks like an s wavefunction, being spherically symmetric. The two forms of $p_{3/2}$ wavefunctions, on the other hand, retain a considerable amount of the usual figure-8 character that we ordinarily associate with p wavefunctions in the non-relativistic limit. It is

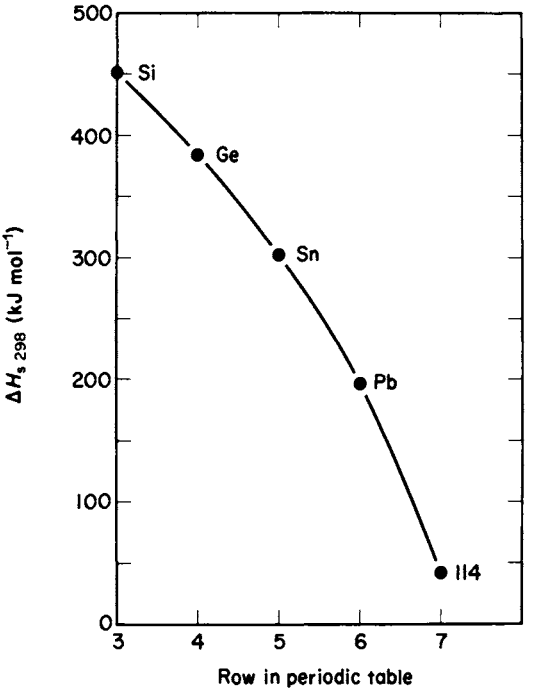

Fig. 24.4 *Heat of sublimation of element* 114.

Table 24.3 *Predicted boiling points for elements* 113 *and* 114.

	S_M (kJ mol^{-1})	B.P. (K)	ΔH_v (kJ mol^{-1})
Cu	339	2855	304
Zn	131	1181	115
Ag	286	2450	255
Cd	118	1038	100
Au	354	2980	324
Hg	61	630	57
113	(142)	(1400)	(130)
114	(42)	(420)	(38)

important to note here that a $p_{1/2}$ shell with two electrons is filled and has a character somewhat like that which we ordinarily associate with an s^2 closed shell. It is this $p^2_{1/2}$ closed-shell character that is so important in the chemistry of eka-lead (element 114). In eka-thallium (element 113), we have one $7p_{1/2}$ electron. In going to eka-lead, we add one more and this closes the shell at element 114. Thus we expect element 114 to be quite volatile, being somewhat like mercury, in fact,

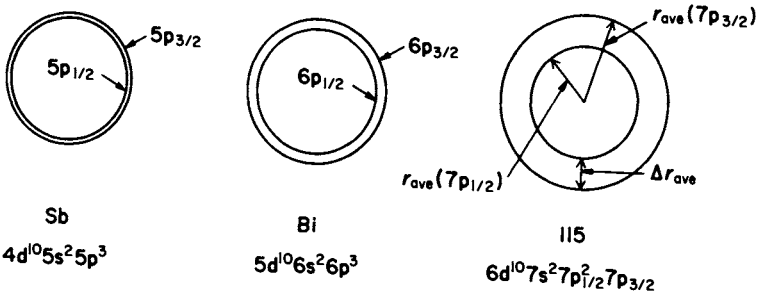

Fig. 24.5 *Relativistic splitting of radii of valence electrons of antimony, bismuth, and element* 115 *(relativistic Hartree–Fock–Slater calculations).*

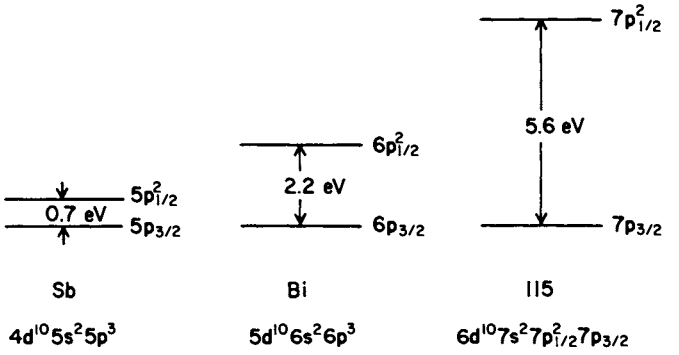

Fig. 24.6 *Relativistic splitting of energy levels of valence electrons of antimony, bismuth, and element* 115 *(relativistic Hartree–Fock–Slater calculations).*

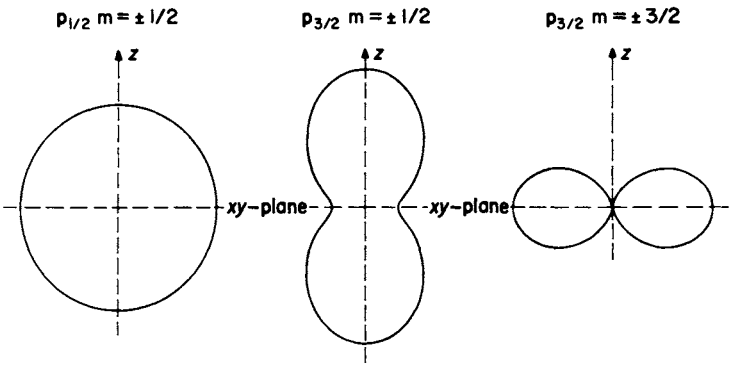

Fig. 24.7 *Angular distribution functions for the wavefunctions.*

rather than lead in this respect. The low boiling point that we predict for eka-lead warns us to watch out for other properties of element 114 that may have a resemblance to mercury or cadmium. For example, 114^{2+} will probably bind anions much more strongly than will Pb^{2+}.

So the something new that is added to chemistry in the superheavy region is relativistic effects. The major importance of the superheavy elements is that they would help us to understand the chemistry of the known elements. Ghostly images of relativity that we see in the chemistry of the known elements, things like Bi^{1+} and Po^{2+}, will come out in full flower in the superheavy region.

Keller, Burnett, Carlson, and Nestor [22] have made detailed predictions of the chemical properties of elements 113 and 114. The group IV elements show increasing stability in oxidation state II relative to the IV state as one goes to higher atomic numbers. Carbon and silicon have very stable tetrapositive oxidation states, and germanium shows a very unstable dipositive oxidation state in addition to a stable tetrapositive state. In tin, both the dipositive and tetrapositive oxidation states are important, and lead is most stable in oxidation state II. Thus, element 114 should be weakly, if at all, tetrapositive and the most stable oxidation state is expected to be the II state. The standard electrode potential for the reaction

$$114^{2+} + 2e^- \rightarrow 114$$

is calculated by Keller *et al.* [22] to be $+0.9$ V, on the scale where the reaction

$$H^+ + e^- \rightarrow \tfrac{1}{2}H_2$$

is assigned the value of 0.0 V.

For reasons similar to those that lead to the expectation of a stable II oxidation state in element 114, element 113 – a member of group III of the periodic system – is expected to have a preferred oxidation state of I; a standard electrode potential of $+0.6$ V is predicted. This means that eka-thallium is expected to be more noble than thallium, being more like silver in this respect. In fact, element 113 should have a chemistry somewhere between the chemistries of Tl^+ and Ag^+. The ion 113^+ is expected to be much more easily complexed in solution than is the case for Tl^+. For example, the solubility of TlCl in water is not increased much by adding excess HCl [24] or NH_3, whereas AgCl dissolves. Element 113 is expected to be more like silver in this respect. We thus see that the relativistic effects on the $7p_{1/2}$ electrons cause a diagonal relationship to be introduced into the periodic table around element 114, causing 114^{2+} to be somewhere between Hg^{2+} or Cd^{2+} and Pb^{2+} in its chemistry and 113^+ to act more like Ag^+ than Tl^+ in its chemistry.

Although all of the superheavy elements will show relativistic effects in their chemistry, the clearest case may be element 115 (eka-bismuth), which we have used for illustration above. Keller, Nestor, and Fricke [25] have made some detailed predictions of the chemical properties of element 115 based on extrapolations of the properties of elements of group V and relativistic calculations of electronic structure. Their results indicate that the chemical

properties of element 115 should be analogous, through a diagonal relationship, to those of thallium (group III) as well as to those of bismuth. As previously noted, relativistic effects on $p_{1/2}$ electrons impart to them (but not to $p_{3/2}$ electrons) some properties analogous to s electrons. On this basis, eka-bismuth will have a single $7p_{3/2}$ electron outside a $7p_{1/2}^2$ closed shell. Thus 115^+ is expected to be stable in analogy with Tl^+ rather than with the unusual and barely stable Bi^+, and is expected to have chemical properties analogous to those of Tl^+; a standard electrode potential of -1.5 V is predicted, indicating 115 metal to be quite reactive. These considerations also suggest that 115(III) should have a relative stability and chemical properties somewhat like Tl(III) but its chemical properties will be more similar to those of Bi(III). Element 115 is not expected to exhibit a stable V oxidation state. Melting and boiling points of the metal should be close to those of element 113.

Certain predicted volatility characteristics of elements 116, 117, and 118 (eka-polonium, eka-astatine, and eka-radon) or their compounds may offer advantages for chemical identification; this, of course, is especially true for element 118. The chemical properties of element 116 should be determined by extrapolation from polonium, and thus it should be stable in the II state with a less stable IV state.

The properties of element 117 have not been predicted in a careful and detailed way. Since there will be three $7p_{3/2}$ electrons outside of a $7p_{1/2}^2$ closed shell, oxidation state III rather than I is expected to be most important. For example, element 117 may be similar to gold(III) in its ion-exchange behavior in halide media.

The properties of element 118 shown in Table 24.2 are those predicted by Grosse [26] in 1965. These properties are obtained chiefly by extrapolation of known properties of lower homologs in the periodic table. Element 118 should be the most electropositive of the noble gases and should certainly exhibit positive oxidation states, such as IV, and should form fluorides and chlorides, and probably bromides and iodides, as well.

The complexity of its calculated electronic structure suggests that element 119 should exhibit an oxidation state or states higher than I, in addition to the stable I state. In other words, element 119 is expected to have core p electrons that are bound loosely enough to allow their removal. Such an expectation is also in accord with Grosse's prediction that element 118 will be the most electropositve of the noble gases. The chemistry of element 120 has not been predicted in detail, but it is expected to follow alkaline-earth-metal chemistry similarly to the manner in which element 119 follows alkali-metal chemistry.

The next element, number 121, might be termed eka-actinium, or perhaps superactinium (because it is followed by 32 rather than 14 inner transition elements), and the following superactinide elements (numbers 122–153, inclusive) might have chemical properties somewhat similar to, but also different from, the actinide elements.

It should be emphasized, however, that the elements beyond the predicted

island of stability (perhaps centered at $Z = 114$ and $N = 184$) do not possess sufficient nuclear stability or accessibility to synthesis via nuclear reactions to allow their synthesis and identification on Earth.

24.4 PREDICTIONS OF NUCLEAR PROPERTIES OF SUPERHEAVY ELEMENTS

Simple extrapolations of radioactive decay properties for elements beyond atomic number 109 suggest that the half-life, especially that for decay by spontaneous fission, would become so short as to make detection very difficult and soon impossible. However, in the period from 1966 to 1972, a number of calculations [27] based on modern theories of nuclear structure showed that in the region of proton number $Z = 114$ and neutron number $N = 184$ the ground states of nuclei should be stabilized against decay by spontaneous fission. This stabilization is due to the complete filling of major spherical proton and neutron shells in this region and is analogous to the stabilization of chemical elements such as the noble gases by the filling of their electronic shells. Such superheavy elements are predicted to form an island of relative stability extending both above and below $Z = 114$ and $N = 184$ and separated from the peninsula of known nuclei by a sea of instability.

Some more recent calculations [28], based on careful consideration of the effect of mass asymmetry on the fission barrier and a reduced spin–orbit coupling strength, have indicated that the $Z = 114$ shell effect is not very large. These calculations do confirm the existence of a shell at $N = 184$, but also suggest less stability for species with $N < 184$; that is, the island of stability has a cliff with a sharp drop-off for $N < 184$. If these considerations are correct, it would become considerably more difficult to synthesize and detect the superheavy elements (defined as those elements stabilized by spherical closed-nucleon shells). A premium would be placed on producing a nucleus with $N = 184$ or, very close to this, $N = 183$, in order that it might have a half-life sufficiently long to make it detectable.

24.5 SYNTHESIS ATTEMPTS AND FUTURE PROSPECTS

Numerous attempts have been made to synthesize and identify superheavy elements through the bombardment of heavy target nuclei with heavy ions. Both the compound-nucleus and deep-inelastic-transfer routes have been attempted. None of these experiments has been successful. A summary and analysis suggests that this failure is not due to failure to produce superheavy intermediate nuclei, but is due to the low survival probabilities of those superheavy precursors (which are lost by undergoing fission before de-excitation to the ground state).

For the compound-nucleus mechanism, the use of ^{48}Ca ions has seemed to offer the best hope because of its tight nuclear binding (closed proton and

neutron shells), neutron excess (allowing an approach toward the 184-neutron shell), and relatively small atomic number (making a fusion reaction possible). Early experiments [29, 30] that gave negative results were carried out at approximately 20 MeV above the classical interaction barrier because theoretical estimates indicated that beyond a certain critical size of projectile and target an extra energy would be required to fuse the nuclei [31–33]. For the inelastic-transfer mechanism, because the heaviest projectiles lead to generally broader primary product distributions, the bombardment of ^{248}Cm with ^{238}U ions seemed to be the best approach, but no products beyond $Z = 101$ were observed [34]. In each case the choice of target was ^{248}Cm because this offered the best combination of high atomic and mass numbers, availability, and relative ease of handling (owing to its relatively long half-life).

Based on the results of these experiments, and the successful synthesis of isotopes of elements 107 and 109 via 'cold fusion' reactions [3, 9], it was decided to pursue further the fusion route with the ^{248}Cm plus ^{48}Ca reaction with lower-energy ^{48}Ca ions. The hope was to produce cold compound nuclei and the ^{248}Cm(^{48}Ca,n)^{295}116 reaction (i.e. the 'one-neutron' channel). Bombarding energies close to the interaction barrier were used on the reasonable assumption that this system is not beyond the critical nuclear size where an 'extra push' is required to effect some degree of fusion. Again, negative results [35] were obtained, extending down to low cross-section limits (10^{-34}–10^{-35} cm^2) over a broad range of half-lives (a microsecond to 10 years).

A possible reason for the negative results from these compound-nucleus experiments is the failure to approach sufficiently close to the required 184 neutrons because ^{295}116 has only 179 neutrons. Because of its larger number of neutrons (155 compared to 152 in ^{248}Cm), the isotope ^{254}Es may offer the best route to the synthesis and identification of superheavy elements, although it is available only in microgram (or perhaps tens of micrograms) amounts. Here the use of ^{48}Ca might produce a nuclear species containing 182 neutrons by a reaction utilizing the one-neutron channel (cold nucleus intermediate), namely ^{254}Es(^{48}Ca,n)^{301}119. The more available ^{252}Cf would give the reaction ^{252}Cf(^{48}Ca,n)^{299}118 to yield a product with 181 neutrons, but this reaction is extremely difficult to handle because of its branching decay by spontaneous fission, giving copious emission of neutrons.

Other possibilities are more difficult to realize. The isotope ^{255}Es as target material could lead to an odd–odd nuclear species with 183 neutrons (even more desirable), but it would be very difficult to produce more than nanogram quantities reasonably free of its intensely radioactive precursor (20 day ^{253}Es) in the chain of neutron-capture reactions required for its production. Also, the 40 day half-life of ^{255}Es is more difficult to deal with than the 275 day half-life of ^{254}Es.

Another desirable target material is ^{250}Cm, with 154 neutrons, but this could be made available only by recovering it from the debris of underground nuclear explosions, an expensive undertaking. Here the one-neutron channel would result

in the reaction $^{250}Cm(^{48}Ca,n)^{297}116$, producing a product of smaller atomic number (presumably an advantage) with 181 neutrons. Eventually it should be possible to use secondary beams produced in sufficient intensity from primary high-energy nuclear reactions, utilizing extremely high-intensity primary beams produced in heavy-ion accelerators of the future. Thus very intense ^{48}Ca ions striking a primary target might produce ^{52}Ca ions in sufficient intensity to effect a reaction like $^{248}Cm(^{52}Ca,n)^{299}116$ with the readily available target isotope ^{248}Cm. The product $^{199}116$ would have the desirable 183 neutrons and a reasonably small atomic number (116). Unfortunately in all of these reactions the 2n or 3n channels are more likely due to the degree of excitation of the compound nucleus.

The perennial goal of ever trying to extend the upper limit of the periodic table of the chemical elements is enticing, and its pursuit should continue to yield very useful information about nuclear and chemical properties that will add to our future knowledge of other elements in the periodic table, as it has in the past.

REFERENCES

1. Seaborg, G. T., Loveland, W., and Morrissey, D. J. (1979) *Science*, **203**, 711–17.
2. Ghiorso, A., Nurmia, M., Harris, J., Eskola, K., and Eskola, P. (1969) *Phys. Rev. Lett.*, **22**, 1317–20.
3. Münzenberg, G., Hofmann, S., Hessberger, F. P., Reisberg, W., Schmidt, K. H., Schneider, J. H. R., Armbruster, P., Sahm, C. C., and Thuma, B. (1981) *Z. Phys. A*, **300**, 107–8.
4. Bemis, C. E., Jr, Silva, R. J., Hensley, D. C., Keller, O. L., Jr, Tarraut, J. R., Hunt, L. D., Dittner, P. J., Hahn, R. L., and Goodman, C. D. (1973) *Phys. Rev. Lett.*, **31**, 647–9.
5. Oganesyan, Yu. Ts., Demin, A. G., Danilov, N. A., Ivanov, M. P., Ilijnov, A. S., Kolesnikov, N. N., Markov, B. N., Plotko, U. M., Tretyakova, S. P., and Flerov, G. N. (1976) *JETP Lett.*, **23**, 277–9.
6. Somerville, L. P., Nurmia, M. J., Nitschke, J. M., Ghiorso, A., Hulet, E. K., and Lougheed, R. W. (1985); *Phys. Rev. C*, **31**, 1801–15. Somerville, L. P. (1982) PhD thesis, Lawrence Berkeley Laboratory Report LBL-14050.
7. Ghiorso, A., Nitschke, J. M., Alonso, C. T., Alonso, J. R., Nurmia, M., Seaborg, G. T., Hulet, E. K., and Lougheed, R. W. (1974) *Phys. Rev. Lett.*, **33**, 1490–3.
8. Oganesyan, Yu. Ts., Demin, A. G., Iljinov, A. S., Tretyakova, S. P., Pleve, A. A., Penionzhkevich, Yu. E., Ivanov, M. P., and Tretyakov, Yu. P. (1975) *Nucl. Phys. A*, **239**, 157–71.
9. Münzenberg, G., Armbruster, P., Hessberger, F. P., Hofmann, S., Poppensieker, K., Reisdorf, W., Schneider, J. R. H., Schneider, W. F. W., Schmidt, K.-H., Sahm, C.-C., and Vermeulen, D. (1982) *Z. Phys. A.*, **309**, 89–90; Münzenberg, G., Reisdorf, W., Hofmann, S., Agarwal, Y. K., Hessberger, F. P., Poppensieker, K., Schneider, J. R. H., Schneider, W. F. W., Schmidt, K.-H., Schött, H.-J., Armbruster, P., Sahm, C.-C., and Vermeulen, D. (1984) *Z. Phys. A*, **315**, 145–58.
10. Brewer, L. (1976) *J. Opt. Soc. Am.*, **61**, 1101–11.
11. Desclaux, J.-P. and Fricke, B. (1980) *J. Phys.*, **41**, 943–6.
12. Hubener, S. and Zvara, I. (1982) *Radiochim. Acta*, **31**, 89–94.

13. Harvey, B. G., Herrmann, G., Hoff, R. W., Hoffman, D. C., Hyde, E. K., Katz, J. J., Keller, O. L., Jr, Lefort, M., and Seaborg, G. T. (1976) *Science*, **193**, 1271–2.
14. Mann, J. B. and Waber, J. T. (1975) *J. Chem. Phys.*, **53**, 2397–406.
15. See, e.g., Fricke, B., Greiner, W., and Waber, J. T. (1970) *Theor. Chem. Acta (Berl.)*, **21**, 235–59.
16. Seaborg, G. T. (1968) *Annu. Rev. Nucl. Sci.*, **18**, 53–152.
17. Penneman, R. A. and Mann, J. B. (1976) *J. Inorg. Chem.*, Suppl., *Proc. Moscow Symp. on Chemistry of the Transuranium Elements* (eds V. I. Spitsyn and J. J. Katz), pp. 257–63.
18. Cunningham, B. B. (1969) *Proc. Robert A. Welch Foundation*, XIII, *The Transuranium Elements* – The Mendeleev Centennial, pp. 307–22.
19. Keller, O. L., Jr, Nestor, C. W., Jr, Carlson, T. A., and Fricke, B. (1973) *J. Phys. Chem.*, **77**, 1806–9.
20. Pitzer, K. S. (1975) *J. Chem. Phys.*, **63**, 1032–3.
21. Keller, O. L. Jr and Seaborg, G. T. (1977) *Annu. Rev. Nucl. Sci.*, **27**, 139–66.
22. Keller, O. L., Jr, Burnett, J. L., Carlson, T. A., and Nestor, C. W., Jr (1970) *J. Phys. Chem.*, **74**, 1127–34.
23. Smith, G. P. and Davis, H. L. (1973) *Inorg. Nucl. Chem. Lett.*, 991–5.
24. Alekseeva, T. E., Arkhipova, N. F., and Rabinovitch, V. A. (1972) *Russ. J. Inorg. Chem.*, **17**, 140–1.
25. Keller, O. L., Jr, Nestor, C. W., Jr, and Fricke, B. (1974) *J. Phys. Chem.*, **78**, 1945–9.
26. Grosse, A. V. (1965) *J. Inorg. Nucl. Chem.*, **27**, 509–20.
27. Bemis, C. E., Jr and Nix, J. R. (1977) *Comm. Nucl. Part. Phys.*, **7**, 65–78.
28. Randrup, I., Larsson, S. E., Möller, P., Sobiczewski, A., and Lukasiak, A. (1974) *Phys. Scr.*, **10A**, 60–4.
29. Hulet, K., Lougheed, R. W., Wild, J. F., Landrum, J. H., Stevenson, P. C., Ghiorso, A., Nitschke, J. M., Otto, R. J., Morrissey, D. J., Baisden, P. A., Gavin, B. F., Lee, D., Silva, R. J., Fowler, M. M., and Seaborg, G. T. (1977) *Phys. Rev. Lett.*, **39**, 385–9.
30. Oganessian, Yu. Ts., Bruchertseifer, H., Buklanov, G. V., Chepigin, V. I., Choi Val Sek, Eichler, B., Gavrilov, K. A., Gaeggeler, H., Korotkin, Yu. S., Orlova, O. A., Reetz, T., Seidel, W., Ter-Akopian, G. M., Tretyakova, S. P., and Zvara, I. (1978) *Nucl. Phys. A*, **294**, 213–24.
31. Nix, J. R. and Sierk, A. J. (1977) *Phys. Rev. C*, **15**, 2072–82.
32. Swiatecki, W. J. (1981) *Phys. Scr.*, **24**, 113–22.
33. Swiatecki, W. J. (1982) *Nucl. Phys. A*, **376**, 275–91.
34. Schädel, M., Brüchle, W., Gäggeler, H., Kratz, J. V., Sümmerer, K., Wirth, G., Herrmann, G., Stakemann, R., Tittel, G., Trautmann, N., Nitschke, J. M., Hulet, E. K., Lougheed, R. W., Hahn, R. L., and Ferguson, R. L. (1982) *Phys. Rev. Lett.*, **48**, 852–5.
35. Armbruster, P., Agarwal, Y. K., Brüchle, W., Brügger, M., Dufour, J. P., Gäggeler, H., Hessberger, F. P., Hofmann, S., Lemmertz, P., Münzenberg, G., Poppensieker, K., Reisdorf, W., Schädel, M., Schmidt, K.-H., Schneider, J. R. H., Schneider, W. F. W., Sümmerer, K., Vermeulen, D., Wirth, G., Ghiorso, A., Gregorich, K. E., Lee, D., Leino, M., Moody, K. J., Seaborg, G. T., Welch, R. B., Wilmarth, P., Yashita, S., Frink, C., Greulich, N., Herrmann, G., Hickmann, U., Hildebrand, N., Kratz, J. V., Trautmann, N., Fowler, M. M., Hoffman, D. C., Daniels, W. R., von Gunten, H. R., and Dornhöfer, H. (1985) *Phys. Rev. Lett.*, **54**, 406–9.
36. Münzenberg, G., Armbruster, P., Folger, H., Hessberger, F. P., Hofmann, S., Keller, J., Poppensieker, K., Reisdorf, W., Schmidt, K.-H., Schött, H.-J., Leino, M. E., and Hingmann, R. (1984) *Z. Phys. A*, **317**, 235–6.

APPENDIX I

NUCLEAR SPINS AND MOMENTS OF THE ACTINIDES

John G. Conway

The table lists the element and atomic mass in the first two columns. The nuclear spin (I) is in column 3. The magnetic dipole moment (μ) in units of nuclear magnetons is in column 4. The spectroscopic electric quadrupole moment (Q) in units of barns is in column 5.

There are several references where this information has been tabulated and reference to the original work may be found. *Nuclear Spins and Moments* by G. H. Fuller and V. W. Cohen, Nuclear Data Tables, **5**, 433 (1969) contains data for all the elements. A later compilation by S. Gerstenkorn, *J. Physique*, **34**, 55 (1973) entitled *Nuclear Properties Deduced from the Optical Spectra of the Atoms, Nuclear Moments and Isotope Shift of the Actinide and Rare Earth Series*, lists the data through 1973. A report *Table of Nuclear Moments* by V. S. Shirley and C. M. Lederer, Lawrence Berkeley Laboratory, LBL-3450 (Dec. 1974) is a listing of all the elements. They have made corrections to the magnetic dipole moments based on a revised proton moment and have also corrected for diamagnetic shielding.

There are two later references to work since 1974. The spin and moment of ^{249}Cf is from N. Edelstein and D. G. Karraker, *J. Chem. Phys.* **62**, 938 (1975). The data for ^{253}Es and ^{254m}Es are from L. S. Goodman, H. Diamond and H. E. Stanton, *Phys. Rev.* **11**, 499 (1975). The sign of the nuclear moment of ^{249}Cf is negative (J. Blaise, private communication, 1979).

Element	*A*	*Nuclear spin I*	*Nuclear magnetic moment μ (nuclear magnetons)*	*Electric quadrupole moment Q (barns)*
Actinium	227	3/2	$+1.1 \pm 0.1$	$+1.7 \pm 0.2$
Thorium	229	5/2	$+0.44 \pm 0.05$	$+4.9 \pm 0.5$
Protactinium	231	3/2	+1.98	−3.0
Protactinium	233	3/2	+3.4	
Uranium	233	5/2	$+0.49 \pm 0.05$	$+4.9 \pm 0.5$
Uranium	235	7/2	-0.31 ± 0.03	$+6.4 \pm 0.7$
Neptunium	237	5/2	+2.9	+5.0
Neptunium	238	2		
Neptunium	239	5/2		
Plutonium	239	1/2	$+0.200 \pm 0.004$	
Plutonium	241	5/2	-0.72 ± 0.02	$+5.6 \pm 0.6$
Americium	241	5/2	$+1.59 \pm 0.03$	+4.9
Americium	242	1	+0.382	−2.74
Americium	243	5/2	$+1.59 \pm 0.03$	+4.9
Curium	243	5/2	0.40	
Curium	245	7/2	0.5 ± 0.1	
Curium	247	9/2	0.36	
Berkelium	249	7/2	2.2 ± 0.4	+5.79
Californium	249	9/2	-0.28 ± 0.06	
Einsteinium	253	7/2	4.10 ± 0.07	6.13
Einsteinium	254m	2	2.87	3.39

APPENDIX II

NUCLEAR PROPERTIES OF ACTINIDE NUCLIDES

Irshad Ahmad and Paul R. Fields

DISCUSSION

In this appendix we first present a brief and elementary discussion of the nuclear properties of heavy elements, mainly for the benefit of those readers who have no previous orientation in nuclear chemistry. For a more detailed understanding of this subject, the reader should refer to a nuclear chemistry textbook [1, 2] and for information on nuclear data he or she should consult the *Table of Isotopes* [3], or the *Table of Radioactive Isotopes* [4].

All nuclei in the actinide region are unstable towards α decay. A few actinide nuclides are stable to β decay, but because of α decay they are radioactive. Thus there are no stable actinide nuclides. The higher-Z elements also decay by spontaneous fission; in particular, ^{248}Cm and ^{252}Cf have significant fission branching.

The most common mode of disintegration for actinide nuclei is by the emission of α particles (^{4}He ions). Alpha decay energies are known [3–5] for most nuclides and they can also be calculated from known atomic masses [6]. This decay process produces daughter nuclei that are two less in atomic number and have four less atomic mass units than the parent nuclei. During α decay, about 2% of the available decay energy is imparted to the recoiling daughter nucleus and the remainder is carried off by the fast-moving α particles. Several groups of α particles, each with a definite energy, are emitted in most α decay processes. For actinide nuclides, α decay energies range from about 4 to about 11 MeV. As a general rule, α decay energy increases with increasing Z and for a given element it decreases with increasing mass number.

The α decay half-life of a nucleus decreases exponentially with increasing decay energy. As a rough guide every 50 keV decrease in the decay energy increases the half-life by a factor of about 2. One useful quantity that facilitates the understanding of the mechanism of the α decay process is the hindrance factor. It is defined as the ratio of the experimental partial half-life to the theoretical half-life calculated on the assumption that the α particle pre-exists in the nucleus as an entity and that during the decay it carries no angular momentum. Alpha transitions in which the ground-state configuration of the parent nucleus remains

unchanged are called 'favored transitions' and these have hindrance factors close to unity. All α transitions between the ground states of even–even nuclei are favored transitions.

Just like elements of lower Z, each actinide element also has one or more β-stable isotopes. Isotopes heavier than the β-stable nucleus decay by emission of β^- particles (electrons) whereas lighter isotopes decay by electron capture (EC). In heavy elements, the β^+/EC ratio is very small and, as a consequence, positron (β^+) emission has been observed only in a few nuclei. The β decay energy usually increases as the nucleus gets further away from the line of β stability. A quantity denoted by ft is very useful in classifying β transitions and estimating β decay half-lives. The log ft value, also called the reduced β transition probability, is the energy-independent transition rate.

Spontaneous fission is a decay process in which a nucleus breaks up into two almost equal fragments. Each fission event is accompanied by the release of about 200 MeV energy and the emission of 2–4 neutrons. Fission half-life depends on the fissility parameter Z^2/A and it is the major mode of decay for many isotopes of elements 100 and beyond.

Recently a new form of radioactivity has been discovered [7] in which nuclei decay by the spontaneous emission of particles heavier than alpha particles but lighter than fission fragments. The branching ratio for this decay mode is extremely small (of the order of 10^{-10}). Examples of such decay modes are the ^{14}C emission [8] by ^{223}Ra, and ^{24}Ne emission [9] by ^{231}Pa and ^{232}U.

Alpha and beta transitions usually populate the ground state as well as several excited states of the daughter nucleus. These excited states de-excite to the ground state by emission of γ rays and conversion electrons. Typical half-lives of these states are between 10^{-9} and 10^{-14} s. However, in some cases, the decay of an excited state is forbidden for fast magnetic dipole (M1), electric dipole (E1), or electric quadrupole (E2) transitions because of the angular momentum selection rule. Such states have lifetimes of 10^{-9} s to years. Excited states that have half-lives of greater than 10^{-9} s are called metastable states or isomers. The isomeric state either de-excites to the ground state of the same nucleus by an internal transition (IT) or it decays by the usual modes of disintegration.

Most isomers occur because of the large difference between the spins of the excited state and the ground state. However, there is a class of isomers that decay by fission, and these are caused not by the difference in the angular momenta of the states but by difference in the shapes. These are called 'fission isomers' or 'shape isomers', and have half-lives in the range of 10^{-9} s to 10^{-3} s. These isomers have deformation almost twice that of the ground-state nucleus. More than 50 fission isomers have been discovered [10].

Extensive research has been done on the nuclear structure of heavy elements using radioactive decay studies and high-resolution nuclear reaction spectroscopy. These investigations have provided important information to test and develop microscopic theoretical models. It has been established that nuclei with $A \gtrsim 225$ have spheroidal shape with major:minor axes in the

approximate ratio of 5:4. The intrinsic electric quadrupole moments of these nuclei have been measured to be about 10^{-23} e cm^2 and their radii are approximately 10^{-12} cm.

Recent investigations indicate that certain nuclei have octupole deformation. These pear-shaped nuclei are axially symmetric but they are reflection asymmetric. Examples [11] of pear-shaped nuclei are ^{229}Pa and ^{225}Ac.

In nuclei, nucleons (protons and neutrons) move in orbits under the influence of the central nuclear potential. Nilsson [12] and others [13] have calculated the eigenvalues and wavefunctions of a nucleon in a deformed potential as a function of deformation β. A plot of eigenvalues versus deformation, commonly known as Nilsson diagram, is extremely useful in understanding the energy levels in deformed nuclei. Each Nilsson state is characterized by Ω, the projection of the single-particle angular momentum on the nuclear symmetry axis; π, the parity; and the asymptotic quantum numbers, N, n_Z and Λ. The quantum number N denotes the oscillator shell number, n_Z represents the number of oscillator quanta along the symmetry axis, and Λ is the projection of the orbital angular momentum on the symmetry axis. In actinide nuclei, neutrons (protons) fill each orbital above the closed shell of 126 (82) pairwise and thus the ground-state spin–parity of an odd-mass nucleus is simply the spin–parity of the state occupied by the last unpaired nucleon. All even–even nuclei have ground-state spin–parity of 0+.

Since the rotation axis of the spheroidal nucleus is perpendicular to the symmetry axis K, the projection of the total angular momentum I, is the same as Ω. The rotation generates a band with spin sequence K, $K+1$, $K+2$, . . . , etc. The rotational energy of a level is given by the expression

$$E_I = \frac{\hbar^2}{2\mathscr{I}} I(I+1)$$

where $\hbar$ is Planck's constant and $\mathscr{I}$ is the nuclear moment of inertia. Typical values of $\hbar^2/2\mathscr{I}$ are 7 keV for even–even nuclei and 6 keV for odd-mass nuclei. The ground-state band of an even–even nucleus has spin–parity sequence of 0+, 2+, 4+, 6+, . . . ; odd spin values are not allowed.

There are several methods for the qualitative and quantitative analysis of actinide samples. The easiest technique is the gross counting in a 2π (50%) geometry gas proportional counter. These counters have very low background for α particles and fission events but have somewhat higher background for β^- particles. Samples with only few disintegrations per minute of α or fission can be easily counted.

A more powerful technique involves the measurement of energy spectra with solid-state detectors. Alpha-particle spectra can be measured with an Au–Si surface barrier detector. For these measurements thin sources are required and both the source and the detector are placed in vacuum. Resolutions (full width at half maximum) of 10–30 keV are easily obtained and usual geometries are 5–30%. By measuring the α-particle spectrum, commonly known as α pulse-height

analysis, one can determine the relative quantities of various nuclides present in a sample.

Gamma-ray spectroscopy with a germanium detector is another powerful and versatile technique for the analysis of radioactive samples. In general, prominent γ rays are present in the decay of odd-mass and odd–odd (odd neutron–odd proton) nuclei, and can be used to assay these nuclides. Also, nuclides that decay by electron capture almost always produce the characteristic K x-rays of the daughter nuclei. These x-rays have convenient energies in the 80–160 keV region. The advantage of γ-ray spectroscopy is that samples in any quantity and in any form (solution or solid) can be assayed. The resolution of Ge detectors can be better than 1 keV and maximum efficiency is about 25%. The efficiency is a function of energy, and between 100 keV and 1 MeV it drops approximately by an order of magnitude.

Because of their long half-lives, ^{232}Th, ^{235}U, and ^{238}U occur in nature. Each of these nuclides starts a decay chain that terminates at stable Pb isotopes. For this reason isotopes of elements between Pb and U are also found in nature. Chemical separation procedures are used to isolate samples of Ac, Th, and Pa nuclides. Enriched samples of elements, like U, for which many isotopes are present together, are commonly obtained using isotope separators.

The main source of transuranium elements is the high-flux reactor, in which ^{238}U or heavier nuclei get transformed into higher-Z elements by multiple neutron capture. In the USA, there is a national program for the production of transuranium elements utilizing the high-flux reactor (HFIR) at Oak Ridge. The heaviest nuclide produced in the reactor is ^{257}Fm. Neutron-deficient nuclides are synthesized in charged-particle accelerators and very neutron-rich nuclides with short half-lives are produced in reactors.

All data in the nuclear properties tables and this appendix have been taken from refs 3–5 except where a more recent reference was found. The cut-off date for literature survey was March 1986.

The notations for various decay modes used in this book are: α for alpha decay, β^- for β^- decay, β^+ for positron decay, EC for electron capture, IT for isomeric transition, and SF for spontaneous fission. The letter 'm' after a mass number denotes an isomer. Isomers with a half-life of less than 1 s and fission isomers are omitted from the tables. Energies are given only for the most abundant α groups and γ rays; for β^- particles the maximum energies β_{max} are tabulated. In the last column, only the convenient methods for the production of nuclides are given: 'nature' denotes that the nuclide occurs in nature and 'multiple neutron capture' means that this nuclide is produced by long irradiation in a high-flux reactor.

The specific activity S in disintegrations per minute per microgram was calculated using the expression

$$S = \frac{4.17449 \times 10^{17}}{T_{1/2} A}$$

The half-lives $T_{1/2}$ were obtained from refs 3–5 and the atomic masses A were taken from ref. 6.

REFERENCES

1. Friedlander, G., Kennedy, J. W., Macias, E. S., and Miller, J. M. (1981) *Nuclear and Radiochemistry*, Wiley, New York.
2. Hyde, E. K., Perlman, I., and Seaborg, G. T. (1964) *The Nuclear Properties of the Heavy Elements*, Vol. I, Prentice-Hall, Inc. Englewood Cliffs, New Jersey.
3. Lederer, C. M. and Shirley, V. S., eds (1978) *Table of Isotopes*, Wiley, New York.
4. Browne, E. and Firestone, R. B. (1986) *Table of Radioactive Isotopes*, (ed. V. S. Shirley) Wiley, New York.
5. Armbruster, P. (1985) *Ann. Rev. Nucl. Part. Sci.*, **35**, 135–94.
6. Wapstra, A. H. and Audi, G. (1985) *Nucl. Phys.*, **A432**, 1–54.
7. Rose, H. J. and Jones, G. A. (1984) *Nature*, **307**, 245–47.
8. Kutschera, W., Ahmad, I., Armato, S. G., III, Friedman, A. M., Gindler, J. E., Henning, W., Ishii, T., Paul, M., and Rehm, K. E. (1985) *Phys. Rev.*, **C32**, 2036–42.
9. Barwick, S. W., Price, P. B., and Stevenson, J. D. (1985) *Phys. Rev.*, **C31**, 1984–6.
10. Vandenbosch, R. (1977) *Ann. Rev. Nucl. Sci.*, **27**, 1–35.
11. Ahmad, I., Gindler, J. E., Betts, R. R., Chasman, R. R., and Friedman, A. M. (1982) *Phys. Rev. Lett.*, **49**, 1758–61.
12. Nilsson, S. G. (1955) *Kgl. Dansk Videnskab. Selskab., Mat.-Fys. Medd.*, **29**, No. 16.
13. Chasman, R. R., Ahmad, I., Friedman, A. M., and Erskine, J. R. (1977) *Rev. Mod. Phys.*, **49**, 833–91.

TABLES

In this appendix we now reproduce, for reference and comparative purposes, the tables in each of chapters 2 through 13 that contained details of the nuclear properties of the isotopes of actinium through lawrencium and of elements 104–109. We then give a table summarizing the specific activities of the nuclides.

Nuclear properties of actinium isotopes.

Mass number	*Half-life*	*Mode of decay*	*Main radiations* (MeV)	*Method of production*
209	0.10 s	α	α 7.59	^{197}Au(^{20}Ne,8n)
210	0.35 s	α	α 7.46	^{197}Au(^{20}Ne,7n) ^{203}Tl(^{16}O,9n)
211	0.25 s	α	α 7.48	^{197}Au(^{20}Ne,6n) ^{203}Tl(^{16}O,8n)
212	0.93 s	α	α 7.38	^{203}Tl(^{16}O,7n) ^{197}Au(^{20}Ne,5n)
213	0.80 s	α	α 7.36	^{197}Au(^{20}Ne,4n) ^{203}Tl(^{16}O,6n)
214	8.2 s	α $\geqslant 86\%$ EC $\leqslant 14\%$	α 7.214 (52%) 7.082 (44%)	^{203}Tl(^{16}O,5n) ^{197}Au(^{20}Ne,3n)
215	0.17 s	α 99.91% EC 0.09%	α 7.604	^{203}Tl(^{16}O,4n) ^{209}Bi(^{12}C,6n)
216	$\approx$ 0.33 ms	α	α 9.07	^{209}Bi(^{12}C,5n)
216 m	0.33 ms	α	α 9.102 (46%) 9.024 (50%)	
217	0.11 μs	α	α 9.65	^{208}Pb(^{14}N,5n)
218	0.27 μs[a]	α	α 9.20	^{222}Pa daughter
219	7 μs	α	α 8.66	^{223}Pa daughter
220	26 ms	α	α 7.85 (24%) 7.68 (21%) 7.61 (23%)	^{208}Pb(^{15}N,3n) ^{224}Pa daughter
221	52 ms	α	α 7.65 (70%) 7.44 (20%)	^{205}Tl(^{22}Na,α2n) ^{208}Pb(^{18}O,p4n)
222	5 s	α	α 7.00	^{226}Ra(p,5n) ^{208}Pb(^{18}O,p3n)
222 m	66 s	α $\leqslant 90\%$ EC $\approx 1\%$ IT $< 10\%$	α 7.00 (15%) 6.81 (27%)	^{208}Pb(^{18}O,p3n) ^{209}Bi(^{18}O,αn)
223	2.2 min	α 99% EC 1%	α 6.662 (32%) 6.647 (45%)	^{227}Pa daughter
224	2.9 h	EC $\approx 90\%$ α $\approx 10\%$	α 6.211 (20%) 6.139 (26%)	^{228}Pa daughter
225	10.0 d	α	α 5.830 (51%) 5.794 (24%) γ 0.100 (1.7%)	^{225}Ra daughter
226	29 h	β^- 83% EC 17% α 6×10^{-3} %	α 5.399 β^- 1.10 γ 0.230 (27%)	^{226}Ra(d,2n)
227	21.773 yr	β^- 98.62% α 1.38%	α 4.950 (47%) 4.938 (40%) β^- 0.045 γ 0.086	nature
228	6.13 h	β^-	β^- 2.18 γ 0.991	nature
229	62.7 min	β^-	β^- 1.09 γ 0.165	^{229}Ra daughter ^{232}Th(γ,p2n)
230	122 s	β^-	β^- 1.4 γ 0.455	^{232}Th(γ,pn)
231	7.5 min	β^-	β^- 2.1 γ 0.282	^{232}Th(γ,p) ^{232}Th(n,pn)
232	35 s	β^-		^{232}Th(n,p)
233	2.3 min	β^-		^{238}U(^{3}He, ^{8}B)

Nuclear properties of thorium isotopes.

Mass number	*Half-life*	*Mode of decay*	*Main radiations* (MeV)	*Method of production*
213 or 214	0.12 s	α	α 7.69	^{206}Pb(^{16}O,8 or 9n)
215	1.2 s	α	α 7.52 (40%) 7.39 (52%)	^{206}Pb(^{16}O,7n)
216	28 ms	α	α 7.92	^{206}Pb(^{16}O,6n)
217	0.25 ms	α	α 9.25	^{206}Pb(^{16}O,5n)
218	0.10 μs	α	α 9.66	^{206}Pb(^{16}O,4n) ^{209}Bi(^{14}N,5n)
219	1.05 μs	α	α 9.34	^{206}Pb(^{16}O,3n)
220	10 μs	α	α 8.79	^{208}Pb(^{16}O,4n)
221	1.7 ms	α	α 8.472 (32%) 8.146 (62%)	^{208}Pb(^{16}O,3n)
222	2.8 ms	α	α 7.98	^{208}Pb(^{16}O,2n)
223	0.66 s	α	α 7.32 (40%) 7.29 (60%)	^{208}Pb(^{18}O,3n)
224	1.043 s	α	α 7.17 (81%) 7.00 (19%) γ 0.177	^{228}U daughter ^{208}Pb(^{22}Ne,α2n)
225	8.0 min	$\alpha \approx 90\%$ EC $\approx 10\%$	α 6.478 (43%) 6.441 (15%) γ 0.321	^{229}U daughter ^{231}Pa(p,α3n)
226	30.9 min	α	α 6.335 (79%) 6.225 (19%) γ 0.1113	^{230}U daughter
227	18.718 d	α	α 6.038 (25%) 5.978 (23%) γ 0.236	nature
228	1.913 yr	α	α 5.423 (72.7%) 5.341 (26.7%) γ 0.084	nature
229	7.3×10^3 yr	α	α 4.901 (11%) 4.845 (56%) γ 0.194	^{233}U daughter
230	8.0×10^4 yr	α	α 4.687 (76.3%) 4.621 (23.4%) γ 0.068	nature
231	25.52 h	β^-	β^- 0.302 γ 0.084	nature ^{230}Th(n,γ)
232	1.41×10^{10} yr $> 1 \times 10^{21}$ yr	α SF	α 4.016 (77%) 3.957 (23%)	nature
233	22.3 min	β^-	β^- 1.23 γ 0.086	^{232}Th(n,γ)
234	24.10 d	β^-	β^- 0.198 γ 0.093	nature
235	6.9 min	β^-		^{238}U(n,α)
236	37 min	β^-	γ 0.111	^{238}U(γ,2p) ^{238}U(p,3p)

Nuclear properties of protactinium isotopes.

Mass number	*Half-life*	*Mode of decay*	*Main radiations* (MeV)	*Method of production*
216	0.20 s	α	α 7.92	^{189}Os(^{31}P,4n) ^{197}Au(^{24}Mg,5n)
222	5.7 ms	α	α 8.54 (~ 30%) ~ 8.18 (~ 50%)	^{209}Bi(^{16}O,3n) ^{206}Pb(^{19}F,3n)
223	6 ms	α	α 8.20 (45%) 8.01 (55%)	^{208}Pb(^{19}F,4n) ^{205}Tl(^{22}Ne,4n)
224	0.9 s	α	α 7.49	^{208}Pb(^{19}F,3n) ^{205}Tl(^{22}Ne,3n) ^{232}Th(p,9n)
225	1.8 s	α	α 7.25 (70%) 7.20 (30%)	^{232}Th(p,8n) ^{209}Bi(^{22}Ne,α2n)
226	1.8 min	α 74% EC 26%	α 6.86 (52%) 6.82 (46%)	^{232}Th(p,7n)
227	38.3 min	α ~ 85% EC ~ 15%	α 6.466 (51%) 6.416 (15%) γ 0.065	^{232}Th(p,6n)
228	22 h	EC ~ 98% α ~ 2%	α 6.105 (12%) 6.078 (21%) γ 0.410	^{232}Th(p,5n) ^{230}Th(p,3n)
229	1.5 d	EC 99.5% α 0.48%	α 5.669 (19%) 5.579 (37%)	^{230}Th(d,3n) ^{229}Th(d,2n)
230	17.7 d	EC 90% β^- 10% α 3.2×10^{-3}%	α 5.345 β^- 0.51 γ 0.952	^{230}Th(d,2n) ^{232}Th(p,3n)
231	3.28×10^4 yr	α	α 5.012 (25%) 4.951 (23%) γ 0.300	nature
232	1.31 d	β^-	β^- 1.29 γ 0.969	^{231}Pa(n,γ) ^{232}Th(d,2n)
233	27.0 d	β^-	β^- 0.568 γ 0.312	^{233}Th daughter ^{237}Np daughter
234	6.75 h	β^-	β^- 1.2 γ 0.570	nature
234m	1.175 min	β^- 99.87% IT 0.13%	β^- 2.29 γ 1.001	nature
235	24.2 min	β^-	β^- 1.41	^{235}Th daughter ^{238}U(γ,p2n) ^{235}U(n,p)
236	9.1 min	β^-	β^- 3.1 γ 0.642	^{236}U(n,p) ^{238}U(d,α)
237	8.7 min	β^-	β^- 2.3 γ 0.854	^{238}U(γ,p) ^{238}U(n,pn)
238	2.3 min	β^-	β^- 2.9 γ 1.014	^{238}U(n,p)

Nuclear properties of uranium isotopes. (Contd.)

Mass number	*Half-life*	*Mode of decay*	*Main radiations* (MeV)	*Method of production*
226	0.5 s	α	α 7.43	^{232}Th(α,10n)
227	1.1 min	α	α 6.87	^{232}Th(α,9n)
				^{208}Pb(^{22}Ne,3n)
228	9.1 min	α ⩾95%	α 6.68 (70%)	^{232}Th(α,8n)
		EC ⩽5%	6.60 (29%)	
			γ 0.152	
229	58 min	EC ~80%	α 6.360 (64%)	^{230}Th(^{3}He,4n)
		α ~20%	6.332 (20%)	^{232}Th(α,7n)
			γ 0.123	
230	20.8 d	α	α 5.888 (67.5%)	^{230}Pa daughter
			5.818 (31.9%)	^{231}Pa (d,3n)
			γ 0.072	
231	4.2 d	EC >99%	α 5.46	^{230}Th(α,3n)
		α 5.5×10^{-3}%	γ 0.084	^{231}Pa(d,2n)
232	68.9 yr	α	α 5.320 (68.6%)	^{232}Th(α,4n)
	≈ 8×10^{13} yr	SF	5.264 (31.2%)	
			γ 0.058	
233	1.592×10^{5} yr	α	α 4.824 (82.7%)	^{233}Pa daughter
	1.2×10^{17} yr	SF	4.783 (14.9%)	
			γ 0.097	
234	2.45×10^{5} yr	α	α 4.777(72%)	nature
	2×10^{16} yr	SF	4.723 (28%)	
235	7.037×10^{8} yr	α	α 4.397 (57%)	nature
	3.5×10^{17} yr	SF	4.367 (18%)	
			γ 0.186	
235 m	26 min	IT		^{239}Pu daughter
236	2.342×10^{7} yr	α	α 4.494 (74%)	^{235}U(n,γ)
	2×10^{16} yr	SF	4.445 (26%)	
237	6.75 d	β^-	β^- 0.519	^{236}U(n,γ)
			γ 0.060	^{241}Pu daughter
238	4.47×10^{9} yr	α	α 4.196 (77%)	nature
	8.19×10^{15} yr	SF	4.149 (23%)	
239	23.5 min	β^-	β^- 1.29	^{238}U(n,γ)
			γ 0.075	
240	14.1 h	β^-	β^- 0.36	^{244}Pu daughter
			γ 0.044	
242	17 min	β^-	β^- 1.2	^{244}Pu(n,2pn)
			γ 0.068	

Nuclear properties of neptunium isotopes.

Mass number	*Half-life*	*Mode of decay*	*Main radiations* (MeV)	*Method of production*
227 or 228	60 s	SF		^{22}Ne on ^{209}Bi
229	4.0 min	$\alpha \geqslant 50\%$ $EC \leqslant 50\%$	α 6.89	^{233}U(p,5n)
230	4.6 min	$\alpha > 99\%$ $EC \leqslant 0.97\%$	α 6.66	^{233}U(p,4n)
231	48.8 min	$EC < 99\%$ $\alpha > 1\%$	α 6.28 γ 0.371	^{233}U(d,4n) ^{235}U(d,6n)
232	14.7 min	EC	γ 0.327	^{233}U(d,3n)
233	36.2 min	$EC < 99\%$ $\alpha \sim 10^{-3}\%$	α 5.54 γ 0.312	^{233}U(d,2n) ^{235}U(d,4n)
234	4.4 d	EC 99.95% β^+ 0.05%	γ 1.559	^{235}U(d,3n)
235	396 d	EC > 99% α $1.6 \times 10^{-3}\%$	α 5.022 (53%) 5.004 (24%)	^{235}U(d,2n)
236[a]	22.5 h	β^- 50% EC 50%	β^- 0.54 γ 0.642	^{235}U(d,n)
236[a]	1.55×10^5 yr	EC 87% β^- 13%	γ 0.163	^{235}U(d,n)
237	2.14×10^6 yr $> 1 \times 10^{18}$ yr	α SF	α 4.788 (51%) 4.770 (19%) γ 0.086	^{237}U daughter ^{241}Am daughter
238	2.117 d	β^-	β^- 1.29 γ 0.984	^{237}Np(n,γ)
239	2.35 d	β^-	β^- 0.72 γ 0.106	^{243}Am daughter ^{239}U daughter
240	1.032 h	β^-	β^- 2.09 γ 0.566	^{238}U(α,pn)
240 m	7.22 min	β^-	β^- 2.05 γ 0.555	^{240}U daughter ^{238}U(α,pn)
241	13.9 min	β^-	β^- 1.31 γ 0.175	^{238}U(α,p) ^{244}Pu(n,p3n)
242 g or m	5.5 min	β^-	β^- 2.7 γ 0.786	^{244}Pu(n,p2n) ^{242}Pu(n,p)
242 g or m	2.2 min	β^-	β^- 2.7 γ 0.736	^{242}U daughter

[a] Not known whether ground-state nuclide or isomer.

Nuclear properties of plutonium isotopes.

Mass number	*Half-life*	*Mode of decay*	*Main radiations* (MeV)	*Method of production*
232	34 min	EC $\geqslant 80\%$	α 6.60 (62%)	^{233}U(α,5n)
		α $\leqslant 20\%$	6.54 (38%)	
233	20.9 min	EC 99.88%	α 6.30	^{233}U(α,4n)
		α 0.12%	γ 0.235	
234	8.8 h	EC 94%	α 6.202 (68%)	^{233}U(α,3n)
		α 6%	6.151 (32%)	
235	25.6 min	EC > 99%	α 5.85	^{235}U(α,4n)
		α 3×10^{-3}%	γ 0.049	^{233}U(α,2n)
236	2.85 yr	α	α 5.768 (69%)	^{235}U(α,3n)
	3.5×10^{9} yr	SF	5.721 (31%)	^{236}Np daughter
237	45.4 d	EC > 99%	α 5.65 (21%)	^{235}U(α,2n)
		α 3.3×10^{-3}%	5.36 (79%)	^{237}Np(d,2n)
			γ 0.059	
238	87.74 yr	α	α 5.499 (70.9%)	^{242}Cm daughter
	4.8×10^{10} yr	SF	5.457 (29.0%)	^{238}Np daughter
239	2.41×10^{4} yr	α	α 5.155 (73.3%)	^{239}Np daughter
	5.5×10^{15} yr	SF	5.143 (15.1%)	n capture
			γ 0.129	
240	6.563×10^{3} yr	α	α 5.168 (72.8%)	multiple n capture
	1.34×10^{11} yr	SF	5.123 (27.1%)	
241	14.4 yr	β^- > 99%	α 4.896 (83.2%)	multiple n capture
		α 2.4×10^{-3}%	4.853 (21.1%)	
			β^- 0.021	
			γ 0.149	
242	3.76×10^{5} yr	α	α 4.901 (74%)	multiple n capture
	6.8×10^{10} yr	SF	4.857 (26%)	
243	4.956 h	β^-	β^- 0.58	multiple n capture
			γ 0.084	
244	8.26×10^{7} yr	α	α 4.589 (81%)	multiple n capture
	6.6×10^{10} yr	SF	4.546 (19%)	
245	10.5 h	β^-	β^- 1.28	^{244}Pu(n,γ)
			γ 0.327	
246	10.85 d	β^-	β^- 0.374	^{245}Pu(n,γ)
			γ 0.224	

Nuclear properties of americium isotopes.

Mass number	*Half-life*	*Mode of decay*	*Main radiations* (MeV)		*Method of production*
234	2.6 min	EC			^{230}Th(^{10}B,6n) ^{10}B, ^{11}B on ^{233}U
237	1.22 h	EC >99%	α	6.042	^{237}Np(α,4n)
		α 0.025%	γ	0.280 (47%)	^{237}Np(^{3}He,3n)
238	1.63 h	EC >99%	α	5.94	^{237}Np(α,3n)
		α 1.0×10^{-4}%	γ	0.963 (29%)	
239	11.9 h	EC >99%	α	5.776 (84%)	^{237}Np(α,2n)
				5.734 (13.8%)	
		α 0.010%	γ	0.278 (15%)	^{239}Pu(d,2n)
240	50.8 h	EC >99%	α	5.378 (87%)	^{237}Np(α,n)
		α 1.9×10^{-4}%		5.337 (12.0%)	^{239}Pu(d, n)
			γ	0.988 (73%)	
241	432.7 yr	α	α	5.486 (84.0%)	^{241}Pu daughter
	1.15×10^{14} yr	SF		5.443 (13.1%)	multiple n capture
			γ	0.059 (35.7%)	
242	16.01 h	β^- 82.7%	β^-	0.667	^{241}Am(n,γ)
		EC 17.3%	γ	0.042 weak	
242 m	141 yr	IT 99.55%	α	5.207 (89%)	^{241}Am(n,γ)
	9.5×10^{11} yr	SF			
		α 0.45%		5.141 (6.0%)	^{241}Am(n,γ)
			γ	0.0493 (41%)	
243	7.38×10^{3} yr	α	α	5.277 (88%)	multiple
	2.0×10^{14} yr	SF		5.234 (10.6%)	n capture
			γ	0.075 (68%)	
244	10.1 h	β^-	β^-	0.387	^{243}Am(n,γ)
			γ	0.746 (67%)	
244 m	26 min	β^- >99% EC 0.041%	β^-	1.50	^{243}Am(n,γ)
245	2.05 h	β^-	β^-	0.895	^{245}Pu daughter
			γ	0.253 (6.1%)	
246[a]	25.0 min	β^-	β^-	2.38	^{246}Pu daughter
			γ	0.799 (25%)	
246[a]	39 min	β^-	γ	0.679 (52%)	^{244}Pu(α,d) ^{244}Pu(^{3}He,p)
247	24 min	β^-	γ	0.285 (23%)	^{244}Pu(α,p)

[a] Not known whether ground-state nuclide or isomer.

Nuclear properties of curium isotopes.

Mass number	*Half-life*	*Mode of decay*	*Main radiations* (MeV)	*Method of production*
238	2.3 h	EC <90%	α 6.52	^{239}Pu(α,5n)
		α >10%		
239	2.9 h	EC	γ 0.188	^{239}Pu(α,4n)
240	27 d	α	α 6.291 (71%)	^{239}Pu(α,3n)
	1.9×10^6 yr	SF	6.248 (29%)	
241	32.8 d	EC 99.0%	α 5.939 (69%)	^{239}Pu(α,2n)
		α 1.0%	5.929 (18%)	
			γ 0.472 (71%)	
242	162.9 d	α	α 6.113 (74.0%)	^{239}Pu(α,n)
	6.1×10^6 yr	SF	6.070 (26.0%)	^{242}Am daughter
243	28.5 yr	α 99.76%	α 5.785 (73.5%)	^{242}Cm(n,γ)
		EC 0.24%	5.741 (10.6%)	
			γ 0.278 (14.0%)	
244	18.11 yr	α	α 5.805 (76.7%)	multiple n capture
	1.35×10^7 yr	SF	5.764 (23.3%)	^{244}Am daughter
245	8.5×10^3 yr	α	α 5.362 (93.2%)	multiple n capture
			5.304 (5.0%)	
			γ 0.175	
246	4.73×10^3 yr	α	α 5.386 (79%)	multiple n capture
	1.80×10^7 yr	SF	5.343 (21%)	
		β stable		
247	1.56×10^7 yr	α	α 5.266 (14%)	multiple n capture
			4.869 (71%)	
			γ 0.402 (72%)	
248	3.40×10^5 yr	α 91.74%	α 5.078 (82%)	multiple n capture
		SF 8.26%	5.034 (18%)	
249	64.2 min	β^-	β^- 0.9	^{248}Cm(n,γ)
			γ 0.634 (1.5%)	
250	$< 1.13 \times 10^4$ yr	SF		multiple n capture
251	16.8 min	β^-	β^- 1.42	^{250}Cm(n,γ)
			γ 0.543 (12%)	

Nuclear properties of berkelium isotopes.

Mass number	*Half-life*	*Mode of decay*	*Main radiations* (MeV)		*Method of production*
240	5 min	EC			^{232}Th(^{14}N,6n)
242	7 min	EC			^{235}U(^{11}B,4n)
					^{232}Th(^{15}N,5n)
243	4.5 h	EC 99.85%	α	6.758 (15%)	^{243}Am(α,4n)
		α 0.15%		6.574 (26%)	
			γ	0.755	
244	4.35 h	EC > 99%	α	6.667 (~ 50%)	^{243}Am(α,3n)
		α 6×10^{-3}%		6.625 (~ 50%)	
			γ	0.218	
245	4.90 d	EC 99.88%	α	6.349 (15.5%)	^{243}Am(α,2n)
		α 0.12%		6.145 (18.3%)	
			γ	0.253 (31%)	
246	1.80 d	EC	γ	0.799 (61%)	^{243}Am(α,n)
247	1.38				
	$\times 10^3$ yr	α	α	5.712 (17%)	^{247}Cf daughter
				5.532 (45%)	^{244}Cm(α,p)
			γ	0.084 (40%)	
248[a]	23.7 h	β^- 70%	β^-	0.86	^{248}Cm(d,2n)
		EC 30%	γ	0.551	
248[a]	> 9 yr	decay not observed			^{246}Cm(α,pn)
249	320 d	β^- > 99%	α	5.417 (74.8%)	multiple n capture
		α 1.45×10^{-3}%		5.390 (16.0%)	
			β^-	0.125	
			γ	0.327 weak	
250	3.217 h	β^-	β^-	1.781	^{254}Es daughter
			γ	0.989 (45%)	^{249}Bk(n,γ)
251	56 min	β^-	β^-	~1.1	^{255}Es daughter
			γ	0.178	

[a] Not known whether ground-state nuclide or isomer.

Nuclear properties of californium isotopes.

Mass number	*Half-life*	*Mode of decay*	*Main radiations* (MeV)	*Method of production*
239	39 s	α	α 7.63	^{243}Fm daughter
240	1.1 min	α	α 7.59	^{233}U(^{12}C,5n)
241	3.8 min	α	α 7.335	^{233}U(^{12}C,4n)
242	3.5 min	α	α 7.385 (~ 80%)	^{233}U(^{12}C,3n)
			7.351 (~ 20%)	^{235}U(^{12}C,5n)
243	10.7 min	EC ~ 86%	α 7.06	^{235}U(^{12}C,4n)
		α ~ 14%		
244	19.4 min	α	α 7.210 (75%)	^{244}Cm(α,4n)
			7.168 (25%)	^{236}U(^{12}C,4n)
245	43.6 min	EC ~ 70%	α 7.137	^{244}Cm(α,3n)
		α ~ 30%		^{238}U(^{12}C,5n)
246	35.7 h	α	α 6.758 (78%)	^{244}Cm(α,2n)
	2.0×10^3 yr	SF	6.719 (22%)	^{246}Cm(α,4n)
		β stable		
247	3.11 h	EC 99.96%	α 6.296 (95%)	^{246}Cm(α,3n)
		α 0.035%	γ 0.294 (1.0%)	^{244}Cm(α,n)
248	334 d	α	α 6.258 (80.0%)	^{246}Cm(α,2n)
	3.2×10^4 yr	SF	6.217 (19.6%)	
		β stable		
249	351 yr	α	α 6.194 (2.2%)	^{249}Bk daughter
	6.9×10^{10} yr	SF	5.812 (84.4%)	
			γ 0.388 (66%)	
250	13.08 yr	α	α 6.031 (83%)	multiple n capture
	1.7×10^4 yr	SF	5.989 (17%)	
251	898 yr	α	α 5.851 (27%)	multiple n capture
			5.677 (35%)	
			γ 0.177 (17%)	
252	2.645 yr	α 96.91%	α 6.118 (84%)	multiple n capture
		SF 3.09%	6.076 (15.8%)	
253	17.81 d	β^- 99.69%	α 5.979 (95%)	multiple n capture
		α 0.31%	5.921 (5%)	
254	60.5 d	SF 99.69%	α 5.834 (83%)	multiple n capture
		α 0.31%	5.792 (17%)	
255	1.4 h	β^-		^{254}Cf(n,γ)
256	12.3 min	SF		^{254}Cf(t,p)

Nuclear properties of einsteinium isotopes.

Mass number	*Half-life*	*Mode of decay*	*Main radiations* (MeV)	*Method of production*
243	21 s	α	α 7.89	^{233}U (^{15}N, 5n)
244	37 s	EC 96 %	α 7.57	^{233}U (^{15}N, 4n)
		α ~ 4 %		^{237}Np (^{12}C, 5n)
245	1.3 min	EC 60 %	α 7.73	^{237}Np (^{12}C, 4n)
		α 40 %		
246	7.7 min	EC 90 %	α 7.35	^{241}Am (^{12}C, α3n)
		α 10 %		
247	4.7 min	EC ~93 %	α 7.32	^{241}Am (^{12}C, α2n)
		α ~ 7 %		^{238}U (^{14}N, 5n)
248	27 min	EC 99.7 %	α 6.87	^{249}Cf (d,3n)
		α ~ 0.3 %	γ 0.551	
249	1.70 h	EC 99.4 %	α 6.770	^{249}Cf (d,2n)
		α 0.57 %	γ 0.380	
250[a]	8.6 h	EC	γ 0.829	^{249}Cf (d,n)
250[a]	2.22 h	EC	γ 0.989	^{249}Cf (d,n)
251	33 h	EC 99.5 %	α 6.492 (81 %)	^{249}Bk (α,2n)
		α 0.49 %	6.463 (9 %)	
252	472 d	α 78 %	α 6.632 (80 %)	^{249}Bk (α,n)
		EC 22 %	6.562 (13.6 %)	
			γ 0.785	
253	20.47 d	α	α 6.633 (89.8 %)	multiple
	6.3×10^5 yr	SF	6.592 (7.3 %)	n capture
		β stable		
254 g	275.7 d	α	α 6.429 (93.2 %)	multiple
	$> 2.5 \times 10^7$ yr	SF	6.359 (2.4 %)	n capture
			γ 0.062	
254 m	39.3 h	β^- 99.6 %	α 6.382 (75 %)	^{253}Es (n,γ)
	$> 1 \times 10^5$ yr	SF	6.357 (8 %)	
		α 0.33 %		
		f 0.08 %		
255	39.8 d	β^- 92.0 %	α 6.300 (88 %)	multiple
		α 8.0 %	6.260 (10 %)	n capture
		SF 4×10^{-3} %		
256[a]	25.0 min	β^-		^{255}Es (n,γ)
256[a]	~ 7.6 h	β^-		^{254}Es (t,p)

[a] Not known whether ground-state nuclide or isomer.

Nuclear properties of fermium isotopes.

Mass number	*Half-life*	*Mode of decay*	*Main radiations* (MeV)	*Method of production*
242	0.8 ms	SF		^{204}Pb(^{40}Ar, 2n)
243	0.18 s	α	α 9.55	^{206}Pb(^{40}Ar, 3n)
244	3.3 ms	SF		^{206}Pb(^{40}Ar, 2n) ^{233}U(^{16}O, 5n)
245	4.2 s	α	α 8.15	^{233}U(^{16}O, 4n)
246	1.1 s	α 92%	α 8.24	^{235}U(^{16}O, 5n)
		SF 8%		^{239}Pu(^{12}C, 5n)
247[a]	35 s	α ⩾ 50%	α 7.93 (~ 30%)	^{239}Pu(^{12}C, 4n)
		EC ⩽ 50%	7.87 (~ 70%)	
247[a]	9 s	α	α 8.18	^{239}Pu(^{12}C, 4n)
248	36 s	α 99.9%	α 7.87 (80%)	^{240}Pu(^{12}C, 4n)
		SF 0.1%	7.83 (20%)	
249	2.6 min	α	α 7.53	^{238}U(^{16}O, 5n) ^{249}Cf(α, 4n)
250	30 min	α	α 7.43	^{249}Cf(α, 3n)
		SF 5.7×10^{-4}%		^{238}U(^{16}O, 4n)
250 m	1.8 s	IT		^{249}Cf(α, 3n)
251	5.30 h	EC 98.2%	α 6.834 (87%)	^{249}Cf(α, 2n)
		α 1.8%	6.783 (4.8%)	
252	25.39 h	α	α 7.039 (84.0%)	^{249}Cf(α, n)
		SF 2.3×10^{-3}%	6.998 (15.0%)	
253	3.0 d	EC 88%	α 6.943 (43%)	^{252}Cf(α, 3n)
		α 12%	6.674 (23%)	
			γ 0.272	
254	3.240 h	α > 99%	α 7.192 (85.0%)	^{254m}Es daughter
		SF 0.0592%	7.150 (14.2%)	
255	20.07 h	α	α 7.022 (93.4%)	^{255}Es daughter
		SF 2.4×10^{-5}%	6.963 (5.0%)	
256	2.63 h	SF 91.9%	α 6.915	^{256}Md daughter
		α 8.1%		^{256}Es daughter
257	100.5 d	α 99.79%	α 6.695 (3.5%)	multiple n capture
		SF 0.21%	6.520 (93.6%)	
			γ 0.241	
258	0.38 ms	SF		^{257}Fm(d, p)
259	1.5 s	SF		^{257}Fm(t, p)

[a] Not known whether ground-state nuclide, isomer, or identification error.

Nuclear properties of mendelevium isotopes.

Mass number	*Half-life*	*Mode of decay*	*Main radiations* (MeV)	*Method of production*
247	2.9 s	α	α 8.43	^{209}Bi(^{40}Ar,2n)
248	7 s	EC ~ 80%	α 8.36 (~ 25%)	^{241}Am(^{12}C,5n)
		α ~ 20%	8.32 (~ 75%)	^{239}Pu(^{14}N,5n)
249	24 s	EC ⩽ 80%	α 8.03	^{241}Am(^{12}C,4n)
		α ⩾ 20%		
250	52 s	EC 94%	α 7.82 (~ 30%)	^{243}Am(^{12}C,5n)
		α 6%	7.75 (~ 70%)	^{240}Pu(^{15}N,5n)
251	4.0 min	EC ⩾ 94%	α 7.55	^{243}Am(^{12}C,4n)
		α ⩽ 6%		^{240}Pu(^{15}N,4n)
252	2.3 min	EC		^{243}Am(^{13}C,4n)
				^{238}U(^{19}F,5n)
254[a]	10 min	EC		^{253}Es(α,3n)
254[a]	28 min	EC		^{253}Es(α,3n)
255	27 min	EC 92%	α 7.333	^{253}Es(α,2n)
		α 8%	γ 0.453	^{254}Es(α,3n)
256	1.27 h	EC 90.7%	α 7.205 (63%)	^{253}Es(α,n)
		α 9.9%	7.139 (16%)	
257	5.4 h	EC 90%	α 7.069	^{254}Es(α,n)
		α 10%		
258[a]	55 d	α	α 6.790 (28%)	^{255}Es(α,n)
			6.716 (72%)	
258[a]	43 min	EC ?		^{255}Es(α,n)
259	1.6 h	SF		^{259}No daughter

[a] Not known whether ground-state nuclide or isomer.

Nuclear properties of nobelium isotopes.

Mass number	*Half-life*	*Mode of decay*	*Main radiations* (MeV)	*Method of production*
250[a]	0.25 ms	SF		$^{233}U(^{22}Ne,5n)$
251	0.8 s	α	α 8.68 (20%) 8.60 (80%)	$^{244}Cm(^{12}C,5n)$
252	2.3 s	α 73% SF 27%	α 8.415 (~75%) 8.372 (~25%)	$^{244}Cm(^{12}C,4n)$ $^{239}Pu(^{18}O,5n)$
253	1.7 min	α	α 8.01	$^{246}Cm(^{12}C,5n)$ $^{242}Pu(^{16}O,5n)$
254	68 s	α	α 8.086	$^{246}Cm(^{12}C,4n)$ $^{242}Pu(^{16}O,4n)$
254 m	0.28 s	IT		$^{246}Cm(^{12}C,4n)$ $^{249}Cf(^{12}C,\alpha 3n)$
255	3.1 min	α 61.4% EC 38.6%	α 8.121 (46%) 8.077 (12%)	$^{248}Cm(^{12}C,5n)$ $^{249}Cf(^{12}C,\alpha 2n)$
256	3.3 s	α ~99.7% SF ~0.3%	α 8.43	$^{248}Cm(^{12}C,4n)$
257	25 s	α	α 8.27 (26%) 8.22 (55%)	$^{248}Cm(^{12}C,3n)$
258	1.2 ms	SF		$^{248}Cm(^{13}C,3n)$
259	1.00 h	α ~78% EC ~22%	α 7.533 (23%) 7.500 (38%)	$^{248}Cm(^{18}O,\alpha 3n)$

[a] The identity of this nuclide is not well-established.

Nuclear properties of lawrencium isotopes.

Mass number	*Half-life*	*Mode of decay*	*Main radiations* (MeV)	*Method of production*
253	1.3 s	α	α 8.800 (56%)	^{257}105 daughter
254	13 s	α	α 8.460 (64%)	^{258}105 daughter
255	22 s	α	α 8.43 (40%) 8.37 (60%)	$^{243}Am(^{16}O,4n)$ $^{249}Cf(^{11}B,5n)$
256	28 s	α	α 8.52 (19%) 8.43 (37%)	$^{243}Am(^{18}O,5n)$ $^{249}Cf(^{11}B,4n)$
257	0.65 s	α	α 8.86 (85%) 8.80 (15%)	$^{249}Cf(^{11}B,3n)$ $^{249}Cf(^{14}N,\alpha 2n)$
258	4.3 s	α	α 8.621 (25%) 8.595 (46%)	$^{248}Cm(^{15}N,5n)$ $^{249}Cf(^{15}N,\alpha 2n)$
259	5.4 s	α	α 8.45	$^{248}Cm(^{15}N,4n)$
260	3.0 min	α	α 8.03	$^{248}Cm(^{15}N,3n)$

Nuclear properties of element 104 isotopes.

Mass number	*Half-life*	*Mode of decay*	*Main radiations (MeV)*	*Method of production*
253[a]	~1.8 s	SF ~50%		$^{206}Pb(^{50}Ti, 3n)$
254[a]	0.5 ms	SF		$^{206}Pb(^{50}Ti, 2n)$
255	1.4 s	α ~55%	α 8.715(70%)	$^{207}Pu(^{50}Ti, 2n)$
		SF ~45%		
256	7.4 ms	SF, α	α 8.812	$^{208}Pb(^{50}Ti, 2n)$
257	4.3 s	α ~70%	α 9.012(18%)	$^{208}Pb(^{50}Ti, n)$
		SF ~14%?	8.977(29%)	$^{249}Cf(^{12}C, 3n)$
		EC ~16%		
258[a]	13 ms	SF		$^{246}Cm(^{16}O, 4n)$
259	3.4 s	α 91%	α 8.87(~40%)	$^{249}Cf(^{13}C, 3n)$
		SF 9%	8.77(~60%)	$^{248}Cm(^{16}O, 5n)$
260[a]	21 ms	SF		$^{248}Cm(^{16}O, 4n)$
261	1.1 min	α	α 8.28	$^{248}Cm(^{18}O, 5n)$
262[a]	47 ms	SF		$^{248}Cm(^{18}O, 4n)$

[a] The identity of this nuclide is not well-established.

Nuclear properties of elements 105–109 isotopes.

Mass number	*Half-life*	*Mode of decay*	*Main radiations (MeV)*	*Method of production*
Element 105				
255[a]	1.5 s	SF ~20%		$^{207}Pb(^{51}V, 3n)$
				$^{206}Pb(^{51}V, 2n)$
257	1.4 s	α 9.16		$^{209}Bi(^{50}Ti, 2n)$
258	4.4 s	α	α 9.19	^{262}107 daughter
			9.07	
260	1.5 s	α ⩾90%	α 9.082 (25%)	$^{249}Cf(^{15}N, 4n)$
		SF ⩽9.6%	9.047 (48%)	$^{243}Am(^{22}Ne, 5n)$
		EC ⩽2.5%		
261	1.8 s	α ~75%	α 8.93	$^{243}Am(^{22}Ne, 4n)$
		SF ~25%		$^{249}Bk(^{16}O, 4n)$
262	34 s	SF ~78%	α 8.66 (~20%)	$^{249}Bk(^{18}O, 5n)$
		α ~22%	8.45 (~80%)	
		EC <5%		
Element 106				
259	0.48 s	α	α 9.63	$^{207}Pb(^{54}Cr, 2n)$
260	3.6 ms	α, SF	α 9.76	$^{208}Pb(^{54}Cr, 2n)$
261	0.26 s	α	α 9.56	$^{208}Pb(^{54}Cr, n)$
263	0.9 s	α	α 9.25	$^{249}Cf(^{18}O, 4n)$
Element 107				
261[a]	1–2 ms	SF		$^{209}Bi(^{54}Cr, 2n)$
				$^{208}Pb(^{55}Mn, 2n)$
262	5 ms	α	α 10.38	$^{209}Bi(^{54}Cr, n)$
Element 108				
265	1–8 ms	α	α 10.36	$^{208}Pb(^{58}Fe, n)$
Element 109				
266	3.5 ms	α	α 11.10	$^{209}Bi(^{58}Fe, n)$

[a] The identity of this nuclide is not well-established.

Specific activities of actinide and transactinide nuclides.

Nuclide		Major decay mode[a]	Half-life[b]	S^c (dis min^{-1} μg^{-1})
Ac	209	α	0.10 s	1.20×10^{18}
	210	α	0.35 s	3.41×10^{17}
	211	α	0.25 s	4.75×10^{17}
	212	α	0.93 s	1.27×10^{17}
	213	α	0.80 s	1.47×10^{17}
	214	α	8.2 s	1.43×10^{16}
	215	α	0.17 s	6.85×10^{17}
	216	α	0.33 ms	3.51×10^{20}
	216 m	α	0.33 ms	3.51×10^{20}
	217	α	0.11 μs	1.05×10^{24}
	218	α	0.27 μs	4.26×10^{23}
	219	α	7 μs	1.60×10^{22}
	220	α	26 ms	4.38×10^{18}
	221	α	52 ms	2.18×10^{18}
	222	α	5 s	2.30×10^{16}
	222 m	α	66 s	1.71×10^{15}
	223	α	2.2 min	8.51×10^{14}
	224	EC	2.9 h	1.07×10^{13}
	225	α	10.0 d	1.29×10^{11}
	226	β^-	29 h	1.06×10^{12}
	227	β^-	21.773 yr	1.6057×10^{8}
	228	β^-	6.13 h	4.98×10^{12}
	229	β^-	62.7 min	2.907×10^{13}
	230	β^-	122 s	8.93×10^{14}
	231	β^-	7.5 min	2.41×10^{14}
	232	β^-	35 s	3.08×10^{15}
Th	213	α	0.12 s	9.8×10^{17}
	214	α	0.12 s	9.8×10^{17}
	215	α	1.2 s	9.71×10^{16}
	216	α	28 ms	4.14×10^{18}
	217	α	0.25 ms	4.62×10^{20}
	218	α	0.10 μs	1.15×10^{24}
	219	α	1.05 μs	1.09×10^{23}
	220	α	10 μs	1.14×10^{22}
	221	α	1.7 ms	6.67×10^{19}
	222	α	2.8 ms	4.03×10^{19}
	223	α	0.66 s	1.70×10^{17}
	224	α	1.04 s	1.08×10^{17}
	225	α	8.0 min	2.32×10^{14}
	226	α	30.9 min	5.98×10^{13}
	227	α	18.72 d	6.821×10^{10}
	228	α	1.91 yr	1.82×10^{9}
	229	α	7.3×10^{3} yr	4.75×10^{5}
	230	α	8.0×10^{4} yr	4.31×10^{4}
	231	β^-	25.52 h	1.180×10^{12}
	232	α	1.41×10^{10} yr	0.243
	233	β^-	22.3 min	8.03×10^{13}

Specific activities of actinide and transactinide nuclides. (Contd.)

Nuclide		*Major decay mode*[a]	*Half-life*[b]	S^c (dis min^{-1} μg^{-1})
	234	β^-	24.10 d	5.140×10^{10}
	235	β^-	6.9 min	2.57×10^{14}
	236	β^-	37 min	4.78×10^{13}
Pa	216	α	0.20 s	5.80×10^{17}
	222	α	5.7 ms	1.98×10^{19}
	223	α	6 ms	1.90×10^{19}
	224	α	0.9 s	1.20×10^{17}
	225	α	1.8 s	6.18×10^{16}
	226	α	1.8 min	1.03×10^{15}
	227	α	38.3 min	4.80×10^{13}
	228	EC	22 h	1.39×10^{12}
	229	EC	1.5 d	8.44×10^{11}
	230	EC	17.7 d	7.12×10^{10}
	231	α	3.28×10^4 yr	1.047×10^5
	232	β^-	1.31 d	9.54×10^{11}
	233	β^-	27.0 d	4.61×10^{10}
	234	β^-	6.75 h	4.40×10^{12}
	234 m	β^-	1.17 min	1.52×10^{15}
	235	β^-	24.2 min	7.34×10^{13}
	236	β^-	9.1 min	1.94×10^{14}
	237	β^-	8.7 min	2.02×10^{14}
	238	β^-	2.3 min	7.63×10^{14}
U	226	α	0.5 s	2.20×10^{17}
	227	α	1.1 min	1.67×10^{15}
	228	α	9.1 min	2.01×10^{14}
	229	EC	58 min	3.14×10^{13}
	230	α	20.8 d	6.06×10^{10}
	231	EC	4.2 d	2.99×10^{11}
	232	α	68.9 yr	4.965×10^7
	233	α	1.591×10^5 yr	2.141×10^4
	234	α	2.45×10^5 yr	1.384×10^4
	235	α	7.04×10^8 yr	4.797
	235 m	IT	26 min	6.83×10^{13}
	236	α	2.342×10^7 yr	1.436×10^2
	237	β^-	6.75 d	1.812×10^{11}
	238	α	4.47×10^9 yr	0.7459
	239	β^-	23.5 min	7.43×10^{13}
	240	β^-	14.1 h	2.06×10^{12}
	242	β^-	17 min	1.01×10^{14}
Np	227 or 228	SF	60 s	1.84×10^{15}
	229	α	4.0 min	4.56×10^{14}
	230	α	4.6 min	3.95×10^{14}
	231	α	48.8 min	3.70×10^{13}
	232	EC	14.7 min	1.22×10^{14}
	233	EC	36.2 min	4.95×10^{13}
	234	EC	4.4 d	2.82×10^{11}
	235	EC	396 d	3.115×10^9

Specific activities of actinide and transactinide nuclides. (Contd.)

Nuclide		*Major decay mode*[a]	*Half-life*[b]	S^c (dis min^{-1} μg^{-1})
	236	β^-	22.5 h	1.31×10^{12}
	236 m	β^-	1.55×10^5 yr	2.17×10^4
	237	α	2.14×10^6 yr	1.565×10^3
	238	β^-	2.117 d	5.752×10^{11}
	239	β^-	2.35 d	5.16×10^{11}
	240	β^-	61.9 min	2.81×10^{13}
	240 m	β^-	7.22 min	2.41×10^{14}
	241	β^-	13.9 min	1.25×10^{14}
	242	β^-	5.5 min	3.14×10^{14}
	242	β^-	2.2 min	7.84×10^{14}
Pu	232	EC	34 min	5.29×10^{13}
	233	EC	20.9 min	8.57×10^{13}
	234	EC	8.8 h	3.38×10^{12}
	235	EC	25.6 min	6.94×10^{13}
	236	α	2.85 yr	1.18×10^9
	237	EC	45.4 d	2.69×10^{10}
	238	α	87.74 yr	3.800×10^7
	239	α	2.41×10^4 yr	1.378×10^5
	240	α	6.563×10^3 yr	5.038×10^5
	241	β^-	14.4 yr	2.29×10^8
	242	α	3.76×10^5 yr	8.721×10^3
	243	β^-	4.96 h	5.77×10^{12}
	244	α	8.26×10^7 yr	39.37
	245	β^-	10.5 h	2.70×10^{12}
	246	β^-	10.85 d	1.086×10^{11}
Am	234	EC	2.6 min	6.9×10^{14}
	237	EC	73.0 min	2.41×10^{13}
	238	EC	98.0 min	1.79×10^{13}
	239	EC	11.9 h	2.45×10^{12}
	240	EC	50.8 h	5.71×10^{11}
	241	α	432.7 yr	7.609×10^6
	242	β^-	16.01 h	1.795×10^{12}
	242 m	IT	141 yr	2.326×10^7
	243	α	7.38×10^3 yr	4.425×10^5
	244	β^-	10.1 h	2.82×10^{12}
	244 m	β^-	26 min	6.58×10^{13}
	245	β^-	2.05 h	1.38×10^{13}
	246	β^-	25.0 min	6.79×10^{13}
	246 m	β^-	39.0 min	4.35×10^{13}
	247	β^-	24 min	7.04×10^{13}
Cm	238	EC	2.3 h	1.27×10^{13}
	239	EC	2.9 h	1.00×10^{13}
	240	α	27 d	4.47×10^{10}
	241	EC	32.8 d	3.67×10^{10}
	242	α	162.9 d	7.352×10^9
	243	α	28.5 yr	1.146×10^8
	244	α	18.11 yr	1.796×10^8
	245	α	8.5×10^3 yr	3.81×10^5

Specific activities of actinide and transactinide nuclides. (Contd.)

Nuclide		*Major decay mode*[a]	*Half-life*[b]	S^c (dis min^{-1} μg^{-1})
	246	α	4.7×10^3 yr	6.86×10^5
	247	α	1.6×10^7 yr	2.01×10^2
	248	α	3.40×10^5 yr	9.410×10^3
	249	β^-	64.2 min	2.61×10^{13}
	250	SF	$< 1.13 \times 10^4$ yr	$> 2.81 \times 10^5$
	251	β^-	16.8 min	9.90×10^{13}
Bk	240	EC	5 min	3.5×10^{14}
	242	EC	7 min	2.5×10^{14}
	243	EC	4.5 h	6.36×10^{12}
	244	EC	4.4 h	6.48×10^{12}
	245	EC	4.90 d	2.41×10^{11}
	246	EC	1.80 d	6.55×10^{11}
	247	α	1.4×10^3 yr	2.30×10^6
	248	β^-	23.7 h	1.183×10^{12}
	249	β^-	320 d	3.637×10^9
	250	β^-	3.22 h	8.64×10^{12}
	251	β^-	56 min	2.97×10^{13}
Cf	239	α	39 s	2.69×10^{15}
	240	α	1.1 min	1.58×10^{15}
	241	α	4 min	4.3×10^{14}
	242	α	3.5 min	4.93×10^{14}
	243	EC	11 min	1.56×10^{14}
	244	α	19 min	9.0×10^{13}
	245	EC	44 min	3.87×10^{13}
	246	α	35.7 h	7.92×10^{11}
	247	EC	3.11 h	9.05×10^{12}
	248	α	334 d	3.50×10^9
	249	α	351 yr	9.079×10^6
	250	α	13.08 yr	2.426×10^8
	251	α	900 yr	3.51×10^6
	252	α	2.645 yr	1.190×10^9
	253	β^-	17.8 d	6.44×10^{10}
	254	SF	60.5 d	1.886×10^{10}
	255	β^-	1.4 h	1.95×10^{13}
	256	β^-	12 min	1.36×10^{14}
Es	243	α	21 s	4.9×10^{15}
	244	EC	37 s	2.77×10^{15}
	245	EC	1.3 min	1.3×10^{15}
	246	EC	7.7 min	2.20×10^{14}
	247	EC	4.7 min	3.60×10^{14}
	248	EC	27 min	6.23×10^{13}
	249	EC	1.70 h	1.64×10^{13}
	250	EC	8.6 h	3.24×10^{13}
	250 m	EC	2.22 h	1.253×10^{13}
	251	EC	33 h	8.40×10^{11}
	252	α	472 d	2.436×10^9
	253	α	20.47 d	5.596×10^{10}

Specific activities of actinide and transactinide nuclides. (Contd.)

Nuclide		*Major decay mode*[a]	*Half-life*[b]	S^c (dis min^{-1} μg^{-1})
	254	α	276 d	4.134×10^9
	254 m	β^-	39.3 h	6.97×10^{11}
	255	β^-	39.8 d	2.86×10^{10}
	256	β^-	25.0 min	6.52×10^{13}
	256	β^-	~ 7.6 h	$\sim 3.57 \times 10^{12}$
Fm	242	SF	0.8 ms	1.30×10^{20}
	243	α	0.18 s	5.73×10^{17}
	244	SF	3.3 ms	3.11×10^{19}
	245	α	4 s	2.60×10^{16}
	246	SF	1.1 s	9.25×10^{16}
	247	α	35 s	2.90×10^{15}
	247	α	9 s	1.1×10^{16}
	248	α	36 s	2.80×10^{15}
	249	α	3 min	5.6×10^{14}
	250	α	30 min	5.57×10^{13}
	250 m	IT	1.8 s	5.57×10^{16}
	251	EC	5.3 h	5.23×10^{12}
	252	α	25.4 h	1.087×10^{12}
	253	EC	3.0 d	3.82×10^{11}
	254	α	3.24 h	8.45×10^{12}
	255	α	20.1 h	1.357×10^{12}
	256	SF	2.63 h	1.033×10^{13}
	257	α	100.5 d	1.122×10^{10}
	258	SF	0.4 ms	2.40×10^{20}
	259	SF	1.5 s	6.45×10^{16}
Md	247	α	2.9 s	3.50×10^{16}
	248	EC	7 s	1.40×10^{16}
	249	EC	24 s	4.19×10^{15}
	250	EC	0.9 min	1.90×10^{15}
	251	EC	4.0 min	4.16×10^{14}
	252	EC	2.3 min	7.2×10^{14}
	254	EC	10 min	1.64×10^{14}
	254 m	EC	28 min	5.87×10^{13}
	255	EC	27 min	6.06×10^{13}
	256	EC	75 min	2.17×10^{13}
	257	EC	5.4 h	5.01×10^{12}
	258	α	55 d	2.04×10^{10}
	258	EC	43 min	3.76×10^{13}
	259	SF	1.6 h	1.68×10^{13}
No	250	SF	0.25 ms	4.01×10^{20}
	251	α	0.8 s	1.20×10^{17}
	252	α	2.3 s	4.32×10^{16}
	253	α	1.7 min	9.70×10^{14}
	254	α	68 s	1.45×10^{15}
	254 m	IT	0.28 s	3.52×10^{17}
	255	α	3.1 min	5.28×10^{14}
	256	α	3.3 s	2.96×10^{16}

Specific activities of actinide and transactinide nuclides. (Contd.)

Nuclide		Major decay mode[a]	Half-life[b]	S[c] (dis min^{-1} μg^{-1})
	257	α	25 s	3.90×10^{15}
	258	SF	1.2 ms	8.09×10^{19}
	259	α	1.00 h	2.69×10^{13}
Lr	253	α	1.3 s	7.6×10^{16}
	254	α	13 s	7.6×10^{15}
	255	α	22 s	4.46×10^{15}
	256	α	28 s	3.5×10^{15}
	257	α	0.65 s	1.50×10^{17}
	258	α	4.3 s	2.26×10^{16}
	259	α	5 s	1.90×10^{16}
	260	α	3.0 min	5.35×10^{14}
104	253	SF	~ 1.8 s	5.5×10^{16}
	254	SF	0.5 ms	2.0×10^{20}
	255	α	1.4 s	7.0×10^{16}
	256	SF	7.4 ms	1.32×10^{19}
	257	α	4.3 s	2.27×10^{16}
	258	SF	13 ms	7.5×10^{18}
	259	α	3 s	3.2×10^{16}
	260	SF	20 ms	4.8×10^{18}
	261	α	1.1 min	1.5×10^{15}
	262	SF	47 ms	2.03×10^{18}
105	255	α	1.5 s	6.5×10^{16}
	257	α	1.4 s	7.0×10^{16}
	258	α	4.4 s	2.21×10^{16}
	260	α	1.5 s	6.4×10^{16}
	261	α	2 s	4.8×10^{16}
	262	SF	34 s	2.8×10^{15}
106	259	SF	0.48 s	2.01×10^{17}
	260	α, SF	3.6 ms	2.7×10^{19}
	261	α	0.26 s	3.7×10^{17}
	263	α	0.9 s	1.1×10^{17}
107	261	SF	1.5 ms	6.4×10^{19}
	262	α	4.7 ms	2.03×10^{19}
108	265	α	1.8 ms	5.3×10^{19}
109	266	α	3.5 ms	2.7×10^{19}

[a] Decay modes are denoted by: α for alpha decay, β^- for beta decay, EC for electron capture, IT for isomeric transition, and SF for spontaneous fission. The decay mode given in this column represents either the major decay mode or the only observed decay mode.

[b] 1 year = 365.243 d.

[c] Specific activity is given in units of disintegrations per minute per microgram and contains one more significant figure than the half-life in order to avoid rounding-off errors. 1 Curie (Ci) = 3.7×10^{10} dis s^{-1} = 3.7×10^{10} Bq.

AUTHOR INDEX

Page numbers in *italic* refer to figures or tables.

SUBJECT INDEX

Page numbers in *italic* refer to information in figures or tables.

Fundamental constants

Quantity	Symbol	Value	SI unit	Auxiliary value
Speed of light in vacuum	c	$2.997\,925 \times 10^{8}$	$m\,s^{-1}$	
Elementary charge	e	$1.602\,189 \times 10^{-19}$	C	
Planck constant	h	$6.626\,18 \times 10^{-34}$	Js	$= 4.135\,70 \times 10^{-15}$ eV s; $\hbar = h/2\pi$
Avogadro constant	N_A	$6.022\,04 \times 10^{23}$	mol^{-1}	
Atomic mass unit	1 u	$1.660\,566 \times 10^{-27}$	kg	= 931.501 6 MeV: mass of $^{12}C = 12$ u
Electron rest mass	m_e	$0.910\,953 \times 10^{-30}$	kg	$M_e = N_A \cdot m_e = 0.000\,548\,580$ u = 0.511 003 4 MeV
Proton rest mass	m_P	$1.672\,649 \times 10^{-27}$	kg	$M_P = N_A \cdot m_P = 1.007\,276\,5$ u = 938.279 6 MeV
Neutron rest mass	m_n	$1.674\,954 \times 10^{-27}$	kg	$M_n = N_A \cdot m_n = 1.008\,665\,0$ u = 939.573 1 MeV
Faraday constant	F	$9.648\,46 \times 10^{4}$	$C\,mol^{-1}$	$= N_A \cdot e$
Rydberg constant	R_∞	$1.097\,373 \times 10^{7}$	m^{-1}	$R_\infty h \cdot c = 13.605\,8$ eV
Bohr radius	a_0	$0.529\,177 \times 10^{-10}$	m	$= \alpha/4\pi R_\infty$
Electron magnetic moment	μ_e	$9.284\,83 \times 10^{-24}$	$J\,T^{-1}$	
Proton magnetic moment	μ_P	$1.410\,617 \times 10^{-26}$	$J\,T^{-1}$	
Bohr magneton	μ_B	$9.274\,08 \times 10^{-24}$	$J\,T^{-1}$	$= e \cdot /2 \cdot m_e$ ($1\,J\,T^{-1} = 10^3$ erg gauss^{-1})
Nuclear magneton	μ_N	$5.050\,82 \times 10^{-27}$	$J\,T^{-1}$	$= e \cdot /2 \cdot m_P$
Molar gas constant	R	8.314 41	$J\,mol^{-1}\,K^{-1}$	= 0.082 057 lit atm $mol^{-1}\,K^{-1}$ = 1.987 2 cal $mol^{-1}\,K^{-1}$
Molar volume of ideal gas (s.t.p.)	V_m	0.022 413 8	$m^3\,mol^{-1}$	$= R \cdot T_0/p_0$, $T_0 = 273.15$ K, $p_0 = 1$ atm
Boltzmann constant	k	$1.380\,662 \times 10^{-23}$	$J\,K^{-1}$	$= R/N_A$; $= 8.617\,35 \times 10^{-5}$ eV K^{-1}; $1/k = 11\,604.5$ K eV^{-1}

Pressure	Pa	bar	kp/m^2
1 Pa (Pascal) = $1\,N/m^2$	1	10^{-5}	1.019716×10^{-1}
1 bar = $10^6\,dyn/cm^2$	10^5	1	10.19716×10^3
$1\,kp/m^2$ = 1 mm H_2O	9.80665	0.980665×10^{-4}	1
1 at = $1\,kp/cm^2$	0.980665×10^5	0.980665	10^4
1 atm = 760 Torr	1.01325×10^5	1.01325	1.033227×10^4
1 Torr = 1 mm Hg	133.3224	1.333224×10^{-3}	13.59510
$1\,lb/in^2$ = 1 psi	6.89476×10^3	68.9476×10^{-3}	703.069

Useful conversion factors

Work, energy, heat	J	kWh	kcal	Btu	MeV
1 J (Joule) = 1 Ws = 1 Nm = 10^7 erg	1	2.778×10^{-7}	2.39006×10^{-4}	9.4781×10^{-4}	6.242×10^{12}
1 kWh	3.6×10^6	1	860.4	3412.14	2.247×10^{19}
1 kcal	4184.0	1.1622×10^{-3}	1	3.96566	2.6117×10^{16}
1 Btu (British thermal unit)	1055.06	2.93071×10^{-4}	0.25164	1	6.5858×10^{15}
1 MeV	1.602×10^{-13}	4.450×10^{-20}	3.8289×10^{-17}	1.51840×10^{-16}	1

Molecular energy	J/mol	cm^{-1}/molecule	K*/molecule	eV/molecule
1 J/mol	1	0.0835935	0.12027	0.0103643
1 cm^{-1}/molecule	11.96266	1	1.43879	1.2398×10^{-4}
1 K/molecule	8.31444	0.69503	1	8.6173×10^{-5}
1 eV/molecule	96484.6	8065.5	11604.5	1

* Kelvin (temperature unit)

Power	kW	PS	kp m/s	kcal/s
1 kW = 10^{10} erg/s	1	1.35962	101.972	0.239006
1 PS	0.73550	1	75	0.17579
1 kp m/s	9.80665×10^{-3}	0.01333	1	2.34384×10^{-3}
1 kcal/s	4.1840	5.6886	426.650	1

at	atm	Torr	lb/in^2
1.019716×10^{-5}	0.986923×10^{-5}	0.750062×10^{-2}	145.0378×10^{-6}
1.019716	0.986923	750.062	14.50378
10^{-4}	0.967841×10^{-4}	0.735559×10^{-1}	1.422335×10^{-3}
1	0.967841	735.559	14.22335
1.033227	1	760	14.69595
1.359510×10^{-3}	1.315789×10^{-3}	1	19.33678×10^{-3}
70.3069×10^{-3}	68.0460×10^{-3}	51.7149	1